2.7 Hypothetical Accident Conditions

The NAC-STC is required to be structurally adequate for the free drop, puncture, fire, crush, and water immersion hypothetical accident scenario in accordance with 10 CFR 71.73. In the free drop analyses, the cask impact orientation evaluated must be that which inflicts the maximum damage to the cask. The cask accident assessment must also be at the most unfavorable ambient temperature in the range from -20°F to 100°F. Likewise, for the Yankee-MPC and CY-MPC canistered fuel or GTCC waste configurations, the NAC-STC has been evaluated for structural adequacy, considering the inclusion of the transportable storage canister in the free drop, puncture, fire, crush, and water immersion hypothetical accident scenario in accordance with 10 CFR 71.73. Where bounded by the directly loaded fuel (uncanistered) configuration analyses, the analyses sections are so noted. The following subsections contain the evaluation of the NAC-STC for structural integrity under hypothetical accident conditions.

NAC-STC Directly Loaded Fuel and Yankee-MPC

After the NAC-STC cask body structural analyses were completed, the cask closure geometry, the fuel basket design and the heat transfer analyses were subsequently reanalyzed. Two- and three-dimensional structural analyses of the cask discussed in this section and summarized in the tables presented in Section 2.10.4 are not influenced by the localized changes to the closure system, the basket design, or the heat transfer analysis and thus, have not been revised to incorporate these design and analyses enhancements.

The revised heat transfer analyses are presented in Chapter 3 for the NAC-STC. Section 2.10.10 presents a comparison of temperature gradients obtained from the original and the revised heat transfer analyses for the NAC-STC and an evaluation of conservative margins of safety identified using original temperature distributions in the cask structural qualification. It has been concluded from the evaluation in Section 2.10.10 that the detailed finite element analyses performed for normal and accident condition loads using the original temperature distribution are conservative. Therefore, the detailed finite element analyses for the NAC-STC have not been changed to incorporate the revised temperature distribution.

Temperature distributions for both normal and accident conditions were recalculated as a result of improvements in the modeling of the boundary conditions used in the heat transfer analyses and design changes made to the fuel basket. These boundary condition improvements better reflect actual conditions than those originally modelled in the cask thermal analyses. The most

significant revisions to the boundary conditions included modeling the gap between the basket and inner shell, and consideration of an adiabatic surface for the area of the cask covered by the impact limiter.

The revised thermal analysis resulted in reduced thermal gradients and the associated secondary stresses applicable to the normal condition structural qualification throughout the cask, and increased the maximum component temperature in the regions of the cask influenced by the insulating effect of the impact limiter (Section 2.10.10). Based on the fact that accident condition structural criteria are based on primary membrane and primary bending stresses, changes in temperature do not create higher stresses in the cask for structural evaluation accident condition loads. Therefore, the resulting influence of the increase in component temperature on the stress qualification is limited to reducing the temperature dependent material allowable stresses. Revisions to the hypothetical accident conditions structural qualification of the cask that result from the newly calculated temperatures are presented as changes in the allowable stresses and the margins of safety in the stress summary tables in Section 2.10.4.

Impact Limiters

As described in Sections 2.3.7 and 2.6.7.4, two impact limiter designs are used with the NAC-STC cask. The redwood impact limiters described in License Drawings 423-209 and 423-210 may be used with the directly loaded fuel and the Yankee-MPC canistered fuel and GTCC waste configurations. The balsa impact limiters described in License Drawings 423-257 and 423-258 must be used with the NAC-STC cask transporting the CY-MPC canistered fuel and GTCC waste configurations, but may also be used in the transport of directly loaded fuel and the Yankee-MPC canistered fuel and GTCC waste configurations.

2.7.1 Free Drop (30 Feet)

The NAC-STC is required by 10 CFR 71.73(c)(1) to demonstrate structural adequacy for a free drop through a distance of 30 feet onto a flat, unyielding, horizontal surface. The cask strikes the surface in an orientation that inflicts maximum damage. In determining which orientation produces the maximum damage, the NAC-STC is evaluated for impact orientations in which the cask strikes the impact surface on its top end, top end oblique, side, bottom end, and bottom end oblique. The redwood and balsa impact limiters and the impact limiter attachments are evaluated in Section 2.6.7.4 for all loading conditions.

Impacts with the maximum and minimum weights of contents are considered. The environmental temperature for the drop is between -20°F and 100°F. Internal heat generation from the contents and solar heating are also considered. Regarding internal pressure, the maximum or minimum normal transport pressure is applied to produce the critical stress condition in conjunction with the other loads previously discussed. Closure lid bolt preload and fabrication stresses are also considered.

The following method and assumptions are adopted in all of the drop analyses:

1. The finite element method is utilized to do the impact analyses. The analyses are performed using the ANSYS computer program.

2. The analyses assume linearly elastic behavior of the cask.

3. The impact loads calculated in Section 2.6.7.4 are statically applied to the impact surface of the cask. The dynamic wave propagation produced by the impact is assumed to spread throughout the cask body simultaneously.

4. The finite element model of the NAC-STC includes only the major structural components of the cask body; thus, the weight of the modeled cask body does not include the weight of the neutron shield material, the neutron shield shell, nor the cavity contents. However, the applied loads on the cask model are based on a cask design weight of 250,000 pounds for the directly loaded and Yankee-MPC configurations, and of 260,000 pounds for the CY-MPC configurations.

5. To account for the lead slump during the drops, and for the differential thermal expansion between the cask stainless steel shells and lead shell, gap elements are used in the finite element model.

6. For the Yankee-MPC and CY-MPC designs, which include a transportable storage canister in the NAC-STC, the same load scenarios, methods and assumptions have been considered.

7. The drop scenarios for the canistered Yankee-MPC class design with spent fuel bound the canistered Yankee-MPC with GTCC contents, as the latter configuration has a lower weight.

8. The redwood impact limiters and the balsa impact limiters are designed to limit the g-loads applied to the NAC-STC to the same values.

The types of loading considered in the accident condition analyses include: (1) thermal, (2) internal pressure, (3) closure lid bolt preload, and (4) impact and inertial loads resulting from the impact event. These loadings and the boundary conditions, used in the finite element analyses, are discussed in Sections 2.7.1.1 through 2.7.1.4. Section 2.10 documents the procedures, analysis and stress results for the 30-foot drop accident conditions.

Note that the fabrication stresses are considered negligible as explained in Section 2.6.11. The puncture analysis is performed using classical hand calculations, as shown in Section 2.7.2.

2.7.1.1 Thirty-Foot End Drop

The NAC-STC is structurally evaluated for the hypothetical accident 30-foot end drop condition in accordance with the requirements of 10 CFR 71.73(c)(1). In this evaluation, the directly loaded NAC-STC (equipped with an impact limiter over each end) falls through a distance of 30 feet onto a flat, unyielding, horizontal surface. The cask strikes the surface in a vertical position; consequently, an end impact on the bottom end or top end of the cask occurs. The types of loading involved in an end drop accident are closure lid bolt preload, internal pressure, thermal, impact load, and inertial body load. There are six credible end impact conditions to be considered, according to Regulatory Guide 7.8:

1. Top end drop with 100°F ambient temperature, maximum decay heat load, and maximum solar insolation.

2. Top end drop with -20°F ambient temperature, maximum decay heat load, and no solar insolation.

3. Top end drop with -20°F ambient temperature, no decay heat load, and no solar insolation.

4. Bottom end drop with 100°F ambient temperature, maximum decay heat load, and maximum solar insolation.

5. Bottom end drop with -20°F ambient temperature, maximum decay heat load, and no solar insolation.

6. Bottom end drop with -20°F ambient temperature, no decay heat load, and no solar insolation.

2.7.1.1.1 Thirty-Foot End Drop—NAC STC Directly Loaded and Yankee-MPC Configurations

The finite element analysis method is utilized to perform the end drop stress evaluations for the NAC-STC. The end drop accident condition can be analyzed using a two-dimensional axisymmetric model, because of the symmetry of both the cask structure and the loads involved in the end drop case. The cask is modeled as an axisymmetric structure using ANSYS STIF42

isoparametric elements. A detailed description of the two-dimensional finite element model of the NAC-STC is provided in Section 2.10.2.1.1.

During an impact event, the cask body will experience a vertical deceleration. Considering the cask as a free body, the impact limiter will apply the load to the cask end to produce the deceleration. Since the deceleration represents an amplification factor for the inertial loading of the cask, the equivalent static method is adopted to perform the impact evaluations. The analyses consider the behavior of the cask to be linearly elastic. Additionally, the fabrication stresses are considered to be negligible (Section 2.6.11).

Five categories of load--closure lid bolt preload, internal pressure, thermal, impact, and inertial body loads--are considered on the cask:

1. Closure lid bolt preload - The required bolt preload on the inner lid bolts is 115,066 pounds per bolt. For the outer lid bolts, the bolt preload is 36,810 pounds per bolt. Individual bolt preload is applied to the model by imposing initial strains to the bolt shafts, as explained in Section 2.10.2.2.3. The bolts are modeled as beam (ANSYS STIF3) elements.

2. Internal pressure - The cask internal pressure is temperature dependent and is evaluated in Section 3.4.4. Pressures of 50 psig and 12 psig are applied on the interior surfaces of the cask cavity for the hot ambient and cold ambient cases, respectively. These pressures envelope the calculated pressures for cask configurations - directly loaded fuel (12 psig), Yankee-MPC canistered fuel (11.3 psig), and Yankee-MPC canistered GTCC waste (<11.3 psig).

3. Thermal - The heat transfer analyses performed in Sections 3.4.2 and 3.4.3 determine the cask temperature distributions for the following three combinations of ambient temperature, heat load, and solar insolation for directly loaded fuel.

   Condition 1. 100°F ambient temperature, with maximum decay heat load, and maximum solar insolation.

Condition 2. -20°F ambient temperature, with maximum decay heat load, and no solar insolation.

Condition 3. -20°F ambient temperature, with no decay heat load, and no solar insolation.

The cask temperatures calculated for each of the three thermal conditions discussed above are used in the ANSYS structural analyses to determine the values of the temperature-dependent material properties.

Additional heat transfer analyses were performed for the Yankee-MPC canistered fuel configuration as described in Section 2.6.7.1.

4. Impact loads - The impact loads are induced by the impact limiter acting on the cask end during an end drop condition. The impact loads are determined from the energy absorbing characteristics of the impact limiters, as described in Section 2.6.7.4. The impact load is expressed in terms of the design cask weight (loaded or empty), multiplied by appropriate deceleration factors (g's). For details, see Section 2.6.7.4.

The impact limiter load is considered to be uniformly applied over the end surface of the finite element model of the cask. The calculation of impact pressure loads is documented in Section 2.10.2.2.2. The following is a summary of the impact pressures applied to the exterior surface of the impacting end, for the different loading scenarios, with the corresponding design deceleration (g) values.

LOADING CONDITION	IMPACT PRESSURE FOR 1g	DECELERATION (g)
End impact with basket and fuel	42.35 psi	56.1
End impact with basket, no fuel	35.74 psi	49.4

For the end impact, with basket and fuel, a uniform pressure of 2376 psi ([42.35 psi][56.1 g/1g]) is applied on the exterior surface of the end of the finite element model of the cask. This pressure value is calculated by dividing the total impact load ([56.1g/1g][250,000 lb] = 14.03×10^6 lb) by the impact area ($p \times (43.35)^2 = 5903.8$ in^2), which is the surface area of the end of the cask.

It should be noted that the design weight of the cask is 250,000 pounds, which includes the weight of the empty cask with impact limiters (194,000 lb), plus the weight of the cavity contents (56,000 lb) for the directly loaded fuel configuration. For those load conditions for which the cask contains no fuel, the basket (design weight = 17,000 lb) is still considered to be in the cask, resulting in a weight of 211,000 pounds for the empty cask with basket. The weights of the cavity contents for the Yankee-MPC canistered fuel and the Yankee-MPC canistered GTCC waste configurations are 55,590 pounds and 54,271 pounds, respectively.

5. Inertial body load - The inertial effects, which occur during the end impact, are represented by equivalent static forces, in accordance with D'Alembert's principle. Inertial body load includes the weight of the empty cask (194,000 lb) and the weight of the cavity contents (56,000 lb) for the directly loaded fuel configuration, which envelopes that of the Yankee-MPC canistered fuel or the Yankee-MPC canistered GTCC waste.

Inertia loads resulting from the weight of the empty cask are imposed by applying an appropriate deceleration factor to the cask mass. The applied decelerations are determined by considering the crush strength and the geometry of the impact limiters, as explained in Section 2.6.7.4.

The inertial load resulting from the 56,000-pound contents design weight is represented as an equivalent static pressure load uniformly applied on the interior surface of the impacting end of the cask. For the load case with no fuel in the cavity, the basket (design weight = 17,000 lb) is considered to be in the cask; the weight of the basket is represented in the ANSYS finite element model in the same manner as that of the contents.

The following is a summary of the inertial body load for a 1g deceleration and the design decelerations for the different loading scenarios. The calculations of content pressures is documented in Section 2.10.2.2.1.

LOADING CONDITION	IMPACT PRESSURE FOR 1g	DECELERATION (g)
End impact with basket and fuel	14.14 psi	56.1
End impact with basket, no fuel	4.29 psi	49.4

In the ANSYS analyses, the inertial body loads are considered together with the impact loads. The results of the two simultaneous loadings are documented as "impact loads."

In all cases, the 30-foot end drop load condition for the canistered Yankee class fuel configuration is bounded by the analyses of the directly loaded fuel configuration. The primary basis for the validity of that statement is that the NAC-STC, with canistered Yankee class fuel, weighs essentially the same as the NAC-STC with directly loaded PWR fuel. Therefore, the crush deceleration from the cask impact limiters for the Yankee-MPC canistered configuration will be essentially equal to that for the NAC-STC directly loaded fuel configuration. The aluminum honeycomb cavity spacers' crush strength is less than that of the impact limiter redwood/balsa design so the spacers will crush first, providing initial deceleration prior to that produced by the impact limiters.

The primary stresses throughout the cask body are calculated for individual and combined loading conditions, for the directly loaded fuel configuration, which envelopes the Yankee-MPC canistered configuration. The individual primary loading conditions are: (1) internal pressure (including bolt preload); (2) top end impact (impact load only); and (3) bottom end impact (impact load only). The combined loading conditions for primary stress evaluations are the: (1) 30-foot top end impact with bolt preload and 50 psig internal pressure; (2) 30-foot top end impact with bolt preload and 12 psig internal pressure; (3) 30-foot top end impact (without contents) with bolt preload and 12 psig internal pressure; (4) 30-foot bottom end impact with bolt preload and 50 psig internal pressure; (5) 30-foot bottom end impact with bolt preload 12 psig internal pressure; and (6) 30-foot bottom end impact (without contents) with bolt preload and 12 psig internal pressure.

Because axisymmetry exists in the cask geometry and in the end-drop loading conditions, axisymmetric boundary conditions are represented in the formulation of the isoparametric elements. A longitudinal support is imposed on the corner node located in the non-impacting end of the cask, to prevent rigid body motion. When the cask system is in equilibrium (i.e., the inertial body loads match the impact loads exactly), then the reaction force at this support will be zero. An examination of the magnitude of the reaction forces provides a check of the validity of the finite element evaluation for the 30-foot end drop condition. The reaction at the longitudinal support is 2,582 pounds/radian for the 56.1g top end drop load condition. This means that the unbalanced force of the cask model system is only (2582)(2p)/56.1 = 289 pounds. Compared to

the cask design weight of 250,000 pounds, the unbalanced force is negligible, amounting to only 0.12 percent of the design weight of the cask.

The allowable stress limit criteria, for containment and noncontainment structures, are provided in Section 2.1.2. These criteria are used to determine the allowable stresses for each cask component, conservatively using the maximum operating temperature within a given component to determine the allowable stress throughout that component. Note that higher temperatures result in lower allowable stresses.

Stress results for the individual loading cases of internal pressure (including bolt preload) are documented in Tables 2.10.4-1 and 2.10.4-2. Stress results for the individual 30-foot top and bottom end drop impact loading cases are documented in Tables 2.10.4-13 and 2.10.4-14. These are nodal stress summaries obtained from the finite element analysis results. As described in Section 2.10.4, the nodal stresses are documented on the representative section cuts. Stress results for the combined loading conditions discussed above are documented in Tables 2.10.4-112 through 2.10.4-129. These tables document the primary, primary membrane (P_m), primary membrane plus primary bending ($P_m + P_b$), and critical P_m and $P_m + P_b$ stresses in accordance with the criteria presented in Regulatory Guide 7.6. As described in Sections 2.10.2.3 and 2.10.2.4, procedures have been implemented to document the nodal and sectional stresses as well as to determine the critical (maximum) stress summary for all cask components.

For the top end impact loading case, the maximum calculated membrane stress intensity is 12.6 ksi. The maximum calculated membrane plus bending stress intensity is 34.4 ksi. By comparison, for the combined loading case, including impact, bolt preload, and internal pressure; the maximum calculated primary membrane stress intensity is 16.4 ksi and the maximum calculated primary membrane plus primary bending stress intensity is 38.5 ksi. The maximum stress intensities due to impact alone are equal to 90 percent of the maximum primary stress intensities due to the combined loading. Therefore, it is concluded that the impact stresses are the governing factor for the 30-foot top end drop condition.

For the 30-foot top end drop scenario, ANSYS analyses were performed at the three different temperature conditions. The results from those three analyses show that the maximum $P_m + P_b$ stress intensities are 37.1 ksi, 38.5 ksi, and 36.2 ksi, as listed in respective Tables 2.10.4-116, 2.10.4-118 and 2.10.4-120.

These three stress results are essentially identical, with the difference between them being less than 6 percent. Since the allowable stress for a component is a function of the component temperature, with higher temperatures resulting in lower allowable stresses, the allowable stress will be lowest for temperature condition 1 because the highest component temperatures occur for condition 1. Therefore, it is concluded that the stress results from temperature condition 1 are the most critical for the end drop accident conditions. The allowable stresses for temperature condition 1 are conservatively used for all of the temperature condition analyses.

A similar set of ANSYS analyses was performed for the 30-foot bottom end drop case. The stress results follow the same pattern as the top end drop. The maximum $P_m + P_b$ stress intensities for the 30-foot bottom end drop are 22.7 ksi, 23.1 ksi, and 21.7 ksi, as listed in Tables 2.10.4-125, 2,10.4-127, and 2.10.4-129, respectively.

As shown in Tables 2.10.4-112 through 2.10.4-129, the margins of safety are positive for all of the end drop accident conditions. The most critically stressed component in the system is the inner lid, for the top end drop. The minimum margin of safety for the top end drop condition is found to be +0.8, as documented in Table 2.10.4-118. The minimum margin of safety for the bottom end drop condition is found to be +1.8, as documented in Table 2.10.4-127.

Satisfaction of the extreme total stress intensity range limit is demonstrated in Section 2.1.3.3. The documentation of the NAC-STC adequacy in satisfying the buckling criteria for the stresses of the end drop condition is presented in Section 2.10.5.

The NAC-STC maintains its containment capability and therefore satisfies the requirements of 10 CFR 71.73 for the hypothetical accident 30-foot end drop condition for the directly loaded fuel configuration, which envelopes the Yankee-MPC canistered fuel and Yankee-MPC canistered GTCC waste configurations for the 30-foot end drop conditions.

2.7.1.1.2 Thirty-Foot End Drop—CY-MPC Configuration

The NAC-STC loaded with the CY-MPC fuel basket is structurally evaluated for the hypothetical accident 30-foot end drop condition in accordance with the requirements of 10 CFR 71.73(c)(1). In this evaluation, the NAC-STC equipped with an impact limiter over each end and loaded with a CY-MPC canister, falls through a distance of 30 feet onto a flat, unyielding, surface.

The finite element analysis method is utilized to perform the end drop stress evaluations for the CY-MPC. With the exception of the loading, the CY-MPC model is the same as the model used to evaluate the Yankee-MPC. A description of the model is included in Section 2.10.2.1.1.

Boundary Conditions—CY-MPC Configuration End Drop Analysis

The maximum internal pressure for the CY-MPC system is 38.1 psig as shown in Section 3.4.4. Since the maximum internal pressure is less than the 50 psig design pressure used for the analyses presented in Sections 2.6 and 2.7, the analyses presented in Sections 2.6 and 2.7 bound the CY-MPC system.

Two cold environment cases are considered. The first case includes -40 °F ambient temperature, no solar insolation, maximum decay heat, and maximum internal pressure. Component temperatures for this case are less than the temperatures used for the NAC-STC analysis. Therefore, the Yankee-MPC analysis envelops the CY-MPC design. The second case, or minimum temperature condition, assumes -40°F ambient temperature, no solar insolation, no decay heat, and maximum internal pressure. An evaluation of the minimum temperature condition is not required since all component temperatures are at -40°F.

For the bottom and top end drops, a surface pressure load equivalent to the weight of the loaded canister and spacer (67,200 lb.) is applied to either the cask bottom or canister lid. The process for applying the pressure load is described in detail in Section 2.10.2.2.1. The pressure load is multiplied by an acceleration of 56.1g to account for the total impact load.

The allowable stress limit criteria, for containment and noncontainment structures, are provided in Section 2.1.2. These criteria are used to determine the allowable stresses for each cask component, conservatively using the maximum operating temperature within a given component to determine the allowable stress throughout that component. Note that higher temperatures result in lower allowable stresses.

Results—CY-MPC Configuration End Drop Analysis

Maximum stress intensities are obtained for the sections shown in Figure 2.7.1.1-1. The coordinate of each section is presented in Table 2.7.1.1-1. Tables 2.7.1.1-2 through 2.7.1.1-5 provide a stress summary at each of the sections listed in Table 2.7.1.1-1. As shown in Tables 2.7.1.1-2 through 2.7.1.1-5, the margins of safety are positive for all of the end drop accident conditions. The most critically stressed component in the system is the outer lid, for the top end

drop. The minimum margin of safety for the top end drop condition is found to be +4.8, as documented in Table 2.7.1.1-3. The minimum margin of safety for the bottom end drop condition is found to be +3.4, as documented in Table 2.7.1.1-5. The stresses that occur at the center of the end plate and lids are artificially high due to the presence of a small hole modeled in the ends (ANSYS modeling technique) and are ignored in the results post-processing.

The NAC-STC maintains its containment capability and therefore satisfies the requirements of 10 CFR 71.73 for the hypothetical accident 30-foot side drop condition for the CY-MPC fuel configuration, which envelopes the canistered fuel and canistered GTCC waste configurations for the 30-foot side drop conditions

Figure 2.7.1.1-1 Location of Sections for CY-MPC Configuration Stress Evaluation

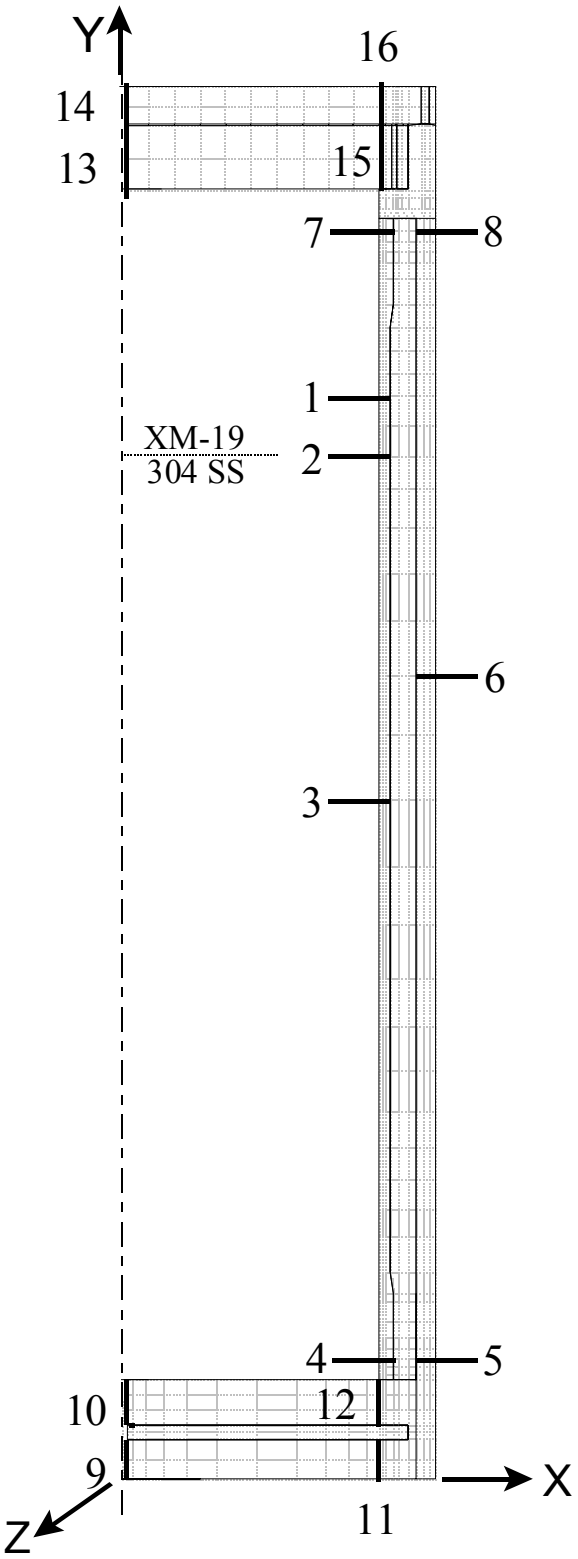

Table 2.7.1.1-1 NAC-STC Section Locations for CY-MPC Stress Evaluation (Maximums)

Section No.	Component Name and Material	Section Location (in.)							
		Inside Node	X	Y	Z	Outside Node	X	Y	Z
1	Transition Shell – XM-19	197	35.5	146.1	0.0	165	37	146.1	0.0
2*	Inner Shell – 304	196	35.5	142.0	0.0	164	37	142.0	0.0
3	Inner Shell – 304	189	35.5	94.2	0.0	157	37	94.2	0.0
4	Bottom Forging – 304	130	35.5	14.5	0.0	123	38	14.5	0.0
5	Outer Shell – 304	280	40.7	14.5	0.0	328	43	14.5	0.0
6	Outer Shell – 304	300	40.7	103.2	0.0	358	43	103.2	0.0
7	Top Forging – 304	271	35.5	173.2	0.0	265	37.5	173.2	0.0
8	Top Forging – 304	317	40.7	173.2	0.0	435	43.4	173.2	0.0
9	Bottom Plate – 304	23	3.16	0.0	0.0	34	3.16	5.45	0.0
10	Bottom Forging – 304	53	3.16	7.45	0.0	65	3.16	13.65	0.0
11	Bottom Plate – 304	22	35.5	0.0	0.0	32	35.5	5.45	0.0
12	Bottom Forging – 304	52	35.5	7.45	0.0	62	35.5	13.65	0.0
13	Inner Lid – 304	486	3.52	178.68	0.0	787	3.52	187.65	0.0
14	Outer Lid – 17-4	514	3.52	187.68	0.0	500	3.52	192.96	0.0
15	Inner Lid – 304	485	35.5	178.68	0.0	796	35.5	187.65	0.0
16	Outer Lid – 17-4	497	35.5	187.68	0.0	495	35.5	192.96	0.0

* This section is at the boundary of transition shell and inner shell.

Table 2.7.1.1-2 NAC-STC Critical P_m Stress Summary for CY-MPC; 30-ft Top End Drop

Section No.	P_m Stresses (ksi)						Stress Intensity Impact (ksi)	Stress Intensity Bolt Preload + Pressure** (ksi)	Stress Intensity Total (ksi)	Allowable Stress* (ksi)	Margin of Safety
	S_X	S_Y	S_Z	S_{XY}	S_{YZ}	S_{XZ}					
1	0.0	-4.4	0.0	0.0	0.0	0.0	4.4	1.9	6.3	65.2	9.3
2	0.0	-4.3	0.0	0.0	0.0	0.0	1.6	1.9	3.5	45.9	12.1
3	0.0	-3.5	0.0	0.0	0.0	0.0	3.5	1.9	5.4	45.9	7.5
4	-0.1	-1.5	0.5	-0.2	0.0	0.0	2.0	1.9	3.9	45.9	10.8
5	0.0	-0.6	0.4	0.0	0.0	0.0	1.1	1.9	3.0	45.9	14.3
6	0.0	-3.5	0.8	0.0	0.0	0.1	4.3	1.9	6.2	45.9	6.4
7	-0.5	-3.6	-0.5	0.1	0.0	-0.1	3.2	1.9	5.1	45.9	8.0
8	-0.3	-5.7	-0.1	-0.5	0.1	0.1	5.6	1.9	7.5	45.9	5.1
9	-0.5	0.0	-0.5	0.0	0.0	0.0	0.5	1.9	2.4	45.9	18.1
10	0.4	0.0	0.4	0.0	0.0	0.0	0.5	1.9	2.4	45.9	18.1
11	-0.5	0.0	-0.5	-0.2	0.0	0.0	0.6	1.9	2.5	45.9	17.4
12	0.4	-0.8	0.2	-0.3	0.0	0.0	1.3	1.9	3.2	45.9	13.3
13	-0.4	-2.8	0.1	1.0	-0.2	0.0	3.3	1.9	5.2	45.9	7.8
14	-1.0	-4.4	0.6	0.5	0.0	0.1	5.1	1.9	7.0	45.9	5.6
15	0.0	-2.9	-0.3	0.0	-0.3	0.0	3.0	1.9	4.9	45.9	8.4
16	-0.1	-3.9	0.0	-0.6	-0.3	0.0	4.1	1.9	6.0	45.9	6.7

* Allowable at 331°F (maximum temperature for inner shell) governed by 0.7Su.

** Based on internal pressure of 50 psi.

Table 2.7.1.1-3 NAC-STC Critical $P_m + P_b$ Stress Summary for CY-MPC; 30-ft Top End Drop

Section No.	P_m Stresses (ksi)						Stress Intensity Impact (ksi)	Stress Intensity Bolt Preload + Pressure** (ksi)	Stress Intensity Total (ksi)	Allowable Stress* (ksi)	Margin of Safety
	S_X	S_Y	S_Z	S_{XY}	S_{YZ}	S_{XZ}					
1	0.0	-4.6	0.0	0.0	0.0	0.0	4.6	1.9	6.5	93.2	13.3
2	0.0	-4.4	0.0	0.0	0.0	0.0	4.4	1.9	6.3	65.6	9.4
3	0.0	-3.5	0.0	0.0	0.0	0.0	1.2	1.9	3.1	65.6	20.2
4	0.0	-3.6	-0.1	-0.4	0.0	0.0	3.7	1.9	5.6	65.6	11.7
5	0.0	-2.1	0.0	-0.2	0.0	0.0	2.2	1.9	4.1	65.6	15.0
6	0.0	-3.5	0.8	0.0	0.0	0.1	4.4	1.9	6.3	65.6	9.4
7	-0.8	-6.1	-1.5	0.1	0.0	-0.2	5.3	1.9	7.2	65.6	8.1
8	0.1	-9.4	-1.0	-0.3	0.1	0.0	9.5	1.9	11.4	65.6	4.8
9	-2.7	0.0	-2.9	0.0	0.0	0.0	2.8	1.9	4.7	65.6	13.0
10	3.1	0.0	3.4	0.0	0.0	0.0	3.4	1.9	5.3	65.6	11.4
11	-1.8	0.0	-0.3	-0.2	0.0	0.1	1.8	1.9	3.7	65.6	16.7
12	2.4	0.3	0.5	-0.1	0.0	-0.1	2.1	1.9	4.0	65.6	15.4
13	8.1	-0.4	8.8	0.3	0.0	0.0	9.3	1.9	11.2	65.6	4.9
14	1.3	-4.0	3.3	-1.0	0.5	0.1	7.5	1.9	9.4	65.6	6.0
15	-0.1	-2.9	2.0	0.6	-0.1	0.0	4.9	1.9	6.8	65.6	8.7
16	5.6	-3.6	4.5	0.0	-0.2	-0.4	9.4	1.9	11.3	65.6	4.8

* Allowable at 331°F (maximum temperature for inner shell) governed by 0.7Su.

** Based on internal pressure of 50 psi.

Table 2.7.1.1-4 NAC-STC Critical P_m Stress Summary for CY-MPC; 30-ft Bottom End Drop

Section No.	P_m Stresses (ksi)						Stress Intensity Impact (ksi)	Stress Intensity Bolt Preload + Pressure** (ksi)	Stress Intensity Total (ksi)	Allowable Stress* (ksi)	Margin of Safety
	S_X	S_Y	S_Z	S_{XY}	S_{YZ}	S_{XZ}					
1	0.0	-3.3	0.0	0.0	0.0	0.0	3.3	1.9	5.2	65.2	11.5
2	0.0	-3.4	0.0	0.0	0.0	0.0	3.4	1.9	5.3	45.9	7.7
3	0.0	-4.2	0.0	0.0	0.0	0.0	4.2	1.9	6.1	45.9	6.5
4	-0.6	-4.4	-1.1	-0.3	0.0	-0.1	3.8	1.9	5.7	45.9	7.1
5	0.0	-7.0	-0.8	0.8	0.0	0.0	7.2	1.9	9.1	45.9	4.0
6	0.0	-4.0	0.6	0.0	0.0	0.1	4.6	1.9	6.5	45.9	6.1
7	-0.1	-2.1	1.1	0.2	0.0	0.1	3.2	1.9	5.1	45.9	8.0
8	0.0	-1.6	1.1	-0.1	0.0	0.1	2.7	1.9	4.6	45.9	9.0
9	-1.6	-5.5	-0.5	-1.8	0.2	0.1	5.8	1.9	7.7	45.9	5.0
10	0.7	-2.9	0.9	-0.7	0.1	0.0	4.0	1.9	5.9	45.9	6.8
11	-0.8	-5.2	-1.1	-0.1	0.8	0.0	4.6	1.9	6.5	45.9	6.1
12	1.0	-2.0	1.1	0.2	0.0	0.0	3.1	1.9	5.0	45.9	8.2
13	-0.3	-0.2	-0.2	0.2	0.0	0.0	0.3	1.9	2.2	45.9	19.8
14	-0.2	-0.4	0.0	0.1	0.0	0.0	0.4	1.9	3.3	45.9	12.9
15	-0.3	-0.8	-0.4	0.5	0.0	0.0	1.1	1.9	3.0	45.9	14.3
16	-0.1	-0.3	-0.1	0.1	0.0	0.0	0.3	1.9	2.2	45.9	19.9

* Allowable at 331°F (maximum temperature for inner shell) governed by 0.7Su.

** Based on internal pressure of 50 psi.

Table 2.7.1.1-5 NAC-STC Critical $P_m + P_b$ Stress Summary for CY-MPC; 30-ft Bottom End Drop

Section No.	P_m Stresses (ksi)						Stress Intensity Impact (ksi)	Stress Intensity Bolt Preload + Pressure** (ksi)	Stress Intensity Total (ksi)	Allowable Stress* (ksi)	Margin of Safety
	S_X	S_Y	S_Z	S_{XY}	S_{YZ}	S_{XZ}					
1	0.0	-3.5	-0.1	0.0	0.0	0.0	3.5	1.9	5.4	93.2	16.3
2	0.0	-3.5	0.0	0.0	0.0	0.0	3.5	1.9	5.4	65.6	11.1
3	0.0	-4.3	0.0	0.0	0.0	0.0	4.3	1.9	6.2	65.6	9.6
4	-1.1	-7.3	-2.2	-0.3	0.0	-0.3	6.3	1.9	8.2	65.6	7.0
5	0.2	-12.9	-2.3	0.3	0.0	-0.1	13.1	1.9	15.0	65.6	3.4
6	0.0	-4.0	0.6	0.0	0.0	0.1	4.6	1.9	6.5	65.6	9.1
7	0.0	-2.9	0.9	0.1	0.0	0.1	3.8	1.9	5.7	65.6	10.5
8	0.0	-3.6	0.6	0.3	0.0	0.1	4.2	1.9	6.1	65.6	10.8
9	3.7	-3.5	5.9	-1.2	-0.2	0.1	9.7	1.9	11.6	65.6	4.7
10	9.3	-1.2	10.7	-0.1	0.0	0.1	11.9	1.9	13.9	65.6	3.7
11	4.1	-3.6	4.0	-0.8	0.6	-0.2	8.1	1.9	10.0	65.6	5.6
12	3.6	-1.7	2.5	0.5	0.1	-0.1	5.4	1.9	7.3	65.6	8.0
13	4.7	0.3	5.0	0.1	0.0	0.0	4.7	1.9	6.6	65.6	8.9
14	2.6	-0.2	2.9	-0.1	0.0	0.0	3.2	1.9	5.1	65.6	11.9
15	-0.6	-1.0	1.5	0.7	0.0	0.1	3.0	1.9	4.9	65.6	12.4
16	-0.1	-0.3	1.0	0.2	0.0	0.0	1.4	1.9	3.3	65.6	18.9

* Allowable at 331°F (maximum temperature for inner shell) governed by 0.7Su.

** Based on internal pressure of 50 psi.

THIS PAGE INTENTIONALLY LEFT BLANK

2.7.1.2 Thirty-Foot Side Drop

The NAC-STC is structurally evaluated for the hypothetical accident 30-foot side drop condition in accordance with the requirements of 10 CFR 71.73(c)(1). In this event the NAC-STC, equipped with an impact limiter over each end, falls through a distance of 30 feet onto a flat, unyielding, horizontal surface. The cask strikes the surface in a horizontal position; consequently, a side impact on the cask occurs. The types of loading involved in a side drop accident are closure lid bolt preload, internal pressure, thermal, impact load, and inertial body load. There are three credible side impact conditions to be considered, according to Regulatory Guide 7.8:

1. Side drop with 100°F ambient temperature, maximum decay heat load, and maximum solar insolation.

2. Side drop with -20°F ambient temperature, maximum decay heat load, and no solar insolation.

3. Side drop with -20°F ambient temperature, no decay heat load, and no solar insolation.

The finite element analysis method is utilized to perform the side drop stress evaluations for the NAC-STC. The side drop accident condition is analyzed using a three-dimensional structural model to accurately represent the non-axisymmetric loads involved in the side drop case. One-half of the cask is modeled as a three-dimensional structure with one plane of symmetry. The ANSYS STIF45 3-D solid element is the primary element type used in the model. In order to reduce the overall problem size, two three-dimensional models have been constructed for the directly loaded fuel configuration--the top fine mesh model and the bottom fine mesh model. A detailed description of the three-dimensional finite element models of the NAC-STC is presented in Section 2.10.2.1.2. The top model contains a fine mesh region at the upper half of the cask with a relatively coarse mesh at the bottom end; the bottom model contains a fine mesh region at the bottom end with relatively coarse mesh at the top end.

Both models are used in the side drop analyses to obtain the detailed stresses throughout the cask for the directly loaded fuel configuration. The stress results from the fine mesh portion of each model are then used to form the final stress summary. For the Yankee-MPC and CY-MPC canistered fuel configurations, the stress results are obtained from the single finite element model of that configuration.

2.7.1.2.1 Thirty-Foot Side Drop—NAC STC and Yankee-MPC Configurations

During a side impact event, the cask body experiences a lateral deceleration. Considering the cask as a free body, the impact limiters apply the load to the side of the cask (in the impact limiter contact area) to produce the deceleration. Since the deceleration represents an amplification factor for the inertial loading of the cask, the equivalent static method is adopted to do the impact evaluations. The analyses consider the behavior of the cask to be linearly elastic. Additionally, fabrication stresses are considered to be negligible (Section 2.6.11).

Five categories of load--closure lid bolt preload, internal pressure, thermal, impact, and body inertia—are considered on the cask:

1. Closure lid bolt preload - The required bolt preload on the inner lid bolts is 115,066 pounds/bolt. For the outer lid bolts, the bolt preload is 36,810 pounds/bolt. Bolt preload is applied to the model by imposing initial strains to the bolt shafts, as explained in Section 2.10.2.2.3.

2. Internal pressure - The cask internal pressure is temperature dependent and is evaluated in Section 3.4.4. Pressures of 50 psig and 12 psig are applied on the interior surfaces of the cask cavity for the hot ambient and cold ambient cases, respectively. These pressures envelope the calculated pressures for all cask configurations—directly loaded fuel (12 psig), Yankee-MPC canistered fuel (11.3 psig), and Yankee-MPC canistered GTCC waste (< 11.3 psig).

3. Thermal - The heat transfer analyses determine the cask temperature distributions for the following three combinations of ambient temperature, heat load, and solar insolation for directly loaded fuel:

   Condition 1. 100°F ambient temperature, with maximum decay heat load, and maximum solar insolation.

   Condition 2. -20°F ambient temperature, with maximum decay heat load, and no solar insolation.

Condition 3. -20°F ambient temperature, with no decay heat load, and no solar insolation.

The cask temperatures calculated for each of the three thermal conditions discussed above are used in the ANSYS structural analyses to determine the values of the temperature-dependent material properties.

Additional heat transfer analyses were performed for the Yankee-MPC canistered fuel configuration as described in Section 2.6.7.2.

4. Impact loads - The impact loads are induced by the impact limiters acting on the cask during a side drop condition. The impact loads are determined from the energy absorbing characteristics of the impact limiters, as described in Section 2.6.7.4. The impact load is expressed in terms of the design cask weight (loaded or empty), multiplied by appropriate deceleration factors (g's). The 30-foot side drop evaluations conservatively consider a deceleration factor of 55g; the calculated deceleration value is 51.7g, as documented in Section 2.6.7.4, Table 2.6.7.4.1-3.

The impact limiter load is applied to the finite element model as a distributed pressure over the contact areas between the impact limiters and the cask. The contact area is defined based on the “crush” geometry of the impact limiter. The distribution of impact pressure is considered to be uniform in the longitudinal direction, and is considered to vary sinusoidally in the circumferential direction. A cosine-shaped pressure distribution is selected, which is peaked at the center, and spread over a 79.4-degree arc on either side of the centerline, around the circumference, as shown in Figure 2.10.2-32 of Section 2.10.2.2.1. The 79.4-degree arc is determined based on the impact limiter test results for a side drop crush geometry. The assumption of a “peaked” pressure distribution is a conservative, classical, stress analysis procedure. Since the center of gravity of the loaded cask is located within 1 inch of the cask middle plane, the impact load is considered to be evenly divided between the two limiters. The impact contact area for a side drop accident consists of the 12.0-inch overlapping region between the impact limiter and the cask, at each end of the cask.

The calculation to determine the pressure applied to the finite element model is documented in Section 2.10.2.2.2. The calculation is based on a 1g deceleration

condition. The following is a summary of the lateral impact pressures for the eight circumferential sectors:

ARC (deg)	LATERAL IMPACT PRESSURE FOR 1g (psi)	DECELERATION (g)
0 - 8.3	163.22	55
8.3 - 17.0	158.67	55
17.0 - 26.2	149.06	55
26.2 - 35.8	133.98	55
35.8 - 45.9	113.17	55
45.9 - 56.5	86.69	55
56.5 - 67.7	54.99	55
67.7 - 79.4	18.96	55

The impact pressures used in the 30-foot side drop analyses are determined by multiplying the pressure values above by the deceleration factor (55g).

It should be noted that the design weight of the cask is 250,000 pounds, which includes the weight of the empty cask (194,000 lb), plus the weight of the cavity contents (56,000 lb), for the directly loaded fuel configuration, which envelopes the Yankee-MPC canistered fuel or Yankee-MPC GTCC waste configurations. For those load conditions in which the cask contains no fuel, the basket (design weight = 17,000 lb) is still considered to be in the cask, resulting in a weight of 211,000 pounds for the cask with basket.

5. Inertial body load - The inertial effects that occur during the impact are represented by equivalent static forces, in accordance with D'Alembert's principle. Inertial body load includes the weight of the empty cask (194,000 lb) and the weight of the cavity contents (56,000 lb) for the directly loaded fuel configuration, which envelopes that of the Yankee-MPC canistered fuel or the Yankee-MPC canistered GTCC waste.

Inertia loads resulting from the weight of the empty cask are imposed by applying an appropriate deceleration factor to the cask mass. The applied deceleration is 55g, and is applied as explained in the discussion of the impact loads.

The inertial load, resulting from the 56,000-pound contents weight, is represented as an equivalent static pressure applied on the interior surface of the cask for the directly loaded fuel configuration. Specifically, the equivalent static pressure is applied with a uniform distribution along the cavity length, and with a cosine-shaped distribution in the circumferential direction. The calculation of the contents pressure, as documented in Section 2.10.2.2.1, uses the identical method as that used in the determination of the impact pressures. In the case of no fuel in the cavity, the design weight of the basket (17,000 lb) is considered, and is represented in the same manner as that of the contents design weight. The following is a summary of the contents pressures for a 1g deceleration, for the eight circumferential sectors:

ARC (deg)	LATERAL CONTENTS PRESSURE FOR 1g (psi)	DECELERATION (g)
0 - 8.3	6.51	55
8.3 - 17.0	6.33	55
17.0 - 26.2	5.95	55
26.2 - 35.8	5.34	55
35.8 - 45.9	4.51	55
45.9 - 56.5	3.46	55
56.5 - 67.7	2.19	55
67.7 - 79.4	0.76	55

Similarly, inertial load pressures are calculated for the Yankee-MPC canistered fuel configuration of the NAC-STC as described in Section 2.6.7.2.

The contents pressures considered in the 30-foot side drop analyses are determined by multiplying the pressure values above by the deceleration factor (55g).

In the ANSYS analyses, the inertial body loads are considered together with the impact loads. The results of the two simultaneous loadings are documented as "impact loads."

The stresses throughout the cask body are calculated for individual and combined loading conditions. The individual loading conditions are (1) internal pressure (including bolt preload); and (2) 30-foot side impact (impact load only). The combined loading condition is the 30-foot side impact with bolt preload and 50 psig internal pressure. This is the most critical combined loading condition for the 30-foot side drop, as will be shown in a discussion later in this report.

The finite element model has one plane of symmetry in the cask geometry and in the side drop loading conditions. Symmetric boundary conditions are applied to the cask finite element model by restraining the nodes on the symmetry plane to prevent translations in the direction normal to the symmetry plane. In addition, two nodes at the outer cask radius on the top and bottom ends of the cask, opposite the points of impact, are restrained laterally (in the drop direction) and the node at the top is restrained in the longitudinal direction to prevent rigid body motion. When the cask system is in equilibrium (i.e., the inertial body loads match the impact loads exactly), then the reaction forces at these supports will be zero. An examination of the magnitude of the reaction forces provides a check of the validity of the finite element evaluation for the 30-foot side drop condition. The sum of reactions in the cask lateral direction for the bottom model is 9,465 pounds, for the application of a 55g-load. This means that the unbalanced force of the cask model system is only 9465/55 = 172.1 pounds. Compared to one-half of the design weight of the cask (125,000 lb), the unbalanced force is negligible, amounting to only 0.1 percent of the design weight of the cask. A similar check done for the top model indicates that the unbalanced force is 0.5 percent of the design weight, which is also negligible.

The allowable stress limit criteria, for containment and noncontainment structures, are provided in Section 2.1.2. These criteria are used to determine the allowable stresses for each cask component, conservatively using the maximum operating temperature within a given component to determine the allowable stress throughout that component. Note that higher component temperatures result in

lower allowable stresses. Table 2.10.2-5 documents the allowable stress values determined for each component, for temperature condition 1.

The stress results for the 30-foot side drop loading cases for the NAC-STC directly loaded fuel configuration are presented as described below.

Stress results for the individual internal pressure loading conditions are documented in Tables 2.10.4-1 and 2.10.4-2. Stress results for the individual 30-foot side impact loading condition are documented in Table 2.10.4-15. These are the nodal stress summaries obtained from the finite element analysis results. As described in Section 2.10.2.4.2, the nodal stresses are documented on the representative section cuts. Stress results for the combined loading condition are documented in Tables 2.10.4-130 through 2.10.4-140. These tables document--the primary stresses for the 0-degree circumferential location, the primary membrane (P_m) stresses for the 0-, 45.9-, 91.7-, and the 180-degree circumferential locations, the primary membrane plus primary bending ($P_m + P_b$) stresses for the 0-, 45.9-, 91.7-, and the 180-degree circumferential locations, and the critical P_m and critical $P_m + P_b$ stresses--in accordance with the criteria presented in Regulatory Guide 7.6. The stress results on the 0-, 45.9-, 91.7-, and the 180-degree circumferential locations document the stress variation in the circumferential direction. The circumferential locations are illustrated in Figure 2.10.2-8. As described in Sections 2.10.2.3 and 2.10.2.4, procedures have been implemented to document the nodal and sectional stresses as well as to determine the critical stress summary for all cask components.

Each of the stress summary tables for the directly loaded fuel configuration are prepared by considering the stress results of two analysis runs, the first using the top fine mesh model and the second using the bottom fine mesh model. The stress results from the fine mesh portion of each model are used to form the nodal and sectional stress summaries. For the critical stress summaries, stresses for the top forging, inner lid and outer lid are determined from the top fine mesh model results; stresses for the bottom plate and the bottom forging are calculated from the bottom fine mesh model results; stresses for the inner shell, the transition sections, and the outer shell are determined as the larger of the stress results from both models. In order to justify the use of stress results from both models for the side drop evaluation, comparisons are made on the combined loading (impact plus internal pressure)

stress results from the two models, at the middle section of the cask (Sections L and M in Figure 2.10.2-34, axial location of 96.15 inches from cask bottom). On the 0-degree, 45-degree, and 90-degree circumferential locations, the stress results from the two models show good agreement, with a difference of less than 10 percent. On the 180-degree circumferential location, where stresses are lower, the stress results from the two models are still reasonably comparable, with a difference of less than 15 percent. An additional check is performed for sections J and K (axial location of 54.90 inches), and sections N and O (axial location of 137.40 inches), which are about 40 inches away from the center of the cask (Figure 2.10.2-34). The stress results from the two models also show good agreement at these sections, with a difference of less than 10 percent for the 0-degree, 45.9-degree and 90-degree circumferential locations. Therefore, it is concluded that the combined stress results from the top fine mesh model and the bottom fine mesh model for the 30-foot side drop condition are valid and conservative.

There are three temperature conditions to be considered in the side drop evaluation. In order to determine the most critical temperature condition, two parametric studies are performed for the NAC-STC, using the three-dimensional bottom fine mesh model. The first parametric study compares the stress results for temperature condition 1 and temperature condition 2. The combined loading stress results show that the maximum stress intensities for conditions 1 and 2 are 34.1 ksi and 34.0 ksi, respectively. Since allowable stress is a function of temperature, higher component temperatures result in lower allowable stresses. The minimum margins of safety for conditions 1 and 2 are +0.87 and +0.93, respectively. It is, therefore, concluded that condition 1 is more critical than condition 2. The second parametric study compares the stress results between the analyses of conditions 1 and 3. The stress results indicate that the minimum margins of safety for temperature conditions 1 and 3 are +0.87 and +1.67, respectively. Therefore, condition 1 is more critical than condition 3. It is concluded, from the stress results of the parametric studies, that condition 1 is the most critical for the side drop accident condition. Therefore, only the stress results for temperature condition 1 for the 30-foot side drop are provided in the stress tables of this section.

It is worthwhile to mention that the most critical stress for the impact loading condition and that for the primary loading condition are essentially identical, with a maximum difference of 3 percent. Therefore it is concluded that the impact stresses are the governing factor, for the 30-foot side drop condition.

As shown in the critical P_m and $P_m + P_b$ stress summaries (Tables 2.10.4-133 and 2.10.4-134) for the directly loaded fuel configuration, the critical stresses for most of the cask components occur on the 0-degree circumferential location, which contains the line of impact. It is also observed that, for the cask inner shell, the maximum calculated stresses are located on the circumferential locations in the 56.5- to 67.7-degree region. This is because the maximum shearing stresses are located near the 56.5-degree circumferential location.

Similarly, the stress results for the Yankee-MPC canistered fuel configuration of the NAC-STC are presented in Tables 2.7.1.2-1 and 2.7.1.2-2. The section locations are defined in Figure 2.6.7.2-1. Only the inner and outer shells and their attachment regions to the top and bottom forgings are evaluated for the Yankee-MPC canistered fuel configuration because the Yankee-MPC canistered contents loading on the cask cavity does not significantly change the stresses in the end components of the cask from those stresses calculated for the directly loaded fuel configuration.

As shown in Tables 2.10.4-133 and 2.10.4-134, the margins of safety are positive for all of the 30-foot side drop accident conditions. The most critically stressed component in the system is the top forging. The minimum margin of safety for the side drop condition is found to be +0.4, as documented in Table 2.10.4-133 for the directly loaded fuel configuration. For the Yankee-MPC canistered fuel configuration, Tables 2.7.1.2-1 and 2.7.1.2-2 show that all margins of safety are positive with a minimum margin of safety, +0.2, located on the inner shell near the bottom.

Satisfaction of the extreme total stress intensity range limit is demonstrated in Section 2.1.3.3.

The documentation of the adequacy of the NAC-STC to satisfy the buckling criteria for the stresses of the side drop condition is presented in Section 2.10.5.

The NAC-STC maintains its containment capability and, therefore, satisfies the requirements of 10 CFR 71.73 for the 30-foot side drop hypothetical accident condition.

2.7.1.2.2 Thirty-Foot Side Drop—CY-MPC Configuration

The NAC-STC loaded with the CY-MPC canister is structurally evaluated for the hypothetical accident 30-foot side drop condition in accordance with the requirements of 10 CFR 71.73(c)(1). In this event the NAC-STC, equipped with an impact limiter over each end, falls through a distance of 30 feet onto a flat, unyielding, horizontal surface. The cask strikes the surface in a horizontal position; consequently, a side impact on the cask occurs. The types of loading involved in a side drop accident are closure lid bolt preload, internal pressure, thermal, impact load, and inertial body load. There are three credible side impact conditions to be considered, according to Regulatory Guide 7.8:

1. Side drop with 100°F ambient temperature, maximum decay heat load, and maximum solar insolation.

2. Side drop with -20°F ambient temperature, maximum decay heat load, and no solar insolation.

3. Side drop with -20°F ambient temperature, no decay heat load, and no solar insolation.

The finite element analysis method is utilized to perform the side drop stress evaluations for the CY-MPC. With the exception of the loading, the CY-MPC model is the same as the model used to evaluate the Yankee-MPC. A description of the model is included in Section 2.10.2.1.1.

Boundary Conditions—CY-MPC Configuration Side Drop Analysis

The maximum internal pressure for the CY-MPC system is 38.1 psig as shown in Section 3.4.4. Since the maximum internal pressure is less than the 50 psig design pressure used for the analyses presented in Sections 2.6 and 2.7, the analyses presented in Sections 2.6 and 2.7 bound the CY-MPC system.

Two cold environment cases are considered. The first case includes -40°F ambient temperature, no solar insolation, maximum decay heat, and maximum internal pressure. Component temperatures for this case are less than the temperatures used for the NAC-STC analysis. Therefore, the Yankee-MPC analysis envelops the CY-MPC design. The second case, or minimum temperature condition, assumes -40°F ambient temperature, no solar insolation, no

decay heat, and maximum internal pressure. An evaluation of the minimum temperature condition is not required since all component temperatures are at -40°F.

The inertial load, resulting from the 67,200-pound contents weight, is represented as an equivalent static pressure applied on the interior surface of the cask for the CY-MPC fuel configuration. Specifically, the equivalent static pressure is applied with a uniform distribution along the cavity length, and with a cosine-shaped distribution in the circumferential direction. Note that the weight of the canister lids is considered separately from the weight of the canister shell and fuel basket. This results in larger load in the region of the canister structural and shield lids. The contents pressures considered in the 30-foot side drop analyses are determined by multiplying the pressure values above by the deceleration factor (55g). In the ANSYS analyses, the inertial body loads are considered together with the impact loads. The results of the two simultaneous loadings are documented as "impact loads."

The stresses throughout the cask body are calculated for individual and combined loading conditions. The individual loading conditions are (1) internal pressure (including bolt preload); and (2) 30-foot side impact (impact load only). The combined loading condition is the 30-foot side impact with bolt preload and 50 psig internal pressure. The peak stress intensity from the internal pressure plus bolt preload is conservatively added to the sectional stresses from the cask body impact results.

The allowable stress limit criteria, for containment and noncontainment structures, are provided in Section 2.1.2. These criteria are used to determine the allowable stresses for each cask component, conservatively using the maximum operating temperature within a given component to determine the allowable stress throughout that component. Note that higher temperatures result in lower allowable stresses.

CY-MPC Configuration Side Drop Analysis Results

The stress results for the CY-MPC configuration of the NAC-STC are presented in Tables 2.7.1.2-4 and 2.7.1.2-5. The section locations are defined in Figure 2.7.1.2-1. The coordinates of each section is presented in Table 2.7.1.2-3. Only the inner and outer shells and their attachment regions to the top and bottom forgings are evaluated for the CY-MPC configuration because the canistered contents loading on the cask cavity does not significantly change the stresses in the end components of the cask from those stresses calculated for the directly loaded fuel configuration.

As shown in Tables 2.7.1.2-4 and 2.7.1.2-5, the margins of safety are positive for all of the 30-foot side drop accident conditions. The most critically stressed component in the system is the inner shell. The minimum margin of safety for the side drop condition is found to be +0.23 as documented in Table 2.7.1.2-5 for the CY-MPC configuration. Tables 2.7.1.2-4 and 2.7.1.2-5 show that all margins of safety are positive with a minimum margin of safety, +0.23, located on the inner shell near the bottom.

Satisfaction of the extreme total stress intensity range limit is demonstrated in Section 2.1.3.3.

The documentation of the adequacy of the NAC-STC loaded with a CY-MPC canister to satisfy the buckling criteria for the stresses of the side drop condition is presented in Section 2.10.5.

The CY-MPC canister maintains its containment capability and, therefore, satisfies the requirements of 10 CFR 71.73 for the 30-foot side drop hypothetical accident condition.

Figure 2.7.1.2-1 Location of Sections for NAC-STC Cask Body Stress Evaluation for CY-MPC

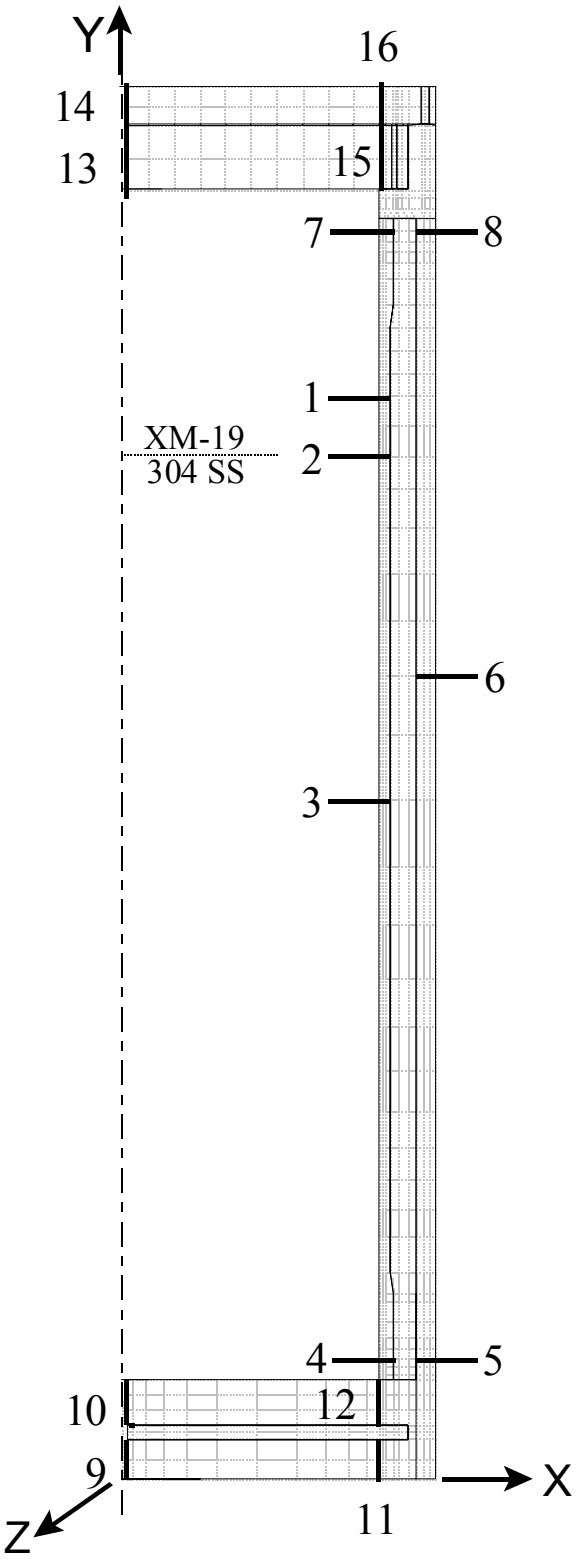

Table 2.7.1.2-1 Yankee-MPC Critical P_m Stress Summary; 30-ft Side Drop; Drop Orientation = 90°

Section No.	P_m Stresses (ksi)						Principal Stresses (ksi)			S.I.	S.I.** Bolt Preload	S.I.	Allowable Stress*	Margin of Safety
	S_X	S_Y	S_Z	S_{XY}	S_{YZ}	S_{XZ}	S1	S2	S3	Impact (ksi)	+ Pressure (ksi)	Total (ksi)	(ksi) $0.7S_u$	
1	-2.4	9.4	15.2	-0.2	-1.6	0.9	15.6	9.0	-2.4	18.1	1.9	20.0	65.7	2.3
2	-1.7	12.0	14.1	0.4	-1.3	0.7	14.7	11.5	-1.7	16.4	1.9	18.3	46.1	1.5
3	-1.1	20.9	6.5	0.0	0.1	0.4	20.9	6.5	-1.1	22.0	1.9	23.9	46.1	0.9
4	-0.4	-12.8	-16.2	3.2	0.9	-1.1	0.4	-13.1	-16.7	17.1	1.9	19.0	46.1	1.4
5	2.0	-2.3	-11.9	3.9	0.9	-0.9	4.3	-4.4	-12.1	16.5	1.9	18.4	46.1	1.5
6	-0.6	22.5	5.3	0.0	0.0	1.0	22.5	5.4	-0.8	23.3	1.9	25.2	46.1	0.8
7	0.0	-8.9	-10.4	-1.7	-0.7	-0.7	0.4	-8.8	-10.8	11.2	1.9	13.1	46.1	2.5
8	0.0	6.5	-3.6	-1.8	-0.7	-0.2	7.0	-0.4	-3.7	10.7	1.9	12.6	46.1	2.7

* Allowable at 311°F (maximum temperature for inner shell).

** Based on internal pressure of 50 psi.

Table 2.7.1.2-2 Yankee-MPC Critical $P_m + P_b$ Stress Summary; 30-ft Side Drop; Drop Orientation = 90°

Section No.	$P_m + P_b$ Stresses (ksi)						Principal Stresses (ksi)			S.I.	S.I. Bolt Preload	S.I.	Allowable Stress*	Margin of Safety
	S_X	S_Y	S_Z	S_{XY}	S_{YZ}	S_{XZ}	S1	S2	S3	Impact (ksi)	+ Pressure** (ksi)	Total (ksi)	(ksi) S_u	
1	-2.7	26.5	33.3	-0.2	-1.0	2.1	33.5	26.4	-2.8	36.3	1.9	38.2	94.0	1.5
2	-1.5	24.8	32.3	0.4	-0.8	2.0	32.5	24.8	-1.6	34.2	1.9	36.1	65.9	0.8
3	-1.0	29.8	29.1	0.0	0.0	1.9	29.8	29.2	-1.1	30.9	1.9	32.8	65.9	1.0
4	1.0	-51.8	-26.6	4.2	0.3	-1.8	1.4	-26.7	-52.1	53.5	1.9	55.4	65.9	0.2
5	3.0	-35.0	-20.3	1.1	0.3	-1.5	3.1	-20.4	-35.1	38.2	1.9	40.1	65.9	0.6
6	-0.5	34.1	34.6	0.0	0.1	2.8	34.8	34.1	-0.7	35.5	1.9	37.4	65.9	0.8
7	0.6	-21.6	-12.0	-2.4	0.0	-0.8	0.9	-12.0	-21.9	22.8	1.9	24.7	65.9	1.7
8	-1.2	17.7	-2.6	-2.4	-1.5	0.0	18.1	-1.5	-2.8	20.9	1.9	22.8	65.9	1.9

* Allowable at 311°F (maximum temperature for inner shell).

** Based on internal pressure of 50 psi.

Table 2.7.1.2-3 CY-MPC Configuration Section Locations for Stress Evaluation (Maximums)

Section No.	Component Name and Material	Section Location (in.)							
		Inside Node	X	Y	Z	Outside Node	X	Y	Z
1	Transition Shell – XM-19	197	35.5	146.1	0.0	165	37	146.1	0.0
2*	Inner Shell – 304	196	35.5	142.0	0.0	164	37	142.0	0.0
3	Inner Shell – 304	189	35.5	94.2	0.0	157	37	94.2	0.0
4	Bottom Forging – 304	130	35.5	14.5	0.0	123	38	14.5	0.0
5	Outer Shell – 304	280	40.7	14.5	0.0	328	43	14.5	0.0
6	Outer Shell – 304	300	40.7	103.2	0.0	358	43	103.2	0.0
7	Top Forging – 304	271	35.5	173.2	0.0	265	37.5	173.2	0.0
8	Top Forging – 304	317	40.7	173.2	0.0	435	43.4	173.2	0.0

***** This section is at the boundary of transition shell and inner shell.

Table 2.7.1.2-4 CY-MPC Configuration Critical P_m Stress Summary; 30-ft Side Drop

Section No.	P_m Stresses (ksi)						Stress Intensity Impact (ksi)	Stress Intensity Bolt Preload + Pressure** (ksi)	Stress Intensity Total (ksi)	Allowable Stress* (ksi)	Margin of Safety
	S_X	S_Y	S_Z	S_{XY}	S_{YZ}	S_{XZ}					
1	-1.2	8.4	7.6	0.0	1.3	0.4	10.5	1.9	12.4	65.2	4.3
2	-1.0	10.6	6.7	-0.1	-1.2	0.2	12.0	1.9	13.9	45.9	2.3
3	-1.1	21.3	5.6	0.0	0.0	0.4	22.4	1.9	24.3	45.9	0.89
4	-0.3	-8.5	-14.7	4.1	1.0	-1.2	16.6	1.9	18.5	45.9	1.5
5	2.5	5.0	-11.3	4.4	0.5	-1.3	19.8	1.9	21.7	45.9	1.1
6	-0.6	24.1	5.2	0.0	0.0	0.9	24.9	1.9	26.8	45.9	0.71
7	-0.9	-10.7	-6.8	-3.6	-1.4	-0.5	12.6	1.9	14.5	45.9	2.2
8	-0.1	9.9	0.3	-1.8	-0.7	0.2	10.6	1.9	12.5	45.9	2.7

* Allowable at 331°F (maximum temperature for inner shell) governed by $0.7S_u$.
** Based on internal pressure of 50 psi.

Table 2.7.1.2-5 CY-MPC Configuration Critical $P_m + P_b$ Stress Summary; 30-ft Side Drop

Section No.	P_m Stresses (ksi)						Stress Intensity Impact (ksi)	Stress Intensity Bolt Preload + Pressure** (ksi)	Stress Intensity Total (ksi)	Allowable Stress* (ksi)	Margin of Safety
	S_X	S_Y	S_Z	S_{XY}	S_{YZ}	S_{XZ}					
1	-1.0	13.7	21.1	0.0	-0.9	1.3	22.4	1.9	24.3	93.2	2.8
2	-0.8	15.7	21.2	-0.1	-0.8	1.2	22.2	1.9	24.1	65.6	1.7
3	-1.0	29.8	26.9	0.0	0.0	1.8	30.9	1.9	32.8	65.6	1.0
4	1.6	-48.8	-25.7	4.9	0.3	-2.1	51.5	1.9	53.4	65.6	0.23
5	1.8	36.7	-1.9	7.9	1.7	-0.8	40.9	1.9	42.8	65.6	0.53
6	-0.5	35.2	33.1	0.0	0.0	2.7	35.9	1.9	37.8	65.6	0.74
7	1.0	-22.9	-7.3	-4.8	-0.4	-0.7	25.8	1.9	27.7	65.6	1.4
8	-1.2	15.3	-0.9	-2.4	-2.0	0.2	17.5	1.9	19.4	65.6	2.4

* Allowable at 331°F (maximum temperature for inner shell) governed by $0.7S_u$.
** Based on internal pressure of 50 psi.

2.7.1.3 Thirty-Foot Corner Drop

The NAC-STC in the directly loaded fuel configuration is structurally evaluated for the hypothetical accident 30-foot corner drop condition in accordance with the requirements of 10 CFR 71.73(c)(1). In this event the NAC-STC, equipped with an impact limiter over each end, falls through a distance of 30 feet onto a flat, unyielding, horizontal surface. The cask strikes the surface on its top or bottom corner. The cask center of gravity is directly above the initial impact point for the corner drop condition. For the NAC-STC, an angle of 24 degrees from vertical is calculated for the corner drop orientation. The types of loading involved in a corner drop accident are closure lid bolt preload, internal pressure, thermal, impact load, and inertial body load. There are six credible corner impact conditions to be considered, according to Regulatory Guide 7.8.

1. Top corner drop with 100°F ambient temperature, maximum decay heat load, and maximum solar insolation.

2. Top corner drop with -20°F ambient temperature, maximum decay heat load, and no solar insolation.

3. Top corner drop with -20°F ambient temperature, no decay heat load, and no solar insolation.

4. Bottom corner drop with 100°F ambient temperature, maximum decay heat load, and maximum solar insolation.

5. Bottom corner drop with -20°F ambient temperature, maximum decay heat load, and no solar insolation.

6. Bottom corner drop with -20°F ambient temperature, no decay heat load, and no solar insolation.

The finite element analysis method is utilized to perform the corner drop stress evaluations for the NAC-STC. The corner drop accident conditions are analyzed using a three-dimensional structural model to accurately represent the non-axisymmetric loads involved in the corner drop case. One-half of the cask is modeled as a three-dimensional structure with one plane of

symmetry. The ANSYS STIF45 3-D solid element type is used in the model. Two finite element models are constructed; a top fine mesh model and a bottom fine mesh model. Each model is a complete representation of the cask, with a fine mesh region at the impacting end and with a relatively coarse mesh at the opposite end. The fine element mesh is modeled at the impacting end of the cask to provide detailed results in that region. The stresses predicted by the coarse element mesh at the non-impacting end of the model are not critical, so less detail is required. The detailed descriptions of the three-dimensional finite element models of the NAC-STC are described in Section 2.10.2.1.2.

Considering the cask as a free body, the impact limiter will apply the load to the cask impacting corner to produce the deceleration. Since the deceleration represents an amplification factor for the inertial loading of the cask, the equivalent static method is adopted to do the impact evaluations. The analyses consider the behavior of the cask to be linear elastic. Additionally, the fabrication stresses are considered to be negligible (Section 2.6.11).

Five categories of load—closure lid bolt preload, internal pressure, thermal, impact, and body inertia--are considered on the cask:

1. Closure lid bolt preload - The required bolt preloads on the inner lid bolts and the outer lid bolts are 115,066 pounds per bolt and 36,810 pounds per bolt, respectively (Section 2.6.7.5). Bolt preload is applied to the model by imposing initial strains to the bolt shafts, as explained in Section 2.10.2.2.3. The bolts are modeled as beam (ANSYS STIF4) elements.

2. Internal pressure - The cask internal pressure is temperature dependent and is evaluated in Section 3.4.4. Pressures of 50 psig and 12 psig are applied on the interior surfaces of the cask cavity for the hot ambient and cold ambient cases, respectively. These pressures envelope the calculated pressures for all cask configurations—directly loaded fuel (12 psig), Yankee-MPC canistered fuel (11.3 psig), and Yankee-MPC canistered GTCC waste (< 11.3 psig).

3. Thermal - The heat transfer analyses performed in Sections 3.4.2 and 3.4.3 determine the cask temperature distributions for the following three combinations of ambient temperature, heat load, and solar insolation for directly loaded fuel:

Condition 1. 100°F ambient temperature, with maximum decay heat load, and maximum solar insolation.

Condition 2. -20°F ambient temperature, with maximum decay heat load, and no solar insolation.

Condition 3. -20°F ambient temperature, with no decay heat load, and no solar insolation.

The cask temperature distributions, calculated for each of the three thermal conditions, are used in the ANSYS structural analyses to determine the values of the temperature-dependent material properties such as modulus of elasticity, density, and Poisson's ratio. These temperatures are also used to evaluate the thermal stress effect on the cask.

4. Impact loads - The impact loads are produced by the impact limiter acting on the cask corner during a corner drop condition. The impact loads are determined from the energy absorbing characteristics of the impact limiters, as described in Section 2.6.7.4. The impact load is expressed in terms of the design cask weight (loaded or empty), multiplied by an appropriate deceleration factor (g's). The design deceleration factor of 55g is used for both top and bottom corner drops. This compares to the actual deceleration factors of 49.3g, and 43.6g, as documented in Section 2.6.7.4, Table 2.6.7.4.1-2.

The impact loads for the corner drop analyses have lateral and longitudinal components, which are calculated from the total impact loads. The lateral component is distributed as a pressure with a circumferential distribution (similar to the side drop pressure) over an arc of 0 to 79.4 degrees on each side of the impact centerline (Section 2.10.2.2.2). The longitudinal component has a uniform distribution on a sector of the impacting end of the cask, over the same arc of 0 to 79.4 degrees on each side of the impact centerline.

Section 2.10.2.2.2 documents the impact pressures for a cask design weight of 250,000 pounds and an impact limiter contact length of 24.0 inches (12.0 inches at each end). In the corner drop case the impact energy is absorbed by only one impact limiter and, hence, the corner drop lateral impact pressures are determined by multiplying the side drop impact limiter by 2 (to account for only half as much impact limiter area), and by multiplying by the sine of the drop angle. For example, the corner drop lateral impact

pressure, for the elements located between the 0- and 8.29-degree circumferential planes, is:

$Press_1$ = (163.22)(2)(sin 24°) = 132.78 psi for 1g
$Press_{55}$ = (132.78)(55g/1g) = 7303.0 psi for 55g

The following is a summary of the lateral impact pressures, for the elements at the various circumferential locations, for a 1g deceleration:

ARC (deg)	LATERAL IMPACT PRESSURE FOR 1g (psi)	DECELERATION (g)
0 - 8.3	132.78	55
8.3 - 17.0	129.07	55
17.0 - 26.2	121.26	55
26.2 - 35.8	108.99	55
35.8 - 45.9	92.06	55
45.9 - 56.5	70.52	55
56.5 - 67.7	44.73	55
67.7 - 79.4	15.42	55

The longitudinal impact pressure is calculated as the cosine component of the total impact load, divided by the sector area within the 0- to 79.4-degree arc.

Therefore:

Weight = 250,000 lb
Area = (79.4/180)(p)$(43.35)^2$ = 2604 in^2
$Press_1$ = (250,000)(cos 24°)/2604 = 87.70 psi for 1g
$Press_{55}$ = (87.70)(55g/1g) = 4824.0 psi for 55g

It should be noted that the design weight of the cask is 250,000 pounds, which includes the weight of the empty cask (194,000 lb) plus the weight of the cavity contents (56,000 lb).

5. Inertial body load - The inertial effects that occur during the impact are represented by equivalent static forces, in accordance with D'Alembert's principle. Inertial body load

includes the weight of the empty cask (194,000 lb) and the weight of the cavity contents (56,000 lb).

Inertia loads resulting from the weight of the empty cask are imposed by applying an appropriate deceleration factor to the cask mass. The lateral and longitudinal components of inertial loading are determined in the same manner as for the impact loading.

The inertial load resulting from the 56,000-pound contents weight is represented as an equivalent static pressure load with both lateral and longitudinal components applied on the interior surface of the cask. The lateral component is applied to the cask model with the same circumferential distribution as that for the side drop pressure (over an arc of 0 degrees to 79.4 degrees on each side of the impact centerline). The lateral component pressure is determined by ratioing the side drop contents pressure values (Section 2.10.2.2.1) by the deceleration factor and by the sine of the drop orientation angle. The longitudinal component has a uniform distribution over the cask cavity end. The longitudinal component pressure is calculated by ratioing the end drop contents pressure by the deceleration factor and by the cosine of the drop orientation angle. The total deceleration factor is constant at 55g for both the top and the bottom corner drops.

Section 2.10.2.2.1 contains the side drop contents pressures for a total contents weight of 56,000 pounds. The corner drop lateral contents pressure for the elements located between the 0- and 8.29-degree circumferential planes is therefore:

$$Press_1 = (6.51)(\sin 24°) = 2.65 \text{ psi for 1g}$$
$$Press_{55} = (2.65)(55g/1g) = 146.0 \text{ psi for 55g}$$

The following is a summary of the applied lateral contents pressures for the corner drop for the directly loaded fuel configuration, for the elements at the various circumferential locations, for a 1g deceleration.

ARC (deg)	LATERAL CONTENTS PRESSURE FOR 1g (psi)	DECELERATION (g)
0 - 8.3	2.65	55
8.3 - 17.0	2.57	55
17.0 - 26.2	2.42	55
26.2 - 35.8	2.17	55
35.8 - 45.9	1.83	55
45.9 - 56.5	1.41	55
56.5 - 67.7	0.89	55
67.7 - 79.4	0.31	55

The longitudinal contents pressure is calculated from the longitudinal component of the total contents weight and the area over which it acts. Therefore:

Weight = 56,000 lb
Area = $(p)(35.5)^2 = 3959$ in^2
$Press_1$ = (56,000)(cos 24°)/3959 = 12.92 psi for 1g
$Press_{55}$ = (12.92)(55g/1g) = 711.0 psi for 55g

In the ANSYS analyses, the inertial body loads are considered together with the impact loads. The results of the two simultaneous loadings are documented as "impact loads".

The stresses throughout the cask body are calculated for individual and combined loading conditions. The individual loading conditions are: (1) internal pressure (including bolt preload); (2) 30-foot drop top corner impact (impact load only); and (3) 30-foot drop bottom corner impact (impact load only). The combined loading conditions are: (1) the 30-foot drop top corner impact with bolt preload and 50 psig internal pressure and (2) the 30-foot drop bottom corner impact with bolt preload and 50 psig internal pressure.

The model has one plane of symmetry in the cask geometry and in the corner drop loading conditions. Symmetric boundary conditions are applied to the cask finite element model by restraining the nodes on the symmetry plane to prevent translations in the direction normal to the

symmetry plane. In addition, two nodes at the outer cask radius on the top and bottom ends of the cask opposite the point of impact are restrained laterally; a longitudinal restraint is applied at one of the nodes opposite the end of impact, i.e., a bottom corner drop is axially restrained at the top node, and vice-versa. These lateral and axial restraints are only to prevent rigid body motion; there should be no significant reaction forces associated with these restraints. When the cask system is in equilibrium (i.e., the inertial body loads match the impact loads exactly), then the reaction forces at these supports will be zero. However, it is difficult to balance the impact limiter pressure resultant with the contents pressure and inertial body load resultant. An eccentricity between the two resultants induces a moment on the cask model. Therefore, non-zero reactions are found at the restraints. The reaction forces cause very high localized stresses (or stress singularities) in the model at the supports. These stresses are unrealistic and do not exist in the real cask. The stress singularity effect is minimized by distributing the reaction forces over the nodes in the top and bottom regions of the model. For the bottom corner drop, the reactions at the supports are 612 pounds laterally and zero longitudinally, for the application of a 55g deceleration. This means that the unbalanced force of the cask model system is only 612/55 = 11.1 pounds. Compared to one-half of the design weight of the cask (125,000 lb), the unbalanced force is negligible, amounting to only 0.009 percent of the design weight of the cask. For the top corner drop, the reactions at the supports are 511 pounds laterally and zero longitudinally, for the application of a 55g deceleration. This means that the unbalanced force of the cask model system is only 511/55 = 9.3 pounds. Compared to one-half of the design weight of the cask (125,000 lb), the unbalanced force is negligible, amounting to only 0.007 percent of the design weight of the cask.

The allowable stress limit criteria, for containment and non-containment structures, are provided in Section 2.1.2. These criteria are used to determined the allowable stresses for each cask component, conservatively using the maximum transport temperature within a given component to determine the allowable stress throughout that component. Note that higher component temperatures result in lower allowable stresses. Table 2.10.2-5 documents the allowable stress values determined for each component, for temperature condition 1.

Based on the discussion in Section 2.6.7.3, it is concluded that the 30-foot corner drop condition is enveloped by the 30-foot end and side drop analyses. Therefore, no additional analysis of the 30-foot corner drop condition is required for the Yankee-MPC or CY-MPC canistered fuel configurations of the NAC-STC. In all cases, the evaluations of the 30-foot corner drop load conditions for the Yankee-MPC and CY-MPC canistered configurations are bounded by the

30-foot corner drop analyses of the directly loaded fuel configurations. The primary basis for this conclusion is that the Yankee-MPC and CY-MPC canistered configurations weigh essentially the same as the directly loaded fuel configuration. Spacers in the cask cavity locate the package center of gravity for the Yankee-MPC and CY-MPC canistered fuel configurations at effectively the same location as that of the directly loaded fuel configuration.

Stress results for the individual loading cases of internal pressure (including bolt preload) are documented in Tables 2.10.4-1 and 2.10.4-2. Stress results for the individual 30-foot top and bottom corner drop impact loading cases are documented in Tables 2.10.4-16 and 2.10.4-17. These are the nodal stress summaries obtained from the finite element analysis results. As described in Section 2.10.2.4.2 and Section 2.10.4, the nodal stresses are documented on the representative section cuts. Primary stress results for the combined loading conditions discussed above are documented in Tables 2.10.4-141 and 2.10.4-152. All of the corner drop analyses are performed at temperature condition 1. The results from Sections 2.7.1.1 and 2.7.1.2 indicate that the stresses associated with temperature condition 1 yield the smallest margins of safety due to the effect of higher temperatures upon the allowable stresses.

These tables document the primary, primary membrane (P_m), primary membrane plus primary bending ($P_m + P_b$), and critical P_m and $P_m + P_b$ stresses in accordance with the criteria presented in Regulatory Guide 7.6. As described in Sections 2.10.2.3 and 2.10.2.4, procedures have been implemented to document the nodal and sectional stresses as well as to determine the critical stress summary for all cask components.

The P_m and the $P_m + P_b$ stresses documented in Tables 2.10.4-142 through 2.10.4-151 and 2.10.4-153 through 2.10.4-162 are stress results on the 0-, 45.9-, 91.7-, and the 180-degree circumferential locations. They indicate that the stress variations in the circumferential direction are similar between the top and the bottom corner drops. Furthermore, it is observed that the maximum calculated stresses are located on the circumferential locations in the 45.9- to 67.7-degree region. This is because the maximum shearing stresses are located near the 56.5-degree circumferential location. This shear stress, which is in the axial to circumferential location, is caused by the cantilever support from the impact limiter pressures and is compounded by the uneven distribution of the impact limiter pressure loading and the contents pressure loading.

The top corner drop cases result in higher maximum stress intensities than the bottom corner drop cases. For the individual impact loading cases, the maximum calculated membrane stress

intensity for the top corner drop is 33.7 ksi. The maximum calculated membrane plus bending stress intensity is 52.8 ksi. By comparison, for the combined loading case, including impact, bolt preload, and internal pressure, the maximum calculated P_m stress intensity is 33.4 ksi and the maximum calculated $P_m + P_b$ stress intensity is 51.8 ksi. The maximum stress intensity due to impact alone is 1.9 percent greater than the maximum stress intensities due to the combined loading. Therefore it is concluded that the impact case is the governing one for the 30-foot corner drop condition.

As shown in Tables 2.10.4-141 through 2.10.4-162, the margins of safety are positive for all of the corner drop accident conditions. The most critically stressed component is the inner lid for the top corner drop, and is the bottom forging for the bottom corner drop. The minimum margin of safety for the top corner drop condition is found to be +0.3, as documented in Table 2.10.4-145. The minimum margin of safety for the bottom corner drop condition is found to be +0.6, as documented in Table 2.10.4-156.

Satisfaction of the extreme total stress intensity range limit is demonstrated in Section 2.1.3.3.

The documentation of the adequacy of the NAC-STC to satisfy the buckling criteria for the stresses of the corner drop condition is presented in Section 2.10.5.

The NAC-STC maintains its containment capability and, therefore, satisfies the requirements of 10 CFR 71.73 for the 30-foot corner drop hypothetical accident condition.

THIS PAGE INTENTIONALLY LEFT BLANK

2.7.1.4 Thirty-Foot Oblique Drop

The NAC-STC is structurally evaluated for the hypothetical accident 30-foot oblique drop condition in accordance with the requirements of 10 CFR 71.73. In this event the NAC-STC, equipped with an impact limiter over each end, falls through a distance of 30 feet onto a flat, unyielding, horizontal surface. The cask strikes the surface obliquely on its top or bottom corner. For the NAC-STC, orientation angles of 15 degrees and 75 degrees are evaluated for the oblique drops. These angles are determined to be the most critical oblique drop orientations, as demonstrated in the following discussion. This section presents the 30-foot oblique drop evaluation for the directly loaded fuel configuration and shows that for the NAC-STC Yankee-MPC and CY-MPC configurations, the side drop results bound the oblique drop results.

The types of loading involved in an oblique drop accident are closure lid bolt preload, internal pressure, thermal, impact load, and inertial body load. There are six credible oblique impact conditions to be considered, according to Regulatory Guide 7.8:

1. Top oblique drop with 100°F ambient temperature, maximum decay heat load, and maximum solar insolation.

2. Top oblique drop with -20°F ambient temperature, maximum decay heat load, and no solar insolation.

3. Top oblique drop with -20°F ambient temperature, no decay heat load, and no solar insolation.

4. Bottom oblique drop with 100°F ambient temperature, maximum decay heat load, and maximum solar insolation.

5. Bottom oblique drop with -20°F ambient temperature, maximum decay heat load, and no solar insolation.

6. Bottom oblique drop with -20°F ambient temperature, no decay heat load, and no solar insolation.

The finite element analysis method is utilized to perform the oblique drop stress evaluations for the NAC-STC. The oblique drop accident conditions are analyzed using a three-dimensional structural model to accurately represent the non-axisymmetric loads involved in the oblique drop case. One-half of the cask is modeled, as a three-dimensional structure with one plane of symmetry. The ANSYS STIF45 3-D solid element is the primary element type used in the model. Two finite element models are constructed--a top fine mesh model and a bottom fine mesh model. Each model is a complete representation of the cask with a fine mesh region at the impacting end and with a relatively coarse mesh at the opposite end. The fine element mesh density is modeled at the impacting end of the cask to provide detailed results in that region. The stresses predicted by the coarse element mesh, at the non-impacting end of the model, are not critical, so less detail is required. The detailed description of the three-dimensional finite element models of the NAC-STC are presented in Section 2.10.2.1.2.

During an impact event, the cask body will experience a deceleration in the oblique drop direction. Considering the cask as a free body, the impact limiter will apply the loads to the impacting corner to produce the deceleration. Since the deceleration represents an amplification factor for the inertial loading of the cask, the equivalent static method is adopted to do the impact evaluations. The analyses consider the behavior of the cask to be linear elastic. Additionally, the fabrication stresses are considered to be negligible (Section 2.6.11).

Five categories of load--closure lid bolt preload, internal pressure, thermal, impact, and body inertial--are considered on the cask:

1. Closure lid bolt preload - The required bolt preloads on the inner lid bolts and the outer lid bolts are 115,066 pounds per bolt and 36,810 pounds per bolt, respectively. Bolt preload is applied to the model by imposing initial strains to the bolt shafts, as explained in Section 2.10.2.2.3. The bolts are modeled as beam (ANSYS STIF4) elements.

2. Internal pressure - The cask internal pressure is temperature dependent and is evaluated in Section 3.4.4. Pressures of 50 psig and 12 psig are applied on the interior surfaces of the cask cavity for the hot ambient and cold ambient cases, respectively. These pressures envelope the calculated pressures for all cask configurations—directly loaded fuel (12 psig), Yankee-MPC canistered fuel (11.3 psig), and Yankee-MPC canistered GTCC waste (< 11.3 psig).

3. Thermal - The heat transfer analyses performed in Sections 3.4.2 and 3.4.3 determine the cask temperature distributions for the following three combinations of ambient temperature, heat load, and solar insolation for directly loaded fuel:

   Condition 1. 100°F ambient temperature, with maximum decay heat load, and maximum solar insolation.

   Condition 2. -20°F ambient temperature, with maximum decay heat load, and no solar insolation.

   Condition 3. -20°F ambient temperature, with no decay heat load, and no solar insolation.

   The cask temperature distributions, calculated for each of the three thermal conditions, are used in the ANSYS structural analyses to determine the values of the temperature-dependent material properties.

4. Impact loads - The impact loads are produced by the impact limiter acting on the cask during an oblique drop condition. The impact loads are determined from the energy absorbing characteristics of the impact limiters, as described in Section 2.6.7.4. The impact load is expressed in terms of the design cask weight (loaded or empty), multiplied by an appropriate deceleration factor (g's).

   The impact load is similar to that discussed in Section 2.7.1.3 and is applied to the cask model by the same method. The design deceleration factor of 55g is used for both the top and the bottom oblique drops. This compares to the actual deceleration factors of 51.6g, and 47.1g, respectively, for the 15-degree drop orientation, and to 28.7g, and 29.9g, respectively, for the 75-degree drop orientation (Section 2.6.7.4). Section 2.10.2.2.2 documents the impact pressures for a cask design weight of 250,000 pounds and a total impact limiter length of 24.0 inches (12.0 inches at each end). In the oblique drop case the impact energy is absorbed by only one impact limiter, and hence the oblique drop lateral impact pressures are determined by multiplying the side drop impact pressures by 2 (to account for having only half as much impact limiter area), and by multiplying by the sine of the drop angle. For example, the oblique drop lateral impact pressure, for elements located between the 0-degree and the 8.29-degree circumferential planes is:

$Press_1$ = (163.22)(2)(sin 15°) = 84.49 psi for 1g

$Press_{55}$ = (84.49)(55g/1g) = 4647 psi for 55g

The following are summaries of lateral impact pressures, for the elements on the various circumferential locations, for a 1g deceleration, at 15-degree and 75-degree drop orientation angles:

15-Degree Drop Orientation

ARC (deg)	LATERAL IMPACT PRESSURE FOR 1g (psi)	DECELERATION (g)
0 - 8.3	84.49	55
8.3 - 17.0	82.13	55
17.0 - 26.2	77.16	55
26.2 - 35.8	69.35	55
35.8 - 45.9	58.58	55
56.9 - 56.5	44.87	55
56.5 - 67.7	28.47	55
67.7 - 79.4	9.81	55

75-Degree Drop Orientation

ARC (deg)	LATERAL IMPACT PRESSURE FOR 1g (psi)	DECELERATION (g)
0 - 8.3	315.32	55
8.3 - 17.0	306.53	55
17.0 - 26.2	287.96	55
26.2 - 35.8	258.83	55
35.8 - 45.9	218.63	55
45.9 - 56.5	167.47	55
56.5 - 67.7	106.23	55
67.7 - 79.4	36.63	55

The longitudinal impact pressure is calculated as the longitudinal component of the total impact load, divided by the sector area within the 0- to 79.4-degree arc on each side of the impact centerline. Therefore, for the 15-degree drop orientation:

Weight	= 250,000 lb	
Area	= (79.4/180)(p)(43.35)^2	= 2604 in^2
$Press_1$	= (250,000)(cos 15°)/2,604	= 92.73 psi for 1g
$Press_{55}$	= (92.73)(55g/1g)	= 5,100 psi for 55g

The longitudinal impact pressure for the 75-degree drop orientation, calculated by the same method, is 24.85 psi for a 1g deceleration, and 1,367 psi for a 55g deceleration.

It should be noted that the design weight of the cask is 250,000 pounds, which includes the weight of the empty cask (194,000 lb), plus the weight of the cavity contents (56,000 lb) for the directly loaded fuel configuration, which envelopes the Yankee-MPC canistered fuel or Yankee-MPC GTCC waste configurations.

5. Inertial body load - The inertial effects that occur during the impact are represented by equivalent static forces, in accordance with D'Alembert's principle. The inertial body load includes the weight of the empty cask (194,000 lb) and the weight of the cavity contents (56,000 lb). Inertia loads resulting from the weight of the empty cask are imposed by applying an appropriate deceleration factor to the cask mass. The lateral and longitudinal components of inertial loading are determined in the same manner as for the impacting loading.

   The inertial load resulting from the 56,000-pound contents design weight is represented as an equivalent static pressure load with both lateral and longitudinal components applied on the interior surface of the cask for the directly loaded fuel configuration. The contents pressure loading is similar to that discussed in Section 2.10.2.2.1 and is applied to the cask model similarly to that in the side drop analyses. The lateral and longitudinal components of the contents pressure are determined in the same manner as for the corner drop analyses (Section 2.7.1.3). The total deceleration factor is constant at 55g for all of the top and bottom oblique drops.

   Section 2.10.2.2.1 contains the side drop contents pressures for a total contents weight of 56,000 pounds. The oblique drop lateral contents pressure for elements located between the 0-degree and the 8.29-degree circumferential planes, for the 15-degree drop orientation, is therefore:

$Press_1$ = (6.51)(sin 15°) = 1.68 psi for 1g
$Press_{55}$ = (1.68)(55g/1g) = 92.4 psi for 55g

The following are summaries of the applied lateral contents pressures, for the elements at the various circumferential locations, for a 1g deceleration, at 15-degree and 75-degree drop orientation angles.

15-Degree Drop Orientation

ARC (deg)	LATERAL CONTENTS PRESSURE FOR 1g (psi)	DECELERATION (g)
0 - 8.3	1.68	55
8.3 - 17.0	1.64	55
17.0 - 26.2	1.54	55
26.2 - 35.8	1.38	55
35.8 - 45.9	1.17	55
56.9 - 56.5	0.90	55
56.5 - 67.7	0.57	55
67.7 - 79.4	0.20	55

75-Degree Drop Orientation

ARC (deg)	LATERAL CONTENTS PRESSURE FOR 1g (psi)	DECELERATION (g)
0 - 8.3	6.29	55
8.3 - 17.0	6.11	55
17.0 - 26.2	5.75	55
26.2 - 35.8	5.16	55
35.8 - 45.9	4.36	55
45.9 - 56.5	3.34	55
56.5 - 67.7	2.12	55
67.7 - 79.4	0.73	55

The longitudinal contents pressure is calculated as the longitudinal component of the total impact load, divided by the sector area within the 0- to 79.4-degree arc on each side of the impact centerline. Therefore, for the 15-degree drop orientation:

Weight = 56,000 lb
Area = $(p)(35.5)^2 = 3959$ in^2
$Press_1$ = (56,000)(cos 15°)/3,959 = 13.66 psi for 1g
$Press_{55}$ = (13.66)(55g/1g) = 751.3 psi for 55g

The longitudinal impact pressure for the 75-degree drop orientation, calculated by the same method, is 3.66 psi for a 1g deceleration, and is 201.3 psi for a 55g deceleration.

In the ANSYS analyses, the inertial body loads are considered together with the impact loads. The results of the two simultaneous loadings are documented as "impact loads."

The stresses throughout the cask body are calculated for individual and combined loading conditions. The individual loading conditions are: (1) the internal pressure (including bolt preload); (2) the 30-foot bottom 15-degree oblique drop impact (impact load only); (3) the 30-foot top 75-degree oblique drop impact (impact load only); and (4) the 30-foot bottom 75-degree oblique drop impact (impact load only). The combined loading conditions are: (1) the 30-foot bottom 15-degree orientation oblique impact with bolt preload and 50 psi internal pressure; (2) the 30-foot top 75-degree oblique drop impact with bolt preload and 50 psi internal pressure; and (3) the 30-foot bottom 75-degree oblique drop impact with bolt preload and 50 psi internal pressure.

The boundary conditions applied to the models are the same as those discussed in Section 2.7.1.3. The lateral and longitudinal restraints are only to prevent rigid body motion; there should be no significant reaction forces associated with these restraints. When the cask system is in equilibrium (i.e., the inertial body loads match the impact loads exactly), the reaction forces at these restraints will be zero. However, it is difficult to balance the impact limiter pressure resultant with the contents pressure and inertial body load resultant. An eccentricity between the two resultants induces a moment on the cask model. Therefore, non-zero reactions are found at the restraints. The reaction forces cause very high localized stresses (or stress singularities) in the model at the restraints. These stresses are unrealistic and do not exist in the real cask. The stress

singularity effect is minimized by distributing the reaction forces over the nodes in the top and bottom regions of the model. For the bottom 15-degree oblique drop, the reactions at the restraints are 136 pounds laterally and essentially zero longitudinally, for the application of a 55g deceleration factor. This means that the unbalanced force of the cask model system is only 136/55 = 2.5 pounds. Compared to one-half of the cask design weight (125,000 lb), the unbalanced force is negligible, amounting to only 0.002 percent of the design weight of the cask. For the top 75-degree oblique drop, the reactions at the restraints are 2312 pounds laterally and essentially zero longitudinally, for the application of a 55g deceleration factor. This means that the unbalanced force of the cask model system is only 2312/55 = 42 pounds. Compared to one-half of the cask design weight (125,000 lb), the unbalanced force is negligible, amounting to only 0.03 percent of the design weight of the cask. For the bottom 75-degree oblique drop, the reactions at the restraints are 2731 pounds laterally and essentially zero longitudinally, for the application of a 55 deceleration factor. This means that the unbalanced force of the cask model system is only 2731/55 = 50 pounds. Compared to one-half of the cask design weight (125,000 lb), the unbalanced force is negligible, amounting to only 0.04 percent of the design weight of the cask.

The allowable stress limit criteria, for containment and noncontainment structures, are provided in Section 2.1.2. These criteria are used to determine the allowable stresses for each cask component, conservatively using the maximum transport temperature within a given component to determine the allowable stress throughout that component. Note that higher component temperatures results in lower allowable stresses. Table 2.10.2-5 documents the allowable stress values for each component for condition 1 temperatures.

Stress results for the directly loaded fuel configuration for the individual loading cases of internal pressure (including bolt preload) are documented in Tables 2.10.4-1 and 2.10.4-2. Stress results for the individual 30-foot top and bottom oblique drop impact loading cases are documented in Tables 2.10.4-18, 2.10.4-19, and 2.10.4-20. These are the nodal stress summaries obtained from the finite element analysis results. As described in Section 2.10.2.4.2 and Section 2.10.4, the nodal stresses are documented on the representative section cuts. Stress results for the combined loading conditions discussed above are documented in Tables 2.10.4-163 through 2.10.4-177. All the oblique drop analyses are performed for temperature condition 1. The results from Sections 2.7.1.1 and 2.7.1.2 both indicate that the stresses associated with temperature condition 1 yield the smallest margins of safety as a result of the effect of higher temperatures upon the allowable stresses. These tables document the primary, primary membrane (P_m), primary membrane plus

primary bending ($P_m + P_b$), and critical P_m and $P_m + P_b$ stresses in accordance with the criteria presented in Regulatory Guide 7.6. As described in Sections 2.10.2.3 and 2.10.2.4, procedures have been implemented to document the nodal and sectional stresses as well as to determine the critical stress summary for all cask components.

The critical oblique drop orientation is determined by the following considerations. First, the deceleration g-loads for different drop orientation angles between 0 and 90 degrees (in 15° increments) are determined by the computer program RBCUBED, as documented in Section 2.6.7.4. The g-load values are highest for the end drop (f = 0°) and the side drop (f = 90°) conditions and are lower for all of the angles in-between. From a plot of the g-load values versus drop orientation angle, it is expected that the most critical oblique drop angle will be adjacent to either the end drop or the side drop and, hence, the 15- and 75-degree oblique drop angles are chosen for further investigation. Also, SCANS (NUREG/CR-4554) analyses are performed for all oblique drop angles from 0 to 90 degrees, in 15-degree increments. A plot of the stress results from the SCANS analyses indicates that the 15-degree drop angle has the highest normal stress intensity, and that the 75-degree drop angle has the highest shear stress intensity; the stress results for the angles between 15 degrees and 75 degrees are all lower. Next, the stress results from the ANSYS analyses of the end, corner, and side drop conditions--f = 0 degrees, 24 degrees, and 90 degrees, respectively--are reviewed. From the stress results documented in Sections 2.7.1.1, 2.7.1.2, and 2.7.1.3--and in Tables 2.10.4-112 through 2.10.4-162--it is observed that the maximum critical P_m and $P_m + P_b$ stresses are always higher for the corner (f = 24°) and side (f = 90°) drop conditions than for the end drop condition (f = 0°). Thus, the results of the ANSYS analyses suggest that the 75-degree drop orientation will result in greater stresses than the 15-degree drop orientation.

Finally, ANSYS analyses are performed for both the 15-degree and 75-degree oblique drop conditions using the three-dimensional bottom fine mesh model. A comparison of the stress results indicates that the 75-degree oblique drop stress results are, in general, more critical than the 15-degree oblique drop stress results. In the few cases where the stresses on an individual cross-section are higher for the 15-degree drop than for the 75-degree drop, the difference between the stress results is negligible. Therefore it is concluded that the 75-degree drop orientation is more critical than the 15-degree drop orientation. For this reason, only the 75-degree drop analysis is performed for the top oblique drop condition. Thus, the determination that the 75-degree orientation is the most critical oblique drop orientation is based upon: (1) the observation that the impact g-loads are highest for drop orientations near 0 degrees and 90

degrees; (2) SCANS analyses for all angles from 0 degrees to 90 degrees, in 15-degree increments, indicate that the 15-degree drop orientation has the highest normal stress intensity and that the 75-degree drop orientation has the highest shear stress intensity; (3) the stress results for the 24-degree and the 90-degree drop orientations are higher than those for the 0-degree drop orientation; and (4) the direct comparison of stress results, between the 15-degree and the 75-degree drop orientations, using the three-dimensional bottom fine mesh model. Based on these observations, the stress results from the oblique drop orientations other than 75 degrees will be lower and, therefore, are not considered further.

The 75-degree top oblique drop case results in higher maximum stress intensities than the other oblique drop cases. For the individual impact loading cases, the maximum calculated membrane stress intensity for the 75-degree top oblique drop is 34.8 ksi. The maximum calculated membrane plus bending stress intensity is 44.6 ksi. By comparison, for the combined loading case, the maximum calculated P_m stress intensity is 34.8 ksi and the maximum calculated $P_m + P_b$ stress intensity is 44.5 ksi. Therefore, it is concluded that the impact case is the governing one for the 30-foot oblique drop condition.

As shown in Tables 2.10.4-166 through 2.10.4-177, the margins of safety are positive for all of the oblique drop accident conditions for the directly loaded fuel configuration. The most critically stressed component in the system, for the top 75-degree oblique drop, is the top forging. The minimum margin of safety for the top oblique drop condition is +0.4, as documented in Table 2.10.4-171. For the bottom oblique drop, the most critically stressed component in the system is the bottom forging. The minimum margin of safety for the bottom oblique drop condition is +0.6, as documented in Table 2.10.4-167.

As described in this section, the directly loaded fuel configuration of the NAC-STC was analyzed for the 30-foot oblique drop conditions and the 75-degree (from vertical) cask drop orientation was determined to be the critical oblique drop orientation. The maximum component stresses are summarized as follows:

	30’ Side Drop Condition 1		30’ Bottom 75° Drop Condition 1		30’ Top 75° Drop Condition 1	
Stress Type	Section ID	S.I.	Section ID	S.I.	Section ID	S.I.
P_m	401 - 1	36.0	12880-12877	4.0	403-3	34.8
	(Table 2.10.4-133)		(Table 2.10.4-166)		(Table 2.10.4-171)	
$P_m + P_b$	403 - 3	49.4	880-877	5.1	404-4	44.5
	(Table 2.10.4-134)		(Table 2.10.4-167)		(Table 2.10.4-172)	

The maximum primary membrane and primary membrane plus bending stresses occur in component 6 (Figure 2.10.2-33) for the 30-foot side, 30-foot bottom 75-degree, and 30-foot top 75-degree drop conditions. These results show that the 30-foot side drop condition envelopes the most critical 30-foot oblique drop conditions (75-degree top and bottom) for the directly loaded fuel configuration of the NAC-STC. Based on the demonstration of the structural adequacy of the NAC-STC in the Yankee-MPC and CY-MPC configurations presented in Sections 2.7.1.1 and 2.7.1.2, and the fact that the same cask body used in the Yankee-MPC and CY-MPC configurations is analyzed and approved for the transport of directly loaded fuel, it is concluded that the 30-foot oblique drop condition is enveloped by the 30-foot side drop analysis and no further evaluation of the Yankee-MPC and CY-MPC canistered configurations of the NAC-STC for the 30-foot oblique drop condition is required.

Satisfaction of the extreme total stress intensity range limit is demonstrated in Section 2.1.3.3.

The documentation of the adequacy of the NAC-STC to satisfy the buckling criteria for the stresses of the oblique drop condition is presented in Section 2.10.5.

The NAC-STC maintains its containment capability and, therefore, satisfies the requirements of 10 CFR 71.73 for the 30-foot oblique drop hypothetical accident condition.

THIS PAGE INTENTIONALLY LEFT BLANK

2.7.1.5 Lead Slump Resulting From a Cask Drop Accident

Following a drop accident, there may be a reduction in the shielding capability of the NAC-STC as a result of lead slump. Some of the fuel also may rupture. The analysis for this accident assumes that all of the fuel rods are ruptured. The three drop accidents evaluated are the bottom end drop, the side drop and the bottom corner drop. The effect of the lead slump that could result from the bottom end drop or the side drop is calculated in this section. The dose rate that could occur as a result of the corner drop is bounded by that for the bottom end drop accident.

Since the previous sections demonstrated that the Yankee-MPC and CY-MPC canistered fuel design is bounded by the NAC-STC directly loaded fuel design, the lead slump results presented herein for the directly loaded fuel design also bound the Yankee-MPC and CY-MPC canistered fuel design. Additionally, the heat load of the fuel transported in the Yankee-MPC and CY-MPC canistered fuel design is less than the 26 kW heat load considered for this evaluation.

The maximum lead slump occurs during the 30-foot bottom end drop accident. The worst case is to assume that the radial gap that exists as a result of the lead contraction following lead pour is completely filled by slumping lead leaving a voided region at the top of the lead annulus adjacent to the upper end-fitting. Prior to lead pour, the inner and outer shells of the cask are heated to approximately the temperature of the molten lead to minimize thermal stress effects. During cooldown, the contraction of the lead shell is significantly greater than that of the stainless steel inner and outer shells due to the difference in material coefficients of thermal expansion; the lead pour continues to fill the contraction gap as the lead solidifies at 620°F. As the stainless steel and lead shells cool down from 620°F to 70°F, a gap is formed. For the cold accident transport conditions (26-kilowatt heat load and -20°F ambient temperature), the shells heat up to an average temperature of 245°F with the gap partially closing. This condition represents the maximum source of radiation combined with its associated maximum contraction gap.

The hypothesized lead slump calculated for the 30-foot end drop accident is 2.35 inches. For the postulated side drop event, a lead thickness reduction of 0.93-inch in the radial lead thickness on the side opposite the impact is used. These calculated worst case values are conservative when considering details of the temperature dependent interaction of the lead gamma shield and both inner and outer steel shells. Differential axial growth between the lead and the steel will reduce and potentially eliminate the radial gap at both ends of the annulus. In addition to this effective increase in lead volume, the slumping action resulting from the 30-foot hypothetical end or side

drop, defined by the detailed finite element analysis presented in Section 2.10.9, shows that the friction forces resulting from differential thermal expansion and lead material properties mitigates the slumping of the lead. Therefore, the dose rate calculation based on the 2.35 inches of lead slump is conservative. Calculations were performed with the three-dimensional Monte Carlo shielding code MORSE, applying the simultaneous end and side drop reductions in lead thickness. The maximum calculated dose rate at 1 meter from the cask surface for directly loaded fuel is 605 mrem/hour (see Table 5.1-5), which bounds the canistered fuel configurations.

Thus, the hypothetical accident dose rate limits of 10 CFR 71.51 are satisfied.

An evaluation of the lead slump for the side drop accident indicates that the nominal lead thickness of 3.20 inches (at the transition regions near the top and bottom end of the inner shell) may be reduced by a maximum of 0.88 inch. This calculated worst case value of 0.88 inches is conservative for the same reasons presented above for the end drop condition. The loss of a 0.88-inch thickness of lead will result in an increase in the primary gamma surface dose rate, which is calculated below:

$$\frac{D_{accident}}{D_{normal}} = (2)^{0.88/0.4} = 4.59$$

The surface dose rate along the lead annulus is highest during normal transport conditions at the fuel midplane. The primary gamma contribution at 1 meter from the cask surface at the fuel midplane would increase by a factor of 4.59 based on a half value layer for lead of 0.4 inch. There is no change in the neutron, secondary gamma and stainless steel gamma dose rate contributions as a result of this accident because they are not significantly affected by a change in lead thickness. The change to the fuel midplane dose rate contribution from the end-fittings is not considered because of their distance from the location of interest. From Section 5.1, the total dose rate 1 meter from the cask surface at the fuel midplane under these conditions would be:

$$\begin{aligned} D_{total} &= (13.53)(4.59) + (3.28)(4.59) + 1.49 \\ &= 62.1 \text{ (fuel gamma)} + 15.06 \text{ (grid spacer gamma)} + 1.49 \\ &\quad \text{(neutron)} \\ &= 78.65 \text{ mrem/hour} \end{aligned}$$

Thus, the dose rate limits of 10 CFR 71.51 are satisfied. The results of this analysis are presented in Table 5.1-7. The analysis shows that the loss of lead shielding resulting from a lead slump accident will not result in a substantial loss in shielding effectiveness and that the dose rates from this accident are small when compared to the allowable dose rates for a hypothetical accident.

THIS PAGE INTENTIONALLY LEFT BLANK

2.7.1.6 Closure Analysis - Hypothetical Accident Conditions

Section 2.6.7.5 provides a general description of the analysis approaches employed to demonstrate the structural integrity of the NAC-STC closure assembly for both normal conditions of transport and hypothetical accident conditions. The materials of construction and the geometry of the components of the closure assembly are also identified in Sections 2.6.7.5 and 2.6.7.5.1.

As discussed in Section 2.6.7.5.2, the analysis of the NAC-STC closure assembly must demonstrate that the inner and outer lids and bolts satisfy two criteria: (1) calculated maximum stresses must be less than the allowable stress limit (material yield strength is conservatively selected); and (2) lid deformation and/or rotation at the o-ring locations must be less than the elastic rebound of the o-rings.

Finite element evaluation of the closure is performed using the ANSYS computer program and a two-dimensional axisymmetric model. Three 10 CFR 71 hypothetical accident condition loadings are conservatively considered: (1) impact limiter crush pressure on the outer lid; (2) pin puncture on the outer lid; and (3) impact of the cavity contents on the inner lid. The inner and outer lids and bolts are evaluated at a temperature of 200°F.

2.7.1.6.1 Finite Element Model

2.7.1.6.1.1 Description

The components of the NAC-STC closure assembly that are considered in the finite element model include the outer lid, the inner lid and NS-4-FR neutron shielding material, the stainless steel coverplate, and the inner and outer lid bolts.

The finite element model of the NAC-STC closure is constructed utilizing the ANSYS PREP7 routine. Because both the geometric configuration and the loading conditions on the closure are axisymmetric, a two-dimensional axisymmetric model is adequate. The finite element model is shown in Figures 2.7.1.6-1 through 2.7.1.6-3. The model utilizes ANSYS STIF42 elements for the lids and STIF1 elements for the bolts. In addition, the interface between the outer lid, the inner lid, and the top forging is represented by two-dimensional interface (gap) elements (STIF12) with the coefficient of friction set to zero.

The gap elements represent two surfaces that may maintain or break physical contact, and may slide relative to each other. Note that the gap element is only capable of supporting compression in the direction normal to the surfaces and friction in the tangential directions. The gap elements transmit compressive loadings, if the surfaces are in contact, but permit no tensile load. This means that the gap elements allow the interface surfaces of the lids to separate from each other, and move relative to each other with no friction.

A large gap element stiffness is specified to maintain the boundary between the interfacing surfaces for compressive loadings.

The NS-4-FR neutron shielding material is considered to be bonded to the steel; which means that common nodes were used to connect two adjacent materials. Its compression modulus of elasticity, 0.56×10^6 psi, is two percent of the modulus of elasticity for steel and too low to have any significant effect on the flexural properties of the inner lid.

The inner and outer lid bolts are modeled as spar elements. The inner lid bolt is connected to the countersink in the lid and to the cask body at the bolt centerline. The outer lid bolt is connected to the countersink in the lid and to the top forging at the bolt centerline. The cross-sectional properties of the bolts are input to ANSYS on a "per radian" basis. The bolt preloads are applied to the finite element model as initial strains on the beam elements.

The material properties of the closure components are presented in Section 2.3.

2.7.1.6.2 Loading Conditions

The NAC-STC closure is analyzed for structural adequacy under hypothetical accident conditions in accordance with 10 CFR 71.73. The three critical accidents considered in the analyses are the 30-foot top end drop and the 30-foot top corner drop in accordance with 10 CFR 71.73(c)(1), and the pin puncture in accordance with 10 CFR 71.73(c)(2).

2.7.1.6.2.1 Loading Condition 1: 30-Foot Top End Drop

During a 30-foot top end drop, the cask (with its attached transport impact limiters) falls through a distance of 30 feet onto a flat, unyielding, horizontal surface. The cask strikes the surface in a vertical position and, consequently, a flat end impact on the top impact limiter occurs. The

compression of the impact limiter energy-absorbing material produces compressive bearing pressure on the top surface of the outer lid.

The nominal dynamic crush strength of the energy absorbing material (redwood) in the end region of the NAC-STC transport impact limiter is 1260 psi. A fabrication tolerance of ±10 percent on the crush strength of the impact limiter material may produce a maximum crush strength equal to 1390 psi. This 1390 psi maximum crush strength occurs as a uniformly distributed, normal bearing pressure load on the top surface of the outer lid. This analysis conservatively uses a bearing pressure of 2376 psi, equivalent to a 56.1g top end impact.

In addition, during the accident, the empty fuel basket and fuel/basket spacer, which are assumed to be in the cask cavity are restrained/decelerated by the inner lid, producing a bearing pressure on the bottom surface of the inner lid. The mass of the basket and spacer, subjected to a 56.1g design deceleration, produces a uniformly distributed bearing pressure of 800 psi on the inside surface of the inner lid. The internal pressure of the cask is about 47 psi, making the total pressure on the inside surface of the inner lid 847 psi. The finite element model with boundary conditions is shown in Figure 2.7.1.6-1.

The 30-foot top end drop for the NAC-STC directly loaded fuel configuration bounds the Yankee-MPC canistered fuel configuration, since the Yankee-MPC canistered contents weight is equal to or less than that of the directly loaded fuel configuration under all scenarios. Additionally, for the Yankee-MPC canistered fuel configuration, the aluminum honeycomb spacers provide additional fuel basket deceleration at impact, further reducing the impact on the cask ends.

2.7.1.6.2.2 Loading Condition 2: Pin Puncture

The NAC-STC outer lid is analyzed for structural adequacy in accordance with the requirements of 10 CFR 71.73(c)(2) for puncture under hypothetical accident conditions. The cask is assumed to be inverted, with the lid downward, when dropped from a height of 1 meter (40 in) onto a 15-centimeter (6-in) diameter, mild steel bar oriented vertically on an unyielding surface.

During the impact, the puncture pin is considered to apply a pressure of 47,000 psi (assumed dynamic flow stress of mild steel) in the inward normal direction on the outer lid over a 6-inch

diameter region at the centerline of the exterior surface. The presence of the top impact limiter is conservatively ignored.

The force exerted by the pin on the cask is:

$$F = (p)(3)^2(47{,}000)$$

$$= 1.329 \times 10^6 \text{ lb}$$

The deceleration of the cask is:

$$a = \frac{F}{W} g$$

$$= 5.3g$$

where

$$W = 250{,}000 \text{ lb}$$

Since the weight (250,000 lb) for the directly loaded fuel configuration envelopes that of the Yankee-MPC canistered fuel configuration of the NAC-STC, the existing pin puncture analysis bounds the Yankee-MPC canistered fuel configuration.

The uniformly distributed internal pressure exerted by the spacer, the fuel assemblies and the basket on the inner lid is:

$$p = \frac{(56{,}350)(5.3)}{\frac{\pi}{4}(71)^2}$$

$$= 75.7 \text{ psi}$$

The finite element model with boundary conditions is shown in Figure 2.7.1.6-2.

2.7.1.6.2.3 Loading Condition 3: 30-Foot Top Corner Drop

During a 30-foot top corner drop, the cask (with its attached transport impact limiters) falls through a distance of 30 feet onto a flat, unyielding horizontal surface. As the corner of the impact limiter contacts the flat, unyielding surface, the cask body impacts on the inside diameter of the impact limiter and the cask cavity contents (spacer, basket and fuel assemblies) impact on the inside surface of the inner lid. The design deceleration of 55g (actual impact load = 44.2g, Table 2.6.7.4.1-2) acting on the cavity contents produces a pressure on the inner surface of the inner lid of:

$$p = \frac{56{,}350 \times 55}{(\pi)(35.50)^2}$$

$$= 785 \text{ psi}$$

Adding the contents pressure to the design internal pressure of 45 psig brings the total pressure on the inner lid to 830 psi. The bearing pressure of the impact limiter on the external surface of the outer lid and the outer lid are conservatively neglected. 847 psi internal pressure, representing 56.1g is conservatively applied to the inner lid. The finite element model with boundary conditions is shown in Figure 2.7.1.6-3.

The 30-foot top corner drop for the directly loaded fuel configuration bounds the Yankee-MPC canistered fuel design, as the total contents weight is equal to, or less than, that of the directly loaded fuel configuration under all accident scenarios. Additionally, the Yankee-MPC canistered fuel configuration includes aluminum honeycomb spacers in the cask cavity that provide additional fuel basket deceleration at impact.

2.7.1.6.3 Analysis Results

Based on the discussion presented for the Yankee-MPC canistered fuel configuration in Section 2.7.1.6.2, the results presented in this subsection for the NAC-STC directly loaded fuel configuration bound the Yankee-MPC canistered fuel configuration.

Table 2.7.1.6-1 provides a summary of the resulting stresses and deformations for the inner and outer lids as determined by the ANSYS finite element analyses for the three loading conditions

defined in Section 2.7.1.6.2. Both the stress and the deformation/rotation limit criteria are satisfied for the inner and the outer lids.

The maximum calculated stress in the outer lid is 52,042 psi, which results in a minimum margin of safety of +0.87 when evaluated with respect to material yield strength for load condition 2, pin puncture on the outer lid. Note that this evaluation is very conservative and that when the outer lid stress results are compared to non-containment structural criteria for the maximum primary membrane stress of 24 ksi with allowable of $0.7S_u$ and the maximum primary membrane plus bending stress of 52 ksi with allowable of S_u, the respective margins of safety are 2.94 and 1.59. The maximum out-of-plane rotational movement of the outer lid is 0.001 inch for load condition 1, impact limiter crush pressure on the outer lid. This elastic deformation is less than the elastic rebound of the Type 321 stainless steel o-ring material (0.005 inches) and is less than the rebound of the EPDM or Viton o-rings (0.03 inches); therefore, the seal is maintained.

The maximum calculated von Mises stress in the inner lid is 22,284 psi, which results in a minimum margin of safety of +0.12 when evaluated with respect to the material yield strength for load condition 1, neglecting impact limiter crush pressure on the outer lid. Note that this evaluation is very conservative and that when the inner lid stress results are compared to containment structural criteria for the maximum primary membrane stress of 2 ksi with allowable 2.4 S_m and the maximum primary membrane plus bending stress of 18 ksi with allowable of S_u, the respective margins of safety are +24.0 and +2.66. The maximum out-of-plane rotational movement of the inner lid is 0.0053 inch for load condition 3, impact of the cavity contents on the inner lid. This rotational movement of 0.0053 inches is calculated for a loading condition that is 27 percent larger than the conservatively postulated loading from the corner drop configuration. The corner drop loading configuration has conservatively ignored the outer lid stiffening effects on the top forging and the impact limiter loading on the top forging. Adjusting this displacement for the ratio of load, 44.2/56.1, Section 2.7.1.6.2.3, the displacement of the inner lid at the sealing surface becomes 0.0042 inches, which is less than the elastic rebound of the metallic o-ring (0.005 inches). The analyses of the inner and outer lid bolts are presented in Section 2.7.1.6.4.

2.7.1.6.4 Lid Bolt Analysis

The NAC-STC inner and outer lid bolts are preloaded at installation to ensure that the sealing function of the o-rings located in the inner and the outer lids is maintained. The lid bolts are

installed with a torque that is calculated to produce a total tensile load that is not less than the total load on the lid; that is, the sum of: (1) internal pressure force on the lid; (2) o-ring compression forces; (3) inertial weight of the lid (calculated weight multiplied by the impact load factor); and (4) inertial weight of any other components that can contact the lid calculated weight multiplied by the impact load factor). Since the total bolt preload exceeds the total load on the lid, there is no movement of the lid relative to its mating component and the status of the seal at the o-ring(s) is maintained.

Inner and outer lid bolt evaluations are prepared for a complete range of impact orientations, from an end impact at 0 degrees to a flat side impact at 90 degrees, in 5-degree increments.

The bounding load condition for the NAC-STC inner lid bolt evaluation for the end drop (0º) is the combined weight of the loaded Yankee-MPC canister, canister spacers, and inner lid multiplied by the acceleration factors applicable to the redwood impact limiter as summarized in Table 2.6.7.4.1-4. Although the loaded CY-MPC canister configuration is heavier, the lower acceleration factor developed by the balsa impact limiters (Table 2.6.7.4.2-2) results in a slightly lower impact load on the inner lid bolts. Using the values from the tables, the Yankee-MPC end drop impact load is (66,690 x 56.1g =) 3.741×10^6 lbs. The corresponding CY-MPC impact load is (77,885 x 48) 3.738×10^6 lbs. The bounding load condition for drop orientations other than 0º (end drop) corresponds to the CY-MPC configuration, since the impact load (77,885 x 48g) is greater than that for the Yankee-MPC (66,690 x 55g).

Hypothetical accident condition results are summarized in Tables 2.7.1.6-2 and 2.7.1.6-3 corresponding to a “hot” initial condition and a “cold” initial condition, respectively, for the inner lid bolts. The details of this analytic evaluation are described and example calculations are performed in Section 2.10.8 for hypothetical accident conditions. Similarly, Table 2.7.1.6-4 summarizes the analysis results for the outer lid bolts. This evaluation is applicable for both the “hot” and “cold” conditions, since the thermal load is negligible. The “hot” condition bolt temperature is taken as 200°F, as summarized in Table 3.4.5. The “cold” condition bolt temperature is assumed to be -20°F, per regulatory requirements. Physical properties for the SB-637, Grade N07718 nickel alloy and the SA-564, H1150, 17-4PH stainless steel bolt materials are conservatively taken at 270°F for both the “hot” and “cold” condition. As defined within Table 2.1.2-1, the allowable bolt stresses are taken as the material yield strength, S_y, yielding allowable direct tension stresses of 141.7 ksi for the inner lid bolts; and 94.2 ksi for the

outer lid bolts. Based on these thorough evaluations, the inner lid bolts and the outer lid bolts incur maximum stress intensities that result in positive margins of safety as shown:

For inner lid bolts: M.S. = (141,700/92,978) - 1 = +0.52

For outer lid bolts: M.S. = (94,200/73,937) - 1 = +0.27

The bolt engagements may be evaluated by calculating shear stresses within the SA-336, Type 304 end forging and inner lid forging materials. At 270°F, the allowable shear stress is $0.42S_u$, or 26.4 ksi, according to Table 2.1.2-1. The maximum bolt tension loads in the inner and outer lid bolts are 138,709 pounds and 39,686 pounds, respectively. The shear area per inch of engagement for 1 1/2 - 8UN internal threads is 3.792 square inches (Section 2.6.7.5.4). The total thread engagement length is 2.39 inches for the inner lid bolts.

The shear stress and the margin of safety for the inner lid bolts are:

S_s = P/A = 138,709/(3.792)(2.39)
= 15,305 psi

M.S. = (26,400/15,305) - 1 = +0.72

For the outer lid bolts, the shear area per inch of engagement for 1-8 UNC internal threads is 2.325 square inches (Section 2.6.7.5.4). The total thread engagement length is 2.0 inches. The shear stress and the margin of safety for the outer lid bolts are:

S_s = P/A = 39,686/(2.325)(2.0)
= 8,535 psi

M.S. = (26,400/8,535) - 1 = + 2.09

2.7.1.6.5 Conclusions

Using consistently conservative assumptions, the NAC-STC closure assembly is shown to satisfy the performance and structural integrity requirements of CFR 71.73(c)(1) for hypothetical accident conditions.

The inner and outer lid bolts are analyzed for the thermal (fire) accident condition in Section 2.7.3.4.

Figure 2.7.1.6-1 Finite Element Model - Lid Assembly (Loading Condition 1 - 56.1g Top Impact)

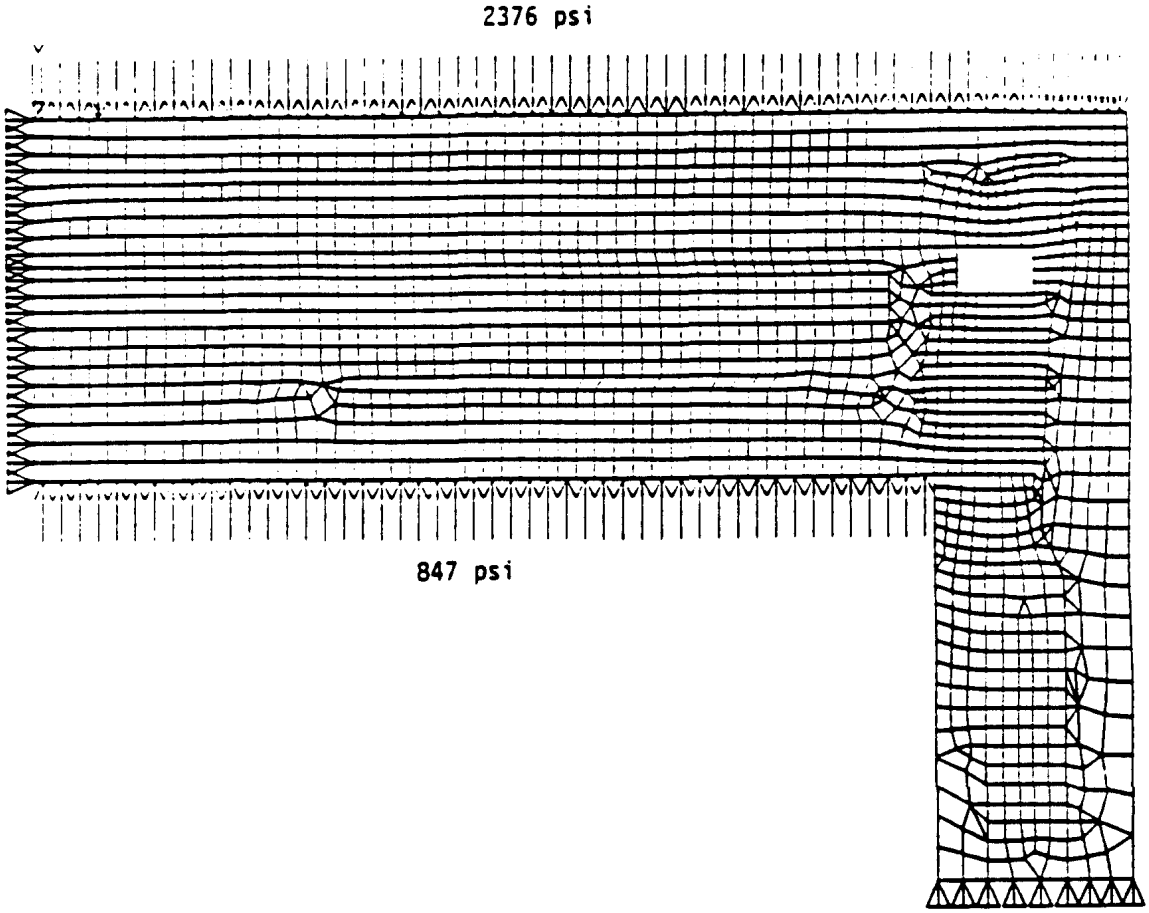

Figure 2.7.1.6-2 Finite Element Model - Lid Assembly (Loading Condition 2 - Pin Puncture)

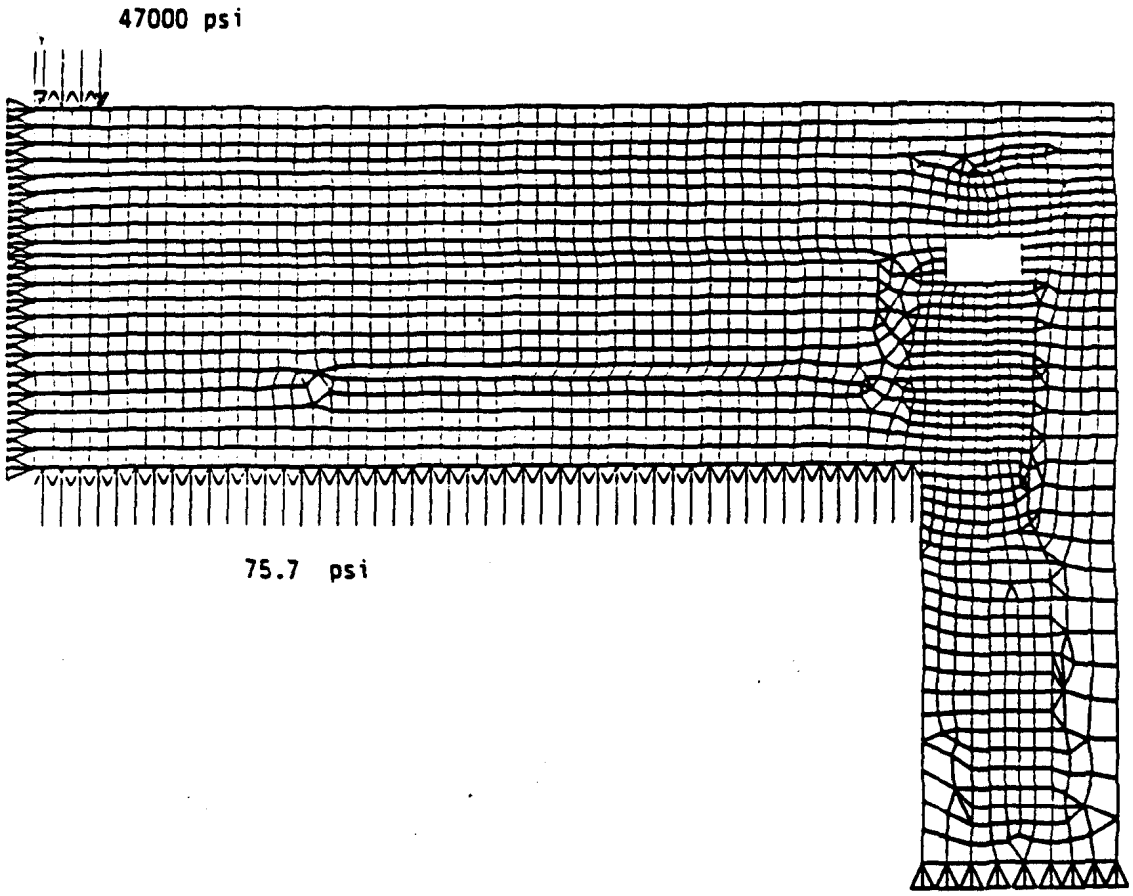

Figure 2.7.1.6-3 Finite Element Model - Lid Assembly (Loading Condition 3 - 56.1g Top Impact of Cavity Contents Plus Internal Pressure)

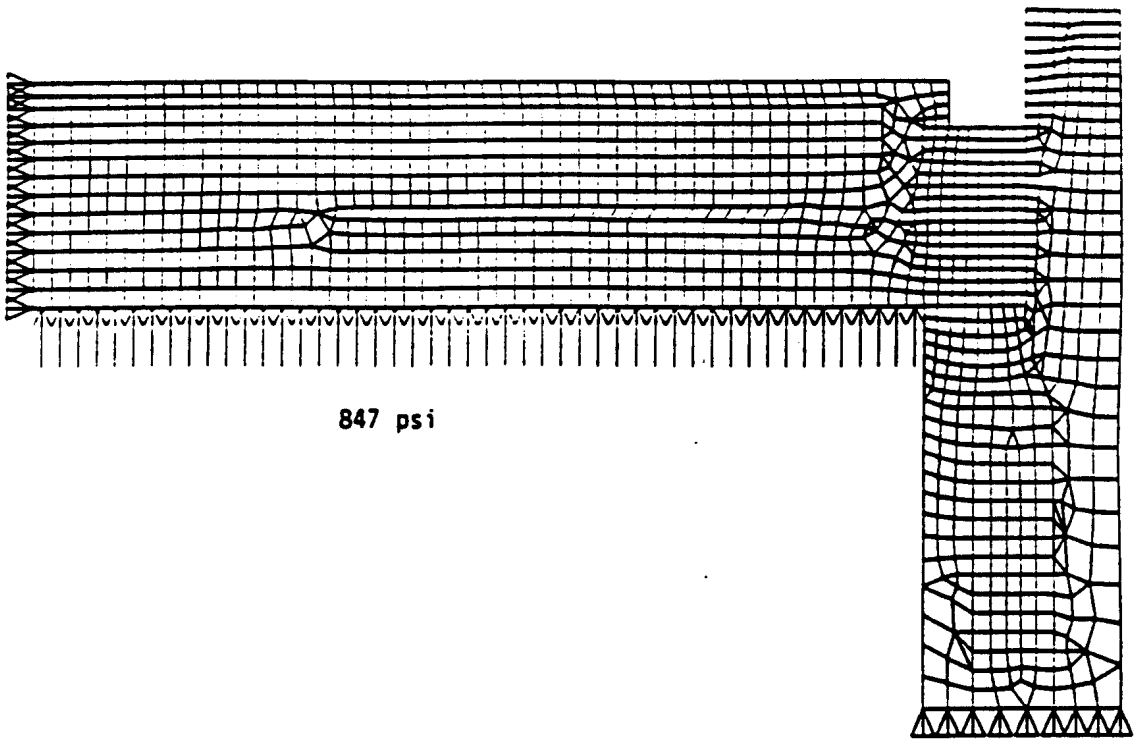

Table 2.7.1.6-1 Stress Summary - Accident Analyses of the NAC-STC Inner and Outer Lids

Load Condition	Maximum Von Mises Stress					
	Outer Lid (S_y = 97.1 ksi @ 200°F)		Inner Lid (S_y = 25.0 ksi @ 200°F)		Displacement at O-ring Location (inches)	
	Stress (psi)	Margin of Safety	Stress (psi)	Margin of Safety	Inner Lid	Outer Lid
1	19,647	+4.94	22,284	+0.12	0.003	0.001
2	52,042	+0.87	20,312	+0.23	0.00162	0.00016
3	-	-	22,080	+0.13	0.0053	

Load Condition	Maximum Primary Membrane Stress			
	Outer Lid 17-4 PH St. Stl. ($0.7S_u$ = 94.5 ksi @ 200°F)		Inner Lid Type 304 St. Stl. ($2.4S_m$ = 48.0 ksi @ 200°F)	
	Stress (psi)	Margin of Safety	Stress (psi)	Margin of Safety
1	1,530	+Large	882	+Large
2	24,000	+2.94	2,000	+Large
3	-	-	147	+Large

Table 2.7.1.6-1 Stress Summary - Accident Analyses of the NAC-STC Inner and Outer Lids (Continued)

Load Condition	Maximum Primary Membrane Plus Primary Bending Stress			
	Outer Lid 17-4 PH St. Stl. (S_u = 135 ksi @ 200°F)		Inner Lid Type 304 St. Stl. (S_u = 66.2 ksi@ 200°F)	
	Stress (psi)	Margin of Safety	Stress (psi)	Margin of Safety
1	19,647	+5.87	18,088	+2.66
2	52,042	+1.59	12,000	+4.52
3	-	-	16,029	+5.13

Table 2.7.1.6-2 NAC-STC "Hot" Inner Lid Bolt Analysis (Hypothetical Accident Condition)

Nominal Bolt Diameter (in):	1.5	Longitudinal Weight (lb) CY-MPC:	77,885
Number of Bolts:	42	Longitudinal Weight (lb) Yankee-MPC*:	66,690
Service Stress, Sy (psi):	141,700	Lateral Weight (lb):	10,690
Bolt Expansion (in/in):	7.30E-06 at a 270°F		
Bolt Modulus of Elasticity (ksi):	28,000 Service Temp.		
Lid Expansion (in/in):	8.94E-06	Calculated Loads and Stiffness	
Lid Modulus of Elasticity (ksi):	27,300	Bolt Thermal Load (lb):	13,703
Bolt Stress Area (in^2):	1.492	Bolt Preload (lb):	115,066
		Bolt Static Load (lb) CY-MPC:	8,308
		Bolt Static Load (lb) Yankee-MPC*:	9,036
Maximum Pressure (psig):	38.1	Bolt Stiffness (lb/in):	4.57E+06
Seal Diameter (in):	73.247	Lid Stiffness (lb/in):	5.40E+07
Preload Torque (ft-lb):	2,540 +200 at room temperature		
Nominal Room Temp. °F:	70		
Bolt Circle Diameter (in):	75.31		
Lid Diameter (in):	79.00		

Angle wrt. Vert. (deg)	Impact Accel. (g)	LOAD (lbs)			STRESS (psi)					Margin of Safety
		Impact			Direct		Principal		Stress	
		Tension	Shear	Bolt Tension	Tension	Shear	S2	S1	Intens.	
0 End*	56.1	98115	0	136425	91438	0	0	91438	91438	0.55
5	48.0	119085	1065	138709	92968	714	-5	92973	92978	0.52
10	48.0	117724	2121	138603	92897	1422	-22	92919	92941	0.52
15	48.0	115467	3162	138427	92779	2119	-48	92827	92875	0.53
20	48.0	112331	4179	138182	92615	2801	-85	92700	92785	0.53
25	48.0	108340	5163	137871	92407	3460	-129	92536	92665	0.53
30	48.0	103525	6109	137495	92155	4095	-182	92337	92519	0.53
35	48.0	97921	7007	137058	91862	4696	-239	92101	92340	0.53
40	48.0	91573	7853	136562	91529	5263	-302	91831	92133	0.54
45	48.0	84528	8639	136013	91162	5790	-366	91528	91894	0.54
50	48.0	76839	9359	135413	90759	6273	-432	91191	91623	0.55
55	48.0	68565	10008	134767	90326	6708	-495	90821	91316	0.55
60	48.0	59770	10580	134081	89867	7091	-556	90423	90979	0.56
65	48.0	50520	11072	133359	89383	7421	-612	89995	90607	0.56
70	48.0	40885	11480	132607	88879	7694	-661	89540	90201	0.57
75	48.0	30939	11801	131831	88359	7910	-703	89062	89765	0.58
80	48.0	20758	12032	131037	87826	8064	-734	88560	89294	0.59
85	48.0	10419	12171	130230	87286	8158	-756	88042	88798	0.60
90 Side	55.0	0	13999	129417	86741	9383	-1003	87744	88747	0.60

* End drop stress is evaluated on the basis of the Yankee-MPC weights and impact load factors. All other drop orientations are bounded by the CY-MPC weights and impact factors.

Table 2.7.1.6-3 NAC-STC "Cold" Inner Lid Bolt Analysis (Hypothetical Accident Condition)

Nominal Bolt Diameter (in):	1.5	Longitudinal Weight (lb) CY-MPC:	77,885
		Longitudinal Weight (lb) Yankee-MPC*:	66,690
Number of Bolts:	42	Lateral Weight (lb):	10,690
Service Stress, Sy (ksi):	141,700		
Bolt Expansion (in/in):	7.30E-06 at a 270°F		
Bolt Modulus of Elasticity (ksi):	28,000 Service Temp.		
Lid Expansion (in/in):	8.94E-06	Calculated Loads and Stiffness	
Lid Modulus of Elasticity (ksi):	27,180	Bolt Thermal Load (lb):	0
Bolt Stress Area (in^2):	1.492	Bolt Preload (lb):	115,066
		Bolt Static Load (lb) CY-MPC:	8,308
		Bolt Static Load (lb) Yankee-MPC*:	9,036
		Bolt Stiffness (lb/in):	4.57E+06
Maximum Pressure (psig):	38.1	Lid Stiffness (lb/in):	5.40E+07
Seal Diameter (in):	73.247		
Preload Torque (ft-lb):	2,540+200 at room temperature		
Nominal Room Temp. °F:	70		
Bolt Circle Diameter (in):	75.31		
Lid Diameter (in):	79.00		

Angle wrt. Vert. (deg)		Impact Accel. (g)	LOAD (lbs)			STRESS (psi)					Margin of Safety
			Impact			Direct		Principal		Stress	
			Tension	Shear	Bolt Tension	Tension	Shear	S2	S1	Intens.	
0	End*	56.1	98115	0	122722	82253	0	0	82253	82253	0.72
5		48.0	119085	1065	125006	83784	714	-6	83790	83796	0.69
10		48.0	117724	2121	124900	83713	1422	-24	83737	83761	0.69
15		48.0	115467	3162	124724	83595	2119	-54	83649	83703	0.69
20		48.0	112331	4179	124479	83431	2801	-94	83525	83619	0.69
25		48.0	108340	5163	124168	83223	3460	-144	83367	83511	0.70
30		48.0	103525	6109	123792	82971	4095	-202	83173	83375	0.70
35		48.0	97921	7007	123355	82678	4696	-266	82944	83210	0.70
40		48.0	91573	7853	122859	82345	5263	-335	82680	83015	0.71
45		48.0	84528	8639	122310	81977	5790	-407	82384	82791	0.71
50		48.0	76839	9359	121710	81575	6273	-480	82055	82535	0.72
55		48.0	68565	10008	121064	81142	6708	-551	81693	82244	0.72
60		48.0	59770	10580	120378	80682	7091	-618	81300	81918	0.73
65		48.0	50520	11072	119656	80198	7421	-681	80879	81560	0.74
70		48.0	40885	11480	118904	79694	7694	-736	80430	81166	0.75
75		48.0	30939	11801	118128	79174	7910	-783	79957	80740	0.76
80		48.0	20758	12032	117334	78642	8064	-818	79460	80278	0.77
85		48.0	10419	12171	116527	78101	8158	-843	78944	79787	0.78
90	Side	55.0	0	13999	115714	77556	9383	-1119	78675	79794	0.78

* End drop stress is evaluated on the basis of the Yankee-MPC weights and impact load factors. All other drop orientations are bounded by the CY-MPC weights and impact factors.

Table 2.7.1.6-4 NAC-STC "Hot and Cold" Outer Lid Bolt Analysis (Hypothetical Accident Condition)

Nominal Bolt Diameter (in):	1	Longitudinal Weight (lb):	16,985
Number of Bolts:	36	Lateral Weight (lb):	8,120
Service Stress, Sy (psi):	94,200		
Bolt Expansion (in/in):	5.90E-06 at a 270°F		
Bolt Modulus of Elasticity (ksi):	27,300 Service Temp.		
Lid Expansion (in/in):	5.90E-06	Calculated Loads and Stiffness	
Lid Modulus of Elasticity (ksi):	27,300	Bolt Thermal Load (lb):	0
		Bolt Preload (lb):	36,810
Bolt Stress Area (in^2):	0.606	Bolt Static Load (lb) CY-MPC:	8,308
		Bolt Static Load (lb) Yankee-MPC:	9,036
		Bolt Stiffness (lb/in):	5.49E+06
Maximum Pressure (psig):	7.35	Lid Stiffness (lb/in):	6.83E+07
Seal Diameter (in):	81.81		
Preload Torque (ft-lb):	550,+50		
Nominal Room Temp. °F:	70		
Bolt Circle Diameter (in):	83.7		
Lid Diameter (in):	86.7		

Angle wrt. Vert. (deg)		Impact Accel. (g)	LOAD (lbs)			STRESS (psi)					Margin of Safety
			Impact			Direct		Principal		Stress	
			Tension	Shear	Bolt Tension	Tension	Shear	S2	S1	Intens.	
0	End	56.1	30468	0	39077	64483	0	0	64483	64483	0.46
5		55.0	34652	1081	39686	65488	1784	-49	65537	65586	0.44
10		55.0	34256	2154	39656	65439	3554	-192	65631	65823	0.43
15		55.0	33600	3211	39607	65358	5299	-427	65785	66212	0.42
20		55.0	32687	4243	39540	65248	7002	-743	65991	66734	0.41
25		55.0	31526	5243	39453	65104	8652	-1130	66234	67364	0.40
30		55.0	30125	6203	39349	64932	10236	-1575	66507	68082	0.38
35		55.0	28494	7116	39228	64733	11743	-2064	66797	68861	0.37
40		55.0	26647	7974	39090	64505	13158	-2581	67086	69667	0.35
45		55.0	24597	8772	38938	64254	14475	-3110	67364	70474	0.34
50		55.0	22359	9503	38771	63979	15682	-3637	67616	71253	0.32
55		55.0	19952	10162	38592	63683	16769	-4146	67829	71975	0.31
60		55.0	17392	10744	38402	63370	17729	-4623	67993	72616	0.30
65		55.0	14701	11243	38201	63038	18553	-5055	68093	73148	0.29
70		55.0	11897	11657	37993	62695	19236	-5431	68126	73557	0.28
75		55.0	9003	11983	37777	62338	19774	-5743	68081	73824	0.28
80		55.0	6040	12217	37557	61975	20160	-5981	67956	73937	0.27
85		55.0	3032	12358	37333	61606	20393	-6139	67745	73884	0.27
90	Side	55.0	0	12406	37108	61234	20472	-6214	67448	73662	0.28

2.7.2 Puncture

The puncture accident outlined in 10 CFR 71 Subpart F requires that the NAC-STC suffer no loss of containment as a result of a 40-inch free fall onto an upright 6-inch diameter mild steel bar (puncture pin), which is supported on an unyielding surface. The impact orientation of the cask is required to be such that maximum damage is inflicted upon the cask.

The maximum cask damage will result from direct impacts of the puncture pin on the following locations: (1) cask side - midpoint, (2) center of the cask lid, (3) center of the cask bottom, and (4) cask port covers. Since an impact at any other location is less severe, the NAC-STC is analyzed for the puncture accident at these four locations.

The canistered Yankee class fuel configuration of the NAC-STC has essentially the same weight and center of gravity location as does the directly loaded fuel configuration. Therefore, the puncture evaluations for the directly loaded fuel configuration are not affected by consideration of canistered fuel or GTCC waste in the cavity of the NAC-STC.

THIS PAGE INTENTIONALLY LEFT BLANK

2.7.2.1 Puncture - Cask Side Midpoint

2.7.2.1.1 Discussion

The NAC-STC is analyzed for structural adequacy in accordance with the requirements of 10 CFR 71 for puncture (hypothetical accident condition). The cask is assumed to be in a horizontal position and dropped through a distance of 40 inches onto a 6-inch diameter, mild steel bar oriented vertically on an unyielding surface. The NAC-STC is analyzed for a cask weight of 250,000 lbs to bound the directly loaded and Yankee-MPC configurations, and for a weight of 260,000 lbs to bound the CY-MPC configuration. The static structural evaluation of the cask is performed by classical analysis and the use of relations derived from destructive testing.

2.7.2.1.2 Analysis Description

Figure 2.7.2.1-1 illustrates the local cask midpoint section that is evaluated for this analysis. It is composed of the initial 2.65-inch design thickness, Type 304 stainless steel outer shell, a 3.70-inch thick chemical lead middle shell, and a 1.50-inch thick, Type 304 stainless steel inner shell.

During impact, the puncture pin is considered to apply a force, based on its assumed 47,000 psi dynamic flow stress, of 1.329×10^6 pounds ($47{,}000 \times \pi \times 6^2/4$) to the cask outer shell midpoint in the inward normal direction. The neutron shield is conservatively not considered.

2.7.2.1.3 Detailed Analysis

For an impact occurring on the cask side, the required local cask outer shell thickness (t_r) for puncture integrity is calculated according to the Nelms equation (Shappert) as:

$$t_r = \left[\frac{W}{S_u}\right]^{0.71} = 2.58 \text{ in}$$

where

W = cask design weight = 250,000 lb
S_u = cask outer shell ultimate tensile strength at 292°F
= 66,400 psi

for the CY-MPC configuration

$$t_r = \left[\frac{W}{S_u}\right]^{0.71} = 2.64 \text{ in}$$

where

W = cask design weight = 260,000 lb
S_u = cask outer shell ultimate tensile strength at 294°F
= 66,400 psi

From the free body diagram in the sketch that follows, it can be determined that:

$$\text{Deceleration} = \frac{\text{Applied Load}}{\text{Cask Design Weight}} = \frac{1.329 \times 10^6}{250{,}000} = 5.32 \text{ g}$$

letting $W_B = W_L$ (Redwood Impact Limiters)

W_B = (weight of bottom assembly and limiter) x 5.32 g
= (20,990 + 8865)(5.32)
= 158,829 lb

W_L = (weight of cask lids and upper limiter) x 5.32 g
= 158,829 lb

P = distributed linear load (lb/in)

$$= \frac{(250{,}000)(5.32) - (2)(158{,}829)}{192.96}$$

= 5,246 lb/in

Then the maximum moment and shear are:

$$M_{max} = 96.48\ W_L + 0.50\ P\ (96.48)^2 = 3.97 \times 10^7 \text{ in-lb}$$

$$V_{max} = (1.329 \times 10^6)(0.50) = 6.645 \times 10^5 \text{ lb}$$

For the CY-MPC:

$$\text{Deceleration} = \frac{\text{Applied Load}}{\text{Cask Design Weight}} = \frac{1.329 \times 10^6}{260{,}000} = 5.11 \text{ g}$$

letting $W_B = W_L$ (Balsa Impact Limiters)

W_B = (weight of bottom assembly and limiter) x 5.11 g
= (20,990 + 6000)(5.11)
= 137,920 lb

W_L = (weight of cask lids and upper limiter) x 5.11 g
= 137,920 lb

P = distributed linear load (lb/in)

$$= \frac{(260{,}000)(5.11) - (2)(137{,}920)}{192.96}$$

= 5,456 lb/in

Then the maximum moment and shear are:

$$M_{max} = 96.48\ W_L + 0.50\ P\ (96.48)^2 = 3.87 \times 10^7 \text{ in-lb}$$

$$V_{max} = (1.329 \times 10^6)(0.50) = 6.645 \times 10^5 \text{ lb}$$

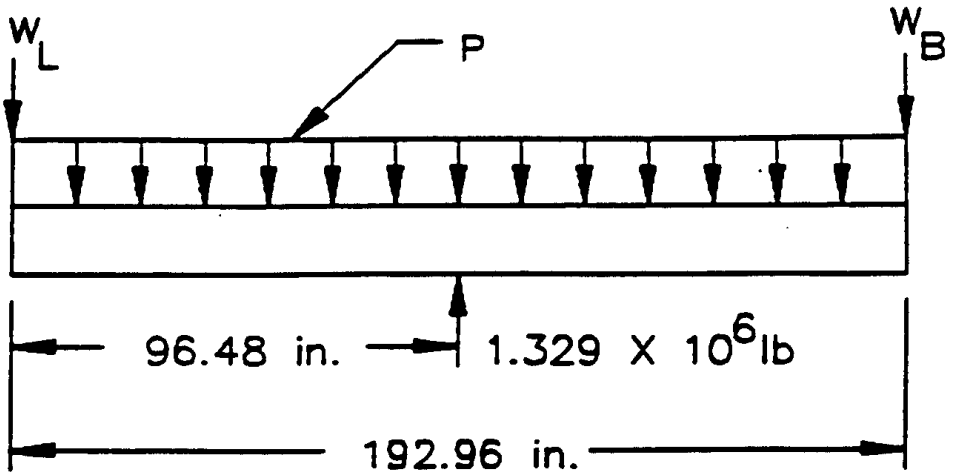

Cask Side Midpoint Puncture - Free Body Diagram

Since this loading is bounded by the 30-foot side drop loading (i.e., a cask deceleration force of 1.375×10^7 lb, which produces $M_{max} = 3.32 \times 10^8$ in-lb and $V_{max} = 6.875 \times 10^6$ lb), the overall cask stresses are bounded by the 30-foot side drop, disregarding the local stresses in the area of the puncture pin. Since the outer shell thickness is 2.65 inches, Nelms Equation, the margin of safety, based on thickness, is +0.03 for NAC-STC and +0.004 for CY-MPC.

2.7.2.1.4 Conclusion

For the pin puncture event at the cask midpoint, local deformation may occur in the region of the impact; however, the cask is demonstrated to have sufficient thickness to resist puncture. Therefore, the NAC-STC satisfies the requirements of 10 CFR 71 for consideration of puncture at the midpoint.

Figure 2.7.2.1-1 NAC-STC Midpoint Section

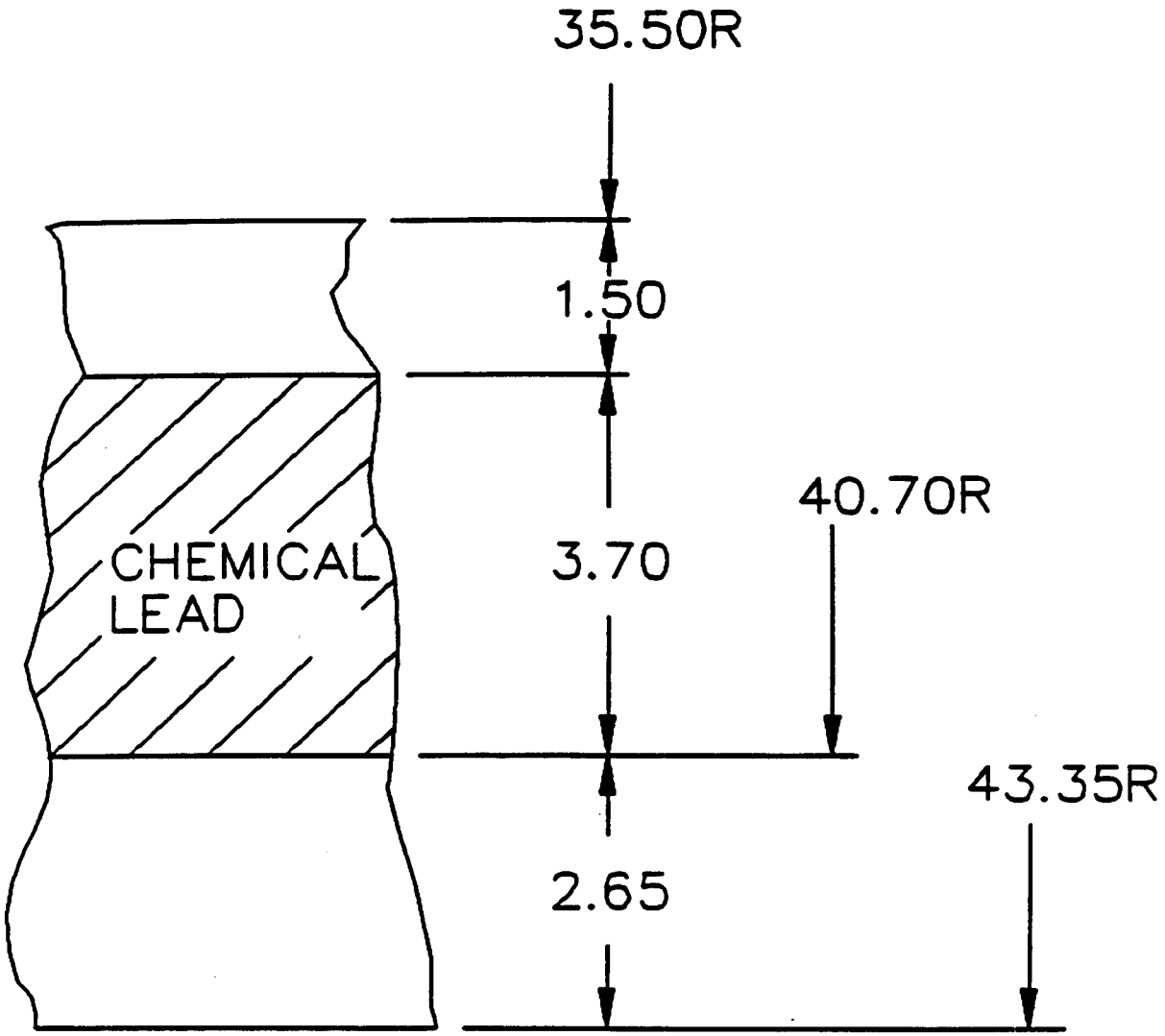

THIS PAGE INTENTIONALLY LEFT BLANK

2.7.2.2 Puncture - Center of Outer Lid

Discussion

The NAC-STC closure lids are analyzed for structural adequacy in accordance with the requirements of 10 CFR 71 for puncture (hypothetical accident condition). The cask is assumed to be inverted, with the lids downward, when dropped through a distance of 40 inches onto a 6-inch diameter, mild steel bar oriented vertically on an unyielding surface. The structural evaluation of the cask lid is performed by finite element analysis and the use of relations derived from destructive testing.

The main closure of the NAC-STC consists of an assembly of a bolted inner lid and a bolted outer lid. The Type 304 stainless steel inner lid is bolted to the top forging by forty-two 1 1/2 - 8 UN bolts fabricated from SB-637, Grade N07718 nickel alloy steel bolting material and is sealed by a metallic o-ring. The 17-4 PH stainless steel outer lid is bolted to the top forging by thirty-six 1-8 UNC bolts fabricated from 17-4 PH stainless steel and is sealed to the top forging by a metallic o-ring.

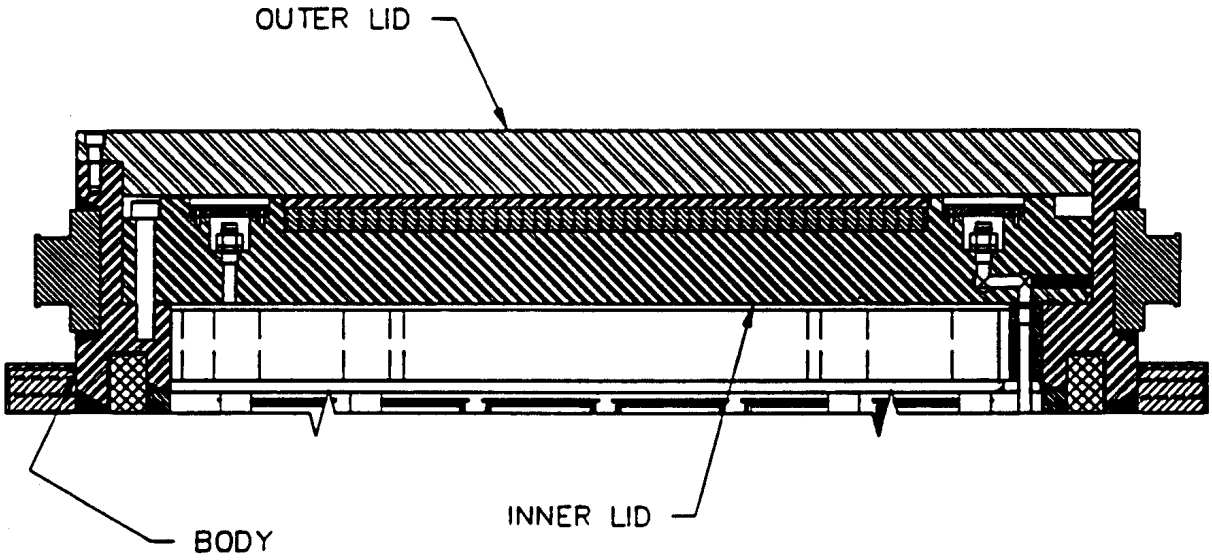

Assembly for NAC-STC Body and Lids

Lid Geometry

The main body of the inner lid is 9.0 inches thick and 79.0 inches in diameter. A 3.0-inch thick, 4.03-inch wide integral outer rim on the top of the inner lid encloses a 2.0-inch thick layer of NS-4-FR neutron shielding material and a 1.0-inch thick, Type 304 stainless steel coverplate.

The outer lid is a plate consisting of a 5.25-inch thick central main body having a 79.08-inch diameter and a 2.50-inch thick integral outer flange having an outside diameter of 86.70 inches. There is a 0.06-inch gap between the inner lid and the outer lid.

2.7.2.2.1 NAC-STC and Yankee-MPC Configuration Outer Lid Puncture Evaluation

Lid Analysis Considerations

The lid analysis must demonstrate that the lids and bolts satisfy two criteria: (1) calculated maximum stresses must be less than the allowable stress limit; the material yield strength is conservatively selected; and (2) lid deformation and/or rotation at the o-ring locations must be less than the elastic rebound of the o-rings.

Finite element evaluations of the combination of the inner and outer lids are performed using ANSYS computer program and a two-dimensional axisymmetric model. During the impact, the puncture pin is considered to apply a pressure of 47,000 psi (assumed dynamic flow stress of mild steel) on the cask lid at the centerline of the exterior surface in the inward normal direction. This is the critical load location on the outer lid because the maximum bending stress and edge rotation occur in the lid. The presence of an impact limiter is conservatively ignored. The lids and bolts are evaluated at a temperature of 200°F.

Finite Element Model Description

The components of the NAC-STC lid assembly that are considered in the finite element model include the outer lid, the inner lid, the NS-4-FR neutron shielding material, the stainless steel coverplate, the top forging, and the inner and outer lid bolts.

The finite element model of the NAC-STC lids is constructed utilizing the ANSYS PREP7 routine. Because both the geometric configuration and loading conditions on the lids are axisymmetric, a two-dimensional axisymmetric model is adequate to represent the lids. The finite element model is shown in Figure 2.7.2.2-1. The model contains ANSYS STIF42 elements for the lids and STIF3 elements for the bolts. In addition, the interfaces between the outer lid, the

inner lid, and the top forging are represented by two-dimensional interface (gap) elements (STIF12) with the coefficient of friction set to zero.

The gap elements represent two surfaces that may maintain, or break, physical contact and may slide relative to each other. Note that the gap element is only capable of supporting compression in the direction normal to the surfaces and friction in the tangential directions. Depending on whether or not there is contact between the two surfaces, the gap elements transmit compressive loadings, but permit no tensile load. This means that the gap elements allow the lid surfaces to separate relative to each other. With the coefficient of friction set to zero, no friction force is developed.

A large gap element stiffness is specified to maintain the boundary between the interfacing surfaces for compressive loadings.

The NS-4-FR neutron shielding material is considered to be bonded to the steel. With respect to a finite element model analysis "bonded" means the use of common nodes to connect two adjacent materials. Its modulus of elasticity, 0.56×10^6 psi, is two percent of the modulus of elasticity for steel and too low to have any significant effect on the flexural properties of the inner lid.

The lid bolts are modeled as spar elements. The outer lid bolt is connected to the countersink in the lid and to the cask body at the bolt centerline. The cross-sectional properties of the bolts are input on a "per radian" basis. The bolt preloads are applied to the finite element model as initial strains on the beam elements.

The material properties of the lids and bolts are from Section 2.3.

Loading Condition

The NAC-STC outer lid is analyzed for structural adequacy in accordance with the requirement of 10 CFR 71, puncture (hypothetical accident condition). During the impact, the puncture pin is considered to apply a pressure of 47,000 psi (assumed dynamic flow stress of mild steel) in the inward normal direction on the outer lid over a 6-inch diameter region at the centerline of the exterior surface. The presence of the top impact limiter is conservatively ignored.

The force exerted by the pin on the cask is:

$$F = (\pi)(3)^2(47{,}000)$$

$= 1.329 \times 10^6$ lb

The deceleration of the cask is:

$$a = \frac{F}{W} g$$
$$= 5.3 \text{ g}$$

where W is equal to 250,000 lb

The uniformly distributed internal pressure exerted by the spacer, basket, and fuel on the inner lid is:

$$p = \frac{(56{,}350)(5.3)}{(\pi/4)(71)^2}$$
$$= 75.7 \text{ psi}$$

Analysis Results

The ANSYS finite element analysis of the NAC-STC closure lids for the pin puncture loading produced the results as summarized in this section.

The maximum primary membrane plus bending calculated stress in the outer lid is 52,000 psi. The ultimate strength of the 17-4 PH stainless steel is 135 ksi at 200°F, providing a margin of safety of +1.59. The maximum gap at the location of the outer o-ring on the outer lid as a result of the out-of-plane rotation of the outer lid is 0.00016 inch. This elastic, short-duration deformation is less than the elastic rebound of the metallic o-ring material (0.005 inches) and is less than the elastic rebound of the non-metallic EPDM or Viton o-rings (0.03 inches); therefore, the seal is maintained.

The maximum primary membrane plus bending calculated stress in the inner lid is 12,000 psi. The ultimate strength of the Type 304 stainless steel is 66.2 ksi at 200°F, providing a margin of safety of +4.52. The maximum gap at the location of the o-rings on the inner lid as a result of the out-of-plane rotation of the edge of the inner lid is 0.00162 inch. This short duration, elastic deformation is less than the elastic rebound of the metallic o-ring material (0.005 inch) and is less than the elastic rebound of the non-metallic EPDM or Viton o-rings (0.03 inches); therefore, the seal is maintained.

The positive margins of safety on the stresses and the small displacements of the lids at the o-ring locations satisfy both stress and displacement/ rotation limit criteria for the lids. Therefore, the NAC-STC satisfies the requirements of 10 CFR 71 for consideration of puncture at the cask closure lids.

Figure 2.7.2.2-1 Finite Element Model - Lid Assembly – Yankee-MPC Pin Puncture

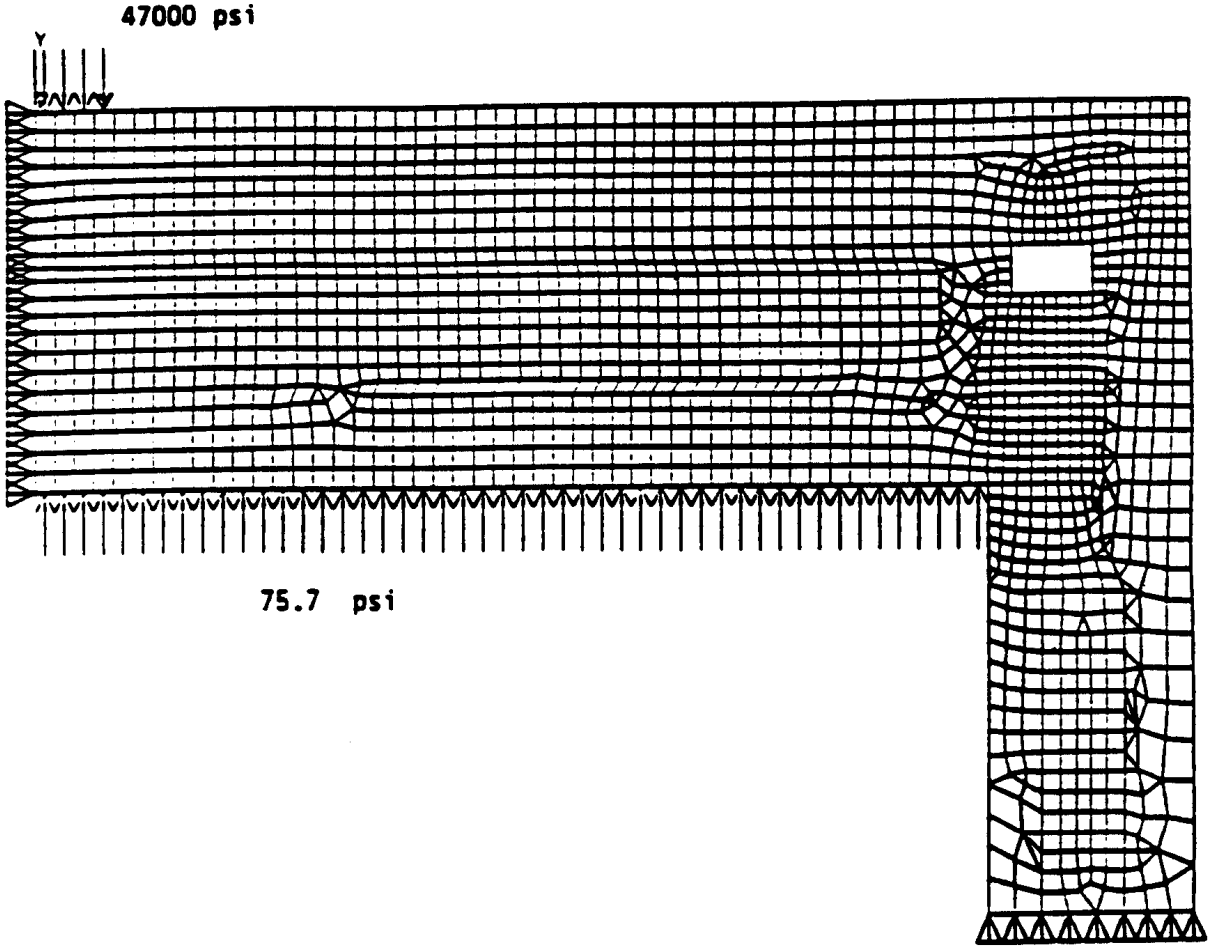

2.7.2.2.2 CY-MPC Configuration Outer Lid Puncture Evaluation

Lid Analysis Considerations

The lid analysis must demonstrate that the lids and bolts satisfy two criteria: (1) calculated maximum stresses must be less than the allowable stress limit; and (2) lid deformation and/or rotation at the o-ring locations must be less than the elastic rebound of the o-rings.

Finite element evaluations of the combination of the inner and outer lids are performed using ANSYS computer program and a two-dimensional axisymmetric model. During the impact, the puncture pin is considered to apply a pressure of 47,000 psi (assumed dynamic flow stress of mild steel) on the cask lid at the centerline of the exterior surface in the inward normal direction. This is the critical load location on the outer lid because the maximum bending stress and edge rotation occur in the lid. The presence of an impact limiter is conservatively ignored. The lids and bolts are evaluated at a temperature of 250°F.

Finite Element Model Description

The components of the NAC-STC lid assembly that are considered in the finite element model include the outer lid, the inner lid, the NS-4-FR neutron shielding material, the stainless steel coverplate, the top forging, and the inner and outer lid bolts.

Because both the geometric configuration and loading conditions on the lids are axisymmetric, the finite element model of the NAC-STC lids is constructed as a two-dimensional axisymmetric model. The finite element model is shown in Figure 2.7.2.2-2. The model contains ANSYS PLANE42 elements for the lids and cask and BEAM3 elements for the bolts. In addition, the interfaces between the outer lid, the inner lid, and the top forging are represented by two-dimensional interface (gap) elements (CONTAC52) with the coefficient of friction set to zero.

The gap elements represent two surfaces that may maintain, or break, physical contact and may slide relative to each other. Note that the gap element is only capable of supporting compression in the direction normal to the surfaces. Depending on whether or not there is contact between the two surfaces, the gap elements transmit compressive loads, but permit no tensile load. A gap element stiffness of 10E9 in-lbs and 1E8 in-lbs is specified for the inner bolt region and outer bolt region, respectively. For the gaps located at the bolting surfaces, the initial gap is specified to be zero. Gap elements are specifically located at the o-ring locations for evaluation of the final

gap. For other surfaces, the initial gap is defined by the initial relative location of the nodes connected, a gap stiffness of 1E6 in-lbs is used.

The NS-4-FR neutron shielding material is considered to be bonded to the steel. With respect to a finite element model analysis "bonded" means the use of common nodes to connect two adjacent materials. Its modulus of elasticity, 0.56×10^6 psi, is two percent of the modulus of elasticity for steel and too low to have any significant effect on the flexural properties of the inner lid.

The lid bolts are modeled as beam elements. The outer lid bolt is connected to the countersink in the lid and to the cask body at the bolt centerline. The bolt preloads are applied to the finite element model as initial strains on the beam elements.

The material properties of the lids and bolts are from Section 2.3.

Loading Condition

The NAC-STC outer lid is analyzed for structural adequacy in accordance with the requirement of 10 CFR 71, puncture (hypothetical accident condition). During the impact, the puncture pin is considered to apply a pressure of 47,000 psi (assumed dynamic flow stress of mild steel) in the inward normal direction on the outer lid over a 6-inch diameter region at the centerline of the exterior surface. The presence of the top impact limiter is conservatively ignored.

The force exerted by the pin on the cask is:

$$F = (\pi)(3)^2(47{,}000)$$

$$= 1.329 \times 10^6 \text{ lb}$$

The deceleration of the cask is:

$$a = \frac{F}{W} \times g = 5.11\,g \text{ (5.3g conservatively used)}$$

where W is equal to 260,000 lbs

The uniformly distributed internal pressure exerted by the spacer, basket, and fuel on the inner lid is:

$$p = \frac{(68{,}000)(5.3)}{(\pi/4)(71)^2} = 91.0 \text{ psi}$$

Analysis Results

The ANSYS finite element analysis of the NAC-STC closure lids for the pin puncture loading produced the results as summarized in this section.

The maximum primary membrane plus bending calculated stress in the outer lid is 81,300 psi. The ultimate strength of the 17-4 PH stainless steel is 135 ksi at 250°F, providing a margin of safety of +0.66. The maximum gap at the location of the outer o-ring on the outer lid as a result of the out-of-plane rotation of the outer lid is 0.004 inch. This elastic, short-duration deformation is less than the elastic rebound of the metallic o-ring material (0.005 inches); therefore, the seal is maintained.

The maximum primary membrane plus bending calculated stress in the inner lid is 23,300 psi. The ultimate strength of the Type 304 stainless steel is 63.8 ksi at 250°F, providing a margin of safety of +1.73. The maximum gap at the location of the o-rings on the inner lid as a result of the out-of-plane rotation of the edge of the inner lid is 0.00001 inch. This short duration, elastic deformation is less than the elastic rebound of the metallic o-ring material (0.005 inch).

The positive margins of safety on the stresses and the small displacements of the lids at the o-ring locations satisfy both stress and displacement/ rotation limit criteria for the lids. Therefore, the NAC-STC satisfies the requirements of 10 CFR 71 for consideration of puncture at the cask closure lids.

Figure 2.7.2.2-2 Lid Assembly Finite Element Model—CY-MPC Pin Puncture

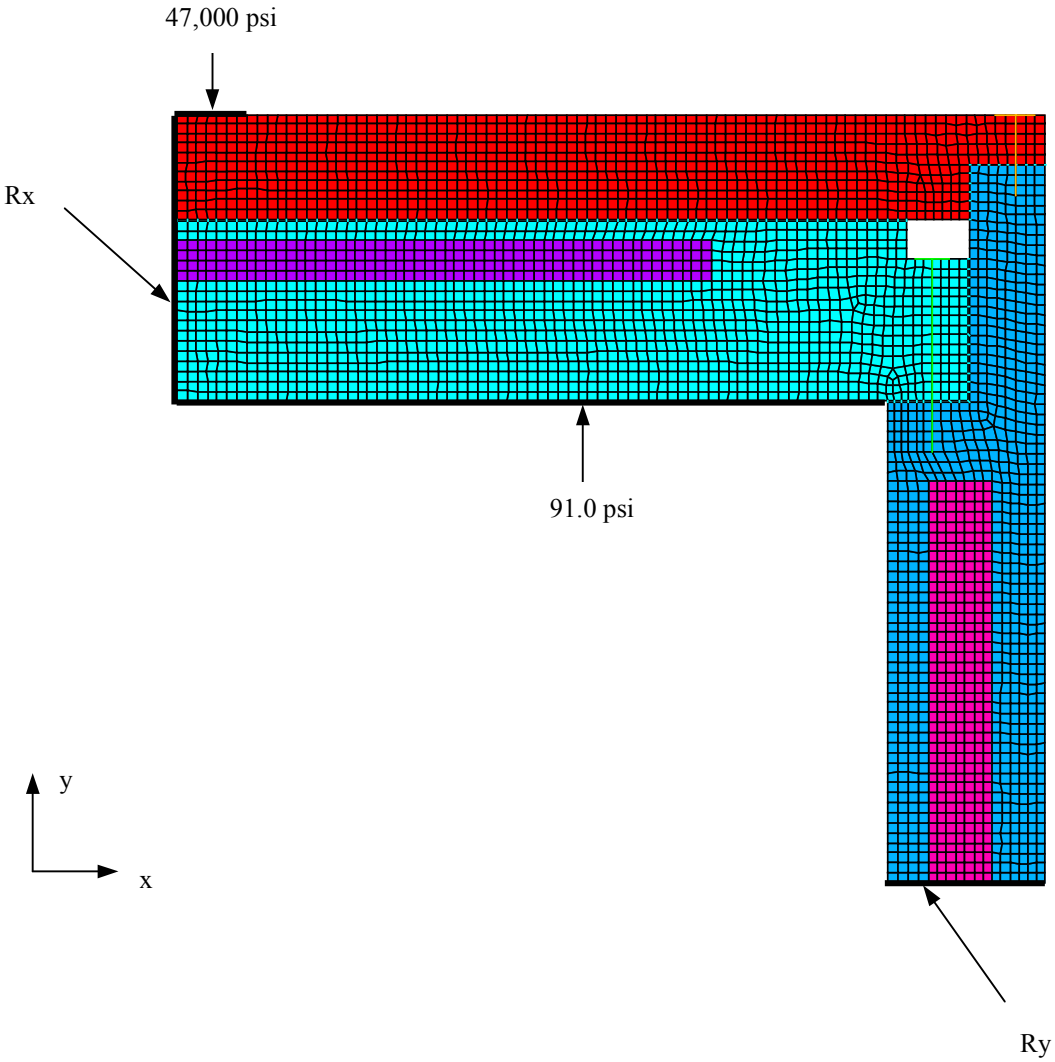

2.7.2.3 Puncture - Center of Cask Bottom

2.7.2.3.1 Discussion

The NAC-STC bottom is analyzed for structural adequacy in accordance with the requirements of 10 CFR 71 for puncture (hypothetical accident condition). The cask is assumed to be vertical and upright when dropped through a distance of 40 inches onto a 6-inch diameter, mild steel bar oriented vertically on an unyielding surface. The NAC-STC is analyzed for a cask weight of 250,000 lb. and 260,000 lb. to bound the current STC design and the CY-MPC configuration. The structural evaluation of the cask bottom is performed by classical elastic analysis and the use of relations derived from destructive testing.

2.7.2.3.2 Analysis Description

The cask bottom geometry shown in Figure 2.7.2.3-1 depicts a 5.45-inch thick outer plate and a 6.20-inch thick inner plate enclosing a 2.0-inch thick layer of NS-4-FR neutron shield material. The plates are made from Type 304 stainless steel. The layer of neutron shield material has a 78.88-inch diameter. The temperature-dependent material properties in Section 2.3 are used in this analysis.

During the impact, the puncture pin is considered to apply a pressure of 47,000 psi (assumed dynamic flow stress of mild steel) on the cask bottom exterior surface in the inward normal direction. The presence of an impact limiter is conservatively ignored.

Vertical and rotational restraints are provided at the 78.88-inch diameter for the composite section by the outer ring of stainless steel, which has an outside diameter of 86.70 inches.

2.7.2.3.3 Detailed Analysis

For the loading and displacement boundary conditions described, the bending behavior of the bottom plates can be assessed by applying formulas from Case 7, (Roark, 4th. ed., page 218) for a fixed edge circular plate, with a concentric uniform load (q) over a circular area of radius (r).

Because of the relatively high stiffness of the NS-4-FR material in compression, any normal displacement of the outer plate due to an inward load on its exterior face will cause a corresponding displacement in the inner plate, as shown in the following analysis.

The bearing stresses in the NS-4-FR material caused by the pin load of 47,000 psi, assuming a 45-degree distribution of pressure through the outer plate to the NS-4-FR, is:

$p = [(3.0)^2/(8.45)^2](47{,}000)$
$= 5924$ psi

This is less than the 8,780 psi yield compressive strength of the NS-4-FR material. The compression deformation of the 2-inch thick NS-4-FR is:

$e = p(2)/E$
$= 0.02$ in

where E = 561,000 psi, the compression modulus of the NS-4-FR.

Conservatively consider that the pin load on the exterior face of the outer plate is equally shared by the outer and inner plates. Then, the effective load on the outer plate is 47,000/2, or 23,500 psi.

The maximum stress at the center of the outer plate is given by:

$$S_r = S_t = \frac{3\,q\gamma^2}{2\,mt^2}\left[(m+1)\ln\left(\frac{a}{\gamma}\right) + (m+1)\left(\frac{\gamma^2}{4a^2}\right)\right]$$

$= 35{,}103$ psi

where:

$q = 23{,}500$ psi
$\gamma = 3$ in
$\upsilon = 0.275$
$m = 1/\upsilon = 3.636$
$t = 5.45$ in
$a = 39.44$ in

The punching shear stress around the periphery of the pin is:

$$S_S = \frac{q\gamma}{2t}$$

$$= 6468 \text{ psi}$$

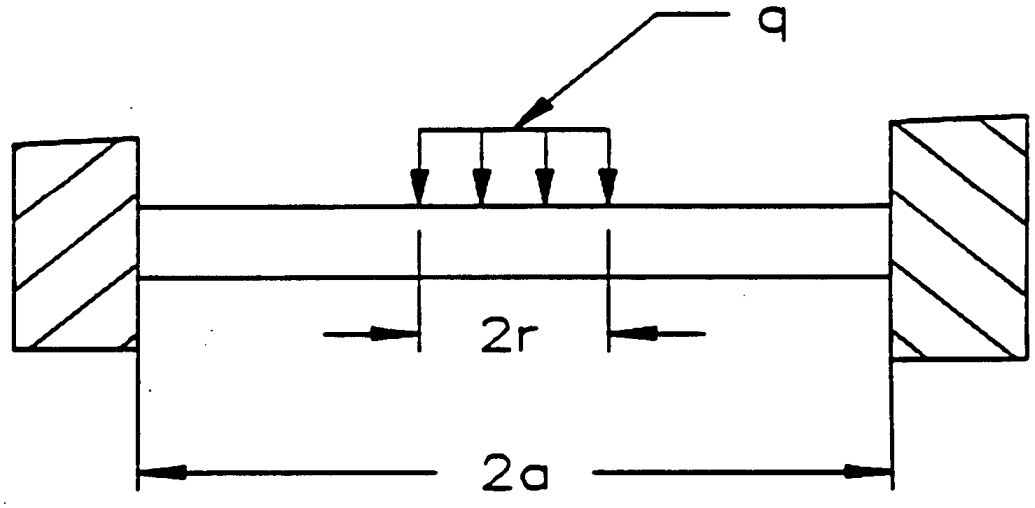

Bottom Plate Loading Diagram

Since the maximum temperature of the cask bottom is less than 420°F for the 100°F ambient temperature hot case, the minimum ultimate strength (S_u) and design stress intensity (S_m) are 64,200 and 18,460 psi, respectively. For accident conditions, the section stress intensity resulting from $P_m + P_b$ stresses must not exceed 64,200 psi (lesser value of 3.6 S_m or S_u); the section stress intensity resulting from P_m stress must not exceed 44,900 psi (lesser value of 2.4 S_m or 0.7 S_u). Averaging the radial bending stress and the tangential bending stresses at the center of the outer plate, the cross section primary bending stresses are:

$$S_t' = S_r' = \frac{S_r}{2} = 17{,}552 \text{ psi}$$

Conservatively, combining the bending stresses and the shear stress, the maximum stress is:

$$S_{smax} = \left[\frac{(S_r' + S_t')^2}{2} + S_s^2 \right]^{0.5} = 25{,}651 \text{ psi}$$

Then the maximum stress intensity and margin of safety associated with $P_m + P_b$ stresses are:

$$SI = 2\, S_{smax} = 51{,}302 \text{ psi}$$

$$\text{M.S.} = \frac{S_u}{SI} - 1 = +0.25$$

Clearly, the addition of S_s and S_t for the P_m stress intensity is less critical than the above stress combination.

The required local bottom plate thickness (t_r) for puncture integrity is calculated according to Shappert as:

$$t_r = \left[\frac{W}{S_u} \right]^{0.71} = 2.60 \text{ in}$$

where:

W = cask design weight = 250,000 lb
S_u = 65,200 psi (bottom plate ultimate tensile strength at 350°F)

$$\text{M.S.} = \frac{5.45}{2.60} - 1 = +1.10$$

For the CY-MPC configuration:

$$t_r = \left[\frac{W}{S_u} \right]^{0.71} = 2.67 \text{ in}$$

where:

W = cask design weight = 260,000 lb
S_u = 65,200 psi (bottom plate ultimate tensile strength at 350°F)

$$MS = \frac{5.45}{2.67} - 1 = +1.04$$

The puncture pin load applied to the cask is:

$$F_{pp} = \pi r^2 S_{DFS}$$

$$= 1.329 \times 10^6 \text{ lb}$$

where:

r = 3.0 in (pin radius)
S_{DFS} = 47,000 psi (assumed dynamic flow stress)

Then, for static equilibrium, the cask deceleration force is a maximum of 1.329×10^6 pounds. Since this loading is bounded by the 30-foot bottom end drop loading (i.e., a cask deceleration force of 1.12×10^7 lb), the cask stresses are bounded by the 30-foot bottom end drop stress calculations.

2.7.2.3.4 Conclusion

For a pin puncture impact on the cask bottom, local deformation may occur in the region of the impact. However, using a conservative loading, it is determined that (1) the minimum margin of safety is +0.25, (2) the bottom plate puncture resistance exceeds puncture requirements, and (3) overall cask stresses are enveloped by the 30-foot bottom end drop analysis. Therefore, the NAC-STC satisfies the requirements of 10 CFR 71 for consideration of puncture on the cask bottom.

Figure 2.7.2.3-1 NAC-STC Bottom Design Configuration

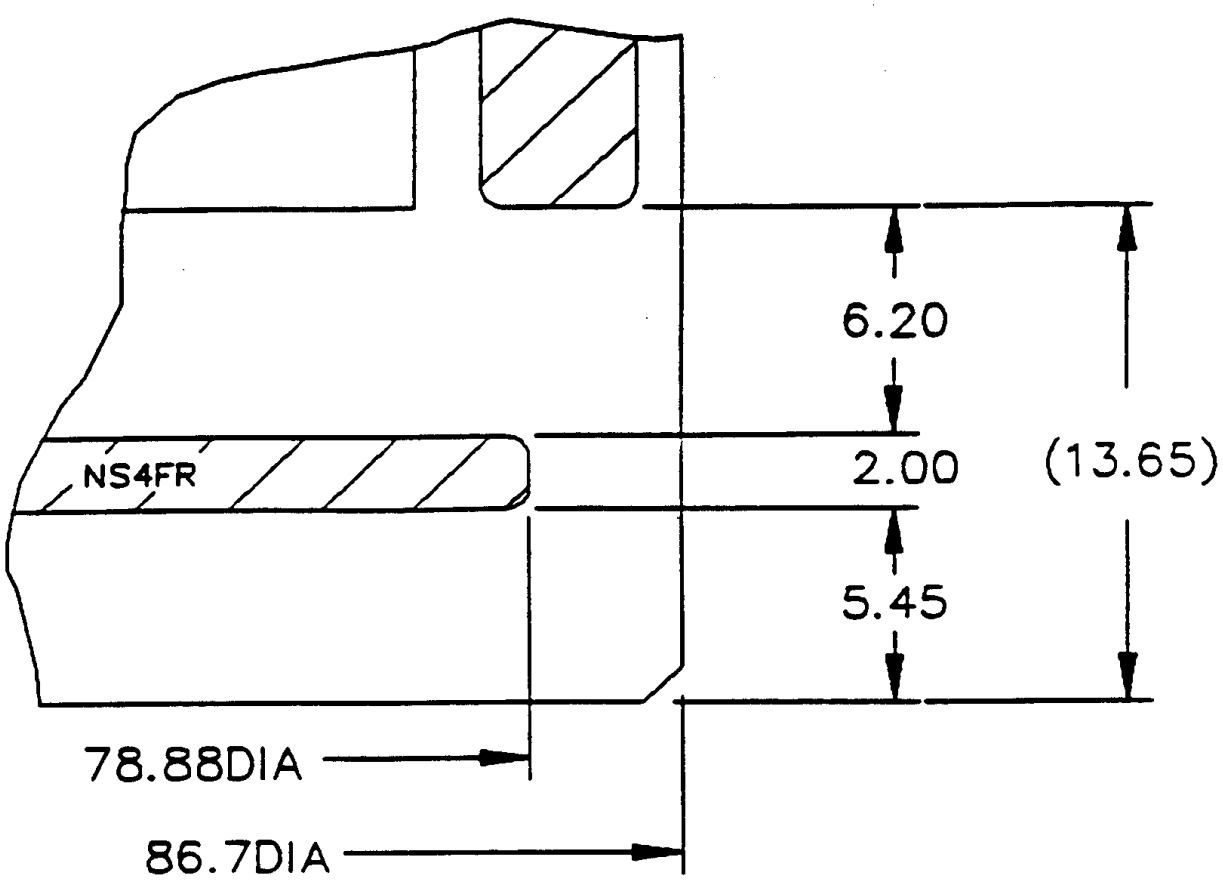

2.7.2.4 Puncture - Port Cover

The port cover of the NAC-STC is analyzed for structural adequacy in accordance with the requirements of 10 CFR 71 for puncture (hypothetical accident condition). The cask is assumed to be in a horizontal position and dropped through a distance of 40 inches onto a 6-inch diameter, mild steel bar oriented vertically on an unyielding surface. The structural evaluation of the port cover is performed by classical elastic analysis methods.

2.7.2.4.1 Analysis Description

The port cover geometry shown in Figure 2.7.2.4-1 is typical for the two port cover locations in the top forging of the cask. Each cover centerline is located 16.4 inches axially below the top of the outer lid. In this region, the cask body is a Type 304 stainless steel ring in excess of 7 inches thick. The port cover material is SA-705, Type 630, precipitation-hardened stainless steel. The vent and drain ports are located in the inner lid where they are protected by the outer lid during normal operation. Therefore, they are not subject to pin puncture loading. The temperature-dependent material properties presented in Section 2.3 are used in this analysis.

During the impact, the puncture pin is considered to apply a pressure of 47,000 psi (assumed dynamic flow stress of mild steel) on the port cover and the surrounding exterior surface of the cask in the inward normal direction.

The port cover rotation at its mating surface with the cask body is restrained by the bolted flange configuration of the cover. The port cover is also restrained from rotation in its flange region due to the puncture pin pressure acting on its exterior surface.

2.7.2.4.2 Detailed Analysis

2.7.2.4.2.1 Local Impact Region - Port Cover

For the loading and displacement boundary conditions described, the bending behavior of the port cover is assessed by applying formulas from Case 6 (Roark, 4th ed., page 217) for a uniformly loaded circular plate with fixed edges. The maximum radial stresses and the inward deflection of the port cover are, respectively:

$$S_r = \frac{3qa^2}{4t^2} = 74{,}569 \text{ psi}$$

$$y = \frac{3qa^4(1-\nu^2)}{16Et^3} = 0.0013 \text{ in}$$

where:

q = 47,000 psi
a = 1.469 in
t = 1.01 in
E = 27.6 x 10^6 psi (at 200°F)
ν = Poisson's ratio = 0.287

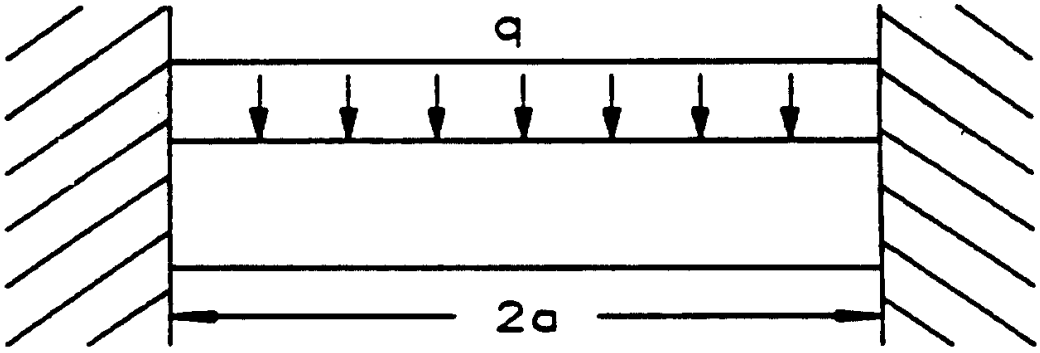

Port Cover Plate Loading Diagram

Since the maximum port cover temperature is less than 300°F for the 100°F ambient temperature hot case (Section 3.4.2), the yield strength of the port cover (conservatively based on 300°F) is 93,000 psi. Therefore, the minimum margin of safety is +0.25. Since the clearance between the port cover and the valve exceeds 0.0013 inch, the port cover does not contact the valve during impact.

2.7.2.4.2.2 Local Impact Region - Upper Ring

Locally, the potential puncture pin force due to its dynamic flow stress is:

$$F_{pp} = (3)^2\pi(47{,}000) = 1.329 \times 10^6 \text{ lb}$$

This force, acting on the 7.85-inch thick stainless steel cask body, produces a maximum shear stress:

$$S_s = F_{pp}/[6\pi(7.85)] = 8{,}982 \text{ psi}$$

As a result of the port cover being recessed 0.06 inches below the cask exterior surface, bearing impact is limited to the annular ring surrounding the port cover (i.e., from 4.53-inch to 6.00-inch diameter), the bearing stress on the cask is:

$$S_{br} = F_{pp}/0.25\ \pi[(6.00)^2 - (4.53)^2] = 109{,}317 \text{ psi}$$

If deformation of the cask and/or pin permits the pin to impact the top of the port cover, the bearing area increases to:

$$A_b = 0.25\pi\ [(6.00)^2 - (4.53)^2 + (4.50)^2 - (2.875)^2] - 0.75\pi\ (.45)^2$$

$$= 21.09 \text{ in}^2$$

Then, the bearing stress on the cask and on the port cover is:

$$S_{br} = \frac{F_{pp}}{A_b} = 63{,}016 \text{ psi}$$

The allowable dynamic yield bearing stress of Type 304 stainless steel is 65,130 psi; i.e., 1.67 x 39,000 psi dynamic yield strength (MIL-HDBK-5A). The allowable dynamic ultimate bearing stress of Type 304 stainless steel is 132,000 psi; i.e., 2.0 x 66,000 psi ultimate tensile strength (MIL-HDBK-5A). Thus, the minimum yield margin of safety is +0.03 and the ultimate margin of safety is +1.09 for the bearing stress state at the cask and port cover mating surface.

For the port cover material, the yield strength is 93,000 psi (Section 2.7.2.4.2.1). The bearing stress of 63,016 psi results in a yield margin of safety of +0.48.

2.7.2.4.2.3 Cask Body Stresses

The NAC-STC is analyzed for structural adequacy during a puncture pin impact on a port cover. The cask is assumed to be in a horizontal position and dropped through a distance of 40 inches, impacting the pin on a port cover, which is located near the upper end of the cask. The static structural evaluation of the cask is performed by classical elastic analysis methods.

During an impact, the puncture pin is considered to apply a total force of 1.329×10^6 pounds (Figure 2.7.2.4-2) to the cask at the port cover in the inward normal direction assuming a pin dynamic flow stress of 47,000 psi. Vertical restraint is provided by the bottom impact limiter and the puncture pin located 16.4 inches from the top of the outer lid.

For the loading and displacement boundary conditions described, the free body diagram (Figure 2.7.2.4-2) is evaluated. For static equilibrium, the cask deceleration force (F_g) and reaction (R_r) are determined by solving the following simultaneous equations:

$$1.329 \times 10^6 - F_g + R_r = 0$$

$$F_g (85.80) - 176.62\ R_r = 0$$

then

$$F_g = 2.585 \times 10^6 \text{ lb}$$

$$R_r = 1.256 \times 10^6 \text{ lb}$$

Since this loading is bounded by the 30-foot side drop loading (a cask deceleration force of 1.35×10^7 lb; Section 2.7.1.2), the cask stresses for the puncture pin impact are bounded by the 30-foot side drop accident.

2.7.2.4.3 Conclusion

For the pin puncture event, local deformation may occur in the region of impact. However, it is demonstrated by use of conservative loading that: (1) the minimum margin of safety is +0.03 for local stresses; (2) the port cover seals are maintained; and (3) cask bending stresses are enveloped by the 30-foot side drop analysis. Therefore, the NAC-STC satisfies the requirements of 10 CFR 71 for puncture of the cask at the port cover.

Figure 2.7.2.4-1 Port Cover Geometry

FIGURE WITHHELD UNDER 10 CFR 2.390

Figure 2.7.2.4-2 Puncture of Cask at Port Cover Location (Free body Diagram)

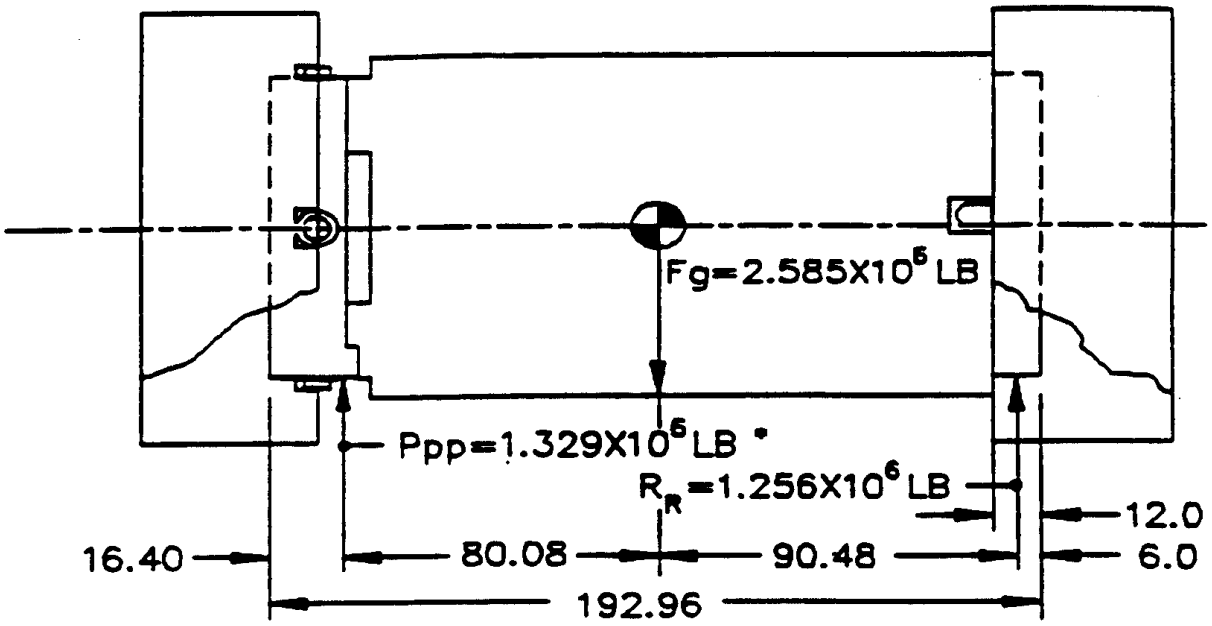

Applied Puncture Pin Load

THIS PAGE INTENTIONALLY LEFT BLANK

2.7.2.5 Puncture Accident - Shielding Consequences

In order to comply with 10 CFR 71, calculations were performed for the hypothetical accidents described in Section 2.7. In this case, a puncture occurs, which causes a localized reduction in the cask shielding. The resulting dose rates are bounded by the loss of neutron shield accident dose rates, which do not exceed the limits of 10 CFR 71.51. Details of the shielding analysis are presented in Section 5.4.

THIS PAGE INTENTIONALLY LEFT BLANK

2.7.2.6 Puncture - Conclusion

The analyses of Section 2.7.2 demonstrate the structural and shielding adequacy of the NAC-STC for a puncture pin impact on the (1) cask side midpoint, (2) center of cask closure, (3) center of cask bottom, and (4) cask port cover. Therefore, the NAC-STC satisfies the structural and the shielding requirements of 10 CFR 71 for the puncture event.

THIS PAGE INTENTIONALLY LEFT BLANK

2.7.3 Thermal

2.7.3.1 Discussion

For the hypothetical fire accident condition, the NAC-STC cask body performs its protection and containment functions identically for both the directly loaded fuel and the canistered fuel or GTCC waste configurations. However, for the fire accident event the canistered configuration components have the advantage of not heating up as rapidly as the fuel and basket in the directly loaded fuel configuration, due to the presence of the canister shell and the gaps, each side of the shell in the heat flow path of the canistered configuration. During the cooldown period following the actual fire, the reverse situation exists so that the canistered configuration contents and basket do not cool down as rapidly as the fuel and basket do in the directly loaded fuel configuration.

The temperature and pressure evaluations of the directly loaded fuel and the canistered fuel configurations of the NAC-STC are presented in Sections 3.5.1, 3.5.3 and 3.5.4.

The NAC-STC is analyzed for structural adequacy in accordance with the requirements of 10 CFR 71.73(c)(3), Thermal, hypothetical accident conditions. The cask is assumed to be subjected to a fire, which produces a surrounding environment of 1475°F for a period of 30 minutes. The thermal evaluation of the hypothetical fire transient is presented Section 3.5. The structural evaluation of the NAC-STC for the Thermal (fire) accident is performed in this section.

THIS PAGE INTENTIONALLY LEFT BLANK

2.7.3.2 Pressure Stress Evaluation

The maximum Thermal (fire) accident condition temperatures, which are calculated in Section 3.5, are summarized in Table 3.5-1 for the various cask components. From Section 3.5.4, the maximum internal cask cavity pressure resulting from the fire transient is 65.5 psig, 42.5 psig and 56 psig for the directly loaded fuel, the Yankee-MPC canistered fuel configuration, and the CY-MPC canistered fuel configuration, respectively. These pressures are based on the assumption that the canister containment fails during the fire transient. The NAC-STC is conservatively evaluated for an internal pressure of 125 psig to protect against an unanticipated pressure buildup. The canister is evaluated for an internal pressure of 50 psig.

Stresses for lid bolt preload plus an internal pressure of 50 psig are calculated at 11 locations on the containment vessel in Section 2.6.1 (Table 2.10.4-1). Table 2.7.3.2-1 presents a tabulation of the principal stresses, the stress intensity, the allowable stress intensity, and the margin of safety at each of those locations for an internal pressure of 125 psig for the directly loaded fuel configuration of the NAC-STC; the tabulated stresses are conservatively calculated by ratioing: $S_{125} = (S_{50})(125/50)$. The allowable stress intensities are based on Table 2.1.1-1 for containment structures for hypothetical accident conditions. Tables 2.7.3.2-2 and 2.7.3.2-3 present a tabulation of the principal stresses, stress intensities, allowable stress intensities and margins of safety at 11 locations in the canister (see Figure 2.6.13.3-1). The stresses are calculated by ratioing: $S_{50} = (S_{20})(50/20)$ from Tables 2.6.13.4-1 and 2.6.13.4-2. The allowable stresses are based on Table 2.1.1-1 for Type 304L stainless steel.

The maximum deflection of the inner lid resulting from the 125 psig pressure is 0.0135 inch. Therefore, there is no loading in the outer lid bolts resulting from a 125 psig internal pressure because of a 0.06 inch gap between the outer and the inner lids.

The stress in the inner lid bolts resulting from a 125 psig internal pressure is:

$$S_{BI} = (\pi/4)(72.331)^2(125)/(42)(1.492)$$
$$= 8{,}197 \text{ psi}$$

The accident condition allowable stress for the inner lid bolts at 400°F is 138,600 psi (S_y), so the margin of safety for the inner lid bolts is:

M.S. = (109,600/8,197) - 1 = + Large

Therefore, the NAC-STC satisfies the accident condition stress intensity limits for the maximum internal cavity pressure that occurs during the Thermal (fire) accident for both the directly loaded fuel configuration and the canistered fuel configuration.

Table 2.7.3.2-1 Cask Internal Pressure Stress Summary - Thermal Accident (125 psig)

Section	Node	Principal Stresses (ksi)			SI (ksi)	Allowable SI[1] (ksi)	Margin of Safety
		S1	S2	S3			
A5	5	1.50	1.50	0.00	1.50	48.0	+Large
C1	251	3.00	1.50	0.75	2.25	48.0	+Large
F1	251	3.00	1.50	0.75	2.25	69.6	+Large
H4	584	2.50	1.75	0.00	2.50	69.6	+Large
J1	971	2.75	1.00	-0.25	3.00	48.0	+Large
L1	1601	2.75	1.00	-0.25	3.00	48.0	+Large
N1	2216	2.75	1.00	-0.25	3.00	48.0	+Large
P4	2549	2.50	1.50	0.00	2.50	69.6	+Large
R4	2774	1.75	0.50	-2.75	4.50	69.6	+Large
V7	3617	1.00	-0.50	-3.50	4.50	94.5	+Large
X7	2807	0.75	0.75	0.00	0.75	94.5	+Large

1. Conservatively assume primary membrane stress intensity.

Table 2.7.3.2-2 Canister Pressure Stress Summary - Thermal Accident (50 psig) (Primary Membrane Stress)

Section	Principal Stresses (ksi)			SI (ksi)	Allowable SI (ksi)	Margin of Safety
	S1	S2	S3			
1	13.332	4.032	-3.355	16.69	35.5	1.12
2	7.210	-4.170	-5.785	13.0	35.5	1.73
3	2.782	1.375	-.005	2.79	35.5	11.7
4	1.151	.962	.317	0.83	35.5	41.7
5	.820	.682	-1.102	1.92	35.5	17.5
6	.302	-.214	-.948	1.25	35.5	27.4
7	1.070	.364	-.317	1.39	35.5	24.5
8	1.071	.343	-.194	1.26	35.5	27.2
9	3.470	1.693	-1.817	5.29	35.5	5.71
10	0.39	-.065	-.074	0.11	42.0	321.7
11	.182	.182	.001	0.18	35.5	196.2

Table 2.7.3.2-3 Canister Pressure Stress Summary - Thermal Accident (50 psig)
(Primary Membrane Stress + Bending Stress)

Section	Principal Stresses (ksi)			SI (ksi)	Allowable SI (ksi)	Margin of Safety
	S1	S2	S3			
1	3.18	0.35	-18.61	21.8	53.3	1.44
2	3.80	-15.79	-39.95	43.8	53.3	0.21
3	2.81	1.38	-0.017	2.83	53.3	17.8
4	0.95	0.78	-0.032	0.98	53.3	53.4
5	5.17	2.15	-0.65	5.82	53.3	8.15
6	-0.58	-3.08	-2.50	2.50	53.3	20.3
7	3.87	1.63	-0.135	4.01	53.3	12.3
8	0.61	-0.26	-1.49	2.10	53.3	24.4
9	42.42	41.35	2.36	40.06	53.3	+0.33
10	-0.12	-2.98	-3.01	2.89	63.0	17.4
11	0.33	0.33	0.01	0.32	53.3	Large

THIS PAGE INTENTIONALLY LEFT BLANK

2.7.3.3 Thermal Stress Evaluation

Differential thermal expansion stresses and through-thickness thermal gradient stresses are induced in the NAC-STC as a result of the Thermal (fire) accident event. All of these thermal stresses are classified as secondary, displacement-limited stresses according to the "ASME Boiler and Pressure Vessel Code." Limits on secondary stresses do not apply for accident conditions (Table 2.1.2-1); the secondary stresses, in themselves, do not compromise the integrity of the cask. To satisfy the requirement regarding the extreme total stress intensity range that is specified in Paragraph C.7 of Regulatory Guide 7.6 (as discussed in Section 2.1.3.3), a finite element analysis is performed to determine the maximum stresses associated with the Thermal (fire) accident transient event.

The thermal analysis of the NAC-STC for the Thermal (fire) accident is presented in Section 3.5. The thermal analysis is performed using the ANSYS finite element computer code. Based on the evaluations performed in Sections 2.6.7.4.7 and 2.10.6, the impact limiters remain attached in position on the NAC-STC throughout the sequence of hypothetical accidents defined in 10 CFR 71.73. Therefore, the impact limiters are included in the finite element thermal analysis model.

The ANSYS finite element computer program is used to calculate the thermal stresses in the NAC-STC for the Thermal (fire) accident. The analysis uses the two-dimensional, axisymmetric finite element model that is described in detail in Section 2.10.2.1.1. The finite element model is constructed of two-dimensional, isoparametric solid elements with two-dimensional beam elements representing the lid bolts and two-dimensional gap elements simulating the interfaces between the lids and the body and between the shielding materials and the body. The model described in Section 2.10.2.1.1 is modified to allow the beam elements representing the bolt head to be coupled in the vertical direction to the solid elements representing the lids.

Time history results of the Thermal (fire) hypothetical accident transient analysis show that maximum gradients occur at 30 minutes into the event (when impinging flame terminates). Accordingly, temperatures at the 30-minute time step are taken

from the appropriate ANSYS file generated by the thermal analysis in Section 3.5 and are linearly interpolated for the proper nodal locations of the structural analysis finite element model. A uniform temperature of 70°F is input as the initial stress free condition of the structural finite element model. Temperature dependent material properties are input in tabular form to allow ANSYS to use the correct properties for each nodal temperature. The temperature dependent material properties are obtained from the "ASME Boiler and Pressure Vessel Code, Section III, Division 1": "Appendix I" for temperatures less than or equal to 800°F. For temperatures over 800°F material properties are obtained from "ASME Boiler and Pressure Vessel Code, Section III, Division 1, Subsection NH" and Section II, Part D, Subpart 2." For material properties not explicitly covered by the code, extrapolated values are used.

The maximum primary plus secondary nodal stress components and principal stresses, calculated by ANSYS in the NAC-STC containment vessel for the directly loaded fuel configuration for the 30-minute time step of the Thermal (fire) Accident, are summarized in Table 2.10.4-178. The detailed results of the ANSYS stress calculations for the NAC-STC during the Thermal (fire) Accident are contained in Tables 2.10.4-178 through 2.10.4-180. Based on the temperature comparison that is discussed in Section 3.5.3 for the canistered fuel configuration and the temperatures tabulated in Table 2.7.3.2-1, the components within the canister (support disk and aluminum heat transfer disk) have higher temperatures than the directly loaded fuel basket, but the cask components (containment boundary) have lower temperatures. Therefore, the thermal evaluation of the canistered fuel configuration of the NAC-STC cask is bounded by that of the directly loaded fuel configuration.

To conservatively evaluate the stress state in the NAC-STC as specified in Paragraph C.7 of Regulatory Guide 7.6, the maximum primary plus secondary (P+Q) stress intensity in the NAC-STC containment vessel for the Thermal Accident will be used (92.2 ksi at Location R on the containment vessel). It is demonstrated in other sections of this Safety Analysis Report that the maximum combined primary membrane plus primary bending stress intensities for all of the other normal conditions of transport and hypothetical accident conditions satisfy Regulatory Guide 7.6, i.e. they are less than 1.0 S_u. It is, therefore, conservative to assume that the maximum allowable value for the primary stresses, 1.0 S_u, actually develops within the NAC-STC containment vessel.

The maximum S_u value for the NAC-STC containment vessel material at Location R is 100.0 ksi (Type XM-19 stainless steel). Adding this maximum S_u value to the maximum P+Q stress

intensity calculated for the Thermal Accident at Location R, the total primary plus secondary stress intensity is 92.2 + 100.0 = 192.2 ksi. The maximum possible stress intensity range is twice this value, or (2)(192.2) = 384.4 ksi. The appropriate alternating stress is one-half of this value, or S_{alt} = (0.5)(384.4) = 192.2 ksi. To account for the temperature effects, the variation in modulus of elasticity of the material is factored into the calculation as follows:

$$S_{alt}(850°F) = (E_{70}/E_{850})(S_{alt})$$
$$= [28.3 \times 10^6/23.8 \times 10^6](192.2)$$
$$= 228.5 \text{ ksi}$$

At 850°F, "ASME Boiler and Pressure Vessel Code, Section III, Division 1, Subsection NH" limits the strain range of Type 316 stainless steel to 0.04080 inch/inch, and the strain range of Type 304 stainless steel to 0.04825 inch/inch. This analysis conservatively applies a strain range limit of 0.0303 inch/inch. For the modulus of elasticity at 850°F of 23,800 ksi, the S_{alt} at 10 cycles is (0.0303)(23,800 ksi) or 721.1 ksi.

$$\text{M.S.} = (721.1/228.5) - 1 = + 2.15$$

Considering the conservative assumptions that were used in the preceding evaluation, i.e. (1) use of the allowable primary stress rather than the actual value; (2) assuming fully reversing primary and secondary stress states to determine stress intensity ranges; and (3) assuming that the worst case primary stresses occur simultaneously with the worst case fire transient stresses, it is apparent that the actual margin of safety is significantly larger than +2.15. Thus, the requirements of Paragraph C.7 of Regulatory Guide 7.6 are satisfied.

THIS PAGE INTENTIONALLY LEFT BLANK

2.7.3.4 Bolts - Closure Lids (Thermal Accident)

During the thermal (fire) hypothetical accident, the NAC-STC inner lid bolts and outer lid bolts are calculated to experience a maximum average temperature of 335°F. This ANSYS analysis of the closure lids and bolts was performed using an average temperature of 310°F. The effect on the stress results due to the temperature difference of 25°F (335-310) is insignificant since the increase of the coefficient of thermal expansion (thermal stress) for the bolt material is less than 0.5%.

The maximum thermal gradients occur at the end of the fire (30 minutes), which produces the largest differential thermal growth between the inner and outer lids of the cask body. Using the results of the ANSYS analysis at the end of the fire (30 minutes), the maximum membrane and bending stresses for the lid bolts, including the combined effects of the 125 psig internal pressure, o-ring compression forces, bolt preload, and thermal accident conditions, are determined as shown in Figure 2.7.3.4-1 to be:

Bolt Location	Maximum Membrane + Bending (ksi)
Inner Lid Bolts:	90.5 + 6.3 = 96.8
Outer Lid Bolts:	82.3 + 1.6 = 83.9

Based on the yield stress at 335°F, the margins of safety are:

Inner Lid bolts (SB-637 Grade N07718)

$$\text{M.S.} = \frac{139.9}{96.8} - 1 = +0.45$$

Outer Lid bolts (17-4PH Stainless Steel)

$$\text{M.S.} = \frac{91.8}{83.9} - 1 = +0.09$$

Figure 2.7.3.4-1 Bolt Stress - Thermal (Fire) Accident

POST1 – INP =
psb1

PRINT ELEMENT STRESS ITEMS PER ELEMENT
***** POST 1 ELEMENT STRESS LISTING *****

LOAD STEP 1 ITERATION = 50 SECTION = 1
TIME = 0 LOAD CASE = 1

ELEM	SDI	SBI	SBJ
2836	13362.	6351.6	-0.54972E – 10
2840	15093.	-1606.4	-0.16855E – 10
2843	0.	-0.2743E – 10	3928.8
2844	-0.10730E – 09	4089.4	0.29950E – 10
2845	82316.	-1606.4	-1606.4
2846	0.12982E – 09	0.20382E – 11	12067.
2847	-0.19442E – 09	11432.	0.64312E – 10
2848	90483.0	6351.6	6351.6
MINIMUMS			
ELEMENT	847	2840	2845
VALUE	-0.19442E – 09	-1606.4	-1606.4
MAXIMUMS			
ELEMENT	2848	2847	2846
VALUE	90483.	11432.	12067.

POST1 – INP =

PRINT NODE LISTING
***** POST1 NODE LISTING *****

NODE	X	Y	Z	THXY	THYZ	THXZ
3057	35.206	187.40	0.	0.000	0.000	0.000
3058	35.206	188.40	0.	0.000	0.000	0.000
7024	37.655	176.90	0.	0.000	0.000	0.000
7064	37.655	179.40	0.	0.000	0.000	0.000
9000	33.705	192.78	0.	0.000	0.000	0.000
9001	35.206	192.78	0.	0.000	0.000	0.000
9002	36.455	192.78	0.	0.000	0.000	0.000
9003	36.833	185.40	0.	0.000	0.000	0.000
9004	37.655	185.40	0.	0.000	0.000	0.000
9005	38.608	185.40	0.	0.000	0.000	0.000

POST1 – INP =

PRINT ELEMENT LISTING
***** POST1 ELEMENT LISTING *****

ELEM	TYPE	STIF	MAT	ESYS	NODES	
2836	3	3	13	0	7064	7024
2840	3	3	12	0	3058	3057
2843	3	3	12	0	9000	9001
2844	3	3	12	0	9001	9002
2845	3	3	12	0	9001	3058
2846	3	3	12	0	9003	9004
2847	3	3	12	0	9004	9005
2848	3	3	12	0	9004	7064

POST1 –INP =

POST DATA FILE = 12
LOAD STEP = 1
ITERATION = 50
CURRENT INPUT FILE = 05

GEOMETRY 3089 NODES 2842 ELEMENTS
STORED FOR
***** STRESS DEFINITIONS *****

LABEL	STIF	ITEM

2.7.3.5 Performance Summary - Thermal Accident

The NAC-STC satisfies all licensing and performance criteria for the Thermal (fire) accident; thus, containment of the cask contents is ensured.

THIS PAGE INTENTIONALLY LEFT BLANK

2.7.3.6 Conclusion

The NAC-STC cask shells, lids, and lid bolts are demonstrated to be structurally adequate against loss of containment. Therefore, the NAC-STC cask satisfies 10 CFR 71 structural requirements for the fire accident scenario.

THIS PAGE INTENTIONALLY LEFT BLANK

2.7.4 Crush

In accordance with 10 CFR 71.73(c)(2) and IAEA Safety Series No. 6, paragraph 627(c), this test is not applicable to the NAC-STC because the mass of the cask and contents is greater than 500 kilograms (1100 lb) and the cask and contents have an overall density greater than 1000 kilograms/cubic meter (62.4 lbs/ft^3).

THIS PAGE INTENTIONALLY LEFT BLANK

2.7.5 Immersion - Fissile Material

According to the requirements of 10 CFR 71.73(c)(5), a package containing fissile material, where water inleakage has not been assumed for criticality analysis, must be subjected to water pressure equivalent to immersion under a head of water of at least 0.9 meters (3 feet) for a period of 8 hours. This immersion is the fifth test in the Hypothetical Accident sequence of tests for the package. Paragraph No. 633 of IAEA Safety Series No. 6 specifies the same requirements for the international shipment of radioactive materials. A head of water of 0.9 meters (3 feet) is equivalent to an external pressure of (3)(0.433) = 1.3 psig.

The analyses presented in Sections 2.7 through 2.7.3 document that the NAC-STC maintains containment of the package contents for the sequence of Hypothetical Accident tests - free drop, puncture, and fire - that precede the immersion test. The outer lid is shown to be structurally adequate for a maximum external dynamic crush pressure of the top impact limiter of 2376 psi (Section 2.7.1.6). For the 2.65-inch thick outer shell with a mean radius of 42.03 inches, an external pressure of 1.3 psig produces a negligible compressive hoop stress. According to the manufacturer's specifications, the metallic o-rings used in the NAC-STC are adequate for pressures in excess of 5000 psi. Therefore, the NAC-STC satisfies the immersion requirement of 10 CFR 71.73(c)(5) for a package containing fissile material.

The criticality analyses of both the directly loaded fuel configuration and the canistered fuel configuration do assume water inleakage, so containment of the package contents is an additional safety consideration.

THIS PAGE INTENTIONALLY LEFT BLANK

2.7.6 Immersion - All Packages

According to the requirements of 10 CFR 71.73(c)(6), a package must be subjected to water pressure equivalent to immersion under a head of water of at least 15 meters (50 ft) for a period of 8 hours. Paragraph 630 of IAEA Safety Series No. 6 requires that a package be immersed under a head of water of at least 200 meters (656 ft) for a period of not less than 1 hour. A head of water of 200 meters (656 ft) is equivalent to an external pressure of (656)(0.433) = 284 psig. Also, 10 CFR 71.61 requires that a package's undamaged containment system be able to withstand an external water pressure of 290 psi for a period of not less than one hour without collapse, buckling or inleakage of water.

The outer lid is shown to be structurally adequate for a maximum external dynamic crush pressure of the top impact limiter of 2376 psi (Section 2.7.1.6). For the 2.65-inch thick outer shell with a mean radius of 42.03 inches, an external pressure of 290 psig produces a compressive hoop stress of -4599 psi, which is much less than the material yield strength. According to the manufacturer's specifications, the metallic o-rings used in the NAC-STC are adequate for pressures in excess of 5000 psi.

Therefore, the NAC-STC satisfies all of the immersion requirements for a package that is used for the international shipment of radioactive materials.

THIS PAGE INTENTIONALLY LEFT BLANK

2.7.7 Damage Summary

The analysis results reported in Sections 2.7.1 through 2.7.6 are summarized in Tables 2.7.7-1 through 2.7.7-3.

These results indicate that the damage incurred by the NAC-STC during the hypothetical accident is minimal and does not diminish the cask's ability to maintain the containment boundary. A 30-foot drop or a 40-inch pin puncture accident may damage the neutron shield and result in a reduction in the cask's neutron shielding ability. However, the gamma shielding remains intact to provide sufficient shielding to satisfy the accident shielding criteria. (Section 2.7.1.5 discusses the shielding consequences of the drop accidents).

Also, in a 30-foot hypothetical drop accident, the impact limiters may crush to a maximum depth of 31.6 inches, and the lead may slump to a maximum of 1.73 inches. These potential consequences have no adverse structural effects.

Based on the analyses of Sections 2.7 through 2.7.6, the NAC-STC fulfills the structural and shielding requirements of 10 CFR 71 for all of the hypothetical accident conditions.

Table 2.7.7-1 Summary of Maximum Calculated Stresses - 30-Foot Free Drop

30-Foot Drop	Conditions*					Maximum Calculated Stress		Allowable Stress	Margin Of
	1	2	3	4	5	Type	Value (ksi)	(ksi)	Safety
Containment**	✓	✓	✓	✓	✓	P_m	16.4	48.0	+1.9
(on end)	✓	✓	✓	✓	✓	$P_m + P_b$	38.5	69.8	+0.8
Noncontainment***	✓	✓	✓	✓	✓	P_m	12.5	44.9	+2.6
(on end)	✓	✓	✓	✓	✓	$P_m + P_b$	23.1	64.2	+1.8
Containment**	✓	✓	✓	✓	✓	P_m	36.0	49.3	+0.4
(on side)	✓	✓	✓	✓	✓	$P_m + P_b$	49.4	70.9	+0.4
	✓	✓	✓	✓	✓		55.4	65.9	+0.2****
Noncontainment***	✓	✓	✓	✓	✓	P_m	24.8	44.9	+0.8
(on side)	✓	✓	✓	✓	✓	$P_m + P_b$	34.1	64.2	+0.9
	✓	✓	✓	✓	✓		37.4	65.9	+0.8****
Containment**	✓	✓	✓	✓	✓	P_m	34.8	49.3	+0.4
(oblique)	✓	✓	✓	✓	✓	$P_m + P_b$	51.8	69.8	+0.3
Noncontainment***	✓	✓	✓	✓	✓	P_m	24.1	44.9	+0.9
(oblique)	✓	✓	✓	✓	✓	$P_m + P_b$	40.3	64.2	+0.6

* Conditions are:

1. Ambient Temperature (100°F)
2. Insolance (-20°F)
3. Decay Heat
4. Internal Pressure
5. Weight of Contents

** The containment structure includes the inner lid, top forging, inner shell, and bottom inner forging.

*** The noncontainment structure includes the outer lid, the outer shell, the bottom outer forging, and the bottom plate.

**** These stresses correspond to the canistered fuel configuration.

Table 2.7.7-2 Summary of Maximum Calculated Stresses - Puncture

40 Inch Drop	Conditions*					Maximum Calculated Stress		Allowable Stress		Margin Of Safety
	1	2	3	4	5	Type	Value (ksi)	Type	Value (ksi)	
Containment**										
(inner lid)	✓	✓	✓	✓	✓	$P_m + P_b$	12.0	1.0 S_u	66.2	+4.52
Noncontainment***										
(on mid-length)	✓	✓	✓		✓	-	-	-		+0.03****
	✓	✓	✓	✓	✓					
Noncontainment***										
(on bottom center)	✓	✓	✓			$P_m + P_b$	51.3	1.0 S_u	64.2	+0.25
(outer lid center)	✓	✓	✓	✓	✓	$P_m + P_b$	52.0	1.0 S_u	135.0	+1.59

* Conditions
1. Ambient Temperature (100°F)
2. Insolance (-20°F)
3. Decay Heat
4. Internal Pressure
5. Weight of Contents

** The containment structure includes the inner lid, top forging, inner shell, and bottom inner forging.

*** The noncontainment structure includes the outer lid, the outer shell, the bottom outer forging and the bottom plate.

**** Result obtained from the displacement criteria, not from the stress criteria.

Table 2.7.7-3 Summary of Maximum Calculated Stresses - Thermal (Fire) Accident

40 Inch Drop	Conditions*					Maximum Calculated Stress		Allowable Stress		Margin Of
	1	2	3	4	5	Type	Value (ksi)	Type	Value (ksi)	Safety
Containment**										
(top forging)			✓	✓	✓	$P_m + P_b + Q$	228.5	S_{alt}	721.1	+2.15
Noncontainment***										
(outer shell)			✓	✓	✓	$P_m + P_b + Q$	216.2	S_{alt}	721.1	+2.33
Inner Lid Bolts			✓	✓	✓	$P_m + Q$	96.8	S_y	140.9	+0.45
Outer Lid Bolts			✓	✓	✓	$P_m + Q$	83.9	S_y	93.0	+0.11

* Conditions
1. Ambient Temperature (100°F)
2. Insolance (-20°F)
3. Decay Heat
4. Internal Pressure
5. Weight of Contents

** The containment structure includes the inner lid, top forging, inner shell, and bottom inner forging.

*** The noncontainment structure includes the outer lid, the outer shell, the bottom outer forging and the bottom plate.

2.7.8 Directly Loaded Fuel Basket Analysis - Accident Conditions

The hypothetical accident condition analyses of the directly loaded fuel basket are presented in this section. The accident condition analyses of the canistered fuel basket and GTCC waste basket are presented in Sections 2.7.9 and 2.7.10, respectively.

The directly loaded fuel basket for the NAC-STC is designed to contain 26 PWR fuel assemblies, each of which produces a 0.85-kilowatt heat load. The basket structure has a right circular cylinder configuration and consists of 26 square fuel tubes supported by 31 circular support disks, a circular top and bottom plate, which are retained by six threaded rods with spacer nuts. The structural design of the NAC-STC 26 PWR fuel assembly basket is illustrated in Figure 2.7.8-1.

Each fuel tube has an 8.78-inch square inside dimension, a 0.142-inch thick wall, and can hold one intact PWR fuel assembly. The fuel assemblies together with the tubes are laterally supported in square holes in the stainless steel support disks. Each circular support disk is 0.5 inches thick, 70.86 inches in diameter, and has 26 holes that are each 9.234 inches square. There are two different web widths in the support disks. One web width is 1.47 inches between the holes, and the other web width is 3.27 inches between the holes. The top and bottom plates are both 1.0 inch thick and have the same diameter as the support disks. The disks are spaced and retained at 4.87-inch center-to-center intervals by threaded rods and spacer nuts at six locations near the periphery of each disk to form an integral basket assembly. The fuel basket contains the fuel and is enclosed by the inner shell of the cask.

The material of the support disks is 17-4 PH stainless steel. The top plate and the bottom plate are fabricated from Type 304 stainless steel. The 26 square fuel tubes are made from Type 304 stainless steel encasing neutron absorber sheets. The threaded rods and spacer nuts are fabricated from 17-4 PH stainless steel. The fuel tubes are not structural components; and are not considered in the basket evaluation. The primary function of the threaded rods and spacer nuts is to locate and structurally assemble the circular support disks, heat transfer disks, and the top and bottom plates to form an integral assembly. The threaded rods and spacer nuts carry the inertial weight of the support disks heat transfer disks, endplate and their own inertial weight for a 30-foot end drop accident loading condition. The end drop loading condition of the threaded rods and spacer nuts represents classical closed form analysis and they are evaluated independent of

the finite element basket model. The support disks structural evaluation is performed using a finite element model of a single disk. Figure 2.7.8-2 shows a support disk cross-sectional configuration.

The directly loaded fuel basket is evaluated for the normal conditions of transport loads in Section 2.6.12 and is evaluated for the hypothetical accident loads in this section. Both stress analyses and buckling evaluations are performed and documented in the subsequent sections. In addition to structural analysis of the basket components qualified to ASME Code, Section III, Division 1, Subsection NG, "Core Support Structures," an evaluation of the stainless steel/BORAL composite fuel tube has been performed for a postulated impact load.

Figure 2.7.8-1 NAC-STC Directly Loaded 26 PWR Fuel Assembly Basket

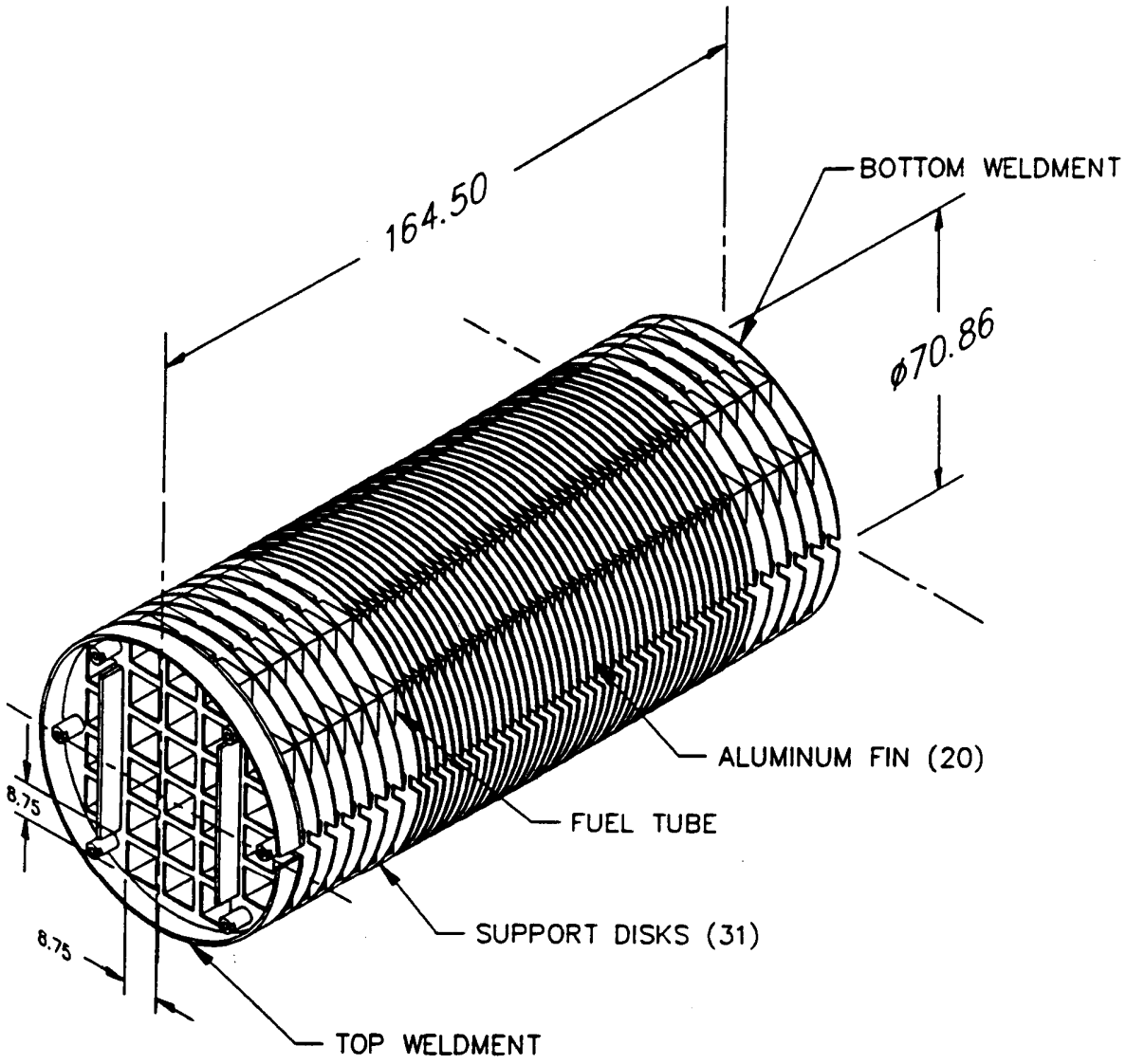

Figure 2.7.8-2 Support Disk Cross-Sectional Configuration for Directly Loaded Fuel Configuration

FIGURE WITHHELD UNDER 10 CFR 2.390

2.7.8.1 Stress Evaluation of Support Disk - Directly Loaded Fuel Configuration

To determine the structural adequacy of the support disks in the 26 PWR fuel assembly basket, the drop accident impact load is evaluated for all cask orientations. The drop accident impact load is analyzed for a 30-foot side drop and a 30-foot end drop and conservatively combined using the square root sum of the squares of the resultant maximum nodal stress intensity values to assure all included orientations are enveloped. A quasi-static impact load equal to the weight of the fuel and tubes multiplied by a 55 g amplification factor is applied to the support disk structure to simulate the side drop accident condition. However, since the support disk does not carry load from the fuel assemblies in the vertical direction, analysis of the 30-foot end drop is limited to consideration of the 56.1 g out-of-plane inertial load from the mass of a single support disk. The 55 g and 56.1 g amplification factors are design values which envelope the calculated deceleration values in Section 2.6.7.4 for a 30-foot drop accident condition. For the side drop condition, the fuel assembly loads are transmitted in direct compression through the tube wall to the web structure of each support disk. These loads are transmitted to the inner shell of the cask by the 31 support disks, the top plate and the bottom plate.

The weights of the PWR fuel assemblies and the basket structure (the support disks and fuel tubes) are applied as a 55 g impact load to simulate a side drop accident scenario for the basket assembly. The value of 55 g for the impact loading is the NAC-STC design deceleration force for a 30-foot side drop accident condition. The support disk configuration (Figure 2.7.8-2) is analyzed for nine drop orientations: 0, 15, 30, 37, 45, 60, 64, 75, and 90 degrees, to bound the possible maximum stress cases. The drop orientations are identified in Figure 2.7.8.1-1. As shown in Figure 2.7.8.1-1 drop orientation, 37 degrees and 64 degrees respectively put each of the support disk ligaments in direct impact.

A finite element analysis is performed, utilizing the ANSYS computer code, to calculate the stresses in a support disk. In accordance with ASME Code, Section III, Subsection NG criteria, the maximum primary stress intensity calculated in the support disk is compared to the allowable stress limit, $0.7S_u$, where S_u is conservatively defined for this analysis evaluation as the material

ultimate strength at a maximum temperature of 600°F. The maximum temperature in the basket support disk is 498°F (Table 3.4-1). Analyses are conservatively performed by calculating the total primary stress intensity at a node point for combined membrane and bending and then employing the 0.7 S_u allowable at 600°F. This enveloping method is conservative since further stress classification dictates that the membrane stress, P_m and the primary membrane plus primary bending stress, $P_m + P_b$ is lower than the total calculated maximum stress intensity, SI, at a node point. The margin of safety is conservatively obtained by evaluating the allowable for the smaller primary membrane stress, 0.7 S_u relative to the total combined primary membrane plus bending stress intensity at a single node. According to the ASME Code, Section III, Division 1, Subsection NG, the allowable for membrane plus bending stress ($P_m + P_b$) is S_u. Using this conservative enveloping methodology to evaluate the fuel basket structural integrity results in large margins of safety. These results document that the fuel basket does not yield under any imposed design load.

2.7.8.1.1 Finite Element Model Description

Two types of finite element analyses were performed for the NAC-STC 26 PWR basket support disk evaluations for hypothetical accident conditions: one for the 30-foot side drop impact condition; and a second for the evaluation of the 30-foot end drop impact condition.

The temperature distribution on the support disk is determined in a separate thermal analysis which uses a three-dimensional finite element model representing one-quarter of the cask. The thermal analysis model is documented in detail in Section 3.4.

The finite element model for the 30-foot side drop impact analysis has the same mesh arrangement and element types as that of the finite element model used for the 1-foot side drop analysis shown in Figure 2.6.12.2-2. The stiffness of the gap elements is 1.0E+6 pounds/inch, as discussed in Section 2.6.12.2.

The finite element model for the 30-foot end drop impact analysis has the same mesh arrangement and element type as that of the finite element model used for

the 1-foot end drop analyses shown in Figure 2.6.12.2-1. The end drop inertial loading is applied in the cask longitudinal direction (lateral to the plane of the support disks). The support disks are separated by spacer nuts on threaded rods at six locations near the periphery of the disks. Displacement restraints are applied at the nodes on the support disk model where the six threaded rods are located.

2.7.8.1.2 Impact Loading Conditions

The lateral impact load applied on the support disk for a side drop accident, includes the inertial weights of the fuel assemblies, the stainless steel tubes, one aluminum heat transfer disk, and the support disk itself. The loads are amplified to account for the side drop impact, a 55 g load factor is used to amplify the weight of the basket components. The load corresponding to the support disk weight is included as the inertial loading resulting from a 55 g acceleration for both the 30-foot side drop and the 30-foot end drop accident conditions.

Each fuel assembly is conservatively assumed to weigh 1525 pounds and is 159.20 inches long. The stainless steel fuel tube has an 8.78-inch square inside dimension and a 9.064-inch square outside dimension. The load at each support disk hole is calculated in Section 2.7.8.1.3.1.

The amplified load from the fuel and the fuel tubes is uniformly applied in the plane of the support disk at the bottom of each hole for the 0-degree and the 90-degree drop orientations. For the other side drop orientations, the load is distributed along the two lower sides of each hole. The mass of the aluminum heat transfer fin is lumped equally at each of the threaded rod locations.

2.7.8.1.2.1 Side Drop Analysis Results

Finite element stress analyses are performed for the 55 g side impact load cases for nine different impact orientations--0, 15, 30, 37, 45, 60, 64, 75, and 90 degrees, as shown in Figure 2.7.8.1-1. The stress evaluations are performed in accordance with the ASME Code, Section III, Division 1, Subsection NG.

The locations of the 20 highest nodal SI stresses in the support disk for each of the nine side impact orientations evaluated are shown in Figures 2.7.8.1-2 through 2.7.8.1-10. Tables 2.7.8.1-1 through 2.7.8.1-9, respectively, provide tabulations of the nodal SI stresses at the 20 locations of maximum stress in the support disk for each of the nine side impact orientations. The tables also show the margin of safety for each analysis location for the 55 g side impact load condition. Table 2.7.8.1-10 presents a summary of the maximum stress locations and margins of safety for the 55 g side impact analysis for the nine impact orientations.

The conservative stress limit chosen for this evaluation of the support disk is 0.7 S_u. The material ultimate strength value is taken at the enveloping temperature of 600°F. Then the allowable stress intensity becomes (0.7)(126.7) = 88.7 ksi.

The total impact loading applied to the finite element model of the support disk is verified in Section 2.7.8.1.3.3 by comparing the reaction forces calculated by ANSYS to those calculated by classical methods. The analysis in Section 2.7.8.1.3.4 evaluates the effect of the stress concentration at the threaded rod holes in the support disk. The minimum margin of safety calculated for the maximum nodal SI stress with a stress concentration factor of 3.0 applied at the threaded rod hole location in the support disk is +3.9, using the stresses resulting from the 55-g side impact load case.

The minimum calculated margin of safety in the support disk of the NAC-STC 26 PWR basket is +0.8 for the 30-degree drop orientation at node number 565 (Figure 2.7.8.1-4) for the 55 g side impact load condition. In addition to the ASME Code, Subsection NG criteria adopted as the design code for the fuel basket, it is noted that the yield strength of 17-4 PH stainless steel at the bounding temperature of 500°F (Table 3.4-1) is 87.0 ksi and, therefore, for the highest impact stress of 50.6 ksi, the basket will not yield. Therefore, the support disks in the NAC-STC 26 PWR fuel basket are structurally adequate for a 55 g side impact load condition.

2.7.8.1.2.2 End Drop Analysis Results

The support disks of the NAC-STC fuel basket are spaced by threaded rods and spacer nuts positioned at six locations near the periphery of each disk. An ANSYS structural analysis is performed to evaluate the effect of a 30-foot end drop impact (out-of-plane loading) on the support disks in the NAC-STC with the cask in the vertical position. The ANSYS eight-node brick element (STIF45) is used in the model as shown in Figure 2.7.8.1-11. The end drop impact loading is applied in the cask longitudinal direction (perpendicular to the plane of the support disk). A load factor of 56.1 g is applied to the mass of the support disk. The value of 56.1 g is the maximum deceleration of the NAC-STC for a 30-foot end drop impact (Table 2.6.7.4-2). Displacement restraints are applied in the ANSYS model at the nodes where the six threaded rods with spacer nuts are located.

Table 2.7.8.1-11 presents a summary of the 20 highest nodal stress intensity results in the support disk for the 30 foot end drop load. Figure 2.7.8.1-12 presents the location of these 20 nodes. The minimum margin of safety is +1.6 for the maximum stress of 36.2 ksi, when evaluated with respect to the conservative NG criteria of 0.7 S_u, where S_u is defined at the node temperature for steady state design basis heat load.

As stated in Section 2.7.8.1, the maximum nodal stress intensity for the side drop, 50.6 ksi at 30 degrees, is combined with the maximum nodal stress intensity for the end drop (36.2 ksi) using the square root sum of the squares assuring a conservative envelope of the stress in the basket support disk under any drop orientation. Using this methodology, the conservative envelope of stress intensity is 62.2 ksi, which is less than the allowable of 0.7 S_u and the material yield strength. Yield strength of 17-4 PH stainless steel at the basket bounding temperature of 500°F (Table 3.4-1) is 87.0 ksi. Therefore, under end drop accident conditions, the fuel basket support disks do not yield and demonstrate significant margin of safety.

2.7.8.1.2.3 Support Disk Web Stresses for a 30-Foot Side Drop Condition

The support disk is analyzed for nine drop orientations in Section 2.7.8.1.2.1. The 20 maximum stress intensities for each drop orientation are listed in Tables 2.7.8.1-1 through 2.7.8.1-9. In this section, a supplementary detailed stress evaluation of the support disk webs is presented for the same drop orientations summarized in Section 2.7.8.1.2.1.

The locations of the nodal stresses in the support disk webs for each of the nine 1-foot side impact orientations evaluated are shown in Figure 2.7.8.1-13. Tables 2.7.8.1-12 through 2.7.8.1-20 provide tabulations of the nodal stress intensities at the defined node locations on the web for each of the nine impact orientations. The tables also show the margin of safety for each analysis location for the 55 g side impact load condition. The minimum margin of safety for this summarized node stress intensity relative to 0.7 S_u at 600°F for the support disk web of the NAC-STC PWR basket for a 30-foot side drop is +2.8 for the 90-degree drop orientation. This margin of safety is greater than the evaluation of maximum stress in the support disk presented in Section 2.7.8.1.2.1 and continues to demonstrate the significant structural integrity of the NAC-STC fuel basket.

2.7.8.1.2.4 Support Disk Shear Stresses for a 30-Foot Side Drop and a 30-Foot End Drop Condition

The maximum stress intensity for the 30-foot side drop is reported in Table 2.7.8.1-3 as 50.58 ksi, (30° drop orientation). Similarly, the maximum stress intensity for the 30-foot end drop is also reported in Table 2.7.8.1-11 as 36.20 ksi. Therefore, the maximum enveloping shear stress anywhere in the basket support disk is 50.58/2 = 25.29 ksi.

According to the ASME Code, Section III, Division 1, Subsection NG, "Core Support Structures," the allowable hypothetical accident loading shear stress is 0.42 S_u. The ultimate stress S_u for 17-4 PH at the bounding operating temperature of 600°F is 126.7 ksi.

Minimum margin of safety for shear is

$$\text{M.S.} = \frac{(2)(0.42 S_u)}{SI} - 1$$
$$= \frac{(2)(0.42)(126.7)}{50.58} - 1 = +1.1$$

Therefore, the structural adequacy of the NAC-STC fuel basket support disk design for the normal conditions of transport 30-foot side drop and 30-foot end drop is demonstrated.

2.7.8.1.3 Supplemental Data - Support Disk Analysis

2.7.8.1.3.1 Calculation of Pressure Loading

The impact pressure loadings on the 26 PWR fuel assembly basket in the side drop condition is calculated based on a fuel assembly weight of 1,525 lbs. This weight is conservative with respect to the maximum weight of 1,500 lbs, shown in Table 2.2.0-1.

The weight per unit length (W/L) of the fuel assembly is:

I = Length of fuel = 159.20 in
W = Weight of one fuel assembly = 1525 lb
W/L = Unit weight = 1525/159.20 = 9.579 lb/in

The weight (W_c) of the tube per linear inch is:

W_{tube} = 141 lb
L_{tube} = 154.7 in
$$W_c = \frac{141}{154.7}$$
= 0.911 lb/in

The fuel assembly plus tube weight per linear inch is:

9.579 + 0.911 = 10.490 lb/in

Distributing the combined weight as a pressure load considering a 4.88-inch spacing between two adjacent support disks and a 55-g load factor:

$$P = \frac{(10.490)(4.88)(55)}{(9.234)(0.5)} = 609.8 \text{ psi}$$

For the 0-degree drop use:

$$P_x = 609.8 \text{ psi}$$

For a 90-degree drop use:

$$P_y = 609.8 \text{ psi}$$

For a q-degree drop use:

$$P_x = (609.8)(\text{Cos } q)$$

$$P_y = (609.8)(\text{Sin } q)$$

2.7.8.1.3.2 Calculation of Lump Masses of the Aluminum Heat Transfer Disk and the Six Threaded Rods and Spacers

The masses of the aluminum heat transfer disk and the six threaded rods and spacer nuts are lumped into the finite element model at the threaded rod locations on the support disk for both the 18.1 g and 55 g side drop analyses. The lump masses applied to the model through ANSYS pointwise generalized mass element (STIF21) is 0.0613 pounds mass.

2.7.8.1.3.3 Verification of Impact Load Applied on the ANSYS Model

The total impact pressure applied on the model is verified by comparing the reaction forces from the ANSYS results versus the hand-calculated method. The 90-degree side drop evaluation is used as an example.

From the ANSYS result, the total reaction force per disk is: F_y = 94,520 lb

Therefore, total weight = 94,520/55 = 1718.55 lb.

This load is verified by the classical-calculation method as described below:

Weight of each support disk = 245.19 lb

Weight of aluminum heat transfer disk
and six threaded rods per support disk = 142.074 lb

Weight of 26 "fuel assemblies plus tubes" = (26)(4.88)(10.49)
= 1330.97 lb/support disk

Total weight = 245.19 + 1330.97 + 142.074 = 1718.234 lb

Total load = 1718.234 lb

The difference between the classical-calculation total load (1718 lb) and the ANSYS total load of 1718.6 pounds is negligible (0.034%).

2.7.8.1.3.4 Evaluation of Stress Concentration at the Threaded Rod Hole Areas in the Support Disks

There are six holes near the periphery of each support disk for the installation of the threaded rods and spacer nuts. The stress concentration effect at these areas is evaluated.

From the ANSYS stress results for the 55-g side impact load condition, the nodal stresses (SI) at the threaded rod hole areas for different loading conditions are listed below.

Nodal SI Stresses (psi)
(55-g Side Impact)

Node[1] Temp	**65**	**374**	**732**	**1041**	**1708**	**2375**
$0.7S_u$[2]	**376**	**405**	**376**	**405**	**405**	**405**
Orientation	**92.58**	**91.88**	**92.58**	**91.88**	**91.88**	**91.88**
0	6.3	3.2	1.4	1.3	3.2	1.3
15	5.9	3.9	1.3	1.7	3.8	1.2
30	5.4	3.8	1.3	2.1	4.3	1.4
37	5.1	3.7	1.3	2.4	4.6	1.7
45	4.6	3.6	1.3	2.6	5.0	2.0
60	3.5	3.0	1.2	2.8	5.6	2.5
64	3.2	2.7	1.2	2.8	5.7	2.6
75	2.2	1.7	1.2	2.5	6.1	2.5
90	1.2	1.4	1.2	1.4	4.7	4.7
Max SI	6.3	3.9	1.4	2.8	6.1	4.7
MS[3]	2.7	4.9	15.5	7.2	2.8	3.9

[1] Node numbers in the finite element model at the threaded rod hole location.

[2] S_u is the ultimate strength of 17-4 PH stainless steel.

[3] Margin of Safety, MS is calculated with respect to 1/3 of the allowable strength to account for stress concentration factor around the holes.

Considering a stress concentration factor of 4.0, the minimum margin of safety for the threaded rod hole areas is +2.7, and occurs at the threaded rod located on node 65 for the 0-degree side drop orientation.

Figure 2.7.8.1-1 Support Disk Drop Orientations

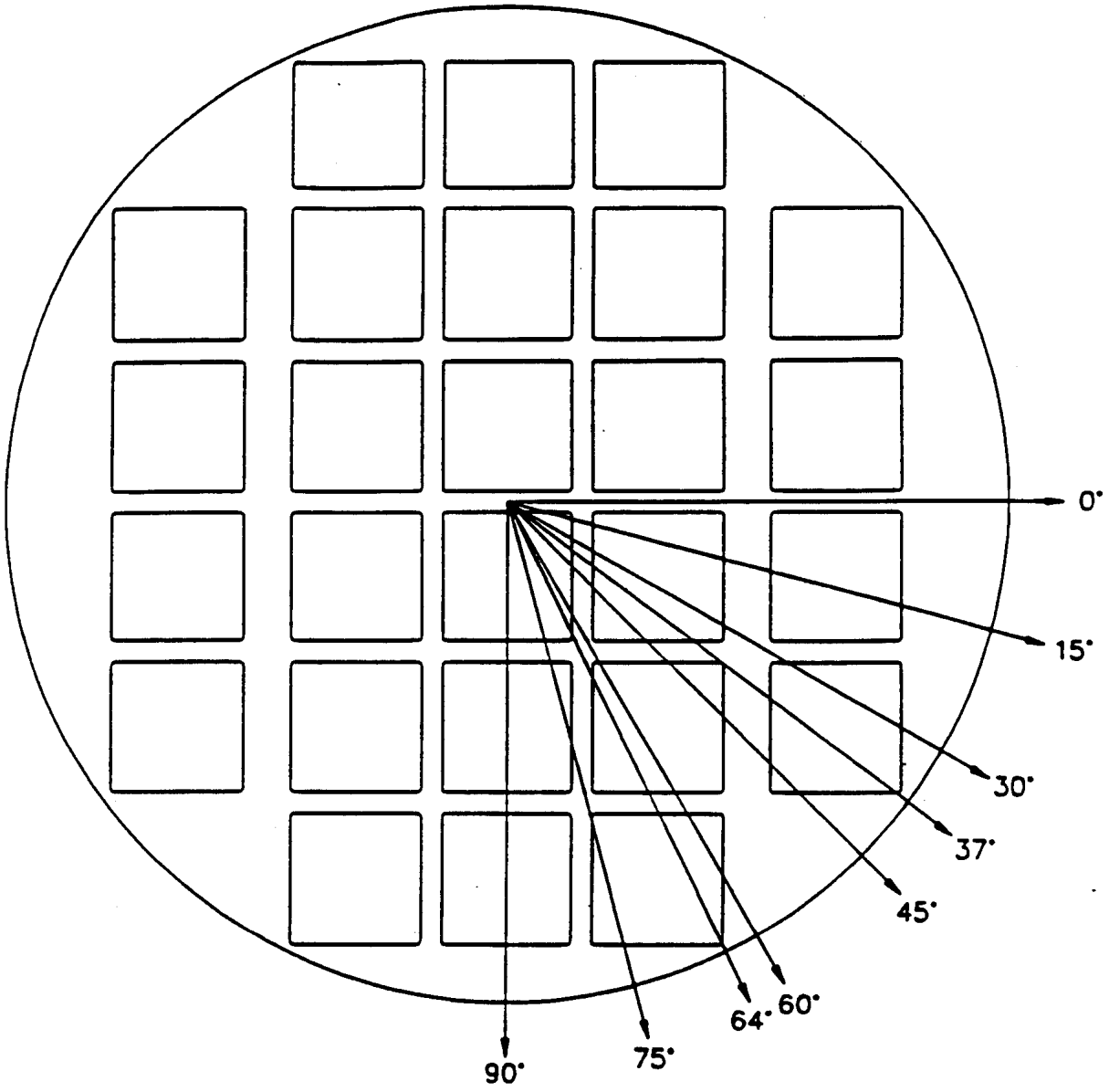

Figure 2.7.8.1-2 Locations of 20 Maximum Nodal SI Stresses - 55-g Side Drop Impact (0° Drop Orientation)

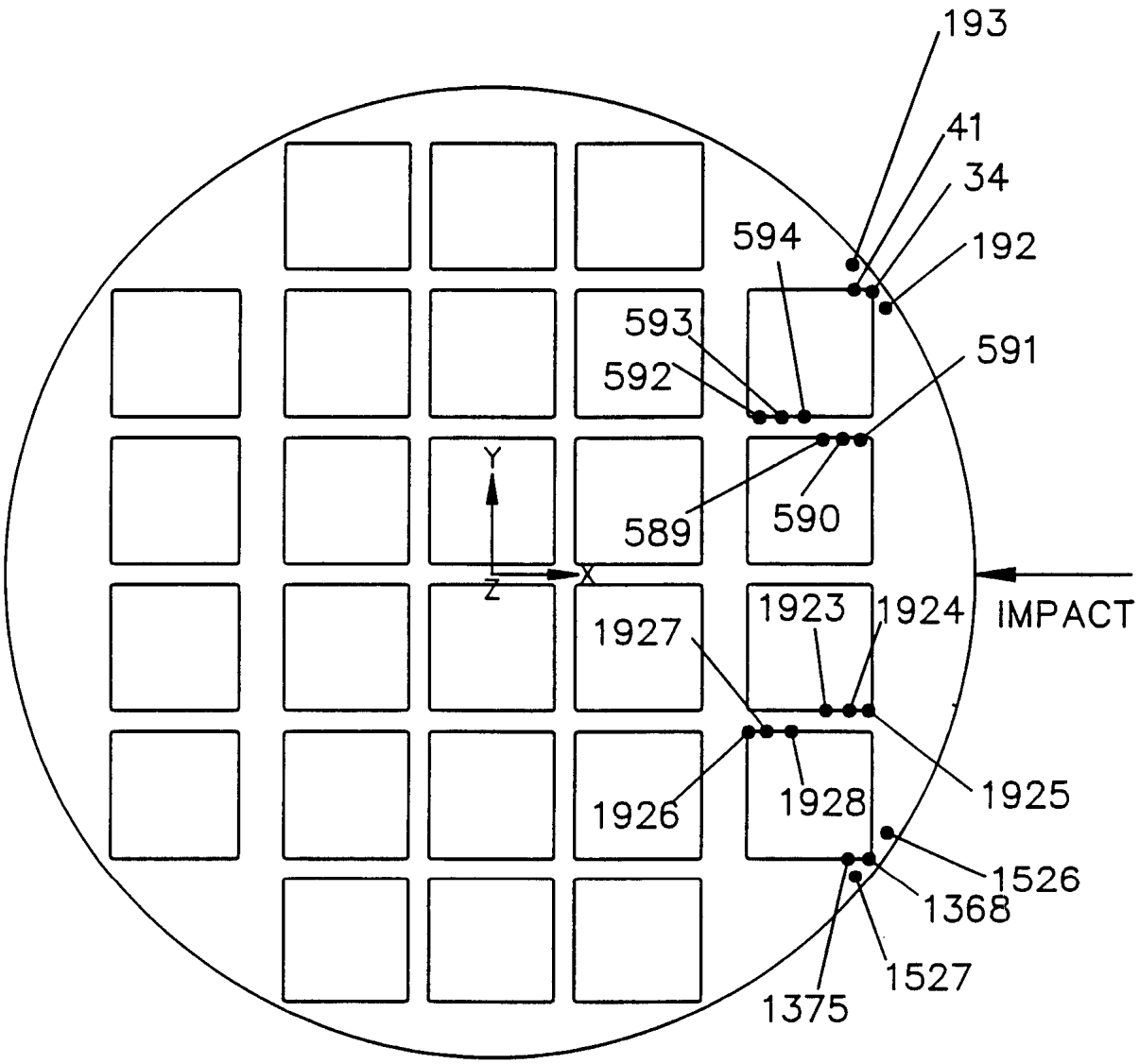

Figure 2.7.8.1-3 Locations of 20 Maximum Nodal SI Stresses - 55-g Side Drop Impact (15° Drop Orientation)

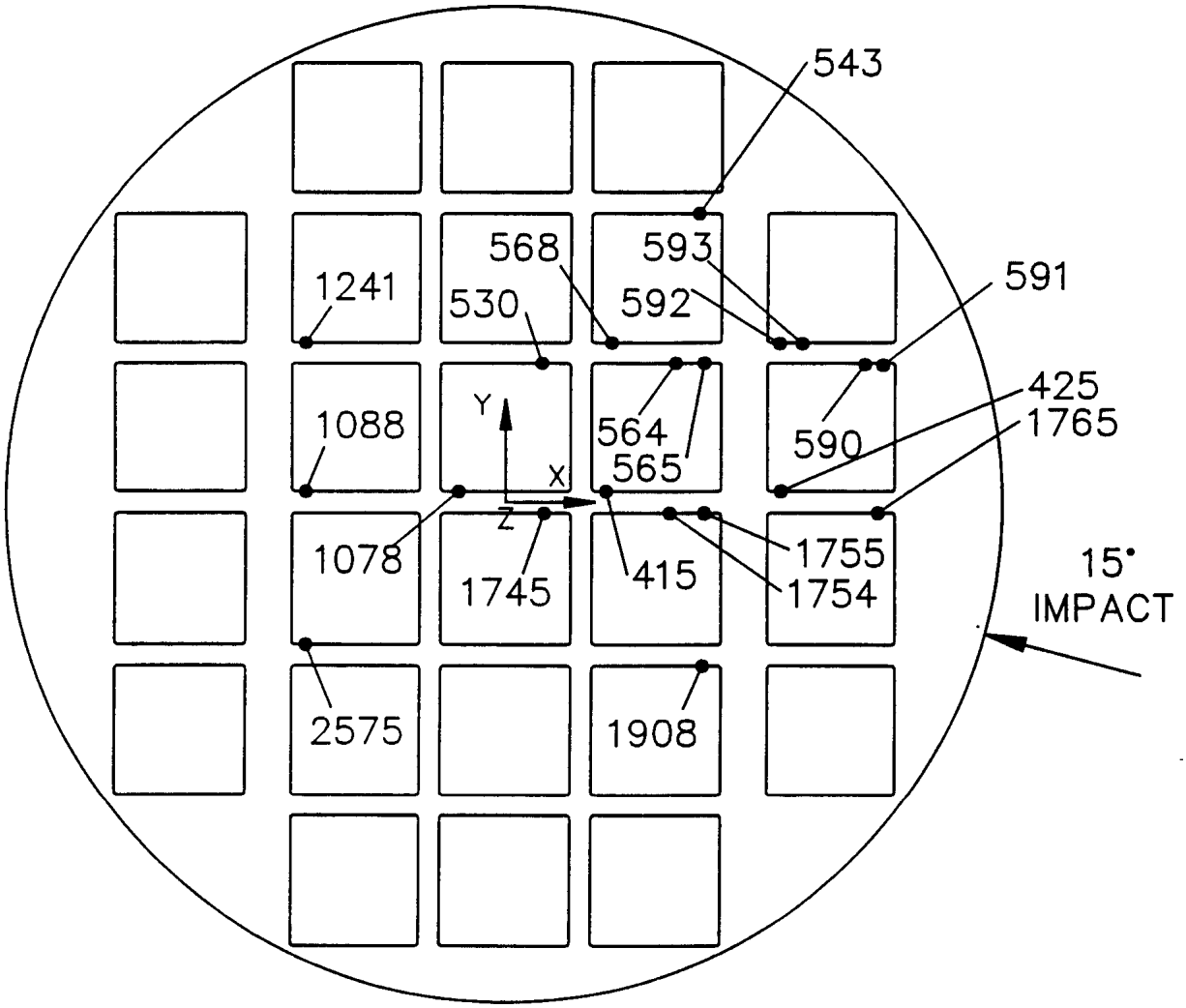

Figure 2.7.8.1-4 Locations of 20 Maximum Nodal SI Stresses - 55-g Side Drop Impact (30° Drop Orientation)

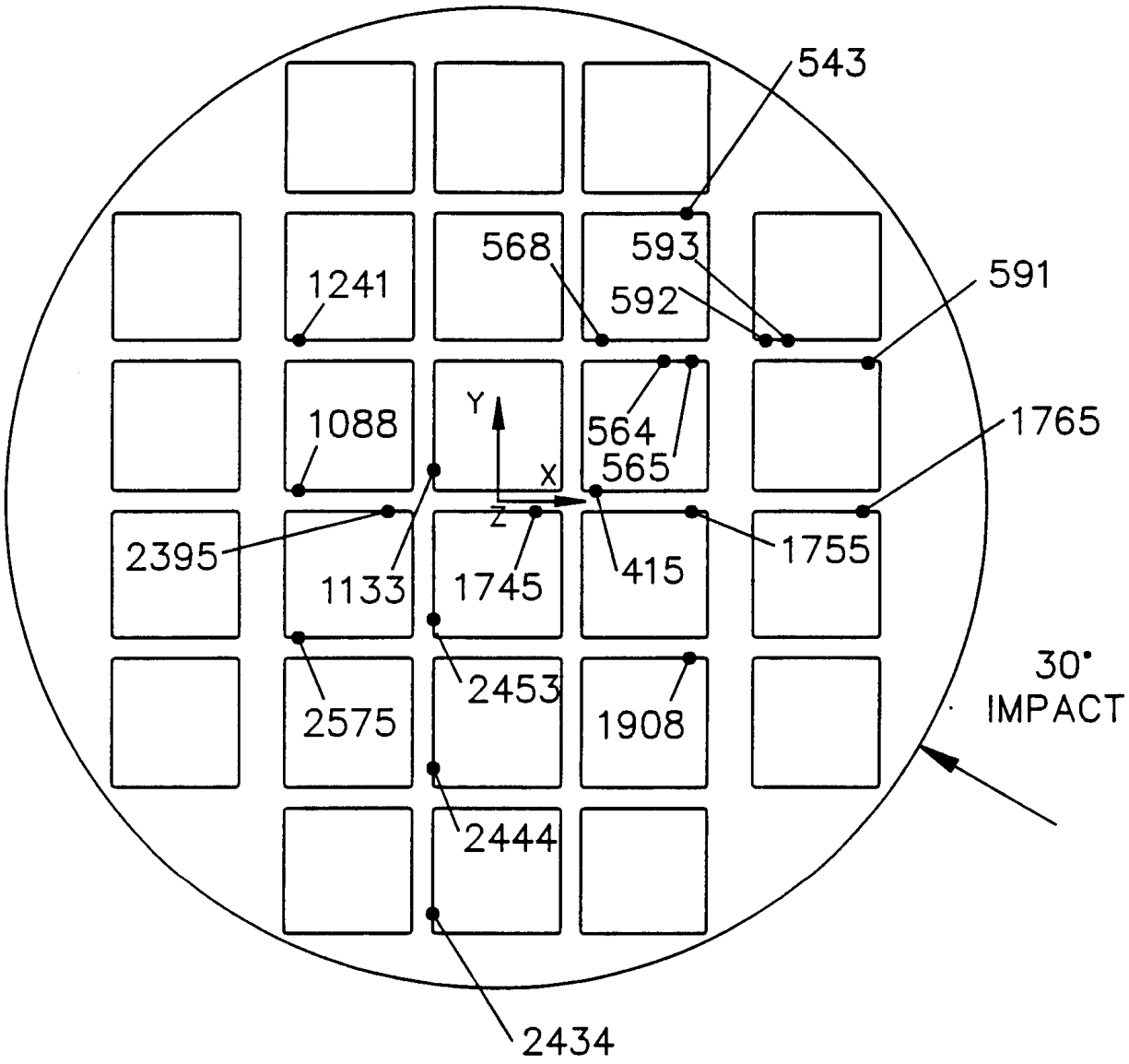

Figure 2.7.8.1-5 Locations of 20 Maximum Nodal SI Stresses - 55-g Side Drop Impact (37° Drop Orientation)

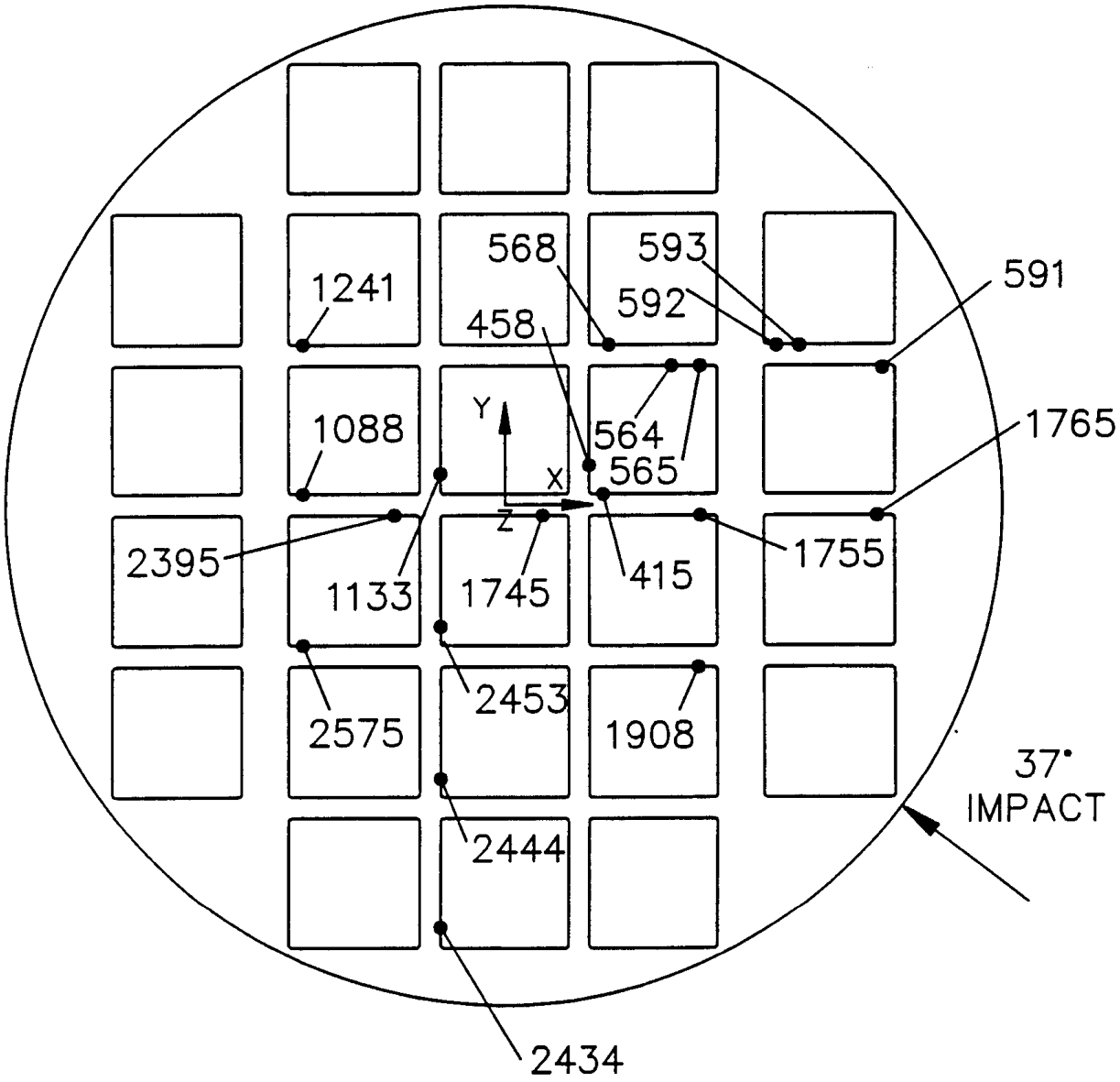

Figure 2.7.8.1-6 Locations of 20 Maximum Nodal SI Stresses - 55-g Side Drop Impact (45° Drop Orientation)

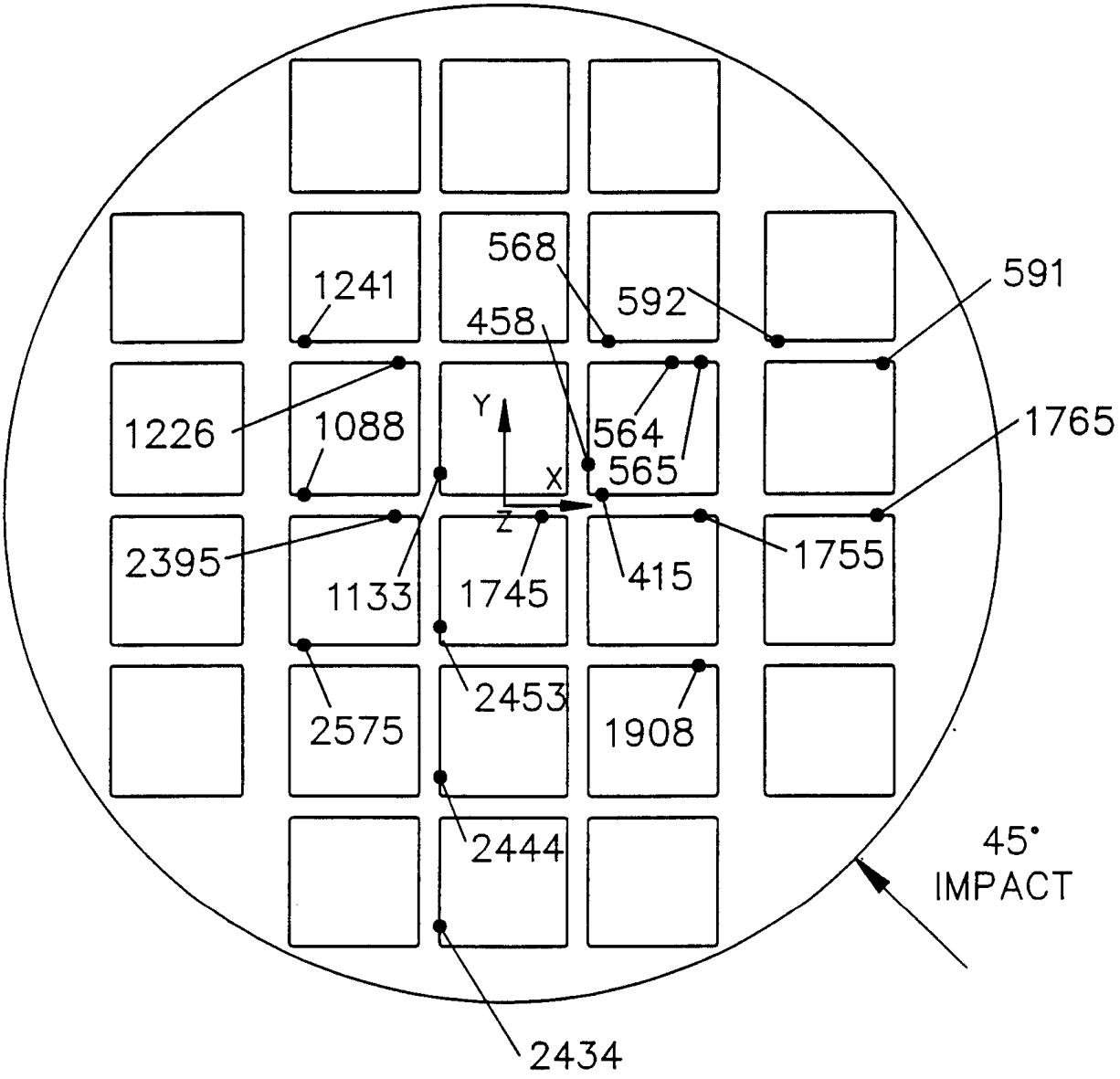

Figure 2.7.8.1-7 Locations of 20 Maximum Nodal Stresses - 55-g Side Drop Impact (60° Drop Orientation)

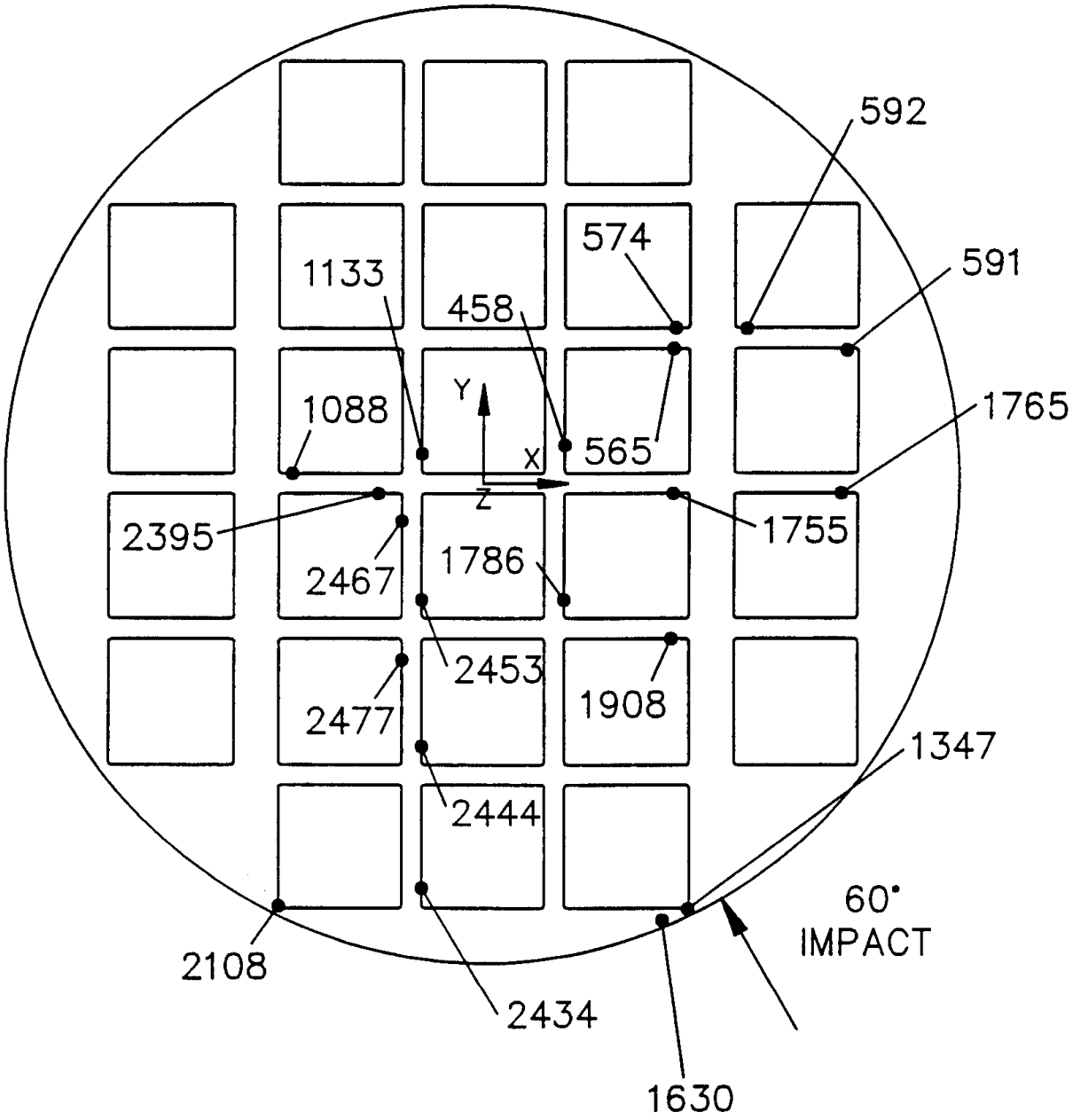

Figure 2.7.8.1-8 Locations of 20 Maximum Nodal SI Stresses - 55-g Side Drop Impact (64° Drop Orientation)

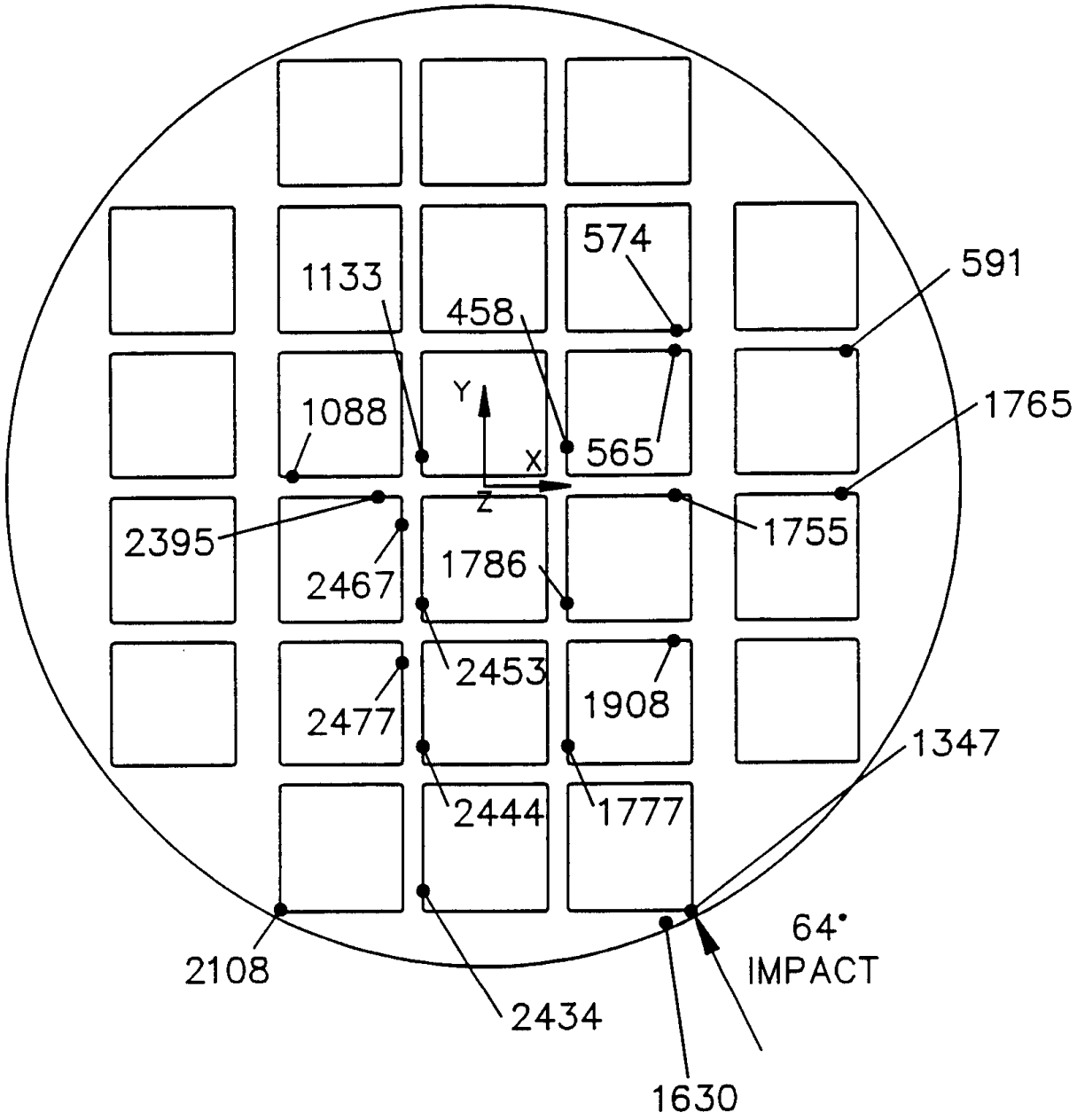

Figure 2.7.8.1-9 Locations of 20 Maximum Nodal SI Stresses - 55-g Side Drop Impact (75° Drop Orientation)

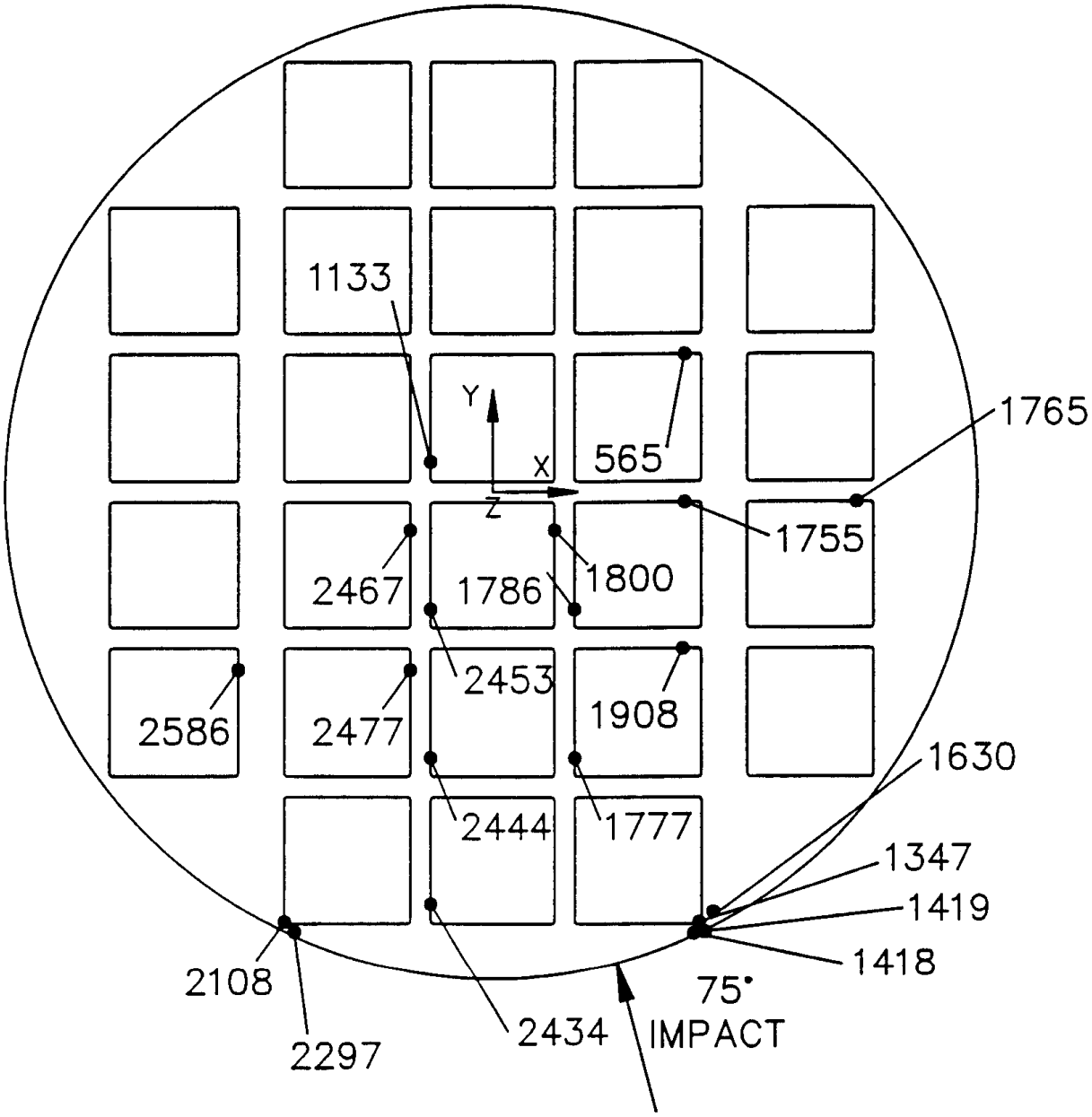

Figure 2.7.8.1-10 Locations of 20 Maximum Nodal SI Stresses - 55-g Side Drop Impact (90° Drop Orientation)

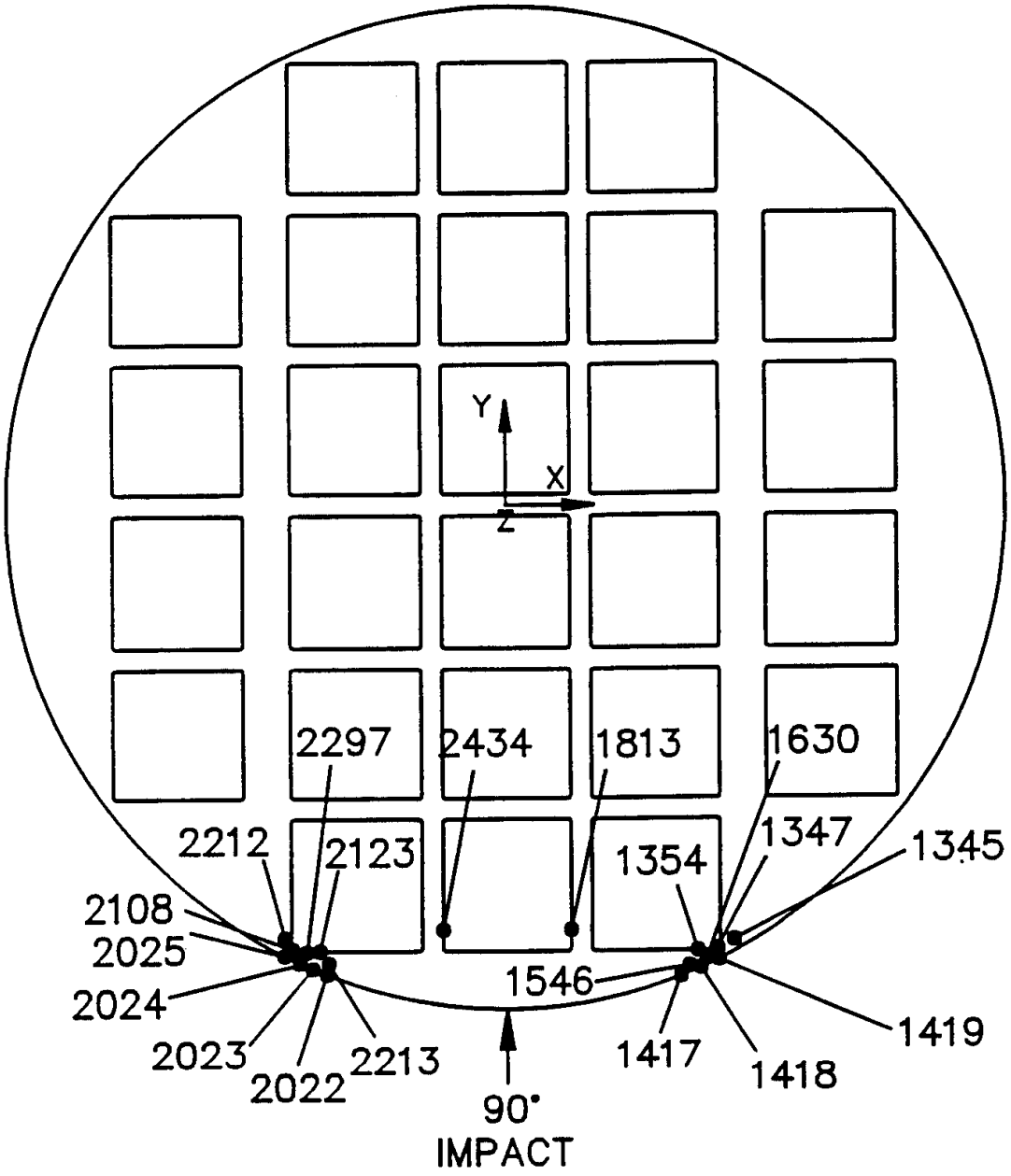

Figure 2.7.8.1-11 Finite Element Model for the Basket Support Disk End Drop

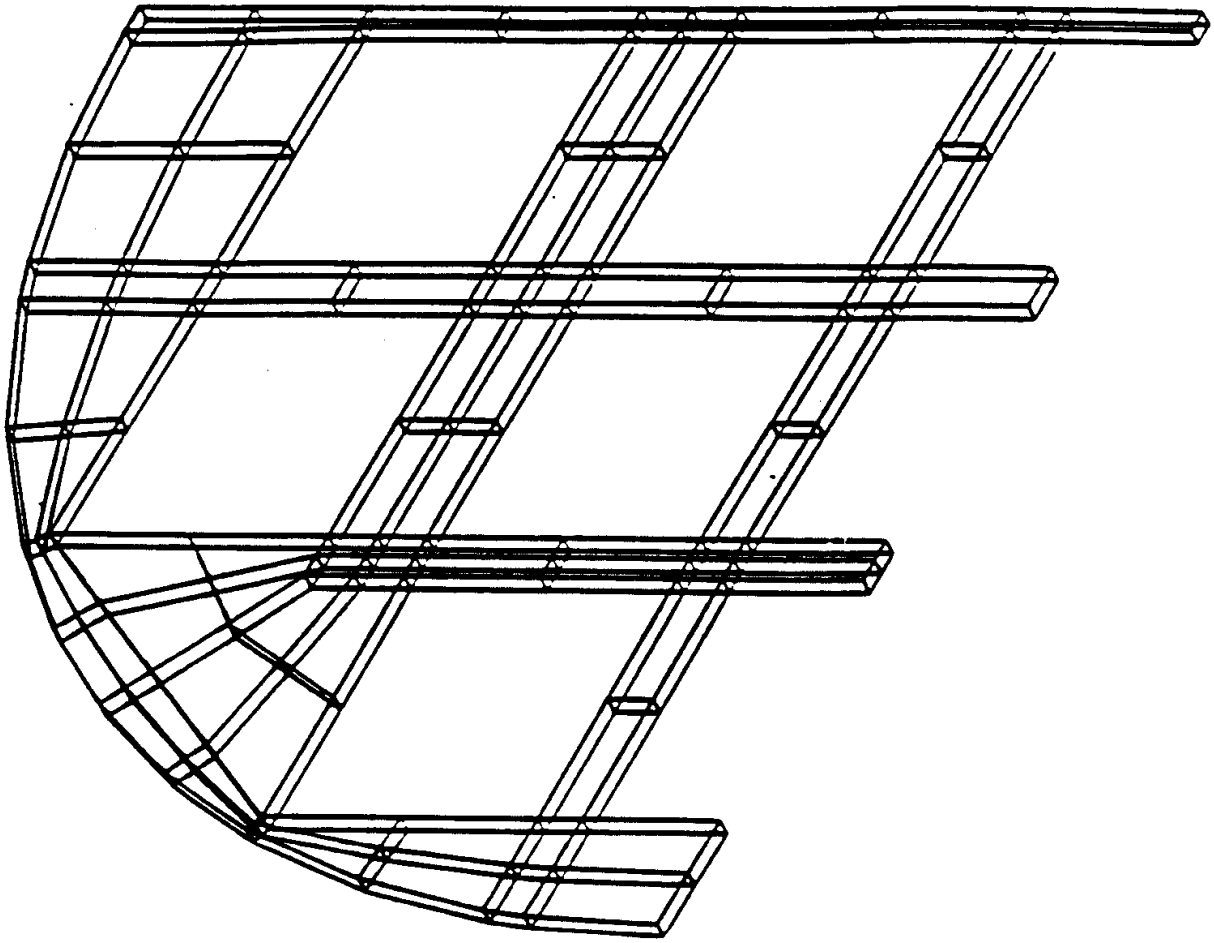

Figure 2.7.8.1-12 Locations of the 20 Maximum Nodal SI Stresses - 56.1-g End Drop

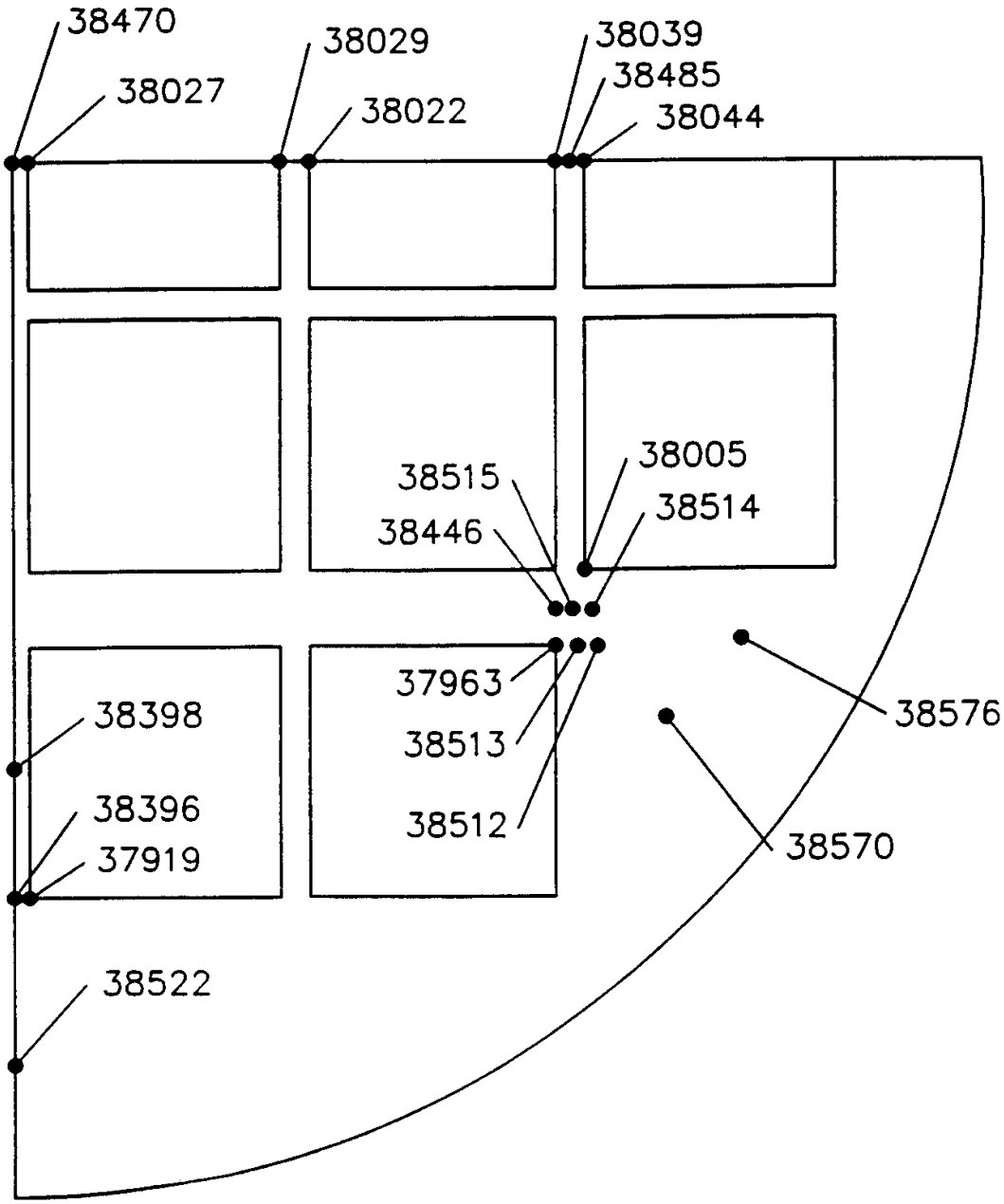

Figure 2.7.8.1-13 Node Point Locations for Basket Web Stress Summaries

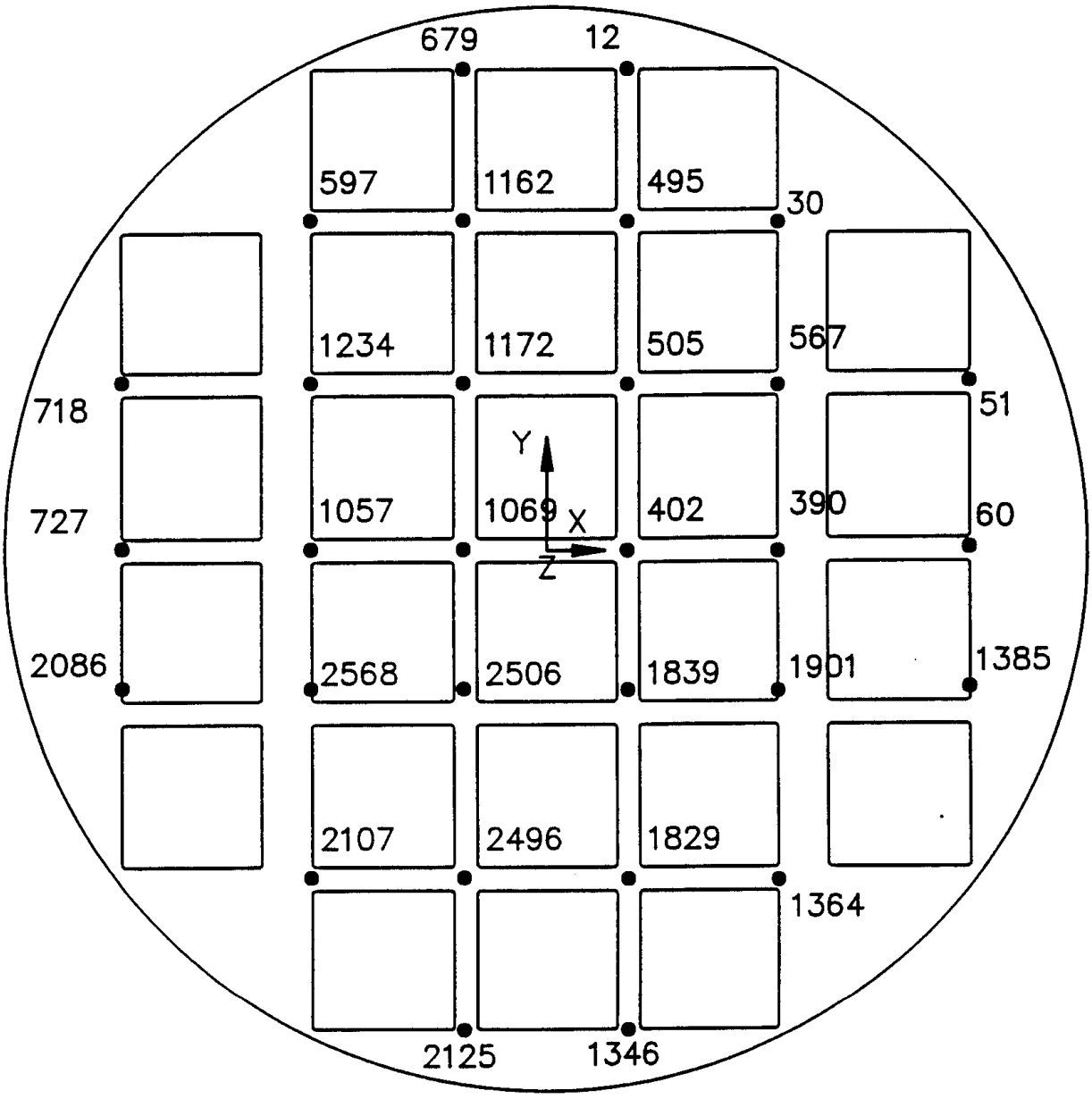

Table 2.7.8.1-1 Basket 55-g Side Impact Stresses for 0-Degree Drop Orientation

Node No.[1]	S_x (ksi)	S_y (ksi)	S_z (ksi)	S_{xy} (ksi)	SI (ksi)	MS[2]
1368	-18.9	-18.2	0.0	-11.2	31.7	1.8
34	-18.9	-18.2	0.0	11.2	31.7	1.8
591	-29.2	0.9	0.0	1.1	30.3	1.9
1925	-29.2	0.9	0.0	-1.1	30.2	1.9
592	-29.5	0.5	0.0	1.1	30.2	1.9
1926	-29.5	0.5	0.0	-1.1	30.2	1.9
593	-25.4	0.2	0.0	0.2	25.6	2.5
1927	-25.4	0.2	0.0	-0.2	25.6	2.5
590	-25.3	0.2	0.0	0.2	25.5	2.5
1924	-25.3	0.2	0.0	-0.2	25.5	2.5
1527	-18.3	-12.9	0.0	-7.4	25.2	2.5
193	-18.3	-12.9	0.0	7.4	25.2	2.5
594	-24.2	-0.1	0.0	0.5	24.2	2.7
1928	-24.2	-0.1	0.0	-0.5	24.2	2.7
589	-24.1	-0.1	0.0	0.5	24.2	2.7
1923	-24.1	-0.1	0.0	-0.5	24.2	2.7
1526	-9.7	-16.0	0.0	-9.2	24.1	2.7
192	-9.7	-16.0	0.0	9.2	24.1	2.7
1375	-21.0	-5.0	-0.0	-6.9	23.9	2.7
41	-21.0	-5.0	0.0	6.9	23.9	2.7

1 Stress components are listed for the nodes with the 20 highest impact nodal point stress intensity values (see Figure 2.7.8.1-2 for locations of these nodes). Note that S_x is the stress in the radial direction, S_y is the stress in the circumferential direction and S_{xy} is the shearing stress.

2 The allowable stress is 0.7 S_u. S_u is the ultimate strength of 17-4 PH stainless steel at a bounding 600°F, S_u = 126.7 ksi.

Table 2.7.8.1-2 Basket 55-g Side Impact Stresses for 15-Degree Drop Orientation

Node No.[1]	S_x (ksi)	S_y (ksi)	S_z (ksi)	S_{xy} (ksi)	SI (ksi)	MS[2]
565	-48.4	0.8	0.0	2.6	49.5	0.8
1755	-44.0	0.6	0.0	2.3	44.9	1.0
591	-42.6	1.4	0.0	2.3	44.3	1.0
592	-40.1	1.1	0.0	1.6	41.4	1.1
568	-36.2	2.4	0.0	2.0	38.9	1.3
1908	-37.8	0.6	0.0	2.0	38.6	1.3
1088	-36.1	1.5	0.0	1.7	37.7	1.3
415	-35.0	2.3	0.0	1.8	37.5	1.4
1241	-35.7	1.6	0.0	1.7	37.5	1.4
564	-36.8	-0.3	0.0	2.2	37.2	1.4
1765	-35.0	1.1	0.0	1.7	36.3	1.4
2575	-32.6	1.6	0.0	1.5	34.3	1.6
1754	-33.8	-0.1	0.0	1.7	34.1	1.6
543	-31.6	1.9	0.0	2.2	33.8	1.6
593	-33.5	0.0	0.0	0.8	33.7	1.6
1745	-32.5	0.9	0.0	1.8	33.6	1.6
590	-33.1	0.0	0.0	1.3	33.4	1.6
425	-32.2	0.7	0.0	1.1	33.1	1.7
1078	-29.9	2.5	0.0	1.4	32.6	1.7
530	-31.1	1.1	0.0	1.9	32.4	1.7

1 Stress components are listed for the nodes with the 20 highest impact nodal point stress intensity values (see Figure 2.7.8.1-3 for locations of these nodes). Note that S_x is the stress in the radial direction, S_y is the stress in the circumferential direction and S_{xy} is the shearing stress.

2 The allowable stress is 0.7 S_u. S_u is the ultimate strength of 17-4 PH stainless steel at a bounding 600°F, S_u = 126.7 ksi.

Table 2.7.8.1-3 Basket 55-g Side Impact Stresses for 30-Degree Drop Orientation

Node No.[1]	S_x (ksi)	S_y (ksi)	S_z (ksi)	S_{xy} (ksi)	SI (ksi)	MS[2]
565	-49.1	1.2	0.0	3.0	50.6	0.8
1755	-44.7	1.0	0.0	2.8	46.0	0.9
591	-44.0	1.5	0.0	2.8	45.9	0.9
592	-39.4	1.0	0.0	1.3	40.6	1.2
1908	-37.9	1.0	0.0	2.4	39.1	1.3
1765	-36.0	1.2	0.0	2.2	37.5	1.4
568	-34.7	2.3	0.0	1.7	37.2	1.4
1088	-35.6	1.5	0.0	1.4	37.2	1.4
1241	-34.8	1.4	0.0	1.4	36.4	1.4
564	-35.8	-0.5	0.0	2.5	36.3	1.4
415	-33.5	2.4	0.0	1.5	36.1	1.5
1745	-32.5	1.5	0.0	2.2	34.2	1.6
2395	-31.7	2.1	0.0	2.6	34.2	1.6
1133	2.6	-30.9	0.0	2.8	34.0	1.6
2575	-32.1	1.7	0.0	1.2	33.9	1.6
593	-33.7	-0.2	0.0	0.8	33.8	1.6
2453	1.2	-32.1	0.0	2.7	33.7	1.6
2444	0.7	-32.5	0.0	2.6	33.5	1.6
2434	1.5	-31.6	0.0	2.5	33.5	1.6
543	-30.8	2.1	0.0	2.5	33.3	1.7

1 Stress components are listed for the nodes with the 20 highest impact nodal point stress intensity values (see Figure 2.7.8.1-4 for locations of these nodes). Note that S_x is the stress in the radial direction, S_y is the stress in the circumferential direction and S_{xy} is the shearing stress.

2 The allowable stress is 0.7 S_u. S_u is the ultimate strength of 17-4 PH stainless steel at a bounding 600°F, S_u = 126.7 ksi.

Table 2.7.8.1-4 Basket 55-g Side Impact Stresses for 37-Degree Drop Orientation

Node No.[1]	S_x (ksi)	S_y (ksi)	S_z (ksi)	S_{xy} (ksi)	SI (ksi)	MS[2]
565	-48.7	1.3	0.0	3.2	50.5	0.8
592	-44.2	1.5	0.0	3.0	46.1	0.9
1755	-44.5	1.2	0.0	2.9	46.0	0.9
592	-38.7	1.0	0.0	1.2	39.9	1.2
1908	-37.5	1.2	0.0	2.6	39.0	1.3
1765	-36.1	1.2	0.0	2.4	37.7	1.4
1088	-35.2	1.5	0.0	1.2	36.8	1.4
568	-33.6	2.3	0.0	1.6	36.0	1.5
1241	-34.2	1.4	0.0	1.3	35.7	1.5
2444	0.5	-34.6	0.0	2.5	35.5	1.5
564	-34.9	-0.5	0.0	2.6	33.4	1.5
2453	1.0	-33.7	0.0	2.6	35.2	1.5
415	-32.5	2.5	0.0	1.3	35.1	1.5
2395	-32.0	2.3	0.0	2.8	34.8	1.5
1133	2.5	-31.9	0.0	2.7	34.8	1.6
2434	1.6	-32.4	0.0	2.4	34.4	1.6
1745	-32.2	1.7	0.0	2.3	34.2	1.6
2575	-31.8	1.7	0.0	1.1	33.6	1.6
458	3.1	-29.9	0.0	3.0	33.6	1.6
593	-33.3	-0.2	0.0	0.8	33.4	1.7

1 Stress components are listed for the nodes with the 20 highest impact nodal point stress intensity values (see Figure 2.7.8.1-5 for locations of these nodes). Note that S_x is the stress in the radial direction, S_y is the stress in the circumferential direction and S_{xy} is the shearing stress.

2 The allowable stress is 0.7 S_u. S_u is the ultimate strength of 17-4 PH stainless steel at a bounding 600°F, S_u = 126.7 ksi.

Table 2.7.8.1-5 Basket 55-g Side Impact Stresses for 45-Degree Drop Orientation

Node No.[1]	S_x (ksi)	S_y (ksi)	S_z (ksi)	S_{xy} (ksi)	SI (ksi)	MS[2]
565	-47.7	1.5	0.0	3.3	49.6	0.8
591	-43.9	1.5	0.0	3.2	45.9	0.9
1755	-43.9	1.3	0.0	3.1	45.6	0.9
1908	-36.7	1.4	0.0	2.7	38.5	1.3
592	-37.4	1.0	0.0	1.1	38.5	1.3
1765	-36.0	1.3	0.0	2.6	37.6	1.4
2444	0.3	-36.5	0.0	2.5	37.2	1.4
2453	0.8	-35.2	0.0	2.6	36.4	1.4
1088	-34.4	1.5	0.0	1.1	36.0	1.5
1133	2.3	-32.6	0.0	2.6	35.3	1.5
2395	-32.1	2.6	0.0	3.0	35.2	1.5
2434	1.7	-33.1	0.0	2.3	35.1	1.5
1241	-33.1	1.3	0.0	1.1	34.5	1.6
458	2.9	-30.8	0.0	2.9	34.2	1.6
568	-31.8	2.2	0.0	1.4	34.2	1.6
564	-33.3	-0.6	0.0	2.8	33.8	1.6
1745	-31.4	2.0	0.0	2.5	33.4	1.6
415	-30.9	2.5	0.0	1.1	33.5	1.6
1226	-30.2	2.3	0.0	3.0	33.0	1.6
2575	-31.2	1.7	0.0	0.9	33.0	1.7

1 Stress components are listed for the nodes with the 20 highest impact nodal point stress intensity values (see Figure 2.7.8.1-6 for locations of these nodes). Note that S_x is the stress in the radial direction, S_y is the stress in the circumferential direction and S_{xy} is the shearing stress.

2 The allowable stress is 0.7 S_u. S_u is the ultimate strength of 17-4 PH stainless steel at a bounding 600°F, S_u = 126.7 ksi.

Table 2.7.8.1-6 Basket 55g Side Impact Stresses for 60-Degree Drop Orientation

Node No.[1]	S_x (ksi)	S_y (ksi)	S_z (ksi)	S_{xy} (ksi)	SI (ksi)	MS[2]
565	-42.7	2.0	0.0	3.4	45.2	1.0
1755	-41.1	1.7	0.0	3.3	43.3	1.0
591	-40.5	1.5	0.0	3.3	42.6	1.1
2444	0.0	-38.5	0.0	2.2	38.8	1.3
2453	0.5	-36.6	0.0	2.3	37.4	1.4
2108	-21.6	-20.1	0.0	12.0	36.9	1.4
1908	-34.4	1.7	0.0	2.9	36.6	1.4
1765	-34.9	1.3	0.0	2.3	36.6	1.4
2434	1.8	-33.4	0.0	1.9	35.5	1.5
1133	1.8	-32.7	0.0	2.3	34.8	1.6
1347	-27.1	-11.1	0.0	-12.0	34.7	1.6
2395	-30.8	3.0	0.0	3.3	34.4	1.6
458	2.4	-31.3	0.0	2.5	34.1	1.6
2467	2.7	-31.2	0.0	1.3	34.0	1.6
1630	-28.2	-7.7	0.0	-10.5	33.5	1.6
2477	1.7	-31.8	0.0	0.9	33.5	1.6
1088	-31.8	1.4	0.0	0.8	33.2	1.7
1786	0.9	-31.9	0.0	2.2	33.1	1.7
574	29.4	-2.7	0.0	3.2	32.7	1.7
592	-31.9	0.7	0.0	0.8	32.7	1.7

1 Stress components are listed for the nodes with the 20 highest impact nodal point stress intensity values (see Figure 2.7.8.1-7 for locations of these nodes). Note that S_x is the stress in the radial direction, S_y is the stress in the circumferential direction and S_{xy} is the shearing stress.

2 The allowable stress is 0.7 S_u. S_u is the ultimate strength of 17-4 PH stainless steel at a bounding 600°F, S_u = 126.7 ksi.

Table 2.7.8.1-7 Basket 55-g Side Impact Stresses for 64-Degree Drop Orientation

Node No.[1]	S_x (ksi)	S_y (ksi)	S_z (ksi)	S_{xy} (ksi)	SI (ksi)	MS[2]
565	-40.4	2.1	0.0	3.3	43.0	1.1
1755	-39.9	1.8	0.0	3.3	42.1	1.1
591	-38.1	1.6	0.0	3.3	40.2	1.2
2444	-0.5	-38.7	0.0	2.1	38.9	1.3
2108	-22.6	-20.4	0.0	12.4	37.9	1.3
2453	0.4	-36.7	0.0	2.2	37.3	1.4
1765	-34.2	1.3	0.0	2.9	36.0	1.5
1908	-33.5	1.8	0.0	3.0	35.8	1.5
1347	-27.8	-11.6	0.0	-12.2	35.6	1.5
2434	1.8	-33.2	0.0	1.8	35.3	1.5
2467	2.6	-31.7	0.0	1.4	34.5	1.6
1630	-28.9	-7.9	0.0	-10.8	34.4	1.6
1133	1.6	-32.2	0.0	2.1	34.2	1.6
2477	1.7	-32.4	0.0	1.0	34.2	1.6
2395	-30.0	3.1	0.0	3.3	33.8	1.6
458	2.2	-31.1	0.0	2.4	33.7	1.6
1786	0.8	-32.1	0.0	2. 2	33.2	1.7
574	29.6	-2.5	0.0	3.2	32.8	1.7
1777	0.2	-31.6	0.0	1.9	32.1	1.8
1088	-30.6	1.4	0.0	0.7	32.0	1.8

1 Stress components are listed for the nodes with the 20 highest impact nodal point stress intensity values (see Figure 2.7.8.1-8 for locations of these nodes). Note that S_x is the stress in the radial direction, S_y is the stress in the circumferential direction and S_{xy} is the shearing stress.

2 The allowable stress is 0.7 S_u. S_u is the ultimate strength of 17-4 PH stainless steel at a bounding 600°F, S_u = 126.7 ksi.

Table 2.7.8.1-8 Basket 55-g Side Impact Stresses for 75-Degree Drop Orientation

Node No.[1]	S_x (ksi)	S_y (ksi)	S_z (ksi)	S_{xy} (ksi)	SI (ksi)	MS[2]
2108	-25.4	-20.9	0.0	13.4	40.5	1.2
2444	-0.2	-38.5	0.0	1.9	38.6	1.3
1347	-29.1	-12.9	0.0	-13.0	37.8	1.3
1755	-33.7	2.1	0.0	3.2	36.4	1.4
1630	-30.3	-8.6	0.0	-11.5	36.3	1.4
2453	0.7	-35.8	0.0	2.0	36.1	1.5
2477	1.6	-33.7	0.0	1.2	35.4	1. 5
2467	2.4	-32.6	0.0	1.6	35.2	1.5
565	-31.7	2.3	0.0	3.1	34.5	1.6
2434	1.8	-32.3	0.0	1.5	34.4	1.6
2297	-25.2	-10.9	0.0	12.2	34.0	1.6
1908	-30.2	2.1	0.0	3.0	32.8	1. 7
1786	0.5	-32.0	0.0	1.9	32.6	1.7
1777	-0.3	-32.0	0.0	1.6	32.2	1.8
1800	2.1	-29.4	0.0	1.3	31.7	1.8
1419	-25.3	-11.4	0.0	-10.7	31.4	1.8
2586	-28.5	2.3	0.0	3.2	31.4	1.8
1765	-29.0	1.5	0.0	2.9	31.1	1.9
1418	-25.9	-8.1	0.0	-10.8	31.0	1.9
1133	1.1	-29.6	0.0	1.7	30.9	1.9

1 Stress components are listed for the nodes with the 20 highest impact nodal point stress intensity values (see Figure 2.7.8-9 for locations of these nodes). Note that S_x in the stress in the radial direction, S_y is the stress in the circumferential direction and S_{xy} is the shearing stress.

2 The allowable stress is $0.7S_u$. S_u is the ultimate strength of 17-4 PH stainless steel at a bounding 600°F, S_u = 126.7 ksi.

Table 2.7.8.1-9 Basket 55-g Side Impact Stresses for 90-Degree Drop Orientation

Node No.[1]	S_x (ksi)	S_y (ksi)	S_z (ksi)	S_{xy} (ksi)	SI (ksi)	MS[2]
2108	-32.6	-17.9	0.0	15.2	44.6	1.0
1347	-32.6	-17.9	0.0	-15.2	44.6	1.0
2297	-33.7	-10.8	0.0	13.6	41.5	1.1
1630	-33.7	-10.8	0.0	-13.6	41.5	1.1
2024	-29.5	-10.1	0.0	12.7	35.9	1.5
1418	-29.5	-10.1	0.0	-12.7	35.9	1.5
2025	-27.8	-14.9	0.0	11.9	35.4	1.5
1419	-27.8	-14.9	0.0	-11.9	35.4	1.5
2123	-30.9	-3.5	0.0	7.8	33.9	1.6
1354	-30.9	-3.5	0.0	-7.7	33.9	1.6
2023	-28.3	-5.6	0.0	9.8	32.0	1.8
1417	-28.3	-5.6	0.0	-9.8	32.0	1.8
2212	-21.0	-17.2	0.0	10.2	31.4	1.8
1545	-21.0	-17.2	0.0	-10.2	31.4	1.8
2213	-25.9	-5.2	0.0	8.1	29.4	2.0
1546	-25.9	-5.2	0.0	-8.1	29.4	2.0
2022	-25.0	-3.7	0.0	7.1	27.3	2.2
1416	-25.0	-3.7	0.0	-7.1	27.3	2.2
1813	1.6	-25.1	0.0	-0.8	27. 0	2.3
2434	1.6	-25.1	0.0	0.8	27.0	2.3

1 Stress components are listed for the nodes with the 20 highest impact nodal point stress intensity values (see Figure 2.7.8.1-10 for locations of these nodes). Note that S_x in the stress in the radial direction, S_y is the stress in the circumferential direction and S_{xy} is the shearing stress.

2 The allowable stress is $0.7S_u$. S_u is the ultimate strength of 17-4 PH stainless steel at a bounding 600°F, S_u = 126.7 ksi.

Table 2.7.8.1-10 Summary of Basket 55-g Side Impact Analysis Results

Drop Orientation (deg)	Maximum Nodal SI Stress[1] (ksi)	Temperature[2] (°F)	Allow Stress[3] (ksi)	Margin of Safety
0	31.74	600	88.69	1.8
15	49.52	600	88.69	0.79
30	50.58	600	88.69	0.75
37	50.46	600	88.69	0.76
45	49.63	600	88.69	0.79
60	45.15	600	88.69	0.96
64	42.97	600	88.69	1.06
75	40.50	600	88.69	1.19
90	44.57	600	88.69	0.99

1 The maximum stress documented is the stress intensity.

2 Conservative envelope temperature of the support disk.

3 The allowable stress is $0.7S_u$. S_u is the ultimate strength of 17-4 PH steel alloy S_u = 126.7 ksi at 600°F.

Table 2.7.8.1-11 End Drop Impact (56.1 g) Basket Stresses

Node No.[1]	S_x (ksi)	S_y (ksi)	S_z (ksi)	S_{xy} (ksi)	S_{yz} (ksi)	S_{xz} (ksi)	SI (ksi)	MS[2]
38512	-21.9	-23.7	5.2	1.9	4.8	-0.1	36.2	1.6
38522	-9.2	-7.0	-1.2	-7.0	-13.2	-2.0	32.6	1.9
38513	-11.3	-14.7	3.6	4.0	-2.4	-2.1	31.2	2.0
38570	-10.4	-11.0	-1.5	1.3	-8.7	3.3	29.8	2.2
38396	-9.4	-23.4	-0.7	5.5	6.8	-0.5	28.9	2.3
38514	-17.3	-15.8	1.4	1.6	2.7	2.5	28.7	2.3
37963	-8.1	-12.9	1.5	8.0	2.3	-2.9	27.7	2.4
37919	-7.6	-16.9	0.1	4.3	-4.4	-0.6	26.0	2.6
38515	-22.6	-20.0	-2.7	1.1	-2.3	4.1	24.9	2.9
38027	-2.0	18.7	-1.8	-0.5	-0.4	2.1	22.7	3.2
38576	-10.8	-16.3	-2.6	2.9	3.2	-1.4	22.6	3.2
38470	-2.3	18.0	-2.1	0.0	0.3	-2.3	22.5	3.2
38005	-14.4	-13.1	-0.1	4.2	2.0	-1.7	22.4	3.2
38029	0.4	20.3	-0.6	0.2	-0.2	-1.4	21.9	3.3
38032	0.3	20.1	-0.7	-0.1	0.1	1.4	21.7	3.3
38039	0.1	21.6	0.2	0.2	-0.2	0.1	21.7	3.4
38044	-0.1	21.2	0.0	0.2	0.1	-0.1	21.3	3.4
38485	-0.2	20.9	0.0	0.2	0.0	0.0	21.2	3.5
38446	-18.6	-14.5	-1.8	4.0	0.2	-0.5	21.2	3.5
38398	2.2	-12.7	1.9	-1.7	-3.1	2.1	20.3	3.6

1 Stress components are listed for the nodes with the 20 highest impact nodal point stress intensity values (see Figure 2.7.8.1-12 for locations of these nodes). Note that S_x is the stress in the radial direction, S_y is the stress in the circumferential direction and S_z is the stress in the longitudinal direction.

2 The allowable stress is $0.7S_u$ at the node temperature for the steady state design basis heat load heat transfer analysis.

Table 2.7.8.1-12 Basket Web Stress 55-g Side Impact for 0-Degree Orientation

Node No.[1]	S_x (ksi)	S_y (ksi)	S_z (ksi)	S_{xy} (ksi)	SI (ksi)	MS[2]
402	-14.3	3.9	0.0	0.0	18.2	3.9
390	-14.4	2.4	0.0	0.0	16.9	4.2
1901	-13.7	3.1	0.0	0.0	16.9	4.3
567	-13.7	3.1	0.0	0.0	16.9	4.3
60	-16.0	-4.6	0.0	0.0	16.5	4.4
1839	-12.5	3.6	0.0	1.2	16.4	4.4
505	-12.5	3.6	0.0	-1.2	16.4	4.4
51	-14.9	-5.7	0.0	-0.1	15.6	4.7
1385	-14.9	-5.7	0.0	0.1	15.6	4.7
1829	-8.2	2.8	0.0	1.4	11.3	6.8
495	-8.2	2.8	0.0	-1.4	11.3	6.8
1069	-9.9	1.2	0.0	0.0	11.2	6.9
2506	-8.2	0.7	0.0	0.9	9.2	8.7
1172	-8.2	0.7	0.0	-0.9	9.2	8.7
1364	-7.2	-0.4	0.0	1.0	8.4	9.6
30	-7.2	-0.4	0.0	-1.0	8.4	9.6
1057	-6.1	-3.6	0.0	-0.1	6.3	13.0
2568	-4.8	-3.6	0.0	0.2	5.3	15.8
1234	-4.8	-3.6	0.0	-0.2	5.3	15.8
2496	-4.1	0.1	0.0	0.9	4.7	18.0
1162	-4.1	0.1	0.0	-0.9	4.7	18.0
727	-2.8	-1.7	0.0	0.0	3.0	28.8
697	-1.7	0.5	0.0	-0.2	2.3	36.9
2107	-1.7	0.5	0.0	0.2	2.3	37.0
1346	0.0	1.0	0.0	0.5	2.1	40.4
12	0.0	1.0	0.0	-0.5	2.1	40.4
2125	-0.3	-0.3	0.0	0.4	2.0	43.2
679	-0.3	-0.3	0.0	-0.4	2.0	43.2
718	-0.8	-1.2	0.0	-0.1	1.4	61.4
2086	-0.8	-1.2	0.0	0.1	1.4	61.4

1 Stress components are listed for the nodes with the 20 highest impact nodal point stress intensity values (see Figure 2.7.8.1-13 for locations of these nodes). Note that S_x is the stress in the radial direction, S_y is the stress in the circumferential direction and S_{xy} is the shearing stress.

2 The allowable stress is $0.7S_u$. S_u is the ultimate strength of 17-4 PH stainless steel at a bounding 600°F, S_u = 126.7 ksi.

Table 2.7.8.1-13 Basket Web Stress 55-g Side Impact for 15-Degree Orientation

Node No.[1]	S_x (ksi)	S_y (ksi)	S_z (ksi)	S_{xy} (ksi)	SI (ksi)	MS[2]
402	-13.0	0.5	0.0	-7.2	19.8	3.5
505	-10.8	0.9	0.0	-7.9	19.8	3.5
567	-12.8	2.5	0.0	-0.8	17.4	4.1
1069	-8.8	-1.7	0.0	-7.7	16.8	4.3
390	-13.5	1.2	0.0	-0.8	16.8	4.3
1172	-6.9	-0.8	0.0	-7.8	16.8	4.3
1839	-11.5	-0.3	0.0	-5.7	16.1	4.5
60	-15.3	-4.1	0.0	-0.3	16.0	4.5
51	-14.8	-4.9	0.0	-0.7	15.9	4.6
1901	-12.5	0.3	0.0	-0.7	14.9	5.0
495	-5.3	0.6	0.0	-6.6	14.5	5.1
2506	-7.3	-3.6	0.0	-6.5	13.8	5.4
1385	-12.9	-4.9	0.0	-0.4	13.6	5.5
1162	-2.0	-0.2	0.0	-6.5	13.1	5.8
1364	-8.8	2.3	0.0	-0.4	11.8	6.5
2496	-4.7	-5.5	0.0	-5.5	11.5	6.6
1829	-9.0	-1.6	0.0	-4.1	11.6	6.6
30	-4.8	-5.1	0.0	-2.2	9.8	8.0
2125	-0.3	-5.1	0.0	-0.8	8.9	8.9
1057	-5.6	-3.2	0.0	-1.2	8.2	9.8
1234	-3.8	-2.6	0.0	-1.3	7.8	10.4
2568	-5.0	-3.6	0.0	-1.1	7.4	10.9
697	-0.4	3.7	0.0	-1.7	6.9	11.9
2107	-2.6	-2.9	0.0	-1.6	6.3	13.0
1346	-1.0	-2.9	0.0	-0.4	5.8	14.2
12	-0.9	0.2	0.0	-1.4	3.3	25.5
727	-2.5	-1.4	0.0	-0.5	3.2	26.3
679	-0.1	0.1	0.0	-1.3	3.1	27.4
718	-0.1	0.1	0.0	-0.7	2.4	35.6
2086	-1.3	-1.9	0.0	-0.4	2.4	36.1

1 Stress components are listed for the nodes with the 20 highest impact nodal point stress intensity values (see Figure 2.7.8.1-13 for locations of these nodes). Note that S_x is the stress in the radial direction, S_y is the stress in the circumferential direction and S_{xy} is the shearing stress.

2 The allowable stress is $0.7S_u$. S_u is the ultimate strength of 17-4 PH stainless steel at a bounding 600°F, S_u = 126.7 ksi.

Table 2.7.8.1-14 Basket Web Stress 55-g Side Impact for 30-Degree Orientation

Node No.[1]	S_x (ksi)	S_y (ksi)	S_z (ksi)	S_{xy} (ksi)	SI (ksi)	MS[2]
505	-9.4	-0.8	0.0	-8.1	18.5	3.8
402	-11.3	-2.0	0.0	-7.5	17.7	4.0
1172	-5.9	-2.4	0.0	-7.9	16.3	4.5
1069	-7.4	-4.3	0.0	-7.9	16.2	4.5
567	-11.5	1.8	0.0	-0.7	16.2	4.5
390	-12.2	0.4	0.0	-0.7	15.4	4.8
51	-13.6	-4.1	0.0	-0.7	15.2	4.8
60	-13.9	-3.4	0.0	-0.3	14.8	5.0
2506	-5.5	-7.2	0.0	-6.8	14.4	5.1
1839	-9.5	-3.8	0.0	-5.9	14.1	5.3
495	-4.1	-0.2	0.0	-6.5	13.6	5.5
2496	-2.7	-10.1	0.0	-5.2	13.6	5.5
1901	-10.8	-0.6	0.0	-0.6	13.4	5.6
1162	-1.2	-0.8	0.0	-6.2	12.5	6.1
1385	-11.3	-4.2	0.0	-0.4	12.1	6.4
2125	-4.6	-8.5	0.0	-0.4	10.4	7.5
1829	-7.0	-5.9	0.0	-3.8	10.3	7.6
30	-3.6	-6.2	0.0	-2.2	10.2	7.7
1364	-7.7	1.0	0.0	-0.4	9.9	7.9
2107	-1.3	-6.9	0.0	-1.6	8.5	9.4
1057	-5.0	-4.0	0.0	-1.5	8.0	10.2
1346	-3.9	-6.2	0.0	-0.3	7.7	10.6
1234	-3.3	-2.8	0.0	-1.5	7.5	10.9
2568	-4.1	-4.7	0.0	-1.3	7.2	11.2
697	-0.3	4.2	0.0	-1.8	6.9	11.9
727	-2.2	-1.3	0.0	-0.8	3.6	23.3
12	-0.6	0.1	0.0	-1.3	3.1	27.9
2086	-1.3	-2.0	0.0	-0.8	3.0	28.4
718	0.1	0.2	0.0	-0.9	2.9	29.4
679	0.2	0.1	0.0	-1.2	2.9	30.0

1 Stress components are listed for the nodes with the 20 highest impact nodal point stress intensity values (see Figure 2.7.8.1-13 for locations of these nodes). Note that S_x is the stress in the radial direction, S_y is the stress in the circumferential direction and S_{xy} is the shearing stress.

2 The allowable stress is $0.7S_u$. S_u is the ultimate strength of 17-4 PH stainless steel at a bounding 600°F, S_u = 126.7 ksi.

Table 2.7.8.1-15 Basket Web Stress 55-g Side Impact for 37-Degree Orientation

Node No.[1]	S_x (ksi)	S_y (ksi)	S_z (ksi)	S_{xy} (ksi)	SI (ksi)	MS[2]
505	-8.5	-1.6	0.0	-8.2	17.8	4.0
402	-10.3	-3.2	0.0	-7.7	16.9	4.3
1069	-6.7	-5.5	0.0	-8.0	16.1	4.5
1172	-5.3	-3.1	0.0	-8.0	16.1	4.5
567	-10.6	1.4	0.0	-0.7	15.4	4.8
2506	-4.6	-8.8	0.0	-6.9	15.2	4.8
2496	-1.9	-12.1	0.0	-5.1	15.1	4.9
390	-11.3	0.0	0.0	-0.6	14.6	5.1
51	-12.7	-3.5	0.0	-0.7	14.6	5.1
60	-12.9	-2.9	0.0	-0.3	14.2	5.3
1839	-8.4	-5.3	0.0	-6.0	13.7	5.5
495	-3.3	-0.6	0.0	-6.4	13.1	5.8
1901	-9.9	-1.0	0.0	-0.5	12.6	6.1
1162	-0.8	-1.1	0.0	-6.1	12.2	6.3
2125	-5.9	-10.0	0.0	-0.4	11.5	6.7
1385	-10.3	-3.7	0.0	-0.4	11.3	6.9
1829	-6.1	-7.7	0.0	-3.7	10.7	7.3
30	-2.9	-6.7	0.0	-2.1	10.5	7.5
2107	-0.9	-8.6	0.0	-1.6	9.9	7.9
1364	-7.1	0.5	0.0	-0.4	9.0	8.9
1346	-5.0	-7.5	0.0	-0.3	8.8	9.1
1057	-4.6	-4.3	0.0	-1.6	7.9	10.2
1234	-3.0	-2.9	0.0	-1.6	7.3	11.2
2568	-3.7	-5.1	0.0	-1.4	7.3	11.2
697	-0.2	4.4	0.0	-1.8	6.9	11.8
727	-2.1	-1.2	0.0	-0.9	3.9	21.8
2086	-1.2	-2.1	0.0	-0.9	3.3	26.0
718	0.2	0.4	0.0	-1.0	3.1	27.2
12	-0.5	0.0	0.0	-1.2	2.9	29.1
679	0.2	-0.1	0.0	-1.2	2.7	31.3

1 Stress components are listed for the nodes with the 20 highest impact nodal point stress intensity values (see Figure 2.7.8.1-13 for locations of these nodes). Note that S_x is the stress in the radial direction, S_y is the stress in the circumferential direction and S_{xy} is the shearing stress.

2 The allowable stress is $0.7S_u$. S_u is the ultimate strength of 17-4 PH stainless steel at a bounding 600°F, S_u = 126.7 ksi.

Table 2.7.8.1-16 Basket Web Stress 55-g Side Impact for 45-Degree Orientation

Node No.[1]	S_x (ksi)	S_y (ksi)	S_z (ksi)	S_{xy} (ksi)	SI (ksi)	MS[2]
505	-7.2	-2.5	0.0	-8.2	17.1	4.2
2496	-1.0	-14.1	0.0	-4.9	16.8	4.3
1069	-5.7	-6.7	0.0	-8.1	16.3	4.5
402	-8.9	-4.5	0.0	-7.7	16.2	4.5
2506	-3.6	-10.4	0.0	-7.0	16.6	4.5
1172	-4.5	-3.9	0.0	-7.9	15.9	4.6
567	-9.4	0.8	0.0	-0.6	14.2	5.3
51	-11.4	-2.7	0.0	-0.8	13.8	5.4
390	-10.1	-0.4	0.0	-0.6	13.7	5.5
1839	-7.0	-7.0	0.0	-6.1	13.5	5.6
60	11.7	2.2	0.0	-0.3	13.5	5.6
2125	-7.2	-11.5	0.0	-0.3	12.9	5.9
495	-2.4	-1.1	0.0	-6.2	12.5	6.1
1162	-0.3	-1.5	0.0	-5.9	11.8	6.5
1829	-4.9	-9.7	0.0	-3.5	11.6	6.6
1901	-8.6	-1.4	0.0	-0.4	11.6	6.7
2107	-0.4	-10.3	0.0	-1.6	11.6	6.7
30	-2.1	-7.2	0.0	-2.0	10.7	7.3
1385	-9.1	-3.0	0.0	-0.4	10.3	7.6
1346	-6.2	-9.0	0.0	-0.3	10.1	7.8
1364	-6.3	-0.2	0.0	-0.5	8.1	10.0
1057	-4.1	-4.5	0.0	-1.7	7.8	10.4
2568	-3.1	-5.5	0.0	-1.6	7.3	11.1
1234	-2.6	-2.8	0.0	-1.7	7.1	11.5
697	-0.1	4.7	0.0	-1.8	6.9	11.9
727	-1.9	-1.2	0.0	-1.1	4.2	20.4
2086	-1.2	-2.2	0.0	-1.1	3.6	23.8
718	0.2	0.6	0.0	-1.1	3.4	25.3
12	-0.4	-0.1	0.0	-1.1	2.8	30.8
679	0.3	-0.1	0.0	-1.1	2.6	33.0

1 Stress components are listed for the nodes with the 20 highest impact nodal point stress intensity values (see Figure 2.7.8.1-13 for locations of these nodes). Note that S_x is the stress in the radial direction, S_y is the stress in the circumferential direction and S_{xy} is the shearing stress.

2 The allowable stress is $0.7S_u$. S_u is the ultimate strength of 17-4 PH stainless steel at a bounding 600°F, S_u = 126.7 ksi.

Table 2.7.8.1-17 Basket Web Stress 55-g Side Impact for 60-Degree Orientation

Node No.[1]	S_x (ksi)	S_y (ksi)	S_z (ksi)	S_{xy} (ksi)	SI (ksi)	MS[2]
2496	0.4	-17.1	0.0	-4.5	19.9	3.5
2506	-1.6	-12.8	0.0	-6.9	18.0	3.9
1069	-3.5	-8.6	0.0	-8.0	16.8	4.3
505	-4.2	-4.1	0.0	-7.8	15.6	4.7
402	-5.6	-6.7	0.0	-7.7	15.5	4.7
1172	-2.3	-5.1	0.0	-7.5	15.3	4.8
2125	-9.0	-13.7	0.0	-0.2	15.0	4.9
1839	-4.2	-9.7	0.0	-6.0	14.3	5.2
2107	0.3	-12.9	0.0	-1.5	14.2	5.2
1829	-2.8	-12.9	0.0	-3.2	13.9	5.4
1346	-8.0	-11.3	0.0	-0.3	12.4	6.2
60	-8.7	-0.7	0.0	-0.3	11.9	6.4
390	-7.2	-1.1	0.0	-0.5	11.5	6.7
51	-7.7	-1.6	0.0	-0.7	11.3	6.9
567	-6.1	-0.9	0.0	-0.5	11.2	6.9
495	-0.7	-1.9	0.0	-5.6	11.2	6.9
1162	0.5	-1.9	0.0	-5.2	10.8	7.3
30	-0.7	-7.2	0.0	-1.8	10.6	7.4
1901	-6.0	-2.2	0.0	-0.3	9.7	8.1
1385	-6.3	-1.4	0.0	-0.4	8.4	9.6
2568	-2.0	-6.1	0.0	-1.7	7.4	11.0
1057	-2.9	-4.6	0.0	-1.9	7.3	11.2
1364	-4.8	-1.3	0.0	-0.6	6.8	12.1
697	0.0	4.7	0.0	-1. 7	6.5	12.7
1234	-1.5	-2.3	0.0	-1.9	6.4	13.0
727	-1.4	-0.9	0.0	-1.3	4.5	18.8
2086	-1.1	-2.3	0.0	-1.3	4.0	21.1
718	0.5	1.1	0.0	-1.3	3.7	23.2
12	-0.2	-0.3	0.0	-0.9	2.5	34.0
679	0.5	-0.1	0.0	-0.9	2.4	36.6

1 Stress components are listed for the nodes with the 20 highest impact nodal point stress intensity values (see Figure 2.7.8.1-13 for locations of these nodes). Note that S_x is the stress in the radial direction, S_y is the stress in the circumferential direction and S_{xy} is the shearing stress.

2 The allowable stress is $0.7S_u$. S_u is the ultimate strength of 17-4 PH stainless steel at a bounding 600°F, S_u = 126.7 ksi.

Table 2.7.8.1-18 Basket Web Stress 55-g Side Impact for 64-Degree Orientation

Node No.[1]	S_x (ksi)	S_y (ksi)	S_z (ksi)	S_{xy} (ksi)	SI (ksi)	MS[2]
2496	0.7	-17.6	0.0	-4.4	20.5	3.3
2506	-1.0	-13.3	0.0	-6.9	18.5	3.8
1069	-2.8	-9.0	0.0	-7.9	17.0	4.2
2125	-9.4	-14.1	0.0	-0.2	15.5	4.7
402	-4.9	-7.3	0.0	-7.6	15.4	4.7
505	-3.2	-4.6	0.0	-7.5	15.1	4.9
1172	-1.6	-5.3	0.0	-7.3	15.1	4.9
2107	0.5	-13.5	0.0	-1.5	14.8	5.0
1839	-3.4	-10.3	0.0	-6.0	14.7	5.0
1829	-2.3	-13.6	0.0	-3.1	14.5	5.1
1346	-8.4	-11.8	0.0	-0.3	12.9	5.9
60	-7.7	-0.3	0.0	-0.3	11.3	6.8
390	-6.3	-1.3	0.0	-0.5	10.8	7.2
495	-0.4	-2.1	0.0	-5.3	10.7	7.3
1162	0.6	-2.0	0.0	-5.0	10.3	7.6
567	-5.0	-1.6	0.0	-0.5	10.3	7.6
30	-0.4	-6.9	0.0	-1.6	10.3	7.6
51	-6.3	-2.1	0.0	-0.7	10.1	7.8
1901	-5.2	-2.4	0.0	-0.3	9.3	8.6
1385	-5.5	-0.9	0.0	-0.4	7.9	10.2
2568	-1.7	-6.1	0.0	-1.7	7.5	10.8
1057	-2.4	-4.5	0.0	-1.9	7.1	11.5
1364	-4.3	-1.6	0.0	-0.6	6.5	12.6
697	-0.1	4.6	0.0	-1.7	6.2	13.3
1234	-1.1	-2.0	0.0	-1.9	6.1	13.7
727	-1.1	-0.8	0.0	-1.3	4.5	18.8
2086	-1.1	-2.3	0.0	-1.3	4.1	20.6
718	0.6	1.3	0.0	-1.3	3.7	23.1
12	-0.1	-0.3	0.0	-0.9	2.5	34.9
679	0.5	-0.2	0.0	-0.8	2.3	37.8

1 Stress components are listed for the nodes with the 20 highest impact nodal point stress intensity values (see Figure 2.7.8.1-13 for locations of these nodes). Note that S_x is the stress in the radial direction, S_y is the stress in the circumferential direction and S_{xy} is the shearing stress.

2 The allowable stress is $0.7S_u$. S_u is the ultimate strength of 17-4 PH stainless steel at a bounding 600°F, S_u = 126.7 ksi.

Table 2.7.8.1-19 Basket Web Stress 55-g Side Impact for 75-Degree Orientation

Node No.[1]	S_x (ksi)	S_y (ksi)	S_z (ksi)	S_{xy} (ksi)	SI (ksi)	MS[2]
2496	1.5	-18.8	0.0	-4.0	22.0	3.0
2506	0.7	-14.4	0.0	-6.5	20.1	3.4
1069	-0.2	-10.0	0.0	-7.3	17.6	4.1
2125	-10.2	-15.0	0.0	-0.2	16.3	4.4
1829	-0.7	-15.3	0.0	-2.9	16.3	4.4
1839	-0.9	-12.0	0.0	-5.8	16.2	4.5
2107	0.9	-14.7	0.0	-1.5	16.1	4.5
402	-1.4	-8.8	0.0	-7.0	15.8	4.6
1346	-9.3	-12.9	0.0	-0.3	14.1	5.3
1172	0.2	-5.9	0.0	-6.3	14.0	5.3
505	-0.5	-5.7	0.0	-6.4	13.7	5.5
495	0.0	-2.5	0.0	-4.3	9.1	8.8
390	-2.9	-2.7	0.0	-0.4	8.7	9.2
1162	0.5	-2.1	0.0	-4.1	8.6	9.3
30	-0.1	-5.3	0.0	-1.2	8.6	9.3
567	-1.9	-3.3	0.0	-0.2	8.4	9.6
60	-3.9	-1.0	0.0	-0.1	8.2	9.8
1901	-2.7	-3.1	0.0	-0.2	8.1	9.9
2568	-0.7	-5.8	0.0	-1.7	7.4	11.0
51	-2.5	-3.2	0.0	-0.5	7.3	11.2
1385	-3.1	0.2	0.0	-0.4	6.6	12.4
1057	-0.8	-3.8	0.0	-1.9	6.2	13.3
1364	-3.1	-2.4	0.0	-0.6	6.0	13.7
697	-0.2	3.8	0.0	-1.4	5.1	16.2
1234	-0.1	-1.2	0.0	-1.8	5.0	16.9
2086	-0.9	-1.9	0.0	-1.4	4.2	20.0
727	-0.2	-0.1	0.0	-1.3	4.2	20.1
718	0.7	1.8	0.0	-1.2	3.5	24.4
12	-0.1	-0.5	0.0	-0.7	2.3	37.0
679	0.6	-0.2	0.0	-0.7	2.1	41.4

1 Stress components are listed for the nodes with the 20 highest impact nodal point stress intensity values (see Figure 2.7.8.1-13 for locations of these nodes). Note that S_x is the stress in the radial direction, S_y is the stress in the circumferential direction and S_{xy} is the shearing stress.

2 The allowable stress is $0.7S_u$. S_u is the ultimate strength of 17-4 PH stainless steel at a bounding 600°F, S_u = 126.7 ksi.

Table 2.7.8.1-20 Basket Web Stress 55-g Side Impact for 90-Degree Orientation

Node No.[1]	S_x (ksi)	S_y (ksi)	S_z (ksi)	S_{xy} (ksi)	SI (ksi)	MS[2]
1829	4.1	-18.8	0.0	0.5	23.1	2.8
2496	4.1	-18.8	0.0	-0.5	23.1	2.8
1839	4.8	-15.0	0.0	0.5	19.8	3.5
2506	4.8	-15.0	0.0	-0.5	19.8	3.5
1346	-11.1	-14.9	0.0	-0.1	16.2	4.5
2125	-11.1	-14.9	0.0	0.1	16.2	4.5
402	2.2	-10.8	0.0	0.4	13.0	5.8
1069	2.2	-10.8	0.0	-0.4	13.0	5.8
1364	1.8	-10.9	0.0	0.3	12.9	5.9
2107	1.8	-10.9	0.0	-0.3	12.9	5.9
2568	2.5	-4.9	0.0	-0.9	7.7	10.6
1901	2.5	-4.9	0.0	0.9	7.7	10.6
1172	-0.5	-6.5	0.0	-0.2	6.7	12.3
505	-0.5	-6.5	0.0	0.2	6.7	12.3
1057	0.6	-3.8	0.0	-0.9	4.9	17.0
390	0.6	-3.8	0.0	0.9	4.9	17.0
1234	-0.9	-2.8	0.0	-1.0	3.4	25.3
567	-0.9	-2.8	0.0	1.0	3.4	25.3
697	-1.2	-0.3	0.0	-0.2	2.8	31.0
30	-1.2	-0.3	0.0	0.2	2.8	31.1
1162	-0.8	-2.6	0.0	0.3	2.7	32.4
495	-0.8	-2.6	0.0	-0.3	2.7	32.4
2086	1.3	-0.3	0.0	-0.8	2.5	35.0
1385	1.3	-0.3	0.0	0.8	2.5	35.0
727	0.3	-0.1	0.0	-0.8	1.7	50.0
60	0.3	-0.1	0.0	0.8	1.7	50.0
51	-0.8	-0.5	0.0	0.7	1.7	50.4
718	-0.8	-0.6	0.0	-0.7	1.7	50.4
679	0.3	-0.6	0.0	0.2	0.9	96.5
12	0.3	-0.6	0.0	-0.2	0.9	96.5

1 Stress components are listed for the nodes with the 20 highest impact nodal point stress intensity values (see Figure 2.7.8.1-13 for locations of these nodes). Note that S_x is the stress in the radial direction, S_y is the stress in the circumferential direction and S_{xy} is the shearing stress.

2 The allowable stress is $0.7S_u$. S_u is the ultimate strength of 17-4 PH stainless steel at a bounding 600°F, S_u = 126.7 ksi.

THIS PAGE INTENTIONALLY LEFT BLANK

2.7.8.2 Stress Evaluation of the Directly Loaded Fuel Basket Threaded Rods and Spacer Nuts - Accident Condition

In accordance with 10 CFR 71.73(c)(1), a spent-fuel shipping cask is subject to a free drop from a height of 30 feet onto a flat, unyielding surface. The design deceleration for the NAC-STC for the hypothetical accident 30-foot end drop is 56.1g (Table 2.6.7.4.1-2).

For a bottom end drop, the threaded rods and spacer nuts are loaded with the weight of the 31 support disks, the top plate, the 20 aluminum heat transfer disks, and the weights of the threaded rods and spacer nuts. These loads are calculated as follows:

Total weight of basket	=	17,000 lb
Less weight of bottom plate	=	-671 lb
Less weight of fuel tubes	=	-3,666 lb
1g load on the tie rods and spacer nuts	=	12,663 lb
Accident load on tie rods and spacer nuts	=	(12,663)(56.1)
	=	710,394 lb

The effective area of one threaded rod and spacer nut at each of the six locations supporting the weight of the support disks is equivalent to the gross area of the square spacer nut and is calculated as:

$$A = (2.5)(2.5)$$

$$= 6.25 \text{ in}^2$$

The average compressive stress in the threaded rods and spacer nuts is:

$$S_c = \frac{710,394}{(6)(6.25)}$$

$$= 18,944 \text{ psi}$$

Then, the margin of safety is:

$$\text{M.S.} = \frac{0.7\,S_u}{S_c} - 1 = +4.11$$

where

S_u = 131.43 ksi (17-4 PH stainless steel at 405°F)

Therefore, the threaded rods and spacer nuts are structurally adequate for a 56.1g end impact.

2.7.8.3 Assessment of Buckling – Directly Loaded Fuel Basket

During the impact of the NAC-STC cask onto an unyielding surface, the basket will be subjected to compressive loading in the plane of the support disks. Depending on the orientation of the basket, loads acting perpendicular to the plane of the support disk (out of plane) will also be applied. These compressive loadings in conjunction with out of plane bending require that buckling of the basket be a design consideration.

To ensure the stability of the basket, the design of the NAC-STC fuel basket is evaluated using Subsection NF of the ASME Boiler and Pressure Vessel Code, Section III, Division 1. The stability of the basket is maintained by 31 17-4 PH steel support disks and six 17-4 PH threaded tie rods. These two components are evaluated separately.

2.7.8.3.1 Assessment of Buckling of the 17-4 PH Stainless Steel Support Disks

The loads of interest are those generated during a lateral impact of any arbitrary angle (other than an end drop). During the lateral impact, the weight of the fuel assembly is transferred to the support disks. The webs of the support disks furthest away from the plane of impact will experience the least loading while the webs nearest the plane of impact which are transferring the weight of the fuel assemblies will be subjected to maximum compression. Loads in the webs of the fuel basket disk transferring the impact forces can be represented as a direct stress (i.e., uniaxial stress). This characterization categorizes the web as a linear support (Section NF-3300).

Within the design rules for linear supports, two levels of loadings are required to be addressed; Service Level A and B loadings, which corresponds to normal transport, and Service Level D loadings, which is associated with the 30 foot (9 meter) drop.

The forces acting on the basket are derived from the deceleration of the basket. The decelerations corresponding to the 30 foot (9 meter) drop are at least 2.8 times larger than the decelerations corresponding to the 1 foot drop. In comparing the allowables for the Service Level D loads to

loads to the allowables for the Service Level A and B Loads, the maximum increase of allowables is 1.7 (NF-3341.1). The Service Level D loading is the limiting condition.

To address the accident condition, Section NF-3340 can be applied which uses limit analyses to establish allowable loads acting on the support disks. Since out of plane loading is present, the governing conditions are detailed in equations (6), (7) and (8) of Section NF-3342.2.

Equation (6) of NF-3342.2 (b)(3) is specified as

$$\frac{P}{P_{cr}} + \frac{C_m M}{[1 - (P/P_e)] M_m} \leq 1.0$$

where:

P = the load acting in the plane of the web

The maximum compressive load is experienced by the web when the cask is subjected to a side impact. The web with the maximum load is the web nearest the plane of impact. The maximum number accumulation of fuel assembly weights is five. Other basket orientations yield a lower accumulation of weights.

The weight of the fuel assemblies and fuel tubes have a weight per unit length of 10.579 lb/in. Since the centerline to centerline distance of the disks is 4.87 inches, the maximum compressive load due to ten fuel assemblies is (5)(10.579)(4.87) or 257.6 pounds.

Additionally, the weights of the webs are also accumulative. This is conservatively considered in this calculation as the addition of eleven webs or 23.07 lbs.

The total amplified load (55g) is (55)(257.6 + 23.07) or 15.44 kips.

P = 15.44 kips

$P_{cr} = 1.7 A F_a$

where:

A = cross sectional area of the web = (1.5)(.5)
A = .75 in²

F_a = as defined by equation (4) in NF-3322.1(c)(1) for non- austenitic stainless steels

$$F_a = \frac{[1 - (Kl/r)^2 / 2C_c^2]S_y}{5/3 + [3(Kl/r)/8C_c] - [(Kl/r)^3/8C_c^3]}$$

where:

Kl/r = slenderness ratio.

For the weak axis of bending, the radius of gyration is 0.1443 for the 1.5 inch wide and 0.5 inch thick web.

The length (l) of the unbraced span is 9.2 inches, which is the length of the slot containing the fuel assembly.

The factor K is taken to be 0.7 (AISC Steel Construction Manual, 8th edition), which corresponds to the condition of the bottom web. For this particular web, one end is connected to the edge of the basket and the other end is considered to be pinned.

l/r = 63.78

Kl/r = 44.6

S_y = yield strength at temperature (400 °F)
S_y = 89.8 ksi

$C_c = \sqrt{2\pi^2 E / S_y}$

At 400° for 17-4 PH (SA 693, Type 630), E = 26,500 ksi, S_y = 89.8 ksi

C_c = 76.32 (Note that $l/r < C_c$ for NF-3342.2 (b)(1))

substituting into the expression for F_a,

F_a = 40.02 ksi

P_{cr} = 51.02 kips

C_m = interaction coefficient = 1.0 (conservatively)

M = maximum bending moment due to the out of plane bending

The moment (M) acting out of plane is due to the axial component of the deceleration. The maximum deceleration for any side or oblique drop, other than the end drop, is 55g. The maximum moment is computed by considering the web with the maximum compression as a simple span beam. Using a length of 9.204 inches, and 0.283 lb/in^3 as the density for steel, the maximum moment acting on the web is:

M = 123.5 lb-in

P_e = 1.92 A F_e'

where F_e is defined by equation NF-3322.1 (e)

$$F_e' = \frac{12\pi^2 E}{23\,Kl/r}$$

F_e' = 68.60

$P_e = 1.92\ (1.5 \times 5)(68.6)$

$P_e = 98.78$

$M_p = S_y Z$

where:

Z = plastic section modulus for the weak axis bending (1.5 inch width, .5 inch thickness), from Roark for a rectangular cross section

$Z = 0.25\ (1.5)\ (0.5^{\,2}) = 0.09375\ \text{inch}^3$

$M_p = 8.4188$ kip-in

The maximum critical moment that can be resisted by a plastically designed member in the absence of axial load, M_m

$$M_m = M_p \left(1.07 - \frac{(1/r\sqrt{S_y})}{3160}\right)$$

$M_m = 0.8787\ M_p$

$M_m = 7.398$ in-kip

By substituting the computed quantities into equation (6) of NF-3342.2 (b)(3),

$$\frac{15.44}{51.02} + \frac{(1)(0.1235)}{(1 - 15.44/98.78)7.398} \leq 1.0$$

$0.283 \leq 1.0$

The margin of safety is:

$$\text{M.S.} = \frac{1.0}{0.283} - 1 = \underline{+2.53}$$

The first term in the above equation is also equation (5) of NF-3342.2 (b)(2) and the corresponding margin of safety is 51.02/15.44 - 1, or +2.30.

Equation (7) of NF-3342.2 (b)(3) is specified as:

$$\frac{P}{P_y} + \frac{M}{1.18\,M_p} \le 1.0$$

where:

P_y = the axial plastic load = yield strength times cross sectional area

P_y = 67.35 kips

substituting

$$\frac{15.44}{67.35} + \frac{0.1235}{1.18(8.4188)} \le 1.0$$

$$0.242 \le 1.0$$

The margin of safety is:

M.S. = 1.0/0.242 - 1 = +3.13

Also note for this equation, that for M = 0.1235 kip-in and M_p = 8.4188 kip-in, $M < M_p$ for which the margin of safety is:

M.S. = 8.4188/0.1235 - 1 = +67.1

2.7.8.3.2 Assessment of Buckling of the 17-4 PH Threaded Rods

2.7.8.3.2.1 Maximum Compressive Load

The maximum compressive load applied to the threaded rods are during the 30 foot (9 meter) end drop, which corresponds to a maximum deceleration of 56.1 g's.

During the end impact, the weight of the support disks, aluminum heat transfer disks, are transferred to the threaded rods. The forces due to the weight of the fuel assemblies is transmitted directly to the end plate of the cask cavity.

The threaded rods transferring the load can be represented as a direct stress (i.e., uniaxial stress). This characterization categorizes the rod as a linear support (Section NF-3300).

To address the accident condition, Section NF-3340 can be applied which uses limit analyses to establish allowable loads acting on the support disks. Since out of plane loading is not present, the governing conditions are detailed in equation (5) of Section NF-3342.2, which specifies the allowable compressive force (P_{cr}).

$$P_{cr} = 1.7 \, A \, F_a$$

The maximum force ($P_{max} \leq P_{cr}$) transmitted to a threaded rod is based on the weight of the basket less the weight of the fuel tubes and the bottom weldment (The bottom weldment weighs 671 pounds while the fuel tubes weight 3,666 pounds). The total weight transmitted by the six rods is 12,663 pounds.

The design of the basket is not sufficiently symmetrical to distribute the loading to the threaded rods in an equal fashion. To determine the distribution of the loads to the threaded rods in an end drop orientation, a finite element model of a single support disk was generated. The model of the entire disk shown in Figure 2.7.8.3-1 uses the ANSYS plate element (STIF63). The material properties for 17-4 PH employed in the model corresponds to the maximum basket temperature at 500°F. While the temperature does vary throughout the basket, the effect on the variation

of the modulus of elasticity and the corresponding effect on the load distribution to the rods is considered to be insignificant.

The support of the threaded rod is simulated by restraining the out of plane degree of freedom at the centerline of the location of the threaded rod connection with the support disk. A 1g load was applied to the elements comprising the support disk. The nodal reactions were used to determine the load distribution to the threaded rods. The four threaded rods at location A in Figure 2.7.8.3-1 have the same reaction value and carry 74.5% of the weight of the support disk, 18.6% per rod. The remaining two threaded rods, which are also of equal value carry 25.5% of the weight of the disk, 12.8% per rod. The limiting load for the threaded rod is 18.6% of the weight of the support disk.

The maximum load to be considered for the threaded rod is 12,663 pounds amplified by 56.1 g and factored by 0.186, or P_{max} = 132.13 kips.

The axial compressive stress permitted in the threaded rod, F_a, is computed in the same manner as in Section 2.7.8.3.1. In the section of the threaded rod experiencing the maximum compressive load, the span is considered as a simple span configuration and the length corresponds to the centerline to centerline distance between the support disks. The simple span condition requires the effective length factor, K, to equal 1.0 (AISC Steel Construction Code, Eight Edition). Using the minor diameter to compute the radius of gyration, $Kl/r = 13.279 < C_c$. Using $C_c = 75.70$, F_a is determined to be 52.87 ksi and P_{cr} is 152.79 kips.

The margin of safety for equation (5) of NF-3342.2 is:

M.S. = 154.58/132.13 - 1 = + 0.17

2.7.8.3.2.2 Maximum Combined Axial and Bending Loads

In drop orientations other than the end drop, the aluminum heat transfer disks, which are supported by the threaded rods, will exert a lateral component on the threaded rods. This will induce bending moment into the threaded rod. It is assumed that the entire weight of one aluminum heat transfer disk will be carried by a single threaded rod carrying the maximum compressive load. This is conservative since the location of the closest aluminum fin to the

bottom of the cask will only experience the weight of 20 support disks instead of 31 disks as in this calculation.

The combined loading is governed by equations NF-3342.2 (6) and (7).

For equation NF-3342.2 (6),

$$\frac{P}{P_{cr}} + \frac{C_m M}{[1 - (P/P_e)]M_m} \leq 1.0$$

Assuming that the mass of the heat transfer disk acts as a point load at the mid span, the maximum moment for a simple span beam is:

$$M = F l / 4$$

where:

F = weight of the heat transfer disk times the lateral deceleration

As the cask assumes other angles, the maximum deceleration varies. Since the maximum decelerations decrease from 56.1 g's at 0° (end drop) to 33.8 g's at 60°, it is conservative to assume the maximum deceleration is 56.1 g's. The lateral deceleration is 56.1 sin q , where q is the angle measured from the vertical to the centerline of the cask body. The weight of the aluminum heat transfer disk is 105 pounds.

$F = 56.1 (.105) \sin q$ (kips)

$l = 4.88$ inches

$M = 7.186 \sin q$ (kip-in)

The axial load on the rod at some angle of notation, q, is determined by 125.63 cos q kips, then P in the above equation is 125.63 cos q.

$$P_e = 1.92\ A\ F_e'$$

where $F_{e\_}$ is defined by equation NF-3322.1 (e)

$$F_{e\_} = \frac{12\pi^2 E}{23(Kl/r)^2}$$

$$F_{e\_} = 773.87$$

$$P_e = 1.92\ A\ F_e'$$

$$P_e = 2644.78$$

$$M_p = S_y Z$$

where

Z = plastic modulus for the weak axis M bending
$1.333\ R^3$

$$Z = 1.333\ (.735)^3\ \text{inch}^3$$

$$M_p = 47.53\ \text{kip-in}$$

The maximum critical moment that can be resisted by a plastically designed member in the absence of axial load, $M_m = M_p$

$$M_m = 47.53\ \text{kip-in}$$

By substituting the computed quantities into equation (6) of NF-3342.2,

$$\frac{125.63\cos\theta}{154.54} + \frac{(1)(7.186\sin\theta)}{(1-125.63\cos\theta/2644.78)\,47.53} \le 1.0$$

or

$$0.81272\cos\theta + \frac{0.1512\sin\theta}{1-.0475\cos\theta} \leq 1.0$$

It is necessary to determine the angle θ which maximizes the left side of the inequality. The maximum ratio of 0.828 occurs at θ = 11.0°.

The margin of safety for equation NF-3342.2 (6) is:

M.S. = 1.0/0.828 - 1 = +0.21

Equation (7) of NF-3342.2 is specified as:

$$\frac{P}{P_y} + \frac{M}{1.18\,M_p} \leq 1.0$$

where:

P_y = the axial plastic load = yield strength times cross sectional area

P_y = (1.78)(89.8) kips

P_y = 159.84 kips

substituting

$$\frac{125.63\cos\theta}{159.84} + \frac{(1)(7.186\sin\theta)}{1.18(47.53)} \leq 1.0$$

or

$$0.7856\cos\theta + 0.1281\sin\theta \leq 1.0$$

By taking the derivative and setting it to zero the maximum angle is determined to be $\theta = 9.26°$.

Substituting for $\theta = 9.26$, Equation (7) of NF-3342.2 becomes:

$$0.796 \leq 1.0$$

The margin of safety for equation NF-3342.2 (7) is:

M.S. = 1.0/0.796 - 1 = +0.26

Also note that for M = 1.156 kip-in and M_p = 47.53 kip-in, $M < M_p$ for which the margin of safety is:

M.S. = 47.53/1.156 - 1 = +40.12

2.7.8.3.3 Summaries of Margins for NF-3400 Evaluation of Buckling

For the 17-4 PH stainless steel support disk and threaded rod, the margins of safety are summarized below:

Equation	Support Disk	Threaded Rod
NF-3342.2 (5)	+2.30	+0.23
NF-3342.2 (6)	+2.11	+0.21
NF-3342.2 (7)	+3.13	+0.26

Based on Subsection NF-3340 of the ASME Boiler and Pressure Vessel Code, Section III, the NAC 17-4 PH stainless steel basket design will maintain stability against buckling for the hypothetical 30 foot (9 meter) drop onto an unyielding surface.

Figure 2.7.8.3-1 Finite Element Model of a Support Disk

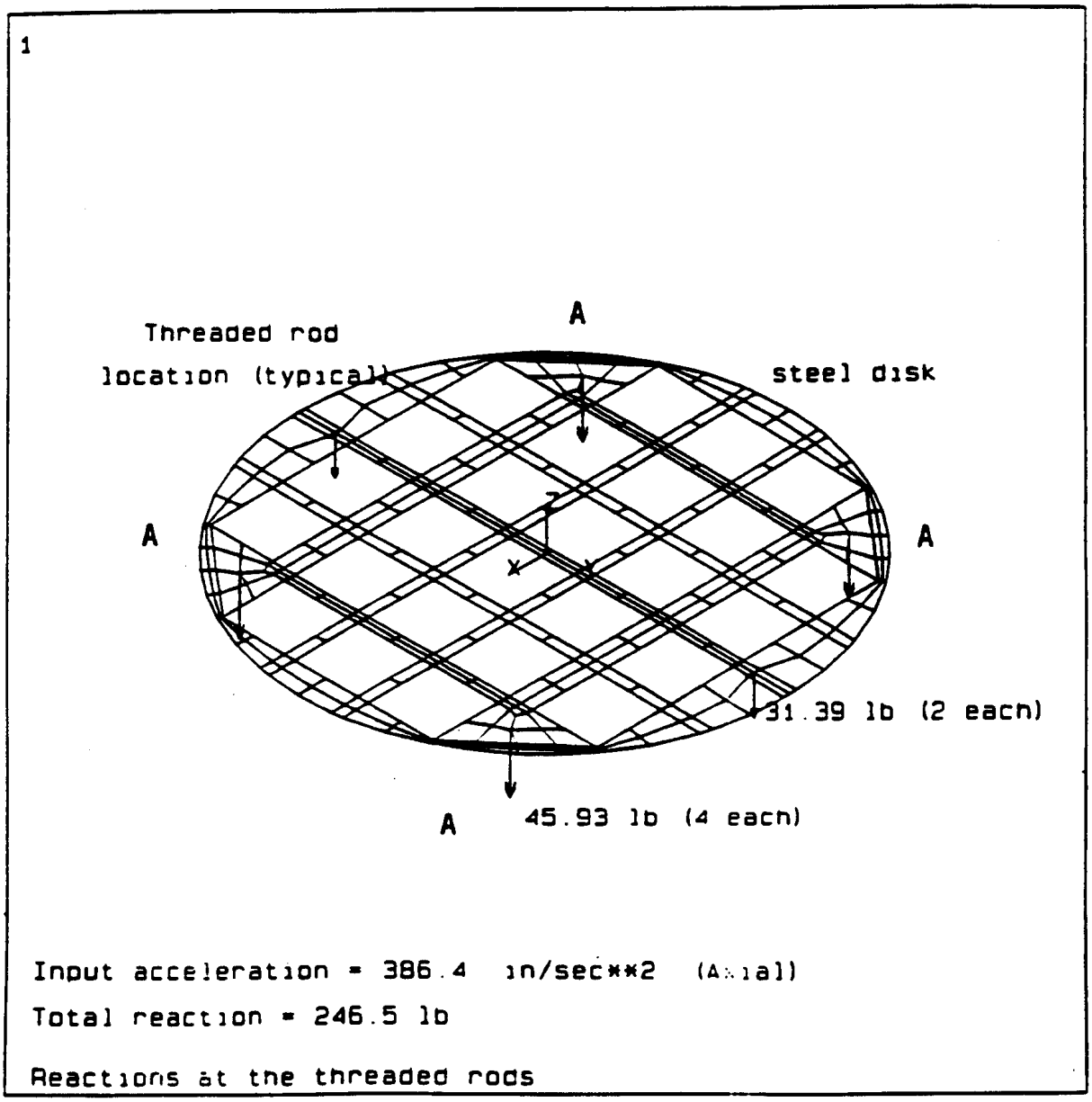

THIS PAGE INTENTIONALLY LEFT BLANK

2.7.8.4 Directly Loaded Fuel Basket Fuel Tube Analysis

The fuel tube provides a foundation and cavity to mount neutron absorber sheets within the fuel basket structure and does not provide a structural function relative to the support of the fuel assembly. The fuel tube design is presented in Figure 2.7.8.4-1. To ensure that the fuel tube remains functional when the cask is subjected to design load conditions, a structural evaluation of the tube has been performed for both the end and side impact load conditions.

2.7.8.4.1 Fuel Tube End Impact Analysis

During the postulated cask end impact, fuel assemblies are supported by the cask bottom plate for the bottom end drop and the inner lid for the top end drop. Fuel assembly load is not carried by the fuel tubes. Therefore, evaluation of the fuel tube for the end impact load is performed considering the weight of the fuel tube subjected to the cask deceleration carried by the minimum tube cross section. The tube minimum cross section is located at the contact point of the tube with the bottom weldment. From the dimensions of the tube shown in Figure 2.7.8.4-1 the minimum cross section area is:

$$\begin{aligned} \text{Area} &= (\text{Thickness})(\text{Mean Perimeter}) \\ &= [0.048][(4)(8.876 - 0.048) - 1] \\ &= 1.647 \text{ in}^2 \end{aligned}$$

The total bearing load on the tube during the cask bottom end impact is 7910 pounds, (56.1 g x 141 lb). The maximum compressive and bearing stress in the fuel tube is 4800 psi, (7910/1.647). Limiting the compressive stress level in the tube to the material yield strength ensures the tube remains in position when the cask is subjected to the postulated end drop. Type 304 stainless steel yield strength is 19,400 psi at a conservatively high temperature of 500°F for the axial location on the fuel tube, which has the minimum cross section area. Using this criteria to evaluate the tube for the end drop load, a positive margin of safety of +3.04 is achieved.

2.7.8.4.2 Fuel Tube Side Impact Analysis

During the cask side impact load configuration the fuel tube is supported by the fuel basket 31 stainless steel support disks. The fuel basket support disks are spaced at 4.37 inches, which is less than one half of the fuel tube width of 8.88 inches, and provide support for the full length of the fuel tube. Considering the fuel tube subjected to the 55 g side impact deceleration and the 31 support locations provided by the basket support disks, the fuel tube shear stress is:

Impact Shear Load = (55)(141)/31 = 250 lb

Shear Area of Tube = (0.048)(8.88)(2) = 1.17 in^2

Shear Stress of Tube = 250/1.17 = 213 psi

The ultimate strength (S_u) of Type 304 stainless steel at 500°F is 63,500 psi. The allowable shear stress of the tube wall material is $0.42S_u$ = 26.7 ksi which results in a large positive margin of safety. It is evident from the conservative evaluation of the tube loading resulting from its own mass during the side impact configuration that the tube structure will maintain position and function.

In addition to the above evaluation, the load transfer of a fuel assembly to the fuel basket support disk when the cask is subjected to a side impact will be through direct bearing and compression of the distributed load of the fuel assembly through the fuel tube to the support disk web. For purposes of the tube evaluation, two load conditions and tube wall thicknesses are evaluated. One analysis postulates that the fuel assembly grid is located at the center of the span between the support disks and produces a localized distributed load over the effective area of the grid. The second analysis considers the fuel assembly load as a distributed pressure on the inside tube surface. The fuel tube structural performance is nonlinear when subjected to either of the postulated impact loadings and is not adequately evaluated using classical methods. Therefore, a finite element model of the tube is developed representing three support disk tube span lengths and analyzed for the imposed loading of the fuel assembly grid at mid-span of the modeled central span

to evaluate maximum accumulated plastic strain. The finite element model was then modified to consider the main tube wall thickness of 0.048 inches as the only material subjected to a distributed pressure load representative of the fuel assembly deceleration of 55g. Figure 2.7.8.4-2 presents the half symmetry fuel tube finite element model for the maximum plastic strain fuel tube grid loading evaluation. Figure 2.7.8.4-3 presents the half symmetry fuel tube finite element model used for the maximum plastic stress fuel assembly distributed loading evaluation. Fuel assembly stiffness is not considered in the development of the imposed load to the fuel tube for either of the two analyses.

The tube is modeled with the ANSYS plastic, quadrilateral shell element (STIF43) with large deflection capability. All energy is absorbed into tube strain by conservatively fixing the displacement of the tube at support disk spacing perpendicular to the direction of load. Material properties reported in NUREG/CR-0481, SAND 77-1872, "An Assessment of Stress-Strain Data Suitable for Finite-Element Elastic-Plastic Analysis of Shipping Containers," are used in these analyses.

Results from the maximum plastic strain evaluation, which loaded the grid surface area and absorbed all energy into the tube wall produced a strain level of 0.036 inch/inch as summarized in Table 2.7.8.4-1. Type 304 stainless steel is a material with high ductility and capacity to absorb significant strain without failure. ASME material specification requirements dictate 40 percent minimum elongation for the defined tube structural material. The maximum strain level of 0.036 inch/inch, or 3.6 percent demonstrates that the fuel tube maintains functional capacity when considering assembly deceleration at the localized fuel assembly grid locations.

Results from the 55g fuel assembly distributed load on the main tube wall, 0.048 inch thick, verifies that the maximum plastic stress in the tube is less than 31 ksi. This maximum plastic stress is local to the sections of the tube resting on the steel support disks. Over 72 percent of the tube does not exceed the material yield strength. Figure 2.7.8.4-4 depicts the elastic-plastic stress distribution over the fuel tube subjected to the side drop distributed pressure load. The maximum plastic stress is more than a factor of two less than the tube wall material minimum ultimate strength of 63.5 ksi.

Defining acceptable elastic-plastic response at one half the material performance permits margins of safety to be evaluated with significant margin beyond the chosen limits relative to actual material failure. Using this methodology to evaluate total cumulative strain shows a margin of safety of:

$$M.S. = \frac{40/2}{4} - 1 = 4.0$$

Similarly, the margin of safety for elastic-plastic stress becomes:

$$M.S. = \frac{(63.5 - 19.4)}{(31-19.4)} - 1 = 0.9$$

More than 72 percent of the tube wall is below the material yield strength. Both evaluations of maximum cumulative plastic strain and maximum elastic-plastic stress result in significant margin when evaluated with respect to an allowable chosen to be 50 percent of the material allowable plastic response.

It is evident from both the maximum cumulative strain, and the elastic-plastic stress analyses that the tube position within the support basket is maintained.

Assurance that the BORAL poison remains within the sealed casing has been evaluated considering loads produced by the BORAL and skin mass decelerated by 55g's being maintained by the seal weld. Total load and resultant stress is calculated as follows:

$F = \text{Volume} \times \text{Density} \times 55$

$F_{BORAL} = (8.18 \times 0.075 \times 4.37) \times 0.10 \times 55$

$= 14.7$ pounds

$F_{Skin} = \{[9.064 - 2(0.019 + 0.075 + 0.13)] \times 0.019 \times 4.37\} \times 0.288 \times 55$

$= 11.3$ pounds

Total load per inch of seal weld becomes:

F_{Weld} = (F_{BORAL} + F_{Skin}) / weld length

= (14.7 + 11.3) / (2 x 4.37)

= 2.97 pounds / inch

The fuel tube skin seal weld provides more material thickness than the skin material thickness. Material stress is calculated based on the thickness of the stainless steel skin. Using the load per unit length acting at the weld area, calculated above, the stress produced in the skin along the seal weld in the stainless steel skin is:

S_{Seal} = 2.97 / 1 x 0.019 = 156 psi

This additional load and material stress, 156 psi, transferred into the main tube wall analyzed for cumulative plastic strain and maximum elastic-plastic stress with a maximum stress intensification factor of 4 remains insignificant relative to the margins of 4.0 and 0.9 respectively. Therefore, it is evident that the fuel tube will remain in position within the fuel basket assembly and that the sealed BORAL remains within the sealed cavity on each outer surface of the tube wall.

This evaluation shows that the impact stress in the seal weld would be less than 200 psi. Therefore the seal weld and outer skin will maintain confinement of the BORAL material.

Figure 2.7.8.4-1 Fuel Tube Configuration

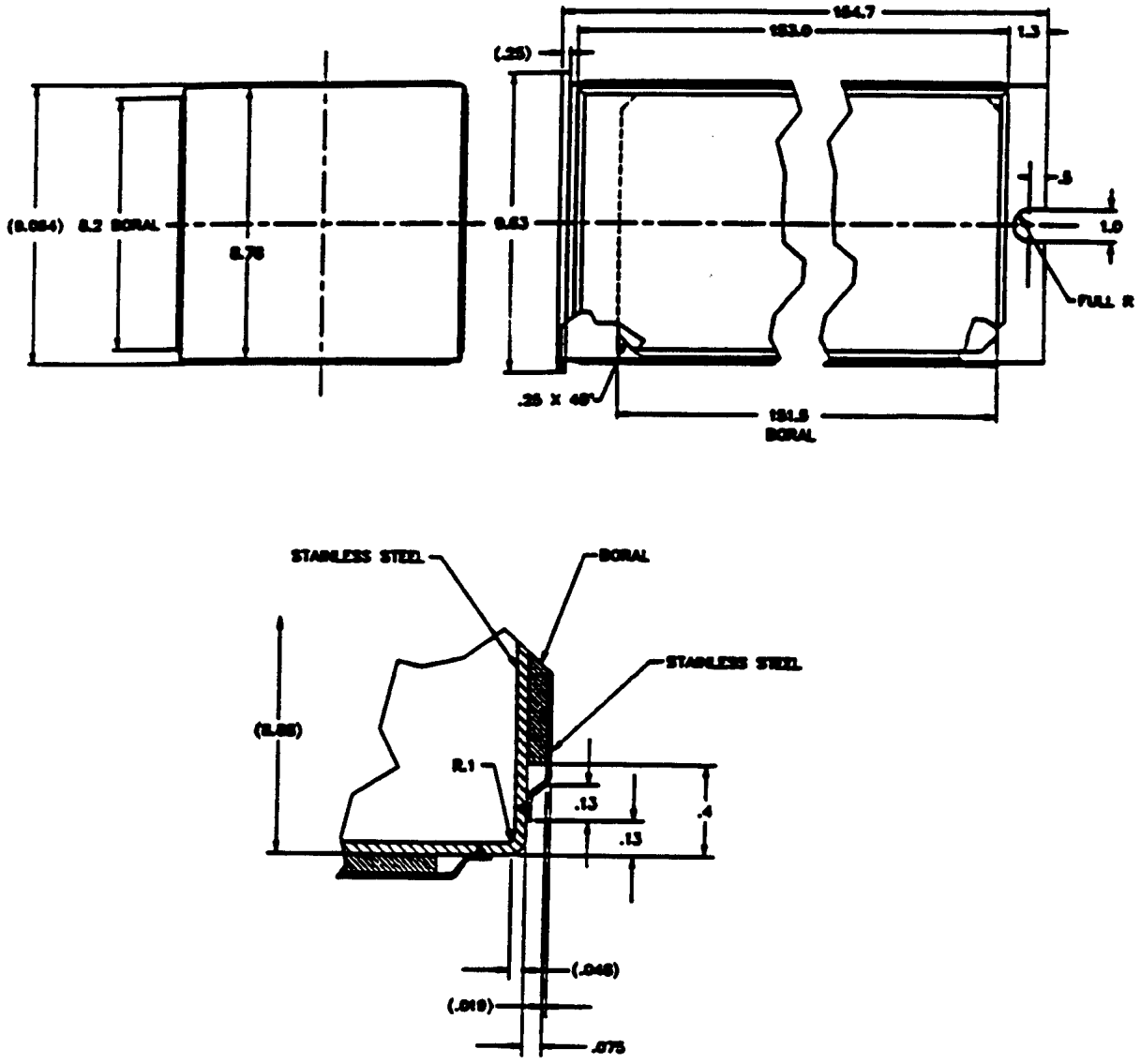

Figure 2.7.8.4-2 Fuel Tube Finite Element Model Grid Loading

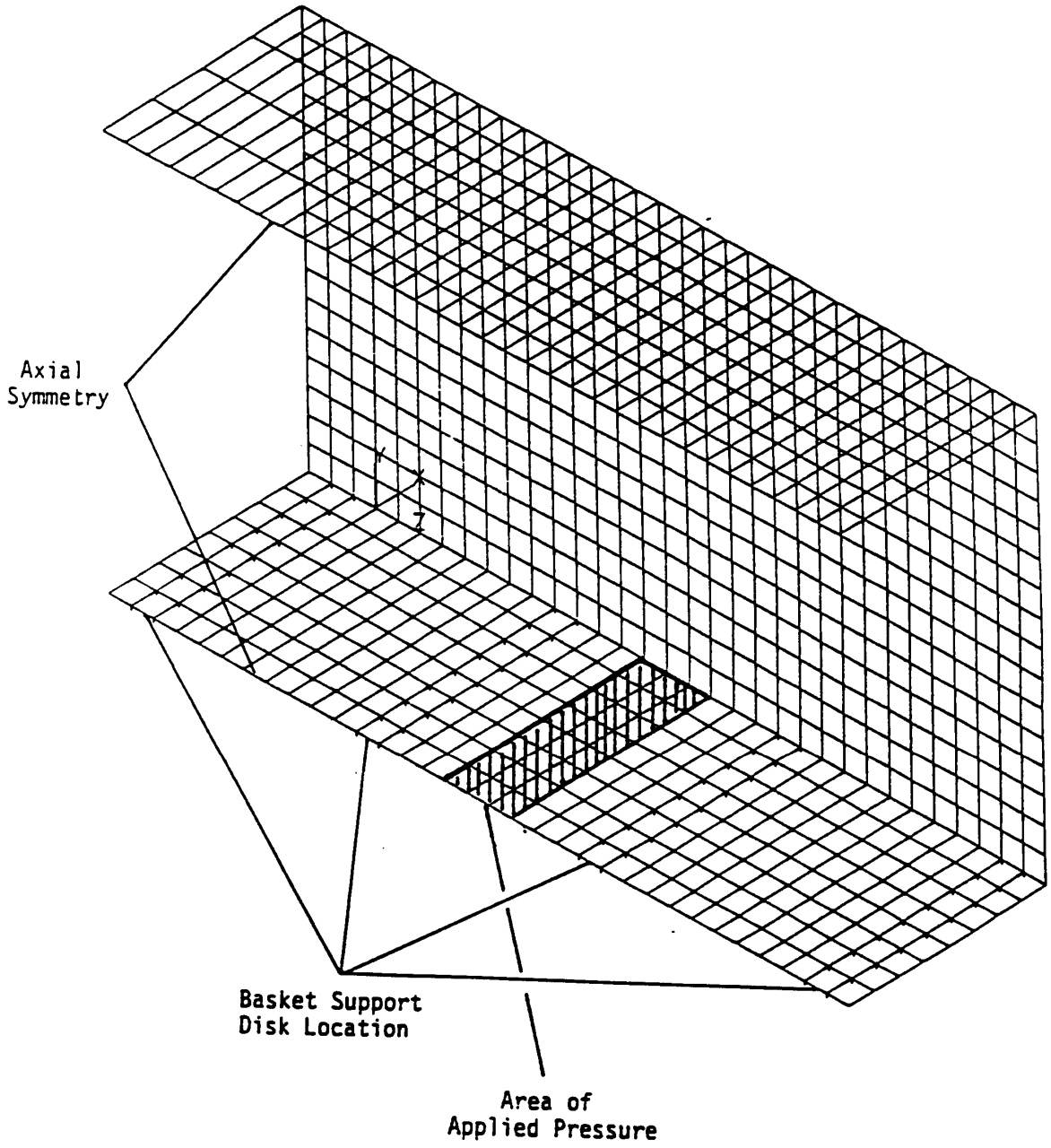

Note: Tube Wall Cumulative Strain Evaluation Considers the Main Tube Wall and Skin Encasement, t = 0.048 + 0.019 = 0.067 inches

Figure 2.7.8.4-3 Fuel Tube Finite Model Distributed Pressure Loading

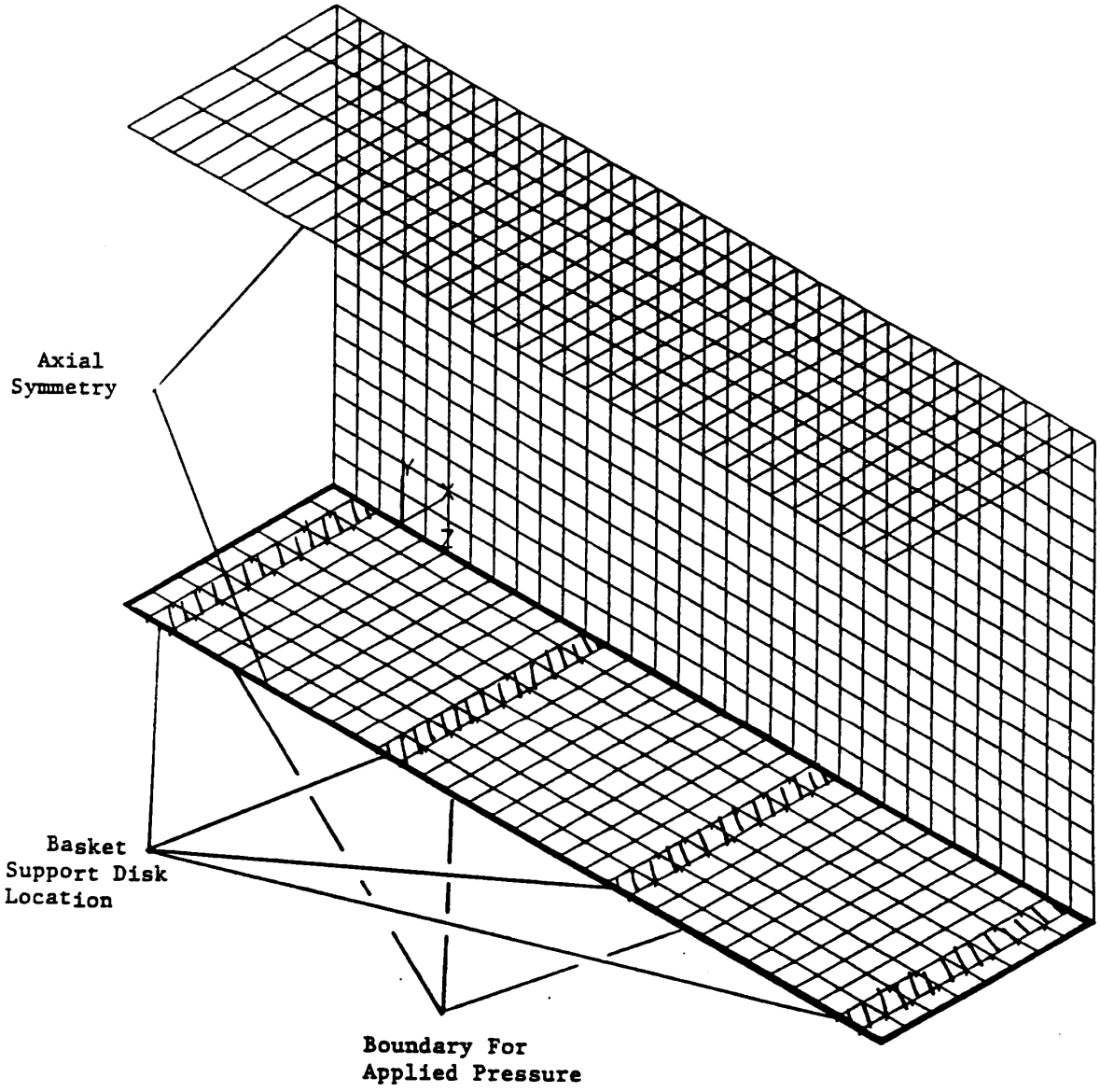

Note: Tube Wall Stress Evaluation Considers the Main Tube Wall Only, t = 0.048 inches

Figure 2.7.8.4-4 Elastic-Plastic Stress Distribution

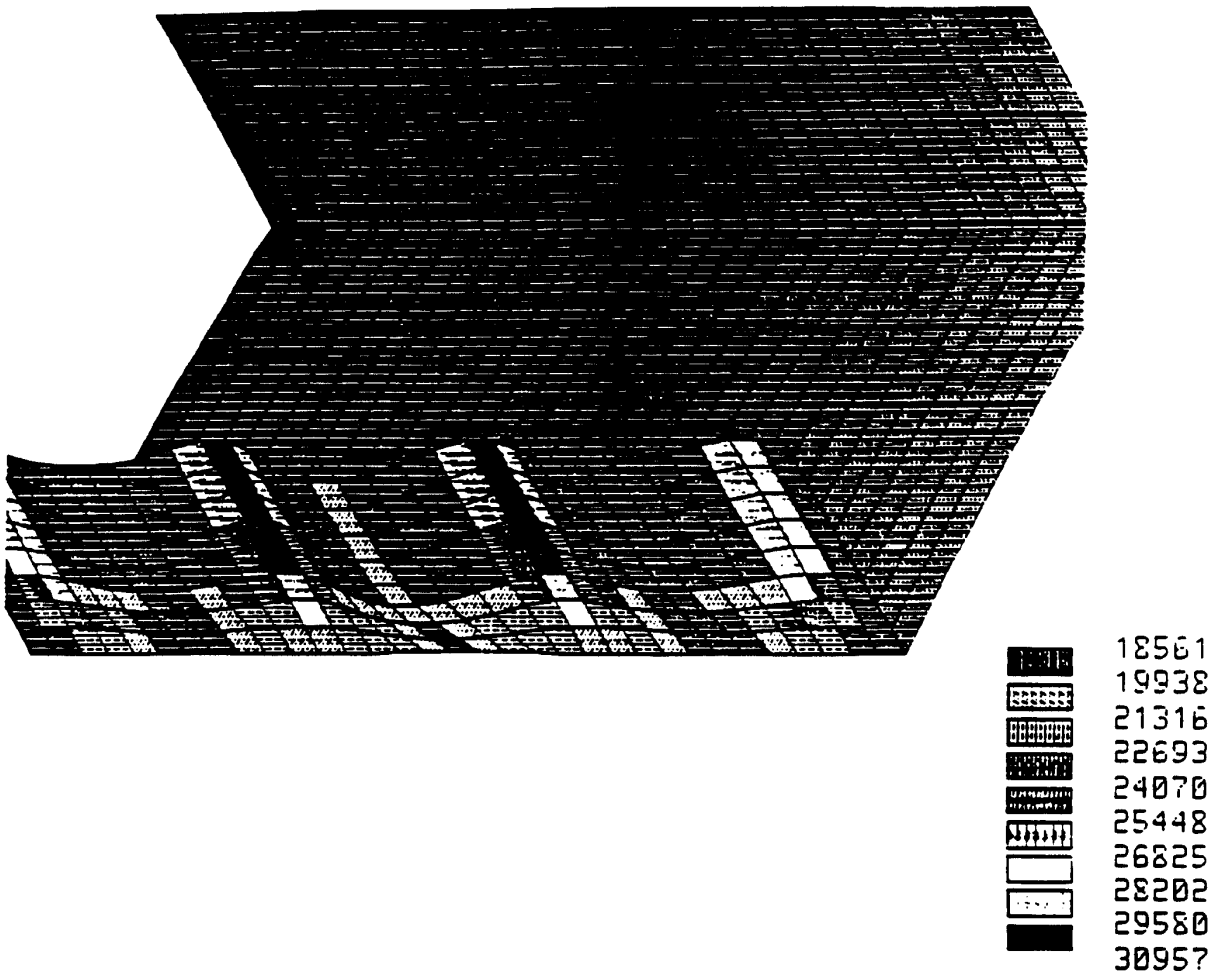

Note: 55g Fuel Assembly Distributed Load

Table 2.7.8.4-1 Ten Highest Strain Points for Total Energy Analysis

ELEMENT	STRAIN IN/IN
51	0.0356
1	0.0356
54	0.0354
4	0.0354
57	0.0354
7	0.0354
60	0.0350
10	0.0350
63	0.0348
13	0.0348

2.7.8.5 Directly Loaded Fuel Basket Weldment Analysis for 30-Foot End Drop

The response of the top and the bottom weldment plates of the fuel basket assembly to a 56.1g accident condition deceleration load are examined. The top and bottom weldment plates are both 1-inch thick and fabricated from SA 240, Type 304 stainless steel. The top weldment supports its own weight as well as the weight of the 26 fuel tubes (without the fuel assemblies) during a 30-foot top end drop. Similarly the bottom weldment supports its own weight and also the weight of the 26 fuel tubes (without the fuel assemblies) during a 30-foot bottom end drop. The responses of the end plates to the 30-foot end drop are analyzed using ANSYS STIF63 three-dimensional, six degrees of freedom, elastic quadrilateral shell elements. The finite element model for both weldment plates and the corresponding boundary condition of each weldment plate are shown in Section 2.6.12.13, Figure 2.6.12.13-1 through Figure 2.6.12.13-3. The evaluation is based on material properties of SA 240, Type 304 at a conservative temperature of 500°F. The hottest steel support disk during normal transport conditions is 498°F, see Table 3.4-1.

The primary membrane plus primary bending stress in the top weldment plate for the 30-foot top end drop is 61.9 ksi. The primary membrane plus primary bending stress in the bottom weldment plate for the 30-foot bottom end drop is 51.3 ksi. At 500°F, the accident condition stress allowable, S_u is 63.5 ksi. The minimum margin of safety for the top weldment plate and the bottom weldment plate are +0.03 and +0.24 respectively. Therefore, the structural adequacy of the NAC-STC fuel basket weldment end plates for the accident condition of transport is demonstrated.

THIS PAGE INTENTIONALLY LEFT BLANK

2.7.9 Yankee-MPC Fuel Basket Analysis - Accident Conditions

The Yankee-MPC fuel basket is a right cylinder structure and is fabricated with the following components: square fuel tubes, circular support disks, heat transfer disks, tie rods with split spacers, and two end weldment plates. The basket components and their geometry are illustrated in Figure 2.7.9-1 and Figure 2.6.14-2.

Three basket configurations incorporate two fuel tube configurations and a damaged fuel can configuration. The three-basket configurations accommodate 36 standard fuel tubes, 32 standard fuel tubes and four enlarged fuel tubes at the four basket corner positions, or 32 standard fuel tubes and four damaged fuel cans at the four basket corner positions. The three basket configurations are not interchangeable.

The standard fuel tube has a 7.80-inch square inside dimension, 0.141-inch thick composite wall, and holds the design basis Yankee Class fuel assembly. Figure 2.6.14-3 shows the details of the stainless steel tube with the encased BORAL. The fuel tubes are open at each end; therefore, longitudinal fuel assembly loads are imparted to the canister body and not the fuel basket structure. The fuel assemblies, together with the tubes, are laterally supported in the holes in the stainless steel support disks. No structural credit is taken for the BORAL sheet.

The enlarged fuel tube has a square interior cross-section of 8.0 inches, but does not have exterior BORAL sheets on the sides. These larger cross-section fuel tubes can accommodate fuel assemblies that exhibit slight physical deformations (e.g., twist, bow) that could preclude loading in the smaller cross-section standard fuel tubes.

The enlarged fuel tubes are restricted to the four corner positions of the basket as shown in Figure 2.6.14-4. When installed, the standard and enlarged fuel tubes are captured between the top and bottom weldments of the fuel basket. To permit full access to the enlarged fuel tubes, the corner positions of the top and bottom weldments used in this basket configuration are also enlarged. However, the enlarged fuel tubes remain captured between the basket top and bottom weldments.

The damaged fuel can is similar to the enlarged fuel tube in that it does not have exterior BORAL sheets on the sides and is restricted to the four corner positions of the basket. The damaged fuel can is closed on its bottom end by a stainless steel bottom plate with screened openings. After being loaded, the can is closed on its top end by a stainless steel lid that also has screened openings. The top plate and can body incorporate lifting fixtures that allow handling of the loaded can, if necessary, and installation and removal of the can lid. The damaged fuel can extends through the bottom and top weldments of the basket, and is captured between the shield lid configured for damaged fuel cans and the canister bottom plate. The damaged fuel can lid is held in place by the canister shield lid, which is machined on the underside in four places to mate with the damaged fuel can lid. The screened openings in the damaged fuel can lid allow for filling, draining, and vacuum drying the damaged fuel can, but preclude the release of gross particulate material to the canister interior. The damaged fuel can may also hold an intact fuel assembly.

The size of the top and bottom weldment openings in the four corner positions of the damaged fuel basket allow removal or insertion (if necessary) of the damaged fuel can with the basket assembled. Consequently, the damaged fuel can is not captured between the weldments.

Since the standard fuel tube has BORAL and stainless steel sheathing attached, the external dimensions of the standard fuel tube, the enlarged fuel tube without BORAL, and the damaged fuel can without BORAL, are identical. Therefore, the support disks and heat transfer disks used in the three basket configurations are identical. In all three basket configurations, the fuel assemblies, together with a combination of fuel tubes and damaged fuel cans, are laterally supported in the holes of the stainless steel support disks. Because the enlarged fuel tube is not equipped with BORAL and stainless steel sheath, the actual weight is less than that of the standard fuel tubes (approximately 20 pounds less). Therefore, the load applied to the basket with enlarged fuel tubes is slightly less than that of the standard fuel tube configuration. The weight of the damaged fuel can is approximately 22 pounds heavier than that of the standard fuel tube. However, as discussed in Section 2.6.14.1, a conservative fuel weight is employed in the basket evaluation and, therefore, the evaluation provided in Section 2.7.9.1 bounds all basket configurations and weights.

Each support disk is 0.5-inch thick, 69.15 inches in diameter and has 37 holes that are each 8.254 inches square. There are three web thicknesses in the support disks: 0.875 inch, 0.810 inch, and 0.75 inch. The widest web is nearest the center of the basket, and the web decreases in width

towards the outer radius of the basket. The support disks are equally spaced at 4.41 inches except for the disk nearest the bottom weldment, which is spaced 6.50 inches from the bottom weldment plate. The weldments are geometrically similar to the support disks and are one-inch thick and 68.98 inches in diameter. The tie rod has 3.0 inches of 1 1/8-8 UN-2B threads at the upper end of the rod, which corresponds to the top of the basket. Fourteen (14) aluminum heat transfer disks are located at the midsection of the cavity to fully optimize the passive heat rejection from the package. Each heat transfer disk is 0.50 inch thick, 68.87 inches in diameter, and has 37 holes that are 8.224 inches square. There are three different web widths: 0.905 inches, 0.84 inch, and 0.78 inch. The widest aluminum web is nearest the center of the basket to optimize the passive heat rejection. The dimensional differences between the heat transfer disk and the support disk accommodate the different rate of thermal growth between aluminum and stainless steel, preventing interference between the tube, the support disk, and heat transfer disks. The heat transfer disks, which serve no structural function, are supported by the eight tie rods with split spacers. The center hole of the support and heat transfer disks is not accessible as the center hole position is blocked by the top end weldment plate, which has only 36 fuel tube positions.

The fuel basket contains the fuel and is laterally supported by the canister shell. The 22 support disks and two (2) end plates are fabricated from Type 17-4 PH and Type 304 stainless steels, respectively. The 14 heat transfer disks are fabricated from Type 6061-T651 aluminum alloy. The 36 fuel tubes are fabricated from Type 304 stainless steel. The tie rods and spacers are fabricated from Type 304 stainless steel. The stainless steel tubes are not considered to be a structural component with respect to the disks and are not included in the basket or weldment analyses. The primary function of the split spacers and the threaded top nut is to locate and structurally assemble the support disks, heat transfer disks, and the top and bottom weldment plates into an integral assembly. The spacers carry the inertial weight of the support disks, heat transfer disks, one end plate, and their own inertial weight for a hypothetical accident condition, 30-foot end drop. The end drop loading of the split spacers and tie rods represents a classical closed form structural analysis. Therefore, the only component that requires a detailed finite element analysis is the support disk.

The fuel basket is evaluated for the hypothetical accident condition loads in this section and is evaluated for the normal transport loads in Section 2.6.14.

Figure 2.7.9-1 Yankee-MPC Fuel Basket Assembly

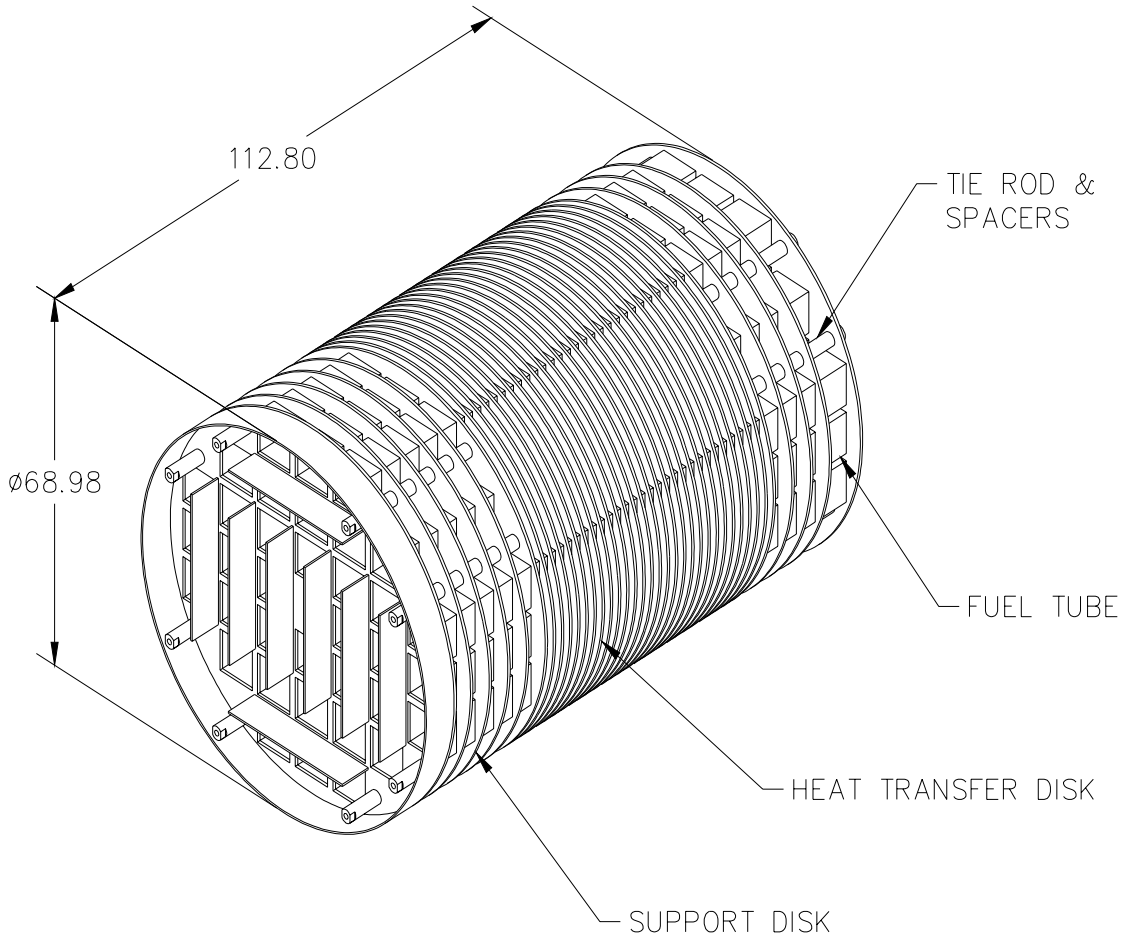

2.7.9.1 Detailed Analysis – Yankee-MPC Fuel Basket

Based on criticality control requirements, the Yankee-MPC basket design criteria requires the maintenance of fuel support and control of spacing of the fuel assemblies for all load conditions. The structural design criteria for the fuel basket is the ASME Boiler and Pressure Vessel Code, Section III, Division 1, Subsection NG, "Core Support Structures." Consistent with this criteria, the main structural component in the fuel basket, the stainless steel support disk, is shown to have a maximum primary membrane stress intensity less than the allowable stress limit, defined as 0.7 S_u, for the accident condition. Likewise the primary membrane plus bending stress intensity is shown to be less than the allowable stress limit, defined as 1.0 S_u. The value of S_u is defined at conservatively high temperatures for the component being analyzed.

The structural evaluation for the support disks considers various cask drop orientations as well as various basket drop orientations. The cask drop orientation is defined in Figure 2.7.9.1-1; end drop (ϕ=0°), side drop (ϕ=90°) and off-angle drops (0° < ϕ < 90°). For the side drop conditions, three basket drop orientations (0°, 22.9°, and 45°) are considered, as shown in Figure 2.6.14.1-1. Angles of 22.9° and 45° were selected because minimum web thickness occurs at those orientations. A parametric study in Section 2.10.11.1 indicates that the 22.9° drop case is bounded by the 45° drop case. Therefore, detailed analysis is performed for the 0° and 45° basket orientations for side drop conditions.

In the side drop, the loads of the fuel assemblies are transferred into the plane of the support disks, from which they are transmitted to the canister shell, and then to the cask body (cask inner shell). For conservatism, a bounding load case is considered where 950 lb/fuel assembly × 36 loading positions for a total 34,200 pounds of fuel is applied to the basket. Therefore, the analyzed weight is greater than the limiting total fuel weight of 30,600 pounds. The load applied to the support disk also considers the weight of the aluminum heat transfer disks and tie-rods/spacers. As previously discussed, there are three basket configurations incorporating two fuel tube configurations (standard and enlarged) and a damaged fuel can configuration. The weight of the enlarged fuel tube is less than that of the standard fuel tube. The weight of the damaged fuel can is approximately 22 pounds heavier than that of the standard fuel tube. Since the fuel weight used in the support disk evaluation is 3,600 pounds (34,200 – 30,600) more than the actual fuel weight, the evaluation is conservative and bounds all three basket configurations. In the end drop, the support disks are loaded by their own inertial weight and do not experience load from the guided, but free standing, fuel assemblies.

Finite element models are used to perform analyses for end drop and side drop conditions using the ANSYS program. Off-angle drops are evaluated by combining the results from the analyses for the end and side drop conditions (Section 2.7.9.1.4). Note that the methodology used for the

off-angle drop evaluation is very conservative given the g loads decrease significantly for off-angle drop orientations (see Table 2.6.7.4.1-3).

In addition to the load from inertial weight, the analyses also consider the stresses due to differential thermal expansion for the buckling evaluation.

Figure 2.7.9.1-1 Cask Orientation

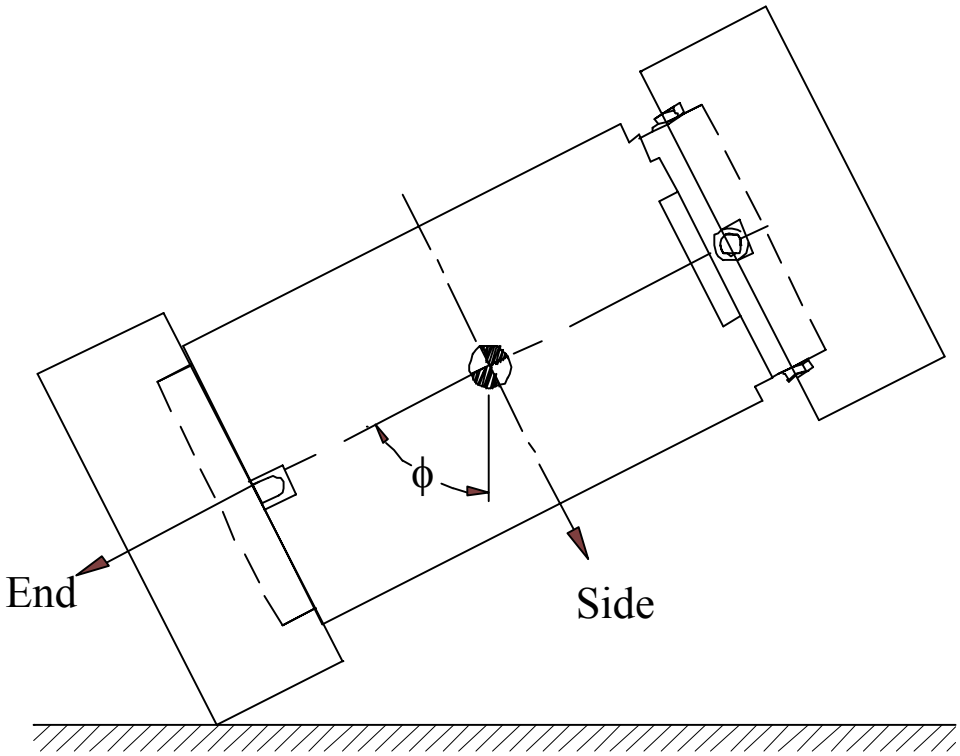

2.7.9.1.1 Finite Element Model Description – Yankee-MPC Fuel Basket

Three finite element models were generated to analyze the canistered Yankee class fuel basket for accident conditions; one for the end drop (Figure 2.6.14.2-1), in which the loads are perpendicular to the plane of the disk and two for the side drop, in which the loads act in the plane of the disk, for two basket orientations, 0° (Figure 2.6.14.2-2) and 45° (Figure 2.6.14.2-3). These are the same models used for the evaluation of the support disk for normal conditions of transport. All models accommodate thermal expansion effects using the temperature distribution from the thermal analysis and the coefficient of thermal expansion. See Section 2.6.14.2 for detailed description of the models. The model for the end drop conditions is constructed using ANSYS SHELL63 elements. It consists of a single support disk with a thickness of 0.5 inch. The finite element models for the side drop evaluation of the support disks are three dimensional models and include the lower section of the canister and cask as well as 14 of the support disks. Similar to the consideration of the normal condition, two bounding thermal conditions (2 and 3) are used in the analysis of the accident condition. See Section 2.6.14.3 for discussion of the thermal considerations. Allowable stresses are determined based on conservative temperatures of 539° F (see Section 2.6.14.3) for Thermal Condition 2 and -40° F for Thermal Condition 3.

To determine the most critical regions, a series of cross sections are considered. The section locations are identified in Figures 2.6.14.2-9 and 2.6.14.2-10 for the 0° and 45° basket drop cases, respectively. Tables 2.6.14.2-1 and 2.6.14.2-2 list the coordinate location of the cross section end points.

2.7.9.1.2 Stress Evaluation of the Yankee-MPC Support Disk for a 30-Foot End Drop Condition

The support disks of the Yankee-MPC fuel basket are located by 8 tie rods with spacers. A structural analysis is performed using ANSYS to evaluate the effect of a 30-foot end drop impact, which corresponds to the most severe out-of-plane loading. The model described in Section 2.7.9.1.1 is used in conjunction with a 56.1g deceleration. Linearized stresses at the cross sections identified in Figure 2.6.14.2-9 are compared to stress allowables per ASME Code, Section III, Subsection NG.

The stress evaluation results for the 30-foot end drop condition are:

Thermal Condition	P_m Stress Intensity (ksi)	M.S.	P_m+P_b Stress Intensity (ksi)	M.S.
2	0	N/A	52.9	1.42
3	0	N/A	53.9	1.51

The margin of safety (M.S.) is:

M.S. = (Allowable Stress/Stress Intensity) –1,

where the allowable stress is 1.0 S_u for 17-4PH Type 630 stainless steel.

The minimum margin of safety is +1.42. The P_m stresses in the support disk for end drop conditions are essentially zero because there is no in-plane loading. Tables 2.7.9.1.2-1 and 2.7.9.1.2-2 list the 40 highest P_m+P_b stress intensities for thermal conditions 2 and 3, respectively.

Table 2.7.9.1.2-1 P_m+P_b Stresses for the Yankee-MPC Support Disk—30-Foot End Drop Thermal Condition 2

Section	Sx (ksi)	Sy (ksi)	Sxy (ksi)	Stress Intensity (ksi)	Allowable Stress (ksi)	Margin of Safety
50	-52.7	-5.6	-3.3	52.9	127.8	1.42
46	-52.6	-17.9	1.3	52.6	127.8	1.43
19	-18.3	-52.5	-0.3	52.5	127.8	1.44
5	-52.4	-27.8	0.1	52.4	127.8	1.44
30	-6.1	-51.5	2.9	51.7	127.8	1.47
56	-18.3	-51.6	0.5	51.6	127.8	1.48
9	-51.3	-19.0	-0.1	51.3	127.8	1.49
7	-51.2	-18.8	-0.6	51.3	127.8	1.49
4	-27.4	-51.2	-0.2	51.2	127.8	1.49
42	-50.8	-27.6	1.0	50.9	127.8	1.51
11	-50.6	-5.9	2.7	50.8	127.8	1.52
3	-50.3	-27.8	-0.2	50.3	127.8	1.54
67	-6.4	-46.7	-1.8	46.8	127.8	1.73
79	-0.1	-46.5	0.3	46.5	127.8	1.75
103	-46.4	0.0	0.3	46.4	127.8	1.75
13	-45.7	-6.6	1.3	45.8	127.8	1.79
94	-45.6	-0.1	-0.1	45.6	127.8	1.80
80	-0.1	-45.5	-0.2	45.5	127.8	1.81
104	-45.5	-0.1	-0.2	45.5	127.8	1.81
95	-44.5	-0.1	-0.2	44.5	127.8	1.87
78	-0.1	-44.0	0.3	44.0	127.8	1.90
102	-44.0	-0.1	0.3	44.0	127.8	1.90
93	-43.8	-0.1	0.1	43.8	127.8	1.92
77	-6.3	-35.1	-10.2	38.3	127.8	2.34
66	-35.1	-6.3	-10.2	38.3	127.8	2.34
89	-0.6	-37.7	-3.3	38.0	127.8	2.36
88	-0.5	-37.5	1.4	37.5	127.8	2.41
20	-37.2	-28.2	0.0	37.2	127.8	2.43
45	-28.1	-36.9	1.0	37.0	127.8	2.46
87	-0.3	-36.0	0.8	36.0	127.8	2.55
82	0.3	-35.7	-0.5	36.0	127.8	2.55
37	8.8	-25.9	3.9	35.5	127.8	2.60
81	0.2	-35.2	-0.3	35.4	127.8	2.61
53	-26.3	8.1	-4.3	35.4	127.8	2.61
106	-34.8	0.4	1.4	35.3	127.8	2.62
107	-34.0	0.5	-3.3	35.1	127.8	2.64
83	0.5	-33.9	2.9	34.9	127.8	2.66
97	-34.4	0.3	-0.7	34.7	127.8	2.68
105	-34.4	0.2	0.8	34.6	127.8	2.69
96	-34.4	0.2	-0.2	34.6	127.8	2.69

Note: See Figure 2.6.14.2-9 for section locations and definition of coordinate system.

Table 2.7.9.1.2-2 P_m+P_b Stresses for the Yankee-MPC Support Disk—30-Foot End Drop Thermal Condition 3

Section	Sx (ksi)	Sy (ksi)	Sxy (ksi)	Stress Intensity (ksi)	Allowable Stress (ksi)	Margin of Safety
5	-53.9	-28.5	0.0	53.9	135.0	1.51
46	-53.1	-18.3	1.6	53.1	135.0	1.54
19	-18.8	-52.9	-0.6	52.9	135.0	1.55
50	-52.6	-5.8	-3.1	52.8	135.0	1.56
4	-28.1	-52.4	-0.4	52.4	135.0	1.58
42	-52.0	-28.3	1.2	52.1	135.0	1.59
56	-18.7	-52.0	0.6	52.0	135.0	1.60
9	-51.7	-19.5	-0.2	51.7	135.0	1.61
7	-51.7	-19.2	-0.9	51.7	135.0	1.61
30	-6.3	-51.4	2.7	51.6	135.0	1.62
3	-51.5	-28.5	-0.3	51.5	135.0	1.62
11	-50.5	-6.1	2.5	50.7	135.0	1.66
79	-0.1	-46.7	0.3	46.7	135.0	1.89
103	-46.7	0.0	0.3	46.7	135.0	1.89
67	-6.6	-46.5	-1.7	46.6	135.0	1.90
94	-45.8	-0.1	-0.1	45.8	135.0	1.95
13	-45.6	-6.8	1.2	45.6	135.0	1.96
80	-0.1	-45.3	-0.2	45.3	135.0	1.98
78	-0.1	-45.3	0.3	45.3	135.0	1.98
104	-45.3	-0.1	-0.2	45.3	135.0	1.98
102	-45.3	-0.1	0.3	45.3	135.0	1.98
93	-45.0	-0.1	0.1	45.0	135.0	2.00
95	-44.3	-0.1	-0.2	44.3	135.0	2.05
20	-38.2	-28.4	-0.2	38.2	135.0	2.53
45	-28.3	-37.9	1.2	38.0	135.0	2.55
88	-0.5	-37.7	1.7	37.8	135.0	2.57
89	-0.6	-37.5	-3.1	37.8	135.0	2.57
77	-6.1	-34.3	-9.9	37.4	135.0	2.61
66	-34.3	-6.1	-9.9	37.4	135.0	2.61
87	-0.3	-36.9	1.0	36.9	135.0	2.66
81	0.2	-36.1	-0.5	36.3	135.0	2.72
82	0.3	-36.0	-0.7	36.3	135.0	2.72
106	-35.1	0.3	1.7	35.6	135.0	2.79
105	-35.3	0.2	1.0	35.5	135.0	2.80
96	-35.3	0.2	-0.3	35.5	135.0	2.80
37	8.7	-25.6	3.8	35.1	135.0	2.85
8	-27.5	-35.0	-0.4	35.0	135.0	2.85
97	-34.7	0.3	-0.9	35.0	135.0	2.86
53	-26.0	7.9	-4.2	35.0	135.0	2.86
107	-33.8	0.5	-3.1	34.9	135.0	2.87

Note: See Figure 2.6.14.2-9 for section locations and definition of coordinate system.

2.7.9.1.3 Stress Evaluation of the Yankee-MPC Support Disk for a 30-Foot Side Drop Load Condition

To determine the structural adequacy of the Yankee-MPC support disk in the canistered Yankee class fuel basket for the 30-foot side drop impact load condition, a quasi-static impact load equal to the weight of the fuel and tubes multiplied by a 55g amplification factor is applied to the support disk structure. The inertial loading of the support disk is also included via the density input for the 17-4 PH stainless steel. The fuel assembly load is transmitted in direct compression through the tube wall to the web structure of the support disk. A finite element analysis is performed using the three dimensional support disk side model described in Section 2.7.9.1.1. As discussed in Section 2.7.9.1, two bounding cases of basket orientation (0° and 45°) are considered in the analysis. The material properties are evaluated at two thermal conditions: Thermal Condition 2, the cold condition (-40°F with 12.5 kW heat load) which has the largest change in temperature from the center of the basket to the outer edge and Thermal Condition 3, extreme cold (-40°F ambient with no heat load). Linearized stresses of the cross-sections (Figures 2.6.14.2-9 and 2.6.14.2-10) at the five critical disks (Section 2.6.14.2 and Figure 2.6.14.2-8) are compared to the stress allowable per the ASME Code, Section III, Subsection NG. The allowable stress is $0.7S_u$ for P_m, and 1.0 S_u for $P_m + P_b$ stresses, respectively.

The stress evaluation results for the 30-foot side drop condition are summarized in Table 2.7.9.1.3-1. The minimum margin of safety is +0.13, which occurs in disk No. 2 for the 45° basket drop orientation (Thermal Condition 2). For the 0° basket drop orientation, the highest P_m stress intensities occur in Disk No. 1 and the highest P_m+P_b stress intensities occur in Disk No. 5 (Thermal Condition 2). Tables 2.7.9.1.3-2 through 2.7.9.1.3-5 list the 40 highest P_m stress intensities for Disk No. 1 (Thermal Conditions 2 and 3) and P_m+P_b stress intensities for Disk No. 5 (Thermal Conditions 2 and 3). For the 45° basket drop orientation, the highest P_m stress intensities occur in Disk No. 3 and the highest P_m+P_b stress intensities occur in Disk No. 2 (Thermal Condition 2). Tables 2.7.9.1.3-6 through 2.7.9.1.3-9 list the 40 highest P_m stress intensities for Disk No.3 and the 40 highest P_m+P_b stress intensities for Disk No. 2 (Thermal Conditions 2 and 3).

Table 2.7.9.1.3-1 Summary of Maximum Yankee-MPC Support Disk Stresses for 30-Foot Side Drop

Thermal Condition	Disk Number	P_m		P_m+P_b	
		S.I. (ksi)	M.S.	S.I. (ksi)	M.S.
0° BASKET DROP ORIENTATION					
2	1	50.57	0.77	66.30	0.93
	2	48.06	0.86	67.74	0.89
	3	43.91	1.04	74.99	0.70
	4	41.96	1.13	80.90	0.58
	5	42.94	1.08	81.14	0.57
3	1	51.12	0.85	66.97	1.02
	2	48.23	0.96	67.78	0.99
	3	44.09	1.14	74.62	0.81
	4	41.83	1.26	80.56	0.68
	5	42.85	1.21	80.76	0.67
45° BASKET DROP ORIENTATION					
2	1	44.67	1.00	112.20	0.14
	2	45.34	0.97	113.40	0.13
	3	48.75	0.83	111.80	0.14
	4	48.15	0.86	112.40	0.14
	5	48.18	0.86	112.30	0.14
3	1	44.84	1.11	114.50	0.18
	2	45.60	1.07	115.70	0.17
	3	49.00	0.93	114.10	0.18
	4	48.38	0.95	114.60	0.18
	5	48.43	0.95	114.60	0.18

Table 2.7.9.1.3-2 P_m Stresses for the Yankee-MPC Support Disk—30-Foot Side Drop, 0° Basket Orientation, Thermal Condition 2, Disk Number 1

Section	Sx (ksi)	Sy (ksi)	Sxy (ksi)	Stress Intensity (ksi)	Allowable Stress (ksi)	Margin of Safety
49	20.88	-29.69	0.08	50.57	89.44	0.77
60	26.26	-24.04	-0.13	50.30	89.44	0.78
45	26.77	-23.21	-0.39	49.99	89.44	0.79
64	13.94	-30.96	0.15	44.90	89.44	0.99
71	23.60	-19.68	-0.04	43.28	89.44	1.07
56	22.91	-16.83	-0.04	39.74	89.44	1.25
53	-24.86	-36.19	-0.18	36.19	89.44	1.47
92	0.02	-36.11	-0.18	36.14	89.44	1.47
51	-31.67	-36.07	-0.18	36.07	89.44	1.48
67	23.56	-12.13	-0.12	35.69	89.44	1.51
4	20.19	-13.50	0.03	33.69	89.44	1.65
66	-25.66	-16.59	-10.73	32.78	89.44	1.73
91	0.00	-30.88	0.15	30.88	89.44	1.90
62	-20.17	-30.83	0.15	30.83	89.44	1.90
72	8.51	-21.58	3.27	30.79	89.44	1.90
8	23.01	-7.06	-0.04	30.07	89.44	1.97
41	9.86	-20.05	-0.38	29.92	89.44	1.99
65	-4.37	-29.12	3.51	29.61	89.44	2.02
90	-0.02	-29.61	0.08	29.61	89.44	2.02
47	-20.75	-29.57	0.08	29.57	89.44	2.02
19	19.25	-10.08	-0.06	29.33	89.44	2.05
63	8.22	-19.64	3.29	28.63	89.44	2.12
48	7.72	-19.78	3.38	28.32	89.44	2.16
23	23.35	-3.25	0.07	26.60	89.44	2.36
10	-26.39	-6.93	-0.04	26.39	89.44	2.39
30	21.61	-4.64	0.07	26.24	89.44	2.41
12	25.60	-0.57	-0.03	26.17	89.44	2.42
61	8.51	-16.01	-3.49	25.49	89.44	2.51
50	-4.37	-24.69	-3.77	25.37	89.44	2.53
46	8.22	-14.76	-3.47	24.01	89.44	2.73
88	-0.01	-23.96	-0.13	23.96	89.44	2.73
58	-22.85	-23.91	-0.13	23.93	89.44	2.74
28	-23.88	-12.00	-0.12	23.88	89.44	2.75
6	-23.83	-13.37	0.03	23.83	89.44	2.75
21	-23.69	-9.95	-0.06	23.69	89.44	2.78
2	-23.38	-19.93	-0.38	23.42	89.44	2.82
87	-0.03	-23.14	-0.39	23.14	89.44	2.87
43	-9.56	-23.09	-0.39	23.10	89.44	2.87
69	-22.81	-19.56	-0.04	22.81	89.44	2.92
52	-4.06	-21.85	3.64	22.56	89.44	2.96

Note: See Figure 2.6.14.2-9 for section locations and definition of coordinate system.

Table 2.7.9.1.3-3 P_m+P_b Stresses for the Yankee-MPC Support Disk—30-Foot Side Drop, 0° Basket Orientation, Thermal Condition 2, Disk Number 5

Section	Sx (ksi)	Sy (ksi)	Sxy (ksi)	Stress Intensity (ksi)	Allowable Stress (ksi)	Margin of Safety
65	-77.07	-40.65	12.83	81.14	127.77	0.57
52	-73.60	-31.56	9.42	75.62	127.77	0.69
50	-71.06	-34.67	-10.47	73.86	127.77	0.73
26	59.32	22.47	6.70	60.50	127.77	1.11
72	-51.22	-40.60	10.85	57.98	127.77	1.20
13	56.55	10.55	3.81	56.87	127.77	1.25
63	49.76	-6.11	-0.96	55.90	127.77	1.29
104	-55.02	-2.64	3.67	55.27	127.77	1.31
107	-54.48	-2.51	3.77	54.75	127.77	1.33
24	53.33	8.84	3.28	53.57	127.77	1.39
11	52.50	8.88	-3.59	52.79	127.77	1.42
33	52.10	3.31	3.83	52.40	127.77	1.44
51	-40.45	-35.06	-13.79	51.80	127.77	1.47
48	42.57	-9.12	-1.11	51.74	127.77	1.47
70	45.76	-5.42	-0.11	51.19	127.77	1.50
59	48.18	-1.39	0.81	49.59	127.77	1.58
71	20.15	-29.02	-2.60	49.45	127.77	1.58
68	45.61	-3.24	-0.67	48.87	127.77	1.61
61	39.17	-9.31	0.30	48.48	127.77	1.64
9	48.16	4.41	2.33	48.29	127.77	1.65
22	46.31	5.14	-2.78	46.50	127.77	1.75
46	41.32	-5.04	-0.24	46.37	127.77	1.76
57	40.84	-5.02	-0.37	45.87	127.77	1.79
62	-29.52	-36.91	10.12	43.99	127.77	1.90
7	43.75	3.56	-2.41	43.89	127.77	1.91
67	23.67	-18.60	5.45	43.65	127.77	1.93
53	-25.97	-37.24	-10.28	43.33	127.77	1.95
60	22.24	-19.91	5.00	43.32	127.77	1.95
31	42.87	1.48	1.62	42.93	127.77	1.98
45	18.17	-23.55	4.62	42.73	127.77	1.99
29	41.78	-0.81	-1.02	42.63	127.77	2.00
20	42.52	1.93	1.48	42.58	127.77	2.00
3	38.39	-3.41	-0.27	41.81	127.77	2.06
56	21.25	-19.01	-5.61	41.79	127.77	2.06
64	-0.11	-41.04	1.35	41.09	127.77	2.11
95	37.86	-2.35	3.54	40.83	127.77	2.13
98	37.46	-2.48	3.66	40.61	127.77	2.15
47	-26.42	-31.97	9.62	39.21	127.77	2.26
37	38.12	11.77	4.41	38.84	127.77	2.29
49	7.36	-31.11	-2.31	38.75	127.77	2.30

Note: See Figure 2.6.14.2-9 for section locations and definition of coordinate system.

Table 2.7.9.1.3-4 P_m Stresses for the Yankee-MPC Support Disk—30-Foot Side Drop, 0° Basket Orientation, Thermal Condition 3, Disk Number 1

Section	Sx (ksi)	Sy (ksi)	Sxy (ksi)	Stress Intensity (ksi)	Allowable Stress (ksi)	Margin of Safety
49	21.17	-29.95	0.07	51.12	94.50	0.85
60	26.38	-24.13	-0.15	50.51	94.50	0.87
45	26.99	-23.46	-0.40	50.45	94.50	0.87
64	14.12	-31.05	0.14	45.17	94.50	1.09
71	23.58	-19.44	-0.04	43.03	94.50	1.20
56	22.79	-16.95	-0.05	39.73	94.50	1.38
53	-24.94	-36.46	-0.18	36.46	94.50	1.59
92	0.04	-36.38	-0.18	36.42	94.50	1.59
51	-31.54	-36.33	-0.18	36.34	94.50	1.60
67	23.52	-11.90	-0.12	35.41	94.50	1.67
4	20.31	-13.70	0.02	34.01	94.50	1.78
66	-25.65	-16.66	-10.73	32.80	94.50	1.88
91	0.01	-30.98	0.14	30.99	94.50	2.05
62	-20.06	-30.93	0.15	30.93	94.50	2.06
72	8.69	-21.37	3.25	30.75	94.50	2.07
41	10.06	-20.28	-0.40	30.35	94.50	2.11
8	23.08	-7.23	-0.05	30.31	94.50	2.12
90	0.00	-29.87	0.07	29.88	94.50	2.16
47	-20.76	-29.82	0.07	29.83	94.50	2.17
65	-4.02	-29.25	3.50	29.72	94.50	2.18
19	19.06	-10.21	-0.07	29.27	94.50	2.23
63	8.40	-19.73	3.28	28.88	94.50	2.27
48	7.89	-19.92	3.38	28.62	94.50	2.30
10	-26.71	-7.11	-0.05	26.71	94.50	2.54
23	23.14	-3.39	0.06	26.54	94.50	2.56
12	25.60	-0.73	-0.04	26.33	94.50	2.59
30	21.52	-4.41	0.07	25.93	94.50	2.64
61	8.69	-16.01	-3.50	25.68	94.50	2.68
50	-4.02	-24.80	-3.78	25.46	94.50	2.71
46	8.40	-14.92	-3.48	24.33	94.50	2.88
6	-24.11	-13.57	0.02	24.11	94.50	2.92
88	0.01	-24.05	-0.15	24.06	94.50	2.93
58	-22.72	-24.01	-0.15	24.02	94.50	2.93
28	-23.83	-11.77	-0.12	23.83	94.50	2.97
2	-23.66	-20.15	-0.40	23.70	94.50	2.99
21	-23.68	-10.09	-0.07	23.68	94.50	2.99
87	-0.01	-23.38	-0.40	23.39	94.50	3.04
43	-9.78	-23.33	-0.40	23.35	94.50	3.05
52	-3.73	-22.02	3.64	22.72	94.50	3.16
69	-22.68	-19.32	-0.04	22.68	94.50	3.17

Note: See Figure 2.6.14.2-9 for section locations and definition of coordinate system.

Table 2.7.9.1.3-5 P_m+P_b Stresses for the Yankee-MPC Support Disk—30-Foot Side Drop, 0° Basket Orientation, Thermal Condition 3, Disk Number 5

Section	Sx (ksi)	Sy (ksi)	Sxy (ksi)	Stress Intensity (ksi)	Allowable Stress (ksi)	Margin of Safety
65	-76.65	-40.81	12.82	80.76	135.00	0.67
52	-73.35	-31.67	9.42	75.38	135.00	0.79
50	-70.92	-34.79	-10.47	73.73	135.00	0.83
26	58.64	22.23	6.63	59.81	135.00	1.26
72	-50.60	-40.42	10.78	57.43	135.00	1.35
13	56.43	10.39	3.77	56.73	135.00	1.38
63	49.88	-6.33	-0.98	56.25	135.00	1.40
104	-54.72	-2.64	3.67	54.98	135.00	1.46
107	-54.24	-2.52	3.77	54.52	135.00	1.48
11	52.80	8.89	-3.57	53.09	135.00	1.54
24	52.84	8.62	3.24	53.08	135.00	1.54
48	42.83	-9.22	-1.11	52.10	135.00	1.59
33	51.70	3.34	3.83	52.01	135.00	1.60
51	-40.32	-35.27	-13.77	51.80	135.00	1.61
70	45.59	-5.39	-0.08	50.98	135.00	1.65
59	47.87	-1.60	0.78	49.49	135.00	1.73
71	20.29	-28.66	-2.64	49.23	135.00	1.74
61	39.69	-9.20	0.27	48.89	135.00	1.76
68	45.73	-3.08	-0.70	48.83	135.00	1.76
9	48.07	4.26	2.29	48.19	135.00	1.80
46	41.67	-5.12	-0.23	46.79	135.00	1.89
22	46.30	5.08	-2.74	46.48	135.00	1.90
57	41.03	-5.02	-0.36	46.05	135.00	1.93
7	43.99	3.53	-2.38	44.13	135.00	2.06
62	-29.32	-36.98	10.10	43.95	135.00	2.07
60	22.30	-20.35	5.03	43.83	135.00	2.08
67	23.62	-18.60	5.45	43.61	135.00	2.10
53	-26.07	-37.44	-10.34	43.55	135.00	2.10
45	18.34	-23.76	4.65	43.11	135.00	2.13
31	42.62	1.51	1.63	42.68	135.00	2.16
29	41.76	-0.66	-1.04	42.48	135.00	2.18
20	42.13	1.69	1.44	42.18	135.00	2.20
3	38.64	-3.45	-0.24	42.09	135.00	2.21
56	21.31	-18.90	-5.60	41.74	135.00	2.23
64	0.13	-41.10	1.32	41.31	135.00	2.27
95	37.65	-2.35	3.54	40.62	135.00	2.32
98	37.42	-2.46	3.64	40.54	135.00	2.33
47	-26.29	-32.10	9.61	39.23	135.00	2.44
49	7.59	-31.24	-2.36	39.11	135.00	2.45
37	37.92	11.74	4.40	38.64	135.00	2.49

Note: See Figure 2.6.14.2-9 for section locations and definition of coordinate system.

Table 2.7.9.1.3-6 P_m Stresses for the Yankee-MPC Support Disk—30-Foot Side Drop, 45° Basket Orientation, Thermal Condition 2, Disk Number 3

Section	Sx (ksi)	Sy (ksi)	Sxy (ksi)	Stress Intensity (ksi)	Allowable Stress (ksi)	Margin of Safety
52	25.34	-22.81	3.80	48.75	89.44	0.83
25	-27.78	17.34	-1.16	45.19	89.44	0.98
21	-31.47	11.47	-0.11	42.94	89.44	1.08
39	-20.92	-41.20	-0.11	41.20	89.44	1.17
58	-4.61	-29.66	-12.71	35.69	89.44	1.51
50	-35.46	-22.72	-1.35	35.60	89.44	1.51
28	-35.49	-16.38	-1.28	35.58	89.44	1.51
32	-35.23	-10.28	-1.00	35.27	89.44	1.54
48	17.27	-16.47	3.87	34.61	89.44	1.58
17	-27.52	5.60	-0.07	33.12	89.44	1.70
49	-12.03	-32.77	-1.61	32.90	89.44	1.72
29	-15.82	-29.77	-1.23	29.88	89.44	1.99
20	-6.66	21.52	4.83	29.80	89.44	2.00
27	-17.01	-2.04	12.65	29.40	89.44	2.04
45	-1.62	25.66	4.54	28.75	89.44	2.11
24	-9.93	16.31	4.60	27.81	89.44	2.22
30	13.66	-10.36	4.15	25.42	89.44	2.52
44	-23.99	-0.15	-1.58	24.09	89.44	2.71
54	0.40	-8.48	-10.71	23.19	89.44	2.86
26	-4.84	16.88	3.81	23.02	89.44	2.89
43	-7.46	-22.88	-0.69	22.91	89.44	2.90
92	-1.76	-22.75	-1.32	22.84	89.44	2.92
10	-14.09	8.30	-1.20	22.52	89.44	2.97
31	-11.15	9.93	3.92	22.48	89.44	2.98
23	18.29	17.25	3.61	21.42	89.44	3.18
42	18.32	5.51	4.71	19.87	89.44	3.50
19	17.18	11.39	4.67	19.78	89.44	3.52
6	-14.88	4.60	0.16	19.48	89.44	3.59
5	-3.41	13.22	4.91	19.32	89.44	3.63
85	-1.76	17.31	-1.13	19.21	89.44	3.66
13	0.11	18.07	3.28	19.11	89.44	3.68
59	-17.54	-0.48	3.31	18.30	89.44	3.89
57	-6.07	-17.95	-1.54	18.15	89.44	3.93
37	-15.91	-12.33	3.20	17.78	89.44	4.03
76	-15.86	-2.08	-5.34	17.69	89.44	4.06
46	-16.71	-0.24	3.20	17.67	89.44	4.06
61	-16.62	-0.39	-1.11	16.69	89.44	4.36
55	-1.06	-16.18	-2.35	16.54	89.44	4.41
80	-1.76	-16.41	-1.25	16.52	89.44	4.41
2	-16.04	-0.01	1.44	16.28	89.44	4.49

Notes: 1. See Figure 2.6.14.2-10 for section locations.
2. Stress components are based on the coordinate system shown in Figure2.6.14.2-10, rotated 45°.

Table 2.7.9.1.3-7 P_m+P_b Stresses for the Yankee-MPC Support Disk—30-Foot Side Drop, 45° Basket Orientation, Thermal Condition 2, Disk Number 2

Section	Sx (ksi)	Sy (ksi)	Sxy (ksi)	Stress Intensity (ksi)	Allowable Stress (ksi)	Margin of Safety
19	47.89	111.70	10.75	113.40	127.77	0.13
42	46.63	106.90	10.51	108.70	127.77	0.18
24	-104.20	-14	1.30	104.20	127.77	0.23
20	-102.10	-11.47	-1.61	102.10	127.77	0.25
53	-100.60	-25.67	7.19	101.30	127.77	0.26
30	-11.87	-100.70	0.84	100.80	127.77	0.27
4	43.29	95.85	8.26	97.12	127.77	0.32
52	-0.48	-96.15	0.43	96.15	127.77	0.33
5	-94.13	-18.70	0.66	94.14	127.77	0.36
48	-3.56	-92.44	-0.23	92.44	127.77	0.38
31	-87.17	-13.64	-0.17	87.17	127.77	0.47
37	-84.18	-24.81	8.42	85.35	127.77	0.50
26	-77.41	7.13	-2.44	84.68	127.77	0.51
45	78.69	54.62	12.52	84.02	127.77	0.52
33	-82.06	-15.48	3.20	82.22	127.77	0.55
51	-79.35	-15.30	0.68	79.36	127.77	0.61
23	40.86	75.23	10.55	78.21	127.77	0.63
9	-75.12	-16.73	2.47	75.23	127.77	0.70
54	-11.19	-48.92	-32.51	75.18	127.77	0.70
21	-13.63	47.86	-7.96	63.52	127.77	1.01
56	-61.61	-21.03	8.59	63.35	127.77	1.02
60	-56.28	-40.21	10.30	61.31	127.77	1.08
62	-61.08	-9.95	1.38	61.12	127.77	1.09
13	-54.40	4.32	-1.69	58.82	127.77	1.17
59	-43.89	-42.89	13.66	57.06	127.77	1.24
8	26.97	54.11	5.66	55.25	127.77	1.31
12	27.69	52.61	7.80	54.85	127.77	1.33
47	-50.28	-34.18	8.43	53.88	127.77	1.37
75	53.17	6.01	-2.62	53.31	127.77	1.40
85	-0.39	52.05	-1.21	52.50	127.77	1.43
32	-47.87	-26.61	8.74	51.00	127.77	1.51
3	-49.19	-35.11	4.74	50.63	127.77	1.52
92	-3.14	-50.22	-1.48	50.26	127.77	1.54
25	-36.72	12.35	5.16	50.13	127.77	1.55
82	0.94	49.47	0.04	49.47	127.77	1.58
106	-49.16	-4.60	0.08	49.16	127.77	1.60
46	-37.90	-36.32	11.84	48.98	127.77	1.61
80	-3.31	-47.86	-1.33	47.90	127.77	1.67
39	-22.53	-44.96	-8.45	47.78	127.77	1.67
49	6.66	-37.66	8.38	47.38	127.77	1.70

Notes: 1. See Figure 2.6.14.2-10 for section locations.
2. Stress components are based on the coordinate system shown in Figure 2.6.14.2-10, rotated 45°.

Table 2.7.9.1.3-8 P_m Stresses for the Yankee-MPC Support Disk—30-Foot Side Drop, 45° Basket Orientation, Thermal Condition 3, Disk Number 3

Section	Sx (ksi)	Sy (ksi)	Sxy (ksi)	Stress Intensity (ksi)	Allowable Stress (ksi)	Margin of Safety
52	25.48	-22.93	3.82	49.00	94.50	0.93
25	-27.63	17.44	-1.15	45.12	94.50	1.09
21	-31.41	11.55	-0.04	42.95	94.50	1.20
39	-21.07	-41.35	-0.36	41.35	94.50	1.29
50	-35.82	-22.84	-1.33	35.95	94.50	1.63
28	-35.80	-16.46	-1.25	35.88	94.50	1.63
58	-4.55	-29.53	-12.67	35.59	94.50	1.66
32	-35.24	-10.32	-0.96	35.28	94.50	1.68
48	17.41	-16.55	3.90	34.84	94.50	1.71
17	-27.82	5.62	0.01	33.44	94.50	1.83
49	-12.18	-32.91	-1.60	33.04	94.50	1.86
20	-6.78	21.55	4.93	29.99	94.50	2.15
29	-15.93	-29.85	-1.21	29.96	94.50	2.15
27	-16.91	-2.03	12.55	29.18	94.50	2.24
45	-1.73	25.90	4.62	29.13	94.50	2.24
24	-9.75	15.99	4.65	27.37	94.50	2.45
30	13.81	-10.41	4.19	25.63	94.50	2.69
44	-24.21	-0.17	-1.54	24.31	94.50	2.89
43	-7.60	-23.13	-0.65	23.15	94.50	3.08
54	0.40	-8.46	-10.68	23.13	94.50	3.09
92	-1.75	-22.87	-1.29	22.95	94.50	3.12
26	-4.82	16.76	3.80	22.88	94.50	3.13
31	-11.25	9.92	3.96	22.60	94.50	3.18
10	-14.13	8.24	-1.19	22.50	94.50	3.20
23	18.52	17.35	3.63	21.61	94.50	3.37
19	17.35	11.46	4.74	19.98	94.50	3.73
42	18.39	5.53	4.79	19.98	94.50	3.73
5	-3.51	13.24	5.02	19.53	94.50	3.84
6	-14.84	4.52	0.27	19.37	94.50	3.88
85	-1.76	17.40	-1.12	19.29	94.50	3.90
59	-18.50	-0.59	3.42	19.17	94.50	3.93
13	0.11	17.81	3.28	18.88	94.50	4.01
57	-6.14	-17.88	-1.53	18.08	94.50	4.23
46	-17.00	-0.26	3.23	17.95	94.50	4.26
37	-16.01	-12.16	3.22	17.84	94.50	4.30
76	-15.74	-2.05	-5.29	17.54	94.50	4.39
80	-1.76	-16.49	-1.22	16.59	94.50	4.70
61	-16.50	-0.50	-1.01	16.57	94.50	4.70
55	-1.08	-16.11	-2.35	16.47	94.50	4.74
2	-16.08	-0.10	1.54	16.28	94.50	4.80

Notes: 1. See Figure 2.6.14.2-10 for section locations.
2. Stress components are based on the coordinate system shown in Figure 2.6.14.2-10, rotated 45°.

Table 2.7.9.1.3-9 P_m+P_b Stresses for the Yankee-MPC Support Disk—30-Foot Side Drop, 45° Basket Orientation, Thermal Condition 3, Disk Number 2

Section	Sx (ksi)	Sy (ksi)	Sxy (ksi)	Stress Intensity (ksi)	Allowable Stress (ksi)	Margin of Safety
19	48.84	114.00	10.87	115.70	135.00	0.17
42	47.42	109.20	10.61	110.90	135.00	0.22
24	-105.20	-14.83	1.44	105.20	135.00	0.28
20	-104.50	-12.4	-1.52	104.50	135.00	0.29
30	-12.16	-102.10	0.85	102.10	135.00	0.32
53	-101.30	-25.79	7.21	101.90	135.00	0.32
4	44.46	99.04	8.33	100.30	135.00	0.35
5	-97.12	-19.89	0.75	97.13	135.00	0.39
52	-0.53	-96.94	0.45	96.94	135.00	0.39
48	-3.76	-93.64	-0.23	93.64	135.00	0.44
31	-88.51	-14.17	-0.12	88.51	135.00	0.53
37	-85.08	-24.82	8.42	86.24	135.00	0.57
45	80.27	55.65	12.67	85.63	135.00	0.58
26	-77.05	7.00	-2.41	84.19	135.00	0.60
33	-82.52	-16.10	3.29	82.68	135.00	0.63
51	-80.58	-15.73	0.72	80.59	135.00	0.68
23	41.39	75.52	10.63	78.55	135.00	0.72
9	-76.75	-18.11	2.74	76.88	135.00	0.76
54	-11.17	-48.80	-32.41	74.96	135.00	0.80
60	-59.33	-42.81	11.04	64.86	135.00	1.08
21	-12.96	49.85	-7.87	64.75	135.00	1.08
56	-62.27	-21.01	8.61	63.99	135.00	1.11
62	-62.41	-11.28	1.65	62.47	135.00	1.16
59	-46.47	-45.96	14.39	60.60	135.00	1.23
13	-54.46	4.08	-1.62	58.63	135.00	1.30
8	27.49	54.09	5.68	55.25	135.00	1.44
47	-51.13	-34.86	8.61	54.84	135.00	1.46
12	27.65	52.18	7.79	54.45	135.00	1.48
3	-52.39	-36.58	4.90	53.79	135.00	1.51
75	53.05	6.03	-2.67	53.20	135.00	1.54
85	-0.37	52.32	-1.20	52.74	135.00	1.56
32	-48.11	-27.89	8.75	51.37	135.00	1.63
92	-3.16	-50.53	-1.46	50.58	135.00	1.67
46	-38.60	-37.12	12.04	49.93	135.00	1.70
82	1.03	49.88	0.11	49.88	135.00	1.71
25	-36.57	12.00	5.10	49.63	135.00	1.72
106	-49.48	-4.62	0.10	49.48	135.00	1.73
17	-9.72	36.28	-7.37	48.31	135.00	1.79
80	-3.35	-48.19	-1.30	48.23	135.00	1.80
39	-22.68	-45.16	-8.82	48.21	135.00	1.80

Notes: 1. See Figure 2.6.14.2-10 for section locations.
2. Stress components are based on the coordinate system shown in Figure 2.6.14.2-10, rotated 45°.

2.7.9.1.4 Stress Evaluation of the Yankee-MPC Support Disk for 30-Foot Off-Angle Drop Load Condition

This section documents the methodology used to calculate the stresses associated with off-angle impacts of the transport cask (Figure 2.7.9.1-1). The results show that the stress criteria is met for all off-angle conditions. Note that the methodology used for the off-angle drop evaluation is very conservative since the g loads decrease significantly for off-angle drop orientations (Table 2.6.7.4.1-3).

To evaluate off-angle impacts, the stress components (i.e., S_x, S_y, S_{xy}) are combined from the side drop and end drop cases for both the 0° basket drop orientation and the 45° basket drop orientation (Figure 2.6.14.1-1). The stresses are combined according to the various cask drop angles (ϕ = 0°, 24°, 30°, 45°, 60°, 73°, 75°, 77°, 80°, 83°, 85°, 88° and 90°) for all five critical support disks (Figure 2.6.14.2-8). The normal stresses (S_x and S_y) and the shear stress (S_{xy}) for a drop with an angle of ϕ (Figure 2.7.9.1-1) are calculated by the following equations:

$$S_{x(\phi)} = S_{x(end)}\mathrm{Cos}\phi + S_{x(side)}\mathrm{Sin}\phi\,,$$

$$S_{y(\phi)} = S_{y(end)}\mathrm{Cos}\phi + S_{y(side)}\mathrm{Sin}\phi\,,$$

$$S_{xy(\phi)} = S_{xy(end)}\mathrm{Cos}\phi + S_{xy(side)}\mathrm{Sin}\phi\,,$$

where:

$S_{x(end)}$, $S_{y(end)}$, and $S_{xy(end)}$ are the sectional stresses resulting from the Support Disk End Drop Model, and $S_{x(side)}$, $S_{y(side)}$, and $S_{xy(side)}$ are the section stresses resulting from the Support Disk Side Drop Model.

Off-angle principle stresses (i.e., S_1, S_2) are calculated by using the following equation:

$$S_1, S_2 = \frac{S_{x(\phi)} + S_{y(\phi)}}{2} \pm \sqrt{\left(\frac{S_{x(\phi)} - S_{y(\phi)}}{2}\right)^2 + S_{xy(\phi)}^2}$$

Once the off-angle principle stresses are calculated, new stress intensities (SI) can be calculated. Summaries of the maximum support disk stress intensities in the 30-foot off-angle drop conditions are given in Table 2.7.9.1.4-1.

Table 2.7.9.1.4-1 Yankee-MPC Support Disk Stress Summary for the 30-Foot Off-Angle Drop

Stress State	Thermal Condition	Section	Cask Drop Angle (°)	Disk Number	Sx (ksi)	Sy (ksi)	Sxy (ksi)	Stress Intensity (ksi)	Allowable Stress[5] (ksi)	Margin of Safety
0° BASKET DROP ORIENTATION										
P_m	2	49	90	1	20.9	-29.7	0.1	50.6	89.4	0.77
P_m+P_b	2	65	90	5	-77.1	-40.7	12.8	81.1	127.8	0.57
P_m	3	49	90	1	21.2	-30.0	0.1	51.1	94.5	0.85
P_m+P_b	3	65	90	5	-76.7	-40.8	12.8	80.8	135.0	0.67
45° BASKET DROP ORIENTATION										
P_m	2	52	90	3	25.3	-22.8	3.8	48.8	89.4	0.83
P_m+P_b	2	19	90	2	47.9	111.7	10.8	113.4	127.8	0.13
P_m	3	52	90	3	25.5	-22.9	3.8	49.0	94.5	0.93
P_m+P_b	3	19	90	2	48.8	114.0	10.9	115.7	135.0	0.17

Notes:

1. P = Primary Stress, $P_m + P_b$ = Primary Membrane + Bending Stress.
2. See Figures 2.6.14.2-9 and 2.6.14.2-10 for section location.
3. See Figure 2.7.9.1-1 for definition of cask drop angle.
4. See Figure 2.6.14.2-8 for disk number.
5. Allowable Stress for 17-4PH, Type 630 stainless steel:

   For P_m, $S_{allow} = 0.7\ S_u = 89.4$ ksi at 539°F

   $= 94.5$ ksi at -40°F

   For $P_m + P_b$, $S_{allow} = S_u = 127.8$ ksi at 539°F

   $= 135.0$ ksi at -40°F

2.7.9.2 Stress Evaluation of the Yankee-MPC Tie Rods and Spacers for a 30-Foot End Drop Load Condition

In accordance with 10 CFR 71.73(c)(1), a spent-fuel shipping cask is subject to a free drop from a height of 30 feet onto a flat, unyielding surface. The design deceleration for the NAC-STC for the hypothetical accident 30-foot end drop is 56.1 g (Table 2.6.7.4.1-2).

The structural capacity of the spacers supporting the basket is evaluated by hand calculations using classical analysis. Accident loading due to the 30-foot drop of the fuel basket is compared to the stress limit of 0.7 S_u in accordance with Article NF 1440 of the ASME Code, assuming membrane stresses.

No detailed evaluation of the tie rods is required. The tie rods serve basket assembly purposes and are not part of the load path for the condition evaluated. The tie rods are loaded during fabrication by a 190 ft-lbs preload. Under drop conditions, the preload will be reduced. The tie rod design is, therefore, acceptable by inspection.

During the end drop, the spacers are loaded with the weight of 22 support disks, the aluminum heat transfer disks, one end plate, and the weight of the spacers. The load is resisted by the effective area of 8 spacers. The compressive stresses are calculated on the effective area of the spacer.

The material allowable stress was conservatively selected at a temperature of 500°F. The temperature near the outer edge of the support disks (at the tie rods) is 387.9°F.

2.7.9.2.1 Design Criteria

Stress limits = 0.7 S_u (accident condition)
(more limiting than 2.4 S_m)
Loading criteria (g) = 56.1g (accident condition)
Evaluation temperature = 500°F

Canister Basket Parameters

Fuel basket weight = 9,530 lbs
Bottom weldment weight = 438 lbs
Fuel tube weight (36 tubes) = 2,164 lbs
Rod diameter = 1.13 in
Spacer outer diameter = 2.50 in

Materials

Tie rod = SA 479 Type 304 Stainless Steel

Spacer = A511 Type 304 Stainless Steel

Material Allowable

Type 304 SS = S_m = 17,500 psi (500°F)

= S_u = 63,500 psi (500°F)

2.7.9.2.2 30-Foot End Drop Condition - Results

The deceleration assumed for the canister basket in the 30-foot end drop is 56.1g. The spacers are loaded with the weight of the 22 support disks, the aluminum heat transfer disks, one end plate and the weight of the spacers. These loads are calculated as:

Total weight of basket = 9,530 lbs

Less weight of bottom weldment = -438 lbs

Less weight of fuel tubes = -2,164 lbs

Therefore,

1-g load on spacers = 6,928 lbs

Applied g level = 56.1g

Therefore,

Accident condition load on spacers = 6,928 x 56.1

= 388,661 lbs

The effective area of one spacer at each of eight locations supporting the weight of the support disks is equal to the net area of the spacer and is calculated as:

$$A = \frac{3.14 \times \left(2.5^2 - 1.25^2\right)}{4}$$

$$= 3.68 \text{ in}^2$$

The average compressive stress, S_c, in the spacer is:

$$S_c = \frac{388,661}{8 \times 3.68}$$

$$= 13,202 \text{ psi}$$

The allowable stress for Type 304 SS under accident conditions of transport is 0.7 S_u.

S_u = 63,500 psi
0.7 S_u = 0.7 x 63,500
= 44,500 psi

The margin of safety (MS), which is defined as $\frac{0.7S_u}{S_c} - 1$, is calculated as:

$$\frac{44,450}{13,202} - 1 = 2.37$$

Therefore, the spacers are structurally adequate for a 56.1g end impact under accident conditions.

2.7.9.3 Yankee-MPC Basket Support Disk - Buckling Evaluation (Accident Conditions)

The Yankee-MPC support disk is subjected to compressive and/or inertia loads during a 30-foot drop of the NAC-STC cask onto an unyielding surface. Depending on the cask orientation for the 30-foot drop impact, the support disk may have both in-plane and out-of-plane loads applied to it. The in-plane loads (basket side impact component) apply compressive forces and in-plane (strong axis) bending moments on the support disk and the out-of-plane inertial loads (basket end-impact component) produce out-of-plane (weak axis) bending moments on the support disk. Buckling of the support disk is evaluated in accordance with the methods and acceptance criteria of NUREG/CR-6322.

The margin of safety is calculated based on the Interaction Equations 31 and 32 in NUREG/CR-6322. These two equations adopt the "Limit Analysis Design" approach for structural members subjected to stresses beyond the yield limit of the material, i.e., for members deformed elastically as a result of axial load or bending moment. Other equations applicable to the calculations are listed later in this section.

The maximum forces and moments are determined from the finite element analysis stress results for the Support Disk End-Drop Model as well as the Support Disk Side Drop Model (two different basket orientations, 0° and 45°). The buckling evaluations account for both in-plane

(about the strong axis of the web) and out-of-plane (about the weak axis of the web) buckling modes. Evaluation of strong axis buckling is performed only for the side drop condition since it is the governing case (side drop always produces maximum compressive force and strong axis bending moment). Evaluation for weak axis buckling is performed for several cask drop angles (Figure 2.7.9.1-1).

Methodology and equations for the buckling evaluation are summarized as follows.

Symbols and Units

P = applied axial compressive loads, kips
M = applied bending moment, kips-inch
P_a = allowable axial compressive load, kips
P_{cr} = critical axial compression load, kips
P_e = Euler buckling loads, kips
P_y = average yield load, equal to profile area times specified minimum yield stress, kips
C_c = column slenderness ratio separating elastic and inelastic buckling
C_m = coefficient applied to bending term in interaction equation
M_m = critical moment that can be resisted by a plastically designed member in the absence of axial load, kip-in.
M_p = plastic moment, kip-in.
F_a = axial compressive stress permitted in the absence of bending moment, ksi
F_e = Euler stress for a prismatic member divided by factor of safety, ksi
k = ratio of effective column length to actual unsupported length
l = unsupported length of member, in.
r = radius of gyration, in.
S_y = yield strength, ksi
A = cross sectional area of member, in^2
Z_x = plastic section modulus, in^3
λ = allowable reduction factor, dimensionless.

From NUREG/CR-6322, the following equations are used to evaluate the support disk for accident condition of transport:

$$\frac{P}{P_{cr}} + \frac{C_m M}{M_m\left[1 - \frac{P}{P_e}\right]} \le 1.0$$

$$\frac{P}{P_y} + \frac{M}{1.18\, M_p} \le 1.0$$

where: $P_{cr} = 1.7 \times A \times F_a$

$$F_a = \frac{P_a}{A} \quad \text{for} \quad P_a = P_y\left[\frac{1 - \frac{\lambda^2}{4}}{1.11 + 0.5\lambda + 0.17\lambda^2 - 0.28\lambda^3}\right]$$

and $\lambda = \frac{1}{\pi}\left(\frac{kl}{r}\right)\sqrt{\frac{S_y}{E}}$

$$F_e = \frac{\pi^2 \cdot E}{1.30 \cdot \left(\frac{k \cdot l}{r}\right)^2}$$

$P_e = 1.92 \times A \times F_e$

$P_y = S_y \times A$

$C_m =$ 0.85 for members with joint translation (sideways).

$M_p = S_y \times Z_x$

$$M_m = M_p \cdot \left(1.07 - \frac{\left(\frac{l}{r}\right) \cdot \sqrt{S_y}}{3160}\right) \le M_p$$

Buckling evaluation is performed for all sections of disk ligaments (Figures 2.6.14.2-9 and 2.6.14.2-10). Using the cross-sectional stresses calculated at each of the sections for each loading condition, the maximum corresponding compressive forces (P) and bending moment (M) are determined as follows:

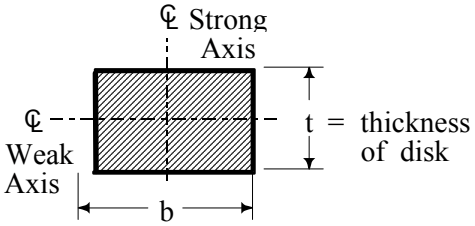

$$P = \sigma_m A,$$

$$M = \sigma_b S,$$

where, σ_m is the membrane stress, σ_b is the strong axis bending stress or weak axis bending stress, A is the area (b × t), and S is the section modulus ($tb^2/6$ for strong axis bending and $bt^2/6$ for weak axis bending).

To determine the margin of safety:

$$P_1 = P/P_{cr} \qquad M_1 = \frac{C_m M}{(1 - P/P_e) M_m} \qquad (P_1 + M_1 \leq 1) \quad \text{(Eq. 31, NUREG/CR-6322)}$$

and $$P_2 = P/P_y \qquad M_2 = \frac{M}{1.18\, M_p} \qquad (P_1 + M_1 \leq 1) \quad \text{(Eq. 32, NUREG/CR-6322)}$$

The margins of safety are calculated as:

$$MS1 = \frac{1}{P_1 + M_1} - 1$$

$$MS2 = \frac{1}{P_2 + M_2} - 1$$

The side drop conditions (cask drop angle ϕ=90°) are the governing conditions for strong axis buckling evaluation since the axial compression for (P) and the strong axis bending moment (M) decrease with the drop angle. Weak axis buckling evaluation is performed for several drop angles (ϕ=0°, 24°, 30°, 45°, 60°, 73°, 75°, 77°, 80°, 83°, 85°, 88° and 90°). For the evaluation of

off-angle drop cases, the forces (P) and bending moments (M) used for the buckling evaluation (weak axis only) are determined as follows:

$$P = P_{side}Sin\phi$$

$$M = M_{end}Cos\phi$$

where:

P_{side} is the compression force from the Side Drop cases

M_{end} is the weak axis bending moment from the End Drop cases

ϕ is the cask drop angle (Figure 2.7.9.1-1)

The results of buckling evaluations for the support disks for the 30-foot drop condition are summarized below. The minimum margin of safety is +0.01 for the strong axis buckling evaluation and +0.54 for weak axis buckling evaluation. As the tables demonstrate, the support disks meet the requirements of NUREG/CR-6322.

Stress State	Thermal Condition	Section Number	Drop Angle	Disk Number	P (kip)	P_{cr} (kip)	M (in-kip)	M_p (in-kip)	M_m (in-kip)	MS1	MS2
Strong Axis, 30-Foot Drop, 0° Basket Drop Orientation											
P	2	65	90	5	7.75	36.23	2.64	6.06	5.80	0.61	0.64
P+Q	2	65	90	5	11.38	36.23	3.01	6.06	5.80	0.26	0.29
P	3	65	90	5	7.64	43.52	2.64	7.38	6.99	0.95	1.01
P+Q	3	65	90	4	10.43	43.52	2.73	7.38	6.99	0.69	0.73
Strong Axis, 30-Foot Drop, 45° Basket Drop Orientation											
P	2	52	90	4	8.40	36.24	3.78	6.06	5.80	0.22	0.27
P+Q	2	52	90	5	11.30	38.79	4.74	6.51	6.21	0.01	0.06
P	3	52	90	4	8.43	43.54	3.81	7.39	6.99	0.47	0.54
P+Q	3	48	90	4	8.44	36.24	4.76	6.06	5.80	0.03	0.08
Weak Axis, 30-Foot Drop, 0° Basket Drop Orientation											
P	2	53	85	1	15.80	35.40	0.00	4.70	4.20	1.23	1.38
P+Q	2	53	85	1	18.70	35.40	0.00	4.70	4.20	0.88	1.00
P	3	50	30	5	3.80	36.20	1.50	4.90	4.40	1.38	1.78
P+Q	3	50	45	5	7.40	36.20	1.30	4.90	4.40	1.10	1.47
Weak Axis, 30-Foot Drop, 45° Basket Drop Orientation											
P	2	39	90	2	11.20	18.00	0.00	2.40	2.20	0.61	0.71
P+Q	2	39	90	1	11.70	18.00	0.00	2.40	2.20	0.54	0.64
P	3	39	90	2	11.20	21.50	0.00	2.90	2.60	0.91	1.08
P+Q	3	39	90	1	11.90	21.50	0.00	2.90	2.60	0.81	0.97

Notes:
1. P = Primary Stress, P+Q = Primary + Secondary Stresses.
2. See Figures 2.6.14.2-9 and 2.6.14.2-10 for section location.
3. See Figure 2.7.9.1-1 for definition of cask drop angle.
4. See Figure 2.6.14.2-8 for disk number.

2.7.9.4 Yankee-MPC Fuel Tube Analysis

The fuel tube provides a foundation and sealed cavity to mount BORAL neutron poison plates within the fuel basket structure. It does not provide a structural function relative to the support of the fuel assembly. The fuel tube configuration is shown in Figure 2.7.9.4-1. To ensure that the fuel tube remains functional when the cask is subjected to design load conditions, a structural evaluation of the tube is performed for both the end and side impact load conditions. Since the enlarged fuel tube design is not equipped with BORAL and stainless steel sheath, the actual weight is less than that of the standard fuel tube (approximately 20 pounds less) and is bounded by the standard fuel tube analysis.

2.7.9.4.1 Fuel Tube Side Impact Analysis

Detailed finite element analysis and classical hand calculations were performed for the fuel tubes for the directly loaded NAC-STC system as documented in Section 2.7.8.4. By comparing the design parameters (dimensions, weight, etc.) of the fuel tube for the canistered fuel to those of fuel tubes for the NAC-STC system, it is concluded that the analyses for the directly loaded uncanistered NAC-STC envelope the design conditions for the fuel tube of the canistered fuel system.

A comparison of the design parameters for the fuel tube of the canistered Yankee class system and the fuel tube of the directly loaded NAC-STC system is shown below:

	Canistered	Directly Loaded
Fuel Tube Material (Stainless steel)	Type 304	Type 304
Fuel Tube Thickness (inch)	0.048	0.048
Fuel Tube Inside Dimension (inch)	7.80	8.78
Fuel Tube Weight (lb)	59	141
Fuel Assembly Weight (lb)	950	1,525
No. of Support Disks	22	31
Fuel Weight Supported by one Disk (lb)	41 (950/22)	49 (1,525/31)
Spacing Between Support Disk (inch)	3.91	4.37

2.7.9.4.2 End Impact Evaluation

The fuel tube end impact analysis for the directly loaded fuel basket configuration of the NAC-STC is documented in Section 2.7.8.4.1. The bearing stress during an end impact condition are proportional to the tube weight, tube cross-sectional area and the design g-load. Since the weight and center of gravity location of the canistered fuel configuration is essentially the same as that of the directly loaded fuel configuration, the same design g-loads (56.1g for end drop and 55g for side drop) are applicable to the canistered basket/tubes. Based on the fuel tube dimensions and loading data presented above, the bearing stress for an end impact condition for the canistered fuel tube is:

$$(S_{br})_{\text{directly loaded}} (59/141) (8.78/7.8) = 0.47 (S_{br})_{\text{directly loaded}}$$

From Section 2.7.8.4.1, the calculated $(S_{br})_{\text{directly loaded}}$ = 4.8 ksi, while the allowable stress (material yield strength) is 19.4 ksi.

Therefore, the canistered fuel tube stress is well below its allowable stress limit during an end impact accident condition.

Figure 2.7.9.4-1 Yankee-MPC Fuel Tube Configuration

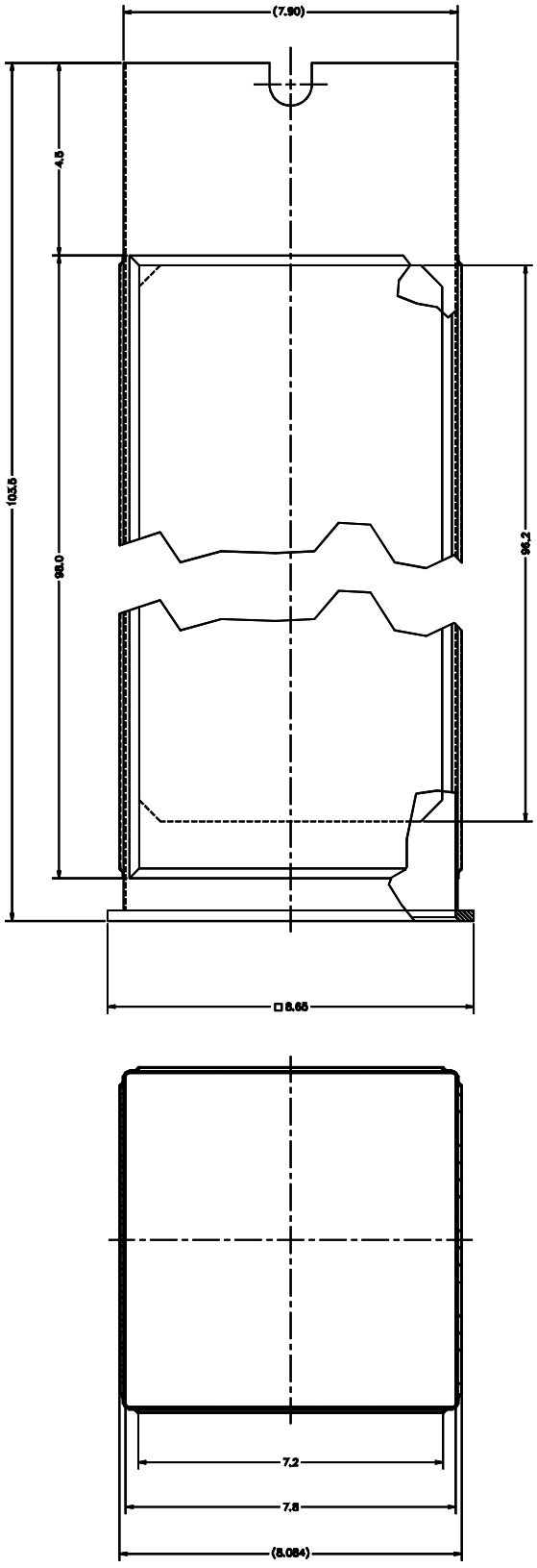

2.7.9.5 Yankee-MPC Basket Weldment Analysis for 30-Foot End Drop

The response of the top and the bottom weldment plates of the Yankee-MPC fuel basket assembly to a 56.1g accident condition deceleration load is examined. Two finite element models representing the PWR basket top and bottom weldments were constructed for structural evaluation. The structural evaluations were performed at normal condition temperatures; therefore, prior to the structural evaluation portion of the analyses, the steady-state temperature distribution in the top and bottom weldment models was determined by applying fixed temperatures to the outer circular edge and a volumetric heat generation rate to all of the elements, then solving for the intermediate temperatures. The fixed temperature of the outer edge of the top and bottom weldments was assumed to be equal to the maximum temperature of the canister lid/bottom plate. During the temperature solution portion of the analyses, the finite element models were constructed using ANSYS three-dimensional thermal shell elements (SHELL57). During the structural evaluation portion of the analyses, the finite element models were constructed using ANSYS three-dimensional, six-degrees-of-freedom, elastic shell elements (SHELL63). The finite element models represent one-quarter sections of the weldments.

The responses of the top and bottom weldments to a hypothetical accident 30-foot end drop were investigated using these two finite element models. For the 30-foot end drop evaluation, a deceleration load of 56.1g was used.

Both the top and bottom weldments are 0.5-inch thick and fabricated from SA240, Type 304 stainless steel. The top weldment supports its own weight and 36 fuel tubes (without the fuel assemblies) during a top end drop. Eight structural ribs, eight tie-rod ends, and a circumferential ring support the top weldment and its loads during a top end drop. These structural components are modeled as zero-translation restraints in the direction of the end drop.

In the four corner positions of the enlarged fuel tube basket configuration, the weldments can accommodate four enlarged fuel tubes. The standard opening size in the weldments is 7.79 inches, but in the four corner positions, the openings are enlarged to 7.97 inches. In the vertical orientation of the basket, the weight of the fuel tubes is transmitted to the bottom weldment and to the canister bottom plate via the stiffeners of the bottom weldment. The increased opening size is considered insignificant. With the net reduction in the weight of the fuel tube (20 pounds

due to the absence of the BORAL and sheath), the evaluation of the bottom weldment using the standard opening bounds the stresses in the bottom weldment with the enlarged fuel tube.

Similarly, to accommodate four damaged fuel cans, the openings are enlarged to 8.25 inches in the four corner positions of both the top and the bottom weldments. In the vertical orientation of the basket, the weight of the damaged fuel can is transmitted directly to the canister bottom plate. Since the weldments are subjected to less load in the damaged fuel can configuration, the evaluation of the weldments using the standard configuration bounds the evaluation of the weldments in the damaged fuel can configuration.

The finite element models of the top weldment and bottom weldment with the applied structural boundary conditions are presented in Figures 2.7.9.5-1 and 2.7.9.5-3, respectively. The finite element models of the top weldment and the bottom weldment with the applied structural forces are presented in Figures 2.7.9.5-2 and 2.7.9.5-4, respectively.

Figure 2.7.9.5-1 Yankee-MPC Top Weldment Finite Element Model with Structural Boundary Conditions

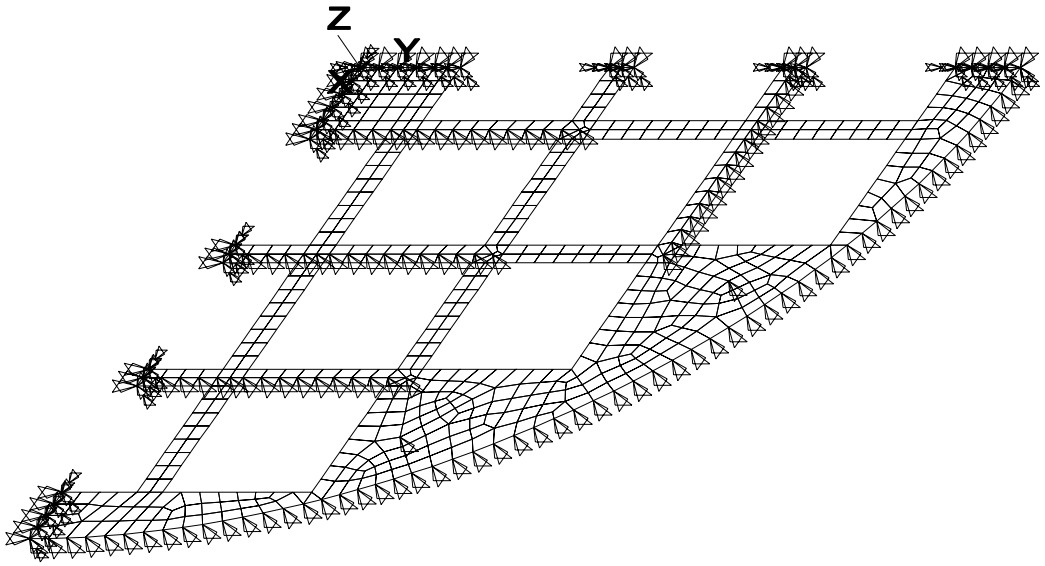

Figure 2.7.9.5-2 Yankee-MPC Top Weldment Finite Element Model with Structural Applied Loads

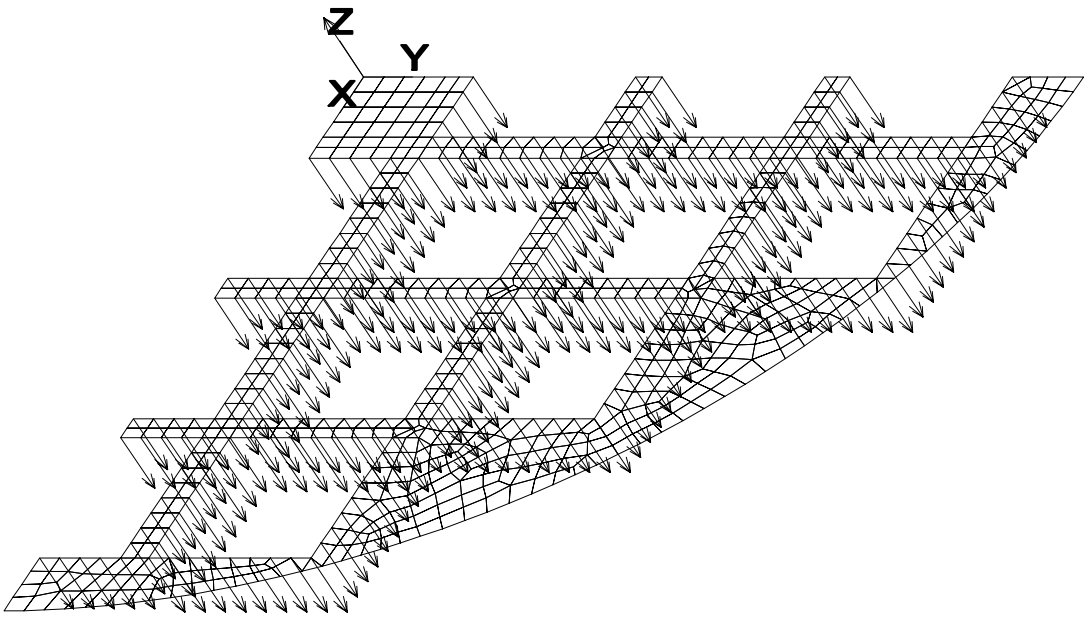

Figure 2.7.9.5-3 Yankee-MPC Bottom Weldment Finite Element Model with Structural Boundary Conditions

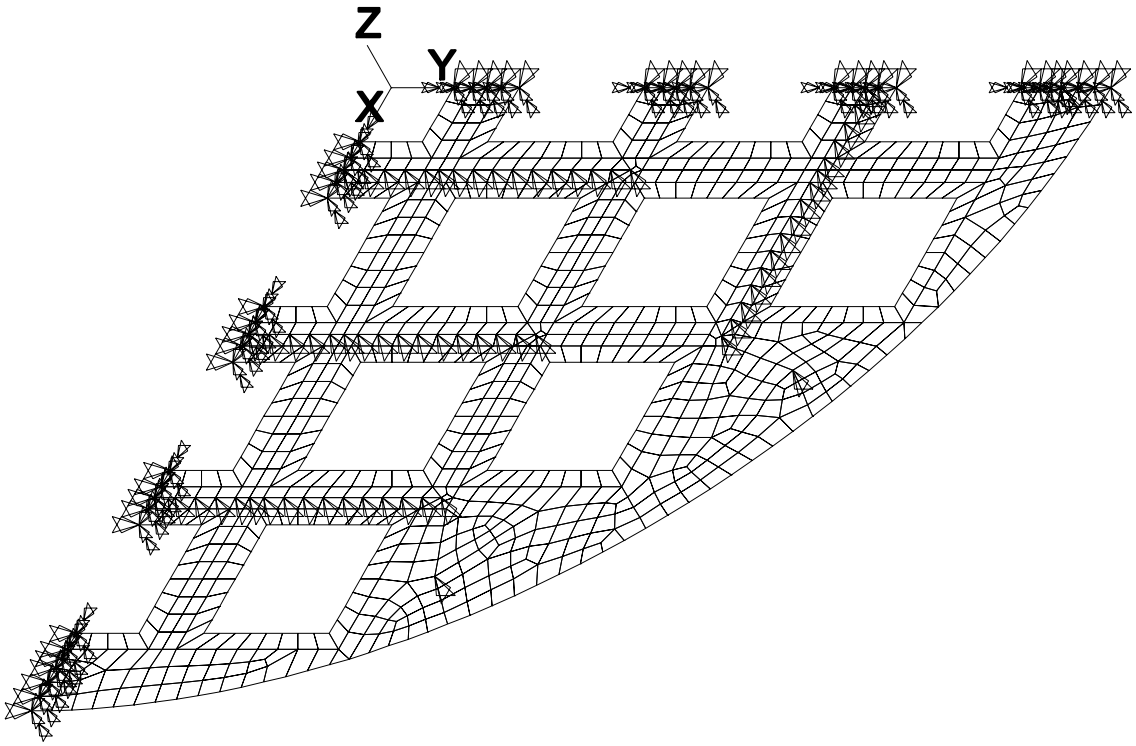

Figure 2.7.9.5-4 Yankee-MPC Bottom Weldment Finite Element Model with Structural Applied Loads

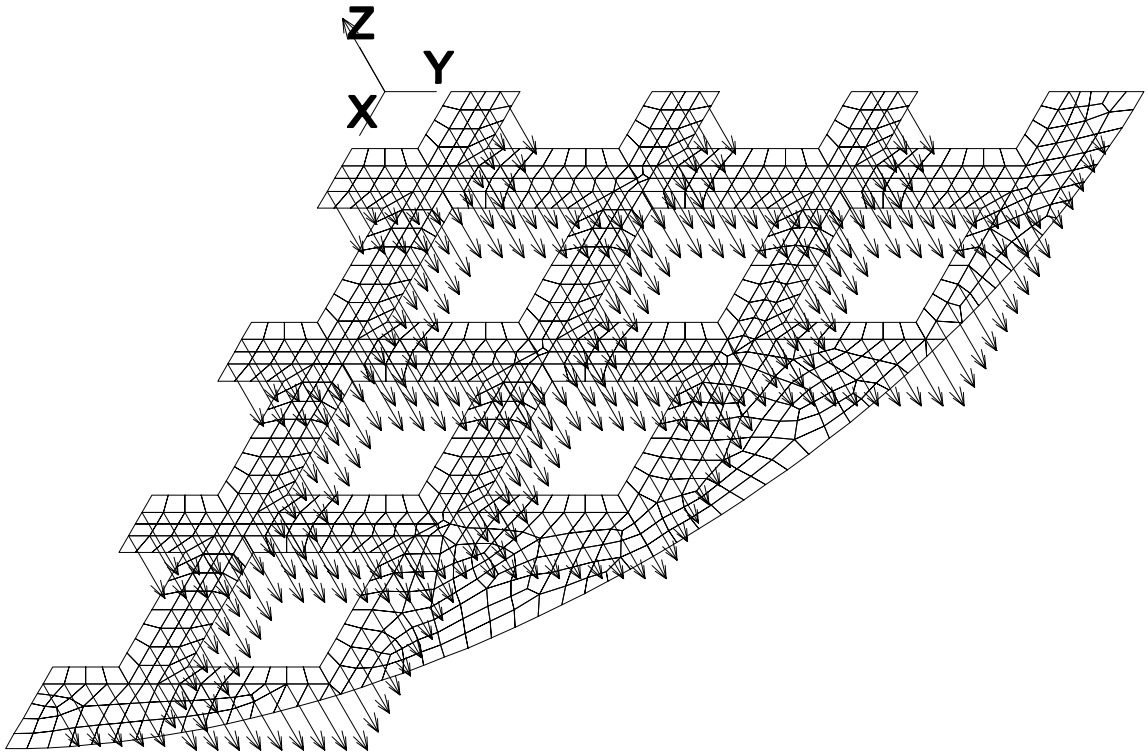

2.7.9.5.1 Results of Yankee-MPC Fuel Basket Weldment Analyses (30-Foot End Drop)

The maximum stress intensity (SI), for primary membrane plus primary bending ($P_m + P_b$), for the 30-foot end drop analysis is 58.0 ksi for the top weldment and 48.1 ksi for the bottom weldment as shown in the table below.

Because there is a large radial temperature gradient through the weldments, the maximum stress intensities do not occur at the maximum temperature of the models, and it is overly conservative to compare these stress intensities to stress allowables based upon the maximum temperature. Therefore, the stress evaluation was performed on a nodal basis. That is, using ANSYS, the maximum stress at each node in each model was compared to the maximum allowable stress at the temperature of the node being evaluated.

For hypothetical accident conditions, the following criteria was used in evaluating the top and bottom weldments nodal stress intensities:

$P_m + P_b < 3.6S_m$ or S_u, whichever is less.

(Note: For Type 304 stainless steel in these temperature ranges, S_u is smaller than $3.6S_m$.)

The margin of safety (M.S.) is calculated as:

M.S. = (Allowable Stress/ Nodal Stress Intensity) - 1

The minimum margins of safety for each weldment for the end drop condition are:

Component/Condition	$P_m + P_b$ (ksi)	Nodal Temp. (°F)	S_u (ksi)	M.S.
Top Weldment/30-ft. Drop	58.0	223	69.9	+0.20
Bottom Weldment/30-ft. Drop	48.1	257	68.1	+0.42

2.7.9.5.2 Yankee-MPC Top Weldment Structural Rib Buckling Evaluation

The structural ribs on the top weldment are subjected to axial loads during a top end drop. End constraints on the ribs during a top end drop consist of: fixed at the end welded to the top weldment, and free at the other end. Because there are no closed solutions readily available for

evaluating a plate for buckling loads with end constraints matching those of the top weldment ribs, a closed-form solution for the buckling of a column was used to analyze a 1-inch section of one of the ribs.

For a column under axial loading with one end fixed and the other end free, the critical load (P_{cr}) is determined by:

$$P_{cr} = \frac{\pi^2 EI}{(KL)^2}$$

where:

I = moment of inertia,
E = modulus of elasticity,
L = length of the column, and
K = effective length factor (K = 2 for a column with one end fixed and the other free).

Evaluating a 1-inch section of one of the ribs at the maximum weldment temperature of 540°F yields:

$$P_{cr} = \frac{\pi^2\left(25.6 \times 10^6 \text{ lb/in}^2\right)\frac{1}{12}(1.0\text{in})(0.38\text{in})^3}{(2 \times 6.80\text{in})^2} = 6{,}241 \text{ lb}$$

For the 30-foot top end drop, the sum of the forces on the nodes representing the ribs is a maximum of 3,681 lbs. Thus, the maximum load (P) on a 1-inch section of one of the structural ribs is:

$$P = \frac{3{,}681}{27.5/2}(1) = 268 \text{ lb}$$

Thus, the margin of safety (M.S.) for buckling of one of the structural ribs of the top weldment during a 30-foot top end drop is:

$$\text{M.S.} = \frac{6{,}241}{268} - 1 = +\text{large}$$

2.7.9.5.3 Conclusions

As shown in this section, both the top and bottom weldments maintain positive margins of safety when subjected to the 30-foot end drop conditions. As shown in the top weldment structural rib buckling calculation, the actual maximum load (P) on one of the structural ribs of the top weldment during a 30-foot drop is much less than the predicted buckling load (P_{cr}). Therefore, the top and bottom weldments are structurally adequate.

2.7.10 Greater Than Class C (GTCC) Basket Analysis - Accident Conditions

The Greater Than Class C (GTCC) basket is evaluated against the requirements of the ASME Code, Section III, Subsection NF (component supports), to ensure that the basket components are structurally adequate for loads imposed during normal conditions of transport in Section 2.6.16 and during hypothetical accident conditions in this section. The evaluation of the GTCC waste basket support disks and the support wall for the 30-ft end drop and side drop accident conditions are presented in this section. As discussed in Section 2.6.16.1, an evaluation of the tubes is not required for accident conditions. Load amplification factors of 55 g and 56.1 g are used for side drop and end drop conditions respectively. Accident condition allowable stresses are based on the normal condition of transport (Level A) in NF-3322 with a factor of 1.7 (NF-3341.1).

The evaluation of the Yankee-MPC and CY-MPC GTCC baskets is provided in Sections 2.7.10.1 and 2.7.10.2, respectively.

2.7.10.1 Yankee-MPC GTCC Basket Evaluation

Support Disk

In the side drop condition, the total basket and contents weight is shared by the eight (8) stainless steel disks. Due to the rigidity of the 2.5-inch thick support wall, the bending and shear stresses over the cross sections of the GTCC basket are not a concern. The in-plane compressive stress on the disk is the limiting factor and is evaluated to demonstrate structural integrity. Loads contributed to the in-plane stress are from the weights of one section (15.60 inches) of the 24 waste containers (baffles), 24 tubes, the wall and one disk. The weights are summarized as:

weight of one disk	= 3,373/8	= 422 pounds
weight of tube contributing to the disk load	= 5,935/7	= 848 pounds
weight of wall contributing to the disk load	= (5,478+8,116+3,507)/7	= 2443 pounds
weight of waste contributing to the disk load	= 12,341/7	= 1763 pounds
TOTAL		= 5476 pounds

The load, P, resulting from the 55 g deceleration experienced during the side drop is:

$$P = (55)(5{,}476) = 301{,}180 \text{ lbs.}$$

The lower portion of the disk (26.4-in. wide, 1-in. thick, and 6.5-in. high) is considered to be a column subjected to the axial force, P. The width of 26.4-in. is determined by considering a contact angle of 45° (between disk and canister shell during drop conditions). The cross-section area, A, considered for the load is:

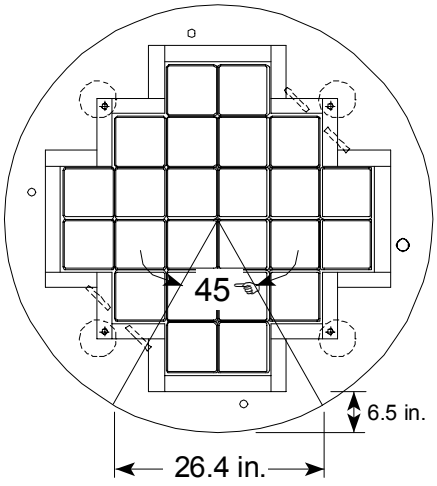

$$A = (1.0)(26.4) = 26.4 \text{ in}^2$$

The normal conditions allowable stress, F_a, for an axially loaded compression member is given by NF-3322.1(c)(2).

$$F_a = S_y\left(0.47 - \frac{Kl/r}{444}\right) = 8{,}331 \text{ psi,}$$

where,

K = 0.8 for the end conditions,

l = 6.5, length of disk to shell,

$$r = \frac{d}{\sqrt{12}} = 0.29.$$

Therefore, Kl/r = 18 < 120.

The allowable load across the section is calculated to be

$$P_y = 1.7\ A\ F_a = (1.7)(26.4)(8331) = 373{,}895 \text{ lb.}$$

The margin of safety is:

$$M.S. = \left(\frac{P_Y}{P}\right) - 1 = \left(\frac{373,895}{301,180}\right) - 1 = +0.24.$$

Side Drop Bearing Stress

In the side drop condition, the weight of the GTCC contents and eight (8) 1-inch thick support disks and the 2.5-inch thick plates that comprise the basket walls transmit the load to the canister shell through the 1-inch thick support disks. As computed in Section 2.7.10.1, the total impact load experienced by a single support disk, when factored by 55g, is 301,180 pounds. This is conservative because according to NF-3223.1, the bearing load evaluation is not required for service level D accident conditions. The bearing stress evaluation is the load divided by the area of contact between the 1-inch support disks and the canister shell. A 45 degree total angular contact is assumed for which the corresponding area of contact is:

$$A_c = \pi D t \theta = 27.08 \text{ in}^2.$$

where,

D = support disk diameter = 68.98 in.,

t = support disk thickness = 1.0 in,

θ = ratio for contact angle = 45/360 = 0.125.

This corresponds to a bearing stress (S_{br}) of

$$S_{br} = \frac{301,180}{27.08} = 11,121 \text{ psi}.$$

The allowable for the bearing stress for a normal condition of transport loading condition is S_y = 19,400 psi. Based on the conservative accident condition loading of 55g, the margin of safety is computed as

$$M.S.=\left(\frac{19,400}{11,121}\right)-1=+0.74.$$

Support Wall - Side Drop Evaluation

In the side drop orientation, the load of the GTCC waste and tubes is transferred into the 2.5-inch thick support walls. This develops a bending stress in the support wall. The deceleration of the contents and basket is 55g. Considering the load of waste baffle and tubes to be transmitted uniformly to the support walls, the maximum moment in the wall is

$$M_{max}=\frac{55(w)(L)^2}{8}=531,878\,in-lb.$$

where,

w = (5,935 + 5,478 + 8,116 + 3,507 + 12,341)/111.3 = 317.9 pounds/inch , which is the weight of the baffle, tubes and support wall per unit length and,

L = 15.60 , distance between the support disks.

The calculation of the sectional modulus (S = 970 in^3) of the support wall conservatively considers the lower portion of the 2.5-inch thick wall only. The bending stress is

$$f_b=\frac{531,799}{970}=548\text{ psi.}$$

The allowable is

$$1.7\times 0.6\,S_y = (1.7)(0.6)(19,400) = 19,788\text{ psi.}$$

The margin of safety is:

$$M.S.=\left(\frac{19,788}{548}\right)-1=+35.1$$

The maximum shear stress is considered to be the load transferred to a single disk divided by the cross sectional area (A_s) of the lower section of 2.5-inch thick wall.

$$A_s = 22.09(2.5) = 55.225 \text{ in}^2$$

Using the distributed weight of 317.9 pounds/inch

$$f_Y = \frac{0.5(55)(317.9)(15.6)}{55.225} = 2{,}470 \text{ psi.}$$

The allowable shear is $F_v = 1.7 \times 0.4S_y = (1.7)(0.4)(19400) = 13{,}192$ psi, and the margin of safety is

$$\text{M.S.} = \left(\frac{13{,}192}{2{,}470}\right) - 1 = +4.3.$$

Support Wall - End Drop Evaluation

In the end drop orientation, the weight of eight 1-inch thick support disks and the 2.5-inch thick plates that comprise the basket walls transmit the load to the canister end through the 2.5-inch thick plates. This represents a total weight of 20,474 pounds (5,478 + 8,116 + 3,507 + 3,373). The GTCC waste and tubes are free standing and will be supported by the canister ends directly.

The axial compressive stress evaluation is the total load times the deceleration (56.1g) divided by the area of contact between the 2.5-inch thick plates and the canister end. The cross sectional area of the wall is computed as the perimeter of the 2.5-inch plates,

$$A = (16)(2.5)(8.44) + (4)(2.5)(22.09) = 558.5 \text{ in}^2.$$

The applied force, P, resulting from the 56.1 g deceleration experienced during the end drop is:

$$P = (56.1)(20{,}474) = 1{,}148{,}591 \text{ lbs.}$$

The allowable stress, F_a, for an axially loaded compression member is given by NF-3322.1(c)(2).

$$F_a = S_y\left(0.47 - \frac{Kl/r}{444}\right) = 8{,}542 \text{ psi},$$

where,

K = 0.65 for the end conditions,

l = 14.6, distance between disks,

r = $\frac{d}{\sqrt{12}}$ = 0.72.

d = 1.0, thickness of support disk

Therefore, Kl/r = 13.18 < 120.

The allowable load across the section is calculated to be

$$P_y = 1.7\ A\ F_a = 1.7(558.5)(8{,}542) = 8{,}110{,}202 \text{ lb}$$

and the associated margin of safety is

$$\text{M.S.} = \left(\frac{8{,}110{,}202}{1{,}148{,}591}\right) - 1 = +6.1.$$

The Yankee-MPC GTCC basket support wall is adequate based on the above calculation.

Basket Support Disk - End Drop Evaluation

In the end drop orientation, the weight of a 1-inch thick support disk will produce a bending moment and shear force in the 3/8 inch weld at the support disk/wall interface. To simplify the evaluation, a 1-inch by 1-inch section is considered. The axial force, F_y, on the weld is

$$F_y = \frac{Wg}{L} = \left(\frac{(422)(56.1)}{235.6}\right) = 100.5 \text{ lb},$$

where,

W = 422 lb, the weight of one disk,

L = 4(25.15) + 16(8.44), the perimeter of the weld,

g = 56.1 g.

The bending moment, M, at the weld is

$$M = F_y\left(\frac{d}{2}\right) = 602.8 \text{ inch} - \text{pounds},$$

where,

d = $\frac{68.96}{2} - \sqrt{\left(\frac{39.03}{2}\right)^2 + \left(\frac{22.15}{2}\right)^2} = 12$ inch, the greatest radial distance to the outer edge of the disk.

$A_w = 2(1) = 2$ in.

The section modulus, S_w, for the weld cross-section is

$$S_w = bh = 1 \text{ in.}^2,$$

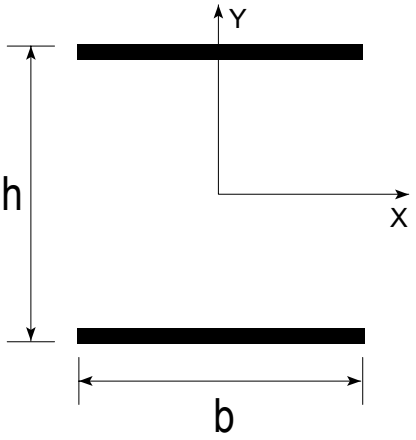

where,

b = 1 in.,

h = 1 in.

Therefore, the resulting bending force is calculated to be

$$F_b = \frac{M}{S_w} = 602.8 \frac{\text{lb}}{\text{in}}$$

and the shear force is

$$F_v = \frac{F_y}{A_w} = 50.3 \frac{\text{lb}}{\text{in.}}.$$

Therefore, the resulting shear force applied to the weld is

$$F_r = \sqrt{F_b^{\,2} + F_v^{\,2}} = 604.9 \frac{\text{lb}}{\text{in.}}.$$

The allowable shear stress in the base metal at the weld junction is

$$F_a = (1.7)(0.4)F_y = (1.7)(0.4)(19{,}400) = 13{,}192 \text{ lb/in}^2.$$

The required weld size is calculated as follows:

$$\frac{F_r}{F_a} = \frac{604.9}{13{,}192} = 0.05 \text{ in.} < \tfrac{3}{8} \text{ in.}$$

The required weld is less than the actual 3/8-inch weld. The support disk has larger cross-sectional area and moment of inertia than the weld and therefore is qualified by comparison to the weld. No further evaluation is required.

2.7.10.2 CY-MPC GTCC Basket Analysis – Accident Conditions

The CY-MPC GTCC basket is evaluated against the requirements of the ASME Code, Section III, Subsection NF (component supports), to ensure that the basket components are structurally adequate for loads imposed during normal conditions of transport (presented in Section 2.6.19.2) and hypothetical accident conditions (presented in this Section).

The GTCC basket is designed to transport up to 24 containers of GTCC waste. The basket (shield shell weldment) is constructed with 1.75-inch thick SA240 Type 304 stainless steel plates that form walls of a cylinder 141.5-inch long with an internal diameter of 60.5 inches and an external diameter of 64 inches. A total of 12 1-1/4 inch (thickness) × 2.4 inch (width) × 141.5 inch (length) plate/bar, also of Type 304 stainless steel material, is welded along the external surface of the shield shell wall. They are evenly spaced at 30° intervals and provide support to the basket wall structure. The GTCC waste containers (tube array weldment) are positioned and supported using 24 stainless steel tubes that are located within the welded wall structure.

Each stainless steel tube has an 8.74-inch square inside dimension, a 0.375-inch thick wall, and can hold one waste container. The tubes inside the basket are stacked together with a maximum of 6 tubes in a row and are welded together. The twelve perimeter locations where the tubes come in contact with each other are reinforced by plates and angles that are welded over the seams. The plates are connected to the tubes by ¼-inch fillet welds. The tube array rests inside of the basket wall supported by the tube corners in contact with the shell when in a horizontal position. The tube array is prevented from rotation by 3-inch tabs located 27 inches apart in the inside of the shield shell wall. The ends of the basket are enclosed by the canister, which provides end support to tubes in case of non-horizontal configurations.

Tube Array Weldment

The tube array weldment is not required to maintain structural integrity during accident conditions of transport. Therefore, no analysis of the Tube Array Weldment is presented in this section.

Shield Shell Weldment Evaluation

The shield shell weldment is a major component for shielding evaluation and, therefore, is required to maintain structural integrity during accident conditions of transport.

End Drop Analysis

During an end drop the entire weight of the shield shell weldment applies a compressive load at the base of the shell weldment. The shield shell weldment consists of the cylindrical shell and the 12 longitudinal ribs. The weight of the assembly is approximately 15,550 lbs., to account for additional hardware, a total weight of 15,700 lbs. will be used in the evaluation. The impact acceleration is 56.1g.

The cross-sectional area of the shell weldment at the base is:

$$A = \frac{\pi}{4} \times \left[64^2 - 60.5^2\right] = 437.8 \text{ in}^2 \qquad \text{(Area of ribs is neglected)}$$

The stress at the base of the assembly is:

$$S_s = \frac{56.1 \times 15{,}700}{437.8} = 2012 \text{ psi}$$

The maximum temperature at the shield shell is 272°F. Conservatively, using the allowable stresses at 300°F S_m = 20,000 psi, therefore, the margin of safety is:

$$\text{M.S.} = \frac{2.4 \times 20{,}000}{2{,}012} - 1 = +\text{large}$$

Side Drop Analysis

For a side-drop scenario, the same two-dimensional finite element model of the shield shell for the normal condition evaluation is used (see Figure 2.6.19-5). The analysis is performed considering an inertia load of 55 g. Four side drop orientations (45°, 60°, 75° and 90°) are considered. A conservative temperature of 300°F is used to determine the material properties and the allowable stresses.

The analysis results indicate that the governing case corresponds to the drop orientation of 75°. The stress results for this drop orientation are summarized in Table 2.7.10.2-1 for the P_m and $P_m + P_b$ stress, respectively. The minimum margin of safety is +4.58 for the P_m stress and +2.74 for the $P_m + P_b$ stress. The locations of the sections with top four P_m+P_b stresses are shown in Figure 2.6.19-7.

Weld Analysis

The longitudinal ribs are connected to the shield shell by 3/16" partial penetration groove welds along the entire length of the shell.

The impact load is transmitted from the ribs to the shell across the two connecting welds on each rib. Subsection NF-3226.2 of the ASME code provides with the requirements for the partial penetration welds to meet the same requirements as for the base metal. Conservatively, the stresses across the weld are treated as membrane stresses and subject to the stress limit of $1.5\times S_m$. For the analyzed drops the minimum number of ribs in contact with the canister is two; therefore, the total load will be resisted by 4 welds. The total applied load of 2,800,000 lbs. is uniformly distributed across the section of each weld.

$$F = (30{,}413 + 18{,}742)\times 55 = 2{,}703{,}525 \text{ lbs.} \quad \text{Use } 2{,}800{,}000 \text{ lbs}.$$

The area of the welds joining the rib to the shell is:

$$A = 4\times 141.5\times \frac{3}{16} = 106.2 \text{ in}^2$$

The average stress is:

$$S_{average} = \frac{2{,}800{,}000}{106.2} = 26{,}365 \text{ psi}$$

The membrane strength (S_m) of SA-240 304 at 300°F is 20 ksi, and the margin of safety is:

$$MS = \frac{1.5\cdot S_m}{S_{average}} - 1 = \frac{30{,}000}{26{,}365} - 1 = 0.14$$

Table 2.7.10.2-1 CY-MPC GTCC Shield Shell Weldment P_m Stress Summary - 75° Side Drop, Accident Condition

Sec	Principal Stress Components (psi)			Stress Intensity (psi)	Allowable Stress (psi)	Margin of Safety
	S1	S2	S3			
1	0	-733	-8276	8276	46200	4.58
2	0	-934	-7499	7499	46200	5.16
3	78	0	-2603	2682	46200	16.23
4	63	0	-2657	2721	46200	15.98

2.7.11 Yankee-MPC Transportable Storage Canister Analysis – Accident Conditions

This section presents the evaluation of the transportable storage canister for the hypothetical accident conditions. The evaluation for normal conditions of transport is presented in Section 2.6.13.

The canistered fuel, or the canistered GTCC waste, configuration consists of the canister together with the top and bottom transport spacers. The spacers position the canister in the NAC-STC cavity to ensure that the center of gravity of the NAC-STC in the canistered configuration is the same as that for the directly loaded fuel configuration.

The principal components of the canister are the canister shell, including the bottom plate, the fuel basket or GTCC waste basket, the shield lid, and the structural lid. A description of the geometry and materials of construction of the canister, baskets, and spacers are provided in Section 1.2.1.2.8.

For damaged fuel can shipments, the damaged fuel can extends through the bottom and top weldments of the basket and is captured between the shield lid for the damaged fuel configuration and canister bottom plate. To accommodate the damaged fuel can, the shield lid is machined on the underside in four places to mate with the damaged fuel can lid. These machined areas occur in regions of low stress and are, therefore, not evaluated.

The general arrangement of the canister, depicted with the fuel basket, is shown in Figure 2.6.13-1. The individual components of the canister are depicted in Figure 2.6.13-2.

A drop accident stress evaluation is performed for the 30-foot side drop condition, and for the 30-foot top and bottom end drop conditions. The stress intensities resulting from these two evaluations bound those that result from the 30-foot corner and oblique drop conditions. This conclusion is based on the analysis results for the directly loaded fuel configurations described in Sections 2.6.12, 2.7.1.3, 2.7.1.4, and 2.7.8.

The transport spacers may crush under the corner, oblique and end drop conditions. In crushing, they reduce the total g load on the fuel or GTCC waste canister that would occur in the hypothetical accident conditions. However, no credit is taken for the presence of the aluminum honeycomb spacers. All of the impact g load - 55 g for the side drop, and 56.1 g for the end drops – is assumed to be applied to the canister. Consequently, the end drop analyses are conservative.

2.7.11.1 Canister - Accident Analysis Description

The canister is a right-circular shell fabricated from rolled 5/8-inch thick, Type 304L stainless steel plate. It is closed on its bottom end with a Type 304L stainless steel circular plate that is 1-inch thick. The canister is closed at the top end by a 5-inch thick, Type 304 stainless steel shield lid, which is seal welded to the canister shell. The shield lid is covered by a 3-inch thick, Type 304L, stainless steel structural lid welded to the canister shell at its top inside edge. The loaded canister is lifted using 6 hoist rings threaded into the top of the structural lid. The canister is the defined confinement boundary for spent fuel or GTCC waste contents during long-term storage, and it is the defined containment boundary for Reconfigured Fuel Assemblies during transport, satisfying the requirements of 10 CFR 71.63(b) for a separate inner container. No credit is taken for containment by the canister for the transport of intact fuel assemblies or GTCC waste. Containment of these contents for transport is provided by the NAC-STC, using the same containment boundary defined for the directly loaded fuel configuration.

The structural design criteria for the canister is the ASME Code Section III, Subsection NB, "Class 1 Components." Consistent with this criteria, the structural components of the canister (shell, bottom plate, and structural lid) are shown to satisfy the allowable stress intensity limits presented in Table 2.1.2-1.

The canister is evaluated using the ANSYS finite element program for the 30-foot drop conditions in the end and side impact orientations. The ANSYS finite element model is the same as that used for the evaluation of the 1-foot drop impacts evaluated for normal conditions of transport. The model is described in Section 2.6.13.2. As described in Section 2.6.13.2, the COMBIN40 elements used between the structural and shield lids and for the backing ring are assigned a gap sizes of 1E-8 inches. The maximum gap size is 0.08 inches. However, use of the smaller gap size results in the highest stresses at critical sections, resulting in the lowest margin of safety. All gap-spring elements are assigned a stiffness of 1E8 lb/in.

2.7.11.2 Analysis Results

The detailed results of the analysis for the 30-foot side, and top and bottom end drops are presented in Tables 2.7.11-1 through 2.7.11-6. The force summation for the side drop analyses indicated that the weight of the canister and contents was 4.86% less than actual (i.e., the

modeled weight (26,098 pounds) was less than the calculated weight (27,365 pounds) by 4.86%). Consequently, the stresses presented in the tables for the side drop, are scaled up 4.86% from those same stresses calculated by the finite element model. The section stresses presented in the tables are identified by a section number. A cross-section of the canister showing the section numbers is presented in Figure 2.7.11-1. A summary of the canister minimum Margins of Safety for the evaluated drop conditions is shown in Table 2.7.11-7.

For the top and bottom end drops, the stresses are essentially uniform around the circumference. For the side drop, the stresses vary around the circumference. Therefore, the circumferential angle at which the maximum stress occurs is noted in the table, (in parentheses) beside the section number. The allowable stresses presented in the tables are for Type 304L stainless steel, except for section 10, which is for Type 304 stainless steel. These allowables are evaluated at 350°F (maximum calculated temperature in the canister is 338°F). The allowable stress for P_m stresses is defined as the lesser of 2.4 S_m or 0.7 S_u. The allowable stress for the $P_m + P_b$ stresses is defined as the lesser of 3.6 S_m or 1.0 S_u.

The minimum margin of safety for the evaluated side and end drops is +0.69 for the primary membrane stress (P_m) in the 30-foot side impact, using the minimum gap size of 1×10^{-8} inches at Section 8. The minimum margin of safety for the evaluated side and end drops is +0.83 for the primary membrane stress at the same section, assuming the maximum gap size of 0.08 inches. Consequently, use of the minimum gap size is conservative.

The canister structural lid closure weld is specifically evaluated for the hypothetical accident conditions. The lid weld is identified as Section 8 in Figure 2.7.11-1. The structural lid weld has a root and final weld surface Liquid Penetrant examination performed in accordance with ASME, Section V, Article 6. Upon completion, the weld is ultrasonically examined in accordance with ASME Section V, Article 5, or multi-pass liquid penetrant examined in accordance with ASME Section V, Article 6. In accordance with NRC guidance, if a multi-pass liquid penetrant examination is performed on the structural lid closure weld, two separate weld stress reduction factors are applied to the structural lid canister shell weld – a 0.8 factor to conservatively consider the weld configuration and a 0.8 factor per NRC ISG-4, Item 5. Thus, a total weld stress reduction factor of 0.64 (0.8 x 0.8) is applied to the stress allowable for the structural lid weld. The canister closure weld evaluation for accident conditions is presented in Section 2.7.11.4. The evaluation, which is based on the finite element analysis stress result as shown in Section 2.7.11.2, shows a minimum margin of safety of +0.69 for the weld.

Figure 2.7.11-1 Identification of the Sections for Evaluating the Linearized Stresses in the Canister

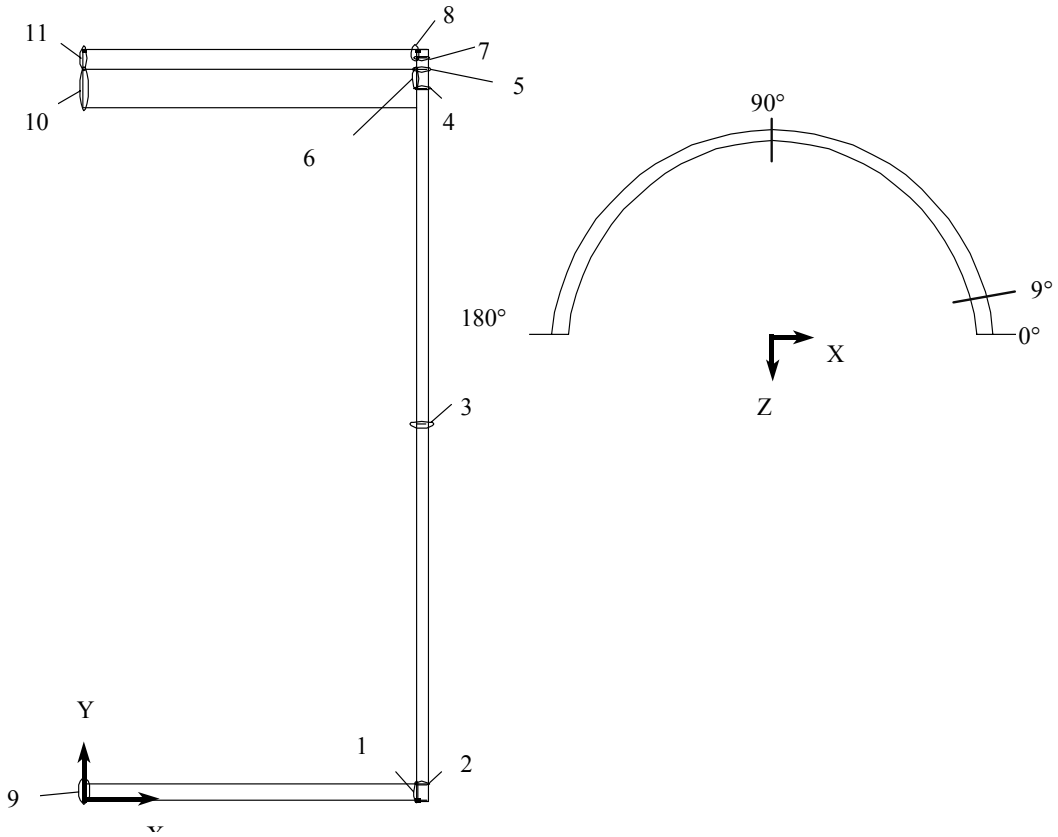

	Node 1		Node 2	
Section	X	Y	X	Y
1	34.695	0.000	34.695	1.000
2	34.695	1.000	35.320	1.000
3	34.695	57.269	35.320	57.269
4	34.695	118.000	35.320	118.000
5	34.695	119.000	35.320	119.000
6	34.695	118.000	34.695	119.000
7	34.695	121.120	35.320	121.120
8	34.695	121.120	34.695	122.000
9	0.000	0.000	0.000	1.000
10	0.000	114.000	0.000	119.000
11	0.000	119.000	0.000	122.000

Table 2.7.11-1 Canister, 30-Foot Side Drop (Primary Membrane Stress) (psi)

Section No.	Component Stresses						Principal Stresses			S.I.	Allow. Stress	Margin of Safety
	SX	SY	SZ	SXY	SYZ	SXZ	S1	S2	S3			
1(0°)	-14680.4	1080.1	-9311.6	-235.5	-21.1	-904.6	1083.2	-9163.7	-14827.2	15917.7	39000	1.45
2(0°)	-3395.4	62.4	-7415.7	-314.3	-438.9	-478.6	111.6	-3358.7	-7501.7	7612.8	39000	4.12
3(180°)	-4.6	-1213.2	586.7	0.1	-4.0	-45.8	590.3	-8.1	-1213.2	1802.5	39000	20.64
4(9°)	-16945.4	3043.0	-4750.2	-336.0	2851.1	2020.7	3978.4	-5329.0	-17301.9	21276.1	39000	0.83
5(0°)	-10863.5	1232.1	-7804.7	-1756.4	1333.8	92.4	1662.0	-7961.0	-11146.6	12803.4	39000	2.05
6(0°)	-23467.7	-3813.8	-11125.6	-2768.3	1168.1	38.0	-3262.2	-11293.4	-23855.7	20594.5	39000	0.89
7(9)	-11503.1	654.7	-4158.7	-31.6	1865.5	961.7	1299.2	-4673.6	-11639.5	12939.7	39000	2.01
8(0°)	-19367.6	-4979.8	-8614.2	-982.6	865.8	-756.5	-4697.7	-8785.2	-19472.5	14774.8	24960*	0.69
9	-2146.5	-15.3	1105.2	-2.9	-14.7	-78.0	1107.3	-15.5	-2148.6	3255.9	39000	10.98
10	-1032.3	-8.4	331.8	-59.4	-2.9	-27.1	332.3	-4.9	-1036.3	1368.4	45640	32.35
11	-1131.4	-1.3	373.3	-25.5	-5.1	-32.8	374.1	-0.7	-1132.5	1506.8	39000	24.88

* Includes two stress reduction factors for weld: 0.8 x 0.8 = 0.64 (See Section 2.7.11.4).

Table 2.7.11-2 Canister, 30-Foot Side Drop (Primary Membrane Plus Primary Bending Stress) (psi)

Section No.	Component Stresses						Principal Stresses			S.I.	Allow. Stress	Margin of Safety
	SX	SY	SZ	SXY	SYZ	SXZ	S1	S2	S3			
1(0°)	-24841.3	457.1	-12761.5	-195.8	106.1	-824.5	459.5	-12709.0	-24904.3	25365.6	58500	1.31
2(0°)	-2630.9	-1326.5	-8993.8	-290.8	-641.0	-126.3	-1218.5	-2682.3	-9050.5	7832.0	58500	6.47
3(0°)	89.9	2039.5	3198.2	2.7	38.7	156.9	3207.7	2038.5	81.9	3125.9	58500	17.71
4(9°)	-13894.0	9446.8	-2019.6	93.3	2241.9	2829.1	9886.2	-1813.0	-14533.6	24421.9	58500	1.40
5(0°)	-14261.0	2077.3	-6923.9	-2052.1	1046.5	-15.1	2446.4	-7037.2	-14512.6	16966.3	58500	2.45
6(0°)	-32968.0	-7832.0	-15215.2	-4140.9	1477.5	185.3	-6920.8	-15456.4	-33639.1	26718.3	58500	1.19
7(9°)	-9079.8	4969.3	-1993.4	53.6	1402.0	1674.6	5250.3	-1894.8	-9460.5	14711.9	58500	2.98
8(0°)	-28144.4	-7245.8	-12646.1	-2107.7	1351.6	-307.9	-6716.3	-12971.2	-28354.1	21643.1	37440*	0.73
9	-2172.7	-33.2	1088.4	-2.9	-14.9	-75.6	1089.5	-33.5	-2174.8	3264.3	58500	16.92
10	-1360.0	-10.9	297.9	-63.0	-2.9	-40.8	299.0	-8.0	-1364.2	1663.1	65200	38.20
11	-1344.3	-1.2	354.1	-25.6	-5.0	-39.5	355.1	-0.7	-1346.4	1700.8	58500	33.40

* Includes two stress reduction factors for weld: 0.8 x 0.8 = 0.64 (See Section 2.7.11.4).

Table 2.7.11-3 Canister, 30-Foot Bottom End Drop (Primary Membrane Stress) (psi)

Section No.	Component Stresses						Principal Stresses			S.I.	Allow. Stress	Margin of Safety
	SX	SY	SZ	SXY	SYZ	SXZ	S1	S2	S3			
1	-70.7	-1971.0	-361.1	176.2	70.3	22.4	-51.8	-360.9	-1990.0	1938.0	39000.0	19.12
2	289.7	-5185.0	-1182.0	91.4	54.3	94.4	297.4	-1187.0	-5187.0	5485.0	39000.0	6.11
3	2.1	-4867.0	0.9	0.0	0.2	0.0	2.1	0.9	-4867.0	4869.0	39000.0	7.01
4	-2131.0	-2251.0	-1084.0	0.0	734.3	0.0	-729.3	-2131.0	-2605.0	1876.0	39000.0	19.79
5	2510.0	-2096.0	-1535.0	-310.9	-0.9	278.1	2549.0	-1553.0	-2117.0	4667.0	39000.0	7.36
6	551.9	1897.0	-676.0	15.4	84.7	-106.6	1900.0	561.0	-688.0	2588.0	39000.0	14.07
7	-3028.0	979.9	-1533.0	-368.1	39.6	55.9	1014.0	-1531.0	-3063.0	4077.0	39000.0	8.57
8	588.3	-3496.0	-2019.0	466.6	119.6	210.4	659.5	-2031.0	-3554.0	4214.0	24960.0*	4.92
9	82.5	-682.0	94.2	6.5	58.3	-0.5	98.5	82.5	-686.4	785.0	39000.0	48.68
10	183.8	-98.9	168.1	43.7	-77.1	5.7	195.2	183.5	-125.7	320.9	45640.0	141.22
11	-469.6	-9.4	-467.5	48.0	-75.2	-1.2	7.4	-470.1	-483.8	491.2	39000.0	78.40

* Includes two stress reduction factors for weld: 0.8 x 0.8 = 0.64 (See Section 2.7.11.4).

Table 2.7.11-4 Canister, 30-Foot Bottom End Drop (Primary Membrane Plus Primary Bending Stress) (psi)

Section No.	Component Stresses						Principal Stresses			S.I.	Allow. Stress	Margin of Safety
	SX	SY	SZ	SXY	SYZ	SXZ	S1	S2	S3			
1	398.0	-2678.0	-380.7	125.9	67.7	37.0	405.2	-380.8	-2685.0	3090.0	58500.0	17.93
2	-1988.0	-7553.0	85.1	0.0	-32.4	0.0	85.2	-1988.0	-7553.0	7638.0	58500.0	6.66
3	2.1	-4867.0	2.9	1.1	0.4	-0.1	3.0	2.1	-4867.0	4870.0	58500.0	11.01
4	-2259.0	-3096.0	-704.5	0.0	805.1	0.0	-458.8	-2259.0	-3342.0	2883.0	58500.0	19.29
5	1450.0	-10380.0	-4379.0	304.5	3.7	410.7	1486.0	-4407.0	-10390.0	11880.0	58500.0	3.92
6	3324.0	5269.0	932.2	817.6	53.3	-170.6	5567.0	3041.0	917.1	4650.0	58500.0	11.58
7	-2361.0	8380.0	938.8	-472.4	41.6	196.1	8401.0	950.4	-2393.0	10790.0	58500.0	4.42
8	4403.0	-1585.0	-491.6	605.7	160.4	345.7	4490.0	-503.9	-1659.0	6149.0	37440.0*	5.09
9	105.1	-686.4	100.3	8.1	60.4	-1.7	106.1	104.0	-691.1	797.2	58500.0	72.38
10	6941.0	230.8	6895.0	28.2	-72.6	35.9	6960.0	6876.0	229.9	6730.0	65200.0	8.69
11	-4093.0	-195.3	-4098.0	47.4	-79.5	-18.6	-193.1	-4079.0	-4115.0	3922.0	58500.0	13.92

* Includes two stress reduction factors for weld: 0.8 x 0.8 = 0.64 (See Section 2.7.11.4).

Table 2.7.11-5 Canister, 30-Foot Top End Drop (Primary Membrane Stress) (psi)

Section No.	Component Stresses						Principal Stresses			S.I.	Allow. Stress	Margin of Safety
	SX	SY	SZ	SXY	SYZ	SXZ	S1	S2	S3			
1	68.2	-371.6	-91.0	-74.7	-19.4	7.7	81.2	-90.6	-385.0	466.2	39000.0	82.66
2	-130.9	110.4	271.9	-75.3	-8.3	-28.6	273.9	131.9	-154.5	428.5	39000.0	90.02
3	-2.9	-975.6	1104.0	0.0	-0.1	-87.6	1110.0	-9.8	-975.6	2086.0	39000.0	17.70
4	185.3	-1596.0	-207.6	-108.1	-29.1	23.1	193.4	-208.6	-1603.0	1796.0	39000.0	20.71
5	-244.0	-1458.0	-78.9	0.0	-55.0	0.0	-76.7	-244.0	-1460.0	1384.0	39000.0	27.18
6	-84.0	-969.1	-40.4	0.0	-65.6	0.0	-35.8	-84.0	-973.7	937.9	39000.0	40.58
7	-18.5	-1372.0	-204.8	2.2	-21.7	-3.1	-18.5	-204.5	-1372.0	1354.0	39000.0	27.80
8	-9.6	-1177.0	-128.4	-6.9	-12.4	-1.4	-9.5	-128.3	-1178.0	1168.0	24960.0*	20.37
9	-3.5	-11.4	-3.7	-25.0	73.7	0.0	70.4	-3.5	-85.5	155.8	39000.0	249.32
10	2.6	-619.2	9.4	-2.6	5.6	-0.6	9.5	2.5	-619.3	628.8	45640.0	71.58
11	-22.9	-703.7	5.2	-2.3	-5.5	-1.9	5.4	-23.0	-703.8	709.1	39000.0	54.00

* Includes two stress reduction factors for weld: 0.8 x 0.8 = 0.64 (See Section 2.7.11.4).

Table 2.7.11-6 Canister, 30-Foot Top End Drop (Primary Membrane Plus Primary Bending Stress) (psi)

Section No.	Component Stresses						Principal Stresses			S.I.	Allow. Stress	Margin of Safety
	SX	SY	SZ	SXY	SYZ	SXZ	S1	S2	S3			
1	-217.7	-703.2	-2.5	-49.8	-15.1	-8.6	-1.9	-212.9	-708.6	706.7	58500.0	81.78
2	-84.3	1053.0	572.2	-92.6	-3.7	-51.7	1061.0	576.2	-95.8	1156.0	58500.0	49.61
3	-7.8	-973.9	1117.0	0.3	-0.2	-89.1	1124.0	-14.8	-973.9	2098.0	58500.0	26.88
4	-502.0	-2503.0	98.7	0.0	-82.4	0.0	101.3	-502.0	-2505.0	2607.0	58500.0	21.44
5	-29.7	-1643.0	-310.5	-74.7	-31.4	25.3	-23.8	-312.3	-1647.0	1623.0	58500.0	35.04
6	-227.9	-1240.0	-231.6	0.0	-33.7	0.0	-227.9	-230.4	-1241.0	1013.0	58500.0	56.75
7	-17.4	-1481.0	-246.9	-20.4	-23.0	-10.0	-16.7	-246.9	-1482.0	1465.0	58500.0	38.93
8	27.1	-1150.0	-107.9	5.8	-7.2	4.9	27.3	-108.0	-1150.0	1177.0	37440.0*	30.81
9	1221.0	66.5	1214.0	-25.0	73.7	12.9	1232.0	1209.0	61.3	1171.0	58500.0	48.96
10	95.9	-619.9	105.1	-0.8	11.4	0.5	105.3	95.9	-620.1	725.4	65200.0	88.88
11	-8.2	-704.4	12.6	3.5	9.8	0.0	12.8	-8.2	-704.6	717.3	58500.0	80.56

* Includes two stress reduction factors for weld: 0.8 x 0.8 = 0.64 (See Section 2.7.11.4).

Table 2.7.11-7 Summary of Minimum Margin of Safety for Canister 30-Foot Drops

Drop Orientation	**Loading Condition**	**Stress Evaluated**	**Minimum Margin of Safety**	**Section No.***
Bottom end	30-ft. impact + pressure (0 psi)	P_m	4.92	8
Bottom end	30-ft. impact + pressure (0 psi)	$P_m + P_b$	3.92	5
Side	30-ft. impact + pressure (20 psi)	P_m	0.69	8
Side	30-ft. impact + pressure (20 psi)	$P_m + P_b$	0.73	8
Top end	30-ft. impact + pressure (20 psi)	P_m	17.70	3
Top end	30-ft. impact + pressure (20 psi)	$P_m + P_b$	21.44	4

* See Figure 2.7.11-1 for section locations.

2.7.11.3 Canister Buckling Evaluation for the 30-Foot End Drop

The canister shell is axially loaded by the weights of the structural lid, the shield lid, and the inertial weight of the shell during a 30-foot end drop impact. The impact load amplification factor is 56.1g's. The shell is evaluated as an unsupported, right circular cylinder using a critical buckling load per Blake, 2nd Edition, "Practical Stress Analysis in Engineering Design."

$$S_{cr} = \frac{E\left(0.605 - 10^{-7} M^2\right)}{M\left(1 + 0.004\phi\right)}$$

$$= 40.3 \text{ ksi}$$

The canister material is Type 304L stainless steel. Conservatively assume the material temperature to be at 400°F for the accident condition.

$E = 26.5E+03$ ksi $R = (69.39 + 0.625)/2$

$= 35.01$ inches (mid-radius of the canister shell)

$S_y = 17.5$ ksi $t = 0.625$ inches. (thickness of the canister)

$\phi = E/S_y$ and $M = R/t$

$= 1514.3$ $= 56.0$

The axial compression load in the canister shell is:

$$P_a = [\,(\pi/4)\,(69.03^2)\,(8)(0.291) + (\pi/4)(\,70.64^2 - 69.39^2\,)(121.5)(0.291)\,]\,(56.1)$$

$P_a = 761{,}457$ pounds

and the axial compression stress is:

$$S_a = \frac{P_A}{\left(\pi/4\right)\left(70.64^2 - 69.39^2\right)}$$

$S_a = 5{,}540$ psi

The margin of safety is:

$(S_{cr}/S_a) - 1 = +\ 6.3$

2.7.11.4 Canister Closure Weld Evaluation – Accident Conditions

2.7.11.4.1 Stress Evaluation for the Canister Closure Weld

The closure weld for the canister is a partial penetration weld with a thickness of 0.9 inches. The evaluation of this weld, in accordance with NRC guidance, is to incorporate two separate weld stress reduction factors: a 0.8 factor based on weld type and a second 0.8 factor based on NRC ISG-4, Item 5. These two weld stress reduction factors are incorporated by applying a factor of 0.64 (0.8 x 0.8) to the stress allowable for this weld.

The stresses for the canister are evaluated using sectional stresses as permitted by Subsection NB. The canister stress results from Section 2.7.11.2 are used for evaluation. The location of the section for the canister weld evaluation is shown in Figure 2.7.11-1 and corresponds to Section 8. The P_m and $P_m + P_b$ stress intensity for Section 8 and the associated allowables are listed below. The factored allowables, incorporating a 0.64 stress reduction factor, and the resulting margin of safety are:

STRESS TYPE	Analysis Stress Intensity (ksi)	0.64 x Allowable Stress (ksi)	Margin of Safety
P_m	14.77	24.96	0.69
$P_m + P_b$	21.64	37.44	0.73

This confirms that the canister closure weld is acceptable for the accident conditions.

2. 7.11.4.1 Critical Flaw Size for the Canister Closure Weld

The closure weld for the canister is comprised of multiple weld beads using a compatible weld material for Type 304L stainless steel. An allowable (critical) flaw evaluation has been performed to determine the critical flaw size in the weld region. The result of the flaw evaluation is used to define the minimum flaw size, which must be identifiable in the nondestructive examination of the weld. Due to the inherent toughness associated with Type 304L stainless steel, a limit load analysis is used in conjunction with a J-integral/tearing modulus approach.

The safety margins used in this evaluation correspond to the stress limits contained in Section XI of the ASME Code.

The stress component used in the evaluation for the critical flaw size is the radial stress component in the weld region of the structural lid. For an accident (Level D) event, in accordance with ASME Code Section XI, a safety factor of $\sqrt{2}$ is required. For the purpose of identifying the stress for the flaw evaluation, the weld region corresponding to Section 8 in Figure 2.7.11-1 is considered. From additional post processing of the tipover analysis, the maximum tensile radial stress is 4.4 ksi. To perform the flaw evaluation, a 10 ksi stress is conservatively used, resulting in a significantly larger safety factor than the required safety factor of $\sqrt{2}$. Using 10 ksi as the basis for the evaluation, the minimum detectable flaw size is 0.52 inch for a flaw that extends 360 degrees around the circumference of the canister. Stress components for the circumferential and axial directions are also determined, which would be associated with flaws oriented in the radial or horizontal directions, respectively. The maximum stress for these components is 0.6 ksi, which is enveloped by the stress value of ksi used for the critical flaw evaluation for radial directions. The 360-degree flaw employed for the circumferential direction is considered to be bounding with respect to any partial flaw in the weld, which could occur in the radial and horizontal directions. Therefore, using a minimum detectable flaw size of 3/8 inch is acceptable, since it is less than the very conservatively determined 0.52-inch critical flaw size.

2.7.11.5 Dyanamic Loading Effect - Structural Lid Weld

In a top end impact accident of the NAC-STC, the fuel assemblies and the basket in the canister bear against the canister shield lid. That load is transmitted to the shield lid weld, to the canister shell, and to the canister structural lid. The impact load occurs for a duration of approximately 100 milliseconds and, depending on the stiffness of the load path, dynamic amplification may occur. Two types of analyses are performed to evaluate the dyanmic effect on the stresses at the canister/structural lid weld: 1) a static analysis using an axial acceleration of 45g; and 2) a transient analysis in which the loading is the time varying acceleration (45g maximum) associated with the compression of the top impact limiter. Note that 45g is selected as being equivalent to the axial component of the acceleration for the 30-foot top corner drop based on the impact limiter analysis (see Table 2.6.7.4.1-3).

2.7.11.5.1 Model Description

The analyses for this evaluation use a two-dimensional model of the upper portion of the canister, which includes the shield lid and the structural lid, as well as the upper 33 inches of the canister shell. ANSYS axisymmetric PLANE42 elements are used in the model. This model is shown in Figure 2.7.11.5-1 and was extracted from the three-dimensional model described in Section 2.6.13.2 for the canister. Instead of using the three-dimensional SOLID45 elements, only one-half of the cross-section of the model in the X-Y plane is required to form the two-dimensional axisymmetric model. The same configuration and stiffness of gap elements between the structural lid and the cask body, betweeen the structural lid and the shield lid, and between the lids and the canister shell, as described in Section 2.6.13.2, are used in this two-dimensional evaluation.

This evaluation addresses an axial load component only. In reviewing the development of the axial load by the fuel, the fuel mass remains constant, and its load on the inner surface of the shield lid is based on the acceleration at each time step. For this reason, the fuel assemblies are represented as a uniform pressure on the inner surface of the shield lid for the static analysis. Also included in the uniform pressure applied to the inner surface of the shield lid is the weight of the basket. For the transient dynamic analysis, the pressure is allowed to vary as the acceleration time history (ATH), which is obtained from the impact limiter analysis for the 30-foot top corner drop. The ATH for this evaluation is shown in Figure 2.7.11.5-2. To restrain the model in the vertical direction, the free end of the gap elements attached to the outer surface of the structural lid are restrained.

To examine the sensitivity of the stiffness for the gap elements between the structural lid and the cask body, two additional values of gap stiffness are considered: a value of 50% of the nominal value and a value of 200% of the nominal value. For each additional case, both the static and the dynamic solutions are recalculated.

To compare the loads transmitted through the structrual lid weld, the stress intensitites in the weld are calculated for the individual cases. To evaluate the dynamic effect, the ratio of the calculated dynamic stress to the calculated static stress (SDLF) is computed for each time step.

2.7.11.5.2 Analysis Results

Since the transient dynamic analysis is initiated as a stress-free condition, the SDLF starts with a zero value. As the impact event proceeds, the SDLF increases to its maximum value and then returns to zero a value at the end of the event. The maximum values are presented below for the three gap-stiffness cases.

Results of the Evaluation of the Dynamic Loading of the Canister Structural Lid Weld

Case-Gap Stiffness	**Maximum SDLF**
Nominal stiffness value	1.006
200% of the nominal value	1.007
50% of the nominal value	1.005

The time history of the SDLF, which corresponds to the analysis using the nominal gap stiffness, is shown in Figure 2.7.11.5-3. The results indicate that the effect of dynamic loading is minimal, which is due to the large stiffness associated with the shield lid and the structural lid.

Figure 2.7.11.5-1 Two-Dimensional Axisymetric Model of the Upper Section of the Yankee-MPC Canister

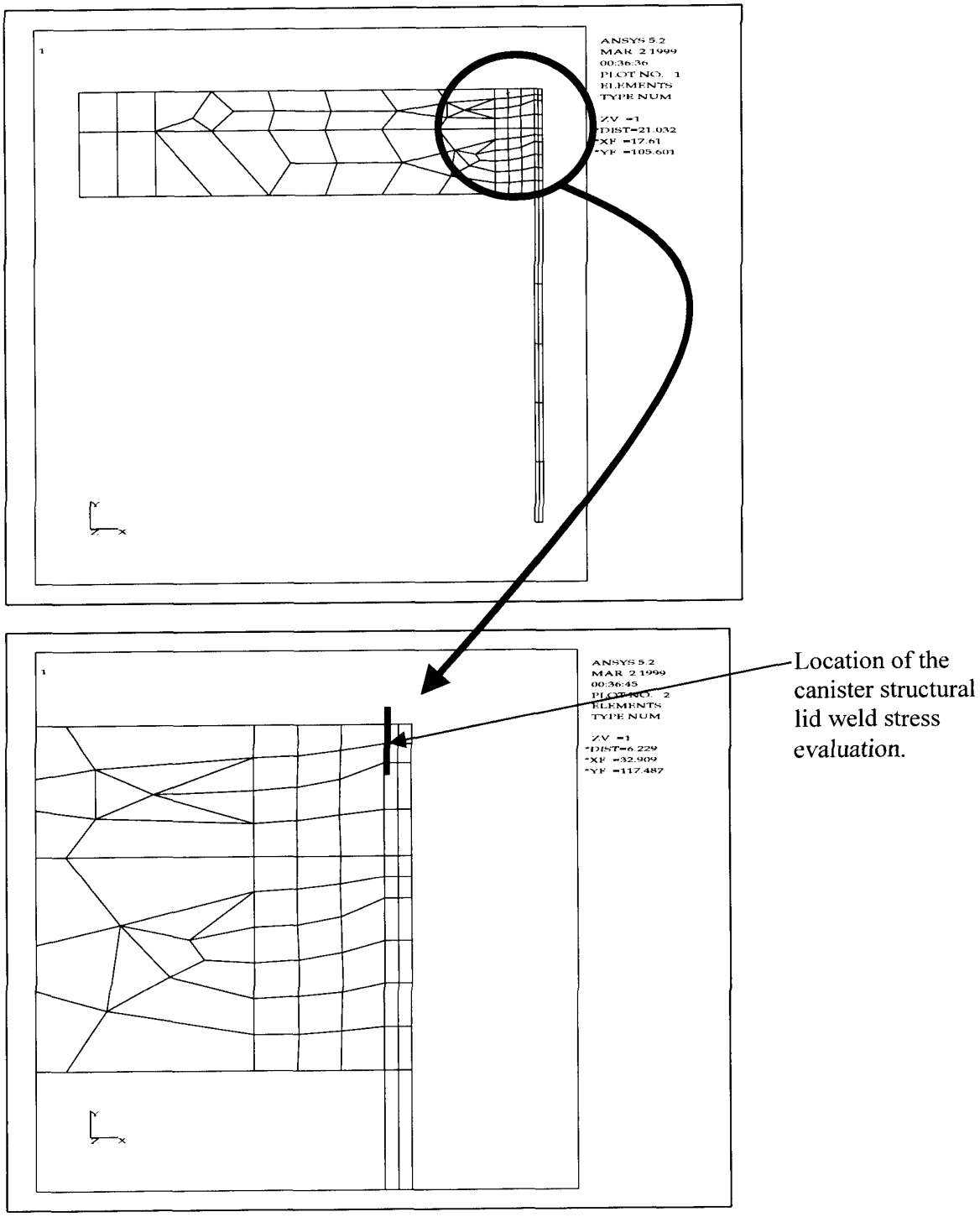

Figure 2.7.11.5-2 Axial Acceleration (g) Time History for a Top End Impact, Yankee-MPC Canister

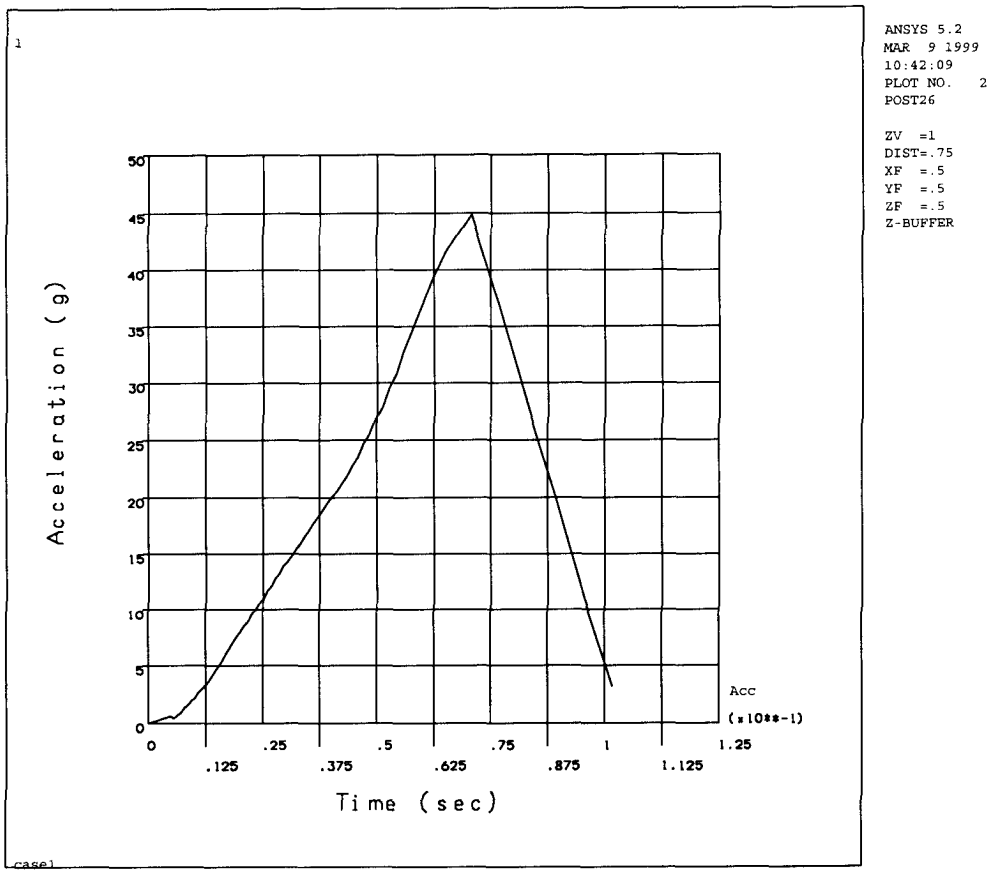

Figure 2.7.11.5-3 Time History for the Ratio of the Dynamic Stress to the Static Stress (SDLF) for the Yankee-MPC Canister Structural Lid Weld (Nominal Gap Stiffness Value)

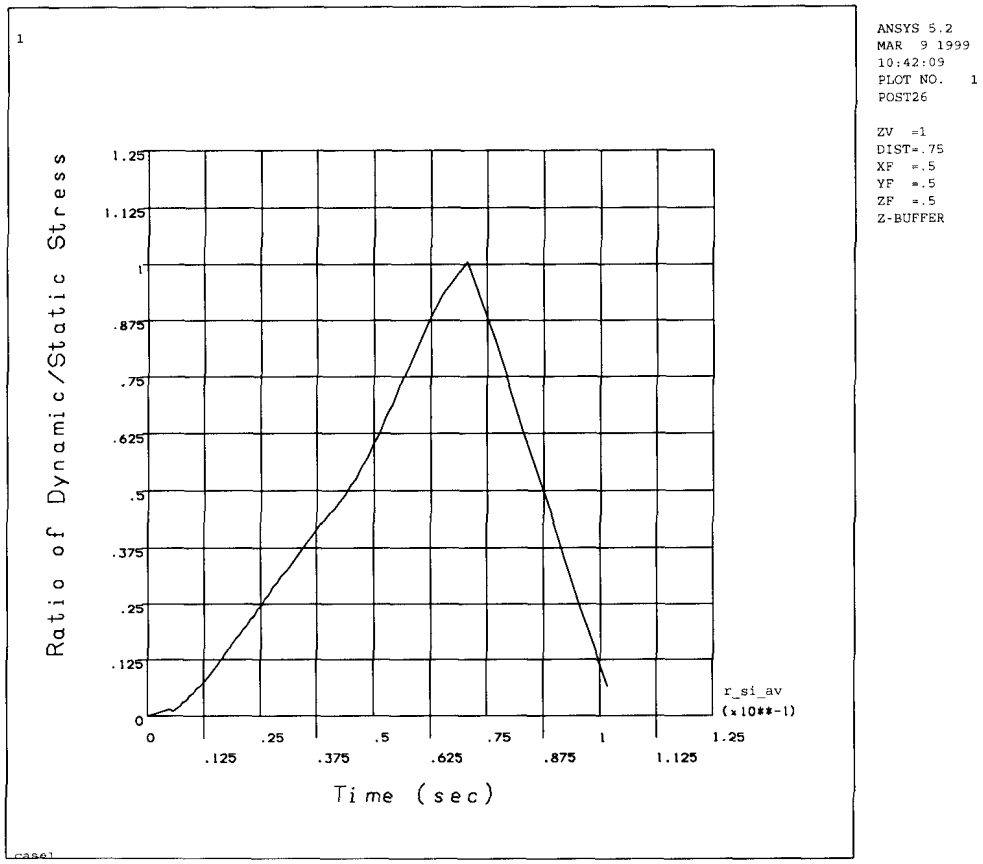

2.7.12 CY-MPC Transportable Storage Canister Analysis – Accident Conditions

This section presents the evaluation of the CY-MPC transportable storage canister for the hypothetical accident conditions. The evaluation for normal conditions of transport is presented in Section 2.6.15.

The principal components of the canister are the canister shell, including the bottom plate, the fuel basket, the shield lid, and the structural lid. A description of the geometry and materials of construction of the canister, baskets, and spacer are provided in Section 1.2.1.2.8.

The general arrangement of the canister, depicted with the fuel basket, is shown in Figure 2.7.13-1.

A drop accident stress evaluation is performed for the 30-foot side drop condition, and for the 30-foot top and bottom end drop conditions. The stress intensities resulting from these two evaluations bound those that result from the 30-foot corner and oblique drop conditions. This conclusion is based on the analysis results for the directly loaded fuel configurations described in Sections 2.6.12, 2.7.1.3, 2.7.1.4, and 2.7.8.

The canister spacer in the cask cavity may crush during the corner, oblique and end drop loading conditions. In crushing, it will reduce the total g load on the fuel and canister that would occur in the hypothetical accident conditions. However, no credit is taken for the presence of the canister spacer. All of the impact g load - 55 g for the side drop, and 56.1 g for the end drops – is assumed to be applied to the canister.

2.7.12.1 Canister - Accident Analysis Description

The canister is a right-circular shell fabricated from rolled 5/8-inch thick, Type 304L stainless steel plate. It is closed on its bottom end with a Type 304L stainless steel circular plate that is 1.75-inches thick. The canister is closed at the top end by a 5-inch thick, Type 304 stainless steel shield lid, which is seal welded to the canister shell. The shield lid is covered by a 3-inch thick, Type 304L, stainless steel structural lid welded to the canister shell at its top inside edge. The canister is the defined confinement boundary for spent fuel or GTCC waste contents during long-term storage, and it is the defined containment boundary for intact fuel and Reconfigured Fuel Assemblies during transport, satisfying the requirements of 10 CFR 71.63(b) for a separate

inner container. The NAC-STC cask, using the same containment boundary defined for the directly loaded fuel configuration, provides the primary containment boundary in transport.

The structural design criteria for the canister is the ASME Code Section III, Subsection NB, "Class 1 Components." Consistent with this criteria, the structural components of the canister (shell, bottom plate, and structural lid) are shown to satisfy the allowable stress intensity limits presented in Table 2.1.2-1.

The canister is evaluated using the ANSYS finite element program for the 30-foot drop conditions in the end and side impact orientations. The ANSYS finite element model is the same as that used for the evaluation of the 1-foot drop impacts evaluated for normal conditions of transport. The model is described in Section 2.6.15.2. As described in Section 2.6.15.2, the COMBIN40 elements used between the structural and shield lids and for the backing ring are assigned a gap sizes of 1E-8 inches. The maximum gap size is 0.08 inches. However, use of the smaller gap size results in the highest stresses at critical sections, resulting in the lowest margin of safety. All gap-spring elements are assigned a stiffness of 1E8 lb/in.

2.7.12.2 Analysis Results

The detailed results of the analysis for the 30-foot side, and top and bottom end drops are presented in Tables 2.7.12-1 through 2.7.12-6. The section stresses presented in the tables are identified by a section number. A cross-section of the canister showing the section numbers is presented in Figure 2.7.12-1. A summary of the canister minimum Margins of Safety for the evaluated drop conditions is shown in Table 2.7.12-7.

For the top and bottom end drops, the stresses are essentially uniform around the circumference. For the side drop, the stresses vary around the circumference. Therefore, the circumferential angle at which the maximum stress occurs is noted in the table, (in parentheses) beside the section number. The allowable stresses presented in the tables are for Type 304L stainless steel, except for section 10, which is for Type 304 stainless steel. These allowables are evaluated at 350°F (maximum calculated temperature in the canister is 349°F). The allowable stress for P_m stresses is defined as the lesser of 2.4 S_m or 0.7 S_u. The allowable stress for the $P_m + P_b$ stresses is defined as the lesser of 3.6 S_m or 1.0 S_u.

The canister structural lid closure weld is specifically evaluated for the hypothetical accident conditions. The lid weld is identified as Section 8 in Figure 2.7.12-1. The structural lid weld has a root and final weld surface Liquid Penetrant examination performed in accordance with ASME Code, Section V, Article 6. The weld is ultrasonically examined in accordance with ASME Code Section V, Article 5, or multi-pass liquid penetrant examined in accordance with ASME Code Section V, Article 6. In accordance with NRC guidance, if a multi-pass liquid penetrant examination is performed on the structural lid closure weld, a weld stress reduction factor is applied to the structural lid canister shell weld – a 0.8 factor to conservatively consider the weld configuration, in accordance with NRC ISG-4, Item 5. Thus, a weld stress reduction factor of 0.8 is applied to the stress allowable for the structural lid weld. The canister closure weld evaluation for accident conditions is presented in Section 2.7.12.4. The evaluation, which is based on the finite element analysis stress result as shown in Section 2.7.12.2, shows a minimum margin of safety of +0.65 for the weld.

2.7.12.3 Canister Buckling Evaluation for the 30-Foot End Drop

The canister shell is axially loaded by the weights of the structural lid, the shield lid, and the inertial weight of the shell during a 30-foot end drop impact. The impact load amplification factor is 56.1g's. The shell is evaluated as an unsupported, right circular cylinder using a critical buckling load per Blake, 2nd Edition, "Practical Stress Analysis in Engineering Design."

$$S_{cr} = \frac{E\left(0.605 - 10^{-7} M^2\right)}{M\left(1 + 0.004\phi\right)}$$

$$= 40.3 \text{ ksi}$$

The canister material is Type 304L stainless steel. Conservatively assume the material temperature to be at 400°F for the accident condition.

$E = 26.5E+03$ ksi $R = (69.39 + 0.625)/2$

$= 35.01$ inches (mid-radius of the canister shell)

$S_y = 17.5$ ksi $t = 0.625$ inches. (thickness of the canister)

$\phi = E/S_y$ and $M = R/t$

$= 1514.3$ $= 56.0$

The axial compression load in the canister shell is:

$$P_a = [\ (\pi/4)\ (69.03^2)\ (8)(0.291)\ +\ (\pi/4)(\ 70.64^2\ -\ 69.39^2\ )(151.75)(0.291)\ ]\quad (56.1)$$

$$P_a = 829{,}350 \text{ pounds}$$

and the axial compression stress is:

$$S_a = \frac{P_A}{\left(\pi/4\right)\left(70.64^2 - 69.39^2\right)}$$

$$S_a = 6{,}033 \text{ psi}$$

The margin of safety is:

$$(S_{cr}/S_a) - 1 = +\ 5.7$$

2.7.12.4 CY-MPC Canister Closure Weld Evaluation – Accident Conditions

2.7.12.4.1 Stress Evaluation for the CY-MPC Canister Closure Weld

The closure weld for the canister is a partial penetration grooveweld. The evaluation of this weld, in accordance with NRC guidance, incorporates a weld stress reduction factor of 0.8 based on NRC ISG-4, Item 5. The weld stress reduction factor is incorporated by applying a factor of 0.8 to the stress allowable for this weld.

The stresses for the canister are evaluated using sectional stresses as permitted by Subsection NB. The canister stress results from Section 2.7.12.2 are used for evaluation. The location of the section for the canister weld evaluation is shown in Figure 2.7.12-1 and corresponds to Section 8. The P_m and $P_m + P_b$ stress intensity for Section 8 and the associated allowables are listed below. The factored allowables, incorporating a 0.8 stress reduction factor, and the resulting margin of safety are:

Stress Type	Analysis Stress Intensity (ksi)	0.8 x Allowable Stress (ksi)	Margin of Safety
P_m	15.14	31.2	1.06
$P_m + P_b$	20.89	46.8	1.24

This confirms that the canister closure weld is acceptable for the accident conditions.

2.7.12.4.2 Critical Flaw Size for the Canister Closure Weld

The closure weld for the canister is comprised of multiple weld beads using a compatible weld material for Type 304L stainless steel. An allowable (critical) flaw evaluation has been performed to determine the critical flaw size in the weld region. The result of the flaw evaluation is used to define the minimum flaw size, which must be identifiable in the nondestructive examination of the weld. Due to the inherent toughness associated with Type 304L stainless steel, a limit load analysis is used in conjunction with a J-integral/tearing modulus approach. The safety margins used in this evaluation correspond to the stress limits contained in Section XI of the ASME Code.

The stress component used in the evaluation for the critical flaw size is the radial stress component in the weld region of the structural lid. For an accident (Level D) event, in accordance with ASME Code Section XI, a safety factor of $\sqrt{2}$ is required. For the purpose of identifying the stress for the flaw evaluation, the weld region corresponding to Section 8 in Figure 2.7.12-1 is considered. From additional post processing of the tipover analysis, the maximum tensile radial stress is 2.6 ksi. To perform the flaw evaluation, a 10 ksi stress is conservatively used, resulting in a significantly larger safety factor than the required safety factor of $\sqrt{2}$. Using 10 ksi as the basis for the evaluation, the minimum detectable flaw size is 0.52 inch for a flaw that extends 360 degrees around the circumference of the canister. Stress components for the circumferential and axial directions are also determined, which would be associated with flaws oriented in the radial or horizontal directions, respectively. The maximum stress for these components is 0.7 ksi, which is enveloped by the stress value used for the critical flaw evaluation for the radial direction. The 360-degree flaw employed for the circumferential direction is considered to be bounding with respect to any partial flaw in the weld, which could occur in the radial and horizontal directions. Therefore, using a minimum detectable flaw size of 3/8 inch is acceptable, since it is less than the very conservatively determined 0.52-inch critical flaw size.

Figure 2.7.12-1 Identification of the Sections for Evaluating the Linearized Stresses in the CY-MPC Canister

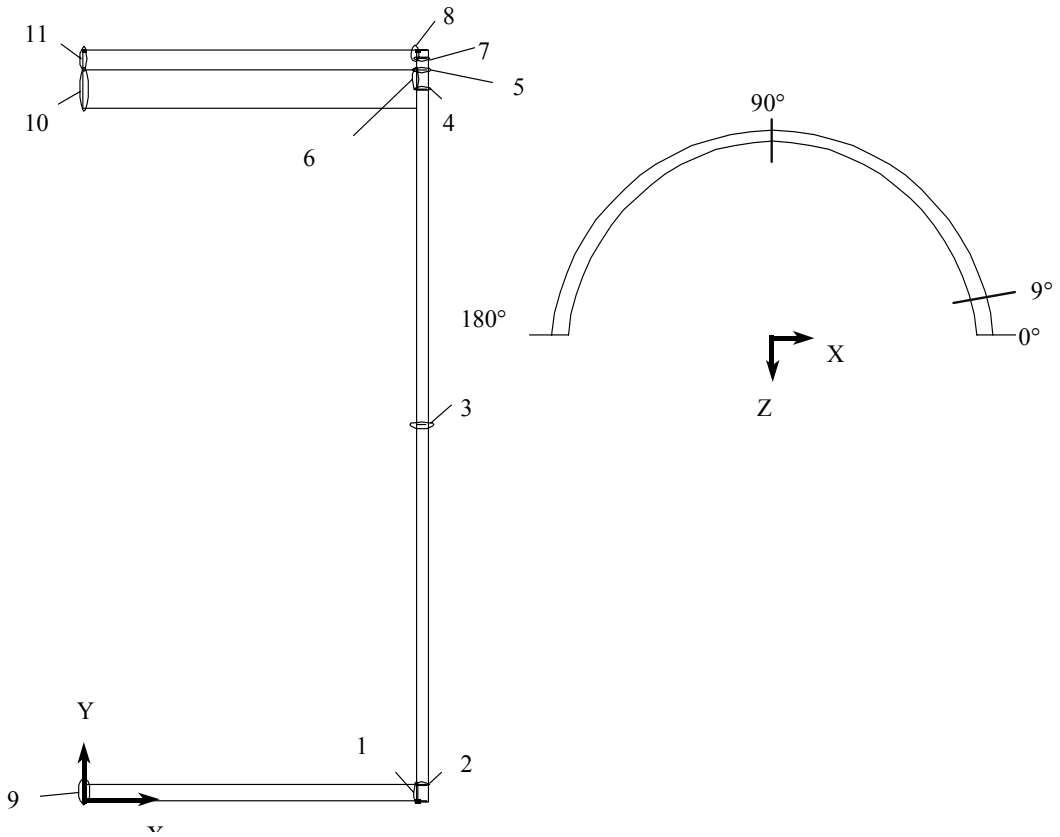

	Node 1		Node 2	
Section	X	Y	X	Y
1	34.695	0.00	34.695	1.75
2	34.695	1.75	35.32	1.75
3	34.695	72.75	35.32	75.75
4	34.695	148.25	35.320	148.25
5	34.695	148.75	35.320	148.75
6	34.695	148.25	34.695	148.75
7	34.695	150.87	35.320	150.87
8	34.695	150.87	34.695	151.75
9	0.10	0.00	0.10	1.75
10	0.10	143.75	0.10	148.73
11	0.10	148.77	0.10	151.75

Table 2.7.12-1 CY-MPC Canister, 30-Foot Side Drop (Primary Membrane Stress) (ksi)

Section No.	Component Stresses						SI	Allow. Stress	Margin of Safety
	SX	SY	SZ	SXY	SYZ	SXZ			
1(0°)	-14.2	0.9	-9.5	0.1	-0.2	-0.8	15.19	39	1.57
2(9°)	3	1.4	-4.3	-0.2	-1.3	-1.7	8.38	39	3.65
3(18°)	-0.9	2.4	1.1	0	0.1	0.7	3.54	39	10.03
4(9°)	-21.9	4.1	-8.3	-1.7	2.5	1.3	26.8	39	0.46
5(0°)	-18.2	2.6	-10	-4.8	1.4	1	23.19	39	0.68
6(0°)	-28.9	-6.9	-13.3	-6	1.2	0.8	25.25	39	0.54
7(9)	-16.0	1.0	-7.7	0.3	1.7	0.5	17.3	39	1.25
8(0°)	-20.4	-5.7	-9.5	-1.2	0.8	-0.5	15.14	31.2*	1.06
9	-2	0.1	0.9	0.1	0	0	2.85	39	12.67
10	-1	0	0.3	-0.1	0	0	1.29	39	29.26
11	-1.2	0	0.4	0	0	0	1.64	39	22.85

* Includes a stress reduction factor for the weld of 0.8 (See Section 2.7.12.4).

Table 2.7.12-2 CY-MPC Canister, 30-Foot Side Drop (Primary Membrane Plus Primary Bending Stress) (ksi)

Section No.	Component Stresses						SI	Allow. Stress	Margin of Safety
	SX	SY	SZ	SXY	SYZ	SXZ			
1(0°)	-24.9	0.2	-13	0.8	0	-0.5	25.16	58.5	1.33
2(36°)	-1.9	-16.9	-4.6	-0.3	1.1	-4.2	18.14	58.5	2.22
3(0°)	-1.1	2.8	2.8	0	0	0.5	4.02	58.5	13.54
4(9°)	-20.0	11.7	-6.7	-0.6	2.8	2.4	32.6	58.5	0.79
5(0°)	-16.5	6.6	-10.3	-3.1	1.9	1.2	24.38	58.5	1.4
6(0°)	-35.6	-9.2	-15.8	-6	1.5	0.8	29.16	58.5	1.01
7(9°)	-14.0	6.1	-6.4	0.9	1.5	1.4	20.6	58.5	1.84
8(0°)	-30	-10.1	-13.7	-2.5	1.4	0	20.89	46.8*	1.24
9	-2.2	0.1	0.9	0.1	0	0	3.08	58.5	17.98
10	-1.2	0	0.4	-0.1	0	0	1.6	58.5	35.63
11	-1.4	0	0.4	0	0	0	1.82	58.5	31.09

* Includes a stress reduction factor for the welds of 0.8 (See Section 2.7.12.4).

Table 2.7.12-3 CY-MPC Canister, 30-Foot Bottom End Drop Without Internal Pressure (Primary Membrane Stress) (ksi)

Section No.	Component Stresses						SI	Allow. Stress	Margin of Safety
	SX	SY	SZ	SXY	SYZ	SXZ			
1	0	-2	-0.3	-0.1	0	0	2.04	39	18.2
2	0.4	-5.1	-1	-0.2	0	-0.1	5.54	39	6.0
3	0	-4.8	0	0	0	0	4.83	39	7.1
4	-1.2	-3.2	-2.8	-0.9	0.1	-0.1	2.64	39	13.8
5	3.1	-2.3	-1.5	0.5	0	-0.3	5.48	39	6.1
6	1.4	3.1	-0.5	0.4	0.1	-0.2	3.67	39	9.6
7	-3.4	1.2	-1.5	-0.3	0	0.1	4.59	39	7.5
8	0.3	-3.3	-2	-0.5	0.1	-0.2	3.78	31.2*	7.3
9	0.1	-0.8	0.1	0	0	0	0.83	39	45.7
10	0.3	-0.1	0.3	0	0	0	0.35	39	109.6
11	-0.4	-0.1	-0.4	0	0	0	0.31	39	125.5

* Includes a stress reduction factor for the weld of 0.8 (See Section 2.7.12.4).

Table 2.7.12-4 CY-MPC Canister, 30-Foot Bottom End Drop (Primary Membrane Plus Primary Bending Stress) (ksi)

Section No.	Component Stresses						SI	Allow. Stress	Margin of Safety
	SX	SY	SZ	SXY	SYZ	SXZ			
1	0.1	-2.7	-0.4	-0.3	0	0	2.81	58.5	19.8
2	0.2	-7.1	-1.5	-0.1	0	-0.1	7.28	58.5	7.0
3	0	-4.8	0	0	0	0	4.83	58.5	11.1
4	-0.8	-6.6	-3.6	-1.2	0.1	-0.2	6.29	58.5	8.3
5	1.1	-11.6	-4.6	-0.4	0	-0.4	12.77	58.5	3.6
6	4.9	6.2	1.2	1.3	0.1	-0.3	5.84	58.5	9.0
7	-2	9.8	1.2	-0.5	0	0.2	11.77	58.5	4.0
8	4.3	-0.4	-0.4	-0.6	0.1	-0.3	4.95	46.8*	8.5
9	0.1	-0.8	0.1	0	0	0	0.93	58.5	61.7
10	5.8	-0.1	5.8	0	0	0	5.85	58.5	9.0
11	-3.9	0	-3.9	0	0	0	3.89	58.5	14.0

* Includes a stress reduction factor for the weld of 0.8 (See Section 2.7.12.4).

Table 2.7.12-5 CY-MPC Canister, 30-Foot Top End Drop (Primary Membrane Stress) (ksi)

Section No.	Component Stresses						SI	Allow. Stress	Margin of Safety
	SX	SY	SZ	SXY	SYZ	SXZ			
1	0	-0.8	-0.3	-0.1	0	0	0.8	39	47.6
2	-0.4	0.5	1	-0.1	0	-0.1	1.46	39	25.8
3	0	-1.4	1.1	0	0	-0.1	2.51	39	14.5
4	0.3	-2.4	-0.3	-0.2	0	0	2.68	39	13.6
5	-0.2	-2.2	-0.4	-0.1	0	0	1.94	39	19.1
6	-0.1	-1.1	-0.1	-0.2	0	0	1.11	39	34.0
7	0	-2	-0.3	0	0	0	1.94	39	19.1
8	0	-1.5	-0.2	0	0	0	1.47	31.2*	20.2
9	-0.1	0	-0.1	0	0	0	0.1	39	391
10	0	-0.8	0	0	0	0	0.78	39	48.7
11	0	-0.8	0	0	0	0	0.76	39	50.2

* Includes a stress reduction factor for the weld of 0.8 (See Section 2.7.12.4).

Table 2.7.12-6 CY-MPC Canister, 30-Foot Top End Drop (Primary Membrane Plus Primary Bending Stress) (ksi)

Section No.	Component Stresses						SI	Allow. Stress	Margin of Safety
	SX	SY	SZ	SXY	SYZ	SXZ			
1	-0.5	-1.9	0.3	0	0	0	2.27	58.5	24.8
2	-0.2	3.6	1.9	-0.3	0	-0.2	3.94	58.5	13.9
3	0	-1.4	1.1	0	0	-0.1	2.52	58.5	22.2
4	0.1	-3.6	-0.7	-0.1	0	0.1	3.69	58.5	14.9
5	-0.1	-3	-0.6	-0.2	0	0	2.95	58.5	18.9
6	0.4	-1	0.1	-0.2	0	0	1.44	58.5	39.7
7	0	-2.3	-0.4	0	0	0	2.22	58.5	25.4
8	0.1	-1.4	-0.1	0	0	0	1.5	46.8*	30.2
9	-3	0	-3	0	0	0	3.04	58.5	18.2
10	0.2	-0.8	0.2	0	0	0	0.96	58.5	60.0
11	0.1	-0.7	0	0	0	0	0.8	58.5	71.9

* Includes a stress reduction factor for the weld of 0.8 (See Section 2.7.12.4).

Table 2.7.12-7 Summary of Minimum Margin of Safety for CY-MPC Canister 30-Foot Drops

Drop Orientation	**Loading Condition**	**Stress Evaluated**	**Minimum Margin of Safety**	**Section No.***
Bottom end	30-ft. impact + pressure (0 psi)	P_m	6.0	2
Bottom end	30-ft. impact + pressure (0 psi)	$P_m + P_b$	3.6	5
Side	30-ft. impact + pressure (20 psi)	P_m	0.46	4
Side	30-ft. impact + pressure (20 psi)	$P_m + P_b$	0.79	4
Top end	30-ft. impact + pressure (20 psi)	P_m	13.6	4
Top end	30-ft. impact + pressure (20 psi)	$P_m + P_b$	13.9	2

* See Figure 2.7.12-1 for section locations.

2.7.13 CY-MPC Fuel Basket Analysis - Accident Conditions

There are two different NAC-STC canistered fuel basket assemblies for Connecticut Yankee class fuel. The first fuel basket is designed to accommodate up to 24 fuel assemblies. The second fuel basket is designed to accommodate up to 26 fuel assemblies. The 26-fuel assembly basket supports the maximum load with the minimum structure. Therefore, only the 26-fuel assembly basket is considered in this analysis.

The fuel basket assembly analyzed herein is a right cylinder structure and is fabricated with the following components: 26 square fuel tubes, 28 circular support disks, 27 heat transfer disks, 6 tie rods with split spacers, and two end weldment plates.

The basket components and their geometry are illustrated in Figure 2.7.13-1 and Figure 2.7.13-2. The basket contains two sizes of fuel tubes. There are 22 standard and 4 oversized fuel tubes. The standard fuel tube has an 8.72-inch square inside dimension, 0.141-inch thick composite wall. The oversized fuel tube has a 9.12-inch square inside dimension, a 0.141-inch thick composite wall. Both fuel tubes hold the design basis Connecticut Yankee Class fuel assembly. The fuel tubes are open at each end. Therefore, longitudinal fuel assembly loads are imparted to the cask body and not the fuel basket structure.

The fuel assemblies, together with the tubes are laterally supported in the holes in the stainless steel support disks. Each support disk is 0.5 inches thick, 69.15 inches in diameter and has 26 holes. There are 22 holes that are each 9.17 inches square and 4 holes that are 9.57 inches square. There are four web thicknesses in the support disks; 1.50 inch, 1.25 inch, 1.10 inch, and 1.00 inch. The widest web is nearest the center of the basket, the web decreases in width towards the outer radius of the basket. The support disks are equally spaced at 4.09 inches.

The weldments are geometrically similar to the support disks and are 68.98 inches in diameter and .50 in thick. The top weldment includes support ribs and an outer ring. The bottom weldment includes support ribs and tie rod support bosses. The total heights of the top and bottom weldments are 6.8 and 2.0 inches, respectively.

Twenty-seven (27) aluminum heat transfer disks are interleaved with the support disks to fully optimize the passive heat rejection from the package. Each heat transfer disk is 0.50-inch thick, 68.9 inches in diameter, and has 26 holes for the fuel tubes. There are 22 standard holes that are 9.14 inches square and 4 oversized holes that are 9.54 inches square. There are five different web widths,

1.56 inches, 1.46 inches, 1.26 inches, 1.16 inches, and 1.06 inches. The widest aluminum web is nearest the center of the basket to optimize passive heat rejection. The dimensional differences between the heat transfer disk and the support disk accommodates the different rate of thermal growth between aluminum and stainless steel preventing interference between the tube, the support disk, and heat transfer disks. The heat transfer disks, which serve no structural function, are supported by the six (6) tie rods with split spacers. Each tie rod has 3.0 inches of 1 5/8-8 UN-2A threads at the upper end of the rod, which thread into the top nuts that clamp against the top weldment. The fuel basket contains the fuel and is laterally supported by the canister shell.

The 28 support disks and 2 end weldments are fabricated from 17-4 PH and Type 304 stainless steels, respectively. The 27 heat transfer disks are fabricated from Type 6061-T651 aluminum alloy. The 26 fuel tubes are fabricated from Type 304 stainless steel. The tie rods and spacers are fabricated from Type 304 stainless steel. The stainless steel tubes are not considered to be a structural component with respect to the disks and are not included in the basket or weldment analyses. The primary function of the split spacers and the threaded top nut is to locate and structurally assemble the support disks, heat transfer disks and the top and bottom weldment plates into an integral assembly. The spacers carry the inertial weight of the support disks, heat transfer disks, one end plate, and their own inertial weight for a normal transport condition 1-foot end drop. The end drop loading of the split spacers and tie rods represent a classical closed form structural analysis. Therefore the only component that requires a detailed finite element analysis is the support disk.

The fuel basket is evaluated for the hypothetical accident loads in this section and is evaluated for the normal transport condition in Section 2.6.16.

Figure 2.7.13-1 CY-MPC Canistered Fuel Basket

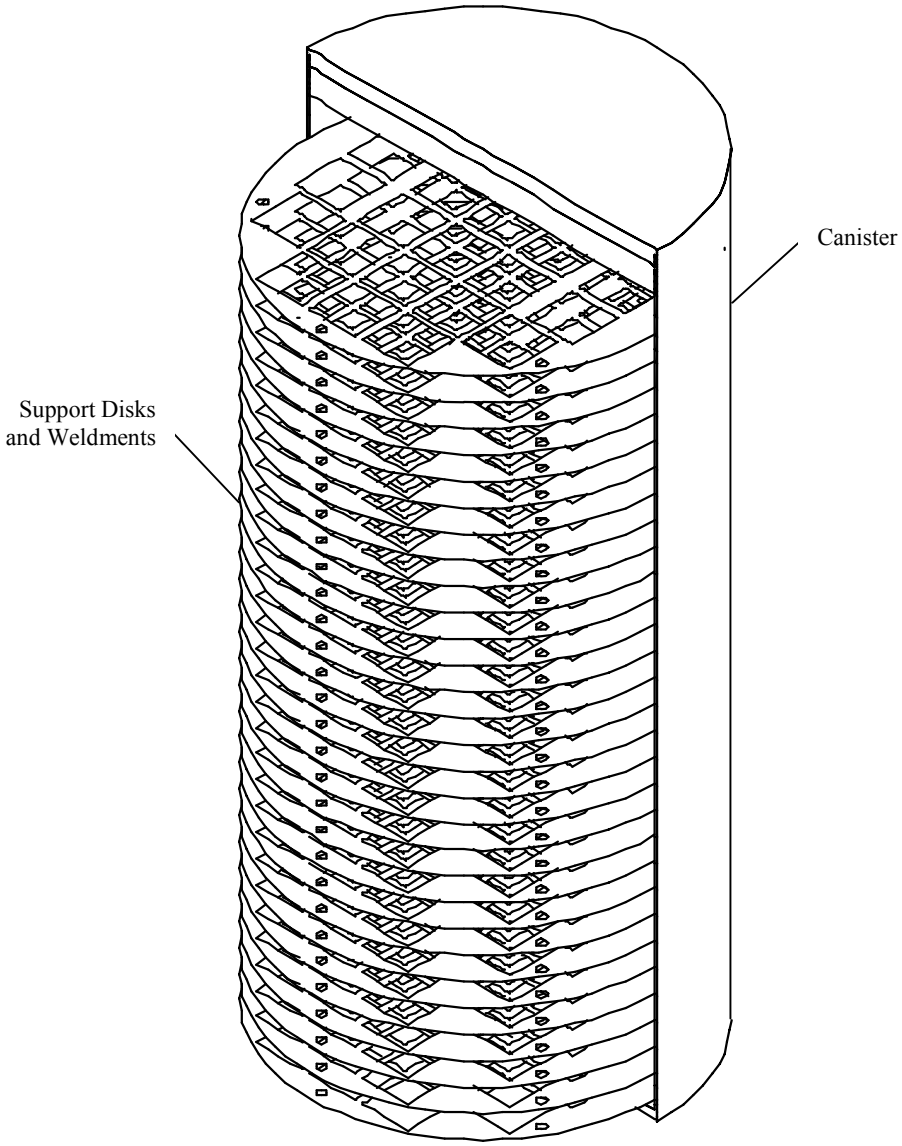

Figure 2.7.13-2 CY-MPC Basket Support Disk Configuration

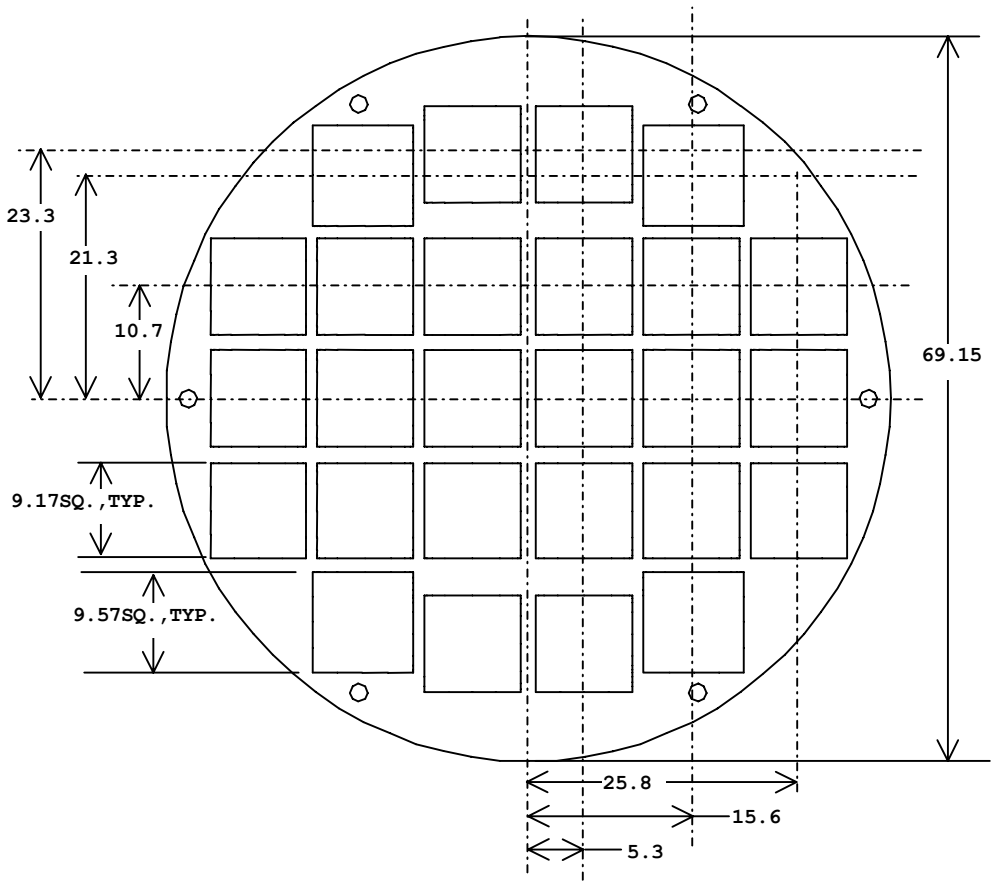

2.7.13.1 Stress Evaluation of CY-MPC Support Disk

Based on criticality control requirements, the canistered fuel basket design criteria requires the maintenance of fuel support and control of spacing of the fuel assemblies for all load conditions. The structural design criteria for the fuel basket is the ASME Boiler and Pressure Vessel Code, Section III, Division 1, Subsection NG, "Core Support Structures." Consistent with this criteria, the main structural component in the fuel basket, the stainless steel support disk, is shown to have a maximum primary membrane stress intensity less than the allowable stress limit, defined as 0.7 S_u, for the accident condition. Likewise the primary membrane plus bending stress intensity is shown to be less than the allowable stress limit, defined as 1.0 S_u. The value of S_u is defined at conservatively high temperatures for the component being analyzed.

For the side drop conditions, four basket drop orientations (0°, 38°, 63°, and 90°) are considered, as shown in Figure 2.7.13.1-1. Angles of 38° and 63° were selected because minimal web thickness occurs at these orientations.

In the side drop, the loads of the fuel assemblies are transferred into the plane of the support disks, from which they are transmitted to the canister shell, and then to the cask body (cask inner shell). In the end drop, the support disks are loaded only by their own inertial mass and do not experience load from the guided, but free standing fuel assemblies.

Finite element models are used to perform analyses for end drop and side-drop conditions using the ANSYS program. In addition to the load from inertial weight, the analyses also consider the stresses due to differential thermal expansion.

Analyses for combined, or oblique angle drops are also performed. The stresses due to the side and end drop load conditions are combined according to the cask angle, as shown in Figure 2.7.13.1-2.

Figure 2.7.13.1-1 Basket Drop Orientations

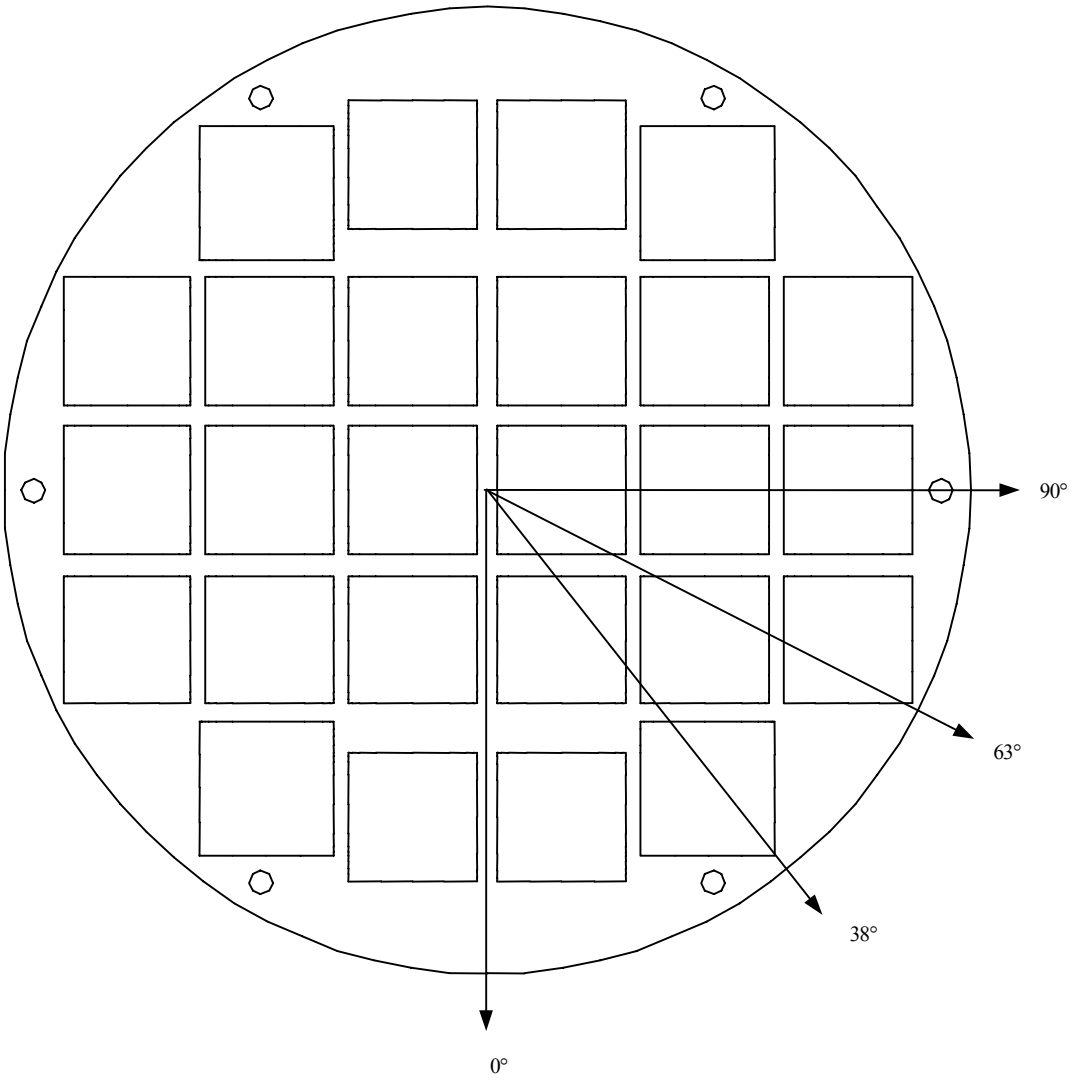

Figure 2.7.13.1-2 Cask Orientation

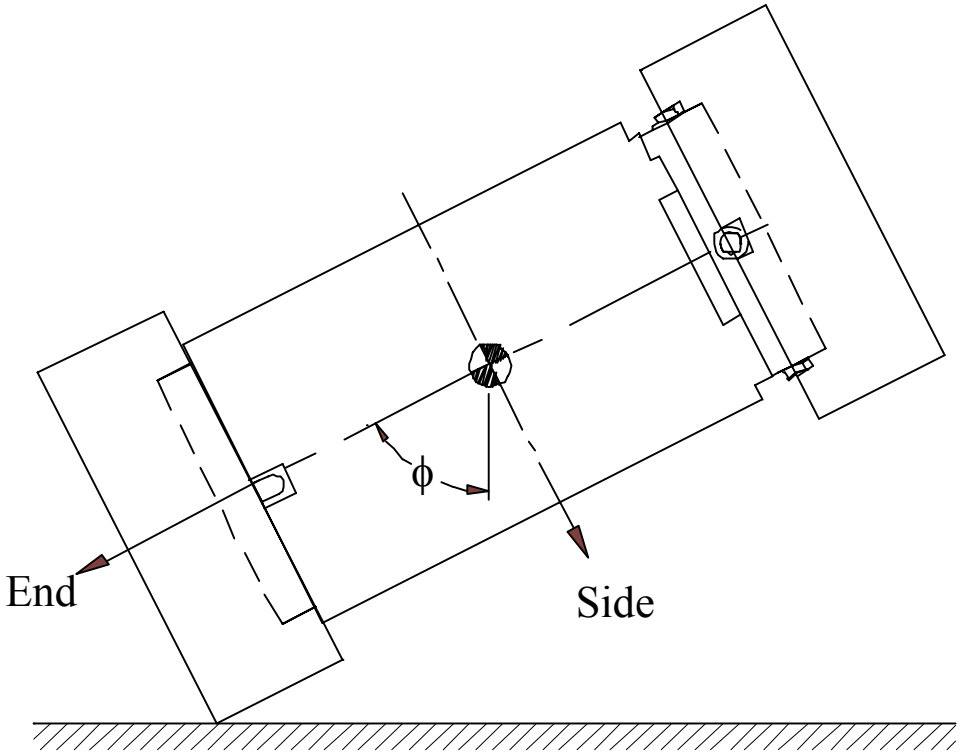

2.7.13.1.1 Finite Element Model Description - CY MPC Fuel Basket

Two finite element models were generated to analyze the CY-MPC fuel basket for the normal operating conditions. The first model simulates the side drop (Figure 2.6.16.2-1) at the basket orientations shown in Figure 2.7.13.1-1. The second model simulates the end drop. These results are then combined to simulate various oblique drops. All calculations accommodate thermal expansion effects using the temperature distribution from the thermal analysis and the coefficient of thermal expansion.

The model for the end drop simulation is constructed using ANSYS SHELL63 elements. It consists of a single support disk with a thickness of 0.5 inch. The shell elements accommodate the out-of-plane bending, which is present in the end-drop condition. The support disk is restrained in the direction of the drop by the split spacers on the six tie rods. Therefore, the nodes corresponding to the location of the tie rods are restrained in the out of plane direction (the cask axial direction) as well as all 5 remaining DOF to stabilize the model. The only loading is the inertial weight of the support disk in the out-of-plane direction.

The finite element model for the side-drop evaluation of the support disk is a three-dimensional model and includes a slice, or section of the canister and cask as well as a single support disk. The canister and the cask body are included in the model to more accurately simulate the boundary conditions for the support disk. The top and bottom portions of the canister and transport cask are not considered in this analysis. Neglecting these end effects is conservative because it allows slightly more deformation of the canister shell and the support disks. In the support disk side drop models, the canister shell and the cask body are modeled with SOLID45 elements. To increase the accuracy of the analysis, the element size is reduced towards the intersections of the ligaments.

While the cask, canister and support disk are modeled explicitly, the impact limiters are represented by CONTAC52 elements. Cask and impact limiter modeling reflect the same approach as described in Section 2.6.7.4. The load from each fuel assembly is modeled as a line-pressure on the inner surfaces of each support disk opening.

To determine the most critical regions, a series of 131 cross sections are considered. To aid in the identification of these sections, Figure 2.6.16.2-5 shows the section locations on a support disk for all of the side drop cases. Table 2.6.16.2-1 lists the geometric locations of the end points for each cross section.

2.7.13.1.2 Stress Evaluation of CY-MPC Support Disk for a 30-Ft End Drop Condition

Six (6) tie rods locate the support disks of the CY-MPC fuel basket with spacers. A structural analysis is performed using ANSYS to evaluate the effect of a 30-foot end drop impact, which corresponds to the most severe out-of-plane loading under hypothetical accident conditions. The model described in Section 2.7.13.1.1 is used with a 56.1g deceleration. Linearized stresses at the cross sections identified in Figure 2.6.16.2-5 are compared to stress allowables in accordance with the ASME Code, Section III, Subsection NG. Table 2.7.13.1.2-1 lists the 10 highest $P_m + P_b$ stress intensities, respectively. For an end drop, there are no membrane stresses in the support disk because there is essentially no in-plane loading.

The worst case results for the 30-foot end drop condition are summarized as:

$P_m + P_b$	
Stress Intensity (ksi)	M.S.
101.3	0.26

The margin of safety (M.S.) is calculated as: M.S. = (Stress Allowable/Stress Intensity) –1.

Table 2.7.13.1.2-1 P_m+P_b Stresses for CY-MPC Support Disk—30-Foot End Drop

Section*	Sx (ksi)	Sy (ksi)	Sxy (ksi)	Stress Intensity (ksi)	Allowable Stress (ksi)	Margin of Safety
61	88.00	-17.10	33.40	101.30	127.60	0.26
63	88.70	-17.80	-31.10	100.40	127.60	0.27
3	88.10	-16.90	33.00	101.00	131.10	0.30
1	88.60	-16.50	-31.20	100.20	131.10	0.31
76	-3.80	-52.40	16.10	64.80	127.80	0.97
93	-4.30	-52.30	-15.50	64.60	127.80	0.98
94	-4.20	-51.70	-15.60	64.00	127.60	0.99
111	-0.90	-55.00	14.10	62.60	127.60	1.04
129	-47.00	11.70	-15.20	52.60	127.60	1.43
125	-46.90	11.70	-15.20	52.50	128.80	1.45

* See Figure 2.6.16.2-5 for section locations and definition of coordinate system.

2.7.13.1.3 Stress Evaluation of CY MPC Support Disk for a 30-Ft Side Drop Condition

The structural adequacy of the support disk in the CY-MPC fuel basket for the 30-foot side-drop impact load condition was determined. A quasi-static impact load equal to the weight of the fuel and tubes multiplied by a 55g-amplification factor is applied to the support disk structure. The inertial loading of the support disk is also included via the density input for the 17-4 PH stainless steel. The fuel assembly load is transmitted in direct compression through the tube wall to the web structure of the support disk. A finite element analysis is performed using the three-dimensional support disk side model described in Section 2.7.13.1.1. As discussed in Section 2.7.13.1, four bounding cases of basket orientation (0°, 38°, 63°, and 90°) are considered in the analysis. The material properties are evaluated at a combined worst case thermal condition. This condition is based on the maximum support disk temperature from Thermal Condition 1 and the maximum temperature gradient across the disk from Thermal Condition 2. Linearized stresses at 131 cross-sections (see Figure 2.6.16.2-5) are compared to the stress allowable per the ASME Code, Section III, Subsection NG. The allowable stress is $0.7S_u$ for P_m, and $1.0\ S_u$ for $P_m + P_b$ stresses, respectively.

The stress evaluation results for the 30-foot side-drop condition are summarized in Table 2.7.13.1.3-1. The minimum margin of safety is +0.26, which occurs for the 38° basket drop orientation. Tables 2.7.13.1.3-2 through 2.7.13.1.3-9 list the 30 highest P_m and P_m+P_b stress intensities for each basket orientation considered.

Table 2.7.13.1.3-1 Summary of CY-MPC Support Disk Stresses for 30-Foot Side Drop

P_m		P_m+P_b	
Section	Margin of Safety	Section	Margin of Safety
0° Basket Orientation			
11	1.13	1	1.48
13	1.15	3	1.49
1	1.48	11	1.63
3	1.49	9	1.64
9	1.58	13	1.66
38° Basket Orientation			
73	0.79	1	0.26
1	1.42	2	0.58
6	1.73	13	0.61
7	1.91	26	0.62
13	2.07	11	0.62
63° Basket Orientation			
73	1.05	43	0.62
24	1.60	106	0.72
39	1.61	13	0.72
108	1.76	3	0.72
66	2.02	28	0.72
90° Basket Orientation			
108	0.86	129	1.17
90	0.88	108	1.48
105	1.54	90	1.51
87	1.55	44	1.65
110	1.94	24	1.68

Note: See Figure 2.6.16.2-5 for section locations and definition of coordinate system.

Table 2.7.13.1.3-2 P_m Stresses for CY-MPC Support Disk 30-Foot Side Drop, 0° Basket Orientation

Section	Sx (ksi)	Sy (ksi)	Sxy (ksi)	Stress Intensity (ksi)	Allowable Stress (ksi)	Margin of Safety
11	-21.3	-21.0	2.0	42.5	90.6	1.13
13	-21.2	-20.7	-1.9	42.1	90.6	1.15
1	-31.6	-5.4	0.7	37.0	91.7	1.48
3	-31.5	-5.3	-0.7	36.8	91.7	1.49
9	-31.4	-3.8	-0.4	35.2	90.9	1.58
7	-31.2	-2.9	0.0	34.1	90.9	1.66
5	-33.4	0.1	0.0	33.4	91.6	1.74
12	-21.4	-9.6	0.0	31.0	90.7	1.92
27	-18.4	-12.0	0.0	30.4	89.6	1.95
4	-30.5	0.0	-1.1	30.6	91.3	1.98
6	-30.4	0.0	1.1	30.5	91.3	1.99
131	-27.3	11.2	7.6	30.4	91.1	2.00
26	-15.4	-12.9	1.1	28.3	89.6	2.17
28	-15.3	-12.7	-1.1	28.1	89.6	2.18
8	-26.2	14.7	0.0	26.2	90.9	2.47
73	-17.5	-8.3	1.1	26.0	90.6	2.49
66	-17.5	-8.4	-1.2	26.0	90.6	2.49
2	-25.5	-0.9	0.0	26.4	92.4	2.51
17	-25.5	0.0	0.0	25.5	90.1	2.54
16	-24.3	0.0	-0.9	24.3	90.1	2.70
18	-24.2	0.0	0.9	24.3	90.1	2.71
69	-19.4	-3.9	-1.2	23.4	90.7	2.87
70	-19.4	-3.9	1.3	23.4	90.7	2.88
42	-13.8	-8.9	0.0	22.7	89.3	2.94
22	-21.7	11.3	0.0	21.7	89.7	3.13
32	-20.1	0.0	0.0	20.1	89.3	3.43
21	-20.1	13.2	1.0	20.2	89.7	3.44
85	-16.8	-3.2	1.4	20.2	89.6	3.44
84	-16.8	-3.2	-1.4	20.2	89.6	3.44
23	-20.0	13.0	-1.0	20.1	89.7	3.45

Note: See Figure 2.6.16.2-5 for section locations and definition of coordinate system.

Table 2.7.13.1.3-3 P_m Stresses for CY-MPC Support Disk 30-Foot Side Drop, 38° Basket Orientation

Section	Sx (ksi)	Sy (ksi)	Sxy (ksi)	Stress Intensity (ksi)	Allowable Stress (ksi)	Margin of Safety
73	-50.3	2.8	3.8	50.6	90.6	0.79
1	-19.1	-18.8	-0.5	38.0	91.7	1.42
6	-32.9	0.4	-3.9	33.5	91.3	1.73
7	-17.8	-13.3	1.3	31.2	90.9	1.91
13	-23.5	-5.9	1.1	29.5	90.6	2.07
24	-12.7	28.1	3.8	29.0	89.6	2.09
39	-7.0	27.2	4.4	28.1	89.3	2.17
114	-25.6	-1.6	1.2	27.3	89.3	2.27
121	22.7	3.5	3.9	27.3	89.3	2.27
5	-25.8	0.3	-4.9	27.4	91.6	2.35
38	-13.2	23.3	6.6	26.6	89.3	2.36
23	-19.3	21.6	5.9	26.4	89.7	2.39
88	-23.8	9.2	6.5	26.3	89.6	2.41
103	-20.4	8.9	9.4	25.7	89.3	2.47
66	24.8	-2.7	1.7	24.9	90.6	2.63
14	-13.1	-11.5	1.6	24.8	90.4	2.64
64	-14.7	-9.1	3.4	24.8	90.4	2.65
18	-23.7	0.3	-3.2	24.2	90.1	2.72
106	-18.8	12.6	7.1	23.5	89.3	2.81
91	-20.5	12.2	5.8	23.4	89.6	2.82
3	-23.4	11.9	-1.3	23.5	91.7	2.90
70	-20.3	0.3	5.0	22.3	90.7	3.06
9	-21.9	9.5	2.2	22.3	90.9	3.07
109	-15.0	15.6	6.6	21.9	89.3	3.07
108	4.8	13.8	4.3	20.5	89.3	3.35
2	-19.4	-1.5	-1.4	21.1	92.4	3.38
55	7.1	13.2	0.9	20.4	89.3	3.38
12	-15.3	-5.3	0.4	20.6	90.7	3.39
17	-18.1	0.3	-5.0	20.5	90.1	3.40
8	-20.1	14.0	1.6	20.5	90.9	3.44

Note: See Figure 2.6.16.2-5 for section locations and definition of coordinate system.

Table 2.7.13.1.3-4 P_m Stresses for CY-MPC Support Disk 30-Foot Side Drop, 63° Basket Orientation

Section	Sx (ksi)	Sy (ksi)	Sxy (ksi)	Stress Intensity (ksi)	Allowable Stress (ksi)	Margin of Safety
73	-43.8	10.0	3.4	44.1	90.6	1.05
24	-7.6	33.8	4.1	34.5	89.6	1.60
39	-3.2	33.4	4.8	34.2	89.3	1.61
108	11.4	19.8	4.4	32.4	89.3	1.76
66	28.8	1.0	1.8	30.0	90.6	2.02
121	20.6	8.0	3.0	29.2	89.3	2.06
54	1.5	26.0	3.2	28.3	89.3	2.16
90	8.9	17.1	2.9	26.7	89.6	2.36
109	-16.5	22.3	6.1	26.2	89.3	2.41
110	-0.3	25.6	-1.7	25.7	89.3	2.48
106	-19.5	18.0	6.4	25.2	89.3	2.54
91	-20.8	19.6	5.0	25.2	89.6	2.55
38	-8.0	22.2	6.9	25.0	89.3	2.57
88	-21.6	15.4	5.7	24.9	89.6	2.60
75	7.7	17.3	0.4	25.0	90.4	2.62
103	-17.8	13.0	8.4	24.1	89.3	2.70
102	10.2	9.3	7.1	24.1	89.3	2.71
23	-11.7	20.9	6.1	23.9	89.7	2.75
105	6.5	15.2	4.3	23.4	89.3	2.82
1	-8.3	-15.2	-1.1	23.6	91.7	2.88
92	-0.3	22.8	-0.9	22.8	89.5	2.92
111	-9.4	22.4	-0.4	22.4	89.3	2.99
6	-21.4	0.5	-4.1	22.5	91.3	3.06
114	-20.2	-1.1	1.6	21.5	89.3	3.15
107	-0.2	20.9	-2.6	21.3	89.3	3.19
55	7.8	12.8	0.5	20.6	89.3	3.33
129	-8.3	18.7	-3.9	20.0	89.3	3.46
130	-15.5	7.1	7.6	20.0	90.1	3.51
99	11.8	5.2	5.0	19.8	89.3	3.52
64	-15.0	-4.0	3.0	19.9	90.4	3.55

Note: See Figure 2.6.16.2-5 for section locations and definition of coordinate system.

Table 2.7.13.1.3-5 P_m Stresses for CY-MPC Support Disk 30-Foot Side Drop, 90° Basket Orientation

Section	Sx (ksi)	Sy (ksi)	Sxy (ksi)	Stress Intensity (ksi)	Allowable Stress (ksi)	Margin of Safety
108	24.0	23.9	0.9	48.0	89.3	0.86
90	23.8	23.9	-0.9	47.7	89.6	0.88
105	16.5	18.7	0.6	35.2	89.3	1.54
87	16.5	18.7	-0.6	35.2	89.6	1.55
110	-0.1	30.4	-0.3	30.4	89.3	1.94
92	-0.1	30.4	0.3	30.4	89.5	1.95
39	9.2	20.6	2.6	30.3	89.3	1.95
29	9.3	20.6	-2.5	30.3	89.6	1.95
44	9.2	19.5	-1.6	28.9	89.3	2.09
14	9.8	19.2	-1.5	29.1	90.4	2.10
24	9.2	19.4	1.6	28.8	89.6	2.11
129	-20.0	20.3	-8.5	28.7	89.3	2.11
54	8.2	19.9	1.1	28.2	89.3	2.17
109	-10.8	26.8	0.9	26.8	89.3	2.33
102	13.9	12.8	0.9	26.8	89.3	2.34
91	-10.6	26.8	-0.9	26.8	89.6	2.34
84	13.8	12.8	-0.8	26.7	89.6	2.35
107	0.0	25.0	-0.3	25.0	89.3	2.57
89	0.0	25.0	0.3	25.0	89.6	2.58
130	-16.0	20.7	5.8	24.6	90.1	2.66
111	-13.1	23.7	-0.5	23.7	89.3	2.76
93	-12.5	23.7	0.6	23.8	89.5	2.76
75	4.9	17.9	0.9	22.9	90.4	2.94
99	13.9	8.3	0.6	22.2	89.3	3.03
81	13.9	8.3	-0.5	22.2	89.6	3.04
123	4.0	17.9	-0.3	22.0	89.3	3.06
106	-14.8	21.8	0.6	21.9	89.3	3.09
88	-14.8	21.8	-0.6	21.9	89.6	3.10
104	0.0	19.5	-0.4	19.6	89.3	3.57
86	0.0	19.6	0.4	19.6	89.7	3.58

Note: See Figure 2.6.16.2-5 for section locations and definition of coordinate system.

Table 2.7.13.1.3-6 $P_m + P_b$ Stresses for CY-MPC Support Disk 30-Foot Side Drop, 0° Basket Orientation

Section	Sx (ksi)	Sy (ksi)	Sxy (ksi)	Stress Intensity (ksi)	Allowable Stress (ksi)	Margin of Safety
1	-52.9	1.6	-0.2	52.9	131.1	1.48
3	-52.6	1.4	0.2	52.6	131.1	1.49
11	-35.1	-13.7	3.1	49.2	129.4	1.63
9	-49.2	0.0	-0.2	49.2	129.8	1.64
13	-34.7	-13.6	-3.0	48.7	129.4	1.66
7	-48.6	2.2	0.0	48.6	129.8	1.67
66	-37.7	15.4	-5.3	38.9	129.4	2.33
131	-34.6	14.7	10.3	38.9	130.2	2.35
73	-37.5	14.9	5.1	38.6	129.4	2.35
81	-33.8	19.0	-3.9	34.7	128.0	2.69
21	-33.0	21.8	-4.6	34.7	128.1	2.69
23	-32.7	21.5	4.6	34.4	128.1	2.73
88	-33.4	18.7	3.9	34.4	128.0	2.73
67	-24.4	-9.7	1.1	34.2	129.5	2.78
72	-24.1	-9.9	-1.1	34.1	129.5	2.79
5	-33.5	0.1	0.0	33.5	130.9	2.91
124	-22.2	15.2	-13.8	33.0	130.3	2.95
70	-14.8	-16.6	-3.8	32.3	129.6	3.01
69	-14.7	-16.6	3.8	32.2	129.6	3.02
4	-32.1	0.0	-1.1	32.2	130.4	3.05
6	-32.0	0.0	1.1	32.1	130.4	3.06
12	-21.5	-9.6	-2.2	31.4	129.6	3.13
27	-18.5	-12.0	0.1	30.4	128.1	3.21
82	-18.2	-12.0	0.3	30.3	128.0	3.23
26	-24.6	-5.4	1.6	30.3	128.0	3.23
28	-24.3	-5.5	-1.6	30.0	128.0	3.27
87	-18.0	-12.0	-0.3	30.0	128.0	3.27
8	-26.3	14.8	-6.6	29.3	129.9	3.43
85	-11.2	-16.1	-1.2	27.3	128.1	3.69
84	-11.0	-16.1	1.3	27.3	128.1	3.69

Note: See Figure 2.6.16.2-5 for section locations and definition of coordinate system.

Table 2.7.13.1.3-7 $P_m + P_b$ Stresses for CY-MPC Support Disk 30-Foot Side Drop, 38° Basket Orientation

Section	Sx (ksi)	Sy (ksi)	Sxy (ksi)	Stress Intensity (ksi)	Allowable Stress (ksi)	Margin of Safety
1	-103.6	4.4	7.0	104.1	131.1	0.26
2	-83.7	14.5	-2.8	83.8	132.1	0.58
13	-80.5	20.4	1.5	80.5	129.4	0.61
26	-78.2	49.7	5.1	79.1	128.0	0.62
11	-79.5	24.3	3.4	79.7	129.4	0.62
41	-77.3	51.8	5.5	78.4	127.6	0.63
3	-78.7	25.4	-9.7	80.4	131.1	0.63
7	-78.7	6.2	7.0	79.4	129.8	0.63
28	-77.9	38.3	2.9	78.1	128.0	0.64
43	-77.2	44.6	4.1	77.7	127.6	0.64
12	-78.1	19.7	-1.2	78.2	129.6	0.66
100	-76.3	38.2	4.2	76.8	127.6	0.66
82	-76.5	36.1	3.8	76.9	128.0	0.67
99	75.9	-38.2	4.1	76.4	127.6	0.67
42	-73.3	58.9	1.9	73.6	127.6	0.73
106	-71.7	30.2	1.8	71.8	127.6	0.78
81	71.1	-38.6	4.9	71.8	128.0	0.78
52	-70.6	30.6	-1.1	70.7	127.6	0.81
88	-70.5	23.2	0.4	70.5	128.0	0.82
103	-68.0	47.2	4.4	68.9	127.6	0.85
70	-68.0	3.2	0.1	68.0	129.6	0.91
105	-66.0	57.6	2.8	66.8	127.6	0.91
66	67.6	-35.8	-1.3	67.6	129.4	0.91
67	-67.5	13.7	2.5	67.6	129.5	0.91
73	-66.8	5.6	-6.7	67.6	129.4	0.92
102	-54.1	62.1	7.3	66.4	127.6	0.92
84	-63.0	59.0	4.5	65.9	128.1	0.94
51	-63.8	36.6	4.5	64.5	127.6	0.98
69	-65.0	22.3	-0.3	65.0	129.6	0.99
37	-47.8	63.7	1.9	64.0	127.6	0.99

Note: See Figure 2.6.16.2-5 for section locations and definition of coordinate system.

Table 2.7.13.1.3-8 $P_m + P_b$ Stresses for CY-MPC Support Disk 30-Foot Side Drop, 63° Basket Orientation

Section	Sx (ksi)	Sy (ksi)	Sxy (ksi)	Stress Intensity (ksi)	Allowable Stress (ksi)	Margin of Safety
43	-78.7	54.6	2.6	79.0	127.6	0.62
106	-74.3	40.8	0.3	74.3	127.6	0.72
13	-75.3	31.2	0.6	75.3	129.4	0.72
3	-74.1	30.5	-9.7	76.2	131.1	0.72
28	-74.1	47.2	1.7	74.2	128.0	0.72
41	73.3	-41.5	4.4	73.9	127.6	0.73
1	-74.6	3.3	5.7	75.0	131.1	0.75
99	71.3	-25.7	2.6	71.4	127.6	0.79
129	-40.3	47.9	-26.6	70.9	127.6	0.80
100	-70.4	41.5	2.2	70.6	127.6	0.81
2	-71.6	18.8	-2.6	71.7	132.1	0.84
105	68.9	-26.0	4.0	69.3	127.6	0.84
88	-68.7	33.8	-0.6	68.7	128.0	0.86
42	-67.2	63.4	0.8	67.4	127.6	0.89
26	-66.9	50.1	3.0	67.4	128.0	0.90
82	-65.9	38.6	1.8	66.0	128.0	0.94
73	-65.3	18.8	-6.7	66.2	129.4	0.95
81	65.2	-23.6	2.7	65.4	128.0	0.96
11	65.5	-33.5	3.6	65.9	129.4	0.96
103	-63.8	52.8	3.3	64.7	127.6	0.97
44	-62.8	33.7	1.2	62.8	127.6	1.03
12	-63.4	24.1	-0.8	63.4	129.6	1.04
102	60.5	-39.0	5.7	61.9	127.6	1.06
52	-60.5	23.9	0.8	60.6	127.6	1.11
66	60.9	-20.9	-2.4	61.1	129.4	1.12
108	58.3	-15.6	3.6	58.6	127.6	1.18
40	58.2	-17.2	1.4	58.3	127.6	1.19
87	57.4	-24.3	3.9	57.9	128.0	1.21
25	57.8	-13.7	1.4	57.9	128.0	1.21
37	-33.2	56.8	3.4	57.3	127.6	1.23

Note: See Figure 2.6.16.2-5 for section locations and definition of coordinate system.

Table 2.7.13.1.3-9 $P_m + P_b$ Stresses for CY-MPC Support Disk 30-Foot Side Drop, 90° Basket Orientation

Section	Sx (ksi)	Sy (ksi)	Sxy (ksi)	Stress Intensity (ksi)	Allowable Stress (ksi)	Margin of Safety
129	-35.4	38.6	-21.7	58.8	127.6	1.17
108	31.3	20.0	-1.9	51.5	127.6	1.48
90	30.7	20.2	2.0	51.0	128.0	1.51
44	41.4	6.8	-0.9	48.2	127.6	1.65
24	40.6	7.1	0.9	47.7	128.0	1.68
39	27.0	16.2	1.8	43.4	127.6	1.94
29	27.2	16.1	-1.8	43.4	128.0	1.95
105	23.3	14.9	-1.5	38.3	127.6	2.33
130	-25.8	27.8	11.8	38.7	128.8	2.33
87	23.1	15.1	1.5	38.3	128.0	2.35
14	10.4	23.1	-3.4	34.1	129.2	2.79
43	30.7	2.4	0.9	33.2	127.6	2.85
23	30.5	2.6	-0.9	33.1	128.1	2.87
54	8.6	23.0	3.7	32.4	127.6	2.94
110	-0.1	31.8	-0.4	31.8	127.6	3.01
111	-15.7	27.7	-8.1	31.8	127.6	3.01
92	-0.1	31.8	0.3	31.8	127.9	3.03
93	-14.7	27.5	8.4	31.7	127.8	3.04
109	-17.9	29.4	-2.8	30.1	127.6	3.24
91	-17.2	29.1	2.8	29.8	128.0	3.30
38	17.7	11.9	0.2	29.7	127.6	3.30
28	18.0	11.7	-0.2	29.7	128.0	3.30
40	-28.4	14.6	-2.4	28.8	127.6	3.42
106	-21.5	25.4	-4.7	28.5	127.6	3.47
20	-28.2	14.5	2.4	28.6	128.0	3.47
88	-21.3	25.2	4.8	28.4	128.0	3.51
102	8.4	18.2	2.5	27.0	127.6	3.72
84	8.6	18.0	-2.4	27.0	128.1	3.74
41	-25.6	21.3	-2.6	26.8	127.6	3.76
42	-19.8	25.0	-3.1	26.5	127.6	3.82

Note: See Figure 2.6.16.2-5 for section locations and definition of coordinate system.

2.7.13.1.4 Stress Evaluation of CY-MPC Support Disk for 30-Ft Oblique Drop

This section documents the methodology used to calculate the stresses associated with oblique impacts of the transport cask (Figure 2.7.13.1-2). The results show that the stress criteria are met for all oblique conditions. Note that the methodology used for the off-angle drop evaluation is very conservative since the g loads decrease significantly for oblique drops (Section 2.6.7.4).

To evaluate oblique impacts, the stress components (i.e., S_x, S_y, S_{xy}) are combined from the side drop and end drop cases for both the 0° the 38° basket drop orientations (Figure 2.7.13.1-1). The stresses are combined according to the following cask drop angles: ϕ = 0°, 24°, 30°, 45°, 60°, 73°, 75°, 77°, 80°, 83°, 85°, 88° and 90°. Note that the 0° and 90° cask drop angles are equivalent to the end- and side- drop cases, respectively. The normal stresses (S_x and S_y) and the shear stress (S_{xy}) for a drop with an angle of ϕ (Figure 2.7.13.1-2) are calculated using the following equations:

$$S_{x(\phi)} = S_{x(end)}\text{Cos}\phi + S_{x(side)}\text{Sin}\phi ,$$

$$S_{y(\phi)} = S_{y(end)}\text{Cos}\phi + S_{y(side)}\text{Sin}\phi ,$$

$$S_{xy(\phi)} = S_{xy(end)}\text{Cos}\phi + S_{xy(side)}\text{Sin}\phi ,$$

where:

$S_{x(end)}$, $S_{y(end)}$, and $S_{xy(end)}$ are the sectional stresses resulting from the Support Disk End Drop Model, and $S_{x(side)}$, $S_{y(side)}$, and $S_{xy(side)}$ are the section stresses resulting from the Support Disk Side Drop Model.

Off-angle principle stresses (i.e., S_1, S_2) are calculated by using the following equation:

$$S_1, S_2 = \frac{S_{x(\phi)} + S_{y(\phi)}}{2} \pm \sqrt{\left(\frac{S_{x(\phi)} - S_{y(\phi)}}{2}\right)^2 + S_{xy(\phi)}^2}$$

Once the principle stresses are calculated, new stress intensities (SI) can be calculated. Summaries of the maximum support-disk stress-intensities in the 30-foot oblique drop conditions are given in Table 2.7.13.1.4-1.

Table 2.7.13.1.4-1 CY-MPC Support Disk Stress Summary for the 30-Foot Oblique Drop

Stress State	Section[2]	Cask Drop Angle (°)[3]	Sx (ksi)	Sy (ksi)	Sxy (ksi)	Stress Intensity (ksi)	Allowable Stress (ksi)	Margin of Safety
0° BASKET DROP ORIENTATION								
P_m	11	90	-21.3	-21.0	2.0	42.5	90.6	1.13
P_m+P_b	61	0	88.0	-17.1	33.4	101.3	127.6	0.26
38° BASKET DROP ORIENTATION								
P_m	73	90	-50.3	2.8	3.8	50.6	90.6	0.79
P_m+P_b	1	30	109.4	-35.3	-30.9	120.6	131.1	0.09

Notes:

1. P_m = Primary Membrane Stress, $P_m + P_b$ = Primary Membrane + Bending Stress.
2. See Figure 2.6.16.2-5 for section locations.
3. See Figure Figure 2.7.13.1-2 for definition of cask drop angle.
4. Allowable Stress for 17-4PH, Type 630 stainless steel:

   For P_m, $S_{allow} = 0.7\ S_u = 89.3$ ksi at 550°F

   $= 94.5$ ksi at -40°F

   For $P_m + P_b$, $S_{allow} = S_u = 127.6$ ksi at 550°F

   $= 135.0$ ksi at -40°F

2.7.13.2 Stress Evaluation of Tie Rods and Spacers for 30-Foot End Drop Load Condition for the CY-MPC

Tie Rod Evaluation

The tie rods serve basket assembly purposes and are not loaded during drop conditions; therefore, no further analysis is required.

Spacer Evaluation

Six tie rods and cylindrical spacers, to maintain disk spacing, connect the basket support disks and heat transfer disks. In a side drop, the load path is through the support disks into the canister wall. In an end drop, the load path is through the spacers to either the canister lid or bottom depending on the drop orientation. The load comprises the weight of the top or bottom weldment (depending on the drop orientation), the weight of the support and heat transfer disks, and the weight of the spacers and washers. The weight of the fuel assemblies is transmitted directly into the canister lid or bottom because the fuel tubes in the basket are open at both ends. In drop orientations between a side drop and an end drop, only a portion of the load acts along the tie rod axis. Thus, the end drop is the critical loading condition for the spacers. The bottom-end drop is the governing case because the top weldment is heavier than the bottom weldment.

During an end drop, the 6 split spacers at the bottom of the heat transfer disk array are loaded by the top weldment, the 27 heat transfer disks, the spacers and washers above, and the 27 support disks above the lowest split spacer at the bottom of the heat transfer disk array. The total weight on the split spacers is 8,225 lbs.

The initial tie rod pre-load tension will be diminished by the compressive effect of the end drop. However, for conservatism, the total compression (2,011 lbs.) induced by the 50±10 ft-lb bolt torque will be included in the load on the split spacers.

The maximum total load (P_{ssp}) on the split spacer is, for accident conditions:

$P_{ssp} = 2{,}011 + (8{,}225)\times 60/6 = 84{,}261$ lb, use 100,000 lb

Note: 60g conservatively used to bound 56g-end drop load

The stress (σ_{ssp}) is determined by applying the total load to the cross-sectional area (A_{ssp}) of the split spacer. A_{ssp} is conservatively taken as the area of the decreased diameter section.

$$\sigma_{ssp} = \frac{P_{ssp}}{A_{ssp}} = \frac{100{,}000\,\text{lb}}{2.45\ \text{in.}^2} = 40{,}816\ \text{psi}$$

Where

$$A_{ssp} = \frac{\pi}{4}\left(2.50^2 - 1.77^2\right) = 2.45\ \text{in.}^2$$

The margin of safety (MS) is:

$$\text{M.S.} = \frac{0.7S_u}{\sigma_{ssp}} - 1 = \frac{0.7(64{,}400)}{40{,}816} - 1 = +0.10 \quad \text{(Accident condition, 400°F)}$$

The load on the bottom spacers comprises the weight of the top weldment, the weight of the support and heat transfer disks, and the weight of the spacers and washers.

During a bottom end drop, the 6 bottom spacers are loaded by the top weldment, the 27 heat transfer disks, the spacers and washers above, and the 28 support disks. The total weight on the spacers is 9,874 lbs.

The initial tie rod pre-load, tension, will be diminished by the compressive effect of the end drop. However, for conservatism, the total compression (2,011 lbs.) induced by the 50±10 ft-lb bolt torque will be included in the load on the bottom spacers.

The maximum total load (P_{bsp}) on the bottom spacer is:

P_{bsp} = 2,011 + (9,874)×60/6 = 100,751 lbs., use 101,000 lbs.
Note: 60g conservatively used to bound 56g-end drop load

The stress on the bottom spacer is:

$$\sigma_{ssp} = \frac{P_{bsp}}{A_{bsp}} = \frac{101{,}000\ \text{lbs}}{4.03\ \text{in.}^2} = 25{,}062\ \text{psi}$$

Where

$$A_{bsp} = \frac{\pi}{4}\left(2.875^2 - 1.77^2\right) = 4.03\ \text{in.}^2$$

The margin of safety (M.S.) is:

$$\text{M.S.} = \frac{0.7S_u}{\sigma_{bsp}} - 1 = \frac{0.7(64{,}400)}{25{,}062} - 1 = +0.80 \quad \text{(Accident condition, 400°F)}$$

2.7.13.3 CY-MPC Fuel Basket Support Disk – Buckling Evaluation (Accident Condition)

The buckling evaluation of the support disk web is based on the Interaction Equations 31 and 32 in NUREG/CR-6322. These two equations adopt the "Limit Analysis Design" approach for structural members subjected to stresses beyond the yield limit of the material, i.e., for members deformed elastically as a result of axial load or bending moment. Other equations applicable to the calculations are listed later in this section.

The maximum forces and moments are determined from the finite element analysis stress results for the Support Disk End-Drop Model as well as the Support Disk Side Drop Models (four different basket orientations, 0°, 38°, 63°, and 90°). The buckling evaluations account for both in-plane (about the strong axis of the web) and out-of-plane (about the weak axis of the web) buckling modes. The methodology and equations used for the buckling evaluation are summarized as follows:

Symbols and Units

- P = applied axial compressive loads, kips
- M = applied bending moment, kips-inch
- P_a = allowable axial compressive load, kips
- P_{cr} = critical axial compression load, kips
- P_e = Euler buckling loads, kips
- P_y = average yield load, equal to profile area times specified minimum yield stress, kips
- C_c = column slenderness ratio separating elastic and inelastic buckling
- C_m = coefficient applied to bending term in interaction equation
- M_m = critical moment that can be resisted by a plastically designed member in the absence of axial load, kip-in.
- M_p = plastic moment, kip-in.
- F_a = axial compressive stress permitted in the absence of bending moment, ksi
- F_e = Euler stress for a prismatic member divided by factor of safety, ksi
- k = ratio of effective column length to actual unsupported length
- l = unsupported length of member, in.
- r = radius of gyration, in.
- S_y = yield strength, ksi
- A = cross sectional area of member, in^2
- Z_x = plastic section modulus, in^3
- λ = allowable reduction factor, dimensionless.

From NUREG/CR-6322, the following equations are used to evaluate the support disk for normal condition of transport:

$$\frac{P}{P_{cr}} + \frac{C_m M}{\left[1 - \frac{P}{P_e}\right] M_m} \le 1.0 \qquad \text{(Eq. 31, NUREG/CR-6322)}$$

$$\frac{P}{P_y} + \frac{M}{1.18 M_p} \le 1.0 \qquad \text{(Eq. 32, NUREG/CR-6322)}$$

where: $P_{cr} = 1.7 \times A \times F_a$

$$F_a = \frac{\left[1 - \frac{1}{2}\left(\frac{k \cdot \ell}{r \cdot C_c}\right)^2\right] \cdot S_y}{\frac{5}{3} + \frac{3}{8}\left(\frac{k \cdot \ell}{r \cdot C_c}\right) - \frac{1}{8}\left(\frac{k \cdot \ell}{r \cdot C_c}\right)^3} \quad \text{for} \quad \frac{k \cdot \ell}{r} < C_c = \sqrt{2 \cdot \pi^2 \frac{E}{S_y}}$$

$P_e = 1.92 \times A \times F_e$

$$F_e = \frac{\pi^2 \cdot E}{1.92\left(\frac{k \cdot \ell}{r}\right)^2} \text{ (non-austenitic)}$$

$P_y = S_y \times A$

$C_m =$ 0.85 for members with joint translation (sideways).

$M_p = S_y \times Z_x$

$$M_m = M_p \cdot \left(1.07 - \frac{\left(\frac{1}{r}\right) \cdot \sqrt{S_y}}{3160}\right) \le M_p$$

Buckling evaluations are performed on all sections in the disk ligaments defined in Figure 2.6.16.2-5. Using the cross-sectional stresses calculated at each of the sections for each loading condition the maximum corresponding compressive forces (P) and bending moment are determined as follows,

$$P = \sigma_m A,$$

$$M = \sigma_b A,$$

where, σ_m is the membrane stress, σ_b is the strong axis bending stress or weak axis bending stress, A is the area (b × t), and S is the section modulus ($tb^2/6$ for strong axis bending and $bt^2/6$ for weak axis bending).

To determine the margin of safety:

$$P_1 = P/P_{cr} \qquad M_1 = \frac{C_m M}{(1 - P/P_e) M_m} \qquad (P_1 + M_1 \leq 1) \quad \text{(Eq. 31, NUREG/CR-6322)}$$

and $$P_2 = P/P_y \qquad M_2 = \frac{M}{1.18\, M_p} \qquad (P_1 + M_1 \leq 1) \quad \text{(Eq. 32, NUREG/CR-6322)}$$

The margins of safety are:

$$M.S._1 = \frac{1}{P_1 + M_1} - 1$$

$$M.S._2 = \frac{1}{P_2 + M_2} - 1$$

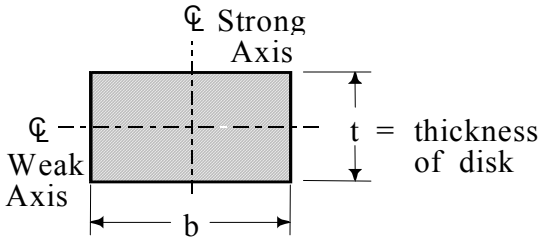

The side drop conditions are the governing conditions for strong axis buckling evaluation since the axial compressive force (P) and the strong axis bending moment (M) decrease with the drop angle. Therefore, evaluation of strong axis buckling is performed for side-drop conditions only.

Buckling analysis was completed only for the 38° basket orientation because this is the worst case angle (See Section 2.7.13.1). The minimum margin of safety is +0.34, which occurs at section number 1. The results for the 20 worst-case sections are summarized in Table 2.7.13.3-1.

Table 2.7.13.3-1 NUREG/CR 6322 Buckling Analysis for CY-MPC Support Disk 30-Foot Side Drop, 38° Basket Orientation

Sect.	P (kip)	Pcr (kip)	Py (kip)	M (in-kip)	Mp (in-kip)	Mm (in-kip)	MS1	MS2
1	10.44	59.07	49.07	8.49	13.49	13.22	0.35	0.34
13	12.90	58.15	48.30	5.74	13.28	13.02	0.64	0.58
2	14.51	87.24	67.61	12.04	25.36	25.36	0.74	0.62
3	12.81	59.07	49.07	5.57	13.49	13.22	0.70	0.64
7	9.71	58.35	48.47	6.13	13.33	13.07	0.73	0.69
28	8.25	57.25	47.54	6.33	13.07	12.83	0.74	0.71
12	11.43	85.12	65.94	11.76	24.73	24.73	0.84	0.73
43	4.85	56.89	47.23	6.89	12.99	12.75	0.82	0.81
11	2.94	58.14	48.29	7.45	13.28	13.02	0.85	0.86
26	2.88	57.25	47.54	7.33	13.07	12.83	0.85	0.87
42	6.73	83.16	64.40	12.04	24.15	24.15	0.97	0.90
41	0.97	56.89	47.23	7.60	12.99	12.75	0.90	0.94
52	5.52	83.16	64.40	11.85	24.15	24.15	1.06	0.99
8	14.98	85.35	66.13	8.01	24.80	24.80	1.20	1.00
9	12.00	58.35	48.47	3.85	13.33	13.07	1.15	1.03
27	9.43	83.72	64.85	9.24	24.32	24.32	1.28	1.14
111	12.98	83.16	64.40	7.55	24.15	24.15	1.35	1.14
23	10.59	57.31	47.59	3.76	13.09	12.84	1.27	1.15
22	11.39	83.83	64.93	8.32	24.35	24.35	1.32	1.15
21	4.41	57.31	47.59	5.46	13.09	12.84	1.26	1.24

Note: See Figure 2.6.16.2-5 for section locations and definition of coordinate system.

2.7.13.4 Fuel Tube Analysis—CY-MPC

The fuel tube provides a foundation and sealed cavity to mount BORAL poison plates within the fuel basket structure. The fuel tube does not serve a structural function relative to the support of the fuel assembly. To ensure that the fuel tube remains functional when the cask is subjected to design load conditions, a structural evaluation of the tube is performed for both end and side-impact load conditions.

Fuel Tube End-Impact Analysis

During the postulated cask end impact, the cask bottom for the bottom-end drop, and the lid for the top-end drop support the CY fuel assemblies. The fuel tubes do not carry fuel assembly load. Therefore, evaluation of the fuel tube for the end-impact load is performed by considering the weight of the fuel tube subjected to the cask deceleration carried by the minimum tube cross-sectional area. The minimum cross-sectional area is located at the contact point of the tube with the bottom weldment. The minimum cross-sectional area is:

$$A = 0.048 \times 4 \times (9.12 + 0.048) = 1.76 \text{ in}^2$$

The total bearing load on the tube during the cask bottom-end impact is 6,820 psi, (55g x 124 lbs). The maximum compressive and bearing stress is (6,820 / 1.76) = 3,875 psi. Limiting the compressive stress level to the material yield strength ensures that the tube remains in position when the cask is subjected to the postulated end-drop. Type 304 stainless steel yield strength is 17,300 psi at a conservatively high temperature of 750°F for the axial location on the fuel tube that has the minimum cross-sectional area. The margin of safety is:

$$\text{M.S.} = \frac{17{,}300}{3{,}875} - 1 = +3.46$$

Fuel Tube Side-Impact Analysis

During the cask side-impact load configuration, the fuel tube is supported by the fuel basket's support disks. The support disks support the full length of the fuel tube, and are spaced at 4.59 inches (center-to-center) which is about one-half of the fuel tube width. Considering the fuel tube is subjected to a 60g side-impact deceleration and the 28 support locations provided by the basket support disk, the fuel tube shear stress is:

Impact Shear Load = 55 x 1590 / 28 = 3,123.2 lbs

Shear Load = 3,123.2 lbs
Area = 0.048 x 9.12 x 2 = 0.876 in^2
Shear Stress = 3123.2 / 0.876 = 3,565.3 psi

Using an allowable shear stress equivalent to half the yield strength of the tube, 8,650 psi (17,300 / 2), the margin of safety is:

$$M.S. = \frac{8,650}{3,565.3} - 1 = \ + 1.43 \text{ at } 750°F$$

The conservative evaluation of the tube loading resulting from its own mass during a side-impact configuration indicates that the tube structure will maintain position and will function.

For transport and storage, the bounding load is the 30-foot side drop condition for transport (55g). ANSYS Finite Element program was used to perform the elastic-plastic analysis on the fuel tubes. ANSYS plastic quadrilateral (SHELL43) shell elements were used to model the fuel tube walls of thickness 0.048 inches. The CY basket's fuel tube is 131.95 inch long and supported by 0.5 inch thick support disks at a 4.59 inch pitch. The BORAL plate (0.075 inch) and stainless steel cover plate (0.018 inch) are conservatively not included in the model. The multi-linear kinematic hardening (kinh) option is used for the non-linear material properties. The stress-strain curve for Type 304 SS is used (R1).

Two loading cases were analyzed: pressure loading and grid loading. Note that only a quarter-symmetry periodic section of the fuel tube was modeled for both the cases (Figure 2.7.13.4-1).

For the pressure loading case, surface pressures were applied to the inside bottom surface of the fuel tubes. The distributed load of the fuel assembly on the fuel tube wall was modeled as a surface pressure loading, determined as follows:

$$\text{Impact Pressure} = \frac{gW_f}{w_f L_f} = 72.67 \text{ psi}$$

where:

g = acceleration load = 55 *g*
W_f = weight of fuel assembly = 1590 lbs
L_f = length of fuel tube = 131.95 in
w_f = width of fuel tube = 9.12 in

For the grid loading case, a bounding load condition for the grid loading case model is simulated by applying a constant displacement of 0.08 inch in the negative Y direction to the nodes corresponding to the grid location in the model. It is assumed that the fuel assembly grid spacer is rigid and therefore a constant displacement is conservatively applied.

From the elastic-plastic analyses of the CY-MPC fuel tube, the maximum equivalent plastic stress is 24,060 psi for the uniform loading case and 30,970 psi for the grid loading case.

Conservatively, comparing the plastic stress of the CY-MPC to the allowable stress of 63,100 psi at 750°F for Type 304 SS, provides margins of safety of:

Pressure Loading: $\text{M.S.} = \frac{63{,}100}{24{,}060} - 1 = +1.62$

Grid Loading: $\text{M.S.} = \frac{63{,}100}{30{,}970} - 1 = +1.04$

The maximum total strain is 0.019 for CY-MPC fuel tube for the uniform loading case and 0.047 for the grid loading case, as shown in Figures 2.7.13.4-2 and 2.7.13.4-3.

Defining the acceptable elastic-plastic response of the stainless steel as one-half the material failure strain of 0.4 in/in at 750°F (R2). Using this methodology to evaluate total cumulative strain shows margins of safety of:

Pressure Loading: $\text{M.S.} = \frac{0.4/2}{0.019} - 1 = +9.53 \text{ at } 750^{o}\text{F}$

Grid Loading: $\text{M.S.} = \frac{0.4/2}{0.047} - 1 = +2.35 \text{ at } 750^{o}\text{F}$

Similarly, the margin of safety for elastic-plastic stress becomes:

Pressure Loading: $\text{M.S.} = \frac{63{,}100 - 17{,}300}{24{,}060 - 17{,}300} - 1 \text{ at } 750^{o}\text{F}$

Grid Loading: $\text{M.S.} = \frac{63{,}100 - 17{,}300}{30{,}970 - 17{,}300} - 1 \text{ at } 750^{o}\text{F}$

Where the yield strength of Type 304 SS at 750°F is 17,300 psi.

The total displacements of the fuel tube are 0.17 inch for the pressure loading case and 0.08 inch for the grid loading case.

Both the maximum total equivalent strain and the elastic-plastic stress analyses indicate that the tube position within the support basket is maintained.

Maximum displacement in the fuel tube was averaged to determine the average displacement. The averaging technique was based on the parabolic shape of the displaced fuel tube bottom wall. The maximum displacement (D) is as follows:

Pressure Loading: D = (2/3)(max displacement) = (2/3)(0.17) = 0.113 inch
Grid Loading: D = (2/3)(max displacement) = (2/3)(0.08) = 0.053 inch

Assurance that the BORAL poison remains within the sealed casing is evaluated by considering that loads produced by the BORAL and skin mass decelerated by 55g are maintained by the seal weld.

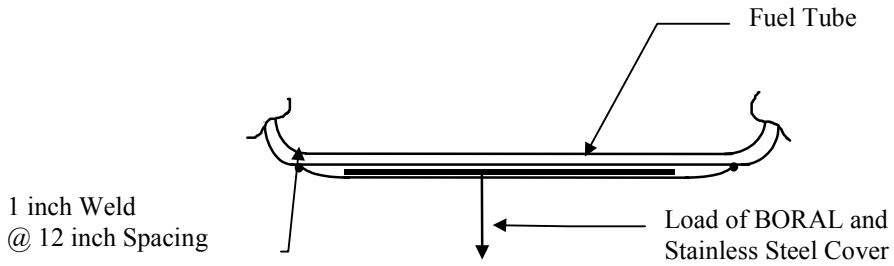

Load exerted by BORAL/Stainless Steel skin is given as follows:

$$F_{b/ss} = g\rho twl$$

where:

g = acceleration due to gravity = 55 g

ρ = density of material

= 0.098 lb/in^3 (BORAL, aluminum density is conservatively used)

= 0.291 lb/in^3 (stainless steel)

t = thickness of material
= 0.075 in (BORAL)
= 0.018 (stainless steel)
w = width of material
= 8.54 in (BORAL) (9.22-0.34x2)
= 9.05 in (stainless steel) (9.22-0.18x2+0.075x2)
l = length of material section = 12.0 in

Loads on a 1-inch weld for a 12-inch section:

F_b = 55 x 0.098 x 0.075 x 8.54 x 12.0 = 41.43 lbs
F_{ss} = 55 x 0.291 x 0.018 x 9.05 x 12.0 = 31.29 lbs

Total load (F_t) on a 1-inch section of fuel tube seal weld:

P = 41.43 + 31.29 = 72.72 lbs

$$\text{Weld stress, } \sigma = \frac{P}{A} = \frac{72.72/2}{1x0.018} = 2{,}020 \text{ psi}$$

Based on the weld material being Type 304 SS the margin of safety is:

σ_{yield} = 17,300 psi at 750°F

$$\text{M.S.} = \frac{17{,}300}{2{,}020} - 1 = +7.56$$

Figure 2.7.13.4-1 CY-MPC Fuel Tube Finite Element Model

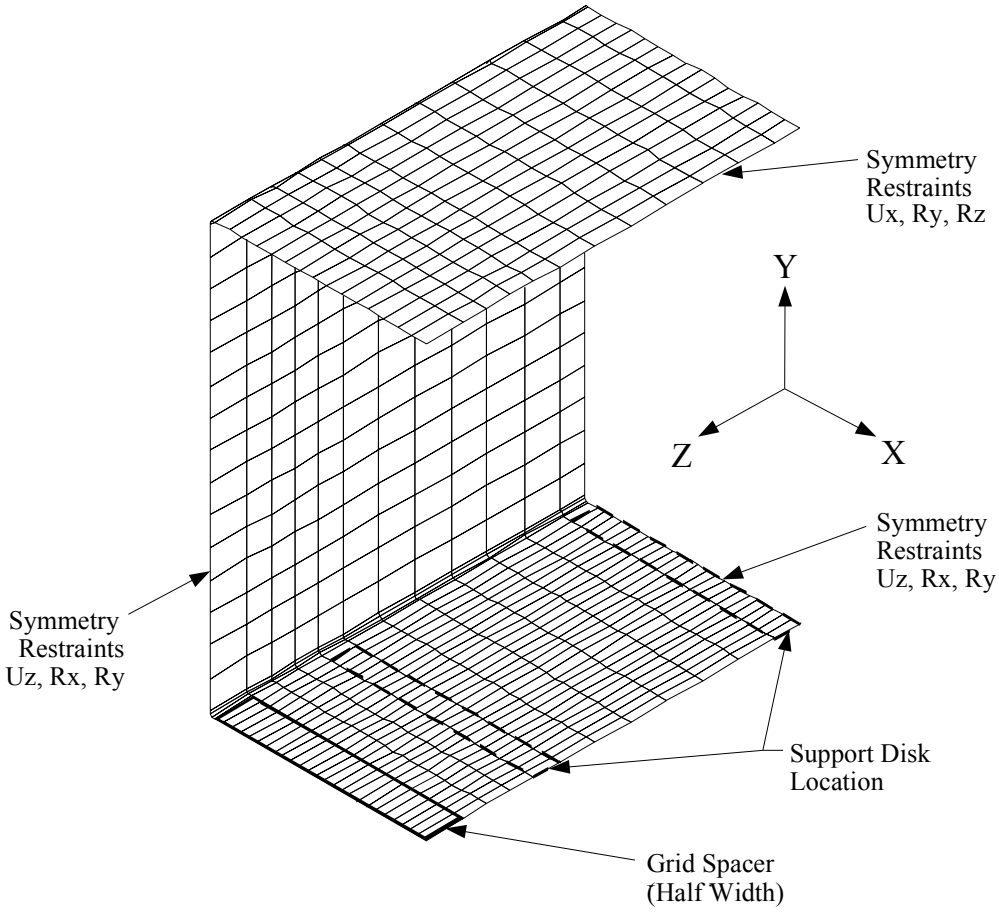

Figure 2.7.13.4-2 CY-MPC Fuel Tube Analysis Results – Total Equivalent Strain (Uniform Loading)

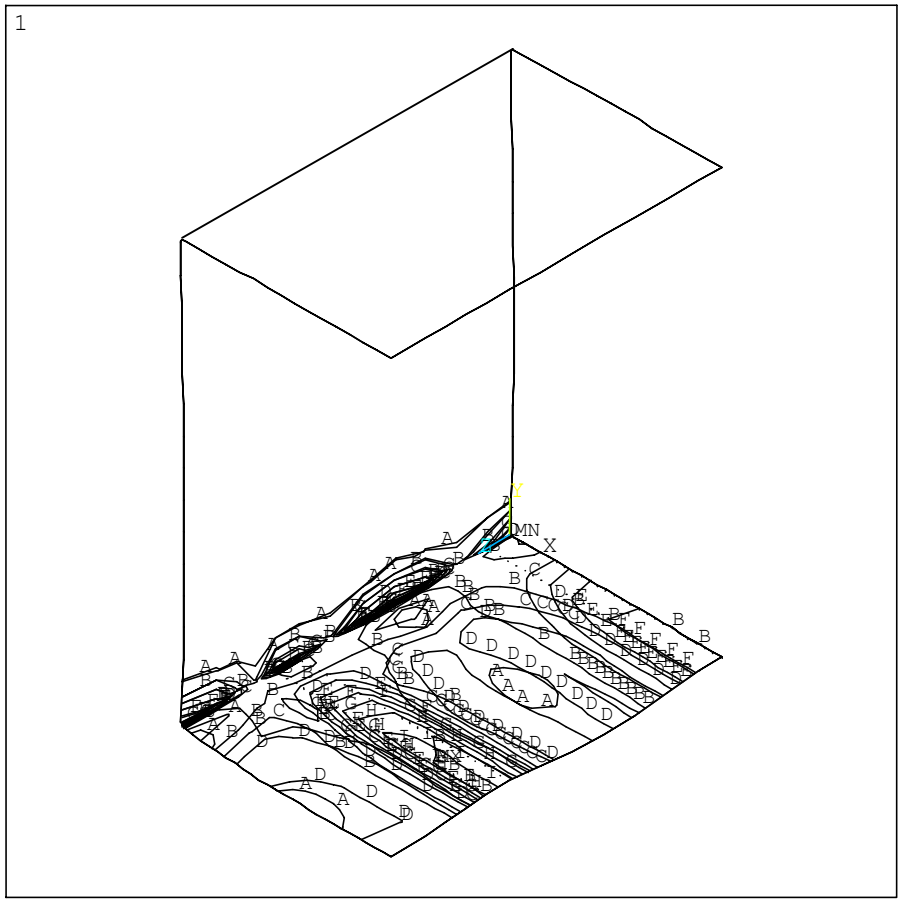

Figure 2.7.13.4-3 CY-MPC Fuel Tube Analysis Results – Total Equivalent Strain (Grid Loading)

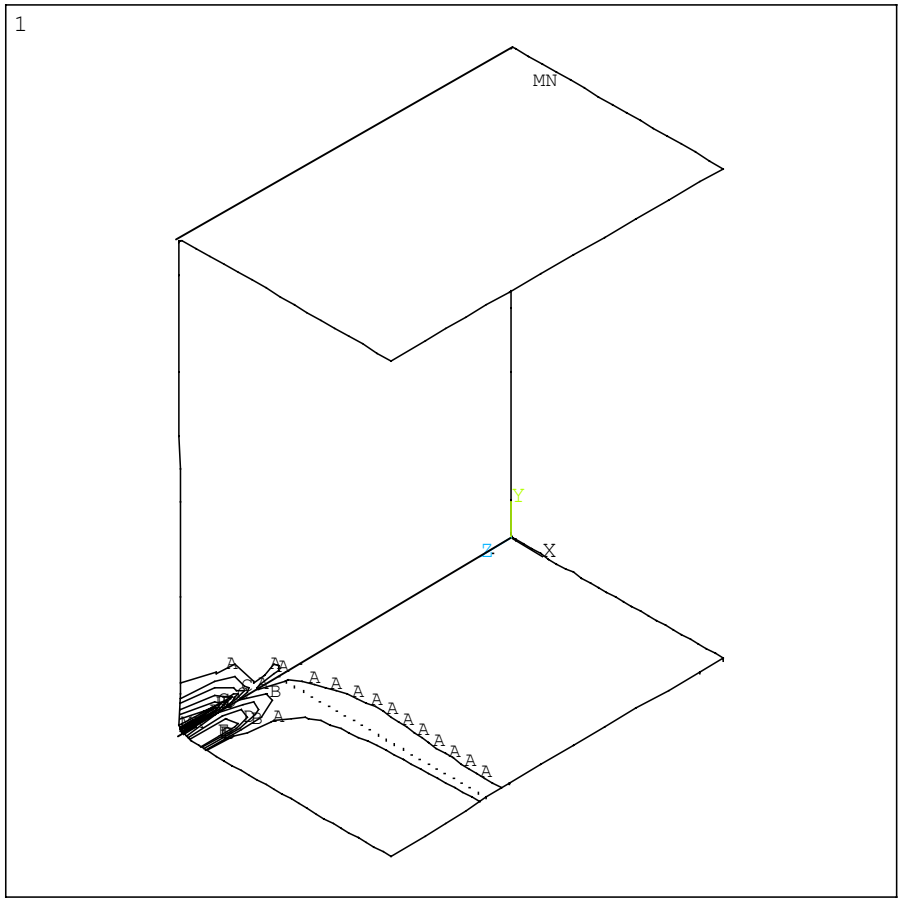

ANSYS 5.5.2
JUL 10 2000
17:17:45
PLOT NO. 1
NODAL SOLUTION
STEP=1
SUB =17
TIME=1
EPTOEQV (AVG)
EffNu=0
TOP
DMX =.080002
SMN =.869E-05
SMX =.047234
A =.002632
B =.00788
C =.013127
D =.018374
E =.023621
F =.028869
G =.034116
H =.039363
I =.044611

2.7.13.5 CY-MPC Fuel Basket Weldment Analysis for 30-Foot End Drop

Two ANSYS finite element models (one for each weldment) are constructed for structural evaluation of the CY-MPC top and bottom weldments when subjected to 1-foot (presented in Section 2.6.16) and 30-foot drop (presented in this Section) conditions. Because of symmetry of the geometry of the weldments and the symmetry of the loading during end-drop conditions, the FE models represent quarter and half sections of the bottom and top weldments, respectively.

The top and bottom weldments are 0.5-inch thick plates of Type 304 stainless steel. The weldments support their own weight plus the weight of 26 fuel assembly tubes. A finite element analysis is performed for both weldments, since the support for each weldment is different due to the location of the support ribs for each. Both models use the SHELL63 element, which permits out of plane loading. Figures 2.7.13.5-1 and 2.7.13.5-2 show the finite element models for the weldments. The ribs supporting the weldment plates were also represented by SHELL63. The top weldment is constrained in the axial direction at the tie rod locations. The bottom weldment is constrained in the axial direction at the support ribs. Evenly distributed nodal forces around the periphery of the fuel assembly slot represent the force on the weldment from each fuel tube. The application of the nodal loads at the slot periphery is accurate since the tube weight is transmitted to the edge of the slot, which provides support to the fuel tubes in the end drop condition. An acceleration of 60g is applied to bound both the transport and storage end-drop conditions.

This analysis demonstrates that the weldment design satisfies the primary membrane (P_m) and the primary membrane plus bending (P_m+P_b) stress criteria.

The weldments are shown to satisfy the stress criteria in ASME Code, Section III Division I, Subsection NG. The margins of safety are conservatively evaluated at the maximum temperature of 500°F. The calculated temperatures and margins of safety are:

Component	Stress (ksi) $P_m + P_b$	Stress Allowable (ksi)	M.S.
Top Weldment	57.62	63.0	+0.09
Bottom Weldment	47.19	63.0	+0.34

Figure 2.7.13.5-1 Finite Element Model of the CY-MPC Top Weldment

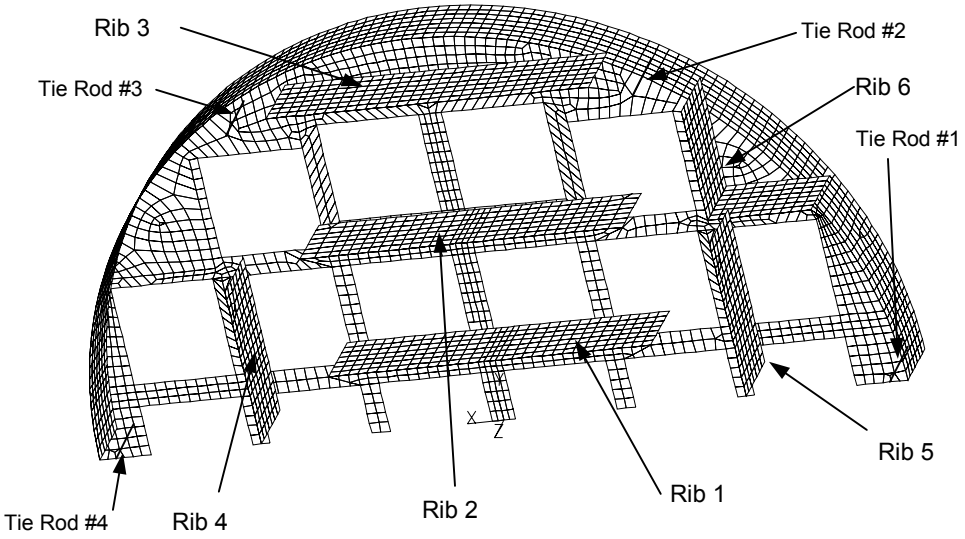

Figure 2.7.13.5-2 Finite Element Model of the CY-MPC Bottom Weldment

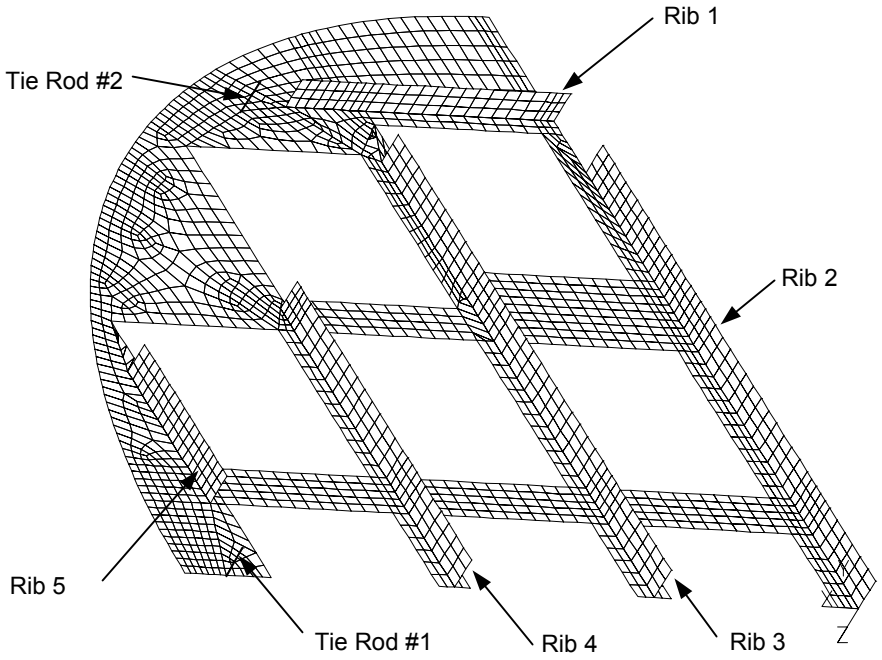

2.7.14 CY-MPC Reconfigured Fuel Assembly and Damaged Fuel Can Evaluation – Accident Conditions

The CY-MPC reconfigured fuel assembly and damaged fuel can are evaluated for the hypothetical accident conditions using 60g impact accelerations for the end-drop and side-drop impacts. Material properties for the reconfigured fuel assembly are taken at 750°F. Material properties for the damaged fuel can are taken at 600°F. These temperatures envelope all operating condition temperatures.

2.7.14.1 CY-MPC Reconfigured Fuel Assembly Weldment Evaluation

2.7.14.1.1 Reconfigured Fuel Assembly End Impact

For the end impact, the corner angle fixtures are evaluated to the criteria specified in NUREG/CR-6322, "Buckling Analysis of Spent Fuel Basket." Length (L) for both corner angles and tubes is conservatively taken as the length of the tube divided into five equal spans by the tube support grids, L=135.09/5 = 27.02 inches.

Corner Angle Evaluation

For Service Level D, the corner angles are evaluated for axial compression in accordance with NUREG/CR-6322 and ASME Code Section III, Appendix F-1334.3.

Because Subsection F-1334.3 specifies no criteria for austenitic stainless steel, the following method from NUREG/CR-6322 is used to determine the criteria for the hypothetical accident condition.

The austenitic stainless steel criteria for the hypothetical accident condition can be expressed as:

$$SS_{\text{Level D}} = \left(\frac{SS}{CS}\right)_{\text{Level A}} \times CS_{\text{Level D}} \qquad \text{(NUREG/CR-6322 Equation 39)}$$

where SS and CS stand for stainless steel and carbon steel, respectively.

The maximum allowable stress for stainless steel (F_a = 6,424.4 lb/in^2) for Level A (normal) conditions was determined previously. The allowable axial load ($P_{SS\text{-normal}}$) can be determined using the relation:

$$P_{SS-\text{normal}} = F_a \times A = 6{,}424.4 \text{ lb/in}^2 \times 0.715 \text{ in}^2 = 4{,}593.4 \text{ lb}$$

The maximum allowable axial load ($P_{CS\text{-}normal}$) for carbon steel (S_y = 25.8 ksi) can be determined using NUREG/CR-6322 Equation 22 as:

$$F_a = \frac{\left[1 - \frac{1}{2}\left(\frac{Kl}{rC_c}\right)^2\right]S_y}{\frac{5}{3} + \frac{3}{8}\frac{Kl}{rC_c} - \frac{1}{8}\left(\frac{Kl}{rC_c}\right)^3} = \frac{0.9498(25{,}800)}{1.667 + 0.1188 - .0039} = 13{,}752.1 \text{ psi}$$

where,

$$\frac{Kl}{r} = 43.8 < C_c = \sqrt{2\pi^2 \frac{E}{S_y}} = 138.85.$$

$$E = 25.2E3 \text{ ksi}$$

$$P_{CS-normal} = F_a A = 13{,}752.1 \text{ lb/in.}^2 \left(0.715 \text{ in.}^2\right) = 9{,}832.8 \text{ lb}$$

The maximum allowable axial compressive load ($P_{CS\text{-}accident}$) for carbon steel accident conditions using NUREG/CR-6322 Equation 33 is:

$$P_{CS-accident} = \frac{\left(1 - \frac{\lambda^2}{4}\right)P_y}{1.11 + 0.50\lambda + 0.17\lambda^2 - 0.28\lambda^3} = \frac{0.9502(18{,}447.0)}{1.11 + 0.223 + 0.0338 - 0.0249} = 13{,}399.8 \text{ lb}$$

where,

P_y = the average yield load ($S_y \times A$ = 25,800 ksi × 0.715 in.^{2} = 18,447.0 lb)

$$\lambda = \frac{1}{\pi}\left(\frac{Kl}{r}\right)\sqrt{\frac{S_y}{E}} = \frac{1}{\pi}(43.8)\sqrt{\frac{25.8}{25.2e3}} = 0.4461 \qquad 0 \le 0.4461 \le 1$$

Using NUREG/CR-6322 Equation 39 to determine the allowable load for stainless steel Level D (accident) conditions:

$$SS_{Level\ D} = \left(\frac{SS}{CS}\right)_{Level\ A} \times CS_{Level\ D} \qquad \text{(NUREG/CR-6322 Equation 39)}$$

and

$$P_{SS-Level\ D} = \frac{P_{SS-Level\ A}}{P_{CS-Level\ A}} \times P_{CS-Level\ D} = \frac{4,593.4}{9,832.8} \times 13,399.8 = 6,259.7 \text{ lb}$$

The load (P_{60g}) on each corner angle for the hypothetical accident condition is:

$$P_{60g} = \frac{225 \text{ lb}(60g)}{4} = 3,375 \text{ lb}$$

The margin of safety (MS) for the hypothetical accident condition is:

$$MS = \frac{P}{P_{60g}} - 1 = \frac{6,259.7}{3,375} - 1 = +0.85$$

Reconfigured Fuel Assembly Tube Evaluation – End Impact

For Service Level D, accident conditions, the tubes are evaluated for axial compression in accordance with NUREG/CR-6322 and ASME Code Section III, Appendix F-1334.3.

Because Subsection F-1334.3 specifies no criteria for austenitic stainless steel, the following method from NUREG/CR-6322 is used to determine the criteria for the hypothetical accident condition (Service Level D).

The austenitic stainless steel criteria for the hypothetical accident condition can be expressed as:

$$SS_{Level\ D} = \left(\frac{SS}{CS}\right)_{Level\ A} \times CS_{Level\ D} \qquad \text{(NUREG/CR-6322 Equation 39)}$$

where SS and CS stand for stainless steel and carbon steel, respectively.

The maximum allowable Service Level A (normal conditions) stress for stainless steel (F_a = 2,750 lb/in.^{2}) was determined previously. The allowable axial load ($P_{SS\text{-}Level\ A}$) can be determined using the relation:

$$P_{SS-norml} = F_a \times A = 2,750 \text{ lb/in.}^2 \times 0.0580 \text{ in.}^2 = 159.5 \text{ lb}$$

The maximum allowable Service Level A axial load ($P_{CS\text{-}Level\ A}$) for carbon steel can be determined as:

$$F_a = \frac{12}{23}\frac{\pi^2 E}{\left(KL/r\right)^2} = \frac{12}{23}\frac{\pi^2\left(25.2E6\right)}{\left(144.57^2\right)} = 6{,}208.7 \text{ psi} \qquad \text{(NUREG/CR-6322 Equation 23)}$$

where,

$$\frac{KL}{r} = 144.57 > C_c = \sqrt{2\pi^2\frac{E}{S_y}} = 138.85$$

$S_y = 25.8$ ksi

$E = 25.2E3$ ksi

$$P_{CS-normal} = F_a A = 6{,}208.7 \text{ lb/in.}^2\left(0.0580 \text{ in.}^2\right) = 360.1 \text{ lb}$$

The maximum allowable axial compressive load ($P_{CS\text{-}Level\ D}$) for carbon steel Level D conditions is:

$$P_{CS-accident} = \frac{2P_y}{3\lambda^2} = \frac{2\left(1496.4\right)}{3\left(1.472^2\right)} = 460.4 \text{ lb} \qquad \text{(NUREG/CR-6322 Equation 35)}$$

where,

P_y = the average yield load ($S_y \times A = 25{,}800$ ksi $\times$ 0.0580 in.^{2} = 1,496.4 lb)

$$\lambda = \frac{1}{\pi}\left(\frac{KL}{r}\right)\sqrt{\frac{S_y}{E}} = \frac{1}{\pi}\left(144.57\right)\sqrt{\frac{25.8}{25.2E3}} = 1.472 > \sqrt{2}$$

Using NUREG/CR-6322 Equation 39 to determine the allowable load for stainless steel Service Level D conditions:

$$SS_{Level\ D} = \left(\frac{SS}{CS}\right)_{Level\ A} \times CS_{Level\ D} \qquad \text{(NUREG/CR-6322 Equation 39)}$$

$$P_{SS-Level\ D} = \frac{P_{SS-Level\ A}}{P_{CS-Level\ A}} \times P_{CS-Level\ D} = \frac{159.5}{360.1} \times 460.4 = 203.9 \text{ lb}$$

The load (P_{60g}) on each tube for the hypothetical accident condition is:

$$P_{60g} = 2.27 \text{ lb}(60g) = 136.2 \text{ lb}$$

The margin of safety (MS) for the hypothetical accident condition is:

$$MS = \frac{P}{P_{60g}} - 1 = \frac{203.9}{136.2} - 1 = +0.50$$

2.7.14.1.2 Reconfigured Fuel Assembly Side Impact

The reconfigured fuel assembly corner angle fixtures and tubes are each evaluated as a continuous beam supported at 6 places-the top and bottom housings and 4 intermediate tube support grids. The beam model for the corner angle is analyzed with a uniformly distributed load that is the self-weight of the angle multiplied by the acceleration factor (60g). The beam model for the tube is analyzed with a uniformly distributed load comprising the weight of the fuel rods and the self weight of the tube multiplied by an acceleration factor (60g).

Reconfigured Fuel Assembly Corner Angle Evaluation – Side Impact

The corner angle length between the top and bottom housing is approximately 135.09 inches. The four intermediate tube support grids divide the corner angle into five equal spans approximately 27.02 inches long.

The maximum moment (M_{max}) in the corner angle is:

$$M_{max} = 0.0779 wl^2 = 0.0779(0.2033)(27.02^2)(60g) = 694 \text{ lb} - \text{in.}$$

The maximum shear force (V) in the corner angle is:

$$V = \frac{23}{38}(wl) = \frac{23}{38}(0.2033)(27.02)(60g) = 200 \text{ lb}$$

The maximum bending stress (σ_b) is:

$$\sigma_b = \frac{M_{max} \times c}{I} = \frac{694(1.431)}{0.272} = 3{,}652 \text{ psi}$$

The maximum shear stress (τ) is:

$$\tau = \frac{V}{A} = \frac{200}{0.715} = 280 \text{ psi}$$

The combined stress is:

$$\sigma_{1,2} = \frac{\sigma_b}{2} \pm \sqrt{\left(\frac{\sigma_b}{2}\right)^2 + \tau^2} = \frac{3{,}652}{2} \pm \sqrt{\left(\frac{3{,}652}{2}\right)^2 + (280)^2} = 1{,}826 \pm 1{,}847 \text{ psi}$$

$\sigma_1 = 3{,}673$ psi

$\sigma_2 = -21$ psi

The maximum combined stress is:

$$\sigma_{max} = |\sigma_1 - \sigma_2| = 3{,}694 \text{ psi}$$

The margin of safety MS is:

$$MS = \frac{3.6S_m}{\sigma_{max}} - 1 = \frac{3.6(15{,}600)}{3{,}694} - 1 = +14.2$$

Reconfigured Fuel Assembly Tube Evaluation – Side Impact

The tube length between the top and bottom housing is approximately 135.09 inches. The four intermediate tube support grids divide the tube into five equal spans approximately 27.02 inches long.

The maximum moment (M_{max}) in the tube is:

$$M_{max} = 0.0779wl^2 = 0.0779(0.076)(27.02^2)(60g) = 260 \text{ lb} - \text{in.}$$

The maximum shear force (V) in the tube is:

$$V = \frac{23}{38}(wl) = \frac{23}{38}(0.076)(27.02)(60g) = 75 \text{ lb}$$

The maximum bending stress (σ_b) is:

$$\sigma_b = \frac{M_{max} \times c}{I} = \frac{260(0.28125)}{.002026} = 35{,}498 \text{ psi}$$

The maximum shear stress (τ) is:

$$\tau = \frac{V}{A} = \frac{75}{0.0580} = 1{,}293 \text{ psi}$$

The combined stress is:

$$\sigma_{1,2} = \frac{\sigma_b}{2} \pm \sqrt{\left(\frac{\sigma_b}{2}\right)^2 + \tau^2} = \frac{35{,}498}{2} \pm \sqrt{\left(\frac{35{,}498}{2}\right)^2 + (1{,}293)^2} = 17{,}749 \pm 17{,}796 \text{ psi}$$

$\sigma_1 = 35{,}545$ psi

$\sigma_2 = -47$ psi

The maximum combined stress is:

$$\sigma_{max} = |\sigma_1 - \sigma_2| = 35{,}592 \text{ psi}$$

The margin of safety, MS, is:

$$MS = \frac{3.6S_m}{\sigma_{max}} - 1 = \frac{3.6(15{,}600)}{35{,}592} - 1 = +0.58$$

2.7.14.1.3 CY-MPC Reconfigured Fuel Assembly Tube Support Grid Evaluation

Analysis of the reconfigured fuel assembly support grid uses an ANSYS finite element model to evaluate the stresses during impact conditions. The model consists of 1/2 of the support grid and is used to evaluate both side and end impacts. The support grid plate is 0.5 inches thick and constructed of 304 stainless steel. Figure 2.7.14-1 shows a plot of the finite element model. The regions where the support grid is welded to the corner angles are shown on the figure as heavy lines. These weld regions are fixed in the appropriate directions to represent the fixity of the angles. A plane of symmetry also exists and is appropriately constrained.

End Drop

During the end drop, the model is loaded using a static gravity load of 60g in the vertical direction (z). For accident conditions the addition of thermal stresses to the primary stresses is not required.

The peak nodal stress calculated for the 60g loading is 5,482 psi. The Service level D (accident) allowable stress at 750°F is 3.6 × 15,600 = 56,160 psi and the resulting margin of safety is +9.2.

Side Drop

During the side-drop, the model (same as used in end-drop) is loaded using a static gravity load of 60g.

The peak nodal stress calculated for the 60g side loading is 43,812 psi. The Service level D allowable stress at 750°F is 3.6 × 15,600 = 56,160 psi and the resulting margin of safety is +0.28.

2.7.14.1.4 CY-MPC Reconfigured Fuel Assembly Weld Analysis

Maximum forces and moments for analysis of the welds joining the tube support grids to the corner angles are taken from the finite element analysis output. Each support grid is welded to the four corner angles with 1/8-in. fillet welds one inch in length both top and bottom. Using Blodgett's (R1) method of considering the weld as a line, the bending force (F_b) on the weld per inch of length is determined as follows:

$$F_b = \frac{M}{S_w} = \frac{46.0 \text{ lb} \cdot \text{in.}}{0.5 \text{ in.}^2} = 92.0 \text{ lb/in.}$$

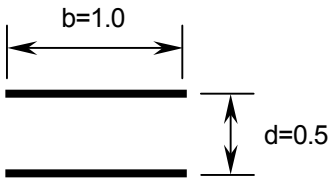

The shear force (F_v) is:

$$F_v = \frac{V}{A_w} = \frac{51.2 \text{ lb}}{2.0 \text{ in.}} = 25.6 \text{ lb/in.}$$

where

$S_w = b \times d$

$A_w = 2 \times b$

The resultant force (F) on the weld is:

$$F = \sqrt{F_b^2 + F_v^2} = 95.5 \text{ lb}$$

The effective throat thickness of the 1/8-in. fillet weld is 0.707(0.125 in.) = 0.088 in., the effective throat area is 0.088 in.^{2}/in., and the stress (f) in the weld is:

$$f = \frac{F}{nA} = \frac{95.5 \text{ lb/in.}}{0.4\left(0.088 \text{ in.}^2/\text{in.}\right)} = 2{,}713.1 \text{ psi}$$

where

n = 0.4 is the minimum quality factor for a Category E Type V weld per ASME Code Section III-NG.

The margin of safety (M.S.) is determined on the basis of the parent metal yield strength:

$$\text{M.S.} = \frac{3S_m}{f} - 1 = \frac{3.6(15{,}600) \text{ psi}}{(2{,}713.1)} - 1 = + \text{large}$$

2.7.14.2 CY-MPC Damaged Fuel Can – Accident Conditions

The CY-MPC damaged fuel can is evaluated for hypothetical accident conditions of concrete cask 6-inch drop and the tip-over event. The concrete cask 30-foot drop is evaluated considering a 60g end-impact and a 60g side-impact.

A bounding temperature of 600°F is used for accident conditions. Material properties for ASME SA240/SA479 Type 304 Stainless Steel, ASME Code Section III, Subsection NG, are:

S_u	63.3 ksi
S_y	18.6 ksi
S_m	16.7 ksi
E	25.2×10^3 ksi

The weight of the damaged fuel can top assembly (lid) is 19.46 lbs, and the weight of the can weldment is 91.6 pounds. Twenty-five lbs and 95 lbs are used in the analysis for the top assembly and can weldment, respectively.

2.7.14.2.1 CY-MPC Damaged Fuel Can Tube Body Evaluation – Side Impact

The majority of the tube body is contained within the fuel tube in the basket assembly. Because both the tube body and the fuel tube have square cross sections, they will be in full contact (for 131.95 in. longitudinally) during the side impact and no significant bending stress will be introduced into the tube body. The last 4.55 in. of the body tube and the 5.0-in. length of the side plates will be unsupported past the fuel tube flange in the side impact configuration.

The tube body will be evaluated as a cantilevered beam with the combined weight (P) of the overhanging tube body, side plates and lid assembly multiplied by a deceleration factor of 60g. The 60g deceleration conservatively bounds the maximum deceleration of 55g for the cask side drop accident (Section 2.6.7.4).

The maximum bending stress (f_b) is determined as follows:

$$f_b = \frac{M_{max} c}{I} = \frac{20{,}055(4.44)}{22.95} \cong 3{,}880 \text{ psi}$$

where:

$M_{max} = Pg \times L = 35(60)(9.55) = 20{,}055$ lb·in.

$g = 60$

The shear stress (τ) is:

$$\tau = \frac{Pg}{A} = \frac{35(60)}{1.766} \cong 1{,}189 \text{ psi}$$

$$\sigma_1, \sigma_2 = \frac{1}{2}\left(f_b \pm \sqrt{f_b^2 + 4\tau^2}\right) = \frac{1}{2}\left(3{,}880 \pm \sqrt{3{,}880^2 + 4(1{,}189)^2}\right) \cong 4{,}215 \text{ psi and } -335 \text{ psi}$$

The stress intensity (σ_{max}) = $|\sigma_1 - \sigma_2|$ = 4,550 psi

The Margin of Safety (M.S.) is:

$$\text{M.S.} = \frac{1.0\ S_u}{\sigma_{max}} - 1 = \frac{1.0(63{,}300)}{4{,}550} - 1 = +12.9$$

2.7.14.2.2 CY-MPC Damaged Fuel Can Weld Evaluation

The welds joining the tube body to the side plates are full penetration welds (Type III, ASME Code Section III, Subsection NG paragraph NG-3352.3). Per Table NG-3352-1 (ASME Code Section III, Subsection NG), the weld quality factor (n) for a Type III weld with visual surface inspection is 0.5.

The margin of safety (M.S.) for the weld is:

$$\text{M.S.} = \frac{(1.0)n \cdot S_u}{\sigma_{max}} - 1 = \frac{(1.0)(0.5)(63{,}300\ \text{psi})}{4{,}550\ \text{psi}} - 1 = +5.9$$

2.7.14.2.3 CY-MPC Damaged Fuel Can Tube Body Evaluation – End Impact

For the bottom end impact, the tube body is subjected to the weight of the top assembly (lid), the side plates, and its self-weight. Because the top assembly is heavier, the bottom end drop is the governing case for tube body compression. The can contents bear against the bottom assembly through which the loads are transferred to the canister bottom plate.

The compressive load (P) on the tube body is:

P = 5,982.6 lb; use 7,500 lb for evaluation

The compressive stress (S_c) in the tube body is:

$$S_c = \frac{P}{A} = \frac{7{,}500\ \text{lb}}{1.766\ \text{in.}^2} \cong 4{,}247\ \text{psi}$$

The margin of safety (M.S.) is:

$$\text{M.S} = \frac{0.7S_u}{S_c} - 1 = \frac{0.7(63{,}300)\ \text{psi}}{4{,}247\ \text{psi}} - 1 = +9.4$$

2.7.14.2.4 Tube Body Buckling Evaluation

The tube is evaluated, using the Euler formula, to determine the critical buckling load (P_{cr}):

$$P_{cr} = \frac{\pi^2 EI}{L_e^2} = \frac{\pi^2 \left(25.2 \times 10^6\right)(22.95)}{2(136.5)^2} = 76{,}587 \text{ lb}$$

where:

$E = 25.2 \times 10^6$ psi

$$I = \frac{8.88^4 - 8.78^4}{12} = 22.95 \text{ in}^4$$

L_e = 2L (worst case condition)

L = unsupported tube body length (136.5 in.)

Because the maximum compressive load (7,500 lb under the accident condition) is much less than the critical buckling load (76,587 lb) the tube has adequate resistance to buckling.

2.7.14.2.5 CY-MPC Damaged Fuel Can Lid Evaluation– End Impact

During a bottom end impact, the top lid will be subjected to bending stresses caused by the weight of the top lid. The top lid assembly conservatively weighs 25 lbs. Under a 60g load, the load on the plate is 1,500 lbs or $(1{,}500/8.77^2) \cong 20$ psi. The maximum stress for the lid is calculated by conservatively assuming a unit width simply supported beam 8.77-inches long with a thickness of 0.75-inches.

$$M = \frac{20(8.77^2)}{8} = 192.3 \text{ in - lbs}$$

$$S_b = \frac{6(192.3)}{1.0(0.75^2)} = 2{,}051 \text{ psi}$$

The Margin of Safety is:

$$\text{M.S.} = \frac{2.4(16{,}700)}{2{,}051} - 1 = +\text{Large}$$

Figure 2.7.14-1 CY-MPC Reconfigured Fuel Assembly Tube Support Grid Finite Element Model

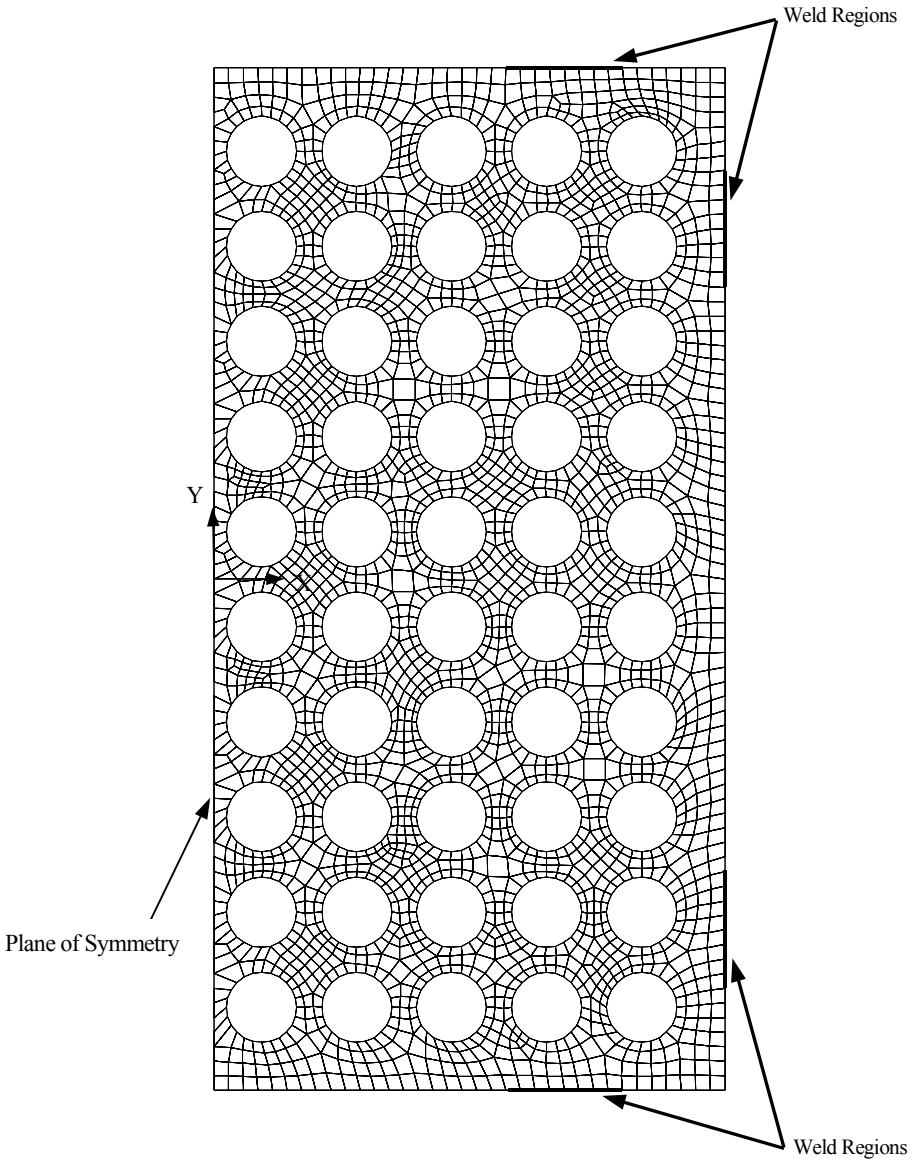

THIS PAGE INTENTIONALLY LEFT BLANK

2.7.15 Yankee-MPC Reconfigured Fuel Assembly and Damaged Fuel Can Analysis– Hypothetical Accident Conditions

The Yankee-MPC reconfigured fuel assembly and damaged fuel can are evaluated for hypothetical accident conditions for a 57g end-drop and 55g side-drop. To envelope all operating condition temperatures, the material properties for the reconfigured fuel assembly evaluation are taken at 750°F and the material properties for the damaged fuel can are taken at 600°F.

2.7.15.1 Yankee-MPC Reconfigured Fuel Assembly (RFA) Evaluation

2.7.15.1.1 Shell Casing Side Drop

Bending in Longitudinal Direction

The shell weldment is analyzed for bending stress as a simple span with distributed load. Because the RFA is supported within the basket tube, the maximum deflection at the weldment center, δ, is limited to 0.107 in., at which time the remaining energy will be transferred into the basket fuel tube assembly. Per ASME III, Subsection NF 3322.2(d), members that are subjected to axial compression or compression due to bending are considered to be fully effective if the width-thickness ratio, b/t, meets the following criterion:

$$\frac{b}{t} \le \frac{238}{\sqrt{S_y}}$$

$$\frac{b}{t} = \frac{7.125 - (2)(0.125)}{0.120} = 57 \le \frac{238}{\sqrt{S_y}}$$

Therefore, the shell casing meets the criterion and no reduction to allowable stress need be applied. The maximum bending stress, f_{bL}, is determined as follows:

$$f_{bL} = \frac{Mc}{I} = \frac{WL}{8} \times \frac{c}{I} = \frac{384 E \delta c}{40 L^2} = 9.66 \text{ ksi}$$

where

$$\delta = \frac{5wL^4}{384EI} = 0.107 \text{ in.}$$

$$W = \frac{384 EI\delta}{5L^3}$$

$$M = \frac{WL}{8} = \frac{wL^2}{8} \text{ (maximum moment)}$$

$E = 24.4 \times 10^3$ ksi, modulus of elasticity for SA240, 304 stainless steel at 750°F

$$c = \frac{7.125 + 2(0.125)}{2} = 3.68 \text{ in.}$$

$L = 97.7$ in. distance between supports (top end fitting and bottom end fitting)

Bending in Transverse Direction

The shell casing sides are evaluated for transverse bending stress, f_{bt}, as follows:

$$f_{bt} = \frac{M}{S} = \frac{wL^2}{12S} = \frac{1.93(7.25^2)}{12(2.40 \times 10^{-3})} = 3.52 \text{ ksi}$$

where

$w = 0.120$ in. $\times$ 0.29 lb/in.^{3} $\times$ 1.0 in. $\times$ 55g $= 1.93$ lb/in for a 1-in.-wide strip

$$S = \frac{1.0 \times 0.120^2}{6} = 2.40 \times 10^{-3} \text{ in.}^3$$

$$M = \frac{wL^2}{12}$$

The combined longitudinal and transverse stress is:

$$f_b = \sqrt{f_{bL}^2 + f_{bt}^2} = \sqrt{9.66^2 + 3.52^2} = 10.28 \text{ ksi}$$

The margin of safety is:

$$M.S. = \frac{S_m}{f_b} - 1 = \frac{37.4 \text{ ksi}}{10.28 \text{ ksi}} - 1 = +2.64$$

Axial Compression and Bending of Sides

Compressive loads are evaluated to the criteria specified in NUREG/CR-6322, "Buckling Analysis of Spent Fuel Basket." For the axial compression of the shell casing sides, the length (L) is 7.25 inches.

$$\frac{KL}{r} = \frac{1 \times 7.25}{0.035} = 207$$

where

K = 1, effective length factor

L = 7.25 in.

$r = \frac{t}{\sqrt{12}} = \frac{0.120}{\sqrt{12}} =$ 0.035, radius of gyration

For accident conditions:

$$f_a = \frac{1.93\left(7.25/2\right)}{0.120} + \frac{1.93(7.25)}{0.120} = 175 \text{ psi}$$

$$\frac{f_a}{F_a} = \frac{0.0707}{1.27} = 0.07 < 0.15$$

$F_b = 1.0\ S_u = 63.1$ ksi

$$\frac{f_a}{F_a} + \frac{f_{bx}}{F_b} + \frac{f_{by}}{F_b} = 0.14 + \frac{3.52}{63.1} + \frac{10.28}{63.1} = 0.36$$

0.36 < 1.0, therefore, the shell casing meets NUREG/CR-6322 acceptance criteria.

Welds Evaluation—Bottom Fitting to Shell Casing

The shear force on the top-ring-to-casing and the bottom-fitting-to-casing welds is equal to 1/2 casing weight + 1/2 basket weight + 1/2 fuel weight = 261.3 lb; therefore, use 265 lb for evaluation. Note: the top fitting design provides a shear key preventing the bolts from being loaded in shear. The weld shear area = 7.25 in. × 0.120 in. × 4 = 3.48 in.^{2} and the dead load shear stress, τ_{DL}, is

$$\tau_{DL} = \frac{265}{3.48} \times 55g = 4.2 \text{ ksi}$$

$F_v = 0.42\ S_u \times$ weld quality factor

$= 0.42 \times 63.1 \times 0.50 = 13.25$ ksi

The margin of safety is:

$$\text{M.S.} = \frac{13.25}{4.2} - 1 = +2.15$$

2.7.15.1.2 Shell Casing Top and Bottom End Drop

For the bottom end drop, the top fitting and casing act against the bottom fitting assembly. For the top end drop, the bottom fitting and casing act against the top fitting assembly. Because the top fitting is heavier, the bottom end drop is the governing case. The allowable compressive force, F_a, is:

$$F_a = S_y\left(0.47 - \frac{\frac{KL}{r}}{444}\right) = 17.3\left(0.47 - \frac{36}{444}\right) = 6.73 \text{ ksi}$$

where

$$\frac{KL}{r} = \frac{1(97.7)}{2.73} = 36 < 120$$

$K = 1$

$L = 97.7$ in.

$$r = \sqrt{\frac{(b+t)^4 - (b-t)^4}{12A}} = 2.73$$

$b = 7.125 - 2(0.125) = 6.875$ in.

$t = 0.120$ in.

Therefore, the axial compressive stress in the shell casing wall is

$$f_a = \frac{P_T}{A} = \frac{124(57g)}{3.48} = 2.03 \text{ ksi}$$

where

P_T = (total weight of top fitting + shell = 124 lb., conservative)

A = cross-sectional area $(7.125 + 2(0.120))^2 - 7.125^2 = 3.48$ in.^{2}

The margin of safety is:

$$\text{M.S.} = \frac{F_a}{f_a} - 1 = \frac{6.73 \text{ ksi}}{2.03 \text{ ksi}} - 1 = +2.31$$

2.7.15.1.3 Lifting Tab Welds

The lifting tabs will be subjected to bending and shear loads in the end drop condition. For accident condition, the bending stress, f_b, on the weld is

$$f_b = \frac{M}{S} = 19.57 \text{ ksi}$$

where

$$M = \frac{Pe}{4} = \frac{0.596 \times (57g)(0.53)}{4} = 4.5 \text{ in.-kips}$$

P = total weight (g)

$$e = \frac{4.813}{2} - \left(\frac{2.0 + 1.75}{2}\right) = 0.53 \text{ in.}$$

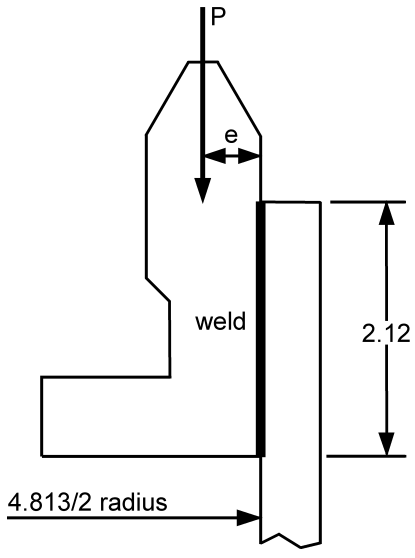

$$S = \frac{bd^2}{6} = \frac{3/8 \times \left(2.12 - 3/16\right)^2}{6} = 0.23 \text{ in.}^3$$

The shear stress, f_v, on the weld is

$$f_v = \frac{P/4}{A_w} = \frac{0.596(57g)}{4(0.72)} = 11.80 \text{ ksi}$$

The total stress, f, on the weld is

$$f = \sqrt{f_b^2 + f_v^2} = \sqrt{19.57^2 + 11.80^2} = 22.85 \text{ ksi}$$

The allowable stress, F_a, for accident conditions is $1.0 \times S_u \times$ weld factor.

$$F_a = 1.0 \times 63.1 \times 0.5 = 31.55 \text{ ksi}$$

The margin of safety is:

$$\text{M.S.} = \frac{F_a}{f} - 1 = \frac{31.55 \text{ ksi}}{22.85 \text{ ksi}} - 1 = +0.38$$

2.7.15.1.4 Corner Leg Angle

Side Drop

The side drop load will be shared by two corner leg angles. The maximum deflection, δ, that a corner leg angle can achieve is 0.102 in. The bending stress is:

$$f_b = \frac{Mc}{I} = \frac{384\,E\delta c}{40L^2} = \frac{384\left(24.4 \times 10^3\right)(0.102)(0.077)}{40\left(97.4^2\right)(0.091)} = 2.13 \text{ ksi}$$

where

$$W = \frac{384EI\delta}{5L^3}$$

$$M = \frac{WL}{8}$$

$$c = \frac{I}{S} = \frac{0.077}{0.091}$$

Using the Service Level B allowable, the margin of safety is:

$$M.S. = \frac{1.5 \times S_m}{f_b} - 1 = \frac{23.4}{2.13} = +\text{large}$$

End Drop

In the end drop, the load from the tie plates will be shared by four corner leg angles. Because the fuel tubes are not attached to the tie plates, their load will not be transferred to the corner leg angles in the end drop condition. From NUREG/CR-6322, the allowable compressive force, F_a, is:

$$F_a = S_y\left(0.47 - \frac{\frac{KL}{r}}{444}\right) = 6.57 \text{ ksi}$$

where

$$\frac{KL}{r} = \frac{1(15)}{0.369} = 40.6 < 120$$

$$r = \sqrt{\frac{I}{A}} = \sqrt{\frac{0.077}{0.563}} = 0.369$$

$$KL/r < 120 \text{ and } \frac{b}{t} = \frac{1.25}{0.25} = 5.0 < \frac{76}{\sqrt{S_y}} = \frac{76}{\sqrt{19.4}} = 17.25$$

The dead load, P_{DL}, on one corner leg angle = (7 × spacer plate weight)/4 +angle weight = 22 lb. For a 57 g acceleration, the compressive load is

$$f_a = (22 \times 57g)/0.56 \text{ in.}^2 = 2.23 \text{ ksi}$$

The margin of safety is:

$$M.S. = \frac{6.57\ \text{ksi}}{2.23\ \text{ksi}} - 1 = +1.95$$

2.7.15.1.5 Fuel Tube

Side Drop Bending Stress

The fuel tube is evaluated for bending as a continuous beam with a uniform load and six equal spans at 15.0-in. on center. The maximum bending stress (f_b) is:

$$f_{b1} = \frac{M_1 c_1}{I_1} = \frac{25.04(0.313)}{2.83 \times 10^{-3}} = 2{,}769 \text{ psi} \qquad \text{(5/8-in. tube)}$$

$$f_{b2} = \frac{M_1 c_1}{I_1} = \frac{30.29(0.375)}{5.04 \times 10^{-3}} = 2{,}254 \text{ psi} \qquad \text{(3/4-in. tube)}$$

where

$$M_{max} = -(0.106 \times wL^2) \qquad \text{(AISC)}$$

$$M_{1\_max} = -0.106(1.05)(15.0^2) = 25.04 \text{ in-lb} \qquad \text{(5/8-in. tube)}$$

$$M_{2\_max} = -0.106(1.27)(15.0^2) = 30.29 \text{ in-lb} \qquad \text{(3/4-in. tube)}$$

w_1 = 0.019 lb/in. × 55g = 1.05 lb/in. (5/8-in. tube)

w_2 = 0.023 lb/in. × 55g = 1.27 lb/in. (3/4-in. tube)

L = 15.0 in.

c_1 = 0.625/2 = 0.313 in. (5/8-in. tube)

c_2 = 0.75/2 = 0.375 in. (3/4-in. tube)

$$I_1 = \frac{\pi}{64}\left(D^4 - d^4\right) = \frac{\pi}{64}\left(0.625^4 - 0.555^4\right) = 2.83\times10^{-3} \text{ in.}^4 \qquad \text{(5/8-in. tube)}$$

$$I_2 = \frac{\pi}{64}\left(D^4 - d^4\right) = \frac{\pi}{64}\left(0.750^4 - 0.680^4\right) = 5.04\times10^{-3} \text{ in.}^4 \qquad \text{(3/4-in. tube)}$$

D_1 = tube outside diameter, 0.625 in. (5/8-in. tube)

d_1 = tube inside diameter, 0.555 in.

D_2 = tube outside diameter, 0.750 in. (3/4-in. tube)

d_2 = tube inside diameter, 0.680 in.

The margin of safety is:

$$\text{M.S.} = \frac{1.0S_u}{f_b} - 1 = \frac{1.0(63.1)}{2.769} - 1 = +\text{ large}$$

End Drop Axial Compression Stress

For accident conditions, the fuel tubes are evaluated for axial compression in accordance with NUREG/CR-6322 and ASME Section III, Appendix F-1334.3. Because Subsection F-1334.3 specifies no criteria for austenitic stainless steel, the following method from NUREG/CR-6322 is used to determine the criteria for the hypothetical accident condition. The maximum allowable axial load, P_{allow}, is

$$\frac{P_{allow}}{P_y} = SS_{LevelD} = \left(\frac{SS}{CS}\right)_{LevelA} \times CS_{LevelD} = 0.51$$

where SS and CS stand for stainless steel and carbon steel, respectively.

$$SS_{Level\,A} = \left(0.47 - \frac{\frac{KL\lambda}{r}}{444\sqrt{2}}\right)$$

$SS_{Level\,A1}$ = 0.40 (5/8-in. tube)

$SS_{Level\,A2}$ = 0.42 (3/4-in. tube)

$$CS_{Level\ A} = \frac{1-\frac{\lambda^2}{4}}{\frac{5}{3}+\frac{3}{8}\left(\frac{\lambda}{\sqrt{2}}\right)-\frac{1}{8}\left(\frac{\lambda}{\sqrt{2}}\right)^3}$$

$CS_{Level\ A1}$ = 0.47 (5/8-in. tube)

$CS_{Level\ A2}$ = 0.50 (3/4-in. tube)

$$CS_{Level\ D} = \frac{1-\frac{\lambda^2}{4}}{1.11+0.5\lambda+0.17\lambda^2-0.28\lambda^3}$$

$CS_{Level\ D1}$ = 0.60 (5/8-in. tube)

$CS_{Level\ D2}$ = 0.64 (3/4-in. tube)

where

$$\lambda = \frac{1}{\pi}\left(\frac{KL}{r}\right)\sqrt{\left(\frac{S_y}{E}\right)}$$

For stainless steel:

λ_{1SS} = 0.61 (5/8-in. tube)

λ_{2SS} = 0.50 (3/4-in. tube)

For carbon steel:

λ_{1CS} = 0.73 (5/8-in. tube)

λ_{2CS} = 0.60 (3/4-in. tube)

$P_{allow\ 1} = P_{y1} \times 0.51 = 1.12\ ksi \times 0.51 = 0.57\ ksi$

$P_{allow\ 2} = P_{y2} \times 0.51 = 1.37\ ksi \times 0.54 = 0.74\ ksi$

where

$P_{y1} = S_y \times A_1 = 17.3 \times 0.065 = 1.12$ ksi

$P_{y2} = S_y \times A_2 = 17.3 \times 0.079 = 1.37$ ksi

The axial load, P, on the fuel tube is (fuel + fuel tube + end cap weight) × end drop acceleration:

$P_1 = 5.84(57g) = 0.33$ kips

$P_2 = 6.27(57g) = 0.36$ kips

The margin of safety for the accident conditions is:

$$\text{M.S.} = \frac{P_{allow}}{P} - 1 = \frac{0.57 \text{ kips}}{0.33 \text{ kips}} - 1 = +0.73$$

2.7.15.1.6 Tie Plate

End Drop

The RFA Tie Plate is analyzed using a finite element model to represent the tie plate during an end drop. The model consists of a square grid of identical stainless steel beams spaced at 0.75 inch. The beams are 0.375 in. deep and 0.23 in. wide (clear space between 0.50 in. diameter holes). The tie plate is welded to four corner angles where the plate is assumed fixed. The tie plate is made of 304 stainless steel. Loads are applied to the nodes to represent the weight time inertial loading of the plate. Because the revised RFA tie plate contains larger tubes than the standard fuel tube, the beam width is reduced to:

Model beam width = 0.75-in.-spacing – 0.645-in.-tube-dia. = 0.105 in.

The revised beam area and moment of inertia are decreased by the factor 0.105/0.23. The new stresses are, therefore, 0.23/0.105 = 2.2 × original stresses. The stress analysis results are summarized as:

Stress State	Standard Fuel Tube Tie Plate (psi)	RFA Fuel Tube Tie Plate Stresses (psi)	Allowable (ksi)	Margin of Safety
Maximum Shear Stress	276	2.2(276)=607	26.5	+large
Maximum Bending Stress	2,070	2.2(2,076)=4,554	63.1	+large

Welds at Tie Plates to Corner Angles

Each tie plate is welded to four corner angles with top and bottom 0.13-in. fillet welds. From the finite element output, the critical shear, torsion, and bending loads are:

Load	Standard Fuel Tube Tie Plate Loads	Effective Throat Area (in.)
Shear	25.72 lb	0.13
Torsion	13.28 in-lb	
Bending	8.36 in-lb	

Therefore:

Shear Stress is: $$F_s = \frac{25.72}{0.23 \times 0.13} + \frac{13.28}{0.0182 \times 0.13} = 6.47 \text{ ksi}$$

Bending Stress is: $$F_b = \frac{8.36}{0.086 \times 0.13} = 0.75 \text{ ksi}$$

The weld allowables, including the ASME Section III-NG minimum quality factor of 0.4 for Category E, Type V, are:

Membrane + Bending: $F = 1.0 \times S_u \times n = 1.0 \times 63.1 \times 0.4 = 25.24$ ksi

Shear: $F = 0.42 \times S_u \times n = 0.42 \times 63.1 \times 0.4 = 4.15$ ksi

Since the weld stresses are less than the accident condition allowables, the 3/16-in. double fillet weld is satisfactory.

Tie Plate Side Drop

The fuel tubes are supported by tie plates at 15 inches on center spacing. During a side drop, the weight of the fuel tube, amplified by the inertial loading, places the bottom edge of the tie plate in compression. The tie plate is analyzed as a compression beam model. The weight of each fuel tube is carried in compression only and does not have the ability to shear to the next row of beams. The weight of each fuel tube at 15-inch spacing is:

$$W_{20g} = \frac{1.84 \text{ lbs/tube}}{97.70 \text{ inches}} \times 15.0 \text{ inch spacing} \times (55g) = 15.54 \text{ lb/tube}$$

The compression and shear load at the bottom of the tie plate during a side drop is:

$$P = 15.54 \times 8 = 124.3 \text{ lb}$$

$$F = \frac{124.3}{0.375 \times 0.105} = 3{,}157 \text{ psi for both shear and compression}$$

The critical margin of safety for shear is:

$$M.S. = \frac{26{,}500}{3{,}157} - 1 = +7.39$$

2.7.15.2 Yankee-MPC Damaged Fuel Can Evaluation

2.7.15.2.1 Yankee Damaged Fuel Can Tube Body–Side Drop

The tube body is directly supported by the steel support disks in the basket assembly. The most critical section of the tube body will be evaluated as an overhang beam with the combined weight (P) of the overhanging tube body, lid, and side plates multiplied by the appropriate deceleration factor. The maximum bending stress (f_b) is determined as follows:

$$f_b = \frac{M_{max} c}{I} = \frac{13{,}678 \times (4.04)}{17.26} \cong 3{,}202 \text{ psi}$$

where

$M_{max} = P \times g \times l = 21.815 \times 60 \times (10.45) = 13{,}678 \text{ lb} - \text{in}$

P = 21.815 lb

g = 60 (bounds accident condition acceleration of 55g)

l = 10.45 in

c = 8.08/2 = 4.04 in.

b = 1 in.

$$I = \frac{bh^3 - b_i h_i^3}{12} = \frac{8.08^4 - 7.98^4}{12} = 17.26 \text{ in.}^4$$

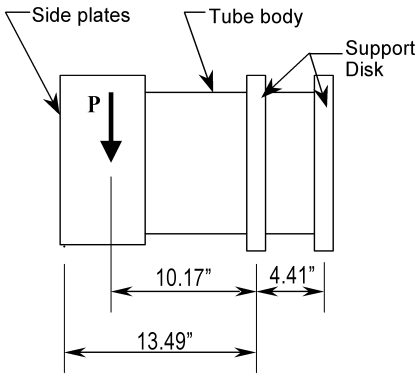

The shear stress (τ) is:

$$\tau = \frac{Pg}{A} = \frac{21.815 \times (60)}{8.08^2 - 7.98^2} \cong 815 \text{ psi}$$

The stress intensity (σ_{max}) = $|\sigma_1 - \sigma_2|$ = 3,594 psi, where

$$\sigma_1, \sigma_2 = \frac{1}{2}\left(f_b \pm \sqrt{f_b^2 + 4\tau^2}\right) = \frac{1}{2}\left(3{,}202 \pm \sqrt{3{,}202^2 + 4(815)^2}\right)$$
$$\cong 3{,}398 \text{ psi and } -196 \text{ psi}$$

The margin of safety is:

$$\text{M.S.} = \frac{1.0\,S_u}{\sigma_{max}} - 1 = \frac{1.0 \cdot (63{,}300) \text{ psi}}{3{,}594 \text{ psi}} - 1 = +16.6 \text{ for accident conditions}$$

Weld Evaluation

The welds joining the tube body to the side plates are full penetration welds. The weld quality factor (n) for a Type III weld with visual surface inspection is 0.5 (Paragraph NG-3352.3 and Table NG-3352-1). The margin of safety for the welds is:

$$\text{M.S.} = \frac{(1.0)\,n\,S_u}{\sigma_{max}} - 1 = \frac{(1.0)(0.5)(63{,}300 \text{ psi})}{3{,}594 \text{ psi}} - 1 = +7.8$$

2.7.15.2.2 Yankee-MPC Damaged Fuel Can Tube Body–End Drop

For the bottom end drop, the top assembly (lid), the side plates, and the tube body act against the bottom assembly. For the top end drop, the bottom assembly, tube body, and side plates act against the top assembly. Because the top assembly is heavier, the bottom end drop is the governing case for tube body compression. The can contents bear against the bottom assembly through which the loads are transferred to the Transportable Storage Canister bottom plate. Under accident conditions, the tube is evaluated for a 60g acceleration, which bounds 30-foot end drop acceleration of 55g. A 10% dynamic load factor is included. The compressive load, P, on the tube is the combined weight of the lid, side plates, and tube body times 60 is:

P = 4,110 lb; use 4,600 lb

The compressive stress (S_c) in the tube body is:

$$S_c = \frac{P}{A} = \frac{4{,}600 \text{ lb}}{1.606 \text{ in.}^2} \cong 2{,}864 \text{ psi}$$

where

$A = 8.08^2 - 7.98^2 = 1.606 \text{ in.}^2$

The margin of safety is:

$$\text{M.S.} = \frac{0.7 S_u}{S_c} - 1 = \frac{0.7(63{,}300) \text{ psi}}{2{,}864 \text{ psi}} - 1 = +14.5$$

Yankee-MPC Damaged Fuel Can Tube Body Buckling

The tube is evaluated using the Euler formula, to determine the critical buckling load, P_{cr}.

$$P_{cr} = \frac{\pi^2 EI}{L_e^2} = \frac{\pi^2 \left(25.2 \times 10^6\right) \cdot (17.26)}{(2 \cdot (114.35))^2} = 82{,}075 \text{ lb}$$

where

$E = 25.2 \times 10^6$ psi

$I = \frac{8.08^4 - 7.98^4}{12} = 17.26 \text{ in.}^4$

L_e = 2L (worst case condition)

L = tube body length (114.35 in.)

Because the maximum compressive load (4,600 lb under accident conditions) is much less than the critical buckling load (82,075 lb) the tube has adequate resistance to buckling.

2.7.15.2.3 Yankee-MPC Damaged Fuel Can Lid–End Drop

Lid Support Ring and Lift Tee Compressive Stress

The lid is analyzed for compressive stresses in a top-end drop where compressive loads are transferred through the lid structure to the Transportable Storage Canister (TSC) shield lid. The compressive load (P) is the weight of the fuel assembly (950 lb bounding) plus the weight of the lid times the appropriate acceleration factor. For accident, conditions an acceleration of 60g is applied that bounds the 56.1g end drop acceleration. The compressive stress (σ_c) is:

$$\sigma_c = \frac{Pg}{A} = \frac{970 \cdot (60) \text{ lb}}{7.66 \text{ in.}^2} \cong 7{,}598 \text{ psi}$$

where A is the combined cross-sectional area of the support ring and the lift tee:

$$A = \frac{\pi}{4}\left(\left(6.63^2 - 6.07^2\right) + 1.625^2\right) = 7.66 \text{ in.}^2$$

The margin of safety is:

$$M.S. = \frac{0.7 S_u}{\sigma_c} - 1 = \frac{0.7(63{,}300 \text{ psi})}{7{,}598 \text{ psi}} - 1 = +4.8$$

Lid Bottom End Impact

During a bottom end impact, the top lid will be subjected to bending stresses caused by the weight of the top lid. The maximum bending stress (f_b) for the lid is calculated by conservatively assuming a one-inch-wide, simply supported beam 7.98-inches long with a thickness of 0.5-inch. The top lid assembly conservatively weighs 11.5 lbs. The load on the plate is 11.5 lb × 60g = 690 lb. The load to consider acting on the beam is ($690/7.98^2$) ≅ 10.86 psi.

$$M = \frac{wl^2}{8} = \frac{10.86 \ (7.98^2)}{8} = 86.3 \text{ in - lb}$$

$$f_b = \frac{6 \times (86.3)}{1.0 \times (0.5^2)} = 2{,}071 \text{ psi}$$

The margin of safety is:

$$M.S. = \frac{2.4(16{,}700)}{2{,}071} - 1 = +18.4$$

2.8 Special Form

This section is not applicable to the NAC-STC because the fuel to be transported in the cask fails to satisfy the definition in 10 CFR 71.4 for special form radioactive material.

THIS PAGE INTENTIONALLY LEFT BLANK

2.9 Fuel Rod Buckling Assessment

The bounding condition for the assessment of the evaluation of the fuel rod buckling is the end drop orientation. This orientation maximizes not only the axial force component that would buckle the fuel rod, but it is also the orientation, which has the maximum axial acceleration. As the cask orientation shifts from the axial end drop condition, the cask body accelerations decrease. Two fuel rod configurations are evaluated: 1) 17 x 17 PWR fuel for the directly loaded fuel case; and 2) Yankee-Class fuel for the canistered fuel case.

2.9.1 Fuel Rod Buckling Assessment for Directly Loaded 17 x 17 PWR Fuel

For this fuel configuration, the fuel rods are laterally restrained by the grids and may come into contact with the fuel assembly base. The only vertical constraint for the fuel rod is the base of the assembly. This is considered to be the bounding condition. Additionally, the weight of the fuel pellets is also included in this evaluation, as it is considered to be vertically supported by the cladding. Use of the fuel pellet weight in the evaluation is considered to be the bounding condition (as opposed to an evaluation that considers the cladding only). Fuel rod buckling is evaluated using the finite element beam model shown in Figure 2.9.1-1.

During the end drop, the fuel rod is expected to impact the fuel assembly base. The fuel rod itself will respond as an elastic bar under a sudden compression load at its bottom end. The duration of this impact is bounded by the first extentional mode shape of the fuel rod. Contribution of higher frequency extentional modes of the rod would tend to shorten the duration of impact of the fuel rod with the fuel assembly base. The fuel rod, upon initiation of impact, corresponds to an undeformed state. In the process of the impact, the compression of the fuel rod will increase to a maximum and then return to a near uncompressed state, at which point the time of impact has been completed. This actually represents half of a cycle of the lowest frequency mode shape of the fuel rod. The frequency of this mode shape is evaluated to be 214.5 Hz using ANSYS Revision 5.2. The shape of the time dependence of the deformation is sinusoidal. The single extentional mode shape can also be considered to be a single degree of freedom (SDOF) with a corresponding mass and stiffness. In viewing such an event as a spring mass system, the time variation of the deformation during the impact is expected to be sinusoidal.

The buckling mode for the fuel rod is governed by the boundary conditions. For this configuration, the eight grids provide a lateral support, but no vertical support. The only vertical restraint is considered to be at the point of contact of the fuel rod and the base of the assembly.

The weight of the fuel rod pellets and cladding is assumed to be uniformly distributed along the length of the fuel rod. In the end drop, this results in the maximum compressive load occurring at the base of the fuel rod. The first buckling mode shape corresponding to these conditions is computed using ANSYS Revision 5.2 and is shown in Figure 2.9.1-2.

Typically eigenvalue buckling is applied for static environments. For dynamic loading, it is assumed that the duration of the loading is sufficiently long to allow the system to experience the complete load, even as the deformation associated with the buckling is commenced. For dynamic loading, the lateral motion, which would correspond to the buckled shape, will correspond to the lowest mode shape. This lowest frequency mode shape is shown in Figure 2.9.1-2 and corresponds to a frequency of 31.31 Hz. The similarity of the two shapes shown in Figure 2.9.1-2 is expected, since both have the same displacement boundary conditions, the same stiffness matrix, and the same governing finite element equations, i.e.,

$$[K]\{\phi_i\} = \lambda_i [A]\{\phi_i\}$$

where:

[K] = structure stiffness matrix
$\{\phi_i\}$ = eigenvector
λ_i = eigenvalue
[A] = mass matrix for the mode shape calculation or stress stiffening matrix for the buckling evaluation

Based on the time duration of the impact and the inherent inability of the fuel rod to rapidly displace in the lateral direction, the effect of the actual lateral motion of buckling can be computed with a dynamic load factor (DLF) (Clough). The expression for the DLF for a half-sine loading for an SDOF is given by

$$\text{DLF} = \frac{2\beta \cos(\pi / 2\beta)}{1 - \beta^2}$$

where:

β = ratio of the first extentional mode frequency to the first lateral mode frequency

These values, computed as described below, are $\beta = 6.85$ and DLF = .2905.

This DLF is applied to the end drop acceleration of 56.1 g for the 30-foot end drop (see Table 2.6.7.4.2-2), which is the driving force to potentially result in the buckling of the fuel rod. The product of 56.1 x DLF = 16.3g is compared to the vertical acceleration corresponding to the first buckling mode shape, computed in Section 2.9.1.2, 28.9g. This indicates that the time duration of the impact of the fuel onto the fuel assembly base is of sufficiently short nature that buckling of the fuel rod cannot occur. The calculational methodology used to determine the acceleration corresponding to the first buckling shape for the PWR 17 by 17 fuel assembly will also be applied to the Yankee-Class fuel assembly using the same vertical restraint location. This calculation is performed in Section 2.9.2, which results in a value of 78g. The increase in this value is primarily due to the difference in the distance between the grids.

Numerical Evaluation of the Fuel Rod Mode Shapes and Buckling Acceleration

The condition is evaluated for the fuel pellet weight being combined with the cladding. To be consistent with this approach, an effective cross-sectional property is used in the evaluation, which incorporates the properties of the fuel pellet and the fuel cladding. The model used in this evaluation is comprised of two-dimensional beam elements in ANSYS Revision 5.2 as shown in Figure 2.9.1-1. In this model, the beam elements considered the weight of the fuel pellet, as well as the cladding. The modulus of elasticity (EX) for the fuel pellet is listed in Rust as having a nominal value of 26.0×10^6 psi. To be conservative, only 50 percent of this value was employed in this evaluation. The EX for the fuel pellet was, therefore, taken to be 13.0×10^6 psi. The EX for the fuel cladding used in the evaluation was also 13.0×10^6 psi, which bounds the EX for the Zircaloy cladding at the end of the fuel assembly. The dimensions and physical data for the fuel rod used in the evaluation are:

Outer diameter of cladding (inches)	.36
Cladding thickness (inches)	.0225
Cladding density (lb/in^3)	.237
Fuel pellet density (lb/in^3)	.396

The elevations of grids are 6.18, 31.08, 51.63, 72.18, 92.73, 113.83, and 153.96 inches as measured from bottom of fuel assembly.

The effective cross-sectional properties (Ei_{eff}) for the beam are computed by adding the value of EI for the cladding and the pellet, where:

E = modulus of elasticity (lb/in^2)
I = cross-sectional moment of inertia (in^4)

The model and the associated displacement boundary conditions for the fuel rod is shown in Figure 2.9.1-1. Using this model, the lowest frequency for the extentional mode shape was computed to be 214.5 Hz. The first mode shape corresponds to a frequency of 31.31 Hz. Using the expression for the DLF in Section 2.9.1.1, the DLF is computed to be $\beta = 6.85$ and DLF = 0.2905.

The buckling calculation used the same model employed for the mode shape calculation. The load that would potentially buckle the fuel rod in the end drop is due to the deceleration of the rod. This loading was implemented by applying a 1g acceleration in the direction that would result in the compressive stress of the fuel rod. The first buckling shape based on the applied boundary conditions is shown in Figure 2.9.1-2. The acceleration corresponding to the first buckling mode for the combined cladding and fuel pellet was computed to be 28.9 g.

Figure 2.9.1-1 Two-dimensional Beam Finite Element Model of the PWR 17 by 17 Fuel Rod

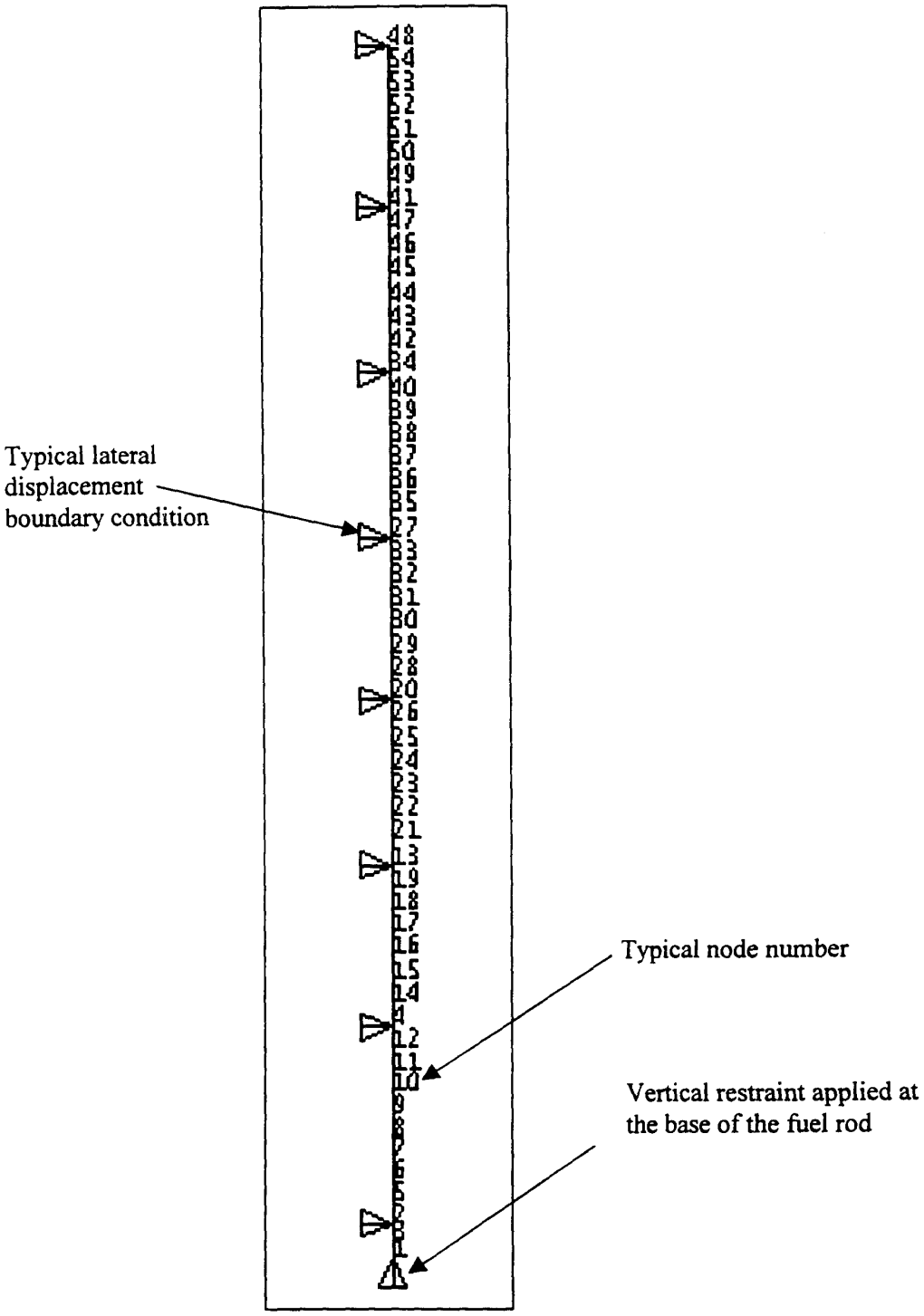

Figure 2.9.1-2 Mode Shape and First Buckling Shape for the PWR 17 by 17 Fuel Rod

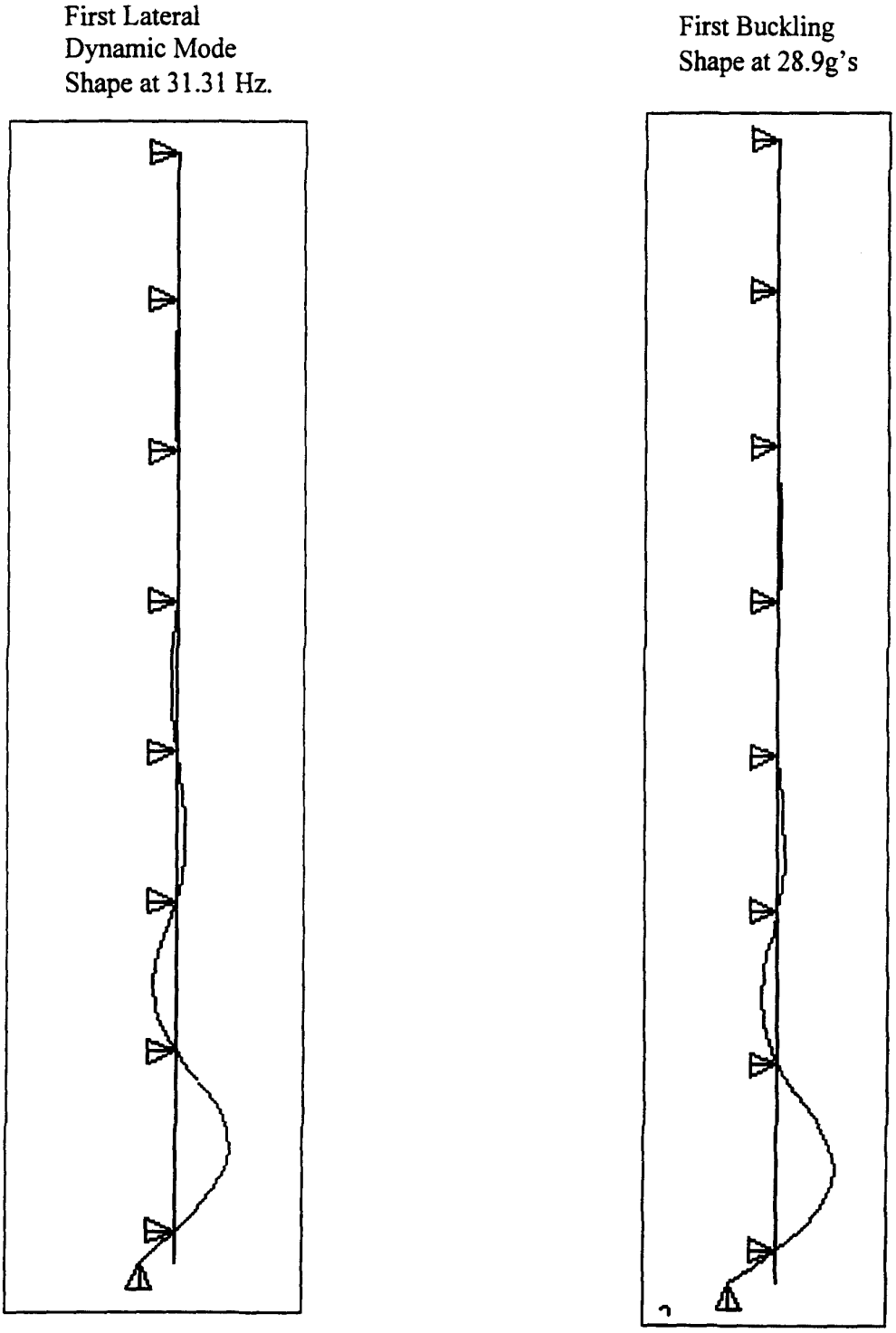

2.9.2 Fuel Rod Buckling Assessment for Yankee-Class Canistered Fuel

For the Yankee-Class fuel, two materials are available for the fuel rod cladding: Zircaloy and stainless steel. For this fuel configuration, the fuel rods are restrained by the grids and are in contact with the fuel assembly base. In the vertical orientation, the weight of the fuel rods is transferred to the base of the fuel assembly. Each of the six grids restraining the fuel rods is considered to provide lateral support, but no rotational resistance to buckling. The calculation of the first buckling mode is performed using ANSYS Revision 5.2. Two models are constructed using beam elements. In the first model, the beam elements use effective cross-sectional properties, which combined the cross-sectional properties of the fuel pellet and the fuel rod cladding. To be consistent with this approach, the beam element considers the weight of the fuel pellet and the cladding. The modulus of elasticity (EX) for the fuel pellet is listed in Rust as having a nominal value of 26×10^6 psi. Conservatively, only 50% of this value is used. The EX for the fuel pellet is therefore taken to be 13×10^6 psi. The EX for zircaloy fuel cladding used in the evaluation is also 13×10^6 psi. The EX for the stainless steel cladding is conservatively taken to be 13×10^6 psi, even though the minimum EX for stainless steels at 600ºF is 25.2×10^6 psi. The fuel rod dimensions and physical data used in the evaluation are:

Fuel Rod Parameters	Stainless Steel Cladding	Zircaloy Cladding
Outer diameter of cladding (inches)	.34	.365
Cladding thickness (inches)	.042	.048
Cladding density (lb/in^3)	.291	.237
Fuel pellet density (lb/in^3)	.396	.396

The elevations of the grids are 2.86, 20.5975, 38.8975, 57.1975, 75.49 and 75.93 inches as measured from bottom of fuel assembly.

The effective cross-sectional properties (EI_{eff}) for the beam are computed by adding the value of EI for the cladding and for the pellet.

where:

E = modulus of elasticity (lb/in^2)
I = cross-sectional moment of inertia (in^4)

For each material, two configurations are evaluated:

- with the weight and the contribution of the cross-section properties of the fuel pellet and cladding, and
- with out the contribution of the fuel pellet (cladding only).

The buckling shapes for each material for the case using the combined cross-sectional properties of the fuel pellet and the cladding, along with the applied boundary conditions are shown in Figure 2.9.2-1. The acceleration corresponding to the first buckling mode for the combined cladding and fuel pellet for both materials are:

Cladding Material	With the cross-sectional properties and weight of the fuel pellet	With the cladding cross-sectional and weight of the fuel cladding only
Zircaloy	94 g	248 g
Stainless Steel	78 g	177 g

This analysis is considered to be conservative. For undamaged fuel the pressure inside the fuel rod actually provides a significant tensile stress in the cladding. For this evaluation, this stress is not considered to stiffen the cladding. Additionally, rotational resistance from each grid is not considered, which would increase the acceleration corresponding to the first buckling mode. Since the impact limiters for the NAC-STC limit the maximum accelerations in the end drop to less than 60g's, based on this evaluation, the fuel rods do not buckle.

Figure 2.9.2-1 First Buckling Mode for the Yankee Class Canistered Fuel

Combined properties for the fuel pellet and for the cladding.

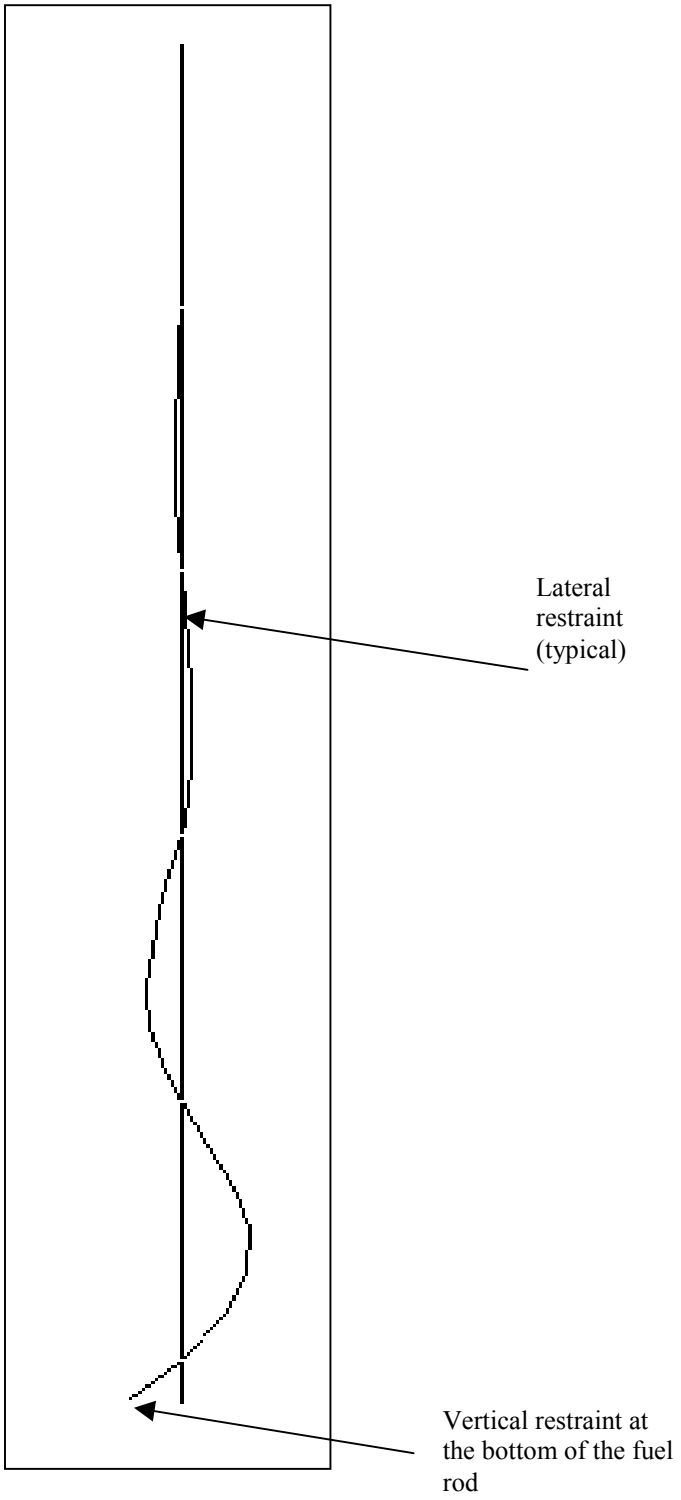

2.9.3 Fuel Rod Buckling Assessment for Connecticut Yankee Canistered Fuel

For the Connecticut Yankee fuel, two materials are available for the fuel rod cladding: Zircaloy and stainless steel. For this fuel configuration, the fuel rods are restrained by the grids and are in contact with the fuel assembly base. In the vertical orientation, the weight of the fuel rods is transferred to the base of the fuel assembly. Each of the grids restraining the fuel rods is considered to provide lateral support, but no rotational resistance to buckling. The calculation of the first buckling mode is performed using ANSYS Revision 5.5. The beam elements use effective cross-sectional properties, which combined the cross-sectional properties of the fuel pellet and the fuel rod cladding. To be consistent with this approach, the beam element considers the weight of the fuel pellet and the cladding. The fuel rod dimensions and physical data used in the evaluation are:

		Cladding				
Case	Fuel Assembly Vendor	Outer Diameter (inch)	Thickness (inch)	Material	Pellet Diameter (inch)	Rod Length (inch)
1	Westinghouse	0.422	0.0242	Zirc-4	0.3659	151.85
2	Westinghouse	0.422	0.0165	SS304	0.3895	126.52
3	B&W	0.43	0.0265	Zirc-4	0.3686	153.68
4	B&W	0.422	0.0165	SS304	0.3825	126.68

The material properties are:

	Density (lb/in^3)	Young's Modulus (psi)
Zircaloy-2 Cladding	0.237	11.5×10^6
UO_2 Fuel	0.396	27.5×10^6

The Young's Modulus used for fuel in the analysis is 13.0×10^6 psi.

The elevations of grids (lateral constraints) vary for each fuel assembly type. The locations of the constraints considered are shown in the table below:

Case	Rod Length (inch)	Lateral Constraints (inch)							
1	151.85	2.93	27.14	53.33	79.52	105.71	131.90	150.57	
2	126.52	1.24	20.12	41.20	62.28	83.36	104.44	125.52	
3	153.68	3.45	25.57	46.70	67.79	88.88	109.98	131.07	153.15
4	126.68	1.84	20.21	41.29	62.27	83.45	104.53	125.51	

The vertical constraint is located at the 0.00-inch location. The lateral constraint locations are adjusted to correspond to a 0.00-inch base location.

The effective cross-sectional properties (EI_{eff}) for the beam is computed by adding the value of EI for the cladding and for the pellet, where:

E = modulus of elasticity (lb/in^2)
I = cross-sectional moment of inertia (in^4)

The acceleration corresponding to the first buckling mode for the combined cladding and fuel pellet for both materials are:

Case	First Extensional Frequency (Hz)	First Lateral Frequency (Hz)	Frequency Ration (β)	Dynamic Load Factor (DLF)	Dynamic Acceleration	First Buckling Mode Acceleration
1	211.5	29.1	7.3	0.279	15.3	41.0
2	231.2	37.1	6.2	0.331	18.2	64.3
3	209.5	41.3	5.1	0.408	22.4	48.2
4	230.4	38.1	6.0	0.343	18.9	60.2

The dynamic acceleration is less than the first buckling mode acceleration for all four cases. Therefore, the fuel assembly will not buckle during a 30-foot end impact.

THIS PAGE INTENTIONALLY LEFT BLANK

2.10 Appendices

2.10.1 Computer Program Descriptions

The structural evaluation of the NAC-STC body, closure lids, canister, baskets, and impact limiters is accomplished using three computer codes, ANSYS, RBCUBED, and LS-DYNA. Each program is described in the following sections.

2.10.1.1 ANSYS

The structural analysis of the main body, the closure lids, the canister, and the baskets of the NAC-STC is performed by the finite element analysis method using the ANSYS structural analysis computer program. The ANSYS computer program is a large-scale, general purpose computer program for the solution of several classes of engineering analyses that include: static and dynamic; elastic, plastic, creep and swelling; buckling; and small and large deflections. The matrix displacement method of analysis based on finite element idealization is employed throughout the program. The large variety of element types available gives ANSYS the capability of analyzing two-dimensional and three-dimensional frame structures, piping systems, two-dimensional plane and axisymmetric solids, three-dimensional solids, flat plates, axisymmetric and three-dimensional shells, and nonlinear problems, including gap element interfaces. A two-dimensional axisymmetric model and two three-dimensional models, a top fine model and a bottom fine model, are used in the analysis of the NAC-STC. The interface gap elements provide the capability of realistic modeling and evaluation of the interactions between the lead layer and the surrounding stainless steel shells; between the top forging, inner lid, and outer lid; and between the neutron shield material and the steel in the inner lid and in the bottom of the cask.

The ANSYS preprocessing routine (PREP7) is used to construct the finite element mesh, describe each cask component material (temperature-dependent) property, assign unique identifiers for cask components, model displacement boundary conditions and prescribe temperature, point loads, or surface tractions of appropriate element faces or nodes. The PREP7 graphics option is a valuable tool that permits the user to check the model for completeness. The ANSYS analysis option uses the PREP7 file to generate a solution file and to provide a user-oriented printout of the solution phase. In general, each solution provides a complete echo of the

model input data, model displacement solution, element stresses, nodal forces, reaction forces, and any warnings or errors related to the analysis.

A variety of ANSYS post-processors (for example, Post1) utilize the solution file to sort, print, or plot selected results from the ANSYS analysis. The post-processors can provide many useful features including a maximum set of variables (such as stress components or displacements) or sectional stresses along a designated path. Additionally, the structural behavior can be viewed by model displacement and stress contour plots.

2.10.1.2 RBCUBED - A Program to Calculate Impact Limiter Dynamics

RBCUBED is an impact limiter analysis computer program developed by NAC (Hardeman) and used in the NAC-STC impact limiter analyses. RBCUBED utilizes quasi-static methodology; that is, each iteration freezes an instant in time during which all calculations are performed, and then, proceeds to the next time increment. The methodology employed in the program sizes the impact limiter and calculates the deceleration forces used to calculate the stresses imposed on the cask structure, but does not implement any load factor. There are several assumptions that are attendant to this methodology:

1. Gravity is the only force that acts on the cask during free fall. While falling, the cask is translating vertically and continues to do so until the initial (first) impacting end has been brought to rest. In oblique and side drop cases, after the first end has been stopped, the cask rotates until the second limiter strikes the unyielding surface and absorbs the remaining kinetic energy.

2. There is no sliding or lateral motion of the cask at any time during the impact(s).

3. The cask weight includes the impact limiters, but the length of the cask does not.

4. The deceleration force generated during crushing of the isotropic energy absorption material acts at the centroid of the area engaged in crushing for that increment in time.

5. Crushing of the energy absorption material occurs from the outside toward the cask body.

6. The component of the cask weight acting downward and the crush force acting upward are assumed to act colinearly. The magnitude of the weight component is very small compared to the crush force.

7. The impact limiter material that is not between the cask and the unyielding surface does not absorb any kinetic energy. The extraneous limiter material is ineffective for the purposes of this impact limiter analysis.

RBCUBED is capable of analyzing any cask impact orientation from vertical (0°) to horizontal (90°).

The input data for RBCUBED includes the following: (1) height of drop; (2) weight of cask system; (3) cask length; (4) impact orientation angle; (5) deflection increment; (6) material crush properties (stress-strain curve or force deflection curve); and (7) impact limiter geometry. Geometric modeling of the impact limiter is performed using combinatorial geometry based on the MORSE-CG computer program.

The output data from RBCUBED includes the following: (1) a verbatim input return; (2) a processed input of general problem parameters and material properties; (3) the results of the RBCUBED execution--deflection; (4) resultant force; (5) remaining kinetic energy; (6) velocity; (7) elapsed time since the beginning of impact; (8) area currently involved in crushing; and (9) a series of crush "footprints" at crush intervals of one inch.

The computer program, RBCUBED--A Program to Calculate Impact Limiter Dynamics, was benchmarked for validity by comparison of analysis results to manual calculations using crush areas determined by drafting methods.

2.10.1.3 LS-DYNA

The structural analysis of balsa impact limiters is performed by the finite element analysis method using the LS-DYNA. LS-DYNA is an explicit general-purpose finite element program for the nonlinear dynamic analysis of three-dimensional structures. It was originally used to simulate permanent deformations of metallic objects impacting hard surfaces at high velocities whose accuracy has been proven through correlation with experimental data. LS-DYNA features include the ability to handle large deformations, sophisticated material models (for steel and

aluminum, rubbers, foams, plastics, and composites), complex contact conditions among multiple components, and short-duration impact dynamics.

Pre- and post-processing is accomplished with FEMB (Finite Element Model Builder). FEMB is a general-purpose finite element pre- and post-processor compatible with most major finite analysis codes and CAD software. FEMB post-processes result data including the real-time animation of stresses, strain energy, displacements, and time history curves.

2.10.2 Finite Element Analysis

2.10.2.1 Model Descriptions

The finite element models of the NAC-STC body are generated utilizing the ANSYS PREP7 routine. The aspect ratio of finite elements and the density of the geometric mesh is carefully arranged, especially at the locations of geometric discontinuities and force boundaries, to minimize the possibility of numerical inaccuracies in the finite element method.

The cask components considered in the finite element models include the cask inner lid and outer lids; the top forging; the NS-4-FR neutron shield layer in the inner lid; the inner shell, transition sections, and outer shell; the lead layer; the bottom forging; the bottom plate; and the NS-4-FR neutron shield layer in the bottom.

Due to the complexity of the cask geometry and the loading conditions, it is apparent that one model is not sufficiently accurate to characterize all loading conditions and still be of a manageable size for available computer resources; therefore, three separate models are used to perform the analysis of the NAC-STC.

A two-dimensional axisymmetric model is used for the axisymmetric loading cases, which include internal pressure, thermal heat load, end drop on top, and end drop on the bottom. The two-dimensional axisymmetric model is described in Section 2.10.2.1.1.

The other two models are three-dimensional, so that they can properly analyze non-axisymmetric loading conditions, which include gravity (with the cask in the horizontal position), the side drop impact, the corner drop impacts, and the oblique drop impacts. The three-dimensional models are described in Section 2.10.2.1.2.

2.10.2.1.1 Two-Dimensional Axisymmetric Model

The ANSYS PREP7 routine is used to generate the finite element model of the NAC-STC. Because of the axisymmetric geometry of the cask, several of the loading conditions can be effectively analyzed using a two-dimensional axisymmetric model. These conditions include bolt preload, internal pressure, thermal expansion, and drops on both the bottom and the top ends of the cask. The model is also described in Section 2.7.1.6.1.

The two-dimensional finite element model of the NAC-STC is constructed of 3083 nodes and 2842 elements. Care is taken when developing the model to maintain adequate mesh density and aspect ratio for the elements in order to minimize any numerical inaccuracies that might result from the finite element method.

The cask components that are considered in the ANSYS model include the inner lid, the outer lid, the bolting for each of the lids, the top forging, the inner shell, the transition sections, and the outer shell, the lead shell, the bottom forging, the bottom plate, and the BISCO NS-4-FR material in the bottom and in the inner lid.

ANSYS STIF3, STIF12, and STIF42 elements are used to construct the two-dimensional finite element model of the NAC-STC. The overall view of the model is shown in Figure 2.10.2-1. Detailed plots showing node numbering patterns and the mesh arrangements in the different regions of the model are included in Figures 2.10.2-2 through 2.10.2-7.

ANSYS STIF42 elements, which are two-dimensional, axisymmetric, isoparametric solid elements, are used to model all of the cask components except the bolts, the interfaces between the lead and the steel, and the interfaces between the neutron shield material and the steel. The bolts are modeled using ANSYS STIF3 elements, which are two-dimensional beam elements. The section properties of the bolts are entered on a “per radian” basis. The bolt preload is included in the model by applying an initial strain to the bolt shaft, which connects the bolt head to the threaded portions of the cask. For a detailed description of how the bolts are modeled, and how the initial strain is determined, see Section 2.10.2.2.3.

The "gap" element, STIF12, represents two surfaces that may maintain or break physical contact and may slide relative to each other. Such surfaces exist between: (1) the lead shell and the inner and outer stainless steel shells, (2) the neutron shield and the cask bottom, (3) the neutron shield and the inner lid, (4) the inner lid, and the outer lid, (5) the inner lid and the cask, and (6) the outer lid and the cask. Note that the gap element is only capable of supporting compression in the direction normal to the surfaces and friction in the tangential direction.

Gap elements completely surround the lead shell in the cask wall. If there is contact between the lead and the stainless steel surfaces, the gap elements transmit compressive load, but permit no tensile load between the lead and the stainless steel. This means that the gap elements allow the lead to move freely inside the space surrounded by the stainless steel. When a deceleration is imposed on the entire mass of the cask model to simulate the inertial effect of a drop impact condition, the deceleration causes the lead to slump and, consequently, creates a lateral pressure on the inner and the outer shells along the lead/shell interfaces.

Similarly, since the lead has a higher coefficient of thermal expansion than the stainless steel, the lead will incur larger thermal expansions and contractions than the stainless steel inner and outer shells; and thus, may be restrained by those shells. The gap element again allows the lead to move freely inside the annulus between the inner and the outer shells. Pressures resulting from the thermal expansion restraints develop wherever the lead contacts the stainless steel shells.

Thus, accurate modeling is achieved for the lead slump during an impact load condition and for the differential thermal expansions and contractions during temperature excursions.

In Figure 2.10.2-1, the elements representing the lead shell and the neutron shield layers are intentionally not shown, in order to improve the clarity of the mesh in the stainless steel components.

A gap element stiffness of 3.0×10^8 psi, approximately 10 times greater than the cask stiffness, is specified to maintain the boundaries between the lead/steel and neutron shield/steel surfaces.

Similar gap elements are used to model theinterfaces between the lids and the top forging. The initial radial gap between the lead shell and the outer shell is calculated to be 0.0428 inch.

The neutron shield that is located around the outer shell of the cask along the length of the cask cavity is not modeled because its structural rigidity is conservatively ignored in the structural analyses of the cask. However, its weight effects are included in the model by using an increased effective density in the region of the cask between the top of the bottom forging and the bottom of the inner lid. Modification of the density of this portion of the cask allows the overall weight of the empty cask to be adjusted to the proper value. Minor density changes are also made to the bottom end forging and bottom plate to allow for proper center of gravity location. The mass of the upper impact limiter is distributed to the top end of the cask by increasing the density of the lids and top forging. The mass of the lower impact limiter is distributed to the cask bottom by increasing the density of the bottom forging and bottom plate. The resulting cask total weight (including impact limiters) and center of gravity are then verified by an ANSYS check run.

The material properties used in the stress analyses include the elastic modulus, the Poisson's ratio, the density and the coefficient of thermal expansion. The elastic moduli and coefficients of thermal expansion are functions of temperature. They are represented by a table of material property values at various temperatures. The material property evaluation for each element is performed by linear interpolation of the tabular data at the element average or integration point temperatures. Thermal expansion is computed relative to a reference temperature (assumed to be 70°F for this analysis). The material property values used are given in Section 2.3.

The nodal temperatures in the structural model are determined from the results of the thermal analysis, which is performed using the HEATING5 computer program. The temperature distribution is considered to be constant around the circumference.

Stability of the finite element analysis requires that one node on the model be restrained in the cask longitudinal (axial) direction to prevent any vertical rigid body motion. Node 7332, located at the top outside corner, is axially restrained for the pressure, thermal, and bottom end impact cases (see Figure 2.10.2-6). Node 360, located at the bottom outside corner, is axially restrained for the top end impact case (see Figure 2.10.2-2).

2.10.2.1.2 Three-Dimensional Finite Element Models (Directly Loaded Fuel Configuration)

There are a number of loading conditions that can only be characterized by a three-dimensional finite element analysis. In order to reduce the overall problem size, two three-dimensional models are developed: (1) the top fine mesh model, to be used in the stress evaluations for the top half of the cask; and (2) the bottom fine mesh model, to be used in the stress evaluations for the bottom half of the cask. In fact, both models are complete representations of the cask, since the entire cask is modeled. The top fine mesh model contains a very detailed representation of the top end of the cask, while the bottom end of the cask is modeled using a coarser mesh density. The top fine mesh model is used in those analyses that are expected to produce larger stresses in the top half of the cask. Similarly, the bottom fine mesh model contains a very detailed representation of the bottom end region of the cask, while the upper end of the cask is modeled with a coarser mesh density. The bottom fine mesh model is used in those analyses that are expected to produce larger stresses in the bottom half of the cask.

For the side drop analysis, both the top and bottom fine mesh models are used separately to obtain the detailed stresses in the upper and lower portions of the NAC-STC, respectively. The stress summary for the entire cask combines the results of the two runs. The oblique drop analyses use the fine mesh model for the impacting end of the cask.

The two three-dimensional models are constructed by first creating a mesh representing a two-dimensional plane of the cask, and then revolving that mesh 180 degrees around the axis of symmetry of the cask to create a model of one-half of the cask. This half-model of the cask is adequate for the drop analyses, because the cask geometry and the imposed loads are also symmetric about the midplane of the cask. The plane of symmetry is chosen to pass through the line of impact in the side, corner, and oblique drop cases. Symmetry boundary conditions (i.e., no translations normal to the plane of symmetry), are imposed on all nodes on the plane of symmetry.

Mesh adequacy in the circumferential direction is ensured by first reviewing the ANSYS reference manual for a recommended mesh size, then adapting a non-uniform circumferential element size to accurately capture the high stresses in the impact region. Finally, a parametric study of mesh density is performed to verify the validity of the chosen mesh arrangement.

The ANSYS reference manual recommends a 15-degree circumferential mesh increment for shell structures. A minimum of twelve (180/15) circumferential elements would be required to model a 180-degree surface, according to this criteria. Since the region of impact will have much higher stresses than the region of the cask remote from the impact, a non-uniform circumferential element spacing is chosen. A very fine mesh near the region of impact varies to a coarse mesh on the side of the cask opposite the impact region. The largest circumferential element size was chosen to be twice that of the smallest, with the element size varying linearly in between. Figure 2.10.2-8 illustrates the resulting non-uniform angular locations of each row of nodes. Table 2.10.2-1 documents the angular location of each plane of nodes, and the circumferential element size for each row of elements. The arc length of the smallest elements, those along the line of impact, is 8.3 degrees. The arc length increases to 16.6 degrees for the elements farthest away from the impact.

A series of parametric studies were performed, which considered a thick-walled cylinder subject to a gravity loading in the lateral direction, in order to examine the results of using different mesh densities. Circumferential mesh densities of 28 uniformly spaced elements and of 15 uniformly spaced elements were considered. The results of the parametric study indicated that maximum stresses as determined by the mesh with 28 circumferential elements were within 1 percent of those determined by the mesh with 15 elements. Therefore, it is concluded that the 15 element non-uniform mesh is adequate to model the structural behavior of the cask. The parametric studies also considered the effects of varying the number of elements through the wall thickness and of varying the element aspect ratio.

Three-dimensional beam elements (STIF4), solid elements (STIF45), and gap elements (STIF52) are used in the construction of the two three-dimensional finite element models. All cask components (forgings, lids, lead shell, shielding, inner and outer shells, etc.) are modeled using the STIF45 element. The STIF45 element is an eight-node, three-dimensional, parametric solid element having three degrees of freedom at each node (translations in X, Y, and Z directions).

Connections and interfaces between the components of the cask are modeled using the ANSYS STIF52 gap element. The STIF52 gap element is a three-dimensional interface element that represents two surfaces that may maintain or break physical contact, and may slide relative to each other. The use of this element is required in areas where contact between adjacent surfaces is not guaranteed by the geometry or loading. Such locations include the lead/steel shell interfaces and lid top forging interfaces. The cask lid bolts are modeled using the ANSYS beam element (STIF4). The STIF4 is a three-dimensional, uniaxial element with tension, compression, torsion, and bending capabilities. The element has six degrees of freedom at each node (translations in the nodal X, Y and Z directions and rotations about the nodal X, Y, and Z axes).

The material properties required by ANSYS for the three-dimensional analyses are those identified in Section 2.10.2.1.1.

2.10.2.1.2.1 Bottom Fine Mesh Model

The complete bottom fine mesh model is shown in Figure 2.10.2-9. A two-dimensional view of the model is shown in Figure 2.10.2-10. The node numbering patterns and mesh arrangement in different regions of the model are provided in Figures 2.10.2-11 through 2.10.2-19. The node numbers shown in these figures are for the 0-degree circumferential plane. A circumferential node number increment of 2000 is used to determine the node numbers on the remaining circumferential planes. The bottom half of the cask contains the finer mesh density. The structural components have a mesh density of at least three elements through their

thicknesses in areas of structural discontinuities to ensure detection of stress gradients in those regions. The lead shell and the neutron shield end layers are modeled with one element through their thickness, which is sufficient to distribute their loads to the surrounding structure. In Figure 2.10.2-10, the elements representing the lead layer and the neutron shield layers are intentionally not shown in order to improve the clarity of the mesh used in modeling the stainless steel components.

The bottom fine mesh model is constructed by first building a two-dimensional mesh of the cask, and then revolving that mesh 180 degrees around the longitudinal axis of the cask to get a three-dimensional model of one-half of the cask.

All of the cask components - cask body, lead, shielding, lids, etc. - are modeled with the three-dimensional solid elements (STIF45). Interaction between the components is modeled by the use of three-dimensional gap elements (STIF52). The cask components which are enclosed by stainless steel, including the lead and the end neutron shields, are surrounded radially and axially by gap elements. Just as for the two-dimensional model, a gap element stiffness of 3.0×10^8 psi is specified to maintain the boundaries between the surfaces. The initial radial gap between the lead layer and the outer shell is set to 0.0428 inches.

The mass densities of some of the cask components are modified to distribute the impact limiter masses onto the cask ends and to distribute the mass of the external neutron shield material to the region between the top of the bottom forging and the bottom of the inner lid, as described in Section 2.10.2.1.1.

2.10.2.1.2.2 Top Fine Mesh Model

The top fine mesh model of the NAC-STC is comprised of 12,601 elements and 15,261 nodes. The maximum in-core wavefront size is 1338, as compared to the maximum permissible wavefront size of 1439, which is based on ANSYS program limitations. The maximum in-core wavefront size is used as a measurement of the ANSYS analysis size. The RMS wavefront size is 664. The three-dimensional model is generated by first creating a mesh for a two-dimensional plane and then revolving the mesh 180 degrees around the longitudinal axis of the cask to create a half model, as described in Section 2.10.2.1.2.

The complete top fine mesh model is shown in Figure 2.10.2-20. The upper half of the model is shown at a larger scale in Figure 2.10.2-21. Figure 2.10.2-22 is a view of the 0-degree circumferential plane of the top fine mesh model. Figures 2.10.2-23 through 2.10.2-31 show in detail the node numbering patterns and the mesh arrangement at different regions of the cask. The node numbers shown in these figures are for the 0-degree circumferential plane. The node numbers on the remaining circumferential planes can be determined by adding 2000 (unless otherwise noted on each plot) to the node numbers on each succeeding circumferential plane. In Figure 2.10.2-22, the elements representing the lead layer and the neutron shield layers are intentionally not shown, in order to improve the clarity of the mesh used in the stainless steel components.

All cask components (cask body, lead, shielding, lids, etc.) are modeled using the ANSYS STIF45 solid elements, as in the bottom fine mesh model. The structural components have a mesh density of at least three elements through their thickness near areas of structural discontinuities to ensure the detection of stress gradients in those regions. The lead shell and the neutron shield end layers are modeled with one element through their thicknesses, which is adequate to distribute their loads to the surrounding structure. The lids are modeled with two or more elements through their thickness near the center of the cask, where stresses are low, and with a finer mesh density near the outer radius of the cask, where the stresses are higher as a result of the bolt loads and the impact loads.

Interaction between the cask components is modeled by use of three-dimensional gap elements (STIF52). The cask components that are enclosed by stainless steel, including the lead and the end neutron shields, are surrounded radially and axially by gap elements. The interface between the inner lid and the cask top forging is modeled using STIF52 gap elements in the axial and radial directions. The outer lid interfaces also use STIF52 gap elements in the radial direction (between the outer lid and the cask top forging) and in the axial direction (between the outer lid and the inner lid and between the outer lid and the top forging). There are 0.03-inch radial gaps between the top forging and the inner lid outside diameter.

There is a 0.06-inch axial gap between the inner lid and the outer lid. Just as for the two-dimensional model, a gap element stiffness of 3.0×10^8 psi is used to maintain the boundaries between the surfaces.

The cask lead shielding is modeled using ANSYS STIF45 elements. The interface between the lead and the cask body is modeled using gap elements in the radial direction along its entire length. All runs are made with an initial gap specification of 0.00 inches at the inside diameter of the lead and 0.0428 inch at the outside diameter of the lead. At locations where the lead surface is angled, the gaps are oriented in such a way that they close in the direction perpendicular to the surface. This allows these gaps to support some axial load, as would be the case in the actual cask. The shielding at the bottom end of the cask is far enough removed from the area of interest for this model, that any gap element effects would be negligible. For this reason, the bottom end shielding is modeled using ANSYS STIF45 brick elements having common nodes with the cask body. The neutron shielding between the lids is also connected to the inner lid with common nodes. Since its modulus of elasticity is small compared to that of steel, the lid stresses are not significantly affected.

The mass densities of some of the cask components are modified to distribute the impact limiter masses onto the cask ends, and to distribute the external neutron shield mass to the region between the top of the bottom forging and the bottom of the inner lid, as described in Section 2.10.2.1.1.

The bolts are modeled using ANSYS STIF4 beam elements and are located on their appropriate radii (connecting the outer lid and the inner lid to the cask top forging), on each circumferential plane location. Since there are 16 circumferential planes contained in the finite element model, this results in 16 equivalent bolts per lid. Each bolt consists of four elements--one element as the bolt shaft, one as the bolt thread, and two as the bolt head.

The effective properties of each bolt are determined by calculating the percentage of the 180-degree arc that each bolt affects, and multiplying that by an overall sum of the actual properties. Table 2.10.2-2 shows the calculated percentages of the 180-degree arc, determined by summing one-half of the angles of the arc of the two elements adjacent to a given node. Tables 2.10.2-3 and 2.10.2-4 document the calculated effective properties for all of the bolts in both lids, including the associated real constant numbers. Following are example calculations for the inner and outer lid bolt properties:

Inner Lid Bolts (42, 1 1/2 - 8 UN)

Tensile area of one bolt = 1.492 in^2
Total tensile area = (42)(1.492) = 62.66 in^2
Bolt minor radius (R) = 1.3444/2 = 0.6722 in
Moment of inertia (I) of one bolt = $\pi R^4/4$ = 0.1604 in^4
Total moment of inertia = (42)(0.1604) = 6.7368 in^4

Referring to Table 2.10.2-3, the inner lid bolt properties for circumferential plane location 4, real constant number 17, are:

Tensile area = (0.0522)(62.66)(0.5) = 1.6354 in^2
I = (0.0522)(6.7368)(0.5) = 0.1758 in
Diameter for stress recovery = $[(1.492)(4)/\pi)]^{0.5}$ = 1.378 in

Additionally, to determine the shear area of the bolt, a shear factor of 10/9 is applied to the bolt tensile area, as recommended by the ANSYS User's Manual, Section 4.0.5. In the ANSYS model, bolt head properties are taken to be 10 times the associated bolt shaft properties.

Outer Lid Bolts (36, 1 - 8 UNC)

Tensile area of one bolt = 0.606 in^2
Total tensile area = (36)(0.606) = 21.816 in^2
Bolt minor radius (R) = 0.8446/2 = 0.4223 in
Moment of inertia (I) of one bolt = $\pi R^4/4$ = 0.0250 in^4
Total moment of inertia = (36)(0.0250) = 0.900 in^4

Referring to Table 2.10.2-4, the outer lid bolt properties for circumferential plane location 8, real constant number 38, are:

Tensile area = (0.0639)(21.816)(0.5) = 0.697 in^2
I = (0.0639)(0.900)(0.5) = 0.02876 in
Diameter for stress recovery = $[(0.606)(4)/\pi)]^{0.5}$ = 0.878 in

Additionally, to determine the shear area of the bolt, a shear factor of 10/9 is applied to the bolt tensile area, as recommended by the ANSYS User's Manual, Section 4.0.5. In the ANSYS model, bolt head properties are taken to be 10 times the associated bolt shaft properties.

The bolt preload is calculated as shown in Section 2.6.7.5. The preload on the inner lid bolts is calculated to be 4.51 x 10^6 pounds for 42 bolts. The preload on the outer lid bolts is calculated to be 6.02 x 10^5 pounds for 36 bolts.

Section 2.10.2.2.3 contains a detailed description of the bolt preload strain calculation for both the inner and outer lids.

2.10.2.1.3 Transport Cask Body Finite Element Model for the Canistered Fuel Configurations

The cask body model used for the Yankee-MPC and CY-MPC analyses is represented using ANSYS SOLID45, BEAM4, CONTAC52, and spring/damper COMBIN14 elements. Gap elements are used to model contact interfaces between components. Friction effects are ignored in the model. Lump mass elements (MASS21) are used to model components such as the impact limiters and NS-4-FR gamma shield.

The loaded canister is represented by a surface pressure load as described in Section 2.10.2.2.1. An acceleration of 20g's is applied to the cask and canister for the 1-ft drop. The pressure load for the canister lid and canister body loaded with fuel is applied to the cask body using a cosine-shaped pressure distribution, where the total pressure applied to the cask body is equal to the total impact load of the contents. The weight of the spacers is included in the weight of the canister and contents. Gap elements are defined at both ends of the cask to simulate the pressure applied by the impact limiters during drop conditions (based on a cosine distribution). The stiffness of the gap elements is varied from a maximum value (1×10^6 lb/in) at the line of impact to a lower

value (2.4×10^5 lb/in) at an angle of 75° from the line of impact, and a minimal value (100 lb/in) from 82.5° to 180°). Element types with ANSYS key options are:

Element Type Number	Description	K1	K2	K3	K4	K5	K6	K7	K8	K9	K10	K11	K12
2	SOLID45	0	0	0	0	0	0	0	0	0	0	0	0
3	BEAM4	0	0	0	0	0	0	0	0	0	0	0	0
4	CONTAC52	0	0	0	0	0	0	0	0	0	0	0	0
5	MASS21	0	0	2	0	0	0	0	0	0	0	0	0
6	COMBIN14	0	0	0	0	0	0	0	0	0	0	0	0

The model consists of the following major regions with appropriate model data.

Region	Material	Mat Num	Type Num	Real Num
Inner Shell	SS304 SA240	1	2	20
Outer Shell	SS304 SA240	1	2	21
Bottom Ring	SS304 SA240	3	2	3
Neutron Shield	NS-4-FR	5	2	5
Bottom Exterior	SS304 SA240	6	2	6
Bottom Forging	SS304 SA336	6	2	6
Gamma Shield	PB ASTM B29	8	2	8
Upper Forging	SS304 SA336	9	2	9
Lid	SS304 SA336	10	2	10
B.C. Hole Annulus	Reduced Modulus	11	2	11

Solid 45 elements have real property numbers assigned but the values are ignored since real properties are not used by this element type. A small hole is modeled in the center of the lid and bottom section to eliminate the need for the generation of prisms or tetrahedrons at these locations. A small stress raiser results in this region but is not significant. The bolt circle annulus region is included in the model to restrain the lids. Since this evaluation is not concerned with bolt preload, the actual bolts are not modeled. Instead, nodes in this region are joined to corresponding nodes in the top forging. Real Property Data for Contact (Gap) elements is as follows:

Real Number	Normal Stiffness	Gap	Start	Tangential Stiffness
2	1.00E+06	0.00E+00	1	0.00E+00
3	1.00E+06	1.00E-05	1	0.00E+00
5	1.00E+06	0.00E+00	1	0.00E+00
6	100	0.00E+00	0.00E+00	0.00E+00
7	100	0.00E+00	0.00E+00	0.00E+00
8	1.00E+06	0.00E+00	0.00E+00	0.00E+00
9	1.00E+06	0.5	0.00E+00	0.00E+00
100	5.00E+05	0.00E+00	0.00E+00	0.00E+00
101	9.89E+05	0.00E+00	0.00E+00	0.00E+00
102	9.57E+05	0.00E+00	0.00E+00	0.00E+00
103	9.04E+05	0.00E+00	0.00E+00	0.00E+00
104	8.32E+05	0.00E+00	0.00E+00	0.00E+00
105	7.41E+05	0.00E+00	0.00E+00	0.00E+00
106	6.34E+05	0.00E+00	0.00E+00	0.00E+00
107	5.14E+05	0.00E+00	0.00E+00	0.00E+00
108	3.83E+05	0.00E+00	0.00E+00	0.00E+00
109	2.43E+05	0.00E+00	0.00E+00	0.00E+00
110	100	0.00E+00	0.00E+00	0.00E+00

Friction is ignored in these analyses. For Start=1, the gap element is initially closed, irrespective of the gap constant or its graphical configuration. For Start=0, the initial condition is based on the Gap constant value. Mass elements are used to model components, which are of little stress interest, yet contribute to the mass and loading of the assembly. This includes items such as the outer neutron shield and the impact limiters. Real property data for this element type is as follows:

Real Number	MASS X	MASS Y	MASS Z	IXX	IYY	IZZ	Region
10	15.032	0.00E+00	0.00E+00	0.00E+00	0.00E+00	0.00E+00	Outer Shell
11	10.051	0.00E+00	0.00E+00	0.00E+00	0.00E+00	0.00E+00	Top
12	9.5942	0.00E+00	0.00E+00	0.00E+00	0.00E+00	0.00E+00	Bottom

These elements are distributed over nodes on the exterior surface of the cask.

The three-dimensional model is similar to the model shown in Fig. 2.10.2-9 and Fig. 2.10.2-20. The mesh is refined to increase element density in the loading area. The canistered fuel configuration model has a higher mesh density at both the top and bottom of the cask body model (as compared to the cask model for directly loaded fuel), eliminating the need for a separate top and bottom model as presented for directly loaded fuel. In the bottom forging (Fig.2.10.2-12), the mesh density of the model for directly loaded fuel transitions from a five element layer to a two

element layer. To avoid triangular and trapezoidal shaped elements, a uniform 3 element layer is used in the canistered fuel model. While the directly loaded fuel model is more conservative, the canistered fuel model is considered to behave accurately in the shell region.

To ensure that the gap elements close properly and apply the total load to the cask outer shell, the gap forces were reviewed at the angular positions to show that the impact limiter loads represent a cosine distribution. The plot below shows the gap forces as a function of angle for the Yankee-MPC configuration 30-ft drop. The angular position of zero corresponds to the point of impact. The value of the gap force represents the sum of all the gap elements at that angle. The CY-MPC configuration evaluation employs the same method of representing the impact limiter, which would, therefore, result in the same contact force distribution shown below.

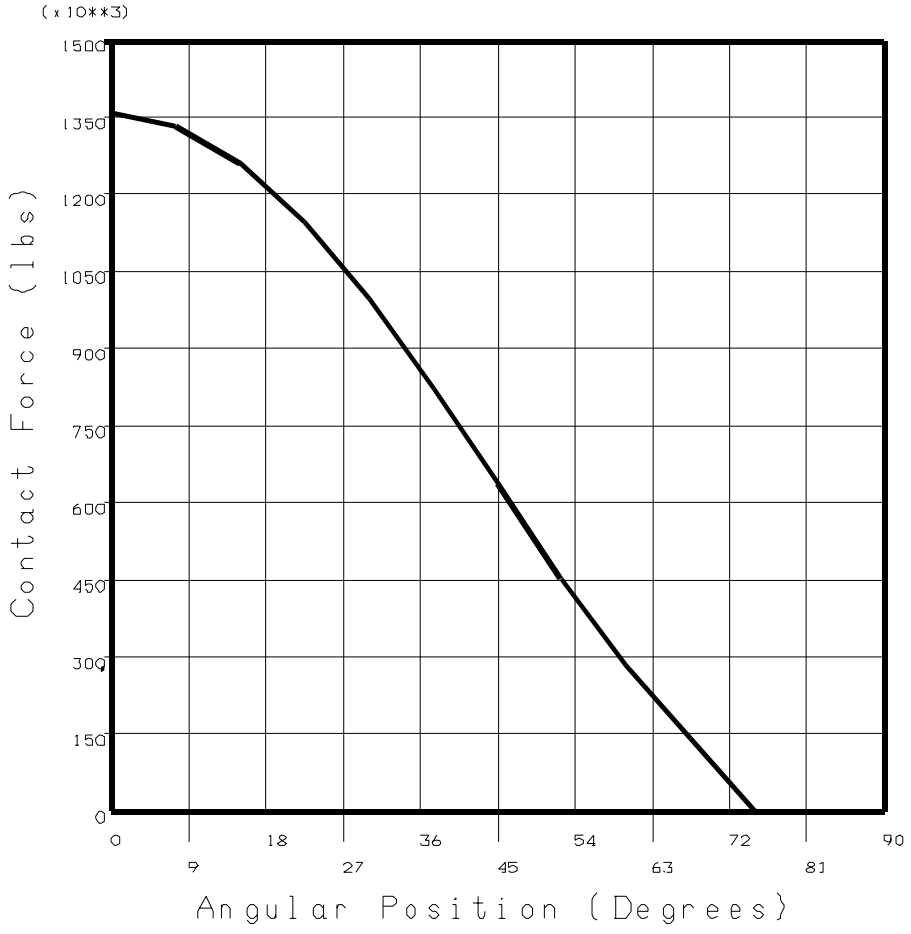

2.10.2.2 Loading Conditions

This section documents the methods of calculating contents pressure loads and impact pressure loads for the end drop, side drop, corner drop, and oblique drop scenarios. Additionally, the use of bolt initial strain to represent the bolt preload and the determination of the bolt initial strain are explained.

2.10.2.2.1 Contents Pressure Calculation for the Directly Loaded and Yankee-MPC Configurations

For the end drop analyses, the contents weight is assumed to be uniformly distributed on the cask end, over an area determined by the inside diameter of the cask. Therefore, the contents weight of 56,000 pounds, and the cask cavity inside radius of 35.5 inches are used to calculate a contact pressure of:

$$p = \frac{56{,}000}{(\pi)(35.5)^2} = 14.14 \text{ psi}$$

The contents weight of the canistered Yankee class fuel configuration is 55,590 pounds. Therefore, the directly loaded fuel configuration bounds the canistered fuel configuration.

This pressure applies to a 1 g loading condition. Pressure values for the 1-foot and 30-foot end drop analyses are determined by ratioing this pressure by the g-load values applicable to the specific case, which are documented in Sections 2.6.7.1 and 2.7.1.1.

For the side drop condition, the basket stress analysis performed in Section 2.7.8 indicates that the contact area between the basket and the cask cavity is approximately 180 degrees (90 degrees on each side of the drop centerline), therefore, for the side drop analyses, the cask contents are conservatively assumed to contact the inner cask diameter on an arc of only 79.4 degrees on either side of the impact centerline. The inertial load produced by the 56,000-pound contents weight is represented as an equivalent static pressure applied on the interior surface of the cask. The pressure is uniformly distributed along the cavity length, and is varied in the circumferential direction as a cosine distribution. The maximum pressure occurs at the impact centerline; the pressure decreases to zero at locations that are 79.4 degrees either side of the impact centerline, as illustrated in Figure 2.10.2-32. The method used to determine the varying pressures on the elements within the 79.4-degree arc is presented in the following paragraphs.

Eight sectors of elements in the ANSYS model are defined within the 79.4-degree arc. The first sector of elements subtends the arc from the 0-degree circumferential plane to the 8.3-degree circumferential plane. The second sector subtends the arc from the 8.3-degree circumferential plane to the 17-degree circumferential plane. The remaining five sectors are defined in the same manner, by the 26.2-, 35.8-, 45.9-, 56.5-, and 67.7-degree circumferential planes, which are shown in Figure 2.10.2-8.

The following formula is used to determine the contents pressures for the side drop analyses, which vary around the circumference. This method uses a summation scheme to approximate the integration of the cosine-shaped pressure distribution:

$$F_{total} = \sum_{i=1}^{8} P_{max} A_i \cos(\theta_i) \cos(\theta_i)$$

where F_{total} = 28,000 lb (cask contents weight is 56,000 lb: therefore, 28,000 lb for a half model)

P_{max} = maximum pressure (at impact centerline)

θ_i = average angle of subtended arc

i = i^{th} circumferential sector

θ = normalized angle to peak at 0° and to be zero at 79.4°

$= \theta_i \left(\frac{90}{79.4}\right) = 1.1335(\theta_i)$

A_i = i^{th} circumferential area over which the pressure is applied

$= R(\Delta\theta_i)(\pi/180) L$

R = inner radius of cask = 35.5 in

L = cask cavity length = 165 in

Therefore, $A_i = (35.5)(\Delta\theta_i)(\pi/180)(165) = 102.23(\Delta\theta_i)$

$\Delta\theta_1 = 8.3 - 0 = 8.3°$

$\Delta\theta_2 = 17.0 - 8.3 = 8.7°$

$\Delta\theta_3 = 26.2 - 17.0 = 9.2°$

$\Delta\theta_4 = 35.8 - 26.2 = 9.6°$

$\Delta\theta_5 = 45.9 - 35.8 = 10.1°$

$\Delta\theta_6 = 56.5 - 45.9 = 10.6°$

$\Delta\theta_7 = 67.7 - 56.5 = 11.2°$

$\Delta\theta_8 = 79.4 - 67.7 = 11.7°$

$\theta_1 = \frac{0 + 8.3}{2} = 4.15°;\ \theta_1 = 4.15°(1.1335) = 4.70°$

$\theta_2 = \frac{8.3 + 17.0}{2} = 12.65°;\ \theta_2 = 12.65°(1.1335) = 14.34°$

$\theta_3 = \frac{17.0 + 26.2}{2} = 21.6°;\ \theta_3 = 21.6°(1.1335) = 24.48°$

$\theta_4 = \frac{26.2 + 35.8}{2} = 31°;\ \theta_4 = 31°(1.1335) = 35.14°$

$\theta_5 = \frac{35.8 + 45.9}{2} = 40.85°;\ \theta_5 = 40.85°(1.1335) = 46.30°$

$\theta_6 = \frac{45.9 + 56.5}{2} = 51.20°;\ \theta_6 = 51.20°(1.1335) = 58.04°$

$\theta_7 = \frac{56.5 + 67.7}{2} = 62.10°;\ \theta_7 = 62.10°(1.1335) = 70.39°$

$\theta_8 = \frac{67.7 + 79.4}{2} = 73.55°;\ \theta_8 = 73.55°(1.1335) = 83.37°$

Define: $F_i = P_{max} A_i \cos(\theta_i) \cos(\theta_i)$

where $i = 1$ through 8

$F_1 = P_{max}(102.23)(8.3°) \cos(4.15°) \cos(4.70°)$
$= 843.4\ (P_{max})$

$F_2 = P_{max}(102.23)(8.7°) \cos(12.65°) \cos(14.34°)$
$= 840.8\ (P_{max})$

$F_3 = P_{max}(102.23)(9.2°) \cos(21.6°) \cos(24.48°)$
$= 795.9\ (P_{max})$

$F_4 = P_{max}(102.23)(9.6°) \cos(31°) \cos(35.14°)$
$= 687.9\ (P_{max})$

$$F_5 = P_{max}(102.23)(10.1°)\cos(40.85°)\cos(46.30°)$$
$$= 539.6\ (P_{max})$$
$$F_6 = P_{max}(102.23)(10.6°)\cos(51.20°)\cos(58.04°)$$
$$= 359.4\ (P_{max})$$
$$F_7 = P_{max}(102.23)(11.2°)\cos(62.10°)\cos(70.39°)$$
$$= 179.8\ (P_{max})$$
$$F_8 = P_{max}(102.23)(11.7°)\cos(73.55°)\cos(83.37°)$$
$$= 39.11\ (P_{max})$$
$$F_{total} = 4286(P_{max})$$

Setting the total load (F_{total}) to 28,000 lb

$$4286(P_{max}) = 28{,}000$$
$$(P_{max}) = 6.533 \text{ psi}$$

P_{max} represents the contents pressure load which would occur along the drop centerline. Given P_{max}, the contents pressure loadings, which are applied to the eight sectors of elements, are calculated as follows:

$$P_1 = P_{max}\cos\theta_1 = 6.533\cos(4.70°) = 6.51 \text{ psi}$$
$$P_2 = P_{max}\cos\theta_2 = 6.533\cos(14.34°) = 6.33 \text{ psi}$$
$$P_3 = P_{max}\cos\theta_3 = 6.533\cos(24.48°) = 5.95 \text{ psi}$$
$$P_4 = P_{max}\cos\theta_4 = 6.533\cos(35.14°) = 5.34 \text{ psi}$$
$$P_5 = P_{max}\cos\theta_5 = 6.533\cos(46.30°) = 4.51 \text{ psi}$$
$$P_6 = P_{max}\cos\theta_6 = 6.533\cos(58.04°) = 3.46 \text{ psi}$$
$$P_7 = P_{max}\cos\theta_7 = 6.533\cos(70.39°) = 2.19 \text{ psi}$$
$$P_8 = P_{max}\cos\theta_8 = 6.533\cos(83.37°) = 0.76 \text{ psi}$$

The following is a summary of the side drop contents pressures applied to the finite element model in the eight circumferential sectors:

ARC (deg)	PRESSURE (psi)
0 - 8.3	6.51
8.3 - 17.0	6.33
17.0 - 26.2	5.95
26.2 - 35.8	5.34
35.8 - 45.9	4.51
45.9 - 56.5	3.46
56.5 - 67.7	2.19
67.7 - 79.4	0.76

The pressures are applied to the cask inner shell, over the length of the cask cavity for the side drop analyses. It should be noted that these pressures consider a 1 g deceleration condition. Pressures for the 1-foot and 30-foot side drop analyses are calculated by ratioing these pressure values by the appropriate deceleration g-loads, which are documented in Sections 2.6.7.2 and 2.7.1.2.

For the corner and oblique drop analyses, the contents pressure loading is a combination of the end drop pressure load and the side drop pressure load. The corner and oblique drop pressure loadings are determined by breaking up the contents pressure load into longitudinal and lateral components, based on the drop angle. The longitudinal component is applied to the cask end, and the lateral component is applied to the cask inner shell as described previously for the side drop case.

Adequacy of this modeling technique has been evaluated by performing a finite element analysis of the cask wall subjected to both a distributed pressure load and a line load along the center line of the support disk contact surface. Analyses results identified a 22 percent more conservative stress value for the distributed pressure load than the results for the discrete line loads. This conservative result is due to higher load being carried over the modeled contact area by piece wise linear pressure. Since the only difference between the corner impact cases and the side impact configuration is the component distribution relative to the angle of impact similarly conservative results are included in the current analysis documentation for all stress combinations using the pressure distribution results.

2.10.2.2.2 Impact Pressure Calculation

For the end drop analysis, the impact pressure is assumed to uniformly contact the cask end over an area determined by the outside diameter of the cask. Therefore, the cask weight (including

contents) of 250,000 pounds and the cask outside radius of 43.35 inches are used to calculate an end drop impact pressure of:

$$P = \frac{250{,}000}{(\pi)(43.35)^2} = 42.35 \text{ psi}$$

For cases when no contents are present, the weight of the empty cask plus basket is 211,000 pounds, therefore the end drop impact pressure is:

$$P = \frac{211{,}000}{(\pi)(43.35)^2} = 35.74 \text{ psi}$$

These pressures apply to a 1 g loading condition. Pressure values for the 1-foot and 30-foot end drop analyses are determined by ratioing these pressure values by the g-loads applicable to the specific case, which are documented in Sections 2.6.7.1 and 2.7.1.1.

For the side drop analyses, the impact pressure load is applied to the finite element model as a distributed pressure over the contact area between the impact limiters and the cask. Since the center of gravity of the loaded cask is located within 1 inch of the cask middle plane, the impact load is assumed to be evenly divided between the two limiters.

The distribution of impact pressure is assumed to be uniform, in the longitudinal direction, over the two 12.0-inch impact limiter contact areas. The distribution of impact limiter pressure is assumed to vary sinusoidally in the circumferential direction. A cosine-shaped pressure distribution is selected, which is "peaked" at the impact centerline, and is spread over a 79.4-degree arc on each side of the impact centerline, as shown in Figure 2.10.2-32. The region of applied pressure (a 158.8° arc) is defined based on the "crush" geometry of the impact limiter. The assumption of a peaked pressure distribution is a conservative, classical, stress analysis procedure since the applied pressure actually is spread over a 180-degree arc (90-degree half-cask arc).

The following calculation is performed to determine the pressure (P_i) to be applied to elements within the eight circumferential sectors defined in Section 2.10.2.2.1. The calculation is based on the weight of a half-model of the cask at 1 g. Pressure forces for the 1-foot and 30-foot side drop analyses are determined by ratioing these pressure forces by the g-load applicable to the specific case.

The following formula can be used to compute the maximum impact pressure. This method uses a summation scheme to approximate the integration of the cosine-shaped pressure distribution:

$$F_{total} = \sum_{i=1}^{8} P_{max} A_i \cos(\theta_i) \cos(\theta_i)$$

where F_{total} = 125,000 lb (the cask design weight for a half model)

P_{max} = maximum impact pressure occurring at the impact centerline

θ_i = average angle of subtended arc

i = i^{th} circumferential sector

$\Delta\theta_i$ = arc length, in degrees, of sector i

θ_i = Normalized angle to peak at 0° and to be zero at 79.4°

= θ_i (90/79.4) = 1.1335 θ_i

A_i = i^{th} circumferential area over which the pressure is applied

= $R(\Delta\theta_i)(\pi/180)L = 0.01745(\Delta\theta_i)(R)(L)$

R = outer radius of the cask at impact limiter contact points

= 43.35 in

L = Impact limiter contact length = 24.03 in (for two limiters, one on each end of the cask)

$\Delta\theta_1$ = 8.3 - 0 = 8.3°

$\Delta\theta_2$ = 17.0 - 8.3 = 8.7°

$\Delta\theta_3$ = 26.2 - 17.0 = 9.2°

$\Delta\theta_4$ = 35.8 - 26.2 = 9.6°

$\Delta\theta_5$ = 45.9 - 35.8 = 10.1°

$\Delta\theta_6$ = 56.5 - 45.9 = 10.6°

$\Delta\theta_7$ = 67.7 - 56.5 = 11.2°

$\Delta\theta_8$ = 79.4 - 67.7 = 11.7°

$$\theta_1 = \frac{0 + 8.3}{2} = 4.15°; \theta_1 = 4.15°(1.1335) = 4.70°$$

$$\theta_2 = \frac{8.3 + 17.0}{2} = 12.65°; \theta_2 = 12.65°(1.1335) = 14.34°$$

$$\theta_3 = \frac{17.0 + 26.2}{2} = 21.6°;\ \theta_3 = 21.6°(1.1335) = 24.48°$$

$$\theta_4 = \frac{26.2 + 35.8}{2} = 31°;\ \theta_4 = 31°(1.1335) = 35.14°$$

$$\theta_5 = \frac{35.8 + 45.9}{2} = 40.85°;\ \theta_5 = 40.85°(1.1335) = 46.30°$$

$$\theta_6 = \frac{45.9 + 56.5}{2} = 51.20°;\ \theta_6 = 51.20°(1.1335) = 58.04°$$

$$\theta_7 = \frac{56.5 + 67.7}{2} = 62.10°;\ \theta_7 = 62.10°(1.1335) = 70.39°$$

$$\theta_8 = \frac{67.7 + 79.4}{2} = 73.55°;\ \theta_8 = 73.55°(1.1335) = 83.37°$$

$F_i = P_{max}\ A_i \cos(q_i) \cos(q)$

$i = 1$ through 8

$F_1 = P_{max}(0.01745)(R)(8.3°)(L) \cos(4.15°) \cos(4.70°)$

$= 0.1440\ (P_{max})(L)(R)$

$F_2 = P_{max}(0.01745)(R)(8.7°)(L) \cos(12.65°) \cos(14.34°)$

$= 0.1435\ (P_{max})(L)(R)$

$F_3 = P_{max}(0.01745)(R)(9.2°)(L) \cos(21.6°) \cos(24.48°)$

$= 0.1359\ (P_{max})(L)(R)$

$F_4 = P_{max}(0.01745)(R)(9.6°)(L) \cos(31°) \cos(35.14°)$

$= 0.1174\ (P_{max})(L)(R)$

$F_5 = P_{max}(0.01745)(R)(10.1°)(L) \cos(40.85°) \cos(46.30°)$

$= 0.0921\ (P_{max})(L)(R)$

$F_6 = P_{max}(0.01745)(R)(10.6°)(L) \cos(51.20°) \cos(58.04°)$

$= 0.0614\ (P_{max})(L)(R)$

$F_7 = P_{max}(0.01745)(R)(11.2°)(L) \cos(62.10°) \cos(70.39°)$

$= 0.0307\ (P_{max})(L)(R)$

$F_8 = P_{max}(0.01745)(R)(11.7°)(L) \cos(73.55°) \cos(83.37°)$

$= 0.0067\ (P_{max})(L)(R)$

$F_{total} = 0.7317\ (P_{max})(L)(R)$

$$P_{max} = \frac{F_{total}}{(0.7317)(L)(R)}$$

The pressures to be applied to the finite element analysis can then be computed as follows:

$$P_i = \frac{F_{Total}\ \cos(\theta_i')}{(0.7317)(L)(R)}$$

where F_{total} = 125,000 lb (for half model)

L = 24.06 in

R = 43.35 in

P_i = 163.7918 cos (θ)

P_1 = 163.7918 cos (4.70°) = 163.22 psi

P_2 = 163.7918 cos (14.34°) = 158.67 psi

P_3 = 163.7918 cos (24.48°) = 149.06 psi

P_4 = 163.7918 cos (35.14°) = 133.98 psi

P_5 = 163.7918 cos (46.30°) = 113.17 psi

P_6 = 163.7918 cos (58.04°) = 86.96 psi

P_7 = 163.7918 cos (70.39°) = 54.99 psi

P_8 = 163.7918 cos (83.37°) = 18.96 psi

The following is a summary of the side drop impact pressures applied to the finite element model in the eight circumferential sectors:

ARC (deg)	PRESSURE (psi)
0 - 8.3	163.22
8.3 - 17.0	158.67
17.0 - 26.2	149.06
26.2 - 35.8	133.98
35.8 - 45.9	113.17
45.9 - 56.5	86.69
56.5 - 67.7	54.99
67.7 - 79.4	18.96

It should be noted that these pressures consider a 1 g deceleration condition. Pressures for the 1-foot and 30-foot side drop analyses are calculated by ratioing these pressure values by the appropriate deceleration or g values, which are documented in Sections 2.6.7.2 and 2.7.1.2.

For the corner and oblique drop analyses, the impact pressure loading is a combination of the end drop impact pressure load and the side drop impact pressure load. The corner and oblique drop impact pressure loadings are determined by breaking up the impact pressure load into longitudinal and lateral components, based on the drop angle. The longitudinal component is applied to the cask end, and the lateral component is applied to the cask inner shell as previously described for the side drop case.

2.10.2.2.3 Bolt Initial Strain Determination

The standard technique for applying bolt preload to a finite element model is employed. The bolts are modeled using beam elements, ANSYS STIF3 elements for the two-dimensional model and ANSYS STIF4 elements for the three-dimensional top fine mesh model. Each bolt is modeled by four beam elements, two that represent the bolt head and two that represent the bolt shaft. The two bolt head elements are defined by three nodes that are an integral part of the non-threaded plate. The bolt head elements are assigned a stiffness of 10 times the actual bolt stiffness. The first bolt shaft element connects the center node of the bolt head with a node located at the top of the threaded hole. This element represents the portion of the bolt that is not engaged in the threaded hole. This portion of the bolt will be in tension due to the bolt preload. The second bolt shaft element connects the node at the top of the threaded hole with a node at the bottom of the threaded hole. This element represents the portion of the bolt that is engaged in the threaded hole. The two bolt shaft elements are assigned material property values (area and stiffness) equal to the actual bolt properties.

The effect of bolt preload is imposed on the model by applying an initial strain to the bolt shaft. The initial strain is applied only to the beam element representing the portion of the bolt shaft not engaged in threads. The initial strain values, which result in the required preload values, are determined by first running ANSYS analyses of both the two-and three-dimensional models with a “trial” initial strain, applied to the bolt shaft element, as the only loading condition. The resulting beam element force (from the element representing the portion of the bolt shaft not engaged in threads), is then used to ratio the trial initial strain to a value that will result in a beam element force closer to the actual bolt preload. This procedure is performed iteratively until the beam element force is effectively equal to the actual bolt preload.

The trial initial strain values are first determined by performing hand calculations of the value of P/nAE for the inner and the outer lid bolts. For the inner lid bolts, the calculation considers a required total bolt preload of 4.51×10^6 pounds, a quantity (n) of 42 bolts, a bolt cross-sectional area (A) of 1.492 square inches per bolt, and a Young’s modulus (E) of 31.0×10^6 psi.

For the outer lid bolts, the calculation considers a required total bolt preload (P) of 6.02×10^5 pounds, a quantity (n) of 36 bolts, a bolt cross-sectional area (A) of 0.606 square inches per bolt, and a Young's modulus (E) of 28.3×10^6 psi.

2.10.2.2.4 Contents Pressure Calculation—CY-MPC Configuration

For the end drop analyses, the contents weight is assumed to be uniformly distributed on the cask end, over an area determined by the inside diameter of the cask. Therefore, the conservatively assumed CY-MPC contents weight of 67,621 pounds (Fuel + Fuel Basket + Canister with lids + Spacer = 35,100 + 14,055 + 16,666 + 1,800), and the cask cavity inside radius of 35.5 inches are used to calculate a contact pressure of:

$$p = \frac{67{,}621}{(\pi)(35.5)^2} = 17.08 \text{ psi}$$

Note a spacer heavier than the weight reported in Table 2.2-4 is conservatively used in this evaluation.

This pressure applies to a 1 g loading condition. Pressure values for the 1-foot and 30-foot end drop analyses are determined by ratioing this pressure by the g-load values applicable to the specific case, which are documented in Sections 2.6.7.1 and 2.7.1.1.

For the side drop condition, the cask contents are conservatively assumed to contact the inner cask diameter on an arc of only 30 degrees during the 1-foot drop and 45 degrees during the 30-foot drop on either side of the impact centerline. The inertial load produced by each component (Lids + Canister body and fuel + Spacer) are represented as equivalent static pressures applied on the interior surface of the cask. The pressures are uniformly distributed along the cavity length, and are varied in the circumferential direction as a cosine distribution. The maximum pressure occurs along the impact centerline and decreases to zero at 30 degrees (1-foot drop) or 45 degrees (30-foot drop) either side of the impact centerline. The method used to determine the varying pressures on the elements within the contact arc is presented in Section 2.10.2.2.1.

2.10.2.3 Finite Element Analysis Procedures

The structural evaluation of the NAC-STC is performed by ANSYS analyses using three finite element models. A two-dimensional axisymmetric model is used for the axisymmetric loading cases, including bolt preload, internal pressure (high and low), thermal hot and cold, thermal fire transient, top end drop, and bottom end drop. A three-dimensional top fine mesh model is used in the non-axisymmetric loading conditions that result in high stresses on the top end of the cask, including the top corner drop and top oblique drops. The three-dimensional bottom fine mesh model is used for the non-axisymmetric loading conditions that result in high stresses on the bottom end of the cask, including the bottom corner drop, and bottom oblique drops. For the side drop analysis, both the top fine mesh model and the bottom fine mesh model are analyzed separately, in order to obtain the detailed stresses for both ends of the cask.

A number of individual and combined loading conditions are evaluated using separate ANSYS analyses. The ANSYS analyses performed for each individual loading condition are for the purpose of studying the structural effects of each individual type of load applied to the cask. The stress results of the ANSYS analysis of each individual load case are documented by nodal stress summaries (for details about finite element stress documentation procedures, see Section 2.10.2.4). The individual loading conditions considered are:

1. Bolt preload plus maximum internal pressure, 50 psig.

2. Bolt preload plus minimum internal pressure, 12 psig.

3. Gravity with 100°F ambient temperature, maximum decay heat load, and maximum insolation.

4. Gravity with -40°F ambient temperature, no decay heat load, and no insolation.

5. Thermal heat with 100°F ambient temperature, maximum decay heat load, and maximum insolation.

6. Thermal cold with -20°F ambient temperature, maximum decay heat load, and no insolation.

7. Thermal cold with -40°F ambient temperature, no decay heat load, and no insolation.

8. Thermal fire transient with 1475°F surrounding environment, 30-minute period.

9. Impact and inertial loads, 1-foot top end drop, 20 g impact load, $\phi = 0$ degrees.

10. Impact and inertial loads, 1-foot bottom end drop, 20 g impact load, $\phi = 0$ degrees.

11. Impact and inertial loads, 1-foot side drop, 20 g impact load, $\phi = 90$ degrees.

12. Impact and inertial loads, 1-foot top corner drop, 20 g impact load, $\phi = 24$ degrees.

13. Impact and inertial loads, 1-foot bottom corner drop, 20 g impact load, $\phi = 24$ degrees.

14. Impact and inertial loads, 30-foot top end drop, 56.1 g impact load, $\phi = 0$ degrees.

15. Impact and inertial loads, 30-foot bottom end drop, 56.1 g impact load, $\phi = 0$ degrees.

16. Impact and inertial loads, 30-foot side drop, 55 g impact load, $\phi = 90$ degrees.

17. Impact and inertial loads, 30-foot top corner drop, 55 g impact load, $\phi = 24$ degrees.

18. Impact and inertial loads, 30-foot bottom corner drop, 55 g impact load, $\phi = 24$ degrees.

19. Impact and inertial loads, 30-foot bottom oblique drop, 55 g impact load, $\phi = 15$ degrees.

20. Impact and inertial loads, 30-foot top critical oblique drop, 55 g impact load, $\phi = 75$ Degrees. ($\phi = 75$ degrees is the angle that results in the most critical stresses for the 30-foot top oblique drops).

21. Impact and inertial loads, 30-foot bottom critical oblique drop, 55 g impact load, $\phi = 75$ degrees. ($\phi = 75$ degrees is the angle that results in the most critical stresses for the 30-foot bottom oblique drops).

Combined load cases are then evaluated by running ANSYS analyses of the combined loading conditions. For example, the 30-foot top corner drop accident condition is evaluated by a single ANSYS analysis with the following loads applied simultaneously:

> 55 g impact and inertial loads (ϕ = 24 degrees), 100°F ambient temperature, maximum decay heat load, maximum solar insolation, bolt preload, and 50 psig internal pressure.

A single analysis with multiple loads is used in contrast to the method of superimposing the stress results from the individual analyses, in order to more accurately evaluate the effect of the simultaneous loads on the cask structure. For combined load cases, the stresses are documented by nodal, sectional, and critical stress summaries. The following combined load cases are considered:

1. Thermal Heat (normal condition), with bolt preload, maximum internal pressure of 50 psig, 100°F ambient temperature, maximum solar insolation, maximum decay heat, 1 g gravity load, still air, loaded and ready for shipment in the horizontal position.

2. Thermal Cold (normal condition) with bolt preload, minimum internal pressure of 12 psig, -40°F ambient temperature, no solar insolation, no decay heat load, 1 g gravity load, still air, loaded and ready for shipment in the horizontal position.

3. Thermal Fire Transient (hypothetical accident condition) with a surrounding environment of 1475°F for a 30-minute period, with bolt preload, internal pressure of 125 psig (conservative; actual internal pressure is 65.5 psig), maximum solar insolation, maximum decay heat load, and 1 g gravity load in the vertical direction.

4. 1-foot Top End Drop (normal condition) with bolt preload, maximum internal pressure of 50 psig, 100°F ambient temperature, maximum solar insolation, maximum decay heat load, 20 g impact and inertial load (ϕ = 0 degrees), still air.

5. 1-foot Top End Drop (normal condition) with bolt preload, minimum internal pressure of 12 psig, -20°F ambient temperature, no solar insolation, maximum decay heat load, 20 g impact and inertial load (ϕ = 0 degrees), still air.

6. 1-foot Top End Drop (normal condition) with bolt preload, minimum internal pressure of 12 psig, -20°F ambient temperature, no solar insolation, no decay heat load, 20 g impact and inertial load (ϕ = 0 degrees), still air.

7. 1-foot Bottom End Drop (normal condition) with bolt preload, maximum internal pressure of 50 psig, 100°F ambient temperature, maximum solar insolation, maximum decay heat load, 20 g impact and inertial load (ϕ = 0 degrees), still air.

8. 1-foot Bottom End Drop (normal condition) with bolt preload, minimum internal pressure of 12 psig, -20°F ambient temperature, no solar insolation, maximum decay heat load, 20 g impact and inertial load (ϕ = 0 degrees), still air.

9. 1-foot Bottom End Drop (normal condition) with bolt preload, minimum internal pressure of 12 psig, -20°F ambient temperature, no solar insolation, no decay heat load, 20 g impact and inertial load (ϕ = 0 degrees), still air.

10. 1-foot Side Drop (normal condition) with bolt preload, maximum internal pressure of 50 psig, 100°F ambient temperature, maximum solar insolation, maximum decay heat load, 20 g impact and inertial load (ϕ = 90 degrees), still air.

11. 1-foot Top Corner Drop (normal condition) with bolt preload, maximum internal pressure of 50 psig, 100°F ambient temperature, maximum solar insolation, maximum decay heat load, 20 g impact and inertial load (ϕ = 24 degrees), still air.

12. 1-foot Bottom Corner Drop (normal condition) with bolt preload, maximum internal pressure of 50 psig, 100°F ambient temperature, maximum solar insolation, 20 g impact and inertial load (ϕ = 24 degrees), still air.

13. 30-foot Top End Drop (hypothetical accident condition) with bolt preload, maximum internal pressure of 50 psig, 100°F ambient temperature, maximum solar insolation, maximum decay heat load, 56.1 g impact and inertial load (ϕ= 0 degrees), still air.

14. 30-foot Top End Drop (hypothetical accident condition) with bolt preload, minimum internal pressure of 12 psig, -20°F ambient temperature, no solar insolation, maximum decay heat load, 56.1 g impact and inertial load (ϕ = 0 degrees), still air.

15. 30-foot Top End Drop (hypothetical accident condition) with bolt preload, minimum internal pressure of 12 psig, -20°F ambient temperature, no solar insolation, no decay heat load, 56.1 g impact and inertial load (ϕ = 0 degrees), still air.

16. 30-foot Bottom End Drop (hypothetical accident condition) with bolt preload, maximum internal pressure of 50 psig, 100°F ambient temperature, maximum solar insolation, maximum decay heat load, 56.1 g impact and inertial load (ϕ = 0 degrees), still air.

17. 30-foot Bottom End Drop (hypothetical accident condition) with bolt preload, minimum internal pressure of 12 psig, -20°F ambient temperature, no solar insolation, maximum decay heat load, 56.1 g impact and inertial load (ϕ = 0 degrees), still air.

18. 30-foot Bottom End Drop (hypothetical accident condition) with bolt preload, minimum internal pressure of 12 psig, -20°F ambient temperature, no solar insolation, no decay heat load, 56.1 g impact and inertial load (ϕ = 0 degrees), still air.

19. 30-foot Side Drop (hypothetical accident condition) with bolt preload, maximum internal pressure of 50 psig, 100°F ambient temperature, maximum solar insolation, maximum decay heat load, 55 g impact and inertial load (ϕ = 90 degrees), still air.

20. 30-foot Top Corner Drop (hypothetical accident condition) with bolt preload, maximum internal pressure of 50 psig, 100°F ambient temperature, maximum solar insolation, maximum decay heat load, 55 g impact and inertial load (ϕ = 24 degrees), still air.

21. 30-foot Bottom Corner Drop (hypothetical accident condition) with bolt preload, maximum internal pressure of 50 psig, 100°F ambient temperature, maximum solar insolation, maximum decay heat load, 55 g impact and inertial load (ϕ = 24 degrees), still air.

22. 30-foot Bottom Oblique Drop (hypothetical accident condition) with bolt preload, maximum internal pressure of 50 psig, 100°F ambient temperature, maximum solar insolation, maximum decay heat load, 55 g impact and inertial load (ϕ = 15 degrees), still air.

23. 30-foot Top Oblique Drop (hypothetical accident condition) with bolt preload, maximum internal pressure of 50 psi, 100°F ambient temperature, maximum solar insolation, maximum decay heat load, 55 g impact and inertial load (ϕ = 75 degrees), still air. (ϕ = 75 degrees is the angle which results in the most critical stresses for 30-foot top oblique drops).

24. 30-foot Bottom Oblique Drop (hypothetical accident condition) with bolt preload, maximum internal pressure of 50 psig, 100°F ambient temperature, maximum solar insolation, maximum decay heat load, 55 g impact and inertial load (ϕ = 75 degrees), still air. (ϕ = 75 degrees is the angle which results in the most critical stresses for 30-foot top oblique drops).

2.10.2.4 Finite Element Documentation Procedures

Documentation of the finite element stress calculations is performed according to the following procedure:

1. A sketch of the cask is prepared showing the points on each shell for which stresses are calculated and tabulated. At given axial locations on the cask, separate points are designated on the inside and outside of each shell. At given radial locations on the end and closure plates, separate points are designated on the inside and outside of each plate. In addition, for thick sections or thin sections at structural discontinuities, the stresses are presented for several points through the thickness in order to adequately define the stress distribution for the stress linearization calculations. Furthermore, for three-dimensional

models, the stress variations around the circumference are documented at several selected circumferential locations.

2. For each stress point identified in step 1, a nodal stress summary, including stress components and principal stresses, is prepared for each individual normal and accident condition loading (e.g., internal pressure, hot and cold temperature, impact, etc.).

3. Summaries are prepared for the combined stresses at each stress point per the load combinations specified in Regulatory Guide 7.8. The combined stresses are classified in the categories of primary, and primary plus secondary stress intensities, as specified in Regulatory Guide 7.6.

4. Stress intensity summaries are prepared for the primary membrane (P_m), primary membrane plus primary bending ($P_m + P_b$), and primary plus secondary (S_n) stress categories. These stress intensity values are obtained by performing stress linearization calculations using the nodal stresses obtained from step 2. This calculation is performed on all of the selected sections.

In order to perform steps 1 through 4, representative section cut locations were chosen based on the critical stress locations. The nodes representing the stress points used in steps 1 through 4 are located on these representative section cuts. The section locations are described in detail in Section 2.10.2.4.2.

5. Stress evaluations are then performed at every feasible cross-section of the cask. Then, the most critical cross-section within each component is determined by searching, on a component basis, for the cross section where the maximum stress intensity is located. Since the stress evaluations and the search are performed by a computer algorithm, every feasible cross-section is identified and evaluated, insuring that the maximum stress location within each component is found. Stress tables are then prepared to summarize the critical primary membrane, primary membrane plus primary bending, primary plus secondary stresses, and the margin of safety, of each cask component, for each loading condition.

In order to perform step 5, the cask is divided into components based on the physical geometry of the cask, such that each component consists of a single material. The details of the cask component identification are given in Section 2.10.2.4.1.

2.10.2.4.1 Structural Component Identification

Cask components are defined so that the qualification of the cask can be performed on a component basis. Stress evaluations are performed at every feasible cask cross-section, and then a computer search is performed to identify the section within each component which has the maximum stress intensity. Critical stress summaries are then prepared on a component basis.

The determination of critical stresses considers the stress results at a total of 3,877 cross-sections on the three-dimensional top fine mesh model, and at a total of 3,188 cross-sections on the three-dimensional bottom fine mesh model. For the two-dimensional axisymmetric model, stress evaluations are performed for a total of 487 cross-sections. These evaluations cover all of the feasible cross-sections of the cask.

Preparation of the critical stress summaries also requires the calculation of allowable stress values. Since allowable stress is a function of material properties (design stress intensity, yield strength and ultimate tensile strength), it is convenient that the components be defined such that each component consists of a single material. This is accomplished by designating the components in a manner consistent with the actual physical construction of the cask, i.e., the components are defined as the unique physical entities which exist prior to the final assembly of the cask.

The material properties used to determine allowable stresses are functions of temperature. If the allowable stresses for all components were determined using the maximum cask temperature, the allowable stresses will be overly conservative in those components which never experience the maximum cask temperature. Maximum temperatures determined on a component basis, rather than on a cask basis, permit the determination of more reasonable, but still conservative, allowable stresses. Therefore, the maximum component temperature is used in calculating the allowable stresses for that component.

The finite element cask components are uniquely designated as shown in Figure 2.10.2.33. Table 2.10.2-5 documents the name of each component, the material of which it is constructed, and an

arbitrary material identification number (used in the ANSYS model). The fifth column of the table documents the maximum temperature which occurs in each individual component, as determined by the 100°F ambient thermal analysis condition.

The sixth and eighth columns of Table 2.10.2-5 documents the design stress intensity (S_m), and the ultimate tensile strength (S_u), for the component material at the maximum component temperature. The values of 1.5 S_m and 0.7 S_u are also provided. These component allowables are conservatively used for the -20°F and -40°F ambient condition load cases.

2.10.2.4.2 Representative Section Locations

The entire NAC-STC body and closure lids are analyzed for structural adequacy. Representative section cut locations are defined, based on the critical stress locations, in order to illustrate the overall structural behavior of the cask. The selected section locations are identified by letters on Figure 2.10.2-34.

Each load case--pressure, thermal, and mechanical--is evaluated separately. The stress components are documented for each of the selected sections and for the nodes on the sections. The individual load cases are then combined to obtain total principal stresses and stress intensities for the primary membrane, primary membrane plus primary bending, and primary plus secondary stress categories.

Figures 2.10.2-35 and 2.10.2-36 show the distribution of nodes and elements in the circumferential direction for the three-dimensional top fine mesh model, and for the three-dimensional bottom fine mesh model, respectively. For the three-dimensional models, stress results are documented for several of the 16 circumferential planes.

The coordinates of the nodes which define the ends of the section cuts for the two-dimensional axisymmetric, three-dimensional bottom fine mesh, and three-dimensional top fine mesh models are provided in Tables 2.10.2-8 through 2.10.2-10, respectively. Tables 2.10.2-11 through 2.10.2-13 contain the node numbers and coordinates of all stress point locations on each section cut, for the three models.

Figure 2.10.2-1 ANSYS Two-Dimensional Finite Element Model - NAC-STC

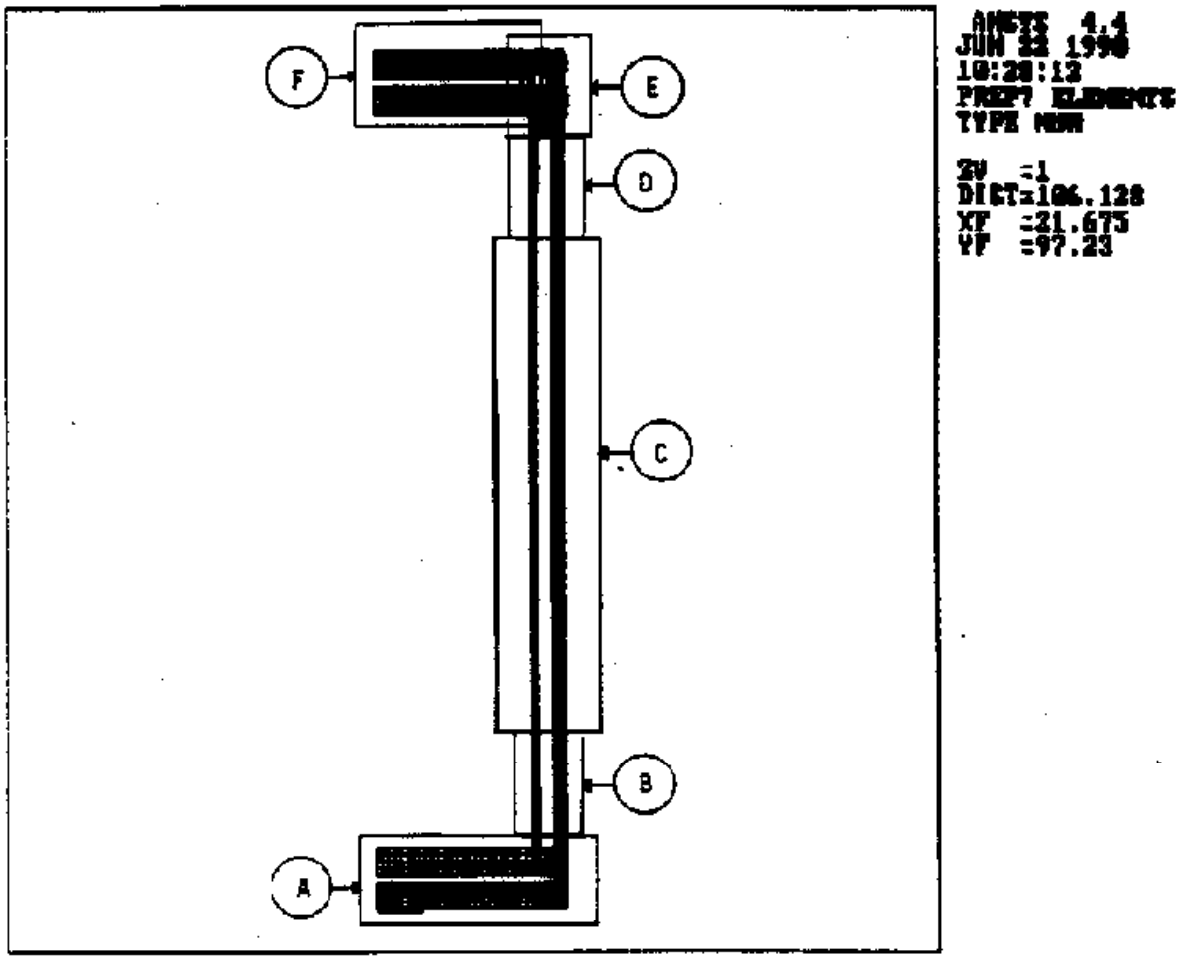

Figure 2.10.2-2 Cask Bottom (Region A) - NAC-STC ANSYS Two-Dimensional Model

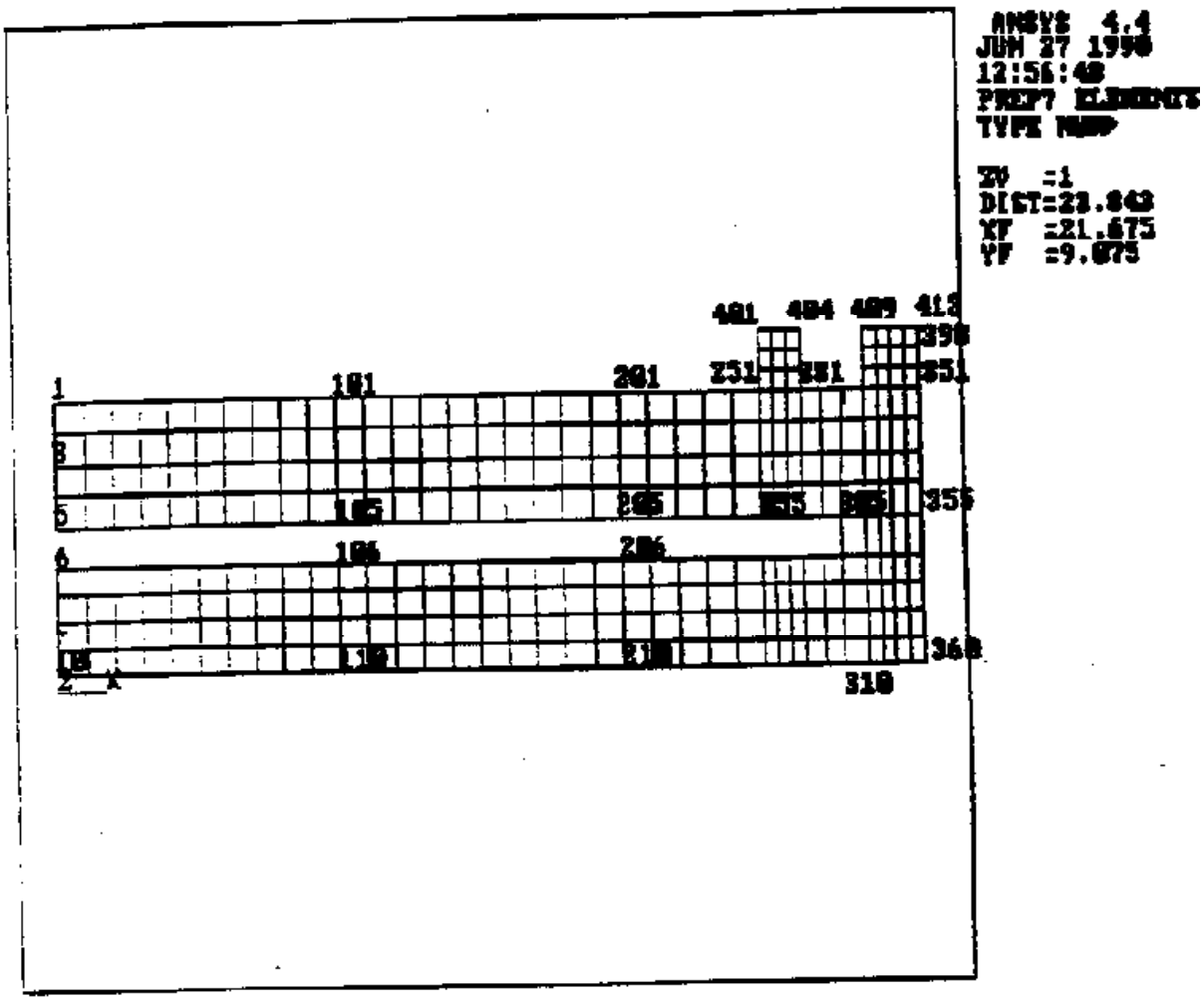

Figure 2.10.2-3 Cask Lower Transition (Region B) - NAC-STC ANSYS Two-Dimensional Model

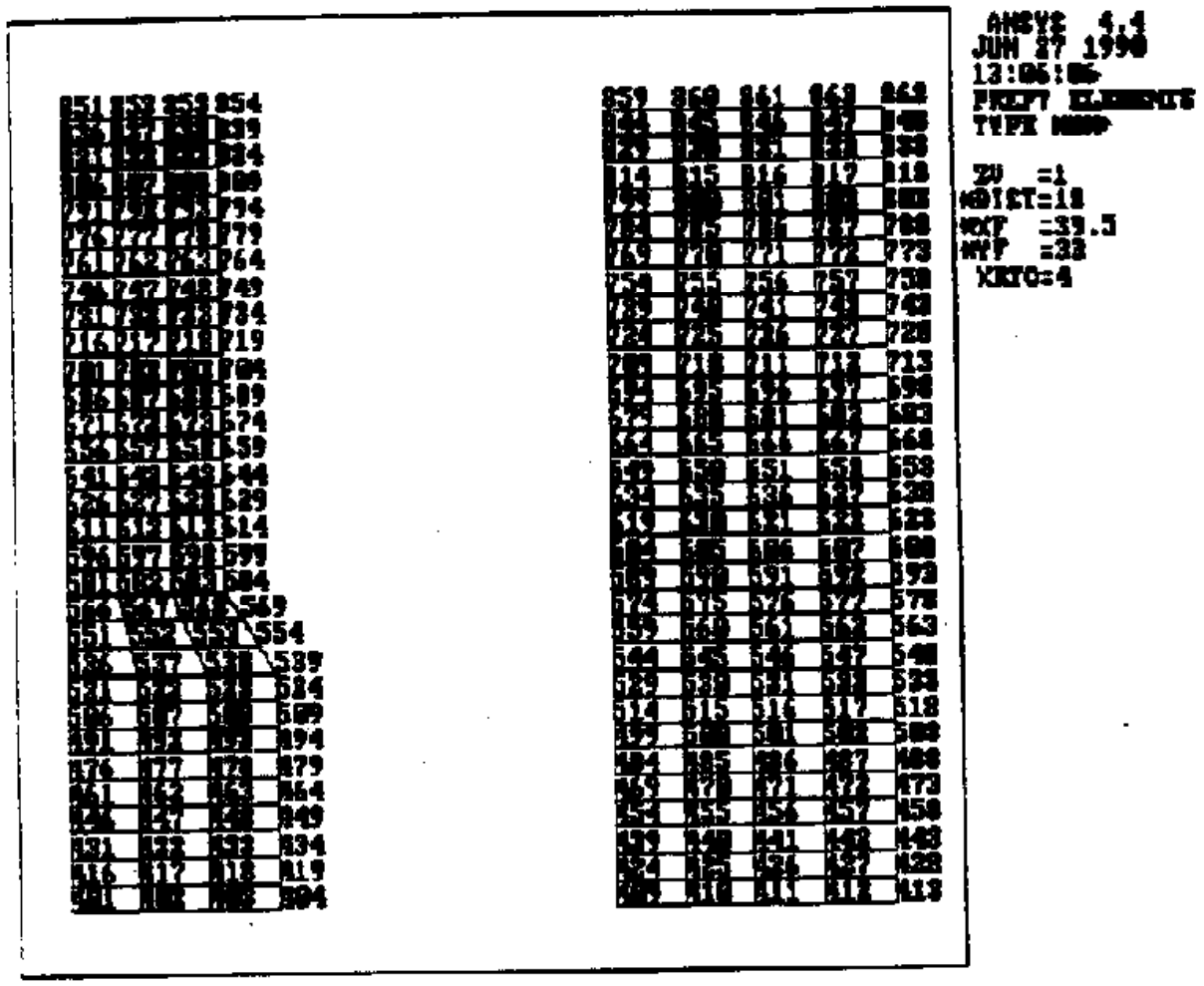

Figure 2.10.2-4 Cask Shells (Region C) - NAC-STC ANSYS Two-Dimensional Model

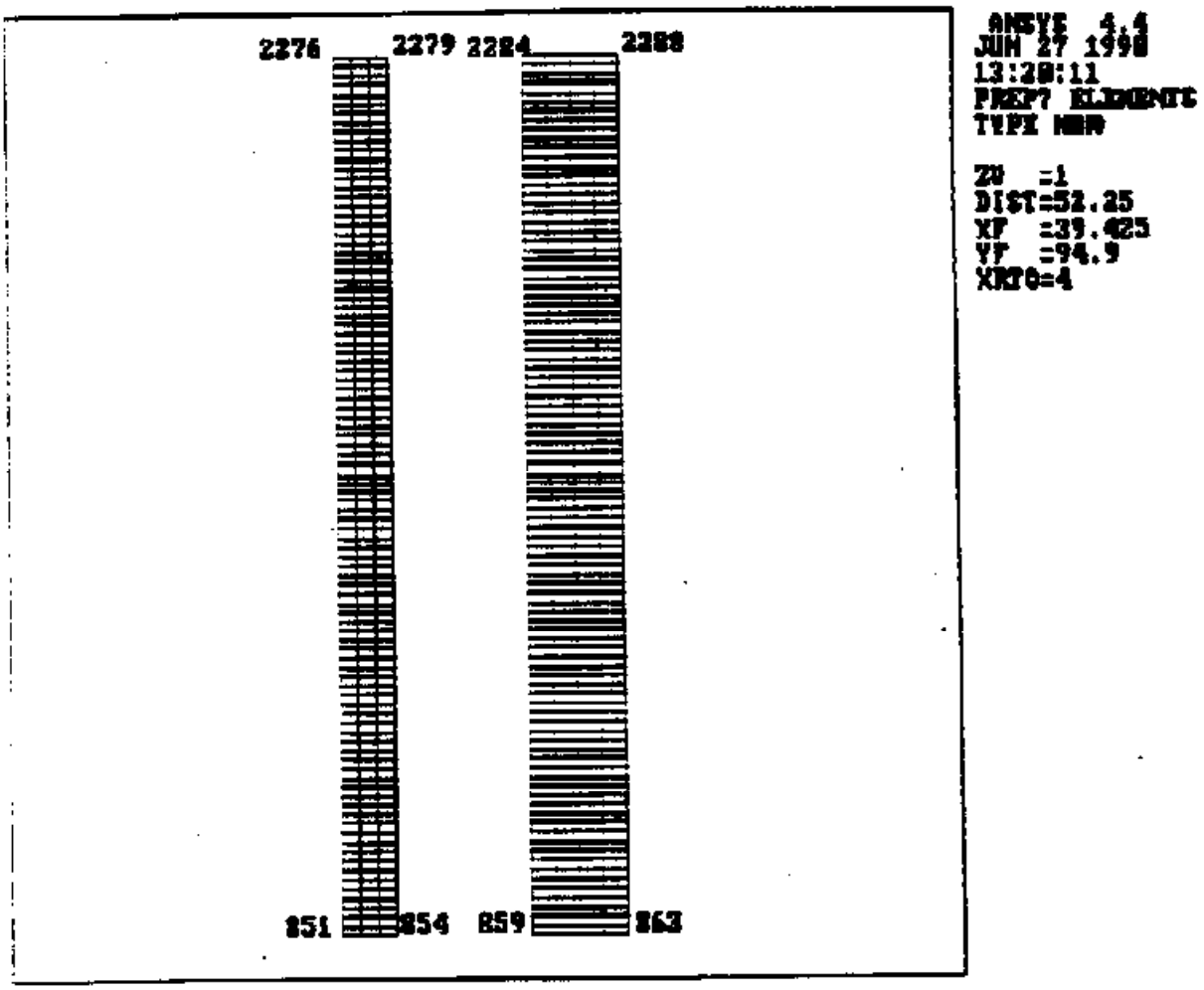

Figure 2.10.2-5 Cask Upper Transition (Region D) - NAC-STC ANSYS Two-Dimensional Model

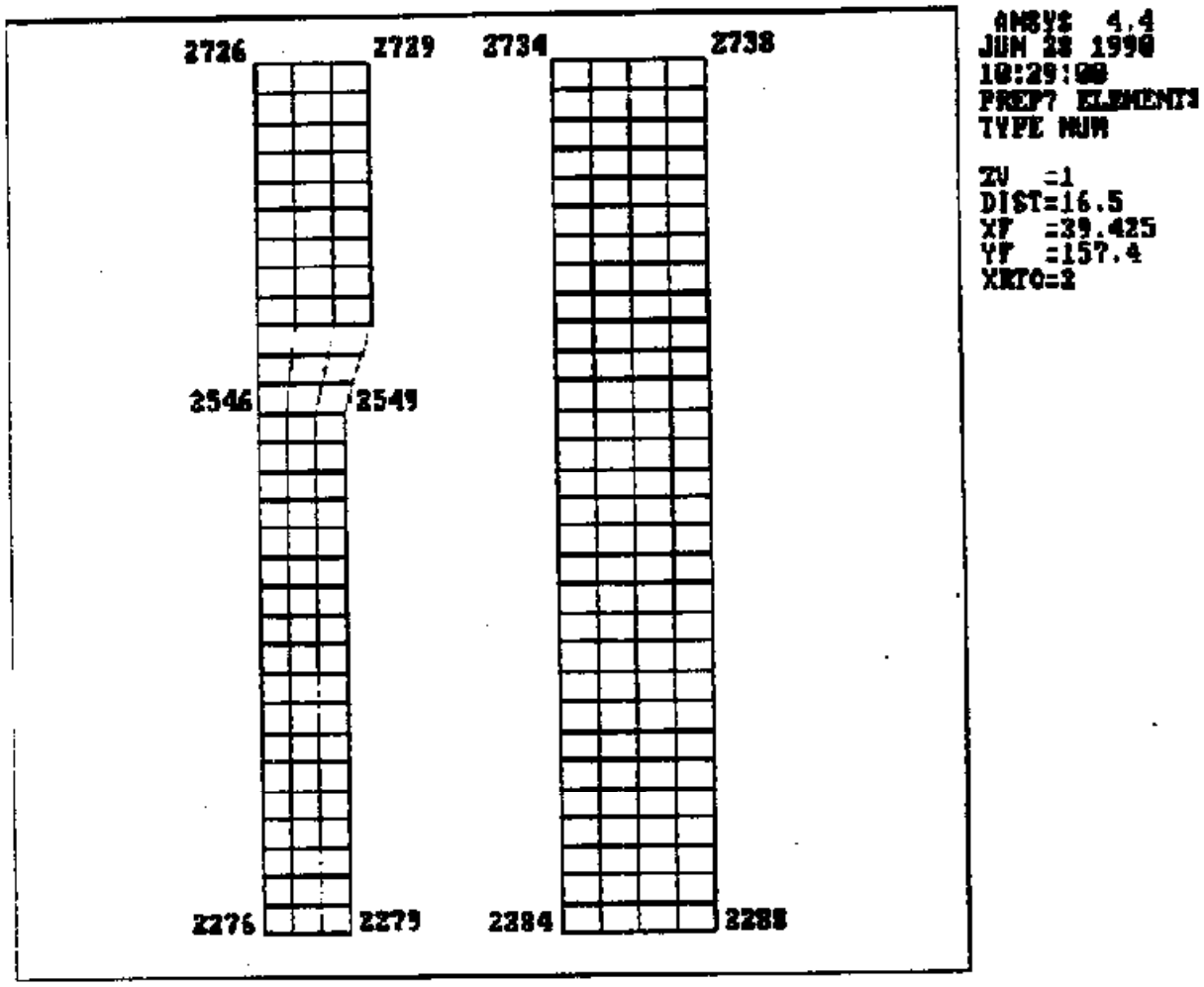

Figure2.10.2-6 Cask Top Forging (Region E) - NAC-STC ANSYS Two-Dimensional Model

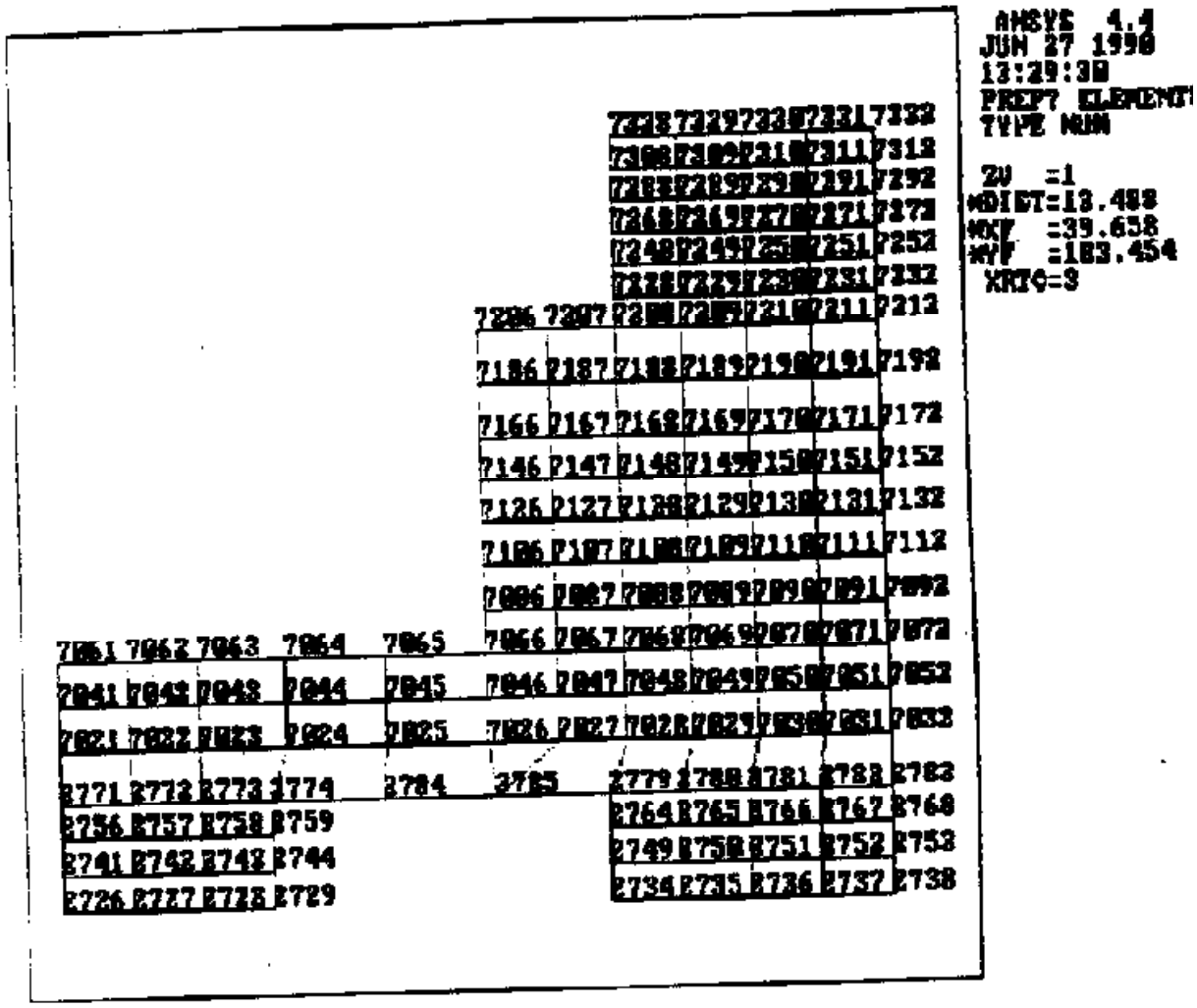

Figure 2.10.2-7 Cask Lids (Region F) - NAC-STC ANSYS Two-Dimensional Model

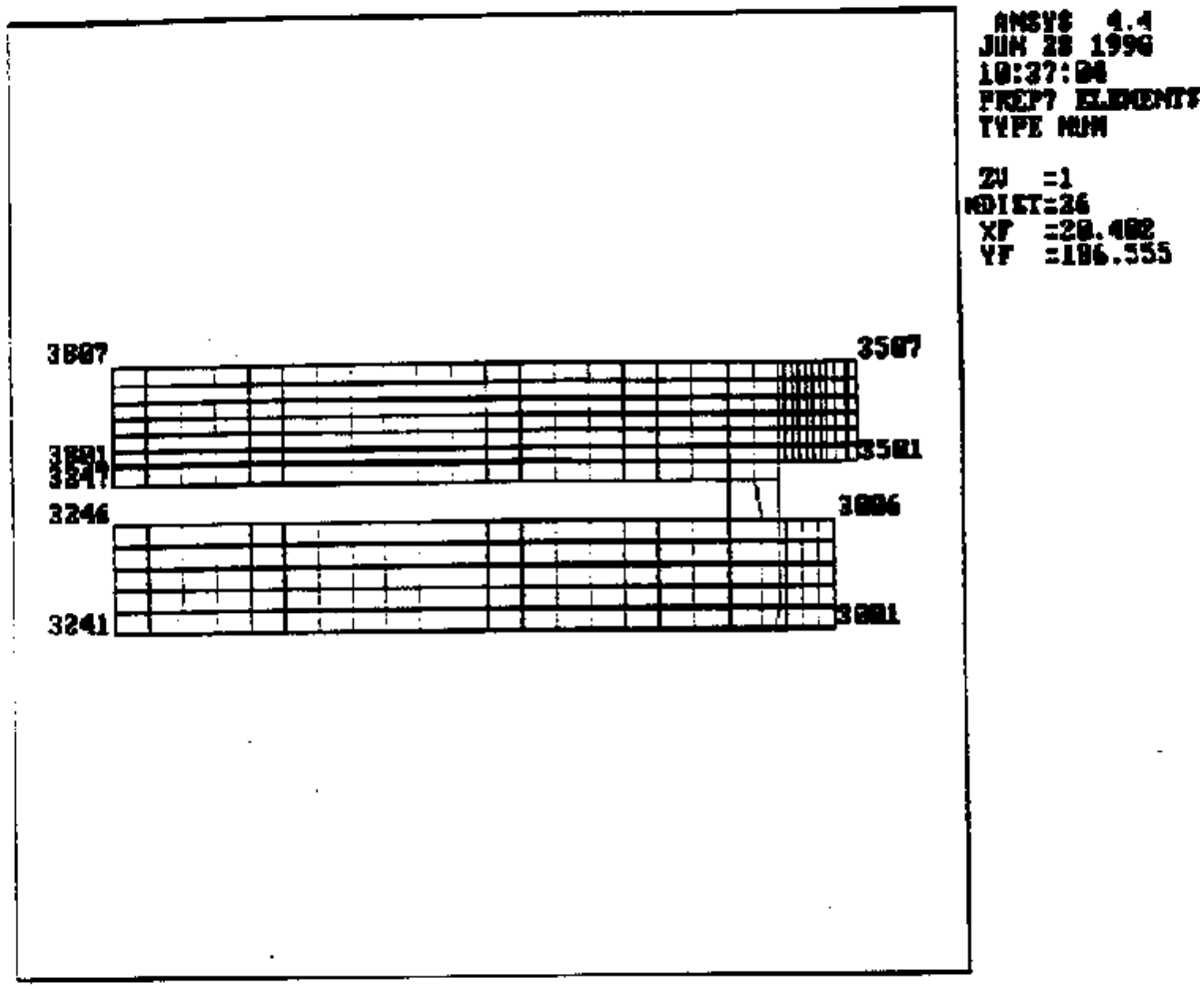

Figure 2.10.2-8 Circumferential Mesh Spacing (End View) - ANSYS Three-Dimensional Top and Bottom Fine Mesh Models

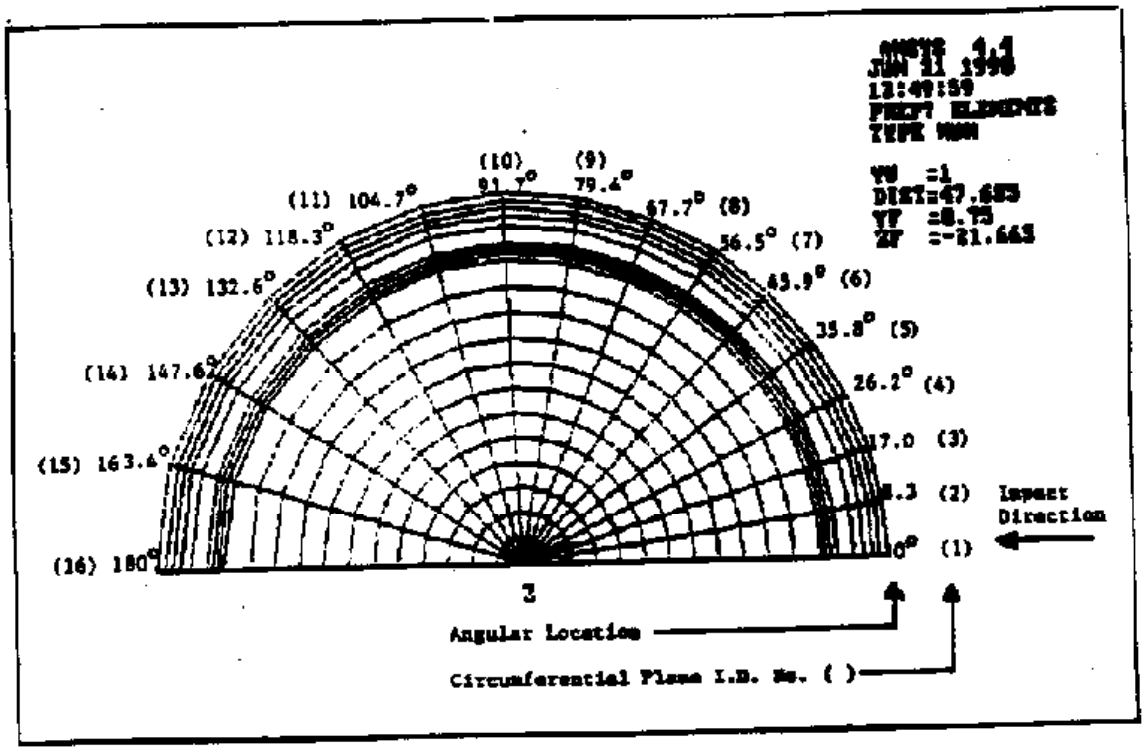

Figure 2.10.2-9 ANSYS Three-Dimensional Bottom Fine Mesh Finite Element Model - NAC-STC

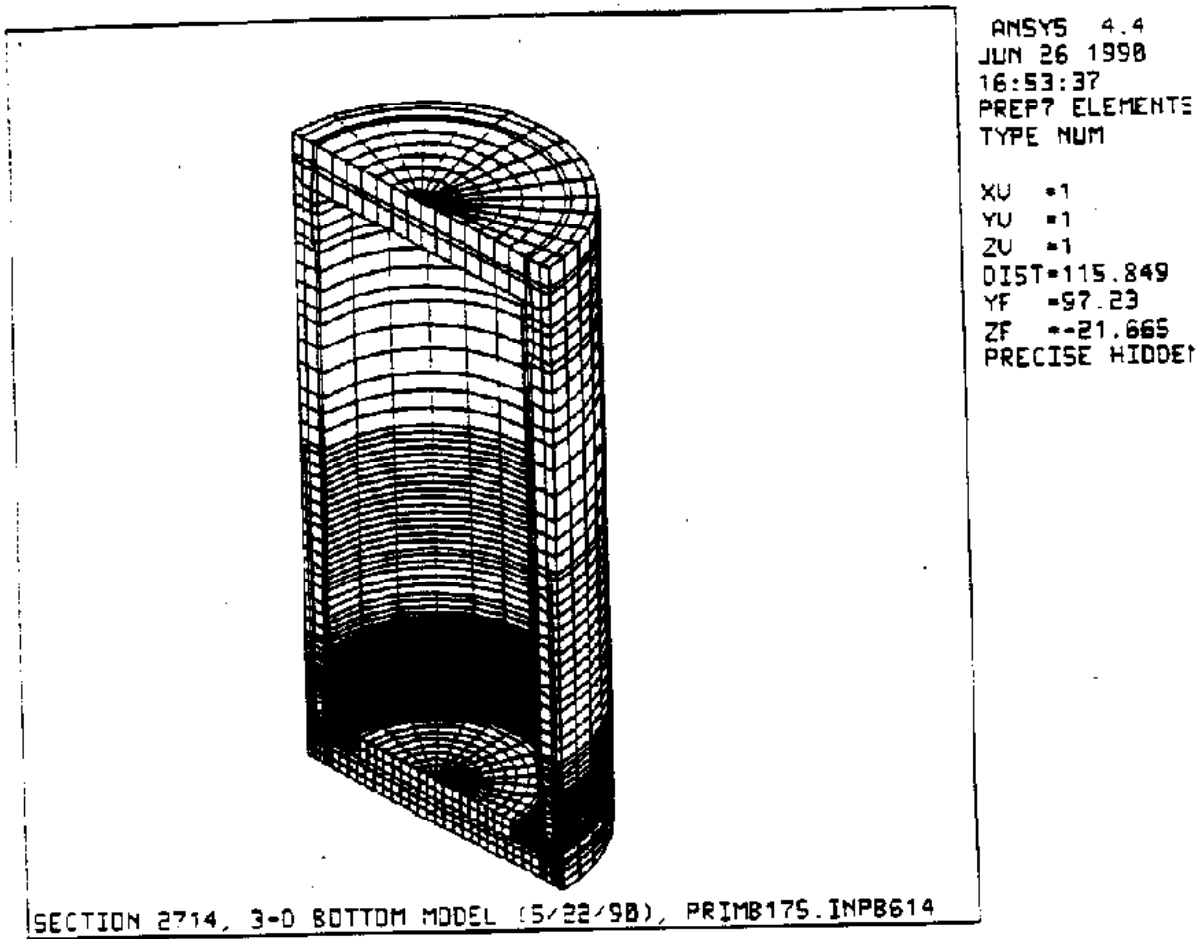

Figure 2.10.2-10 Details - NAC-STC ANSYS Three-Dimensional Bottom Fine Mesh Model

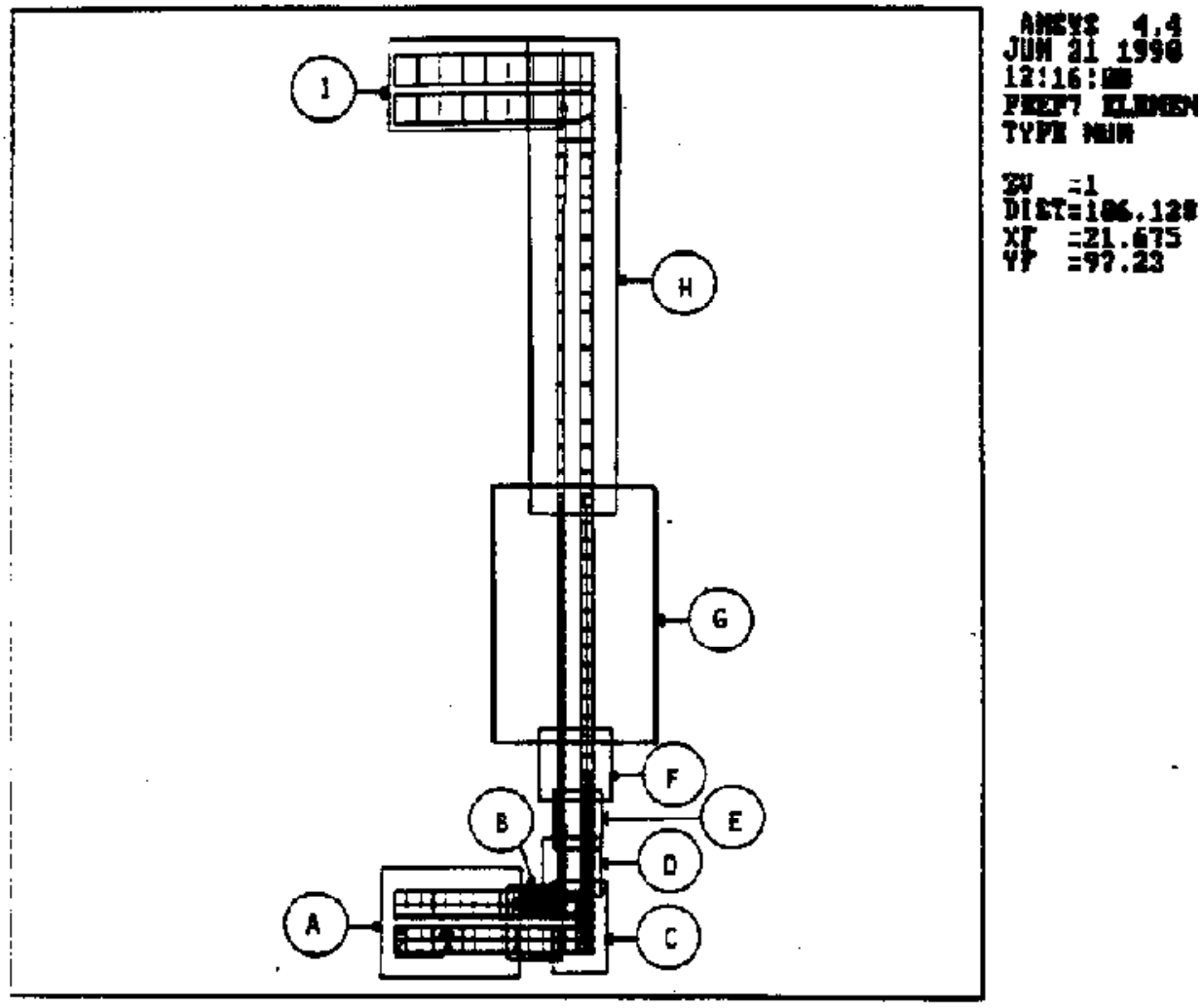

Figure2.10.2-11 Cask Bottom (Region A) - NAC-STC ANSYS Bottom Fine Mesh Three-Dimensional Model

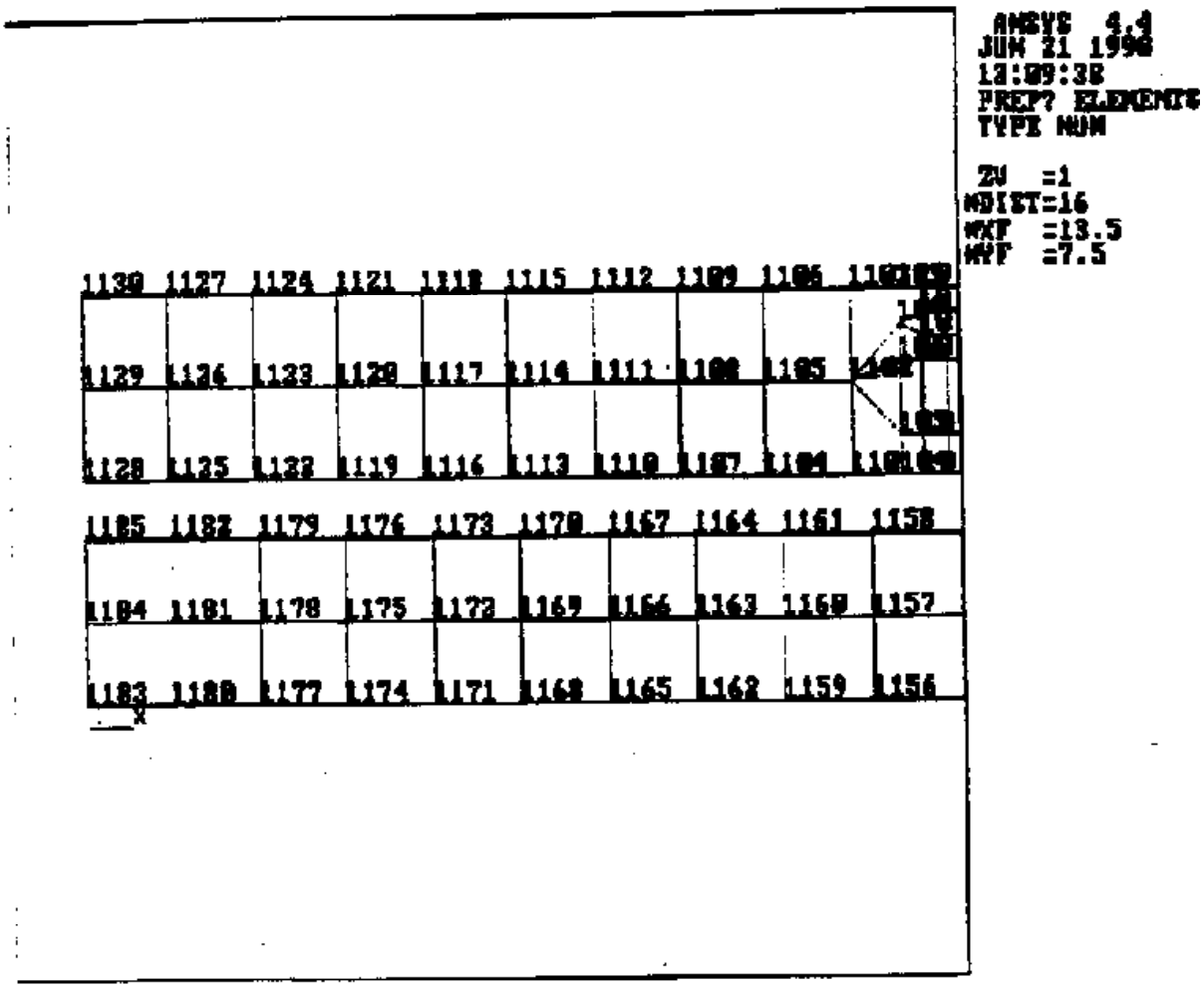

Figure 2.10.2-12 Cask Bottom (Region B) - NAC-STC ANSYS Bottom Fine Mesh Three-Dimensional Model

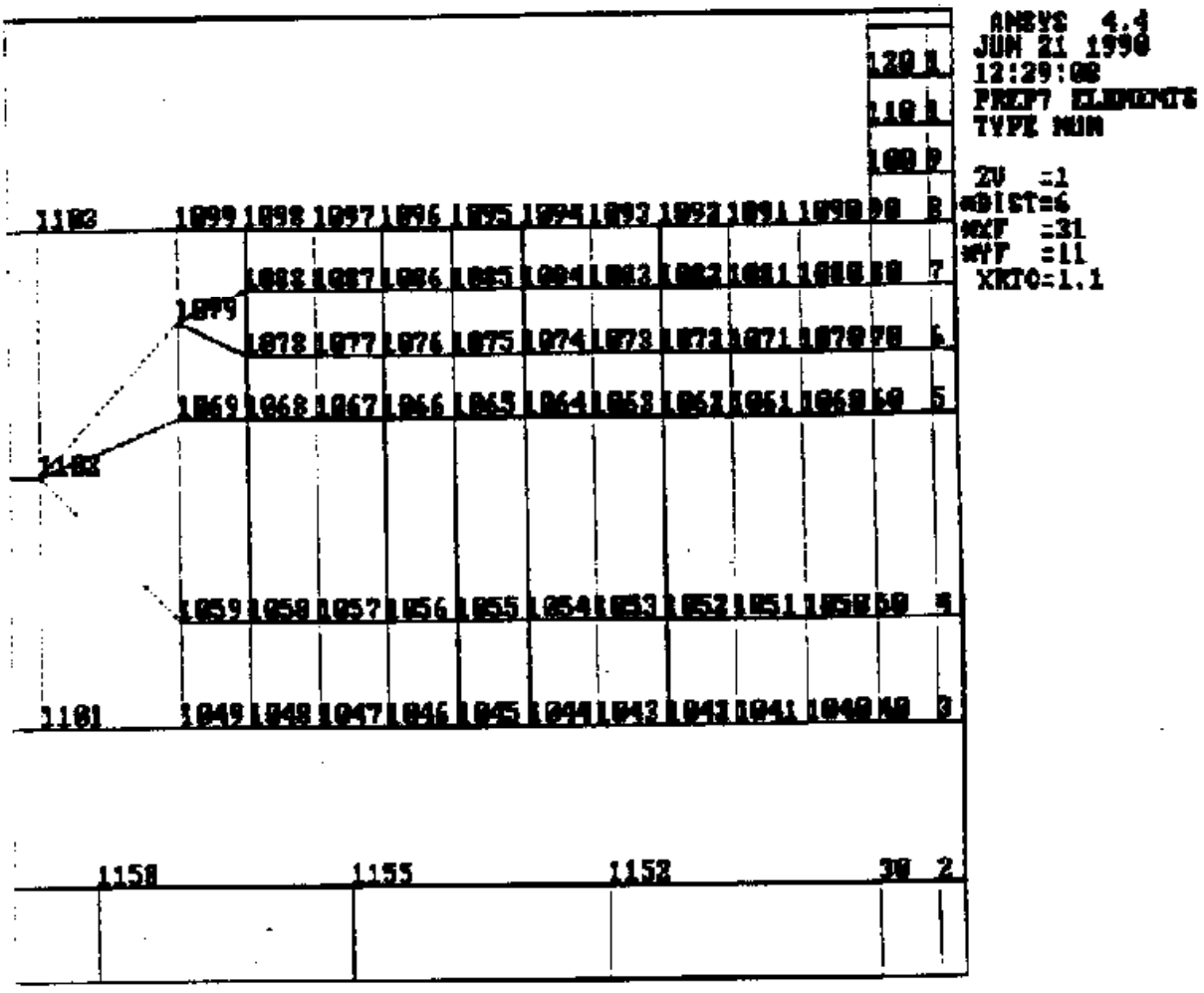

Figure 2.10.2-13 Cask Bottom (Region C) - NAC-STC ANSYS Bottom Fine Mesh Three-Dimensional Model

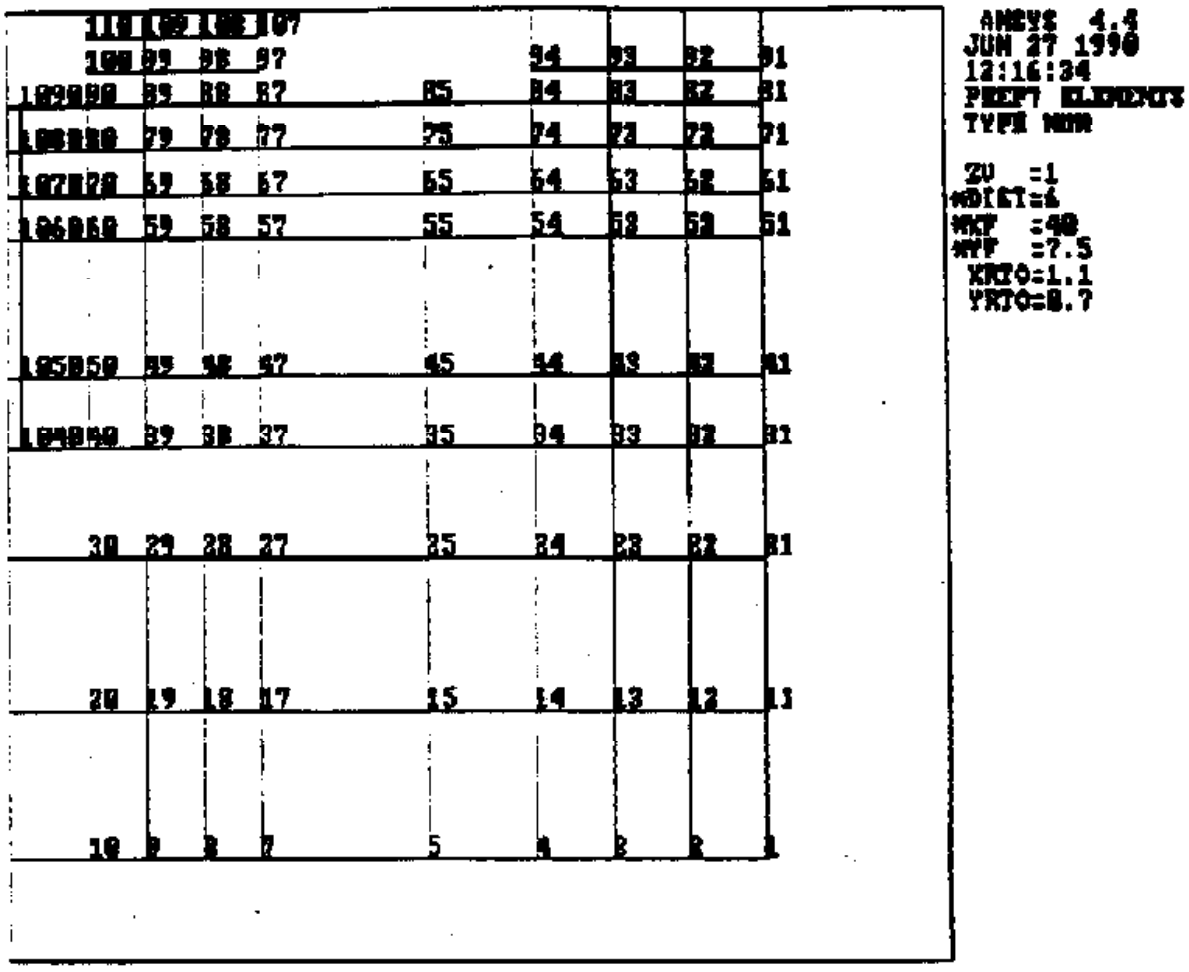

Figure 2.10.2-14 Cask Lower Transition (Region D) - NAC-STC ANSYS Bottom Fine Mesh Three-Dimensional Model

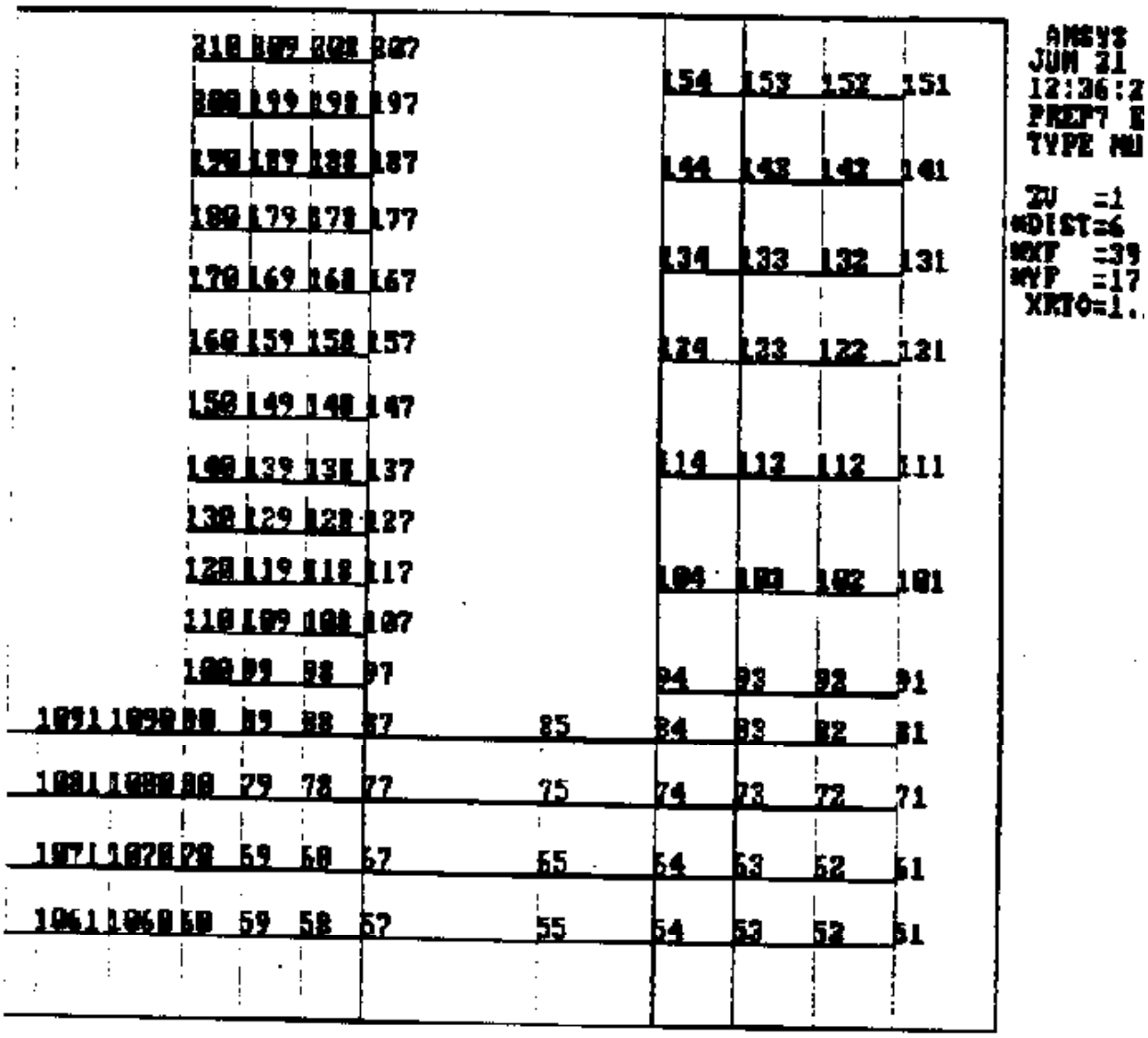

Figure 2.10.2-15 Cask Lower Transition (Region E) - NAC-STC ANSYS Bottom Fine Mesh Three-Dimensional Model

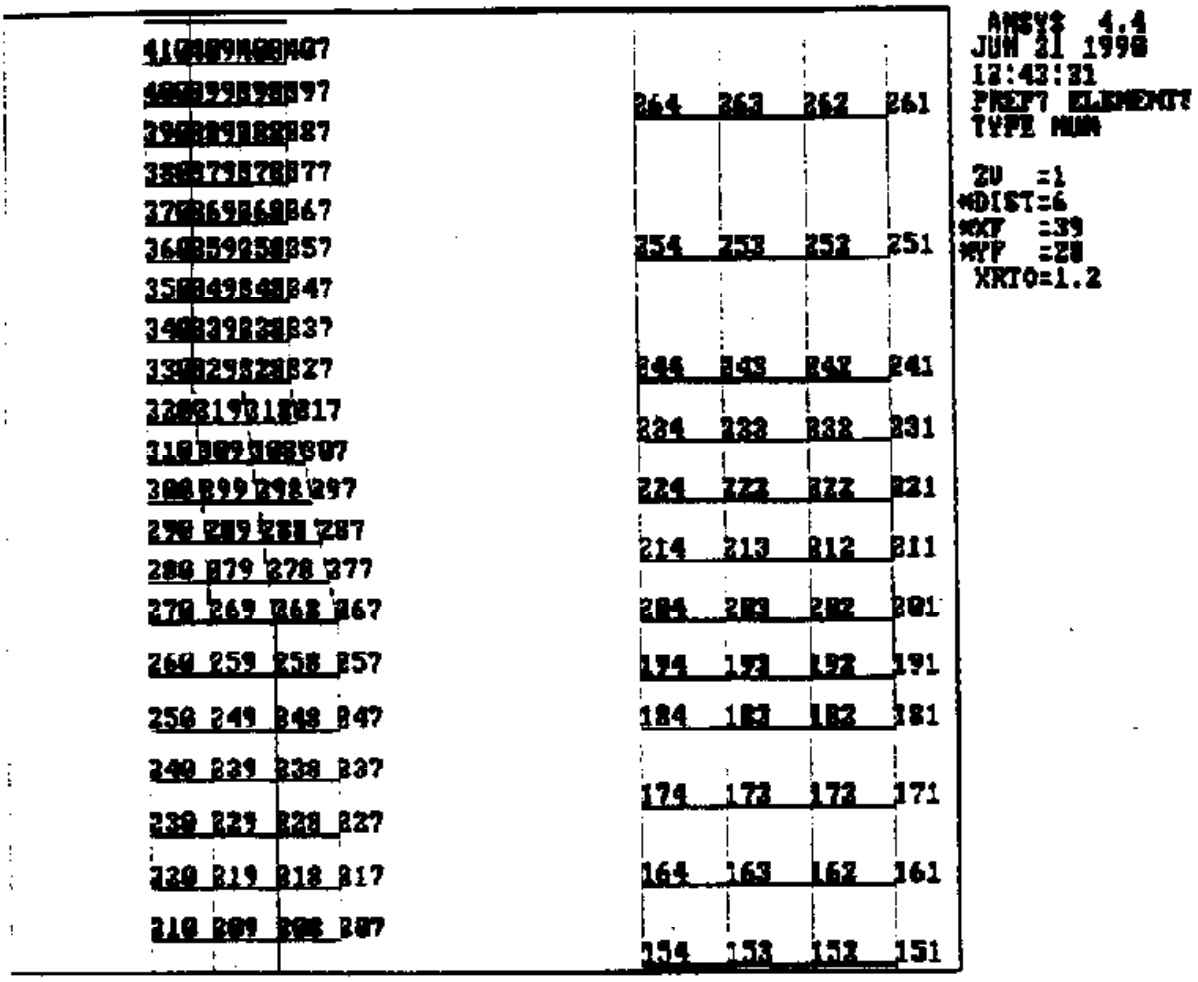

Figure 2.10.2-16 Cask Lower Shell (Region F) - NAC-STC ANSYS Bottom Fine Mesh Three-Dimensional Model

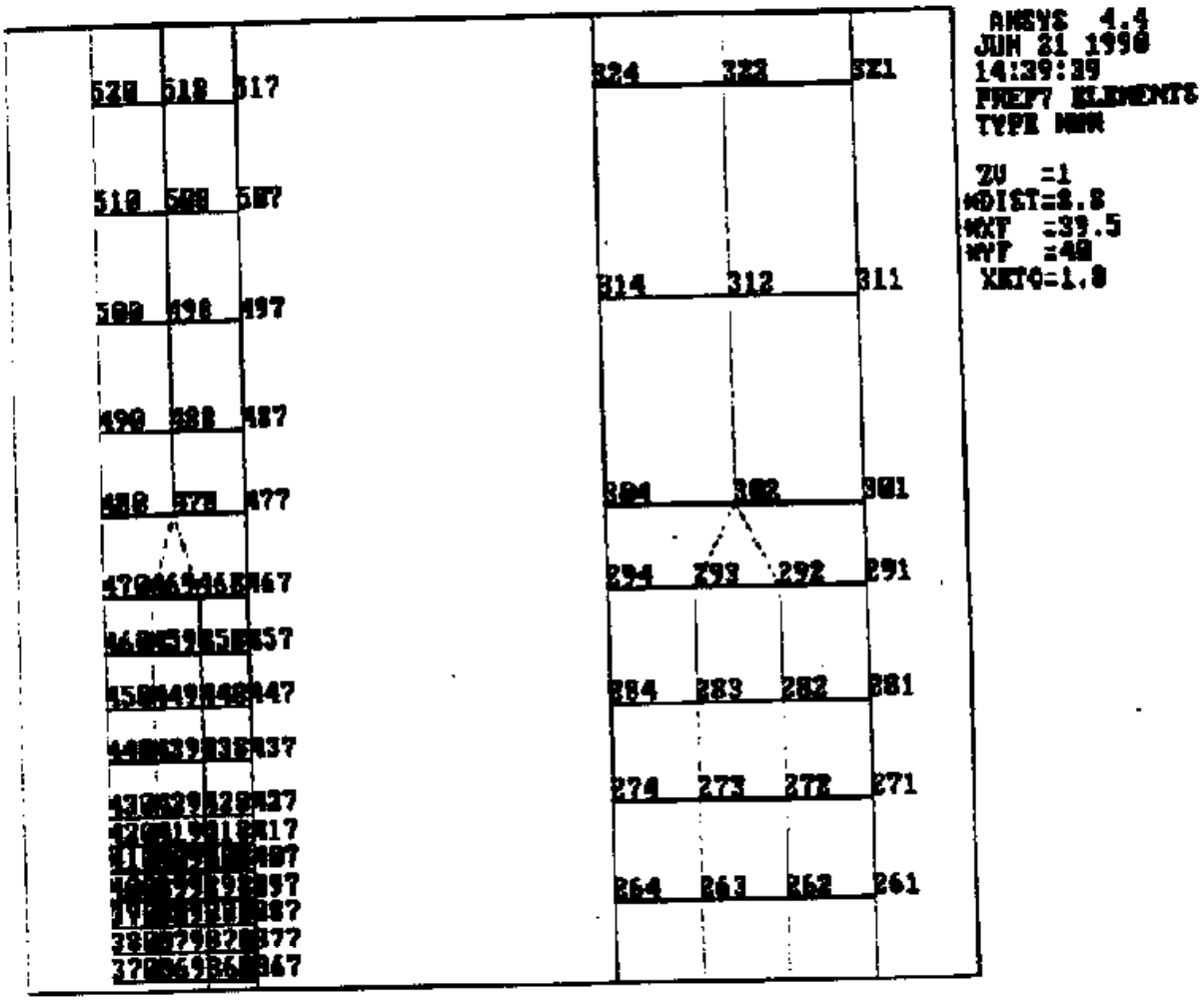

Figure 2.10.2-17 Cask Lower Shell (Region G) - NAC-STC ANSYS Bottom Fine Mesh Three-Dimensional Model

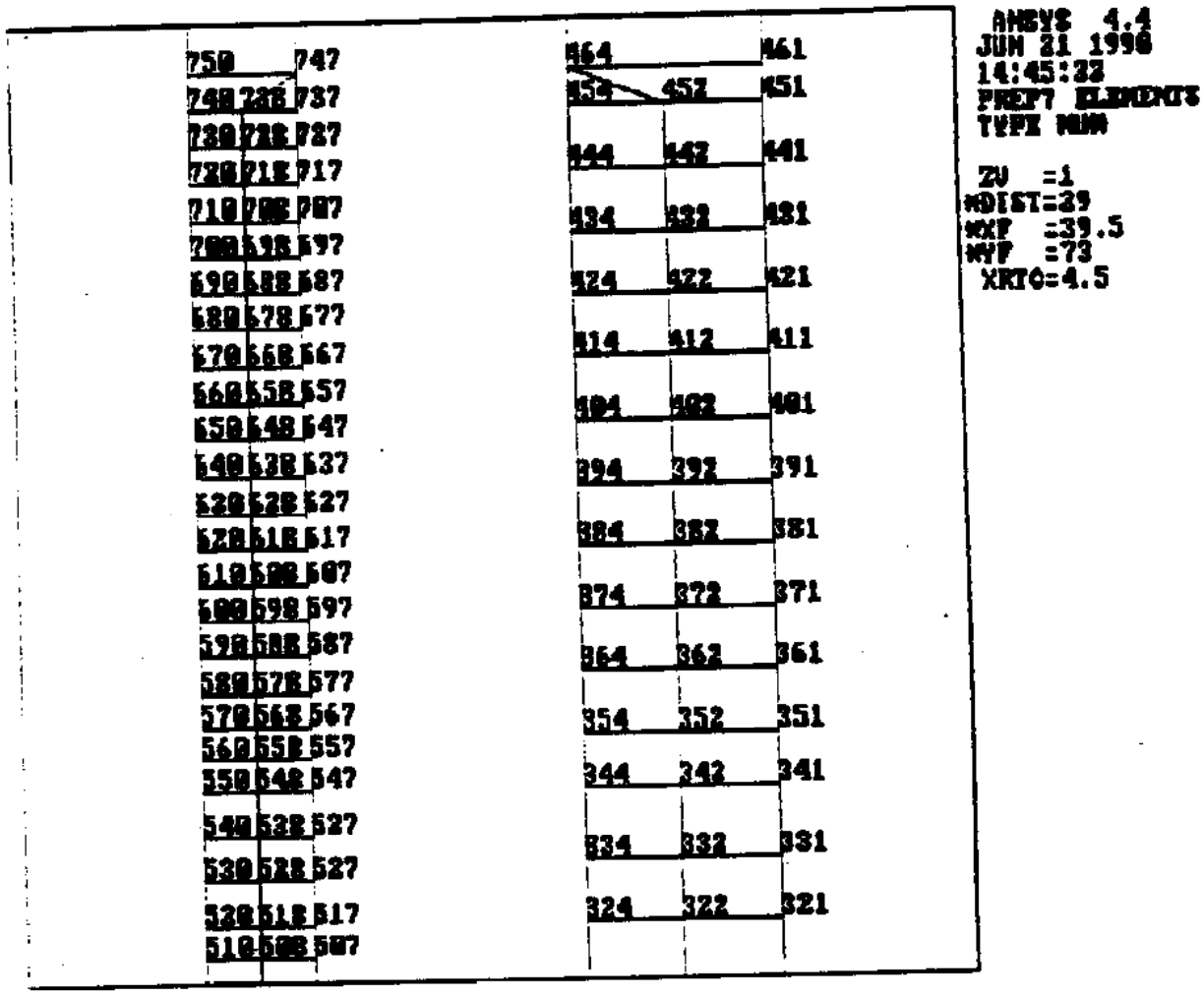

Figure 2.10.2-18 Cask Upper Shell (Region H) - NAC-STC ANSYS Bottom Fine Mesh Three-Dimensional Model

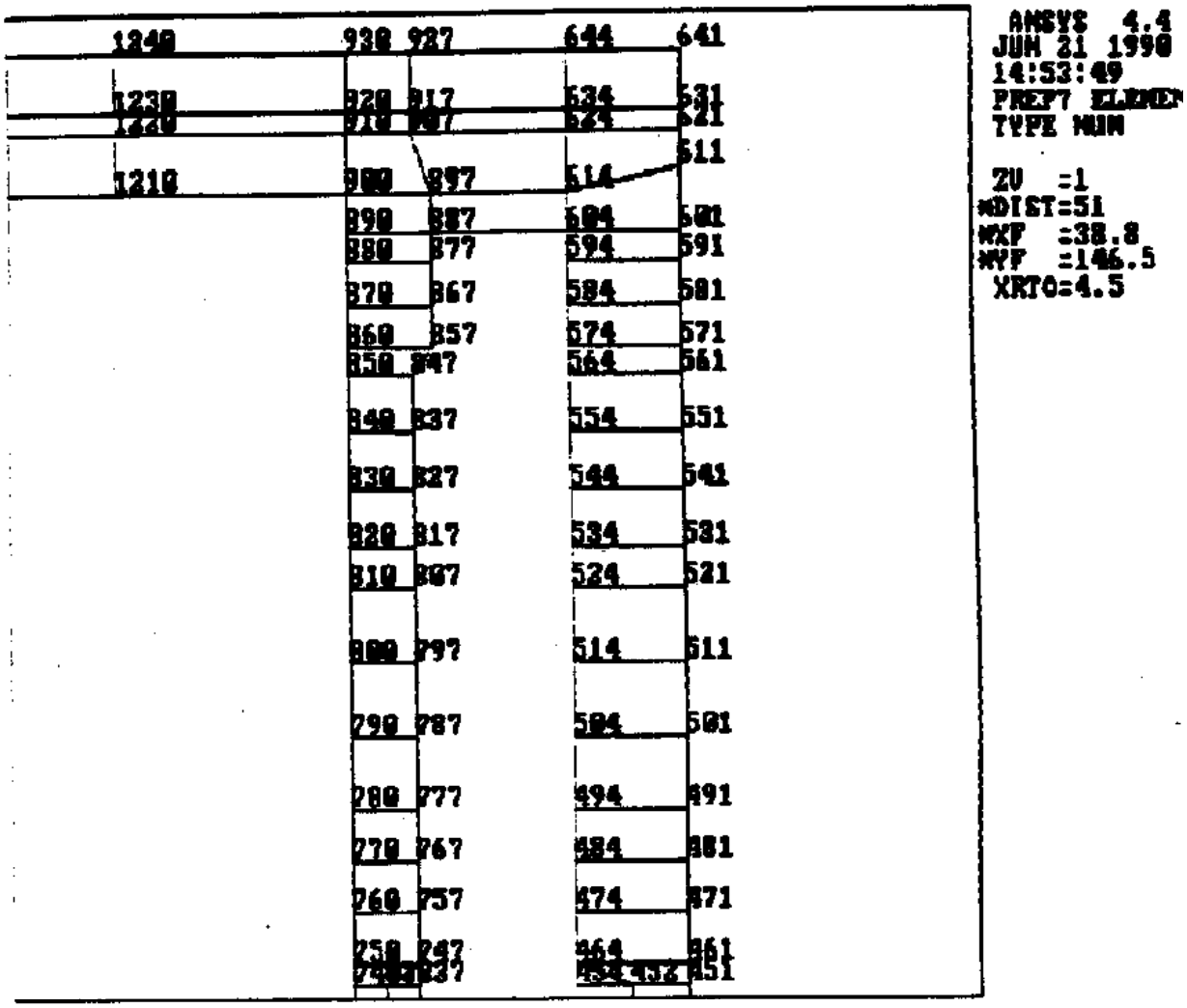

Figure 2.10.2-19 Cask Lids (Region I) - NAC-STC ANSYS Bottom Fine Mesh Three-Dimensional Model

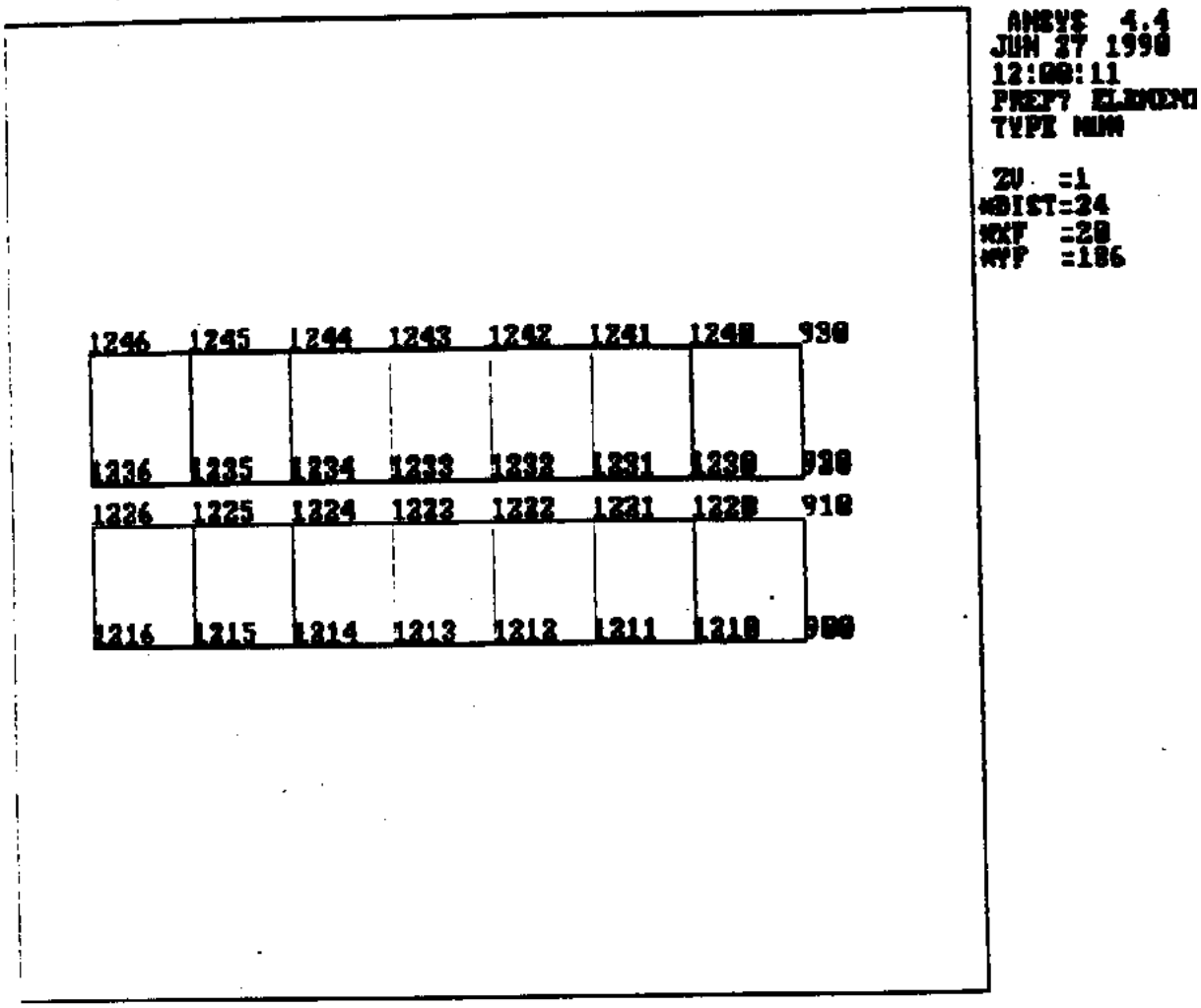

Figure 2.10.2-20 ANSYS Three-Dimensional Top Fine Mesh Finite Element Model - NAC-STC

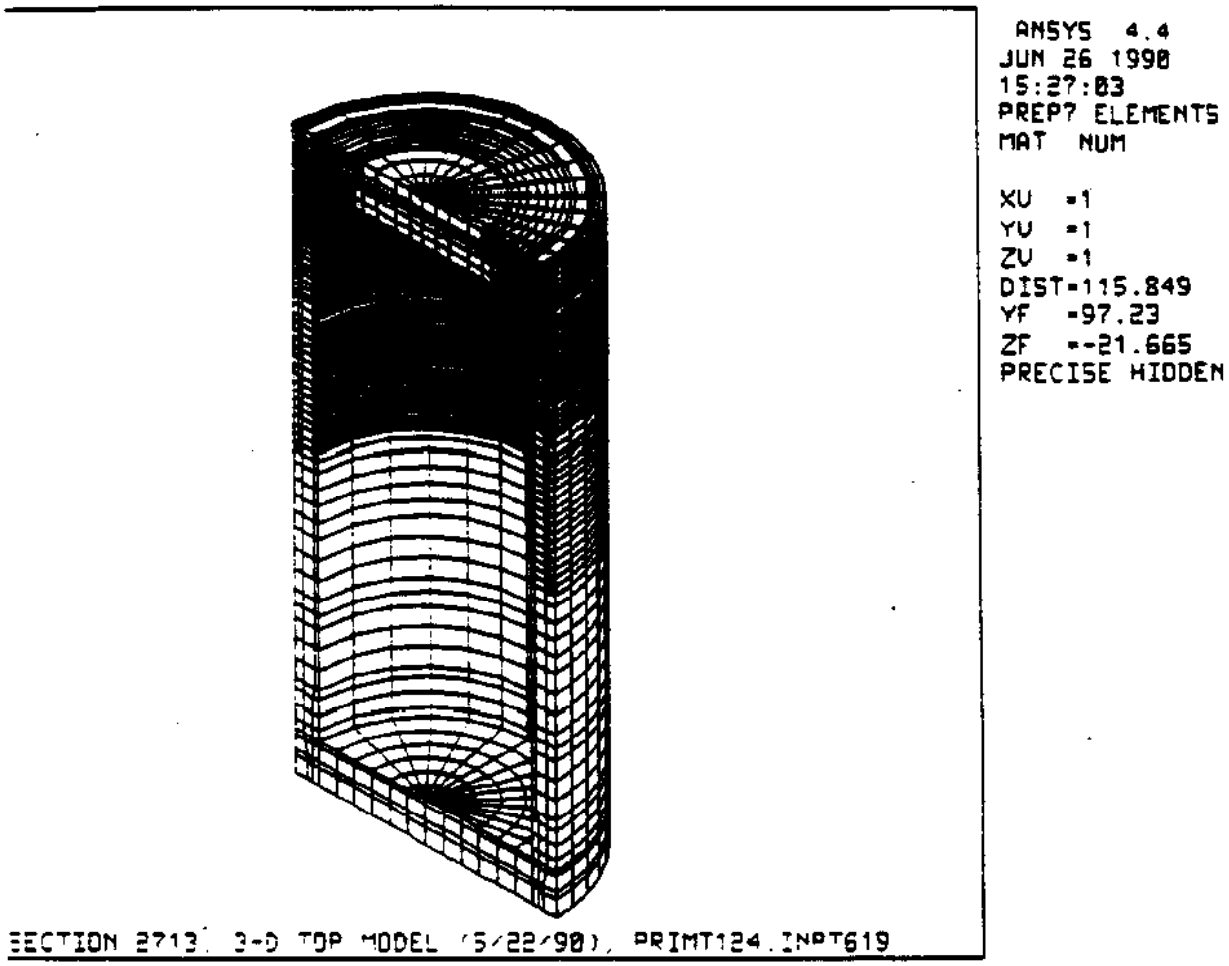

Figure 2.10.2-21 Upper Half of NAC-STC ANSYS Three-Dimensional Top Fine Mesh Finite Element Model

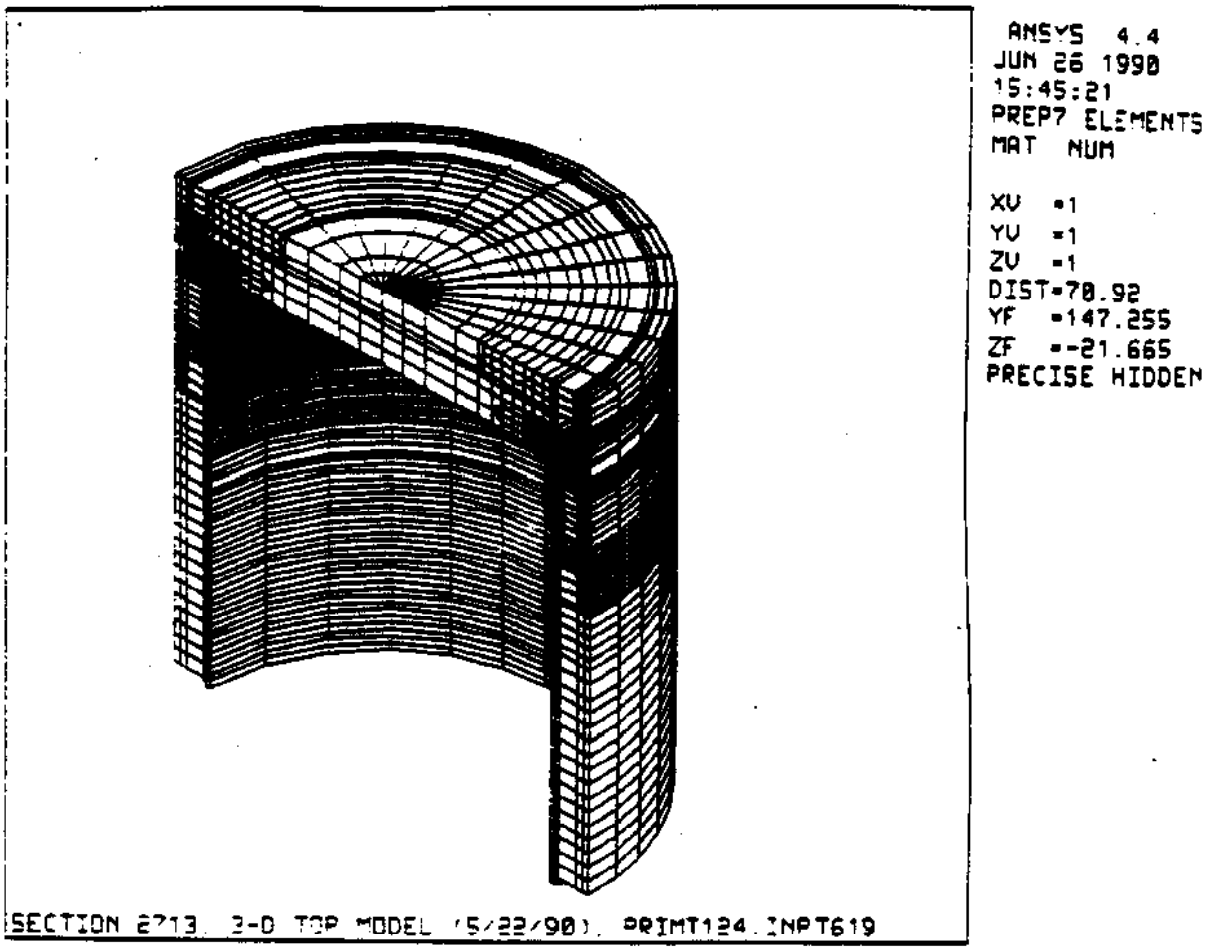

Figure 2.10.2-22 Details - NAC-STC ANSYS Three-Dimensional Top Fine Mesh Model

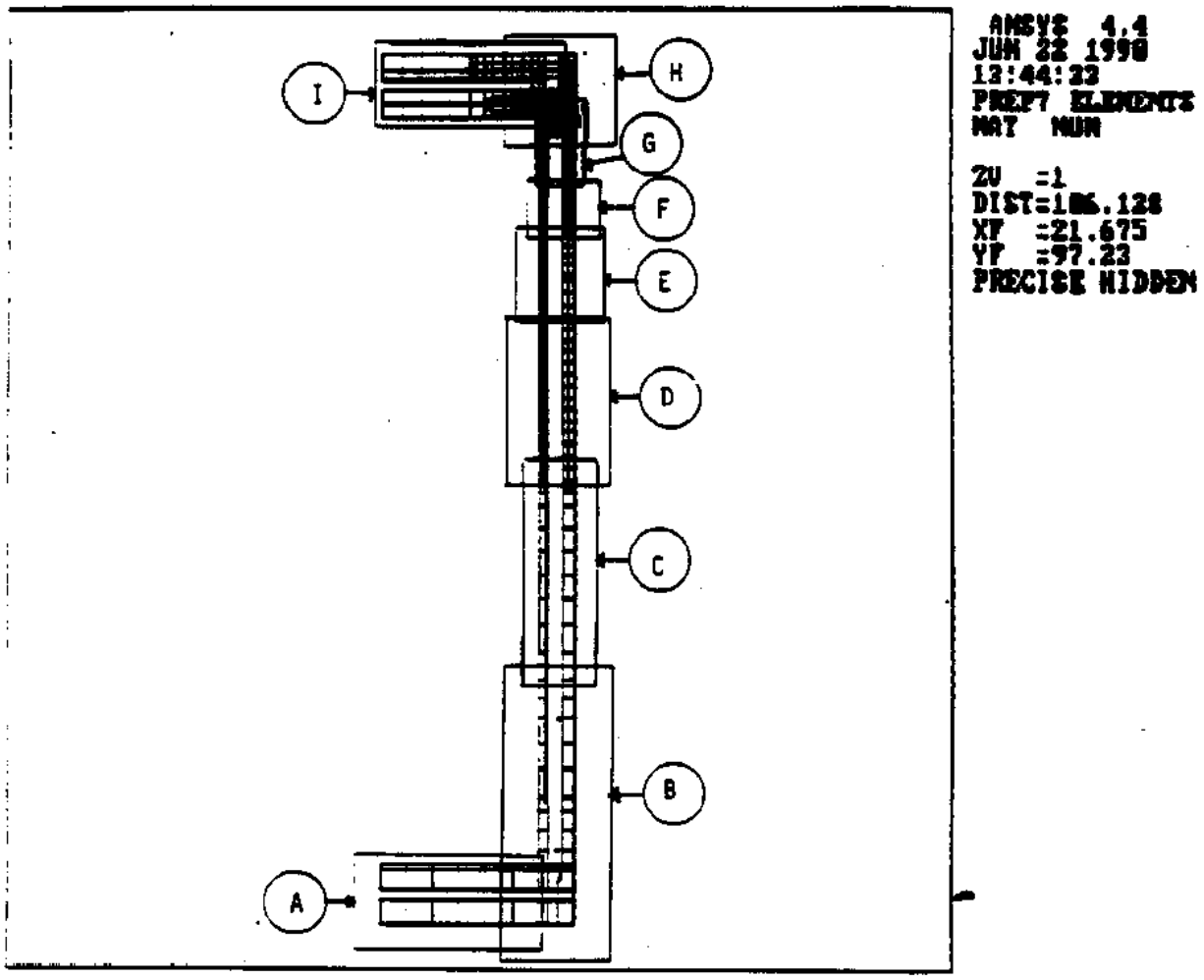

Figure 2.10.2-23 Cask Bottom (Region A) - NAC-STC ANSYS Top Fine Mesh Three-Dimensional Model

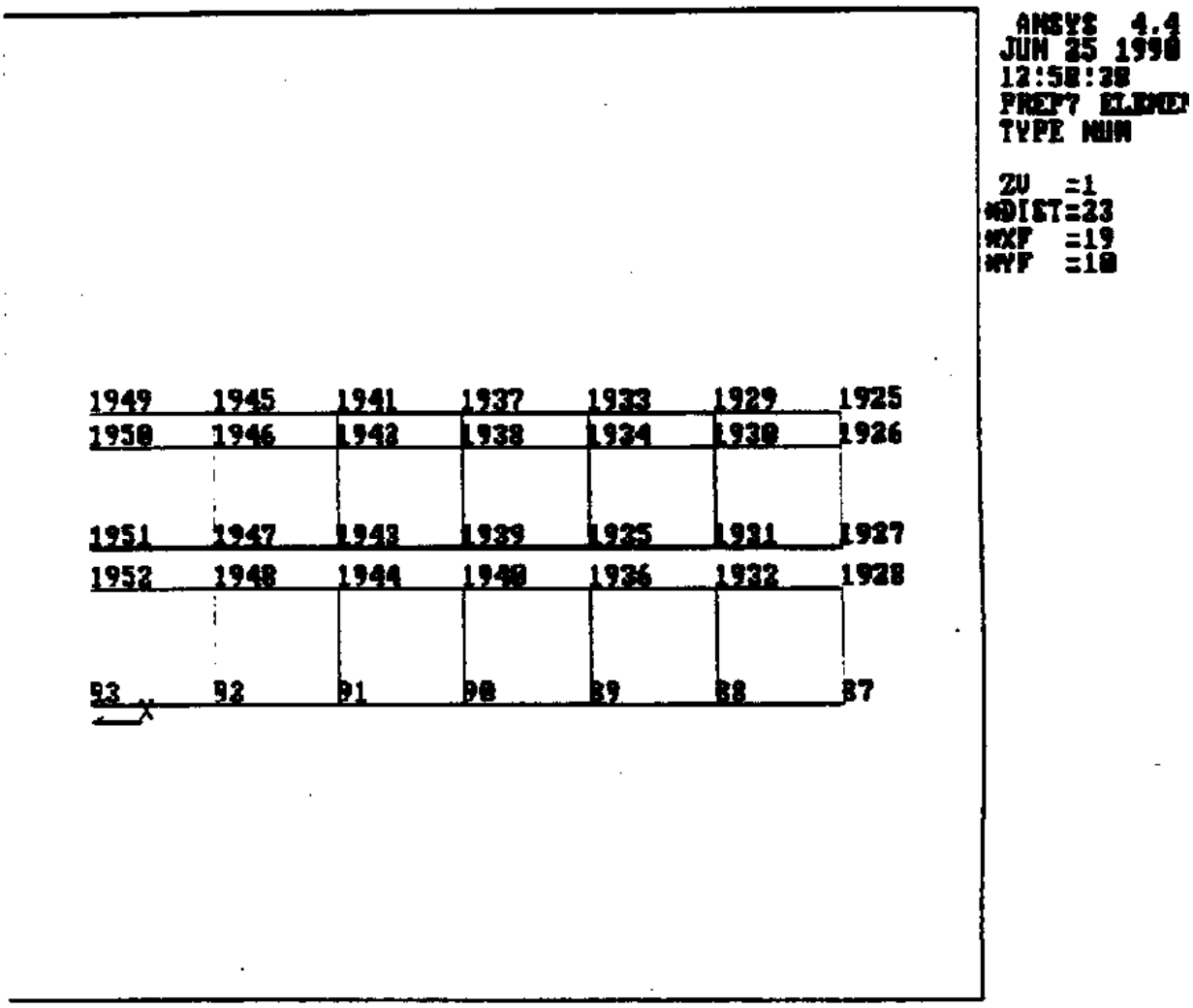

Figure 2.10.2-24 Cask Lower Transition (Region B) - NAC-STC ANSYS Top Fine Mesh Three-Dimensional Model

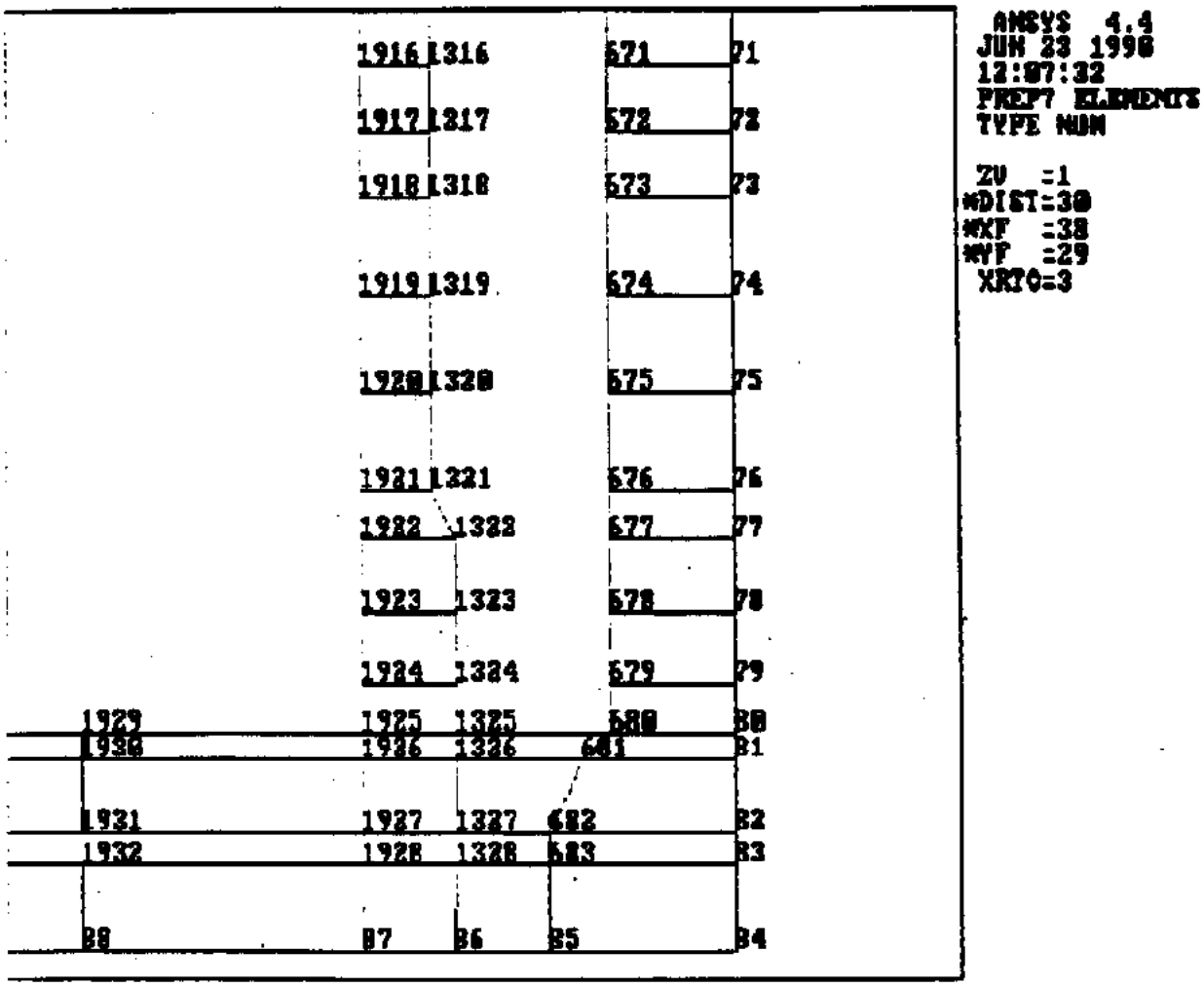

Figure 2.10.2-25 Cask Lower Shell (Region C) - NAC-STC ANSYS Top Fine Mesh Three-Dimensional Model

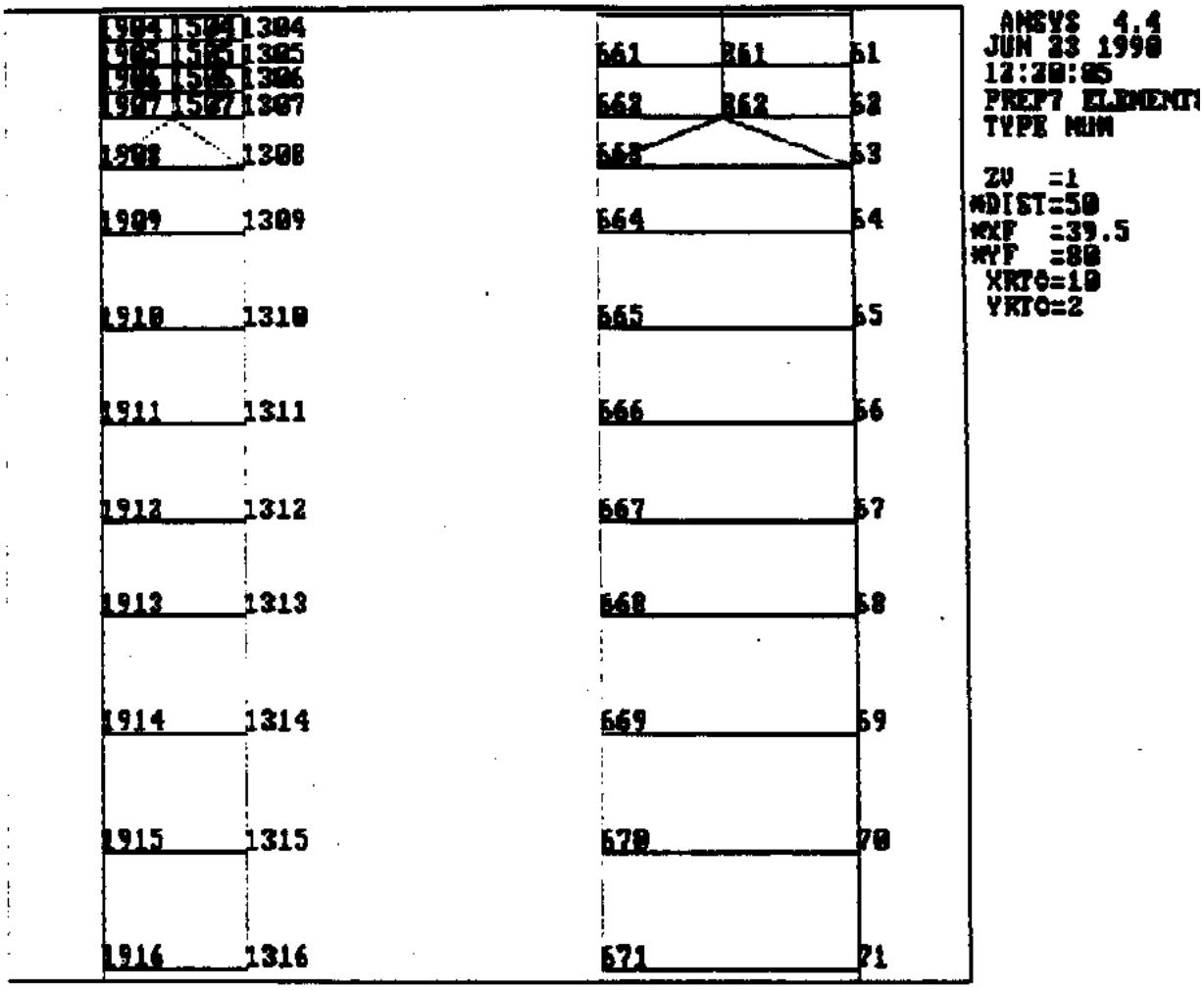

Figure 2.10.2-26 Cask Middle Shell (Region D) - NAC-STC ANSYS Top Fine Mesh Three-Dimensional Model

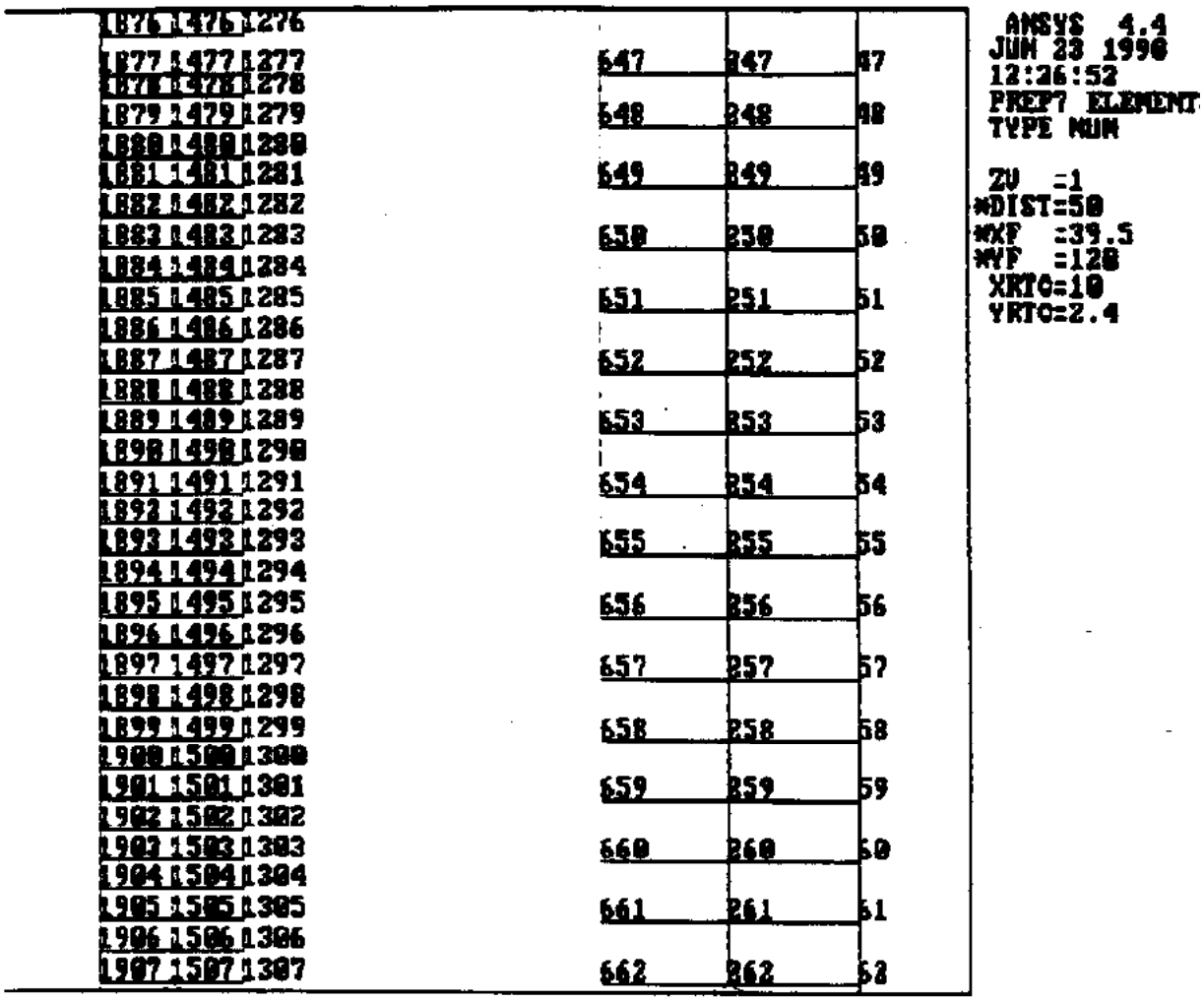

Figure 2.10.2-27 Cask Upper Shell (Region E) - NAC-STC ANSYS Top Fine Mesh Three-Dimensional Model

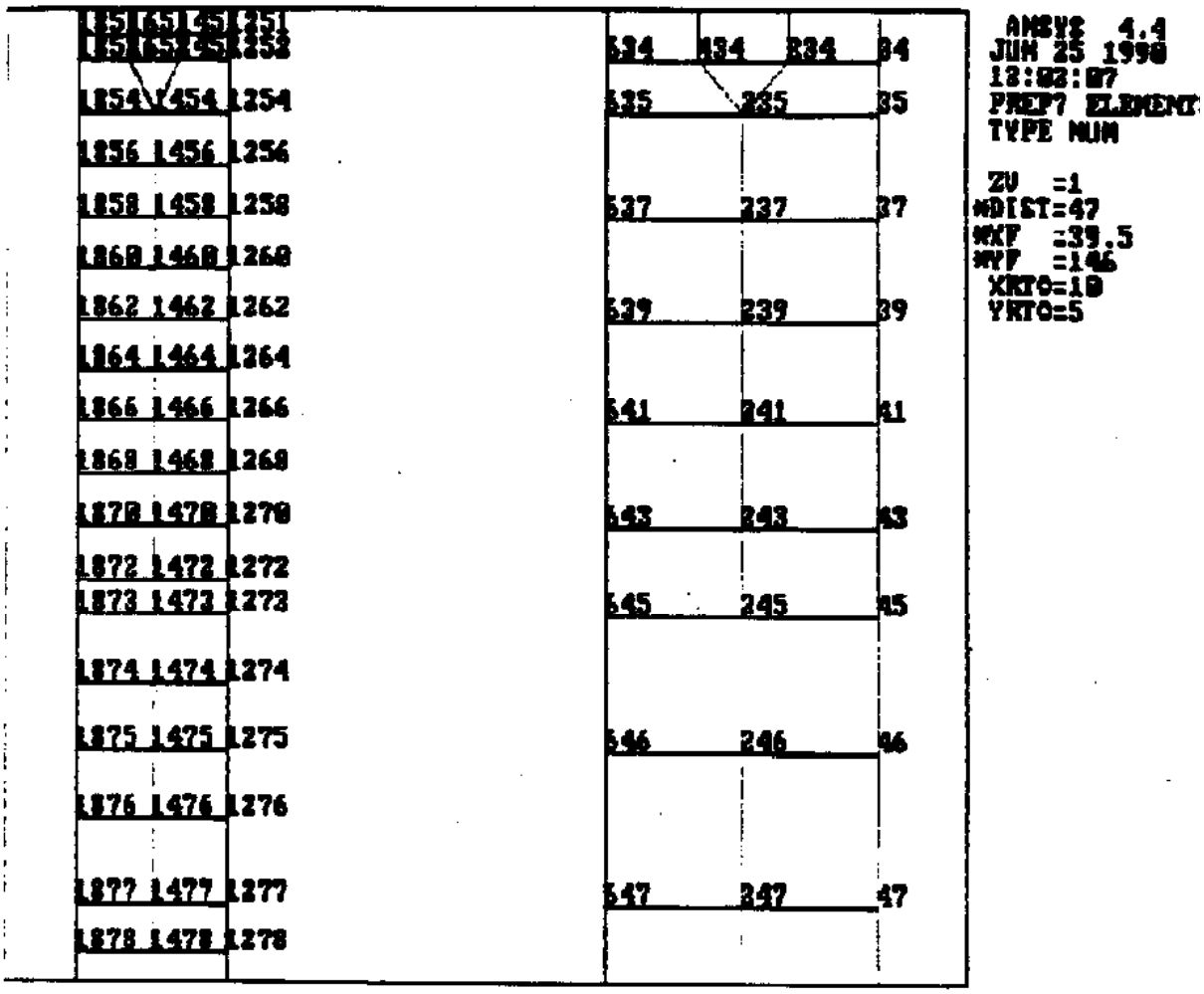

Figure 2.10.2-28 Cask Upper Transition (Region F) - NAC-STC ANSYS Top Fine Mesh Three-Dimensional Model

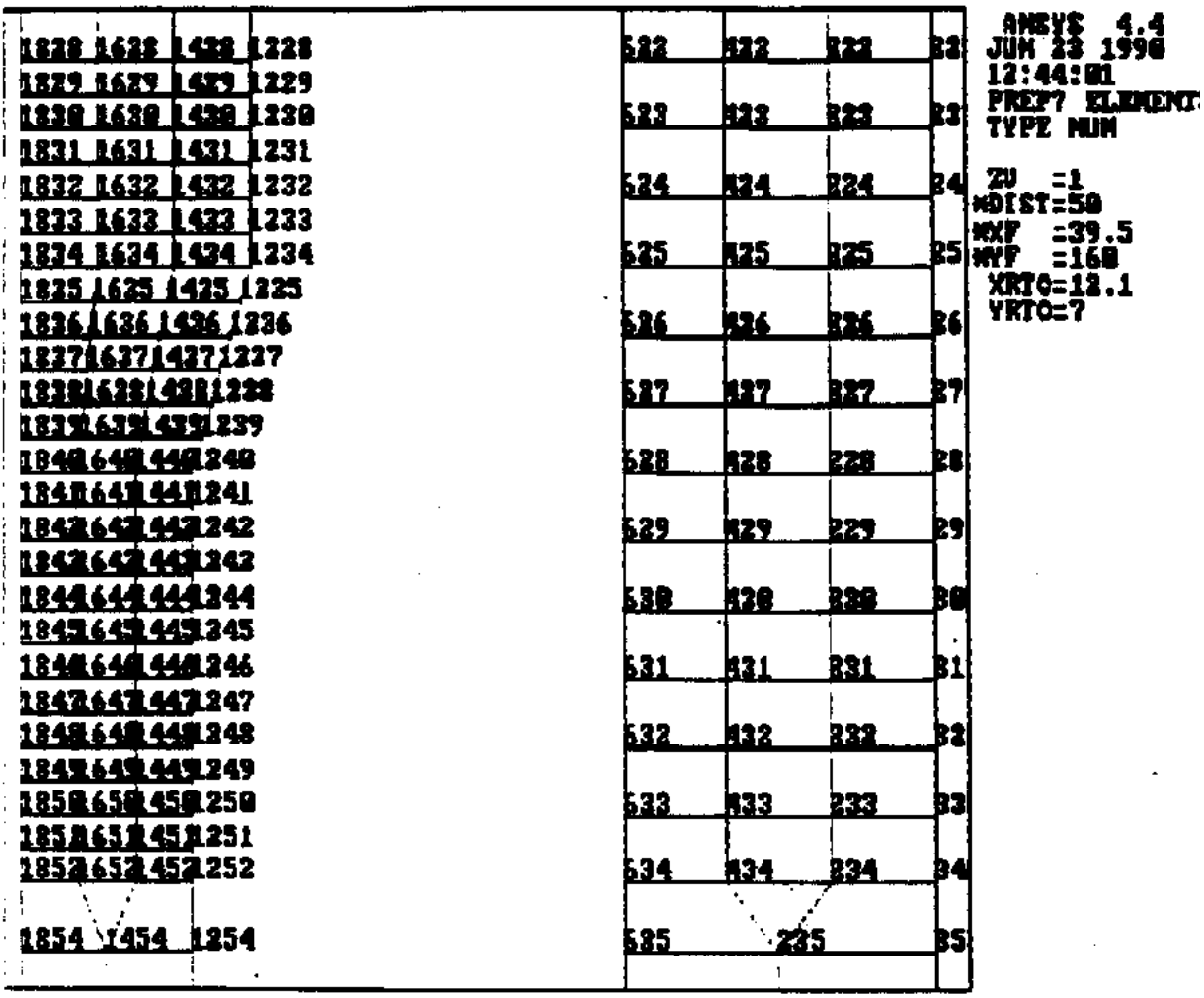

Figure 2.10.2-29 Cask Upper Transition (Region G) - NAC-STC ANSYS Top Fine Mesh Three-Dimensional Model

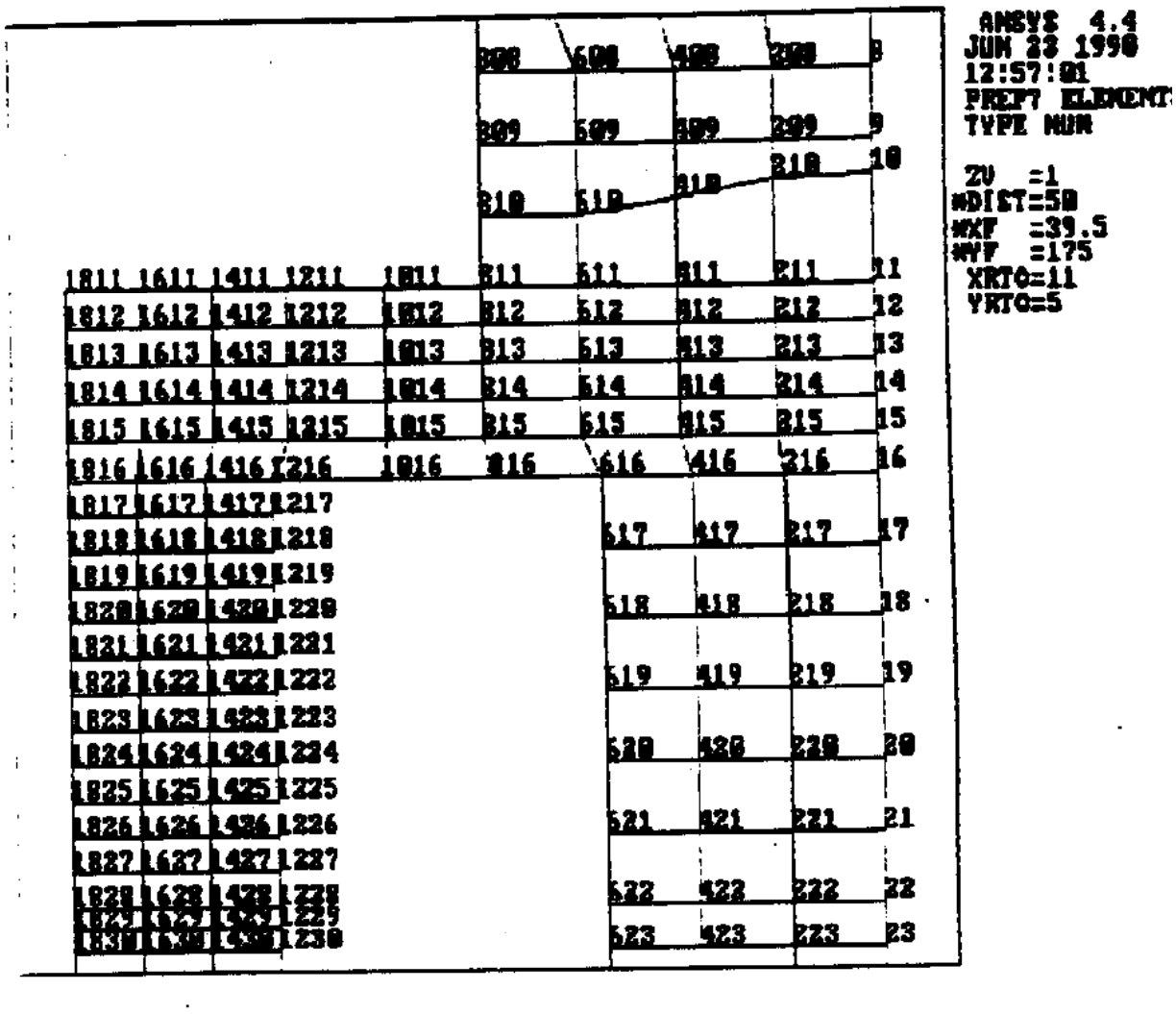

Figure 2.10.2-30 Cask Top Forging (Region H) - NAC-STC ANSYS Top Fine Mesh Three-Dimensional Model

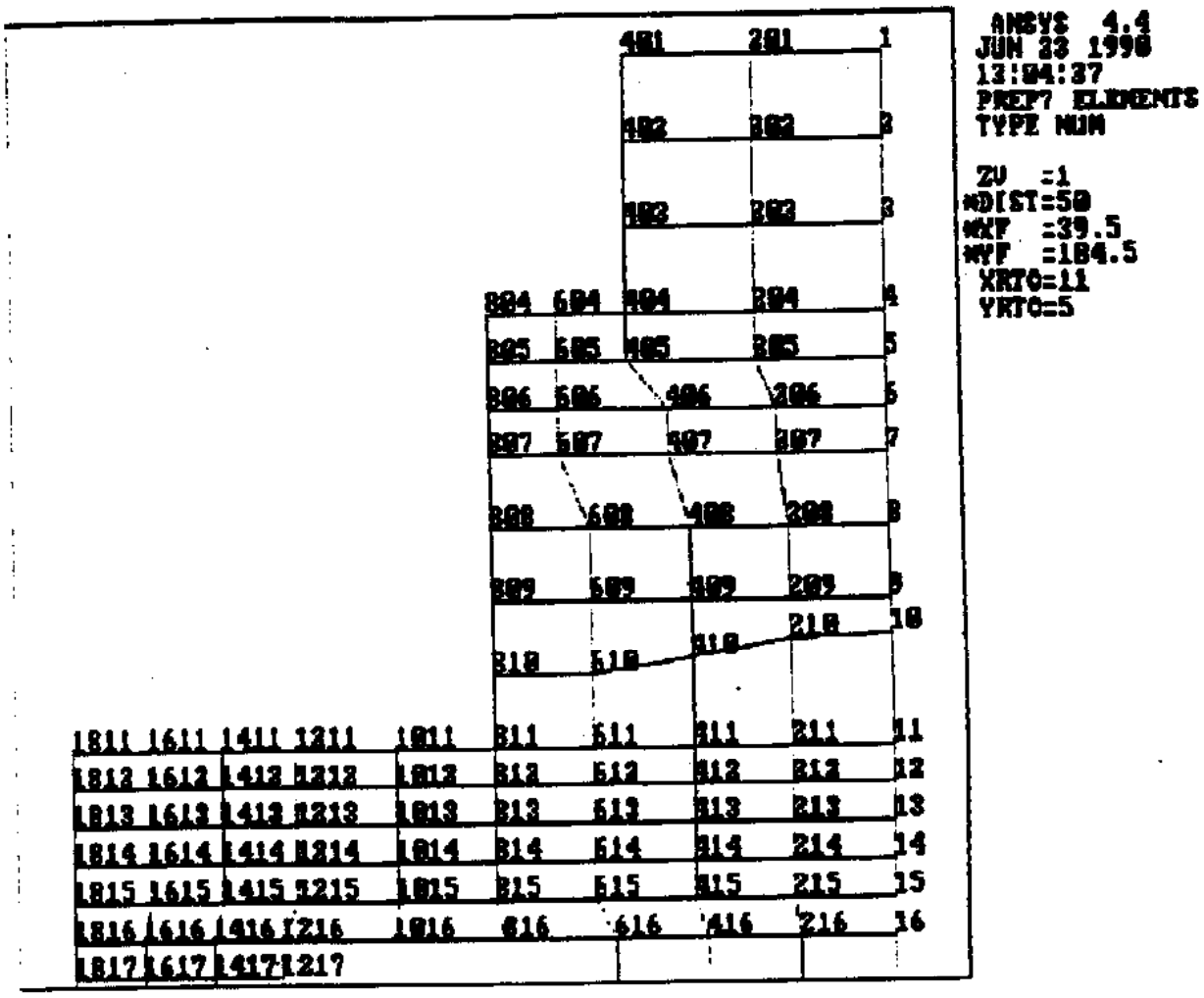

Figure 2.10.2-31 Cask Lids (Region I) - NAC-STC ANSYS Top Fine Mesh Three-Dimensional Model

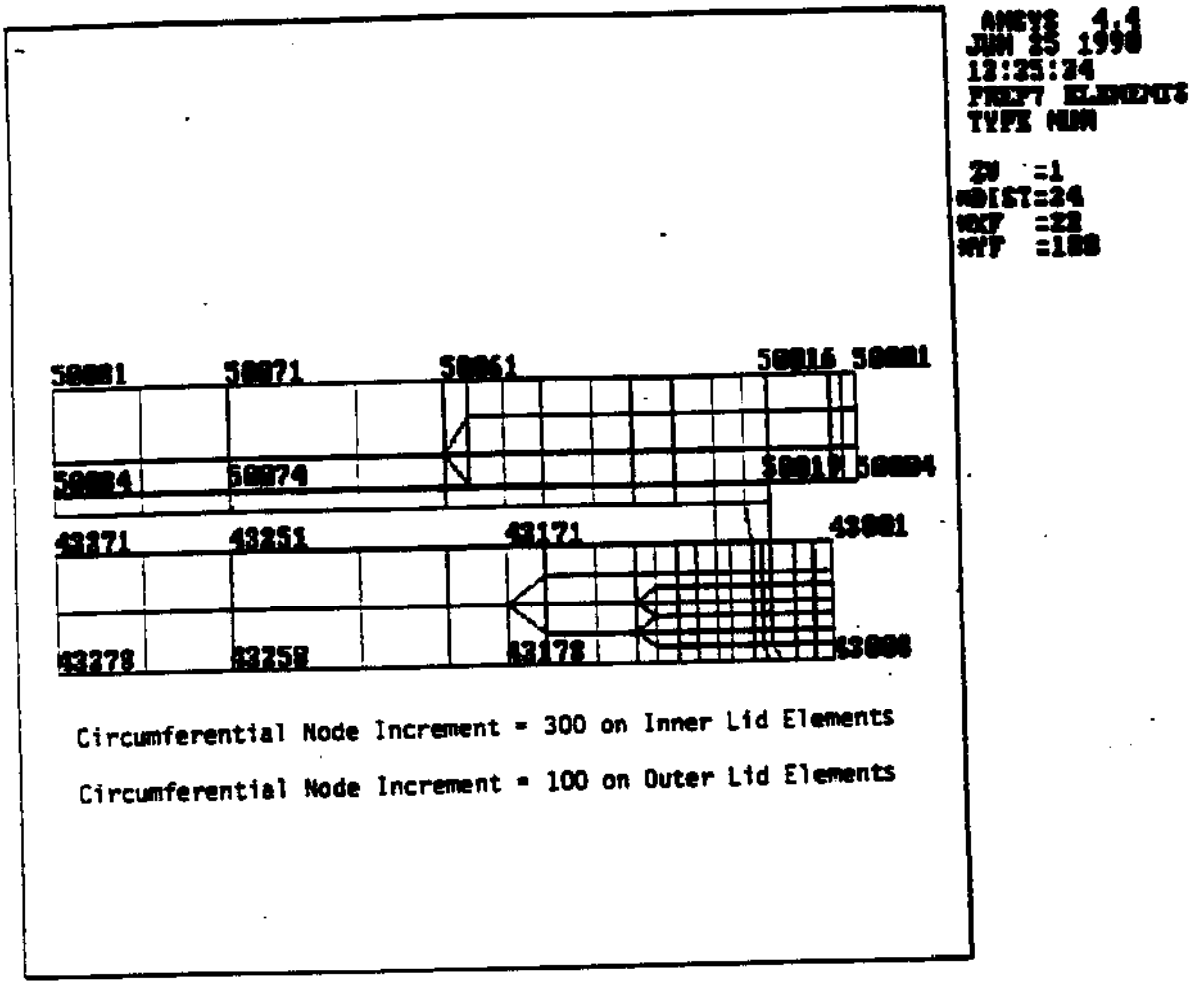

Figure 2.10.2-32 Load Distribution for Cask Side Drop Impact

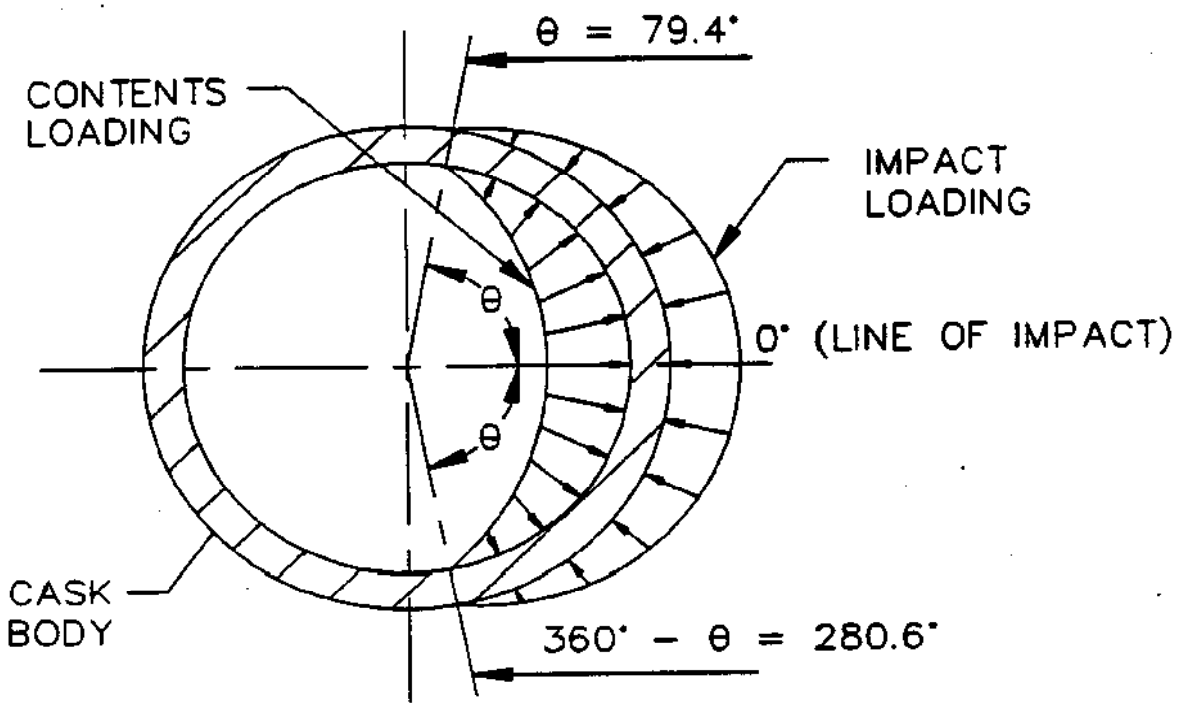

Figure 2.10.2-33 ANSYS Finite Element Model - Structural Component Identification

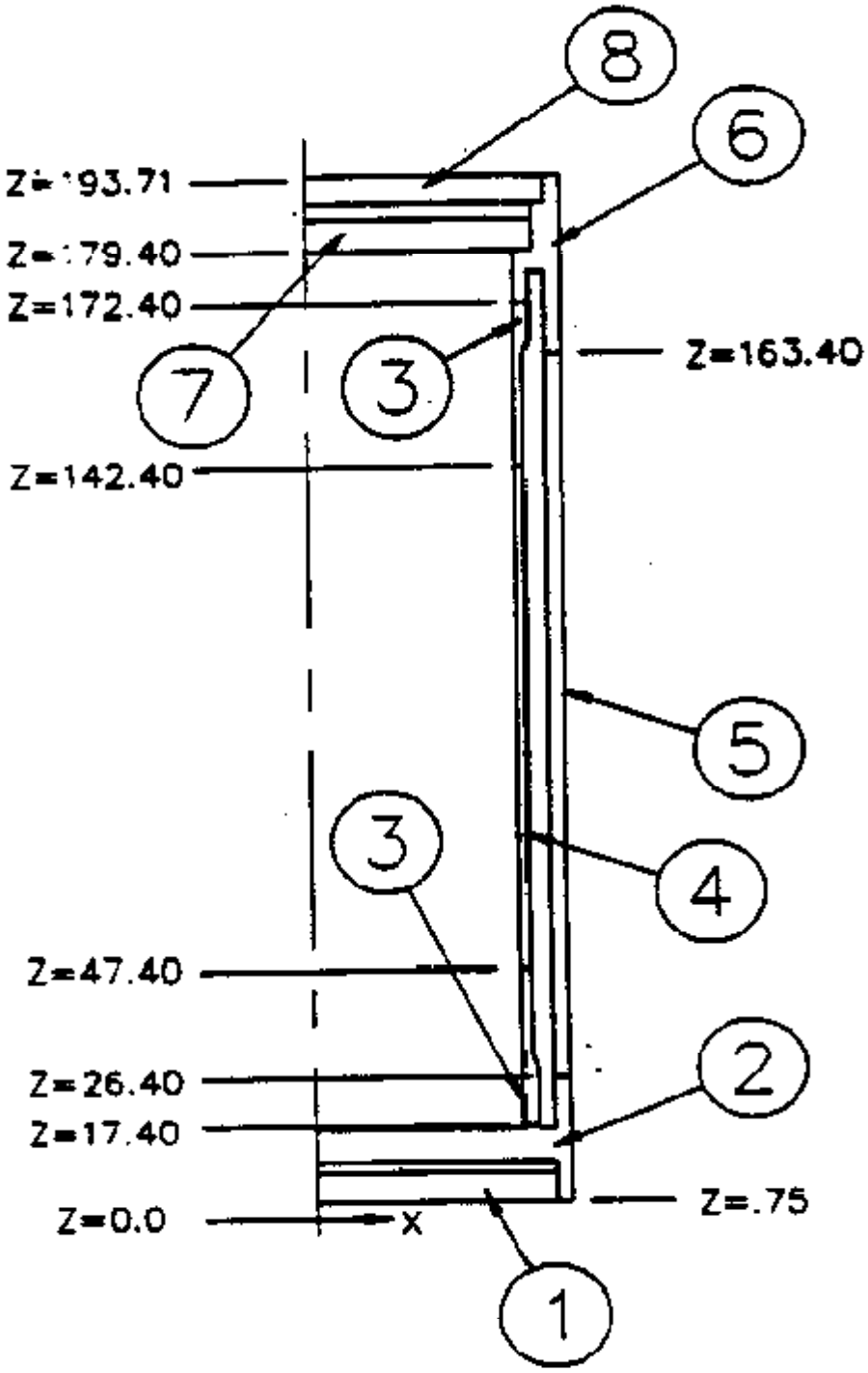

Figure 2.10.2-34 ANSYS Finite Element Model - Representative Section Locations

FIGURE WITHHELD UNDER 10 CFR 2.390

Figure 2.10.2-35 Circular Nodal Locations - NAC-STC ANSYS Three-Dimensional Model

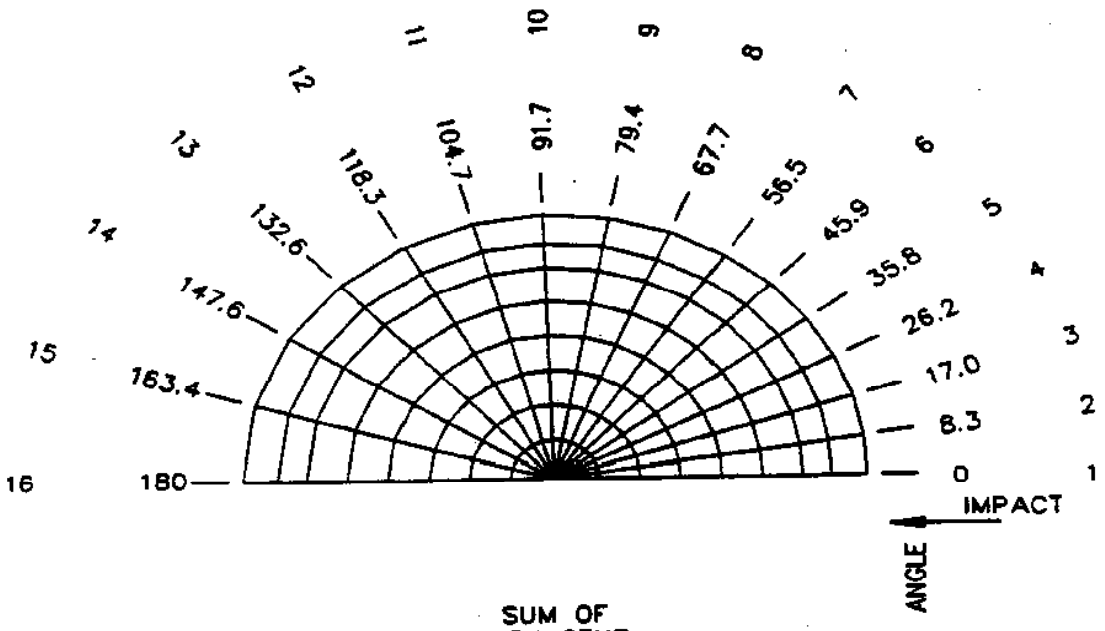

NODE LOCATION	SUM OF ADJACENT HALF ANGLES	CIRCUMFERENCE %
1	4.2	2.33
2	8.5	4.72
3	9.0	5.00
4	9.4	5.22
5	9.9	5.50
6	10.4	5.77
7	10.9	6.05
8	11.5	6.39
9	12.0	6.67
10	12.7	7.06
11	13.3	7.38
12	14.0	7.78
13	14.7	8.17
14	15.4	8.56
15	16.2	9.00
16	8.3	4.61

Figure 2.10.2-36 Nodal Identification - NAC-STC ANSYS Three-Dimensional Model

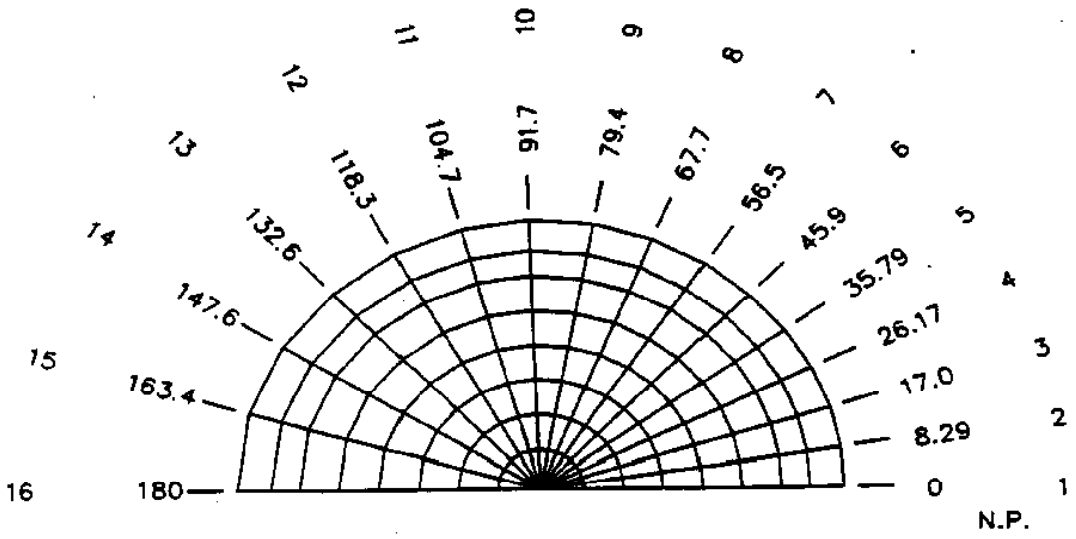

NODE LOCATION	ANGLE	NODES
1	0	1–2000
2	8.29	2001–4000
3	17.0	4001–6000
4	26.17	6001–8000
5	35.79	8001–10000
6	45.9	10001–12000
7	56.5	12001–14000
8	67.7	14001–16000
9	79.4	16001–18000
10	91.7	18001–20000
11	104.7	20001–22000
12	118.3	22001–24000
13	132.6	24001–26000
14	147.6	26001–28000
15	163.4	28001–30000
16	180.0	30001–32000

Table 2.10.2-1 Tabulation of Circumferential Mesh Spacing - ANSYS Three-Dimensional Top and Bottom Fine Mesh Models

Circumferential Plane Identification Number	Angular Location θ (degrees)	Angular Spacing Increment (degrees)
1	0.0	---
2	8.3	8.3
3	17.0	8.7
4	26.2	9.2
5	35.8	9.6
6	45.9	10.1
7	56.5	10.6
8	67.7	11.2
9	79.4	11.7
10	91.7	12.3
11	104.7	13.0
12	118.3	13.6
13	132.6	14.3
14	147.6	15.0
15	163.4	15.8
16	180.0	16.6

Table 2.10.2-2 Circumferential Plane - Percentage of 180° Arc

Circumferential Plane Identification No.	Real Constant Numbers		Sum of Adjacent Half-Angles	Percentage of 180° Arc
	Inner Bolts	Outer Bolts		
1	14	31	(1/2)(8.3) = 4.2	0.0233
2	15	32	(1/2)(8.3 + 8.7) = 8.5	0.0472
3	16	33	(1/2)(8.7 + 9.2) = 9.0	0.0500
4	17	34	(1/2)(9.2 + 9.6) = 9.4	0.0522
5	18	35	(1/2)(9.6 + 10.1) = 9.9	0.0550
6	19	36	(1/2)(10.1 + 10.6) = 10.4	0.0577
7	20	37	(1/2)(10.6 + 11.2) = 10.9	0.0605
8	21	38	(1/2)(11.2 + 11.7) = 11.5	0.0639
9	22	39	(1/2)(11.7 + 12.3) = 12.0	0.0667
10	23	40	(1/2)(12.3 + 13.0) = 12.7	0.0706
11	24	41	(1/2)(13.0 + 13.6) = 13.3	0.0738
12	25	42	(1/2)(13.6 + 14.3) = 14.0	0.0778
13	26	43	(1/2)(14.3 + 15.0) = 14.7	0.0817
14	27	44	(1/2)(15.0 + 15.8) = 15.4	0.0856
15	28	45	(1/2)(15.8 + 16.6) = 16.2	0.0900
16	29	46	(1/2)(16.6) = 8.3	0.0461

Table 2.10.2-3 Effective Inner Lid Bolt Properties

Circumferential Plane Identification No.	Real Constant Numbers	Area	I_{zz}/I_{yy}	T_{kz}/T_{ky}	$\left(\frac{\text{Shear z}}{\text{Shear y}}\right)$
1	14	0.7300	0.0785	1.378	1.11
2	15	1.4790	0.1590	1.378	1.11
3	16	1.5665	0.1684	1.378	1.11
4	17	1.6354	0.1758	1.378	1.11
5	18	1.723	0.1852	1.378	1.11
6	19	1.8077	0.1943	1.378	1.11
7	20	1.8955	0.2037	1.378	1.11
8	21	2.0020	0.2152	1.378	1.11
9	22	2.0897	0.2246	1.378	1.11
10	23	2.2119	0.2377	1.378	1.11
11	24	2.3122	0.2485	1.378	1.11
12	25	2.4375	0.2620	1.378	1.11
13	26	2.5500	0.2751	1.378	1.11
14	27	2.6818	0.2883	1.378	1.11
15	28	2.8197	0.3031	1.378	1.11
16	29	1.4443	0.1552	1.378	1.11

Table 2.10.2-4 Outer Lid Effective Bolt Properties

Circumferential Plane Identification No.	Real Constant Numbers	Area	I_{zz}/I_{yy}	T_{kz}/T_{ky}	$\left(\frac{\text{Shear z}}{\text{Shear y}}\right)$
1	31	0.2342	0.0105	0.879	1.11
2	32	0.5149	0.2124	0.879	1.11
3	33	0.5454	0.0225	0.879	1.11
4	34	0.5694	0.0235	0.879	1.11
5	35	0.5999	0.0248	0.879	1.11
6	36	0.6294	0.0260	0.879	1.11
7	37	0.6599	0.0272	0.879	1.11
8	38	0.6970	0.0288	0.879	1.11
9	39	0.7276	0.0300	0.879	1.11
10	40	0.7701	0.0318	0.879	1.11
11	41	0.8050	0.0332	0.879	1.11
12	42	0.8486	0.0350	0.879	1.11
13	43	0.8912	0.0378	0.879	1.11
14	44	0.9337	0.0385	0.879	1.11
15	45	0.9817	0.0405	0.879	1.11
16	46	0.5029	0.0207	0.879	1.11

Table 2.10.2-5 Identification of ANSYS Model Structural Components, Material and Allowables; Condition 1

Condition 1: 100°F Ambient with Contents

Comp ID.	Description	Material	Mat ID	Max Temp.	Allowable Stress (ksi) Normal P_m (S_m)	Normal P_m+P_b ($1.5S_m$)	Accident P_m ($0.7S_u$)	Accident P_m+P_b (S_u)
1	Bottom Plate	304SS	5	350	19.2	28.7	45.6	65.2
2	Bottom Forging	304SS	6	417	18.5	27.7	44.9	64.2
3	Transition Shell	XM-19SS	15	300	31.4	47.1	66.0	94.3
4	Inner Shell	304SS	7	331	19.6	29.4	45.8	65.5
5	Outer Shell	304SS	8	292	20.0	30.0	46.4	66.4
6	Top Forging	304SS	9	211	20.0	30.0	49.3	70.9
7	Inner Lid	304SS	10	223	20.0	30.0	48.0[1]	69.8
8	Outer Lid	17-4 PH SS	11	178	45.0	67.5	94.5	135.0
9	Inner Lid Bolt	SB-637 Ni	13	190		144.4[2]		144.4[2]
10	Outer Lid Bolt	17-4 PH SS	12	178		98.8[2]		98.8[2]

[1] 2.4 S_m governs.

[2] Bolt allowables based on material yield strength.

Table 2.10.2-6 Deleted

Table 2.10.2-7 Deleted

Table 2.10.2-8 Section Cut Identification - (2-D Model)

Section[1]	Inside Node Radial (in)	Inside Node Axial (in)	Outside Node Radial (in)	Outside Node Axial (in)
A	0.00	14.40	0.00	8.20
B	0.00	6.20	0.00	0.75
C	35.50	14.40	35.50	8.20
D	39.44	6.20	39.44	0.75
E	39.44	8.20	43.35	8.20
F	35.50	14.40	37.50	14.40
G	40.70	14.40	43.35	14.40
H	35.50	29.40	37.00	29.40
I	40.70	29.40	43.35	29.40
J	35.50	55.65	37.00	55.65
K	40.70	55.65	43.35	55.65
L	35.50	96.90	37.00	96.90
M	40.70	96.90	43.35	96.90
N	35.50	138.15	37.00	138.15
O	40.70	138.15	43.35	138.15
P	35.50	160.40	37.00	160.40
Q	40.70	160.40	43.35	160.40
R	35.50	175.40	37.00	175.40
S	40.70	175.40	43.35	175.40
T	39.56	179.40	43.35	179.40
U	35.50	179.40	35.50	185.40
V	35.21	188.40	35.21	193.71
W	0.00	179.40	0.00	185.40
X	0.00	188.46	0.00	193.71

[1] Refer to Figure 2.10.2-34 for the section cut locations.

Table 2.10.2-9 Section Cut Identification - (3-D Bottom Fine Mesh Model)

Section[1]	Inside Node Radial (in)	Inside Node Axial (in)	Outside Node Radial (in)	Outside Node Axial (in)
A	0.00	14.40	0.00	8.20
B	0.00	6.20	0.00	0.75
C	35.50	14.40	35.50	8.20
D	39.44	6.20	39.44	0.75
E	39.44	8.20	43.35	8.20
F	35.50	15.00[2]	37.50	15.00[2]
G	40.70	15.00[2]	43.35	15.00[2]
H	35.50	29.40	37.00	29.40
I	40.70	29.40	43.35	29.40
J	35.50	55.65	37.00	55.65
K	40.70	55.65	43.35	55.65
L	35.50	96.90	37.00	96.90
M	40.70	96.90	43.35	96.90
N	35.50	138.15	37.00	138.15
O	40.70	138.15	43.35	138.15
P	35.50	160.40	37.00	160.40
Q	40.70	160.40	43.35	160.40
R	35.50	175.40	37.50	175.40
S	40.70	175.40	43.35	175.40
T	40.70	179.40	43.35	181.68[3]
U	35.50	179.40	35.50	185.40
V	35.50[4]	187.40	35.50[4]	193.71
W	0.00	179.40	0.00	185.40
X	0.00	187.40	0.00	193.71

1 Refer to Figure 2.10.2-34 for the section cut locations

2 Moved one section up from the root (Y = 14.40”) to pick up higher stresses

3 Moved up for impact pressure specification

4 No nodes at outer lid bolt circle for three-dimensional bottom model

Table 2.10.2-10 Section Cut Identification - (3-D Top Fine Mesh Model)

Section[1]	Inside Node Radial (in)	Inside Node Axial (in)	Outside Node Radial (in)	Outside Node Axial (in)
A	0.00	14.40	0.00	8.20
B	0.00	6.20	0.00	0.75
C	35.50	14.40	35.50	8.20
D	39.44	6.20	39.44	0.75
E	39.44	8.20	43.35	8.20
F	35.50	14.40	37.50	14.40
G	40.70	14.40	43.35	14.40
H	35.50	29.40	37.00	29.40
I	40.70	29.40	43.35	29.40
J	35.50	55.65	37.00	55.65
K	40.70	55.65	43.35	55.65
L	35.50	96.90	37.00	96.90
M	40.70	96.90	43.35	96.90
N	35.50	138.15	37.00	138.15
O	40.70	138.15	43.35	138.15
P	35.50	160.40	37.00	160.40
Q	40.70	160.40	43.35	160.40
R	35.50	175.40	37.50	175.40
S	40.70	175.40	43.35	175.40
T	39.56	179.40	43.35	179.40
U	35.50	179.41	35.50	185.40
V	35.21	188.40	35.21	193.71
W	0.00	179.40	0.00	185.40
X	0.00	188.46	0.00	193.71

[1] Refer to Figure 2.10.2-34 for the section cut locations

Table 2.10.2-11 Stress Point Locations - 2-D Model

Stress Point ID	Node	Location Radial (in)	Location Axial (in)
A-1	1	0.00	14.40
A-2	2	0.00	12.95
A-3	3	0.00	11.30
A-4	4	0.00	9.75
A-5	5	0.00	8.20
B-1	6	0.00	6.20
B-2	7	0.00	4.84
B-3	8	0.00	3.48
B-4	9	0.00	2.11
B-5	10	0.00	0.75
C-1	251	35.50	14.40
C-2	252	35.50	12.85
C-3	253	35.50	11.30
C-4	254	35.50	9.75
C-5	255	35.50	8.20
D-1	306	39.44	6.20
D-2	307	39.44	4.84
D-3	308	39.44	3.48
D-4	309	39.44	2.11
D-5	310	39.44	0.75
E-1	305	39.44	8.20
E-2	315	40.70	8.20
E-3	325	41.36	8.20
E-4	335	42.03	8.20
E-5	345	42.69	8.20
E-6	355	43.35	8.20

Table 2.10.2-11 Stress Point Locations - 2-D Model (continued)

Stress Point		Location	
		Radial	Axial
ID	Node	(in)	(in)
F-1	251	35.50	14.40
F-2	261	36.17	14.40
F-3	271	36.83	14.40
F-4	281	37.50	14.40
G-1	311	40.70	14.40
G-2	321	41.36	14.40
G-3	331	42.03	14.40
G-4	341	42.69	14.40
G-5	351	43.35	14.40
H-1	581	35.50	29.40
H-2	582	36.00	29.40
H-3	583	36.50	29.40
H-4	584	37.00	29.40
I-1	589	40.70	29.40
I-2	590	41.36	29.40
I-3	591	42.03	29.40
I-4	592	42.69	29.40
I-5	593	43.35	29.40
J-1	971	35.50	55.65
J-2	972	36.00	55.65
J-3	973	36.50	55.65
J-4	974	37.00	55.65
K-1	979	40.70	55.65
K-2	980	41.36	55.65
K-3	981	42.03	55.65

Table 2.10.2-11 Stress Point Locations - 2-D Model (continued)

Stress Point		Location	
		Radial	Axial
ID	Node	(in)	(in)
K-4	982	42.69	55.65
K-5	983	43.35	55.65
L-1	1601	35.50	96.90
L-2	1602	36.00	96.90
L-3	1603	36.50	96.90
L-4	1604	37.00	96.90
M-1	1609	40.70	96.90
M-2	1610	41.36	96.90
M-3	1611	42.03	96.90
M-4	1612	42.69	96.90
M-5	1613	43.35	96.90
N-1	2216	35.50	138.15
N-2	2217	36.00	138.15
N-3	2218	36.50	138.15
N-4	2219	37.00	138.15
O-1	2224	40.70	138.15
O-2	2225	41.36	138.15
O-3	2226	42.03	138.15
O-4	2227	42.69	138.15
O-5	2228	43.35	138.15
P-1	2546	35.50	160.40
P-2	2547	36.00	160.40
P-3	2548	36.50	160.40
P-4	2549	37.00	160.40

Table 2.10.2-11 Stress Point Locations - 2-D Model (continued)

Stress Point		Location	
		Radial	Axial
ID	Node	(in)	(in)
Q-1	2554	40.70	160.40
Q-2	2555	41.36	160.40
Q-3	2556	42.03	160.40
Q-4	2557	42.69	160.40
Q-5	2558	43.35	160.40
R-1	2771	35.50	175.40
R-2	2772	36.17	175.40
R-3	2773	36.83	175.40
R-4	2774	37.50	175.40
S-1	2779	40.70	175.40
S-2	2780	41.36	175.40
S-3	2781	42.03	175.40
S-4	2782	42.69	175.40
S-5	2783	43.35	175.40
T-1	7066	39.56	179.40
T-2	7067	40.22	179.40
T-3	7068	40.88	179.40
T-4	7069	41.50	179.40
T-5	7070	42.11	179.40
T-6	7071	42.73	179.40
T-7	7072	43.35	179.40
U-1	3051	35.50	179.40
U-2	3052	35.50	180.60
U-3	3053	35.50	181.80
U-4	3054	35.50	183.00
U-5	3055	35.50	184.20
U-6	3056	35.50	185.40

Table 2.10.2-11 Stress Point Locations - 2-D Model (continued)

Stress Point		Location	
		Radial	Axial
ID	Node	(in)	(in)
V-1	3611	35.21	188.40
V-2	3612	35.21	189.28
V-3	3613	35.21	190.15
V-4	3614	35.21	191.03
V-5	3615	35.21	191.90
V-6	3616	35.21	192.78
V-7	3617	35.21	193.71
W-1	3241	0.00	179.40
W-2	3242	0.00	180.60
W-3	3243	0.00	181.80
W-4	3244	0.00	183.00
W-5	3245	0.00	184.20
W-6	3246	0.00	185.40
X-1	3801	0.00	188.46
X-2	3802	0.00	189.28
X-3	3803	0.00	190.15
X-4	3804	0.00	191.03
X-5	3805	0.00	191.90
X-6	3806	0.00	192.78
X-7	3807	0.00	193.71

Table 2.10.2-12 Stress Point Locations - 3-D Bottom Fine Mesh Model

Stress Point		Location	
		Radial	Axial
ID	Node	(in)	(in)
A-1	1130	0.00	14.40
A-2	1129	0.00	11.35
A-3	1128	0.00	8.20
B-1	1185	0.00	6.20
B-2	1184	0.00	3.48
B-3	1183	0.00	0.75
C-1	90	35.50	14.40
C-2	80	35.50	13.60
C-3	70	35.50	12.80
C-4	60	35.50	12.00
C-5	50	35.50	9.50
C-6	40	35.50	8.20
D-1	25	39.44	6.20
D-2	15	39.44	3.48
D-3	5	39.44	0.75
E-1	35	39.44	8.20
E-2	34	40.70	8.20
E-3	33	41.58	8.20
E-4	32	42.47	8.20
E-5	31	43.35	8.20
F-1	100	35.50	15.07
F-2	99	36.17	15.07
F-3	98	36.83	15.07
F-4	97	37.50	15.07

Table 2.10.2-12 Stress Point Locations - 3-D Bottom Fine Mesh Model (continued)

Stress Point		Location	
		Radial	Axial
ID	Node	(in)	(in)
G-1	94	40.70	15.52
G-2	93	41.58	15.52
G-3	92	42.47	15.52
G-4	91	43.35	15.52
H-1	330	35.50	29.40
H-2	329	36.00	29.40
H-3	328	36.50	29.40
H-4	327	37.00	29.40
I-1	244	40.70	29.40
I-2	243	41.58	29.40
I-3	242	42.47	29.40
I-4	241	43.35	29.40
J-1	550	35.50	55.65
J-2	548	36.25	55.65
J-3	547	37.00	55.65
K-1	344	40.70	55.65
K-2	342	42.03	55.65
K-3	341	43.35	55.65
L-1	740	35.50	96.90
L-2	738	36.25	96.90
L-3	737	37.00	96.90
M-1	454	40.70	96.90
M-2	452	42.03	96.90

Table 2.10.2-12 Stress Point Locations - 3-D Bottom Fine Mesh Model (continued)

Stress Point		Location	
		Radial	Axial
ID	Node	(in)	(in)
M-3	451	43.35	96.90
N-1	810	35.50	138.15
N-2	807	37.00	138.15
O-1	524	40.70	138.15
O-2	521	43.35	138.15
P-1	850	35.50	160.40
P-2	847	37.00	160.40
Q-1	564	40.70	160.40
Q-2	561	43.35	160.40
R-1	890	35.50	175.40
R-2	887	37.50	175.40
S-1	604	40.70	175.40
S-2	601	43.35	175.40
T-1	614	40.70	179.40
T-2	611	43.35	179.40
U-1	900	35.50	179.40
U-2	910	35.50	185.40
V-1	920	35.50	187.40
V-2	930	35.50	193.71

Table 2.10.2-12 Stress Point Locations - 3-D Bottom Fine Mesh Model (continued)

Stress Point		Location	
		Radial	Axial
ID	Node	(in)	(in)
W-1	1216	0.00	179.40
W-2	1226	0.00	185.40
X-1	1236	0.00	187.40
X-2	1246	0.00	193.71

Table 2.10.2-13 Stress Point Locations - 3-D Top Fine Mesh Model

Stress Point		Location	
		Radial	Axial
ID	Node	(in)	(in)
A-1	1949	0.00	14.40
A-2	1950	0.00	12.78
A-3	1951	0.00	8.20
B-1	1952	0.00	6.20
B-2	93	0.00	0.75
C-1	1925	35.50	14.40
C-2	1926	35.50	12.78
C-3	1927	35.50	8.20
D-1	683	39.44	6.20
D-2	85	39.44	0.75
E-1	682	39.44	8.20
E-2	82	43.35	8.20
F-1	1925	35.50	14.40
F-2	1325	37.50	14.40
G-1	680	40.70	14.40
G-2	80	43.35	14.40
H-1	1921	35.50	29.40
H-2	1321	37.00	29.40
I-1	676	40.70	29.40
I-2	76	43.35	29.40

Table 2.10.2-13 Stress Point Locations - 3-D Top Fine Mesh Model (continued)

Stress Point		Location	
		Radial	Axial
ID	Node	(in)	(in)
J-1	1916	35.50	55.65
J-2	1316	37.00	55.65
K-1	671	40.70	55.65
K-2	71	43.50	55.65
L-1	1908	35.50	96.90
L-2	1308	37.00	96.90
M-1	663	40.70	96.90
M-2	63	43.50	96.90
N-1	1877	35.50	138.15
N-2	1477	36.25	138.15
N-3	1277	37.00	138.15
O-1	647	40.70	138.15
O-2	247	42.03	138.15
O-3	47	43.35	138.15
P-1	1840	35.50	160.40
P-2	1640	36.00	160.40
P-3	1440	36.50	160.40
P-4	1240	37.00	160.40
Q-1	628	40.70	160.40
Q-2	428	41.58	160.40
Q-3	228	42.47	160.40
Q-4	28	43.35	160.40

Table 2.10.2-13 Stress Point Locations - 3-D Top Fine Mesh Model (continued)

Stress Point		Location	
		Radial	Axial
ID	Node	(in)	(in)
R-1	1816	35.50	175.40
R-2	1616	36.17	175.40
R-3	1416	36.83	175.40
R-4	1216	37.50	175.40
S-1	616	40.70	175.40
S-2	416	41.58	175.40
S-3	216	42.47	175.40
S-4	16	43.35	175.40
T-1	811	39.56	179.40
T-2	611	40.51	179.40
T-3	411	41.46	179.40
T-4	211	42.40	179.40
T-5	11	43.35	179.40
U-1	43058	35.50	179.40
U-2	43057	35.50	180.15
U-3	43056	35.50	180.90
U-4	43055	35.50	181.65
U-5	43054	35.50	182.40
U-6	43053	35.50	183.15
U-7	43052	35.50	183.90
U-8	43051	35.50	185.40
V-1	50024	35.21	188.40
V-2	50023	35.21	190.15
V-3	50022	35.21	191.90
V-4	50021	35.21	193.71

Table 2.10.2-13 Stress Point Locations - 3-D Top Fine Mesh Model (continued)

Stress Point		Location	
		Radial	Axial
ID	Node	(in)	(in)
W-1	43278	0.00	179.40
W-2	43274	0.00	182.40
W-3	43271	0.00	185.40
X-1	50084	0.00	188.46
X-2	50083	0.00	190.15
X-3	50081	0.00	193.71

2.10.3 LS-DYNA Computer Code

Two separate cases are used to verify the LS-DYNA program as a tool to predict the deceleration of the cask body during normal and accident conditions. LS-DYNA provides two strain rate dependent material models that adequately simulate the behavior of wood crushing during a dynamic impact event. Benchmarking of the two material properties and the method of analysis are presented in the following sections. The first verification problem is designed to determine the accuracy of the modeling methodology when compared to closed form solutions. The second verification problem shows that strain rate dependent material models properly interpolate between inputted stress-strain curves at a given strain rate.

2.10.3.1 Predicting Impact Deceleration using Strain Rate Sensitive Properties

The validation of the use of LS-DYNA to represent the behavior of the balsa impact limiters was accomplished by using the balsa stress strain curve for a simple geometry for which the crushing and acceleration could be determined. The geometry used is shown in Figure 2.10.3.2-1, which corresponds to a right circular cylinder 50 inches in diameter and 50 inches in length. The model employed symmetry boundary conditions for the quarter symmetry model. The stress strain curve representative of balsa material is shown in Figure 2.10.3.2-2. The material model used in this evaluation is the FU_CHANG_FOAM (material 83), which is the material model employed in the balsa impact limiter evaluation. The impacting object is a quarter symmetry circular plate of the same diameter with an assigned weight of 257 kips. The interface between the balsa cylinder and the plate is modeled using automatic surface to surface, while the unyielding surface was modeled using the RIGIDWALL_GEOMETRIC_FLAT option. The system has an initial velocity of 150 in/sec. To compute the crush, an energy balance is used.

$$\frac{mv_o^2}{2} = AL\int_0^{\varepsilon_i} \sigma_i \, d\varepsilon$$

where:

A = area of the block being crushed
L = total original height of the block
$d\varepsilon_i$ = the incremental strain as the block crushes
σ_i = the stress at the given incremental strain value

The acceleration is computed by σ A/W (g), where W is the weight of the modeled plate. The peak crush strength is 2,090 psi obtained from Figure 2.10.3.2-2. The results of the calculation are:

Item	LS-DYNA	Calculation	% Difference
Crush (in)	12.9	12.6	2
Acceleration (maximum) (g)	4.04	3.99	1

This demonstrates that the material model and numerical methodology employed in LS-DYNA for the balsa impact limiters is acceptable.

2.10.3.2 Accounting for Strain Rate Sensitivity by Interpolation

The strain rate sensitive foam/wood is modeled using the LS-DYNA finite element model builder (FEMB). The model is comprised of a steel block and a wooden cube. The model as shown in Figure 2.10.3.2-3 is constructed of solid brick elements. The wooden cube measures 5 inches by 5 inches. The impacting steel plate is 5 inches tall and 7.5 inches across. Surface-to-surface contact interfaces are employed between the steel block and the wooden cube. The wooden cube sits on a rigid plane.

The Piecewise_Linear_Plasticity material model is used to represent the steel block. The wooden cube is represented as a homogeneous isotropic material, type number 163 in LS-DYNA (Modified_Crushable_Foam). For this example, three strain rates are inputted into the material model, 0 ε/sec, 20 ε/sec, 60 ε/sec, with corresponding constant stress values of 2000 psi, 7000 psi and 10,000 psi, respectively. A prescribed motion is applied to the steel block to apply a constant strain rate to the wood cube after 0.01 seconds.

To demonstrate that the correct strain rate curve is used during the crushing of the wood cube two cases are considered. The first case uses 20 ε/sec, and the second case uses 40 ε/sec. The stress in the wood block should compare to the applied stress-strain curve at the strain rate of interest. For the 20 ε/sec case, the compressive stress in the cube is approximately 7,000 psi, which agrees with the LS-DYNA result. For the 40 ε/sec case, the compressive stress in the cube is a value of 8,000 psi, due to logarithmetic interpolation that agrees with the LS-DYNA result in

Figure 2.10.3.2-5. Therefore, the Modified_Crushable_Foam material model is an acceptable method of accounting for the strain rate variability of foam and wood crushable materials.

Figure 2.10.3.2-1 LS-DYNA Model used to Verify the Material Model

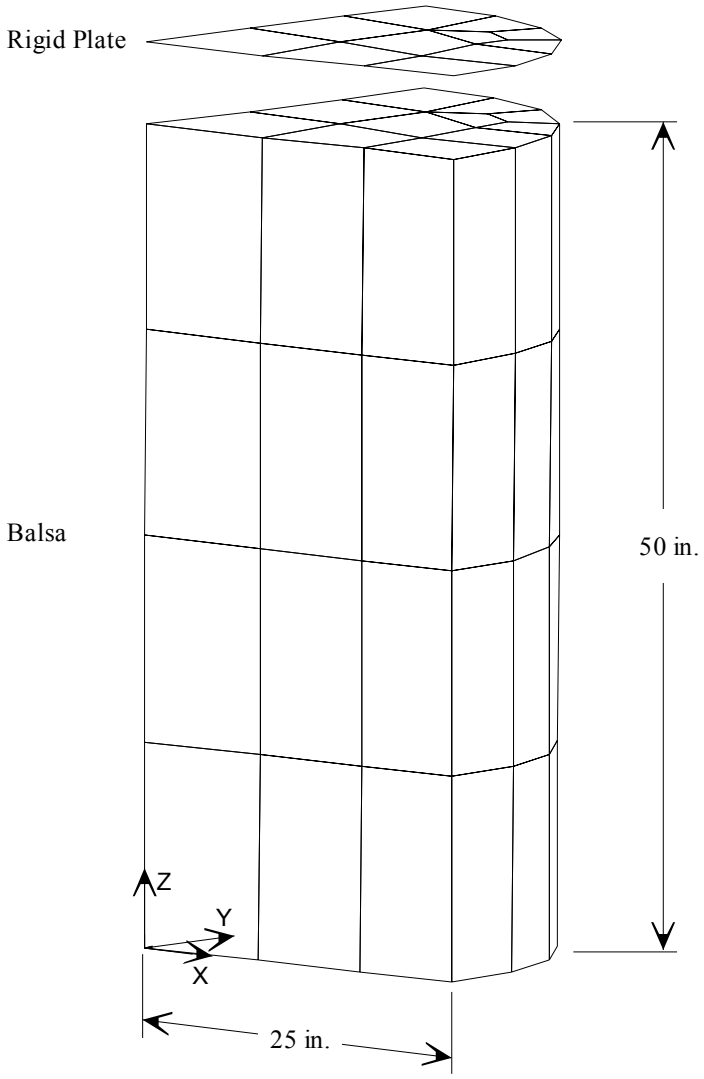

Note: XZ and YZ planes are planes of symmetry.

Figure 2.10.3.2-2 Stress-Strain Curve used for the Balsa Material

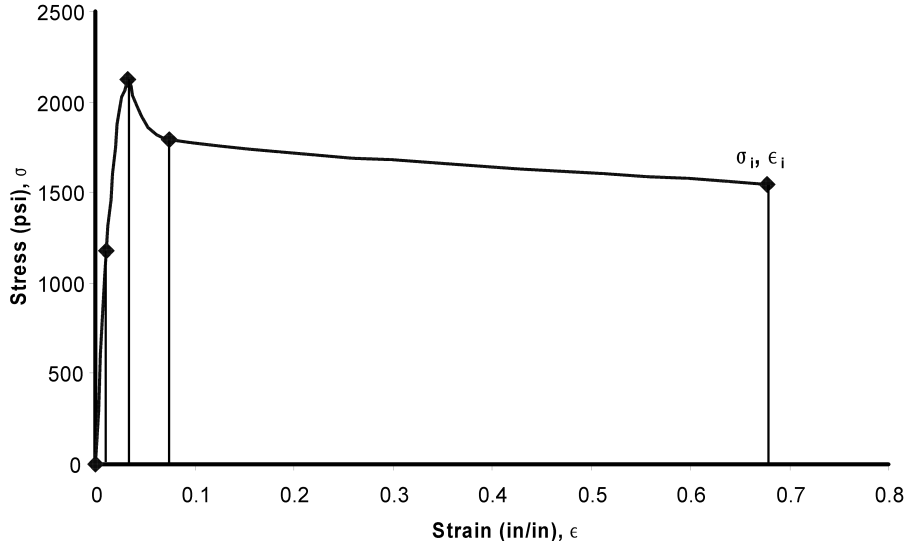

Figure 2.10.3.2-3 Finite Element Model for Strain-Rate Dependent Crushable Foam/Wood Block Impact

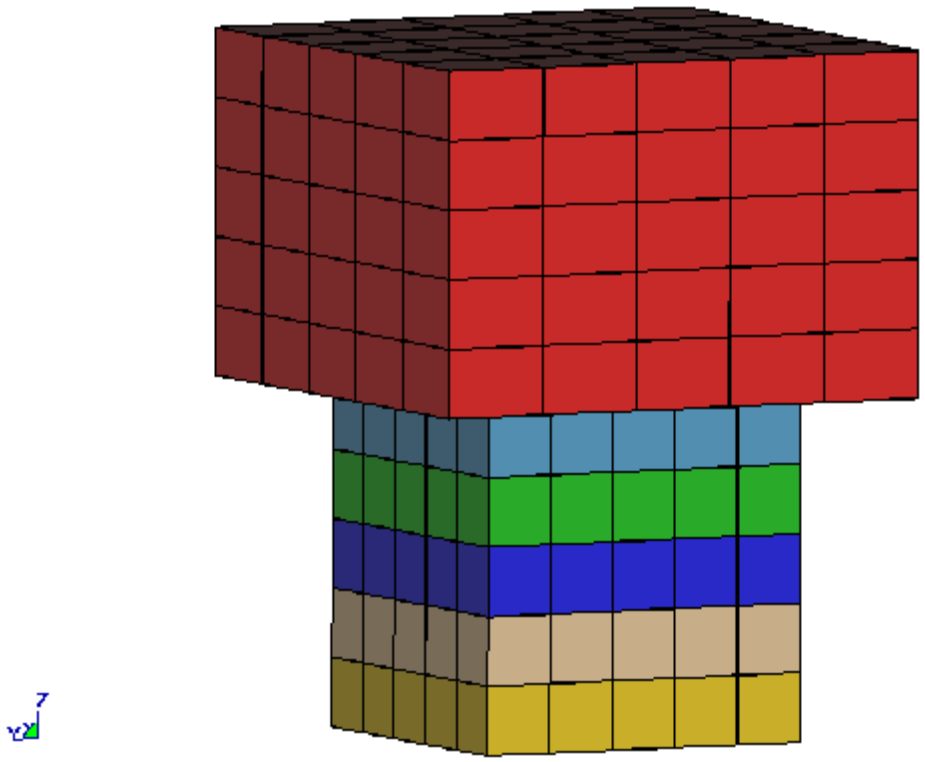

Figure 2.10.3.2-4 Stress Time History at 20 ε/sec

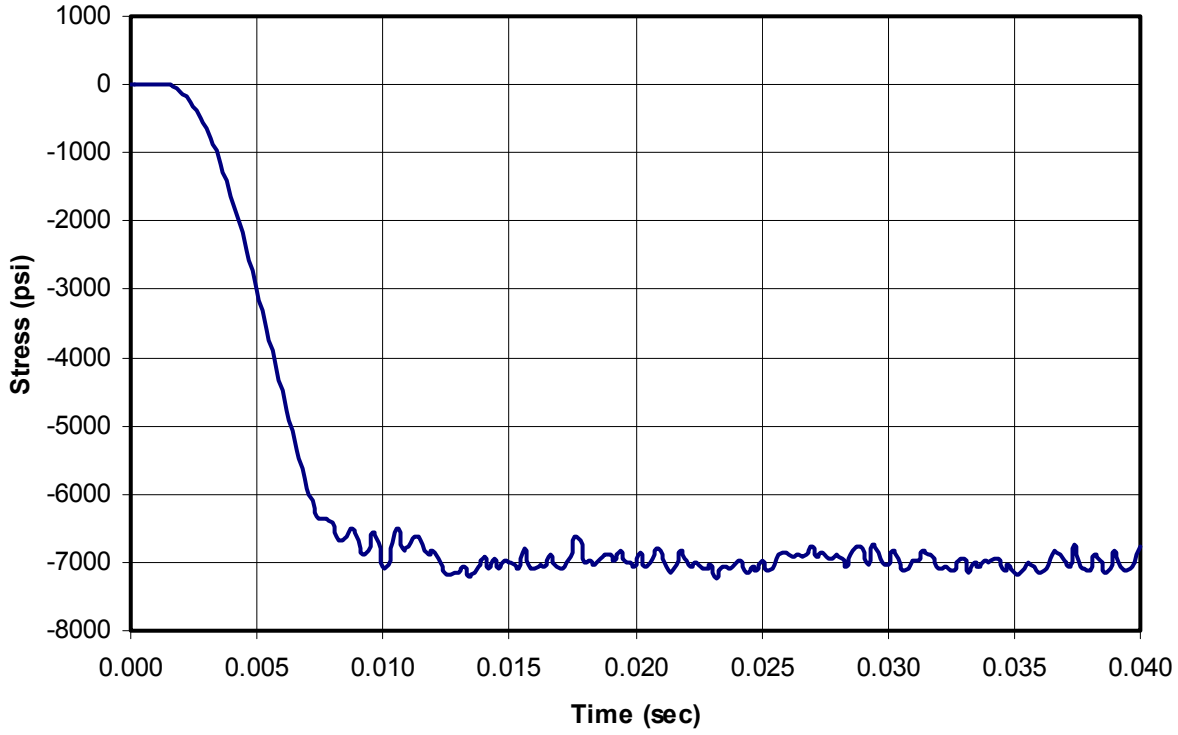

Figure 2.10.3.2-5 Stress Time History at 40 ε/sec

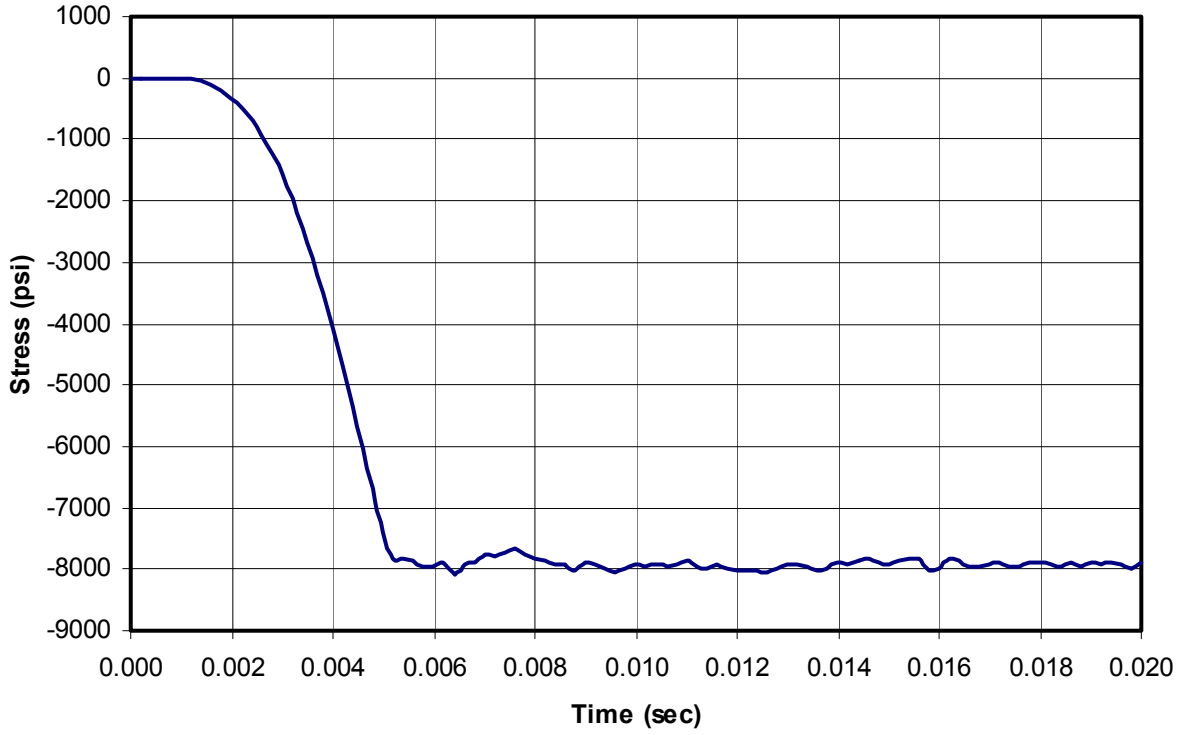

2.10.4 Detailed Finite Element Stress Summaries - Directly Loaded Fuel Configuration

This section documents the finite element stress results from the different loading cases for the normal condition of transport and hypothetical accident conditions for the directly loaded fuel configuration of the NAC-STC. Nodal and sectional stress summaries are presented for the representative sections as defined in Section 2.10.2.4.2. Critical stress summaries are presented for the critical component sections determined as described in Section 2.10.2.4.1. The maximum stress intensity is the maximum value of (S1-S3), where S1 and S3 are the maximum and minimum principle stresses, respectively.

A summary of the individual and combined loading conditions is provided, followed by the stress summary tables. The values for S_x, S_y, and S_z shown in the tables are normal stresses corresponding to radial, longitudinal and circumferential stresses, respectively. Allowable stresses, in tables where these data items appear, are based on maximum component temperature for normal conditions.

SUMMARY OF INDIVIDUAL LOADING ANALYSES

(The following are individual loading analyses, nodal stress summaries are prepared for each)

ANALYSIS NO.	LOADING DESCRIPTION	SAR SECTION	TABLE NO.
1.	50 psi Maximum Internal Pressure plus Bolt Preload, 100°F		2.10.4-1
2.	12 psi Minimum Internal Pressure plus Bolt Preload, -40°F		2.10.4-2
3.	Gravity, 100°F, Decay Heat, Solar Insolation	2.6.1	2.10.4-3
4.	Gravity, -40°F, no Decay Heat, No Solar Insolation	2.6.2	2.10.4-4
5.	Thermal Heat, 100°F, Decay Heat, Solar Insolation	2.6.1	2.10.4-5
6.	Thermal Cold, -20°F, Decay Heat		2.10.4-6
7.	Thermal Cold, -40°F, No Decay Heat	2.6.2	2.10.4-7
8.	Impact, 1 Ft Top End Drop, 20 g, $\phi = 0°$	2.6.7.1	2.10.4-8
9.	Impact, 1 Ft Bottom End Drop, 20 g, $\phi = 0°$	2.6.7.1	2.10.4-9
10.	Impact, 1 Ft Side Drop, 20 g, $\phi = 90°$	2.6.7-2	2.10.4-10
11.	Impact, 1 Ft Top Corner Drop, 20 g, $\phi = 24°$	2.6.7.3	2.10.4-11
12.	Impact, 1 Ft Bottom Corner Drop, 20 g, $\phi = 24°$	2.6.7.3	2.10.4-12
13.	Impact, 30 Ft Top End Drop, 56.1 g, $\phi = 0°$	2.7.1.1	2.10.4-13
14.	Impact, 30 Ft Bottom End Drop, 56.1 g, $\phi = 0°$	2.7.1.1	2.10.4-14
15.	Impact, 30 Ft Side Drop, 55 g, $\phi = 90°$	2.7.1.2	2.10.4-15
16.	Impact, 30 Ft Top Corner Drop, 55 g, $\phi = 24°$	2.7.1.3	2.10.4-16
17.	Impact, 30 Ft Bottom Corner Drop, 55 g, $\phi = 24°$	2.7.1.3	2.10.4-17
18.	Impact, 30 Ft Bottom Oblique Drop, 55 g, $\phi = 15°$	2.7.1.4	2.10.4-18
19.	Impact, 30 Ft Top Oblique Drop, 55 g, $\phi = 75°$	2.7.1.4	2.10.4-19
20.	Impact, 30 Ft Bottom Oblique Drop, 55 g, $\phi = 75°$	2.7.1.4	2.10.4-20
21.	Thermal Fire Transient, 1475°F, 30 Minutes	2.7.3	2.10.4-178 through 2.10.4-180

SUMMARY OF COMBINED LOADING ANALYSES

ANALYSIS NO.	LOADING DESCRIPTION	SAR SECTION	TABLE NO.
22.	Thermal Heat 50 psi Internal Pressure, Bolt Preload 1 g Gravity with Cask in Horizontal Position 100°F, Solar Insolation, Decay Heat	2.6.1	2.10.4-21 through 2.10.4-28
23.	Thermal Cold 12 psi Internal Pressure, Bolt Preload 1 g Gravity with Cask in Horizontal Position -40°F, no Solar Insolation, no Decay Heat	2.6.2	2.10.4-29 through 2.10.4-36
24.	1 Ft Top End Drop 50 psi Internal Pressure, Bolt Preload Impact (20 g, f = 0°) 100°F, Solar Insolation, Decay Heat	2.6.7.1	2.10.4-37 through 2.10.4-44
25.	1 Ft Top End Drop 12 psi Internal Pressure, Bolt Preload Impact (20 g, f = 0°) -20°F, no Solar Insolation, Decay Heat	2.6.7.1	2.10.4-45 through 2.10.4-47
26.	1 Ft Top End Drop 12 psi Internal Pressure, Bolt Preload Impact (20 g, f = 0°) -20°F, no Solar Insolation, no Contents	2.6.7.1	2.10.4-48 through 2.10.4-50
27.	1 Ft Bottom End Drop 50 psi Internal Pressure, Bolt Preload Impact (20 g, f = 0°) 100°F, Solar Insolation, Decay Heat	2.6.7.1	2.10.4-51 through 2.10.4-58

SUMMARY OF COMBINED LOADING ANALYSES (Continued)

ANALYSIS NO.	LOADING DESCRIPTION	SAR SECTION	TABLE NO.
28.	1 Ft Bottom End Drop 12 psi Internal Pressure, Bolt Preload Impact (20 g, f = 0°) -20°F, no Solar Insolation, Decay Heat	2.6.7.1	2.10.4-59 through 2.10.4-61
29.	1 Ft Bottom End Drop 12 psi Internal Pressure, Bolt Preload Impact (20 g, f = 0°) -20°F, no Solar Insolation, no Contents	2.6.7.1	2.10.4-62 through 2.10.4-64
30.	1 Ft Side Drop 50 psi Internal Pressure, Bolt Preload Impact (20 g, f = 90°) 100°F, Solar Insolation, Decay Heat	2.6.7.2	2.10.4-65 through 2.10.4-83
31.	1 Ft Top Corner Drop 50 psi Internal Pressure, Bolt Preload Impact (20 g, f = 24°) 100°F, Solar Insolation, Decay Heat	2.6.7.3	2.10.4-84 through 2.10.4-97
32.	1 Ft Bottom Corner Drop 50 psi Internal Pressure, Bolt Preload Impact (20 g, f = 24°) 100°F, Solar Insolation, Decay Heat	2.6.7.3	2.10.4-98 through 2.10.4-111
33.	30 Ft Top End Drop 50 psi Internal Pressure, Bolt Preload Impact (56.1 g, f = 0°) 100°F, Solar Insolation, Decay Heat	2.7.7.1	2.10.4-112 through 2.10.4-116

SUMMARY OF COMBINED LOADING ANALYSES (Continued)

ANALYSIS NO.	LOADING DESCRIPTION	SAR SECTION	TABLE NO.
34.	30 Ft Top End Drop 12 psi Internal Pressure, Bolt Preload Impact (56.1 g, f = 0°) -20°F, no Solar Insolation, Decay Heat	2.7.1.1	2.10.4-117 through 2.10.4-118
35.	30 Ft Top End Drop 12 psi Internal Pressure, Bolt Preload Impact (56.1 g, f = 0°) -20°F, no Solar Insolation, no Contents	2.7.1.1	2.10.4-119 through 2.10.4-120
36.	30 Ft Bottom End Drop 50 psi Internal Pressure, Bolt Preload Impact (56.1 g, f = 0°) 100°F, Solar Insolation, Decay Heat	2.7.1.1	2.10.4-121 through 2.10.4-125
37.	30 Ft Bottom End Drop 12 psi Internal Pressure, Bolt Preload Impact (56.1 g, f = 0°) -20°F, no Solar Insolation, Decay Heat	2.7.1.1	2.10.4-126 through 2.10.4-127
38.	30 Ft Bottom End Drop 12 psi Internal Pressure, Bolt Preload Impact (56.1 g, f = 0°) -20°F, no Solar Insolation, no Contents	2.7.1.1	2.10.4-128 through 2.10.4-129
39.	30 Ft Side Drop 50 psi Internal Pressure, Bolt Preload Impact, (55 g, f = 90°) 100°F, Solar Insolation, Decay Heat	2.7.1.2	2.10.4-130 through 2.10.4-140

SUMMARY OF COMBINED LOADING ANALYSES (Continued)

ANALYSIS NO.	LOADING DESCRIPTION	SAR SECTION	TABLE NO.
40.	30 Ft Top Corner Drop 50 psi Internal Pressure, Bolt Preload Impact, (55 g, f = 24°) 100°F, Solar Insolation, Decay Heat	2.7.1.3	2.10.4-141 through 2.10.4-151
41.	30 Ft Bottom Corner Drop 50 psi Internal Pressure, Bolt Preload Impact, (55 g, f = 24°) 100°F, Solar Insolation, Decay Heat	2.7.1.3	2.10.4-152 through 2.10.4-162
42.	30 Ft Bottom Critical Oblique Drop 50 psi Internal Pressure, Bolt Preload Impact (55 g, f = 15°) 100°F, Solar Insolation, Decay Heat	2.7.1.4	2.10.4-163 through 2.10.4-167
43.	30 Ft Top Critical Oblique Drop 50 psi Internal Pressure, Bolt Preload Impact (55 g, f = 75°) 100°F, Solar Insolation, Decay Heat	2.7.1.4	2.10.4-168 through 2.10.4-172
44.	30 Ft Bottom Critical Oblique Drop 50 psi Internal Pressure, Bolt Preload Impact (55 g, f = 75°) 100°F, Solar Insolation, Decay Heat	2.7.1.4	2.10.4-173 through 2.10.4-177
45.	Thermal Fire Transient 125 psi Internal Pressure, Bolt Preload 1 g Gravity with Cask in Vertical Position 1475°F, 30 Minute Period, Decay Heat	2.7.3	2.10.4-178 through 2.10.4-180

Table 2.10.4-1 Stress Components – 50 psig Internal Pressure + Bolt Preload; 2-D Model; Condition 1

Condition 1: 100°F Ambient with Contents

Stress Points		Stress Components (ksi)						Principal Stresses (ksi)		
Section[1]	Node	S_x	S_y	S_z	S_{xy}	S_{yz}	S_{zx}	S1	S2	S3
A1	1	-0.7	0.0	-0.7	0.0	0.0	0.0	0.0	-0.7	-0.7
A2	2	-0.4	0.0	-0.4	0.0	0.0	0.0	0.0	-0.4	-0.4
A3	3	0.0	0.0	0.0	0.0	0.0	0.0	0.0	0.0	0.0
A4	4	0.3	0.0	0.3	0.0	0.0	0.0	0.3	0.3	0.0
A5	5	0.6	0.0	0.6	0.0	0.0	0.0	0.6	0.6	0.0
B1	6	-0.5	0.0	-0.5	0.0	0.0	0.0	0.0	-0.5	-0.5
B2	7	-0.2	0.0	-0.2	0.0	0.0	0.0	0.0	-0.2	-0.2
B3	8	0.1	0.0	0.1	0.0	0.0	0.0	0.1	0.1	0.0
B4	9	0.4	0.0	0.4	0.0	0.0	0.0	0.4	0.4	0.0
B5	10	0.7	0.0	0.7	0.0	0.0	0.0	0.7	0.7	0.0
C1	251	0.7	1.1	0.3	0.2	0.0	0.0	1.2	0.6	0.3
C2	252	0.1	0.4	0.0	0.1	0.0	0.0	0.4	0.1	0.0
C3	253	-0.1	0.1	0.0	0.0	0.0	0.0	0.1	0.0	-0.1
C4	254	-0.3	0.0	0.0	0.0	0.0	0.0	0.0	0.0	-0.3
C5	255	-0.6	0.0	-0.1	0.0	0.0	0.0	0.0	-0.1	-0.6
D1	306	0.5	0.2	0.2	0.1	0.0	0.0	0.0	0.2	0.2
D2	307	0.2	0.2	0.1	0.0	0.0	0.0	0.2	0.1	0.1
D3	308	0.0	0.1	0.1	0.0	0.0	0.0	0.1	0.1	0.0
D4	309	-0.1	0.0	0.1	0.0	0.0	0.0	0.1	0.0	-0.1
D5	310	-0.2	0.0	0.1	0.0	0.0	0.0	0.1	0.0	-0.2
E1	305	-0.5	-0.1	-0.1	0.1	0.0	0.0	-0.1	-0.1	-0.5
E2	315	-0.3	0.1	0.0	0.1	0.0	0.0	0.1	0.0	-0.3
E3	325	-0.1	0.1	0.0	0.1	0.0	0.0	0.1	0.0	-0.2
E4	335	-0.1	0.1	0.0	0.1	0.0	0.0	0.1	0.0	-0.1
E5	345	0.0	0.1	0.0	0.1	0.0	0.0	0.1	0.0	0.0
E6	355	0.0	0.1	0.0	0.0	0.0	0.0	0.1	0.0	0.0
F1	251	0.7	1.1	0.3	0.2	0.0	0.0	1.2	0.6	0.3
F2	261	0.5	0.4	0.1	0.0	0.0	0.0	0.5	0.4	0.1
F3	271	0.2	-0.1	-0.1	0.0	0.0	0.0	0.2	-0.1	-0.1
F4	281	0.1	-0.6	-0.3	0.0	0.0	0.0	0.1	-0.3	-0.6
G1	311	0.2	0.3	0.0	0.0	0.0	0.0	0.3	0.2	0.0

Table 2.10.4-1 Stress Components – 50 psig Internal Pressure + Bolt Preload; 2-D Model; Condition 1 (continued)

Stress Points		Stress Components (ksi)						Principal Stresses (ksi)		
Section[1]	Node	S_x	S_y	S_z	S_{xy}	S_{yz}	S_{xz}	S1	S2	S3
G2	321	0.1	0.2	0.0	0.0	0.0	0.0	0.2	0.1	0.0
G3	331	0.1	0.1	0.0	0.0	0.0	0.0	0.1	0.0	0.0
G4	341	0.0	0.0	-0.1	0.0	0.0	0.0	0.0	0.0	-0.1
G5	351	0.0	-0.1	-0.0	0.0	0.0	0.0	0.0	-0.1	-0.1
H1	581	0.0	0.1	0.9	0.0	0.0	0.0	0.9	0.1	0.0
H2	582	0.0	0.3	0.9	0.0	0.0	0.0	0.9	0.3	0.0
H3	583	0.0	0.5	1.0	0.0	0.0	0.0	1.0	0.5	0.0
H4	584	0.0	0.7	1.0	0.0	0.0	0.0	1.0	0.7	0.0
I1	589	0.0	0.1	0.0	0.0	0.0	0.0	0.1	0.0	0.0
I2	590	0.0	0.1	0.0	0.0	0.0	0.0	0.1	0.0	0.0
I3	591	0.0	0.1	0.0	0.0	0.0	0.0	0.1	0.0	0.0
I4	592	0.0	0.1	0.0	0.0	0.0	0.0	0.1	0.0	0.0
I5	593	0.0	0.1	0.0	0.0	0.0	0.0	0.1	0.0	0.0
J1	971	-0.1	0.4	1.1	0.0	0.0	0.0	1.1	0.4	-0.1
J2	972	0.0	0.4	1.0	0.0	0.0	0.0	1.0	0.4	0.0
J3	973	0.0	0.4	1.0	0.0	0.0	0.0	1.0	0.4	0.0
J4	974	0.0	0.4	1.0	0.0	0.0	0.0	1.0	0.4	0.0
K1	979	0.0	0.1	0.0	0.0	0.0	0.0	0.1	0.0	0.0
K2	980	0.0	0.1	0.0	0.0	0.0	0.0	0.1	0.0	0.0
K3	981	0.0	0.1	0.0	0.0	0.0	0.0	0.1	0.0	0.0
K4	982	0.0	0.1	0.0	0.0	0.0	0.0	0.1	0.0	0.0
K5	983	0.0	0.1	0.0	0.0	0.0	0.0	0.1	0.0	0.0
L1	160	-0.1	0.4	1.1	0.0	0.0	0.0	1.1	0.0	-0.1
L2	1602	0.0	0.4	1.0	0.0	0.0	0.0	1.0	0.4	0.0
L3	1603	0.0	0.4	1.0	0.0	0.0	0.0	1.0	0.4	0.0
L4	1604	0.0	0.4	1.0	0.0	0.0	0.0	1.0	0.4	0.0
M1	1609	0.0	0.1	0.0	0.0	0.0	0.0	0.1	0.0	0.0
M2	1610	0.0	0.1	0.0	0.0	0.0	0.0	0.1	0.0	0.0
M3	1611	0.0	0.1	0.0	0.0	0.0	0.0	0.1	0.0	0.0
M4	1612	0.0	0.1	0.0	0.0	0.0	0.0	0.1	0.0	0.0
M5	1613	0.0	0.1	0.0	0.0	0.0	0.0	0.1	0.0	0.0
N1	2216	-0.1	0.4	1.1	0.0	0.0	0.0	1.1	0.4	-0.1
N2	2217	0.0	0.4	1.0	0.0	0.0	0.0	1.0	0.4	0.0

Table 2.10.4-1 Stress Components – 50 psig Internal Pressure + Bolt Preload; 2-D Model; Condition 1 (continued)

Stress Points		Stress Components (ksi)						Principal Stresses (ksi)		
Section[1]	Node	S_x	S_y	S_z	S_{xy}	S_{yz}	S_{zx}	S1	S2	S3
N3	2218	0.0	0.4	1.0	0.0	0.0	0.0	1.0	0.4	0.0
N4	2219	0.0	0.4	1.0	0.0	0.0	0.0	1.0	0.4	0.0
O1	2224	0.0	0.1	0.0	0.0	0.0	0.0	0.1	0.0	0.0
O2	2225	0.0	0.1	0.0	0.0	0.0	0.0	0.1	0.0	0.0
O3	2226	0.0	0.1	0.0	0.0	0.0	0.0	0.1	0.0	0.0
O4	2227	0.0	0.1	0.0	0.0	0.0	0.0	0.1	0.0	0.0
O5	2228	0.0	0.1	0.0	0.0	0.0	0.0	0.1	0.0	0.0
P1	2546	0.0	0.2	1.0	0.0	0.0	0.0	1.0	0.2	0.0
P2	2547	0.0	0.3	1.0	0.0	0.0	0.0	1.0	0.3	0.0
P3	2548	0.0	0.4	1.0	0.0	0.0	0.0	1.0	0.4	0.0
P4	2549	0.0	0.6	1.0	0.0	0.0	0.0	1.0	0.6	0.0
Q1	2554	0.0	0.1	0.0	0.0	0.0	0.0	0.1	0.0	0.0
Q2	2555	0.0	0.1	0.0	0.0	0.0	0.0	0.1	0.0	0.0
Q3	2556	0.0	0.1	0.0	0.0	0.0	0.0	0.1	0.0	0.0
Q4	2557	0.0	0.1	0.0	0.0	0.0	0.0	0.1	0.0	0.0
Q5	2558	0.0	0.0	0.0	0.0	0.0	0.0	0.0	0.0	0.0
R1	2771	-0.3	0.1	0.3	0.1	0.0	0.0	0.3	0.2	-0.3
R2	2772	-0.3	0.2	0.3	0.2	0.0	0.0	0.3	0.2	-0.3
R3	2773	-0.5	0.2	0.2	0.2	0.0	0.0	0.3	0.2	-0.6
R4	2774	-1.1	0.7	0.2	0.1	0.0	0.0	0.7	0.2	-1.1
S1	2775	-0.3	0.0	0.1	-0.1	0.0	0.0	0.1	0.0	-0.3
S2	2780	-0.1	0.0	0.2	0.0	0.0	0.0	0.2	0.0	-0.1
S3	2781	0.0	0.1	0.2	0.0	0.0	0.0	0.2	0.1	0.0
S4	2782	0.0	0.1	0.2	0.0	0.0	0.0	0.2	0.1	0.0
S5	2783	0.0	0.1	0.2	0.0	0.0	0.0	0.2	0.1	0.0
T1	7066	-0.3	-0.2	0.1	0.1	0.0	0.0	0.1	-0.2	-0.3
T2	7067	0.1	-0.6	0.1	-0.1	0.0	0.0	0.1	0.1	-0.6
T3	7068	0.1	-0.4	0.1	0.0	0.0	0.0	0.1	0.1	-0.4
T4	7069	0.0	-0.2	0.2	0.0	0.0	0.0	0.2	0.0	-0.2
T5	7070	0.0	-0.1	0.2	0.0	0.0	0.0	0.2	0.0	-0.1
T6	7071	0.0	0.1	0.2	0.0	0.0	0.0	0.2	0.1	0.0
T7	7072	0.0	0.2	0.3	0.0	0.0	0.0	0.3	0.2	0.0
U1	3051	0.3	-1.4	-0.6	0.4	0.0	0.0	0.4	-0.6	-1.5

Table 2.10.4-1 Stress Components – 50 psig Internal Pressure + Bolt Preload; 2-D Model; Condition 1 (continued)

Stress Points		Stress Components (ksi)						Principal Stresses (ksi)		
Section[1]	Node	S_x	S_y	S_z	S_{xy}	S_{yz}	S_{zx}	S1	S2	S3
U2	3052	-0.4	-1.8	-0.9	0.4	0.0	0.0	-0.3	-0.9	-1.9
U3	3053	-0.1	-2.0	-0.7	0.1	0.0	0.0	-0.1	-0.7	-2.0
U4	3054	0.0	-1.5	-0.4	-0.4	0.0	0.0	0.1	-0.4	-1.7
U5	3055	-0.5	-0.7	-0.1	-0.5	0.0	0.0	0.0	-0.1	-1.2
U6	3056	0.9	0.2	0.7	-0.4	0.0	0.0	1.1	0.7	0.0
V1	3611	1.2	0.0	0.3	0.0	0.0	0.0	1.2	0.3	0.0
V2	3612	0.7	-0.1	0.2	0.0	0.0	0.0	0.7	0.2	-0.1
V3	3613	0.3	-0.2	0.0	0.0	0.0	0.0	0.4	0.0	-0.2
V4	3614	0.1	-0.5	-0.1	0.0	0.0	0.0	0.1	-0.1	-0.5
V5	3615	-0.2	-1.0	-0.3	0.0	0.0	0.0	-0.2	-0.3	-1.0
V6	3616	-0.4	-0.5	-0.2	0.0	0.0	0.0	-0.2	-0.4	-0.5
V7	3617	-1.4	0.4	-0.2	0.0	0.0	0.0	0.4	-0.2	-1.4
W1	3241	-1.2	0.0	-1.2	0.0	0.0	0.0	0.0	-1.2	-1.2
W2	3242	-0.8	0.0	-0.8	0.0	0.0	0.0	0.0	-0.8	-0.8
W3	3243	-0.3	0.0	-0.3	0.0	0.0	0.0	0.0	-0.3	-0.3
W4	3244	0.2	0.0	0.2	0.0	0.0	0.0	0.2	0.2	0.0
W5	3245	0.7	0.0	0.7	0.0	0.0	0.0	0.7	0.7	0.0
W6	3246	1.1	0.0	1.1	0.0	0.0	0.0	1.1	1.1	0.0
X1	3801	-0.3	0.0	-0.3	0.0	0.0	0.0	0.0	-0.3	-0.3
X2	3802	-0.2	0.0	-0.2	0.0	0.0	0.0	0.0	-0.2	-0.2
X3	3803	-0.1	0.0	-0.1	0.0	0.0	0.0	0.0	-0.1	-0.1
X4	3804	0.0	0.0	0.0	0.0	0.0	0.0	0.0	0.0	0.0
X5	3805	0.1	0.0	0.1	0.0	0.0	0.0	0.1	0.1	0.0
X6	3806	0.2	0.0	0.2	0.0	0.0	0.0	0.2	0.2	0.0
X7	3807	0.3	0.0	0.3	0.0	0.0	0.0	0.3	0.3	0.0

[1] Refer to Figure 2.10.2-34 for the identification of the representative section.

Table 2.10.4-2 Stress Components – 12 psig Internal Pressure + Bolt Preload; 2-D Model; Condition 4

Condition 4: -40°F Ambient, No Decay Heat

Stress Points		Stress Components (ksi)						Principal Stresses (ksi)		
Section[1]	Node	S_x	S_y	S_z	S_{xy}	S_{yz}	S_{xz}	S1	S2	S3
A1	1	-0.2	0.0	-0.2	0.0	0.0	0.0	0.0	-0.2	-0.2
A2	2	-0.1	0.0	-0.1	0.0	0.0	0.0	0.0	-0.1	-0.1
A3	3	0.0	0.0	0.0	0.0	0.0	0.0	0.0	0.0	0.0
A4	4	0.1	0.0	0.1	0.0	0.0	0.0	0.1	0.1	0.0
A5	5	0.1	0.0	0.1	0.0	0.0	0.0	0.1	0.1	0.0
B1	6	-0.1	0.0	-0.1	0.0	0.0	0.0	0.0	-0.1	-0.1
B2	7	0.0	0.0	0.0	0.0	0.0	0.0	0.0	0.0	0.0
B3	8	0.0	0.0	0.0	0.0	0.0	0.0	0.0	0.0	0.0
B4	9	0.1	0.0	0.1	0.0	0.0	0.0	0.1	0.1	0.0
B5	10	0.2	0.0	0.2	0.0	0.0	0.0	0.2	0.2	0.0
C1	251	0.2	0.3	0.1	0.0	0.0	0.0	0.3	0.1	0.1
C2	252	0.0	0.1	0.0	0.0	0.0	0.0	0.1	0.0	0.0
C3	253	0.0	0.0	0.0	0.0	0.0	0.0	0.0	0.0	0.0
C4	254	-0.1	0.0	0.0	0.0	0.0	0.0	0.0	0.0	-0.1
C5	255	-0.1	0.0	0.0	0.0	0.0	0.0	0.0	0.0	-0.1
D1	306	0.1	0.1	0.1	0.0	0.0	0.0	0.1	0.1	0.0
D2	307	0.0	0.0	0.0	0.0	0.0	0.0	0.1	0.0	0.0
D3	308	0.0	0.0	0.0	0.0	0.0	0.0	0.0	0.0	0.0
D4	309	0.0	0.0	0.0	0.0	0.0	0.0	0.0	0.0	0.0
D5	310	-0.1	0.0	0.0	0.0	0.0	0.0	0.0	0.0	-0.1
E1	305	-0.1	0.0	0.0	0.0	0.0	0.0	0.0	0.0	-0.1
E2	315	-0.1	0.0	0.0	0.0	0.0	0.0	0.0	0.0	-0.1
E3	325	0.0	0.0	0.0	0.0	0.0	0.0	0.0	0.0	0.0
E4	335	0.0	0.0	0.0	0.0	0.0	0.0	0.0	0.0	0.0
E5	345	0.0	0.0	0.0	0.0	0.0	0.0	0.0	0.0	0.0
E6	355	0.0	0.0	0.0	0.0	0.0	0.0	0.0	0.0	0.0
F1	251	0.2	0.3	0.1	0.0	0.0	0.0	0.3	0.1	0.1
F2	261	0.1	0.1	0.0	0.0	0.0	0.0	0.1	0.1	0.0
F3	271	0.0	0.0	0.0	0.0	0.0	0.0	0.0	0.0	0.0
F4	281	0.0	-0.2	-0.1	0.0	0.0	0.0	0.0	-0.1	-0.2
G1	311	0.1	0.1	0.0	0.0	0.0	0.0	0.1	0.0	0.0

Table 2.10.4-2 Stress Components – 12 psig Internal Pressure + Bolt Preload; 2-D Model; Condition 4 (continued)

Stress Points		Stress Components (ksi)						Principal Stresses (ksi)		
Section[1]	Node	S_x	S_y	S_z	S_{xy}	S_{yz}	S_{xz}	S1	S2	S3
G2	321	0.0	0.0	0.0	0.0	0.0	0.0	0.0	0.0	0.0
G3	331	0.0	0.0	0.0	0.0	0.0	0.0	0.0	0.0	0.0
G4	341	0.0	0.0	0.0	0.0	0.0	0.0	0.0	0.0	0.0
G5	351	0.0	0.0	0.0	0.0	0.0	0.0	0.0	0.0	0.0
H1	581	0.0	0.0	0.2	0.0	0.0	0.0	0.2	0.0	0.0
H2	582	0.0	0.1	0.2	0.0	0.0	0.0	0.2	0.1	0.0
H3	583	0.0	0.1	0.2	0.0	0.0	0.0	0.2	0.1	0.0
H4	584	0.0	0.2	0.2	0.0	0.0	0.0	0.2	0.2	0.0
I1	589	0.0	0.0	0.0	0.0	0.0	0.0	0.0	0.0	0.0
I2	590	0.0	0.0	0.0	0.0	0.0	0.0	0.0	0.0	0.0
I3	591	0.0	0.0	0.0	0.0	0.0	0.0	0.0	0.0	0.0
I4	592	0.0	0.0	0.0	0.0	0.0	0.0	0.0	0.0	0.0
I5	593	0.0	0.0	0.0	0.0	0.0	0.0	0.0	0.0	0.0
J1	971	0.0	0.1	0.2	0.0	0.0	0.0	0.2	0.1	0.0
J2	972	0.0	0.1	0.2	0.0	0.0	0.0	0.2	0.1	0.0
J3	973	0.0	0.1	0.2	0.0	0.0	0.0	0.2	0.1	0.0
J4	974	0.0	0.1	0.2	0.0	0.0	0.0	0.2	0.1	0.0
K1	979	0.0	0.0	0.0	0.0	0.0	0.0	0.0	0.0	0.0
K2	980	0.0	0.0	0.0	0.0	0.0	0.0	0.0	0.0	0.0
K3	981	0.0	0.0	0.0	0.0	0.0	0.0	0.0	0.0	0.0
K4	982	0.0	0.0	0.0	0.0	0.0	0.0	0.0	0.0	0.0
K5	983	0.0	0.0	0.0	0.0	0.0	0.0	0.0	0.0	0.0
L1	1601	0.0	0.1	0.2	0.0	0.0	0.0	0.2	0.1	0.0
L2	1602	0.0	0.1	0.2	0.0	0.0	0.0	0.2	0.1	0.0
L3	1603	0.0	0.1	0.2	0.0	0.0	0.0	0.2	0.1	0.0
L4	1604	0.0	0.1	0.2	0.0	0.0	0.0	0.2	0.1	0.0
M1	1609	0.0	0.0	0.0	0.0	0.0	0.0	0.0	0.0	0.0
M2	1610	0.0	0.0	0.0	0.0	0.0	0.0	0.0	0.0	0.0
M3	1611	0.0	0.0	0.0	0.0	0.0	0.0	0.0	0.0	0.0
M4	1612	0.0	0.0	0.0	0.0	0.0	0.0	0.0	0.0	0.0
M5	1613	0.0	0.0	0.0	0.0	0.0	0.0	0.0	0.0	0.0
N1	2216	0.0	0.1	0.2	0.0	0.0	0.0	0.2	0.1	0.0
N2	2217	0.0	0.1	0.2	0.0	0.0	0.0	0.2	0.1	0.0

Table 2.10.4-2 Stress Components – 12 psig Internal Pressure + Bolt Preload; 2-D Model; Condition 4 (continued)

Stress Points		Stress Components (ksi)						Principal Stresses (ksi)		
Section[1]	Node	S_x	S_y	S_z	S_{xy}	S_{yz}	S_{xz}	S1	S2	S3
N3	2218	0.0	0.1	0.2	0.0	0.0	0.0	0.2	0.1	0.0
N4	2219	0.0	0.1	0.2	0.0	0.0	0.0	0.2	0.1	0.0
O1	2224	0.0	0.0	0.0	0.0	0.0	0.0	0.0	0.0	0.0
O2	2225	0.0	0.0	0.0	0.0	0.0	0.0	0.0	0.0	0.0
O3	2226	0.0	0.0	0.0	0.0	0.0	0.0	0.0	0.0	0.0
O4	2227	0.0	0.0	0.0	0.0	0.0	0.0	0.0	0.0	0.0
O5	2228	0.0	0.0	0.0	0.0	0.0	0.0	0.0	0.0	0.0
P1	2546	0.0	0.1	0.3	0.0	0.0	0.0	0.3	0.1	0.0
P2	2547	0.0	0.1	0.3	0.0	0.0	0.0	0.3	0.1	0.0
P3	2548	0.0	0.1	0.2	0.0	0.0	0.0	0.2	0.1	0.0
P4	2549	0.0	0.1	0.2	0.0	0.0	0.0	0.2	0.1	0.0
Q1	2554	0.0	0.1	0.0	0.0	0.0	0.0	0.1	0.0	0.0
Q2	2555	0.0	0.0	0.0	0.0	0.0	0.0	0.0	0.0	0.0
Q3	2556	0.0	0.0	0.0	0.0	0.0	0.0	0.0	0.0	0.0
Q4	2557	0.0	0.0	0.0	0.0	0.0	0.0	0.0	0.0	0.0
Q5	2558	0.0	0.0	0.0	0.0	0.0	0.0	0.0	0.0	0.0
R1	2771	-0.2	-0.8	0.0	0.2	0.0	0.0	0.0	-0.2	-0.8
R2	2772	-0.2	-0.3	0.1	0.2	0.0	0.0	0.1	0.0	-0.5
R3	2773	-0.4	0.1	0.1	0.3	0.0	0.0	0.2	0.1	-0.5
R4	2774	-0.9	1.1	0.2	0.2	0.0	0.0	1.1	0.2	-1.0
S1	2779	-0.4	0.0	0.0	-0.1	0.0	0.0	0.0	0.0	-0.4
S2	2780	-0.1	0.0	0.0	0.0	0.0	0.0	0.0	0.0	-0.2
S3	2781	-0.1	0.0	0.1	0.0	0.0	0.0	0.1	0.0	-0.1
S4	2782	0.0	0.0	0.1	0.0	0.0	0.0	0.1	0.0	0.0
S5	2783	0.0	0.1	0.1	0.0	0.0	0.0	0.1	0.1	0.0
T1	7066	0.0	0.0	0.1	0.1	0.0	0.0	0.1	0.1	-0.1
T2	7067	0.2	-0.5	0.0	0.0	0.0	0.0	0.2	0.0	-0.5
T3	7068	0.2	-0.4	0.0	0.0	0.0	0.0	0.2	0.0	-0.4
T4	7069	0.1	-0.3	0.1	0.0	0.0	0.0	0.1	0.1	-0.3
T5	7070	0.0	-0.2	0.1	0.0	0.0	0.0	0.1	0.0	-0.2
T6	7071	0.0	-0.1	0.1	0.0	0.0	0.0	0.1	0.0	-0.1
T7	7072	0.0	0.0	0.1	0.0	0.0	0.0	0.1	0.0	0.0
U1	3051	-0.1	-1.8	-0.6	0.5	0.0	0.0	0.0	-0.6	-1.9

Table 2.10.4-2 Stress Components – 12 psig Internal Pressure + Bolt Preload; 2-D Model; Condition 4 (continued)

Stress Points		Stress Components (ksi)						Principal Stresses (ksi)		
Section[1]	Node	S_x	S_y	S_z	S_{xy}	S_{yz}	S_{zx}	S1	S2	S3
U2	3052	-0.4	-2.1	-0.8	0.4	0.0	0.0	-0.3	-0.8	-2.2
U3	3053	-0.1	-2.3	-0.7	0.1	0.0	0.0	-0.1	-0.7	-2.3
U4	3054	0.1	-1.7	-0.5	-0.5	0.0	0.0	0.2	-0.5	-1.9
U5	3055	-0.4	-0.9	-0.2	-0.6	0.0	0.0	0.0	-0.2	-1.3
U6	3056	1.0	0.1	0.6	-0.4	0.0	0.0	1.1	0.6	-0.1
V1	3611	1.2	0.0	0.5	0.0	0.0	0.0	1.2	0.5	0.0
V2	3612	0.7	-0.1	0.3	0.0	0.0	0.0	0.7	0.3	-0.1
V3	3613	0.4	-0.3	0.1	0.0	0.0	0.0	0.4	0.1	-0.3
V4	3614	0.1	-0.5	-0.1	0.0	0.0	0.0	0.1	-0.1	-0.5
V5	3615	-0.2	-1.1	-0.4	0.1	0.0	0.0	-0.2	-0.4	-1.1
V6	3616	-0.4	-0.5	-0.3	0.0	0.0	0.0	-0.3	-0.4	-0.5
V7	3617	-1.4	0.4	-0.4	0.0	0.0	0.0	0.4	-0.4	-1.4
W1	3241	-0.3	0.0	-0.3	0.0	0.0	0.0	0.0	-0.3	-0.3
W2	3242	-0.2	0.0	-0.2	0.0	0.0	0.0	0.0	-0.2	-0.2
W3	3243	0.0	0.0	0.0	0.0	0.0	0.0	0.0	0.0	0.0
W4	3244	0.1	0.0	0.1	0.0	0.0	0.0	0.1	0.1	0.0
W5	3245	0.2	0.0	0.2	0.0	0.0	0.0	0.2	0.2	0.0
W6	3246	0.3	0.0	0.3	0.0	0.0	0.0	0.3	0.3	0.0
X1	3801	0.0	0.0	0.0	0.0	0.0	0.0	0.0	0.0	0.0
X2	3802	0.0	0.0	0.0	0.0	0.0	0.0	0.0	0.0	0.0
X3	3803	0.0	0.0	0.0	0.0	0.0	0.0	0.0	0.0	0.0
X4	3804	0.0	0.0	0.0	0.0	0.0	0.0	0.0	0.0	0.0
X5	3805	0.0	0.0	0.0	0.0	0.0	0.0	0.0	0.0	0.0
X6	3806	0.0	0.0	0.0	0.0	0.0	0.0	0.0	0.0	0.0
X7	3807	0.0	0.0	0.0	0.0	0.0	0.0	0.0	0.0	0.0

[1] Refer to Figure 2.10.2-34 for the identification of the representative sections.

Table 2.10.4-3 Stress Components – Gravity; 1 g; 3-D Top Model; 0-Degree Circumferential Location; Condition 1

Condition 1: 100°F Ambient with Contents

Stress Points		Stress Components (ksi)						Principal Stresses (ksi)		
Section[1]	Node	S_x	S_y	S_z	S_{xy}	S_{yz}	S_{xz}	S1	S2	S3
A1	1949	0.0	0.0	0.0	0.0	0.0	0.0	0.0	0.0	0.0
A2	1950	0.0	0.0	0.0	0.0	0.0	0.0	0.0	0.0	0.0
A3	1951	0.0	0.0	0.0	0.0	0.0	0.0	0.0	0.0	0.0
B1	1952	0.0	0.0	0.0	0.0	0.0	0.0	0.0	0.0	0.0
B2	93	0.0	0.0	0.0	0.0	0.0	0.0	0.0	0.0	0.0
C1	1925	0.0	0.0	0.1	0.0	0.0	0.0	0.1	0.0	0.0
C2	1926	0.0	0.0	0.0	0.0	0.0	0.0	0.0	0.0	0.0
C3	1927	0.0	0.0	0.0	0.0	0.0	0.0	0.0	0.0	0.0
D1	683	0.0	0.0	0.0	0.0	0.0	0.0	0.0	0.0	0.0
D2	85	0.0	0.1	0.0	0.0	0.0	0.0	0.1	0.0	0.0
E1	682	0.0	0.0	0.0	0.0	0.0	0.0	0.0	0.0	0.0
E2	82	0.0	0.1	0.1	0.0	0.0	0.0	0.1	0.1	0.0
F1	1925	0.0	0.0	0.1	0.0	0.0	0.0	0.1	0.0	0.0
F2	1325	-0.1	-0.1	-0.3	0.0	0.0	0.0	-0.1	-0.1	-0.3
G1	680	0.0	0.0	0.1	0.0	0.0	0.0	0.1	0.0	0.0
G2	80	0.0	0.0	0.1	0.0	0.0	0.0	0.1	0.0	0.0
H1	1921	0.0	0.1	-0.1	0.0	0.0	0.0	0.1	0.0	-0.1
H2	1321	0.0	0.2	0.0	0.0	0.0	0.0	0.2	0.0	0.0
I1	676	0.0	0.0	0.1	0.0	0.0	0.0	0.1	0.0	0.0
I2	76	0.0	0.0	0.2	0.0	0.0	0.0	0.2	0.0	0.0
J1	1916	0.0	0.1	0.2	0.0	0.0	0.0	0.2	0.1	0.0
J2	1316	0.0	0.2	0.3	0.0	0.0	0.0	0.3	0.2	0.0
K1	671	0.0	0.0	0.1	0.0	0.0	0.0	0.1	0.0	0.0
K2	71	0.0	0.1	0.1	0.0	0.0	0.0	0.1	0.1	0.0
L1	1908	0.0	0.1	0.4	0.0	0.0	0.0	0.4	0.1	0.0
L2	1308	0.0	0.2	0.5	0.0	0.0	0.0	0.5	0.3	0.0
M1	663	0.0	0.0	0.1	0.0	0.0	0.0	0.1	0.0	0.0
M2	63	0.0	0.0	0.1	0.0	0.0	0.0	0.1	0.0	0.0
N1	1877	0.0	0.2	0.2	0.0	0.0	0.0	0.3	0.1	0.0

Table 2.10.4-3 Stress Components – Gravity; 1 g; 3-D Top Model; 0-Degree Circumferential Location; Condition 1 (continued)

Stress Points		Stress Components (ksi)						Principal Stresses (ksi)		
Section[1]	Node	S_x	S_y	S_z	S_{xy}	S_{yz}	S_{xz}	S1	S2	S3
N2	1477	0.0	0.2	0.3	0.0	0.0	0.0	0.3	0.2	0.0
N3	1277	0.0	0.2	0.3	0.0	0.0	0.0	0.3	0.2	0.0
O1	647	0.0	0.1	0.0	0.0	0.0	0.0	0.1	0.0	0.0
O2	247	0.0	0.0	0.0	0.0	0.0	0.0	0.0	0.0	0.0
O3	47	0.0	0.0	0.0	0.0	0.0	0.0	0.0	0.0	0.0
P1	1840	0.0	0.1	-0.2	0.0	0.0	0.0	0.1	0.0	-0.2
P2	1640	0.0	0.1	-0.1	0.0	0.0	0.0	0.1	0.0	-0.1
P3	1440	0.0	0.2	0.1	0.0	0.0	0.0	0.2	0.1	0.0
P4	1240	0.0	0.2	0.3	0.0	0.0	0.0	0.3	0.2	0.0
Q1	628	0.0	-0.3	-0.3	0.0	0.0	0.0	0.0	-0.3	-0.3
Q2	428	0.0	-0.2	-0.1	0.0	0.0	0.0	0.0	-0.1	-0.2
Q3	228	0.0	-0.2	0.0	0.0	0.0	0.0	0.0	0.0	-0.2
Q4	28	0.0	-0.1	0.2	0.0	0.0	0.0	0.2	0.0	-0.1
R1	1816	-0.1	-0.2	1.6	0.0	0.0	0.1	1.6	-0.1	-0.2
R2	1616	-0.2	-0.5	0.5	0.0	0.0	0.1	0.5	-0.2	-0.5
R3	1416	-0.6	-0.9	-0.4	0.0	0.0	0.0	-0.4	-0.6	-0.9
R4	1216	-1.1	-1.3	-1.5	0.0	0.0	-0.3	-1.0	-1.3	-1.6
S1	616	-0.8	-0.7	0.4	0.0	0.0	0.3	0.5	-0.7	-0.9
S2	416	-0.5	-0.6	0.3	0.0	0.0	0.5	0.6	-0.6	-0.7
S3	216	0.0	-0.7	-0.3	0.0	0.0	0.5	0.4	-0.7	-0.7
S4	16	0.3	-0.7	-0.8	0.0	0.0	0.4	0.4	-0.7	-0.9
T1	811	0.1	-0.2	-0.5	0.0	0.0	0.1	0.1	-0.2	-0.5
T2	611	-0.3	-0.3	-0.2	0.0	0.0	0.1	-0.2	-0.3	-0.3
T3	411	-0.1	-0.2	-0.1	0.0	0.0	0.0	0.0	-0.1	-0.2
T4	211	0.0	-0.1	0.2	0.0	0.0	0.0	0.2	0.0	-0.1
T5	11	0.0	0.0	0.5	0.0	0.0	0.0	0.5	0.0	0.0
U1	43058	-0.7	-0.5	-0.4	0.0	0.0	0.0	-0.4	-0.5	-0.7
U2	43057	-0.4	-0.4	-0.3	0.0	0.0	0.0	-0.3	-0.4	-0.5
U3	43056	-0.3	-0.3	-0.2	0.0	0.0	0.1	-0.2	-0.3	-0.3
U4	43055	-0.2	-0.2	-0.1	0.0	0.0	0.0	-0.1	-0.2	-0.2
U5	43054	-0.1	-0.2	-0.1	0.0	0.0	0.0	-0.1	-0.1	-0.2

Table 2.10.4-3 Stress Components – Gravity; 1 g; 3-D Top Model; 0-Degree Circumferential Location; Condition 1 (continued)

Stress Points		Stress Components (ksi)						Principal Stresses (ksi)		
Section[1]	Node	S_x	S_y	S_z	S_{xy}	S_{yz}	S_{zx}	S1	S2	S3
U6	43053	0.0	-0.1	-0.1	0.0	0.0	0.0	0.0	-0.1	-0.1
U7	43052	0.0	0.0	-0.1	0.0	0.0	0.0	0.0	0.0	-0.1
U8	43051	0.1	0.1	0.0	0.0	0.0	0.0	0.1	0.1	0.0
V1	50024	-0.1	-0.1	0.0	0.0	0.0	0.0	0.0	-0.1	-0.1
V2	50023	-0.1	-0.1	0.0	0.0	0.0	0.0	0.0	-0.1	-0.1
V3	50022	0.0	0.0	0.0	0.0	0.0	0.0	0.0	0.0	0.0
V4	50021	0.1	0.1	0.0	0.0	0.0	0.0	0.1	0.1	0.0
W1	43278	-0.1	-0.1	0.0	0.0	0.0	0.0	0.0	-0.1	-0.1
W2	43274	0.0	-0.1	0.0	0.0	0.0	0.0	0.0	0.0	-0.1
W3	43271	0.0	-0.1	0.0	0.0	0.0	0.0	0.0	0.0	-0.1
X1	50084	-0.1	0.0	0.0	0.0	0.0	0.0	0.0	0.0	-0.1
X2	50083	0.0	0.0	0.0	0.0	0.0	0.0	0.0	0.0	0.0
X3	50081	0.1	0.0	0.0	0.0	0.0	0.0	0.1	0.0	0.0

[1] Refer to Figure 2.10.2-34 for the identification of the representative sections.

Table 2.10.4-4 Stress Components – Gravity; 1 g; 3-D Top Model; 0-Degree Circumferential Location; Condition 4

Condition 4: -40°F Ambient, No Decay Heat

Stress Points		Stress Components (ksi)						Principal Stresses (ksi)		
Section[1]	Node	S_x	S_y	S_z	S_{xy}	S_{yz}	S_{xz}	S1	S2	S3
A1	1949	0.0	0.0	0.0	0.0	0.0	0.0	0.0	0.0	0.0
A2	1950	0.0	0.0	0.0	0.0	0.0	0.0	0.0	0.0	0.0
A3	1951	0.0	0.0	0.0	0.0	0.0	0.0	0.0	0.0	0.0
B1	1952	0.0	0.0	0.0	0.0	0.0	0.0	0.0	0.0	0.0
B2	93	0.0	0.0	0.0	0.0	0.0	0.0	0.0	0.0	0.0
C1	1925	0.0	0.0	0.1	0.0	0.0	0.0	0.1	0.0	0.0
C2	1926	0.0	0.0	0.0	0.0	0.0	0.0	0.0	0.0	0.0
C3	1927	0.0	0.0	0.0	0.0	0.0	0.0	0.0	0.0	0.0
D1	683	0.0	0.0	0.0	0.0	0.0	0.0	0.0	0.0	0.0
D2	85	0.0	0.1	0.0	0.0	0.0	0.0	0.1	0.0	0.0
E1	682	0.0	0.0	0.0	0.0	0.0	0.0	0.0	0.0	0.0
E2	82	0.0	0.1	0.1	0.0	0.0	0.0	0.1	0.1	0.0
F1	1925	0.0	0.0	0.1	0.0	0.0	0.0	0.1	0.0	0.0
F2	1325	-0.1	-0.1	-0.3	0.0	0.0	0.0	-0.1	-0.1	-0.3
G1	680	0.0	0.0	0.1	0.0	0.0	0.0	0.1	0.0	0.0
G2	80	0.0	0.0	0.1	0.0	0.0	0.0	0.1	0.0	0.0
H1	1921	0.0	0.1	-0.1	0.0	0.0	0.0	0.1	0.0	-0.1
H2	1321	0.0	0.2	0.1	0.0	0.0	0.0	0.2	0.0	0.0
I1	676	0.0	0.0	0.1	0.0	0.0	0.0	0.1	0.0	0.0
I2	76	0.0	0.0	0.2	0.0	0.0	0.0	0.2	0.0	0.0
J1	1916	0.0	0.1	0.2	0.0	0.0	0.0	0.2	0.1	0.0
J2	1316	0.0	0.2	0.3	0.0	0.0	0.0	0.3	0.2	0.0
K1	671	0.0	0.0	0.1	0.0	0.0	0.0	0.1	0.0	0.0
K2	71	0.0	0.1	0.1	0.0	0.0	0.0	0.1	0.1	0.0
L1	1908	0.0	0.1	0.4	0.0	0.0	0.0	0.4	0.1	0.0
L2	1308	0.0	0.2	0.5	0.0	0.0	0.0	0.5	0.3	0.0
M1	663	0.0	0.0	0.1	0.0	0.0	0.0	0.1	0.0	0.0
M2	63	0.0	0.0	0.1	0.0	0.0	0.0	0.1	0.0	0.0
N1	1877	0.0	0.1	0.2	0.0	0.0	0.0	0.3	0.1	0.0

Table 2.10.4-4 Stress Components – Gravity; 1 g; 3-D Top Model; 0-Degree Circumferential Location; Condition 4 (continued)

Stress Points		Stress Components (ksi)						Principal Stresses (ksi)		
Section[1]	Node	S_x	S_y	S_z	S_{xy}	S_{yz}	S_{xz}	S1	S2	S3
N2	1477	0.0	0.2	0.3	0.0	0.0	0.0	0.3	0.2	0.0
N3	1277	0.0	0.2	0.3	0.0	0.0	0.0	0.3	0.2	0.0
O1	647	0.0	0.1	0.0	0.0	0.0	0.0	0.1	0.0	0.0
O2	247	0.0	0.0	0.0	0.0	0.0	0.0	0.0	0.0	0.0
O3	47	0.0	0.0	0.0	0.0	0.0	0.0	0.0	0.0	0.0
P1	1840	0.0	0.1	-0.2	0.0	0.0	0.0	0.1	0.0	-0.2
P2	1640	0.0	0.1	-0.1	0.0	0.0	0.0	0.1	0.0	-0.1
P3	1440	0.0	0.2	0.1	0.0	0.0	0.0	0.2	0.1	0.0
P4	1240	0.0	0.2	0.3	0.0	0.0	0.0	0.3	0.2	0.0
Q1	628	0.0	-0.3	-0.3	0.0	0.0	0.0	0.0	-0.3	-0.3
Q2	428	0.0	-0.2	-0.1	0.0	0.0	0.0	0.0	-0.1	-0.2
Q3	228	0.0	-0.2	0.0	0.0	0.0	0.0	0.0	0.0	-0.2
Q4	28	0.0	-0.1	0.2	0.0	0.0	0.0	0.2	0.0	-0.1
R1	1816	-0.1	-0.2	1.6	0.0	0.0	0.1	1.6	-0.1	-0.2
R2	1616	-0.2	-0.5	0.5	0.0	0.0	0.1	0.5	-0.2	-0.5
R3	1416	-0.6	-0.9	-0.4	0.0	0.0	0.0	-0.4	-0.6	-0.9
R4	1216	-1.1	-1.3	-1.5	0.0	0.0	-0.3	-1.0	-1.3	-1.6
S1	616	-0.8	-0.7	0.4	0.0	0.0	0.3	0.5	-0.7	-0.9
S2	416	-0.5	-0.6	0.3	0.0	0.0	0.5	0.5	-0.6	-0.7
S3	216	0.0	-0.7	-0.3	0.0	0.0	0.5	0.4	-0.7	-0.7
S4	16	0.3	-0.7	-0.8	0.0	0.0	0.4	0.4	-0.7	-0.9
T1	811	0.1	-0.2	-0.5	0.0	0.0	0.1	0.1	-0.2	-0.5
T2	611	-0.3	-0.3	-0.2	0.0	0.0	0.1	-0.2	-0.3	-0.3
T3	411	-0.1	-0.2	-0.1	0.0	0.0	0.0	0.0	-0.1	-0.2
T4	211	0.0	-0.1	0.2	0.0	0.0	0.0	0.2	0.0	-0.1
T5	11	0.0	0.0	0.5	0.0	0.0	0.0	0.5	0.0	0.0
U1	43058	-0.7	-0.5	-0.4	0.0	0.0	0.0	-0.4	-0.5	-0.7
U2	43057	-0.4	-0.4	-0.3	0.0	0.0	0.0	-0.3	-0.4	-0.5
U3	43056	-0.3	-0.3	-0.2	0.0	0.0	0.1	-0.2	-0.3	-0.3
U4	43055	-0.2	-0.2	-0.1	0.0	0.0	0.0	-0.1	-0.2	-0.2
U5	43054	-0.1	-0.2	-0.1	0.0	0.0	0.0	-0.1	-0.1	-0.2

Table 2.10.4-4 Stress Components – Gravity; 1 g; 3-D Top Model; 0-Degree Circumferential Location; Condition 4 (continued)

Stress Points		Stress Components (ksi)						Principal Stresses (ksi)		
Section[1]	Node	S_x	S_y	S_z	S_{xy}	S_{yz}	S_{zx}	S1	S2	S3
U6	43053	0.0	-0.1	-0.1	0.0	0.0	0.0	0.0	-0.1	-0.1
U7	43052	0.0	0.0	-0.1	0.0	0.0	0.0	0.0	0.0	-0.1
U8	43051	0.1	0.1	0.0	0.0	0.0	0.0	0.1	0.1	0.0
V1	50024	-0.1	-0.1	0.0	0.0	0.0	0.0	0.0	-0.1	-0.1
V2	50023	-0.1	-0.1	0.0	0.0	0.0	0.0	0.0	-0.1	-0.1
V3	50022	0.0	0.0	0.0	0.0	0.0	0.0	0.0	0.0	0.0
V4	50021	0.1	0.1	0.0	0.0	0.0	0.0	0.1	0.1	0.0
W1	43278	-0.1	-0.1	0.0	0.0	0.0	0.0	0.0	-0.1	-0.1
W2	43274	0.0	-0.1	0.0	0.0	0.0	0.0	0.0	0.0	-0.1
W3	43271	0.0	-0.1	0.0	0.0	0.0	0.0	0.0	0.0	-0.1
X1	50084	-0.1	0.0	0.0	0.0	0.0	0.0	0.0	0.0	-0.1
X2	50083	0.0	0.0	0.0	0.0	0.0	0.0	0.0	0.0	0.0
X3	50081	0.1	0.0	0.0	0.0	0.0	0.0	0.1	0.0	0.0

[1] Refer to Figure 2.10.2-34 for the identification of the representative sections.

Table 2.10.4-5 Stress Components – Thermal Heat, 100°F; 2-D Model; Condition 1

Condition 1: 100°F Ambient with Contents

Stress Points		Stress Components (ksi)						Principal Stresses (ksi)		
Section[1]	Node	S_x	S_y	S_z	S_{xy}	S_{yz}	S_{xz}	S1	S2	S3
A1	1	0.8	0.0	0.8	0.0	0.0	0.0	0.8	0.8	0.0
A2	2	0.1	0.0	0.1	0.0	0.0	0.0	0.1	0.1	0.0
A3	3	-0.5	0.0	-0.5	0.0	0.0	0.0	0.0	-0.5	-0.5
A4	4	-1.2	0.0	-1.2	0.0	0.0	0.0	0.0	-1.2	-1.2
A5	5	-1.8	0.0	-1.8	0.0	0.0	0.0	0.0	-1.8	-1.8
B1	6	0.8	0.0	0.8	0.0	0.0	0.0	0.8	0.8	0.0
B2	7	1.1	0.0	1.1	0.0	0.0	0.0	1.1	1.1	0.0
B3	8	1.3	0.0	1.3	0.0	0.0	0.0	1.3	1.3	0.0
B4	9	1.6	0.0	1.6	0.0	0.0	0.0	1.6	1.6	0.0
B5	10	1.8	0.0	1.8	0.0	0.0	0.0	1.8	1.8	0.0
C1	251	-0.7	-2.7	-0.5	-0.5	0.0	0.0	-0.5	-0.5	-2.8
C2	252	0.1	-1.2	-0.3	-0.4	0.0	0.0	0.3	-0.3	-1.4
C3	253	-0.3	-0.9	-0.8	-0.4	0.0	0.0	-0.1	-0.8	-1.1
C4	254	-0.6	-1.0	-1.3	-0.3	0.0	0.0	-0.5	-1.1	-1.3
C5	255	-1.2	-1.0	-1.9	-0.1	0.0	0.0	-1.0	-1.2	-1.9
D1	306	5.7	6.6	3.5	2.0	0.0	0.0	8.2	4.1	3.5
D2	307	1.0	3.7	1.5	1.3	0.0	0.0	4.3	1.5	0.5
D3	308	0.3	1.4	0.9	0.4	0.0	0.0	1.5	0.9	0.2
D4	309	-0.5	0.5	0.6	0.1	0.0	0.0	0.6	0.5	-0.5
D5	310	-1.7	0.2	0.4	0.0	0.0	0.0	0.4	0.2	-1.7
E1	305	-1.0	3.6	0.3	0.6	0.0	0.0	3.7	0.3	-1.1
E2	315	-0.7	2.4	0.2	1.5	0.0	0.0	3.1	0.2	-1.3
E3	325	0.0	1.5	0.2	1.7	0.0	0.0	2.6	0.2	-1.1
E4	335	0.1	0.8	0.1	1.4	0.0	0.0	1.8	0.1	-1.0
E5	345	0.1	0.0	-0.1	0.8	0.0	0.0	0.8	-0.1	-0.8
E6	355	0.1	-1.0	-0.3	0.5	0.0	0.0	0.3	-0.3	-1.1
F1	251	-0.7	-2.7	-0.5	-0.5	0.0	0.0	-0.5	-0.5	-2.8
F2	261	-0.2	-0.9	0.1	-0.4	0.0	0.0	0.1	0.0	-1.1
F3	271	0.7	0.5	0.6	-0.6	0.0	0.0	1.2	0.6	-0.1
F4	281	1.0	2.5	1.0	-1.2	0.0	0.0	3.1	1.0	0.4
G1	311	-3.5	0.5	-0.8	1.5	0.0	0.0	1.1	-0.8	-4.1
G2	321	-3.2	3.4	0.1	1.1	0.0	0.0	3.6	0.1	-3.4

Table 2.10.4-5 Stress Components – Thermal Heat, 100°F; 2-D Model; Condition 1 (continued)

Stress Points		Stress Components (ksi)						Principal Stresses (ksi)		
Section[1]	Node	S_x	S_y	S_z	S_{xy}	S_{yz}	S_{xz}	S1	S2	S3
G3	331	-1.6	4.7	0.9	0.2	0.0	0.0	4.7	0.9	-1.6
G4	341	-0.6	6.0	1.5	-0.1	0.0	0.0	6.0	1.5	-0.6
G5	351	-0.2	7.9	2.2	-0.1	0.0	0.0	7.9	2.2	-0.2
H1	581	0.0	1.1	-0.2	0.1	0.0	0.0	1.1	0.0	-0.2
H2	582	0.0	0.4	-0.3	0.1	0.0	0.0	0.4	0.0	-0.3
H3	583	0.0	-0.2	-0.3	0.1	0.0	0.0	0.1	-0.3	-0.3
H4	584	-0.1	-1.0	-0.4	0.1	0.0	0.0	-0.1	-0.4	-1.0
I1	589	-0.3	5.7	2.1	0.1	0.0	0.0	5.7	2.1	-0.3
I2	590	-0.2	5.8	2.3	0.1	0.0	0.0	5.8	2.3	-0.2
I3	591	-0.1	5.8	2.4	0.1	0.0	0.0	5.9	2.4	-0.2
I4	592	-0.1	5.9	2.5	0.1	0.0	0.0	5.9	2.5	-0.1
I5	593	0.0	5.9	2.7	0.1	0.0	0.0	5.9	2.7	0.0
J1	971	0.0	-1.8	-1.1	0.0	0.0	0.0	0.0	-1.1	-1.8
J2	972	0.0	-0.6	-0.4	0.0	0.0	0.0	0.0	-0.4	-0.6
J3	973	0.0	0.7	0.4	0.0	0.0	0.0	0.7	0.4	0.0
J4	974	0.0	1.9	1.1	0.0	0.0	0.0	1.9	1.1	0.0
K1	979	-0.3	3.6	3.7	0.0	0.0	0.0	3.7	3.6	-0.3
K2	980	-0.2	4.7	4.3	0.0	0.0	0.0	4.7	4.3	-0.2
K3	981	-0.2	5.8	4.9	0.0	0.0	0.0	5.8	4.9	-0.2
K4	982	-0.1	6.9	5.5	0.0	0.0	0.0	6.9	5.5	-0.1
K5	983	0.0	7.9	6.0	0.0	0.0	0.0	7.9	6.0	0.0
L1	1601	0.0	-1.3	-1.1	0.0	0.0	0.0	0.0	-1.1	-1.3
L2	1602	0.0	-0.4	-0.3	0.0	0.0	0.0	0.0	-0.3	-0.4
L3	1603	0.0	0.5	0.4	0.0	0.0	0.0	0.5	0.4	0.0
L4	1604	0.0	1.4	1.1	0.0	0.0	0.0	1.4	1.1	0.0
M1	1609	-0.4	3.8	4.6	0.0	0.0	0.0	4.6	3.8	-0.4
M2	1610	-0.3	4.8	5.3	0.0	0.0	0.0	5.3	4.8	-0.3
M3	1611	-0.2	5.8	5.9	0.0	0.0	0.0	5.9	5.8	-0.2
M4	1612	-0.1	6.9	6.6	0.0	0.0	0.0	6.9	6.6	-0.1
M5	1613	0.0	7.9	7.2	0.0	0.0	0.0	7.9	7.2	0.0
N1	2216	0.0	-1.6	-1.4	0.0	0.0	0.0	0.0	-1.4	-1.6
N2	2217	0.0	-0.5	-0.7	0.0	0.0	0.0	0.0	-0.5	-0.7
N3	2218	0.0	0.6	-0.1	0.0	0.0	0.0	0.6	0.0	-0.1

Table 2.10.4-5 Stress Components – Thermal Heat, 100°F; 2-D Model; Condition 1 (continued)

Stress Points		Stress Components (ksi)						Principal Stresses (ksi)		
Section[1]	Node	S_x	S_y	S_z	S_{xy}	S_{yz}	S_{zx}	S1	S2	S3
N4	2219	0.0	1.7	0.6	0.0	0.0	0.0	1.7	0.6	0.0
O1	2224	-0.3	4.2	3.7	0.0	0.0	0.0	4.2	3.7	-0.3
O2	2225	-0.2	5.0	4.2	0.0	0.0	0.0	5.0	4.2	-0.2
O3	2226	-0.2	5.8	4.8	0.0	0.0	0.0	5.8	4.8	-0.2
O4	2227	-0.1	6.6	5.3	0.0	0.0	0.0	6.6	5.3	-0.1
O5	2228	0.0	7.4	5.7	0.0	0.0	0.0	7.4	5.7	0.0
P1	2546	0.0	-0.3	-0.5	0.0	0.0	0.0	0.0	-0.4	-0.5
P2	2547	0.0	-0.1	-0.2	0.0	0.0	0.0	0.0	-0.1	-0.2
P3	2548	0.1	0.2	0.0	0.0	0.0	0.0	0.2	0.1	0.0
P4	2549	-0.2	0.4	0.2	0.1	0.0	0.0	0.5	0.2	-0.2
Q1	2554	-0.1	5.1	2.3	0.0	0.0	0.0	5.1	2.3	-0.1
Q2	2555	-0.1	5.4	2.6	0.1	0.0	0.0	5.4	2.6	-0.1
Q3	2556	-0.1	5.8	2.9	0.1	0.0	0.0	5.8	2.9	-0.1
Q4	2557	0.0	6.2	3.2	0.1	0.0	0.0	6.2	3.2	0.0
Q5	2558	0.0	6.6	3.4	0.0	0.0	0.0	6.6	3.4	0.0
R1	2771	-0.3	3.4	-3.0	0.1	0.0	0.0	3.4	-0.3	-3.0
R2	2772	-0.7	0.9	-3.2	0.1	0.0	0.0	0.9	-0.7	-3.2
R3	2773	-1.6	-1.0	-3.5	0.2	0.0	0.0	-1.0	-1.7	-3.5
R4	2774	-3.0	-3.4	-3.9	0.0	0.0	0.0	-3.0	-3.4	-3.9
S1	2779	2.5	8.3	2.0	-2.2	0.0	0.0	9.1	2.0	1.8
S2	2780	2.3	6.2	1.7	-0.9	0.0	0.0	6.4	2.1	1.7
S3	2781	1.2	4.4	1.2	0.3	0.0	0.0	4.5	1.2	1.2
S4	2782	0.5	2.7	0.8	0.4	0.0	0.0	2.8	0.8	0.4
S5	2783	0.3	0.7	0.5	0.3	0.0	0.0	0.8	0.5	0.1
T1	7066	-1.8	-5.8	-0.7	-1.8	0.0	0.0	-0.7	-1.1	-6.5
T2	7067	-1.6	-3.1	0.2	-1.1	0.0	0.0	0.2	-1.1	-3.6
T3	7068	-1.2	-0.9	1.0	-0.6	0.0	0.0	1.0	-0.4	-1.7
T4	7069	-0.7	0.7	1.6	-0.3	0.0	0.0	1.6	0.8	-0.8
T5	7070	-0.4	2.2	2.2	-0.2	0.0	0.0	2.2	2.2	-0.4
T6	7071	-0.2	3.8	2.8	0.0	0.0	0.0	3.8	2.8	-0.2
T7	7072	-0.1	5.6	3.4	0.0	0.0	0.0	5.6	3.4	-0.1
U1	3051	-0.7	-1.2	-2.1	0.0	0.0	0.0	-0.7	-1.2	-2.1
U2	3052	0.2	-0.8	-1.6	-0.1	0.0	0.0	0.2	-0.9	-1.6

Table 2.10.4-5 Stress Components – Thermal Heat, 100°F; 2-D Model; Condition 1 (continued)

Stress Points		Stress Components (ksi)						Principal Stresses (ksi)		
Section[1]	Node	S_x	S_y	S_z	S_{xy}	S_{yz}	S_{zx}	S1	S2	S3
U3	3053	0.2	-0.4	-1.3	-0.2	0.0	0.0	0.2	-0.4	-1.3
U4	3054	0.2	-0.1	-1.2	-0.3	0.0	0.0	0.3	-0.3	-1.2
U5	3055	0.1	0.3	-1.0	-0.2	0.0	0.0	0.4	-0.1	-1.0
U6	3056	0.5	0.0	-0.8	0.0	0.0	0.0	0.5	-0.1	-0.8
V1	3611	0.1	0.0	-2.1	0.0	0.0	0.0	0.2	-0.1	-2.1
V2	3612	0.2	-0.1	-1.5	-0.1	0.0	0.0	0.2	-0.1	-1.5
V3	3613	0.1	-0.2	-1.0	-0.2	0.0	0.0	0.2	-0.3	-1.0
V4	3614	0.1	-0.4	-0.6	-0.2	0.0	0.0	0.2	-0.4	-0.6
V5	3615	0.1	-0.7	-0.2	-0.1	0.0	0.0	0.2	-0.2	-0.7
V6	3616	0.1	-0.3	0.3	-0.1	0.0	0.0	0.3	0.1	-0.3
V7	3617	-0.2	0.3	0.9	0.0	0.0	0.0	0.9	0.3	-0.2
W1	3241	1.9	0.0	1.9	0.0	0.0	0.0	1.9	1.9	0.0
W2	3242	1.7	0.0	1.7	0.0	0.0	0.0	1.7	1.7	0.0
W3	3243	1.4	0.0	1.4	0.0	0.0	0.0	1.4	1.4	0.0
W4	3244	1.2	0.0	1.2	0.0	0.0	0.0	1.2	1.2	0.0
W5	3245	1.0	0.0	1.0	0.0	0.0	0.0	1.0	1.0	0.0
W6	3246	0.7	0.0	0.7	0.0	0.0	0.0	0.7	0.7	0.0
X1	3801	-1.8	0.0	-1.8	0.0	0.0	0.0	0.0	-1.8	-1.8
X2	3802	-1.1	0.0	-1.1	0.0	0.0	0.0	0.0	-1.1	-1.1
X3	3803	-0.3	0.0	-0.3	0.0	0.0	0.0	0.0	-0.3	-0.3
X4	3804	0.4	0.0	0.4	0.0	0.0	0.0	0.4	0.4	0.0
X5	3805	1.2	0.0	1.2	0.0	0.0	0.0	1.2	1.2	0.0
X6	3806	2.0	0.0	2.0	0.0	0.0	0.0	2.0	2.0	0.0
X7	3807	2.8	-0.1	2.8	0.0	0.0	0.0	2.8	2.8	-0.1

[1] Refer to Figure 2.10.2-34 for the identification of the representative sections.

Table 2.10.4-6 Stress Components – Thermal Cold, -20°F; 2-D Model; Condition 2

Condition 2: -20°F Ambient with Contents

Stress Points		Stress Components (ksi)						Principal Stresses (ksi)		
Section[1]	Node	S_x	S_y	S_z	S_{xy}	S_{yz}	S_{xz}	S1	S2	S3
A1	1	0.0	0.0	0.0	0.0	0.0	0.0	0.0	0.0	0.0
A2	2	-0.3	0.0	-0.3	0.0	0.0	0.0	0.0	-0.3	-0.3
A3	3	-0.6	0.0	-0.6	0.0	0.0	0.0	0.0	-0.6	-0.6
A4	4	-0.9	0.0	-0.9	0.0	0.0	0.0	0.0	-0.9	-0.9
A5	5	-1.2	0.0	-1.2	0.0	0.0	0.0	0.0	-1.2	-1.2
B1	6	1.6	0.0	1.6	0.0	0.0	0.0	1.6	1.6	0.0
B2	7	1.3	0.0	1.3	0.0	0.0	0.0	1.3	1.3	0.0
B3	8	0.9	0.0	0.9	0.0	0.0	0.0	0.9	0.9	0.0
B4	9	0.6	0.0	0.6	0.0	0.0	0.0	0.6	0.6	0.0
B5	10	0.2	0.0	0.2	0.0	0.0	0.0	0.2	0.2	0.0
C1	251	-0.4	-0.1	-0.6	-0.1	0.0	0.0	-0.1	-0.5	-0.6
C2	252	-0.6	-0.3	-0.8	-0.1	0.0	0.0	-0.3	-0.6	-0.8
C3	253	-0.6	-0.3	-0.9	0.0	0.0	0.0	-0.3	-0.6	-0.9
C4	254	-0.7	-0.2	-0.9	0.0	0.0	0.0	-0.2	-0.7	-0.9
C5	255	-0.3	-0.1	-0.9	0.0	0.0	0.0	-0.1	-0.4	-0.9
D1	306	2.2	-1.1	0.9	0.7	0.0	0.0	2.4	0.9	-1.3
D2	307	1.1	0.0	0.8	0.1	0.0	0.0	1.2	0.8	0.0
D3	308	0.9	0.0	0.6	-0.1	0.0	0.0	0.9	0.6	0.0
D4	309	-1.0	-0.5	-1.4	-0.1	0.0	0.0	-0.5	-1.0	-1.4
D5	310	0.6	0.2	0.2	0.0	0.0	0.0	0.6	0.2	0.2
E1	305	-3.0	-3.3	-1.7	1.2	0.0	0.0	-1.7	-1.9	-4.4
E2	315	-1.7	-0.3	-0.3	0.9	0.0	0.0	0.2	-0.3	-2.2
E3	325	-1.0	0.4	0.1	0.8	0.0	0.0	0.8	0.1	-1.3
E4	335	-0.5	1.2	0.5	0.6	0.0	0.0	1.4	0.5	-0.7
E5	345	-0.2	2.0	0.8	0.4	0.0	0.0	2.1	0.8	-0.3
E6	355	-0.1	3.0	1.1	0.2	0.0	0.0	3.0	1.1	-0.1
F1	251	-0.4	-0.1	-0.6	-0.1	0.0	0.0	-0.1	-0.5	-0.6
F2	261	-0.4	-0.7	-0.8	-0.1	0.0	0.0	-0.4	-0.8	-0.8
F3	271	-0.7	-1.6	-1.3	0.0	0.0	0.0	-0.7	-1.3	-1.6
F4	281	-1.0	-2.3	-1.8	0.1	0.0	0.0	-1.0	-1.8	-2.4
G1	311	-0.6	1.9	-0.5	0.7	0.0	0.0	2.0	-0.5	-0.8
G2	321	-0.3	2.5	-0.1	0.3	0.0	0.0	2.5	-0.1	-0.3

Table 2.10.4-6 Stress Components – Thermal Cold, -20°F; 2-D Model; Condition 2 (continued)

Stress Points		Stress Components (ksi)						Principal Stresses (ksi)		
Section[1]	Node	S_x	S_y	S_z	S_{xy}	S_{yz}	S_{xz}	S1	S2	S3
G3	331	-0.1	2.7	0.1	-0.1	0.0	0.0	2.7	0.1	-0.1
G4	341	-0.1	3.0	0.2	-0.2	0.0	0.0	3.0	0.2	-0.1
G5	351	0.0	3.3	0.3	-0.1	0.0	0.0	3.3	0.3	0.0
H1	581	0.0	-1.1	-0.4	0.0	0.0	0.0	0.0	-0.4	-1.1
H2	582	0.0	-1.6	-0.5	0.1	0.0	0.0	0.0	-0.5	-1.6
H3	583	0.0	-2.0	-0.4	0.1	0.0	0.0	0.0	-0.4	-2.0
H4	584	-0.1	-2.7	-0.6	0.2	0.0	0.0	-0.1	-0.6	-2.7
I1	589	0.0	3.3	-0.2	0.0	0.0	0.0	3.3	0.0	-0.2
I2	590	0.0	3.3	-0.1	0.1	0.0	0.0	3.3	0.0	-0.1
I3	591	0.0	3.2	0.0	0.1	0.0	0.0	3.2	0.0	0.0
I4	592	0.0	3.2	0.2	0.1	0.0	0.0	3.2	0.2	0.0
I5	593	0.0	3.1	0.3	0.0	0.0	0.0	3.1	0.3	0.0
J1	971	0.0	-3.5	-1.0	0.0	0.0	0.0	0.0	-1.0	-3.5
J2	972	0.0	-2.4	-0.3	0.0	0.0	0.0	0.0	-0.3	-2.4
J3	973	0.0	-1.4	0.4	0.0	0.0	0.0	0.4	0.0	-1.4
J4	974	0.0	-0.4	1.1	0.0	0.0	0.0	1.1	0.0	-0.4
K1	979	-0.1	1.0	-0.7	0.0	0.0	0.0	1.0	-0.1	-0.7
K2	980	-0.1	2.1	0.0	0.0	0.0	0.0	2.1	0.0	-0.1
K3	981	-0.1	3.2	0.7	0.1	0.0	0.0	3.2	0.7	-0.1
K4	982	0.0	4.3	1.3	0.0	0.0	0.0	4.3	1.3	0.0
K5	983	0.0	5.3	1.9	0.0	0.0	0.0	5.3	1.9	0.0
L1	1601	0.0	-3.3	-1.1	0.0	0.0	0.0	0.0	-1.1	-3.3
L2	1602	0.0	-2.4	-0.3	0.0	0.0	0.0	0.0	-0.3	-2.4
L3	1603	0.0	-1.5	0.4	0.0	0.0	0.0	0.4	0.0	-1.5
L4	1604	0.0	-0.6	1.1	0.0	0.0	0.0	1.1	0.0	-0.6
M1	1609	-0.1	1.1	0.3	0.0	0.0	0.0	1.1	0.3	-0.1
M2	1610	-0.1	2.2	1.1	0.0	0.0	0.0	2.2	1.1	-0.1
M3	1611	-0.1	3.2	1.8	0.0	0.0	0.0	3.2	1.8	-0.1
M4	1612	0.0	4.2	2.5	0.0	0.0	0.0	4.2	2.5	0.0
M5	1613	0.0	5.3	3.2	0.0	0.0	0.0	5.3	3.2	0.0
N1	2216	0.0	-3.2	-1.1	0.0	0.0	0.0	0.0	-1.1	-3.2
N2	2217	0.0	-2.3	-0.5	0.0	0.0	0.0	0.0	-0.5	-2.3
N3	2218	0.0	-1.5	0.1	0.0	0.0	0.0	0.1	0.0	-1.5

Table 2.10.4-6 Stress Components – Thermal Cold, -20°F; 2-D Model; Condition 2 (continued)

Stress Points		Stress Components (ksi)						Principal Stresses (ksi)		
Section[1]	Node	S_x	S_y	S_z	S_{xy}	S_{yz}	S_{zx}	S1	S2	S3
N4	2219	0.0	-0.7	0.7	0.0	0.0	0.0	0.7	0.0	-0.7
O1	2224	-0.1	1.6	-0.5	0.0	0.0	0.0	1.6	-0.1	-0.5
O2	2225	-0.1	2.4	0.0	0.0	0.0	0.0	2.4	0.0	-0.1
O3	2226	-0.1	3.2	0.6	0.0	0.0	0.0	3.2	0.6	-0.1
O4	2227	0.0	4.0	1.2	0.0	0.0	0.0	4.0	1.2	0.0
O5	2228	0.0	4.8	1.7	0.0	0.0	0.0	4.8	1.7	0.0
P1	2546	0.0	-2.4	-0.6	0.0	0.0	0.0	0.0	-0.6	-2.4
P2	2547	0.0	-2.1	-0.3	0.0	0.0	0.0	0.0	-0.3	-2.1
P3	2548	0.1	-1.6	0.0	0.0	0.0	0.0	0.1	0.0	-1.6
P4	2549	-0.2	-1.4	0.1	0.0	0.0	0.0	0.1	-0.2	-1.4
Q1	2554	0.0	2.8	-0.8	0.0	0.0	0.0	2.8	0.0	-0.8
Q2	2555	0.0	3.0	-0.5	0.0	0.0	0.0	3.0	0.0	-0.5
Q3	2556	0.0	3.2	-0.2	0.0	0.0	0.0	3.2	0.0	-0.2
Q4	2557	0.0	3.4	0.0	0.0	0.0	0.0	3.4	0.0	0.0
Q5	2558	0.0	3.6	0.3	0.0	0.0	0.0	3.6	0.3	0.0
R1	2771	-0.3	3.8	-3.2	0.1	0.0	0.0	3.8	-0.3	-3.2
R2	2772	-0.8	0.4	-3.7	0.1	0.0	0.0	0.5	-0.8	-3.7
R3	2773	-1.7	-2.2	-4.2	-0.2	0.0	0.0	-1.6	-2.2	-4.2
R4	2774	-2.7	-5.3	-4.7	-0.7	0.0	0.0	-2.5	-4.7	-5.5
S1	2779	1.2	4.0	0.1	-0.9	0.0	0.0	4.3	0.9	0.1
S2	2780	1.1	3.3	0.2	-0.2	0.0	0.0	3.3	1.0	0.2
S3	2781	0.6	2.6	0.2	0.3	0.0	0.0	2.7	0.5	0.2
S4	2782	0.2	1.9	0.2	0.3	0.0	0.0	2.0	0.2	0.2
S5	2783	0.1	1.2	0.2	0.2	0.0	0.0	1.2	0.2	0.1
T1	7066	-1.9	-4.5	-0.9	-1.3	0.0	0.0	-0.9	-1.3	-5.0
T2	7067	-1.5	-2.3	-0.2	-0.8	0.0	0.0	-0.2	-1.1	-2.8
T3	7068	-1.1	-0.7	0.5	-0.4	0.0	0.0	0.5	-0.5	-1.3
T4	7069	-0.6	0.5	1.0	-0.2	0.0	0.0	1.0	0.6	-0.7
T5	7070	-0.3	1.7	1.5	-0.1	0.0	0.0	1.7	1.5	-0.3
T6	7071	-0.2	2.9	2.0	0.0	0.0	0.0	2.9	2.0	-0.2
T7	7072	-0.1	4.2	2.5	0.0	0.0	0.0	4.2	2.5	-0.1
U1	3051	0.1	-0.6	-2.0	0.0	0.0	0.0	0.1	-0.6	-2.0
U2	3052	0.3	-0.4	-1.7	0.0	0.0	0.0	0.3	-0.4	-1.7

Table 2.10.4-6 Stress Components – Thermal Cold, -20°F; 2-D Model; Condition 2 (continued)

Stress Points		Stress Components (ksi)						Principal Stresses (ksi)		
Section[1]	Node	S_x	S_y	S_z	S_{xy}	S_{yz}	S_{zx}	S1	S2	S3
U3	3053	0.2	-0.2	-1.5	0.0	0.0	0.0	0.2	-0.2	-1.5
U4	3054	0.1	-0.2	-1.4	0.0	0.0	0.0	0.1	-0.2	-1.4
U5	3055	0.0	-0.1	-1.3	0.0	0.0	0.0	0.0	-0.1	-1.3
U6	3056	0.0	-0.1	-1.2	-0.1	0.0	0.0	0.1	-0.2	-1.2
V1	3611	0.0	0.0	-0.7	0.0	0.0	0.0	0.0	0.0	-0.7
V2	3612	0.1	0.0	-0.6	0.0	0.0	0.0	0.1	0.0	-0.6
V3	3613	0.1	0.0	-0.6	0.0	0.0	0.0	0.1	0.0	-0.6
V4	3614	0.1	0.0	-0.6	0.0	0.0	0.0	0.1	-0.1	-0.6
V5	3615	0.0	-0.1	-0.6	0.0	0.0	0.0	0.0	-0.1	-0.6
V6	3616	0.0	0.0	-0.6	0.0	0.0	0.0	0.0	0.0	-0.6
V7	3617	0.0	0.0	-0.6	0.0	0.0	0.0	0.0	0.0	-0.6
W1	3241	1.1	0.0	1.1	0.0	0.0	0.0	1.1	1.1	0.0
W2	3242	1.0	0.0	1.0	0.0	0.0	0.0	1.0	1.0	0.0
W3	3243	0.9	0.0	0.9	0.0	0.0	0.0	0.9	0.9	0.0
W4	3244	0.8	0.0	0.8	0.0	0.0	0.0	0.8	0.8	0.0
W5	3245	0.6	0.0	0.6	0.0	0.0	0.0	0.6	0.6	0.0
W6	3246	0.5	0.0	0.5	0.0	0.0	0.0	0.5	0.5	0.0
X1	3801	0.5	0.0	0.5	0.0	0.0	0.0	0.5	0.5	0.0
X2	3802	0.5	0.0	0.5	0.0	0.0	0.0	0.5	0.5	0.0
X3	3803	0.5	0.0	0.5	0.0	0.0	0.0	0.5	0.5	0.0
X4	3804	0.4	0.0	0.4	0.0	0.0	0.0	0.4	0.4	0.0
X5	3805	0.4	0.0	0.4	0.0	0.0	0.0	0.4	0.4	0.0
X6	3806	0.4	0.0	0.4	0.0	0.0	0.0	0.4	0.4	0.0
X7	3807	0.4	0.0	0.4	0.0	0.0	0.0	0.4	0.4	0.0

[1] Refer to Figure 2.10.2-34 for the identification of the representative sections.

Table 2.10.4-7 Stress Components – Thermal Cold, -40°F; 2-D Model; Condition 4

Condition 4: -40°F Ambient, No Decay Heat

Stress Points		Stress Components (ksi)						Principal Stresses (ksi)		
Section[1]	Node	S_x	S_y	S_z	S_{xy}	S_{yz}	S_{xz}	S1	S2	S3
A1	1	-0.5	0.0	-0.5	0.0	0.0	0.0	0.0	-0.5	-0.5
A2	2	-0.3	0.0	-0.3	0.0	0.0	0.0	0.0	-0.3	-0.3
A3	3	-0.2	0.0	-0.2	0.0	0.0	0.0	0.0	-0.2	-0.2
A4	4	0.0	0.0	0.0	0.0	0.0	0.0	0.0	0.0	0.0
A5	5	0.1	0.0	0.1	0.0	0.0	0.0	0.1	0.1	0.0
B1	6	0.1	0.0	0.1	0.0	0.0	0.0	0.1	0.1	0.0
B2	7	0.1	0.0	0.1	0.0	0.0	0.0	0.1	0.1	0.0
B3	8	0.1	0.0	0.1	0.0	0.0	0.0	0.1	0.1	0.0
B4	9	0.1	0.0	0.1	0.0	0.0	0.0	0.1	0.1	0.0
B5	10	0.1	0.0	0.1	0.0	0.0	0.0	0.1	0.1	0.0
C1	251	-0.7	-1.7	-1.0	-0.2	0.0	0.0	-0.7	-1.0	-1.7
C2	252	0.0	-0.6	-0.4	0.0	0.0	0.0	0.0	-0.4	-0.6
C3	253	-0.1	-0.2	-0.2	0.2	0.0	0.0	0.0	-0.2	-0.3
C4	254	-0.1	-0.1	0.0	0.1	0.0	0.0	0.0	0.0	-0.2
C5	255	0.0	0.0	0.1	0.1	0.0	0.0	0.1	0.1	-0.1
D1	306	0.1	-0.5	0.0	0.1	0.0	0.0	0.1	0.0	-0.5
D2	307	0.1	-0.1	0.1	0.0	0.0	0.0	0.1	0.1	-0.1
D3	308	0.1	-0.1	0.1	0.0	0.0	0.0	0.1	0.1	-0.1
D4	309	0.1	0.0	0.1	0.0	0.0	0.0	0.1	0.1	0.0
D5	310	0.1	0.0	0.1	0.0	0.0	0.0	0.1	0.1	0.0
E1	305	-0.6	-0.7	-0.3	0.2	0.0	0.0	-0.3	-0.5	-0.8
E2	315	-0.4	-0.1	-0.1	0.1	0.0	0.0	-0.1	-0.1	-0.4
E3	325	-0.2	0.1	0.0	0.0	0.0	0.0	0.1	0.0	-0.2
E4	335	-0.1	0.2	0.1	0.0	0.0	0.0	0.2	0.1	-0.1
E5	345	-0.1	0.4	0.1	0.0	0.0	0.0	0.4	0.1	-0.1
E6	355	0.0	0.7	0.2	0.0	0.0	0.0	0.7	0.2	0.0
F1	251	-0.7	-1.7	-1.0	-0.2	0.0	0.0	-0.7	-1.0	-1.7
F2	261	-0.3	-0.7	-0.6	-0.1	0.0	0.0	-0.3	-0.6	-0.7
F3	271	0.2	0.1	-0.2	0.0	0.0	0.0	0.2	0.1	-0.2
F4	281	0.5	1.1	0.1	-0.1	0.0	0.0	1.1	0.5	0.1
G1	311	0.4	0.7	0.1	0.1	0.0	0.0	0.7	0.4	0.1
G2	321	0.3	0.4	-0.1	0.0	0.0	0.0	0.4	0.3	-0.1

Table 2.10.4-7 Stress Components – Thermal Cold, -40°F; 2-D Model; Condition 4 (continued)

Stress Points		Stress Components (ksi)						Principal Stresses (ksi)		
Section[1]	Node	S_x	S_y	S_z	S_{xy}	S_{yz}	S_{xz}	S1	S2	S3
G3	331	0.1	0.2	-0.1	0.0	0.0	0.0	0.2	0.1	-0.1
G4	341	0.1	0.0	-0.2	0.0	0.0	0.0	0.1	-0.1	-0.2
G5	351	0.0	-0.3	-0.3	0.0	0.0	0.0	0.0	-0.3	-0.3
H1	581	0.0	-0.2	-3.4	0.0	0.0	0.0	0.0	-0.2	-3.4
H2	582	0.0	-0.4	-3.3	0.0	0.0	0.0	0.0	-0.4	-3.3
H3	583	0.0	-0.6	-3.3	0.1	0.0	0.0	0.0	-0.6	-3.3
H4	584	0.0	-0.8	-3.4	0.1	0.0	0.0	0.0	-0.8	-3.4
I1	589	0.0	0.2	-0.1	0.0	0.0	0.0	0.2	0.0	-0.1
I2	590	0.0	0.2	-0.1	0.0	0.0	0.0	0.2	0.0	-0.1
I3	591	0.0	0.2	-0.1	0.0	0.0	0.0	0.2	0.0	-0.1
I4	592	0.0	0.3	0.0	0.0	0.0	0.0	0.3	0.0	0.0
I5	593	0.0	0.3	0.0	0.0	0.0	0.0	0.3	0.0	0.0
J1	971	0.0	-0.5	-3.9	0.0	0.0	0.0	0.0	-0.5	-3.9
J2	972	-0.1	-0.5	-3.9	0.0	0.0	0.0	-0.1	-0.5	-3.9
J3	973	-0.1	-0.5	-3.8	0.0	0.0	0.0	-0.1	-0.5	-3.8
J4	974	-0.2	-0.5	-3.8	0.0	0.0	0.0	-0.2	-0.5	-3.8
K1	979	0.0	0.2	0.0	0.0	0.0	0.0	0.2	0.0	0.0
K2	980	0.0	0.2	0.0	0.0	0.0	0.0	0.2	0.0	0.0
K3	981	0.0	0.2	0.0	0.0	0.0	0.0	0.2	0.0	0.0
K4	982	0.0	0.2	0.0	0.0	0.0	0.0	0.2	0.0	0.0
K5	983	0.0	0.2	0.0	0.0	0.0	0.0	0.2	0.0	0.0
L1	1601	0.0	-0.5	-3.9	0.0	0.0	0.0	0.0	-0.5	-3.9
L2	1602	-0.1	-0.5	-3.9	0.0	0.0	0.0	-0.1	-0.5	-3.9
L3	1603	-0.1	-0.5	-3.8	0.0	0.0	0.0	-0.1	-0.5	-3.8
L4	1604	-0.2	-0.5	-3.8	0.0	0.0	0.0	-0.2	-0.5	-3.8
M1	1609	0.0	0.2	0.0	0.0	0.0	0.0	0.2	0.0	0.0
M2	1610	0.0	0.2	0.0	0.0	0.0	0.0	0.2	0.0	0.0
M3	1611	0.0	0.2	0.0	0.0	0.0	0.0	0.2	0.0	0.0
M4	1612	0.0	0.2	0.0	0.0	0.0	0.0	0.2	0.0	0.0
M5	1613	0.0	0.2	0.0	0.0	0.0	0.0	0.2	0.0	0.0
N1	2216	0.0	-0.5	-4.0	0.0	0.0	0.0	0.0	-0.5	-4.0
N2	2217	-0.1	-0.5	-3.9	0.0	0.0	0.0	-0.1	-0.5	-3.9
N3	2218	-0.1	-0.5	-3.8	0.0	0.0	0.0	-0.1	-0.5	-3.8

Table 2.10.4-7 Stress Components – Thermal Cold, -40°F; 2-D Model; Condition 4 (continued)

Stress Points		Stress Components (ksi)						Principal Stresses (ksi)		
Section[1]	Node	S_x	S_y	S_z	S_{xy}	S_{yz}	S_{zx}	S1	S2	S3
N4	2219	-0.2	-0.5	-3.8	0.0	0.0	0.0	-0.2	-0.5	-3.8
O1	2224	0.0	0.2	0.0	0.0	0.0	0.0	0.2	0.0	0.0
O2	2225	0.0	0.2	0.0	0.0	0.0	0.0	0.2	0.0	0.0
O3	2226	0.0	0.2	0.0	0.0	0.0	0.0	0.2	0.0	0.0
O4	2227	0.0	0.2	0.0	0.0	0.0	0.0	0.2	0.0	0.0
O5	2228	0.0	0.2	0.0	0.0	0.0	0.0	0.2	0.0	0.0
P1	2546	0.0	-0.3	-3.4	0.0	0.0	0.0	0.0	-0.3	-3.4
P2	2547	0.0	-0.4	-3.4	0.0	0.0	0.0	0.0	-0.4	-3.4
P3	2548	0.0	-0.5	-3.4	-0.1	0.0	0.0	0.0	-0.5	-3.4
P4	2549	0.0	-0.7	-3.4	-0.1	0.0	0.0	0.0	-0.7	-3.4
Q1	2554	0.0	0.1	-0.2	0.0	0.0	0.0	0.1	0.0	-0.2
Q2	2555	0.0	0.1	-0.1	0.0	0.0	0.0	0.1	0.0	-0.1
Q3	2556	0.0	0.2	-0.1	0.0	0.0	0.0	0.2	0.0	-0.1
Q4	2557	0.0	0.3	-0.1	0.0	0.0	0.0	0.3	0.0	-0.1
Q5	2558	0.0	0.4	-0.1	0.0	0.0	0.0	0.4	0.0	-0.1
R1	2771	0.1	-1.1	-1.0	0.0	0.0	0.0	0.1	-1.0	-1.1
R2	2772	0.2	-0.6	-0.8	0.0	0.0	0.0	0.2	-0.6	-0.8
R3	2773	0.5	-0.2	-0.6	0.0	0.0	0.0	0.5	-0.2	-0.6
R4	2774	1.0	0.2	-0.4	0.0	0.0	0.0	1.0	0.1	-0.4
S1	2779	1.1	1.2	0.1	-0.1	0.0	0.0	1.3	1.0	0.1
S2	2780	0.7	0.6	-0.2	0.0	0.0	0.0	0.7	0.6	-0.2
S3	2781	0.3	0.1	-0.4	0.1	0.0	0.0	0.4	0.1	-0.4
S4	2782	0.1	-0.3	-0.5	0.1	0.0	0.0	0.2	-0.4	-0.5
S5	2783	0.1	-0.9	-0.7	0.1	0.0	0.0	0.1	-0.7	-0.9
T1	7066	-1.0	-0.7	-0.6	-0.2	0.0	0.0	-0.6	-0.6	-1.1
T2	7067	-0.7	-0.3	-0.4	0.0	0.0	0.0	-0.3	-0.4	-0.7
T3	7068	-0.4	0.0	-0.3	0.1	0.0	0.0	0.0	-0.3	-0.5
T4	7069	-0.3	0.1	-0.2	0.1	0.0	0.0	0.1	-0.2	-0.3
T5	7070	-0.1	0.2	-0.1	0.1	0.0	0.0	0.3	-0.1	-0.2
T6	7071	-0.1	0.4	-0.1	0.1	0.0	0.0	0.4	-0.1	-0.1
T7	7072	0.0	0.6	0.0	0.0	0.0	0.0	0.6	0.0	0.0
U1	3051	-0.1	0.0	-0.1	0.0	0.0	0.0	0.0	-0.1	-0.1
U2	3052	-0.1	0.0	0.0	0.0	0.0	0.0	0.0	0.0	-0.1

Table 2.10.4-7 Stress Components – Thermal Cold, -40°F; 2-D Model; Condition 4 (continued)

Stress Points		Stress Components (ksi)						Principal Stresses (ksi)		
Section[1]	Node	S_x	S_y	S_t	S_{xy}	S_{yz}	S_{zx}	S1	S2	S3
U3	3053	0.0	0.0	0.0	0.0	0.0	0.0	0.0	0.0	0.0
U4	3054	0.1	-0.1	0.0	0.0	0.0	0.0	0.1	0.0	-0.1
U5	3055	0.3	-0.1	0.1	-0.1	0.0	0.0	0.3	0.1	-0.1
U6	3056	-0.3	-0.1	-0.1	-0.1	0.0	0.0	0.0	-0.1	-0.3
V1	3611	0.0	0.0	-0.1	0.0	0.0	0.0	0.0	0.0	-0.1
V2	3612	0.0	0.0	0.0	0.0	0.0	0.0	0.0	0.0	0.0
V3	3613	0.0	0.0	0.0	0.0	0.0	0.0	0.0	0.0	0.0
V4	3614	0.0	0.0	0.0	0.0	0.0	0.0	0.0	0.0	0.0
V5	3615	0.0	0.0	0.0	-0.1	0.0	0.0	0.1	0.0	-0.1
V6	3616	0.0	0.0	0.0	0.0	0.0	0.0	0.0	0.0	0.0
V7	3617	0.0	0.0	0.0	0.0	0.0	0.0	0.0	0.0	0.0
W1	3241	-0.1	0.0	-0.1	0.0	0.0	0.0	0.0	-0.1	-0.1
W2	3242	0.0	0.0	0.0	0.0	0.0	0.0	0.0	0.0	0.0
W3	3243	0.0	0.0	0.0	0.0	0.0	0.0	0.0	0.0	0.0
W4	3244	0.0	0.0	0.0	0.0	0.0	0.0	0.0	0.0	0.0
W5	3245	0.0	0.0	0.0	0.0	0.0	0.0	0.0	0.0	0.0
W6	3246	0.1	0.0	0.1	0.0	0.0	0.0	0.1	0.1	0.0
X1	3801	-0.1	0.0	-0.1	0.0	0.0	0.0	0.0	-0.1	-0.1
X2	3802	-0.1	0.0	-0.1	0.0	0.0	0.0	0.0	-0.1	-0.1
X3	3803	0.0	0.0	0.0	0.0	0.0	0.0	0.0	0.0	0.0
X4	3804	0.0	0.0	0.0	0.0	0.0	0.0	0.0	0.0	0.0
X5	3805	0.0	0.0	0.0	0.0	0.0	0.0	0.0	0.0	0.0
X6	3806	0.0	0.0	0.0	0.0	0.0	0.0	0.0	0.0	0.0
X7	3807	0.0	0.0	0.0	0.0	0.0	0.0	0.0	0.0	0.0

[1] Refer to Figure 2.10.2-34 for the identification of the representative sections.

Table 2.10.4-8 Stress Components – Impact; 1-Foot Top End Drop; Drop Orientation = 0 Degrees; 2-D Model; Condition 1

Condition 1: 100°F Ambient with Contents

Stress Points		Stress Components (ksi)						Principal Stresses (ksi)		
Section[1]	Node	S_x	S_y	S_z	S_{xy}	S_{yz}	S_{xz}	S1	S2	S3
A1	1	1.6	0.0	1.6	0.0	0.0	0.0	1.6	1.6	0.0
A2	2	0.9	0.0	0.9	0.0	0.0	0.0	0.9	0.9	0.0
A3	3	0.2	0.0	0.2	0.0	0.0	0.0	0.2	0.2	0.0
A4	4	-0.5	0.0	-0.5	0.0	0.0	0.0	0.0	-0.5	-0.5
A5	5	-1.2	0.0	-1.2	0.0	0.0	0.0	0.0	-1.2	-1.2
B1	6	1.0	0.0	1.0	0.0	0.0	0.0	1.0	1.0	0.0
B2	7	0.4	0.0	0.4	0.0	0.0	0.0	0.4	0.4	0.0
B3	8	-0.3	0.0	-0.3	0.0	0.0	0.0	0.0	-0.3	-0.3
B4	9	-0.9	0.0	-0.9	0.0	0.0	0.0	0.0	-0.9	-0.9
B5	10	-1.5	0.0	-1.5	0.0	0.0	0.0	0.0	-1.5	-1.5
C1	251	-1.0	-1.2	-0.2	-0.2	0.0	0.0	-0.2	-0.8	-1.4
C2	252	-0.2	-0.5	0.1	-0.2	0.0	0.0	0.1	-0.1	-0.6
C3	253	0.2	-0.2	0.1	-0.2	0.0	0.0	0.3	0.1	-0.3
C4	254	0.7	-0.1	0.2	-0.1	0.0	0.0	0.7	0.2	-0.1
C5	255	1.2	-0.1	0.1	-0.1	0.0	0.0	1.2	0.1	-0.1
D1	306	-1.2	-0.7	-0.5	-0.3	0.0	0.0	-0.5	-0.5	-1.4
D2	307	-0.4	-0.5	-0.3	-0.1	0.0	0.0	-0.3	-0.3	-0.6
D3	308	-0.1	-0.2	-0.3	0.0	0.0	0.0	-0.1	-0.2	-0.3
D4	309	0.2	-0.1	-0.2	0.1	0.0	0.0	0.2	-0.1	-0.2
D5	310	0.5	0.0	-0.2	0.1	0.0	0.0	0.5	0.0	-0.2
E1	305	1.1	0.0	0.3	-0.3	0.0	0.0	1.2	0.3	0.0
E2	315	0.6	-0.3	0.1	-0.3	0.0	0.0	0.7	0.1	-0.4
E3	325	0.3	-0.2	0.0	-0.3	0.0	0.0	0.4	0.0	-0.3
E4	335	0.1	-0.2	0.0	-0.2	0.0	0.0	0.2	0.0	-0.3
E5	345	0.1	-0.2	0.0	-0.1	0.0	0.0	0.1	0.0	-0.3
E6	355	0.0	-0.3	-0.1	-0.1	0.0	0.0	0.0	-0.1	-0.3
F1	251	-1.0	-1.2	-0.2	-0.2	0.0	0.0	-0.2	-0.8	-1.4
F2	261	-0.8	-0.7	0.0	-0.1	0.0	0.0	0.0	-0.6	-0.8
F3	271	-0.6	-0.3	0.2	0.1	0.0	0.0	0.2	-0.3	-0.6
F4	281	-0.6	0.0	0.2	0.1	0.0	0.0	0.2	0.0	-0.6
G1	311	-0.5	-0.8	-0.1	-0.1	0.0	0.0	-0.1	-0.5	-0.8

Table 2.10.4-8 Stress Components – Impact; 1-Foot Top End Drop; Drop Orientation = 0 Degrees; 2-D Model; Condition 1 (continued)

Stress Points		Stress Components (ksi)						Principal Stresses (ksi)		
Section[1]	Node	S_x	S_y	S_z	S_{xy}	S_{yz}	S_{xz}	S1	S2	S3
G2	321	-0.3	-0.5	0.1	0.0	0.0	0.0	0.1	-0.3	-0.5
G3	331	-0.2	-0.3	0.2	0.1	0.0	0.0	0.2	-0.2	-0.3
G4	341	-0.1	-0.1	0.3	0.1	0.0	0.0	0.3	0.0	-0.1
G5	351	0.0	0.2	0.3	0.0	0.0	0.0	0.3	0.2	0.0
H1	581	0.0	-0.8	0.0	0.0	0.0	0.0	0.0	0.0	-0.8
H2	582	0.0	-1.0	0.0	0.0	0.0	0.0	0.0	0.0	-1.0
H3	583	0.0	-1.2	-0.1	0.0	0.0	0.0	0.0	-0.1	-1.2
H4	584	0.0	-1.6	-0.2	0.1	0.0	0.0	0.0	-0.2	-1.6
I1	589	0.0	-0.4	0.1	0.0	0.0	0.0	0.1	0.0	-0.4
I2	590	0.0	-0.4	0.1	0.0	0.0	0.0	0.1	0.0	-0.4
I3	591	0.0	-0.5	0.1	0.0	0.0	0.0	0.1	0.0	-0.5
I4	592	0.0	-0.5	0.0	0.0	0.0	0.0	0.0	0.0	-0.5
I5	593	0.0	-0.6	0.0	0.0	0.0	0.0	0.0	0.0	-0.6
J1	971	0.0	-1.4	0.0	0.0	0.0	0.0	0.0	0.0	-1.4
J2	972	0.0	-1.4	0.0	0.0	0.0	0.0	0.0	0.0	-1.4
J3	973	0.0	-1.4	0.0	0.0	0.0	0.0	0.0	0.0	-1.4
J4	974	0.0	-1.4	0.0	0.0	0.0	0.0	0.0	0.0	-1.4
K1	979	0.0	-0.7	0.0	0.0	0.0	0.0	0.0	0.0	-0.7
K2	980	0.0	-0.7	0.0	0.0	0.0	0.0	0.0	0.0	-0.7
K3	981	0.0	-0.7	0.0	0.0	0.0	0.0	0.0	0.0	-0.7
K4	982	0.0	-0.7	0.0	0.0	0.0	0.0	0.0	0.0	-0.7
K5	983	0.0	-0.7	0.0	0.0	0.0	0.0	0.0	0.0	-0.7
L1	1601	0.0	-1.8	0.0	0.0	0.0	0.0	0.0	0.0	-1.8
L2	1602	0.0	-1.8	0.0	0.0	0.0	0.0	0.0	0.0	-1.8
L3	1603	0.0	-1.8	0.0	0.0	0.0	0.0	0.0	0.0	-1.8
L4	1604	0.0	-1.8	0.0	0.0	0.0	0.0	0.0	0.0	-1.8
M1	1609	0.0	-1.0	0.0	0.0	0.0	0.0	0.0	0.0	-1.0
M2	1610	0.0	-1.0	0.0	0.0	0.0	0.0	0.0	0.0	-1.0
M3	1611	0.0	-1.0	0.0	0.0	0.0	0.0	0.0	0.0	-1.0
M4	1612	0.0	-1.0	0.0	0.0	0.0	0.0	0.0	0.0	-1.0
M5	1613	0.0	-1.0	0.0	0.0	0.0	0.0	0.0	0.0	-1.0
N1	2216	0.0	-2.1	0.0	0.0	0.0	0.0	0.0	0.0	-2.1
N2	2217	0.0	-2.1	0.0	0.0	0.0	0.0	0.0	0.0	-2.1

Table 2.10.4-8 Stress Components – Impact; 1-Foot Top End Drop; Drop Orientation = 0 Degrees; 2-D Model; Condition 1 (continued)

Stress Points		Stress Components (ksi)						Principal Stresses (ksi)		
Section[1]	Node	S_x	S_y	S_z	S_{xy}	S_{yz}	S_{xz}	S1	S2	S3
N3	2218	0.0	-2.1	0.0	0.0	0.0	0.0	0.0	0.0	-2.1
N4	2219	0.0	-2.1	0.0	0.0	0.0	0.0	0.0	0.0	-2.1
O1	2224	0.0	-1.4	0.0	0.0	0.0	0.0	0.0	0.0	-1.4
O2	2225	0.0	-1.4	0.0	0.0	0.0	0.0	0.0	0.0	-1.4
O3	2226	0.0	-1.4	0.0	0.0	0.0	0.0	0.0	0.0	-1.4
O4	2227	0.0	-1.4	0.0	0.0	0.0	0.0	0.0	0.0	-1.4
O5	2228	0.0	-1.4	0.0	0.0	0.0	0.0	0.0	0.0	-1.4
P1	2546	0.0	-1.2	0.3	0.0	0.0	0.0	0.3	0.0	-1.2
P2	2547	0.0	-1.9	0.1	0.0	0.0	0.0	0.1	0.0	-1.9
P3	2548	0.0	-2.5	-0.1	-0.1	0.0	0.0	0.0	-0.1	-2.5
P4	2549	0.0	-3.4	-0.3	-0.2	0.0	0.0	0.0	-0.3	-3.4
Q1	2554	0.0	-1.3	0.5	0.0	0.0	0.0	0.5	0.0	-1.3
Q2	2555	0.0	-1.4	0.4	0.0	0.0	0.0	0.4	0.0	-1.4
Q3	2556	0.0	-1.6	0.4	0.0	0.0	0.0	0.4	0.0	-1.6
Q4	2557	0.0	-1.7	0.3	0.0	0.0	0.0	0.3	0.0	-1.7
Q5	2558	0.0	-1.9	0.3	0.0	0.0	0.0	0.3	0.0	-1.9
R1	2771	0.1	-6.5	-0.3	0.0	0.0	0.0	0.1	-0.3	-6.5
R2	2772	0.2	-3.8	0.4	0.0	0.0	0.0	0.4	0.2	-3.8
R3	2773	0.6	-1.3	1.2	0.4	0.0	0.0	1.2	0.7	-1.4
R4	2774	0.6	1.7	2.0	1.0	0.0	0.0	2.3	2.0	-0.1
S1	2779	-3.3	-4.5	-1.0	0.3	0.0	0.0	-1.0	-3.3	-4.6
S2	2780	-2.1	-2.7	-0.2	-0.1	0.0	0.0	-0.2	-2.1	-2.7
S3	2781	-1.1	-1.4	0.4	-0.4	0.0	0.0	0.4	-0.8	-1.7
S4	2782	-0.4	-0.1	0.9	-0.3	0.0	0.0	0.9	0.1	-0.6
S5	2783	-0.2	1.6	1.4	-0.2	0.0	0.0	1.6	1.4	-0.2
T1	7066	4.1	3.6	1.7	1.1	0.0	0.0	5.0	2.8	1.7
T2	7067	2.8	1.3	0.8	0.4	0.0	0.0	2.9	1.2	0.8
T3	7068	1.9	-0.1	0.2	-0.1	0.0	0.0	1.9	0.2	-0.1
T4	7069	1.1	-1.0	-0.3	-0.3	0.0	0.0	1.2	-0.3	-1.0
T5	7070	0.6	-1.8	-0.6	-0.4	0.0	0.0	0.7	-0.6	-1.8
T6	7071	0.3	-2.7	-0.9	-0.3	0.0	0.0	0.3	-0.9	-2.7
T7	7072	0.1	-3.8	-1.2	-0.2	0.0	0.0	0.1	-1.2	-3.8
U1	3051	0.0	-3.1	2.3	0.7	0.0	0.0	2.3	0.1	-3.3

Table 2.10.4-8 Stress Components – Impact; 1-Foot Top End Drop; Drop Orientation = 0 Degrees; 2-D Model; Condition 1 (continued)

Stress Points		Stress Components (ksi)						Principal Stresses (ksi)		
Section[1]	Node	S_x	S_y	S_z	S_{xy}	S_{yz}	S_{xz}	S1	S2	S3
U2	3052	1.1	-2.9	1.7	1.0	0.0	0.0	1.7	1.3	-3.1
U3	3053	0.9	-2.4	0.9	1.2	0.0	0.0	1.3	0.9	-2.8
U4	3054	0.6	-2.3	-0.1	1.1	0.0	0.0	1.0	-0.1	-2.7
U5	3055	0.4	-2.8	-1.2	1.2	0.0	0.0	0.8	-1.2	-3.2
U6	3056	-0.8	-2.0	-2.1	1.6	0.0	0.0	0.3	-2.1	-3.1
V1	3611	-3.4	-0.9	2.3	-0.6	0.0	0.0	2.3	-0.7	-3.5
V2	3612	-2.3	-1.0	1.6	-0.8	0.0	0.0	1.6	-0.6	-2.7
V3	3613	-1.2	-1.1	0.8	-1.1	0.0	0.0	0.8	-0.1	-2.2
V4	3614	-0.2	-1.1	-0.1	-1.0	0.0	0.0	0.5	-0.1	-1.8
V5	3615	0.7	-0.9	-0.9	-0.9	0.0	0.0	1.1	-0.9	-1.3
V6	3616	0.9	-0.7	-1.9	-0.6	0.0	0.0	1.0	-0.8	-1.9
V7	3617	3.0	-0.6	-2.4	-0.3	0.0	0.0	3.0	-0.6	-2.4
W1	3241	1.1	-0.2	1.1	0.0	0.0	0.0	1.1	1.1	-0.2
W2	3242	1.1	-0.2	1.1	0.0	0.0	0.0	1.1	1.1	-0.2
W3	3243	1.1	-0.2	1.1	0.0	0.0	0.0	1.1	1.1	-0.2
W4	3244	1.0	-0.1	1.0	0.0	0.0	0.0	1.0	1.0	-0.1
W5	3245	1.0	-0.1	1.0	0.0	0.0	0.0	1.0	1.0	-0.1
W6	3246	1.0	0.0	1.0	0.0	0.0	0.0	1.0	1.0	0.0
X1	3801	18.9	-0.6	18.9	0.0	0.0	0.0	18.9	18.9	-0.6
X2	3802	12.8	-0.5	12.8	0.0	0.0	0.0	12.8	12.8	-0.5
X3	3803	6.6	-0.3	6.6	0.0	0.0	0.0	6.6	6.6	-0.3
X4	3804	0.4	-0.4	0.4	0.0	0.0	0.0	0.4	0.4	-0.4
X5	3805	-5.8	-0.5	-5.8	0.0	0.0	0.0	-0.5	-5.8	-5.8
X6	3806	-12.0	-0.4	-12.0	0.0	0.0	0.0	-0.4	-12.0	-12.0
X7	3807	-18.8	-0.3	-18.8	0.0	0.0	0.0	-0.3	-18.8	-18.8

[1] Refer to Figure 2.10.2-34 for the identification of the representative sections.

Table 2.10.4-9 Stress Components – Impact; 1-Foot Bottom End Drop; Drop Orientation = 0 Degrees; 2-D Model; Condition 1

Condition 1: 100°F Ambient with Contents

Stress Points		Stress Components (ksi)						Principal Stresses (ksi)		
Section[1]	Node	S_x	S_y	S_z	S_{xy}	S_{yz}	S_{xz}	S1	S2	S3
A1	1	7.7	-0.3	7.7	0.0	0.0	0.0	7.7	7.7	-0.3
A2	2	4.4	-0.4	4.4	0.0	0.0	0.0	4.4	4.4	-0.4
A3	3	1.1	-0.5	1.1	0.0	0.0	0.0	1.1	1.1	-0.5
A4	4	-2.3	-0.5	-2.3	0.0	0.0	0.0	-0.5	-2.3	-2.3
A5	5	-5.6	-0.6	-5.6	0.0	0.0	0.0	-0.6	-5.6	-5.6
B1	6	4.5	-0.6	4.5	0.0	0.0	0.0	4.5	4.5	-0.6
B2	7	1.6	-0.7	1.6	0.0	0.0	0.0	1.6	1.6	-0.7
B3	8	-1.3	-0.7	-1.3	0.0	0.0	0.0	-0.7	-1.3	-1.3
B4	9	-4.3	-0.8	-4.3	0.0	0.0	0.0	-0.8	-4.3	-4.3
B5	10	-7.1	-0.8	-7.1	0.0	0.0	0.0	-0.8	-7.1	-7.1
C1	251	-4.2	-5.2	-0.3	-0.9	0.0	0.0	-0.3	-3.7	-5.7
C2	252	-0.7	-2.1	0.8	-0.6	0.0	0.0	0.8	-0.4	-2.4
C3	253	1.1	-0.9	1.0	-0.7	0.0	0.0	1.3	1.0	-1.1
C4	254	3.4	-0.6	1.0	-0.5	0.0	0.0	3.5	1.0	-0.6
C5	255	5.9	-0.5	0.9	-0.4	0.0	0.0	6.0	0.9	-0.5
D1	306	-6.6	-5.5	-3.1	-1.9	0.0	0.0	-3.1	-4.0	-8.1
D2	307	-1.7	-4.0	-1.7	-0.8	0.0	0.0	-1.5	-1.7	-4.2
D3	308	-0.4	-2.0	-1.4	0.0	0.0	0.0	-0.4	-1.4	-2.0
D4	309	0.8	-1.3	-1.4	0.2	0.0	0.0	0.8	-1.3	-1.4
D5	310	2.4	-1.0	-1.4	0.2	0.0	0.0	2.4	-1.0	-1.4
E1	305	5.6	-1.6	1.3	-1.3	0.0	0.0	5.8	1.3	-1.9
E2	315	2.7	-2.5	0.4	-1.7	0.0	0.0	3.2	0.4	-3.0
E3	325	1.1	-2.0	0.1	-1.6	0.0	0.0	1.8	0.1	-2.6
E4	335	0.6	-1.6	0.1	-1.3	0.0	0.0	1.1	0.1	-2.2
E5	345	0.2	-1.3	0.1	-0.7	0.0	0.0	0.5	0.1	-1.6
E6	355	0.1	-1.3	0.0	-0.4	0.0	0.0	0.2	0.0	-1.4
F1	251	-4.2	-5.2	-0.3	-0.9	0.0	0.0	-0.3	-3.7	-5.7
F2	261	-3.1	-2.3	0.7	-0.3	0.0	0.0	0.7	-2.2	-3.2
F3	271	-2.0	-0.2	1.5	0.1	0.0	0.0	1.5	-0.2	-2.0
F4	281	-2.0	1.6	2.0	-0.1	0.0	0.0	2.0	1.6	-2.0
G1	311	-2.9	-4.6	-0.4	-0.1	0.0	0.0	-0.4	-2.8	-4.6

Table 2.10.4-9 Stress Components – Impact; 1-Foot Bottom End Drop; Drop Orientation = 0 Degrees; 2-D Model; Condition 1 (continued)

Stress Points		Stress Components (ksi)						Principal Stresses (ksi)		
Section[1]	Node	S_x	S_y	S_z	S_{xy}	S_{yz}	S_{xz}	S1	S2	S3
G2	321	-2.0	-2.9	0.3	0.1	0.0	0.0	0.3	-2.0	-2.9
G3	331	-1.0	-1.7	0.8	0.3	0.0	0.0	0.8	-0.9	-1.8
G4	341	-0.4	-0.5	1.3	0.2	0.0	0.0	1.3	-0.2	-0.7
G5	351	-0.2	1.0	1.7	0.2	0.0	0.0	1.7	1.0	-0.2
H1	581	0.0	-1.1	0.3	0.0	0.0	0.0	0.3	0.0	-1.1
H2	582	0.0	-1.8	0.0	0.0	0.0	0.0	0.0	0.0	-1.8
H3	583	-0.1	-2.5	-0.2	0.1	0.0	0.0	0.0	-0.2	-2.5
H4	584	0.0	-3.5	-0.4	0.2	0.0	0.0	0.0	-0.4	-3.6
I1	589	0.0	-1.3	0.4	0.0	0.0	0.0	0.4	0.0	-1.3
I2	590	0.0	-1.5	0.3	0.0	0.0	0.0	0.3	0.0	-1.5
I3	591	0.0	-1.7	0.3	0.0	0.0	0.0	0.3	0.0	-1.7
I4	592	0.0	-1.9	0.2	0.0	0.0	0.0	0.2	0.0	-1.9
I5	593	0.0	-2.1	0.2	0.0	0.0	0.0	0.2	0.0	-2.1
J1	971	0.0	-2.1	0.0	0.0	0.0	0.0	0.0	0.0	-2.1
J2	972	0.0	-2.1	0.0	0.0	0.0	0.0	0.0	0.0	-2.1
J3	973	0.0	-2.1	0.0	0.0	0.0	0.0	0.0	0.0	-2.1
J4	974	0.0	-2.1	0.0	0.0	0.0	0.0	0.0	0.0	-2.1
K1	979	0.0	-1.5	0.0	0.0	0.0	0.0	0.0	0.0	-1.5
K2	980	0.0	-1.5	0.0	0.0	0.0	0.0	0.0	0.0	-1.5
K3	981	0.0	-1.5	0.0	0.0	0.0	0.0	0.0	0.0	-1.5
K4	982	0.0	-1.5	0.0	0.0	0.0	0.0	0.0	0.0	-1.5
K5	983	0.0	-1.5	0.0	0.0	0.0	0.0	0.0	0.0	-1.5
L1	1601	0.0	-1.7	0.0	0.0	0.0	0.0	0.0	0.0	-1.7
L2	1602	0.0	-1.7	0.0	0.0	0.0	0.0	0.0	0.0	-1.7
L3	1603	0.0	-1.7	0.0	0.0	0.0	0.0	0.0	0.0	-1.7
L4	1604	0.0	-1.7	0.0	0.0	0.0	0.0	0.0	0.0	-1.7
M1	1609	0.0	-1.2	0.0	0.0	0.0	0.0	0.0	0.0	-1.2
M2	1610	0.0	-1.2	0.0	0.0	0.0	0.0	0.0	0.0	-1.2
M3	1611	0.0	-1.2	0.0	0.0	0.0	0.0	0.0	0.0	-1.2
M4	1612	0.0	-1.2	0.0	0.0	0.0	0.0	0.0	0.0	-1.2
M5	1613	0.0	-1.2	0.0	0.0	0.0	0.0	0.0	0.0	-1.2
N1	2216	0.0	-1.4	0.0	0.0	0.0	0.0	0.0	0.0	-1.4
N2	2217	0.0	-1.4	0.0	0.0	0.0	0.0	0.0	0.0	-1.4

Table 2.10.4-9 Stress Components – Impact; 1-Foot Bottom End Drop; Drop Orientation = 0 Degrees; 2-D Model; Condition 1 (continued)

Stress Points		Stress Components (ksi)						Principal Stresses (ksi)		
Section[1]	Node	S_x	S_y	S_z	S_{xy}	S_{yz}	S_{xz}	S1	S2	S3
N3	2218	0.0	-1.4	0.0	0.0	0.0	0.0	0.0	0.0	-1.4
N4	2219	0.0	-1.4	0.0	0.0	0.0	0.0	0.0	0.0	-1.4
O1	2224	0.0	-0.8	0.0	0.0	0.0	0.0	0.0	0.0	-0.8
O2	2225	0.0	-0.8	0.0	0.0	0.0	0.0	0.0	0.0	-0.8
O3	2226	0.0	-0.8	0.0	0.0	0.0	0.0	0.0	0.0	-0.8
O4	2227	0.0	-0.8	0.0	0.0	0.0	0.0	0.0	0.0	-0.8
O5	2228	0.0	-0.8	0.0	0.0	0.0	0.0	0.0	0.0	-0.8
P1	2546	0.0	-0.8	0.0	0.0	0.0	0.0	0.0	0.0	-0.8
P2	2547	0.0	-1.0	0.0	0.0	0.0	0.0	0.0	0.0	-1.0
P3	2548	0.0	-1.2	-0.1	0.0	0.0	0.0	0.0	-0.1	-1.2
P4	2549	0.0	-1.5	-0.2	-0.1	0.0	0.0	0.0	-0.2	-1.5
Q1	2554	0.0	-0.6	0.1	0.0	0.0	0.0	0.1	0.0	-0.6
Q2	2555	0.0	-0.6	0.1	0.0	0.0	0.0	0.1	0.0	-0.6
Q3	2556	0.0	-0.6	0.1	0.0	0.0	0.0	0.1	0.0	-0.6
Q4	2557	0.0	-0.7	0.1	0.0	0.0	0.0	0.1	0.0	-0.7
Q5	2558	0.0	-0.7	0.1	0.0	0.0	0.0	0.1	0.0	-0.7
R1	2771	0.0	-1.6	-0.1	0.0	0.0	0.0	0.0	-0.1	-1.6
R2	2772	0.0	-1.1	0.0	0.0	0.0	0.0	0.0	0.0	-1.1
R3	2773	0.1	-0.6	0.2	0.1	0.0	0.0	0.2	0.1	-0.6
R4	2774	0.1	0.1	0.4	0.1	0.0	0.0	0.4	0.2	0.0
S1	2779	-0.6	-1.0	-0.2	0.1	0.0	0.0	-0.2	-0.6	-1.0
S2	2780	-0.4	-0.7	0.0	0.0	0.0	0.0	0.0	-0.4	-0.7
S3	2781	-0.2	-0.4	0.1	-0.1	0.0	0.0	0.1	-0.2	-0.4
S4	2782	-0.1	-0.1	0.2	-0.1	0.0	0.0	0.2	0.0	-0.2
S5	2783	0.0	0.2	0.3	0.0	0.0	0.0	0.3	0.2	0.0
T1	7066	0.7	0.6	0.3	0.2	0.0	0.0	0.9	0.5	0.3
T2	7067	0.5	0.2	0.2	0.1	0.0	0.0	0.5	0.2	0.2
T3	7068	0.3	0.0	0.0	0.0	0.0	0.0	0.3	0.0	0.0
T4	7069	0.2	-0.2	0.0	0.0	0.0	0.0	0.2	0.0	-0.2
T5	7070	0.1	-0.4	-0.1	-0.1	0.0	0.0	0.1	-0.1	-0.4
T6	7071	0.0	-0.5	-0.2	0.0	0.0	0.0	0.0	-0.2	-0.5
T7	7072	0.0	-0.8	-0.2	0.0	0.0	0.0	0.0	-0.2	-0.8
U1	3051	-0.5	-0.8	0.4	0.1	0.0	0.0	0.4	-0.5	-0.8

Table 2.10.4-9 Stress Components – Impact; 1-Foot Bottom End Drop; Drop Orientation = 0 Degrees; 2-D Model; Condition 1 (continued)

Stress Points		Stress Components (ksi)						Principal Stresses (ksi)		
Section[1]	Node	S_x	S_y	S_z	S_{xy}	S_{yz}	S_{xz}	S1	S2	S3
U2	3052	0.0	-0.7	0.4	0.1	0.0	0.0	0.4	0.0	-0.7
U3	3053	0.1	-0.5	0.2	0.1	0.0	0.0	0.2	0.2	-0.5
U4	3054	0.2	-0.5	0.0	0.0	0.0	0.0	0.2	0.0	-0.5
U5	3055	0.3	-0.6	-0.3	0.1	0.0	0.0	0.3	-0.3	-0.6
U6	3056	0.1	-0.4	-0.5	0.3	0.0	0.0	0.2	-0.5	-0.5
V1	3611	-0.2	0.0	0.5	0.0	0.0	0.0	0.5	0.0	-0.2
V2	3612	-0.1	0.0	0.4	0.0	0.0	0.0	0.4	0.0	-0.2
V3	3613	-0.1	-0.1	0.2	0.0	0.0	0.0	0.2	0.0	-0.1
V4	3614	0.0	-0.1	0.0	0.0	0.0	0.0	0.0	0.0	-0.1
V5	3615	0.0	0.0	-0.2	0.0	0.0	0.0	0.0	0.0	-0.2
V6	3616	0.0	0.0	-0.4	0.0	0.0	0.0	0.0	0.0	-0.4
V7	3617	0.2	0.0	-0.5	0.0	0.0	0.0	0.2	0.0	-0.5
W1	3241	2.1	0.0	2.1	0.0	0.0	0.0	2.1	2.1	0.0
W2	3242	1.4	0.0	1.4	0.0	0.0	0.0	1.4	1.4	0.0
W3	3243	0.6	0.0	0.6	0.0	0.0	0.0	0.6	0.6	0.0
W4	3244	-0.1	0.0	-0.1	0.0	0.0	0.0	0.0	-0.1	-0.1
W5	3245	-0.9	0.0	-0.9	0.0	0.0	0.0	0.0	-0.9	-0.9
W6	3246	-1.7	0.0	-1.7	0.0	0.0	0.0	0.0	-1.7	-1.7
X1	3801	1.7	0.0	1.7	0.0	0.0	0.0	1.7	1.7	0.0
X2	3802	1.2	0.0	1.2	0.0	0.0	0.0	1.2	1.2	0.0
X3	3803	0.6	0.0	0.6	0.0	0.0	0.0	0.6	0.6	0.0
X4	3804	0.0	0.0	0.0	0.0	0.0	0.0	0.0	0.0	0.0
X5	3805	-0.5	0.0	-0.5	0.0	0.0	0.0	0.0	-0.5	-0.5
X6	3806	-1.1	0.0	-1.1	0.0	0.0	0.0	0.0	-1.1	-1.1
X7	3807	-1.8	0.0	-1.8	0.0	0.0	0.0	0.0	-1.8	-1.8

[1] Refer to Figure 2.10.2-34 for the identification of the representative sections.

Table 2.10.4-10 Stress Components – Impact; 1-Foot Side Drop; Drop Orientation = 90 Degrees; 3-D Model; 0-Degree Circumferential Location; Condition 1

Condition 1: 100°F Ambient with Contents

Stress Points		Stress Components (ksi)						Principal Stresses (ksi)		
Section[1]	Node	S_x	S_y	S_z	S_{xy}	S_{yz}	S_{xz}	S1	S2	S3
A1	1130	-0.4	-0.7	-0.1	0.0	0.0	0.0	-0.1	-0.4	-0.7
A2	1129	-0.4	-1.2	0.0	0.0	0.0	0.0	0.0	-0.4	-1.2
A3	1128	-0.4	-1.7	0.1	0.0	0.0	0.0	0.1	-0.4	-1.7
B1	1185	-0.4	-1.9	0.0	0.0	0.0	-0.1	0.0	-0.4	-1.9
B2	1184	-0.2	-2.1	0.0	0.0	0.0	-0.1	0.0	-0.2	-2.1
B3	1183	0.1	-2.3	0.0	0.0	0.0	-0.1	0.1	0.0	-2.3
C1	90	1.6	-1.3	5.6	0.0	-0.3	0.4	5.6	1.6	-1.3
C2	80	-1.3	-2.9	2.3	0.0	-0.2	-0.1	2.3	-1.3	-2.9
C3	70	-1.6	-3.4	0.6	0.0	-0.1	-0.3	0.6	-1.7	-3.4
C4	60	-1.8	-3.6	0.0	0.1	-0.1	-0.2	0.0	-1.9	-3.6
C5	50	-3.3	-4.1	-0.1	0.1	0.0	0.0	-0.1	-3.3	-4.1
C6	40	-3.8	-4.2	-0.1	0.1	0.0	0.0	-0.1	-3.8	-4.2
D1	25	-1.8	-3.5	1.5	0.1	0.0	0.1	1.5	-1.8	-3.5
D2	15	-3.5	-4.0	0.6	0.1	0.0	-0.2	0.6	-3.5	-4.0
D3	5	-3.9	-4.1	0.1	0.1	0.0	-0.1	0.1	-3.9	-4.1
E1	35	-4.1	-4.3	1.0	0.1	0.0	0.8	1.1	-4.1	-4.3
E2	34	-2.9	-4.1	0.6	0.1	0.0	0.8	0.8	-3.1	-4.1
E3	33	-3.0	-4.4	0.0	0.1	0.0	0.7	0.2	-3.1	-4.4
E4	32	-3.2	-4.6	-0.6	0.1	0.0	0.4	-0.5	-3.2	-4.6
E5	31	-3.2	-4.9	-1.2	0.1	0.0	0.2	-1.2	-3.2	-4.9
F1	100	-0.5	-1.1	8.7	0.0	-0.5	0.8	8.8	-0.6	-1.1
F2	99	-0.7	-3.4	0.3	0.2	-0.4	0.9	0.8	-1.2	-3.5
F3	98	-0.3	-4.8	-5.2	0.3	-0.3	1.4	0.0	-4.6	-5.7
F4	97	0.2	-7.5	-16.1	0.6	-0.3	1.7	0.4	-7.5	-16.3
G1	94	0.3	-0.8	8.2	0.1	-0.1	1.2	8.4	0.1	-0.8
G2	93	0.5	-2.1	3.1	0.2	-0.1	0.8	3.3	0.3	-2.1
G3	92	0.5	-2.5	1.4	0.2	-0.1	0.3	1.5	0.5	-2.5
G4	91	0.3	-3.1	-0.5	0.2	0.0	0.1	0.3	-0.5	-3.1
H1	330	-0.1	2.3	-2.3	-0.2	-0.7	0.0	2.4	-0.1	-2.4
H2	329	0.0	2.9	-1.1	-0.2	-0.6	0.0	3.0	-0.1	-1.2

Table 2.10.4-10 Stress Components – Impact; 1-Foot Side Drop; Drop Orientation = 90 Degrees; 3-D Model; 0-Degree Circumferential Location; Condition 1 (continued)

Stress Points		Stress Components (ksi)						Principal Stresses (ksi)		
Section[1]	Node	S_x	S_y	S_z	S_{xy}	S_{yz}	S_{xz}	S1	S2	S3
H3	328	0.0	3.5	0.1	-0.2	-0.6	0.0	3.6	0.1	-0.1
H4	327	0.1	4.1	1.5	-0.3	-0.6	-0.1	4.3	1.4	0.0
I1	244	-0.1	-0.6	2.1	0.0	-0.3	0.0	2.1	-0.1	-0.6
I2	243	-0.1	0.1	3.0	0.0	-0.2	0.0	3.0	0.1	-0.1
I3	242	0.0	0.7	3.9	0.0	-0.1	0.0	3.9	0.7	0.0
I4	241	0.0	1.4	4.9	-0.1	-0.1	0.0	4.9	1.4	0.0
J1	550	-0.1	2.3	4.1	-0.2	-0.4	0.0	4.2	2.2	-0.1
J2	548	-0.1	3.3	4.8	-0.3	-0.4	0.0	4.9	3.2	-0.1
J3	547	0.0	4.3	5.4	-0.3	-0.4	0.0	5.5	4.2	0.0
K1	344	-0.1	-0.9	3.8	0.1	-0.1	0.0	3.8	-0.1	-0.9
K2	342	0.0	0.6	4.6	-0.1	-0.1	0.0	4.6	0.6	0.0
K3	341	0.0	2.1	5.3	-0.2	-0.1	0.0	5.3	2.1	0.0
L1	740	0.0	1.9	7.0	0.2	0.0	-0.1	7.1	1.9	0.0
L2	738	-0.2	3.3	8.0	-0.5	0.0	0.0	8.0	3.3	-0.3
L3	737	0.2	4.7	8.8	-1.2	0.0	0.0	8.8	5.0	-0.1
M1	663	-0.4	-1.5	4.6	0.1	0.0	0.0	4.6	-0.4	-1.5
M2	63	0.2	2.7	6.4	0.8	0.0	0.0	6.4	2.9	-0.1
N1	1877	-0.1	2.1	3.3	-0.2	0.5	0.0	3.5	2.0	-0.1
N2	1477	-0.1	3.3	3.9	-0.3	0.4	0.0	4.2	3.1	-0.1
N3	1277	0.0	4.5	4.6	-0.3	0.4	0.0	4.9	4.1	0.0
O1	647	-0.1	-1.1	4.5	0.1	0.1	0.0	4.5	-0.1	-1.1
O2	247	0.0	0.5	5.3	0.0	0.1	0.0	5.3	0.5	0.0
O3	47	0.0	2.0	6.0	-0.2	0.0	0.0	6.0	2.0	0.0
P1	1840	-0.1	2.3	-2.1	-0.2	0.7	0.0	2.4	-0.1	-2.2
P2	1640	-0.1	3.0	-1.1	-0.2	0.7	0.0	3.1	-0.1	-1.2
P3	1440	0.0	3.7	-0.2	-0.2	0.6	0.0	3.8	0.0	-0.3
P4	1240	0.0	4.4	0.9	-0.3	0.6	0.1	4.5	0.8	0.0
Q1	628	0.0	-0.3	3.9	0.0	0.2	0.0	3.9	0.0	-0.3
Q2	428	0.0	0.4	4.4	0.0	0.2	0.0	4.4	0.4	0.0
Q3	228	0.0	1.0	4.8	-0.1	0.1	0.0	4.8	1.0	0.0
Q4	28	0.0	1.6	5.3	-0.1	0.0	0.0	5.3	1.6	0.0
R1	1816	-0.4	-2.8	2.1	0.2	0.4	0.0	2.1	-0.4	-2.8

Table 2.10.4-10 Stress Components – Impact; 1-Foot Side Drop; Drop Orientation = 90 Degrees; 3-D Model; 0-Degree Circumferential Location; Condition 1 (continued)

Stress Points		Stress Components (ksi)						Principal Stresses (ksi)		
Section[1]	Node	S_x	S_y	S_z	S_{xy}	S_{yz}	S_{xz}	S1	S2	S3
R2	1616	-0.8	-3.5	-1.0	0.3	0.4	-0.1	-0.7	-0.9	-3.6
R3	1416	-1.9	-4.4	-3.6	0.3	0.3	-0.8	-1.6	-3.7	-4.6
R4	1216	-2.6	-5.3	-7.3	0.4	0.2	-1.8	-2.0	-5.3	-7.9
S1	616	0.5	-1.7	0.2	0.1	0.2	-0.1	0.5	0.2	-1.7
S2	416	-0.2	-1.1	2.7	0.0	0.1	-0.1	2.7	-0.2	-1.1
S3	216	0.0	-0.3	4.8	0.0	0.1	0.1	4.8	0.0	-0.3
S4	16	0.0	0.4	7.0	0.0	0.0	0.1	7.0	0.4	0.0
T1	811	-6.5	-7.8	-8.0	0.4	0.1	-2.5	-4.7	-7.8	-9.9
T2	611	-3.6	-5.2	-2.0	0.2	0.1	-1.7	-0.9	-4.6	-5.3
T3	411	-1.7	-3.7	1.1	0.2	0.1	-1.3	1.6	-2.1	-3.7
T4	211	-0.4	-2.4	3.9	0.1	0.0	-0.7	4.1	-0.5	-2.4
T5	11	0.1	-1.1	8.0	0.1	0.0	-0.4	8.0	0.1	-1.1
U1	43058	1.4	-0.2	0.0	0.1	0.0	0.0	1.4	0.0	-0.2
U2	43057	0.8	-0.5	-0.1	0.1	0.0	0.0	0.8	-0.1	-0.5
U3	43056	0.3	-0.7	-0.2	0.1	0.0	0.0	0.3	-0.2	-0.7
U4	43055	-0.2	-1.0	-0.4	0.0	0.0	-0.2	0.0	-0.5	-1.0
U5	43054	-0.7	-1.3	-0.5	0.0	0.0	-0.4	-0.2	-1.1	-1.3
U6	43053	-1.3	-1.6	-0.7	0.0	-0.1	-0.9	-0.1	-1.6	-1.9
U7	43052	-2.3	-1.9	-0.4	0.0	-0.1	-1.1	0.2	-1.9	-2.8
U8	43051	-5.0	-2.8	0.0	-0.1	0.0	0.0	0.0	-2.8	-5.0
V1	50024	0.5	-0.6	0.1	0.0	0.0	0.0	0.5	0.1	-0.6
V2	50023	-1.5	-1.5	-0.1	0.0	0.0	0.0	-0.1	-1.5	-1.5
V3	50022	-2.4	-2.1	-0.2	0.0	0.0	-0.1	-0.1	-2.1	-2.4
V4	50021	-5.6	-3.3	0.0	0.0	0.0	0.0	0.0	-3.3	-5.6
W1	43278	-0.8	-1.1	0.0	0.0	0.0	0.1	0.0	-0.8	-1.1
W2	43274	-0.5	-1.2	0.0	0.0	-0.1	0.1	0.0	-0.6	-1.2
W3	43271	-0.1	-0.7	0.0	0.0	-0.1	0.0	0.0	-0.2	-0.7
X1	50084	-0.4	-2.0	0.0	0.0	0.0	0.1	0.1	-0.4	-2.0
X2	50083	-0.2	-2.1	0.0	0.0	0.0	0.1	0.1	-0.2	-2.1
X3	50081	0.2	-2.3	-0.1	0.0	0.0	0.1	0.3	-0.1	-2.3

[1] Refer to Figure 2.10.2-34 for the identification of the representative sections.

Table 2.10.4-11 Stress Components – Impact; 1-Foot Top Corner Drop; Drop Orientation = 24 Degrees; 3-D Top Model; 0-Degree Circumferential Location; Condition 1

Condition 1: 100°F Ambient with Contents

Stress Points		Stress Components (ksi)						Principal Stresses (ksi)		
Section[1]	Node	S_x	S_y	S_z	S_{xy}	S_{yz}	S_{xz}	S1	S2	S3
A1	1949	0.8	1.1	-0.1	0.0	0.0	0.1	1.1	0.8	-0.1
A2	1950	0.4	0.7	-0.1	0.0	0.0	0.1	0.7	0.5	-0.1
A3	1951	-0.2	-0.1	0.2	0.0	0.0	0.1	0.2	-0.1	-0.2
B1	1952	0.0	0.0	-0.2	0.0	0.0	0.1	0.0	0.0	-0.2
B2	93	-0.7	-1.0	0.4	0.0	0.0	0.1	0.5	-0.8	-1.0
C1	1925	-0.3	-0.1	0.2	0.0	-0.1	0.0	0.2	-0.1	-0.3
C2	1926	-0.1	-0.1	-0.1	0.0	0.0	-0.1	0.1	-0.1	-0.2
C3	1927	0.3	-0.1	-0.1	0.0	0.0	-0.1	0.3	-0.1	-0.1
D1	683	0.0	-0.2	-0.2	0.0	0.0	0.0	0.0	-0.2	-0.2
D2	85	0.0	-0.4	-0.2	0.1	0.0	0.0	0.0	-0.2	-0.4
E1	682	0.2	-0.1	-0.3	0.0	0.0	0.1	0.2	-0.1	-0.3
E2	82	0.2	0.1	0.5	0.0	0.0	0.1	0.5	0.1	0.1
F1	1925	-0.3	-0.1	0.2	0.0	-0.1	0.0	0.2	-0.1	-0.3
F2	1325	-0.7	-0.9	-2.2	0.0	-0.1	0.1	-0.7	-0.9	-2.2
G1	680	-0.4	0.0	0.2	0.0	0.0	0.2	0.3	0.0	-0.5
G2	80	0.0	0.2	0.6	0.0	0.0	0.0	0.6	0.2	0.0
H1	1921	0.0	1.1	-1.6	-0.1	-0.2	0.0	1.1	0.0	-1.6
H2	1321	0.0	1.4	-0.8	-0.1	-0.1	0.0	1.4	0.0	-0.8
I1	676	0.0	0.0	0.1	0.0	0.0	0.0	0.1	0.0	0.0
I2	76	0.0	0.3	0.3	0.0	0.0	0.0	0.3	0.2	0.0
J1	1916	0.0	1.1	-0.5	-0.1	-0.1	0.0	1.1	0.0	-0.5
J2	1316	0.0	1.7	-0.1	-0.1	-0.1	0.0	1.7	0.0	-0.1
K1	671	0.0	-0.2	-0.4	0.0	0.0	0.0	0.0	-0.2	-0.4
K2	71	0.0	0.4	-0.1	0.0	0.0	0.0	0.4	0.0	-0.1
L1	1908	-0.2	0.6	-1.3	-0.1	0.1	0.0	0.6	-0.2	-1.3
L2	1308	0.0	2.1	-0.7	0.4	0.1	0.0	2.2	0.0	-0.7
M1	663	-0.2	-0.5	-1.4	0.0	0.0	0.0	-0.2	-0.5	-1.4
M2	63	0.1	0.9	-0.9	0.3	0.1	0.0	1.0	0.0	-0.9
N1	1877	0.0	0.7	-4.6	-0.1	0.3	0.0	0.7	0.0	-4.6
N2	1477	0.0	1.4	-4.3	-0.1	0.3	0.0	1.4	0.0	-4.3

Table 2.10.4-11 Stress Components – Impact; 1-Foot Top Corner Drop; Drop Orientation = 24 Degrees; 3-D Top Model; 0-Degree Circumferential Location; Condition 1 (continued)

Stress Points		Stress Components (ksi)						Principal Stresses (ksi)		
Section[1]	Node	S_x	S_y	S_z	S_{xy}	S_{yz}	S_{zx}	S1	S2	S3
N3	1277	0.0	2.0	-4.0	-0.2	0.2	0.0	2.1	0.0	-4.0
O1	647	0.0	-0.5	-2.5	0.0	0.1	0.0	0.0	-0.5	-2.5
O2	247	0.0	0.1	-2.3	0.0	0.1	0.0	0.1	0.0	-2.3
O3	47	0.0	0.6	-2.1	-0.1	0.1	0.0	0.6	0.0	-2.1
P1	1840	-0.1	1.1	-5.2	-0.1	0.4	0.0	1.1	-0.1	-5.2
P2	1640	-0.2	1.0	-6.3	-0.1	0.4	0.0	1.0	-0.2	-6.3
P3	1440	-0.2	1.0	-7.3	-0.1	0.3	-0.2	1.0	-0.2	-7.3
P4	1240	-0.2	0.6	-9.4	0.0	0.3	-0.5	0.6	-0.2	-9.5
Q1	628	0.0	0.8	-2.5	-0.1	0.1	0.0	0.9	0.0	-2.5
Q2	428	0.0	0.9	-2.9	-0.1	0.1	0.0	0.9	0.0	-2.9
Q3	228	0.0	1.0	-3.2	-0.1	0.1	0.0	1.0	0.0	-3.2
Q4	28	0.0	1.0	-3.5	-0.1	0.0	0.0	1.0	0.0	-3.5
R1	1816	0.1	-1.2	-11.4	0.1	0.2	0.0	0.1	-1.2	-11.5
R2	1616	0.2	-0.3	-8.4	0.1	-0.2	0.1	0.2	-0.3	-8.5
R3	1416	0.2	0.5	-5.7	0.0	0.2	0.3	0.5	0.2	-5.7
R4	1216	2.8	2.0	-3.1	0.1	0.1	0.3	2.8	1.9	-3.1
S1	616	-3.6	-2.1	-11.8	-0.1	0.2	1.5	-2.1	-3.3	-12.1
S2	416	-3.6	-0.4	-5.3	-0.2	0.0	-0.3	-0.4	-3.5	-5.4
S3	216	-1.3	1.4	-0.8	-0.2	0.0	-0.5	1.4	-0.5	-1.6
S4	16	-0.5	3.0	4.5	-0.3	0.0	-0.4	4.5	3.0	-0.5
T1	811	0.1	-1.6	-1.4	0.2	0.2	0.3	0.2	-1.4	-1.7
T2	611	0.4	-1.8	-2.6	0.2	0.1	-0.1	0.4	-1.8	-2.6
T3	411	0.3	-1.8	-2.6	0.2	0.1	-0.2	0.3	-1.8	-2.6
T4	211	0.3	-1.7	-2.3	0.1	0.1	-0.2	0.3	-1.7	-2.3
T5	11	0.3	-1.5	-1.7	0.1	0.0	-0.1	0.3	-1.5	-1.7
U1	43058	0.5	3.0	-5.0	-0.3	0.2	1.1	3.0	0.7	-5.2
U2	43057	1.5	2.5	-4.4	-0.2	0.1	1.6	2.5	1.8	-4.8
U3	43056	1.2	1.7	-3.7	-0.1	0.1	2.1	2.0	1.7	-4.5
U4	43055	0.8	0.8	-3.4	0.0	0.1	2.2	1.7	0.8	-4.4
U5	43054	0.3	-0.1	-3.4	0.0	0.1	2.1	1.3	-0.1	-4.4
U6	43053	-0.3	-0.9	-2.7	0.1	0.1	1.7	0.6	-0.9	-3.5
U7	43052	-0.5	-2.4	-4.7	0.2	0.1	1.7	0.2	-2.4	-5.3

Table 2.10.4-11 Stress Components – Impact; 1-Foot Top Corner Drop; Drop Orientation = 24 Degrees; 3-D Top Model; 0-Degree Circumferential Location; Condition 1 (continued)

Stress Points		Stress Components (ksi)						Principal Stresses (ksi)		
Section[1]	Node	S_x	S_y	S_z	S_{xy}	S_{yz}	S_{xz}	S1	S2	S3
UB	43051	-3.5	-4.8	-4.6	0.2	0.2	2.8	-1.1	-4.8	-6.9
V1	50024	-6.9	0.2	-1.8	-0.6	-0.1	-0.9	0.2	-1.7	-7.1
V2	50023	-4.4	-1.6	-1.9	-0.3	-0.1	-0.7	-1.5	-1.7	-4.6
V3	50022	-1.6	-3.3	-1.9	0.1	0.0	-0.3	-1.4	-2.0	-3.3
V4	50021	1.4	-5.0	-1.8	0.4	0.0	-0.1	1.4	-1.8	-5.1
W1	43278	1.0	0.2	-0.3	-0.1	-0.3	-0.1	1.0	0.3	-0.5
W2	43274	0.4	-0.2	-0.1	0.0	-0.3	-0.1	0.4	0.1	-0.5
W3	43271	-0.1	-0.3	0.1	0.0	-0.4	0.0	0.3	-0.1	-0.6
X1	50084	13.8	11.1	-3.4	-0.4	0.2	-3.3	14.5	11.1	-4.0
X2	50083	4.3	2.2	-2.2	-0.1	0.2	-3.3	5.7	2.2	-3.6
X3	50081	-13.0	-13.8	6.9	0.4	-0.2	-3.3	7.4	-13.3	-14.0

[1] Refer to Figure 2.10.2-33 for the identification of the representative sections.

Table 2.10.4-12 Stress Components – Impact; 1-Foot Bottom Corner Drop; Drop Orientation = 24 Degrees; 3-D Bottom Model; 0-Degree Circumferential Location; Condition 1

Condition 1: 100°F Ambient with Contents

Stress Points		Stress Components (ksi)						Principal Stresses (ksi)		
Section[1]	Node	S_x	S_y	S_z	S_{xy}	S_{yz}	S_{xz}	S1	S2	S3
A1	1130	6.6	5.0	-2.4	-0.2	0.8	0.8	6.7	5.1	-2.6
A2	1129	0.9	0.1	-0.5	0.0	0.6	0.8	1.3	0.3	-1.1
A3	1128	-4.8	-4.9	1.5	0.2	0.8	0.8	1.7	-4.9	-5.1
B1	1185	3.8	1.5	-2.5	-0.2	0.8	0.8	3.9	1.7	-2.8
B2	1184	-1.4	-2.9	-0.7	0.0	0.6	0.9	-0.1	-1.9	-3.1
B3	1183	-6.7	-7.3	1.1	0.1	0.6	0.8	1.2	-6.8	-7.3
C1	90	-7.0	-2.1	-8.5	-0.4	-0.3	-1.7	-2.0	-5.9	-9.7
C2	80	-3.3	-0.6	-5.0	-0.4	-0.2	-1.3	-0.6	-2.7	-5.7
C3	70	-2.1	-0.4	-3.1	-0.2	-0.1	-1.0	-0.4	-1.6	-3.7
C4	60	-1.1	-0.3	-1.8	0.0	-0.1	-0.9	-0.3	-0.5	-2.4
C5	50	2.5	-0.9	-0.6	0.3	-0.1	-0.6	2.7	-0.7	-1.0
C6	40	5.8	-0.9	-0.1	0.6	0.0	-0.4	5.9	-0.1	-1.0
D1	25	-12.4	-9.3	-15.2	-0.1	-0.3	-3.3	-9.3	-10.2	-17.4
D2	15	-2.0	-7.0	-6.5	0.2	-0.1	-1.6	-1.5	-7.0	-7.0
D3	5	0.9	-8.6	-3.0	0.6	0.0	-0.5	1.0	-3.1	-8.7
E1	35	2.9	-3.8	-11.7	0.5	-0.1	-1.2	3.1	-3.9	-11.8
E2	34	0.0	-3.4	-7.8	0.2	-0.3	-3.0	1.0	-3.4	-8.8
E3	33	-2.4	-3.0	-4.0	0.0	-0.3	-3.3	0.2	-3.0	-6.6
E4	32	-2.7	-2.4	-1.1	0.0	-0.2	-2.0	0.3	-2.4	-4.1
E5	31	-2.8	-1.6	1.9	-0.1	-0.1	-1.2	2.2	-1.6	-3.1
F1	100	0.0	-0.8	-11.1	0.0	-0.4	-1.1	0.1	-0.8	-11.2
F2	99	-1.0	0.1	-6.7	-0.1	-0.3	-0.5	0.2	-1.0	-6.8
F3	98	-1.1	0.5	-5.2	-0.1	-0.2	0.4	0.5	-1.0	-5.3
F4	97	0.0	0.9	-4.6	-0.1	-0.2	0.8	1.0	0.1	-4.7
G1	94	0.1	-0.8	-8.1	0.0	-0.1	-0.3	0.1	-0.8	-8.1
G2	93	-0.2	-0.1	-5.3	0.0	-0.1	-0.2	-0.1	-0.2	-5.3
G3	92	-0.3	0.4	-3.2	-0.1	-0.1	0.0	0.4	-0.4	-3.2
G4	91	-0.2	1.1	-0.6	-0.1	0.0	0.0	1.1	-0.2	-0.6

Table 2.10.4-12 Stress Components – Impact; 1-Foot Bottom Corner Drop; Drop Orientation = 24 Degrees; 3-D Bottom Model; 0-Degree Circumferential Location; Condition 1 (continued)

Stress Points		Stress Components (ksi)						Principal Stresses (ksi)		
Section[1]	Node	S_x	S_y	S_z	S_{xy}	S_{yz}	S_{zx}	S1	S2	S3
H1	330	-0.1	1.1	-5.0	-0.1	-0.4	0.0	1.2	-0.1	-5.0
H2	329	-0.2	1.0	-6.0	-0.1	-0.3	0.0	1.0	-0.2	-6.1
H3	328	-0.2	0.9	-7.0	-0.1	-0.3	0.2	0.9	-0.2	-7.0
H4	327	-0.2	0.6	-9.0	0.0	-0.3	0.5	0.6	-0.2	-9.1
I1	244	0.0	0.1	-3.6	0.0	-0.2	0.0	0.1	0.0	-3.7
I2	243	0.0	0.4	-3.7	0.0	-0.1	0.0	0.4	0.0	-3.7
I3	242	0.0	0.6	-3.7	0.0	-0.1	0.0	0.6	0.0	-3.7
I4	241	0.0	0.8	-3.7	-0.1	0.0	0.0	0.8	0.0	-3.7
J1	550	0.0	0.8	-3.9	-0.1	-0.3	0.0	0.9	0.0	-3.9
J2	548	0.0	1.4	-3.7	-0.1	-0.2	0.0	1.4	0.0	-3.7
J3	547	0.0	1.9	-3.5	-0.1	-0.2	0.0	1.9	0.0	-3.5
K1	344	0.0	-0.7	-3.1	0.0	-0.1	0.0	0.0	-0.7	-3.1
K2	342	0.0	0.2	-2.7	0.0	-0.1	0.0	0.0	0.0	-2.7
K3	341	0.0	1.1	-2.4	-0.1	-0.1	0.0	1.1	0.0	-2.4
L1	740	0.0	0.9	-0.9	0.0	-0.1	0.0	0.9	0.0	-0.9
L2	738	-0.1	1.3	-0.6	-0.2	-0.1	0.0	1.4	-0.1	-0.6
L3	737	0.0	1.8	-0.3	-0.4	-0.1	0.0	1.9	0.0	-0.3
M1	454	0.0	-0.7	-1.8	-0.3	0.0	0.0	0.1	-0.9	-1.8
M2	452	0.1	0.2	-1.4	-0.1	-0.1	0.0	0.3	0.0	-1.4
M3	451	-0.1	0.9	-1.2	0.0	-0.1	0.0	0.9	-0.1	-1.2
N1	810	0.0	1.2	-0.5	-0.1	0.1	0.0	1.2	0.0	-0.5
N2	807	0.0	1.6	-0.1	-0.1	0.1	0.0	1.6	0.0	-0.1
O1	524	0.0	-0.2	-0.6	0.0	0.0	0.0	0.0	-0.2	-0.6
O2	521	0.0	0.4	-0.3	0.0	-0.1	0.0	0.4	0.0	-0.3
P1	850	0.0	1.0	-1.6	-0.1	0.2	0.0	1.1	0.0	-1.6
P2	847	0.0	1.4	-0.7	-0.1	0.2	0.0	1.5	0.0	-0.8
Q1	564	0.0	0.1	0.0	0.0	0.0	0.0	0.1	0.0	0.0
Q2	561	0.0	0.3	0.1	0.0	0.0	0.0	0.3	0.1	0.0
R1	890	-0.3	-0.1	0.2	0.0	0.1	0.0	0.2	-0.2	-0.3
R2	887	-0.4	-0.7	-2.1	0.0	0.1	-0.1	-0.4	-0.7	-2.1

Table 2.10.4-12 Stress Components – Impact; 1-Foot Bottom Corner Drop; Drop Orientation = 24 Degrees; 3-D Bottom Model; 0-Degree Circumferential Location; Condition 1 (continued)

Stress Points		Stress Components (ksi)						Principal Stresses (ksi)		
Section[1]	Node	S_x	S_y	S_z	S_{xy}	S_{yz}	S_{xz}	S1	S2	S3
S1	604	-0.2	0.1	0.0	0.0	0.0	-0.1	0.2	0.1	-0.2
S2	601	0.0	0.4	0.7	0.0	0.0	0.0	0.7	0.4	0.0
T1	897	0.1	-0.1	-0.7	0.0	0.0	-0.1	0.1	-0.1	-0.7
T2	614	0.1	0.1	0.0	0.0	0.0	-0.2	0.2	0.1	-0.1
T3	611	0.0	0.1	0.3	0.0	0.0	-0.1	0.3	0.1	0.0
U1	900	0.1	0.0	-0.4	0.0	0.0	0.1	0.1	0.0	-0.4
U2	910	0.3	-0.1	-0.3	0.0	0.0	0.1	0.3	-0.1	-0.3
V1	920	-0.1	-0.2	-0.2	0.0	0.0	0.1	-0.1	-0.2	-0.2
V2	930	-0.1	-0.4	-0.1	0.1	0.0	0.0	0.0	-0.1	-0.4
W1	1216	0.5	0.9	-0.4	0.0	0.0	-0.1	0.9	0.5	-0.4
W2	1226	-0.1	-0.1	0.2	0.0	0.0	-0.1	0.2	-0.1	-0.1
X1	1236	0.0	0.0	-0.2	0.0	0.0	-0.1	0.1	0.0	-0.3
X2	1246	-0.7	-1.0	0.5	0.0	0.0	-0.1	0.5	-0.7	-1.0

[1] Refer to Figure 2.10.2-34 for the identification of the representative sections.

Table 2.10.4-13 Stress Components – Impact; 30-Foot Top End Drop; Drop Orientation = 0 Degrees; 2-D Model; Condition 1

Condition 1: 100°F Ambient with Contents

Stress Points		Stress Components (ksi)						Principal Stresses (ksi)		
Section[1]	Node	S_x	S_y	S_z	S_{xy}	S_{yz}	S_{xz}	S1	S2	S3
A1	1	4.4	0.0	4.4	0.0	0.0	0.0	4.4	4.4	0.0
A2	2	2.4	0.0	2.4	0.0	0.0	0.0	2.4	2.4	0.0
A3	3	0.5	0.0	0.5	0.0	0.0	0.0	0.5	0.5	0.0
A4	4	-1.4	0.0	-1.4	0.0	0.0	0.0	0.0	-1.4	-1.4
A5	5	-3.3	0.0	-3.3	0.0	0.0	0.0	0.0	-3.3	-3.3
B1	6	2.7	0.0	2.7	0.0	0.0	0.0	2.7	2.7	0.0
B2	7	1.0	0.0	1.0	0.0	0.0	0.0	1.0	1.0	0.0
B3	8	-0.7	0.0	-0.7	0.0	0.0	0.0	0.0	-0.7	-0.7
B4	9	-2.4	0.0	-2.4	0.0	0.0	0.0	0.0	-2.4	-2.4
B5	10	-4.1	0.0	-4.1	0.0	0.0	0.0	0.0	-4.1	-4.1
C1	251	-2.8	-3.5	-0.5	-0.7	0.0	0.0	-0.5	-2.4	-3.9
C2	252	-0.5	-1.4	0.3	-0.5	0.0	0.0	0.3	-0.3	-1.6
C3	253	0.6	-0.6	0.4	-0.4	0.0	0.0	0.8	0.4	-0.7
C4	254	1.9	-0.2	0.4	-0.3	0.0	0.0	2.0	0.4	-0.3
C5	255	3.4	-0.2	0.4	-0.2	0.0	0.0	3.4	0.4	-0.2
D1	306	-3.4	-1.9	-1.5	-0.9	0.0	0.0	-1.4	-1.5	-3.8
D2	307	-1.0	-1.5	-0.9	-0.3	0.0	0.0	-0.9	-0.9	-1.6
D3	308	-0.3	-0.6	-0.7	0.1	0.0	0.0	-0.3	-0.6	-0.7
D4	309	0.4	-0.2	-0.7	0.2	0.0	0.0	0.5	-0.3	-0.7
D5	310	1.3	-0.1	-0.7	0.1	0.0	0.0	1.3	-0.1	-0.7
E1	305	3.2	0.1	0.9	-0.7	0.0	0.0	3.4	0.9	0.0
E2	315	1.6	-0.7	0.3	-0.8	0.0	0.0	1.9	0.3	-1.0
E3	325	0.8	-0.6	0.1	-0.8	0.0	0.0	1.1	0.1	-1.0
E4	335	0.4	-0.6	0.0	-0.6	0.0	0.0	0.7	0.0	-0.9
E5	345	0.2	-0.6	-0.1	-0.4	0.0	0.0	0.3	-0.1	-0.8
E6	355	0.1	-0.8	-0.2	-0.2	0.0	0.0	0.1	-0.2	-0.9
F1	251	-2.8	-3.5	-0.5	-0.7	0.0	0.0	-0.5	-2.4	-3.9
F2	261	-2.1	-1.9	0.1	-0.2	0.0	0.0	0.1	-1.8	-2.3
F3	271	-1.6	-0.9	0.5	0.2	0.0	0.0	0.5	-0.8	-1.7
F4	281	-1.7	-0.1	0.6	0.3	0.0	0.0	0.6	0.0	-1.7
G1	311	-1.5	-2.3	-0.2	-0.2	0.0	0.0	-0.2	-1.4	-2.4

Table 2.10.4-13 Stress Components – Impact; 30-Foot Top End Drop; Drop Orientation = 0 Degrees; 2-D Model; Condition 1 (continued)

Stress Points		Stress Components (ksi)						Principal Stresses (ksi)		
Section[1]	Node	S_x	S_y	S_z	S_{xy}	S_{yz}	S_{zx}	S1	S2	S3
G2	321	-1.0	-1.5	0.2	0.0	0.0	0.0	0.2	-1.0	-1.5
G3	331	-0.5	-0.8	0.5	0.2	0.0	0.0	0.5	-0.4	-0.9
G4	341	-0.2	-0.2	0.7	0.1	0.0	0.0	0.7	-0.1	-0.3
G5	351	-0.1	0.7	1.0	0.1	0.0	0.0	1.0	0.7	-0.1
H1	581	0.0	-2.3	0.1	0.0	0.0	0.0	0.1	0.0	-2.3
H2	582	-0.1	-2.9	-0.1	0.0	0.0	0.0	-0.1	-0.1	-2.9
H3	583	-0.1	-3.5	-0.3	0.1	0.0	0.0	-0.1	-0.3	-3.5
H4	584	0.0	-4.4	-0.5	0.2	0.0	0.0	0.0	-0.5	-4.4
I1	589	0.0	-1.1	0.2	0.0	0.0	0.0	0.2	0.0	-1.1
I2	590	0.0	-1.2	0.2	0.0	0.0	0.0	0.2	0.0	-1.2
I3	591	0.0	-1.4	0.2	0.0	0.0	0.0	0.2	0.0	-1.4
I4	592	0.0	-1.5	0.1	0.0	0.0	0.0	0.1	0.0	-1.5
I5	593	0.0	-1.6	0.1	0.0	0.0	0.0	0.1	0.0	-1.6
J1	971	0.0	-3.9	0.0	0.0	0.0	0.0	0.0	0.0	-3.9
J2	972	0.0	-3.9	0.0	0.0	0.0	0.0	0.0	0.0	-3.9
J3	973	0.0	-3.9	0.0	0.0	0.0	0.0	0.0	0.0	-3.9
J4	974	0.0	-3.9	0.0	0.0	0.0	0.0	0.0	0.0	-3.9
K1	979	0.0	-2.0	0.0	0.0	0.0	0.0	0.0	0.0	-2.0
K2	980	0.0	-2.0	0.0	0.0	0.0	0.0	0.0	0.0	-2.0
K3	981	0.0	-2.0	0.0	0.0	0.0	0.0	0.0	0.0	-2.0
K4	982	0.0	-2.0	0.0	0.0	0.0	0.0	0.0	0.0	-2.0
K5	983	0.0	-2.0	0.0	0.0	0.0	0.0	0.0	0.0	-2.0
L1	1601	0.0	-4.9	0.0	0.0	0.0	0.0	0.0	0.0	-4.9
L2	1602	0.0	-4.9	0.0	0.0	0.0	0.0	0.0	0.0	-4.9
L3	1603	0.0	-4.9	0.0	0.0	0.0	0.0	0.0	0.0	-4.9
L4	1604	0.0	-4.9	0.0	0.0	0.0	0.0	0.0	0.0	-4.9
M1	1609	0.0	-3.0	0.0	0.0	0.0	0.0	0.0	0.0	-3.0
M2	1610	0.0	-3.0	0.0	0.0	0.0	0.0	0.0	0.0	-3.0
M3	1611	0.0	-3.0	0.0	0.0	0.0	0.0	0.0	0.0	-3.0
M4	1612	0.0	-3.0	0.0	0.0	0.0	0.0	0.0	0.0	-3.0
M5	1613	0.0	-3.0	0.0	0.0	0.0	0.0	0.0	0.0	-3.0
N1	2216	0.0	-6.0	0.0	0.0	0.0	0.0	0.0	0.0	-6.0
N2	2217	0.0	-5.9	0.0	0.0	0.0	0.0	0.0	0.0	-5.9

Table 2.10.4-13 Stress Components – Impact; 30-Foot Top End Drop; Drop Orientation = 0 Degrees; 2-D Model; Condition 1 (continued)

Stress Points		Stress Components (ksi)						Principal Stresses (ksi)		
Section[1]	Node	S_x	S_y	S_z	S_{xy}	S_{yz}	S_{zx}	S1	S2	S3
N3	2218	0.0	-5.9	0.0	0.0	0.0	0.0	0.0	0.0	-5.9
N4	2219	0.0	-5.9	0.0	0.0	0.0	0.0	0.0	0.0	-5.9
O1	2224	0.0	-3.9	-0.1	0.0	0.0	0.0	0.0	-0.1	-3.9
O2	2225	0.0	-3.9	-0.1	0.0	0.0	0.0	0.0	-0.1	-3.9
O3	2226	0.0	-3.9	-0.1	0.0	0.0	0.0	0.0	-0.1	-3.9
O4	2227	0.0	-3.9	-0.1	0.0	0.0	0.0	0.0	-0.1	-3.9
O5	2228	0.0	-3.9	-0.1	0.0	0.0	0.0	0.0	-0.1	-3.9
P1	2546	-0.1	-3.5	0.7	0.0	0.0	0.0	0.7	-0.1	-3.5
P2	2547	-0.1	-5.3	0.2	0.0	0.0	0.0	0.2	-0.1	-5.3
P3	2548	-0.1	-7.0	-0.3	-0.2	0.0	0.0	-0.1	-0.3	-7.0
P4	2549	-0.1	-9.5	-0.9	-0.5	0.0	0.0	-0.1	-0.9	-9.5
Q1	2554	0.0	-3.6	1.3	0.0	0.0	0.0	1.3	0.0	-3.6
Q2	2555	0.0	-4.0	1.1	0.0	0.0	0.0	1.1	0.0	-4.0
Q3	2556	0.0	-4.4	1.0	0.1	0.0	0.0	1.0	0.0	-4.4
Q4	2557	0.0	-4.9	0.9	0.0	0.0	0.0	0.9	0.0	-4.9
Q5	2558	0.0	-5.3	0.7	0.0	0.0	0.0	0.7	0.0	-5.3
R1	2771	0.2	-18.3	-0.9	-0.1	0.0	0.0	0.2	-0.9	-18.3
R2	2772	0.6	-10.8	1.3	0.1	0.0	0.0	1.3	0.6	-10.8
R3	2773	1.7	-3.7	3.5	1.2	0.0	0.0	3.5	1.9	-3.9
R4	2774	1.4	4.6	5.6	2.9	0.0	0.0	6.4	5.6	-0.3
S1	2779	-9.2	-12.6	-2.8	0.8	0.0	0.0	-2.8	-9.1	-12.7
S2	2780	-5.9	-7.5	-0.6	-0.3	0.0	0.0	-0.6	-5.8	-7.6
S3	2781	-3.0	-4.0	1.1	-1.1	0.0	0.0	1.1	-2.3	-4.8
S4	2782	-1.2	-0.4	2.5	-0.9	0.0	0.0	2.5	0.2	-1.8
S5	2783	-0.5	4.2	3.8	-0.6	0.0	0.0	4.3	3.8	-0.6
T1	7066	11.5	9.1	4.7	2.7	0.0	0.0	13.3	7.3	4.7
T2	7067	7.7	2.8	2.0	1.0	0.0	0.0	7.9	2.6	2.0
T3	7068	5.1	-0.7	0.5	-0.2	0.0	0.0	5.1	0.5	-0.7
T4	7069	3.0	-3.0	-0.6	-0.9	0.0	0.0	3.2	-0.6	-3.1
T5	7070	1.6	-5.1	-1.5	-1.0	0.0	0.0	1.8	-1.5	-5.2
T6	7071	0.7	-7.4	-2.4	-0.7	0.0	0.0	0.8	-2.4	-7.4
T7	7072	0.4	-10.5	-3.3	-0.4	0.0	0.0	0.4	-3.3	-10.5
U1	3051	-1.9	-9.3	6.3	1.8	0.0	0.0	6.3	-1.5	-9.7

Table 2.10.4-13 Stress Components – Impact; 30-Foot Top End Drop; Drop Orientation = 0 Degrees; 2-D Model; Condition 1 (continued)

Stress Points		Stress Components (ksi)						Principal Stresses (ksi)		
Section[1]	Node	S_x	S_y	S_z	S_{xy}	S_{yz}	S_{xz}	S1	S2	S3
U2	3052	2.1	-8.6	4.7	2.2	0.0	0.0	4.7	2.5	-9.0
U3	3053	2.5	-7.2	2.4	2.5	0.0	0.0	3.1	2.4	-7.8
U4	3054	2.2	-7.1	-0.3	2.3	0.0	0.0	2.8	-0.3	-7.7
U5	3055	2.1	-8.6	-3.5	2.7	0.0	0.0	2.7	-3.5	-9.3
U6	3056	-1.6	-6.8	-6.4	4.4	0.0	0.0	0.9	-6.4	-9.2
V1	3611	-8.4	-4.6	5.3	-1.5	0.0	0.0	5.3	-4.2	-8.9
V2	3612	-5.0	-4.5	3.7	-1.8	0.0	0.0	3.7	-2.9	-6.6
V3	3613	-2.4	-4.0	1.8	-2.3	0.0	0.0	1.8	-0.9	-5.6
V4	3614	-0.3	-3.6	-0.3	-2.1	0.0	0.0	0.7	-0.3	-4.6
V5	3615	1.6	-2.7	-2.3	-1.8	0.0	0.0	2.3	-2.3	-3.4
V6	3616	1.7	-2.0	-4.9	-1.1	0.0	0.0	2.0	-2.3	-4.9
V7	3617	6.9	-1.9	-6.3	-0.7	0.0	0.0	6.9	-1.9	-6.3
W1	3241	21.5	-1.0	21.5	0.0	0.0	0.0	21.5	21.5	-1.0
W2	3242	13.9	-1.3	13.9	0.0	0.0	0.0	13.9	13.9	-1.3
W3	3243	6.5	-1.8	6.5	0.0	0.0	0.0	6.5	6.5	-1.8
W4	3244	-0.8	-2.3	-0.8	0.0	0.0	0.0	-0.8	-0.8	-2.3
W5	3245	-8.3	-2.8	-8.3	0.0	0.0	0.0	-2.8	-8.3	-8.3
W6	3246	-16.2	-3.0	-16.2	0.0	0.0	0.0	-3.0	-16.2	-16.2
X1	3801	27.5	-3.5	27.5	0.0	0.0	0.0	27.5	27.5	-3.5
X2	3802	19.0	-3.3	19.0	0.0	0.0	0.0	19.0	19.0	-3.3
X3	3803	9.8	-3.0	9.8	0.0	0.0	0.0	9.8	9.8	-3.0
X4	3804	0.5	-2.8	0.5	0.0	0.0	0.0	0.5	0.5	-2.8
X5	3805	-8.9	-2.6	-8.9	0.0	0.0	0.0	-2.6	-8.9	-8.9
X6	3806	-18.2	-2.1	-18.2	0.0	0.0	0.0	-2.1	-18.2	-18.2
X7	3807	-28.0	-1.8	-28.0	0.0	0.0	0.0	-1.8	-28.0	-28.0

[1] Refer to Figure 2.10.2-34 for the identification of the representative sections.

Table 2.10.4-14 Stress Components – Impact; 30-Foot Bottom End Drop; Drop Orientation = 0 Degrees; 2-D Model; Condition 1

Condition 1: 100°F Ambient with Contents

Stress Points		Stress Components (ksi)						Principal Stresses (ksi)		
Section[1]	Node	S_x	S_y	S_z	S_{xy}	S_{yz}	S_{zx}	S1	S2	S3
A1	1	21.7	-0.9	21.7	0.0	0.0	0.0	21.7	21.7	-0.9
A2	2	12.3	-1.0	12.3	0.0	0.0	0.0	12.3	12.3	-1.0
A3	3	3.0	-1.3	3.0	0.0	0.0	0.0	3.0	3.0	-1.3
A4	4	-6.3	-1.5	-6.3	0.0	0.0	0.0	-1.5	-6.3	-6.3
A5	5	-15.9	-1.6	-15.9	0.0	0.0	0.0	-1.6	-15.9	-15.9
B1	6	12.7	-1.8	12.7	0.0	0.0	0.0	12.7	12.7	-1.8
B2	7	4.5	-1.9	4.5	0.0	0.0	0.0	4.5	4.5	-1.9
B3	8	-3.7	-2.1	-3.7	0.0	0.0	0.0	-2.1	-3.7	-3.7
B4	9	-11.9	-2.2	-11.9	0.0	0.0	0.0	-2.2	-11.9	-11.9
B5	10	-20.0	-2.4	-20.0	0.0	0.0	0.0	-2.4	-20.0	-20.0
C1	251	-11.9	-14.6	-0.8	-2.5	0.0	0.0	-0.8	-10.4	-16.1
C2	252	-1.9	-6.0	2.4	-1.8	0.0	0.0	2.4	-1.2	-6.6
C3	253	3.1	-2.6	2.7	-1.8	0.0	0.0	3.7	2.7	-3.1
C4	254	9.6	-1.6	2.7	-1.5	0.0	0.0	9.8	2.7	-1.8
C5	255	16.7	-1.5	2.6	-1.0	0.0	0.0	16.7	2.6	-1.5
D1	306	-18.4	-15.6	-8.6	-5.5	0.0	0.0	-8.6	-11.3	-22.6
D2	307	-4.9	-11.2	-4.9	-2.3	0.0	0.0	-4.1	-4.9	-11.9
D3	308	-1.2	-5.7	-3.8	0.0	0.0	0.0	-1.2	-3.8	-5.7
D4	309	2.3	-3.7	-3.9	0.5	0.0	0.0	2.4	-3.7	-3.9
D5	310	6.8	-2.9	-4.0	0.6	0.0	0.0	6.8	-2.9	-4.0
E1	305	15.7	-4.6	3.6	-3.6	0.0	0.0	16.3	3.6	-5.2
E2	315	7.6	-6.9	1.1	-4.7	0.0	0.0	8.9	1.1	-8.3
E3	325	3.2	-5.5	0.3	-4.6	0.0	0.0	5.1	0.3	-7.4
E4	335	1.6	-4.5	0.2	-3.5	0.0	0.0	3.2	0.2	-6.1
E5	345	0.6	-3.8	0.2	-2.1	0.0	0.0	1.4	0.2	-4.6
E6	355	0.3	-3.7	0.1	-1.2	0.0	0.0	0.6	0.1	-4.0
F1	251	-11.9	-14.6	-0.8	-2.5	0.0	0.0	-0.8	-10.4	-16.1
F2	261	-8.6	-6.5	2.1	-0.8	0.0	0.0	2.1	-6.2	-8.9
F3	271	-5.6	-0.5	4.3	0.2	0.0	0.0	4.3	-0.5	-5.6
F4	281	-5.6	4.6	5.5	-0.2	0.0	0.0	5.5	4.6	-5.6
G1	311	-8.0	-12.9	-1.1	-0.4	0.0	0.0	-1.1	-8.0	-12.9

Table 2.10.4-14 Stress Components – Impact; 30-Foot Bottom End Drop; Drop Orientation = 0 Degrees; 2-D Model; Condition 1 (continued)

Stress Points		Stress Components (ksi)						Principal Stresses (ksi)		
Section[1]	Node	S_x	S_y	S_z	S_{xy}	S_{yz}	S_{zx}	S1	S2	S3
G2	321	-5.6	-8.0	0.8	0.3	0.0	0.0	0.8	-5.6	-8.1
G3	331	-2.9	-4.8	2.3	0.9	0.0	0.0	2.3	-2.5	-5.2
G4	341	-1.2	-1.5	3.6	0.7	0.0	0.0	3.6	-0.6	-2.1
G5	351	-0.5	2.8	4.9	0.4	0.0	0.0	4.9	2.8	-0.6
H1	581	-0.1	-3.0	0.7	0.0	0.0	0.0	0.7	-0.1	-3.0
H2	582	-0.1	-5.1	0.1	0.0	0.0	0.0	0.1	-0.1	-5.1
H3	583	-0.1	-7.1	-0.5	0.3	0.0	0.0	-0.1	-0.5	-7.1
H4	584	-0.1	-9.9	-1.2	0.6	0.0	0.0	-0.1	-1.2	-10.0
I1	589	0.0	-3.6	1.1	0.0	0.0	0.0	1.1	0.0	-3.6
I2	590	0.0	-4.2	1.0	0.0	0.0	0.0	1.0	0.0	-4.2
I3	591	0.0	-4.8	0.8	0.0	0.0	0.0	0.8	0.0	-4.8
I4	592	0.0	-5.4	0.6	0.0	0.0	0.0	0.6	0.0	-5.4
I5	593	0.0	-6.0	0.4	0.0	0.0	0.0	0.4	0.0	-6.0
J1	971	0.0	-5.8	0.0	0.0	0.0	0.0	0.0	0.0	-5.8
J2	972	0.0	-5.8	0.0	0.0	0.0	0.0	0.0	0.0	-5.8
J3	973	0.0	-5.8	0.0	0.0	0.0	0.0	0.0	0.0	-5.8
J4	974	0.0	-5.8	0.0	0.0	0.0	0.0	0.0	0.0	-5.8
K1	979	0.0	-4.3	0.0	0.0	0.0	0.0	0.0	0.0	-4.3
K2	980	0.0	-4.2	0.0	0.0	0.0	0.0	0.0	0.0	-4.2
K3	981	0.0	-4.2	0.0	0.0	0.0	0.0	0.0	0.0	-4.2
K4	982	0.0	-4.2	0.0	0.0	0.0	0.0	0.0	0.0	-4.2
K5	983	0.0	-4.2	0.0	0.0	0.0	0.0	0.0	0.0	-4.2
L1	1601	0.0	-4.8	0.0	0.0	0.0	0.0	0.0	0.0	-4.8
L2	1602	0.0	-4.8	0.0	0.0	0.0	0.0	0.0	0.0	-4.8
L3	1603	0.0	-4.8	0.0	0.0	0.0	0.0	0.0	0.0	-4.8
L4	1604	0.0	-4.8	0.0	0.0	0.0	0.0	0.0	0.0	-4.8
M1	1609	0.0	-3.2	0.0	0.0	0.0	0.0	0.0	0.0	-3.2
M2	1610	0.0	-3.2	0.0	0.0	0.0	0.0	0.0	0.0	-3.2
M3	1611	0.0	-3.2	0.0	0.0	0.0	0.0	0.0	0.0	-3.2
M4	1612	0.0	-3.2	0.0	0.0	0.0	0.0	0.0	0.0	-3.2
M5	1613	0.0	-3.2	0.0	0.0	0.0	0.0	0.0	0.0	-3.2
N1	2216	0.0	-3.8	0.0	0.0	0.0	0.0	0.0	0.0	-3.8
N2	2217	0.0	-3.8	0.0	0.0	0.0	0.0	0.0	0.0	-3.8

Table 2.10.4-14 Stress Components – Impact; 30-Foot Bottom End Drop; Drop Orientation = 0 Degrees; 2-D Model; Condition 1 (continued)

Stress Points		Stress Components (ksi)						Principal Stresses (ksi)		
Section[1]	Node	S_x	S_y	S_z	S_{xy}	S_{yz}	S_{xz}	S1	S2	S3
N3	2218	0.0	-3.8	0.0	0.0	0.0	0.0	0.0	0.0	-3.8
N4	2219	0.0	-3.8	0.0	0.0	0.0	0.0	0.0	0.0	-3.8
O1	2224	0.0	-2.3	0.0	0.0	0.0	0.0	0.0	0.0	-2.3
O2	2225	0.0	-2.3	0.0	0.0	0.0	0.0	0.0	0.0	-2.3
O3	2226	0.0	-2.3	0.0	0.0	0.0	0.0	0.0	0.0	-2.3
O4	2227	0.0	-2.3	0.0	0.0	0.0	0.0	0.0	0.0	-2.3
O5	2228	0.0	-2.3	0.0	0.0	0.0	0.0	0.0	0.0	-2.3
P1	2546	0.0	-2.3	0.1	0.0	0.0	0.0	0.1	0.0	-2.3
P2	2547	-0.1	-2.9	-0.1	0.0	0.0	0.0	-0.1	-0.1	-2.9
P3	2548	-0.1	-3.4	-0.2	-0.1	0.0	0.0	-0.1	-0.2	-3.4
P4	2549	0.0	-4.3	-0.5	-0.2	0.0	0.0	0.0	-0.5	-4.3
Q1	2554	0.0	-1.6	0.3	0.0	0.0	0.0	0.3	0.0	-1.6
Q2	2555	0.0	-1.6	0.3	0.0	0.0	0.0	0.3	0.0	-1.6
Q3	2556	0.0	-1.7	0.2	0.0	0.0	0.0	0.2	0.0	-1.7
Q4	2557	0.0	-1.8	0.2	0.0	0.0	0.0	0.2	0.0	-1.8
Q5	2558	0.0	-1.9	0.2	0.0	0.0	0.0	0.2	0.0	-1.9
R1	2771	0.0	-4.4	-0.3	0.0	0.0	0.0	0.0	-0.3	-4.4
R2	2772	0.1	-3.0	0.1	0.1	0.0	0.0	0.1	0.1	-3.0
R3	2773	0.3	-1.6	0.6	0.2	0.0	0.0	0.6	0.3	-1.6
R4	2774	0.4	0.2	1.1	0.3	0.0	0.0	1.1	0.7	-0.1
S1	2779	-1.7	-2.8	-0.5	0.3	0.0	0.0	-0.5	-1.6	-2.9
S2	2780	-1.1	-1.9	-0.1	0.0	0.0	0.0	-0.1	-1.1	-1.9
S3	2781	-0.6	-1.1	0.2	-0.2	0.0	0.0	0.2	-0.5	-1.2
S4	2782	-0.2	-0.4	0.5	-0.2	0.0	0.0	0.5	-0.1	-0.5
S5	2783	-0.1	0.5	0.8	-0.1	0.0	0.0	0.8	0.6	-0.1
T1	7066	2.1	1.8	0.9	0.5	0.0	0.0	2.4	1.5	0.9
T2	7067	1.3	0.6	0.4	0.2	0.0	0.0	1.4	0.6	0.4
T3	7068	0.9	-0.1	0.1	0.0	0.0	0.0	0.9	0.1	-0.1
T4	7069	0.5	-0.6	-0.1	-0.1	0.0	0.0	0.5	-0.1	-0.6
T5	7070	0.3	-1.0	-0.3	-0.1	0.0	0.0	0.3	-0.3	-1.0
T6	7071	0.1	-1.5	-0.4	-0.1	0.0	0.0	0.1	-0.4	-1.5
T7	7072	0.1	-2.1	-0.6	-0.1	0.0	0.0	0.1	-0.6	-2.1
U1	3051	-1.4	-2.3	1.3	0.3	0.0	0.0	1.3	-1.3	-2.3

Table 2.10.4-14 Stress Components – Impact; 30-Foot Bottom End Drop; Drop Orientation = 0 Degrees; 2-D Model; Condition 1 (continued)

Stress Points		Stress Components (ksi)						Principal Stresses (ksi)		
Section[1]	Node	S_x	S_y	S_z	S_{xy}	S_{yz}	S_{xz}	S1	S2	S3
U2	3052	0.1	-2.0	1.0	0.3	0.0	0.0	1.0	0.1	-2.0
U3	3053	0.4	-1.5	0.5	0.2	0.0	0.0	0.5	0.4	-1.5
U4	3054	0.6	-1.3	-0.1	0.1	0.0	0.0	0.6	-0.1	-1.3
U5	3055	0.9	-1.5	-0.8	0.2	0.0	0.0	0.9	-0.8	-1.6
U6	3056	0.2	-1.1	-1.5	0.8	0.0	0.0	0.6	-1.5	-1.5
V1	3611	-0.5	-0.1	1.5	-0.1	0.0	0.0	1.5	0.0	-0.5
V2	3612	-0.4	-0.1	1.0	-0.1	0.0	0.0	1.0	-0.1	-0.4
V3	3613	-0.2	-0.2	0.5	-0.1	0.0	0.0	0.5	0.0	-0.3
V4	3614	0.0	-0.2	0.0	-0.1	0.0	0.0	0.0	0.0	-0.2
V5	3615	0.1	-0.1	-0.5	-0.1	0.0	0.0	0.1	-0.1	-0.5
V6	3616	0.0	0.0	-1.1	-0.1	0.0	0.0	0.1	0.0	-1.1
V7	3617	0.5	0.0	-1.5	0.0	0.0	0.0	0.5	0.0	-1.5
W1	3241	6.0	0.0	6.0	0.0	0.0	0.0	6.0	6.0	0.0
W2	3242	3.8	0.0	3.8	0.0	0.0	0.0	3.8	3.8	0.0
W3	3243	1.7	0.0	1.7	0.0	0.0	0.0	1.7	1.7	0.0
W4	3244	-0.4	0.0	-0.4	0.0	0.0	0.0	0.0	-0.4	-0.4
W5	3245	-2.5	0.0	-2.5	0.0	0.0	0.0	0.0	-2.5	-2.5
W6	3246	-4.7	0.0	-4.7	0.0	0.0	0.0	0.0	-4.7	-4.7
X1	3801	4.9	-0.1	4.9	0.0	0.0	0.0	4.9	4.9	-0.1
X2	3802	3.3	-0.1	3.3	0.0	0.0	0.0	3.3	3.3	-0.1
X3	3803	1.7	0.0	1.7	0.0	0.0	0.0	1.7	1.7	0.0
X4	3804	0.1	0.0	0.1	0.0	0.0	0.0	0.1	0.1	0.0
X5	3805	-1.5	0.0	-1.5	0.0	0.0	0.0	0.0	-1.5	-1.5
X6	3806	-3.2	0.1	-3.2	0.0	0.0	0.0	0.1	-3.2	-3.2
X7	3807	-4.9	0.1	-4.9	0.0	0.0	0.0	0.1	-4.9	-4.9

[1] Refer to Figure 2.10.2-34 for the identification of the representative sections.

Table 2.10.4-15 Stress Components – Impact; 30-Foot Side Drop; Drop Orientation = 90 Degrees; 3-D Model; 0-Degree Circumferential Location; Condition 1

Condition 1: 100°F Ambient with Contents

Stress Points		Stress Components (ksi)						Principal Stresses (ksi)		
Section[1]	Node	S_x	S_y	S_z	S_{xy}	S_{yz}	S_{xz}	S1	S2	S3
A1	1130	-0.9	-2.0	-0.3	-0.1	0.1	0.0	-0.3	-0.9	-2.0
A2	1129	-1.1	-3.2	0.0	-0.1	0.1	0.0	0.0	-1.1	-3.2
A3	1128	-1.3	-4.4	0.2	0.0	0.1	0.0	0.2	-1.3	-4.4
B1	1185	-1.1	-5.3	0.0	-0.1	0.0	-0.2	0.0	-1.1	-5.3
B2	1184	-0.3	-6.0	0.0	-0.1	0.0	-0.2	0.1	-0.4	-6.0
B3	1183	0.5	-6.7	0.0	-0.1	0.1	-0.2	0.5	-0.1	-6.7
C1	90	5.6	-2.8	14.7	0.0	-0.8	1.4	14.9	5.4	-2.8
C2	80	-2.4	-7.2	6.3	-0.1	-0.5	0.0	6.3	-2.4	-7.2
C3	70	-3.6	-8.7	2.0	0.1	-0.4	-0.8	2.1	-3.7	-8.7
C4	60	-4.7	-9.5	0.2	0.2	-0.2	-0.5	0.3	-4.7	-9.6
C5	50	-9.8	-11.5	-0.1	0.2	-0.1	0.0	-0.1	-9.8	-11.6
C6	40	-12.0	-12.5	-0.1	0.2	0.0	0.0	-0.1	-11.9	-12.5
D1	25	-4.9	-9.6	5.4	0.3	-0.1	0.1	5.4	-4.9	-9.6
D2	15	-9.7	-11.3	1.8	0.1	-0.1	-0.5	1.8	-9.8	-11.3
D3	5	-10.8	-11.6	0.4	0.2	0.0	-0.4	0.4	-10.8	-11.6
E1	35	-10.7	-11.5	4.6	0.2	-0.1	1.6	4.8	-10.8	-11.6
E2	34	-7.6	-11.5	2.1	0.3	0.0	1.8	2.4	-7.9	-11.5
E3	33	-8.0	-12.4	-0.3	0.3	0.0	1.6	0.0	-8.3	-12.4
E4	32	-8.6	-13.3	-2.7	0.4	0.0	0.9	-2.6	-8.7	-13.4
E5	31	-8.8	-14.2	-5.2	0.4	0.0	0.5	-5.1	-8.8	-14.2
F1	100	-1.2	-2.7	22.2	0.0	-1.2	2.2	22.5	-1.4	-2.8
F2	99	-1.5	-8.3	1.9	0.4	-0.9	2.4	3.2	-2.6	-8.5
F3	98	-0.5	-11.5	-11.1	0.8	-0.7	3.2	0.4	-10.9	-12.6
F4	97	0.6	-17.8	-36.4	1.3	-0.7	3.8	1.0	-17.9	-36.8
G1	94	0.8	-2.2	21.7	0.2	-0.5	3.3	22.2	0.3	-2.3
G2	93	1.5	-6.0	7.2	0.5	-0.3	2.5	8.2	0.6	-6.0
G3	92	1.5	-7.1	2.5	0.6	-0.3	1.0	3.2	0.9	-7.2
G4	91	0.7	-8.7	-3.1	0.7	-0.2	0.4	0.8	-3.1	-8.8
H1	330	-0.2	6.2	-4.5	-0.4	-1.6	0.1	6.5	-0.3	-4.8
H2	329	-0.1	8.0	-0.9	-0.5	-1.6	0.0	8.3	-0.1	-1.2

Table 2.10.4-15 Stress Components – Impact; 30-Foot Side Drop; Drop Orientation = 90 Degrees; 3-D Model; 0-Degree Circumferential Location; Condition 1 (continued)

Stress Points		Stress Components (ksi)						Principal Stresses (ksi)		
Section[1]	Node	S_x	S_y	S_z	S_{xy}	S_{yz}	S_{xz}	S1	S2	S3
H3	328	0.1	9.7	2.6	-0.6	-1.5	-0.1	10.0	2.3	0.0
H4	327	0.2	11.6	6.9	-0.7	-1.4	-0.5	12.0	6.6	0.1
I1	244	-0.2	-0.4	4.9	0.0	-0.8	0.0	5.0	-0.2	-0.5
I2	243	-0.1	1.2	7.5	-0.1	-0.7	0.0	7.6	1.2	-0.1
I3	242	-0.1	2.8	10.1	-0.2	-0.5	0.0	10.1	2.8	-0.1
I4	241	0.0	4.2	12.7	-0.3	-0.4	0.0	12.7	4.3	0.0
J1	550	-0.3	6.7	10.7	-0.5	-0.8	0.0	10.8	6.6	-0.3
J2	548	-0.2	9.2	12.6	-0.7	-0.8	0.0	12.8	9.1	-0.2
J3	547	-0.1	11.6	14.4	-0.9	-0.7	0.0	14.6	11.4	-0.1
K1	344	-0.1	-1.2	11.3	0.0	-0.5	0.0	11.3	-0.1	-1.2
K2	342	-0.1	2.5	13.1	-0.2	-0.4	0.0	13.1	2.5	-0.1
K3	341	0.0	6.0	14.8	-0.5	-0.3	0.0	14.8	6.0	-0.1
L1	740	-0.1	3.8	16.6	0.3	0.0	-0.2	16.6	3.8	-0.1
L2	738	-0.6	6.6	18.2	-1.1	0.0	0.0	18.2	6.8	-0.7
L3	737	0.2	9.6	19.9	-2.5	0.0	0.0	19.9	10.2	-0.4
M1	663	-1.3	-2.6	14.1	0.1	0.0	0.0	14.1	-1.3	-2.6
M2	63	0.5	9.3	19.4	2.2	0.0	0.0	19.4	9.8	0.0
N1	1877	-0.3	6.2	8.7	-0.5	1.0	0.0	9.1	5.9	-0.3
N1	1877	-0.3	6.2	8.7	-0.5	1.0	0.0	9.1	5.9	-0.3
N2	1477	-0.2	9.2	10.6	-0.7	0.9	0.0	11.1	8.7	-0.2
N3	1277	-0.1	12.0	12.4	-0.9	0.9	0.0	13.1	11.3	-0.1
O1	647	-0.1	-1.7	12.9	0.1	0.4	0.0	12.9	-0.1	-1.7
O2	247	-0.1	2.4	14.9	-0.2	0.3	0.0	14.9	2.4	-0.1
O3	47	0.0	6.1	16.8	-0.5	0.2	0.0	16.8	6.2	-0.1
P1	1840	-0.3	6.5	-4.5	-0.5	1.7	0.0	6.8	-0.3	-4.7
P2	1640	-0.1	8.5	-1.6	-0.6	1.6	0.0	8.7	-0.2	-1.9
P3	1440	0.0	10.4	1.2	-0.7	1.5	0.1	10.6	1.0	-0.1
P4	1240	0.1	12.4	4.5	-0.8	1.5	0.3	12.7	4.3	0.0
Q1	628	-0.3	0.5	8.8	-0.1	0.6	0.1	8.8	0.5	-0.3
Q2	428	-0.2	2.4	11.0	-0.2	0.5	0.1	11.1	2.4	-0.2
Q3	228	-0.1	4.3	13.3	-0.3	0.4	0.1	13.3	4.3	-0.1
Q4	28	0.0	6.0	15.5	-0.4	0.3	0.1	15.5	6.1	-0.1
R1	1816	-0.9	-8.3	3.0	0.6	1.2	-0.2	3.1	-0.9	-8.4

Table 2.10.4-15 Stress Components – Impact; 30-Foot Side Drop; Drop Orientation = 90 Degrees; 3-D Model; 0-Degree Circumferential Location; Condition 1 (continued)

Stress Points		Stress Components (ksi)						Principal Stresses (ksi)		
Section[1]	Node	S_x	S_y	S_z	S_{xy}	S_{yz}	S_{zx}	S1	S2	S3
R2	1616	-1.8	-9.5	-2.6	0.7	1.0	-0.6	-1.5	-2.7	-9.7
R3	1416	-4.1	-10.8	-7.4	0.8	0.7	-2.0	-3.2	-8.0	-11.2
R4	1216	-5.5	-12.4	-14.5	0.8	0.4	-3.8	-4.0	-12.4	-16.0
S1	616	1.3	-4.9	0.6	0.1	0.6	-0.1	1.3	0.7	-4.9
S2	416	-0.2	-3.4	6.5	0.1	0.5	-0.2	6.6	-0.3	-3.5
S3	216	0.1	-1.6	11.8	0.1	0.3	0.2	11.8	0.1	-1.6
S4	16	0.1	0.2	17.0	0.0	0.2	0.1	17.0	0.2	0.1
T1	811	-16.0	-21.2	-18.8	1.1	0.5	-6.0	-11.2	-20.8	-24.0
T2	611	-8.9	-14.6	-4.4	0.7	0.4	-4.4	-1.7	-11.4	-14.8
T3	411	-4.1	-11.0	2.8	0.6	0.3	-3.4	4.2	-5.4	-11.0
T4	211	-0.9	-8.0	9.3	0.5	0.2	-1.9	9.7	-1.2	-8.0
T5	11	0.3	-4.7	19.0	0.3	0.1	-1.0	19.1	0.3	-4.8
U1	43058	3.9	-0.7	-0.1	0.2	0.0	0.1	3.9	-0.1	-0.7
U2	43057	2.2	-1.4	-0.2	0.1	0.0	0.1	2.2	-0.2	-1.4
U3	43056	0.8	-2.1	-0.6	0.1	0.0	-0.1	0.8	-0.6	-2.1
U4	43055	-0.5	-2.8	-1.0	0.1	0.0	-0.5	-0.1	-1.3	-2.8
U5	43054	-2.1	-3.6	-1.4	0.1	-0.1	-1.2	-0.5	-3.0	-3.6
U6	43053	-3.6	-4.5	-1.9	0.1	-0.2	-2.4	-0.2	-4.5	-5.3
U7	43052	-6.2	-5.2	-0.9	0.0	-0.2	-3.1	0.5	-5.2	-7.6
U8	43051	-13.6	-7.5	0.2	-0.2	0.0	0.0	0.2	-7.5	-13.6
V1	50024	1.5	-1.8	0.2	0.1	0.0	-0.1	1.5	0.2	-1.8
V2	50023	-4.0	-4.2	-0.3	0.1	0.0	0.0	-0.3	-4.0	-4.3
V3	50022	-6.7	-5.7	-0.4	0.1	0.0	0.0	-0.4	-5.7	-6.7
V4	50021	-15.8	-9.0	0.0	-0.1	0.0	-0.1	0.0	-9.0	-15.8
W1	43278	-2.2	-3.1	0.1	-0.1	-0.1	0.2	0.1	-2.2	-3.1
W2	43274	-1.5	-3.4	0.0	0.0	-0.2	0.2	0.0	-1.5	-3.4
W3	43271	-0.4	-1.9	0.0	0.0	-0.2	0.1	0.0	-0.4	-1.9
X1	50084	-1.0	-5.6	0.1	-0.1	0.0	0.3	0.1	-1.0	-5.6
X2	50083	-0.4	-5.8	0.0	-0.1	0.0	0.3	0.2	-0.6	-5.8
X3	50081	0.7	-6.4	-0.1	0.0	-0.1	0.3	0.7	-0.2	-6.4

[1] Refer to Figure 2.10.2-34 for the identification of the representative sections.

Table 2.10.4-16 Stress Components – Impact; 30-Foot Top Corner Drop; Drop Orientation = 24 Degrees; 3-D Top Model; 0-Degree Circumferential Location; Condition 1

Condition 1: 100°F Ambient with Contents

Stress Points		Stress Components (ksi)						Principal Stresses (ksi)		
Section[1]	Node	S_x	S_y	S_z	S_{xy}	S_{yz}	S_{xz}	S1	S2	S3
A1	1949	2.2	3.2	-0.4	0.0	-0.1	0.4	3.2	2.2	-0.4
A2	1950	1.2	2.0	-0.3	0.0	-0.1	0.4	2.0	1.3	-0.4
A3	1951	-0.4	-0.4	0.5	0.0	0.1	0.2	0.6	-0.4	-0.5
B1	1952	0.1	0.0	-0.6	0.0	0.0	0.2	0.1	0.0	-0.7
B2	93	-2.0	-2.9	1.2	-0.1	-0.1	0.4	1.3	-2.1	-3.0
C1	1925	-0.4	-0.1	0.7	-0.1	-0.1	0.0	0.7	-0.1	-0.4
C2	1926	0.2	-0.3	-0.2	0.0	-0.1	-0.3	0.4	-0.2	-0.4
C3	1927	0.7	-0.2	-0.2	0.1	0.0	-0.2	0.7	-0.2	-0.2
D1	683	-0.3	-0.6	-0.6	0.1	0.0	0.0	-0.3	-0.6	-0.6
D2	85	0.0	-1.1	-0.5	0.2	0.0	0.0	0.0	-0.5	-1.1
E1	682	0.6	-0.3	-0.6	0.1	0.0	0.2	0.6	-0.3	-0.6
E2	82	0.5	-0.1	0.5	0.1	0.1	0.1	0.7	0.4	-0.1
F1	1925	-0.4	-0.1	0.7	-0.1	-0.1	0.0	0.7	-0.1	-0.4
F2	1325	-1.3	-2.0	-5.2	0.1	-0.1	0.4	-1.3	-1.9	-5.2
G1	680	-0.4	0.0	1.0	0.0	0.0	0.6	1.2	0.0	-0.6
G2	80	0.2	0.0	-0.1	0.0	0.0	0.0	0.2	0.0	-0.1
H1	1921	0.0	2.5	-3.9	-0.1	-0.4	0.1	2.5	0.0	-3.9
H2	1321	-0.1	4.2	-1.8	-0.2	-0.3	0.0	4.2	-0.1	-1.8
I1	676	0.0	-0.2	-0.2	0.0	-0.1	0.0	0.0	-0.1	-0.3
I2	76	0.0	1.4	1.0	-0.1	0.0	0.0	1.4	1.0	0.0
J1	1916	-0.1	2.1	-1.8	-0.1	-0.2	0.0	2.1	-0.1	-1.8
J2	1316	-0.1	5.3	-0.3	-0.4	-0.1	0.0	5.3	-0.1	-0.3
K1	671	0.0	-0.6	-1.0	0.0	0.0	0.0	0.0	-0.6	-1.0
K2	71	0.0	2.1	0.4	-0.2	0.1	0.0	2.1	0.4	0.0
L1	1908	-0.7	0.5	-4.4	-0.1	0.3	0.0	0.5	-0.7	-4.4
L2	1308	0.1	6.9	-2.1	1.8	0.3	0.0	7.4	-0.3	-2.1
M1	663	-0.4	-0.8	-3.2	0.0	0.2	0.0	-0.4	-0.8	-3.2
M2	63	0.2	2.6	-1.9	0.6	0.2	0.0	2.8	0.0	-1.9

Table 2.10.4-16 Stress Components – Impact; 30-Foot Top Corner Drop; Drop Orientation = 24 Degrees; 3-D Top Model; 0-Degree Circumferential Location; Condition 1 (continued)

Stress Points		Stress Components (ksi)						Principal Stresses (ksi)		
Section[1]	Node	S_x	S_y	S_z	S_{xy}	S_{yz}	S_{zx}	S1	S2	S3
N1	1877	-0.1	1.2	-12.8	-0.1	0.8	0.0	1.3	-0.1	-12.8
N2	1477	-0.1	3.7	-11.8	-0.3	0.7	0.0	3.8	-0.1	-11.8
N3	1277	0.0	6.1	-10.9	-0.5	0.6	0.0	6.1	-0.1	-10.9
O1	647	-0.1	-0.2	-6.5	0.0	0.3	0.0	-0.1	-0.2	-6.5
O2	247	0.0	1.0	-6.1	-0.1	0.2	0.0	1.1	0.0	-6.1
O3	47	0.0	2.2	-5.7	-0.2	0.2	0.0	2.3	0.0	-5.7
P1	1840	-0.3	2.8	-13.9	-0.2	1.0	0.1	2.9	-0.3	-14.0
P2	1640	-0.5	2.7	-16.9	-0.2	0.9	0.0	2.8	-0.5	-17.0
P3	1440	-0.5	2.7	-19.7	-0.2	0.8	-0.6	2.7	-0.5	-19.8
P4	1240	-0.5	1.9	-25.4	-0.1	0.7	-1.3	1.9	-0.5	-25.5
Q1	628	-0.2	2.9	-7.9	-0.2	0.4	0.1	2.9	-0.2	-8.0
Q2	428	-0.1	3.2	-8.3	-0.2	0.3	0.1	3.2	-0.1	-8.3
Q3	228	0.0	3.5	-8.7	-0.3	0.3	0.1	3.5	-0.1	-8.7
Q4	28	0.0	3.7	-9.0	-0.3	0.2	0.1	3.7	0.0	-9.0
R1	1816	0.1	-3.5	-30.8	0.3	0.6	0.0	0.1	-3.5	-30.8
R2	1616	0.3	-1.1	-22.7	0.2	0.6	0.1	0.3	-1.1	-22.7
R3	1416	0.2	1.0	-15.2	0.1	0.5	0.7	1.0	0.2	-15.3
R4	1216	7.2	4.9	-8.4	0.3	0.4	0.9	7.2	4.9	-8.4
S1	616	-8.8	-5.4	-30.7	-0.3	0.7	4.1	-5.4	-8.1	-31.5
S2	416	-8.8	-1.4	-14.7	-0.5	0.2	-0.7	-1.3	-8.8	-14.8
S3	216	-3.2	3.1	-3.3	-0.5	0.1	-1.2	3.1	-2.1	-4.4
S4	16	-1.2	7.1	10.0	-0.6	0.0	-0.9	10.1	7.1	-1.3
T1	811	0.2	-5.1	-4.5	0.7	0.5	0.7	0.4	-4.4	-5.4
T2	611	0.9	-5.5	-7.5	0.6	0.3	-0.2	1.0	-5.5	-7.6
T3	411	0.6	-5.4	-7.4	0.5	0.3	-0.3	0.7	-5.4	-7.4
T4	211	0.8	-5.1	-6.6	0.4	0.2	-0.3	0.8	-5.1	-6.7
T5	11	0.8	-4.6	-4.9	0.4	0.1	-0.2	0.8	-4.6	-5.0
U1	43058	0.5	8.1	-13.5	-0.8	0.6	3.0	8.2	1.0	-14.1
U2	43057	3.3	6.7	-12.1	-0.6	0.1	4.1	6.8	4.2	-13.1
U3	43056	2.7	4.6	-10.2	-0.3	0.4	5.4	4.8	4.4	-12.2

Table 2.10.4-16 Stress Components – Impact; 30-Foot Top Corner Drop; Drop Orientation = 24 Degrees; 3-D Top Model; 0-Degree Circumferential Location; Condition 1 (continued)

Stress Points		Stress Components (ksi)						Principal Stresses (ksi)		
Section[1]	Node	S_x	S_y	S_z	S_{xy}	S_{yz}	S_{xz}	S1	S2	S3
U4	43055	1.8	2.2	-9.4	-0.1	0.4	5.6	4.1	2.2	-11.8
U5	43054	0.8	-0.4	-9.3	0.1	0.4	5.4	3.1	-0.4	-11.7
U6	43053	-0.7	-2.6	-7.3	0.2	0.3	4.2	1.4	-2.6	-9.4
U7	43052	-1.0	-6.6	-13.0	0.5	0.2	4.3	0.5	-6.6	-14.3
U8	43051	-9.0	-13.2	-13.1	0.5	0.5	7.5	-3.2	-13.3	-18.9
V1	50024	-16.7	0.7	-5.9	-1.4	-0.2	-2.1	0.8	-5.5	-17.2
V2	50023	-11.0	-4.2	-5.8	-0.7	-0.2	-1.3	-4.2	-5.5	-11.4
V3	50022	-4.9	-9.2	-5.4	0.4	0.0	-0.1	-4.9	-5.4	-9.2
V4	50021	1.3	-14.3	-5.0	1.1	0.0	0.3	1.3	-5.0	-14.4
W1	43278	10.5	7.2	-3.9	-0.6	-1.3	-2.1	10.9	7.3	-4.4
W2	43274	1.7	-0.1	-1.2	-0.1	-1.3	-2.1	3.0	0.4	-2.8
W3	43271	-4.0	-4.2	-0.1	0.2	-1.7	-1.1	0.7	-4.2	-4.8
X1	50084	23.6	17.8	-8.5	-0.5	0.2	-5.3	24.5	17.7	-9.3
X2	50083	7.0	1.6	-6.0	-0.2	0.3	-5.4	9.0	1.6	-8.0
X3	50081	-23.8	-27.6	11.0	0.5	-0.1	-5.3	11.8	-24.5	-27.7

[1] Refer to Figure 2.10.2-34 for the identification of the representative sections.

Table 2.10.4-17 Stress Components – Impact; 30-Foot Bottom Corner Drop; Drop Orientation = 24 Degrees; 3-D Bottom Model; 0-Degree Circumferential Location; Condition 1

Condition 1: 100°F Ambient with Contents

Stress Points		Stress Components (ksi)						Principal Stresses (ksi)		
Section[1]	Node	S_x	S_y	S_z	S_{xy}	S_{yz}	S_{xz}	S1	S2	S3
A1	1130	18.0	13.9	-6.7	-0.5	2.0	2.1	18.2	14.1	-7.1
A2	1129	2.3	-0.1	-1.2	0.0	1.5	2.1	3.4	0.5	-2.8
A3	1128	-13.5	-14.1	4.4	0.5	2.0	2.1	4.8	-13.7	-14.4
B1	1185	10.5	3.7	-6.6	-0.5	2.4	2.3	10.8	4.3	-7.5
B2	1184	-3.7	-7.9	-1.9	0.0	1.8	2.3	0.0	-5.0	-8.5
B3	1183	-18.1	-19.4	2.9	0.4	1.9	2.3	3.3	-18.4	-19.5
C1	90	-20.6	-6.2	-26.3	-1.3	-0.8	-5.4	-6.1	-17.4	-29.6
C2	80	-9.1	-1.7	-15.1	-1.0	-0.5	-4.3	-1.6	-6.9	-17.4
C3	70	-5.8	-1.2	-9.4	-0.5	-0.4	-3.8	-1.1	-3.4	-11.9
C4	60	-3.0	-1.2	-5.6	-0.1	-0.4	-3.7	-0.3	-1.2	-8.2
C5	50	6.9	-4.1	-3.6	1.0	-0.2	-2.5	7.5	-4.2	-4.2
C6	40	14.3	-5.4	-3.6	1.7	-0.1	-1.5	14.5	-3.7	-5.6
D1	25	-30.8	-23.1	-32.0	-0.4	-0.7	-8.5	-22.8	-23.2	-39.9
D2	15	-6.7	-18.6	-14.9	0.6	-0.3	-3.8	-5.2	-16.4	-18.6
D3	5	0.7	-22.4	-7.5	1.4	-0.1	-1.2	0.9	-7.7	-22.5
E1	35	11.0	-8.2	-21.9	1.3	-0.4	-3.9	11.5	-8.3	-22.3
E2	34	2.0	-8.9	-17.6	0.7	-0.8	-7.5	4.6	-8.9	-20.1
E3	33	-5.1	-9.1	-11.2	0.3	-0.7	-7.9	0.4	-9.1	-16.6
E4	32	-6.7	-8.4	-6.8	0.1	-0.4	-4.9	-1.8	-8.4	-11.6
E5	31	-7.2	-7.6	-2.6	0.0	-0.3	-2.9	-1.1	-7.6	-8.7
F1	100	0.0	-2.5	-34.8	-0.1	-0.9	-3.4	0.3	-2.5	-35.1
F2	99	-2.8	0.9	-19.5	-0.4	-0.8	-1.7	1.0	-2.7	-19.7
F3	98	-2.8	2.5	-13.4	-0.5	-0.4	0.9	2.5	-2.8	-13.5
F4	97	0.1	5.0	-6.8	-0.5	-0.4	1.9	5.1	0.5	-7.3
G1	94	0.3	-2.6	-24.6	0.1	-0.4	-1.2	0.4	-2.6	-24.7
G2	93	-0.7	-0.2	-15.0	-0.1	-0.4	-0.6	-0.2	-0.7	-15.0
G3	92	-1.1	1.4	-8.4	-0.2	-0.2	0.1	1.4	-1.1	-8.4
G4	91	-0.5	3.6	-0.5	-0.3	-0.1	0.1	3.6	-0.4	-0.7
H1	330	-0.3	3.0	-13.1	-0.2	-1.0	-0.1	3.1	-0.3	-13.2
H2	329	-0.4	2.8	-16.3	-0.2	-0.9	0.0	2.8	-0.5	-16.4

Table 2.10.4-17 Stress Components – Impact; 30-Foot Bottom Corner Drop; Drop Orientation = 24 Degrees; 3-D Bottom Model; 0-Degree Circumferential Location; Condition 1 (continued)

Stress Points		Stress Components (ksi)						Principal Stresses (ksi)		
Section[1]	Node	Sx	S_y	S_z	S_{xy}	S_{yz}	S_{xz}	S1	S2	S3
H3	328	-0.5	2.6	-19.3	-0.2	-0.8	0.6	2.7	-0.5	-19.4
H4	327	-0.5	1.7	-25.2	-0.1	-0.7	1.3	1.8	-0.5	-25.3
I1	244	0.0	1.9	-10.2	-0.1	-0.4	-0.1	1.9	0.0	-10.2
I2	243	0.0	2.3	-10.1	-0.2	-0.4	-0.1	2.4	0.0	-10.2
I3	242	0.0	2.8	-10.0	-0.2	-0.3	-0.1	2.8	0.0	-10.0
I4	241	0.0	3.2	-10.0	-0.2	-0.2	-0.1	3.2	0.0	-10.0
J1	550	-0.1	1.2	-11.2	-0.1	-0.7	0.0	1.3	-0.1	-11.2
J2	548	-0.1	3.7	-10.3	-0.3	-0.6	0.0	3.7	-0.1	-10.3
J3	547	0.0	6.0	-9.4	-0.5	-0.6	0.0	6.1	-0.1	-9.4
K1	344	-0.1	-0.3	-7.7	0.0	-0.3	0.0	-0.1	-0.3	-7.7
K2	342	0.0	1.2	-7.1	-0.1	-0.3	0.0	1.2	0.0	-7.1
K3	341	0.0	2.6	-6.5	-0.2	-0.2	0.0	2.6	0.0	-6.5
L1	740	0.1	1.1	-3.3	0.5	-0.2	-0.1	1.3	-0.1	-3.3
L2	738	-0.3	3.5	-2.4	-0.8	-0.2	0.0	3.7	-0.5	-2.4
L3	737	0.3	6.1	-1.2	-2.0	-0.2	0.0	6.7	-0.3	-1.3
M1	454	-0.1	-0.8	-3.9	-0.6	-0.2	0.0	0.3	-1.2	-3.9
M2	452	0.2	1.0	-3.2	-0.3	-0.2	0.0	1.1	0.1	-3.2
M3	451	-0.2	2.4	-2.8	0.0	-0.2	-0.1	2.4	-0.2	-2.8
N1	810	-0.1	2.2	-1.9	-0.1	0.2	0.0	2.2	-0.1	-1.9
N2	807	-0.1	5.2	-0.5	-0.3	0.1	0.0	5.2	-0.1	-0.5
O1	524	0.0	-0.6	-1.3	0.0	-0.1	0.0	0.0	-0.6	-1.3
O2	521	0.0	2.0	0.0	-0.1	-0.1	0.0	2.0	0.0	0.0
P1	850	0.0	2.4	-4.1	-0.1	0.4	-0.1	2.4	0.0	-4.1
P2	847	-0.1	4.2	-1.9	-0.2	0.3	0.0	4.2	-0.1	-1.9
Q1	564	0.0	-0.1	-0.3	0.0	0.0	0.0	0.0	-0.1	-0.3
Q2	561	0.0	1.5	0.6	-0.1	0.0	0.0	1.5	0.6	0.0
R1	890	-0.8	-0.4	0.6	0.0	0.2	-0.2	0.6	-0.4	-0.8
R2	887	-1.0	-1.6	-5.0	0.1	0.1	-0.4	-0.9	-1.6	-5.1
S1	604	-0.3	0.4	0.3	0.0	0.0	-0.3	0.5	0.4	-0.5
S2	601	0.1	0.7	0.5	-0.1	0.0	-0.1	0.7	0.5	0.0
T1	897	0.3	-0.3	-1.7	0.0	0.1	-0.2	0.4	-0.3	-1.7

Table 2.10.4-17 Stress Components – Impact; 30-Foot Bottom Corner Drop; Drop Orientation = 24 Degrees; 3-D Bottom Model; 0-Degree Circumferential Location; Condition 1 (continued)

Stress Points		Stress Components (ksi)						Principal Stresses (ksi)		
Section[1]	Node	Sx	S_y	S_z	S_{xy}	S_{yz}	S_{zx}	S1	S2	S3
T2	614	0.2	0.3	0.0	0.0	0.0	-0.4	0.4	0.3	-0.3
T3	611	-0.1	0.1	0.1	0.0	-0.1	-0.2	0.3	0.1	-0.3
U1	900	0.4	-0.1	-0.8	0.0	0.1	0.2	0.5	-0.1	-0.8
U2	910	0.7	-0.2	-0.5	0.1	0.0	0.2	0.7	-0.2	-0.5
V1	920	-0.4	-0.4	-0.4	0.1	0.0	0.2	-0.2	-0.5	-0.6
V2	930	-0.3	-1.1	-0.2	0.2	0.0	0.1	-0.1	-0.4	-1.1
W1	1216	1.5	2.6	-1.2	0.0	0.0	-0.3	2.6	1.5	-1.2
W2	1226	-0.3	-0.1	0.6	0.0	-0.1	-0.1	0.6	-0.1	-0.3
X1	1236	0.1	0.1	-0.7	0.0	-0.1	-0.1	0.2	0.1	-0.7
X2	1246	-1.8	-2.8	1.4	-0.1	0.0	-0.3	1.4	-1.9	-2.8

[1] Refer to Figure 2.10.2-34 for the identification of the representative sections.

Table 2.10.4-18 Stress Components – Impact; 30-Foot Bottom Oblique Drop; Drop Orientation = 15 Degrees; 3-D Bottom Model; 0-Degree Circumferential Location; Condition 1

Condition 1: 100°F Ambient with Contents

Stress Points		Stress Components (ksi)						Principal Stresses (ksi)		
Section[1]	Node	S_x	S_y	S_z	S_{xy}	S_{yz}	S_{xz}	S1	S2	S3
A1	1130	19.2	15.7	-7.0	-0.5	2.2	2.3	19.5	15.9	-7.4
A2	1129	2.6	1.1	-1.2	0.0	1.6	2.3	3.8	1.5	-2.8
A3	1128	-14.1	-13.4	4.6	0.5	2.1	2.3	5.1	-13.6	-14.4
B1	1185	11.3	5.2	-6.9	-0.6	2.6	2.5	11.6	5.8	-7.8
B2	1184	-3.7	-6.7	-2.0	-0.1	1.9	2.5	0.1	-4.9	-7.7
B3	1183	-19.0	-18.7	3.0	0.4	2.0	2.5	3.5	-18.8	-19.3
C1	90	-22.2	-5.3	-31.5	-1.4	-0.7	-6.0	-5.2	-19.4	-34.5
C2	80	-8.2	0.4	-17.5	-1.0	-0.5	-4.6	0.6	-6.4	-19.5
C3	70	-4.6	1.3	-10.5	-0.6	-0.4	-4.0	1.3	-2.6	-12.6
C4	60	-1.5	1.4	-6.1	-0.1	-0.4	-3.9	1.4	0.7	-8.4
C5	50	9.6	-1.6	-4.1	1.0	-0.2	-2.7	10.2	-1.7	-4.6
C6	40	17.6	-3.1	-4.3	1.8	-0.1	-1.6	17.9	-3.3	-4.4
D1	25	-28.5	-21.0	-33.9	-0.3	-0.7	-8.4	-21.0	-22.4	-40.1
D2	15	-3.9	-16.6	-15.6	0.7	-0.3	-3.8	-2.8	-16.6	-16.8
D3	5	3.1	-21.1	-7.8	1.6	-0.1	-1.2	3.3	-8.0	-21.2
E1	35	13.7	-5.8	-23.9	1.4	-0.4	-4.1	14.3	-5.9	-24.4
E2	34	4.0	-6.4	-18.5	0.7	-0.8	-7.8	6.4	-6.4	-21.0
E3	33	-2.9	-6.3	-11.3	0.2	-0.8	-8.1	2.1	-6.3	-16.3
E4	32	-4.2	-5.3	-6.1	0.1	-0.4	-5.0	0.0	-5.3	-10.3
E5	31	-4.6	-4.1	-1.1	0.0	-0.3	-3.0	0.7	-4.1	-6.4
F1	100	0.2	-1.7	-42.5	-0.1	-0.8	-4.1	0.6	-1.7	-42.9
F2	99	-2.6	3.4	-21.1	-0.6	-0.7	-2.4	3.4	-2.3	-21.5
F3	98	-2.8	5.8	-11.4	-0.7	-0.4	0.1	5.9	-2.9	-11.4
F4	97	-0.1	10.1	2.1	-0.8	-0.3	1.0	10.2	2.5	-0.5
G1	94	0.1	-1.9	-31.3	0.0	-0.4	-2.2	0.2	-1.9	-31.4
G2	93	-1.1	1.6	-17.1	-0.3	-0.4	-1.3	1.7	-1.0	-17.2
G3	92	-1.5	3.6	-9.0	-0.4	-0.2	-0.2	3.7	-1.6	-9.0
G4	91	-0.7	6.4	0.8	-0.5	-0.1	0.0	6.5	0.8	-0.8
H1	330	-0.2	2.3	-12.5	-0.2	-0.7	-0.1	2.3	-0.2	-12.5
H2	329	-0.4	1.6	-16.6	-0.1	-0.7	0.0	1.7	-0.5	-16.6

Table 2.10.4-18 Stress Components – Impact; 30-Foot Bottom Oblique Drop; Drop Orientation = 15 Degrees; 3-D Bottom Model; 0-Degree Circumferential Location; Condition 1 (continued)

Stress Points		Stress Components (ksi)						Principal Stresses (ksi)		
Section[1]	Node	S_x	S_y	S_z	S_{xy}	S_{yz}	S_{xz}	S1	S2	S3
H3	328	-0.6	1.1	-20.5	-0.1	-0.6	0.6	1.1	-0.6	-20.5
H4	327	-0.6	-0.2	-27.5	0.0	-0.5	1.5	-0.2	-0.5	-27.5
I1	244	0.0	2.1	-11.3	-0.1	-0.3	-0.1	2.1	0.0	-11.3
I2	243	0.0	2.3	-11.9	-0.2	-0.3	-0.1	2.3	0.0	-11.9
I3	242	0.0	2.5	-12.4	-0.2	-0.2	-0.1	2.6	0.0	-12.4
I4	241	0.0	2.7	-12.9	-0.2	-0.2	-0.1	2.8	0.0	-12.9
J1	550	-0.1	0.6	-13.6	-0.1	-0.5	0.0	0.7	-0.1	-13.6
J2	548	0.0	2.3	-13.1	-0.2	-0.5	0.0	2.4	-0.1	-13.1
J3	547	0.0	4.0	-12.6	-0.3	-0.5	0.0	4.0	0.0	-12.6
K1	344	0.0	-0.4	-9.9	0.0	-0.2	0.0	0.0	-0.4	-9.9
K2	342	0.0	0.7	-9.6	-0.1	-0.2	0.0	0.7	0.0	-9.6
K3	341	0.0	1.8	-9.3	-0.1	-0.2	0.0	1.8	0.0	-9.3
L1	740	0.1	0.8	-6.7	0.3	-0.2	0.0	0.9	0.0	-6.7
L2	738	-0.2	2.2	-6.2	-0.5	-0.2	0.0	2.3	-0.3	-6.2
L3	737	0.2	3.8	-5.6	-1.2	-0.2	0.0	4.2	-0.2	-5.6
M1	454	-0.1	-0.7	-6.4	-0.4	-0.2	0.0	0.1	-0.9	-6.4
M2	452	0.1	0.5	-6.0	-0.2	-0.2	0.0	0.6	0.0	-6.0
M3	451	-0.2	1.5	-5.8	0.0	-0.2	0.0	1.5	-0.2	-5.8
N1	810	0.0	1.6	-3.8	-0.1	0.0	0.0	1.6	-0.1	-3.8
N2	807	-0.1	3.1	-3.1	-0.2	0.0	0.0	3.2	-0.1	-3.1
O1	524	0.0	-0.7	-3.5	0.0	-0.1	0.0	0.0	-0.7	-3.5
O2	521	0.0	1.3	-2.6	-0.1	-0.1	0.0	1.3	0.0	-2.6
P1	850	0.0	1.6	-3.9	-0.1	0.2	-0.1	1.6	0.0	-3.9
P2	847	0.0	2.4	-3.0	-0.1	0.1	0.0	2.4	0.0	-3.0
Q1	564	0.0	0.1	-1.6	0.0	-0.1	0.0	0.1	0.0	-1.6
Q2	561	0.0	0.7	-2.0	0.0	-0.1	0.0	0.7	0.0	-2.0
R1	890	-0.2	0.4	-1.2	0.0	0.1	0.0	0.4	-0.2	-1.2
R2	887	-0.4	0.0	-3.1	0.0	0.0	-0.1	0.0	-0.4	-3.1
S1	604	-0.4	0.7	-1.5	0.0	-0.1	-0.1	0.7	-0.4	-1.5
S2	601	-0.1	1.4	0.4	-0.1	-0.1	0.0	1.4	0.4	-0.1
T1	897	-0.2	0.4	-1.3	0.0	0.0	0.0	0.4	-0.2	-1.3
T2	614	0.0	0.7	-0.6	0.0	-0.1	-0.1	0.7	0.0	-0.6

Table 2.10.4-18 Stress Components – Impact; 30-Foot Bottom Oblique Drop; Drop Orientation = 15 Degrees; 3-D Bottom Model; 0-Degree Circumferential Location; Condition 1 (continued)

Stress Points		Stress Components (ksi)						Principal Stresses (ksi)		
Section[1]	Node	S_x	S_y	S_z	S_{xy}	S_{yz}	S_{zx}	S1	S2	S3
T3	611	0.0	0.6	-0.2	0.0	-0.1	-0.1	0.6	0.0	-0.3
U1	900	-0.5	0.4	-1.2	0.0	0.0	0.2	0.4	-0.4	-1.2
U2	910	1.2	0.3	-0.5	0.0	0.0	0.4	1.2	0.3	-0.6
V1	920	-1.0	-0.3	-0.5	0.0	0.0	0.4	-0.3	-0.3	-1.2
V2	930	0.4	-0.5	-0.4	0.1	0.0	0.2	0.4	-0.4	-0.5
W1	1216	1.8	2.4	-1.2	0.0	0.1	-0.3	2.4	1.9	-1.2
W2	1226	-0.3	-0.2	0.6	0.0	0.0	-0.2	0.7	-0.2	-0.3
X1	1236	0.2	0.2	-0.7	0.0	0.0	-0.2	0.2	0.2	-0.7
X2	1246	-2.1	-2.4	1.4	0.0	0.1	-0.3	1.4	-2.1	-2.5

[1] Refer to Figure 2.10.2-34 for the identification of the representative sections.

Table 2.10.4-19 Stress Components – Impact; 30-Foot Top Oblique Drop; Drop Orientation = 75 Degrees; 3-D Top Model; 0-Degree Circumferential Location; Condition 1

Condition 1: 100°F Ambient with Contents

Stress Points		Stress Components (ksi)						Principal Stresses (ksi)		
Section[1]	Node	S_x	S_y	S_z	S_{xy}	S_{yz}	S_{xz}	S1	S2	S3
A1	1949	-0.5	2.2	-0.1	-0.2	0.0	-0.1	2.2	-0.1	-0.6
A2	1950	-0.6	1.5	-0.1	-0.2	0.2	-0.1	1.6	-0.1	-0.6
A3	1951	-0.3	-0.1	0.2	-0.1	0.5	0.0	0.6	-0.3	-0.5
B1	1952	0.0	-0.7	-0.2	-0.2	0.5	-0.1	0.2	-0.1	-1.0
B2	93	0.2	-3.4	0.5	-0.4	0.2	-0.1	0.5	0.2	-3.5
C1	1925	2.2	-2.4	6.8	0.1	-0.5	0.4	6.9	2.2	-2.4
C2	1926	2.3	-3.6	1.3	0.2	-0.2	-0.2	2.3	1.3	-3.6
C3	1927	-1.1	-2.2	0.2	0.1	-0.1	0.2	0.2	-1.2	-2.3
D1	683	2.3	-2.0	0.3	0.5	-0.1	0.8	2.6	0.0	-2.0
D2	85	-3.2	-4.1	0.8	0.8	-0.1	0.2	0.8	-2.7	-4.5
E1	682	-1.8	-3.2	0.0	0.2	-0.1	1.1	0.6	-2.3	-3.3
E2	82	-1.5	-3.6	2.6	0.3	0.2	1.3	3.0	-1.9	-3.6
F1	1925	2.2	-2.4	6.8	0.1	-0.5	0.4	6.9	2.2	-2.4
F2	1325	0.5	-8.3	-13.6	0.5	-0.4	1.0	0.7	-8.3	-13.7
G1	680	2.2	-1.3	9.9	0.1	-0.1	2.0	10.4	1.7	-1.3
G2	80	2.0	-4.4	-2.3	0.4	-0.3	-0.2	2.1	-2.2	-4.4
H1	1921	-0.1	6.2	-3.0	-0.3	-1.3	0.1	6.4	-0.1	-3.1
H2	1321	-0.2	10.9	5.9	-0.7	-1.1	-0.3	11.1	5.7	-0.3
I1	676	-0.1	-0.2	5.4	0.1	-0.6	0.0	5.5	-0.1	-0.3
I2	76	-0.1	3.8	11.0	-0.2	-0.4	0.0	11.0	3.8	-0.1
J1	1916	-0.2	6.4	9.2	-0.5	-0.6	0.0	9.4	6.3	-0.3
J2	1316	-0.2	11.4	13.1	-0.8	-0.6	0.0	13.2	11.3	-0.2
K1	671	-0.1	-1.2	9.8	0.1	-0.4	0.0	9.9	-0.1	-1.2
K2	71	-0.1	5.9	13.2	-0.4	-0.2	0.0	13.2	5.9	-0.1
L1	1908	-0.9	3.5	12.6	-0.3	0.2	0.0	12.6	3.5	-0.9
L2	1308	0.0	10.4	15.5	1.8	0.2	0.0	15.5	10.7	-0.3
M1	663	-1.2	-2.2	10.7	0.1	0.1	0.0	10.7	-1.2	-2.2
M2	63	0.4	8.8	15.7	2.0	0.1	0.0	15.7	9.3	0.0

Table 2.10.4-19 Stress Components – Impact; 30-Foot Top Oblique Drop; Drop Orientation = 75 Degrees; 3-D Top Model; 0-Degree Circumferential Location; Condition 1 (continued)

Stress Points		Stress Components (ksi)						Principal Stresses (ksi)		
Section[1]	Node	S_x	S_y	S_z	S_{xy}	S_{yz}	S_{xz}	S1	S2	S3
N1	1877	-0.3	6.1	3.9	-0.5	1.1	0.0	6.6	3.5	-0.3
N2	1477	-0.2	8.9	5.7	-0.7	1.0	0.0	9.2	5.4	-0.2
N3	1277	-0.1	11.5	7.4	-0.8	1.0	0.0	11.8	7.2	-0.1
O1	647	-0.1	-1.1	8.2	0.0	0.5	0.0	8.3	-0.1	-1.1
O2	247	-0.1	2.5	9.9	-0.2	0.4	0.0	9.9	2.5	-0.1
O3	47	0.0	5.7	11.4	-0.4	0.2	0.0	11.4	5.8	-0.1
P1	1840	-0.3	6.2	-9.5	-0.4	1.7	0.0	6.4	-0.3	-9.7
P2	1640	-0.2	7.9	-6.8	-0.5	1.6	0.0	8.1	-0.3	-7.0
P3	1440	-0.1	9.5	-4.2	-0.6	1.5	0.0	9.8	-0.1	-4.4
P4	1240	0.0	11.1	-1.8	-0.7	1.5	0.1	11.4	0.0	-2.0
Q1	628	-0.4	0.3	2.1	-0.1	0.7	0.1	2.4	0.1	-0.4
Q2	428	-0.3	2.2	5.0	-0.2	0.6	0.1	5.1	2.0	-0.3
Q3	228	-0.1	3.9	7.8	-0.3	0.5	0.1	7.8	3.9	-0.1
Q4	28	0.0	5.6	10.6	-0.4	0.4	0.0	10.6	5.6	-0.1
R1	1816	-0.9	-10.4	2.3	0.8	1.1	0.2	2.4	-0.8	-10.6
R2	1616	-1.7	-12.4	-5.2	0.9	1.0	-0.1	-1.6	-5.0	-12.6
R3	1416	-4.1	-14.5	-12.0	1.0	0.7	-2.1	-3.5	-12.2	-15.0
R4	1216	-4.5	-16.5	-20.5	1.2	0.4	-4.9	-3.0	-16.5	-22.0
S1	616	4.3	-7.6	-2.1	0.6	0.6	-0.8	4.5	-2.1	-7.7
S2	416	0.1	-7.8	1.3	0.5	0.4	-1.0	1.9	-0.4	-7.9
S3	216	0.4	-6.7	4.5	0.5	0.3	-0.2	4.5	0.4	-6.8
S4	16	0.2	-5.7	7.6	0.4	0.2	-0.1	7.6	0.2	-5.8
T1	811	-18.9	-24.8	-16.4	1.1	0.3	-6.7	-10.8	-23.6	-25.7
T2	611	-10.2	-18.9	-4.8	0.9	0.1	-6.4	-0.6	-14.3	-19.1
T3	411	-4.8	-16.6	-2.5	1.0	0.1	-5.6	2.1	-9.3	-16.7
T4	211	-0.5	-14.7	-0.7	1.0	0.1	-3.3	2.7	-3.8	-14.8
T5	11	1.0	-12.3	5.7	0.9	0.1	-1.7	6.2	0.5	-12.4
U1	43058	5.2	1.5	-0.2	0.1	0.1	0.0	5.2	1.5	-0.2
U2	43057	2.6	0.0	-0.3	0.0	-0.1	0.0	2.6	0.0	-0.3
U3	43056	0.4	-1.5	-0.5	0.0	0.0	-0.1	0.4	-0.5	-1.5

Table 2.10.4-19 Stress Components – Impact; 30-Foot Top Oblique Drop; Drop Orientation = 75 Degrees; 3-D Top Model; 0-Degree Circumferential Location; Condition 1 (continued)

Stress Points		Stress Components (ksi)						Principal Stresses (ksi)		
Section[1]	Node	S_x	S_y	S_z	S_{xy}	S_{yz}	S_{xz}	S1	S2	S3
U4	43055	-1.8	-3.0	-0.8	0.1	0.0	-0.4	-0.6	-2.0	-3.0
U5	43054	-4.1	-4.6	-1.3	0.1	-0.1	-1.0	-1.0	-4.4	-4.6
U6	43053	-6.1	-6.2	-1.8	0.1	-0.2	-2.1	-0.9	-6.2	-7.0
U7	43052	-8.7	-7.7	-1.5	0.0	-0.2	-2.5	-0.7	-7.7	-9.5
U8	43051	-16.8	-11.1	-0.2	-0.1	0.1	1.8	0.0	-11.1	-17.0
V1	50024	-19.9	-13.2	0.1	-1.1	0.0	0.6	0.2	-13.0	-20.1
V2	50023	-20.2	-15.6	-0.8	-0.8	0.1	1.5	-0.7	-15.5	-20.5
V3	50022	-13.2	-15.8	-1.4	-0.3	0.1	2.0	-1.1	-13.5	-15.8
V4	50021	-16.0	-18.6	-1.0	-0.2	0.1	1.6	-0.8	-16.2	-18.7
W1	43278	-0.9	-4.5	-0.2	-0.2	-0.3	0.2	-0.1	-0.9	-4.5
W2	43274	-0.6	-5.1	-0.1	-0.1	-0.3	0.2	0.0	-0.6	-5.1
W3	43271	-0.1	-2.9	0.0	0.0	-0.5	0.1	0.1	-0.1	-3.0
X1	50084	9.7	0.0	-2.7	-0.2	0.2	-2.4	10.2	0.0	-3.2
X2	50083	2.5	-7.5	-1.7	0.0	0.2	-2.4	3.6	-2.8	-7.5
X3	50081	-10.5	-20.7	5.4	0.4	-0.3	-2.4	5.7	-10.8	-20.7

[1] Refer to Figure 2.10.2-34 for the identification of the representative sections.

Table 2.10.4-20 Stress Components – Impact; 30-Foot Bottom Oblique Drop; Drop Orientation = 75 Degrees; 3-D Bottom Model; 0-Degree Circumferential Location; Condition 1

Condition 1: 100°F Ambient with Contents

Stress Points		Stress Components (ksi)						Principal Stresses (ksi)		
Section[1]	Node	S_x	S_y	S_z	S_{xy}	S_{yz}	S_{xz}	S1	S2	S3
A1	1130	4.3	-0.8	-2.2	-0.3	0.5	0.6	4.3	-0.6	-2.4
A2	1129	-0.3	-5.8	-0.4	-0.1	0.4	0.6	0.2	-0.9	-5.8
A3	1128	-4.9	-10.8	1.4	0.0	0.6	0.6	1.4	-4.9	-10.8
B1	1185	2.1	-5.4	-2.3	0.2	0.7	0.6	2.2	-2.3	-5.6
B2	1184	-2.1	-10.3	-0.5	0.3	0.4	0.6	-0.3	-2.3	-10.3
B3	1183	-6.3	-14.4	1.0	0.4	0.4	0.6	1.0	-6.3	-14.4
C1	90	-1.5	-7.1	10.9	-0.2	-0.8	0.3	10.9	-1.5	-7.1
C2	80	-7.9	-11.0	3.9	-0.2	-0.5	-0.6	3.9	-7.9	-11.0
C3	70	-8.3	-12.3	0.5	0.0	-0.4	-1.0	0.7	-8.4	-12.3
C4	60	-8.5	-13.0	-0.5	0.2	-0.2	-0.7	-0.5	-8.6	-13.1
C5	50	-10.8	-15.1	-0.4	0.3	-0.1	-0.2	-0.4	-10.8	-15.1
C6	40	-11.1	-15.9	-0.2	0.5	0.0	-0.1	-0.2	-11.0	-16.0
D1	25	-29.4	-23.7	-8.4	-0.6	-0.2	-5.0	-7.3	-23.6	-30.6
D2	15	-17.6	-20.4	-4.9	-0.3	0.0	-2.2	-4.6	-18.0	-20.5
D3	5	-10.8	-19.6	-2.4	-0.1	0.0	-0.7	-2.4	-10.9	-19.6
E1	35	-7.6	-16.4	-1.5	0.5	-0.1	-1.5	-1.1	-7.9	-16.5
E2	34	-8.4	-17.6	-5.0	0.5	-0.2	-3.3	-3.0	-10.4	-17.6
E3	33	-14.0	-19.4	-5.4	0.3	-0.3	-3.7	-4.0	-15.4	-19.4
E4	32	-16.2	-20.6	-7.0	0.3	-0.2	-2.4	-6.4	-16.8	-20.7
E5	31	-17.0	-21.6	-8.9	0.3	-0.2	-1.4	-8.7	-17.2	-21.6
F1	100	-1.1	-5.1	18.0	0.2	-1.2	1.6	18.2	-1.3	-5.1
F2	99	-2.4	-10.9	-1.9	0.5	-0.9	2.2	0.0	-4.2	-11.0
F3	98	-1.4	-14.2	-15.2	0.9	-0.6	3.9	-0.4	-14.0	-16.5
F4	97	0.6	-20.9	-42.5	1.5	-0.6	5.0	1.3	-20.9	-43.1
G1	94	1.3	-5.2	18.1	0.4	-0.4	4.1	19.0	0.4	-5.2
G2	93	1.8	-9.6	1.3	0.8	-0.3	3.2	4.8	-1.6	-9.7
G3	92	1.6	-10.8	-3.1	0.9	-0.2	1.5	2.0	-3.5	-10.9
G4	91	0.7	-12.3	-7.9	0.9	-0.2	0.6	0.8	-8.0	-12.4

Table 2.10.4-20 Stress Components – Impact; 30-Foot Bottom Oblique Drop; Drop Orientation = 75 Degrees; 3-D Bottom Model; 0-Degree Circumferential Location; Condition 1 (continued)

Stress Points		Stress Components (ksi)						Principal Stresses (ksi)		
Section[1]	Node	S_x	S_y	S_z	S_{xy}	S_{yz}	S_{zx}	S1	S2	S3
H1	330	-0.3	5.9	-9.2	-0.4	-1.7	0.0	6.1	-0.3	-9.4
H2	329	-0.2	7.5	-6.2	-0.5	-1.6	0.0	7.7	-0.2	-6.4
H3	328	0.0	9.1	-3.2	-0.6	-1.5	0.0	9.3	-0.1	-3.4
H4	327	0.1	10.6	-0.2	-0.7	-1.4	-0.1	10.9	0.1	-0.5
I1	244	-0.2	-0.8	-0.9	0.1	-0.8	0.0	0.0	-0.2	-1.7
I2	243	-0.1	1.0	2.2	-0.1	-0.7	-0.1	2.5	0.6	-0.1
I3	242	-0.1	2.6	5.3	-0.2	-0.5	-0.1	5.4	2.5	-0.1
I4	241	0.0	4.2	8.4	-0.3	-0.4	-0.1	8.5	4.1	0.0
J1	550	-0.3	6.3	5.9	-0.5	-0.9	0.0	7.0	5.2	-0.3
J2	548	-0.2	8.9	7.7	-0.7	-0.9	0.0	9.4	7.3	-0.2
J3	547	-0.1	11.3	9.5	-0.8	-0.8	0.0	11.7	9.2	-0.1
K1	344	-0.1	-0.9	6.9	0.0	-0.6	0.0	7.0	-0.1	-1.0
K2	342	-0.1	2.6	8.5	-0.2	-0.4	0.0	8.5	2.6	-0.1
K3	341	0.0	5.8	10.0	-0.5	-0.3	0.0	10.0	5.9	-0.1
L1	740	-0.1	3.8	13.3	0.3	-0.1	-0.1	13.3	3.9	-0.1
L2	738	-0.5	6.5	14.8	-1.1	-0.1	0.0	14.8	6.7	-0.7
L3	737	0.2	9.4	16.3	-2.4	-0.1	0.0	16.3	10.0	-0.4
M1	454	-0.3	-2.0	9.7	-1.9	-0.1	0.0	9.7	0.9	-3.2
M2	452	0.4	3.5	12.4	-0.9	-0.1	0.2	12.4	3.7	0.2
M3	451	-0.7	8.0	14.8	0.0	-0.1	-0.3	14.8	8.0	-0.7
N1	810	-0.2	6.6	9.0	-0.5	0.7	-0.1	9.2	6.4	-0.3
N2	807	-0.2	11.2	12.5	-0.8	0.7	0.0	12.8	11.0	-0.3
O1	524	-0.1	-0.8	9.6	0.1	0.4	0.0	9.6	-0.1	-0.9
O2	521	-0.1	5.7	12.9	-0.4	0.2	0.0	12.9	5.8	-0.1
P1	850	-0.1	6.3	-2.0	-0.3	1.3	-0.1	6.5	-0.2	-2.2
P2	847	-0.2	11.0	6.4	-0.7	1.1	0.3	11.3	6.2	-0.3
Q1	564	-0.1	0.0	6.3	0.0	0.5	0.0	6.3	0.0	-0.1
Q2	561	-0.1	4.0	11.1	-0.3	0.3	0.0	11.1	4.0	-0.1
R1	890	-3.0	-3.3	9.3	0.1	0.8	-0.6	9.4	-3.0	-3.4
R2	887	-2.9	-7.7	-10.2	0.4	0.5	-1.6	-2.6	-7.6	-10.7

Table 2.10.4-20 Stress Components – Impact; 30-Foot Bottom Oblique Drop; Drop Orientation = 75 Degrees; 3-D Bottom Model; 0-Degree Circumferential Location; Condition 1 (continued)

Stress Points		Stress Components (ksi)						Principal Stresses (ksi)		
Section[1]	Node	S_x	S_y	S_z	S_{xy}	S_{yz}	S_{zx}	S1	S2	S3
S1	604	-0.1	-1.2	8.1	0.0	0.2	-1.4	8.3	-0.4	-1.2
S2	601	0.7	-2.6	0.6	0.2	0.1	-0.6	1.3	0.1	-2.6
T1	897	3.0	-3.3	-2.3	0.3	0.3	-1.0	3.2	-2.3	-3.4
T2	614	0.8	-2.1	2.5	0.1	0.0	-1.2	3.2	0.2	-2.1
T3	611	-0.2	-2.5	1.3	0.1	-0.1	-0.7	1.5	-0.5	-2.5
U1	900	4.8	-1.7	1.9	0.2	0.4	-0.1	4.8	1.9	-1.7
U2	910	-2.0	-2.8	0.1	0.1	0.2	-0.9	0.4	-2.3	-2.8
V1	920	2.6	-1.1	0.8	0.4	0.1	-0.7	2.9	0.6	-1.2
V2	930	-4.0	-3.8	0.6	0.6	0.1	-0.2	0.6	-3.3	-4.5
W1	1216	-0.8	2.1	-0.4	-0.1	-0.3	0.1	2.2	-0.5	-0.8
W2	1226	-0.4	0.1	0.2	-0.1	-0.5	0.0	0.6	-0.3	-0.4
X1	1236	0.0	-0.7	-0.2	-0.2	-0.5	0.0	0.2	-0.1	-1.0
X2	1246	0.2	-3.3	0.5	-0.4	-0.3	0.0	0.6	0.2	-3.3

[1] Refer to Figure 2.10.2-34 for the identification of the representative sections.

Table 2.10.4-21 Primary Stresses; Heat Condition; 3-D Top Model; 0-Degree Circumferential Location; Condition 1

Condition 1: 100°F Ambient with Contents

Stress Points		Stress Components (ksi)						Principal Stresses (ksi)		
Section[1]	Node	S_x	S_y	S_z	S_{xy}	S_{yz}	S_{xz}	S1	S2	S3
A1	1949	-0.4	-0.4	0.0	0.0	0.0	-0.1	0.0	-0.4	-0.5
A2	1950	-0.3	-0.2	0.0	0.0	0.0	-0.1	0.0	-0.2	-0.3
A3	1951	0.1	0.1	-0.1	0.0	0.0	0.0	0.1	0.1	-0.1
B1	1952	0.0	0.0	0.1	0.0	0.0	0.0	0.1	0.0	-0.1
B2	93	0.4	0.4	-0.2	0.0	0.0	-0.1	0.4	0.4	-0.2
C1	1925	0.2	0.1	0.8	0.0	0.0	0.1	0.8	0.2	0.1
C2	1926	0.1	0.0	0.2	0.0	0.0	0.0	0.2	0.1	0.0
C3	1927	-0.1	0.0	0.1	0.0	0.0	0.0	0.1	0.0	-0.1
D1	683	0.1	0.1	0.0	0.0	0.0	0.0	0.2	0.1	0.0
D2	85	-0.1	0.2	0.1	0.0	0.0	0.0	0.2	0.1	-0.1
E1	682	-0.1	0.0	0.0	0.0	0.0	0.0	0.0	0.0	-0.1
E2	82	-0.1	0.0	0.1	0.0	0.0	0.1	0.1	0.0	-0.1
F1	1925	0.2	0.1	0.8	0.0	0.0	0.1	0.8	0.2	0.1
F2	1325	0.0	-0.4	-0.8	0.0	0.0	0.1	0.1	-0.4	-0.8
G1	680	0.0	0.0	0.3	0.0	0.0	0.1	0.3	0.0	0.0
G2	80	0.1	-0.1	0.0	0.0	0.0	0.0	0.1	0.0	-0.1
H1	1921	0.0	1.1	0.0	-0.1	0.0	0.0	1.1	0.0	0.0
H2	1321	0.0	1.3	0.7	-0.1	0.0	0.0	1.3	0.7	0.0
I1	676	0.0	-0.1	0.2	0.0	0.0	0.0	0.2	0.0	-0.1
I2	76	0.0	0.0	0.3	0.0	0.0	0.0	0.3	0.0	0.0
J1	1916	0.0	1.2	0.6	-0.1	0.0	0.0	1.2	0.6	0.0
J2	1316	0.0	1.3	0.7	-0.1	0.0	0.0	1.3	0.7	0.0
K1	671	0.0	0.0	0.2	0.0	0.0	0.0	0.2	0.0	0.0
K2	71	0.0	0.1	0.2	0.0	0.0	0.0	0.2	0.1	0.0
L1	1908	0.0	1.2	0.8	-0.1	0.0	0.0	1.2	0.8	-0.1
L2	1308	0.0	1.3	0.9	0.0	0.0	0.0	1.3	0.9	0.0
M1	663	0.0	0.0	0.2	0.0	0.0	0.0	0.2	0.0	0.0
M2	63	0.0	0.0	0.2	0.0	0.0	0.0	0.2	0.0	0.0
N1	1877	0.0	1.2	0.6	-0.1	0.0	0.0	1.2	0.6	0.0

Table 2.10.4-21 Primary Stresses; Heat Condition; 3-D Top Model; 0-Degree Circumferential Location; Condition 1 (continued)

Stress Points		Stress Components (ksi)						Principal Stresses (ksi)		
Section[1]	Node	S_x	S_y	S_z	S_{xy}	S_{yz}	S_{zx}	S1	S2	S3
N2	1477	0.0	1.3	0.6	-0.1	0.0	0.0	1.3	0.6	0.0
N3	1277	0.0	1.3	0.7	-0.1	0.0	0.0	1.3	0.7	0.0
O1	647	0.0	0.1	0.1	0.0	0.0	0.0	0.1	0.1	0.0
O2	247	0.0	0.0	0.1	0.0	0.0	0.0	0.1	0.0	0.0
O3	47	0.0	0.0	0.1	0.0	0.0	0.0	0.1	0.0	0.0
P1	1840	0.0	1.1	-0.1	-0.1	0.0	0.0	1.1	0.0	-0.1
P2	1640	0.0	1.2	0.2	-0.1	0.0	0.0	1.2	0.2	0.0
P3	1440	0.0	1.3	0.5	-0.1	0.0	0.0	1.3	0.5	0.0
P4	1240	0.0	1.4	0.9	-0.1	0.0	0.1	1.4	0.9	0.0
Q1	628	0.0	-0.3	-0.2	0.0	0.0	0.0	0.0	-0.2	-0.3
Q2	428	0.0	-0.3	0.0	0.0	0.0	0.0	0.0	0.0	-0.3
Q3	228	0.0	-0.2	0.1	0.0	0.0	0.0	0.1	0.0	-0.2
Q4	28	0.0	-0.1	0.3	0.0	0.0	0.0	0.3	0.0	-0.2
R1	1816	-0.2	0.1	2.1	0.0	0.0	0.1	2.1	0.1	-0.2
R2	1616	-0.5	-0.3	0.7	0.0	0.0	0.2	0.7	-0.3	-0.5
R3	1416	-1.2	-0.8	-0.3	0.0	0.0	0.1	-0.3	-0.8	-1.2
R4	1216	-2.3	-1.4	-1.2	0.0	0.0	-0.2	-1.2	-1.4	-2.3
S1	616	-1.1	-0.7	0.6	0.0	0.0	0.2	0.6	-0.7	-1.1
S2	416	-0.5	-0.5	0.4	0.0	0.0	0.4	0.6	-0.5	-0.7
S3	216	0.0	-0.6	-0.3	0.0	0.0	0.5	0.3	-0.6	-0.7
S4	16	0.3	-0.6	-0.8	0.0	0.0	0.4	0.4	-0.6	-0.9
T1	811	0.3	0.1	0.2	0.0	0.0	0.4	0.6	0.1	-0.1
T2	611	0.5	-0.1	-0.6	0.0	0.0	0.1	0.5	-0.1	-0.6
T3	411	0.2	0.0	-0.2	0.0	0.0	0.1	0.2	0.0	-0.2
T4	211	0.1	0.0	0.1	0.0	0.0	0.1	0.1	0.0	0.0
T5	11	0.0	0.1	0.4	0.0	0.0	0.0	0.4	0.1	0.0
U1	43058	0.7	-0.6	-1.6	0.1	0.0	0.3	0.7	-0.6	-1.6
U2	43057	-0.4	-0.9	-1.7	0.0	0.0	0.4	-0.3	-0.9	-1.8
U3	43056	-0.6	-1.0	-2.0	0.0	0.0	0.6	-0.4	-1.0	-2.2
U4	43055	-0.3	-0.9	-2.3	0.0	0.0	0.4	-0.3	-0.9	-2.4
U5	43054	-0.2	-0.8	-2.4	0.0	0.0	-0.1	-0.2	-0.8	-2.4

Table 2.10.4-21 Primary Stresses; Heat Condition; 3-D Top Model; 0-Degree Circumferential Location; Condition 1 (continued)

Stress Points		Stress Components (ksi)						Principal Stresses (ksi)		
Section[1]	Node	S_x	S_y	S_z	S_{xy}	S_{yz}	S_{xz}	S1	S2	S3
U6	43053	-0.4	-0.7	-2.0	0.0	0.0	-0.4	-0.3	-0.7	-2.1
U7	43052	-0.7	-0.5	-1.3	0.0	0.0	-0.5	-0.5	-0.5	-1.6
U8	43051	0.8	0.5	-0.4	0.0	0.0	-0.4	0.9	0.5	-0.5
V1	50024	0.4	-0.2	-0.6	0.1	0.0	-0.1	0.5	-0.2	-0.6
V2	50023	0.2	-0.2	-0.8	0.0	0.0	0.0	0.2	-0.2	-0.8
V3	50022	-0.1	0.0	-0.2	0.0	0.0	0.0	0.0	-0.1	-0.2
V4	50021	-0.7	0.1	0.6	-0.1	0.0	0.0	0.6	0.1	-0.7
W1	43278	-0.8	-0.9	0.3	0.0	0.0	0.2	0.3	-0.9	-0.9
W2	43274	-0.1	-0.2	0.0	0.0	0.0	0.2	0.1	-0.2	-0.2
W3	43271	0.4	0.3	-0.2	0.0	0.0	0.1	0.4	0.3	-0.2
X1	50084	-0.4	-0.3	0.1	0.0	0.0	0.1	0.1	-0.3	-0.4
X2	50083	-0.1	-0.1	0.0	0.0	0.0	0.1	0.1	-0.1	-0.1
X3	50081	0.3	0.3	-0.2	0.0	0.0	0.1	0.4	0.3	-0.2

[1] Refer to Figure 2.10.2-34 for the identification of the representative sections.

Table 2.10.4-22 Primary + Secondary Stresses; Heat Condition; 3-D Top Model; 0-Degree Circumferential Location; Condition 1

Condition 1: 100°F Ambient with Contents

Stress Points		Stress Components (ksi)						Principal Stresses (ksi)		
Section[1]	Node	S_x	S_y	S_z	S_{xy}	S_{yz}	S_{xz}	S1	S2	S3
A1	1949	-0.8	-0.7	0.6	0.0	-0.1	0.6	0.9	-0.7	-1.0
A2	1950	-0.7	-0.6	0.5	0.0	-0.1	0.6	0.8	-0.7	-1.0
A3	1951	-1.5	-1.5	-0.8	0.0	-0.1	0.3	-0.7	-1.5	-1.7
B1	1952	0.7	0.7	0.7	0.0	-0.1	0.3	1.0	0.7	0.3
B2	93	0.6	0.5	-1.8	0.0	-0.2	0.7	0.8	0.5	-2.0
C1	1925	-1.0	-0.6	-0.6	0.0	-0.1	-0.8	0.0	-0.6	-1.7
C2	1926	0.8	-0.4	-0.8	0.1	-0.1	-0.7	1.1	-0.4	-1.1
C3	1927	-2.0	-2.1	-1.2	0.0	0.0	0.0	-1.2	-2.0	-2.1
D1	683	1.8	1.3	3.4	0.0	0.1	0.8	3.7	1.5	1.3
D2	85	-1.5	1.7	3.4	-0.1	0.1	0.6	3.5	1.7	-1.6
E1	682	-1.5	-0.4	2.4	-0.1	0.1	0.6	2.5	-0.4	-1.6
E2	82	-1.0	-0.5	-0.4	0.0	0.0	1.2	0.6	-0.5	-1.9
F1	1925	-1.0	-0.6	-0.6	0.0	-0.1	-0.8	0.0	-0.6	-1.7
F2	1325	0.6	-0.8	-1.5	0.1	0.0	-0.7	0.8	-0.8	-1.7
G1	680	0.0	0.2	1.0	0.0	0.0	0.2	1.1	0.2	-0.1
G2	80	-2.6	1.2	7.1	-0.2	0.1	1.3	7.2	1.2	-2.7
H1	1921	0.0	0.9	0.6	-0.1	0.1	0.0	1.0	0.6	0.0
H2	1321	-0.1	1.0	-0.4	-0.1	0.0	0.1	1.0	-0.1	-0.4
I1	676	-0.1	2.5	5.7	-0.2	0.1	0.1	5.7	2.5	-0.1
I2	76	-0.1	3.2	6.5	-0.2	-0.1	0.1	6.5	3.2	-0.2
J1	1916	-0.1	0.1	-1.5	0.0	0.0	0.0	0.1	-0.1	-1.5
J2	1316	-0.1	2.5	2.2	-0.2	0.0	0.0	2.5	2.2	-0.1
K1	671	-0.1	3.7	4.0	-0.3	0.0	0.0	4.0	3.7	-0.2
K2	71	-0.1	6.1	8.2	-0.5	0.0	0.0	8.2	6.2	-0.2
L1	1908	-0.9	-0.2	-1.1	0.0	0.0	0.0	-0.2	-0.9	-1.1
L2	1308	0.6	2.8	1.8	0.0	0.0	0.0	2.8	1.8	0.6
M1	663	-1.3	4.1	3.9	-0.4	0.0	0.0	4.1	3.9	-1.3
M2	63	0.7	7.7	8.0	-0.5	0.0	0.0	8.0	7.7	0.7
N1	1877	0.0	-0.6	-1.6	0.0	0.0	0.0	0.0	-0.6	-1.6

Table 2.10.4-22 Primary + Secondary Stresses; Heat Condition; 3-D Top Model; 0-Degree Circumferential Location; Condition 1 (continued)

Stress Points		Stress Components (ksi)						Principal Stresses (ksi)		
Section[1]	Node	S_x	S_y	S_z	S_{xy}	S_{yz}	S_{xz}	S1	S2	S3
N2	1477	0.0	1.0	0.1	-0.1	0.0	0.0	1.0	0.1	0.0
N3	1277	0.0	2.5	1.7	-0.2	0.1	0.0	2.5	1.7	0.0
O1	647	-0.2	2.9	4.5	-0.2	-0.1	0.0	4.5	2.9	-0.3
O2	247	-0.1	4.7	6.2	-0.4	0.0	0.0	6.2	4.8	-0.2
O3	47	-0.1	6.4	7.9	-0.5	0.0	0.0	7.9	6.5	-0.1
P1	1840	0.0	-0.9	-1.7	0.1	0.0	0.0	0.0	-0.9	-1.7
P2	1640	0.0	0.3	-0.7	0.0	0.0	0.0	0.3	0.0	-0.7
P3	1440	0.1	1.6	0.3	-0.1	0.0	0.0	1.6	0.3	0.1
P4	1240	-0.2	2.7	1.5	-0.2	0.1	0.2	2.8	1.5	-0.2
Q1	628	-0.2	1.5	5.4	-0.1	0.0	0.1	5.4	1.5	-0.2
Q2	428	-0.2	2.6	6.1	-0.2	0.0	0.1	6.1	2.7	-0.2
Q3	228	-0.1	3.8	6.9	-0.3	0.0	0.1	6.9	3.8	-0.1
Q4	28	0.0	4.8	7.7	-0.4	0.0	0.0	7.7	4.9	0.0
R1	1816	0.0	-7.9	-1.0	0.6	0.0	1.0	0.7	-1.7	-7.9
R2	1616	-0.2	-6.7	-1.6	0.5	0.0	1.7	0.9	-2.7	-6.7
R3	1416	-2.0	-5.8	-1.7	0.2	0.0	2.8	1.0	-4.6	-5.8
R4	1216	-0.1	-3.5	0.4	0.1	0.0	2.2	2.4	-2.0	-3.5
S1	616	-3.2	-0.7	-2.4	-0.3	0.1	-1.7	-0.6	-1.1	-4.5
S2	416	-5.9	1.4	4.4	-0.5	-0.1	-2.3	4.9	1.4	-6.4
S3	216	-1.6	3.8	5.1	-0.4	0.1	-0.1	5.1	3.9	-1.7
S4	16	-0.7	5.6	7.4	-0.6	0.2	0.1	7.4	5.7	-0.8
T1	811	-1.8	-1.3	-4.8	-0.1	-0.1	-1.3	-1.3	-1.3	-5.2
T2	611	-1.0	0.8	-2.0	-0.1	-0.1	-0.7	0.8	-0.6	-2.3
T3	411	-0.4	2.5	0.1	-0.3	0.0	-0.4	2.5	0.3	-0.6
T4	211	-0.1	4.1	2.0	-0.3	0.0	-0.2	4.1	2.1	-0.2
T5	11	-0.1	5.6	3.9	-0.4	0.0	-0.1	5.6	3.9	-0.1
U1	43058	-2.6	-2.7	-7.4	0.1	0.2	1.0	-2.4	-2.7	-7.6
U2	43057	-0.1	-2.3	-6.4	0.2	0.1	1.2	0.1	-2.3	-6.6
U3	43056	-0.1	-2.3	-4.8	0.2	0.2	1.3	0.3	-2.3	-5.2
U4	43055	-0.1	-2.5	-4.2	0.2	0.2	0.9	0.1	-2.5	-4.4
U5	43054	-0.4	-2.8	-3.6	0.1	0.2	0.3	-0.4	-2.8	-3.6

Table 2.10.4-22 Primary + Secondary Stresses; Heat Conditions; 3-D Top Model; 0-Degree Circumferential Location; Condition 1 (continued)

Stress Points		Stress Components (ksi)						Principal Stresses (ksi)		
Section[1]	Node	S_x	S_y	S_z	S_{xy}	S_{yz}	S_{zx}	S1	S2	S3
U6	43053	-1.2	-3.2	-2.7	0.1	0.3	-0.1	-1.2	-2.6	-3.3
U7	43052	-2.6	-3.5	-1.6	0.1	0.5	-0.2	-1.5	-2.6	-3.7
U8	43051	3.1	3.7	5.3	-0.3	0.7	-1.1	6.0	3.5	2.6
V1	50024	1.3	0.2	0.0	0.1	-0.1	0.3	1.4	0.2	-0.1
V2	50023	0.6	-0.3	-0.5	0.1	-0.2	0.2	0.6	-0.2	-0.6
V3	50022	-0.3	-0.8	-0.3	0.0	-0.2	0.1	-0.2	-0.4	-0.9
V4	50021	-1.4	-1.2	0.5	-0.1	-0.1	0.1	0.5	-1.2	-1.4
W1	43278	1.9	2.0	-1.1	0.0	0.2	-0.6	2.0	1.9	-1.2
W2	43274	-0.9	-0.8	-0.6	0.0	0.2	-0.7	0.0	-0.8	-1.5
W3	43271	-2.8	-2.7	0.3	0.0	0.1	-0.3	0.3	-2.7	-2.8
X1	50084	1.6	1.7	-0.2	0.0	0.1	-0.3	1.7	1.7	-0.2
X2	50083	0.9	0.9	-0.1	0.0	0.1	-0.3	1.0	0.9	-0.2
X3	50081	-0.6	-0.7	0.4	0.0	0.1	-0.3	0.5	-0.7	-0.7

[1] Refer to Figure 2.10.2-34 for the identification of the representative sections.

Table 2.10.4-23 P_m Stresses; Heat Condition; 3-D Top Model; 0-Degree Circumferential Location; Condition 1

Condition 1: 100°F Ambient with Contents

			Stress Components (ksi)						Principal Stresses (ksi)			
Section[1]	Node -	Node	S_x	S_y	S_z	S_{xy}	S_{yz}	S_{zx}	S1	S2	S3	S.I.
A	1949 -	1951	-0.2	-0.1	0.0	0.0	0.0	-0.1	0.0	-0.1	-0.2	0.2
B	1952 -	93	0.2	0.2	-0.1	0.0	0.0	-0.1	0.2	0.2	-0.1	0.3
C	1925 -	1927	0.0	0.0	0.2	0.0	0.0	0.0	0.2	0.0	0.0	0.2
D	683 -	85	0.0	0.1	0.1	0.0	0.0	0.0	0.1	0.1	0.0	0.1
E	682 -	82	-0.1	0.0	0.1	0.0	0.0	0.1	0.1	0.0	-0.1	0.2
F	1925 -	1325	0.1	-0.1	0.0	0.0	0.0	0.1	0.1	0.0	-0.1	0.3
G	680 -	80	0.1	0.0	0.2	0.0	0.0	0.0	0.2	0.0	0.0	0.2
H	1921 -	1321	0.0	1.2	0.3	-0.1	0.0	0.0	1.2	0.3	0.0	1.3
I	676 -	76	0.0	0.0	0.2	0.0	0.0	0.0	0.2	0.0	0.0	0.2
J	1916 -	1316	0.0	1.3	0.7	-0.1	0.0	0.0	1.3	0.7	0.0	1.3
K	671 -	71	0.0	0.0	0.2	0.0	0.0	0.0	0.2	0.0	0.0	0.2
L	1908 -	1308	0.0	1.2	0.8	-0.1	0.0	0.0	1.2	0.8	0.0	1.3
M	663 -	63	0.0	0.0	0.2	0.0	0.0	0.0	0.2	0.0	0.0	0.2
N	1877 -	1277	0.0	1.3	0.6	-0.1	0.0	0.0	1.3	0.6	0.0	1.3
O	647 -	47	0.0	0.0	0.1	0.0	0.0	0.0	0.1	0.0	0.0	0.1
P	1840 -	1240	0.0	1.2	0.4	-0.1	0.0	0.0	1.2	0.4	0.0	1.2
Q	628 -	28	0.0	-0.2	0.1	0.0	0.0	0.0	0.1	0.0	-0.2	0.3
R	1816 -	1216	-1.0	-0.6	0.3	0.0	0.0	0.1	0.3	-0.6	-1.0	1.3
S	616 -	16	-0.3	-0.6	0.0	0.0	0.0	0.4	0.3	-0.6	-0.6	0.9
T	811 -	11	0.2	0.0	-0.1	0.0	0.0	0.1	0.3	0.0	-0.1	0.4
U	43058 -	43051	-0.2	-0.6	-1.7	0.0	0.0	0.0	-0.2	-0.6	-1.7	1.5
V	50024 -	50021	0.0	-0.1	-0.3	0.0	0.0	0.0	0.0	-0.1	-0.3	0.3
W	43278 -	43271	-0.1	-0.2	0.0	0.0	0.0	0.1	0.1	-0.2	-0.3	0.4
X	50084 -	50081	0.0	0.0	0.0	0.0	0.0	0.1	0.1	0.0	-0.1	0.2

[1] Refer to Figure 2.10.2-34 for the identification of the representative sections.

Table 2.10.4-24 $P_m + P_b$ Stresses; Heat Condition; 3-D Top Model; 0-Degree Circumferential Location; Condition 1

Condition 1: 100°F Ambient with Contents

			Stress Components (ksi)						Principal Stresses (ksi)			
Section[1]	Node -	Node	S_x	S_y	S_z	S_{xy}	S_{yz}	S_{xz}	S1	S2	S3	S.I.
A I	1949 -	1951	-0.4	-0.4	0.0	0.0	0.0	-0.1	0.1	-0.4	-0.4	0.5
B O	1952 -	93	0.4	0.4	-0.2	0.0	0.0	-0.1	0.4	0.4	-0.2	0.7
C I	1925 -	1927	0.2	0.0	0.5	0.0	0.0	0.0	0.5	0.2	0.0	0.5
D O	683 -	85	-0.1	0.2	0.1	0.0	0.0	0.0	0.2	0.1	-0.1	0.3
E O	682	82	-0.1	0.0	0.1	0.0	0.0	0.1	0.1	0.0	-0.1	0.2
F O	1925 -	1325	0.0	-0.4	-0.8	0.0	0.0	0.1	0.1	-0.4	-0.8	0.8
G I	680 -	80	0.0	0.0	0.3	0.0	0.0	0.1	0.3	0.0	0.0	0.3
H O	1921 -	1321	0.0	1.3	0.7	-0.1	0.0	0.0	1.3	0.7	0.0	1.4
I O	676 -	76	0.0	0.0	0.3	0.0	0.0	0.0	0.3	0.0	0.0	0.3
J O	1916 -	1316	0.0	1.3	0.7	-0.1	0.0	0.0	1.3	0.7	0.0	1.3
K O	671 -	71	0.0	0.1	0.2	0.0	0.0	0.0	0.2	0.1	0.0	0.2
L O	1908 -	1308	0.0	1.3	0.9	0.0	0.0	0.0	1.3	0.9	0.0	1.3
M O	663 -	63	0.0	0.0	0.2	0.0	0.0	0.0	0.2	0.0	0.0	0.2
N O	1877 -	1277	0.0	1.3	0.7	-0.1	0.0	0.0	1.3	0.7	0.0	1.3
O I	647 -	47	0.0	0.1	0.1	0.0	0.0	0.0	0.1	0.1	0.0	0.1
P O	1840 -	1240	0.0	1.4	0.8	-0.1	0.0	0.0	1.4	0.8	0.0	1.3
Q O	628 -	28	0.0	-0.1	0.3	0.0	0.0	0.0	0.3	0.0	-0.1	0.5
R I	1816 -	1216	0.1	0.2	1.9	0.0	0.0	0.2	1.9	0.2	0.1	1.9
S I	616 -	16	-1.0	-0.6	0.8	0.0	0.0	0.3	0.8	-0.6	-1.1	1.9
T I	811 -	11	0.5	0.0	-0.4	0.0	0.0	0.2	0.6	0.0	-0.5	1.0
U I	43058 -	43051	-0.4	-1.1	-2.3	0.1	0.0	0.6	-0.2	-1.1	-2.4	2.2
V I	50024 -	50021	0.5	-0.3	-1.0	0.1	0.0	-0.1	0.5	-0.3	-1.0	1.5
W I	43278 -	43271	-0.8	-0.8	0.2	0.0	0.0	0.2	0.3	-0.8	-0.8	1.1
X O	50084 -	50081	0.3	0.3	-0.2	0.0	0.0	0.1	0.4	0.3	-0.2	0.5

[1] Refer to Figure 2.10.2-34 for the identification of the representative section.

Table 2.10.4-25 S_n Stresses; Heat Condition; 3-D Top Model; 0-Degree Circumferential Location; Condition 1

Condition 1: 100°F Ambient with Contents

			Stress Components (ksi)						Principal Stresses (ksi)			
Section[1]	Node -	Node	S_x	S_y	S_z	S_{xy}	S_{yz}	S_{xz}	S1	S2	S3	S.I.
A I	1949 -	1951	-0.6	-0.5	0.8	0.0	-0.2	0.7	1.1	-0.5	-0.9	2.0
B O	1952 -	93	0.6	0.5	-1.8	0.0	-0.2	0.7	0.8	0.5	-2.0	2.8
C I	1925 -	1927	0.5	-0.1	-0.7	0.0	-0.1	-0.9	1.0	-0.1	-1.2	2.1
D O	683 -	85	-1.5	1.7	3.4	-0.1	0.1	0.6	3.5	1.7	-1.6	5.1
E I	682 -	82	-1.5	-0.4	2.4	-0.1	0.1	0.6	2.5	-0.4	-1.6	4.1
F O	1925 -	1325	0.6	-0.8	-1.5	0.1	0.0	-0.7	0.8	-0.8	-1.7	2.5
G O	680 -	80	-2.6	1.2	7.1	-0.2	0.1	1.3	7.2	1.2	-2.7	10.0
H O	1921 -	1321	-0.1	1.0	-0.4	-0.1	0.0	0.1	1.0	-0.1	-0.4	1.4
I O	676 -	76	-0.1	3.2	6.5	-0.2	-0.1	0.1	6.5	3.2	-0.2	6.6
J O	1916 -	1316	-0.1	2.5	2.2	-0.2	0.0	0.0	2.5	2.2	-0.1	2.6
K O	671 -	71	-0.1	6.1	8.2	-0.5	0.0	0.0	8.2	6.2	-0.2	8.4
L O	1908 -	1308	0.6	2.8	1.8	0.0	0.0	0.0	2.8	1.8	0.6	2.2
M O	663 -	63	0.7	7.7	8.0	-0.5	0.0	0.0	8.0	7.7	0.7	7.4
N O	1877 -	1277	0.0	2.5	1.8	-0.2	0.1	0.0	2.5	1.8	0.0	2.5
O O	647 -	47	-0.1	6.5	7.9	-0.5	0.0	0.0	7.9	6.5	-0.1	8.0
P O	1840 -	1240	0.0	2.8	1.5	-0.2	0.1	0.1	2.8	1.5	0.0	2.8
Q O	628 -	28	0.0	4.9	7.7	-0.4	0.0	0.1	7.7	4.9	0.0	7.7
R I	1816 -	1216	-0.1	-8.1	-1.8	0.6	0.1	1.2	0.5	-2.4	-8.1	8.6
S O	616 -	16	-0.8	5.8	8.0	-0.6	0.2	0.3	8.0	5.9	-0.9	8.9
T O	811 -	11	0.3	5.7	4.1	-0.4	0.0	0.0	5.8	4.1	0.2	5.6
U I	43058 -	43051	-1.0	-3.5	-8.0	0.2	0.0	1.6	-0.6	-3.5	-8.4	7.7
V I	50024 -	50021	1.4	0.2	-0.5	0.2	-0.1	0.3	1.5	0.2	-0.5	2.0
W O	43278 -	43271	-3.0	-2.9	0.2	0.0	0.1	-0.4	0.3	-2.9	-3.0	3.3
X I	50084 -	50081	1.6	1.7	-0.3	0.0	0.1	-0.3	1.7	1.6	-0.3	2.0

[1] Refer to Figure 2.10.2-34 for the identification of the representative sections.

Table 2.10.4-26 Critical P_m Stress Summary; Heat Condition; 3-D Top Model; Condition 1

Condition 1: 100°F Ambient with Contents

Comp. No.[1]	Section Cut Node-Node	P_m Stresses (ksi) S_x	S_y	S_z	S_{xy}	S_{yz}	S_{xz}	Principal Stresses (ksi) S1	S2	S3	S.I.	Allow. Stress	Margin of Safety
1	1952- 93	0.2	0.2	-0.1	0.0	0.0	-0.1	0.2	0.2	-0.1	0.3	19.2	63.0
2	18679-18079	0.0	0.0	0.0	1.9	0.2	0.0	2.0	0.0	-1.9	3.9	18.5	3.7
3	1920- 1320	0.0	1.4	0.4	-0.1	0.0	0.0	1.4	0.4	0.0	1.4	31.4	21.4
4	1918- 1318	0.0	1.3	0.6	-0.1	0.0	0.0	1.3	0.6	0.0	1.3	19.6	14.1
5	625- 25	0.0	-0.4	0.1	0.0	0.0	0.0	0.1	0.0	-0.4	0.5	20.0	39.0
6	29216-29211	0.1	1.3	3.7	0.0	0.0	0.1	3.7	1.3	0.1	3.6	20.0	4.5
7	43021-43028	0.2	-2.5	-9.0	0.2	0.0	-0.1	-0.2	-2.5	-9.0	8.9	20.0	1.2
8	50916-50919	0.0	0.0	-0.1	0.0	0.0	0.2	0.2	0.0	-0.2	0.4	45.0	105.2

Locations of the most critical sections for each component are provided in the following:

Comp. No.[1]	Section Location Inside Node x (in)	y (deg)	z (in)	Outside Node x (in)	y (deg)	z (in)
1	0.00	0.0	6.20	0.00	0.0	0.75
2	40.70	91.7	17.40	43.35	91.7	17.40
3	35.50	0.0	35.40	37.00	0.0	35.40
4	35.50	0.0	47.40	37.00	0.0	47.40
5	40.70	0.0	163.40	43.35	0.0	163.40
6	37.50	163.4	175.40	37.66	163.4	179.40
7	37.66	0.0	185.40	37.66	0.0	179.40
8	36.46	91.7	193.71	36.46	91.7	188.40

[1] Refer to Figure 2.10.2-33 for cask component identification.

Table 2.10.4-27 Critical $P_m + P_b$ Stress Summary; Heat Condition; 3-D Top Model; Condition 1

Condition 1: 100°F Ambient with Contents

Comp. No.[1]	Section Cut Node-Node	$P_m + P_b$ Stresses (ksi) S_x	S_y	S_z	S_{xy}	S_{yz}	S_{xz}	Principal Stresses (ksi) S1	S2	S3	S.I.	Allow. Stress	Margin of Safety
1	1952- 93	0.4	0.4	-0.2	0.0	0.0	-0.1	0.4	0.4	-0.2	0.7	28.7	40.0
2	18679-18079	0.1	0.1	0.0	2.1	0.4	0.0	2.2	0.0	-2.0	4.2	27.7	5.6
3	1920- 1320	0.0	1.4	0.6	-0.1	0.0	0.0	1.4	0.6	0.0	1.5	47.1	30.4
4	1911- 1311	0.0	1.3	0.9	-0.1	0.0	0.0	1.3	0.9	0.0	1.4	29.4	20.0
5	625- 25	0.0	-0.3	0.2	0.0	0.0	0.0	0.2	0.0	-0.3	0.5	30.0	59.0
6	29216-29211	1.8	3.7	10.5	0.0	0.0	0.1	10.6	3.7	1.8	8.8	30.0	2.4
7	43021-43028	-0.9	-3.4	-10.6	0.2	0.0	0.7	-0.9	-3.4	-10.6	9.8	30.0	2.1
8	50921-50924	1.0	0.1	-0.6	0.0	0.0	0.0	1.0	0.1	-0.6	1.6	67.5	41.2

Locations of the most critical sections for each component are provided in the following:

Comp. No.[1]	Section Location Inside Node x (in)	y (deg)	z (in)	Outside Node x (in)	y (deg)	z (in)
1	0.00	0.0	6.20	0.00	0.0	0.75
2	40.70	91.7	17.40	43.35	91.7	17.40
3	35.50	0.0	35.40	37.00	0.0	35.40
4	35.50	0.0	83.69	37.00	0.0	83.69
5	40.70	0.0	163.40	43.35	0.0	163.40
6	37.50	163.4	175.40	37.66	163.4	179.40
7	37.66	0.0	185.40	37.66	0.0	179.40
8	35.21	91.7	193.71	35.21	91.7	188.40

[1] Refer to Figure 2.10.2-33 for cask component identification.

Table 2.10.4-28 Critical S_n Stress Summary; Heat Condition; 3-D Top Model; Condition 1

Condition 1: 100°F Ambient with Contents

Comp. No.[1]	Section Cut Node-Node	S_n Stresses (ksi)						Principal Stresses (ksi)				Allow. Stress 3.0 S_m
		S_x	S_y	S_z	S_{xy}	S_{yz}	S_{xz}	S1	S2	S3	S.I.	
1	16683-16085	-1.5	1.4	3.5	0.0	0.0	0.6	3.5	1.4	-1.6	5.1	57.6
2	18680-18080	-2.6	1.3	7.3	-0.3	1.4	1.3	7.7	1.1	-2.8	10.6	55.5
3	1821-1221	-0.1	-4.6	1.0	0.3	0.0	-0.4	1.2	-0.2	-4.6	5.7	94.2
4	1881-1281	0.0	2.8	1.7	-0.2	0.1	0.0	2.8	1.7	0.0	2.8	58.8
5	669-69	-0.1	6.9	8.3	-0.5	0.0	0.0	8.3	6.9	-0.2	8.4	60.0
6	10618-10018	-2.2	5.6	16.6	0.0	0.2	-1.4	16.7	5.6	-2.3	19.0	60.0
7	64571-64531	6.2	24.7	1.0	-0.1	0.0	-1.8	24.7	6.7	0.4	24.3	60.0
8	50036-50039	0.0	-0.7	-2.5	0.1	-0.5	-0.3	0.0	-0.6	-2.6	2.6	135.0

Locations of the most critical sections for each component are provided in the following:

Comp. No.[1]	Section Location					
	Inside Node			Outside Node		
	x (in)	y (deg)	z (in)	x (in)	y (deg)	z (in)
1	39.44	0.0	6.20	39.44	0.0	0.75
2	40.70	91.7	14.40	43.35	91.7	14.40
3	35.50	0.0	171.65	37.50	0.0	171.65
4	35.50	0.0	133.30	37.00	0.0	133.30
5	40.70	0.0	67.80	43.35	0.0	67.80
6	40.70	45.9	172.40	43.35	45.9	172.40
7	33.71	45.9	187.40	36.46	45.9	187.40
8	29.54	0.0	193.71	29.54	0.0	193.71

[1] Refer to Figure 2.10.2-33 for cask component identification.

Table 2.10.4-29 Primary Stresses; Cold Condition; 3-D Top Model; 0-Degree Circumferential Location; Condition 4

Condition 4: -40°F Ambient, No Decay Heat

Stress Points		Stress Components (ksi)						Principal Streases (ksi)		
Section[1]	Node	S_z	S_y	S_x	S_{xy}	S_{yz}	S_{xz}	S1	S2	S3
A1	1949	-0.1	-0.1	0.0	0.0	0.0	0.0	0.0	-0.1	-0.1
A2	1950	-0.1	0.0	0.0	0.0	0.0	0.0	0.0	0.0	-0.1
A3	1951	0.0	0.0	0.0	0.0	0.0	0.0	0.0	0.0	0.0
B1	1952	0.0	0.0	0.0	0.0	0.0	0.0	0.0	0.0	0.0
B2	93	0.1	0.1	-0.1	0.0	0.0	0.0	0.1	0.1	-0.1
C1	1925	0.0	0.0	0.3	0.0	0.0	0.0	0.3	0.0	0.0
C2	1926	0.0	0.0	0.1	0.0	0.0	0.0	0.1	0.0	0.0
C3	1927	0.0	0.0	0.0	0.0	0.0	0.0	0.0	0.0	0.0
D1	683	0.0	0.0	0.0	0.0	0.0	0.0	0.0	0.0	0.0
D2	85	0.0	0.1	0.0	0.0	0.0	0.0	0.1	0.0	0.0
E1	682	0.0	0.0	0.0	0.0	0.0	0.0	0.0	0.0	0.0
E2	82	0.0	0.0	0.1	0.0	0.0	0.0	0.1	0.0	0.0
F1	1925	0.0	0.0	0.3	0.0	0.0	0.0	0.3	0.0	0.0
F2	1325	0.0	-0.2	-0.4	0.0	0.0	0.0	0.0	-0.2	-0.4
G1	680	0.0	0.0	0.2	0.0	0.0	0.0	0.2	0.0	0.0
G2	80	0.0	0.0	0.1	0.0	0.0	0.0	0.1	0.0	0.0
H1	1921	0.0	0.4	-0.1	0.0	0.0	0.0	0.4	0.0	-0.1
H2	1321	0.0	0.5	0.2	0.0	0.0	0.0	0.5	0.2	0.0
I1	676	0.0	0.0	0.1	0.0	0.0	0.0	0.1	0.0	0.0
I2	76	0.0	0.0	0.2	0.0	0.0	0.0	0.2	0.0	0.0
J1	1916	0.0	0.4	0.3	0.0	0.0	0.0	0.4	0.3	0.0
J2	1316	0.0	0.5	0.4	0.0	0.0	0.0	0.5	0.4	0.0
K1	671	0.0	0.0	0.1	0.0	0.0	0.0	0.1	0.0	0.0
K2	71	0.0	0.1	0.2	0.0	0.0	0.0	0.2	0.1	0.0
L1	1908	0.0	0.3	0.5	0.0	0.0	0.0	0.5	0.3	0.0
L2	1308	0.0	0.6	0.6	0.0	0.0	0.0	0.6	0.6	0.0
M1	663	0.0	0.0	0.1	0.0	0.0	0.0	0.1	0.0	0.0
M2	63	0.0	0.0	0.1	0.0	0.0	0.0	0.1	0.0	0.0
N1	1877	0.0	0.4	0.3	0.0	0.0	0.0	0.4	0.3	0.0

Table 2.10.4-29 Primary Stresses; Cold Condition; 3-D Top Model; 0-Degree Circumferential Location; Condition 4 (continued)

Stress Points		Stress Components (ksi)						Principal Stresses (ksi)		
Section[1]	Node	S_z	S_y	S_x	S_{xy}	S_{yz}	S_{xz}	S1	S2	S3
N2	1477	0.0	0.5	0.3	0.0	0.0	0.0	0.5	0.3	0.0
N3	1277	0.0	0.5	0.4	0.0	0.0	0.0	0.5	0.4	0.0
O1	647	0.0	0.0	0.0	0.0	0.0	0.0	0.0	0.0	0.0
O2	247	0.0	0.0	0.0	0.0	0.0	0.0	0.0	0.0	0.0
O3	47	0.0	0.0	0.0	0.0	0.0	0.0	0.0	0.0	0.0
P1	1840	0.0	0.4	-0.1	0.0	0.0	0.0	0.4	0.0	-0.2
P2	1640	0.0	0.4	0.0	0.0	0.0	0.0	0.4	0.0	0.0
P3	1440	0.0	0.4	0.1	0.0	0.0	0.0	0.5	0.1	0.0
P4	1240	0.0	0.5	0.3	0.0	0.0	0.0	0.5	0.3	0.0
Q1	628	0.0	-0.3	-0.2	0.0	0.0	0.0	0.0	-0.2	-0.3
Q2	428	0.0	-0.2	-0.1	0.0	0.0	0.0	0.0	-0.1	-0.2
Q3	228	0.0	-0.2	0.1	0.0	0.0	0.0	0.1	0.0	-0.2
Q4	28	0.0	-0.1	0.2	0.0	0.0	0.0	0.2	0.0	-0.1
R1	1816	-0.2	-0.1	1.1	0.0	0.0	0.1	1.1	-0.1	-0.2
R2	1616	-0.3	-0.4	0.2	0.0	0.0	0.2	0.2	-0.4	-0.4
R3	1416	-0.9	-0.7	-0.3	0.0	0.0	0.1	-0.3	-0.7	-1.0
R4	1216	-1.9	-1.1	-0.7	0.0	0.0	-0.1	-0.7	-1.1	-1.9
S1	616	-1.2	-0.7	0.4	0.0	0.0	0.2	0.4	-0.7	-1.2
S2	416	-0.6	-0.6	0.4	0.0	0.0	0.4	0.5	-0.6	-0.8
S3	216	0.0	-0.6	-0.3	0.0	0.0	0.5	0.3	-0.6	-0.7
S4	16	0.3	-0.6	-0.7	0.0	0.0	0.3	0.4	-0.6	-0.8
T1	811	0.5	0.1	0.2	0.0	0.0	0.4	0.8	0.1	-0.1
T2	611	0.6	-0.1	-0.6	0.0	0.0	0.2	0.6	-0.1	-0.6
T3	411	0.2	-0.1	-0.2	0.0	0.0	0.2	0.3	-0.1	-0.3
T4	211	0.1	0.0	0.1	0.0	0.0	0.1	0.2	0.0	0.0
T5	11	0.0	0.0	0.4	0.0	0.0	0.1	0.4	0.0	0.0
U1	43058	0.2	-0.7	-2.1	0.0	0.0	0.3	0.2	-0.7	-2.1
U2	43057	-0.6	-0.9	-2.1	0.0	0.0	0.5	-0.5	-0.9	-2.2
U3	43056	-0.7	-1.0	-2.3	0.0	0.0	0.7	-0.5	-1.0	-2.5
U4	43055	-0.4	-0.9	-2.6	0.0	0.0	0.4	-0.3	-0.9	-2.6
U5	43054	-0.2	-0.8	-2.6	0.1	0.0	0.0	-0.2	-0.8	-2.6

Table 2.10.4-29 Primary Stresses; Cold Condition; 3-D Top Model; 0-Degree Circumferential Location; Condition 4 (continued)

Stress Points		Stress Components (ksi)						Principal Stresses (ksi)		
Section[1]	Node	S_x	S_y	S_z	S_{xy}	S_{yz}	S_{xz}	S1	S2	S3
U6	43053	-0.3	-0.7	-2.2	0.0	0.0	-0.4	-0.2	-0.7	-2.3
U7	43052	-0.6	-0.5	-1.5	0.0	0.0	-0.4	-0.4	-0.5	-1.7
U8	43051	1.0	0.3	-0.6	0.0	0.0	-0.3	1.0	0.3	-0.6
V1	50024	0.4	-0.1	-0.7	0.0	0.0	-0.1	0.4	-0.1	-0.7
V2	50023	0.2	-0.2	-0.9	0.0	0.0	0.0	0.2	-0.2	-0.9
V3	50022	-0.1	-0.1	-0.2	0.0	0.0	0.0	-0.1	-0.1	-0.2
V4	50021	-0.7	0.0	0.6	0.0	0.0	0.0	0.6	0.0	-0.7
W1	43278	-0.2	-0.3	0.1	0.0	0.0	0.1	0.1	-0.2	-0.3
W2	43274	0.0	-0.1	0.0	0.0	0.0	0.1	0.1	0.0	-0.1
W3	43271	0.2	0.1	0.0	0.0	0.0	0.0	0.2	0.1	-0.1
X1	50084	-0.1	-0.1	0.0	0.0	0.0	0.0	0.0	-0.1	-0.1
X2	50083	0.0	0.0	0.0	0.0	0.0	0.0	0.0	0.0	-0.1
X3	50081	0.1	0.1	-0.1	0.0	0.0	0.0	0.1	0.1	-0.1

[1] Refer to Figure 2.10.2-34 for the identification of the representative sections.

Table 2.10.4-30 Primary + Secondary Stresses; Cold Condition; 3-D Top Model; 0-Degree Circumferential Location; Condition 4

Condition 4: -40°F Ambient, No Decay Heat

Stress Points		Stress Components (ksi)						Principal Stresses (ksi)		
Section[1]	Node	S_x	S_y	S_z	S_{xy}	S_{yz}	S_{zx}	S1	S2	S3
A1	1949	0.1	0.1	0.0	0.0	0.0	0.1	0.1	0.1	-0.1
A2	1950	-0.1	-0.1	0.0	0.0	0.0	0.1	0.0	-0.1	-0.1
A3	1951	0.9	0.9	0.1	0.0	0.0	0.0	0.9	0.9	0.1
B1	1952	0.8	0.8	0.2	0.0	0.0	0.0	0.8	0.8	0.2
B2	93	-0.2	-0.2	-0.2	0.0	0.0	-0.1	-0.1	-0.2	-0.3
C1	1925	-1.1	-1.1	1.0	0.0	0.0	0.3	1.1	-1.1	-1.2
C2	1926	-1.3	-0.7	0.9	0.0	0.1	0.5	1.0	-0.7	-1.4
C3	1927	2.3	2.2	1.4	0.0	0.0	0.3	2.4	2.2	1.3
D1	683	-0.1	-0.6	-5.3	0.1	0.0	-0.4	0.0	-0.7	-5.3
D2	85	0.8	-2.3	-4.5	0.2	0.0	-0.7	0.9	-2.3	-4.6
E1	682	0.0	-0.5	-5.0	0.1	0.0	0.2	0.1	-0.5	-5.0
E2	82	-0.5	1.8	5.2	-0.2	0.0	-0.3	5.2	1.8	-0.5
F1	1925	-1.1	-1.1	1.0	0.0	0.0	0.3	1.1	-1.1	-1.2
F2	1325	0.2	-1.4	-1.7	0.1	0.0	0.4	0.2	-1.4	-1.7
G1	680	0.6	0.0	2.2	0.0	0.0	0.3	2.3	0.5	0.0
G2	80	0.4	-1.2	-2.4	0.1	0.0	-0.1	0.5	-1.2	-2.4
H1	1921	0.0	-3.0	-0.1	0.2	0.0	0.0	0.0	-0.1	-3.0
H2	1321	0.0	-2.8	-0.1	0.2	0.0	0.0	0.0	-0.1	-2.8
I1	676	0.0	-0.4	-0.1	0.0	0.0	0.0	0.0	-0.1	-0.4
I2	76	0.0	-0.2	0.6	0.0	0.0	0.0	0.6	0.0	-0.2
J1	1916	-0.1	-3.5	0.1	0.2	0.0	0.0	0.1	-0.1	-3.5
J2	1316	-0.1	-3.1	0.3	0.2	0.0	0.0	0.3	-0.1	-3.2
K1	671	0.0	0.1	0.2	0.0	0.0	0.0	0.2	0.1	0.0
K2	71	0.0	-0.1	0.2	0.0	0.0	0.0	0.2	0.0	-0.1
L1	1908	-0.1	-3.5	0.4	0.2	0.0	0.0	0.4	-0.1	-3.5
L2	1308	-0.1	-3.2	0.5	0.3	0.0	0.0	0.5	-0.1	-3.2
M1	663	0.1	0.5	0.2	0.0	0.0	0.0	0.5	0.2	0.1
M2	63	0.0	-0.4	-0.1	-0.2	0.0	0.0	0.0	-0.1	-0.5
N1	1877	-0.1	-3.2	0.3	0.2	0.0	0.0	0.3	-0.1	-3.2

Table 2.10.4-30 Primary + Secondary Stresses; Cold Condition; 3-D Top Model; 0-Degree Circumferential Location; Condition 4 (continued)

Stress Points		Stress Components (ksi)						Principal Stresses (ksi)		
Section[1]	Node	S_x	S_y	S_z	S_{xy}	S_{yz}	S_{zx}	S1	S2	S3
N2	1477	-0.3	-3.4	0.4	0.2	0.0	0.0	0.4	-0.3	-3.4
N3	1277	-0.4	-3.6	0.4	0.2	0.0	0.0	0.4	-0.4	-3.6
O1	647	0.0	1.1	-0.1	-0.1	0.1	0.0	1.1	0.0	-0.1
O2	247	0.0	0.1	-0.4	0.0	0.1	0.0	0.2	0.0	-0.4
O3	47	0.0	-0.8	-0.6	0.1	0.0	0.0	0.0	-0.6	-0.8
P1	1840	0.0	-2.2	0.0	0.2	0.1	0.0	0.0	-0.1	-2.2
P2	1640	0.0	-2.6	0.1	0.2	0.1	0.0	0.1	0.0	-2.6
P3	1440	0.0	-3.0	0.1	0.2	0.1	0.0	0.2	0.0	-3.0
P4	1240	0.0	-3.3	0.3	0.2	0.0	0.0	0.3	0.0	-3.3
Q1	628	0.0	0.2	-1.2	0.0	0.1	0.0	0.2	0.0	-1.2
Q2	428	0.0	-0.4	-1.0	0.0	0.1	0.0	0.0	-0.4	-1.0
Q3	228	0.0	-1.0	-0.8	0.1	0.1	0.0	0.0	-0.8	-1.0
Q4	28	0.0	-1.6	-0.7	0.1	0.1	0.0	0.0	-0.7	-1.6
R1	1816	-0.2	2.2	1.8	-0.2	0.0	0.5	2.2	1.9	-0.3
R2	1616	-0.4	1.2	0.2	-0.1	0.1	0.7	1.2	0.6	-0.9
R3	1416	-1.2	0.2	-0.7	-0.1	0.1	0.7	0.3	-0.3	-1.7
R4	1216	-2.9	-0.9	-1.5	0.0	0.1	0.3	-0.8	-1.4	-2.9
S1	616	-2.3	-1.0	3.4	0.1	-0.2	0.1	3.4	-1.0	-2.3
S2	416	-0.9	-1.8	1.0	0.1	0.0	1.0	1.4	-1.3	-1.8
S3	216	0.2	-3.0	-2.9	0.2	0.1	1.3	0.7	-3.0	-3.3
S4	16	1.1	-3.9	-5.9	0.4	0.1	0.9	1.3	-4.0	-6.1
T1	811	3.5	3.2	3.3	-0.2	-0.1	1.1	4.6	3.1	2.2
T2	611	0.6	1.2	0.8	-0.1	-0.1	0.5	1.3	1.0	0.2
T3	411	0.5	0.2	-0.8	0.0	0.0	0.1	0.5	0.2	-0.8
T4	211	0.2	-0.7	-2.2	0.1	0.0	0.0	0.2	-0.7	-2.2
T5	11	0.1	-1.5	-3.9	0.1	0.1	0.0	0.1	-1.5	-3.9
U1	43058	-4.1	-3.5	-5.2	0.2	0.0	0.8	-3.4	-3.8	-5.6
U2	43057	-2.5	-2.8	-4.6	0.2	0.0	1.0	-2.0	-2.8	-5.1
U3	43056	-1.7	-2.2	-4.0	0.2	0.0	1.2	-1.2	-2.2	-4.5
U4	43055	-0.8	-1.7	-3.8	0.2	0.0	0.8	-0.6	-1.8	-4.0
U5	43054	-0.2	-1.3	-3.5	0.2	-0.1	0.3	-0.1	-1.3	-3.6

Table 2.10.4-30 Primary + Secondary Stresses; Cold Condition; 3-D Top Model; 0-Degree Circumferential Location; Condition 4 (continued)

Stress Points		Stress Components (ksi)						Principal Stresses (ksi)		
Section[1]	Node	S_x	S_y	S_z	S_{xy}	S_{yz}	S_{xz}	S1	S2	S3
U6	43053	-0.1	-0.9	-2.6	0.1	-0.1	-0.2	-0.1	-0.9	-2.7
U7	43052	0.4	-0.7	-3.1	0.1	-0.1	-0.4	0.5	-0.7	-3.1
U8	43051	1.3	0.4	-1.1	0.0	-0.1	-0.8	1.5	0.4	-1.4
V1	50024	-3.1	-2.5	-0.1	0.0	0.0	0.3	-0.1	-2.5	-3.2
V2	50023	-2.2	-1.8	-0.6	0.0	0.0	0.4	-0.6	-1.8	-2.3
V3	50022	-0.4	-0.6	-0.3	0.0	0.0	0.3	0.0	-0.6	-0.7
V4	50021	0.9	0.6	0.5	0.0	0.0	0.2	1.0	0.6	0.4
W1	43278	-1.0	-1.0	0.2	0.0	0.0	0.1	0.2	-1.0	-1.0
W2	43274	-0.5	-0.6	0.0	0.0	0.0	0.1	0.0	-0.5	-0.6
W3	43271	1.2	1.0	-0.1	0.0	0.0	0.1	1.2	1.0	-0.1
X1	50084	-1.6	-1.7	0.2	0.0	0.0	0.2	0.2	-1.6	-1.7
X2	50083	-1.1	-1.3	0.1	0.0	0.0	0.2	0.1	-1.1	-1.3
X3	50081	-0.1	-0.6	-0.4	0.0	0.0	0.2	0.0	-0.5	-0.6

[1] Refer to Figure 2.10.2-34 for the identification of the representative sections.

Table 2.10.4-31 P_m Stresses; Cold Condition; 3-D Top Model; 0-Degree Circumferential Location; Condition 4

Condition 4: -40°F Ambient, No Decay Heat

		Stress Components (ksi)						Principal Stresses (ksi)			
Section[1]	Node - Node	S_x	S_y	S_z	S_{xy}	S_{yz}	S_{xz}	S1	S2	S3	S.I.
A	1949 - 1951	0.0	0.0	0.0	0.0	0.0	0.0	0.0	0.0	0.0	0.0
B	1952 - 93	0.0	0.0	0.0	0.0	0.0	0.0	0.0	0.0	0.0	0.1
C	1925 - 1927	0.0	0.0	0.1	0.0	0.0	0.0	0.1	0.0	0.0	0.1
D	683 - 85	0.0	0.1	0.0	0.0	0.0	0.0	0.1	0.0	0.0	0.1
E	682 - 82	0.0	0.0	0.0	0.0	0.0	0.0	0.0	0.0	0.0	0.1
F	1925 - 1325	0.0	-0.1	-0.1	0.0	0.0	0.0	0.0	-0.1	-0.1	0.1
G	680 - 80	0.0	0.0	0.1	0.0	0.0	0.0	0.1	0.0	0.0	0.1
H	1921 - 1321	0.0	0.4	0.1	0.0	0.0	0.0	0.4	0.1	0.0	0.4
I	676 - 76	0.0	0.0	0.2	0.0	0.0	0.0	0.2	0.0	0.0	0.2
J	1916 - 1316	0.0	0.4	0.4	0.0	0.0	0.0	0.5	0.4	0.0	0.5
K	671 - 71	0.0	0.0	0.1	0.0	0.0	0.0	0.1	0.0	0.0	0.1
L	1908 - 1308	0.0	0.4	0.5	0.0	0.0	0.0	0.5	0.4	0.0	0.6
M	663 - 63	0.0	0.0	0.1	0.0	0.0	0.0	0.1	0.0	0.0	0.1
N	1877 - 1277	0.0	0.5	0.3	0.0	0.0	0.0	0.5	0.3	0.0	0.5
O	647 - 47	0.0	0.0	0.0	0.0	0.0	0.0	0.0	0.0	0.0	0.0
P	1840 - 1240	0.0	0.4	0.1	0.0	0.0	0.0	0.4	0.1	0.0	0.4
Q	628 - 28	0.0	-0.2	0.0	0.0	0.0	0.0	0.0	0.0	-0.2	0.2
R	1816 - 1216	-0.8	-0.6	0.0	0.0	0.0	0.1	0.0	-0.6	-0.8	0.8
S	616 - 16	-0.4	-0.6	0.0	0.0	0.0	0.4	0.2	-0.6	-0.6	0.9
T	811 - 11	0.3	0.0	-0.1	0.0	0.0	0.2	0.4	0.0	-0.2	0.5
U	43058 - 43051	-0.3	-0.6	-1.9	0.0	0.0	0.0	-0.3	-0.6	-1.9	1.7
V	50024 - 50021	0.0	-0.1	-0.4	0.0	0.0	0.0	0.0	-0.1	-0.4	0.4
W	43278 - 43271	0.0	-0.1	0.0	0.0	0.0	0.1	0.1	-0.1	-0.1	0.2
X	50084 - 50081	0.0	0.0	0.0	0.0	0.0	0.0	0.0	0.0	0.0	0.1

[1] Refer to Figure 2.10.2-34 for the identification of the representative sections.

Table 2.10.4-32 $P_m + P_b$ Stresses; Cold Condition; 3-D Top Model; 0-Degree Circumferential Location; Condition 4

Condition 4: -40°F Ambient, No Decay Heat

		Stress Components (ksi)						Principal Stresses (ksi)			
Section[1]	Node - Node	S_x	S_y	S_z	S_{xy}	S_{yz}	S_{xz}	S1	S2	S3	S.I.
A I	1949 - 1951	-0.1	0.1	0.0	0.0	0.0	0.0	0.0	-0.1	-0.1	0.1
B O	1952 - 93	0.1	0.1	-0.1	0.0	0.0	0.0	0.1	0.1	-0.1	0.2
C I	1925 - 1927	0.0	0.0	0.2	0.0	0.0	0.0	0.2	0.0	0.0	0.2
D O	683 - 85	0.0	0.1	0.0	0.0	0.0	0.0	0.1	0.0	0.0	0.1
E O	682 - 82	0.0	0.0	0.1	0.0	0.0	0.0	0.1	0.0	0.0	0.1
F O	1925 - 1325	0.0	-0.2	-0.4	0.0	0.0	0.0	0.0	-0.2	-0.4	0.4
G I	680 - 80	0.0	0.0	0.2	0.0	0.0	0.0	0.2	0.0	0.0	0.2
H O	1921 - 1321	0.0	0.5	0.2	0.0	0.0	0.0	0.5	0.2	0.0	0.5
I O	676 - 76	0.0	0.0	0.2	0.0	0.0	0.0	0.2	0.0	0.0	0.2
J O	1916 - 1316	0.0	0.5	0.4	0.0	0.0	0.0	0.5	0.4	0.0	0.5
K O	671 - 71	0.0	0.1	0.2	0.0	0.0	0.0	0.2	0.1	0.0	0.2
L O	1908 - 1308	0.0	0.6	0.6	0.0	0.0	0.0	0.6	0.6	0.0	0.6
M O	663 - 63	0.0	0.0	0.1	0.0	0.0	0.0	0.1	0.0	0.0	0.1
N O	1877 - 1277	0.0	0.5	0.4	0.0	0.0	0.0	0.5	0.4	0.0	0.5
O I	647 - 47	0.0	0.0	0.0	0.0	0.0	0.0	0.0	0.0	0.0	0.0
P I	1840 - 1240	0.0	0.4	-0.2	0.0	0.0	0.0	0.4	0.0	-0.2	0.5
Q O	628 - 28	0.0	-0.1	0.2	0.0	0.0	0.0	0.2	0.0	-0.1	0.4
R I	1816 - 1216	0.1	-0.1	0.9	0.0	0.0	0.2	0.9	0.1	-0.1	1.0
S I	616 - 16	-1.1	-0.6	0.6	0.0	0.0	0.3	0.7	-0.6	-1.2	1.9
T I	811 - 11	0.7	0.0	-0.4	0.0	0.0	0.3	0.8	0.0	-0.5	1.3
U I	43058 - 43051	-0.6	-1.1	-2.7	0.0	0.0	0.7	-0.4	-1.2	-2.9	2.4
V I	50024 - 50021	0.5	-0.2	-1.1	0.1	0.0	-0.1	0.5	-0.2	-1.1	1.5
W I	43278 - 43271	-0.2	-0.3	0.1	0.0	0.0	0.1	0.1	-0.2	-0.3	0.4
X O	50084 - 50081	0.1	0.1	-0.1	0.0	0.0	0.0	0.1	0.1	-0.1	0.2

[1] Refer to Figure 2.10.2-34 for the identification of the representative sections.

Table 2.10.4-33 S_n Stresses; Cold Condition; 3-D Top Model; 0-Degree Circumferential Location; Condition 4

Condition 4: -40°F Ambient, No Decay Heat

		Stress Components (ksi)						Principal Stresses (ksi)			
Section[1]	Node - Node	S_x	S_y	S_z	S_{xy}	S_{yz}	S_{zx}	S1	S2	S3	S.I.
A O	1949 - 1951	0.8	0.8	0.1	0.0	0.0	0.0	0.8	0.8	0.1	0.8
B I	1952 - 93	0.8	0.8	0.2	0.0	0.0	0.0	0.8	0.8	0.2	0.6
C I	1925 - 1927	-1.9	-1.4	0.9	0.0	0.1	0.5	0.9	-1.4	-2.0	2.9
D O	683 - 85	0.8	-2.3	-4.5	0.2	0.0	-0.7	0.9	-2.3	-4.6	5.5
E O	682 - 82	-0.5	1.8	5.2	-0.2	0.0	-0.3	5.2	1.8	-0.5	5.8
F I	1925 - 1325	-1.1	-1.1	1.0	0.0	0.0	0.3	1.1	-1.1	-1.2	2.2
G O	680 - 80	0.4	-1.2	-2.4	0.1	0.0	-0.1	0.5	-1.2	-2.4	2.8
H I	1921 - 1321	0.0	-3.0	-0.1	0.2	0.0	0.0	0.0	-0.1	-3.0	3.0
I O	676 - 76	0.0	-0.2	0.6	0.0	0.0	0.0	0.6	0.0	-0.2	0.8
J I	1916 - 1316	-0.1	-3.5	0.1	0.2	0.0	0.0	0.1	-0.1	-3.5	3.6
K O	671 - 71	0.0	-0.1	0.2	0.0	0.0	0.0	0.2	0.0	-0.1	0.2
L I	1908 - 1308	-0.1	-3.5	0.4	0.2	0.0	0.0	0.4	-0.1	-3.5	3.9
M O	663 - 63	0.0	-0.4	-0.1	-0.2	0.0	0.0	0.0	-0.1	-0.5	0.5
N O	1877 - 1277	-0.4	-3.6	0.4	0.2	0.0	0.0	0.4	-0.4	-3.6	4.0
O I	647 - 47	0.0	1.1	-0.1	-0.1	0.1	0.0	1.1	0.0	-0.1	1.2
P O	1840 - 1240	0.0	-3.3	0.3	0.2	0.0	0.0	0.3	0.0	-3.3	3.6
Q O	628 - 28	0.0	-1.6	-0.7	0.1	0.1	0.0	0.0	-0.7	-1.6	1.6
R I	1816 - 216	0.2	2.2	1.4	-0.2	0.0	0.6	2.2	1.7	0.0	2.3
S O	616 - 16	1.3	-4.0	-6.0	0.4	0.1	1.4	1.5	-4.0	-6.2	7.8
T O	811 - 11	-0.5	-1.8	-4.0	0.1	0.1	-0.2	-0.4	-1.8	-4.0	3.6
U O	43058 - 43051	1.6	0.4	-1.7	0.1	-0.1	-0.9	1.8	0.4	-1.9	3.7
V I	50024 - 50021	-3.4	-2.7	-0.6	0.0	0.0	0.3	-0.6	-2.7	-3.4	2.9
W I	43278 - 43271	-1.3	-1.3	0.1	0.0	0.0	0.1	0.2	-1.3	-1.3	1.4
X I	50084 - 50081	-1.5	-1.7	0.2	0.0	0.0	0.2	0.3	-1.6	-1.7	1.9

[1] Refer to Figure 2.10.2-34 for the identification of the representative sections.

Table 2.10.4-34 Critical P_m Stress Summary; Cold Condition; 3-D Top Model; Condition 4

Condition 4: -40°F Ambient, No Decay Heat

Comp. No.[1]	Section Cut Node-Node	P_m Stresses (ksi) S_x	S_y	S_z	S_{xy}	S_{yz}	S_{xz}	Principal Stresses (ksi) S1	S2	S3	S.I.	Allow. Stress	Margin of Safety
1	683- 85	0.0	0.1	0.0	0.0	0.0	0.0	0.1	0.0	0.0	0.1	19.2	191.0
2	18679-18079	0.1	0.1	0.0	1.9	0.2	0.0	2.0	0.0	-1.9	3.9	18.5	3.7
3	15841-15241	0.0	0.3	0.2	0.0	0.3	0.0	0.6	0.0	-0.1	0.7	31.4	43.9
4	1907- 1307	0.0	0.4	0.5	-0.1	0.0	0.0	0.5	0.5	0.0	0.6	19.6	31.7
5	625- 25	0.0	-0.4	0.0	0.0	0.0	0.0	0.0	0.0	-0.4	0.4	20.0	49.0
6	29216-29211	0.1	1.3	3.9	0.0	0.0	0.2	3.9	1.3	0.1	3.8	20.0	4.3
7	43021-43028	-0.2	-2.5	-9.4	0.2	0.0	-0.1	-0.2	-2.6	-9.4	9.2	20.0	1.2
8	50916-50919	0.0	0.0	-0.1	0.0	0.0	0.2	0.2	0.0	-0.2	0.4	45.0	111.5

Locations of the most critical sections for each component are provided in the following:

Comp. No.[1]	Section Location Inside Node x (in)	y (deg)	z (in)	Outside Node x (in)	y (deg)	z (in)
1	39.44	0.0	6.20	39.44	0.0	0.75
2	40.70	91.7	17.40	43.35	91.7	17.40
3	35.50	67.7	159.90	37.00	67.7	159.90
4	35.50	0.0	99.50	37.00	0.0	99.50
5	40.70	0.0	163.40	43.35	0.0	163.40
6	37.50	163.4	175.40	37.66	163.4	179.40
7	37.66	0.0	185.40	37.66	0.0	179.40
8	36.46	91.7	193.71	36.46	91.7	188.40

[1] Refer to Figure 2.10.2-33 for cask component identification.

Table 2.10.4-35 Critical $P_m + P_b$ Stress Summary; Cold Condition; 3-D Top Model; Condition 4

Condition 4: -40°F Ambient, No Decay Heat

Comp. No.[1]	Section Cut Node-Node	$P_m + P_b$ Stresses (ksi) S_x	S_y	S_z	S_{xy}	S_{yz}	S_{xz}	Principal Stresses (ksi) S1	S2	S3	S.I.	Allow. Stress	Margin of Safety
1	1952- 93	0.1	0.1	-0.1	0.0	0.0	0.0	0.1	0.1	-0.1	0.2	28.7	142.5
2	18679-18079	0.1	0.2	0.1	2.1	0.4	0.0	2.3	0.1	-2.0	4.2	27.7	5.6
3	13841-13241	0.0	0.3	0.0	0.0	0.4	0.0	0.6	0.0	-0.3	0.8	47.1	57.9
4	1909- 1309	0.0	0.5	0.6	0.0	0.0	0.0	0.6	0.5	0.0	0.6	29.4	48.0
5	625- 25	0.0	-0.3	0.1	0.0	0.0	0.0	0.1	0.0	-0.3	0.5	30.0	59.0
6	29216-29211	1.9	3.7	10.8	0.0	0.0	0.2	10.8	3.7	1.9	8.9	30.0	2.4
7	43021-43028	-1.2	-3.4	-10.9	0.2	0.0	0.7	-1.2	-3.4	-10.9	9.8	30.0	2.1
8	50921-50924	1.0	0.2	-0.7	0.0	0.0	0.0	1.0	0.2	-0.7	1.7	67.5	38.7

Locations of the most critical sections for each component are provided in the following:

Comp. No.[1]	Section Location Inside Node x (in)	y (deg)	z (in)	Outside Node x (in)	y (deg)	z (in)
1	0.00	0.0	6.20	0.00	0.0	0.75
2	40.70	91.7	17.40	43.35	91.7	17.40
3	35.50	56.5	159.90	37.00	56.5	159.90
4	35.50	0.0	93.56	37.00	0.0	93.56
5	40.70	0.0	163.40	43.35	0.0	163.40
6	37.50	163.4	175.40	37.66	163.4	179.40
7	37.66	0.0	185.40	37.66	0.0	179.40
8	35.21	91.7	193.71	35.21	91.7	188.40

[1] Refer to Figure 2.10.2-33 for cask component identification.

Table 2.10.4-36 Critical S_n Stress Summary; Cold Condition; 3-D Top Model; Condition 4

Condition 4: -40°F Ambient, No Decay Heat

Comp. No.[1]	Section Cut Node-Node	S_n Stresses (ksi) S_x	S_y	S_z	S_{xy}	S_{yz}	S_{xz}	Principal Stresses (ksi) S1	S2	S3	S.I.	Allow. Stress 3.0 S_m
1	20683-20085	0.8	-2.3	-4.5	0.0	0.0	-0.7	0.9	-2.3	-4.6	5.5	57.6
2	682- 82	-0.5	1.8	5.2	-0.2	0.0	-0.3	5.2	1.8	-0.5	5.8	55.5
3	15847-15247	-0.1	-3.7	0.5	0.0	0.3	0.0	0.5	-0.1	-3.7	4.2	94.2
4	1875- 1275	-0.5	-3.6	0.4	0.2	0.0	0.0	0.4	-0.4	-3.6	4.1	58.8
5	10625-10025	0.1	-1.9	0.8	0.0	0.3	0.0	0.9	0.1	-2.0	2.9	60.0
6	11216-11211	1.3	2.0	11.4	-0.3	-0.3	-0.4	11.5	2.1	1.2	10.2	60.0
7	50030-63071	11.7	2.0	-3.5	0.5	-0.1	1.2	11.8	2.0	-3.6	15.4	60.0
8	50001-50004	-4.6	-1.8	3.5	-0.1	0.0	0.5	3.5	-1.8	-4.6	8.1	135.0

Locations of the most critical sections for each component are provided in the following:

Comp. No.[1]	Section Location Inside Node x (in)	y (deg)	z (in)	Outside Node x (in)	y (deg)	z (in)
1	39.44	104.7	6.20	39.44	104.7	0.75
2	39.44	0.0	8.20	43.35	0.0	8.20
3	35.50	67.7	156.90	37.00	67.7	156.90
4	35.50	0.0	141.10	37.00	0.0	141.10
5	40.70	45.9	163.40	43.35	45.9	163.40
6	37.50	45.9	175.40	37.66	45.9	179.40
7	33.71	0.0	188.40	33.71	0.0	187.40
8	40.88	0.0	193.71	40.88	0.0	188.40

[1] Refer to Figure 2.10.2-33 for cask component identification.

Table 2.10.4-37 Primary Stresses; 1-Foot Top End Drop; Drop Orientation = 0 Degrees; 2-D Model; Condition 1

Condition 1: 100°F Ambient with Contents

Stress Points		Stress Components (ksi)						Principal Stresses (ksi)		
Section[1]	Node	S_x	S_y	S_z	S_{xy}	S_{yz}	S_{xz}	S1	S2	S3
A1	1	-0.7	0.0	-0.7	0.0	0.0	0.0	0.0	-0.7	-0.7
A1	1	0.9	0.0	0.9	0.0	0.0	0.0	0.9	0.9	0.0
A2	2	0.5	0.0	0.5	0.0	0.0	0.0	0.5	0.5	0.0
A3	3	0.1	0.0	0.1	0.0	0.0	0.0	0.1	0.1	0.0
A4	4	-0.2	0.0	-0.2	0.0	0.0	0.0	0.0	-0.2	-0.2
A5	5	-0.6	0.0	-0.6	0.0	0.0	0.0	0.0	-0.6	-0.6
B1	6	0.5	0.0	0.5	0.0	0.0	0.0	0.5	0.5	0.0
B2	7	0.2	0.0	0.2	0.0	0.0	0.0	0.2	0.2	0.0
B3	8	-0.1	0.0	-0.1	0.0	0.0	0.0	0.0	-0.1	-0.1
B4	9	-0.5	0.0	-0.5	0.0	0.0	0.0	0.0	-0.5	-0.5
B5	10	-0.8	0.0	-0.8	0.0	0.0	0.0	0.0	-0.8	-0.8
C1	251	-0.3	-0.1	0.2	-0.1	0.0	0.0	0.2	-0.1	-0.3
C2	252	-0.1	-0.1	0.2	-0.1	0.0	0.0	0.2	0.0	-0.2
C3	253	0.1	-0.1	0.1	-0.1	0.0	0.0	0.2	0.1	-0.1
C4	254	0.4	-0.1	0.1	-0.1	0.0	0.0	0.4	0.1	-0.1
C5	255	0.6	0.0	0.1	-0.1	0.0	0.0	0.6	0.1	0.0
D1	306	-0.7	-0.5	-0.3	-0.2	0.0	0.0	-0.3	-0.3	-0.8
D2	307	-0.2	-0.3	-0.2	-0.1	0.0	0.0	-0.2	-0.2	-0.4
D3	308	-0.1	-0.1	-0.1	0.0	0.0	0.0	-0.1	-0.1	-0.1
D4	309	0.1	-0.1	-0.1	0.0	0.0	0.0	0.1	-0.1	-0.1
D5	310	0.2	0.0	-0.2	0.0	0.0	0.0	0.3	0.0	-0.2
E1	305	0.7	0.0	0.2	-0.1	0.0	0.0	0.7	0.2	-0.1
E2	315	0.3	-0.2	0.1	-0.2	0.0	0.0	0.4	0.1	-0.2
E3	325	0.1	-0.2	0.0	-0.2	0.0	0.0	0.2	0.0	-0.2
E4	335	0.1	-0.1	0.0	-0.1	0.0	0.0	0.1	0.0	-0.2
E5	345	0.0	-0.1	0.0	-0.1	0.0	0.0	0.1	0.0	-0.2
E6	355	0.0	-0.2	0.0	0.0	0.0	0.0	0.0	0.0	-0.2
F1	251	-0.3	-0.1	0.2	-0.1	0.0	0.0	0.2	-0.1	-0.3
F2	261	-0.3	-0.2	0.1	0.0	0.0	0.0	0.1	-0.2	-0.3
F3	271	-0.4	-0.4	0.1	0.1	0.0	0.0	0.1	-0.3	-0.4
F4	281	-0.5	-0.6	0.0	0.1	0.0	0.0	0.0	-0.4	-0.7

Table 2.10.4-37 Primary Stresses; 1-Foot Top End Drop; Drop Orientation = 0 Degrees; 2-D Model; Condition 1 (continued)

Stress Points		Stress Components (ksi)						Principal Stresses (ksi)		
Section[1]	Node	S_x	S_y	S_z	S_{xy}	S_{yz}	S_{xz}	S1	S2	S3
G1	311	-0.3	-0.6	0.0	-0.1	0.0	0.0	0.0	-0.3	-0.6
G2	321	-0.2	-0.4	0.1	0.0	0.0	0.0	0.1	-0.2	-0.4
G3	331	-0.1	-0.2	0.1	0.0	0.0	0.0	0.1	-0.1	-0.2
G4	341	0.0	-0.1	0.2	0.0	0.0	0.0	0.2	0.0	-0.1
G5	351	0.0	0.1	0.2	0.0	0.0	0.0	0.2	0.1	0.0
H1	581	-0.1	-0.8	1.0	0.0	0.0	0.0	1.0	-0.1	-0.8
H2	582	0.0	-0.8	1.0	0.0	0.0	0.0	1.0	0.0	-0.8
H3	583	0.0	-0.8	1.0	0.0	0.0	0.0	1.0	0.0	-0.8
H4	584	0.0	-0.8	0.9	0.0	0.0	0.0	0.9	0.0	-0.8
I1	589	0.0	-0.3	0.1	0.0	0.0	0.0	0.1	0.0	-0.3
I2	590	0.0	-0.4	0.0	0.0	0.0	0.0	0.0	0.0	-0.4
I3	591	0.0	-0.4	0.0	0.0	0.0	0.0	0.0	0.0	-0.4
I4	592	0.0	-0.4	0.0	0.0	0.0	0.0	0.0	0.0	-0.4
I5	593	0.0	-0.4	0.0	0.0	0.0	0.0	0.0	0.0	-0.4
J1	971	-0.1	-1.0	1.2	0.0	0.0	0.0	1.2	-0.1	-1.0
J2	972	0.0	-1.0	1.2	0.0	0.0	0.0	1.2	0.0	-1.0
J3	973	0.0	-1.0	1.2	0.0	0.0	0.0	1.2	0.0	-1.0
J4	974	0.0	-1.0	1.2	0.0	0.0	0.0	1.2	0.0	-1.0
K1	979	0.0	-0.6	0.0	0.0	0.0	0.0	0.0	0.0	-0.6
K2	980	0.0	-0.6	0.0	0.0	0.0	0.0	0.0	0.0	-0.6
K3	981	0.0	-0.6	0.0	0.0	0.0	0.0	0.0	0.0	-0.6
K4	982	0.0	-0.6	0.0	0.0	0.0	0.0	0.0	0.0	-0.6
K5	983	0.0	-0.6	0.0	0.0	0.0	0.0	0.0	0.0	-0.6
L1	1601	-0.1	-1.4	1.2	0.0	0.0	0.0	1.2	-0.1	-1.4
L2	1602	0.0	-1.4	1.2	0.0	0.0	0.0	1.2	0.0	-1.4
L3	1603	0.0	-1.4	1.2	0.0	0.0	0.0	1.2	0.0	-1.4
L4	1604	0.0	-1.4	1.2	0.0	0.0	0.0	1.2	0.0	-1.4
M1	1609	0.0	-1.0	0.0	0.0	0.0	0.0	0.0	0.0	-1.0
M2	1610	0.0	-1.0	0.0	0.0	0.0	0.0	0.0	0.0	-1.0
M3	1611	0.0	-1.0	0.0	0.0	0.0	0.0	0.0	0.0	-1.0
M4	1612	0.0	-1.0	0.0	0.0	0.0	0.0	0.0	0.0	-1.0
M5	1613	0.0	-1.0	0.0	0.0	0.0	0.0	0.0	0.0	-1.0
N1	2216	-0.1	-1.7	1.2	0.0	0.0	0.0	1.2	-0.1	-1.7

Table 2.10.4-37 Primary Stresses; 1-Foot Top End Drop; Drop Orientation = 0 Degrees; 2-D Model; Condition 1 (continued)

Stress Points		Stress Components (ksi)						Principal Stresses (ksi)		
Section[1]	Node	S_x	S_y	S_z	S_{xy}	S_{yz}	S_{zx}	S1	S2	S3
N2	2217	0.0	-1.7	1.2	0.0	0.0	0.0	1.2	0.0	-1.7
N3	2218	0.0	-1.7	1.2	0.0	0.0	0.0	1.2	0.0	-1.7
N4	2219	0.0	-1.7	1.2	0.0	0.0	0.0	1.2	0.0	-1.7
O1	2224	0.0	-1.3	0.0	0.0	0.0	0.0	0.0	0.0	-1.3
O2	2225	0.0	-1.3	0.0	0.0	0.0	0.0	0.0	0.0	-1.3
O3	2226	0.0	-1.3	0.0	0.0	0.0	0.0	0.0	0.0	-1.3
O4	2227	0.0	-1.3	0.0	0.0	0.0	0.0	0.0	0.0	-1.3
O5	2228	0.0	-1.3	0.0	0.0	0.0	0.0	0.0	0.0	-1.3
P1	2546	-0.1	-1.0	1.4	0.0	0.0	0.0	1.4	-0.1	-1.0
P2	2547	-0.1	-1.6	1.2	0.0	0.0	0.0	1.2	-0.1	-1.6
P3	2548	-0.1	-2.1	1.0	-0.1	0.0	0.0	1.0	-0.1	-2.1
P4	2549	0.0	-2.8	0.8	-0.2	0.0	0.0	0.8	0.0	-2.8
Q1	2554	0.0	-1.1	0.5	0.0	0.0	0.0	0.5	0.0	-1.1
Q2	2555	0.0	-1.3	0.4	0.0	0.0	0.0	0.4	0.0	-1.3
Q3	2556	0.0	-1.5	0.4	0.0	0.0	0.0	0.4	0.0	-1.5
Q4	2557	0.0	-1.7	0.3	0.0	0.0	0.0	0.3	0.0	-1.7
Q5	2558	0.0	-1.9	0.3	0.0	0.0	0.0	0.3	0.0	-1.9
R1	2771	-0.2	-6.5	0.0	0.1	0.0	0.0	0.0	-0.2	-6.5
R2	2772	0.0	-3.7	0.8	0.2	0.0	0.0	0.8	0.0	-3.7
R3	2773	0.1	-1.1	1.5	0.6	0.0	0.0	1.5	0.4	-1.4
R4	2774	-0.5	2.4	2.2	1.2	0.0	0.0	2.9	2.2	-0.9
S1	2779	-3.7	-4.7	-1.0	0.2	0.0	0.0	-1.0	-3.7	-4.7
S2	2780	-2.3	-2.7	-0.1	-0.1	0.0	0.0	-0.1	-2.3	-2.7
S3	2781	-1.2	-1.3	0.6	-0.4	0.0	0.0	0.6	-0.8	-1.7
S4	2782	-0.5	0.1	1.1	-0.3	0.0	0.0	1.1	0.2	-0.6
S5	2783	-0.2	1.9	1.6	-0.2	0.0	0.0	1.9	1.6	-0.2
T1	7066	4.0	3.7	1.9	1.2	0.0	0.0	5.0	2.6	1.9
T2	7067	3.0	0.8	0.9	0.3	0.0	0.0	3.0	0.9	0.8
T3	7068	2.0	-0.4	0.3	-0.1	0.0	0.0	2.0	0.3	-0.4
T4	7069	1.2	-1.2	-0.1	-0.4	0.0	0.0	1.2	-0.1	-1.2
T5	7070	0.6	-1.8	-0.4	-0.4	0.0	0.0	0.7	-0.4	-1.9
T6	7071	0.3	-2.6	-0.7	-0.3	0.0	0.0	0.3	-0.7	-2.6
T7	7072	0.1	-3.7	-1.0	-0.2	0.0	0.0	0.2	-1.0	-3.7

Table 2.10.4-37 Primary Stresses; 1-Foot Top End Drop; Drop Orientation = 0 Degrees; 2-D Model; Condition 1 (continued)

Stress Points		Stress Components (ksi)						Principal Stresses (ksi)		
Section[1]	Node	S_x	S_y	S_z	S_{xy}	S_{yz}	S_{xz}	S1	S2	S3
U1	3051	0.4	-4.5	1.7	1.2	0.0	0.0	1.7	0.7	-4.8
U2	3052	0.7	-4.7	0.8	1.4	0.0	0.0	1.1	0.8	-5.0
U3	3053	0.9	-4.4	0.2	1.3	0.0	0.0	1.2	0.2	-4.8
U4	3054	0.6	-3.9	-0.5	0.7	0.0	0.0	0.7	-0.5	-4.0
U5	3055	-0.2	-3.6	-1.3	0.7	0.0	0.0	0.0	-1.3	-3.7
U6	3056	0.0	-2.0	-1.4	1.2	0.0	0.0	0.6	-1.4	-2.5
V1	3611	-2.7	-1.2	2.3	-0.6	0.0	0.0	2.3	-1.0	-2.9
V2	3612	-1.8	-1.3	1.5	-0.8	0.0	0.0	1.5	-0.7	-2.4
V3	3613	-0.9	-1.5	0.7	-1.1	0.0	0.0	0.7	-0.1	-2.3
V4	3614	-0.1	-1.7	-0.2	-1.0	0.0	0.0	0.4	-0.2	-2.2
V5	3615	0.6	-2.0	-1.1	-0.9	0.0	0.0	0.9	-1.1	-2.2
V6	3616	0.6	-1.1	-1.9	-0.5	0.0	0.0	0.8	-1.3	-1.9
V7	3617	2.0	-0.2	-2.4	-0.3	0.0	0.0	2.1	-0.2	-2.4
W1	3241	-0.2	-0.3	-0.2	0.0	0.0	0.0	-0.2	-0.2	-0.3
W2	3242	0.3	-0.3	0.3	0.0	0.0	0.0	0.3	0.3	-0.3
W3	3243	0.8	-0.2	0.8	0.0	0.0	0.0	0.8	0.8	-0.2
W4	3244	1.2	-0.1	1.2	0.0	0.0	0.0	1.2	1.2	-0.1
W5	3245	1.7	-0.1	1.7	0.0	0.0	0.0	1.7	1.7	-0.1
W6	3246	2.2	0.0	2.2	0.0	0.0	0.0	2.2	2.2	0.0
X1	3801	18.5	-0.6	18.5	0.0	0.0	0.0	18.5	18.5	-0.6
X2	3802	12.5	-0.5	12.5	0.0	0.0	0.0	12.5	12.5	-0.5
X3	3803	6.5	-0.3	6.5	0.0	0.0	0.0	6.5	6.5	-0.3
X4	3804	0.4	-0.4	0.4	0.0	0.0	0.0	0.4	0.4	-0.4
X5	3805	-5.6	-0.5	-5.6	0.0	0.0	0.0	-0.5	-5.6	-5.6
X6	3806	-11.7	-0.4	-11.7	0.0	0.0	0.0	-0.4	-11.7	-11.7
X7	3807	-18.3	-0.3	-18.3	0.0	0.0	0.0	-0.3	-18.3	-18.3

[1] Refer to Figure 2.10.2-34 for the identification of the representative sections.

Table 2.10.4-38 Primary + Secondary Stresses; 1-Foot Top End Drop; Drop Orientation = 0 Degrees; 2-D Model; Condition 1

Condition 1: 100°F Ambient with Contents

Stress Points		Stress Components (ksi)						Principal Stresses (ksi)		
Section[1]	Node	S_x	S_y	S_z	S_{xy}	S_{yz}	S_{zx}	S1	S2	S3
A1	1	1.3	-0.1	1.3	0.0	0.0	0.0	1.3	1.3	-0.1
A2	2	0.4	0.0	0.4	0.0	0.0	0.0	0.4	0.4	0.0
A3	3	-0.4	0.0	-0.4	0.0	0.0	0.0	0.0	-0.4	-0.4
A4	4	-1.2	0.0	-1.2	0.0	0.0	0.0	0.0	-1.2	-1.2
A5	5	-2.0	0.0	-2.0	0.0	0.0	0.0	0.0	-2.0	-2.0
B1	6	1.9	0.0	1.9	0.0	0.0	0.0	1.9	1.9	0.0
B2	7	1.5	0.0	1.5	0.0	0.0	0.0	1.5	1.5	0.0
B3	8	1.2	0.0	1.2	0.0	0.0	0.0	1.2	1.2	0.0
B4	9	0.8	0.0	0.8	0.0	0.0	0.0	0.8	0.8	0.0
B5	10	0.5	0.0	0.5	0.0	0.0	0.0	0.5	0.5	0.0
C1	251	-0.8	-2.9	-0.3	-0.6	0.0	0.0	-0.3	-0.6	-3.0
C2	252	0.1	-1.4	-0.1	-0.6	0.0	0.0	0.3	-0.1	-1.6
C3	253	-0.2	-1.1	-0.6	-0.6	0.0	0.0	0.1	-0.6	-1.3
C4	254	-0.4	-1.1	-1.2	-0.4	0.0	0.0	-0.2	-1.2	-1.2
C5	255	-0.8	-1.1	-1.9	-0.2	0.0	0.0	-0.7	-1.1	-1.9
D1	306	4.9	6.1	3.1	1.8	0.0	0.0	7.4	3.6	3.1
D2	307	0.8	3.4	1.3	1.3	0.0	0.0	3.9	1.3	0.2
D3	308	0.3	1.3	0.8	0.5	0.0	0.0	1.4	0.8	0.1
D4	309	-0.4	0.5	0.5	0.1	0.0	0.0	0.5	0.5	-0.4
D5	310	-1.3	0.2	0.2	0.0	0.0	0.0	0.2	0.2	-1.3
E1	305	-0.4	3.6	0.4	0.4	0.0	0.0	3.6	0.4	-0.5
E2	315	-0.4	2.3	0.3	1.3	0.0	0.0	2.8	0.3	-0.9
E3	325	0.2	1.3	0.2	1.5	0.0	0.0	2.3	0.2	-0.9
E4	335	0.1	0.6	0.1	1.2	0.0	0.0	1.6	0.1	-0.8
E5	345	0.1	-0.2	-0.1	0.7	0.0	0.0	0.7	-0.1	-0.7
E6	355	0.1	-1.1	-0.3	0.4	0.0	0.0	0.2	-0.3	-1.2
F1	251	-0.8	-2.9	-0.3	-0.6	0.0	0.0	-0.3	-0.6	-3.0
F2	261	-0.4	-1.3	0.2	-0.5	0.0	0.0	0.2	-0.2	-1.5
F3	271	0.3	-0.2	0.5	-0.5	0.0	0.0	0.6	0.5	-0.5
F4	281	0.5	1.5	0.9	-0.9	0.0	0.0	2.0	0.9	0.0
G1	311	-3.7	-0.3	-0.8	1.3	0.0	0.0	0.2	-0.8	-4.1

Table 2.10.4-38 Primary + Secondary Stresses; 1-Foot Top End Drop; Drop Orientation = 0 Degrees; 2-D Model; Condition 1 (continued)

Stress Points		Stress Components (ksi)						Principal Stresses (ksi)		
Section[1]	Node	S_x	S_y	S_z	S_{xy}	S_{yz}	S_{xz}	S1	S2	S3
G2	321	-3.3	2.7	0.1	0.9	0.0	0.0	2.9	0.1	-3.4
G3	331	-1.6	4.2	1.0	0.2	0.0	0.0	4.2	1.0	-1.6
G4	341	-0.6	5.6	1.6	0.0	0.0	0.0	5.6	1.6	-0.6
G5	351	-0.2	7.7	2.3	-0.1	0.0	0.0	7.7	2.3	-0.2
H1	581	-0.1	-0.1	0.9	0.1	0.0	0.0	0.9	0.0	-0.2
H2	582	-0.1	-0.8	0.8	0.1	0.0	0.0	0.8	-0.1	-0.9
H3	583	0.0	-1.5	0.7	0.1	0.0	0.0	0.7	0.0	-1.5
H4	584	-0.2	-2.3	0.5	0.2	0.0	0.0	0.5	-0.1	-2.4
I1	589	-0.3	5.1	2.0	0.1	0.0	0.0	5.1	2.0	-0.3
I2	590	-0.2	5.1	2.1	0.1	0.0	0.0	5.1	2.1	-0.2
I3	591	-0.1	5.0	2.2	0.2	0.0	0.0	5.0	2.2	-0.2
I4	592	-0.1	4.9	2.4	0.1	0.0	0.0	4.9	2.4	-0.1
I5	593	0.0	4.9	2.5	0.1	0.0	0.0	4.9	2.5	0.0
J1	971	-0.1	-3.3	0.1	0.0	0.0	0.0	0.1	-0.1	-3.3
J2	972	0.0	-2.1	0.8	0.0	0.0	0.0	0.8	0.0	-2.1
J3	973	0.0	-0.8	1.6	0.0	0.0	0.0	1.6	0.0	-0.8
J4	974	0.0	0.4	2.3	0.0	0.0	0.0	2.3	0.4	0.0
K1	979	-0.3	2.6	3.5	0.0	0.0	0.0	3.5	2.6	-0.3
K2	980	-0.2	3.7	4.1	0.0	0.0	0.0	4.1	3.7	-0.2
K3	981	-0.2	4.8	4.8	0.0	0.0	0.0	4.8	4.8	-0.2
K4	982	-0.1	5.9	5.4	0.0	0.0	0.0	5.9	5.4	-0.1
K5	983	0.0	6.9	5.9	0.0	0.0	0.0	6.9	5.9	0.0
L1	1601	-0.1	-3.1	0.1	0.0	0.0	0.0	0.1	-0.1	-3.1
L2	1602	0.0	-2.2	0.8	0.0	0.0	0.0	0.8	0.0	-2.2
L3	1603	0.0	-1.3	1.5	0.0	0.0	0.0	1.5	0.0	-1.3
L4	1604	0.0	-0.5	2.2	0.0	0.0	0.0	2.2	0.0	-0.5
M1	1609	-0.4	2.4	4.6	0.0	0.0	0.0	4.6	2.4	-0.4
M2	1610	-0.3	3.4	5.3	0.0	0.0	0.0	5.3	3.4	-0.3
M3	1611	-0.2	4.4	6.0	0.0	0.0	0.0	6.0	4.4	-0.2
M4	1612	-0.1	5.5	6.6	0.0	0.0	0.0	6.6	5.5	-0.1
M5	1613	0.0	6.5	7.2	0.0	0.0	0.0	7.2	6.5	0.0

Table 2.10.4-38 Primary + Secondary Stresses; 1-Foot Top End Drop; Drop Orientation = 0 Degrees; 2-D Model; Condition 1 (continued)

Stress Points		Stress Components (ksi)						Principal Stresses (ksi)		
Section[1]	Node	S_x	S_y	S_z	S_{xy}	S_{yz}	S_{zx}	S1	S2	S3
N1	2216	-0.1	-3.8	-0.2	0.0	0.0	0.0	-0.1	-0.2	-3.8
N2	2217	0.0	-2.7	0.5	0.0	0.0	0.0	0.5	0.0	-2.7
N3	2218	0.0	-1.6	1.1	0.0	0.0	0.0	1.1	0.0	-1.6
N4	2219	0.0	-0.5	1.8	0.0	0.0	0.0	1.8	0.0	-0.5
O1	2224	-0.3	2.5	3.9	0.0	0.0	0.0	3.9	2.5	-0.3
O2	2225	-0.3	3.3	4.4	0.0	0.0	0.0	4.4	3.3	-0.3
O3	2226	-0.2	4.1	4.9	0.0	0.0	0.0	4.9	4.1	-0.2
O4	2227	-0.1	4.9	5.4	0.0	0.0	0.0	5.4	4.9	-0.1
O5	2228	0.0	5.7	5.9	0.0	0.0	0.0	5.9	5.7	0.0
P1	2546	-0.1	-1.7	0.9	0.0	0.0	0.0	0.9	-0.1	-1.7
P2	2547	-0.1	-2.1	0.9	0.0	0.0	0.0	0.9	-0.1	-2.1
P3	2548	0.1	-2.3	1.0	-0.1	0.0	0.0	1.0	0.1	-2.3
P4	2549	-0.2	-2.9	0.9	-0.1	0.0	0.0	0.9	-0.2	-2.9
Q1	2554	-0.1	3.5	3.2	0.1	0.0	0.0	3.5	3.2	-0.1
Q2	2555	-0.1	3.7	3.4	0.1	0.0	0.0	3.7	3.4	-0.1
Q3	2556	-0.1	3.9	3.6	0.1	0.0	0.0	3.9	3.6	-0.1
Q4	2557	0.0	4.2	3.8	0.1	0.0	0.0	4.2	3.8	0.0
Q5	2558	0.0	4.3	4.0	0.1	0.0	0.0	4.3	4.0	0.0
R1	2771	-0.5	-3.6	-3.0	0.2	0.0	0.0	-0.5	-3.0	-3.6
R2	2772	-0.7	-3.2	-2.4	0.4	0.0	0.0	-0.7	-2.4	-3.3
R3	2773	-1.5	-2.4	-1.9	0.9	0.0	0.0	-0.9	-1.9	-2.9
R4	2774	-3.5	-1.0	-1.5	1.1	0.0	0.0	-0.5	-1.5	-4.0
S1	2779	-0.9	3.8	1.3	-1.9	0.0	0.0	4.5	1.3	-1.6
S2	2780	0.2	3.3	1.7	-0.9	0.0	0.0	3.6	1.7	-0.1
S3	2781	0.1	2.7	1.8	-0.1	0.0	0.0	2.7	1.8	0.1
S4	2782	0.0	2.2	1.9	0.1	0.0	0.0	2.2	1.9	0.0
S5	2783	0.1	1.7	2.0	0.1	0.0	0.0	2.0	1.7	0.1
T1	7066	2.1	-2.8	1.2	-0.8	0.0	0.0	2.3	1.2	-2.9
T2	7067	1.1	-2.6	1.0	-0.8	0.0	0.0	1.3	1.0	-2.7
T3	7068	0.7	-1.6	1.3	-0.6	0.0	0.0	1.3	0.8	-1.7
T4	7069	0.4	-0.7	1.6	-0.6	0.0	0.0	1.6	0.6	-0.9
T5	7070	0.2	0.2	1.8	-0.4	0.0	0.0	1.8	0.6	-0.3
T6	7071	0.1	1.0	2.1	-0.2	0.0	0.0	2.1	1.0	0.0

Table 2.10.4-38 Primary + Secondary Stresses; 1-Foot Top End Drop; Drop Orientation = 0 Degrees; 2-D Model; Condition 1 (continued)

Stress Points		Stress Components (ksi)						Principal Stresses (ksi)		
Section[1]	Node	S_x	S_y	S_z	S_{xy}	S_{yz}	S_{xz}	S1	S2	S3
T7	7072	0.0	1.6	2.4	-0.1	0.0	0.0	2.4	1.7	0.0
U1	3051	-1.5	-5.9	-0.7	1.2	0.0	0.0	-0.7	-1.2	-6.2
U2	3052	0.4	-5.6	-0.9	1.3	0.0	0.0	0.7	-0.9	-5.9
U3	3053	0.9	-4.8	-1.2	1.0	0.0	0.0	1.1	-1.2	-4.9
U4	3054	0.8	-3.7	-1.6	0.2	0.0	0.0	0.8	-1.6	-3.7
U5	3055	0.3	-2.9	-2.1	0.1	0.0	0.0	0.3	-2.1	-2.9
U6	3056	1.2	-1.5	-2.0	1.0	0.0	0.0	1.6	-1.8	-2.0
V1	3611	-0.6	-0.2	1.1	-0.3	0.0	0.0	1.1	0.0	-0.8
V2	3612	-0.7	-0.3	0.6	-0.5	0.0	0.0	0.6	0.1	-1.0
V3	3613	-0.5	-0.6	0.0	-0.8	0.0	0.0	0.3	0.0	-1.4
V4	3614	-0.1	-1.1	-0.5	-0.9	0.0	0.0	0.5	-0.5	-1.6
V5	3615	0.4	-1.7	-1.2	-0.8	0.0	0.0	0.6	-1.2	-1.9
V6	3616	0.2	-1.1	-1.7	-0.5	0.0	0.0	0.4	-1.2	-1.7
V7	3617	0.6	-0.2	-1.9	-0.3	0.0	0.0	0.7	-0.2	-1.9
W1	3241	1.9	-0.3	1.9	0.0	0.0	0.0	1.9	1.9	-0.3
W2	3242	2.1	-0.3	2.1	0.0	0.0	0.0	2.1	2.1	-0.3
W3	3243	2.2	-0.2	2.2	0.0	0.0	0.0	2.2	2.2	-0.2
W4	3244	2.3	-0.1	2.3	0.0	0.0	0.0	2.3	2.3	-0.1
W5	3245	2.5	-0.1	2.5	0.0	0.0	0.0	2.5	2.5	-0.1
W6	3246	2.6	0.0	2.6	0.0	0.0	0.0	2.6	2.6	0.0
X1	3801	16.4	-0.4	16.4	0.0	0.0	0.0	16.4	16.4	-0.4
X2	3802	11.3	-0.4	11.3	0.0	0.0	0.0	11.3	11.3	-0.4
X3	3803	6.1	-0.3	6.1	0.0	0.0	0.0	6.1	6.1	-0.3
X4	3804	0.9	-0.4	0.9	0.0	0.0	0.0	0.9	0.9	-0.4
X5	3805	-4.3	-0.5	-4.3	0.0	0.0	0.0	-0.5	-4.3	-4.3
X6	3806	-9.6	-0.5	-9.6	0.0	0.0	0.0	-0.5	-9.6	-9.6
X7	3807	-15.4	-0.3	-15.4	0.0	0.0	0.0	-0.3	-15.4	-15.4

[1] Refer to Figure 2.10.2-34 for the identification of the representative sections.

Table 2.10.4-39 P_m Stresses; 1-Foot Top End Drop; Drop Orientation = 0 Degrees; 2-D Model; Condition 1

Condition 1: 100°F Ambient with Contents

Section[1]	Node - Node	Stress Components (ksi)						Principal Stresses (ksi)			
		S_x	S_y	S_z	S_{xy}	S_{yz}	S_{xz}	S1	S2	S3	S.I.
A	1 - 5	0.1	0.0	0.1	0.0	0.0	0.0	0.1	0.1	0.0	0.2
B	6 - 10	-0.1	0.0	-0.1	0.0	0.0	0.0	0.0	-0.1	-0.1	0.1
C	251 - 255	0.2	-0.1	0.1	-0.1	0.0	0.0	0.2	0.1	-0.1	0.3
D	306 - 310	-0.1	-0.2	-0.2	0.0	0.0	0.0	-0.1	-0.2	-0.2	0.1
E	305 - 355	0.2	-0.1	0.0	-0.1	0.0	0.0	0.3	0.0	-0.2	0.5
F	251 - 281	-0.4	-0.3	0.1	0.0	0.0	0.0	0.1	-0.3	-0.4	0.5
G	311 - 351	-0.1	-0.2	0.1	0.0	0.0	0.0	0.1	-0.1	-0.2	0.3
H	581 - 584	0.0	-0.8	1.0	0.0	0.0	0.0	1.0	0.0	-0.8	1.7
I	589 - 593	0.0	-0.4	0.0	0.0	0.0	0.0	0.0	0.0	-0.4	0.4
J	971 - 974	0.0	-1.0	1.2	0.0	0.0	0.0	1.2	0.0	-1.0	2.2
K	979 - 983	0.0	-0.6	0.0	0.0	0.0	0.0	0.0	0.0	-0.6	0.6
L	1601 - 1604	0.0	-1.4	1.2	0.0	0.0	0.0	1.2	0.0	-1.4	2.6
M	1609 - 1613	0.0	-1.0	0.0	0.0	0.0	0.0	0.0	0.0	-1.0	1.0
N	2216 - 2219	0.0	-1.7	1.2	0.0	0.0	0.0	1.2	0.0	-1.7	2.9
O	2224 - 2228	0.0	-1.3	0.0	0.0	0.0	0.0	0.0	0.0	-1.3	1.3
P	2546 - 2549	-0.1	-1.9	1.1	0.0	0.0	0.0	1.1	-0.1	-1.9	3.0
Q	2554 - 2558	0.0	-1.5	0.4	0.0	0.0	0.0	0.4	0.0	-1.5	1.9
R	2771 - 2774	-0.1	-2.2	1.1	0.5	0.0	0.0	1.1	0.0	-2.4	3.5
S	2779 - 2783	-1.5	-1.3	0.5	-0.2	0.0	0.0	0.5	-1.2	-1.6	2.1
T	7066 - 7072	1.6	-0.9	0.1	0.0	0.0	0.0	1.6	0.1	-0.9	2.4
U	3051 - 3056	0.4	-4.1	-0.2	1.0	0.0	0.0	0.7	-0.2	-4.3	5.0
V	3611 - 3617	-0.3	-1.4	-0.2	-0.8	0.0	0.0	0.2	-0.2	-1.8	1.9
W	3241 - 3246	1.0	-0.2	1.0	0.0	0.0	0.0	1.0	1.0	-0.2	1.2
X	3801 - 3807	0.0	-0.4	0.0	0.0	0.0	0.0	0.0	0.0	-0.4	0.5

[1] Refer to Figure 2.10.2-34 for the identification of the representative sections.

Table 2.10.4-40 $P_m + P_b$ Stresses; 1-Foot Top End Drop; Drop Orientation = 0 Degrees; 2-D Model; Condition 1

Condition 1: 100°F Ambient with Contents

Section[1]	Node - Node	Stress Components (ksi) S_x	S_y	S_z	S_{xy}	S_{yz}	S_{xz}	Principal Stresses (ksi) S1	S2	S3	S.I.
A I	1 - 5	0.9	0.0	0.9	0.0	0.0	0.0	0.9	0.9	0.0	0.9
B O	6 - 10	-0.8	0.0	-0.8	0.0	0.0	0.0	0.0	-0.8	-0.8	0.8
C O	251 - 255	0.6	0.0	0.1	-0.1	0.0	0.0	0.6	0.1	-0.1	0.7
D O	306 - 310	0.3	0.0	-0.1	0.0	0.0	0.0	0.3	0.0	-0.1	0.4
E I	305 - 355	0.7	-0.1	0.1	-0.1	0.0	0.0	0.7	0.1	-0.1	0.8
F O	251 - 281	-0.5	-0.6	0.0	0.0	0.0	0.0	0.0	-0.5	-0.6	0.6
G I	311 - 351	-0.3	-0.5	0.0	0.0	0.0	0.0	0.0	-0.3	-0.5	0.5
H I	581 - 584	-0.1	-0.8	1.0	0.0	0.0	0.0	1.0	-0.1	-0.8	1.7
I O	589 - 593	0.0	-0.4	0.0	0.0	0.0	0.0	0.0	0.0	-0.4	0.5
J I	971 - 974	-0.1	-1.0	1.2	0.0	0.0	0.0	1.2	-0.1	-1.0	2.2
K I	979 - 983	0.0	-0.6	0.0	0.0	0.0	0.0	0.0	0.0	-0.6	0.6
L I	1601 - 1604	-0.1	-1.4	1.2	0.0	0.0	0.0	1.2	-0.1	-1.4	2.6
M O	1609 - 1613	0.0	-1.0	0.0	0.0	0.0	0.0	0.0	0.0	-1.0	1.0
N I	2216 - 2219	-0.1	-1.7	1.2	0.0	0.0	0.0	1.2	-0.1	-1.7	2.9
O I	2224 - 2228	0.0	-1.3	0.0	0.0	0.0	0.0	0.0	0.0	-1.3	1.3
P O	2546 - 2549	0.0	-2.7	0.9	0.0	0.0	0.0	0.9	0.0	-2.7	3.6
Q O	2554 - 2558	0.0	-1.9	0.3	0.0	0.0	0.0	0.3	0.0	-1.9	2.1
R I	2771 - 2774	-0.2	-6.6	0.0	0.5	0.0	0.0	0.0	-0.2	-6.7	6.7
S I	2779 - 2783	-3.7	-4.4	-0.8	-0.2	0.0	0.0	-0.8	-3.7	-4.5	3.7
T O	7066 - 7072	0.1	-3.9	-1.2	0.0	0.0	0.0	0.1	-1.2	-3.9	4.0
U I	3051 - 3056	0.9	-13.1	1.3	1.0	0.0	0.0	1.3	1.0	-13.2	14.5
V O	3611 - 3617	1.7	-0.2	-2.6	-0.8	0.0	0.0	2.0	-0.5	-2.6	4.6
W O	3241 - 3246	2.2	0.0	2.2	0.0	0.0	0.0	2.2	2.2	0.0	2.2
X I	3801 - 3807	18.3	-0.6	18.3	0.0	0.0	0.0	18.3	18.3	-0.6	18.9

[1] Refer to Figure 2.10.2-34 for the identification of the representative sections.

Table 2.10.4-41 S_n Stresses; 1-Foot Top End Drop; Drop Orientation = 0 Degrees; 2-D Model; Condition 1

Condition 1: 100°F Ambient with Contents

Section[1]	Node - Node	Stress Components (ksi)						Principal Stresses (ksi)			
		S_x	S_y	S_z	S_{xy}	S_{yz}	S_{xz}	S1	S2	S3	S.I.
A O	1 - 5	-2.0	0.0	-2.0	0.0	0.0	0.0	0.0	-2.0	-2.0	2.0
B I	6 - 10	1.9	0.0	1.9	0.0	0.0	0.0	1.9	1.9	0.0	1.9
C I	251 - 255	-0.1	-2.9	0.1	-0.5	0.0	0.0	0.1	0.0	-2.9	3.1
D I	306 - 310	3.0	6.1	2.3	0.7	0.0	0.0	6.3	2.8	2.3	4.0
E I	305 - 355	-0.4	3.7	0.5	1.0	0.0	0.0	3.9	0.5	-0.6	4.5
F I	251 - 281	-0.8	-2.8	-0.2	-0.6	0.0	0.0	-0.2	-0.6	-2.9	2.7
G O	311 - 351	-0.2	7.6	2.4	0.4	0.0	0.0	7.6	2.4	-0.3	7.9
H O	581 - 584	-0.2	-2.2	0.6	0.1	0.0	0.0	0.6	-0.1	-2.2	2.8
I I	589 - 593	-0.3	5.1	2.0	0.1	0.0	0.0	5.1	2.0	-0.3	5.4
J I	971 - 974	-0.1	-3.3	0.1	0.0	0.0	0.0	0.1	-0.1	-3.3	3.4
K O	979 - 983	0.0	6.9	5.9	0.0	0.0	0.0	6.9	5.9	0.0	6.9
L I	1601 - 1604	-0.1	-3.1	0.2	0.0	0.0	0.0	0.2	-0.1	-3.1	3.3
M O	1609 - 1613	0.0	6.5	7.3	0.0	0.0	0.0	7.3	6.5	0.0	7.3
N I	2216 - 2219	-0.1	-3.8	-0.2	0.0	0.0	0.0	-0.1	-0.2	-3.8	3.7
O O	2224 - 2228	0.0	5.7	5.9	0.0	0.0	0.0	5.9	5.7	0.0	5.9
P O	2546 - 2549	-0.2	-2.8	1.0	-0.1	0.0	0.0	1.0	-0.2	-2.8	3.8
Q O	2554 - 2558	0.0	4.4	4.0	0.1	0.0	0.0	4.4	4.0	0.0	4.4
R I	2771 - 2774	-0.5	-3.9	-2.9	0.7	0.0	0.0	-0.4	-2.9	-4.0	3.7
S I	2779 - 2783	-0.9	3.8	1.5	-0.5	0.0	0.0	3.9	1.5	-1.0	4.8
T I	7066 - 7072	2.1	-3.2	0.9	-0.5	0.0	0.0	2.2	0.9	-3.3	5.4
U I	3051 - 3056	0.0	-17.1	-0.7	0.7	0.0	0.0	0.0	-0.7	-17.1	17.1
V O	3611 - 3617	0.6	-0.2	-2.1	-0.6	0.0	0.0	1.0	-0.5	-2.1	3.1
W O	3241 - 3246	2.6	0.0	2.6	0.0	0.0	0.0	2.6	2.6	0.0	2.6
X I	3801 - 3807	16.3	-0.4	16.3	0.0	0.0	0.0	16.3	16.3	-0.4	16.7

[1] Refer to Figure 2.10.2-34 for the identification of the representative sections.

Table 2.10.4-42 Critical P_m Stress Summary; 1-Foot Top End Drop; Drop Orientation = 0 Degrees; 2-D Model; Condition 1

Condition 1: 100°F Ambient with Contents

Comp. No.[1]	Section Cut Node-Node	P_m Stresses (ksi)						Principal Stresses (ksi)			S.I.	Allow. Stress	Margin of Safety
		S_x	S_y	S_z	S_{xy}	S_{yz}	S_{xz}	S1	S2	S3			
1	256- 260	-0.1	0.0	-0.1	-0.1	0.0	0.0	0.0	-0.1	-0.2	0.2	19.2	95.0
2	386- 389	0.0	-0.5	0.3	0.1	0.0	0.0	0.3	0.0	-0.5	0.8	18.5	22.1
3	2711- 2714	0.0	-1.5	2.2	0.2	0.0	0.0	2.2	0.0	-1.5	3.7	31.4	7.5
4	2276- 2279	0.0	-1.8	1.2	0.0	0.0	0.0	1.2	0.0	-1.8	2.9	19.6	5.8
5	2599- 2603	-1.5	0.0	0.6	-0.1	0.0	0.0	0.6	0.0	-1.5	2.1	20.0	8.5
6	7064- 2774	0.1	3.4	1.6	1.0	0.0	0.0	3.7	1.6	-0.2	3.9	20.0	4.1
7	3021- 3026	0.2	-8.8	-1.5	0.2	0.0	0.0	0.2	-1.5	-8.8	9.1	20.0	1.2
8	3661- 3667	-0.2	-3.4	-0.9	1.0	0.0	0.0	0.1	-0.9	-3.7	3.8	45.0	10.8

Locations of the most critical sections for each component are provided in the following:

Comp. No.[1]	Section Location			
	Inside Node		Outside Node	
	x (in)	y (in)	z (in)	x (in)
1	35.50	6.20	35.50	0.75
2	35.50	16.40	37.50	16.40
3	35.50	171.40	37.50	171.40
4	35.50	142.40	37.00	142.40
5	40.70	163.40	43.35	163.40
6	37.655	179.40	37.50	175.40
7	37.655	179.40	37.655	185.40
8	26.158	188.40	26.158	193.71

[1] Refer to Figure 2.10.2-33 for cask component identification.

Table 2.10.4-43 Critical $P_m + P_b$ Stress Summary; 1-Foot Top End Drop; Drop Orientation = 0 Degrees; 2-D Model; Condition 1

Condition 1: 100°F Ambient with Contents

Comp. No.[1]	Section Cut Node-Node	$P_m + P_b$ Stresses (ksi) S_x	S_y	S_z	S_{xy}	S_{yz}	S_{xz}	Principal Stresses (ksi) S1	S2	S3	S.I.	Allow. Stress	Margin of Safety
1	16- 20	-0.8	0.0	-0.8	0.0	0.0	0.0	0.0	-0.8	-0.8	0.8	28.7	34.9
2	371- 374	0.0	-0.8	0.1	0.1	0.0	0.0	0.1	0.0	-0.8	0.9	27.7	29.8
3	2711- 2714	-0.1	-4.0	1.6	0.2	0.0	0.0	1.6	0.0	-4.0	5.6	47.1	7.4
4	2276- 2279	-0.1	-1.8	1.2	0.0	0.0	0.0	1.2	-0.1	-1.8	3.0	29.4	8.8
5	2599- 2603	-1.7	0.0	0.6	-0.1	0.0	0.0	0.6	0.0	-1.7	2.2	30.0	12.6
6	7065- 2784	4.0	-7.6	-0.8	0.5	0.0	0.0	4.1	-0.8	-7.6	11.6	30.0	1.6
7	3107- 3108	14.6	-6.1	-0.3	0.2	0.0	0.0	14.6	-0.3	-6.1	20.7	30.0	0.4
8	3801- 3807	18.3	-0.6	18.3	0.0	0.0	0.0	18.3	18.3	-0.6	18.9	67.5	2.6

Locations of the most critical sections for each component are provided in the following:

Comp. No.[1]	Section Location Inside Node x (in)	y (in)	Outside Node z (in)	x (in)
1	1.42	6.20	1.42	0.75
2	35.50	15.40	37.50	15.40
3	35.50	171.40	37.50	171.40
4	35.50	142.40	37.00	142.40
5	40.70	163.40	43.35	163.40
6	38.608	179.40	38.567	175.40
7	26.158	187.40	26.158	188.40
8	0.0	188.46	0.0	193.71

[1] Refer to Figure 2.10.2-33 for cask component identification.

Table 2.10.4-44 Critical S_n Stress Summary; 1-Foot Top End Drop; Drop Orientation = 0 Degrees; 2-D Model; Condition 1

Condition 1: 100°F Ambient with Contents

Comp. No.[1]	Section Cut Node-Node	S_n Stresses (ksi) S_x	S_y	S_z	S_{xy}	S_{yz}	S_{xz}	Principal Stresses (ksi) S1	S2	S3	S.I.	Allow. Stress 3.0 S_m
1	296- 300	4.1	-0.8	1.4	1.1	0.0	0.0	4.3	1.4	-1.1	5.4	57.6
2	311- 351	-0.2	7.6	2.4	0.4	0.0	0.0	7.6	2.4	-0.3	7.9	55.5
3	2291- 2294	-0.4	-2.8	1.4	-0.1	0.0	0.0	1.4	-0.4	-2.9	4.2	94.2
4	2156- 2159	-0.1	-3.7	0.2	0.0	0.0	0.0	0.2	-0.1	-3.7	3.8	58.8
5	1534- 1538	6.6	0.0	7.3	0.0	0.0	0.0	7.3	6.6	0.0	7.3	60.0
6	7065- 2784	5.7	-6.1	1.4	-0.9	0.0	0.0	5.8	1.4	-6.2	12.0	60.0
7	3107- 3108	15.2	-6.3	0.5	0.1	0.0	0.0	15.2	0.5	-6.3	21.6	60.0
8	3801- 3807	16.3	-0.4	16.3	0.0	0.0	0.0	16.3	16.3	-0.4	16.7	135.0

Locations of the most critical sections for each component are provided in the following:

Comp. No.[1]	Section Location Inside Node x (in)	y (in)	Outside Node z (in)	x (in)
1	38.567	6.20	38.567	0.75
2	40.700	14.40	43.35	14.40
3	35.50	143.40	37.00	143.40
4	35.50	134.40	37.00	134.40
5	40.70	92.40	43.35	92.40
6	38.608	179.40	38.567	175.40
7	26.158	187.40	26.158	188.40
8	0.0	188.46	0.0	193.71

[1] Refer to Figure 2.10.2-33 for cask component identification.

Table 2.10.4-45 Critical P_m Stress Summary; 1-Foot Top End Drop; Drop Orientation = 0 Degrees; 2-D Model; Condition 2

Condition 2: -20°F Ambient with Contents

Comp. No.[1]	Section Cut Node-Node	P_m Stresses (ksi) S_x	S_y	S_z	S_{xy}	S_{yz}	S_{xz}	Principal Stresses (ksi) S1	S2	S3	S.I.	Allow. Stress	Margin of Safety
1	216- 220	-0.2	0.0	-0.2	-0.1	0.0	0.0	0.0	-0.2	-0.2	0.3	19.2	63.0
2	386- 389	0.0	-0.7	0.3	0.0	0.0	0.0	0.3	0.0	-0.7	1.0	18.5	17.5
3	2711-2714	0.0	-1.7	1.9	0.3	0.0	0.0	1.9	0.0	-1.8	3.7	31.4	7.5
4	2276-2279	0.0	-2.1	0.3	0.0	0.0	0.0	0.3	0.0	-2.1	2.4	19.6	7.2
5	2599-2603	-1.6	0.0	0.6	-0.1	0.0	0.0	0.6	0.0	-1.6	2.2	20.0	8.1
6	7064-2774	0.1	3.5	1.5	1.1	0.0	0.0	3.9	1.5	-0.2	4.1	20.0	3.9
7	3021-3026	0.2	-9.1	-1.5	0.2	0.0	0.0	0.2	-1.5	-9.1	9.3	20.0	1.1
8	3671-3677	0.0	-0.5	0.0	1.8	0.0	0.0	1.7	0.0	-2.1	3.7	45.0	11.1

Locations of the most critical sections for each component are provided in the following:

Comp. No.[1]	Section Location Inside Node x (in)	y (in)	Outside Node z (in)	x (in)
1	29.820	6.20	29.820	0.75
2	35.50	16.40	37.50	16.40
3	35.50	171.40	37.50	171.40
4	35.50	142.40	37.00	142.40
5	40.70	163.40	43.35	163.40
6	37.655	179.40	37.50	175.40
7	37.655	179.40	37.655	185.40
8	24.289	188.46	24.289	193.71

[1] Refer to Figure 2.10.2-33 for cask component identification.

Table 2.10.4-46 Critical $P_m + P_b$ Stress Summary; 1-Foot Top End Drop; Drop Orientation = 0 Degrees; 2-D Model; Condition 2

Condition 2: -20°F Ambient with Contents

Comp. No.[1]	Section Cut Node-Node	$P_m + P_b$ Stresses (ksi) S_x	S_y	S_z	S_{xy}	S_{yz}	S_{xz}	Principal Stresses (ksi) S1	S2	S3	S.I.	Allow. Stress	Margin of Safety
1	16- 20	-1.3	0.0	-1.3	0.0	0.0	0.0	0.0	-1.3	-1.3	1.3	28.7	21.1
2	371- 374	0.1	-1.3	0.1	-0.1	0.0	0.0	0.1	0.1	-1.3	1.4	27.7	18.8
3	2711-2714	0.0	-4.4	1.2	0.3	0.0	0.0	1.2	0.0	-4.4	5.6	47.1	7.4
4	2276-2279	0.0	-2.1	0.3	0.0	0.0	0.0	0.3	0.0	-2.1	2.4	29.4	11.3
5	2599-2603	-1.7	0.0	0.6	-0.1	0.0	0.0	0.6	0.0	-1.7	2.3	30.0	12.0
6	7065-2784	4.2	-7.5	-0.9	0.6	0.0	0.0	4.3	-0.9	-7.5	11.8	30.0	1.6
7	3107-3108	14.0	-6.0	-0.6	0.2	0.0	0.0	14.0	-0.6	-6.0	20.0	30.0	0.5
8	3801-3807	18.6	-0.6	18.6	0.0	0.0	0.0	18.6	18.6	-0.6	19.2	67.5	2.5

Locations of the most critical sections for each component are provided in the following:

Comp. No.[1]	Section Location Inside Node x (in)	y (in)	z (in)	Outside Node x (in)
1	1.42	6.20	1.42	0.75
2	35.50	15.40	37.50	15.40
3	35.50	171.40	37.50	171.40
4	35.50	142.40	37.00	142.40
5	40.70	163.40	43.35	163.40
6	38.608	179.40	38.567	175.40
7	26.158	187.40	26.158	188.40
8	0.0	188.46	0.0	193.71

[1] Refer to Figure 2.10.2-33 for cask component identification.

Table 2.10.4-47 Critical S_n Stress Summary; 1-Foot Top End Drop; Drop Orientation = 0 Degrees; 2-D Model; Condition 2

Condition 2: -20°F Ambient with Contents

Comp. No.[1]	Section Cut Node-Node	S_n Stresses (ksi)						Principal Stresses (ksi)				Allow. Stress 3.0 S_m
		S_x	S_y	S_z	S_{xy}	S_{yz}	S_{xz}	S1	S2	S3	S.I.	
1	306- 310	1.1	-2.0	0.8	0.0	0.0	0.0	1.1	0.8	-2.0	3.1	57.6
2	371- 374	0.1	-4.0	-1.3	0.1	0.0	0.0	0.1	-1.3	-4.0	4.1	55.5
3	2531-2534	0.0	-5.4	0.0	-0.1	0.0	0.0	0.0	0.0	-5.4	5.4	94.2
4	2201-2204	0.0	-5.8	-0.7	0.0	0.0	0.0	0.0	-0.7	-5.8	5.7	58.8
5	1039-1043	0.0	4.4	2.0	0.0	0.0	0.0	4.4	2.0	0.0	4.4	60.0
6	7065-2784	4.8	-7.4	-0.2	-0.4	0.0	0.0	4.8	-0.2	-7.4	12.1	60.0
7	3107-3108	14.4	-5.8	-0.4	0.2	0.0	0.0	14.4	-0.4	-5.8	20.1	60.0
8	3801-3807	19.2	-0.6	19.2	0.0	0.0	0.0	19.2	19.2	-0.6	19.7	135.0

Locations of the most critical sections for each component are provided in the following:

Comp. No.[1]	Section Location			
	Inside Node		Outside Node	
	x (in)	y (in)	z (in)	x (in)
1	39.44	6.20	39.44	0.75
2	35.50	15.40	37.50	15.40
3	35.50	159.40	37.00	159.40
4	35.50	137.40	37.00	137.40
5	40.70	59.40	43.35	59.40
6	38.608	179.40	38.567	175.40
7	26.158	187.40	26.158	188.40
8	0.0	188.46	0.0	193.71

[1] Refer to Figure 2.10.2-33 for cask component identification.

Table 2.10.4-48 Critical P_m Stress Summary; 1-Foot Top End Drop; Drop Orientation = 0 Degrees; 2-D Model; Condition 3

Condition 3: -20°F ambient without Contents

Comp. No.[1]	Section Cut Node-Node	P_m Stresses (ksi)						Principal Stresses (ksi)			S.I.	Allow. Stress	Margin of Safety
		S_x	S_y	S_z	S_{xy}	S_{yz}	S_{xz}	S1	S2	S3			
1	206- 210	-0.2	0.0	-0.2	-0.1	0.0	0.0	0.0	-0.2	-0.2	0.3	19.2	63.0
2	386- 389	0.0	-0.8	0.3	0.0	0.0	0.0	0.3	0.0	-0.8	1.0	18.5	17.5
3	2711-2714	0.0	-1.8	2.0	0.3	0.0	0.0	2.0	0.0	-1.8	3.9	31.4	7.1
4	2261-2264	0.0	-2.1	0.3	0.0	0.0	0.0	0.3	0.0	-2.1	2.4	19.6	7.2
5	2599-2603	-1.5	0.0	0.7	-0.1	0.0	0.0	0.7	0.0	-1.6	2.2	20.0	8.1
6	7064-2774	0.1	3.8	1.6	1.3	0.0	0.0	4.2	1.6	-0.3	4.5	20.0	3.4
7	3021-3026	0.2	-9.1	-1.5	0.1	0.0	0.0	0.2	-1.5	-9.1	9.3	20.0	1.1
8	3671-3677	0.0	-0.4	0.0	1.5	0.0	0.0	1.4	0.0	-1.7	3.1	45.0	13.4

Locations of the most critical sections for each component are provided in the following:

Comp. No.[1]	Section Location: Inside Node x (in)	Inside Node y (in)	Inside Node z (in)	Outside Node x (in)
1	28.40	6.20	28.40	0.75
2	35.50	16.40	37.50	16.40
3	35.50	171.40	37.50	171.40
4	35.50	141.40	37.00	141.40
5	40.70	163.40	43.35	163.40
6	37.655	179.40	37.50	175.40
7	37.655	179.40	37.655	185.40
8	24.289	188.46	24.289	193.71

[1] Refer to Figure 2.10.2-33 for cask component identification.

Table 2.10.4-49 Critical $P_m + P_b$ Stress Summary; 1-Foot Top End Drop; Drop Orientation = 0 Degrees; 2-D Model; Condition 3

Condition 3: -20°F Ambient without Contents

Comp. No.[1]	Section Cut Node-Node	$P_m + P_b$ Stresses (ksi) S_x	S_y	S_z	S_{xy}	S_{yz}	S_{xz}	Principal Stresses (ksi) S1	S2	S3	S.I.	Allow. Stress	Margin of Safety
1	6- 20	-1.3	0.0	-1.3	0.0	0.0	0.0	0.0	-1.3	-1.3	1.3	28.7	21.1
2	371- 374	0.1	-1.3	0.1	-0.1	0.0	0.0	0.1	0.1	-1.3	1.4	27.7	18.8
3	2711-2714	0.0	-4.7	1.3	0.3	0.0	0.0	1.3	0.0	-4.7	6.0	47.1	6.9
4	2276-2279	0.0	-2.2	0.3	0.0	0.0	0.0	0.3	0.0	-2.2	2.5	29.4	10.8
5	2599-2603	-1.7	0.0	0.6	-0.1	0.0	0.0	0.6	0.0	-1.7	2.3	30.0	12.0
6	7065-2784	4.8	-6.8	-0.6	0.6	0.0	0.0	4.8	-0.6	-6.9	11.7	30.0	1.6
7	3051-3056	0.2	-16.3	1.7	0.9	0.0	0.0	1.7	0.3	-16.3	18.0	30.0	0.7
8	3801-3807	16.8	-0.7	16.8	0.0	0.0	0.0	16.8	16.8	-0.7	17.6	67.5	2.8

Locations of the most critical sections for each component are provided in the following:

Comp. No.[1]	Section Location Inside Node x (in)	y (in)	Outside Node z (in)	x (in)
1	1.42	6.20	1.42	0.75
2	35.50	15.40	37.50	15.40
3	35.50	171.40	37.50	171.40
4	35.50	142.40	37.00	142.40
5	40.70	163.40	43.35	163.40
6	38.608	179.40	38.567	175.40
7	35.50	179.40	35.50	185.40
8	0.0	188.46	0.0	193.71

[1] Refer to Figure 2.10.2-33 for cask component identification.

Table 2.10.4-50 Critical S_n Stress Summary; 1-Foot Top End Drop; Drop Orientation = 0 Degrees; 2-D Model; Condition 3

Condition 3: -20°F Ambient without Contents

Comp. No.[1]	Section Cut Node-Node	S_n Stresses (ksi)						Principal Stresses (ksi)				Allow. Stress 3.0 S_m
		S_x	S_y	S_z	S_{xy}	S_{yz}	S_{zx}	S1	S2	S3	S.I.	
1	16- 20	-1.5	0.0	-1.5	0.0	0.0	0.0	0.0	-1.5	-1.5	1.5	57.6
2	371- 374	0.1	-2.7	-0.8	-0.3	0.0	0.0	0.2	-0.8	-2.8	2.9	55.5
3	2711-2714	0.0	-4.9	0.3	0.2	0.0	0.0	0.3	0.0	-4.9	5.2	94.2
4	851- 854	0.0	-1.7	-2.9	0.0	0.0	0.0	0.0	-1.7	-2.9	2.9	58.8
5	2599-2603	-1.4	0.0	0.6	-0.1	0.0	0.0	0.6	0.0	-1.4	2.0	60.0
6	7065-2784	4.1	-7.1	-1.1	0.7	0.0	0.0	4.1	-1.1	-7.1	11.3	60.0
7	3051-3056	0.7	-15.9	1.4	1.1	0.0	0.0	1.4	0.8	-16.0	17.4	60.0
8	3801-3807	17.9	-0.5	17.9	0.0	0.0	0.0	17.9	17.9	-0.5	18.4	135.0

Locations of the most critical sections for each component are provided in the following:

Comp. No.[1]	Section Location			
	Inside Node		Outside Node	
	x (in)	y (in)	z (in)	x (in)
1	1.42	6.20	1.42	0.75
2	35.50	15.40	37.50	15.40
3	35.50	171.40	37.50	171.40
4	35.50	47.40	37.00	47.40
5	40.70	163.40	43.35	163.40
6	38.608	179.40	38.567	175.40
7	35.50	179.40	35.50	185.40
8	0.0	188.46	0.0	193.71

[1] Refer to Figure 2.10.2-33 for cask component identification.

Table 2.10.4-51 Primary Stresses; 1-Foot Bottom End Drop; Drop Orientation = 0 Degrees; 2-D Model; Condition 1

Condition 1: 100°F Ambient with Contents

Stress Points		Stress Components (ksi)						Principal Stresses (ksi)		
Section[1]	Node	S_x	S_y	S_z	S_{xy}	S_{yz}	S_{xz}	S1	S2	S3
A1	1	7.0	-0.4	7.0	0.0	0.0	0.0	7.0	7.0	-0.4
A2	2	4.0	-0.4	4.0	0.0	0.0	0.0	4.0	4.0	-0.4
A3	3	1.0	-0.5	1.0	0.0	0.0	0.0	1.0	1.0	-0.5
A4	4	-2.0	-0.6	-2.0	0.0	0.0	0.0	-0.6	-2.0	-2.0
A5	5	-5.0	-0.6	-5.0	0.0	0.0	0.0	-0.6	-5.0	-5.0
B1	6	4.0	-0.7	4.0	0.0	0.0	0.0	4.0	4.0	-0.7
B2	7	1.4	-0.7	1.4	0.0	0.0	0.0	1.4	1.4	-0.7
B3	8	-1.2	-0.7	-1.2	0.0	0.0	0.0	-0.7	-1.2	-1.2
B4	9	-3.9	-0.8	-3.9	0.0	0.0	0.0	-0.8	-3.9	-3.9
B5	10	-6.4	-0.8	-6.4	0.0	0.0	0.0	-0.8	-6.4	-6.4
C1	251	-3.5	-4.1	0.1	-0.7	0.0	0.0	0.1	-3.0	-4.6
C2	252	-0.6	-1.7	0.9	-0.5	0.0	0.0	0.9	-0.4	-1.9
C3	253	1.0	-0.8	0.9	-0.6	0.0	0.0	1.2	0.9	-1.0
C4	254	3.1	-0.5	0.9	-0.5	0.0	0.0	3.2	0.9	-0.6
C5	255	5.4	-0.5	0.9	-0.3	0.0	0.0	5.4	0.9	-0.5
D1	306	-6.0	-5.3	-2.8	-1.8	0.0	0.0	-2.8	-3.8	-7.5
D2	307	-1.6	-3.8	-1.6	-0.8	0.0	0.0	-1.3	-1.6	-4.0
D3	308	-0.4	-2.0	-1.3	0.0	0.0	0.0	-0.4	-1.3	-2.0
D4	309	0.8	-1.3	-1.3	0.2	0.0	0.0	0.8	-1.3	-1.3
D5	310	2.2	-1.0	-1.3	0.2	0.0	0.0	2.2	-1.0	-1.3
E1	305	5.1	-1.7	1.1	-1.2	0.0	0.0	5.3	1.1	-1.9
E2	315	2.4	-2.4	0.4	-1.5	0.0	0.0	2.9	0.4	-2.9
E3	325	1.0	-1.9	0.1	-1.5	0.0	0.0	1.7	0.1	-2.5
E4	335	0.5	-1.5	0.1	-1.2	0.0	0.0	1.0	0.1	-2.1
E5	345	0.2	-1.3	0.1	-0.7	0.0	0.0	0.5	0.1	-1.5
E6	355	0.1	-1.2	0.1	-0.4	0.0	0.0	0.2	0.1	-1.3
F1	251	-3.5	-4.1	0.1	-0.7	0.0	0.0	0.1	-3.0	-4.6
F2	261	-2.6	-1.9	0.9	-0.3	0.0	0.0	0.9	-1.8	-2.7
F3	271	-1.8	-0.2	1.5	0.0	0.0	0.0	1.5	-0.2	-1.8
F4	281	-1.8	1.1	1.7	-0.1	0.0	0.0	1.7	1.1	-1.8
G1	311	-2.7	-4.3	-0.3	-0.1	0.0	0.0	-0.3	-2.6	-4.3

Table 2.10.4-51 Primary Stresses; 1-Foot Bottom End Drop; Drop Orientation = 0 Degrees; 2-D Model; Condition 1 (continued)

Stress Points		Stress Components (ksi)						Principal Stresses (ksi)		
Section[1]	Node	S_x	S_y	S_z	S_{xy}	S_{yz}	S_{xz}	S1	S2	S3
G2	321	-1.9	-2.7	0.3	0.1	0.0	0.0	0.3	-1.9	-2.7
G3	331	-1.0	-1.6	0.8	0.3	0.0	0.0	0.8	-0.8	-1.8
G4	341	-0.4	-0.6	1.2	0.2	0.0	0.0	1.2	-0.2	-0.7
G5	351	-0.2	0.9	1.6	0.1	0.0	0.0	1.6	0.9	-0.2
H1	581	-0.1	-1.0	1.3	0.0	0.0	0.0	1.3	-0.1	-1.0
H2	582	-0.1	-1.5	1.1	0.0	0.0	0.0	1.1	-0.1	-1.5
H3	583	-0.1	-2.0	1.0	0.1	0.0	0.0	1.0	-0.1	-2.0
H4	584	0.0	-2.7	0.8	0.2	0.0	0.0	0.8	0.0	-2.7
I1	589	0.0	-1.2	0.4	0.0	0.0	0.0	0.4	0.0	-1.2
I2	590	0.0	-1.4	0.3	0.0	0.0	0.0	0.3	0.0	-1.4
I3	591	0.0	-1.6	0.3	0.0	0.0	0.0	0.3	0.0	-1.6
I4	592	0.0	-1.8	0.2	0.0	0.0	0.0	0.2	0.0	-1.8
I5	593	0.0	-2.0	0.1	0.0	0.0	0.0	0.1	0.0	-2.0
J1	971	-0.1	-1.7	1.2	0.0	0.0	0.0	1.2	-0.1	-1.7
J2	972	0.0	-1.7	1.2	0.0	0.0	0.0	1.2	0.0	-1.7
J3	973	0.0	-1.7	1.2	0.0	0.0	0.0	1.2	0.0	-1.7
J4	974	0.0	-1.7	1.2	0.0	0.0	0.0	1.2	0.0	-1.7
K1	979	0.0	-1.4	0.0	0.0	0.0	0.0	0.0	0.0	-1.4
K2	980	0.0	-1.4	0.0	0.0	0.0	0.0	0.0	0.0	-1.4
K3	981	0.0	-1.4	0.0	0.0	0.0	0.0	0.0	0.0	-1.4
K4	982	0.0	-1.4	0.0	0.0	0.0	0.0	0.0	0.0	-1.4
K5	983	0.0	-1.4	0.0	0.0	0.0	0.0	0.0	0.0	-1.4
L1	1601	-0.1	-1.3	1.2	0.0	0.0	0.0	1.2	-0.1	-1.3
L2	1602	0.0	-1.3	1.2	0.0	0.0	0.0	1.2	0.0	-1.3
L3	1603	0.0	-1.3	1.2	0.0	0.0	0.0	1.2	0.0	-1.3
L4	1604	0.0	-1.3	1.2	0.0	0.0	0.0	1.2	0.0	-1.3
M1	1609	0.0	-1.1	0.0	0.0	0.0	0.0	0.0	0.0	-1.1
M2	1610	0.0	-1.1	0.0	0.0	0.0	0.0	0.0	0.0	-1.1
M3	1611	0.0	-1.1	0.0	0.0	0.0	0.0	0.0	0.0	-1.1
M4	1612	0.0	-1.1	0.0	0.0	0.0	0.0	0.0	0.0	-1.1
M5	1613	0.0	-1.1	0.0	0.0	0.0	0.0	0.0	0.0	-1.1
N1	2216	-0.1	-1.0	1.2	0.0	0.0	0.0	1.2	-0.1	-1.0
N2	2217	0.0	-1.0	1.2	0.0	0.0	0.0	1.2	0.0	-1.0

Table 2.10.4-51 Primary Stresses; 1-Foot Bottom End Drop; Drop Orientation = 0 Degrees; 2-D Model; Condition 1 (continued)

Stress Points		Stress Components (ksi)						Principal Stresses (ksi)		
Section[1]	Node	S_x	S_y	S_z	S_{xy}	S_{yz}	S_{xz}	S1	S2	S3
N3	2218	0.0	-0.9	1.2	0.0	0.0	0.0	1.2	0.0	-0.9
N4	2219	0.0	-0.9	1.2	0.0	0.0	0.0	1.2	0.0	-0.9
O1	2224	0.0	-0.7	0.0	0.0	0.0	0.0	0.0	0.0	-0.7
O2	2225	0.0	-0.7	0.0	0.0	0.0	0.0	0.0	0.0	-0.7
O3	2226	0.0	-0.7	0.0	0.0	0.0	0.0	0.0	0.0	-0.7
O4	2227	0.0	-0.7	0.0	0.0	0.0	0.0	0.0	0.0	-0.7
O5	2228	0.0	-0.7	0.0	0.0	0.0	0.0	0.0	0.0	-0.7
P1	2546	-0.1	-0.6	1.0	0.0	0.0	0.0	1.0	-0.1	-0.6
P2	2547	0.0	-0.7	1.0	0.0	0.0	0.0	1.0	0.0	-0.7
P3	2548	0.0	-0.8	1.0	0.0	0.0	0.0	1.0	0.0	-0.8
P4	2549	0.0	-0.9	0.9	0.0	0.0	0.0	0.9	0.0	-0.9
Q1	2554	0.0	-0.4	0.1	0.0	0.0	0.0	0.1	0.0	-0.4
Q2	2555	0.0	-0.5	0.1	0.0	0.0	0.0	0.1	0.0	-0.5
Q3	2556	0.0	-0.5	0.1	0.0	0.0	0.0	0.1	0.0	-0.5
Q4	2557	0.0	-0.6	0.1	0.0	0.0	0.0	0.1	0.0	-0.6
Q5	2558	0.0	-0.7	0.0	0.0	0.0	0.0	0.0	0.0	-0.7
R1	2771	-0.3	-1.5	0.2	0.2	0.0	0.0	0.2	-0.3	-1.5
R2	2772	-0.2	-0.9	0.4	0.2	0.0	0.0	0.4	-0.2	-1.0
R3	2773	-0.4	-0.4	0.4	0.3	0.0	0.0	0.4	-0.1	-0.7
R4	2774	-1.0	0.8	0.6	0.3	0.0	0.0	0.9	0.6	-1.0
S1	2779	-0.9	-1.0	-0.1	0.0	0.0	0.0	-0.1	-0.9	-1.0
S2	2780	-0.5	-0.6	0.1	0.0	0.0	0.0	0.1	-0.5	-0.6
S3	2781	-0.3	-0.3	0.3	-0.1	0.0	0.0	0.3	-0.2	-0.4
S4	2782	-0.1	0.0	0.4	-0.1	0.0	0.0	0.4	0.0	-0.1
S5	2783	0.0	0.4	0.5	0.0	0.0	0.0	0.5	0.4	0.0
T1	7066	0.5	0.4	0.5	0.2	0.0	0.0	0.7	0.5	0.2
T2	7067	0.6	-0.3	0.2	0.0	0.0	0.0	0.6	0.2	-0.3
T3	7068	0.4	-0.4	0.2	0.0	0.0	0.0	0.4	0.2	-0.4
T4	7069	0.2	-0.4	0.1	0.0	0.0	0.0	0.2	0.1	-0.4
T5	7070	0.1	-0.4	0.1	0.0	0.0	0.0	0.1	0.1	-0.4
T6	7071	0.1	-0.5	0.1	0.0	0.0	0.0	0.1	0.1	-0.5
T7	7072	0.0	-0.6	0.1	0.0	0.0	0.0	0.1	0.0	-0.6
U1	3051	-0.3	-2.2	-0.2	0.5	0.0	0.0	-0.1	-0.2	-2.3

Table 2.10.4-51 Primary Stresses; 1-Foot Bottom End Drop; Drop Orientation = 0 Degrees; 2-D Model; Condition 1 (continued)

Stress Points		Stress Components (ksi)						Principal Stresses (ksi)		
Section[1]	Node	S_x	S_y	S_z	S_{xy}	S_{yz}	S_{xz}	S1	S2	S3
U2	3052	-0.4	-2.5	-0.5	0.5	0.0	0.0	-0.3	-0.5	-2.6
U3	3053	0.0	-2.5	-0.5	0.2	0.0	0.0	0.0	-0.5	-2.5
U4	3054	0.2	-2.0	-0.5	-0.4	0.0	0.0	0.2	-0.5	-2.1
U5	3055	-0.2	-1.3	-0.4	-0.5	0.0	0.0	0.0	-0.4	-1.4
U6	3056	1.0	-0.2	0.2	-0.1	0.0	0.0	1.0	0.2	-0.2
V1	3611	1.0	0.0	0.9	0.0	0.0	0.0	1.0	0.9	0.0
V2	3612	0.5	-0.1	0.5	0.0	0.0	0.0	0.5	0.5	-0.1
V3	3613	0.3	-0.3	0.2	0.0	0.0	0.0	0.3	0.2	-0.3
V4	3614	0.1	-0.6	-0.1	0.0	0.0	0.0	0.1	-0.1	-0.6
V5	3615	-0.2	-1.0	-0.5	0.0	0.0	0.0	-0.2	-0.5	-1.0
V6	3616	-0.4	-0.5	-0.6	0.0	0.0	0.0	-0.4	-0.5	-0.6
V7	3617	-1.2	0.4	-0.7	0.0	0.0	0.0	0.4	-0.7	-1.2
W1	3241	0.9	0.0	0.9	0.0	0.0	0.0	0.9	0.9	0.0
W2	3242	0.6	0.0	0.6	0.0	0.0	0.0	0.6	0.6	0.0
W3	3243	0.3	0.0	0.3	0.0	0.0	0.0	0.3	0.3	0.0
W4	3244	0.0	0.0	0.0	0.0	0.0	0.0	0.0	0.0	0.0
W5	3245	-0.2	0.0	-0.2	0.0	0.0	0.0	0.0	-0.2	-0.2
W6	3246	-0.5	0.0	-0.5	0.0	0.0	0.0	0.0	-0.5	-0.5
X1	3801	1.4	0.0	1.4	0.0	0.0	0.0	1.4	1.4	0.0
X2	3802	1.0	0.0	1.0	0.0	0.0	0.0	1.0	1.0	0.0
X3	3803	0.5	0.0	0.5	0.0	0.0	0.0	0.5	0.5	0.0
X4	3804	0.0	0.0	0.0	0.0	0.0	0.0	0.0	0.0	0.0
X5	3805	-0.4	0.0	-0.4	0.0	0.0	0.0	0.0	-0.4	-0.4
X6	3806	-0.9	0.0	-0.9	0.0	0.0	0.0	0.0	-0.9	-0.9
X7	3807	-1.4	0.0	-1.4	0.0	0.0	0.0	0.0	-1.4	-1.4

[1] Refer to Figure 2.10.2-34 for the identification of the representative sections.

Table 2.10.4-52 Primary + Secondary Stresses; 1-Foot Bottom End Drop; Drop Orientation = 0 Degrees; 2-D Model; Condition 1

Condition 1: 100°F Ambient with Contents

Stress Points		Stress Components (ksi)						Principal Stresses (ksi)		
Section[1]	Node	S_x	S_y	S_z	S_{xy}	S_{yz}	S_{xz}	S1	S2	S3
A1	1	6.9	-0.4	6.9	0.0	0.0	0.0	6.9	6.9	-0.4
A2	2	3.7	-0.4	3.7	0.0	0.0	0.0	3.7	3.7	-0.4
A3	3	0.5	-0.5	0.5	0.0	0.0	0.0	0.5	0.5	-0.5
A4	4	-2.7	-0.6	-2.7	0.0	0.0	0.0	-0.6	-2.7	-2.7
A5	5	-6.0	-0.6	-6.0	0.0	0.0	0.0	-0.6	-6.0	-6.0
B1	6	6.0	-0.7	6.0	0.0	0.0	0.0	6.0	6.0	-0.7
B2	7	3.1	-0.7	3.1	0.0	0.0	0.0	3.1	3.1	-0.7
B3	8	0.1	-0.7	0.1	0.0	0.0	0.0	0.1	0.1	-0.7
B4	9	-2.9	-0.8	-2.9	0.0	0.0	0.0	-0.8	-2.9	-2.9
B5	10	-5.8	-0.8	-5.8	0.0	0.0	0.0	-0.8	-5.8	-5.8
C1	251	-3.9	-6.8	-0.4	-1.3	0.0	0.0	-0.4	-3.4	-7.3
C2	252	-0.3	-3.0	0.6	-1.1	0.0	0.0	0.6	0.1	-3.4
C3	253	0.7	-1.8	0.2	-1.1	0.0	0.0	1.1	0.2	-2.2
C4	254	2.2	-1.6	-0.4	-0.8	0.0	0.0	2.4	-0.4	-1.7
C5	255	3.8	-1.6	-1.1	-0.5	0.0	0.0	3.8	-1.1	-1.6
D1	306	-0.5	1.3	0.6	0.2	0.0	0.0	1.3	0.6	-0.6
D2	307	-0.7	0.0	-0.1	0.6	0.0	0.0	0.3	-0.1	-1.0
D3	308	-0.1	-0.5	-0.4	0.5	0.0	0.0	0.2	-0.4	-0.8
D4	309	0.4	-0.7	-0.7	0.3	0.0	0.0	0.4	-0.7	-0.8
D5	310	0.7	-0.8	-0.9	0.2	0.0	0.0	0.7	-0.8	-0.9
E1	305	4.0	1.9	1.4	-0.6	0.0	0.0	4.1	1.7	1.4
E2	315	1.7	0.1	0.6	-0.1	0.0	0.0	1.7	0.6	0.1
E3	325	1.0	-0.4	0.3	0.1	0.0	0.0	1.0	0.3	-0.4
E4	335	0.5	-0.7	0.2	0.2	0.0	0.0	0.6	0.2	-0.7
E5	345	0.2	-1.2	0.0	0.1	0.0	0.0	0.3	0.0	-1.2
E6	355	0.2	-2.0	-0.2	0.0	0.0	0.0	0.2	-0.2	-2.0
F1	251	-3.9	-6.8	-0.4	-1.3	0.0	0.0	-0.4	-3.4	-7.3
F2	261	-2.6	-2.9	0.9	-0.7	0.0	0.0	0.9	-2.0	-3.5
F3	271	-1.0	-0.1	1.9	-0.6	0.0	0.0	1.9	0.2	-1.3
F4	281	-0.7	3.1	2.6	-1.1	0.0	0.0	3.4	2.6	-1.0
G1	311	-5.7	-3.6	-1.0	1.3	0.0	0.0	-1.0	-3.0	-6.3

Table 2.10.4-52 Primary + Secondary Stresses; 1-Foot Bottom End Drop; Drop Orientation = 0 Degrees; 2-D Model; Condition 1 (continued)

Stress Points		Stress Components (ksi)						Principal Stresses (ksi)		
Section[1]	Node	S_x	S_y	S_z	S_{xy}	S_{yz}	S_{xz}	S1	S2	S3
G2	321	-4.7	0.6	0.4	1.1	0.0	0.0	0.8	0.4	-4.9
G3	331	-2.3	2.8	1.7	0.4	0.0	0.0	2.8	1.7	-2.4
G4	341	-0.9	5.0	2.6	0.2	0.0	0.0	5.0	2.6	-0.9
G5	351	-0.4	8.0	3.6	0.0	0.0	0.0	8.0	3.6	-0.4
H1	581	-0.1	-0.4	1.1	0.0	0.0	0.0	1.1	-0.1	-0.4
H2	582	-0.1	-1.6	0.8	0.1	0.0	0.0	0.8	-0.1	-1.6
H3	583	0.0	-2.8	0.6	0.2	0.0	0.0	0.6	0.0	-2.8
H4	584	-0.2	-4.3	0.3	0.3	0.0	0.0	0.3	-0.2	-4.3
I1	589	-0.3	3.8	2.8	0.0	0.0	0.0	3.8	2.8	-0.3
I2	590	-0.2	3.8	2.9	0.0	0.0	0.0	3.8	2.9	-0.2
I3	591	-0.1	3.8	3.0	0.1	0.0	0.0	3.8	3.0	-0.1
I4	592	-0.1	3.8	3.1	0.1	0.0	0.0	3.8	3.1	-0.1
I5	593	0.0	3.8	3.2	0.0	0.0	0.0	3.8	3.2	0.0
J1	971	-0.1	-3.9	0.1	0.0	0.0	0.0	0.1	-0.1	-3.9
J2	972	0.0	-2.7	0.8	0.0	0.0	0.0	0.8	0.0	-2.7
J3	973	0.0	-1.5	1.6	0.0	0.0	0.0	1.6	0.0	-1.5
J4	974	0.0	-0.3	2.3	0.0	0.0	0.0	2.3	0.0	-0.3
K1	979	-0.3	1.8	3.8	0.0	0.0	0.0	3.8	1.8	-0.3
K2	980	-0.3	2.9	4.5	0.0	0.0	0.0	4.5	2.9	-0.3
K3	981	-0.2	4.0	5.1	0.0	0.0	0.0	5.1	4.0	-0.2
K4	982	-0.1	5.1	5.7	0.0	0.0	0.0	5.7	5.1	-0.1
K5	983	0.0	6.1	6.2	0.0	0.0	0.0	6.2	6.1	0.0
L1	1601	-0.1	-3.1	0.1	0.0	0.0	0.0	0.1	-0.1	-3.1
L2	1602	0.0	-2.2	0.8	0.0	0.0	0.0	0.8	0.0	-2.2
L3	1603	0.0	-1.3	1.5	0.0	0.0	0.0	1.5	0.0	-1.3
L4	1604	0.0	-0.4	2.2	0.0	0.0	0.0	2.2	0.0	-0.4
M1	1609	-0.4	2.3	4.6	0.0	0.0	0.0	4.6	2.3	-0.4
M2	1610	-0.3	3.3	5.3	0.0	0.0	0.0	5.3	3.3	-0.3
M3	1611	-0.2	4.3	6.0	0.0	0.0	0.0	6.0	4.3	-0.2
M4	1612	-0.1	5.4	6.6	0.0	0.0	0.0	6.6	5.4	-0.1
M5	1613	0.0	6.4	7.2	0.0	0.0	0.0	7.2	6.4	0.0
N1	2216	-0.1	-3.0	-0.2	0.0	0.0	0.0	-0.1	-0.2	-3.0
N2	2217	0.0	-1.9	0.5	0.0	0.0	0.0	0.5	0.0	-1.9

Table 2.10.4-52 Primary + Secondary Stresses; 1-Foot Bottom End Drop; Drop Orientation = 0 Degrees; 2-D Model; Condition 1 (continued)

Stress Points		Stress Components (ksi)						Principal Stresses (ksi)		
Section[1]	Node	S_x	S_y	S_z	S_{xy}	S_{yz}	S_{zx}	S1	S2	S3
N3	2218	0.0	-0.9	1.1	0.0	0.0	0.0	1.1	0.0	-0.9
N4	2219	0.0	0.2	1.7	0.0	0.0	0.0	1.7	0.2	0.0
O1	2224	-0.3	3.1	3.6	0.0	0.0	0.0	3.6	3.1	-0.3
O2	2225	-0.2	3.9	4.1	0.0	0.0	0.0	4.1	3.9	-0.2
O3	2226	-0.2	4.7	4.6	0.0	0.0	0.0	4.7	4.6	-0.2
O4	2227	-0.1	5.5	5.1	0.0	0.0	0.0	5.5	5.1	-0.1
O5	2228	0.0	6.3	5.6	0.0	0.0	0.0	6.3	5.6	0.0
P1	2546	0.0	-1.4	0.7	0.0	0.0	0.0	0.7	0.0	-1.4
P2	2547	0.0	-1.3	0.8	0.0	0.0	0.0	0.8	0.0	-1.3
P3	2548	0.1	-1.1	1.1	0.0	0.0	0.0	1.1	0.1	-1.1
P4	2549	-0.2	-1.1	1.1	0.0	0.0	0.0	1.1	-0.2	-1.1
Q1	2554	-0.1	4.3	2.3	0.0	0.0	0.0	4.3	2.3	-0.1
Q2	2555	-0.1	4.6	2.6	0.1	0.0	0.0	4.6	2.6	-0.1
Q3	2556	-0.1	4.9	2.8	0.1	0.0	0.0	4.9	2.8	-0.1
Q4	2557	0.0	5.2	3.1	0.1	0.0	0.0	5.2	3.1	0.0
Q5	2558	0.0	5.5	3.3	0.0	0.0	0.0	5.5	3.3	0.0
R1	2771	-0.6	1.3	-2.9	0.3	0.0	0.0	1.4	-0.6	-2.9
R2	2772	-0.9	-0.5	-2.9	0.4	0.0	0.0	-0.3	-1.2	-2.9
R3	2773	-2.0	-1.7	-3.1	0.5	0.0	0.0	-1.3	-2.4	-3.1
R4	2774	-4.0	-2.6	-3.3	0.3	0.0	0.0	-2.5	-3.3	-4.0
S1	2779	1.2	6.7	1.6	-2.0	0.0	0.0	7.4	1.6	0.6
S2	2780	1.5	5.1	1.6	-0.8	0.0	0.0	5.3	1.6	1.4
S3	2781	0.8	3.8	1.4	0.2	0.0	0.0	3.8	1.4	0.8
S4	2782	0.3	2.5	1.1	0.3	0.0	0.0	2.6	1.1	0.3
S5	2783	0.2	1.1	1.0	0.3	0.0	0.0	1.1	1.0	0.1
T1	7066	-0.9	-5.0	-0.1	-1.5	0.0	0.0	-0.1	-0.4	-5.5
T2	7067	-0.9	-3.1	0.4	-1.0	0.0	0.0	0.4	-0.5	-3.5
T3	7068	-0.6	-1.2	1.1	-0.6	0.0	0.0	1.1	-0.3	-1.6
T4	7069	-0.4	0.3	1.7	-0.4	0.0	0.0	1.7	0.4	-0.6
T5	7070	-0.2	1.6	2.2	-0.2	0.0	0.0	2.2	1.6	-0.3
T6	7071	-0.1	3.0	2.7	-0.1	0.0	0.0	3.0	2.7	-0.1
T7	7072	-0.1	4.5	3.2	0.0	0.0	0.0	4.5	3.2	-0.1
U1	3051	-1.4	-3.4	-2.5	0.6	0.0	0.0	-1.2	-2.5	-3.6

Table 2.10.4-52 Primary + Secondary Stresses; 1-Foot Bottom End Drop; Drop Orientation = 0 Degrees; 2-D Model; Condition 1 (continued)

Stress Points		Stress Components (ksi)						Principal Stresses (ksi)		
Section[1]	Node	S_x	S_y	S_z	S_{xy}	S_{yz}	S_{xz}	S1	S2	S3
U2	3052	-0.4	-3.4	-2.3	0.5	0.0	0.0	-0.3	-2.3	-3.5
U3	3053	0.2	-3.0	-1.9	0.0	0.0	0.0	0.2	-1.9	-3.0
U4	3054	0.4	-2.1	-1.6	-0.7	0.0	0.0	0.6	-1.6	-2.3
U5	3055	0.0	-1.0	-1.3	-0.8	0.0	0.0	0.4	-1.3	-1.4
U6	3056	1.7	-0.3	-0.5	-0.2	0.0	0.0	1.7	-0.3	-0.5
V1	3611	1.2	-0.1	-1.3	-0.1	0.0	0.0	1.2	-0.1	-1.3
V2	3612	0.8	-0.1	-1.0	-0.1	0.0	0.0	0.8	-0.1	-1.0
V3	3613	0.4	-0.4	-0.8	-0.1	0.0	0.0	0.5	-0.4	-0.8
V4	3614	0.2	-0.8	-0.7	-0.1	0.0	0.0	0.2	-0.7	-0.8
V5	3615	-0.1	-1.5	-0.7	-0.1	0.0	0.0	-0.1	-0.7	-1.6
V6	3616	-0.3	-0.7	-0.2	0.0	0.0	0.0	-0.2	-0.3	-0.7
V7	3617	-1.5	0.7	0.2	0.0	0.0	0.0	0.7	0.2	-1.5
W1	3241	2.7	0.0	2.7	0.0	0.0	0.0	2.7	2.7	0.0
W2	3242	2.2	0.0	2.2	0.0	0.0	0.0	2.2	2.2	0.0
W3	3243	1.7	0.0	1.7	0.0	0.0	0.0	1.7	1.7	0.0
W4	3244	1.2	0.0	1.2	0.0	0.0	0.0	1.2	1.2	0.0
W5	3245	0.7	0.0	0.7	0.0	0.0	0.0	0.7	0.7	0.0
W6	3246	0.2	0.0	0.2	0.0	0.0	0.0	0.2	0.2	0.0
X1	3801	-0.5	0.0	-0.5	0.0	0.0	0.0	0.0	-0.5	-0.5
X2	3802	-0.2	0.0	-0.2	0.0	0.0	0.0	0.0	-0.2	-0.2
X3	3803	0.2	0.0	0.2	0.0	0.0	0.0	0.2	0.2	0.0
X4	3804	0.5	0.0	0.5	0.0	0.0	0.0	0.5	0.5	0.0
X5	3805	0.8	0.0	0.8	0.0	0.0	0.0	0.8	0.8	0.0
X6	3806	1.1	0.0	1.1	0.0	0.0	0.0	1.1	1.1	0.0
X7	3807	1.5	0.0	1.5	0.0	0.0	0.0	1.5	1.5	0.0

[1] Refer to Figure 2.10.2-34 for the identification of the representative sections.

Table 2.10.4-53 P_m Stresses; 1-Foot Bottom End Drop; Drop Orientation = 0 Degrees; 2-D Model; Condition 1

Condition 1: 100°F Ambient with Contents

Section[1]	Node - Node	Stress Components (ksi)						Principal Stresses (ksi)			
		S_x	S_y	S_z	S_{xy}	S_{yz}	S_{zx}	S1	S2	S3	S.I.
A	1 - 5	1.0	-0.5	1.0	0.0	0.0	0.0	1.0	1.0	-0.5	1.5
B	6 - 10	-1.2	-0.7	-1.2	0.0	0.0	0.0	-0.7	-1.2	-1.2	0.5
C	251 - 255	1.1	-1.3	0.8	-0.5	0.0	0.0	1.2	0.8	-1.5	2.7
D	306 - 310	-0.8	-2.5	-1.6	-0.4	0.0	0.0	-0.7	-1.6	-2.6	1.9
E	305 - 355	1.7	-1.8	0.3	-1.2	0.0	0.0	2.1	0.3	-2.1	4.2
F	251 - 281	-2.4	-1.2	1.1	-0.2	0.0	0.0	1.1	-1.2	-2.4	3.5
G	311 - 351	-1.2	-1.6	0.7	0.2	0.0	0.0	0.7	-1.1	-1.7	2.4
H	581 - 584	-0.1	-1.8	1.0	0.1	0.0	0.0	1.0	-0.1	-1.8	2.9
I	589 - 593	0.0	-1.6	0.3	0.0	0.0	0.0	0.3	0.0	-1.6	1.9
J	971 - 974	0.0	-1.7	1.2	0.0	0.0	0.0	1.2	0.0	-1.7	2.8
K	979 - 983	0.0	-1.4	0.0	0.0	0.0	0.0	0.0	0.0	-1.4	1.4
L	1601 - 1604	0.0	-1.3	1.2	0.0	0.0	0.0	1.2	0.0	-1.3	2.5
M	1609 - 1613	0.0	-1.1	0.0	0.0	0.0	0.0	0.0	0.0	-1.1	1.1
N	2216 - 2219	0.0	-1.0	1.2	0.0	0.0	0.0	1.2	0.0	-1.0	2.1
O	2224 - 2228	0.0	-0.7	0.0	0.0	0.0	0.0	0.0	0.0	-0.7	0.7
P	2546 - 2549	0.0	-0.7	1.0	0.0	0.0	0.0	1.0	0.0	-0.7	1.7
Q	2554 - 558	0.0	-0.5	0.1	0.0	0.0	0.0	0.1	0.0	-0.5	0.6
R	2771 - 2774	-0.4	-0.5	0.4	0.2	0.0	0.0	0.4	-0.2	-0.7	1.1
S	2779 - 2783	-0.3	-0.3	0.2	0.0	0.0	0.0	0.2	-0.3	-0.4	0.6
T	7066 - 7072	0.3	-0.4	0.2	0.0	0.0	0.0	0.3	0.2	-0.4	0.6
U	3051 - 3056	0.0	-1.9	-0.4	0.0	0.0	0.0	0.0	-0.4	-1.9	1.9
V	3611 - 3617	0.0	-0.3	-0.1	0.0	0.0	0.0	0.0	-0.1	-0.3	0.4
W	3241 - 3246	0.2	0.0	0.2	0.0	0.0	0.0	0.2	0.2	0.0	0.2
X	3801 - 3807	0.0	0.0	0.0	0.0	0.0	0.0	0.0	0.0	0.0	0.0

[1] Refer to Figure 2.10.2-34 for the identification of the representative sections.

Table 2.10.4-54 $P_m + P_b$ Stresses; 1-Foot Bottom End Drop; Drop Orientation = 0 Degrees; 2-D Model; Condition 1

Condition 1: 100°F Ambient with Contents

		Stress Components (ksi)						Principal Stresses (ksi)			
Section[1]	Node - Node	S_x	S_y	S_z	S_{xy}	S_{yz}	S_{zx}	S1	S2	S3	S.I.
A I	1 - 5	7.0	-0.4	7.0	0.0	0.0	0.0	7.0	7.0	-0.4	7.4
B O	6 - 10	-6.5	-0.8	-6.5	0.0	0.0	0.0	-0.8	-6.5	-6.5	5.6
C O	251 - 255	5.3	-0.5	1.1	-0.5	0.0	0.0	5.3	1.1	-0.6	5.9
D O	306 - 310	2.7	-1.0	-1.0	-0.4	0.0	0.0	2.7	-1.0	-1.1	3.8
E I	305 - 355	5.1	-2.3	0.8	-1.2	0.0	0.0	5.3	0.8	-2.5	7.8
F I	251 - 281	-3.5	-3.7	0.2	-0.2	0.0	0.0	0.2	-3.4	-3.9	4.1
G I	311 - 351	-2.7	-4.1	-0.2	0.2	0.0	0.0	-0.2	-2.6	-4.1	3.9
H O	581 - 584	0.0	-2.6	0.8	0.1	0.0	0.0	0.8	0.0	-2.6	3.4
I O	589 - 593	0.0	-2.0	0.1	0.0	0.0	0.0	0.1	0.0	-2.0	2.2
J I	971 - 974	-0.1	-1.7	1.2	0.0	0.0	0.0	1.2	-0.1	-1.7	2.9
K I	979 - 983	0.0	-1.4	0.0	0.0	0.0	0.0	0.0	0.0	-1.4	1.4
L I	1601 - 1604	-0.1	-1.3	1.2	0.0	0.0	0.0	1.2	-0.1	-1.3	2.5
M O	1609 - 1613	0.0	-1.1	0.0	0.0	0.0	0.0	0.0	0.0	-1.1	1.1
N I	2216 - 2219	-0.1	-1.0	1.2	0.0	0.0	0.0	1.2	-0.1	-1.0	2.2
O I	2224 - 2228	0.0	-0.7	0.0	0.0	0.0	0.0	0.0	0.0	-0.7	0.7
P O	2546 - 2549	0.0	-0.9	0.9	0.0	0.0	0.0	0.9	0.0	-0.9	1.8
Q O	2554 - 2558	0.0	-0.7	0.0	0.0	0.0	0.0	0.0	0.0	-0.7	0.7
R I	2771 - 2774	-0.3	-1.6	0.2	0.2	0.0	0.0	0.2	-0.2	-1.7	1.9
S I	2779 - 2783	-0.9	-1.0	0.0	0.0	0.0	0.0	0.0	-0.9	-1.0	1.0
T O	7066 - 7072	0.0	-0.6	0.0	0.0	0.0	0.0	0.0	0.0	-0.6	0.6
U I	3051 - 3056	-0.4	-6.5	-0.6	0.0	0.0	0.0	-0.4	-0.6	-6.5	6.1
V I	3611 - 3617	0.9	2.5	0.8	0.0	0.0	0.0	2.5	0.9	0.8	1.8
W I	3241 - 3246	0.9	0.0	0.9	0.0	0.0	0.0	0.9	0.9	0.0	0.9
X I	3801 - 3807	1.4	0.0	1.4	0.0	0.0	0.0	1.4	1.4	0.0	1.5

[1] Refer to Figure 2.10.2-34 for the identification of the representative sections.

Table 2.10.4-55 S_n Stresses; 1-Foot Bottom End Drop; Drop Orientation = 0 Degrees; 2-D Model; Condition 1

Condition 1: 100°F Ambient with Contents

Section[1]	Node - Node	Stress Components (ksi) S_x	S_y	S_z	S_{xy}	S_{yz}	S_{xz}	Principal Stresses (ksi) S1	S2	S3	S.I.
A I	1 - 5	6.9	-0.4	6.9	0.0	0.0	0.0	6.9	6.9	-0.4	7.3
B I	6 - 10	6.1	-0.7	6.1	0.0	0.0	0.0	6.1	6.1	-0.7	6.7
C I	251 - 255	-2.7	-6.8	0.5	-1.0	0.0	0.0	0.5	-2.4	-7.0	7.5
D I	306 - 310	-0.9	1.3	0.4	0.4	0.0	0.0	1.4	0.4	-0.9	2.3
E I	305 - 355	4.0	1.5	1.2	0.0	0.0	0.0	4.0	1.5	1.2	2.8
F I	251 - 281	-3.9	-6.4	-0.2	-0.8	0.0	0.0	-0.2	-3.6	-6.7	6.5
G O	311 - 351	-0.4	7.9	3.8	0.6	0.0	0.0	7.9	3.8	-0.4	8.4
H O	581 - 584	-0.2	-4.1	0.3	0.2	0.0	0.0	0.3	-0.2	-4.1	4.5
I I	589 - 593	-0.3	3.8	2.8	0.0	0.0	0.0	3.8	2.8	-0.3	4.1
J I	971 - 974	-0.1	-3.9	0.1	0.0	0.0	0.0	0.1	-0.1	-3.9	4.0
K O	979 - 983	0.0	6.2	6.3	0.0	0.0	0.0	6.3	6.2	0.0	6.3
L I	1601 - 1604	-0.1	-3.1	0.2	0.0	0.0	0.0	0.2	-0.1	-3.1	3.2
M O	1609 - 1613	0.0	6.4	7.2	0.0	0.0	0.0	7.2	6.4	0.0	7.2
N I	2216 - 2219	-0.1	-3.0	-0.2	0.0	0.0	0.0	-0.1	-0.2	-3.0	3.0
O O	2224 - 2228	0.0	6.3	5.6	0.0	0.0	0.0	6.3	5.6	0.0	6.3
P O	2546 - 2549	-0.2	-1.0	1.2	0.0	0.0	0.0	1.2	-0.2	-1.0	2.2
Q O	2554 - 2558	0.0	5.5	3.3	0.1	0.0	0.0	5.5	3.3	0.0	5.5
R I	2771 - 2774	-0.6	1.0	-2.8	0.4	0.0	0.0	1.1	-0.7	-2.8	3.9
S I	2779 - 2783	1.2	6.6	1.8	-0.3	0.0	0.0	6.6	1.8	1.2	5.4
T O	7066 - 7072	-0.1	4.6	3.2	-0.5	0.0	0.0	4.7	3.2	-0.1	4.8
U I	3051 - 3056	-0.8	-10.0	-2.5	-0.2	0.0	0.0	-0.8	-2.5	-10.0	9.2
V I	3611 - 3617	1.1	2.4	-1.2	-0.1	0.0	0.0	2.4	1.0	-1.2	3.6
W I	3241 - 3246	2.7	0.0	2.7	0.0	0.0	0.0	2.7	2.7	0.0	2.7
X O	3801 - 3807	1.5	0.0	1.5	0.0	0.0	0.0	1.5	1.5	0.0	1.5

Table 2.10.4-56 Critical P_m Stress Summary; 1-Foot Bottom End Drop; Drop Orientation = 0 Degrees; 2-D Model; Condition 1

Condition 1: 100°F Ambient with Contents

Comp. No.[1]	Section Cut Node-Node	P_m Stresses (ksi) S_x	S_y	S_z	S_{xy}	S_{yz}	S_{xz}	Principal Stresses (ksi) S1	S2	S3	S.I.	Allow. Stress	Margin of Safety
1	306- 310	-0.8	-2.5	-1.6	-0.4	0.0	0.0	-0.7	-1.6	-2.6	1.9	19.2	9.1
2	305- 355	1.7	-1.8	0.3	-1.2	0.0	0.0	2.1	0.3	-2.1	4.2	18.5	3.4
3	416- 419	0.0	-1.5	2.1	-0.2	0.0	0.0	2.1	0.0	-1.5	3.6	31.4	7.7
4	851- 854	0.0	-1.7	1.2	0.0	0.0	0.0	1.2	0.0	-1.7	2.9	19.6	5.8
5	544- 548	0.0	-1.7	0.5	0.0	0.0	0.0	0.5	0.0	-1.7	2.1	20.0	8.5
6	7064-2774	0.0	4.0	1.5	0.1	0.0	0.0	4.0	1.5	0.0	4.0	20.0	4.0
7	3021-3026	0.2	-7.6	-1.8	-0.2	0.0	0.0	0.2	-1.8	-7.6	7.8	20.0	1.6
8	3521-3527	0.0	-0.4	-0.1	0.2	0.0	0.0	0.1	-0.1	-0.4	0.5	45.0	89.0

Locations of the most critical sections for each component are provided in the following:

Comp. No.[1]	Section Location Inside Node x (in)	y (in)	Outside Node z (in)	x (in)
1	39.44	6.20	39.44	0.75
2	39.44	8.20	43.35	8.20
3	35.50	18.40	37.50	18.40
4	35.50	47.40	37.00	47.40
5	40.70	26.40	43.35	26.40
6	37.655	179.40	37.50	175.40
7	37.655	179.40	37.655	185.40
8	39.56	188.40	39.56	193.71

[1] Refer to Figure 2.10.2-33 for cask component identification.

Table 2.10.4-57 Critical $P_m + P_b$ Stress Summary; 1-Foot Bottom End Drop; Drop Orientation = 0 Degrees; 2-D Model; Condition 1

Condition 1: 100°F Ambient with Contents

Comp. No.[1]	Section Cut Node-Node	$P_m + P_b$ Stresses (ksi) S_x	S_y	S_z	S_{xy}	S_{yz}	S_{xz}	Principal Stresses (ksi) S1	S2	S3	S.I.	Allow. Stress	Margin of Safety
1	16- 20	-6.4	-0.8	-6.4	0.0	0.0	0.0	-0.8	-6.4	-6.4	5.7	28.7	4.0
2	305- 355	5.1	-2.3	0.8	-1.2	0.0	0.0	5.3	0.8	-2.5	7.8	27.7	2.6
3	416- 419	-0.1	-3.3	1.7	-0.2	0.0	0.0	1.7	-0.1	-3.3	5.0	47.1	8.4
4	851- 854	-0.1	-1.8	1.2	0.0	0.0	0.0	1.2	-0.1	-1.8	3.0	29.4	8.8
5	544- 548	0.0	-2.0	0.4	0.0	0.0	0.0	0.4	0.0	-2.0	2.3	30.0	12.0
6	7064-2774	2.2	12.7	3.5	0.1	0.0	0.0	12.7	3.5	2.2	10.5	30.0	1.9
7	3021-3026	0.1	12.7	-1.1	-0.2	0.0	0.0	12.7	0.1	-1.1	13.8	30.0	1.2
8	3521-3527	0.1	-2.2	0.3	0.2	0.0	0.0	0.3	0.1	-2.2	2.5	67.5	26.0

Locations of the most critical sections for each component are provided in the following:

Comp. No.[1]	Section Location Inside Node x (in)	y (in)	Outside Node z (in)	x (in)
1	1.42	6.20	1.42	0.75
2	39.44	8.20	43.35	8.20
3	35.50	18.40	37.50	18.40
4	35.50	47.40	37.00	47.40
5	40.70	26.40	43.35	26.40
6	37.655	179.40	37.50	175.40
7	37.655	179.40	37.655	185.40
8	39.56	188.40	39.56	193.71

[1] Refer to Figure 2.10.2-33 for cask component identification.

Table 2.10.4-58 Critical S_n Stress Summary; 1-Foot Bottom End Drop; Drop Orientation = 0 Degrees; 2-D Model; Condition 1

Condition 1: 100°F Ambient with Contents

Comp. No.[1]	Section Cut Node-Node	S_n Stresses (ksi)						Principal Stresses (ksi)				Allow. Stress 3.0 S_m
		S_x	S_y	S_z	S_{xy}	S_{yz}	S_{xz}	S1	S2	S3	S.I.	
1	16- 20	6.0	-0.7	6.1	0.0	0.0	0.0	6.1	6.0	-0.7	6.8	57.6
2	371- 374	0.5	-8.9	1.2	-1.0	0.0	0.0	1.2	0.6	-9.0	10.1	55.5
3	416- 419	-0.2	-3.8	3.3	-0.4	0.0	0.0	3.3	-0.1	-3.9	7.2	94.2
4	971- 974	-0.1	-3.9	0.1	0.0	0.0	0.0	0.1	-0.1	-3.9	4.0	58.8
5	1519-1523	6.4	0.0	7.3	0.0	0.0	0.0	7.3	6.4	0.0	7.3	60.0
6	2764-2768	10.5	-0.4	2.2	0.5	0.0	0.0	0.5	2.2	-0.5	11.0	60.0
7	3021-3026	1.0	12.2	-2.9	-0.5	0.0	0.0	12.2	1.0	-2.9	15.2	60.0
8	3611-3617	1.1	2.4	-1.2	-0.1	0.0	0.0	2.4	1.0	-1.2	3.6	135.0

Locations of the most critical sections for each component are provided in the following:

Comp. No.[1]	Section Location			
	Inside Node		Outside Node	
	x (in)	y (in)	z (in)	x (in)
1	1.42	6.20	1.42	0.75
2	35.50	15.40	37.50	15.40
3	35.50	18.40	37.50	18.40
4	35.50	55.65	37.00	55.65
5	40.70	91.40	43.35	91.40
6	40.70	174.40	43.35	174.40
7	37.655	179.40	37.655	185.40
8	35.206	188.40	35.206	193.71

[1] Refer to Figure 2.10.2-33 for cask component identification.

Table 2.10.4-59 Critical P_m Stress Summary; 1-Foot Bottom End Drop; Drop Orientation = 0 Degrees; 2-D Model; Condition 2

Condition 2: -20°F Ambient with Contents

Comp. No.[1]	Section Cut Node-Node	P_m Stresses (ksi)						Principal Stresses (ksi)			S.I.	Allow. Stress	Margin of Safety
		S_x	S_y	S_z	S_{xy}	S_{yz}	S_{xz}	S1	S2	S3			
1	306- 310	-0.8	-2.6	-1.7	-0.4	0.0	0.0	-0.8	-1.7	-2.7	1.9	19.2	9.1
2	305- 355	1.8	-1.8	0.3	-1.2	0.0	0.0	2.2	0.3	-2.2	4.4	18.5	3.2
3	416- 419	0.0	-1.7	2.0	-0.2	0.0	0.0	2.0	0.0	-1.8	3.7	31.4	7.5
4	851- 854	0.0	-2.0	0.3	0.0	0.0	0.0	0.3	0.0	-2.0	2.3	19.6	7.5
5	544- 548	0.0	-1.7	0.5	0.0	0.0	0.0	0.5	0.0	-1.7	2.2	20.0	8.1
6	7064- 2774	0.1	4.2	1.4	0.2	0.0	0.0	4.2	1.4	0.1	4.1	20.0	3.8
7	3021- 3026	0.2	-7.8	-1.8	-0.3	0.0	0.0	0.2	-1.8	-7.8	8.0	20.0	1.5
8	3521- 3527	0.0	-0.4	-0.1	0.2	0.0	0.0	0.1	-0.1	-0.5	0.5	45.0	89.0

Locations of the most critical sections for each component are provided in the following:

Comp. No.[1]	Section Location			
	Inside Node			Outside Node
	x (in)	y (in)	z (in)	x (in)
1	39.44	6.20	39.44	0.75
2	39.44	8.20	43.35	8.20
3	35.50	18.40	37.50	18.40
4	35.50	47.40	37.00	47.40
5	40.70	26.40	43.35	26.40
6	37.655	179.40	37.50	175.40
7	37.655	179.40	37.655	185.40
8	39.56	188.40	39.56	193.71

[1] **Refer to Figure 2.10.2-33 for cask component identification.**

Table 2.10.4-60 Critical $P_m + P_b$ Stress Summary; 1-Foot Bottom End Drop; Drop Orientation = 0 Degrees; 2-D Model; Condition 2

Condition 2: -20°F Ambient with Contents

Comp. No.[1]	Section Cut Node-Node	$P_m + P_b$ Stresses (ksi) S_x	S_y	S_z	S_{xy}	S_{yz}	S_{xz}	Principal Stresses (ksi) S1	S2	S3	S.I.	Allow. Stress	Margin of Safety
1	16- 20	-6.9	-0.8	-7.0	0.0	0.0	0.0	-0.8	-6.9	-7.0	6.2	28.7	3.6
2	305- 355	5.5	-2.3	0.9	-1.2	0.0	0.0	5.7	0.9	-2.5	8.2	27.7	2.4
3	416- 419	0.0	-3.8	1.5	-0.2	0.0	0.0	1.5	0.0	-3.8	5.3	47.1	7.9
4	851- 854	0.0	-2.1	0.3	0.0	0.0	0.0	0.3	0.0	-2.1	2.4	29.4	11.3
5	544- 548	0.0	-2.0	0.4	0.0	0.0	0.0	0.4	0.0	-2.0	2.4	30.0	11.5
6	7064-2774	2.3	13.0	3.4	0.2	0.0	0.0	13.0	3.4	2.3	10.7	30.0	1.8
7	3021-3026	0.1	13.0	-1.0	-0.3	0.0	0.0	13.0	0.1	-1.0	14.0	30.0	1.1
8	3521-3527	0.1	-2.5	0.4	0.2	0.0	0.0	0.4	0.1	-2.5	2.9	67.5	22.3

Locations of the most critical sections for each component are provided in the following:

Comp. No.[1]	Section Location Inside Node x (in)	y (in)	Outside Node z (in)	x (in)
1	1.42	6.20	1.42	0.75
2	39.44	8.20	43.35	8.20
3	35.50	18.40	37.50	18.40
4	35.50	47.40	37.00	47.40
5	40.70	26.40	43.35	26.40
6	37.655	179.40	37.50	175.40
7	37.655	179.40	37.655	185.40
8	39.56	188.40	39.56	193.71

[1] Refer to Figure 2.10.2-33 for cask component identification.

Table 2.10.4-61 Critical S_n Stress Summary; 1-Foot Bottom End Drop; Drop Orientation = 0 Degrees; 2-D Model; Condition 2

Condition 2: -20°F Ambient with Contents

Comp. No.[1]	Section Cut Node-Node	S_n Stresses (ksi) S_x	S_y	S_z	S_{xy}	S_{yz}	S_{zx}	Principal Stresses (ksi) S1	S2	S3	S.I.	Allow. Stress 3.0 S_m
1	306- 310	-2.7	-8.1	-1.4	-0.5	0.0	0.0	-1.4	-2.7	-8.1	6.7	57.6
2	301- 305	3.4	-6.3	0.0	0.8	0.0	0.0	3.5	0.0	-6.4	9.9	55.5
3	596- 599	0.0	-6.2	-0.8	0.2	0.0	0.0	0.0	-0.8	-6.2	6.2	94.2
4	926- 929	0.0	-6.0	-0.9	0.0	0.0	0.0	0.0	-0.9	-6.0	6.0	58.8
5	1579- 1583	3.8	0.0	3.2	0.0	0.0	0.0	3.8	3.2	0.0	3.8	60.0
6	7064- 2774	3.4	12.6	4.4	-0.1	0.0	0.0	12.6	4.4	3.4	9.2	60.0
7	3021- 3026	0.3	12.6	-3.3	-0.3	0.0	0.0	12.6	0.3	-3.3	15.9	60.0
8	3801- 3807	2.3	0.0	2.3	0.0	0.0	0.0	2.3	2.3	0.0	2.3	135.0

Locations of the most critical sections for each component are provided in the following:

Comp. No.[1]	Section Location Inside Node x (in)	y (in)	Outside Node z (in)	x (in)
1	39.44	6.20	39.44	0.75
2	39.633	14.40	39.44	8.20
3	35.50	30.40	37.00	30.40
4	35.50	52.40	37.00	52.40
5	40.70	95.40	43.35	95.40
6	37.655	179.40	37.50	175.40
7	37.655	179.40	37.655	185.40
8	0.0	188.46	0.0	193.71

[1] Refer to Figure 2.10.2-33 for cask component identification.

Table 2.10.4-62 Critical P_m Stress Summary; 1-Foot Bottom End Drop; Drop Orientation = 0 Degrees; 2-D Model; Condition 3

Condition 3: -20°F Ambient without Contents

Comp. No.[1]	Section Cut Node-Node	P_m Stresses (ksi)						Principal Stresses (ksi)			S.I.	Allow. Stress	Margin of Safety
		S_x	S_y	S_z	S_{xy}	S_{yz}	S_{xz}	S1	S2	S3			
1	306- 310	-1.0	-2.5	-1.8	-0.4	0.0	0.0	-0.9	-1.8	-2.6	1.7	19.2	10.3
2	305- 355	2.2	-1.7	0.4	-1.4	0.0	0.0	2.6	0.4	-2.1	4.7	18.5	2.9
3	416- 419	0.0	-1.8	2.2	-0.3	0.0	0.0	2.2	0.0	-1.8	4.0	31.4	6.9
4	866- 869	0.0	-2.1	0.3	0.0	0.0	0.0	0.3	0.0	-2.1	2.4	19.6	7.2
5	544- 548	0.0	-1.7	0.6	0.0	0.0	0.0	0.6	0.0	-1.7	2.3	20.0	7.7
6	7064-2774	0.1	4.2	1.4	0.2	0.0	0.0	4.2	1.4	0.1	4.2	20.0	3.8
7	3021-3026	0.2	-7.8	-1.8	-0.3	0.0	0.0	0.2	-1.8	-7.8	8.0	20.0	1.5
8	3521-3527	0.0	-0.4	-0.1	0.2	0.0	0.0	0.1	-0.1	-0.5	0.5	45.0	89.0

Locations of the most critical sections for each component are provided in the following:

Comp. No.[1]	Section Location			
	Inside Node		Outside Node	
	x (in)	y (in)	z (in)	x (in)
1	39.44	6.20	39.44	0.75
2	39.44	8.20	43.35	8.20
3	35.50	18.40	37.50	18.40
4	35.50	48.40	37.00	48.40
5	40.70	26.40	43.35	26.40
6	37.655	179.40	37.50	175.40
7	37.655	179.40	37.655	185.40
8	39.56	188.40	39.56	193.71

[1] Refer to Figure 2.10.2-33 for cask component identification.

Table 2.10.4-63 Critical $P_m + P_b$ Stress Summary; 1-Foot Bottom End Drop; Drop Orientation = 0 Degrees; 2-D Model; Condition 3

Condition 3: -20°F Ambient without Contents

Comp. No.[1]	Section Cut Node-Node	$P_m + P_b$ Stresses (ksi) S_x	S_y	S_z	S_{xy}	S_{yz}	S_{xz}	Principal Stresses (ksi) S1	S2	S3	S.I.	Allow. Stress	Margin of Safety
1	16- 20	-7.9	-0.6	-7.9	0.0	0.0	0.0	-0.6	-7.9	-7.9	7.3	28.7	2.9
2	1- 5	8.6	-0.1	8.6	0.0	0.0	0.0	8.6	8.6	-0.1	8.7	27.7	2.2
3	416- 419	0.0	-4.2	1.6	-0.3	0.0	0.0	1.6	0.0	-4.3	5.9	47.1	7.0
4	851- 854	0.0	-2.2	0.3	0.0	0.0	0.0	0.3	0.0	-2.2	2.4	29.4	11.3
5	544- 548	0.0	-2.0	0.5	0.0	0.0	0.0	0.5	0.0	-2.0	2.5	30.0	11.0
6	7064-2774	2.4	13.1	3.5	0.2	0.0	0.0	13.1	3.5	2.4	10.7	30.0	1.8
7	3021-3026	0.1	13.1	-1.0	-0.3	0.0	0.0	13.1	0.1	-1.0	14.1	30.0	1.1
8	3521-3527	0.1	-2.5	0.4	0.2	0.0	0.0	0.4	0.1	-2.5	2.9	67.5	22.3

Locations of the most critical sections for each component are provided in the following:

Comp. No.[1]	Section Location Inside Node x (in)	y (in)	Outside Node z (in)	x (in)
1	1.42	6.20	1.42	0.75
2	0.0	14.40	0.0	8.20
3	35.50	18.40	37.50	18.40
4	35.50	47.40	37.00	47.40
5	40.70	26.40	43.35	26.40
6	37.655	179.40	37.50	175.40
7	37.655	179.40	37.655	185.40
8	39.56	188.40	39.56	193.71

[1] Refer to Figure 2.10.2-33 for cask component identification.

Table 2.10.4-64 Critical S_n Stress Summary; 1-Foot Bottom End Drop; Drop Orientation = 0 Degrees; 2-D Model; Condition 3

Condition 3: -20°F Ambient without Contents

Comp. No.	Section Cut Node-Node	S_n Stresses (ksi) S_x	S_y	S_z	S_{xy}	S_{yz}	S_{zx}	Principal Stresses (ksi) S1	S2	S3	S.I.	Allow. Stress 3.0 S_m
1	296- 300	-7.3	-0.4	-1.7	-1.2	0.0	0.0	-0.2	-1.7	-7.5	7.4	57.6
2	305- 355	5.1	-5.2	0.2	-1.5	0.0	0.0	5.3	0.2	-5.5	10.7	55.5
3	416- 419	0.0	-4.1	0.6	-0.2	0.0	0.0	0.6	0.0	-4.1	4.7	94.2
4	2276-2279	0.0	-1.7	-2.9	0.0	0.0	0.0	0.0	-1.7	-2.9	2.9	58.8
5	544- 548	0.0	-1.8	0.3	0.0	0.0	0.0	0.3	0.0	-1.8	2.1	60.0
6	7064-2774	1.8	13.2	3.2	0.1	0.0	0.0	13.2	3.2	1.8	11.4	60.0
7	3021-3026	-0.5	13.2	-1.3	-0.2	0.0	0.0	13.2	-0.5	-1.3	14.5	60.0
8	3621-3627	0.2	-2.3	0.4	-0.1	0.0	0.0	0.4	0.2	-2.3	2.7	135.0

Locations of the most critical sections for each component are provided in the following:

Comp. No.[1]	Section Location Inside Node x (in)	y (in)	Outside Node z (in)	x (in)
1	38.567	6.20	38.567	0.75
2	39.44	8.20	43.35	8.20
3	35.50	18.40	37.50	18.40
4	35.50	142.40	37.00	142.40
5	40.70	26.40	43.35	26.40
6	37.655	179.40	37.50	175.40
7	37.655	179.40	37.655	185.40
8	33.705	188.40	33.705	193.71

[1] Refer to Figure 2.10.2-33 for cask component identification.

Table 2.10.4-65 Primary Stresses; 1-Foot Side Drop; Drop Orientation = 90 Degrees; 3-D Model; 0-Degree Circumferential Location; Condition 1

Condition 1: 100°F Ambient with Contents

Stress Points		Stress Components (ksi)						Principal Stresses (ksi)		
Section[1]	Node	S_x	S_y	S_z	S_{xy}	S_{yz}	S_{zx}	S1	S2	S3
A1	1130	-0.3	-0.6	-0.1	0.0	0.0	0.0	-0.1	-0.3	-0.6
A2	1129	-0.3	-1.2	0.0	0.0	0.0	0.0	0.0	-0.3	-1.2
A3	1128	-0.4	-1.7	0.1	0.0	0.0	0.0	0.1	-0.4	-1.7
B1	1185	-0.5	-1.9	0.0	0.0	0.0	-0.1	0.0	-0.5	-1.9
B2	1184	-0.2	-2.1	0.0	0.0	0.0	-0.1	0.0	-0.2	-2.1
B3	1183	0.1	-2.4	0.0	0.0	0.0	-0.1	0.1	0.0	-2.4
C1	90	1.9	-0.9	6.3	0.0	-0.3	0.5	6.3	1.9	-0.9
C2	80	-1.3	-2.7	2.6	-0.1	-0.2	-0.1	2.6	-1.3	-2.7
C3	70	-1.6	-3.3	0.8	0.0	-0.2	-0.4	0.8	-1.7	-3.3
C4	60	-1.8	-3.5	0.0	0.1	-0.1	-0.2	0.1	-1.9	-3.5
C5	50	-3.3	-4.0	-0.1	0.1	0.0	0.0	-0.1	-3.3	-4.1
C6	40	-3.7	-4.3	-0.1	0.1	0.0	0.0	-0.1	-3.7	-4.3
D1	25	-1.8	-3.5	1.6	0.1	0.0	0.1	1.6	-1.8	-3.5
D2	15	-3.5	-4.0	0.6	0.1	0.0	-0.2	0.6	-3.5	-4.0
D3	5	-3.9	-4.1	0.1	0.1	0.0	-0.1	0.1	-3.9	-4.1
E1	35	-3.9	-4.2	1.2	0.1	0.0	0.7	1.3	-4.0	-4.2
E2	34	-2.8	-4.1	0.6	0.1	0.0	0.8	0.8	-3.0	-4.1
E3	33	-3.0	-4.4	0.0	0.1	0.0	0.7	0.1	-3.1	-4.4
E4	32	-3.1	-4.6	-0.7	0.1	0.0	0.4	-0.6	-3.2	-4.6
E5	31	-3.2	-4.9	-1.4	0.1	0.0	0.2	-1.4	-3.2	-4.9
F1	100	-0.6	-0.7	9.6	0.0	-0.5	0.9	9.7	-0.6	-0.7
F2	99	-0.7	-3.2	0.6	0.2	-0.4	1.0	1.1	-1.2	-3.3
F3	98	-0.3	-4.7	-5.3	0.3	-0.3	1.5	0.1	-4.6	-5.8
F4	97	0.3	-7.6	-16.9	0.6	-0.3	1.8	0.5	-7.6	-17.1
G1	94	0.3	-0.8	7.9	0.1	-0.1	1.1	8.0	0.1	-0.8
G2	93	0.5	-2.1	3.0	0.2	-0.1	0.8	3.2	0.3	-2.1
G3	92	0.5	-2.4	1.5	0.2	-0.1	0.3	1.5	0.4	-2.4
G4	91	0.2	-2.9	-0.3	0.2	0.0	0.1	0.3	-0.3	-3.0
H1	330	-0.1	3.4	-2.4	-0.2	-0.7	0.0	3.5	-0.1	-2.5
H2	329	-0.1	4.0	-1.0	-0.3	-0.7	0.0	4.1	-0.1	-1.1

Table 2.10.4-65 Primary Stresses; 1-Foot Side Drop; Drop Orientation = 90 Degrees; 3-D Model; 0-Degree Circumferential Location; Condition 1 (continued)

Stress Points		Stress Components (ksi)						Principal Stresses (ksi)		
Section[1]	Node	S_x	S_y	S_z	S_{xy}	S_{yz}	S_{zx}	S1	S2	S3
H3	328	0.0	4.6	0.3	-0.3	-0.6	0.0	4.7	0.2	0.0
H4	327	0.1	5.2	1.9	-0.3	-0.6	-0.1	5.4	1.8	0.0
I1	244	-0.1	-0.6	2.0	0.0	-0.3	0.0	2.1	0.0	-0.7
I2	243	0.0	0.1	3.0	0.0	-0.2	0.0	3.0	0.1	0.0
I3	242	0.0	0.7	3.9	0.0	-0.1	0.0	3.9	0.7	0.0
I4	241	0.0	1.4	4.8	-0.1	-0.1	0.0	4.8	1.4	0.0
J1	550	-0.1	3.6	4.3	-0.3	-0.4	0.0	4.5	3.4	-0.2
J2	548	-0.1	4.5	4.9	-0.3	-0.4	0.0	5.2	4.3	-0.1
J3	547	0.0	5.4	5.6	-0.4	-0.4	0.0	5.9	5.1	-0.1
K1	344	-0.1	-1.0	3.7	0.1	-0.1	0.0	3.7	-0.1	-1.0
K2	342	0.0	0.6	4.5	-0.1	-0.1	0.0	4.5	0.6	0.0
K3	341	0.0	2.1	5.3	-0.2	-0.1	0.0	5.3	2.1	0.0
L1	740	0.0	3.1	7.3	0.0	0.0	-0.1	7.3	3.1	0.0
L2	738	-0.2	4.4	8.2	-0.6	0.0	0.0	8.2	4.5	-0.3
L3	737	0.1	5.8	9.0	-1.2	0.0	0.0	9.0	6.1	-0.1
M1	663	-0.4	-1.5	4.5	0.1	0.0	0.0	4.5	-0.4	-1.5
M2	63	0.2	2.7	6.2	0.8	0.0	0.0	6.2	2.9	-0.1
N1	1877	-0.1	3.4	3.6	-0.3	0.5	0.0	4.0	3.0	-0.1
N2	1477	-0.1	4.5	4.3	-0.3	0.4	0.0	4.8	3.9	-0.1
N3	1277	0.0	5.6	4.9	-0.4	0.4	0.0	5.8	4.7	-0.1
O1	647	0.0	-1.1	4.3	0.1	0.1	0.0	4.3	0.0	-1.1
O2	247	0.0	0.5	5.1	0.0	0.1	0.0	5.1	0.5	0.0
O3	47	0.0	2.0	5.8	-0.2	0.0	0.0	5.8	2.0	0.0
P1	1840	-0.1	3.4	-2.1	-0.2	0.7	0.0	3.5	-0.1	-2.2
P2	1640	-0.1	4.1	-0.9	-0.3	0.7	0.0	4.2	-0.1	-1.0
P3	1440	0.0	4.8	0.2	-0.3	0.6	0.0	4.9	0.2	0.0
P4	1240	0.1	5.5	1.6	-0.4	0.6	0.1	5.6	1.5	0.0
Q1	628	0.0	-0.3	3.8	0.0	0.2	0.0	3.8	0.0	-0.3
Q2	428	0.0	0.3	4.2	0.0	0.2	0.0	4.2	0.3	0.0
Q3	228	0.0	0.9	4.6	-0.1	0.1	0.0	4.6	0.9	0.0
Q4	28	0.0	1.5	5.0	-0.1	0.0	0.0	5.0	1.5	0.0
R1	1816	-0.5	-2.1	3.9	0.1	0.4	0.1	3.9	-0.5	-2.1

Table 2.10.4-65 Primary Stresses; 1-Foot Side Drop; Drop Orientation = 90 Degrees; 3-D Model; 0-Degree Circumferential Location; Condition 1 (continued)

Stress Points		Stress Components (ksi)						Principal Stresses (ksi)		
Section[1]	Node	S_x	S_y	S_z	S_{xy}	S_{yz}	S_{zx}	S1	S2	S3
R2	1616	-1.0	-3.2	-0.2	0.2	0.4	-0.1	-0.1	-1.0	-3.3
R3	1416	-2.5	-4.4	-3.7	0.3	0.3	-0.9	-2.0	-3.9	-4.7
R4	1216	-3.5	-5.7	-8.2	0.4	0.2	-2.1	-2.7	-5.7	-9.0
S1	616	1.1	-1.3	0.4	0.1	0.2	-0.1	1.2	0.4	-1.3
S2	416	0.1	-0.9	2.6	0.1	0.1	-0.1	2.6	0.1	-0.9
S3	216	0.1	-0.3	4.5	0.0	0.1	0.1	4.5	0.1	-0.3
S4	16	0.1	0.3	6.3	0.0	0.0	0.1	6.4	0.3	0.1
T1	811	-8.3	-8.0	-8.5	0.3	0.2	-2.2	-6.2	-8.0	-10.7
T2	611	-4.0	-5.1	-2.7	0.2	0.1	-1.8	-1.4	-5.0	-5.4
T3	411	-1.9	-3.5	0.9	0.1	0.1	-1.3	1.4	-2.3	-3.5
T4	211	-0.5	-2.1	4.0	0.1	0.0	-0.7	4.1	-0.5	-2.1
T5	11	0.0	-0.7	8.6	0.0	0.0	-0.3	8.6	0.0	-0.7
U1	43058	4.1	0.8	-0.1	0.1	0.0	-0.1	4.1	0.8	-0.1
U2	43057	1.2	-0.3	-0.4	0.1	0.0	0.1	1.2	-0.3	-0.4
U3	43056	0.1	-0.9	-1.0	0.0	0.0	0.4	0.2	-0.9	-1.1
U4	43055	-0.3	-1.3	-1.8	0.1	0.0	0.2	-0.3	-1.3	-1.8
U5	43054	-0.9	-1.7	-2.3	0.1	0.0	-0.4	-0.8	-1.7	-2.4
U6	43053	-1.7	-2.1	-2.3	0.1	-0.1	-1.1	-0.8	-2.1	-3.2
U7	43052	-2.9	-2.3	-1.4	0.0	-0.1	-1.4	-0.6	-2.3	-3.8
U8	43051	-4.2	-2.5	-0.1	0.0	0.0	-0.1	-0.1	-2.5	-4.2
V1	50024	1.4	-0.3	0.0	0.1	0.0	0.0	1.4	0.0	-0.3
V2	50023	-1.2	-1.6	-0.6	0.0	0.0	0.0	-0.6	-1.2	-1.6
V3	50022	-2.6	-2.2	-0.3	0.0	0.0	0.0	-0.3	-2.2	-2.6
V4	50021	-6.8	-3.6	0.5	-0.1	0.0	0.0	0.5	-3.6	-6.8
W1	43278	-0.7	-0.9	0.0	0.0	-0.1	0.1	0.0	-0.7	-0.9
W2	43274	-0.4	-1.1	0.0	0.0	-0.1	0.1	0.0	-0.4	-1.1
W3	43271	-0.1	-0.6	0.0	0.0	-0.1	0.0	0.0	-0.1	-0.7
X1	50084	-0.2	-1.9	0.0	0.0	0.0	0.1	0.0	-0.2	-1.9
X2	50083	-0.1	-2.1	0.0	0.0	0.0	0.1	0.0	-0.2	-2.1
X3	50081	0.1	-2.5	0.0	0.0	0.0	0.1	0.1	0.0	-2.5

[1] Refer to Figure 2.10.2-34 for the identification of the representative sections.

Table 2.10.4-66 Primary Plus Secondary Stresses; 1-Foot Side Drop; Drop Orientation = 90 Degrees; 3-D Model; 0-Degree Circumferential Location; Condition 1

Condition 1: 100°F Ambient with Contents

Stress Points		Stress Components (ksi)						Principal Stresses (ksi)		
Section[1]	Node	S_x	S_y	S_z	S_{xy}	S_{yz}	S_{xz}	S1	S2	S3
A1	1130	-0.1	-0.4	1.0	0.0	-0.1	0.3	1.1	-0.2	-0.4
A2	1129	-0.9	-1.7	0.0	0.0	-0.1	0.3	0.1	-1.0	-1.7
A3	1128	-1.6	-3.0	-1.0	0.0	-0.1	0.3	-0.9	-1.8	-3.0
B1	1185	1.7	0.4	0.8	-0.1	-0.1	0.3	1.8	0.7	0.4
B2	1184	0.9	-1.0	0.0	0.0	-0.1	0.3	1.0	-0.1	-1.0
B3	1183	0.2	-2.3	-0.8	0.0	0.0	0.3	0.2	-0.9	-2.3
C1	90	1.8	-1.3	6.1	0.0	-0.3	0.5	6.1	1.7	-1.3
C2	80	-1.9	-3.3	2.4	0.0	-0.2	-0.2	2.4	-1.9	-3.3
C3	70	-2.1	-3.9	0.3	0.0	-0.2	-0.5	0.4	-2.2	-4.0
C4	60	-2.2	-4.2	-0.4	0.1	-0.1	-0.3	-0.3	-2.3	-4.2
C5	50	-4.0	-4.7	-0.3	0.1	0.0	0.0	-0.3	-3.9	-4.7
C6	40	-3.8	-4.7	-0.1	0.1	0.0	0.0	-0.1	-3.8	-4.7
D1	25	0.2	-2.8	-0.2	0.2	0.0	0.9	1.0	-0.9	-2.8
D2	15	-2.7	-3.7	0.4	0.1	0.0	0.0	0.4	-2.7	-3.7
D3	5	-4.2	-4.7	0.0	0.1	0.0	-0.1	0.0	-4.1	-4.7
E1	35	-7.3	-6.1	-3.0	0.0	0.0	2.0	-2.3	-6.1	-8.1
E2	34	-5.2	-4.5	0.3	0.0	0.1	1.8	0.8	-4.5	-5.7
E3	33	-4.1	-4.0	1.1	0.0	0.1	1.4	1.5	-4.0	-4.5
E4	32	-3.6	-3.7	1.9	0.0	0.0	0.8	2.0	-3.7	-3.7
E5	31	-3.4	-3.4	2.9	0.0	0.0	0.5	3.0	-3.4	-3.4
F1	100	-0.6	-0.7	9.3	0.0	-0.4	1.0	9.4	-0.6	-0.8
F2	99	-0.6	-3.4	0.2	0.2	-0.3	1.1	0.9	-1.3	-3.5
F3	98	0.1	-5.0	-5.9	0.4	-0.3	1.2	0.4	-4.9	-6.2
F4	97	0.8	-7.3	-14.2	0.6	-0.3	1.3	0.9	-7.3	-14.3
G1	94	1.3	2.5	21.4	-0.1	0.0	2.7	21.8	2.5	1.0
G2	93	1.4	-1.2	7.6	0.2	0.0	1.6	8.0	1.0	-1.2
G3	92	1.0	-1.6	6.1	0.2	-0.1	0.3	6.2	1.0	-1.6
G4	91	0.3	-2.5	3.3	0.2	-0.1	0.0	3.3	0.3	-2.5
H1	330	-0.1	2.9	-1.7	-0.2	-0.6	0.1	3.0	-0.2	-1.8
H2	329	-0.1	3.6	-0.8	-0.2	-0.6	0.1	3.7	-0.1	-0.9

Table 2.10.4-66 Primary Plus Secondary Stresses; 1-Foot Side Drop; Drop Orientation = 90 Degrees; 3-D Model; 0-Degree Circumferential Location; Condition 1 (continued)

Stress Points		Stress Components (ksi)						Principal Streases (ksi)		
Section[1]	Node	S_x	S_y	S_z	S_{xy}	S_{yz}	S_{xz}	S1	S2	S3
H3	328	0.0	4.3	0.1	-0.3	-0.6	0.1	4.4	0.0	0.0
H4	327	-0.1	4.9	1.1	-0.3	-0.6	0.0	5.0	1.0	-0.1
I1	244	-0.1	2.4	8.1	-0.2	-0.2	0.0	8.1	2.4	-0.1
I2	243	-0.1	3.0	8.9	-0.2	-0.2	0.0	8.9	3.0	-0.1
I3	242	0.0	3.6	9.9	-0.3	-0.2	0.0	9.9	3.6	0.0
I4	241	0.0	4.2	10.8	-0.3	-0.1	0.0	10.8	4.2	0.0
J1	550	-0.1	2.4	1.9	-0.2	-0.3	0.0	2.6	1.7	-0.2
J2	548	-0.1	4.6	4.5	-0.3	-0.3	0.0	4.9	4.2	-0.1
J3	547	0.0	6.6	7.1	-0.5	-0.3	0.0	7.3	6.5	0.0
K1	344	-0.3	3.9	8.0	-0.3	-0.1	0.0	8.1	3.9	-0.3
K2	342	-0.2	6.2	10.8	-0.5	-0.1	0.0	10.8	6.2	-0.2
K3	341	-0.1	8.3	13.4	-0.6	-0.1	0.0	13.4	8.3	-0.1
L1	740	0.4	2.0	5.2	0.0	0.0	-0.1	5.2	2.0	0.4
L2	738	-0.6	3.5	6.5	-0.5	0.0	0.0	6.5	3.5	-0.7
L3	737	0.1	5.4	8.3	-0.8	0.0	0.0	8.3	5.5	0.0
M1	454	-0.8	4.2	8.6	-0.9	0.0	0.0	8.6	4.4	-1.0
M2	452	0.4	7.6	11.7	-0.7	0.0	0.2	11.7	7.7	0.3
M3	451	-0.9	10.0	14.2	-0.6	0.0	-0.4	14.2	10.1	-0.9
N1	1877	-0.2	1.9	1.4	-0.2	0.4	0.0	2.2	1.2	-0.2
N2	1477	-0.1	4.1	3.8	-0.3	0.4	0.0	4.4	3.6	-0.1
N3	1277	0.0	6.3	6.1	-0.5	0.4	0.0	6.6	5.8	-0.1
O1	647	-0.3	3.9	9.2	-0.3	0.1	0.0	9.2	3.9	-0.3
O2	247	-0.2	5.9	11.3	-0.4	0.1	0.0	11.3	5.9	-0.2
O3	47	-0.1	7.7	13.4	-0.6	0.1	0.0	13.4	7.7	-0.1
P1	1840	-0.1	2.8	-2.5	-0.2	0.7	0.0	2.9	-0.1	-2.6
P2	1640	-0.1	3.7	-1.3	-0.3	0.6	0.0	3.8	-0.1	-1.3
P3	1440	0.1	4.7	0.0	-0.3	0.6	0.0	4.8	0.1	0.0
P4	1240	-0.2	5.6	1.4	-0.4	0.6	0.1	5.7	1.4	-0.2
Q1	628	-0.3	3.6	8.5	-0.3	0.2	0.1	8.5	3.6	-0.3
Q2	428	-0.2	4.4	9.7	-0.3	0.2	0.1	9.7	4.4	-0.2
Q3	228	0.0	5.2	11.0	-0.4	0.2	0.1	11.0	5.2	-0.1
Q4	28	0.0	5.9	12.2	-0.4	0.1	0.1	12.2	6.0	0.0
R1	1816	-0.1	-6.4	-1.2	0.5	0.4	0.9	0.5	-1.7	-6.4

Table 2.10.4-66 Primary Plus Secondary Stresses; 1-Foot Side Drop; Drop Orientation = 90 Degrees; 3-D Model; 0-Degree Circumferential Location; Condition 1 (continued)

Stress Points		Stress Components (ksi)						Principal Stresses (ksi)		
Section[1]	Node	S_x	S_y	S_z	S_{xy}	S_{yz}	S_{xz}	S1	S2	S3
R2	1616	-0.4	-6.3	-3.1	0.5	0.4	1.4	0.3	-3.7	-6.3
R3	1416	-2.1	-6.5	-4.8	0.5	0.4	2.0	-1.0	-5.8	-6.6
R4	1216	0.6	-5.0	-4.8	0.5	0.3	0.7	0.7	-4.8	-5.1
S1	616	-0.9	-2.2	-2.3	0.1	0.2	-1.5	0.0	-2.2	-3.2
S2	416	-5.0	-0.7	6.5	-0.3	0.0	-2.1	6.8	-0.7	-5.4
S3	216	-1.2	1.6	9.4	-0.2	0.1	0.1	9.4	1.6	-1.2
S4	16	-0.4	3.3	13.6	-0.3	0.1	0.2	13.6	3.4	-0.4
T1	811	-10.6	-10.4	-15.3	0.3	0.0	-3.9	-8.4	-10.4	-17.5
T2	611	-5.6	-5.9	-5.0	0.1	0.0	-2.1	-3.2	-5.9	-7.5
T3	411	-2.4	-3.1	1.3	0.1	0.1	-1.1	1.6	-2.7	-3.1
T4	211	-0.6	-0.7	7.2	0.0	0.1	-0.5	7.2	-0.7	-0.7
T5	11	-0.1	1.7	14.5	-0.1	0.1	-0.2	14.5	1.7	-0.1
U1	43058	1.1	-1.0	-4.3	0.1	0.2	0.8	1.2	-1.0	-4.4
U2	43057	0.8	-1.7	-4.0	0.1	0.1	1.1	1.1	-1.7	-4.3
U3	43056	0.2	-2.3	-3.6	0.2	0.1	1.3	0.7	-2.4	-4.1
U4	43055	-0.3	-3.1	-3.6	0.2	0.1	0.9	-0.1	-3.1	-3.9
U5	43054	-1.3	-3.9	-3.5	0.2	0.1	0.1	-1.3	-3.4	-3.9
U6	43053	-2.7	-4.7	-3.0	0.1	0.2	-0.7	-2.1	-3.5	-4.7
U7	43052	-4.9	-5.4	-1.3	0.1	0.3	-1.0	-1.0	-5.1	-5.5
U8	43051	-2.2	0.7	5.9	-0.4	0.5	-0.7	6.0	0.7	-2.3
V1	50024	4.2	1.3	0.0	0.2	-0.1	-0.1	4.2	1.3	0.0
V2	50023	0.4	-0.8	-0.5	0.1	-0.1	-0.1	0.4	-0.5	-0.8
V3	50022	-2.4	-2.5	-0.3	0.0	-0.1	0.0	-0.3	-2.4	-2.5
V4	50021	-7.0	-4.6	0.5	-0.1	-0.1	0.0	0.5	-4.6	-7.0
W1	43278	3.0	2.4	-1.4	0.0	0.2	-0.8	3.1	2.4	-1.6
W2	43274	-0.6	-1.7	-0.6	0.0	0.2	-0.9	0.3	-1.4	-1.7
W3	43271	-3.0	-3.9	0.5	0.0	0.0	-0.4	0.6	-3.1	-3.9
X1	50084	2.3	1.6	-0.4	0.0	0.1	-0.4	2.4	1.6	-0.4
X2	50083	1.2	0.1	-0.2	0.0	0.1	-0.4	1.3	0.1	-0.4
X3	50081	-1.0	-2.9	0.9	0.0	0.1	-0.4	0.9	-1.0	-2.9

[1] Refer to Figure 2.10.2-34 for the identification of the representative sections.

Table 2.10.4-67 P_m Stresses; 1-Foot Side Drop; Drop Orientation = 90 Degrees; 3-D Model; 0-Degree Circumferential Location; Condition 1

Condition 1: 100°F Ambient with Contents

Section[1]	Node - Node	Stress Components (ksi)						Principal Stresses (ksi)			
		S_x	S_y	S_z	S_{xy}	S_{yz}	S_{zx}	S1	S2	S3	S.I.
A	1130 - 1128	-0.3	-1.2	0.0	0.0	0.0	0.0	0.0	-0.3	-1.2	1.2
B	1185 - 1183	-0.2	-2.1	0.0	0.0	0.0	-0.1	0.0	-0.2	-2.1	2.1
C	90 - 40	-2.1	-3.5	0.8	0.0	-0.1	-0.1	0.8	-2.1	-3.5	4.3
D	25 - 5	-3.2	-3.9	0.7	0.1	0.0	-0.1	0.7	-3.2	-3.9	4.6
E	35 - 31	-3.1	-4.4	0.0	0.1	0.0	0.6	0.2	-3.2	-4.4	4.5
F	100 - 97	-0.4	-4.0	-2.8	0.3	-0.3	1.3	0.1	-3.2	-4.2	4.4
G	94 - 91	0.4	-2.1	2.7	0.2	-0.1	0.6	2.9	0.3	-2.1	5.0
H	330 - 327	0.0	4.3	-0.3	-0.3	-0.6	0.0	4.4	0.0	-0.4	4.8
I	244 - 241	0.0	0.4	3.4	0.0	-0.2	0.0	3.4	0.4	0.0	3.5
J	550 - 547	-0.1	4.5	4.9	-0.3	-0.4	0.0	5.2	4.3	-0.1	5.3
K	344 - 341	0.0	0.6	4.5	-0.1	-0.1	0.0	4.5	0.6	0.0	4.5
L	740 - 737	-0.1	4.5	8.2	-0.6	0.0	0.0	8.2	4.5	-0.2	8.3
M	663 - 63	-0.1	0.6	5.4	0.5	0.0	0.0	5.4	0.8	-0.3	5.7
N	1877 - 1277	-0.1	4.5	4.2	-0.3	0.4	0.0	4.8	3.9	-0.1	4.9
O	647 - 47	0.0	0.5	5.1	0.0	0.1	0.0	5.1	0.5	0.0	5.1
P	1840 - 1240	0.0	4.4	-0.3	-0.3	0.6	0.0	4.5	0.0	-0.4	5.0
Q	628 - 28	0.0	0.6	4.4	-0.1	0.1	0.0	4.4	0.6	0.0	4.4
R	1816 - 1216	-1.8	-3.8	-2.0	0.3	0.3	-0.7	-1.3	-2.5	-3.9	2.7
S	616 - 16	0.3	-0.6	3.5	0.0	0.1	0.0	3.5	0.3	-0.6	4.1
T	811 - 11	-2.6	-3.8	0.5	0.2	0.1	-1.3	1.0	-3.0	-3.8	4.8
U	43058 - 43051	-1.0	-1.5	-1.3	0.0	0.0	-0.4	-0.7	-1.5	-1.6	0.8
V	50024 - 50021	-2.2	-1.9	-0.2	0.0	0.0	0.0	-0.2	-1.9	-2.2	2.0
W	43278 - 43271	-0.4	-0.9	0.0	0.0	-0.1	0.1	0.0	-0.4	-0.9	0.9
X	50084 - 50081	-0.1	-2.2	0.0	0.0	0.0	0.1	0.0	-0.1	-2.2	2.2

[1] Refer to Figure 2.10.2-34 for the identification of the representative sections.

Table 2.10.4-68 $P_m + P_b$ Stresses; 1-Foot Side Drop; Drop Orientation = 90 Degrees; 3-D Model; 0-Degree Circumferential Location; Condition 1

Condition 1: 100°F Ambient with Contents

Section[1]	Node - Node	Stress Components (ksi) S_x	S_y	S_z	S_{xy}	S_{yz}	S_{xz}	Principal Stresses (ksi) S1	S2	S3	S.I.
A O	1130 - 1128	-0.4	-1.7	0.1	0.0	0.0	0.0	0.1	-0.4	1.7	1.8
B O	1185 - 1183	0.1	-2.4	0.0	0.0	0.0	-0.1	0.1	0.0	-2.4	2.5
C I	90 - 40	-0.2	-2.3	2.9	0.0	-0.2	-0.1	2.9	-0.2	-2.3	5.2
D I	25 - 5	-2.1	-3.6	1.5	0.1	0.0	0.0	1.5	-2.1	-3.6	5.1
E I	35 - 31	-3.3	-4.0	1.4	0.1	0.0	0.9	1.5	-3.5	-4.0	5.5
F O	100 - 97	0.1	-7.2	-15.1	0.5	-0.3	1.8	0.3	-7.2	-15.3	15.6
G I	94 - 91	0.4	-1.2	6.4	0.1	-0.1	1.1	6.6	0.2	-1.2	7.8
H I	330 - 327	-0.1	3.4	-2.5	-0.2	-0.7	0.0	3.5	-0.1	-2.5	6.0
I O	244 - 241	0.0	1.4	4.8	-0.1	-0.1	0.0	4.8	1.4	0.0	4.8
J O	550 - 547	0.0	5.4	5.6	-0.4	-0.4	0.0	5.9	5.1	-0.1	5.9
K O	344 - 341	0.0	2.1	5.3	-0.2	-0.1	0.0	5.3	2.1	0.0	5.3
L O	740 - 737	0.0	5.8	9.0	-1.2	0.0	0.0	9.0	6.1	-0.2	9.3
M O	663 - 63	0.2	2.7	6.2	0.8	0.0	0.0	6.2	2.9	-0.1	6.3
N O	1877 - 1277	0.0	5.6	4.9	-0.4	0.4	0.0	5.8	4.7	-0.1	5.8
O O	647 - 47	0.0	2.0	5.8	-0.2	0.0	0.0	5.8	2.1	0.0	5.9
P I	1840 - 1240	-0.1	3.4	-2.2	-0.2	0.7	0.0	3.5	-0.1	-2.2	5.7
Q O	628 - 28	0.0	1.5	5.0	-0.1	0.0	0.0	5.0	1.5	0.0	5.1
R I	1816 - 1216	-0.2	-2.0	3.9	0.2	0.5	0.4	4.0	-0.2	-2.1	6.0
S O	616 - 16	-0.1	0.3	6.4	0.0	0.0	0.2	6.4	0.3	-0.1	6.6
T O	811 - 11	1.3	-0.4	8.4	0.1	0.0	-0.2	8.4	1.3	-0.4	8.8
U O	43058 - 43051	-4.5	-3.0	-1.5	0.0	-0.1	-1.1	-1.1	-3.0	-4.8	3.7
V O	50024 - 50021	-5.8	-3.4	0.1	0.0	0.0	0.0	0.1	-3.4	-5.8	6.0
W I	43278 - 43271	-0.7	-1.0	0.0	0.0	-0.1	0.1	0.0	-0.7	-1.0	1.0
X O	50084 - 50081	0.1	-2.5	0.0	0.0	0.0	0.1	0.1	0.0	-2.5	2.6

[1] Refer to Figure 2.10.2-34 for the identification of the representative sections.

Table 2.10.4-69 S_n Stresses; 1-Foot Side Drop; Drop Orientation = 90 Degrees; 3-D Model; 0-Degree Circumferential Location; Condition 1

Condition 1: 100°F Ambient with Contents

Section[1]	Node - Node	Stress Components (ksi) S_x	S_y	S_z	S_{xy}	S_{yz}	S_{zx}	Principal Stresses (ksi) S1	S2	S3	S.I.
A O	1130 - 1128	-1.6	-3.0	-1.1	0.0	-0.1	0.3	-0.9	-1.8	-3.0	2.1
B O	1185 - 1183	0.2	-2.3	-0.8	0.0	0.0	0.3	0.2	-0.9	-2.3	2.6
C I	90 - 40	-0.6	-2.9	2.5	0.0	-0.2	-0.2	2.5	-0.6	-2.9	5.5
D O	25 - 5	-4.5	-4.7	0.3	0.1	0.0	-0.3	0.3	-4.5	-4.7	5.0
E O	35 - 31	-2.7	-3.1	3.2	0.0	0.0	0.6	3.3	-2.8	-3.1	6.4
F O	100 - 97	0.6	-7.2	-13.9	0.5	-0.3	1.3	0.8	-7.2	-14.0	14.8
G I	94 - 91	1.6	1.1	16.2	0.0	0.0	2.6	16.6	1.2	1.1	15.5
H O	330 - 327	0.0	4.9	1.0	-0.3	-0.6	0.0	5.0	1.0	0.0	5.1
I O	244 - 241	0.0	4.2	10.8	-0.3	-0.1	0.0	10.8	4.2	0.0	10.8
J O	550 - 547	0.0	6.7	7.1	-0.5	-0.3	0.0	7.3	6.5	0.0	7.3
K O	344 - 341	-0.1	8.3	13.4	-0.6	-0.1	0.0	13.4	8.3	-0.1	13.6
L O	740 - 737	-0.3	5.3	8.2	-0.8	0.0	0.0	8.2	5.4	-0.4	8.6
M O	454 - 451	-0.3	10.3	14.3	-0.6	0.0	-0.2	14.3	10.3	-0.3	14.6
N O	1877 - 1277	0.0	6.3	6.1	-0.5	0.4	0.0	6.6	5.8	-0.1	6.7
O O	647 - 47	-0.1	7.7	13.4	-0.6	0.1	0.0	13.4	7.8	-0.1	13.5
P O	1840 - 1240	0.0	5.6	1.4	-0.4	0.6	0.1	5.7	1.3	0.0	5.8
Q O	628 - 28	0.0	6.0	12.2	-0.4	0.1	0.1	12.2	6.0	0.0	12.2
R I	1816 - 1216	-0.4	-6.6	-1.7	0.5	0.5	1.3	0.4	-2.5	-6.7	7.1
S O	616 - 16	-0.8	3.4	14.3	-0.3	0.1	0.5	14.3	3.4	-0.8	15.2
T O	811 - 11	1.7	2.2	14.6	-0.1	0.1	0.3	14.6	2.2	1.6	13.0
U I	43058 - 43051	1.4	-2.3	-6.0	0.3	0.0	1.5	1.8	-2.3	-6.3	8.1
V O	50024 - 50021	-6.5	-4.6	0.1	-0.1	-0.1	0.0	0.1	-4.6	-6.5	6.6
W O	43278 - 43271	-3.3	-4.4	0.5	0.0	0.0	-0.5	0.6	-3.4	-4.4	4.9
X O	50084 - 50081	-1.0	-2.9	0.8	0.0	0.1	-0.4	0.9	-1.1	-2.9	3.8

[1] Refer to Figure 2.10.2-34 for the identification of the representative sections.

Table 2.10.4-70 Critical P_m Stress Summary; 1-Foot Side Drop; Drop Orientation = 90 Degrees; 3-D Model; Condition 1

Condition 1: 100°F Ambient with Contents

Comp. No.[1]	Section Cut Node-Node	P_m Stresses (ksi) S_x	S_y	S_z	S_{xy}	S_{yz}	S_{xz}	Principal Stresses (ksi) S1	S2	S3	S.I.	Allow. Stress	Margin of Safety
1	25- 5	-3.2	-3.9	0.7	0.1	0.0	-0.1	0.7	-3.2	-3.9	4.6	19.2	3.2
2	14140-14137	0.0	0.3	0.5	0.0	-5.4	0.0	5.8	0.0	-5.0	10.9	18.5	0.7
3	14340-14337	0.0	1.8	0.7	0.1	-6.8	0.0	8.1	0.0	-5.6	13.7	31.4	1.3
4	14520-14517	0.0	1.9	0.6	0.0	-4.7	0.0	6.0	0.0	-3.5	9.5	19.6	1.1
5	662- 62	0.1	0.4	5.4	-0.9	0.0	0.0	5.4	1.1	-0.6	6.0	20.0	2.3
6	401- 1	-3.9	-12.7	0.1	0.6	0.1	0.6	0.1	-3.9	-12.7	12.9	20.0	0.6
7	43021-43028	-0.6	-3.5	-9.5	0.2	0.0	0.4	-0.6	-3.6	-9.5	8.9	20.0	1.2
8	51501-51504	-1.7	-1.2	1.2	0.1	0.0	0.0	1.2	-1.2	-1.7	2.8	45.0	15.0

Locations of the most critical sections for each component are provided in the following:

Comp. No.[1]	Section Location Inside Node x (in)	y (deg)	z (in)	Outside Node x (in)	y (deg)	z (in)
1	39.44	0.0	6.20	39.44	0.0	0.75
2	35.50	67.7	17.40	37.50	67.7	17.40
3	35.50	67.7	29.90	37.00	67.7	29.90
4	35.50	67.7	47.40	37.00	67.7	47.40
5	40.70	0.0	99.50	43.35	0.0	99.50
6	40.88	0.0	193.71	43.35	0.0	193.71
7	37.66	0.0	185.40	37.66	0.0	179.40
8	40.88	180.0	193.71	40.88	180.0	188.40

[1] Refer to Figure 2.10.2-33 for cask component identification.

Table 2.10.4-71 Critical $P_m + P_b$ Stress Summary; 1-Foot Side Drop; Drop Orientation = 90 Degrees; 3-D Model; Condition 1

Condition 1: 100°F Ambient with Contents

Comp. No.[1]	Section Cut Node-Node	$P_m + P_b$ Stresses (ksi) S_x	S_y	S_z	S_{xy}	S_{yz}	S_{xz}	Principal Stresses (ksi) S1	S2	S3	S.I.	Allow. Stress	Margin of Safety
1	25- 5	-2.1	-3.6	1.5	0.1	0.0	0.0	1.5	-2.1	-3.6	5.1	28.7	4.6
2	100- 97	0.1	-7.2	-15.1	0.5	-0.3	1.8	0.3	-7.2	-15.3	15.6	27.7	0.8
3	14350- 14347	0.0	2.0	0.2	0.0	-7.4	0.0	8.6	0.0	-6.3	14.8	47.1	2.2
4	14520- 14517	0.0	2.6	0.9	0.0	-5.0	0.0	6.8	0.0	-3.4	10.2	29.4	1.9
5	662- 62	0.2	2.4	6.3	-1.0	0.0	0.0	6.3	2.8	-0.2	6.5	30.0	3.6
6	403- 3	-2.8	-9.8	7.5	0.5	0.2	1.2	7.6	-2.9	-9.8	17.4	30.0	0.7
7	43021- 43028	0.9	-3.0	-11.1	0.2	0.1	1.9	1.2	-3.0	-11.4	12.6	30.0	1.4
8	51501- 51504	-5.0	-2.8	1.8	0.3	0.0	0.3	1.8	-2.7	-5.0	6.8	67.5	8.9

Locations of the most critical sections for each component are provided in the following:

Comp. No.[1]	Section Location Inside Node x (in)	y (deg)	z (in)	Outside Node x (in)	y (deg)	z (in)
1	39.44	0.0	6.20	39.44	0.0	0.75
2	35.50	0.0	15.00	37.50	0.0	15.00
3	35.50	67.7	30.40	37.00	67.7	30.40
4	35.50	67.7	47.40	37.00	67.7	47.40
5	40.70	0.0	99.50	43.35	0.0	99.50
6	40.88	0.0	190.15	43.35	0.0	190.15
7	37.66	0.0	185.40	37.66	0.0	179.40
8	40.88	180.0	193.71	40.88	180.0	188.40

[1] Refer to Figure 2.10.2-33 for cask component identification.

Table 2.10.4-72 Critical S_n Stress Summary; 1-Foot Side Drop; Drop Orientation = 90 Degrees; 3-D Model; Condition 1

Condition 1: 100°F Ambient with Contents

Comp. No.[1]	Section Cut Node-Node	S_x Stresses (ksi) S_x	S_y	S_z	S_{xy}	S_{yz}	S_{xz}	Principal Stresses (ksi) S1	S2	S3	S.I.	Allow. Stress 3.0 S_m
1	20025- 20005	1.6	0.9	-1.1	-1.4	-1.6	0.6	3.3	0.2	-2.0	5.2	57.6
2	104- 101	-1.3	0.1	14.2	-0.1	-0.1	1.1	14.3	0.1	-1.4	15.7	55.5
3	13842- 13242	-0.1	2.7	-0.1	0.0	6.0	0.0	7.5	-0.1	-4.9	12.4	94.2
4	13874- 13274	0.0	2.7	-0.1	-0.1	4.3	0.0	5.9	0.0	-3.2	9.1	58.8
5	664- 64	-0.2	10.4	15.2	-0.8	0.0	0.0	15.2	10.4	-0.2	15.4	60.0
6	401- 1	-8.5	-22.6	4.0	1.1	0.1	1.9	4.2	-8.7	-22.7	26.9	60.0
7	67571- 67531	6.2	24.0	-0.1	1.8	0.1	-1.8	24.2	6.5	-0.6	24.8	60.0
8	50001- 50004	-5.7	-3.9	2.4	-0.1	0.0	-0.3	2.4	-3.9	-5.7	8.1	135.0

Locations of the most critical sections for each component are provided in the following:

Comp. No.[1]	Section Location Inside Node x (in)	y (deg)	z (in)	Outside Node x (in)	y (deg)	z (in)
1	39.44	104.7	6.20	39.44	104.7	0.75
2	40.70	0.0	16.20	43.35	0.0	16.20
3	35.50	56.5	159.40	37.00	56.5	159.40
4	35.50	56.5	142.40	37.00	56.5	142.40
5	40.70	0.0	93.56	43.35	0.0	93.56
6	40.88	0.0	193.71	43.35	0.0	193.71
7	33.71	180.0	187.40	36.46	180.0	187.40
8	40.88	0.0	193.71	40.88	0.0	188.40

[1] Refer to Figure 2.10.2-33 for cask component identification.

Table 2.10.4-73 P_m Stresses; 1-Foot Side Drop; Drop Orientation = 90 Degrees; 3-D Model; 45.9-Degree Circumferential Location; Condition 1

Condition 1: 100°F Ambient with Contents

Section[1]	Node - Node	Stress Components (ksi)						Principal Stresses (ksi)			
		S_x	S_y	S_z	S_{xy}	S_{yz}	S_{xz}	S1	S2	S3	S.I.
A	1130 - 1128	-0.3	-1.2	0.0	0.0	0.0	0.0	0.0	-0.3	-1.2	1.2
B	1185 - 1183	-0.2	-2.1	0.0	0.0	0.0	-0.1	0.0	-0.2	-2.1	2.1
C	10090 - 10040	-1.5	-2.1	0.5	-0.4	-1.0	-0.1	0.8	-1.4	-2.6	3.4
D	10025 - 10005	-1.9	-2.9	0.6	-0.1	-0.3	0.0	0.6	-1.9	-3.0	3.5
E	10035 - 10031	-1.9	-2.8	0.1	0.3	-0.6	0.5	0.3	-1.9	-3.0	3.3
F	10100 - 10097	-0.2	-1.9	-1.3	0.0	-4.3	0.7	2.8	-0.3	-5.9	8.7
G	10094 - 10091	0.1	-0.9	1.6	0.0	-0.9	0.1	1.9	0.1	-1.2	3.1
H	10330 - 10327	0.0	3.1	0.2	0.2	-5.9	0.0	7.8	0.0	-4.5	12.2
I	10244 - 10241	0.0	0.3	1.8	0.0	-1.3	0.0	2.5	0.0	-0.4	2.9
J	10550 - 10547	0.0	3.2	2.7	0.0	-3.5	0.0	6.4	0.0	-0.6	7.0
K	10344 - 10341	0.0	0.4	2.2	0.0	-0.8	0.0	2.5	0.1	0.0	2.5
L	10740 - 10737	0.0	3.2	3.9	0.1	0.1	0.0	3.9	3.1	0.0	4.0
M	10663 - 10063	0.1	0.3	2.6	-0.1	-0.1	0.0	2.6	0.4	0.0	2.6
N	11877 - 11277	0.0	3.2	2.4	0.0	3.8	0.0	6.6	0.0	-1.1	7.6
O	10647 - 10047	0.0	0.3	2.5	0.0	0.5	0.0	2.6	0.2	0.0	2.6
P	11840 - 11240	0.0	3.2	0.3	0.2	5.8	0.0	7.7	0.0	-4.2	11.9
Q	10628 - 10028	0.0	0.5	2.2	0.0	0.9	0.0	2.6	0.1	0.0	2.6
R	11816 - 11216	-0.9	-1.3	-0.8	1.0	3.5	-0.3	2.6	-0.8	-4.8	7.4
S	10616 - 10016	-0.2	-0.2	2.0	-0.2	0.8	0.0	2.3	-0.1	-0.6	2.9
T	10811 - 10011	.3	-2.2	0.4	0.6	1.6	-0.6	1.2	-1.0	-3.3	4.4
U	44558 - 44551	-0.8	-1.2	-1.3	0.0	0.0	-0.2	-0.7	-1.2	-1.4	0.7
V	50524 - 50521	-1.1	-1.3	-0.2	0.3	0.1	0.0	-0.2	-0.9	-1.5	1.4
W	43278 - 43271	-0.4	-0.9	0.0	0.0	-0.1	0.1	0.0	-0.4	-0.9	0.9
X	50084 - 50081	-0.1	-2.2	0.0	0.0	0.0	0.1	0.0	-0.1	-2.2	2.2

[1] Refer to Figure 2.10.2-34 for the identification of the representative sections.

Table 2.10.4-74 $P_m + P_b$ Stresses; 1-Foot Side Drop; Drop Orientation = 90 Degrees; 3-D Model; 45.9-Degree Circumferential Location; Condition 1

Condition 1: 100°F Ambient with Contents

		Stress Components (ksi)						Principal Stresses (ksi)			
Section[1]	Node - Node	S_x	S_y	S_z	S_{xy}	S_{yz}	S_{zx}	S1	S2	S3	S.I.
A O	1130 - 1128	-0.4	-1.7	0.1	0.0	0.0	0.0	0.1	-0.4	-1.7	1.8
B O	1185 - 1183	0.1	-2.4	0.0	0.0	0.0	-0.1	0.1	0.0	-2.4	2.5
C I	10090 - 10040	-0.4	-1.1	1.6	-1.5	-2.2	0.0	3.0	0.1	-3.0	6.0
D I	10025 - 10005	-1.0	-2.4	1.1	-0.4	-0.6	0.1	1.2	-0.9	-2.6	3.8
E I	10035 - 10031	-2.1	-2.6	1.0	0.6	-0.9	0.7	1.3	-1.7	-3.3	4.6
F I	10100 - 10097	-0.5	-0.3	5.0	0.0	-4.8	0.5	7.9	-0.5	-3.1	11.0
G I	10094 - 10091	0.1	-0.8	1.6	0.0	-1.4	0.2	2.3	0.1	-1.5	3.8
H I	10330 - 10327	-0.1	2.5	-1.2	0.1	-6.4	0.1	7.2	-0.1	-6.0	13.2
I I	10244 - 10241	0.0	0.6	1.5	0.0	-1.8	0.0	2.8	0.0	-0.8	3.6
J I	10550 - 10547	-0.1	2.8	2.4	0.0	-3.9	0.0	6.5	-0.1	-1.3	7.8
K I	10344 - 10341	0.0	1.1	2.3	0.0	-1.1	0.0	2.9	0.5	0.0	2.9
L O	10740 - 10737	0.0	3.4	4.1	0.2	0.1	0.0	4.1	3.4	0.0	4.1
M O	10663 - 10063	-0.1	-0.7	2.3	-0.2	-0.1	0.0	2.4	0.0	-0.7	3.1
N I	11877 - 11277	-0.1	2.9	2.1	0.0	4.2	0.0	6.8	-0.1	-1.7	8.4
O I	10647 - 10047	0.0	0.9	2.6	0.0	0.8	0.0	2.9	0.6	0.0	2.9
P I	11840 - 11240	-0.1	2.9	-0.7	0.0	6.2	0.0	7.5	-0.1	-5.4	12.9
Q I	10628 - 10028	0.0	0.8	2.2	0.0	1.3	0.0	2.9	0.0	0.0	3.0
R I	11816 - 11216	-0.1	-0.5	1.4	0.0	4.0	0.1	4.5	-0.1	-3.6	8.1
S O	10616 - 10016	0.0	0.5	4.8	0.1	0.4	0.0	4.8	0.5	-0.1	4.9
T I	10811 - 10011	-3.5	-4.1	-4.5	1.6	2.9	-1.1	-1.3	-2.8	-8.0	6.8
U I	44558 - 44551	1.4	0.0	-1.3	-0.5	0.1	0.5	1.7	-0.1	-1.4	3.0
V O	50524 - 50521	-3.8	-2.6	0.2	1.0	0.1	0.0	0.2	-2.1	-4.4	4.5
W I	43278 - 43271	-0.7	-1.0	0.0	0.0	-0.1	0.1	0.0	-0.7	-1.0	1.0
X O	50084 - 50081	0.1	-2.5	0.0	0.0	0.0	0.1	0.1	0.0	-2.5	2.6

[1] Refer to Figure 2.10.2-34 for the identification of the representative sections.

Table 2.10.4-75 S_n Stresses; 1-Foot Side Drop; Drop Orientation = 90 Degrees; 3-D Model; 45.9-Degree Circumferential Location; Condition 1

Condition 1: 100°F Ambient with Contents

		Stress Components (ksi)						Principal Stresses (ksi)			
Section[1]	Node - Node	S_x	S_y	S_z	S_{xy}	S_{yz}	S_{xz}	S1	S2	S3	S.I.
A O	1130 - 1128	-1.6	-3.0	-1.1	0.0	-0.1	0.3	-0.9	-1.8	-3.0	2.1
B O	1185 - 1183	0.2	-2.3	-0.8	0.0	0.0	0.3	0.2	-0.9	-2.3	2.6
C I	10090 - 10040	-0.4	-1.6	1.1	-1.4	-1.8	-0.1	2.2	0.0	-3.1	5.3
D O	10025 - 10005	-3.0	-3.9	0.2	0.3	0.0	-0.3	0.3	-2.9	-4.0	4.2
E I	10035 - 10031	-5.4	-4.2	-2.1	0.5	-1.0	1.8	-1.2	-4.0	-6.5	5.4
F I	10100 - 10097	-0.4	-0.6	2.9	0.0	-4.1	0.7	5.7	-0.4	-3.3	9.0
G I	10094 - 10091	1.3	1.5	11.9	-0.1	-2.2	1.9	12.7	1.3	0.8	11.9
H I	10330 - 10327	0.0	2.4	-0.1	0.0	-5.7	0.1	7.0	0.0	-4.7	11.7
I O	10244 - 10241	0.0	3.5	8.4	0.0	-1.4	0.0	8.8	3.2	0.0	8.8
J I	10550 - 10547	0.0	1.5	-0.3	-0.1	-3.4	0.0	4.1	0.0	-2.9	7.0
K O	10344 - 10341	0.0	6.7	10.8	0.0	-1.0	0.0	11.0	6.5	0.0	11.1
L O	10740 - 10737	-0.1	5.1	4.8	0.6	0.0	0.1	5.2	4.8	-0.1	5.3
M O	10454 - 10451	-0.1	7.3	10.5	0.0	0.0	-0.1	10.5	7.3	-0.1	10.6
N I	11877 - 11277	0.0	1.4	-0.3	0.0	3.8	0.0	4.5	0.0	-3.3	7.8
O O	10647 - 10047	0.0	6.3	10.3	0.0	0.6	0.0	10.4	6.2	0.0	10.5
P I	11840 - 11240	0.0	2.7	-0.7	0.0	5.7	-0.1	7.0	0.0	-5.0	12.0
Q O	10628 - 10028	0.0	5.0	9.7	0.0	1.1	0.1	10.0	4.8	0.0	9.9
R I	11816 - 11216	-0.5	-4.2	-4.5	0.0	3.6	0.8	0.0	-1.2	-7.9	7.9
S O	10616 - 10016	-0.7	2.9	12.4	0.1	1.1	0.3	12.6	2.8	-0.7	13.3
T O	10811 - 10011	1.3	1.4	11.3	-0.4	0.8	0.3	11.4	1.8	0.8	10.6
U I	44558 - 44551	1.7	-1.1	-5.2	-0.6	0.1	1.9	2.3	-1.2	-5.7	8.0
V O	50524 - 50521	-5.0	-4.5	0.3	1.0	0.1	0.2	0.3	-3.7	-5.7	6.0
W O	43278 - 43271	-3.3	-4.4	0.5	0.0	0.0	-0.5	0.6	-3.4	-4.4	4.9
X O	50084 - 50081	-1.0	-2.9	0.8	0.0	0.1	-0.4	0.9	-1.1	-2.9	3.8

[1] Refer to Figure 2.10.2-34 for the identification of the representative sections.

Table 2.10.4-76 P_m Stresses; 1-Foot Side Drop; Drop Orientation = 90 Degrees; 3-D Model; 91.7-Degree Circumferential Location; Condition 1

Condition 1: 100°F Ambient with Contents

		Stress Components (ksi)						Principal Stresses (ksi)			
Section[1]	Node - Node	S_x	S_y	S_z	S_{xy}	S_{yz}	S_{xz}	S1	S2	S3	S.I.
A	1130 - 1128	-0.3	-1.2	0.0	0.0	0.0	0.0	0.0	-0.3	-1.2	1.2
B	1185 - 1183	-0.2	-2.1	0.0	0.0	0.0	-0.1	0.0	-0.2	-2.1	2.1
C	18090 - 18040	-0.2	-0.1	-0.2	-0.5	-1.1	0.1	1.0	-0.3	-1.4	2.4
D	18025 - 18005	0.0	-0.8	0.3	-0.8	-0.7	0.0	0.8	0.2	-1.5	2.3
E	18035 - 18031	0.2	-0.2	0.0	0.3	-1.4	-0.1	1.4	0.2	-1.5	2.9
F	18100 - 18097	0.1	1.3	1.8	0.0	-4.7	-0.5	6.3	0.2	-3.2	9.6
G	18094 - 18091	-0.2	0.5	-1.0	-0.1	-1.4	-0.2	1.3	-0.1	-1.9	3.2
H	18330 - 18327	-0.1	0.4	0.8	0.3	-5.9	-0.1	6.4	-0.1	-5.3	11.7
I	18244 - 18241	0.0	0.2	-1.0	0.0	-1.3	0.0	1.0	0.0	-1.8	2.8
J	18550 - 18547	-0.2	0.6	-1.4	0.0	-3.5	0.0	3.2	-0.2	-4.0	7.2
K	18344 - 18341	0.0	0.0	-1.2	0.0	-0.8	0.0	0.4	0.0	-1.6	2.0
L	18740 - 18737	-0.2	1.0	-2.4	0.0	0.1	0.0	1.0	-0.2	-2.4	3.4
M	18663 - 18063	0.1	0.0	-1.3	0.1	-0.1	0.0	0.1	-0.1	-1.4	1.5
N	19877 - 19277	-0.2	0.7	-1.1	0.0	3.7	0.0	3.6	-0.2	-4.0	7.5
O	18647 - 18047	0.0	0.0	-1.3	0.0	0.6	0.0	0.2	0.0	-1.6	1.8
P	19840 - 19240	-0.1	0.6	0.8	0.3	5.7	0.1	6.4	-0.1	-5.0	11.3
Q	18628 - 18028	0.0	0.1	-1.3	0.0	1.1	0.0	0.7	0.0	-1.8	2.6
R	19816 - 19216	0.9	2.4	1.1	1.3	4.0	0.4	6.1	0.7	-2.3	8.4
S	18616 - 18016	-0.5	0.5	-1.1	-0.1	1.1	0.1	1.1	-0.5	-1.7	2.8
T	18811 - 18011	0.5	0.7	-0.3	0.8	2.0	0.5	2.7	0.2	-1.9	4.6
U	45758 - 45751	-0.5	-0.9	-1.6	-0.2	0.1	0.0	-0.5	-0.9	-1.7	1.2
V	50924 - 50921	0.0	-0.6	-0.2	-0.1	0.1	0.0	0.0	-0.2	-0.7	0.7
W	43278 - 43271	-0.4	-0.9	0.0	0.0	-0.1	0.1	0.0	-0.4	-0.9	0.9
X	50084 - 50081	-0.1	-2.2	0.0	0.0	0.0	0.1	0.0	-0.1	-2.2	2.2

[1] Refer to Figure 2.10.2-34 for the identification of the representative sections.

Table 2.10.4-77 $P_m + P_b$ Stresses; 1-Foot Side Drop; Drop Orientation = 90 Degrees; 3-D Model; 91.7-Degree Circumferential Location; Condition 1

Condition 1: 100°F Ambient with Contents

		Stress Components (ksi)						Principal Stresses (ksi)			
Section[1]	Node - Node	S_x	S_y	S_z	S_{xy}	S_{yz}	S_{xz}	S1	S2	S3	S.I.
A O	1130 - 1128	-0.4	-1.7	0.1	0.0	0.0	0.0	0.1	-0.4	-1.7	1.8
B O	1185 - 1183	0.1	-2.4	0.0	0.0	0.0	-0.1	0.1	0.0	-2.4	2.5
C I	18090 - 18040	0.0	0.4	-1.0	-1.5	-2.4	0.1	2.8	-0.4	-3.1	5.9
D I	18025 - 18005	0.0	-0.4	0.7	-1.2	-1.3	0.0	1.9	0.3	-1.9	3.8
E I	18035 - 18031	0.4	0.0	1.0	0.8	-1.7	-0.2	2.5	0.3	-1.5	3.9
F O	18100 - 18097	0.0	2.8	7.5	0.1	-4.6	-0.8	10.3	0.3	-0.4	10.7
G I	18094 - 18091	-0.2	-0.2	-3.3	-0.1	-1.6	-0.4	0.5	-0.1	-4.0	4.5
H O	18330 - 18327	0.0	-0.6	0.4	0.4	-6.0	-0.1	6.0	0.0	-6.1	12.1
I O	18244 - 18241	0.0	-0.1	-1.3	0.0	-1.4	0.0	0.8	0.0	-2.2	3.0
J I	18550 - 18547	-0.2	2.6	-0.7	0.0	-3.5	0.0	4.8	-0.2	-2.9	7.7
K I	18344 - 18341	0.0	0.5	-0.9	0.0	-0.8	0.0	0.9	0.0	-1.2	2.1
L I	19908 - 19308	0.4	3.3	-1.4	0.0	0.3	0.0	3.3	0.4	-1.4	4.7
M I	18663 - 18063	0.2	0.9	-1.0	0.0	-0.1	0.0	0.9	0.2	-1.0	1.9
N I	19877 - 19277	-0.2	2.5	-0.4	0.0	3.7	0.0	5.0	-0.2	-2.9	7.9
O O	18647 - 18047	0.0	-0.7	-1.6	0.0	0.7	0.0	0.0	-0.3	-2.0	2.0
P O	19840 - 19240	0.0	-0.4	0.4	0.4	5.8	0.1	5.8	0.0	-5.8	11.7
Q O	18628 - 18028	0.0	-0.3	-1.8	0.0	1.2	0.0	0.3	0.0	-2.4	2.7
R O	19816 - 19216	1.8	3.7	5.7	2.6	3.9	1.1	9.5	2.1	-0.5	10.0
S I	18616 - 18016	-1.0	0.3	-2.1	-0.2	1.2	0.3	0.8	-0.9	-2.7	3.5
T I	18811 - 18011	1.2	1.3	0.6	1.9	2.9	0.9	4.9	0.2	-2.1	7.0
U I	45758 - 45751	-1.1	-1.0	-2.3	-0.6	0.1	0.6	-0.4	-1.4	-2.6	2.2
V I	50924 - 50921	0.8	-0.1	-0.7	-0.6	0.1	-0.1	1.1	-0.4	-0.7	1.8
W I	43278 - 43271	-0.7	-1.0	0.0	0.0	-0.1	0.1	0.0	-0.7	-1.0	1.0
X O	50084 - 50081	0.1	-2.5	0.0	0.0	0.0	0.1	0.1	0.0	-2.5	2.6

[1] Refer to Figure 2.10.2-34 for the identification of the representative sections.

Table 2.10.4-78 S_n Stresses; 1-Foot Side Drop; Drop Orientation = 90 Degrees; 3-D Model; 91.7-Degree Circumferential Location; Condition 1

Condition 1: 100°F Ambient with Contents

Section[1]	Node - Node	Stress Components (ksi)						Principal Stresses (ksi)			
		S_x	S_y	S_z	S_{xy}	S_{yz}	S_{xz}	S1	S2	S3	S.I.
A O	1130 - 1128	-1.6	-3.0	-1.1	0.0	-0.1	0.3	-0.9	-1.8	-3.0	2.1
B O	1185 - 1183	0.2	-2.3	-0.8	0.0	0.0	0.3	0.2	-0.9	-2.3	2.6
C I	18090 - 18040	-0.5	-0.1	-0.7	-1.5	-1.6	0.0	1.9	-0.6	-2.6	4.4
D I	18025 - 18005	2.0	0.5	-0.9	-1.4	-1.5	0.7	3.2	0.2	-1.8	5.1
E I	18035 - 18031	-3.0	-1.6	-2.6	0.8	-1.9	1.1	-0.1	-2.1	-5.0	4.9
F O	18100 - 18097	0.8	2.6	7.8	-0.1	-2.4	-1.1	8.9	1.9	0.4	8.5
G I	18094 - 18091	0.9	2.1	6.6	-0.3	-3.4	0.9	8.5	0.8	0.2	8.3
H O	18330 - 18327	-0.1	0.3	0.3	0.3	-3.6	0.0	3.9	0.0	-3.3	7.2
I I	18244 - 18241	0.0	2.7	5.4	0.0	-2.6	0.0	7.0	1.2	0.0	7.0
J I	18550 - 18547	-0.1	2.5	-2.7	0.1	-2.0	0.0	3.2	-0.1	-3.4	6.6
K O	18344 - 18341	0.0	5.6	6.8	0.0	-1.5	0.0	7.9	4.5	0.0	7.9
M O	18454 - 18451	-0.1	6.4	6.3	0.0	0.0	-0.1	6.4	6.3	-0.1	6.5
L I	19908 - 19308	-0.2	3.5	-3.6	0.2	0.2	0.0	3.5	-0.2	-3.6	7.1
N I	19877 - 19277	-0.1	2.0	-2.4	0.1	2.2	0.0	2.9	-0.1	-3.3	6.2
O O	18647 - 18047	0.0	4.9	5.3	0.0	1.4	0.0	6.5	3.7	0.0	6.6
P O	19840 - 19240	0.0	0.9	1.1	0.3	3.7	0.1	4.7	0.0	-2.7	7.4
Q O	18628 - 18028	0.0	3.5	4.1	0.0	2.4	0.1	6.2	1.4	0.0	6.2
R O	19816 - 19216	0.9	0.7	6.1	0.9	2.0	4.1	9.0	0.1	-1.4	10.4
S I	18616 - 18016	-6.3	-1.5	-3.1	-1.5	2.8	-2.2	1.4	-4.9	-7.5	8.9
T I	18811 - 18011	1.3	-0.4	-1.6	1.4	3.0	0.1	2.9	0.5	-4.1	7.0
U I	45758 - 45751	-0.1	-1.8	-7.6	-0.2	0.0	1.9	0.4	-1.8	-8.1	8.5
V O	50924 - 50921	-2.1	-3.1	0.4	0.4	0.0	0.3	0.4	-2.0	-3.3	3.7
W O	43278 - 43271	-3.3	-4.4	0.5	0.0	0.0	-0.5	0.6	-3.4	-4.4	4.9
X O	50084 - 50081	-1.0	-2.9	0.8	0.0	0.1	-0.4	0.9	-1.1	-2.9	3.8

[1] Refer to Figure 2.10.2-34 for the identification of the representative sections.

Table 2.10.4-79 P_m Stresses; 1-Foot Side Drop; Drop Orientation = 90 Degrees; 3-D Model; 180-Degree Circumferential Location; Condition 1

Condition 1: 100°F Ambient with Contents

		Stress Components (ksi)						Principal Stresses (ksi)			
Section[1]	Node - Node	S_x	S_y	S_z	S_{xy}	S_{yz}	S_{zx}	S1	S2	S3	S.I.
A	1130 - 1128	-0.3	-1.2	0.0	0.0	0.0	0.0	0.0	-0.3	-1.2	1.2
B	1185 - 1183	-0.2	-2.1	0.0	0.0	0.0	-0.1	0.0	-0.2	-2.1	2.1
C	30090 - 30040	0.0	0.9	-0.3	0.1	-0.1	0.0	0.9	0.0	-0.4	1.3
D	30025 - 30005	-0.9	1.5	-0.2	0.1	-0.1	0.0	1.5	-0.2	-0.9	2.4
E	30035 - 30031	0.6	1.1	-0.3	0.1	-0.2	-0.4	1.2	0.7	-0.5	1.7
F	30100 - 30097	0.0	0.8	0.3	0.1	-0.4	-0.5	1.2	0.4	-0.3	1.5
G	30094 - 30091	-0.1	0.3	-1.3	0.0	-0.2	-0.1	0.3	-0.1	-1.4	1.7
H	30330 - 30327	-0.1	-1.8	-0.9	-0.2	-0.4	0.0	0.0	-0.7	-2.0	2.0
I	30244 - 30241	0.0	-0.3	-1.8	0.0	-0.2	0.0	0.0	-0.3	-1.8	1.8
J	30550 - 30547	-0.2	-1.3	-2.6	-0.2	-0.2	0.0	-0.2	-1.3	-2.6	2.4
K	30344 - 30341	0.0	-0.3	-2.4	0.0	-0.1	0.0	0.0	-0.3	-2.4	2.4
L	30740 - 30737	0.0	-1.2	-3.5	0.3	0.0	0.0	0.1	-1.2	-3.5	3.6
M	30663 - 30063	-0.1	-0.3	-2.8	-0.4	0.0	0.0	0.2	-0.6	-2.8	3.0
N	31877 - 31277	-0.2	-1.2	-2.0	-0.2	0.3	0.0	-0.2	-1.2	-2.1	1.9
O	30647 - 30047	0.0	-0.3	-2.6	0.0	0.1	0.0	0.0	-0.3	-2.6	2.6
P	31840 - 31240	-0.1	-1.8	-0.6	-0.2	0.4	0.0	-0.1	-0.5	-2.0	1.9
Q	30628 - 30028	0.0	-0.5	-2.2	-0.1	0.1	0.0	0.0	-0.5	-2.2	2.2
R	31816 - 31216	0.2	2.4	0.3	0.4	0.3	0.6	2.5	0.6	-0.4	2.9
S	30616 - 30016	-0.2	1.6	-1.8	0.3	0.2	0.0	1.7	-0.2	-1.8	3.5
T	30811 - 30011	0.3	3.6	-0.9	0.6	0.2	0.4	3.7	0.3	-1.0	4.7
U	47558 - 47551	-1.1	-1.6	-2.6	-0.1	0.0	0.1	-1.1	-1.7	-2.6	1.4
V	51524 - 51521	-1.6	-1.4	-0.4	0.0	0.0	0.2	-0.4	-1.4	-1.7	1.3
W	43278 - 43271	-0.4	-0.9	0.0	0.0	-0.1	0.1	0.0	-0.4	-0.9	0.9
X	50084 - 50081	-0.1	-2.2	0.0	0.0	0.0	0.1	0.0	-0.1	-2.2	2.2

[1] Refer to Figure 2.10.2-34 for the identification of the representative sections.

Table 2.10.4-80 $P_m + P_b$ Stresses; 1-Foot Side Drop; Drop Orientation = 90 Degrees; 3-D Model; 180-Degree Circumferential Location; Condition 1

Condition 1: 100°F Ambient with Contents

		Stress Components (ksi)						Principal Stresses (ksi)			
Section[1]	Node - Node	S_x	S_y	S_z	S_{xy}	S_{yz}	S_{xz}	S1	S2	S3	S.I.
A O	1130 - 1128	-0.4	-1.7	0.1	0.0	0.0	0.0	0.1	-0.4	-1.7	1.8
B O	1185 - 1183	0.1	-2.4	0.0	0.0	0.0	-0.1	0.1	0.0	-2.4	2.5
C I	30090 - 30040	-0.9	0.2	-1.1	0.0	-0.2	-0.1	0.2	-0.9	-1.1	1.4
D O	30025 - 30005	-0.7	2.0	-0.3	0.1	0.0	0.3	2.0	-0.1	-0.9	2.9
E O	30035 - 30031	-0.1	0.6	-1.2	0.1	-0.2	-0.2	0.7	-0.1	-1.2	1.9
F O	30100 - 30097	-0.1	1.7	3.6	0.3	-0.4	-0.5	3.8	1.6	-0.2	4.0
G I	30094 - 30091	-0.1	0.1	-1.8	0.0	-0.2	-0.2	0.1	0.0	-1.8	2.0
H O	30330 - 30327	-0.1	-1.7	-1.4	-0.2	-0.5	0.0	0.0	-1.0	-2.1	2.0
I O	30244 - 30241	0.0	-0.2	-2.0	0.0	-0.2	0.0	0.0	-0.1	-2.0	2.0
J I	30550 - 30547	-0.2	-2.0	-2.8	-0.3	-0.2	0.0	-0.1	-2.0	-2.8	2.7
K I	30344 - 30341	0.0	-0.8	-2.5	-0.1	-0.1	0.0	0.0	-0.8	-2.5	2.5
L O	31908 - 31308	-0.4	0.7	-2.7	-1.7	0.0	0.0	2.0	-1.7	-2.7	4.7
M O	30663 - 30063	-0.1	0.5	-2.6	-0.6	0.0	0.0	0.9	-0.5	-2.6	3.5
N I	31877 - 31277	-0.1	-1.9	-2.2	-0.3	0.2	0.0	-0.1	-1.8	-2.3	2.2
O I	30647 - 30047	0.0	-0.8	-2.7	-0.1	0.1	0.0	0.0	-0.8	-2.7	2.7
P I	31840 - 31240	-0.1	-1.9	0.1	-0.3	0.4	0.0	0.1	-0.1	-2.0	2.1
Q O	30628 - 30028	0.0	-0.4	-2.7	-0.1	0.2	0.0	0.0	-0.4	-2.7	2.7
R I	31816 - 31216	0.1	1.9	-1.7	0.3	0.3	0.2	1.9	0.1	-1.7	3.7
S O	30616 - 30016	0.1	1.3	-3.4	0.2	0.1	0.1	1.4	0.0	-3.4	4.8
T O	30811 - 30011	-0.3	2.6	-3.8	0.4	0.2	-0.2	2.7	-0.4	-3.8	6.5
U O	47558 - 47551	1.3	0.4	-1.1	-0.1	0.2	-0.8	1.6	0.4	-1.4	3.0
V I	51524 - 51521	-4.0	-3.1	-1.2	0.0	0.0	0.1	-1.2	-3.1	-4.0	2.8
W I	43278 - 43271	-0.7	-1.0	0.0	0.0	-0.1	0.1	0.0	-0.7	-1.0	1.0
X O	50084 - 50081	0.1	-2.5	0.0	0.0	0.0	0.1	0.1	0.0	-2.5	2.6

[1] Refer to Figure 2.10.2-34 for the identification of the representative sections.

Table 2.10.4-81 S_n Stresses; 1-Foot Side Drop; Drop Orientation = 90 Degrees; 3-D Model; 180-Degree Circumferential Location; Condition 1

Condition 1: 100°F Ambient with Contents

Section[1]	Node - Node	Stress Components (ksi) S_x	S_y	S_z	S_{xy}	S_{yz}	S_{zx}	Principal Stresses (ksi) S1	S2	S3	S.I.
A O	1130 - 1128	-1.6	-3.0	-1.1	0.0	-0.1	0.3	-0.9	-1.8	-3.0	2.1
B O	1185 - 1183	0.2	-2.3	-0.8	0.0	0.0	0.3	0.2	-0.9	-2.3	2.6
C I	30090 - 30040	-2.6	-0.9	-0.2	0.1	-0.1	-0.4	-0.2	-0.9	-2.6	2.4
D I	30025 - 30005	1.1	2.1	-2.1	0.0	-0.3	0.6	2.1	1.2	-2.2	4.3
E O	30035 - 30031	0.1	3.0	4.7	0.4	-0.3	0.1	4.8	3.0	0.0	4.7
F O	30100 - 30097	0.5	-0.9	-3.1	-0.1	-0.1	0.0	0.5	-0.9	-3.1	3.6
G I	30094 - 30091	0.9	2.2	8.1	0.2	-0.7	0.8	8.2	2.2	0.8	7.4
H O	30330 - 30327	-0.1	0.3	-3.0	0.1	-0.1	0.2	0.3	-0.1	-3.0	3.3
I I	30244 - 30241	0.0	1.0	5.2	0.1	-0.4	0.0	5.3	1.0	0.0	5.3
J I	30550 - 30547	-0.1	-0.6	-4.0	-0.1	0.0	0.0	-0.1	-0.6	-4.0	3.9
K O	30344 - 30341	0.0	5.5	5.6	0.8	-0.2	0.0	5.8	5.4	-0.1	5.8
L I	30740 - 30737	-0.2	-0.6	-3.4	-0.4	0.0	-0.1	0.0	-0.8	-3.4	3.4
M O	30454 - 30451	-0.1	6.6	4.3	0.9	0.0	-0.1	6.8	4.3	-0.2	6.9
N I	31877 - 31277	-0.1	-0.9	-3.3	-0.1	0.0	0.0	-0.1	-0.9	-3.3	3.3
O O	30647 - 30047	0.0	4.9	4.9	0.7	0.2	0.0	5.2	4.8	-0.1	5.2
P O	31840 - 31240	-0.1	0.7	-1.7	0.1	0.1	-0.1	0.7	-0.1	-1.7	2.4
Q I	30628 - 30028	-0.1	1.6	4.3	0.2	0.3	0.0	4.4	1.6	-0.1	4.5
R O	31816 - 31216	-0.9	-0.2	-1.4	0.1	-0.3	3.4	2.2	-0.2	-4.5	6.8
S O	30616 - 30016	-0.6	5.2	6.8	0.9	0.3	0.4	6.8	5.3	-0.7	7.5
T I	30811 - 30011	-2.9	2.4	-4.2	0.8	0.5	-0.6	2.5	-2.7	-4.6	7.1
U I	47558 - 47551	-3.2	-5.0	-9.8	-0.3	-0.4	2.6	-2.3	-5.1	-10.7	8.5
V O	51524 - 51521	-0.7	-1.5	0.1	-0.1	0.0	0.2	0.2	-0.7	-1.6	1.8
W O	43278 - 43271	-3.3	-4.4	0.5	0.0	0.0	-0.5	0.6	-3.4	-4.4	4.9
X O	50084 - 50081	-1.0	-2.9	0.8	0.0	0.1	-0.4	0.9	-1.1	-2.9	3.8

[1] Refer to Figure 2.10.2-34 for the identification of the representative sections.

Table 2.10.4-82 P_m Stresses; 1-Foot Side Drop; Drop Orientation = 90 Degrees; 3-D Model; 67.7-Degree Circumferential Location; Condition 1

Condition 1: 100°F Ambient with Contents

		Stress Components (ksi)						Principal Stresses (ksi)			
Section[1]	Node - Node	S_x	S_y	S_z	S_{xy}	S_{yz}	S_{xz}	S1	S2	S3	S.I.
A	1130 - 1128	0.3	-1.2	0.0	0.0	0.0	0.0	0.0	-0.3	-1.2	1.2
B	1185 - 1183	-0.2	-2.1	0.0	0.0	0.0	-0.1	0.0	-0.2	-2.1	2.1
C	14090 -14040	-0.7	-1.1	0.1	-0.4	-1.2	0.0	0.9	-0.6	-1.9	2.8
D	14025 -14005	-0.6	-1.9	0.4	-0.3	-0.5	0.0	0.5	-0.6	-2.1	2.6
E	14035 -14031	-0.7	-1.3	0.1	0.3	-1.0	0.2	0.6	-0.5	-1.9	2.6
F	14100 -14097	0.0	-0.1	0.4	0.1	-5.2	0.1	5.3	0.0	-5.0	10.3
G	14094 -14091	-0.1	0.0	0.3	-0.1	-1.2	-0.1	1.3	-0.1	-1.1	2.4
H	14330 -14327	0.0	1.8	0.7	0.2	-6.8	0.0	8.1	0.0	-5.6	13.6
I	14244 -14241	0.0	0.3	0.4	0.0	-1.4	0.0	1.7	0.0	-1.0	2.7
J	14550 -14547	0.0	2.0	0.6	0.0	-3.9	0.0	5.2	0.0	-2.7	7.9
K	14344 -14341	0.0	0.2	0.4	0.0	-0.9	0.0	1.2	0.0	-0.6	1.8
L	14740 -14737	-0.1	2.1	0.5	0.1	0.1	0.0	2.1	0.5	-0.1	2.2
M	14454 -14451	-0.1	0.3	0.4	0.0	-0.1	0.0	0.4	0.2	-0.1	0.5
N	15877 -15277	0.0	2.0	0.6	0.0	4.2	0.0	5.5	0.0	-3.0	8.5
O	14647 -14047	0.0	0.2	0.4	0.0	0.6	0.0	0.9	0.0	-0.3	1.3
P	15840 -15240	0.0	2.0	0.7	0.2	6.6	0.0	8.0	0.0	-5.2	13.2
Q	14628 -14028	0.0	0.4	0.4	0.0	1.0	0.0	1.4	0.0	-0.7	2.0
R	15816 -15216	-0.1	0.8	0.3	1.3	4.2	0.0	4.9	-0.1	-3.8	8.8
S	14616 -14016	0.3	0.0	0.3	-0.2	1.0	0.1	1.2	-0.3	-0.9	2.2
T	14811 -14011	-0.2	-0.9	0.1	0.7	2.0	0.0	1.7	-0.2	-2.6	4.3
U	45158 -45151	-0.5	-0.9	-1.5	0.0	0.0	-0.1	-0.5	-0.9	-1.5	1.0
V	50724 -50721	-0.2	-0.8	-0.2	0.2	0.1	0.0	-0.1	-0.2	-0.9	0.8
W	43278 -43271	-0.4	-0.9	0.0	0.0	-0.1	0.1	0.0	-0.4	-0.9	0.9
X	50084 -50081	-0.1	-2.2	0.0	0.0	0.0	0.1	0.0	-0.1	-2.2	2.2

[1] Refer to Figure 2.10.2-34 for the identification of the representative sections.

Table 2.10.4-83 $P_m + P_b$ Stresses; 1-Foot Side Drop; Drop Orientation = 90 Degrees; 3-D Model; 67.7-Degree Circumferential Location; Condition 1

Condition 1: 100°F Ambient with Contents

Section[1]	Node - Node	Stress Components (ksi) S_x	S_y	S_z	S_{xy}	S_{yz}	S_{xz}	Principal Stresses (ksi) S1	S2	S3	S.I.
A O	1130 - 1128	-0.4	-1.7	0.1	0.0	0.0	0.0	0.1	-0.4	-1.7	1.8
B O	1185 - 1183	0.1	-2.4	0.0	0.0	0.0	-0.1	0.1	0.0	-2.4	2.5
C I	14090 - 14040	0.0	-0.3	0.3	-1.6	-2.7	0.1	3.1	0.0	-3.1	6.3
D I	14025 - 14005	-0.1	-1.3	0.9	-0.8	-1.0	0.1	1.3	0.1	-2.0	3.3
E I	14035 - 14031	-0.7	-1.3	0.9	0.8	-1.4	0.2	1.6	-0.3	-2.4	3.9
F I	14100 - 14097	-0.1	-0.2	0.4	0.0	-5.7	0.2	5.8	-0.1	-5.6	11.5
G I	14094 - 14091	-0.1	-0.5	-1.3	-0.1	-1.5	-0.2	0.7	-0.1	-2.5	3.2
H I	14330 - 14327	0.0	1.9	0.2	0.0	-7.3	0.0	8.4	0.0	-6.3	14.6
I I	14244 - 14241	0.0	0.6	0.5	0.0	-1.6	0.0	2.1	0.0	-1.0	3.2
J I	14550 - 14547	0.0	2.9	0.9	0.0	-4.1	0.0	6.1	0.0	-2.4	8.5
K I	14344 - 14341	0.0	1.1	0.7	0.0	-1.0	0.0	1.9	0.0	-0.1	2.0
M I	14454 - 14451	-0.2	1.6	0.8	0.0	0.0	0.0	1.6	0.8	-0.2	1.8
L I	15908 - 15308	0.3	3.8	1.1	-0.1	0.4	0.0	3.8	1.0	0.3	3.5
N I	15877 - 15277	0.0	2.9	0.9	0.0	4.5	0.0	6.5	0.0	-2.7	9.2
O I	14647 - 14047	0.0	1.1	0.8	0.0	0.7	0.0	1.7	0.2	0.0	1.7
P I	15840 - 15240	0.0	2.3	0.5	0.0	6.9	0.0	8.4	0.0	-5.6	14.0
Q I	14628 - 14028	0.0	0.9	0.6	0.0	1.2	0.0	2.0	0.0	-0.4	2.3
R O	15816 - 15216	-0.2	1.0	1.6	2.5	3.8	0.2	5.7	0.2	-3.5	9.3
S I	14616 - 14016	-0.7	-0.4	-1.5	-0.4	1.4	0.2	0.6	-0.6	-2.5	3.1
T I	14811 - 14011	-0.7	-1.3	-1.5	1.9	3.3	0.0	2.5	-0.9	-5.1	7.6
U I	45158 - 45151	0.4	-0.2	-1.9	-0.5	0.1	0.5	0.8	-0.5	-2.0	2.8
V O	50724 - 50721	-1.8	-1.9	0.3	0.9	0.1	0.0	0.3	-1.0	-2.7	3.0
W I	43278 - 43271	-0.7	-1.0	0.0	0.0	-0.1	0.1	0.0	-0.7	-1.0	1.0
X O	50084 - 50081	0.1	-2.5	0.0	0.0	0.0	0.1	0.1	0.0	-2.5	2.6

[1] Refer to Figure 2.10.2-34 for the identification of the representative sections.

Table 2.10.4-84 Primary Stresses; 1-Foot Top Corner Drop; Drop Orientation = 24 Degrees; 3-D Top Model; 0-Degree Circumferential Location; Condition 1

Condition 1: 100°F Ambient with Contents

Stress Points		Stress Components (ksi)						Principal Stresses (ksi)		
Section[1]	Node	S_x	S_y	S_z	S_{xy}	S_{yz}	S_{xz}	S1	S2	S3
A1	1949	0.3	0.7	-0.1	0.0	0.0	0.1	0.7	0.3	-0.1
A2	1950	0.2	0.5	-0.1	0.0	0.0	0.1	0.5	0.2	-0.1
A3	1951	-0.1	-0.1	0.1	0.0	0.0	0.0	0.1	-0.1	-0.1
B1	1952	0.0	0.0	-0.1	0.0	0.0	0.0	0.0	0.0	-0.1
B2	93	-0.3	-0.6	0.2	0.0	0.0	0.0	0.2	-0.3	-0.6
C1	1925	-0.1	0.0	0.9	0.0	-0.1	0.0	0.9	0.0	-0.1
C2	1926	0.0	-0.1	0.1	0.0	0.0	-0.1	0.2	-0.1	-0.2
C3	1927	0.2	0.0	0.0	0.0	0.0	0.0	0.2	0.0	-0.1
D1	683	0.1	-0.1	-0.2	0.0	0.0	0.1	0.1	-0.1	-0.2
D2	85	-0.1	-0.3	-0.1	0.1	0.0	0.0	-0.1	-0.1	-0.3
E1	682	0.1	-0.1	-0.3	0.0	0.0	0.1	0.1	-0.1	-0.3
E2	82	0.1	0.1	0.5	0.0	0.0	0.2	0.6	0.1	0.0
F1	1925	-0.1	0.0	0.9	0.0	-0.1	0.0	0.9	0.0	-0.1
F2	1325	-0.6	-1.1	-2.7	0.1	-0.1	0.2	-0.6	-1.1	-2.7
G1	680	-0.3	-0.1	0.4	0.0	0.0	0.2	0.5	-0.1	-0.4
G2	80	0.0	0.1	0.5	0.0	0.0	0.0	0.5	0.1	0.0
H1	1921	0.0	2.1	-1.6	-0.1	-0.2	0.0	2.2	0.0	-1.6
H2	1321	0.0	2.6	-0.2	-0.2	-0.2	0.0	2.6	0.0	-0.2
I1	676	0.0	0.0	0.2	0.0	0.0	0.0	0.2	0.0	0.0
I2	76	0.0	0.3	0.4	0.0	0.0	0.0	0.4	0.2	0.0
J1	1916	0.0	2.3	-0.1	-0.2	-0.1	0.0	2.3	-0.1	-0.1
J2	1316	0.0	2.8	0.3	-0.2	-0.1	0.0	2.8	0.3	-0.1
K1	671	0.0	-0.1	-0.3	0.0	0.0	0.0	0.0	-0.1	-0.3
K2	71	0.0	0.4	0.0	0.0	0.0	0.0	0.4	0.0	0.0
L1	1908	-0.2	1.9	-0.8	-0.1	0.1	0.0	1.9	-0.2	-0.8
L2	1308	0.0	3.2	-0.2	0.3	0.1	0.0	3.3	0.0	-0.2
M1	663	-0.1	-0.5	-1.3	0.0	0.0	0.0	-0.1	-0.5	-1.3
M2	63	0.1	0.8	-0.9	0.2	0.1	0.0	0.9	0.0	-0.9

Table 2.10.4-84 Primary Stresses; 1-Foot Top Corner Drop; Drop Orientation = 24 Degrees; 3-D Top Model; 0-Degree Circumferential Location; Condition 1 (continued)

Stress Points		Stress Components (ksi)						Principal Stresses (ksi)		
Section[1]	Node	S_x	S_y	S_z	S_{xy}	S_{yz}	S_{zx}	S1	S2	S3
N1	1877	-0.1	1.9	-4.1	-0.1	0.3	0.0	1.9	-0.1	-4.1
N2	1477	0.0	2.5	-3.9	-0.2	0.3	0.0	2.6	-0.1	-3.9
N3	1277	0.0	3.2	-3.6	-0.2	0.3	0.0	3.2	0.0	-3.6
O1	647	0.0	-0.4	-2.4	0.0	0.1	0.0	0.0	-0.4	-2.4
O2	247	0.0	0.1	-2.2	0.0	0.1	0.0	0.1	0.0	-2.2
O3	47	0.0	0.5	-2.1	0.0	0.0	0.0	0.6	0.0	-2.1
P1	1840	-0.1	2.2	-5.0	-0.2	0.4	0.0	2.2	-0.1	-5.0
P2	1640	-0.2	2.1	-5.9	-0.2	0.4	0.0	2.2	-0.2	-6.0
P3	1440	-0.2	2.1	-6.8	-0.1	0.3	-0.2	2.1	-0.2	-6.8
P4	1240	-0.2	1.8	-8.6	-0.1	0.3	-0.5	1.8	-0.2	-8.7
Q1	628	0.0	0.8	-2.4	-0.1	0.1	0.0	0.8	0.0	-2.4
Q2	428	0.0	0.9	-2.8	-0.1	0.1	0.0	0.9	0.0	-2.8
Q3	228	0.0	0.9	-3.1	-0.1	0.1	0.0	0.9	0.0	-3.1
Q4	28	0.0	1.0	-3.4	-0.1	0.0	0.0	1.0	0.0	-3.4
R1	1816	-0.1	-1.0	-10.7	0.1	0.3	0.1	0.0	-1.0	-10.7
R2	1616	0.0	-0.2	-8.1	0.0	0.2	0.2	0.0	-0.2	-8.1
R3	1416	-0.2	0.5	-5.6	0.0	0.2	0.4	0.5	-0.2	-5.6
R4	1216	1.8	1.8	-2.8	0.1	0.2	0.4	1.9	1.8	-2.8
S1	616	-3.7	-2.0	-11.6	-0.1	0.2	1.4	-2.0	-3.4	-11.8
S2	416	-3.6	-0.4	-5.2	-0.2	0.0	-0.4	-0.4	-3.5	-5.3
S3	216	-1.3	1.4	-0.8	-0.2	0.0	-0.5	1.4	-0.5	-1.6
S4	16	-0.5	3.0	4.4	-0.3	0.0	-0.4	4.5	3.0	-0.5
T1	811	-0.6	-1.7	-1.3	0.2	0.2	0.5	-0.3	-1.4	-1.8
T2	611	0.4	-1.8	-2.9	0.2	0.1	-0.3	0.4	-1.8	-2.9
T3	411	0.3	-1.8	-2.8	0.2	0.1	-0.3	0.3	-1.8	-2.8
T4	211	0.3	-1.6	-2.4	0.1	0.1	-0.2	0.3	-1.6	-2.4
T5	11	0.3	-1.5	-1.8	0.1	0.0	-0.1	0.3	-1.5	-1.8
U1	43058	2.1	3.0	-6.1	-0.2	0.2	1.3	3.1	2.2	-6.3
U2	43057	1.6	2.0	-5.7	-0.1	0.1	1.9	2.1	1.9	-6.2
U3	43056	1.0	1.1	-5.4	-0.1	0.2	2.6	1.9	1.1	-6.4

Table 2.10.4-84 Primary Stresses; 1-Foot Top Corner Drop; Drop Orientation = 24 Degrees; 3-D Top Model; 0-Degree Circumferential Location; Condition 1 (continued)

Stress Points		Stress Components (ksi)						Principal Stresses (ksi)		
Section[1]	Node	S_x	S_y	S_z	S_{xy}	S_{yz}	S_{zx}	S1	S2	S3
U4	43055	0.7	0.2	-5.5	0.0	0.2	2.5	1.6	0.2	-6.4
U5	43054	0.3	-0.8	-5.6	0.1	0.1	2.0	0.9	-0.8	-6.2
U6	43053	-0.6	-1.5	-4.5	0.1	0.1	1.2	-0.3	-1.5	-4.9
U7	43052	-1.2	-2.8	-5.8	0.2	0.1	1.2	-0.9	-2.8	-6.1
U8	43051	-2.9	-4.3	-4.8	0.2	0.1	2.4	-1.2	-4.3	-6.4
V1	50024	-5.8	0.4	-2.1	-0.5	-0.1	-0.9	0.4	-1.9	-6.1
V2	50023	-4.0	-1.6	-2.5	-0.2	-0.1	-0.7	-1.6	-2.2	-4.3
V3	50022	-1.8	-3.3	-2.1	0.1	0.0	-0.2	-1.6	-2.2	-3.4
V4	50021	0.2	-5.1	-1.2	0.4	0.0	0.0	0.2	-1.2	-5.1
W1	43278	0.2	-0.7	-0.1	-0.1	-0.3	0.1	0.3	0.0	-0.9
W2	43274	0.4	-0.3	-0.1	0.0	-0.4	0.1	0.4	0.1	-0.6
W3	43271	0.3	0.1	-0.1	0.0	-0.4	0.0	0.4	0.3	-0.5
X1	50084	13.3	10.5	-3.2	-0.4	0.1	-3.2	13.9	10.5	-3.8
X2	50083	4.1	2.0	-2.1	-0.1	0.1	-3.2	5.5	2.0	-3.4
X3	50081	-12.5	-13.2	6.6	0.4	-0.3	-3.2	7.1	-12.8	-13.5

[1] Refer to Figure 2.10.2-34 for the identification of the representative sections.

Table 2.10.4-85 Primary + Secondary Stresses; 1-Foot Top Corner Drop; Drop Orientation = 24 Degrees; 3-D Top Model; 0-Degree Circumferential Location; Condition 1

Condition 1: 100°F Ambient with Contents

Stress Points		Stress Components (ksi)						Principal Stresses (ksi)		
Section[1]	Node	S_x	S_y	S_z	S_{xy}	S_{yz}	S_{xz}	S1	S2	S3
A1	1949	0.0	0.4	0.5	0.0	-0.2	0.7	1.1	0.4	-0.5
A2	1950	-0.3	0.0	0.4	0.0	-0.2	0.7	0.9	0.0	-0.8
A3	1951	-1.7	-1.7	-0.6	0.0	0.0	0.4	-0.5	-1.7	-1.8
B1	1952	0.7	0.7	0.4	0.0	-0.1	0.4	1.0	0.7	0.1
B2	93	-0.2	-0.5	-1.4	0.0	-0.2	0.8	0.3	-0.5	-1.8
C1	1925	-1.1	-0.6	-0.7	0.0	-0.1	-0.8	-0.1	-0.6	-1.7
C2	1926	0.7	-0.5	-1.0	0.1	-0.1	-0.8	1.0	-0.5	-1.3
C3	1927	-1.7	-2.2	-1.3	0.0	0.0	-0.1	-1.3	-1.7	-2.2
D1	683	1.7	1.1	3.1	0.0	0.1	0.8	3.5	1.3	1.1
D2	85	-1.5	1.1	3.2	-0.1	0.1	0.6	3.3	1.1	-1.6
E1	682	-1.3	-0.5	2.1	0.0	0.1	0.7	2.3	-0.5	-1.4
E2	82	-0.7	-0.5	-0.1	0.0	0.0	1.3	0.9	-0.5	-1.7
F1	1925	-1.1	-0.6	-0.7	0.0	-0.1	-0.8	-0.1	-0.6	-1.7
F2	1325	-0.1	-1.5	-3.5	0.1	-0.1	-0.5	0.0	-1.5	-3.5
G1	680	-0.4	0.1	1.2	0.0	0.0	0.4	1.3	0.1	-0.5
G2	80	-2.3	1.2	7.1	-0.2	0.1	1.2	7.3	1.2	-2.5
H1	1921	0.0	1.7	-1.4	-0.1	-0.1	0.1	1.7	0.0	-1.4
H2	1321	-0.1	2.3	-1.8	-0.2	-0.1	0.1	2.3	-0.1	-1.8
I1	676	-0.1	2.6	5.5	-0.2	0.1	0.1	5.5	2.6	-0.1
I2	76	-0.1	3.4	6.5	-0.3	-0.1	0.1	6.5	3.4	-0.2
J1	1916	-0.2	0.6	-2.9	0.0	-0.1	0.0	0.6	-0.2	-2.9
J2	1316	-0.1	4.3	1.3	-0.3	-0.1	0.0	4.3	1.3	-0.2
K1	671	-0.1	3.8	3.5	-0.3	0.1	0.0	3.8	3.5	-0.2
K2	71	-0.1	6.5	8.0	-0.5	0.0	0.0	8.0	6.5	-0.2
L1	1908	-1.1	-0.2	-3.5	-0.1	0.1	0.0	-0.1	-1.1	-3.5
L2	1308	0.6	5.1	0.3	0.7	0.1	0.0	5.2	0.5	0.3
M1	663	-1.3	4.4	2.7	-0.4	0.0	0.0	4.5	2.7	-1.3
M2	63	0.7	8.1	6.9	-0.5	0.0	0.0	8.1	6.9	0.6

Table 2.10.4-85 Primary + Secondary Stresses; 1-Foot Top Corner Drop; Drop Orientation = 24 Degrees; 3-D Top Model; 0-Degree Circumferential Location; Condition 1 (continued)

Stress Points		Stress Components (ksi)						Principal Stresses (ksi)		
Section[1]	Node	S_x	S_y	S_z	S_{xy}	S_{yz}	S_{xz}	S1	S2	S3
N1	1877	-0.1	0.2	-6.7	0.0	0.3	0.0	0.2	-0.1	-6.7
N2	1477	0.0	2.2	-4.7	-0.2	0.3	0.0	2.2	-0.1	-4.8
N3	1277	0.0	4.0	-2.8	-0.3	0.3	0.0	4.0	0.0	-2.8
O1	647	-0.3	4.1	2.0	-0.3	0.1	0.0	4.1	2.0	-0.3
O2	247	-0.2	5.4	3.7	-0.4	0.1	0.0	5.4	3.7	-0.2
O3	47	-0.1	6.5	5.3	-0.5	0.1	0.0	6.6	5.3	-0.1
P1	1840	-0.1	1.7	-5.9	-0.1	0.4	0.0	1.7	-0.1	-5.9
P2	1640	-0.2	1.8	-6.9	-0.1	0.3	0.0	1.8	-0.2	-6.9
P3	1440	-0.1	2.1	-7.7	-0.1	0.3	-0.2	2.1	-0.1	-7.7
P4	1240	-0.4	1.9	-9.6	-0.1	0.3	-0.5	1.9	-0.4	-9.7
Q1	628	-0.2	4.3	2.2	-0.3	0.1	0.1	4.4	2.2	-0.2
Q2	428	-0.1	4.7	2.5	-0.4	0.1	0.2	4.8	2.6	-0.2
Q3	228	0.0	5.2	3.0	-0.4	0.1	0.2	5.2	3.0	-0.1
Q4	28	0.0	5.5	3.5	-0.4	0.1	0.1	5.6	3.5	0.0
R1	1816	0.2	-5.5	-15.6	0.4	0.3	0.8	0.3	-5.6	-15.6
R2	1616	0.2	-3.7	-11.4	0.3	0.3	1.4	0.4	-3.7	-11.6
R3	1416	-0.8	-2.3	-7.2	0.2	0.4	2.9	0.4	-2.3	-8.4
R4	1216	4.4	1.4	-1.0	0.2	0.3	2.7	5.5	1.4	-2.1
S1	616	-5.7	-3.1	-13.9	-0.2	0.3	0.2	-3.1	-5.7	-13.9
S2	416	-8.3	-0.2	-1.4	-0.5	-0.1	-2.2	-0.2	-0.7	-9.0
S3	216	-2.5	3.2	4.1	-0.4	0.0	-0.5	4.1	3.2	-2.6
S4	16	-0.9	5.9	11.7	-0.5	0.0	-0.3	11.8	6.0	-1.0
T1	811	-2.5	-4.3	-8.0	0.3	0.1	-1.3	-2.2	-4.4	-8.3
T2	611	-1.1	-2.9	-5.1	0.2	0.0	-0.6	-1.0	-2.9	-5.2
T3	411	-0.3	-1.7	-2.2	0.1	0.1	-0.3	-0.3	-1.7	-2.3
T4	211	0.1	-0.5	0.8	0.0	0.1	-0.1	0.8	0.1	-0.5
T5	11	0.2	0.7	4.3	0.0	0.1	0.0	4.3	0.7	0.2
U1	43058	-2.1	1.0	-11.9	-0.3	0.5	2.2	1.0	-1.6	-12.4
U2	43057	0.9	0.6	-10.6	-0.1	0.2	2.9	1.6	0.6	-11.3
U3	43056	0.8	-0.3	-8.7	0.0	0.4	3.6	2.0	-0.3	-9.9

Table 2.10.4-85 Primary + Secondary Stresses; 1-Foot Top Corner Drop; Drop Orientation = 24 Degrees; 3-D Top Model; 0-Degree Circumferential Location; Condition 1 (continued)

Stress Points		Stress Components (ksi)						Principal Stresses (ksi)		
Section[1]	Node	S_x	S_y	S_z	S_{xy}	S_{yz}	S_{zx}	S1	S2	S3
U4	43055	0.6	-1.5	-7.9	0.1	0.4	3.2	1.7	-1.5	-9.0
U5	43054	-0.2	-2.8	-7.3	0.2	0.5	2.5	0.6	-2.8	-8.1
U6	43053	-1.6	-4.0	-5.7	0.2	0.6	1.6	-1.0	-4.0	-6.3
U7	43052	-3.0	-5.9	-7.0	0.3	0.8	1.5	-2.5	-5.7	-7.7
U8	43051	-0.9	-1.2	-0.7	-0.3	1.3	2.1	1.5	-0.9	-3.5
V1	50024	-2.7	1.8	-5.0	-0.3	-0.7	-1.0	1.9	-2.4	-5.4
V2	50023	-1.7	-0.5	-4.1	-0.2	-0.6	-0.7	-0.3	-1.5	-4.4
V3	50022	-1.8	-3.6	-2.6	0.0	-0.5	-0.4	-1.6	-2.6	-3.8
V4	50021	-1.7	-6.5	-1.5	0.2	-0.3	-0.1	-1.4	-1.8	-6.5
W1	43278	4.0	2.9	-1.6	-0.1	-0.1	-0.8	4.1	2.9	-1.7
W2	43274	0.1	-0.9	-0.7	0.0	-0.1	-0.9	0.7	-0.8	-1.4
W3	43271	-2.8	-3.3	0.5	0.0	-0.3	-0.4	0.6	-2.9	-3.3
X1	50084	16.7	14.6	-3.7	-0.4	0.3	-3.7	17.4	14.6	-4.3
X2	50083	5.9	4.5	-2.4	-0.1	0.3	-3.7	7.4	4.5	-3.8
X3	50081	-13.5	-13.9	7.6	0.4	-0.1	-3.7	8.3	-13.6	-14.4

[1] Refer to Figure 2.10.2-34 for the identification of the representative sections.

Table 2.10.4-86 P_m Stresses; 1-Foot Top Corner Drop; Drop Orientation = 24 Degrees; 3-D Top Model; 0-Degree Circumferential Location; Condition 1

Condition 1: 100°F Ambient with Contents

Section[1]	Node - Node	Stress Components (ksi)						Principal Stresses (ksi)			
		S_x	S_y	S_z	S_{xy}	S_{yz}	S_{xz}	S1	S2	S3	S.I.
A	1949 - 1951	0.1	0.3	0.0	0.0	0.0	0.0	0.3	0.1	-0.1	0.4
B	1952 - 93	-0.2	-0.3	0.0	0.0	0.0	0.0	0.1	-0.2	-0.3	0.4
C	1925 - 1927	0.1	-0.1	0.2	0.0	0.0	-0.1	0.2	0.0	-0.1	0.3
D	683 - 85	0.0	-0.2	-0.1	0.0	0.0	0.0	0.0	-0.1	-0.2	0.2
E	682 - 82	0.1	0.0	0.1	0.0	0.0	0.2	0.3	0.0	-0.1	0.3
F	1925 - 1325	-0.4	-0.5	-0.9	0.0	-0.1	0.1	-0.4	-0.5	-0.9	0.6
G	680 - 80	-0.2	0.0	0.5	0.0	0.0	0.1	0.5	0.0	-0.2	0.7
H	1921 - 1321	0.0	2.4	-0.9	-0.2	-0.2	0.0	2.4	0.0	-0.9	3.3
I	676 - 76	0.0	0.1	0.3	0.0	0.0	0.0	0.3	0.1	0.0	0.3
J	1916 - 1316	0.0	2.6	0.1	-0.2	-0.1	0.0	2.6	0.1	-0.1	2.6
K	671 - 71	0.0	0.1	-0.2	0.0	0.0	0.0	0.1	0.0	-0.2	0.3
L	1908 - 1308	-0.1	2.5	-0.5	0.1	0.1	0.0	2.6	-0.1	-0.5	3.1
M	663 - 63	0.0	0.2	-1.1	0.1	0.1	0.0	0.2	-0.1	-1.1	1.3
N	1877 - 1277	0.0	2.5	-3.9	-0.2	0.3	0.0	2.6	-0.1	-3.9	6.4
O	647 - 47	0.0	0.1	-2.2	0.0	0.1	0.0	0.1	0.0	-2.2	2.3
P	1840 - 1240	-0.2	2.1	-6.5	-0.1	0.3	-0.1	2.1	-0.2	-6.5	8.6
Q	628 - 28	0.0	0.9	-2.9	-0.1	0.1	0.0	0.9	0.0	-2.9	3.8
R	1816 - 1216	0.2	0.2	-6.8	0.0	0.2	0.3	0.3	0.2	-6.8	7.1
S	616 - 16	-2.3	0.5	-3.2	-0.2	0.1	-0.1	0.5	-2.3	-3.2	3.7
T	811 - 11	0.2	-1.7	-2.4	0.2	0.1	-0.1	0.2	-1.7	-2.4	2.7
U	43058 - 43051	-0.1	-0.7	-5.4	0.0	0.1	1.9	0.5	-0.8	-6.0	6.5
V	50024 - 50021	-2.8	-2.5	-2.1	-0.1	-0.1	-0.5	-1.9	-2.4	-3.1	1.2
W	43278 - 43271	0.3	-0.3	-0.1	0.0	-0.4	0.1	0.3	0.2	-0.6	0.9
X	50084 - 50081	-0.1	-1.8	0.7	0.0	0.0	-3.2	3.5	-1.8	-2.9	6.4

[1] Refer to Figure 2.10.2-34 for the identification of the representative sections.

Table 2.10.4-87 $P_m + P_b$ Stresses; 1-Foot Top Corner Drop; Drop Orientation = 24 Degrees; 3-D Top Model; 0-Degree Circumferential Location; Condition 1

Condition 1: 100°F Ambient with Contents

Section[1]	Node - Node	Stress Components (ksi) S_x	S_y	S_z	S_{xy}	S_{yz}	S_{xz}	Principal Stresses (ksi) S1	S2	S3	S.I.
A I	1949 - 1951	0.3	0.7	-0.1	0.0	0.0	0.1	0.7	0.3	-0.1	0.8
B O	1952 - 93	-0.3	-0.6	0.2	0.0	0.0	0.0	0.2	-0.3	-0.6	0.9
C I	1925 - 1927	-0.1	-0.1	0.5	0.0	-0.1	-0.1	0.5	-0.1	-0.1	0.6
D I	683 - 85	0.1	-0.1	-0.2	0.0	0.0	0.1	0.1	-0.1	-0.2	0.3
E O	682 - 82	0.1	0.1	0.5	0.0	0.0	0.2	0.6	0.1	0.0	0.6
F O	1925 - 1325	-0.6	-1.1	-2.7	0.1	-0.1	0.2	-0.6	-1.1	-2.7	2.1
G I	680 - 80	-0.3	-0.1	0.4	0.0	0.0	0.2	0.5	-0.1	-0.4	0.9
H I	1921 - 1321	0.0	2.1	-1.6	-0.1	-0.2	0.0	2.2	0.0	-1.6	3.7
I O	676 - 76	0.0	0.3	0.4	0.0	0.0	0.0	0.4	0.2	0.0	0.4
J O	1916 - 1316	0.0	2.8	0.3	-0.2	-0.1	0.0	2.8	0.3	-0.1	2.9
K O	671 - 71	0.0	0.4	0.0	0.0	0.0	0.0	0.4	0.0	0.0	0.4
L O	1908 - 1308	0.0	3.2	-0.2	0.3	0.1	0.0	3.3	0.0	-0.2	3.5
M O	663 - 63	0.1	0.8	-0.9	0.2	0.1	0.0	0.9	0.0	-0.9	1.7
N O	1877 - 1277	0.0	3.2	-3.6	-0.2	0.3	0.0	3.2	0.0	-3.6	6.8
O O	647 - 47	0.0	0.6	-2.1	0.0	0.0	0.0	0.6	0.0	-2.1	2.7
P O	1840 - 1240	-0.2	1.9	-8.2	-0.1	0.3	-0.4	1.9	-0.2	-8.2	10.2
Q O	628 - 28	0.0	1.0	-3.4	-0.1	0.0	0.0	1.0	0.0	-3.4	4.4
R I	1816 - 1216	-0.4	-1.1	-10.7	0.1	0.3	0.1	-0.4	-1.1	-10.7	10.3
S I	616 - 16	-4.3	-2.0	-10.9	-0.1	0.2	0.6	-2.0	-4.3	-10.9	8.9
T O	811 - 11	0.5	-1.5	-2.4	0.1	0.0	-0.3	0.5	-1.6	-2.4	2.9
U I	43058 - 43051	2.3	2.9	-5.8	-0.2	0.2	2.1	3.0	2.7	-6.3	9.3
V I	50024 - 50021	-5.9	0.3	-2.6	-0.5	-0.1	-1.0	0.3	-2.3	-6.2	6.6
W I	43278 - 43271	0.3	-0.7	-0.1	-0.1	-0.3	0.1	0.3	0.0	-0.8	1.2
X O	50084 - 50081	-12.8	-13.5	5.9	0.4	-0.2	-3.2	6.5	13.0	13.8	20.2

[1] Refer to Figure 2.10.2-34 for the identification of the representative sections.

Table 2.10.4-88 S_n Stresses; 1-Foot Top Corner Drop; Drop Orientation = 24 Degrees; 3-D Top Model; 0-Degree Circumferential Location; Condition 1

Condition 1: 100°F Ambient with Contents

		Stress Components (ksi)						Principal Stresses (ksi)			
Section[1]	Node - Node	S_x	S_y	S_z	S_{xy}	S_{yz}	S_{xz}	S1	S2	S3	S.I.
A I	1949 - 1951	0.1	0.6	0.6	0.0	-0.2	0.8	1.3	0.5	-0.5	1.7
B O	1952 - 93	-0.2	-0.5	-1.4	0.0	-0.2	0.8	0.3	-0.5	-1.8	2.1
C I	1925 - 1927	0.4	-0.2	-0.8	0.0	-0.1	-0.9	0.9	-0.2	-1.3	2.2
D O	683 - 85	-1.5	1.1	3.2	-0.1	0.1	0.6	3.3	1.1	-1.6	4.9
E I	682 - 82	-1.3	-0.5	2.1	0.0	0.1	0.7	2.3	-0.5	-1.4	3.7
F O	1925 - 1325	-0.1	-1.5	-3.5	0.1	-0.1	-0.5	0.0	-1.5	-3.5	3.5
G O	680 - 80	-2.3	1.2	7.1	-0.2	0.1	1.2	7.3	1.2	-2.5	9.8
H O	1921 - 1321	-0.1	2.3	-1.8	-0.2	-0.1	0.1	2.3	-0.1	-1.8	4.2
I O	676 - 76	-0.1	3.4	6.5	-0.3	-0.1	0.1	6.5	3.4	-0.2	6.7
J O	1916 - 1316	-0.1	4.3	1.3	-0.3	-0.1	0.0	4.3	1.3	-0.2	4.5
K O	671 - 71	-0.1	6.5	8.0	-0.5	0.0	0.0	8.0	6.5	-0.2	8.1
L O	1908 - 1308	0.6	5.1	0.3	0.7	0.1	0.0	5.2	0.5	0.3	4.8
M O	663 - 63	0.7	8.1	6.9	-0.5	0.0	0.0	8.1	6.9	0.6	7.5
N I	1877 - 1277	-0.1	0.3	-6.7	0.0	0.3	0.0	0.3	-0.1	-6.7	7.0
O O	647 - 47	-0.1	6.6	5.3	-0.5	0.1	0.0	6.6	5.3	-0.1	6.7
P O	1840 - 1240	-0.3	2.1	-9.1	-0.1	0.3	-0.4	2.1	-0.3	-9.2	11.3
Q O	628 - 28	0.0	5.5	3.5	-0.4	0.1	0.2	5.6	3.5	0.0	5.6
R I	1816 - 1216	-0.7	-5.9	-16.0	0.4	0.3	0.8	-0.6	-5.9	16.1	15.4
S O	616 - 16	-0.9	6.1	12.3	-0.5	0.0	-0.6	12.4	6.1	-1.0	13.3
T I	811 - 11	-1.9	-4.2	-8.2	0.3	0.0	-1.0	-1.7	-4.2	-8.3	6.6
U I	43058 - 43051	0.8	0.6	-11.5	0.0	0.1	3.3	1.6	0.6	-12.3	13.9
V I	50024 - 50021	-2.2	2.1	-5.2	-0.3	-0.7	-1.0	2.2	-1.9	-5.6	7.8
W I	43278 - 43271	3.7	2.5	-1.7	-0.1	-0.1	-1.0	3.9	2.5	-1.9	5.8
X I	50084 - 50081	16.0	14.0	-5.2	-0.4	0.4	-3.7	16.7	13.9	-5.9	22.6

[1] Refer to Figure 2.10.2-34 for the identification of the representative sections.

Table 2.10.4-89 Critical P_m Stress Summary; 1-Foot Top Corner Drop; Drop Orientation = 24 Degrees; 3-D Top Model; Condition 1

Condition 1: 100°F Ambient with Contents

Comp. No.[1]	Section Cut Node-Node	P_m Stresses (ksi) S_x	S_y	S_z	S_{xy}	S_{xz}	S_{yz}	Principal Stresses (ksi) S1	S2	S3	S.I.	Allow. Stress	Margin of Safety
1	1952- 93	-0.2	-0.3	0.0	0.0	0.0	0.0	0.1	-0.2	-0.3	0.4	19.2	47.0
2	13924-13324	0.0	0.5	-0.3	0.0	-1.5	0.1	1.6	0.0	-1.4	3.0	18.5	5.2
3	11841-11241	-0.1	1.7	-5.2	0.0	3.3	-0.1	3.0	-0.1	-6.5	9.5	31.4	2.3
4	13874-13274	0.0	1.8	-3.3	0.0	3.1	0.0	3.2	0.0	-4.8	8.0	19.6	1.5
5	10625-10025	0.0	1.2	-3.2	0.0	0.9	0.1	1.4	0.0	-3.4	4.8	20.0	3.2
6	401- 1	-2.0	-13.7	-1.7	0.8	0.0	-0.2	-1.6	-2.0	13.7	12.1	20.0	0.7
7	43021-43028	-0.9	-2.8	-12.3	0.1	0.0	1.2	-0.7	-2.8	-12.4	11.7	20.0	0.7
8	50081-50084	-0.1	-1.8	0.7	0.0	0.0	-3.2	3.5	-1.8	-2.9	6.4	45.0	6.0

Locations of the most critical sections for each component are provided in the following:

Comp. No.[1]	Section Location Inside Node x (in)	y (deg)	z (in)	Outside Node x (in)	y (deg)	z (in)
1	0.00	0.0	6.20	0.00	0.0	0.75
2	35.50	56.5	17.40	37.50	56.5	17.40
3	35.50	45.9	159.90	37.00	45.9	159.90
4	35.50	56.5	142.40	37.00	56.5	142.40
5	40.70	45.9	163.40	43.35	45.9	163.40
6	40.88	0.0	193.71	43.35	0.0	193.71
7	37.66	0.0	185.40	37.66	0.0	179.40
8	0.00	0.0	193.71	0.00	0.0	188.46

[1] Refer to Figure 2.10.2-33 for cask component identification.

Table 2.10.4-90 Critical $P_m + P_b$ Stress Summary; 1-Foot Top Corner Drop; Drop Orientation = 24 Degrees; 3-D Top Model; Condition 1

Condition 1: 100°F Ambient with Contents

Comp. No.[1]	Section Cut Node-Node	$P_m + P_b$ Stresses (ksi) S_x	S_y	S_z	S_{xy}	S_{yz}	S_{xz}	Principal Stresses (ksi) S1	S2	S3	S.I.	Allow. Stress	Margin of Safety
1	1952- 93	-0.3	-0.6	0.2	0.0	0.0	0.0	0.2	-0.3	-0.6	0.9	28.7	30.9
2	13924-13324	0.0	0.6	-0.1	0.0	-1.9	0.1	2.2	0.0	-1.7	3.9	27.7	6.1
3	11821-11221	-0.1	1.8	-7.7	0.0	3.1	0.2	2.7	-0.1	-8.6	11.3	47.1	3.2
4	13874-13274	0.0	2.1	-3.3	0.0	3.3	0.0	3.7	0.0	-4.8	8.5	29.4	2.5
5	12625-12025	0.0	0.9	-3.4	0.0	1.1	0.1	1.1	0.0	-3.7	4.9	30.0	5.1
6	401- 1	-1.7	-13.9	-2.1	0.8	0.0	-0.1	-1.6	-2.2	-13.9	12.3	30.0	1.4
7	50150-63451	-29.1	-14.5	-8.2	0.3	0.0	-0.4	-8.2	-14.4	-29.1	20.9	30.0	0.4
8	50071-50074	-25.5	-20.0	-1.5	0.0	0.0	0.0	-1.5	-20.0	-25.5	23.9	67.5	1.8

Locations of the most critical sections for each component are provided in the following:

Comp. No.[1]	Section Location Inside Node x (in)	y (deg)	z (in)	Outside Node x (in)	y (deg)	z (in)
1	0.00	0.0	6.20	0.00	0.0	0.75
2	35.50	56.5	17.40	37.50	56.5	17.40
3	35.50	45.9	171.65	37.00	45.9	171.65
4	35.50	56.5	142.40	37.00	56.5	142.40
5	40.70	56.5	163.40	43.35	56.5	163.40
6	40.88	0.0	193.71	43.35	0.0	193.71
7	25.00	8.3	188.40	25.00	8.3	187.40
8	9.00	0.0	193.71	9.00	0.0	188.46

[1] Refer to Figure 2.10.2-33 for cask component identification.

Table 2.10.4-91 Critical S_n Stress Summary; 1-Foot Top Corner Drop; Drop Orientation = 24 Degrees; 3-D Top Model; Condition 1

Condition 1: 100°F Ambient with Contents

Comp. No.[1]	Section Cut Node-Node	S_x Stresses (ksi) S_x	S_y	S_z	S_{xy}	S_{yz}	S_{xz}	Principal Stresses (ksi) S1	S2	S3	S.I.	Allow. Stress 3.0 S_m
1	683- 85	-1.5	1.1	3.2	-0.1	0.1	0.6	3.3	1.1	-1.6	4.9	57.6
2	16680- 16080	-2.6	1.7	7.1	-0.1	-0.2	1.2	7.3	1.6	-2.7	10.0	55.5
3	1841- 1241	-0.1	2.1	-9.2	-0.2	0.3	-0.2	2.1	-0.1	-9.2	11.3	94.2
4	13874- 13274	0.0	1.8	-5.0	0.0	3.0	0.0	3.0	0.0	-6.1	9.1	58.8
5	664- 64	-0.2	7.9	7.3	-0.6	0.0	0.0	8.0	7.2	-0.2	8.2	60.0
6	401- 1	-2.1	-22.4	-1.4	1.4	0.0	0.2	-1.4	-2.0	-22.4	21.0	60.0
7	50050- 63151	-26.9	-0.9	3.9	-0.9	-0.2	-0.5	3.9	-0.9	-27.0	30.8	60.0
8	50071- 50074	-26.8	-21.4	-1.6	0.0	0.0	0.0	-1.6	-21.4	-26.8	25.2	135.0

Locations of the most critical sections for each component are provided in the following:

Comp. No.[1]	Section Location Inside Node x (in)	y (deg)	z (in)	Outside Node x (in)	y (deg)	z (in)
1	39.44	0.0	6.20	39.44	0.0	0.75
2	40.70	79.4	14.40	43.35	79.4	14.40
3	35.50	0.0	159.90	37.00	0.0	159.90
4	35.50	56.5	142.40	37.00	56.5	142.40
5	40.70	0.0	93.56	43.35	0.0	93.56
6	40.88	0.0	193.71	43.35	0.0	193.71
7	25.00	0.0	188.40	25.00	0.0	187.40
8	9.00	0.0	193.71	9.00	0.0	188.46

[1] Refer to Figure 2.10.2-33 for cask component identification.

Table 2.10.4-92 P_m Stresses; 1-Foot Top Corner Drop; Drop Orientation = 24 Degrees; 3-D Top Model; 45.9-Degree Circumferential Location; Condition 1

Condition 1: 100°F Ambient with Contents

Section[1]	Node - Node	Stress Components (ksi)						Principal Stresses (ksi)			
		S_x	S_y	S_z	S_{xy}	S_{yz}	S_{xz}	S1	S2	S3	S.I.
A	1949 - 1951	0.1	0.3	0.0	0.0	0.0	0.0	0.3	0.1	-0.1	0.4
B	1952 - 93	-0.2	-0.3	0.0	0.0	0.0	0.0	0.1	-0.2	-0.3	0.4
C	11925 - 11927	0.0	0.1	0.1	-0.1	-0.2	0.0	0.3	0.1	-0.2	0.5
D	10683 - 10085	0.0	-0.3	-0.1	0.0	0.0	0.0	0.0	-0.1	-0.3	0.3
E	10682 - 10082	0.1	0.0	0.0	0.0	0.0	0.0	0.1	0.0	0.0	0.1
F	11925 - 11325	-0.2	0.0	-0.4	0.0	-0.7	0.1	0.5	-0.2	-0.9	1.4
G	10680 - 10080	-0.2	0.1	0.1	0.2	0.2	0.0	0.4	0.0	-0.2	0.6
H	11921 - 11321	0.0	1.7	-0.5	0.0	-1.5	0.0	2.5	0.0	-1.3	3.8
I	10676 - 10076	0.0	0.1	-0.1	0.0	0.3	0.0	0.3	0.0	-0.3	0.6
J	11916 - 11316	0.0	1.9	-0.5	0.0	-0.5	0.0	2.0	0.0	-0.5	2.6
K	10671 - 10071	0.0	0.1	-0.5	0.0	0.4	0.0	0.3	0.0	-0.7	1.0
L	11908 - 11308	0.0	2.0	-1.4	-0.1	1.1	0.0	2.3	0.0	-1.7	4.0
M	10663 - 10063	0.0	0.1	-1.3	0.0	0.6	0.0	0.3	0.0	-1.5	1.8
N	11877 - 11277	0.0	2.0	-3.5	0.0	2.6	0.0	3.0	0.0	-4.5	7.5
O	10647 - 10047	0.0	0.1	-2.3	0.0	0.8	0.0	0.3	0.0	-2.6	2.9
P	11840 - 11240	-0.1	1.8	-5.2	0.1	3.2	-0.1	3.0	-0.1	-6.4	9.5
Q	10628 - 10028	0.0	0.8	-3.1	0.0	0.9	0.0	1.0	0.0	-3.3	4.3
R	11816 - 11216	0.4	1.1	-5.6	0.5	2.2	0.4	2.0	0.2	-6.2	8.2
S	10616 - 10016	-2.2	0.8	-3.4	-0.3	0.9	0.0	1.0	-2.2	-3.6	4.6
T	10811 - 10011	0.6	-0.8	-2.3	0.6	1.3	0.1	0.9	-0.3	-3.0	4.0
U	44558 - 44551	0.2	-0.4	-5.2	-0.1	-0.1	1.8	0.8	-0.4	-5.7	6.5
V	50524 - 50521	-2.1	-1.9	-2.3	0.2	0.0	-0.4	-1.6	-2.0	-2.6	1.0
W	43278 - 43271	0.3	-0.3	-0.1	0.0	-0.4	0.1	0.3	0.2	-0.6	0.9
X	50084 - 50081	-0.1	-1.8	0.7	0.0	0.0	-3.2	3.5	-1.8	-2.9	6.4

[1] Refer to Figure 2.10.2-34 for the identification of the representative sections.

Table 2.10.4-93 $P_m + P_b$ Stresses; 1-Foot Top Corner Drop; Drop Orientation = 24 Degrees; 3-D Top Model; 45.9-Degree Circumferential Location; Condition 1

Condition 1: 100°F Ambient with Contents

Section[1]	Node - Node	Stress Components (ksi)						Principal Stresses (ksi)			
		S_x	S_y	S_z	S_{xy}	S_{yz}	S_{xz}	S1	S2	S3	S.I.
A I	1949 - 1951	0.3	0.7	-0.1	0.0	0.0	0.1	0.7	0.3	-0.1	0.8
B O	1952 - 93	-0.3	-0.6	0.2	0.0	0.0	0.0	0.2	-0.3	-0.6	0.9
C I	11925 - 11927	0.0	0.2	0.2	-0.1	-0.5	0.0	0.7	0.0	-0.3	1.1
D O	10683 - 10085	0.0	-0.4	-0.1	0.1	0.0	0.0	0.0	-0.1	-0.4	0.4
E I	10682 - 10082	0.1	-0.1	-0.2	0.0	0.0	0.0	0.1	-0.1	-0.2	0.3
F O	11925 - 11325	-0.4	-0.3	-1.3	0.1	-0.6	0.1	0.0	-0.4	-1.6	1.6
G O	10680 - 10080	-0.1	0.3	0.4	0.1	0.2	0.0	0.6	0.1	-0.1	0.7
H I	11921 - 11321	0.0	1.4	-1.0	0.0	-1.9	0.0	2.4	0.0	-2.0	4.4
I O	10676 - 10076	0.0	0.1	-0.1	0.0	0.3	0.0	0.3	0.0	-0.4	0.7
J O	11916 - 11316	0.0	2.3	-0.3	0.0	-0.4	0.0	2.3	0.0	-0.3	2.7
K I	10671 - 10071	0.0	0.2	-0.5	0.0	0.3	0.0	0.3	0.0	-0.6	1.0
L I	11908 - 11308	0.0	1.9	-1.4	-0.1	1.1	0.0	2.3	0.0	-1.7	4.0
M I	10663 - 10063	0.1	0.4	-1.2	0.0	0.6	0.0	0.5	0.1	-1.4	1.9
N I	11877 - 11277	0.0	2.2	-3.4	0.0	2.7	0.0	3.3	0.0	-4.5	7.9
O I	10647 - 10047	0.0	0.3	-2.2	0.0	0.8	0.0	0.6	0.0	-2.5	3.1
P O	11840 - 11240	-0.2	1.1	-7.0	0.2	3.1	-0.3	2.2	-0.2	-8.1	10.3
Q O	10628 - 10028	0.0	0.5	-3.8	0.0	0.8	0.0	0.6	0.0	-4.0	4.6
R I	11816 - 11216	-0.4	-0.4	-10.5	0.0	2.6	-0.1	0.2	-0.4	-11.1	11.3
S I	10616 - 10016	-4.2	-1.5	-10.3	-0.7	1.3	0.7	-1.2	-4.2	-10.6	9.4
T I	10811 - 10011	1.1	-0.4	-1.4	1.4	2.3	0.5	2.7	-0.1	-3.3	6.0
U I	44558 - 44551	1.4	2.9	-5.6	-1.1	0.0	2.1	3.6	1.3	-6.2	9.8
V I	50524 - 50521	-5.2	0.7	-3.1	-1.1	0.0	-0.8	0.9	-2.9	-5.6	6.6
W I	43278 - 43271	0.3	-0.7	-0.1	-0.1	-0.3	0.1	0.3	0.0	-0.8	1.2
X O	50084 - 50081	-12.8	-13.5	5.9	0.4	-0.2	-3.2	6.5	-13.0	-13.8	20.2

[1] Refer to Figure 2.10.2-34 for the identification of the representative sections.

Table 2.10.4-94 P_m Stresses; 1-Foot Top Corner Drop; Drop Orientation = 24 Degrees; 3-D Top Model; 91.7-Degree Circumferential Location; Condition 1

Condition 1: 100°F Ambient with Contents

Section[1]	Node - Node	Stress Components (ksi)						Principal Stresses (ksi)			
		S_x	S_y	S_z	S_{xy}	S_{yz}	S_{xz}	S1	S2	S3	S.I.
A	1949 - 1951	0.1	0.3	0.0	0.0	0.0	0.0	0.3	0.1	-0.1	0.4
B	1952 - 93	-0.2	-0.3	0.0	0.0	0.0	0.0	0.1	-0.2	-0.3	0.4
C	19925 - 19927	0.0	0.2	-0.1	0.0	-0.2	0.0	0.3	0.0	-0.2	0.6
D	18683 - 18085	0.0	-0.3	-0.1	-0.1	-0.1	-0.1	0.0	0.0	-0.4	0.4
E	18682 - 18082	0.1	0.0	-0.2	0.1	-0.1	-0.1	0.2	0.0	-0.3	0.5
F	19925 - 19325	0.1	0.7	0.3	0.1	-0.6	-0.1	1.1	0.1	-0.1	1.2
G	18680 - 18080	-0.1	0.2	-0.5	0.1	0.1	-0.1	0.3	-0.1	-0.6	0.8
H	19921 - 19321	0.0	0.6	-0.2	0.1	-0.9	0.0	1.2	0.0	-0.8	2.1
I	18676 - 18076	0.0	0.1	-0.8	0.0	0.3	0.0	0.2	0.0	-0.9	1.0
J	19916 - 19316	0.0	0.8	-1.4	0.0	-0.1	0.0	0.8	0.0	-1.4	2.2
K	18671 - 18071	0.0	0.0	-0.9	0.0	0.5	0.0	0.2	0.0	-1.1	1.3
L	19908 - 19308	0.1	0.9	-1.9	0.2	1.4	0.0	1.4	0.1	-2.5	3.9
M	18663 - 18063	0.0	0.0	-1.1	0.0	0.8	0.0	0.4	0.0	-1.6	1.9
N	19877 - 19277	-0.1	0.9	-1.3	0.0	2.9	0.0	2.9	-0.1	-3.3	6.2
O	18647 - 18047	0.0	0.0	-1.3	0.0	1.1	0.0	0.6	0.0	-2.0	2.6
P	19840 - 19240	-0.3	0.6	-0.4	0.2	3.6	0.0	3.8	-0.3	-3.6	7.3
Q	18628 - 18028	0.0	0.2	-1.3	0.0	1.4	0.0	1.0	0.0	-2.2	3.2
R	19816 - 19216	0.1	1.9	-0.4	0.6	2.9	0.7	4.1	-0.1	-2.4	6.5
S	18616 - 18016	-1.4	0.8	-1.2	-0.6	1.6	-0.2	1.8	-1.5	-2.1	3.9
T	18811 - 18011	0.7	1.0	-0.5	0.8	2.1	0.2	2.8	0.4	-2.0	4.8
U	45758 - 45751	-0.1	-0.8	-2.9	-0.2	0.2	0.5	0.0	-0.8	-3.0	3.0
V	50924 - 50921	-0.4	-0.9	0.0	-0.2	0.1	-0.4	0.3	-0.6	-1.0	1.3
W	43278 - 43271	0.3	-0.3	-0.1	0.0	-0.4	0.1	0.3	0.2	-0.6	0.9
X	50084 - 50081	-0.1	-1.8	0.7	0.0	0.0	-3.2	3.5	-1.8	-2.9	6.4

[1] Refer to Figure 2.10.2-34 for the identification of the representative sections.

Table 2.10.4-95 $P_m + P_b$ Stresses; 1-Foot Top Corner Drop; Drop Orientation = 24 Degrees; 3-D Top Model; 91.7-Degree Circumferential Location; Condition 1

Condition 1: 100°F Ambient with Contents

		Stress Components (ksi)						Principal Stresses (ksi)			
Section[1]	Node - Node	S_x	S_y	S_z	S_{xy}	S_{yz}	S_{xz}	S1	S2	S3	S.I.
A I	1949 - 1951	0.3	0.7	-0.1	0.0	0.0	0.1	0.7	0.3	-0.1	0.8
B O	1952 - 93	-0.3	-0.6	0.2	0.0	0.0	0.0	0.2	-0.3	-0.6	0.9
C I	19925 - 19927	0.0	0.5	-0.3	0.0	-0.4	0.0	0.7	0.0	-0.5	1.1
D O	18683 - 18085	0.1	-0.4	-0.1	0.0	-0.1	0.0	0.1	-0.1	-0.4	0.6
E O	18682 - 18082	0.1	0.0	-0.3	0.1	-0.1	-0.1	0.2	-0.1	-0.4	0.6
F O	19925 - 19325	0.2	0.9	1.2	0.2	-0.6	-0.1	1.7	0.4	0.1	1.6
G I	18680 - 18080	-0.1	0.1	-0.9	0.2	0.1	-0.2	0.3	-0.1	-1.0	1.3
H O	19921 - 19321	0.0	0.3	-0.4	0.1	-1.0	0.0	1.0	0.0	-1.1	2.2
I I	18676 - 18076	0.0	0.2	-0.6	0.0	0.3	0.0	0.3	0.0	-0.8	1.1
J I	19916 - 19316	0.0	1.6	-1.1	0.0	-0.1	0.0	1.6	0.0	-1.1	2.6
K I	18671 - 18071	0.0	0.1	-0.9	0.0	0.5	0.0	0.4	0.0	-1.1	1.4
L I	19908 - 19308	0.1	2.0	-1.6	0.1	1.4	0.0	2.4	0.1	-2.0	4.5
M I	18663 - 18063	0.0	0.1	-1.1	0.0	0.8	0.0	0.5	0.0	-1.5	2.0
N I	19877 - 19277	-0.1	1.5	-1.1	0.0	2.9	0.0	3.3	-0.1	-3.0	6.3
O I	18647 - 18047	0.0	0.0	-1.3	0.0	1.1	0.0	0.6	0.0	-2.0	2.6
P O	19840 - 19240	-0.6	0.1	-1.5	0.3	3.9	-0.1	3.3	-0.6	-4.7	8.0
Q O	18628 - 18028	0.0	0.1	-1.8	0.0	1.5	0.0	0.9	0.0	-2.6	3.6
R I	19816 - 19216	-0.1	0.9	-4.1	-0.1	3.3	-0.1	2.6	-0.1	-5.7	8.3
S I	18616 - 18016	-2.7	-0.2	-3.7	-1.2	2.1	-0.1	1.1	-2.9	-4.8	5.9
T I	18811 - 18011	1.6	1.9	2.0	2.0	3.3	0.8	6.1	1.0	-1.6	7.7
U I	45758 - 45751	-1.3	-0.7	-4.6	-1.5	0.1	1.1	0.6	-2.2	-5.0	5.6
V I	50924 - 50921	-2.2	-0.6	-0.3	-1.8	0.1	-0.4	0.7	-0.4	-3.4	4.1
W I	43278 - 43271	0.3	-0.7	-0.1	-0.1	-0.3	0.1	0.3	0.0	-0.8	1.2
X O	50084 - 50081	-12.8	-13.5	5.9	0.4	-0.2	-3.2	6.5	-13.0	-13.8	20.2

[1] Refer to Figure 2.10.2-34 for the identification of the representative sections.

Table 2.10.4-96 P_m Stresses; 1-Foot Top Corner Drop; Drop Orientation = 24 Degrees; 3-D Top Model; 180-Degree Circumferential Location; Condition 1

Condition 1: 100°F Ambient with Contents

Section[1]	Node - Node	Stress Components (ksi) S_x	S_y	S_z	S_{xy}	S_{yz}	S_{xz}	Principal Stresses (ksi) S1	S2	S3	S.I.
A	1949 - 95	0.1	0.3	0.0	0.0	0.0	0.0	0.3	0.1	-0.1	0.4
B	1952 - 93	-0.2	-0.3	0.0	0.0	0.0	0.0	0.1	-0.2	-0.3	0.4
C	31925 - 31927	0.0	0.1	-0.1	0.0	0.0	-0.1	0.1	0.1	-0.2	0.2
D	30683 - 30085	0.0	0.0	-0.3	0.0	0.0	0.0	0.1	0.0	-0.3	0.3
E	30682 - 30082	0.3	0.1	-0.3	0.0	0.0	0.0	0.3	0.1	-0.3	0.6
F	31925 - 31325	-0.3	0.0	-0.3	0.0	0.0	0.0	0.0	-0.3	-0.3	0.3
G	30680 - 30080	0.0	-0.1	-0.6	0.0	0.1	0.0	0.0	-0.1	-0.7	0.6
H	31921 - 31321	0.0	0.0	-0.8	0.0	0.0	0.0	0.0	0.0	-0.8	0.8
I	30676 - 30076	0.0	-0.1	-0.7	0.0	0.1	0.0	0.0	-0.1	-0.7	0.7
J	31916 - 31316	-0.1	0.1	-0.7	0.0	0.1	0.0	0.1	-0.1	-0.8	0.9
K	30671 - 30071	0.0	-0.1	-0.6	0.0	0.1	0.0	0.0	-0.1	-0.6	0.6
L	31908 - 31308	-0.1	0.3	-0.1	-0.1	0.2	0.0	0.3	-0.1	-0.2	0.5
M	30663 - 30063	0.0	-0.1	-0.4	0.0	0.1	0.0	0.0	-0.1	-0.4	0.4
N	31877 - 31277	-0.1	0.2	1.1	0.0	0.2	0.0	1.1	0.1	-0.1	1.2
O	30647 - 30047	0.0	-0.1	0.0	0.0	0.1	0.0	0.1	0.0	-0.2	0.3
P	31840 - 31240	-0.4	-0.4	2.0	0.0	0.3	0.0	2.0	-0.4	-0.5	2.5
Q	30628 - 30028	0.0	-0.3	0.3	0.0	0.1	0.0	0.3	0.0	-0.3	0.7
R	31816 - 31216	-0.4	2.5	1.3	0.5	0.1	0.9	2.6	1.6	-0.9	3.5
S	30616 - 30016	-0.8	1.7	0.1	0.3	0.1	-0.2	1.8	0.2	-0.9	2.7
T	30811 - 30011	0.1	3.4	-0.2	0.5	0.1	0.2	3.5	0.1	-0.3	3.7
U	47558 - 47551	-1.2	-1.4	-2.6	-0.1	0.0	-0.1	-1.1	-1.4	-2.6	1.5
V	51524 - 51521	-1.5	-1.2	-0.2	0.0	0.0	-0.2	-0.1	-1.2	-1.6	1.4
W	43278 - 43271	0.3	-0.3	-0.1	0.0	-0.4	0.1	0.3	0.2	-0.6	0.9
X	50084 - 50081	-0.1	-1.8	0.7	0.0	0.0	-3.2	3.5	-1.8	-2.9	6.4

[1] Refer to Figure 2.10.2-34 for the identification of the representative sections.

Table 2.10.4-97 $P_m + P_b$ Stresses; 1-Foot Top Corner Drop; Drop Orientation = 24 Degrees; 3-D Top Model; 180-Degree Circumferential Location; Condition 1

Condition 1: 100°F Ambient with Contents

		Stress Components (ksi)						Principal Stresses (ksi)			
Section[1]	Node - Node	S_x	S_y	S_z	S_{xy}	S_{yz}	S_{xz}	S1	S2	S3	S.I.
A I	1949 - 1951	0.3	0.7	-0.1	0.0	0.0	0.1	0.7	0.3	-0.1	0.8
B O	1952 - 93	-0.3	-0.6	0.2	0.0	0.0	0.0	0.2	-0.3	-0.6	0.9
C O	31925 - 31927	0.3	0.1	0.0	0.0	0.0	-0.1	0.3	0.1	-0.1	0.4
D O	30683 - 30085	0.4	0.1	-0.3	0.0	0.0	0.0	0.4	0.1	-0.3	0.7
E O	30682 - 30082	0.3	0.1	-0.4	0.0	0.1	0.0	0.3	0.1	-0.4	0.7
F O	31925 - 31325	-0.3	0.0	-0.3	0.0	0.0	0.0	0.0	-0.3	-0.4	0.3
G O	30680 - 30080	0.0	-0.2	-1.0	0.0	0.1	0.0	0.0	-0.2	-1.0	1.0
H O	31921 - 31321	0.0	0.0	-0.9	0.0	0.0	0.0	0.0	0.0	-0.9	0.9
I O	30676 - 30076	0.0	-0.1	-0.7	0.0	0.0	0.0	0.0	-0.1	-0.7	0.7
J O	31916 - 31316	-0.1	0.2	-0.7	0.0	0.1	0.0	0.3	-0.1	-0.7	1.0
K I	30671 - 30071	0.0	-0.2	-0.6	0.0	0.1	0.0	0.0	-0.2	-0.6	0.6
L O	31908 - 31308	-0.1	0.5	0.0	-0.2	0.2	0.0	0.6	0.0	-0.2	0.8
M I	30663 - 30063	0.0	-0.1	-0.4	0.0	0.1	0.0	0.0	-0.1	-0.4	0.4
N O	31877 - 31277	-0.1	0.1	1.1	0.0	0.2	0.0	1.1	0.1	-0.1	1.2
O O	30647 - 30047	0.0	-0.2	0.0	0.0	0.1	0.0	0.1	0.0	-0.2	0.3
P I	31840 - 31240	0.0	0.1	3.3	0.0	0.3	0.0	3.3	0.1	0.0	3.3
Q I	30628 - 30028	0.0	-0.1	0.9	0.0	0.2	0.0	0.9	0.0	-0.1	1.0
R O	31816 - 31216	-0.9	2.5	2.2	0.6	-0.1	1.5	2.9	2.5	-1.6	4.5
S I	30616 - 30016	-1.6	1.7	0.5	0.4	0.2	-0.6	1.7	0.7	-1.8	3.5
T O	30811 - 30011	-0.2	2.7	-1.9	0.4	0.1	-0.3	2.7	-0.2	-2.0	4.7
U O	47558 - 47551	2.0	0.5	-0.5	-0.1	0.2	-1.1	2.4	0.5	-0.9	3.3
V I	51524 - 51521	-5.2	-2.4	-0.6	0.1	0.0	-0.2	-0.6	-2.4	-5.2	4.6
W I	43278 - 43271	0.3	-0.7	-0.1	-0.1	-0.3	0.1	0.3	0.0	-0.8	1.2
X O	50084 - 50081	-12.8	-13.5	5.9	0.4	-0.2	-3.2	6.5	-13.0	-13.8	20.2

[1] Refer to Figure 2.10.2-34 for the identification of the representative sections.

Table 2.10.4-98 Primary Stresses; 1-Foot Bottom Corner Drop; Drop Orientation = 24 Degrees; 3-D Bottom Model; 0-Degree Circumferential Location; Condition 1

Condition 1: 100°F Ambient with Contents

Stress Points		Stress Components (ksi)						Principal Stresses (ksi)		
Section[1]	Node	S_x	S_y	S_z	S_{xy}	S_{yz}	S_{xz}	S1	S2	S3
A1	1130	6.1	4.5	-2.3	-0.2	0.8	0.7	6.1	4.6	-2.4
A2	1129	0.9	0.0	-0.5	0.0	0.6	0.7	1.2	0.2	-1.1
A3	1128	-4.3	-4.5	1.3	0.2	0.8	0.7	1.5	-4.4	-4.6
B1	1185	3.4	1.1	-2.3	-0.2	0.9	0.8	3.5	1.3	-2.6
B2	1184	-1.3	-2.8	-0.7	0.0	0.6	0.8	-0.1	-1.8	-3.0
B3	1183	-6.1	-6.6	0.9	0.1	0.7	0.8	1.0	-6.2	-6.7
C1	90	-6.2	-1.6	-7.1	-0.4	-0.3	-1.5	-1.6	-5.1	-8.2
C2	80	-3.1	-0.5	-4.3	-0.3	-0.2	-1.1	-0.5	-2.4	-5.0
C3	70	-2.0	-0.4	-2.8	-0.2	-0.1	-0.9	-0.3	-1.4	-3.4
C4	60	-1.1	-0.3	-1.6	0.0	-0.1	-0.8	-0.3	-0.5	-2.2
C5	50	2.2	-1.0	-0.5	0.3	-0.1	-0.6	2.3	-0.7	-1.0
C6	40	5.3	-1.0	-0.1	0.5	0.0	-0.4	5.4	-0.1	-1.0
D1	25	-12.0	-9.1	-15.0	-0.1	-0.2	-3.2	-9.1	-9.9	-17.1
D2	15	-2.0	-6.9	-6.4	0.2	-0.1	-1.6	-1.5	-6.9	-6.9
D3	5	0.7	-8.5	-3.0	0.6	0.0	-0.5	0.8	-3.1	-8.6
E1	35	2.5	-4.0	-11.8	0.5	-0.1	-1.1	2.6	-4.0	-11.8
E2	34	-0.3	-3.4	-7.7	0.2	-0.3	-2.9	0.7	-3.4	-8.7
E3	33	-2.5	-3.0	-4.0	0.0	-0.3	-3.2	0.0	-3.0	-6.5
E4	32	-2.7	-2.3	-1.1	0.0	-0.2	-2.0	0.2	-2.3	-4.0
E5	31	-2.8	-1.6	2.0	-0.1	-0.1	-1.2	2.3	-1.6	-3.1
F1	100	-0.1	-0.4	-9.1	-0.1	-0.3	-0.9	0.0	-0.4	-9.2
F2	99	-1.0	0.2	-6.1	-0.1	-0.3	-0.4	0.2	-1.0	-6.1
F3	98	-1.0	0.3	-5.3	-0.1	-0.2	0.6	0.4	-0.9	-5.4
F4	97	0.0	0.5	-5.8	-0.1	-0.1	0.9	0.5	0.1	-6.0
G1	94	0.1	-0.8	-7.7	0.0	-0.1	-0.3	0.1	-0.8	-7.7
G2	93	-0.2	-0.2	-5.2	0.0	-0.1	-0.2	-0.2	-0.2	-5.2
G3	92	-0.3	0.3	-3.1	0.0	-0.1	0.0	0.3	-0.3	-3.1
G4	91	-0.2	1.0	-0.7	-0.1	0.0	0.0	1.0	-0.2	-0.7

Table 2.10.4-98 Primary Stresses; 1-Foot Bottom Corner Drop; Drop Orientation = 24 Degrees; 3-D Bottom Model; 0-Degree Circumferential Location; Condition 1 (continued)

Stress Points		Stress Components (ksi)						Principal Stresses (ksi)		
Section[1]	Node	S_x	S_y	S_z	S_{xy}	S_{yz}	S_{xz}	S1	S2	S3
H1	330	-0.1	2.2	-5.0	-0.2	-0.4	0.0	2.2	-0.1	-5.0
H2	329	-0.2	2.1	-5.8	-0.2	-0.3	0.0	2.1	-0.2	-5.8
H3	328	-0.2	2.1	-6.6	-0.1	-0.3	0.2	2.1	-0.2	-6.6
H4	327	-0.2	1.8	-8.3	-0.1	-0.3	0.4	1.8	-0.1	-8.3
I1	244	0.0	0.1	-3.6	0.0	-0.1	0.0	0.1	0.0	-3.6
I2	243	0.0	0.4	-3.6	0.0	-0.1	0.0	0.4	0.0	-3.6
I3	242	0.0	0.6	-3.6	0.0	-0.1	0.0	0.6	0.0	-3.6
I4	241	0.0	0.8	-3.6	-0.1	0.0	0.0	0.8	0.0	-3.6
J1	550	-0.1	2.1	-3.4	-0.2	-0.3	0.0	2.1	-0.1	-3.5
J2	548	0.0	2.5	-3.3	-0.2	-0.3	0.0	2.6	-0.1	-3.3
J3	547	0.0	3.0	-3.1	-0.2	-0.2	0.0	3.0	0.0	-3.1
K1	344	0.0	-0.7	-3.0	0.0	-0.1	0.0	0.0	-0.7	-3.0
K2	342	0.0	0.2	-2.6	0.0	-0.1	0.0	0.2	0.0	-2.6
K3	341	0.0	1.0	-2.3	-0.1	-0.1	0.0	1.0	0.0	-2.3
L1	740	0.0	2.1	-0.4	-0.1	-0.1	0.0	2.1	0.0	-0.4
L2	738	-0.1	2.5	-0.1	-0.3	-0.1	0.0	2.6	-0.1	-0.1
L3	737	0.0	3.0	0.1	-0.5	-0.1	0.0	3.1	0.1	0.0
M1	454	0.0	-0.6	-1.7	-0.3	0.0	0.0	0.1	-0.7	-1.7
M2	452	0.1	0.2	-1.4	-0.1	-0.1	0.0	0.3	0.0	-1.4
M3	451	-0.1	0.8	-1.2	0.0	-0.1	0.0	0.8	-0.1	-1.2
N1	810	0.0	2.4	0.0	-0.2	0.1	0.0	2.4	0.0	-0.1
N2	807	-0.1	2.7	0.3	-0.2	0.1	0.0	2.7	0.3	-0.1
O1	524	0.0	-0.2	-0.5	0.0	0.0	0.0	0.0	-0.2	-0.5
O2	521	0.0	0.4	-0.2	0.0	-0.1	0.0	0.4	0.0	-0.2
P1	850	0.0	2.1	-1.5	-0.1	0.2	0.0	2.2	0.0	-1.5
P2	847	0.0	2.6	-0.2	-0.2	0.2	0.0	2.6	0.0	-0.2
Q1	564	0.0	0.1	0.1	0.0	0.0	0.0	0.2	0.0	0.0
Q2	561	0.0	0.3	0.2	0.0	0.0	0.0	0.3	0.2	0.0
R1	890	-0.5	0.0	1.1	0.0	0.1	-0.1	1.1	0.0	-0.5
R2	887	-0.6	-0.8	-2.3	0.0	0.1	-0.2	-0.6	-0.8	-2.3

Table 2.10.4-98 Primary Stresses; 1-Foot Bottom Corner Drop; Drop Orientation = 24 Degrees; 3-D Bottom Model; 0-Degree Circumferential Location; Condition 1 (continued)

Stress Points		Stress Components (ksi)						Principal Stresses (ksi)		
Section[1]	Node	S_x	S_y	S_z	S_{xy}	S_{yz}	S_{xz}	S1	S2	S3
S1	604	-0.3	0.1	0.1	0.0	0.0	-0.2	0.2	0.1	-0.4
S2	601	0.0	0.4	0.7	0.0	0.0	-0.1	0.7	0.4	0.0
T1	897	0.3	-0.1	-0.7	0.0	0.0	-0.1	0.3	-0.1	-0.7
T2	614	0.2	0.1	0.1	0.0	0.0	-0.2	0.3	0.1	-0.1
T3	611	0.0	0.1	0.3	0.0	0.0	-0.1	0.3	0.1	0.0
U1	900	0.3	0.1	-0.1	0.0	0.0	0.1	0.3	0.1	-0.1
U2	910	0.1	-0.1	-0.2	0.0	0.0	0.0	0.1	-0.1	-0.2
V1	920	0.0	-0.1	-0.1	0.0	0.0	0.0	0.0	-0.1	-0.1
V2	930	-0.2	-0.3	0.0	0.1	0.0	0.0	0.0	-0.2	-0.3
W1	1216	0.3	0.7	-0.3	0.0	0.0	0.0	0.7	0.3	-0.3
W2	1226	-0.1	0.0	0.1	0.0	0.0	0.0	0.1	0.0	-0.1
X1	1236	0.0	0.0	-0.2	0.0	0.0	0.0	0.0	0.0	-0.2
X2	1246	-0.4	-0.7	0.3	0.0	0.0	0.0	0.3	-0.4	-0.7

[1] Refer to Figure 2.10.2-34 for the identification of the representative sections.

Table 2.10.4-99 Primary + Secondary Stresses; 1-Foot Bottom Corner Drop; Drop Orientation = 24 Degrees; 3-D Bottom Model; 0-Degree Circumferential Location; Condition 1

Condition 1: 100°F Ambient with Contents

Stress Points		Stress Components (ksi)						Principal Stresses (ksi)		
Section[1]	Node	S_x	S_y	S_z	S_{xy}	S_{yz}	S_{xz}	S1	S2	S3
A1	1130	6.2	4.8	-1.2	-0.2	0.7	1.0	6.4	4.9	-1.4
A2	1129	0.2	-0.7	-0.5	0.0	0.5	1.1	1.0	-0.5	-1.4
A3	1128	-5.9	-6.2	0.3	0.2	0.6	1.0	0.5	-6.0	-6.2
B1	1185	5.3	3.0	-1.3	-0.2	0.8	1.1	5.5	3.1	-1.6
B2	1184	-0.1	-1.5	-0.7	0.0	0.6	1.1	0.8	-1.1	-2.0
B3	1183	-5.5	-5.9	-0.1	0.1	0.6	1.1	0.2	-5.7	-6.0
C1	90	-7.7	-2.7	-9.0	-0.4	-0.3	-2.0	-2.6	-6.3	-10.5
C2	80	-4.2	-1.4	-5.5	-0.4	-0.2	-1.8	-1.3	-2.9	-6.8
C3	70	-2.9	-1.3	-3.9	-0.2	-0.2	-1.7	-1.3	-1.6	-5.2
C4	60	-1.7	-1.3	-2.6	0.0	-0.1	-1.5	-0.5	-1.3	-3.7
C5	50	1.8	-2.4	-1.9	0.4	-0.1	-1.0	2.1	-2.1	-2.4
C6	40	5.1	-2.7	-1.9	0.6	0.0	-0.6	5.2	-2.0	-2.8
D1	25	-7.8	-6.8	-11.4	0.0	-0.2	-1.9	-6.8	-7.0	-12.2
D2	15	-1.8	-6.0	-5.0	0.2	-0.1	-1.1	-1.4	-5.3	-6.0
D3	5	-0.7	-8.2	-2.7	0.5	0.0	-0.5	-0.5	-2.8	-8.2
E1	35	0.4	-4.6	-10.7	0.4	-0.1	0.0	0.4	-4.7	-10.7
E2	34	-1.7	-3.6	-5.9	0.1	-0.2	-1.3	-1.3	-3.6	-6.3
E3	33	-2.9	-3.0	-2.8	0.0	-0.2	-1.6	-1.2	-3.0	-4.5
E4	32	-2.8	-2.3	-0.3	0.0	-0.1	-1.0	0.0	-2.3	-3.2
E5	31	-2.8	-1.6	2.3	-0.1	-0.1	-0.6	2.4	-1.6	-2.9
F1	100	-0.1	-0.8	-11.7	0.0	-0.3	-1.1	0.0	-0.8	-11.8
F2	99	-1.1	-0.1	-7.6	-0.1	-0.3	-0.5	0.0	-1.0	-7.6
F3	98	-0.7	0.2	-6.4	-0.1	-0.2	0.3	0.2	-0.7	-6.4
F4	97	0.6	1.3	-2.5	-0.1	-0.2	0.5	1.3	0.6	-2.6
G1	94	1.0	2.1	4.2	-0.1	0.0	1.0	4.5	2.1	0.7
G2	93	0.6	0.8	-0.5	-0.1	-0.1	0.5	0.9	0.7	-0.7
G3	92	0.0	1.3	1.7	-0.1	-0.1	0.0	1.7	1.3	0.0
G4	91	-0.1	1.7	3.4	-0.1	-0.1	-0.1	3.4	1.7	-0.1

Table 2.10.4-99 Primary + Secondary Stresses; 1-Foot Bottom Corner Drop; Drop Orientation = 24 Degrees; 3-D Bottom Model; 0-Degree Circumferential Location; Condition 1 (continued)

Stress Points		Stress Components (ksi)						Principal Stresses (ksi)		
Section[1]	Node	S_x	S_y	S_z	S_{xy}	S_{yz}	S_{xz}	S1	S2	S3
H1	330	-0.1	1.8	-4.8	-0.1	-0.4	0.0	1.8	-0.1	-4.8
H2	329	-0.2	1.7	-6.4	-0.1	-0.3	0.1	1.7	-0.2	-6.4
H3	328	-0.2	1.7	-7.8	-0.1	-0.3	0.3	1.7	-0.2	-7.8
H4	327	-0.4	1.3	-10.4	-0.1	-0.3	0.6	1.3	-0.3	-10.5
I1	244	0.0	3.3	2.2	-0.2	-0.1	0.0	3.3	2.2	-0.1
I2	243	0.0	3.5	2.2	-0.3	-0.1	-0.1	3.5	2.2	0.0
I3	242	0.0	3.8	2.3	-0.3	-0.1	-0.1	3.9	2.3	0.0
I4	241	0.0	4.1	2.4	-0.3	-0.1	0.0	4.1	2.4	0.0
J1	550	-0.1	0.5	-6.4	0.0	-0.3	0.0	0.5	-0.1	-6.4
J2	548	0.0	2.6	-4.2	-0.2	-0.2	0.0	2.6	0.0	-4.2
J3	547	0.0	4.5	-2.0	-0.3	-0.2	0.0	4.6	0.0	-2.0
K1	344	-0.3	4.1	1.0	-0.3	-0.1	0.0	4.1	1.0	-0.3
K2	342	-0.2	5.7	3.3	-0.4	-0.1	0.0	5.7	3.3	-0.2
K3	341	-0.1	7.2	5.6	-0.5	-0.1	0.0	7.2	5.6	-0.1
L1	740	0.4	0.5	-2.6	0.2	-0.1	-0.1	0.7	0.3	-2.6
L2	738	-0.6	2.3	-1.2	-0.4	-0.1	0.1	2.4	-0.7	-1.2
L3	737	0.3	4.7	0.7	-1.0	-0.1	0.0	4.9	0.7	0.1
M1	454	-0.7	4.7	2.4	-0.4	0.0	0.0	4.7	2.4	-0.8
M2	452	0.3	6.6	4.7	-0.5	0.0	0.1	6.7	4.7	0.2
M3	451	-0.7	7.8	6.3	-0.6	-0.1	-0.3	7.8	6.3	-0.7
N1	810	0.3	0.6	-2.6	0.0	0.1	0.0	0.6	0.3	-2.6
N2	807	0.3	3.8	0.9	-0.3	0.1	0.0	3.8	0.9	0.3
O1	524	-0.1	3.9	4.0	-0.3	-0.1	0.0	4.0	3.9	-0.2
O2	521	-0.1	6.3	7.4	-0.5	0.0	0.0	7.4	6.3	-0.2
P1	850	0.2	1.9	-1.7	-0.1	0.1	0.0	1.9	0.2	-1.7
P2	847	-0.3	2.7	-1.7	-0.2	0.1	0.0	2.7	-0.4	-1.7
Q1	564	0.0	3.4	5.7	-0.2	0.0	0.1	5.7	3.4	0.0
Q2	561	-0.1	4.3	6.4	-0.3	0.0	0.0	6.4	4.4	-0.1
R1	890	-0.4	-4.2	-4.3	0.2	0.1	0.3	-0.4	-4.2	-4.4
R2	887	0.1	-1.7	-2.2	0.1	0.1	0.2	0.1	-1.7	-2.2

Table 2.10.4-99 Primary + Secondary Stresses; 1-Foot Bottom Corner Drop; Drop Orientation = 24 Degrees; 3-D Bottom Model; 0-Degree Circumferential Location; Condition 1 (continued)

Stress Points		Stress Components (ksi)						Principal Stresses (ksi)		
Section[1]	Node	S_x	S_y	S_z	S_{xy}	S_{yz}	S_{xz}	S1	S2	S3
S1	604	0.1	0.5	1.5	0.0	-0.1	-0.5	1.7	0.5	-0.1
S2	601	0.2	3.3	7.3	-0.3	0.1	-0.7	7.3	3.3	0.1
T1	897	-1.0	-1.7	-1.1	0.1	0.0	-0.3	-0.8	-1.3	-1.7
T2	614	-0.4	-0.8	0.3	0.1	-0.1	-1.2	1.2	-0.8	-1.3
T3	611	0.9	-0.3	2.5	0.1	-0.1	-1.1	3.1	0.3	-0.3
U1	900	-1.0	-1.0	-1.3	0.0	0.1	1.2	0.1	-1.0	-2.4
U2	910	0.8	-0.3	3.7	0.1	0.0	0.6	3.8	0.7	-0.3
V1	920	6.3	5.3	4.6	0.0	0.0	-0.9	6.7	5.3	4.2
V2	930	-5.8	-2.6	0.5	-0.1	0.0	-1.7	0.9	-2.6	-6.2
W1	1216	1.9	2.4	-1.7	0.0	0.1	-0.6	2.4	2.0	-1.8
W2	1226	-2.5	-2.4	1.0	0.0	0.0	-0.3	1.0	-2.4	-2.5
X1	1236	1.8	1.8	-1.1	0.0	0.1	-0.4	1.9	1.8	-1.1
X2	1246	-0.1	-0.5	2.4	0.0	0.2	-0.8	2.7	-0.4	-0.5

[1] Refer to Figure 2.10.2-34 for the identification of the representative sections.

Table 2.10.4-100 P_m Stresses; 1-Foot Bottom Corner Drop; Drop Orientation = 24 Degrees; 3-D Bottom Model; 0-Degree Circumferential Location; Condition 1

Condition 1: 100°F Ambient with Contents

		Stress Components (ksi)						Principal Stresses (ksi)			
Section[1]	Node - Node	S_x	S_y	S_z	S_{xy}	S_{yz}	S_{xz}	S1	S2	S3	S.I.
A	1130 - 1128	0.9	0.0	-0.5	0.0	0.7	0.7	1.2	0.3	-1.2	2.4
B	1185 - 1183	-1.4	-2.8	-0.7	0.0	0.7	0.8	-0.1	-1.8	-3.0	3.0
C	90 - 40	-0.1	-0.7	-2.0	0.0	-0.1	-0.8	0.2	-0.7	-2.3	2.5
D	25 - 5	-3.8	-7.8	-7.7	0.2	-0.1	-1.7	-3.2	-7.9	-8.4	5.2
E	35 - 31	-1.2	-3.0	-4.9	0.1	-0.2	-2.3	-0.1	-3.0	-6.0	5.9
F	100 - 97	-0.7	0.2	-6.3	-0.1	-0.2	0.1	0.2	-0.7	-6.3	6.5
G	94 - 91	-0.2	0.1	-4.2	0.0	-0.1	-0.1	0.1	-0.2	-4.2	4.3
H	330 - 327	-0.2	2.0	-6.3	-0.1	-0.3	0.1	2.1	-0.2	-6.3	8.4
I	244 - 241	0.0	0.5	-3.6	0.0	-0.1	0.0	0.5	0.0	-3.6	4.1
J	550 - 547	0.0	2.5	-3.3	-0.2	-0.3	0.0	2.6	-0.1	-3.3	5.8
K	344 - 341	0.0	0.2	-2.6	0.0	-0.1	0.0	0.2	0.0	-2.6	2.8
L	740 - 737	0.0	2.5	-0.1	-0.3	-0.1	0.0	2.6	-0.1	-0.1	2.7
M	454 - 451	0.0	0.1	-1.4	-0.1	-0.1	0.0	0.2	-0.1	-1.4	1.6
N	810 - 807	-0.1	2.6	0.1	-0.2	0.1	0.0	2.6	0.1	-0.1	2.6
O	524 - 521	0.0	0.1	-0.3	0.0	0.0	0.0	0.1	0.0	-0.3	0.5
P	850 - 847	0.0	2.4	-0.8	-0.2	0.2	0.0	2.4	0.0	-0.8	3.2
Q	564 - 561	0.0	0.2	0.2	0.0	0.0	0.0	0.2	0.1	0.0	0.2
R	890 - 887	-0.6	-0.4	-0.6	0.0	0.1	-0.1	-0.4	-0.5	-0.7	0.4
S	604 - 601	-0.2	0.2	0.4	0.0	0.0	-0.1	0.4	0.2	-0.2	0.6
T	614 - 611	0.1	0.1	0.2	0.0	0.0	-0.1	0.3	0.1	0.0	0.3
U	900 - 910	0.2	0.0	-0.1	0.0	0.0	0.0	0.2	0.0	-0.1	0.4
V	920 - 930	-0.1	-0.2	-0.1	0.0	0.0	0.0	-0.1	-0.1	-0.2	0.1
W	1216 - 1226	0.1	0.3	-0.1	0.0	0.0	0.0	0.3	0.1	-0.1	0.4
X	1236 - 1246	-0.2	-0.3	0.1	0.0	0.0	0.0	0.1	-0.2	-0.3	0.4

[1] Refer to Figure 2.10.2-34 for the identification of the representative sections.

Table 2.10.4-101 $P_m + P_b$ Stresses; 1-Foot Bottom Corner Drop; Drop Orientation = 24 Degrees; 3-D Bottom Model; 0-Degree Circumferential Location; Condition 1

Condition 1: 100°F Ambient with Contents

		Stress Components (ksi)						Principal Stresses (ksi)			
Section[1]	Node - Node	S_x	S_y	S_z	S_{xy}	S_{yz}	S_{xz}	S1	S2	S3	S.I.
A I	1130 - 1128	6.1	4.5	-2.3	-0.2	0.7	0.7	6.1	4.6	-2.4	8.5
B O	1185 - 1183	-6.1	-6.7	0.9	0.1	0.6	0.8	1.0	-6.2	-6.7	7.7
C O	90 - 40	4.6	-0.9	0.8	0.5	0.0	-0.4	4.7	0.8	-0.9	5.6
D O	25 - 5	2.5	-7.6	-1.7	0.6	0.0	-0.3	2.5	-1.7	-7.6	10.1
E I	35 - 31	1.7	-4.1	-11.9	0.4	-0.3	-2.4	2.1	-4.1	-12.4	14.5
F I	100 - 97	-0.7	-0.2	-7.8	-0.1	-0.4	-1.0	-0.2	-0.6	-8.0	7.8
G I	94 - 91	0.0	-0.8	-7.6	0.0	-0.1	-0.3	0.0	-0.8	-7.6	7.6
H O	330 - 327	-0.2	1.9	-7.8	-0.1	-0.3	0.4	1.9	-0.2	-7.9	9.8
I O	244 - 241	0.0	0.8	-3.6	-0.1	0.0	0.0	0.8	0.0	-3.6	4.4
J O	550 - 547	0.0	3.0	-3.1	-0.2	-0.2	0.0	3.0	0.0	-3.1	6.1
K O	344 - 341	0.0	1.0	-2.3	-0.1	-0.1	0.0	1.1	0.0	-2.3	3.4
L O	740 - 737	0.0	3.0	0.1	-0.5	-0.1	0.0	3.0	0.1	-0.1	3.1
M O	454 - 451	0.0	0.8	-1.2	0.0	-0.1	0.0	0.9	0.0	-1.2	2.0
N O	810 - 807	-0.1	2.7	0.3	-0.2	0.1	0.0	2.7	0.3	-0.1	2.8
O O	524 - 521	0.0	0.4	-0.2	0.0	-0.1	0.0	0.4	0.0	-0.2	0.6
P I	850 - 847	0.0	2.1	-1.5	-0.1	0.2	0.0	2.2	0.0	-1.5	3.7
Q O	564 - 561	0.0	0.3	0.2	0.0	0.0	0.0	0.3	0.2	0.0	0.3
R O	890 - 887	-0.6	-0.8	-2.3	0.0	0.1	-0.2	-0.6	-0.8	-2.3	1.7
S O	604 - 601	0.0	0.4	0.7	0.0	0.0	-0.1	0.7	0.4	0.0	0.7
T O	614 - 611	0.0	0.1	0.3	0.0	0.0	-0.1	0.3	0.1	0.0	0.4
U I	900 - 910	0.3	0.1	-0.1	0.0	0.0	0.1	0.3	0.1	-0.1	0.4
V O	920 - 930	-0.2	-0.3	0.0	0.1	0.0	0.0	0.0	-0.2	-0.3	0.3
W I	1216 - 1226	0.3	0.7	-0.3	0.0	0.0	0.0	0.7	0.3	-0.3	0.9
X O	1236 - 1246	-0.4	-0.7	0.3	0.0	0.0	0.0	0.3	-0.4	-0.7	0.9

[1] Refer to Figure 2.10.2-34 for the identification of the representative sections.

Table 2.10.4-102 S_n Stresses; 1-Foot Bottom Corner Drop; Drop Orientation = 24 Degrees; 3-D Bottom Model; 0-Degree Circumferential Location; Condition 1

Condition 1: 100°F Ambient with Contents

Section[1]	Node - Node	Stress Components (ksi) S_x	S_y	S_z	S_{xy}	S_{yz}	S_{xz}	Principal Stresses (ksi) S1	S2	S3	S.I.
A I	1130 - 1128	6.2	4.8	-1.2	-0.2	0.6	1.0	6.4	4.9	-1.4	7.8
B I	1185 - 1183	5.3	3.0	-1.3	-0.2	0.8	1.1	5.5	3.1	-1.6	7.1
C O	90 - 40	4.6	-2.4	-0.5	0.6	0.0	-0.6	4.7	-0.6	-2.5	7.2
D O	25 - 5	0.6	-7.4	-1.6	0.5	0.0	-0.4	0.7	-1.7	-7.4	8.1
E I	35 - 31	-0.4	-4.6	-10.3	0.3	-0.1	-0.8	-0.3	-4.6	-10.4	10.0
F I	100 - 97	-0.9	-0.8	-11.0	-0.1	-0.3	-1.0	-0.7	-0.8	-11.1	10.4
G O	94 - 91	-0.3	1.3	2.1	-0.1	-0.1	-0.3	2.1	1.3	-0.3	2.4
H O	330 - 327	-0.3	1.5	-9.9	-0.1	-0.3	0.5	1.5	-0.3	-9.9	11.4
I O	244 - 241	0.0	4.1	2.4	-0.3	-0.1	-0.1	4.1	2.4	0.0	4.1
J I	550 - 547	-0.1	0.5	-6.4	0.0	-0.3	0.0	0.5	-0.1	-6.4	6.9
K O	344 - 341	-0.1	7.2	5.6	-0.5	-0.1	0.0	7.3	5.6	-0.1	7.4
L O	740 - 737	-0.2	4.5	0.5	-1.0	0.0	0.1	4.7	0.5	-0.4	5.1
M O	454 - 451	-0.2	8.0	6.5	-0.6	-0.1	-0.1	8.0	6.5	-0.2	8.2
N O	810 - 807	0.3	3.8	0.9	-0.3	0.1	0.0	3.8	0.9	0.3	3.6
O O	524 - 521	-0.1	6.3	7.4	-0.5	0.0	0.0	7.4	6.3	-0.2	7.6
P O	850 - 847	-0.3	2.7	-1.7	-0.2	0.1	0.0	2.7	-0.4	-1.7	4.4
Q O	564 - 561	-0.1	4.3	6.4	-0.3	0.0	0.0	6.4	4.4	-0.1	6.4
R I	890 - 887	-0.4	-4.2	-4.3	0.2	0.1	0.3	-0.4	-4.2	-4.4	4.0
S O	604 - 601	0.2	3.3	7.3	-0.3	0.1	-0.7	7.3	3.3	0.1	7.2
T O	614 - 611	0.9	-0.3	2.5	0.1	-0.1	-1.1	3.1	0.3	-0.3	3.4
U O	900 - 910	0.8	-0.3	3.7	0.1	0.0	0.6	3.8	0.7	-0.3	4.1
V O	920 - 930	-5.8	-2.6	0.5	-0.1	0.0	-1.7	0.9	-2.6	-6.2	7.1
W I	1216 - 1226	1.9	2.4	-1.7	0.0	0.1	-0.6	2.4	2.0	-1.8	4.2
X O	1236 - 1246	-0.1	-0.5	2.4	0.0	0.2	-0.8	2.7	-0.4	-0.5	3.1

[1] Refer to Figure 2.10.2-34 for the identification of the representative sections.

Table 2.10.4-103 Critical P_m Stress Summary; 1-Foot Bottom Corner Drop; Drop Orientation = 24 Degrees; 3-D Bottom Model; Condition 1

Condition 1: 100°F Ambient with Contents

Comp. No.[1]	Section Cut Node-Node	P_m Stresses (ksi) S_x	S_y	S_z	S_{xy}	S_{yz}	S_{xz}	Principal Stresses (ksi) S1	S2	S3	S.I.	Allow. Stress	Margin of Safety
1	14025-14005	-1.5	-4.9	-6.9	-0.7	-1.1	-1.4	-1.1	-4.4	-7.8	6.7	19.2	1.9
2	12140-12137	0.0	1.8	-3.8	0.0	-3.3	-0.1	3.3	0.0	-5.3	8.6	18.5	1.2
3	12340-12337	-0.1	1.5	-4.0	0.1	-3.8	0.1	3.4	-0.1	-6.0	9.4	31.4	2.3
4	12520-12517	0.0	1.8	-3.0	0.0	-3.1	0.0	3.3	0.0	-4.5	7.8	19.6	1.5
5	12204-12201	0.0	0.6	-3.5	0.0	-1.3	0.0	1.0	0.0	-3.9	4.9	20.0	3.1
6	12880-12877	0.0	0.6	-0.3	0.0	1.5	-0.1	1.8	0.0	-1.4	3.2	20.0	5.3
7	897-907	0.2	-0.1	-0.4	0.0	0.0	-0.1	0.2	-0.1	-0.4	0.6	20.0	32.3
8	31234-31244	-0.4	-0.2	0.0	0.0	0.0	0.0	0.0	-0.2	-0.4	0.4	45.0	111.5

Locations of the most critical sections for each component are provided in the following:

Comp. No.[1]	Section Location Inside Node x (in)	y (deg)	z (in)	Outside Node x (in)	y (deg)	z (in)
1	39.44	67.7	6.20	39.44	67.7	0.75
2	35.50	56.5	17.40	37.45	56.5	17.40
3	35.50	56.5	29.90	37.00	56.5	29.90
4	35.50	56.5	47.40	37.00	56.5	47.40
5	40.70	56.5	26.40	43.35	56.5	26.40
6	35.50	56.5	172.40	37.50	56.5	175.40
7	37.50	0.0	179.40	37.00	0.0	185.40
8	10.00	180.0	187.40	10.00	180.0	193.71

[1] Refer to Figure 2.10.2-33 for cask component identification.

Table 2.10.4-104 Critical $P_m + P_b$ Stress Summary; 1-Foot Bottom Corner Drop; Drop Orientation = 24 Degrees; 3-D Bottom Model; Condition 1

Condition 1: 100°F Ambient with Contents

Comp. No.[1]	Section Cut Node-Node	$P_m + P_b$ Stresses (ksi) S_x	S_y	S_z	S_{xy}	S_{yz}	S_{xz}	Principal Stresses (ksi) S1	S2	S3	S.I.	Allow. Stress	Margin of Safety
1	1167- 1165	-16.2	-12.3	-1.7	0.0	0.0	-0.1	-1.7	-12.3	-16.2	14.5	28.7	1.0
2	12035-12031	1.9	-2.8	-11.9	1.6	-2.4	-2.1	2.9	-3.0	-12.7	15.6	27.7	0.8
3	12150-12147	-0.1	1.5	-5.5	0.0	-3.6	-0.1	3.0	-0.1	-7.1	10.1	47.1	3.7
4	12520-12517	0.0	1.9	-3.0	0.0	-3.3	0.0	3.5	0.0	-4.7	8.2	29.4	2.6
5	10204-10201	0.0	0.9	-3.6	0.0	-1.2	-0.1	1.2	0.0	-3.9	5.0	30.0	5.0
6	12880-12877	0.0	0.7	-0.1	0.0	1.9	-0.1	2.3	0.0	-1.6	3.9	30.0	6.7
7	897- 907	0.3	-0.1	-0.7	0.0	0.0	-0.1	0.3	-0.1	-0.7	1.0	30.0	29.0
8	1236- 1246	-0.4	-0.7	0.3	0.0	0.0	0.0	0.3	-0.4	-0.7	0.9	67.5	74.0

Locations of the most critical sections for each component are provided in the following:

Comp. No.[1]	Section Location Inside Node x (in)	y (deg)	z (in)	Outside Node x (in)	y (deg)	z (in)
1	17.67	0.0	6.20	17.67	0.0	0.75
2	39.44	56.5	8.20	43.35	56.5	8.20
3	35.50	56.5	18.15	37.50	56.5	18.15
4	35.50	56.5	47.40	37.00	56.5	47.40
5	40.70	45.9	26.40	43.35	45.9	26.40
6	35.50	56.5	172.40	37.50	56.5	172.40
7	37.50	0.0	179.40	37.00	0.0	185.40
8	0.0	0.0	187.40	0.0	0.0	193.71

[1] Refer to Figure 2.10.2-33 for cask component identification.

Table 2.10.4-105 Critical S_n Stress Summary; 1-Foot Bottom Corner Drop; Drop Orientation = 24 Degrees; 3-D Bottom Model; Condition 1

Condition 1: 100°F Ambient with Contents

Comp. No.[1]	Section Cut Node-Node	S_x Stresses (ksi) S_x	S_y	S_z	S_{xy}	S_{yz}	S_{xz}	Principal Stresses (ksi) S1	S2	S3	S.I.	Allow. Stress 3.0 S_m
1	1170- 1168	-14.9	-10.8	-1.7	0.0	0.0	0.0	-1.7	-10.8	-14.9	13.2	57.6
2	12100- 12097	-0.5	-0.2	-11.4	-0.2	-3.6	-0.8	0.9	-0.4	-12.5	13.4	55.5
3	10150- 10147	-0.1	3.0	-7.7	0.0	-3.0	-0.4	3.7	-0.1	-8.5	12.2	94.2
4	10520- 10517	0.2	1.5	-5.8	0.0	-2.8	0.0	2.4	0.2	-6.7	9.1	58.8
5	424- 421	-0.1	8.2	6.6	-0.6	-0.1	0.0	8.2	6.6	-0.1	8.3	60.0
6	14644- 14641	-1.9	-9.9	-1.2	0.1	0.0	1.3	-0.2	-2.9	-9.9	9.7	60.0
7	1211- 1221	6.4	4.1	0.0	0.1	0.0	0.1	6.4	4.1	0.0	6.3	60.0
8	920- 930	-5.8	-2.6	0.5	-0.1	0.0	-1.7	0.9	-2.6	-6.2	7.1	135.0

Locations of the most critical sections for each component are provided in the following:

Comp. No.[1]	Section Location Inside Node x (in)	y (deg)	z (in)	Outside Node x (in)	y (deg)	z (in)
1	14.72	0.0	6.20	14.72	0.0	0.75
2	35.50	56.5	15.00	37.50	56.5	15.00
3	35.50	45.9	18.15	37.50	45.9	18.15
4	35.50	45.9	47.40	37.00	45.9	47.40
5	40.70	0.0	85.50	43.35	0.0	85.50
6	40.70	67.7	193.71	43.35	67.7	193.71
7	25.00	0.0	179.40	25.00	0.0	185.40
8	35.50	0.0	187.40	35.50	0.0	193.71

[1] Refer to Figure 2.10.2-33 for cask component identification.

Table 2.10.4-106 P_m Stresses; 1-Foot Bottom Corner Drop; Drop Orientation = 24 Degrees; 3-D Bottom Model; 45.9-Degree Circumferential Location; Condition 1

Condition 1: 100°F Ambient with Contents

		Stress Components (ksi)						Principal Stresses (ksi)			
Section[1]	Node - Node	S_x	S_y	S_z	S_{xy}	S_{yz}	S_{xz}	S1	S2	S3	S.I.
A	1130 - 1128	0.9	0.0	-0.5	0.0	0.7	0.7	1.2	0.3	-1.2	2.4
B	1185 - 1183	-1.4	-2.8	-0.7	0.0	0.7	0.8	-0.1	-1.8	-3.0	3.0
C	10090 - 10040	0.4	-0.1	-1.8	0.1	-0.7	-0.6	0.7	0.0	-2.2	2.9
D	10025 - 10005	-2.7	-6.7	-7.6	-0.4	-0.6	-1.6	-2.2	-6.5	-8.3	6.1
E	10035 - 10031	-0.5	-1.8	-4.7	0.5	-0.9	-2.1	0.6	-2.0	-5.7	6.3
F	10100 - 10097	-0.5	0.9	-5.0	-0.1	-2.7	-0.1	2.0	-0.5	-6.0	8.0
G	10094 - 10091	-0.3	0.5	-4.3	-0.1	-1.0	-0.3	0.7	-0.2	-4.5	5.3
H	10330 - 10327	-0.1	1.7	-4.9	0.1	-3.3	0.1	3.1	-0.1	-6.2	9.3
I	10244 - 10241	0.0	0.5	-3.6	0.0	-1.0	0.0	0.7	0.0	-3.9	4.6
J	10550 - 10547	0.0	2.0	-2.9	0.0	-2.4	0.0	3.0	0.0	-3.9	6.9
K	10344 - 10341	0.0	0.1	-2.7	0.0	-0.9	0.0	0.4	0.0	-3.0	3.4
L	10740 - 10737	0.0	2.0	-1.0	0.0	-0.9	0.0	2.2	0.0	-1.3	3.4
M	10454 - 10451	0.0	0.1	-1.5	0.0	-0.7	0.0	0.4	0.0	-1.7	2.1
N	10810 - 10807	0.0	1.9	-0.4	0.0	0.7	0.0	2.1	0.0	-0.6	2.7
O	10524 - 10521	0.0	0.1	-0.6	0.0	-0.5	0.0	0.3	0.0	-0.9	1.2
P	10850 - 10847	0.0	1.7	-0.5	0.0	1.6	0.0	2.5	0.0	-1.3	3.9
Q	10564 - 10561	0.0	0.2	-0.2	0.0	-0.4	0.0	0.4	0.0	-0.5	0.9
R	10890 - 10887	-0.3	0.2	-0.3	0.4	0.9	-0.1	0.9	-0.3	-1.1	1.9
S	10604 - 10601	-0.1	0.3	0.1	0.2	-0.2	0.0	0.5	-0.1	-0.2	0.7
T	10614 - 10611	0.1	0.2	0.0	0.0	-0.1	-0.1	0.2	0.1	-0.1	0.3
U	10900 - 10910	0.1	0.1	-0.1	-0.1	0.2	0.0	0.2	0.1	-0.2	0.5
V	10920 - 10930	0.0	-0.3	-0.1	0.0	0.0	0.0	0.0	-0.1	-0.3	0.3
W	1216 - 1226	0.1	0.3	-0.1	0.0	0.0	0.0	0.3	0.1	-0.1	0.4
X	1236 - 1246	-0.2	-0.3	0.1	0.0	0.0	0.0	0.1	-0.2	-0.3	0.4

[1] Refer to Figure 2.10.2-34 for the identification of the representative sections.

Table 2.10.4-107 P_m Stresses; 1-Foot Bottom Corner Drop; Drop Orientation = 24 Degrees; 3-D Bottom Model; 45.9-Degree Circumferential Location; Condition 1

Condition 1: 100°F Ambient with Contents

Section[1]	Node - Node	Stress Components (ksi) S_x	S_y	S_z	S_{xy}	S_{yz}	S_{xz}	Principal Stresses (ksi) S1	S2	S3	S.I.
A I	1130 - 1128	6.1	4.5	-2.3	-0.2	0.7	0.7	6.1	4.6	-2.4	8.5
B O	1185 - 1183	-6.1	-6.7	0.9	0.1	0.6	0.8	1.0	-6.2	-6.7	7.7
C I	10090 - 10040	-4.5	-0.1	-4.5	-1.7	-1.6	-1.0	0.8	-3.5	-6.3	7.1
D O	10025 - 10005	3.1	-6.6	-1.6	0.8	0.1	-0.4	3.2	-1.6	-6.7	9.8
E I	10035 - 10031	1.8	-3.3	-12.1	1.3	-1.8	-2.2	2.6	-3.5	-12.7	15.3
F I	10100 - 10097	-0.5	0.2	-7.8	-0.2	-3.4	-0.9	1.4	-0.5	-9.2	10.6
G I	10094 - 10091	-0.2	-0.4	-8.1	-0.2	-1.6	-0.6	0.0	-0.2	-8.4	8.4
H O	10330 - 10327	-0.2	1.2	-6.4	0.2	-3.2	0.3	2.4	-0.1	-7.6	10.0
I I	10244 - 10241	0.0	0.8	-3.2	0.0	-1.1	0.0	1.1	0.0	-3.5	4.6
J I	10550 - 10547	0.0	2.0	-2.9	0.0	-2.6	0.0	3.1	0.0	-4.0	7.1
K I	10344 - 10341	0.0	0.6	-2.5	0.0	-1.0	0.0	0.8	0.0	-2.8	3.6
L O	10740 - 10737	0.0	2.1	-1.0	0.1	-0.8	0.0	2.3	0.0	-1.2	3.5
M I	10454 - 10451	0.0	0.4	-1.4	0.0	-0.7	0.0	0.6	0.0	-1.7	2.3
N O	10810 - 10807	0.0	2.3	-0.2	0.0	0.6	0.0	2.4	0.0	-0.3	2.8
O O	10524 - 10521	0.0	0.0	-0.6	0.0	-0.5	0.0	0.3	0.0	-0.9	1.2
P I	10850 - 10847	0.0	1.4	-1.0	0.0	1.9	0.0	2.4	0.0	-2.0	4.5
Q O	10564 - 10561	0.0	0.1	-0.3	0.0	-0.5	0.0	0.4	0.0	-0.6	1.0
R I	10890 - 10887	-0.3	0.4	0.5	0.3	1.0	-0.1	1.5	-0.1	-0.8	2.3
S O	10604 - 10601	-0.1	0.5	0.5	0.1	-0.3	0.0	0.7	0.2	-0.1	0.8
T I	10614 - 10611	0.1	0.2	-0.1	0.0	-0.1	-0.1	0.2	0.1	-0.1	0.4
U I	10900 - 10910	0.1	0.2	-0.1	-0.2	0.3	0.0	0.5	0.1	-0.3	0.8
V O	10920 - 10930	0.0	-0.4	-0.1	0.1	0.0	0.0	0.0	-0.1	-0.5	0.5
W I	1216 - 1226	0.3	0.7	-0.3	0.0	0.0	0.0	0.7	0.3	-0.3	0.9
X O	1236 - 1246	-0.4	-0.7	0.3	0.0	0.0	0.0	0.3	-0.4	-0.7	0.9

[1] Refer to Figure 2.10.2-34 for the identification of the representative sections.

Table 2.10.4-108 P_m Stresses; 1-Foot Bottom Corner Drop; Drop Orientation = 24 Degrees; 3-D Bottom Model; 91.7-Degree Circumferential Location; Condition 1

Condition 1: 100°F Ambient with Contents

		Stress Components (ksi)						Principal Stresses (ksi)			
Section[1]	Node - Node	S_x	S_y	S_z	S_{xy}	S_{yz}	S_{xz}	S1	S2	S3	S.I.
A	1130 - 1128	0.9	0.0	-0.5	0.0	0.7	0.7	1.2	0.3	-1.2	2.4
B	1185 - 1183	-1.4	-2.8	-0.7	0.0	0.7	0.8	-0.1	-1.8	-3.0	3.0
C	18090 - 18040	1.0	0.7	-0.3	0.0	-0.9	0.1	1.2	1.0	-0.8	2.0
D	18025 - 18005	-0.7	-1.7	-2.7	-1.1	-1.2	-0.2	0.1	-1.4	-3.7	3.8
E	18035 - 18031	1.0	0.3	-0.8	0.5	-2.1	-1.4	2.9	0.3	-2.6	5.5
F	18100 - 18097	0.0	1.1	0.5	-0.2	-3.5	-0.3	4.2	0.1	-2.7	7.0
G	18094 - 18091	-0.1	0.4	-1.0	-0.2	-2.0	-0.1	1.8	-0.1	-2.4	4.2
H	18330 - 18327	-0.5	0.3	-0.4	0.2	-3.7	0.0	3.7	-0.5	-3.7	7.4
I	18244 - 18241	0.0	0.0	-1.3	0.0	-1.5	0.0	1.1	0.0	-2.3	3.3
J	18550 - 18547	-0.1	0.9	-1.4	0.0	-2.7	0.0	2.6	-0.1	-3.2	5.8
K	18344 - 18341	0.0	0.0	-1.4	0.0	-1.3	0.0	0.7	0.0	-2.1	2.9
L	18740 - 18737	-0.1	1.0	-1.9	0.0	-1.1	0.0	1.4	-0.1	-2.3	3.7
M	18454 - 18451	0.0	0.0	-1.2	0.0	-0.9	0.0	0.5	0.0	-1.7	2.2
N	18810 - 18807	0.0	0.8	-1.2	0.0	0.3	0.0	0.9	0.0	-1.3	2.1
O	18524 - 18521	0.0	0.0	-1.1	0.0	-0.6	0.0	0.3	0.0	-1.3	1.6
P	18850 - 18847	0.0	0.6	-0.2	0.1	1.0	0.0	1.3	0.0	-0.9	2.3
Q	18564 - 18561	0.0	0.1	-0.9	0.0	-0.5	0.0	0.2	0.0	-1.1	1.4
R	18890 - 18887	0.2	0.9	0.2	0.3	0.7	0.1	1.4	0.1	-0.3	1.7
S	18604 - 18601	-0.1	0.3	-0.6	0.2	-0.1	0.1	0.4	-0.1	-0.7	1.1
T	18614 - 18611	0.0	0.1	-0.4	0.0	0.0	0.1	0.2	0.0	-0.4	0.6
U	18900 - 18910	0.0	0.2	0.0	0.0	0.2	0.0	0.3	0.0	-0.2	0.5
V	18920 - 18930	-0.1	-0.3	-0.1	-0.1	0.1	0.1	0.0	-0.1	-0.3	0.3
W	1216 - 1226	0.1	0.3	-0.1	0.0	0.0	0.0	0.3	0.1	-0.1	0.4
X	1236 - 1246	-0.2	-0.3	0.1	0.0	0.0	0.0	0.1	-0.2	-0.3	0.4

[1] Refer to Figure 2.10.2-34 for the identification of the representative sections.

Table 2.10.4-109 $P_m + P_b$ Stresses; 1-Foot Bottom Corner Drop; Drop Orientation = 24 Degrees; 3-D Bottom Model; 91.7-Degree Circumferential Location; Condition 1

Condition 1: 100°F Ambient with Contents

Section[1]	Node - Node	Stress Components (ksi) S_x	S_y	S_z	S_{xy}	S_{yz}	S_{xz}	Principal Stresses (ksi) S1	S2	S3	S.I.
A I	1130 - 1128	6.1	4.5	-2.3	-0.2	0.7	0.7	6.1	4.6	-2.4	8.5
B O	1185 - 1183	-6.1	-6.7	0.9	0.1	0.6	0.8	1.0	-6.2	-6.7	7.7
C I	18090 - 18040	-2.3	-0.1	-1.0	-2.0	-2.0	0.1	2.1	-1.6	-3.8	5.9
D I	18025 - 18005	-5.2	-2.9	-5.3	-3.3	-2.6	-1.0	0.0	-4.3	-9.1	9.1
E I	18035 - 18031	2.6	-0.2	-4.3	1.6	-3.2	-1.7	4.4	-0.2	-6.2	10.6
F I	18100 - 18097	0.0	0.3	-2.6	-0.2	-4.0	-0.2	3.1	0.0	-5.5	8.6
G I	18094 - 18091	0.0	0.1	-2.1	-0.3	-2.4	-0.2	1.7	0.0	-3.7	5.4
H O	18330 - 18327	-1.0	-0.5	-1.8	0.3	-3.9	0.0	2.8	-1.0	-5.1	7.9
I O	18244 - 18241	0.0	0.1	-1.4	0.0	-1.6	0.0	1.2	0.0	-2.4	3.6
J I	18550 - 18547	-0.1	1.6	-1.2	0.0	-2.7	0.0	3.2	-0.1	-2.8	6.0
K I	18344 - 18341	0.0	-0.1	-1.4	0.0	-1.3	0.0	0.7	0.0	-2.2	2.9
L I	18740 - 18737	0.0	1.8	-1.6	0.1	-1.1	0.0	2.2	0.0	-1.9	4.1
M I	18454 - 18451	0.0	0.1	-1.2	0.0	-1.0	0.0	0.6	0.0	-1.7	2.4
N I	18810 - 18807	0.0	1.5	-0.9	0.0	0.3	0.0	1.5	0.0	-1.0	2.5
O I	18524 - 18521	0.0	0.1	-1.0	0.0	-0.7	0.0	0.4	0.0	-1.3	1.7
P O	18850 - 18847	0.0	0.3	-0.4	0.1	1.1	0.0	1.1	0.0	-1.2	2.3
Q I	18564 - 18561	0.0	0.2	-0.8	0.0	-0.5	0.0	0.4	0.0	-1.0	1.4
R I	18890 - 18887	0.1	0.7	-0.8	0.3	0.8	0.0	1.1	0.1	-1.1	2.2
S I	18604 - 18601	0.0	0.3	-1.0	0.2	-0.2	0.1	0.4	-0.1	-1.0	1.4
T I	18614 - 18611	0.0	0.2	-0.4	0.0	0.0	0.1	0.2	0.0	-0.4	0.6
U I	18900 - 18910	-0.2	0.4	0.0	-0.1	0.3	0.0	0.5	-0.2	-0.2	0.7
V O	18920 - 18930	0.1	-0.4	-0.1	0.0	0.1	0.0	0.1	-0.1	-0.5	0.6
W I	1216 - 1226	0.3	0.7	-0.3	0.0	0.0	0.0	0.7	0.3	-0.3	0.9
X O	1236 - 1246	-0.4	-0.7	0.3	0.0	0.0	0.0	0.3	-0.4	-0.7	0.9

[1] Refer to Figure 2.10.2-34 for the identification of the representative sections.

Table 2.10.4-110 P_m Stresses; 1-Foot Bottom Corner Drop; Drop Orientation = 24 Degrees; 3-D Bottom Model; 180-Degree Circumferential Location; Condition 1

Condition 1: 100°F Ambient with Contents

		Stress Components (ksi)						Principal Stresses (ksi)			
Section[1]	Node - Node	S_x	S_y	S_z	S_{xy}	S_{yz}	S_{xz}	S1	S2	S3	S.I.
A	1130 - 1128	0.9	0.0	-0.5	0.0	0.7	0.7	1.2	0.3	-1.2	2.4
B	1185 - 1183	-1.4	-2.8	-0.7	0.0	0.7	0.8	-0.1	-1.8	-3.0	3.0
C	30090 - 30040	0.4	1.0	0.4	0.1	-0.1	0.4	1.0	0.8	0.0	1.0
D	30025 - 30005	-0.6	1.0	-1.0	0.1	-0.1	0.1	1.0	-0.5	-1.1	2.1
E	30035 - 30031	0.6	1.2	0.0	0.1	-0.1	-0.6	1.3	0.9	-0.4	1.7
F	30100 - 30097	0.2	0.6	1.8	0.0	-0.3	-0.1	1.8	0.5	0.1	1.7
G	30094 - 30091	0.1	0.2	0.9	0.0	-0.2	0.0	0.9	0.1	0.1	0.8
H	30330 - 30327	-0.5	-0.6	1.7	0.0	-0.3	0.0	1.7	-0.5	-0.6	2.3
I	30244 - 30241	0.0	-0.3	0.6	0.0	-0.2	0.0	0.6	0.0	-0.3	0.9
J	30550 - 30547	-0.1	0.0	0.7	0.0	-0.2	0.0	0.7	0.0	-0.1	0.9
K	30344 - 30341	0.0	-0.1	0.2	0.0	-0.1	0.0	0.2	0.0	-0.2	0.4
L	30740 - 30737	-0.1	0.2	-0.4	0.1	-0.1	0.0	0.2	-0.1	-0.4	0.6
M	30454 - 30451	0.0	-0.1	-0.3	0.0	-0.1	0.0	0.0	-0.1	-0.3	0.3
N	30810 - 30807	-0.1	0.1	-0.8	0.0	-0.1	0.0	0.1	-0.1	-0.8	0.9
O	30524 - 30521	0.0	-0.1	-0.6	0.0	-0.1	0.0	0.0	-0.1	-0.6	0.6
P	30850 - 30847	0.0	0.0	-0.7	0.0	0.0	0.0	0.0	0.0	-0.7	0.7
Q	30564 - 30561	0.0	-0.1	-0.6	0.0	-0.1	0.0	0.0	-0.1	-0.7	0.7
R	30890 - 30887	0.0	0.0	-0.3	0.0	0.0	0.0	0.1	0.0	-0.3	0.3
S	30604 - 30601	0.0	0.0	-0.5	0.0	0.0	0.0	0.0	0.0	-0.5	0.5
T	30614 - 30611	0.0	0.0	-0.4	0.0	0.0	0.1	0.0	0.0	-0.4	0.4
U	30900 - 30910	0.1	0.1	-0.1	0.0	0.0	0.1	0.2	0.1	-0.1	0.3
V	30920 - 30930	-0.1	0.1	-0.1	0.0	0.0	0.1	0.1	0.0	-0.2	0.3
W	1216 - 1226	0.1	0.3	-0.1	0.0	0.0	0.0	0.3	0.1	-0.1	0.4
X	1236 - 1246	-0.2	-0.3	0.1	0.0	0.0	0.0	0.1	-0.2	-0.3	0.4

[1] Refer to Figure 2.10.2-34 for the identification of the representative sections.

Table 2.10.4-111 $P_m + P_b$ Stresses; 1-Foot Bottom Corner Drop; Drop Orientation = 24 Degrees; 3-D Bottom Model; 180-Degree Circumferential Location; Condition 1

Condition 1: 100°F Ambient with Contents

		Stress Components (ksi)						Principal Stresses (ksi)			
Section[1]	Node - Node	S_x	S_y	S_z	S_{xy}	S_{yz}	S_{xz}	S1	S2	S3	S.I.
A I	1130 - 1128	6.1	4.5	-2.3	-0.2	0.7	0.7	6.1	4.6	-2.4	8.5
B O	1185 - 1183	-6.1	-6.7	0.9	0.1	0.6	0.8	1.0	-6.2	-6.7	7.7
C I	30090 - 30040	-1.8	-0.1	1.0	0.0	-0.2	0.5	1.2	-0.2	-1.9	3.1
D I	30025 - 30005	-3.3	-0.1	-2.0	0.2	-0.1	-0.3	-0.1	-2.0	-3.4	3.3
E I	30035 - 30031	1.5	1.1	-1.4	0.1	-0.1	-0.8	1.7	1.1	-1.6	3.3
F I	30100 - 30097	0.1	0.6	1.9	0.0	-0.4	0.1	2.0	0.5	0.1	2.0
G I	30094 - 30091	0.2	0.6	2.2	0.0	-0.3	0.2	2.3	0.6	0.2	2.1
H I	30330 - 30327	0.0	-0.1	2.8	0.0	-0.3	0.0	2.8	0.0	-0.1	2.9
I O	30244 - 30241	0.0	-0.4	0.5	-0.1	-0.1	0.0	0.5	0.0	-0.4	0.9
J O	30550 - 30547	-0.1	0.0	0.7	0.0	-0.2	0.0	0.8	0.0	-0.1	0.9
K O	30344 - 30341	0.0	-0.2	0.1	0.0	-0.1	0.0	0.2	0.0	-0.3	0.5
L O	30740 - 30737	0.0	0.3	-0.3	0.3	-0.1	0.0	0.5	-0.1	-0.3	0.8
M I	30454 - 30451	0.0	-0.1	-0.3	0.0	-0.1	0.0	0.0	-0.1	-0.3	0.3
N O	30810 - 30807	0.0	0.2	-0.8	0.0	0.0	0.0	0.2	-0.1	-0.8	1.0
O I	30524 - 30521	0.0	-0.2	-0.6	0.0	-0.1	0.0	0.0	-0.2	-0.6	0.6
P O	30850 - 30847	0.0	0.0	-0.8	0.0	0.0	0.0	0.0	0.0	-0.8	0.8
Q O	30564 - 30561	0.0	-0.1	-0.6	0.0	0.0	0.0	0.0	-0.1	-0.7	0.7
R I	30890 - 30887	0.0	0.0	-0.3	0.0	0.0	0.0	0.0	0.0	-0.3	0.4
S O	30604 - 30601	0.0	-0.1	-0.6	0.0	0.0	0.0	0.0	-0.1	-0.6	0.5
T O	30614 - 30611	0.0	0.0	-0.4	0.0	0.0	0.1	0.0	0.0	-0.4	0.5
U O	30900 - 30910	0.4	0.2	0.0	0.0	0.0	0.1	0.4	0.2	-0.1	0.5
V I	30920 - 30930	-0.4	-0.1	-0.1	0.0	0.0	0.2	0.0	-0.1	-0.5	0.5
W I	1216 - 1226	0.3	0.7	-0.3	0.0	0.0	0.0	0.7	0.3	-0.3	0.9
X O	1236 - 1246	-0.4	-0.7	0.3	0.0	0.0	0.0	0.3	-0.4	-0.7	0.9

[1] Refer to Figure 2.10.2-34 for the identification of the representative sections.

Table 2.10.4-112 Primary Stresses; 30-Foot Top End Drop; Drop Orientation = 0 Degrees; 2-D Model; Condition 1

Condition 1: 100°F Ambient with Contents

Stress Points		Stress Components (ksi)						Principal Stresses (ksi)		
Section[1]	Node	S_x	S_y	S_z	S_{xy}	S_{yz}	S_{xz}	S1	S2	S3
A1	1	3.7	-0.1	3.7	0.0	0.0	0.0	3.7	3.7	-0.1
A2	2	2.1	0.0	2.1	0.0	0.0	0.0	2.1	2.1	0.0
A3	3	0.5	0.0	0.5	0.0	0.0	0.0	0.5	0.5	0.0
A4	4	-1.1	0.0	-1.1	0.0	0.0	0.0	0.0	-1.1	-1.1
A5	5	-2.7	0.0	-2.7	0.0	0.0	0.0	0.0	-2.7	-2.7
B1	6	2.3	0.0	2.3	0.0	0.0	0.0	2.3	2.3	0.0
B2	7	0.8	0.0	0.8	0.0	0.0	0.0	0.8	0.8	0.0
B3	8	-0.6	0.0	-0.6	0.0	0.0	0.0	0.0	-0.6	-0.6
B4	9	-2.0	0.0	-2.0	0.0	0.0	0.0	0.0	-2.0	-2.0
B5	10	-3.5	0.0	-3.5	0.0	0.0	0.0	0.0	-3.5	-3.5
C1	251	-2.1	-2.4	-0.1	-0.5	0.0	0.0	-0.1	-1.7	-2.7
C2	252	-0.4	-1.0	0.4	-0.4	0.0	0.0	0.4	-0.2	-1.2
C3	253	0.6	-0.5	0.4	-0.4	0.0	0.0	0.7	0.4	-0.6
C4	254	1.6	-0.2	0.4	-0.3	0.0	0.0	1.7	0.4	-0.3
C5	255	2.8	-0.1	0.3	-0.2	0.0	0.0	2.8	0.3	-0.2
D1	306	-2.9	-1.7	-1.2	-0.8	0.0	0.0	-1.2	-1.3	-3.3
D2	307	-0.9	-1.3	-0.8	-0.3	0.0	0.0	-0.7	-0.8	-1.4
D3	308	-0.2	-0.5	-0.6	0.1	0.0	0.0	-0.2	-0.5	-0.6
D4	309	0.4	-0.2	-0.6	0.1	0.0	0.0	0.4	-0.2	-0.6
D5	310	1.1	-0.1	-0.6	0.1	0.0	0.0	1.1	-0.1	-0.6
E1	305	2.7	0.1	0.7	-0.6	0.0	0.0	2.9	0.7	-0.1
E2	315	1.4	-0.7	0.2	-0.7	0.0	0.0	1.6	0.2	-0.9
E3	325	0.6	-0.6	0.1	-0.7	0.0	0.0	0.9	0.1	-0.9
E4	335	0.3	-0.5	0.0	-0.5	0.0	0.0	0.6	0.0	-0.8
E5	345	0.1	-0.5	-0.1	-0.3	0.0	0.0	0.2	-0.1	-0.7
E6	355	0.1	-0.7	-0.1	-0.2	0.0	0.0	0.1	-0.1	-0.7
F1	251	-2.1	-2.4	-0.1	-0.5	0.0	0.0	-0.1	-1.7	-2.7
F2	261	-1.7	-1.5	0.2	-0.2	0.0	0.0	0.2	-1.4	-1.8
F3	271	-1.4	-0.9	0.4	0.2	0.0	0.0	0.4	-0.9	-1.5
F4	281	-1.6	-0.7	0.4	0.3	0.0	0.0	0.4	-0.6	-1.7
G1	311	-1.2	-2.1	-0.1	-0.2	0.0	0.0	-0.1	-1.2	-2.1

Table 2.10.4-112 Primary Stresses; 30-Foot Top End Drop; Drop Orientation = 0 Degrees; 2-D Model; Condition 1 (continued)

Stress Points		Stress Components (ksi)						Principal Stresses (ksi)		
Section[1]	Node	S_x	S_y	S_z	S_{xy}	S_{yz}	S_{zx}	S1	S2	S3
G2	321	-0.8	-1.3	0.2	0.0	0.0	0.0	0.2	-0.8	-1.3
G3	331	-0.4	-0.8	0.4	0.1	0.0	0.0	0.4	-0.4	-0.8
G4	341	-0.2	-0.2	0.6	0.1	0.0	0.0	0.6	-0.1	-0.3
G5	351	-0.1	0.5	0.8	0.1	0.0	0.0	0.8	0.5	-0.1
H1	581	-0.1	-2.2	1.1	0.0	0.0	0.0	1.1	-0.1	-2.2
H2	582	-0.1	-2.6	1.0	0.0	0.0	0.0	1.0	-0.1	-2.6
H3	583	-0.1	-2.9	0.9	0.1	0.0	0.0	0.9	-0.1	-2.9
H4	584	0.0	-3.5	0.7	0.2	0.0	0.0	0.7	0.0	-3.6
I1	589	0.0	-1.1	0.2	0.0	0.0	0.0	0.2	0.0	-1.1
I2	590	0.0	-1.2	0.2	0.0	0.0	0.0	0.2	0.0	-1.2
I3	591	0.0	-1.3	0.1	0.0	0.0	0.0	0.1	0.0	-1.3
I4	592	0.0	-1.4	0.1	0.0	0.0	0.0	0.1	0.0	-1.4
I5	593	0.0	-1.5	0.1	0.0	0.0	0.0	0.1	0.0	-1.5
J1	971	-0.1	-3.5	1.2	0.0	0.0	0.0	1.2	-0.1	-3.5
J2	972	0.0	-3.5	1.2	0.0	0.0	0.0	1.2	0.0	-3.5
J3	973	0.0	-3.5	1.2	0.0	0.0	0.0	1.2	0.0	-3.5
J4	974	0.0	-3.5	1.2	0.0	0.0	0.0	1.2	0.0	-3.5
K1	979	0.0	-1.9	0.0	0.0	0.0	0.0	0.0	0.0	-1.9
K2	980	0.0	-1.9	0.0	0.0	0.0	0.0	0.0	0.0	-1.9
K3	981	0.0	-1.9	0.0	0.0	0.0	0.0	0.0	0.0	-1.9
K4	982	0.0	-1.9	0.0	0.0	0.0	0.0	0.0	0.0	-1.9
K5	983	0.0	-1.9	0.0	0.0	0.0	0.0	0.0	0.0	-1.9
L1	1601	-0.1	-4.5	1.2	0.0	0.0	0.0	1.2	-0.1	-4.5
L2	1602	0.0	-4.5	1.2	0.0	0.0	0.0	1.2	0.0	-4.5
L3	1603	0.0	-4.5	1.2	0.0	0.0	0.0	1.2	0.0	-4.5
L4	1604	0.0	-4.5	1.2	0.0	0.0	0.0	1.2	0.0	-4.5
M1	1609	0.0	-2.9	0.0	0.0	0.0	0.0	0.0	0.0	-2.9
M2	1610	0.0	-2.9	0.0	0.0	0.0	0.0	0.0	0.0	-2.9
M3	1611	0.0	-2.9	0.0	0.0	0.0	0.0	0.0	0.0	-2.9
M4	1612	0.0	-2.9	0.0	0.0	0.0	0.0	0.0	0.0	-2.9
M5	1613	0.0	-2.9	0.0	0.0	0.0	0.0	0.0	0.0	-2.9
N1	2216	-0.1	-5.6	1.2	0.0	0.0	0.0	1.2	-0.1	-5.6
N2	2217	0.0	-5.5	1.2	0.0	0.0	0.0	1.2	0.0	-5.5

Table 2.10.4-112 Primary Stresses; 30-Foot Top End Drop; Drop Orientation = 0 Degrees; 2-D Model; Condition 1 (continued)

Stress Points		Stress Components (ksi)						Principal Stresses (ksi)		
Section[1]	Node	S_x	S_y	S_z	S_{xy}	S_{yz}	S_{xz}	S1	S2	S3
N3	2218	0.0	-5.5	1.2	0.0	0.0	0.0	1.2	0.0	-5.5
N4	2219	0.0	-5.5	1.2	0.0	0.0	0.0	1.2	0.0	-5.5
O1	2224	0.0	-3.8	-0.1	0.0	0.0	0.0	0.0	-0.1	-3.8
O2	2225	0.0	-3.8	-0.1	0.0	0.0	0.0	0.0	-0.1	-3.8
O3	2226	0.0	-3.8	-0.1	0.0	0.0	0.0	0.0	-0.1	-3.8
O4	2227	0.0	-3.8	-0.1	0.0	0.0	0.0	0.0	-0.1	-3.8
O5	2228	0.0	-3.8	-0.1	0.0	0.0	0.0	0.0	-0.1	-3.8
P1	2546	-0.1	-3.3	1.8	0.0	0.0	0.0	1.8	-0.1	-3.3
P2	2547	-0.2	-4.9	1.3	0.0	0.0	0.0	1.3	-0.2	-4.9
P3	2548	-0.1	-6.6	0.9	-0.2	0.0	0.0	0.9	-0.1	-6.6
P4	2549	-0.1	-8.8	0.2	-0.5	0.0	0.0	0.2	-0.1	-8.9
Q1	2554	0.0	-3.4	1.3	0.0	0.0	0.0	1.3	0.0	-3.4
Q2	2555	0.0	-3.9	1.1	0.0	0.0	0.0	1.1	0.0	-3.9
Q3	2556	0.0	-4.4	1.0	0.1	0.0	0.0	1.0	0.0	-4.4
Q4	2557	0.0	-4.8	0.8	0.0	0.0	0.0	0.8	0.0	-4.8
Q5	2558	0.0	-5.3	0.7	0.0	0.0	0.0	0.7	0.0	-5.3
R1	2771	-0.1	-18.1	-0.6	0.0	0.0	0.0	-0.1	-0.6	-18.1
R2	2772	0.3	-10.6	1.6	0.3	0.0	0.0	1.6	0.4	-10.6
R3	2773	1.1	-3.5	3.7	1.4	0.0	0.0	3.7	1.5	-3.9
R4	2774	0.3	5.4	5.8	3.1	0.0	0.0	6.8	5.8	-1.1
S1	2779	-9.6	-12.6	-2.7	0.7	0.0	0.0	-2.7	-9.4	-12.7
S2	2780	-6.0	-7.5	-0.4	-0.3	0.0	0.0	-0.4	-5.9	-7.6
S3	2781	-3.1	-3.9	1.2	-1.1	0.0	0.0	1.2	-2.3	-4.7
S4	2782	-1.2	-0.3	2.7	-0.9	0.0	0.0	2.7	0.3	-1.8
S5	2783	-0.5	4.4	4.1	-0.6	0.0	0.0	4.4	4.1	-0.6
T1	7066	11.2	8.9	4.8	2.8	0.0	0.0	13.1	7.0	4.8
T2	7067	7.8	2.2	2.1	0.9	0.0	0.0	7.9	2.1	2.1
T3	7068	5.2	-1.1	0.6	-0.2	0.0	0.0	5.2	0.6	-1.1
T4	7069	3.1	-3.2	-0.5	-0.9	0.0	0.0	3.2	-0.5	-3.3
T5	7070	1.6	-5.1	-1.3	-1.0	0.0	0.0	1.8	-1.3	-5.3
T6	7071	0.7	-7.3	-2.1	-0.7	0.0	0.0	0.8	-2.1	-7.3
T7	7072	0.4	-10.3	-3.0	-0.4	0.0	0.0	0.4	-3.0	-10.3
U1	3051	-1.7	-10.7	5.7	2.2	0.0	0.0	5.7	-1.2	-11.2

Table 2.10.4-112 Primary Stresses; 30-Foot Top End Drop; Drop Orientation = 0 Degrees; 2-D Model; Condition 1 (continued)

Stress Points		Stress Components (ksi)						Principal Stresses (ksi)		
Section[1]	Node	S_x	S_y	S_z	S_{xy}	S_{yz}	S_{zx}	S1	S2	S3
U2	3052	1.7	-10.3	3.8	2.6	0.0	0.0	3.8	2.2	-10.9
U3	3053	2.4	-9.2	1.7	2.6	0.0	0.0	2.9	1.7	-9.8
U4	3054	2.2	-8.7	-0.8	1.9	0.0	0.0	2.5	-0.8	-9.0
U5	3055	1.6	-9.4	-3.6	2.1	0.0	0.0	2.0	-3.6	-9.8
U6	3056	-0.6	-6.6	-5.7	3.9	0.0	0.0	1.3	-5.7	-8.6
V1	3611	-7.3	-4.7	5.5	-1.4	0.0	0.0	5.5	-4.1	-8.0
V2	3612	-4.3	-4.6	3.8	-1.8	0.0	0.0	3.8	-2.7	-6.3
V3	3613	-2.1	-4.3	1.8	-2.2	0.0	0.0	1.8	-0.7	-5.7
V4	3614	-0.2	-4.1	-0.4	-2.1	0.0	0.0	0.7	-0.4	-5.0
V5	3615	1.4	-3.7	-2.6	-1.7	0.0	0.0	2.0	-2.6	-4.3
V6	3616	1.4	-2.5	-5.1	-1.1	0.0	0.0	1.6	-2.7	-5.1
V7	3617	5.6	-1.5	-6.4	-0.6	0.0	0.0	5.6	-1.5	-6.4
W1	3241	20.7	-1.1	20.7	0.0	0.0	0.0	20.7	20.7	-1.1
W2	3242	13.4	-1.3	13.4	0.0	0.0	0.0	13.4	13.4	-1.3
W3	3243	6.2	-1.8	6.2	0.0	0.0	0.0	6.2	6.2	-1.8
W4	3244	-0.7	-2.3	-0.7	0.0	0.0	0.0	-0.7	-0.7	-2.3
W5	3245	-7.9	-2.8	-7.9	0.0	0.0	0.0	-2.8	-7.9	-7.9
W6	3246	-15.5	-3.0	-15.5	0.0	0.0	0.0	-3.0	-15.5	-15.5
X1	3801	26.5	-3.5	26.5	0.0	0.0	0.0	26.5	26.5	-3.5
X2	3802	18.4	-3.3	18.4	0.0	0.0	0.0	18.4	18.4	-3.3
X3	3803	9.5	-3.1	9.5	0.0	0.0	0.0	9.5	9.5	-3.1
X4	3804	0.5	-2.9	0.5	0.0	0.0	0.0	0.5	0.5	-2.9
X5	3805	-8.6	-2.6	-8.6	0.0	0.0	0.0	-2.6	-8.6	-8.6
X6	3806	-17.5	-2.2	-17.5	0.0	0.0	0.0	-2.2	-17.5	-17.5
X7	3807	-27.0	-1.8	-27.0	0.0	0.0	0.0	-1.8	-27.0	-27.0

[1] Refer to Figure 2.10.2-34 for the identification of the representative sections.

Table 2.10.4-113 P_m Stresses; 30-Foot Top End Drop; Drop Orientation = 0 Degrees; 2-D Model; Condition 1

Condition 1: 100°F Ambient with Contents

Section[1]	Node - Node	Stress Components (ksi) S_x	S_y	S_z	S_{xy}	S_{yz}	S_{xz}	Principal Stresses (ksi) S1	S2	S3	S.I.
A	1 - 5	0.5	0.0	0.5	0.0	0.0	0.0	0.5	0.5	0.0	0.5
B	6 - 10	-0.6	0.0	-0.6	0.0	0.0	0.0	0.0	-0.6	-0.6	0.6
C	251 - 255	0.5	-0.7	0.3	-0.3	0.0	0.0	0.6	0.3	-0.8	1.5
D	306 - 310	-0.4	-0.7	-0.7	-0.1	0.0	0.0	-0.4	-0.7	-0.8	0.4
E	305 - 355	1.0	-0.5	0.2	-0.5	0.0	0.0	1.1	0.2	-0.7	1.8
F	251 - 281	-1.6	-1.3	0.2	0.0	0.0	0.0	0.2	-1.3	-1.6	1.9
G	311 - 351	-0.5	-0.8	0.4	0.0	0.0	0.0	0.4	-0.5	-0.8	1.2
H	581 - 584	-0.1	-2.8	0.9	0.1	0.0	0.0	0.9	-0.1	-2.8	3.7
I	589 - 593	0.0	-1.3	0.2	0.0	0.0	0.0	0.2	0.0	-1.3	1.4
J	971 - 974	0.0	-3.5	1.2	0.0	0.0	0.0	1.2	0.0	-3.5	4.7
K	979 - 983	0.0	-1.9	0.0	0.0	0.0	0.0	0.0	0.0	-1.9	1.9
L	1601 - 1604	0.0	-4.5	1.2	0.0	0.0	0.0	1.2	0.0	-4.5	5.7
M	1609 - 1613	0.0	-2.9	0.0	0.0	0.0	0.0	0.0	0.0	-2.9	2.9
N	2216 - 2219	0.0	-5.5	1.2	0.0	0.0	0.0	1.2	0.0	-5.5	6.7
O	2224 - 2228	0.0	-3.8	-0.1	0.0	0.0	0.0	0.0	-0.1	-3.8	3.8
P	2546 - 2549	-0.1	-5.9	1.1	-0.2	0.0	0.0	1.1	-0.1	-5.9	6.9
Q	2554 - 2558	0.0	-4.4	1.0	0.0	0.0	0.0	1.0	0.0	-4.4	5.4
R	2771 - 2774	0.5	-6.7	2.7	1.1	0.0	0.0	2.7	0.7	-6.9	9.5
S	2779 - 2783	-3.8	-3.9	1.0	-0.6	0.0	0.0	1.0	-3.3	-4.4	5.5
T	7066 - 7072	4.1	-2.5	0.0	-0.1	0.0	0.0	4.1	0.0	-2.5	6.7
U	3051 - 3056	1.4	-9.5	0.1	2.4	0.0	0.0	1.9	0.1	-10.0	11.9
V	3611 - 3617	-0.6	-3.7	-0.7	-1.6	0.0	0.0	0.1	-0.7	-4.4	4.5
W	3241 - 3246	2.7	-2.1	2.7	0.0	0.0	0.0	2.7	2.7	-2.1	4.8
X	3801 - 3807	-0.2	-2.8	-0.2	0.0	0.0	0.0	-0.2	-0.2	-2.8	2.6

[1] Refer to Figure 2.10.2-34 for the identification of the representative sections.

Table 2.10.4-114 $P_m + P_b$ Stresses; 30-Foot Top End Drop; Drop Orientation = 0 Degrees; 2-D Model; Condition 1

Condition 1: 100°F Ambient with Contents

Section[1]	Node - Node	Stress Components (ksi) S_x	S_y	S_z	S_{xy}	S_{yz}	S_{xz}	Principal Stresses (ksi) S1	S2	S3	S.I.
A I	1 - 5	3.7	-0.1	3.7	0.0	0.0	0.0	3.7	3.7	-0.1	3.7
B O	6 - 10	-3.5	0.0	-3.5	0.0	0.0	0.0	0.0	-3.5	-3.5	3.5
C O	251 - 255	2.8	-0.1	0.5	-0.3	0.0	0.0	2.9	0.5	-0.2	3.0
D O	306 - 310	1.3	-0.1	-0.5	-0.1	0.0	0.0	1.3	-0.1	-0.5	1.8
E I	305 - 355	2.7	-0.3	0.6	-0.5	0.0	0.0	2.8	0.6	-0.4	3.2
F I	251 - 281	-2.1	-2.2	0.0	0.0	0.0	0.0	0.0	-2.1	-2.2	2.2
G I	311 - 351	-1.2	-2.0	-0.1	0.0	0.0	0.0	-0.1	-1.2	-2.0	1.9
H O	581 - 584	0.0	-3.4	0.7	0.1	0.0	0.0	0.7	0.0	-3.4	4.2
I O	589 - 593	0.0	-1.5	0.1	0.0	0.0	0.0	0.1	0.0	-1.5	1.6
J I	971 - 974	-0.1	-3.5	1.2	0.0	0.0	0.0	1.2	-0.1	-3.5	4.7
K I	979 - 983	0.0	-1.9	0.0	0.0	0.0	0.0	0.0	0.0	-1.9	1.9
L I	1601 - 1604	-0.1	-4.5	1.2	0.0	0.0	0.0	1.2	-0.1	-4.5	5.7
M O	1609 - 1613	0.0	-2.9	0.0	0.0	0.0	0.0	0.0	0.0	-2.9	2.9
N I	2216 - 2219	-0.1	-5.6	1.2	0.0	0.0	0.0	1.2	-0.1	-5.6	6.8
O I	2224 - 2228	0.0	-3.8	-0.1	0.0	0.0	0.0	0.0	-0.1	-3.8	3.8
P O	2546 - 2549	-0.1	-8.6	0.3	-0.2	0.0	0.0	0.3	-0.1	-8.6	8.8
Q O	2554 - 2558	0.0	-5.3	0.7	0.0	0.0	0.0	0.7	0.0	-5.3	6.0
R I	2771 - 2774	-0.1	-18.3	-0.5	1.1	0.0	0.0	0.0	-0.5	-18.4	18.4
S I	2779 - 2783	-9.6	-12.0	-2.3	-0.6	0.0	0.0	-2.3	-9.4	-12.1	9.8
T O	7066 - 7072	0.4	-10.5	-3.5	-0.1	0.0	0.0	0.4	-3.5	-10.6	10.9
U I	3051 - 3056	1.3	-31.4	5.5	2.4	0.0	0.0	5.5	1.5	-31.6	37.1
V I	3611 - 3617	-5.7	-3.5	5.2	-1.6	0.0	0.0	5.2	-2.7	-6.6	11.8
W I	3241 - 3246	20.6	-1.1	20.6	0.0	0.0	0.0	20.6	20.6	-1.1	21.7
X I	3801 - 3807	26.7	-3.5	26.7	0.0	0.0	0.0	26.7	26.7	-3.5	30.2

[1] Refer to Figure 2.10.2-34 for the identification of the representative sections.

Table 2.10.4-115 Critical P_m Stress Summary; 30-Foot Top End Drop; Drop Orientation = 0 Degrees; 2-D Model; Condition 1

Condition 1: 100°F Ambient with Contents

Comp. No.[1]	Section Cut Node-Node	P_m Stresses (ksi) S_x	S_y	S_z	S_{xy}	S_{yz}	S_{xz}	Principal Stresses (ksi) S1	S2	S3	S.I.	Allow. Stress	Margin of Safety
1	246- 250	-0.6	0.0	-0.6	-0.2	0.0	0.0	0.0	-0.6	-0.7	0.7	45.6	64.1
2	386- 389	0.0	-1.9	0.9	-0.1	0.0	0.0	0.9	0.0	-1.9	2.7	44.9	15.6
3	2711- 2714	0.0	-4.7	4.9	0.6	0.0	0.0	4.9	0.1	-4.8	9.7	66.0	5.8
4	2276- 2279	0.0	-5.6	1.2	0.0	0.0	0.0	1.2	0.0	-5.6	6.8	45.8	5.7
5	2599- 2603	-4.4	0.0	1.6	-0.1	0.0	0.0	1.6	0.0	-4.4	6.1	46.4	6.6
6	2726- 2729	-0.1	-4.8	4.8	0.7	0.0	0.0	4.8	0.0	-4.9	9.7	49.3	4.1
7	3117- 3118	-13.1	1.1	-12.6	-3.7	0.0	0.0	2.0	-12.6	-14.0	16.0	48.0	2.0
8	3661- 3667	-0.4	-6.7	-1.6	2.5	0.0	0.0	0.5	-1.6	-7.6	8.1	94.5	10.7

Locations of the most critical sections for each component are provided in the following:

Comp. No.[1]	Section Location Inside Node x (in)	y (in)	z (in)	Outside Node x (in)
1	34.08	6.20	34.08	0.75
2	35.50	16.40	37.50	16.40
3	35.50	171.40	37.50	171.40
4	35.50	142.20	37.00	142.40
5	40.70	163.40	43.35	163.40
6	35.50	172.40	37.50	172.40
7	24.289	187.40	24.289	188.40
8	26.158	188.40	26.158	193.71

[1] Refer to Figure 2.10.2-33 for cask component identification.

Table 2.10.4-116 Critical $P_m + P_b$ Stress Summary; 30-Foot Top End Drop; Drop Orientation = 0 Degrees; 2-D Model; Condition 1

Condition 1: 100°F Ambient with Contents

Comp. No.[1]	Section Cut Node-Node	$P_m + P_b$ Stresses (ksi) S_x	S_y	S_z	S_{xy}	S_{yz}	S_{xz}	Principal Stresses (ksi) S1	S2	S3	S.I.	Allow. Stress	Margin of Safety
1	16- 20	-3.5	0.0	-3.5	0.0	0.0	0.0	0.0	-3.5	-3.5	3.5	65.2	17.6
2	1- 5	3.7	-0.1	3.7	0.0	0.0	0.0	3.7	3.7	-0.1	3.7	64.2	16.4
3	2711- 2714	-0.1	-11.3	3.3	0.6	0.0	0.0	3.3	0.0	-11.4	14.6	94.3	5.5
4	2276- 2279	-0.1	-5.7	1.2	0.0	0.0	0.0	1.2	-0.1	-5.7	6.9	65.5	8.5
5	2599- 2603	-4.8	0.0	1.5	-0.1	0.0	0.0	1.5	0.0	-4.8	6.2	66.4	9.7
6	2756- 2759	-18.5	0.3	0.5	-0.9	0.0	0.0	0.5	0.4	-18.5	19.0	70.9	2.7
7	3051- 3056	1.3	-31.4	5.5	2.4	0.0	0.0	5.5	1.5	-31.6	37.1	69.8	0.9
8	3761- 3767	28.5	-2.4	27.9	-0.4	0.0	0.0	28.5	27.9	-2.4	30.9	135.0	3.4

Locations of the most critical sections for each component are provided in the following:

Comp. No.[1]	Section Location Inside Node x (in)	y (in)	Outside Node z (in)	x (in)
1	1.42	6.20	1.42	0.75
2	0.00	14.40	0.00	8.20
3	35.50	171.40	37.50	171.40
4	35.50	142.40	37.00	142.40
5	40.70	163.40	43.35	163.40
6	35.50	174.40	37.50	174.40
7	35.50	179.40	35.50	185.40
8	7.4737	188.46	7.4737	193.71

[1] Refer to Figure 2.10.2-33 for cask component identification.

Table 2.10.4-117 Critical P_m Stress Summary; 30-Foot Top End Drop; Drop Orientation = 0 Degrees; 2-D Model; Condition 2

Condition 2: -20°F Ambient with Contents

Comp. No.[1]	Section Cut Node-Node	P_m Stresses (ksi) S_x	S_y	S_z	S_{xy}	S_{yz}	S_{xz}	Principal Stresses (ksi) S1	S2	S3	S.I.	Allow. Stress	Margin of Safety
1	206- 210	-0.7	0.0	-0.7	-0.2	0.0	0.0	0.1	-0.7	-0.8	0.8	45.6	56.0
2	386- 389	0.0	-2.1	0.8	-0.2	0.0	0.0	0.8	0.0	-2.1	2.9	44.9	14.5
3	2711- 2714	0.0	-5.0	4.6	0.7	0.0	0.0	4.6	0.1	-5.1	9.6	66.0	5.9
4	2276- 2279	0.0	-5.9	0.3	0.0	0.0	0.0	0.3	0.0	-5.9	6.2	45.8	6.4
5	2599- 2603	-4.5	0.0	1.6	-0.1	0.0	0.0	1.6	0.0	-4.5	6.1	46.4	6.6
6	2771- 2774	-7.0	0.7	2.5	-1.2	0.0	0.0	2.5	0.8	-7.2	9.7	49.3	4.1
7	3117- 3118	-13.5	1.1	-13.0	-3.7	0.0	0.0	2.0	-13.0	-14.4	16.4	48.0	1.9
8	3661- 3667	-0.4	-6.7	-1.7	2.6	0.0	0.0	0.5	-1.7	-7.6	8.1	94.5	10.7

Locations of the most critical sections for each component are provided in the following:

Comp. No.[1]	Section Location Inside Node x (in)	y (in)	Outside Node z (in)	x (in)
1	28.40	6.20	28.40	0.75
2	35.50	16.40	37.50	16.40
3	35.50	171.40	37.50	171.40
4	35.50	142.40	37.00	142.40
5	40.70	163.40	43.35	163.40
6	35.50	175.40	37.50	175.40
7	24.289	187.40	24.289	188.40
8	26.158	188.40	26.158	193.71

[1] Refer to Figure 2.10.2-33 for cask component identification.

Table 2.10.4-118 Critical $P_m + P_b$ Stress Summary; 30-Foot Top End Drop; Drop Orientation = 0 Degrees; 2-D Model; Condition 2

Condition 2: -20°F Ambient with Contents

Comp. No.[1]	Section Cut Node-Node	$P_m + P_b$ Stresses (ksi) S_x	S_y	S_z	S_{xy}	S_{yz}	S_{xz}	Principal Stresses (ksi) S1	S2	S3	S.I.	Allow. Stress	Margin of Safety
1	16- 20	-4.0	0.0	-4.0	0.0	0.0	0.0	0.0	-4.0	-4.0	4.0	65.2	15.3
2	371- 374	0.3	-4.4	0.2	-0.2	0.0	0.0	0.3	0.2	-4.4	4.7	64.2	12.7
3	2711- 2714	0.0	-11.7	2.9	0.7	0.0	0.0	2.9	0.0	-11.8	14.7	94.3	5.4
4	2276- 2279	0.0	-6.1	0.3	0.0	0.0	0.0	0.3	0.0	-6.1	6.3	65.5	9.4
5	2599- 2603	-4.8	0.0	1.5	-0.1	0.0	0.0	1.5	0.0	-4.8	6.2	66.4	9.7
6	2756- 2759	-19.3	0.4	0.1	-1.0	0.0	0.0	0.4	0.1	-19.3	19.8	70.9	2.6
7	3051- 3056	1.2	-32.7	5.6	2.5	0.0	0.0	5.6	1.4	-32.9	38.5	69.8	0.8
8	3761- 3767	29.4	-2.4	28.8	-0.4	0.0	0.0	29.4	28.8	-2.4	31.7	135.0	3.3

Locations of the most critical sections for each component are provided in the following:

Comp. No.[1]	Section Location Inside Node x (in)	Inside Node y (in)	Outside Node z (in)	Outside Node x (in)
1	1.42	6.20	1.42	0.75
2	35.50	15.40	37.50	15.40
3	35.50	171.40	37.50	171.40
4	35.50	142.40	37.00	142.40
5	40.70	163.40	43.35	163.40
6	35.50	174.40	37.50	174.40
7	35.50	179.40	35.50	185.40
8	7.4737	188.46	7.4737	193.71

[1] Refer to Figure 2.10.2-33 for cask component identification.

Table 2.10.4-119 Critical P_m Stress Summary; 30-Foot Top End Drop; Drop Orientation = 0 Degrees; 2-D Model; Condition 3

Condition 3: -20°F Ambient without Contents

Comp. No.[1]	Section Cut Node-Node	P_m Stresses (ksi)						Principal Stresses (ksi)			S.I.	Allow. Stress	Margin of Safety
		S_x	S_y	S_z	S_{xy}	S_{yz}	S_{xz}	S1	S2	S3			
1	206- 210	-0.5	0.0	-0.5	-0.2	0.0	0.0	0.0	-0.5	-0.6	0.6	45.6	75.0
2	386- 389	0.0	-1.8	0.6	-0.1	0.0	0.0	0.6	0.0	-1.8	2.5	44.7	17.0
3	2711- 2714	0.0	-4.2	4.2	0.6	0.0	0.0	4.2	0.1	-4.2	8.5	66.0	6.8
4	2276- 2279	0.0	-5.0	0.3	0.0	0.0	0.0	0.3	0.0	-5.0	5.2	45.8	7.8
5	2599- 2603	-3.6	0.0	1.5	-0.1	0.0	0.0	1.5	0.0	-3.6	5.1	46.4	8.1
6	2771- 2774	-6.1	0.5	2.3	-1.1	0.0	0.0	2.3	0.7	-6.2	8.5	49.3	4.8
7	3117- 3118	-12.7	0.9	-12.4	-2.8	0.0	0.0	1.4	-12.4	-13.2	14.6	48.0	2.3
8	3671- 3677	0.0	-0.9	0.0	3.2	0.0	0.0	2.8	0.0	-3.7	6.5	94.5	13.5

Locations of the most critical sections for each component are provided in the following:

Comp. No.[1]	Section Location			
	Inside Node		Outside Node	
	x (in)	y (in)	z (in)	x (in)
1	28.40	6.20	28.40	0.75
2	35.50	16.40	37.50	16.40
3	35.50	171.40	37.50	171.40
4	35.50	142.40	37.00	142.40
5	40.70	163.40	43.35	163.40
6	35.50	175.40	37.50	175.40
7	24.289	187.40	24.289	188.40
8	24.289	188.46	24.289	193.71

[1] Refer to Figure 2.10.2-33 for cask component identification.

Table 2.10.4-120 Critical $P_m + P_b$ Stress Summary; 30-Foot Top End Drop; Drop Orientation = 0 Degrees; 2-D Model; Condition 3

Condition 3: -20°F Ambient without Contents

Comp. No.[1]	Section Cut Node-Node	$P_m + P_b$ Stresses (ksi) S_x	S_y	S_z	S_{xy}	S_{yz}	S_{xz}	Principal Stresses (ksi) S1	S2	S3	S.I.	Allow. Stress	Margin of Safety
1	16- 20	-3.2	0.0	-3.2	0.0	0.0	0.0	0.0	-3.2	-3.2	3.2	65.2	19.4
2	371- 374	0.2	-3.5	0.1	-0.2	0.0	0.0	0.2	0.1	-3.5	3.7	64.2	16.4
3	2711- 2714	0.0	-10.5	2.6	0.6	0.0	0.0	2.6	0.0	-10.5	13.2	94.3	6.1
4	2276- 2279	0.0	-5.1	0.3	0.0	0.0	0.0	0.3	0.0	-5.1	5.3	65.5	11.4
5	2599- 2603	-3.9	0.0	1.4	-0.1	0.0	0.0	1.4	0.0	-3.9	5.2	66.4	11.8
6	2756- 2759	-17.5	0.4	0.1	-0.9	0.0	0.0	0.4	0.1	-17.6	18.0	70.9	2.9
7	3051- 3056	0.5	-31.0	5.1	2.1	0.0	0.0	5.1	0.	-31.1	36.2	69.8	0.9
8	3801- 3807	29.7	-2.3	29.7	0.0	0.0	0.0	29.7	29.7	-2.3	32.0	135.0	3.2

Locations of the most critical sections for each component are provided in the following:

Comp. No.[1]	Section Location Inside Node x (in)	y (in)	Outside Node z (in)	x (in)
1	1.42	6.20	1.42	0.75
2	35.50	15.40	37.50	15.40
3	35.50	171.40	37.50	171.40
4	35.50	142.40	37.00	142.40
5	40.70	163.40	43.35	163.40
6	35.50	174.40	37.50	174.40
7	35.50	179.40	35.50	185.40
8	0.0	188.46	0.0	193.71

[1] Refer to Figure 2.10.2-33 for cask component identification.

Table 2.10.4-121 Primary Stresses; 30-Foot Bottom End Drop; Drop Orientation = 0 Degrees; 2-D Model; Condition 1

Condition 1: 100°F Ambient with Contents

Stress Points		Stress Components (ksi)						Principal Stresses (ksi)		
Section[1]	Node	S_x	S_y	S_z	S_{xy}	S_{yz}	S_{zx}	S1	S2	S3
A1	1	21.0	-1.0	21.0	0.0	0.0	0.0	21.0	21.0	-1.0
A2	2	11.9	-1.1	11.9	0.0	0.0	0.0	11.9	11.9	-1.1
A3	3	2.9	-1.3	2.9	0.0	0.0	0.0	2.9	2.9	-1.3
A4	4	-6.1	-1.5	-6.1	0.0	0.0	0.0	-1.5	-6.1	-6.1
A5	5	-15.2	-1.6	-15.2	0.0	0.0	0.0	-1.6	-15.2	-15.2
B1	6	12.2	-1.8	12.2	0.0	0.0	0.0	12.2	12.2	-1.8
B2	7	4.3	-1.9	4.3	0.0	0.0	0.0	4.3	4.3	-1.9
B3	8	-3.6	-2.1	-3.6	0.0	0.0	0.0	-2.1	-3.6	-3.6
B4	9	-11.5	-2.2	-11.5	0.0	0.0	0.0	-2.2	-11.5	-11.5
B5	10	-19.3	-2.4	-19.3	0.0	0.0	0.0	-2.4	-19.3	-19.3
C1	251	-11.2	-13.5	-0.4	-2.3	0.0	0.0	-0.4	-9.7	-14.9
C2	252	-1.8	-5.6	2.4	-1.7	0.0	0.0	2.4	-1.2	-6.2
C3	253	3.1	-2.5	2.7	-1.8	0.0	0.0	3.6	2.7	-3.0
C4	254	9.3	-1.6	2.7	-1.4	0.0	0.0	9.4	2.7	-1.8
C5	255	16.1	-1.4	2.5	-1.0	0.0	0.0	16.2	2.5	-1.5
D1	306	-17.9	-15.3	-8.4	-5.3	0.0	0.0	-8.4	-11.1	-22.1
D2	307	-4.7	-11.0	-4.7	-2.3	0.0	0.0	-4.0	-4.7	-11.7
D3	308	-1.2	-5.6	-3.7	0.0	0.0	0.0	-1.2	-3.7	-5.6
D4	309	2.3	-3.6	-3.8	0.5	0.0	0.0	2.3	-3.7	-3.8
D5	310	6.6	-2.9	-3.9	0.5	0.0	0.0	6.6	-2.9	-3.9
E1	305	15.2	-4.7	3.5	-3.5	0.0	0.0	15.8	3.5	-5.3
E2	315	7.3	-6.9	1.0	-4.5	0.0	0.0	8.6	1.0	-8.2
E3	325	3.1	-5.4	0.3	-4.4	0.0	0.0	5.0	0.3	-7.3
E4	335	1.5	-4.4	0.2	-3.4	0.0	0.0	3.1	0.2	-6.0
E5	345	0.6	-3.7	0.2	-2.0	0.0	0.0	1.4	0.2	-4.5
E6	355	0.2	-3.6	0.1	-1.2	0.0	0.0	0.6	0.1	-3.9
F1	251	-11.2	-13.5	-0.4	-2.3	0.0	0.0	-0.4	-9.7	-14.9
F2	261	-8.1	-6.1	2.2	-0.8	0.0	0.0	2.2	-5.8	-8.4
F3	271	-5.4	-0.6	4.2	0.1	0.0	0.0	4.2	-0.6	-5.4
F4	281	-5.4	4.0	5.3	-0.2	0.0	0.0	5.3	4.0	-5.4
G1	311	-7.8	-12.6	-1.0	-0.4	0.0	0.0	-1.0	-7.8	-12.6

Table 2.10.4-121 Primary Stresses; 30-Foot Bottom End Drop; Drop Orientation = 0 Degrees; 2-D Model; Condition 1 (continued)

Stress Points		Stress Components (ksi)						Principal Stresses (ksi)		
Section[1]	Node	S_x	S_y	S_z	S_{xy}	S_{yz}	S_{zx}	S1	S2	S3
G2	321	-5.5	-7.9	0.8	0.3	0.0	0.0	0.8	-5.4	-7.9
G3	331	-2.8	-4.7	2.3	0.9	0.0	0.0	2.3	-2.5	-5.1
G4	341	-1.1	-1.5	3.5	0.7	0.0	0.0	3.5	-0.6	-2.0
G5	351	-0.5	2.6	4.7	0.4	0.0	0.0	4.7	2.7	-0.6
H1	581	-0.1	-3.0	1.7	0.0	0.0	0.0	1.7	-0.1	-3.0
H2	582	-0.2	-4.8	1.2	0.0	0.0	0.0	1.2	-0.2	-4.8
H3	583	-0.1	-6.6	0.7	0.2	0.0	0.0	0.7	-0.1	-6.6
H4	584	-0.1	-9.1	0.0	0.5	0.0	0.0	0.0	-0.1	-9.2
I1	589	0.0	-3.6	1.1	0.0	0.0	0.0	1.1	0.0	-3.6
I2	590	0.0	-4.2	0.9	0.0	0.0	0.0	0.9	0.0	-4.2
I3	591	0.0	-4.7	0.8	0.0	0.0	0.0	0.8	0.0	-4.7
I4	592	0.0	-5.3	0.6	0.0	0.0	0.0	0.6	0.0	-5.3
I5	593	0.0	-5.9	0.4	0.0	0.0	0.0	0.4	0.0	-5.9
J1	971	-0.1	-5.4	1.2	0.0	0.0	0.0	1.2	-0.1	-5.4
J2	972	0.0	-5.4	1.2	0.0	0.0	0.0	1.2	0.0	-5.4
J3	973	0.0	-5.4	1.2	0.0	0.0	0.0	1.2	0.0	-5.4
J4	974	0.0	-5.4	1.2	0.0	0.0	0.0	1.2	0.0	-5.4
K1	979	0.0	-4.2	0.0	0.0	0.0	0.0	0.0	0.0	-4.2
K2	980	0.0	-4.2	0.0	0.0	0.0	0.0	0.0	0.0	-4.2
K3	981	0.0	-4.1	0.0	0.0	0.0	0.0	0.0	0.0	-4.1
K4	982	0.0	-4.1	0.0	0.0	0.0	0.0	0.0	0.0	-4.1
K5	983	0.0	-4.1	0.0	0.0	0.0	0.0	0.0	0.0	-4.1
L1	1601	-0.1	-4.4	1.2	0.0	0.0	0.0	1.2	-0.1	-4.4
L2	1602	0.0	-4.4	1.2	0.0	0.0	0.0	1.2	0.0	-4.4
L3	1603	0.0	-4.4	1.2	0.0	0.0	0.0	1.2	0.0	-4.4
L4	1604	0.0	-4.4	1.2	0.0	0.0	0.0	1.2	0.0	-4.4
M1	1609	0.0	-3.2	0.0	0.0	0.0	0.0	0.0	0.0	-3.2
M2	1610	0.0	-3.2	0.0	0.0	0.0	0.0	0.0	0.0	-3.2
M3	1611	0.0	-3.2	0.0	0.0	0.0	0.0	0.0	0.0	-3.2
M4	1612	0.0	-3.2	0.0	0.0	0.0	0.0	0.0	0.0	-3.2
M5	1613	0.0	-3.2	0.0	0.0	0.0	0.0	0.0	0.0	-3.2
N1	2216	-0.1	-3.4	1.2	0.0	0.0	0.0	1.2	-0.1	-3.4
N2	2217	0.0	-3.4	1.2	0.0	0.0	0.0	1.2	0.0	-3.4

Table 2.10.4-121 Primary Stresses; 30-Foot Bottom End Drop; Drop Orientation = 0 Degrees; 2-D Model; Condition 1 (continued)

Stress Points		Stress Components (ksi)						Principal Stresses (ksi)		
Section[1]	Node	S_x	S_y	S_z	S_{xy}	S_{yz}	S_{zx}	S1	S2	S3
N3	2218	0.0	-3.4	1.2	0.0	0.0	0.0	1.2	0.0	-3.4
N4	2219	0.0	-3.4	1.2	0.0	0.0	0.0	1.2	0.0	-3.4
O1	2224	0.0	-2.2	0.0	0.0	0.0	0.0	0.0	0.0	-2.2
O2	2225	0.0	-2.2	0.0	0.0	0.0	0.0	0.0	0.0	-2.2
O3	2226	0.0	-2.2	0.0	0.0	0.0	0.0	0.0	0.0	-2.2
O4	2227	0.0	-2.2	0.0	0.0	0.0	0.0	0.0	0.0	-2.2
O5	2228	0.0	-2.2	0.0	0.0	0.0	0.0	0.0	0.0	-2.2
P1	2546	-0.1	-2.1	1.1	0.0	0.0	0.0	1.1	-0.1	-2.1
P2	2547	-0.1	-2.6	1.0	0.0	0.0	0.0	1.0	-0.1	-2.6
P3	2548	-0.1	-3.0	0.9	-0.1	0.0	0.0	0.9	-0.1	-3.0
P4	2549	0.0	-3.6	0.7	-0.2	0.0	0.0	0.7	0.0	-3.7
Q1	2554	0.0	-1.4	0.3	0.0	0.0	0.0	0.3	0.0	-1.4
Q2	2555	0.0	-1.5	0.3	0.0	0.0	0.0	0.3	0.0	-1.5
Q3	2556	0.0	-1.7	0.2	0.0	0.0	0.0	0.2	0.0	-1.7
Q4	2557	0.0	-1.8	0.2	0.0	0.0	0.0	0.2	0.0	-1.8
Q5	2558	0.0	-1.9	0.1	0.0	0.0	0.0	0.1	0.0	-1.9
R1	2771	-0.3	-4.4	0.0	0.2	0.0	0.0	0.0	-0.3	-4.4
R2	2772	-0.1	-2.9	0.4	0.3	0.0	0.0	0.4	-0.1	-2.9
R3	2773	-0.2	-1.4	0.8	0.4	0.0	0.0	0.8	-0.1	-1.5
R4	2774	-0.7	1.0	1.3	0.5	0.0	0.0	1.3	1.2	-0.9
S1	2779	-2.1	-2.9	-0.4	0.2	0.0	0.0	-0.4	-2.0	-2.9
S2	2780	-1.3	-1.8	0.1	0.0	0.0	0.0	0.1	-1.3	-1.8
S3	2781	-0.7	-1.1	0.4	-0.2	0.0	0.0	0.4	-0.5	-1.2
S4	2782	-0.3	-0.3	0.7	-0.2	0.0	0.0	0.7	-0.1	-0.5
S5	2783	-0.1	0.7	1.0	-0.1	0.0	0.0	1.0	0.8	-0.1
T1	7066	1.9	1.6	1.1	0.5	0.0	0.0	2.3	1.2	1.1
T2	7067	1.5	0.1	0.5	0.1	0.0	0.0	1.5	0.5	0.1
T3	7068	1.0	-0.5	0.3	0.0	0.0	0.0	1.0	0.3	-0.5
T4	7069	0.6	-0.8	0.1	-0.1	0.0	0.0	0.6	0.1	-0.8
T5	7070	0.3	-1.1	-0.1	-0.1	0.0	0.0	0.3	-0.1	-1.1
T6	7071	0.1	-1.4	-0.2	-0.1	0.0	0.0	0.1	-0.2	-1.4
T7	7072	0.1	-1.9	-0.3	-0.1	0.0	0.0	0.1	-0.3	-1.9
U1	3051	-1.2	-3.6	0.6	0.7	0.0	0.0	0.6	-1.0	-3.8

Table 2.10.4-121 Primary Stresses; 30-Foot Bottom End Drop; Drop Orientation = 0 Degrees; 2-D Model; Condition 1 (continued)

Stress Points		Stress Components (ksi)						Principal Stresses (ksi)		
Section[1]	Node	S_x	S_y	S_z	S_{xy}	S_{yz}	S_{xz}	S1	S2	S3
U2	3052	-0.4	-3.7	0.1	0.7	0.0	0.0	0.1	-0.2	-3.9
U3	3053	0.3	-3.5	-0.2	0.3	0.0	0.0	0.3	-0.2	-3.5
U4	3054	0.6	-2.9	-0.5	-0.3	0.0	0.0	0.6	-0.5	-2.9
U5	3055	0.4	-2.3	-0.9	-0.3	0.0	0.0	0.4	-0.9	-2.3
U6	3056	1.2	-1.0	-0.7	0.4	0.0	0.0	1.2	-0.7	-1.0
V1	3611	0.6	-0.1	1.8	-0.1	0.0	0.0	1.8	0.6	-0.1
V2	3612	0.3	-0.2	1.1	-0.1	0.0	0.0	1.1	0.3	-0.2
V3	3613	0.1	-0.4	0.5	-0.1	0.0	0.0	0.5	0.2	-0.5
V4	3614	0.0	-0.7	-0.1	-0.1	0.0	0.0	0.0	-0.1	-0.7
V5	3615	-0.1	-1.1	-0.8	0.0	0.0	0.0	-0.1	-0.8	-1.1
V6	3616	-0.3	-0.5	-1.2	0.0	0.0	0.0	-0.3	-0.5	-1.2
V7	3617	-0.8	0.4	-1.7	0.0	0.0	0.0	0.4	-0.8	-1.7
W1	3241	4.7	0.0	4.7	0.0	0.0	0.0	4.7	4.7	0.0
W2	3242	3.0	0.0	3.0	0.0	0.0	0.0	3.0	3.0	0.0
W3	3243	1.4	0.0	1.4	0.0	0.0	0.0	1.4	1.4	0.0
W4	3244	-0.2	0.0	-0.2	0.0	0.0	0.0	0.0	-0.2	-0.2
W5	3245	-1.9	0.0	-1.9	0.0	0.0	0.0	0.0	-1.9	-1.9
W6	3246	-3.5	0.0	-3.5	0.0	0.0	0.0	0.0	-3.5	-3.5
X1	3801	4.6	-0.1	4.6	0.0	0.0	0.0	4.6	4.6	-0.1
X2	3802	3.1	-0.1	3.1	0.0	0.0	0.0	3.1	3.1	-0.1
X3	3803	1.6	0.0	1.6	0.0	0.0	0.0	1.6	1.6	0.0
X4	3804	0.1	0.0	0.1	0.0	0.0	0.0	0.1	0.1	0.0
X5	3805	-1.4	0.0	-1.4	0.0	0.0	0.0	0.0	-1.4	-1.4
X6	3806	-2.9	0.1	-2.9	0.0	0.0	0.0	0.1	-2.9	-2.9
X7	3807	-4.6	0.1	-4.6	0.0	0.0	0.0	0.1	-4.6	-4.6

[1] Refer to Figure 2.10.2-34 for the identification of the representative sections.

Table 2.10.4-122 P_m Stresses; 30-Foot Bottom End Drop; Drop Orientation = 0 Degrees; 2-D Model; Condition 1

Condition 1: 100°F Ambient with Contents

		Stress Components (ksi)						Principal Stresses (ksi)			
Section[1]	Node - Node	S_x	S_y	S_z	S_{xy}	S_{yz}	S_{xz}	S1	S2	S3	S.I.
A	1 - 5	2.9	-1.3	2.9	0.0	0.0	0.0	2.9	2.9	-1.3	4.2
B	6 - 10	-3.6	-2.1	-3.6	0.0	0.0	0.0	-2.1	-3.6	-3.6	1.5
C	251 - 255	3.2	-4.3	2.2	-1.6	0.0	0.0	3.6	2.2	-4.6	8.2
D	306 - 310	-2.3	-7.3	-4.6	-1.1	0.0	0.0	-2.1	-4.6	-7.5	5.4
E	305 - 355	5.1	-5.0	1.0	-3.4	0.0	0.0	6.2	1.0	-6.1	12.3
F	251 - 281	-7.3	-3.7	3.0	-0.6	0.0	0.0	3.0	-3.6	-7.4	10.3
G	311 - 351	-3.4	-4.7	2.1	0.5	0.0	0.0	2.1	-3.2	-4.9	7.0
H	581 - 584	-0.1	-5.9	0.9	0.2	0.0	0.0	0.9	-0.1	-5.9	6.8
I	589 - 593	0.0	-4.8	0.8	0.0	0.0	0.0	0.8	0.0	-4.8	5.5
J	971 - 974	0.0	-5.4	1.2	0.0	0.0	0.0	1.2	0.0	-5.4	6.6
K	979 - 983	0.0	-4.1	0.0	0.0	0.0	0.0	0.0	0.0	-4.1	4.1
L	1601 - 1604	0.0	-4.4	1.2	0.0	0.0	0.0	1.2	0.0	-4.4	5.6
M	1609 - 1613	0.0	-3.2	0.0	0.0	0.0	0.0	0.0	0.0	-3.2	3.2
N	2216 - 2219	0.0	-3.4	1.2	0.0	0.0	0.0	1.2	0.0	-3.4	4.6
O	2224 - 2228	0.0	-2.2	0.0	0.0	0.0	0.0	0.0	0.0	-2.2	2.2
P	2546 - 2549	-0.1	-2.8	0.9	-0.1	0.0	0.0	0.9	-0.1	-2.8	3.7
Q	2554 - 2558	0.0	-1.7	0.2	0.0	0.0	0.0	0.2	0.0	-1.7	1.9
R	2771 - 2774	-0.3	-2.0	0.6	0.3	0.0	0.0	0.6	-0.2	-2.0	2.7
S	2779 - 2783	-0.8	-1.0	0.4	-0.1	0.0	0.0	0.4	-0.8	-1.1	1.5
T	7066 - 7072	0.8	-0.6	0.2	0.0	0.0	0.0	0.8	0.2	-0.6	1.4
U	3051 - 3056	0.2	-3.0	-0.4	0.2	0.0	0.0	0.2	-0.4	-3.0	3.2
V	3611 - 3617	0.0	-0.4	-0.1	-0.1	0.0	0.0	0.0	-0.1	-0.4	0.4
W	3241 - 3246	0.6	0.0	0.6	0.0	0.0	0.0	0.6	0.6	0.0	0.6
X	3801 - 3807	0.0	0.0	0.0	0.0	0.0	0.0	0.0	0.0	0.0	0.0

[1] Refer to Figure 2.10.2-34 for the identification of the representative sections.

Table 2.10.4-123 $P_m + P_b$ Stresses; 30-Foot Bottom End Drop; Drop Orientation = 0 Degrees; 2-D Model; Condition 1

Condition 1: 100°F Ambient with Contents

		Stress Components (ksi)						Principal Stresses (ksi)			
Section[1]	Node - Node	S_x	S_y	S_z	S_{xy}	S_{yz}	S_{xz}	S1	S2	S3	S.I.
A I	1 - 5	21.0	-1.0	21.0	0.0	0.0	0.0	21.0	21.0	-1.0	22.0
B O	6 - 10	-19.4	-2.4	-19.4	0.0	0.0	0.0	-2.4	-19.4	-19.4	17.0
C O	251 - 255	15.9	-1.4	3.2	-1.6	0.0	0.0	16.1	3.2	-1.6	17.7
D O	306 - 310	7.9	-2.9	-2.8	-1.1	0.0	0.0	8.0	-2.8	-3.0	11.0
E I	305 - 355	15.2	-6.4	2.5	-3.4	0.0	0.0	15.7	2.5	-7.0	22.7
F I	251 - 281	-11.2	-12.4	0.1	-0.6	0.0	0.0	0.1	-10.9	-12.7	12.7
G I	311 - 351	-7.8	-11.9	-0.7	0.5	0.0	0.0	-0.7	-7.8	-12.0	11.3
H O	581 - 584	-0.1	-8.8	0.1	0.2	0.0	0.0	0.1	-0.1	-8.8	8.9
I O	589 - 593	0.0	-5.9	0.4	0.0	0.0	0.0	0.4	0.0	-5.9	6.3
J I	971 - 974	-0.1	-5.4	1.2	0.0	0.0	0.0	1.2	-0.1	-5.4	6.6
K I	979 - 983	0.0	-4.2	0.0	0.0	0.0	0.0	0.0	0.0	-4.2	4.2
L I	1601 - 1604	-0.1	-4.4	1.2	0.0	0.0	0.0	1.2	-0.1	-4.4	5.6
M O	1609 - 1613	0.0	-3.2	0.0	0.0	0.0	0.0	0.0	0.0	-3.2	3.2
N I	2216 - 2219	-0.1	-3.4	1.2	0.0	0.0	0.0	1.2	-0.1	-3.4	4.6
O I	2224 - 2228	0.0	-2.2	0.0	0.0	0.0	0.0	0.0	0.0	-2.2	2.2
P O	2546 - 2549	0.0	-3.5	0.7	-0.1	0.0	0.0	0.7	0.0	-3.5	4.2
Q O	2554 - 2558	0.0	-1.9	0.1	0.0	0.0	0.0	0.1	0.0	-1.9	2.1
R I	2771 - 2774	-0.3	-4.6	0.0	0.3	0.0	0.0	0.0	-0.2	-4.6	4.6
S I	2779 - 2783	-2.1	-2.8	-0.3	-0.1	0.0	0.0	-0.3	-2.0	-2.8	2.5
T O	7066 - 7072	0.1	-2.0	-0.4	0.0	0.0	0.0	0.1	-0.4	-2.0	2.1
U I	3051 - 3056	-0.7	-11.2	0.3	0.2	0.0	0.0	0.3	-0.7	-11.2	11.4
V O	3611 - 3617	-0.6	0.4	-1.8	-0.1	0.0	0.0	0.4	-0.6	-1.8	2.2
W I	3241 - 3246	4.7	0.0	4.7	0.0	0.0	0.0	4.7	4.7	0.0	4.7
X O	3801 - 3807	-4.5	0.1	-4.5	0.0	0.0	0.0	0.1	-4.5	-4.5	4.7

[1] Refer to Figure 2.10.2-34 for the identification of the representative sections.

Table 2.10.4-124 Critical P_m Stress Summary; 30-Foot Bottom End Drop; Drop Orientation = 0 Degrees; 2-D Model; Condition 1

Condition 1: 100°F Ambient with Contents

Comp. No.[1]	Section Cut Node-Node	P_m Stresses (ksi) S_x	S_y	S_z	S_{xy}	S_{yz}	S_{xz}	Principal Stresses (ksi) S1	S2	S3	S.I.	Allow. Stress	Margin of Safety
1	306- 310	-2.3	-7.3	-4.6	-1.1	0.0	0.0	-2.1	-4.6	-7.5	5.4	45.6	7.4
2	305- 355	5.1	-5.0	1.0	-3.4	0.0	0.0	6.2	1.0	-6.1	12.3	44.9	2.7
3	416- 419	-0.1	-4.7	5.6	-0.6	0.0	0.0	5.6	0.0	-4.8	10.4	66.0	5.3
4	851- 854	0.0	-5.6	1.2	0.0	0.0	0.0	1.2	0.0	-5.6	6.8	45.8	5.7
5	544- 548	0.0	-4.8	1.4	-0.1	0.0	0.0	1.4	0.0	-4.8	6.2	46.4	6.5
6	7064- 2774	0.0	3.8	1.7	0.4	0.0	0.0	3.8	1.7	0.0	3.9	49.3	11.6
7	3021- 3026	0.2	-8.0	-1.7	-0.2	0.0	0.0	0.2	-1.7	-8.0	8.3	48.0	4.8
8	3621- 3627	0.0	-0.6	-0.2	-0.1	0.0	0.0	0.0	-0.2	-0.6	0.6	94.5	156.5

Locations of the most critical sections for each component are provided in the following:

Comp. No.[1]	Section Location Inside Node x (in)	y (in)	Outside Node z (in)	x (in)
1	39.44	6.20	39.44	0.75
2	39.44	8.20	43.35	8.20
3	35.50	18.40	37.50	18.40
4	35.50	47.40	37.00	47.40
5	40.70	26.40	43.35	26.40
6	37.655	179.40	37.50	175.40
7	37.655	179.40	37.655	185.40
8	33.705	188.40	33.705	193.71

[1] Refer to Figure 2.10.2-33 for cask component identification.

Table 2.10.4-125 Critical $P_m + P_b$ Stress Summary; 30-Foot Bottom End Drop; Drop Orientation = 0 Degrees; 2-D Model; Condition 1

Condition 1: 100°F Ambient with Contents

Comp. No.[1]	Section Cut Node-Node	$P_m + P_b$ Stresses (ksi) S_x	S_y	S_z	S_{xy}	S_{yz}	S_{xz}	Principal Stresses (ksi) S1	S2	S3	S.I.	Allow. Stress	Margin of Safety
1	16- 20	-19.3	-2.2	-19.3	-0.1	0.0	0.0	-2.2	-19.3	-19.3	17.1	65.2	2.8
2	305- 355	15.2	-6.4	2.5	-3.4	0.0	0.0	15.7	2.5	-7.0	22.7	64.2	1.8
3	416- 419	-0.1	-10.5	4.2	-0.6	0.0	0.0	4.2	-0.1	-10.5	14.7	94.3	5.4
4	851- 854	-0.1	-5.7	1.2	0.0	0.0	0.0	1.2	-0.1	-5.7	6.9	65.5	8.5
5	544- 548	0.0	-5.6	1.1	-0.1	0.0	0.0	1.1	0.0	-5.6	6.7	66.4	8.9
6	7064- 2774	2.6	12.2	3.3	0.4	0.0	0.0	12.2	3.3	2.6	9.6	70.9	6.4
7	3021- 3026	0.1	12.2	-0.1	-0.2	0.0	0.0	12.2	0.1	-0.1	12.3	69.8	4.7
8	3801- 3807	-4.5	0.1	-4.5	0.0	0.0	0.0	0.1	-4.5	-4.5	4.7	135.0	27.7

Locations of the most critical sections for each component are provided in the following:

Comp. No.[1]	Section Location Inside Node x (in)	y (in)	Outside Node z (in)	x (in)
1	1.42	6.20	1.42	0.75
2	39.44	8.20	43.35	8.20
3	35.50	18.40	37.50	18.40
4	35.50	47.40	37.00	47.40
5	40.70	26.40	43.35	26.40
6	37.655	179.40	37.50	175.40
7	37.655	179.40	37.655	185.40
8	0.0	188.46	0.0	193.71

[1] Refer to Figure 2.10.2-33 for cask component identification.

Table 2.10.4-126 Critical P_m Stress Summary; 30-Foot Bottom End Drop; Drop Orientation = 0 Degrees; 2-D Model; Condition 2

Condition 2: -20°F Ambient with Contents

Comp. No.[1]	Section Cut Node-Node	P_m Stresses (ksi)						Principal Stresses (ksi)				Allow. Stress	Margin of Safety
		S_x	S_y	S_z	S_{xy}	S_{yz}	S_{xz}	S1	S2	S3	S.I.		
1	306- 310	-2.4	-7.4	-4.7	-1.1	0.0	0.0	-2.2	-4.7	-7.6	5.5	45.6	7.3
2	305- 355	5.3	-5.1	1.0	-3.5	0.0	0.0	6.3	1.0	-6.1	12.5	44.9	2.6
3	416- 419	0.0	-5.0	5.4	-0.7	0.0	0.0	5.4	0.1	-5.1	10.5	66.0	5.3
4	851- 854	0.0	-5.9	0.3	0.0	0.0	0.0	0.3	0.0	-5.9	6.2	45.8	6.4
5	544- 548	0.0	-4.9	1.4	-0.1	0.0	0.0	1.4	0.0	-4.9	6.3	46.4	6.4
6	7064- 2774	0.1	4.0	1.6	0.5	0.0	0.0	4.0	1.6	0.0	4.0	49.3	11.3
7	3021- 3026	0.2	-8.3	-1.7	-0.3	0.0	0.0	0.2	-1.7	-8.3	8.5	48.0	4.6
8	3621- 3627	0.0	-0.6	-0.2	-0.1	0.0	0.0	0.0	-0.2	-0.7	0.7	94.5	134.0

Locations of the most critical sections for each component are provided in the following:

Comp. No.[1]	Section Location			
	Inside Node			Outside Node
	x (in)	y (in)	z (in)	x (in)
1	39.44	6.20	39.44	0.75
2	39.44	8.20	43.35	8.20
3	35.50	18.40	37.50	18.40
4	35.50	47.40	37.00	47.40
5	40.70	26.40	43.35	26.40
6	37.655	179.40	37.50	175.40
7	37.655	179.40	37.655	185.40
8	33.705	188.40	33.705	193.716

[1] Refer to Figure 2.10.2-33 for cask component identification.

Table 2.10.4-127 Critical $P_m + P_b$ Stress Summary; 30-Foot Bottom End Drop; Drop Orientation = 0 Degrees; 2-D Model; Condition 2

Condition 2: -20°F Ambient with Contents

Comp. No.[1]	Section Cut Node-Node	$P_m + P_b$ Stresses (ksi) S_x	S_y	S_z	S_{xy}	S_{yz}	S_{xz}	Principal Stresses (ksi) S1	S2	S3	S.I.	Allow. Stress	Margin of Safety
1	16- 20	-19.8	-2.2	-19.8	-0.1	0.0	0.0	-2.2	-19.8	-19.8	17.6	65.2	2.7
2	305- 355	15.5	-6.5	2.5	-3.5	0.0	0.0	16.1	2.5	-7.0	23.1	64.2	1.8
3	416- 419	-0.1	-11.0	4.0	-0.7	0.0	0.0	4.0	0.0	-11.0	15.0	94.3	5.3
4	851- 854	0.0	-6.1	0.3	0.0	0.0	0.0	0.3	0.0	-6.1	6.3	65.5	9.4
5	544- 548	0.0	-5.7	1.1	-0.1	0.0	0.0	1.1	0.0	-5.7	6.8	66.4	8.8
6	7064- 2774	2.8	12.5	3.3	0.5	0.0	0.0	12.6	3.3	2.8	9.8	70.9	6.2
7	3051- 3056	-0.8	-12.6	0.4	0.2	0.0	0.0	0.4	-0.8	-12.6	12.9	69.8	4.4
8	3801- 3807	-4.8	0.1	-4.8	0.0	0.0	0.0	0.1	-4.8	-4.8	5.0	135.0	26.0

Locations of the most critical sections for each component are provided in the following:

Comp. No.[1]	Section Location Inside Node x (in)	y (in)	z (in)	Outside Node x (in)
1	1.42	6.20	1.42	0.75
2	39.44	8.20	43.35	8.20
3	35.50	18.40	37.50	18.40
4	35.50	47.40	37.00	47.40
5	40.70	26.40	43.35	26.40
6	37.655	179.40	37.50	175.40
7	35.50	179.40	35.50	185.40
8	0.0	188.46	0.0	193.71

[1] Refer to Figure 2.10.2-33 for cask component identification.

Table 2.10.4-128 Critical P_m Stress Summary; 30-Foot Bottom End Drop; Drop Orientation = 0 Degrees; 2-D Model; Condition 3

Condition 3: -20°F Ambient without Contents

Comp. No.[1]	Section Cut Node-Node	P_m Stresses (ksi) S_x	S_y	S_z	S_{xy}	S_{yz}	S_{xz}	Principal Stresses (ksi) S1	S2	S3	S.I.	Allow. Stress	Margin of Safety
1	306- 310	-2.4	-6.3	-4.5	-0.9	0.0	0.0	-2.2	-4.5	-6.5	4.3	45.6	9.6
2	305- 355	5.5	-4.2	0.9	-3.4	0.0	0.0	6.5	0.9	-5.3	11.8	44.9	2.8
3	416- 419	0.0	-4.5	5.5	-0.7	0.0	0.0	5.5	0.1	-4.6	10.1	66.0	5.5
4	866- 869	0.0	-5.3	0.3	0.0	0.0	0.0	0.3	0.0	-5.3	5.6	45.8	7.2
5	544- 548	0.0	-4.2	1.4	-0.1	0.0	0.0	1.4	0.0	-4.2	5.7	46.4	7.1
6	7064- 2774	0.1	4.0	1.5	0.4	0.0	0.0	4.0	1.5	0.0	4.0	49.7	11.3
7	3021- 3026	0.2	-8.2	-1.7	-0.3	0.0	0.0	0.2	-1.7	-8.2	8.4	48.0	4.7
8	3621- 3627	0.0	-0.6	-0.2	-0.1	0.0	0.0	0.0	-0.2	-0.6	0.6	94.5	156.5

Locations of the most critical sections for each component are provided in the following:

Comp. No.[1]	Section Location Inside Node x (in)	y (in)	Outside Node z (in)	x (in)
1	39.44	6.20	39.44	0.75
2	39.44	8.20	43.35	8.20
3	35.50	18.40	37.50	18.40
4	35.50	48.40	37.00	48.40
5	40.70	26.40	43.35	26.40
6	35.50	79.40	37.50	175.40
7	37.65	179.40	37.66	185.40
8	33.05	188.40	33.71	193.71

[1] Refer to Figure 2.10.2-33 for cask component identification.

Table 2.10.4-129 Critical $P_m + P_b$ Stress Summary; 30-Foot Bottom End Drop; Drop Orientation = 0 Degrees; 2-D Model; Condition 3

Condition 3: -20°F Ambient without Contents

Comp. No.[1]	Section Cut Node-Node		$P_m + P_b$ Stresses (ksi) S_x	S_y	S_z	S_{xy}	S_{yz}	S_{xz}	Principal Stresses (ksi) S1	S2	S3	S.I.	Allow. Stress	Margin of Safety
1	16-	20	-19.8	-1.5	-19.8	-0.1	0.0	0.0	-1.5	-19.8	-19.8	18.3	65.2	2.6
2	1-	5	21.4	-0.4	21.4	0.0	0.0	0.0	21.4	21.4	-0.4	21.7	64.2	2.0
3	416-	419	-0.1	10.7	4.0	-0.7	0.0	0.0	4.0	0.0	-10.7	14.7	94.3	5.4
4	851-	854	0.0	-5.5	0.3	0.0	0.0	0.0	0.3	0.0	-5.5	5.7	65.5	10.5
5	544-	548	0.0	-5.1	1.2	-0.1	0.0	0.0	1.2	0.0	-5.1	6.2	66.4	9.7
6	7064-	2774	2.7	12.7	3.4	0.4	0.0	0.0	12.7	3.4	2.7	10.0	70.9	6.1
7	3021-	3026	0.1	12.7	-0.1	-0.3	0.0	0.0	12.7	0.1	-0.1	12.8	69.8	4.5
8	3521-	3527	0.0	-3.6	0.9	0.1	0.0	0.0	0.9	0.0	-3.6	4.5	135.0	29.0

Locations of the most critical sections for each component are provided in the following:

Comp. No.[1]	Section Location Inside Node x (in)	y (in)	z (in)	Outside Node x (in)
1	1.42	6.20	1.42	0.75
2	0.0	14.40	0.0	8.20
3	35.50	18.40	37.50	18.40
4	35.50	47.40	37.00	47.40
5	40.70	26.40	43.35	26.40
6	37.66	179.40	37.50	175.40
7	37.66	179.40	37.66	185.40
8	39.56	188.40	39.56	193.71

[1] Refer to Figure 2.10.2-33 for cask component identification.

Table 2.10.4-130 Primary Stresses; 30-Foot Side Drop; Drop Orientation = 90 Degrees; 3-D Model; 0-Degree Circumferential Location; Condition 1

Condition 1: 100°F Ambient with Contents

Stress Points		Stress Components (ksi)						Principal Stresses (ksi)		
Section[1]	Node	S_x	S_y	S_z	S_{xy}	S_{yz}	S_{xz}	S1	S2	S3
A1	1130	-0.8	-1.9	-0.3	-0.1	0.1	0.0	-0.3	-0.7	-1.9
A2	1129	-1.0	-3.2	0.0	-0.1	0.1	0.0	0.0	-1.0	-3.2
A3	1128	-1.3	-4.4	0.3	0.0	0.1	0.0	0.3	-1.3	-4.4
B1	1185	-1.1	-5.3	0.0	-0.1	0.0	-0.2	0.0	-1.1	-5.3
B2	1184	-0.3	-6.0	0.0	-0.1	0.0	-0.2	0.1	-0.4	-6.0
B3	1183	0.4	-6.7	0.0	-0.1	0.1	-0.2	0.5	-0.1	-6.7
C1	90	5.9	-2.4	15.3	0.0	-0.8	1.5	15.6	5.7	-2.5
C2	80	-2.4	-7.0	6.6	-0.1	-0.5	0.0	6.6	-2.4	-7.0
C3	70	-3.5	-8.6	2.2	0.1	-0.4	-0.8	2.3	-3.6	-8.6
C4	60	-4.6	-9.5	0.3	0.2	-0.2	-0.5	0.4	-4.7	-9.5
C5	50	-9.8	-11.5	-0.1	0.2	-0.1	-0.1	-0.1	-9.8	-11.6
C6	40	-12.0	-12.5	-0.1	0.2	0.0	0.0	-0.1	-12.0	-12.6
D1	25	-4.9	-9.6	5.6	0.3	-0.1	0.1	5.6	-4.9	-9.6
D2	15	-9.8	-11.4	1.8	0.1	-0.1	-0.5	1.9	-9.8	-11.4
D3	5	-10.8	-11.6	0.4	0.2	0.0	-0.4	0.4	-10.8	-11.7
E1	35	-10.5	-11.4	4.9	0.2	-0.2	1.6	5.0	-10.6	-11.5
E2	34	-7.5	-11.5	2.1	0.3	0.0	1.8	2.5	-7.8	-11.5
E3	33	-8.0	-12.4	-0.3	0.3	0.0	1.5	0.0	-8.2	-12.4
E4	32	-8.6	-13.4	-2.8	0.4	0.0	0.9	-2.7	-8.7	-13.4
E5	31	-8.8	-14.3	-5.4	0.4	0.0	0.5	-5.3	-8.8	-14.3
F1	100	-1.3	-2.3	23.1	0.0	-1.2	2.3	23.4	-1.5	-2.4
F2	99	-1.5	-8.1	2.3	0.4	-0.9	2.5	3.5	-2.6	-8.2
F3	98	-0.5	-11.3	-11.0	0.8	-0.7	3.3	0.5	-10.7	-12.6
F4	97	0.6	-17.8	-36.7	1.3	-0.7	3.9	1.1	-17.8	-37.1
G1	94	0.8	-2.3	21.3	0.2	-0.5	3.3	21.8	0.3	-2.3
G2	93	1.5	-5.9	7.1	0.5	-0.3	2.4	8.0	0.6	-6.0
G3	92	1.5	-7.1	2.4	0.6	-0.3	1.0	3.1	0.9	-7.1
G4	91	0.7	-8.6	-3.1	0.7	-0.2	0.4	0.8	-3.1	-8.7
H1	330	-0.3	7.3	-4.6	-0.5	-1.6	0.1	7.6	-0.3	-4.8
H2	329	-0.1	9.1	-0.8	-0.6	-1.5	0.0	9.4	-0.2	-1.0

Table 2.10.4-130 Primary Stresses; 30-Foot Side Drop; Drop Orientation = 90 Degrees; 3-D Model; 0-Degree Circumferential Location; Condition 1 (continued)

Stress Points		Stress Components (ksi)						Principal Stresses (ksi)		
Section[1]	Node	S_x	S_y	S_z	S_{xy}	S_{yz}	S_{xz}	S1	S2	S3
H3	328	0.1	10.8	2.9	-0.7	-1.5	-0.2	11.1	2.7	0.0
H4	327	0.2	12.8	7.4	-0.8	-1.4	-0.5	13.1	7.1	0.1
I1	244	-0.2	-0.4	4.8	0.0	-0.8	0.0	5.0	-0.2	-0.5
I2	243	-0.1	1.2	7.4	-0.1	-0.7	0.0	7.5	1.2	-0.1
I3	242	-0.1	2.8	10.0	-0.2	-0.5	0.0	10.0	2.7	-0.1
I4	241	0.0	4.2	12.5	-0.3	-0.4	0.0	12.6	4.3	0.0
J1	550	-0.3	7.9	10.8	-0.6	-0.8	0.0	11.0	7.7	-0.4
J2	548	-0.2	10.3	12.7	-0.8	-0.8	0.0	12.9	10.2	-0.2
J3	547	-0.1	12.7	14.5	-0.9	-0.7	0.0	14.8	12.5	-0.1
K1	344	-0.1	-1.3	11.2	0.0	-0.5	0.0	11.2	-0.1	-1.3
K2	342	-0.1	2.5	13.0	-0.2	-0.4	0.0	13.0	2.5	-0.1
K3	341	0.0	6.0	14.7	-0.5	-0.3	0.0	14.7	6.0	-0.1
L1	740	-0.1	4.8	16.7	0.3	0.0	-0.2	16.7	4.8	-0.1
L2	738	-0.6	7.7	18.3	-1.2	0.0	0.0	18.3	7.8	-0.7
L3	737	0.2	10.7	20.0	-2.6	0.0	0.0	20.0	11.3	-0.4
M1	663	-1.3	-2.5	13.9	0.1	0.0	0.0	13.9	-1.3	-2.5
M2	63	0.5	9.3	19.3	2.2	0.0	0.0	19.3	9.8	0.0
N1	1877	-0.3	7.6	9.2	-0.6	1.0	0.0	9.6	7.2	-0.4
N2	1477	-0.2	10.4	10.9	-0.8	0.9	0.0	11.6	9.7	-0.2
N3	1277	-0.1	13.0	12.7	-1.0	0.9	0.0	13.8	12.0	-0.1
O1	647	-0.1	-1.7	12.7	0.1	0.4	0.0	12.7	-0.1	-1.7
O2	247	-0.1	2.4	14.6	-0.2	0.3	0.0	14.6	2.4	-0.1
O3	47	0.0	6.1	16.5	-0.5	0.2	0.0	16.5	6.2	-0.1
P1	1840	-0.3	7.6	-4.4	-0.5	1.6	0.0	7.8	-0.3	-4.6
P2	1640	-0.2	9.5	-1.2	-0.7	1.6	0.0	9.8	-0.2	-1.4
P3	1440	0.0	11.4	1.9	-0.7	1.5	0.1	11.7	1.7	0.0
P4	1240	0.2	13.5	5.6	-0.9	1.5	0.4	13.8	5.4	0.1
Q1	628	-0.3	0.4	8.4	-0.1	0.7	0.1	8.5	0.3	-0.3
Q2	428	-0.2	2.3	10.7	-0.2	0.6	0.1	10.7	2.3	-0.2
Q3	228	-0.1	4.1	12.9	-0.3	0.4	0.1	12.9	4.2	-0.1
Q4	28	0.0	5.9	15.2	-0.4	0.3	0.1	15.2	5.9	-0.1
R1	1816	-1.0	-7.5	5.9	0.5	1.1	-0.2	6.0	-1.0	-7.6
R2	1616	-2.0	-9.2	-1.2	0.6	1.0	-0.5	-0.9	-2.1	-9.4

Table 2.10.4-130 Primary Stresses; 30-Foot Side Drop; Drop Orientation = 90 Degrees; 3-D Model; 0-Degree Circumferential Location; Condition 1 (continued)

Stress Points		Stress Components (ksi)						Principal Stresses (ksi)		
Section[1]	Node	S_x	S_y	S_z	S_{xy}	S_{yz}	S_{xz}	S1	S2	S3
R3	1416	-4.8	-11.1	-7.4	0.7	0.7	-2.1	-3.6	-8.2	-11.4
R4	1216	-6.4	-13.1	-15.7	0.8	0.4	-4.3	-4.6	-13.1	-17.5
S1	616	2.8	-4.3	1.3	0.2	0.6	-0.2	2.8	1.3	-4.4
S2	416	0.4	-3.3	6.4	0.2	0.5	-0.1	6.4	0.4	-3.4
S3	216	0.4	-1.7	11.1	0.1	0.3	0.3	11.1	0.4	-1.7
S4	16	0.2	-0.2	15.6	0.0	0.2	0.2	15.6	0.2	-0.2
T1	811	-19.4	-21.7	-19.3	0.9	0.5	-5.4	-13.9	-21.4	-25.0
T2	611	-9.6	-14.7	-5.4	0.7	0.4	-4.5	-2.5	-12.2	-14.9
T3	411	-4.5	-10.8	2.5	0.5	0.3	-3.3	3.8	-5.7	-10.8
T4	211	-1.0	-7.6	9.5	0.5	0.2	-1.8	9.8	-1.3	-7.6
T5	11	0.2	-4.2	20.0	0.3	0.1	-0.9	20.0	0.2	-4.2
U1	43058	6.9	0.4	-0.1	0.2	0.0	-0.1	6.9	0.4	-0.1
U2	43057	3.3	-0.9	-0.4	0.2	0.0	-0.1	3.3	-0.4	-0.9
U3	43056	1.0	-2.0	-1.0	0.1	0.0	-0.1	1.0	-1.1	-2.0
U4	43055	-0.6	-2.9	-1.9	0.1	0.0	-0.4	-0.4	-2.0	-3.0
U5	43054	-2.3	-3.9	-2.7	0.1	-0.1	-1.3	-1.1	-3.8	-3.9
U6	43053	-4.1	-4.9	-3.2	0.1	-0.2	-2.7	-0.9	-4.9	-6.4
U7	43052	-7.0	-5.6	-1.6	0.0	-0.3	-3.4	0.0	-5.6	-8.6
U8	43051	-13.1	-7.3	0.2	-0.1	0.0	-0.1	0.2	-7.3	-13.1
V1	50024	2.4	-1.4	0.1	0.1	0.0	0.0	2.4	0.1	-1.4
V2	50023	-3.7	-4.3	-0.8	0.1	0.0	0.1	-0.8	-3.7	-4.3
V3	50022	-6.9	-6.0	-0.6	0.1	0.0	0.1	-0.6	-6.0	-6.9
V4	50021	-17.1	-9.5	0.6	-0.1	0.0	0.0	0.6	-9.5	-17.1
W1	43278	-2.1	-2.8	0.1	-0.1	-0.2	0.2	0.1	-2.1	-2.8
W2	43274	-1.4	-3.2	0.0	0.0	-0.2	0.2	0.0	-1.4	-3.2
W3	43271	-0.3	-1.8	0.0	0.0	-0.3	0.1	0.0	-0.4	-1.9
X1	50084	-0.7	-5.6	0.0	-0.1	0.0	0.2	0.1	-0.7	-5.6
X2	50083	-0.3	-5.9	0.0	-0.1	0.0	0.2	0.1	-0.4	-5.9
X3	50081	0.4	-6.6	0.0	0.0	-0.1	0.2	0.5	-0.1	-6.6

[1] Refer to Figure 2.10.2-34 for the identification of the representative sections.

Table 2.10.4-131 P_m Stresses; 30-Foot Side Drop; Drop Orientation = 90 Degrees; 3-D Model; 0-Degree Circumferential Location; Condition 1

Condition 1: 100°F Ambient with Contents

		Stress Components (ksi)						Principal Stresses (ksi)			
Section[1]	Node - Node	S_x	S_y	S_z	S_{xy}	S_{yz}	S_{zx}	S1	S2	S3	S.I.
A	1130 - 1128	-1.0	-3.2	0.0	-0.1	0.1	0.0	0.0	-1.0	-3.2	3.1
B	1185 - 1183	-0.3	-6.0	0.0	-0.1	0.0	-0.2	0.1	-0.4	-6.0	6.0
C	90 - 40	-5.9	-9.5	2.2	0.1	-0.3	-0.2	2.2	-5.9	-9.5	11.7
D	25 - 5	-8.8	-11.0	2.4	0.2	-0.1	-0.3	2.4	-8.8	-11.0	13.4
E	35 - 31	-8.5	-12.4	0.1	0.3	0.0	1.4	0.3	-8.6	-12.5	12.7
F	100 - 97	-0.8	-9.8	-5.2	0.6	-0.8	3.0	0.7	-6.4	-10.1	10.8
G	94 - 91	1.2	-6.2	6.2	0.5	-0.3	1.8	6.8	0.7	-6.2	13.0
H	330 - 327	0.0	10.0	1.2	-0.7	-1.5	-0.1	10.3	1.0	-0.1	10.4
I	244 - 241	-0.1	2.0	8.7	-0.1	-0.6	0.0	8.8	1.9	-0.1	8.9
J	550 - 547	-0.2	10.3	12.7	-0.8	-0.8	0.0	12.9	10.1	-0.2	13.2
K	344 - 341	-0.1	2.4	13.0	-0.2	-0.4	0.0	13.0	2.4	-0.1	13.1
L	740 - 737	-0.3	7.7	18.3	-1.2	0.0	0.0	18.3	7.9	-0.4	18.8
M	663 - 63	-0.4	3.4	16.6	1.1	0.0	0.0	16.6	3.7	-0.7	17.3
N	1877 - 1277	-0.2	10.3	10.9	-0.8	0.9	0.0	11.6	9.7	-0.2	11.9
O	647 - 47	-0.1	2.3	14.6	-0.2	0.3	0.0	14.6	2.3	-0.1	14.7
P	1840 - 1240	-0.1	10.5	0.4	-0.7	1.5	0.1	10.8	0.3	-0.2	11.0
Q	628 - 28	-0.2	3.2	11.8	-0.3	0.5	0.1	11.8	3.2	-0.2	12.0
R	1816 - 1216	-3.5	-10.2	-4.5	0.7	0.8	-1.6	-2.3	-5.5	-10.4	8.1
S	616 - 16	0.8	-2.4	8.6	0.1	0.4	0.1	8.7	0.8	-2.5	11.1
T	811 - 11	-6.2	-11.5	1.7	0.6	0.3	-3.2	2.9	-7.2	-11.6	14.5
U	43058 - 43051	-2.9	-3.8	-1.4	0.1	-0.1	-1.2	-0.7	-3.6	-3.8	3.0
V	50024 - 50021	-6.1	-5.2	-0.3	0.1	0.0	0.0	-0.3	-5.2	-6.1	5.7
W	43278 - 43271	-1.3	-2.7	0.0	0.0	-0.2	0.2	0.1	-1.3	-2.8	2.8
X	50084 - 50081	-0.1	-6.1	0.0	0.0	0.0	0.2	0.1	-0.3	-6.1	6.2

[1] Refer to Figure 2.10.2-34 for the identification of the representative sections.

Table 2.10.4-132 $P_m + P_b$ Stresses; 30-Foot Side Drop; Drop Orientation = 90 Degrees; 3-D Model; 0-Degree Circumferential Location; Condition 1

Condition 1: 100°F Ambient with Contents

		Stress Components (ksi)						Principal Stresses (ksi)			
Section[1]	Node - Node	S_x	S_y	S_z	S_{xy}	S_{yz}	S_{xz}	S1	S2	S3	S.I.
A O	1130 - 1128	-1.3	-4.4	0.3	0.0	0.1	0.0	0.3	-1.3	-4.4	4.7
B O	1185 - 1183	0.4	-6.7	0.0	-0.1	0.1	-0.2	0.5	-0.1	-6.7	7.2
C I	90 - 40	1.0	-5.7	7.3	0.0	-0.6	0.0	7.3	1.0	-5.7	13.1
D I	25 - 5	-5.9	-10.0	5.0	0.2	-0.1	-0.1	5.0	-5.9	-10.0	15.0
E I	35 - 31	-8.8	-10.8	5.3	0.3	-0.1	2.0	5.5	-9.1	-10.9	16.4
F O	100 - 97	0.3	-16.9	-32.8	1.2	-0.6	3.8	0.8	-16.9	-33.3	34.1
G I	94 - 91	1.3	-3.3	17.2	0.3	-0.5	3.4	17.9	0.6	-3.3	21.2
H O	330 - 327	0.2	12.7	7.1	-0.8	-1.4	-0.4	13.0	6.8	0.1	12.9
I O	244 - 241	0.0	4.3	12.6	-0.3	-0.4	0.0	12.6	4.3	0.0	12.6
J O	550 - 547	-0.1	12.7	14.6	-0.9	-0.7	0.0	14.8	12.5	-0.1	14.9
K O	344 - 341	0.0	6.1	14.7	-0.5	-0.3	0.0	14.7	6.1	-0.1	14.8
L O	740 - 737	-0.1	10.6	20.0	-2.6	0.0	0.0	20.0	11.2	-0.7	20.7
M O	663 - 63	0.5	9.3	19.3	2.2	0.0	0.0	19.3	9.8	0.0	19.3
N O	1877 - 1277	-0.1	13.0	12.7	-1.0	0.9	0.0	13.8	12.0	-0.1	13.9
O O	647 - 47	0.0	6.2	16.5	-0.5	0.2	0.0	16.5	6.2	-0.1	16.6
P O	1840 - 1240	0.2	13.4	5.4	-0.8	1.5	0.3	13.7	5.2	0.1	13.6
Q O	628 - 28	0.0	6.0	15.2	-0.4	0.3	0.1	15.2	6.0	0.0	15.2
R I	1816 - 1216	-0.5	-7.4	5.9	0.5	1.2	0.5	6.1	-0.5	-7.5	13.6
S O	616 - 16	-0.3	-0.3	15.8	0.0	0.2	0.4	15.8	-0.2	-0.3	16.1
T O	811 - 11	3.2	-3.4	19.6	0.3	0.1	-0.8	19.6	3.1	-3.4	23.0
U O	43058 - 43051	-11.9	-7.5	-1.7	-0.1	-0.2	-2.5	-1.1	-7.5	-12.5	11.4
V O	50024 - 50021	-14.8	-9.0	0.0	0.0	0.0	0.1	0.0	-9.0	-14.8	14.7
W I	43278 - 43271	-2.2	-3.2	0.1	-0.1	-0.1	0.2	0.1	-2.2	-3.3	3.4
X O	50084 - 50081	0.4	-6.6	0.0	0.0	-0.1	0.2	0.5	-0.1	-6.6	7.1

[1] Refer to Figure 2.10.2-34 for the identification of the representative sections.

Table 2.10.4-133 Critical P_m Stress Summary; 30-Foot Side Drop; Drop Orientation = 90 Degrees; 3-D Model; Condition 1

Condition 1: 100°F Ambient with Contents

Comp. No.[1]	Section Cut Node-Node	P_m Stresses (ksi) S_x	S_y	S_z	S_{xy}	S_{yz}	S_{xz}	Principal Stresses (ksi) S1	S2	S3	S.I.	Allow. Stress	Margin of Safety
1	25- 5	-8.8	-11.0	2.4	0.2	-0.1	-0.3	2.4	-8.8	-11.0	13.4	45.6	2.4
2	16140-16137	0.0	1.5	1.1	0.0	-12.4	-0.2	13.7	0.0	-11.1	24.8	44.9	0.8
3	14340-14337	-0.1	3.9	0.7	0.2	-15.4	-0.1	17.8	-0.1	-13.2	31.0	66.0	1.1
4	14520-14517	-0.1	3.7	0.9	0.0	-10.7	0.0	13.1	-0.1	-8.5	21.6	45.8	1.1
5	662- 62	0.2	2.9	16.7	-2.6	0.0	0.1	16.7	4.5	-1.4	18.0	46.4	1.6
6	401- 1	-10.7	-35.5	0.1	1.8	0.2	1.6	0.4	-10.8	-35.6	36.0	49.3	0.4
7	43071-43031	-12.0	-6.9	-0.5	-0.1	-0.2	-2.0	-0.1	-6.9	-12.3	12.2	48.0	2.9
8	51501-51504	-4.5	-3.3	3.2	0.2	0.1	0.1	3.2	-3.3	-4.6	7.8	94.5	11.1

Locations of the most critical sections for each component are provided in the following:

Comp. No.[1]	Section Location Inside Node x (in)	y (deg)	z (in)	Outside Node x (in)	y (deg)	z (in)
1	39.44	0.0	6.20	39.44	0.0	0.75
2	35.50	79.4	17.40	37.50	79.4	17.40
3	35.50	67.7	29.90	37.00	67.7	29.90
4	35.50	67.7	47.40	37.00	67.7	47.40
5	40.70	0.0	99.50	43.35	0.0	99.50
6	40.88	0.0	193.71	43.35	0.0	193.71
7	33.71	0.0	185.40	36.46	0.0	185.40
8	40.88	180.0	193.71	40.88	180.0	188.40

[1] Refer to Figure 2.10.2-33 for cask component identification.

Table 2.10.4-134 Critical $P_m + P_b$ Stress Summary; 30-Foot Side Drop; Drop Orientation = 90 Degrees; 3-D Model; Condition 1

Condition 1: 100°F Ambient with Contents

Comp. No.[1]	Section Cut Node-Node	$P_m + P_b$ Stresses (ksi) S_x	S_y	S_z	S_{xy}	S_{yz}	S_{xz}	Principal Stresses (ksi) S1	S2	S3	S.I.	Allow. Stress	Margin of Safety
1	25- 5	-5.9	-10.0	5.0	0.2	-0.1	-0.1	5.0	-5.9	-10.0	15.0	65.2	3.3
2	100- 97	0.3	-16.9	-32.8	1.2	-0.6	3.8	0.8	-16.9	-33.3	34.1	64.2	0.9
3	12350- 12347	-0.2	6.0	-0.7	0.0	-16.0	-0.1	18.9	-0.2	-13.7	32.6	94.3	1.9
4	14520- 14517	-0.2	6.4	1.9	0.0	-11.4	0.0	15.7	-0.2	-7.5	23.2	65.5	1.8
5	662- 62	0.5	8.5	19.6	-2.9	0.0	0.0	19.6	9.5	-0.4	20.0	66.4	2.3
6	403- 3	-7.4	-27.7	21.2	1.5	0.5	3.4	21.6	-7.7	-27.8	49.4	70.9	0.4
7	43001- 43008	-20.3	-7.0	10.0	-0.7	0.3	1.0	10.1	-7.0	-20.3	30.4	69.8	1.3
8	51501- 51504	-13.3	-7.9	4.9	0.7	0.0	0.8	4.9	-7.8	-13.5	18.4	135.0	6.3

Locations of the most critical sections for each component are provided in the following:

Comp. No.[1]	Section Location Inside Node x (in)	y (deg)	z (in)	Outside Node x (in)	y (deg)	z (in)
1	39.44	0.0	6.20	39.44	0.0	0.75
2	35.50	0.0	15.00	37.50	0.0	15.00
3	35.50	56.5	30.40	37.00	56.5	30.40
4	35.50	67.7	142.40	37.00	67.7	142.40
5	40.70	0.0	99.50	43.35	0.0	99.50
6	40.88	0.0	190.15	43.35	0.0	190.15
7	39.53	0.0	185.40	39.53	0.0	179.40
8	40.88	180.0	193.71	40.88	180.0	188.40

[1] Refer to Figure 2.10.2-33 for cask component identification.

Table 2.10.4-135 P_m Stresses; 30-Foot Side Drop; Drop Orientation = 90 Degrees; 3-D Model; 45.9-Degree Circumferential Location; Condition 1

Condition 1: 100°F Ambient with Contents

		Stress Components (ksi)						Principal Stresses (ksi)			
Section[1]	Node - Node	S_x	S_y	S_z	S_{xy}	S_{yz}	S_{xz}	S1	S2	S3	S.I.
A	1130 - 1128	-1.0	-3.2	0.0	-0.1	0.1	0.0	0.0	-1.0	-3.2	3.1
B	1185 - 1183	-0.3	-6.0	0.0	-0.1	0.0	-0.2	0.1	-0.4	-6.0	6.0
C	10090 - 10040	-4.1	-5.9	0.9	-1.1	-2.4	0.0	1.7	-3.7	-7.1	8.8
D	10025 - 10005	-5.2	-8.2	1.7	-0.2	-0.9	-0.2	1.8	-5.2	-8.2	10.0
E	10035 - 10031	-5.3	-7.8	0.3	0.8	-1.7	1.1	0.8	-5.1	-8.5	9.3
F	10100 - 10097	-0.4	-4.6	-2.5	-0.1	-9.7	1.5	6.5	-0.6	-13.4	19.9
G	10094 - 10091	0.4	-2.5	3.8	-0.3	-4.2	0.7	6.0	0.3	-4.6	10.7
H	10330 - 10327	0.0	6.8	0.7	0.4	-13.4	-0.1	17.5	0.0	-10.0	27.5
I	10244 - 10241	0.0	1.5	4.9	-0.1	-5.1	0.0	8.5	0.0	-2.1	10.6
J	10550 - 10547	0.0	6.7	6.3	0.0	-7.4	0.0	13.9	0.0	-0.9	14.9
K	10344 - 10341	0.0	1.6	6.4	-0.1	-3.3	0.0	8.0	0.1	-0.1	8.1
L	10740 - 10737	0.1	5.7	9.9	0.1	0.1	0.0	10.0	5.7	0.1	9.8
M	10663 - 10063	0.1	2.0	7.6	-0.6	-0.2	0.0	7.7	2.2	-0.1	7.8
N	11877 - 11277	0.0	6.7	5.4	0.0	8.4	0.0	14.5	0.0	-2.4	16.9
O	10647 - 10047	0.0	1.6	7.1	-0.1	2.5	0.0	8.1	0.6	0.0	8.1
P	11840 - 11240	0.0	7.0	0.7	0.4	13.5	0.0	17.7	0.0	-10.0	27.7
Q	10628 - 10028	0.0	2.0	6.0	-0.1	4.1	0.0	8.6	0.0	-0.5	9.1
R	11816 - 11216	-1.4	-3.3	-1.7	1.9	8.8	-0.8	6.4	-1.0	-11.7	18.1
S	10616 - 10016	-0.3	-1.2	5.0	-1.3	3.7	0.1	6.7	0.2	-3.4	10.1
T	10811 - 10011	-3.4	-6.6	1.2	1.8	4.7	-1.5	3.5	-2.6	-9.7	13.1
U	44558 - 44551	-2.3	-2.7	-1.2	-0.1	-0.1	-0.9	-0.7	-2.6	-2.9	2.2
V	50524 - 50521	-3.1	-3.4	-0.2	0.9	0.2	-0.1	-0.2	-2.3	-4.2	3.9
W	43278 - 43271	-1.3	-2.7	0.0	0.0	-0.2	0.2	0.1	-1.3	-2.8	2.8
X	50084 - 50081	-0.1	-6.1	0.0	0.0	0.0	0.2	0.1	-0.3	-6.1	6.2

[1] Refer to Figure 2.10.2-34 for the identification of the representative sections.

Table 2.10.4-136 $P_m + P_b$ Stresses; 30-Foot Side Drop; Drop Orientation = 90 Degrees; 3-D Model; 45.9-Degree Circumferential Location; Condition 1

Condition 1: 100°F Ambient with Contents

Section[1]	Node - Node	Stress Components (ksi)						Principal Stresses (ksi)			
		S_x	S_y	S_z	S_{xy}	S_{yz}	S_{xz}	S1	S2	S3	S.I.
A O	1130 - 1128	-1.3	-4.4	0.3	0.0	0.1	0.0	0.3	-1.3	-4.4	4.7
B O	1185 - 1183	0.4	-6.7	0.0	-0.1	0.1	-0.2	0.5	-0.1	-6.7	7.2
C I	10090 - 10040	-0.3	-3.1	3.2	-4.3	-5.5	0.0	7.1	0.8	-8.1	15.3
D I	10025 - 10005	-2.9	-6.6	3.4	-1.3	-1.8	0.1	3.8	-2.6	-7.3	11.1
E I	10035 - 10031	-5.8	-7.1	3.3	1.9	-2.9	1.6	4.1	-4.4	-9.3	13.4
F I	10100 - 10097	-1.0	-1.4	9.9	-0.2	-11.7	1.0	17.3	-1.0	-8.8	26.1
G I	10094 - 10091	0.5	-2.0	5.5	-0.4	-6.6	1.3	9.5	0.4	-5.9	15.4
H I	10330 - 10327	-0.1	6.1	-2.2	0.0	-14.5	0.1	17.0	-0.1	-13.2	30.2
I I	10244 - 10241	-0.1	1.2	3.3	-0.2	-6.8	0.0	9.2	-0.1	-4.7	13.9
J I	10550 - 10547	-0.1	6.4	6.0	-0.1	-8.2	0.0	14.4	-0.1	-2.0	16.3
K I	10344 - 10341	0.0	2.0	6.2	-0.2	-4.2	0.0	8.8	0.0	-0.6	9.4
L O	10740 - 10737	0.2	6.9	10.6	0.2	0.2	0.0	10.6	6.9	0.2	10.4
M O	10663 - 10063	-0.1	0.6	7.4	-0.9	-0.2	0.0	7.4	1.2	-0.8	8.1
N I	11877 - 11277	-0.1	6.6	5.2	-0.1	9.2	0.0	15.2	-0.1	-3.4	18.5
O I	10647 - 10047	0.0	2.0	7.0	-0.2	3.4	0.0	8.7	0.3	-0.1	8.8
P I	11840 - 11240	-0.1	6.6	-1.4	0.0	14.5	-0.1	17.6	-0.1	-12.4	30.0
Q I	10628 - 10028	-0.1	2.2	5.4	-0.2	5.7	0.0	9.7	-0.1	-2.1	11.9
R I	11816 - 11216	-0.3	-2.0	1.9	0.0	10.6	0.1	10.7	-0.3	-10.8	21.5
S I	10616 - 10016	-0.4	-2.9	-2.0	-3.0	5.6	0.3	4.1	-0.5	-8.7	12.8
T I	10811 - 10011	-8.6	-11.2	-10.7	4.9	8.7	-2.9	-1.9	-6.7	-21.9	20.0
U O	44558 - 44551	-8.6	-6.1	-1.4	1.3	-0.3	-1.8	-0.9	-5.8	-9.4	8.5
V O	50524 - 50521	-9.0	-6.7	0.1	2.9	0.2	-0.1	0.1	-4.7	-11.0	11.1
W I	43278 - 43271	-2.2	-3.2	0.1	-0.1	-0.1	0.2	0.1	-2.2	-3.3	3.4
X O	50084 - 50081	0.4	-6.6	0.0	0.0	-0.1	0.2	0.5	-0.1	-6.6	7.1

[1] Refer to Figure 2.10.2-34 for the identification of the representative sections.

Table 2.10.4-137 P_m Stresses; 30-Foot Side Drop; Drop Orientation = 90 Degrees; 3-D Model; 91.7-Degree Circumferential Location; Condition 1

Condition 1: 100°F Ambient with Contents

Section[1]	Node - Node	Stress Components (ksi) S_x	S_y	S_z	S_{xy}	S_{yz}	S_{xz}	Principal Stresses (ksi) S1	S2	S3	S.I.
A	1130 - 1128	-1.0	-3.2	0.0	-0.1	0.1	0.0	0.0	-1.0	-3.2	3.1
B	1185 - 1183	-0.3	-6.0	0.0	-0.1	0.0	-0.2	0.1	-0.4	-6.0	6.0
C	18090 - 18040	-0.6	-0.4	-0.7	-1.5	-2.7	0.1	2.6	-0.7	-3.6	6.2
D	18025 - 18005	0.1	-2.0	0.4	-2.3	-2.0	0.0	2.4	0.3	-4.1	6.5
E	18035 - 18031	0.3	-0.1	0.2	0.8	-4.0	0.1	4.1	0.3	-4.1	8.2
F	18100 - 18097	0.1	2.3	1.9	-0.1	-11.6	-0.8	13.7	0.2	-9.5	23.2
G	18094 - 18091	-0.5	1.7	-1.1	-0.4	-4.9	-0.6	5.4	-0.4	-4.9	10.3
H	18330 - 18327	0.0	0.4	0.2	0.6	-14.1	0.0	14.4	0.0	-13.8	28.1
I	18244 - 18241	0.0	0.5	-1.9	0.0	-4.5	-0.1	4.0	0.0	-5.3	9.3
J	18550 - 18547	0.1	0.7	-3.2	0.1	-8.2	0.0	7.2	0.1	-9.7	16.9
K	18344 - 18341	0.0	0.1	-3.6	0.1	-2.9	0.0	1.7	0.0	-5.2	6.9
L	19908 - 19308	0.6	0.8	-4.9	0.8	0.8	0.0	1.6	-0.1	-5.0	6.6
M	18663 - 18063	0.4	-0.1	-4.7	0.5	-0.3	0.0	0.7	-0.4	-4.7	5.4
N	19877 - 19277	0.1	0.7	-2.7	0.1	8.9	0.0	8.1	0.1	-10.1	18.2
O	18647 - 18047	0.0	0.1	-4.0	0.1	2.4	0.0	1.2	0.0	-5.1	6.3
P	19840 - 19240	0.1	0.4	0.5	0.6	13.8	0.0	14.3	0.1	-13.4	27.7
Q	18628 - 18028	0.0	0.4	-3.0	0.0	3.9	0.0	2.9	0.0	-5.5	8.4
R	19816 - 19216	1.7	5.3	1.2	3.1	9.8	0.7	13.9	1.2	-7.1	21.0
S	18616 - 18016	-1.2	1.7	-1.9	-0.5	3.9	0.2	4.2	-1.2	-4.5	8.7
T	18811 - 18011	0.5	2.0	-0.3	2.0	5.8	1.0	7.5	-0.1	-5.1	12.6
U	45758 - 45751	-1.4	-1.9	-2.4	-0.5	0.2	0.2	-1.1	-1.9	-2.6	1.5
V	50924 - 50921	-0.1	-1.7	-0.5	-0.3	0.2	-0.1	0.0	-0.5	-1.8	1.8
W	43278 - 43271	-1.3	-2.7	0.0	0.0	-0.2	0.2	0.1	-1.3	-2.8	2.8
X	50084 - 50081	-0.1	-6.1	0.0	0.0	0.0	0.2	0.1	-0.3	-6.1	6.2

[1] Refer to Figure 2.10.2-34 for the identification of the representative sections.

Table 2.10.4-138 $P_m + P_b$ Stresses; 30-Foot Side Drop; Drop Orientation = 90 Degrees; 3-D Model; 91.7-Degree Circumferential Location; Condition 1

Condition 1: 100°F Ambient with Contents

Section[1]	Node - Node	Stress Components (ksi) S_x	S_y	S_z	S_{xy}	S_{yz}	S_{xz}	Principal Stresses (ksi) S1	S2	S3	S.I.
A O	1130 - 1128	-1.3	-4.4	0.3	0.0	0.1	0.0	0.3	-1.3	-4.4	4.7
B O	1185 - 1183	0.4	-6.7	0.0	-0.1	0.1	-0.2	0.5	-0.1	-6.7	7.2
C I	18090 - 18040	-1.4	0.4	-2.4	-4.1	-6.1	0.0	6.6	-1.7	-8.3	14.9
D I	18025 - 18005	0.3	-0.9	0.9	-3.5	-3.8	0.0	5.1	0.6	-5.4	10.5
E I	18035 - 18031	0.5	-0.2	1.2	2.2	-4.9	0.0	5.8	0.6	-5.0	10.8
F I	18100 - 18097	0.3	-0.2	-7.7	-0.2	-12.4	-0.6	9.0	0.4	-16.9	25.9
G I	18094 - 18091	-0.4	-0.1	-8.2	-0.5	-5.6	-1.2	2.7	-0.3	-11.2	13.9
H O	18330 - 18327	0.1	-0.9	-0.8	1.1	-14.4	0.0	13.6	0.1	-15.2	28.8
I O	18244 - 18241	0.0	-0.8	-3.1	0.0	-4.8	-0.1	3.0	0.0	-6.9	9.9
J I	18550 - 18547	0.1	3.1	-2.2	0.1	-8.1	0.0	9.0	0.1	-8.1	17.1
K I	18344 - 18341	0.0	2.8	-2.3	0.1	-2.7	0.0	4.0	0.0	-3.4	7.4
L I	19908 - 19308	0.9	5.4	-3.3	0.3	0.8	0.0	5.5	0.9	-3.4	8.9
M I	18663 - 18063	0.9	4.3	-3.0	0.2	-0.3	0.0	4.3	0.9	-3.0	7.3
N I	19877 - 19277	0.1	3.2	-1.7	0.1	8.8	0.0	9.9	0.1	-8.4	18.2
O I	18647 - 18047	0.0	3.1	-2.6	0.1	2.2	0.0	3.8	0.0	-3.3	7.1
P O	19840 - 19240	0.1	-1.2	-1.1	1.1	14.2	-0.1	13.1	0.1	-15.4	28.5
Q O	18628 - 18028	0.0	-1.5	-4.5	0.0	4.2	0.0	1.5	0.0	-7.5	9.0
R O	19816 - 19216	3.3	7.1	8.5	6.4	9.5	1.9	19.4	3.3	-3.8	23.2
S I	18616 - 18016	-2.6	0.9	-5.2	-1.2	4.1	0.8	3.0	-2.3	-7.6	10.6
T I	18811 - 18011	1.5	2.7	-0.1	5.0	7.8	1.8	11.7	-0.5	-7.1	18.8
U I	45758 - 45751	-3.8	-2.3	-3.5	-1.7	0.2	1.0	-1.2	-3.1	-5.4	4.2
V I	50924 - 50921	0.0	-1.3	-1.4	-1.5	0.2	-0.2	1.0	-1.4	-2.3	3.3
W I	43278 - 43271	-2.2	-3.2	0.1	-0.1	-0.1	0.2	0.1	-2.2	-3.3	3.4
X O	50084 - 50081	0.4	-6.6	0.0	0.0	-0.1	0.2	0.5	-0.1	-6.6	7.1

[1] Refer to Figure 2.10.2-34 for the identification of the representative sections.

Table 2.10.4-139 P_m Stresses; 30-Foot Side Drop; Drop Orientation = 90 Degrees; 3-D Model; 180-Degree Circumferential Location; Condition 1

Condition 1: 100°F Ambient with Contents

Section[1]	Node - Node	Stress Components (ksi)						Principal Stresses (ksi)			
		S_x	S_y	S_z	S_{xy}	S_{yz}	S_{zx}	S1	S2	S3	S.I.
A	1130 - 1128	-1.0	-3.2	0.0	-0.1	0.1	0.0	0.0	-1.0	-3.2	3.1
B	1185 - 1183	-0.3	-6.0	0.0	-0.1	0.0	-0.2	0.1	-0.4	-6.0	6.0
C	30090 - 30040	0.0	2.4	-0.9	0.3	-0.3	0.0	2.5	-0.1	-0.9	3.4
D	30025 - 30005	-2.4	4.2	-0.4	0.3	-0.2	0.0	4.2	-0.5	-2.4	6.6
E	30035 - 30031	1.6	3.0	-0.8	0.3	-0.6	-1.3	3.3	1.9	-1.4	4.7
F	30100 - 30097	0.2	2.5	1.7	0.4	-1.1	-1.4	3.6	1.3	-0.7	4.3
G	30094 - 30091	-0.2	0.6	-4.0	0.1	-0.6	-0.2	0.6	-0.2	-4.1	4.7
H	30330 - 30327	-0.2	-5.4	-1.9	-0.7	-1.3	0.0	0.0	-1.5	-6.0	5.9
I	30244 - 30241	0.0	-0.9	-5.1	-0.1	-0.4	0.0	0.0	-0.9	-5.2	5.2
J	30550 - 30547	-0.4	-4.4	-7.2	-0.6	-0.8	-0.1	-0.4	-4.2	-7.4	7.1
K	30344 - 30341	0.0	-0.9	-6.3	-0.1	-0.2	0.0	0.0	-0.9	-6.3	6.3
L	30740 - 30737	0.0	-4.0	-10.4	0.4	0.0	0.0	0.1	-4.1	-10.4	10.5
M	30663 - 30063	-0.4	-0.6	-7.2	-1.3	0.0	0.0	0.7	-1.8	-7.2	8.0
N	31877 - 31277	-0.4	-4.4	-5.6	-0.6	0.9	0.0	-0.3	-4.0	-6.0	5.7
O	30647 - 30047	0.0	-0.9	-6.9	-0.1	0.1	0.0	0.0	-0.9	-6.9	6.9
P	31840 - 31240	-0.4	-5.7	-1.0	-0.8	1.3	-0.1	-0.1	-0.8	-6.2	6.1
Q	30628 - 30028	0.0	-1.5	-6.1	-0.2	0.3	-0.1	0.0	-1.5	-6.1	6.2
R	31816 - 31216	1.3	6.6	1.3	1.1	0.8	1.3	7.0	2.2	-0.1	7.0
S	30616 - 30016	-0.3	4.3	-5.1	0.7	0.4	0.1	4.4	-0.4	-5.1	9.6
T	30811 - 30011	0.4	9.6	-2.1	1.6	0.6	1.1	9.9	0.5	-2.5	12.4
U	47558 - 47551	-3.1	-3.8	-3.7	-0.1	0.0	0.2	-3.0	-3.7	-3.9	0.9
V	51524 - 51521	-4.5	-3.5	-0.2	-0.1	0.0	0.4	-0.2	-3.5	-4.6	4.4
W	43278 - 43271	-1.3	-2.7	0.0	0.0	-0.2	0.2	0.1	-1.3	-2.8	2.8
X	50084 - 50081	-0.1	-6.1	0.0	0.0	0.0	0.2	0.1	-0.3	-6.1	6.2

[1] Refer to Figure 2.10.2-34 for the identification of the representative sections.

Table 2.10.4-140 $P_m + P_b$ Stresses; 30-Foot Side Drop; Drop Orientation = 90 Degrees; 3-D Model; 180-Degree Circumferential Location; Condition 1

Condition 1: 100°F Ambient with Contents

Section[1]	Node - Node	Stress Components (ksi) S_x	S_y	S_z	S_{xy}	S_{yz}	S_{zx}	Principal Stresses (ksi) S1	S2	S3	S.I.
A O	1130 - 1128	-1.3	-4.4	0.3	0.0	0.1	0.0	0.3	-1.3	-4.4	4.7
B O	1185 - 1183	0.4	-6.7	0.0	-0.1	0.1	-0.2	0.5	-0.1	-6.7	7.2
C I	30090 - 30040	-2.1	0.5	-3.0	0.1	-0.6	-0.2	0.6	-2.1	-3.1	3.7
D O	30025 - 30005	-1.9	5.7	-0.7	0.2	-0.1	0.8	5.7	-0.3	-2.3	8.0
E O	30035 - 30031	-0.4	1.6	-3.4	0.3	-0.7	-0.7	1.7	-0.3	-3.6	5.3
F O	30100 - 30097	-0.1	5.2	12.1	0.9	-1.2	-1.5	12.5	5.1	-0.4	12.9
G I	30094 - 30091	-0.1	0.3	-4.6	0.0	-0.5	-0.4	0.3	-0.1	-4.7	5.0
H O	30330 - 30327	-0.2	-5.2	-3.3	-0.7	-1.5	0.1	0.0	-2.6	-6.1	6.0
I O	30244 - 30241	0.0	-0.4	-5.6	-0.1	-0.5	0.0	0.0	-0.3	-5.6	5.7
J I	30550 - 30547	-0.3	-5.9	-7.6	-0.8	-0.7	-0.1	-0.2	-5.8	-7.8	7.7
K I	30344 - 30341	-0.1	-2.3	-6.7	-0.3	-0.2	0.0	0.0	-2.4	-6.7	6.7
L O	31908 - 31308	-0.9	0.0	-8.5	-4.1	0.1	0.0	3.7	-4.6	-8.5	12.2
M O	30663 - 30063	-0.3	1.9	-6.5	-2.1	0.0	0.0	3.2	-1.5	-6.5	9.7
N I	31877 - 31277	-0.2	-6.0	-5.9	-0.8	0.8	0.1	-0.1	-5.2	-6.8	6.7
O I	30647 - 30047	-0.1	-2.5	-7.4	-0.4	0.1	0.0	0.0	-2.5	-7.4	7.3
P I	31840 - 31240	-0.1	-5.9	0.9	-0.9	1.2	0.0	1.1	0.0	-6.3	7.4
Q O	30628 - 30028	0.0	-0.9	-7.4	-0.1	0.4	-0.1	0.0	-0.9	-7.4	7.4
R I	31816 - 31216	0.3	4.8	-4.2	0.7	1.0	0.3	5.0	0.2	-4.3	9.3
S O	30616 - 30016	0.1	3.4	-10.0	0.5	0.4	0.2	3.5	0.1	-10.0	13.5
T O	30811 - 30011	-1.0	7.0	-10.5	1.1	0.6	-0.5	7.2	-1.1	-10.5	17.7
U O	47558 - 47551	3.6	1.5	-1.0	-0.3	0.3	-1.2	4.0	1.5	-1.3	5.3
V I	51524 - 51521	-11.7	-8.5	-0.5	0.1	0.0	0.4	-0.5	-8.5	-11.7	11.2
W I	43278 - 43271	-2.2	-3.2	0.1	-0.1	-0.1	0.2	0.1	-2.2	-3.3	3.4
X O	50084 - 50081	0.4	-6.6	0.0	0.0	-0.1	0.2	0.5	-0.1	-6.6	7.1

[1] Refer to Figure 2.10.2-34 for the identification of the representative sections.

Table 2.10.4-141 Primary Stresses; 30-Foot Top Corner Drop; Drop Orientation = 24 Degrees; 3-D Top Model; 0-Degree Circumferential Location; Condition 1

Condition 1: 100°F Ambient with Contents

Stress Points		Stress Components (ksi)						Principal Stresses (ksi)		
Section[1]	Node	S_x	S_y	S_z	S_{xy}	S_{yz}	S_{zx}	S1	S2	S3
A1	1949	1.7	2.7	-0.3	0.0	-0.1	0.3	2.7	1.8	-0.4
A2	1950	1.0	1.7	-0.3	0.0	-0.1	0.3	1.8	1.0	-0.4
A3	1951	-0.4	-0.3	0.4	0.0	0.1	0.2	0.4	-0.3	-0.4
B1	1952	0.0	0.0	-0.5	0.0	0.1	0.1	0.1	0.0	-0.6
B2	93	-1.6	-2.5	1.0	-0.1	0.0	0.3	1.0	-1.6	-2.5
C1	1925	-0.2	0.0	1.3	-0.1	-0.1	0.0	1.3	0.0	-0.2
C2	1926	0.3	-0.3	0.0	0.0	-0.1	-0.3	0.5	-0.2	-0.3
C3	1927	0.5	-0.2	-0.1	0.0	0.0	-0.2	0.6	-0.2	-0.2
D1	683	-0.1	-0.5	-0.5	0.1	0.0	0.0	-0.1	-0.5	-0.5
D2	85	-0.2	-0.9	-0.4	0.2	0.0	0.0	-0.1	-0.4	-1.0
E1	682	0.4	-0.3	-0.6	0.1	0.0	0.2	0.5	-0.3	-0.6
E2	82	0.4	-0.1	0.6	0.1	0.1	0.2	0.7	0.3	-0.1
F1	1925	-0.2	0.0	1.3	-0.1	-0.1	0.0	1.3	0.0	-0.2
F2	1325	-1.2	-2.2	-5.6	0.1	-0.1	0.4	-1.2	-2.2	-5.7
G1	680	-0.4	0.0	1.2	0.0	0.0	0.6	1.4	0.0	-0.6
G2	80	0.3	-0.1	-0.2	0.0	0.0	0.0	0.3	-0.1	-0.2
H1	1921	0.0	3.6	-3.9	-0.2	-0.4	0.1	3.6	0.0	-3.9
H2	1321	-0.1	5.3	-1.2	-0.3	-0.3	0.0	5.3	-0.1	-1.2
I1	676	0.0	-0.3	-0.1	0.0	-0.1	0.0	0.0	-0.1	-0.3
I2	76	0.0	1.4	1.1	-0.1	0.0	0.0	1.4	1.1	0.0
J1	1916	-0.1	3.3	-1.4	-0.2	-0.2	0.0	3.4	-0.1	-1.4
J2	1316	-0.1	6.4	0.1	-0.5	-0.1	0.0	6.4	0.1	-0.1
K1	671	0.0	-0.7	-0.9	0.0	0.0	0.0	0.0	-0.7	-0.9
K2	71	0.0	2.1	0.5	-0.2	0.1	0.0	2.1	0.5	0.0
L1	1908	-0.7	1.8	-3.9	-0.2	0.3	0.0	1.9	-0.7	-3.9
L2	1308	0.1	7.9	-1.6	1.7	0.3	0.0	8.3	-0.2	-1.6
M1	663	-0.4	-0.9	-3.2	0.0	0.2	0.0	-0.4	-0.8	-3.2
M2	63	0.2	2.7	-1.8	0.7	0.2	0.0	2.9	0.0	-1.8

Table 2.10.4-141 Primary Stresses; 30-Foot Top Corner Drop; Drop Orientation = 24 Degrees; 3-D Top Model; 0-Degree Circumferential Location; Condition 1 (continued)

Stress Points		Stress Components (ksi)						Principal Stresses (ksi)		
Section[1]	Node	S_x	S_y	S_z	S_{xy}	S_{yz}	S_{zx}	S1	S2	S3
N1	1877	-0.1	2.5	-12.2	-0.2	0.7	0.0	2.6	-0.2	-12.3
N2	1477	-0.1	4.9	-11.3	-0.4	0.7	0.0	4.9	-0.1	-11.3
N3	1277	0.0	7.1	-10.4	-0.5	0.6	0.0	7.2	-0.1	-10.4
O1	647	-0.1	-0.3	-6.5	0.0	0.3	0.0	-0.1	-0.3	-6.5
O2	247	0.0	1.0	-6.0	-0.1	0.2	0.0	1.0	0.0	-6.0
O3	47	0.0	2.3	-5.6	-0.2	0.2	0.0	2.3	0.0	-5.6
P1	1840	-0.3	3.9	-13.7	-0.3	1.0	0.1	4.0	-0.3	-13.8
P2	1640	-0.5	3.8	-16.5	-0.3	0.9	0.0	3.9	-0.5	-16.6
P3	1440	-0.5	3.8	-19.1	-0.3	0.8	-0.6	3.9	-0.5	-19.1
P4	1240	-0.5	3.1	-24.5	-0.2	0.7	-1.3	3.1	-0.4	-24.6
Q1	628	-0.2	2.7	-7.9	-0.2	0.4	0.1	2.8	-0.2	-7.9
Q2	428	-0.1	3.1	-8.2	-0.2	0.3	0.1	3.1	-0.1	-8.3
Q3	228	0.0	3.4	-8.6	-0.3	0.3	0.1	3.4	-0.1	-8.6
Q4	28	0.0	3.7	-8.9	-0.3	0.2	0.0	3.7	0.0	-8.9
R1	1816	0.0	-3.3	-29.9	0.3	0.6	0.1	0.0	-3.3	-29.9
R2	1616	0.1	-1.1	-22.3	0.2	0.6	0.2	0.1	-1.1	-22.3
R3	1416	-0.2	0.9	-15.0	0.1	0.6	0.9	0.9	-0.2	-15.1
R4	1216	6.1	4.7	-8.1	0.2	0.4	0.9	6.2	4.6	-8.1
S1	616	-8.8	-5.4	-30.4	-0.3	0.7	4.0	-5.4	-8.1	-31.1
S2	416	-8.8	-1.4	-14.6	-0.5	0.2	-0.7	-1.4	-8.7	-14.7
S3	216	-3.1	3.1	-3.4	-0.4	0.1	-1.2	3.1	-2.1	-4.4
S4	16	-1.2	7.0	9.8	-0.6	0.0	-0.9	9.9	7.1	-1.3
T1	811	-0.5	-5.2	-4.3	0.7	0.5	0.8	-0.3	-4.3	-5.5
T2	611	0.9	-5.6	-7.8	0.6	0.3	-0.4	0.9	-5.6	-7.9
T3	411	0.6	-5.5	-7.6	0.5	0.3	-0.4	0.7	-5.5	-7.7
T4	211	0.8	-5.2	-6.8	0.4	0.2	-0.4	0.8	-5.2	-6.9
T5	11	0.8	-4.6	-5.1	0.4	0.1	-0.2	0.9	-4.6	-5.2
U1	43058	2.1	8.2	-14.5	-0.7	0.6	3.2	8.3	2.6	-15.1
U2	43057	3.4	6.2	-13.2	-0.5	0.1	4.4	6.4	4.4	-14.3
U3	43056	2.5	4.0	-11.8	-0.3	0.4	5.9	4.6	4.0	-13.9
U4	43055	1.8	1.6	-11.5	-0.1	0.4	5.9	4.0	1.6	-13.7
U5	43054	0.7	-1.0	-11.5	0.1	0.3	5.3	2.7	-1.0	-13.4
U6	43053	-1.0	-3.1	-9.2	0.2	0.2	3.7	0.5	-3.1	-10.6

Table 2.10.4-141 Primary Stresses; 30-Foot Top Corner Drop; Drop Orientation = 24 Degrees; 3-D Top Model; 0-Degree Circumferential Location; Condition 1 (continued)

Stress Points		Stress Components (ksi)						Principal Stresses (ksi)		
Section[1]	Node	S_x	S_y	S_z	S_{xy}	S_{yz}	S_{xz}	S1	S2	S3
U7	43052	-1.7	-6.9	-14.0	0.5	0.2	3.8	-0.6	-6.9	-15.1
U8	43051	-8.3	-12.7	-13.2	0.5	0.4	7.1	-3.2	-12.7	-18.2
V1	50024	-15.6	0.8	-6.2	-1.3	-0.2	-2.2	0.9	-5.7	-16.2
V2	50023	-10.7	-4.3	-6.3	-0.6	-0.2	-1.2	-4.3	-6.0	-11.1
V3	50022	-5.1	-9.3	-5.5	0.3	0.0	0.0	-5.1	-5.5	-9.3
V4	50021	0.0	-14.4	-4.4	1.0	0.0	0.3	0.1	-4.4	-14.5
W1	43278	9.6	6.1	-3.6	-0.7	-1.4	-2.0	10.0	6.3	-4.1
W2	43274	1.7	-0.2	-1.2	-0.1	-1.4	-2.0	2.8	0.4	-2.8
W3	43271	-3.6	-3.7	-0.3	0.2	-1.7	-1.0	0.6	-3.8	-4.5
X1	50084	22.8	16.8	-8.2	-0.5	0.1	-5.1	23.7	16.8	-9.1
X2	50083	6.7	1.3	-5.9	-0.2	0.3	-5.2	8.6	1.3	-7.8
X3	50081	-23.0	-26.8	10.5	0.5	-0.1	-5.1	11.3	-23.7	-26.9

[1] Refer to Figure 2.10.2-34 for the identification of the representative sections.

Table 2.10.4-142 P_m Stresses; 30-Foot Top Corner Drop; Drop Orientation = 24 Degrees; 3-D Top Model; 0-Degree Circumferential Location; Condition 1

Condition 1: 100°F Ambient with Contents

		Stress Components (ksi)						Principal Stresses (ksi)			
Section[1]	Node - Node	S_x	S_y	S_z	S_{xy}	S_{yz}	S_{xz}	S1	S2	S3	S.I.
A	1949 - 1951	0.6	1.1	0.0	0.0	0.0	0.2	1.1	0.7	-0.1	1.2
B	1952 - 93	-0.8	-1.3	0.2	-0.1	0.0	0.2	0.3	-0.8	-1.3	1.6
C	1925 - 1927	0.3	-0.2	0.1	0.0	-0.1	-0.2	0.5	0.0	-0.2	0.7
D	683 - 85	-0.1	-0.7	-0.4	0.2	0.0	0.0	-0.1	-0.4	-0.8	0.7
E	682 - 82	0.4	-0.2	0.0	0.1	0.0	0.2	0.5	-0.1	-0.2	0.7
F	1925 - 1325	-0.7	-1.1	-2.2	0.0	-0.1	0.2	-0.7	-1.1	-2.2	1.5
G	680 - 80	-0.1	0.0	0.5	0.0	0.0	0.3	0.6	0.0	-0.2	0.8
H	1921 - 1321	0.0	4.4	-2.5	-0.2	-0.4	0.0	4.5	-0.1	-2.6	7.0
I	676 - 76	0.0	0.6	0.5	0.0	0.0	0.0	0.6	0.5	0.0	0.6
J	1916 - 1316	-0.1	4.9	-0.6	-0.3	-0.1	0.0	4.9	-0.1	-0.6	5.5
K	671 - 71	0.0	0.7	-0.2	-0.1	0.1	0.0	0.7	0.0	-0.2	0.9
L	1908 - 1308	-0.3	4.9	-2.8	0.7	0.3	0.0	5.0	-0.4	-2.8	7.8
M	663 - 63	-0.1	0.9	-2.5	0.4	0.2	0.0	1.0	-0.2	-2.5	3.6
N	1877 - 1277	-0.1	4.9	-11.3	-0.4	0.7	0.0	4.9	-0.1	-11.3	16.2
O	647 - 47	0.0	1.0	-6.0	-0.1	0.2	0.0	1.0	0.0	-6.0	7.0
P	1840 - 1240	-0.5	3.7	-18.2	-0.3	0.9	-0.4	3.8	-0.5	-18.3	22.0
Q	628 - 28	-0.1	3.2	-8.4	-0.2	0.3	0.1	3.3	-0.1	-8.4	11.7
R	1816 - 1216	1.0	0.2	-18.8	0.2	0.5	0.5	1.0	0.2	-18.8	19.8
S	616 - 16	-5.7	0.8	-9.4	-0.5	0.2	-0.1	0.9	-5.7	-9.4	10.3
T	811 - 11	0.6	-5.3	-6.8	0.5	0.3	-0.2	0.7	-5.3	-6.8	7.5
U	43058 - 43051	-0.3	-1.4	-12.3	0.1	0.3	4.9	1.5	-1.4	-14.1	15.6
V	50024 - 50021	-7.8	-6.9	-5.7	-0.1	-0.1	-0.7	-5.5	-6.8	-8.1	2.6
W	43278 - 43271	2.4	0.5	-1.6	-0.2	-1.5	-1.7	3.1	1.1	-2.9	5.9
X	50084 - 50081	-0.8	-5.7	-0.7	0.0	0.1	-5.2	4.4	-5.7	-6.0	10.4

[1] Refer to Figure 2.10.2-34 for the identification of the representative sections.

Table 2.10.4-143 $P_m + P_b$ Stresses; 30-Foot Top Corner Drop; Drop Orientation = 24 Degrees; 3-D Top Model; 0-Degree Circumferential Location; Condition 1

Condition 1: 100°F Ambient with Contents

			Stress Components (ksi)						Principal Stresses (ksi)			
Section[1]	Node -	Node	S_x	S_y	S_z	S_{xy}	S_{yz}	S_{xz}	S1	S2	S3	S.I.
A I	1949 -	1951	1.6	2.6	-0.4	0.0	-0.1	0.3	2.6	1.6	-0.5	3.1
B O	1952 -	93	-1.6	-2.5	1.0	-0.1	0.0	0.3	1.0	-1.6	-2.5	3.6
C O	1925 -	1927	0.6	-0.3	-0.4	0.1	0.0	-0.2	0.7	-0.3	-0.4	1.1
D O	683 -	85	-0.2	-0.9	-0.4	0.2	0.0	0.0	-0.1	-0.4	-1.0	0.9
E I	682 -	82	0.4	-0.3	-0.6	0.1	0.0	0.2	0.5	-0.3	-0.6	1.1
F O	1925 -	1325	-1.2	-2.2	-5.6	0.1	-0.1	0.4	-1.2	-2.2	-5.7	4.5
G I	680 -	80	-0.4	0.0	1.2	0.0	0.0	0.6	1.4	0.0	-0.6	2.0
H I	1921 -	1321	0.0	3.6	-3.9	-0.2	-0.4	0.1	3.6	0.0	-3.9	7.5
I O	676 -	76	0.0	1.4	1.1	-0.1	0.0	0.0	1.4	1.1	0.0	1.4
J O	1916 -	1316	-0.1	6.4	0.1	-0.5	-0.1	0.0	6.4	0.1	-0.1	6.5
K O	671 -	71	0.0	2.1	0.5	-0.2	0.1	0.0	2.1	0.5	0.0	2.1
L O	1908 -	1308	0.1	7.9	-1.6	1.7	0.3	0.0	8.3	-0.2	-1.6	9.9
M O	663 -	63	0.2	2.7	-1.8	0.7	0.2	0.0	2.9	0.0	-1.8	4.7
N O	1877 -	1277	0.0	7.2	-10.4	-0.5	0.6	0.0	7.2	-0.1	-10.4	17.6
O O	647 -	47	0.0	2.3	-5.6	-0.2	0.2	0.0	2.3	0.0	-5.6	7.9
P O	1840 -	1240	-0.6	3.4	-23.3	-0.2	0.7	-1.1	3.4	-0.5	-23.4	26.8
Q O	628 -	28	0.0	3.7	-8.9	-0.3	0.2	0.1	3.7	0.0	-8.9	12.7
R I	1816 -	1216	-1.3	-3.6	-29.7	0.2	0.7	0.0	-1.3	-3.6	-29.7	28.4
S I	616 -	16	-10.5	-5.5	-28.8	-0.3	0.5	1.9	-5.5	-10.3	-29.0	23.5
T O	811 -	11	1.0	-4.9	-6.6	0.4	0.1	-0.5	1.0	-5.0	-6.7	7.7
U I	43058 -	43051	4.9	9.1	-12.2	-0.6	0.3	4.6	9.2	5.9	-13.4	22.6
V I	50024 -	50021	-15.8	0.7	-6.7	-1.4	-0.2	-2.1	0.8	-6.2	-16.4	17.2
W I	43278 -	43271	9.0	5.4	-3.2	-0.6	-1.3	-2.2	9.4	5.6	-3.8	13.2
X O	50084 -	50081	-23.5	-27.3	9.3	0.5	-0.1	-5.2	10.1	-24.2	-27.4	37.5

[1] Refer to Figure 2.10.2-34 for the identification of the representative sections.

Table 2.10.4-144 Critical P_m Stress Summary; 30-Foot Top Corner Drop; Drop Orientation = 24 Degrees; 3-D Top Model; Condition 1

Condition 1: 100°F Ambient with Contents

Comp. No.[1]	Section Cut Node-Node	P_m Stresses (ksi) S_x	S_y	S_z	S_{xy}	S_{yz}	S_{xz}	Principal Stresses (ksi) S1	S2	S3	S.I.	Allow. Stress	Margin of Safety
1	1952- 93	-0.8	-1.3	0.2	-0.1	0.0	0.2	0.3	-0.8	-1.3	1.6	45.6	27.5
2	1592- 15324	0.1	1.7	-0.7	0.1	-3.2	-0.1	3.9	0.1	-2.9	6.8	44.9	5.6
3	11841- 11241	-0.2	2.7	-14.7	0.1	8.2	-0.3	6.0	-0.2	-18.0	24.0	66.0	1.8
4	13874- 13274	-0.1	3.0	-10.2	0.0	7.8	0.0	6.6	-0.1	-13.8	20.4	45.8	1.2
5	10625- 10025	0.0	3.7	-9.0	0.0	3.4	0.2	4.6	0.0	-9.9	14.5	46.4	2.2
6	401- 1	-5.4	-37.8	-4.7	2.2	0.0	-0.5	-4.5	-5.5	-37.9	33.4	49.3	0.5
7	50055- 63171	-24.1	-15.3	-0.1	-0.2	-1.8	-4.2	0.8	-15.5	-24.9	25.7	48.0	0.9
8	50051- 50054	-7.3	-3.8	-2.1	-0.2	0.5	6.2	2.0	-3.8	-11.5	13.5	94.5	6.0

Locations of the most critical sections for each component are provided in the following:

Comp. No.[1]	Section Location Inside Node x (in)	y (deg)	z (in)	Outside Node x (in)	y (deg)	z (in)
1	0.00	0.0	6.20	0.00	0.0	0.75
2	35.50	67.7	17.40	37.50	67.7	17.40
3	35.50	45.9	159.90	37.50	45.9	159.90
4	35.50	56.5	142.40	37.00	56.5	142.40
5	40.70	45.9	163.40	43.35	45.9	163.40
6	40.88	0.0	193.71	43.35	0.0	193.71
7	23.00	8.3	188.40	23.00	8.3	187.40
8	23.00	0.0	193.71	23.00	0.0	188.46

[1] Refer to Figure 2.10.2-33 for cask component identification.

Table 2.10.4-145 Critical $P_m + P_b$ Stresses; 30-Foot Top Corner Drop; Drop Orientation = 24 Degrees; 3-D Top Model; Condition 1

Condition 1: 100°F Ambient with Contents

Comp. No.[1]	Section Cut Node-Node	$P_m + P_b$ Stresses (ksi) S_x	S_y	S_z	S_{xy}	S_{yz}	S_{xz}	Principal Stresses (ksi) S1	S2	S3	S.I.	Allow. Stress	Margin of Safety
1	1952- 93	-1.6	-2.5	1.0	-0.1	0.0	0.3	1.0	-1.6	-2.5	3.6	65.2	17.1
2	15924-15324	0.0	1.4	-2.5	0.1	-4.0	-0.1	3.9	0.0	-5.0	8.9	64.2	6.2
3	11821-11221	-0.1	4.3	-21.8	0.0	8.1	0.7	6.6	-0.1	-24.1	30.7	94.3	2.1
4	13874-13274	-0.1	5.1	-9.6	0.0	8.2	0.0	8.7	-0.1	-13.2	21.9	65.5	2.0
5	10625-10025	0.0	4.1	-8.1	-0.1	4.1	0.2	5.4	0.1	-9.4	14.7	66.4	3.5
6	401- 1	-4.7	-38.3	-5.8	2.3	0.0	-0.4	-4.4	-6.0	-38.4	34.0	70.9	1.1
7	50150-63451	-69.2	-37.5	-17.4	1.0	0.0	-0.8	-17.4	-37.5	-69.2	51.8	69.8	0.3
8	50071-50074	-55.0	-38.4	-4.8	-0.2	-0.3	-1.4	-4.8	-38.4	-55.1	50.3	135.0	1.7

Locations of the most critical sections for each component are provided in the following:

Comp. No.[1]	Section Location Inside Node x (in)	y (deg)	z (in)	Outside Node x (in)	y (deg)	z (in)
1	0.00	0.0	6.20	0.00	0.0	0.75
2	35.50	67.7	17.40	37.50	67.7	17.40
3	35.50	45.9	171.65	37.50	45.9	171.65
4	35.50	56.5	142.40	37.00	56.5	142.40
5	40.70	45.9	163.40	43.35	45.9	163.40
6	40.88	0.0	193.71	43.35	0.0	193.71
7	25.00	8.3	188.40	25.00	8.3	187.40
8	9.00	0.0	193.71	9.00	0.0	188.46

[1] Refer to Figure 2.10.2-33 for cask component identification.

Table 2.10.4-146 P_m Stresses; 30-Foot Top Corner Drop; Drop Orientation = 24 Degrees; 3-D Top Model; 45.9-Degree Circumferential Location; Condition 1

Condition 1: 100°F Ambient with Contents

		Stress Components (ksi)						Principal Stresses (ksi)			
Section[1]	Node - Node	S_x	S_y	S_z	S_{xy}	S_{yz}	S_{zx}	S1	S2	S3	S.I.
A	1949 - 1951	0.6	1.1	0.0	0.0	0.0	0.2	1.1	0.7	-0.1	1.2
B	1952 - 93	-0.8	-1.3	0.2	-0.1	0.0	0.2	0.3	-0.8	-1.3	1.6
C	11925 - 11927	0.1	0.2	-0.2	-0.2	-0.6	-0.2	0.6	0.2	-0.6	1.3
D	10683 - 10085	0.0	-1.0	-0.4	0.1	-0.1	0.0	0.0	-0.4	-1.0	1.0
E	10682 - 10082	0.5	0.0	0.0	0.1	0.0	0.0	0.5	0.0	0.0	0.5
F	11925 - 11325	-0.8	0.3	-1.1	-0.2	-1.4	0.1	1.2	-0.8	-2.0	3.2
G	10680 - 10080	-0.6	0.5	0.2	0.1	0.2	0.0	0.6	0.1	-0.7	1.3
H	11921 - 11321	0.0	3.2	-1.7	0.1	-3.1	0.0	4.7	0.0	-3.2	7.9
I	10676 - 10076	0.0	0.5	-0.6	0.0	0.1	0.0	0.5	0.0	-0.6	1.1
J	11916 - 11316	0.0	3.4	-2.0	0.0	-0.8	0.0	3.6	0.0	-2.1	5.7
K	10671 - 10071	0.0	0.4	-1.6	0.0	0.6	0.0	0.6	0.0	-1.8	2.4
L	11908 - 11308	0.1	3.4	-4.8	-0.4	3.0	0.0	4.4	0.1	-5.8	10.2
M	10663 - 10063	0.0	0.6	-3.6	-0.3	1.5	0.0	1.2	0.0	-4.1	5.2
N	11877 - 11277	0.0	3.6	-10.6	0.0	6.5	0.0	6.1	0.0	-13.1	19.2
O	10647 - 10047	0.0	0.7	-6.5	0.0	2.5	0.0	1.5	0.0	-7.3	8.8
P	11840 - 11240	-0.4	3.0	-14.6	0.3	8.1	-0.3	6.2	-0.4	-17.8	23.9
Q	10628 - 10028	0.0	2.7	-8.6	0.0	3.3	0.0	3.6	0.0	-9.5	13.1
R	11816 - 11216	1.8	3.1	-15.5	1.1	5.6	0.9	5.1	1.3	-17.0	22.2
S	10616 - 10016	-5.9	2.0	-9.8	-1.1	3.1	0.0	2.9	-6.0	-10.6	13.5
T	10811 - 10011	1.4	-2.4	-6.2	1.5	3.7	0.4	2.3	-1.0	-8.5	10.9
U	44558 - 44551	0.5	-0.4	-11.8	-0.2	-0.3	4.9	2.3	-0.5	-13.5	15.8
V	50524 - 50521	-5.7	-5.2	-6.3	0.7	0.0	-0.6	-4.6	-5.8	-6.7	2.1
W	43278 - 43271	2.4	0.5	-1.6	-0.2	-1.5	-1.7	3.1	1.1	-2.9	5.9
X	50084 - 50081	-0.8	-5.7	-0.7	0.0	0.1	-5.2	4.4	-5.7	-6.0	10.4

[1] Refer to Figure 2.10.2-34 for the identification of the representative sections.

Table 2.10.4-147 $P_m + P_b$ Stresses; 30-Foot Top Corner Drop; Drop Orientation = 24 Degrees; 3-D Top Model; 45.9-Degree Circumferential Location; Condition 1

Condition 1: 100°F Ambient with Contents

		Stress Components (ksi)						Principal Stresses (ksi)			
Section[1]	Node - Node	S_x	S_y	S_z	S_{xy}	S_{yz}	S_{xz}	S1	S2	S3	S.I.
A I	1949 - 1951	1.6	2.6	-0.4	0.0	-0.1	0.3	2.6	1.6	-0.5	3.1
B O	1952 - 93	-1.6	-2.5	1.0	-0.1	0.0	0.3	1.0	-1.6	-2.5	3.6
C I	11925 - 11927	-0.4	0.6	-0.2	-0.5	-1.1	-0.1	1.5	-0.2	-1.2	2.6
D O	10683 - 10085	0.2	-1.5	-0.4	0.2	-0.1	0.0	0.2	-0.4	-1.5	1.8
E I	10682 - 10082	0.5	-0.2	-0.6	0.1	-0.2	0.0	0.5	-0.1	-0.6	1.1
F I	11925 - 11325	-0.4	0.7	-0.1	-0.5	-1.6	0.0	2.0	-0.4	-1.5	3.4
G O	10680 - 10080	-0.3	1.0	1.6	0.0	0.3	0.1	1.7	0.8	-0.3	2.0
H I	11921 - 11321	0.0	3.0	-2.4	0.1	-3.7	0.1	4.9	0.0	-4.4	9.2
I O	10676 - 10076	0.0	0.1	-0.9	0.0	0.5	0.0	0.3	0.0	-1.1	1.4
J I	11916 - 11316	0.0	3.8	-2.0	0.0	-1.2	0.0	4.0	0.0	-2.3	6.3
K I	10671 - 10071	0.0	1.2	-1.4	-0.1	0.3	0.0	1.2	0.0	-1.4	2.7
L I	11908 - 11308	0.2	4.7	-4.4	-0.1	3.0	0.0	5.6	0.2	-5.3	11.0
M I	10663 - 10063	0.1	1.2	-3.4	-0.1	1.6	0.0	1.7	0.1	-3.9	5.6
N I	11877 - 11277	-0.1	4.8	-10.1	-0.1	7.0	0.0	7.5	-0.1	-12.9	20.4
O I	10647 - 10047	0.0	1.0	-6.3	-0.1	2.8	0.0	2.0	0.0	-7.2	9.3
P O	11840 - 11240	-0.5	0.8	-20.2	0.5	7.7	-0.9	3.4	-0.4	-22.8	26.1
Q O	10628 - 10028	0.0	2.0	-10.4	0.0	2.8	0.0	2.6	0.0	-11.0	13.6
R I	11816 - 11216	-1.2	-1.7	-30.1	0.0	6.8	-0.5	-0.1	-1.2	-31.6	31.5
S I	10616 - 10016	-11.1	-4.1	-28.2	-2.5	4.4	2.1	-2.8	-11.3	-29.3	26.6
T I	10811 - 10011	2.6	-1.5	-4.0	3.9	6.5	1.4	7.2	-0.6	-9.6	16.8
U I	44558 - 44551	2.6	9.2	-11.9	-3.2	0.1	4.6	10.6	2.6	-13.3	23.8
V O	50524 - 50521	2.8	-12.4	-4.3	4.5	0.0	0.6	4.0	-4.4	-13.6	17.7
W I	43278 - 43271	9.0	5.4	-3.2	-0.6	-1.3	-2.2	9.4	5.6	-3.8	13.2
X O	50084 - 50081	-23.5	-27.3	9.3	0.5	-0.1	-5.2	10.1	-24.2	-27.4	37.5

[1] Refer to Figure 2.10.2-34 for the identification of the representative sections.

Table 2.10.4-148 P_m Stresses; 30-Foot Top Corner Drop; Drop Orientation = 24 Degrees; 3-D Top Model; 91.7-Degree Circumferential Location; Condition 1

Condition 1: 100°F Ambient with Contents

		Stress Components (ksi)						Principal Stresses (ksi)			
Section[1]	Node - Node	S_x	S_y	S_z	S_{xy}	S_{yz}	S_{zx}	S1	S2	S3	S.I.
A	1949 - 1951	0.6	1.1	0.0	0.0	0.0	0.2	1.1	0.7	-0.1	1.2
B	1952 - 93	-0.8	-1.3	0.2	-0.1	0.0	0.2	0.3	-0.8	-1.3	1.6
C	19925 - 19927	-0.1	0.6	-0.7	0.1	-0.5	-0.1	0.8	-0.1	-0.9	1.7
D	18683 - 18085	-0.1	-0.9	-0.4	-0.2	-0.4	-0.2	0.0	-0.2	-1.1	1.1
E	18682 - 18082	0.6	0.1	-0.5	0.2	-0.5	-0.3	0.8	0.1	-0.7	1.6
F	19925 - 19325	-0.4	1.6	0.2	0.2	-1.4	-0.2	2.5	-0.4	-0.7	3.2
G	18680 - 18080	-0.5	0.8	-1.1	0.3	0.1	-0.2	0.8	-0.5	-1.2	2.0
H	19921 - 19321	0.0	0.3	-1.8	0.1	-2.2	0.0	1.7	0.0	-3.2	4.9
I	18676 - 18076	0.0	0.2	-2.1	0.0	0.6	0.0	0.4	0.0	-2.2	2.6
J	19916 - 19316	0.0	0.8	-4.1	0.0	0.2	0.0	0.9	0.0	-4.1	5.0
K	18671 - 18071	0.0	0.0	-2.8	0.0	1.1	0.0	0.4	0.0	-3.2	3.6
L	19908 - 19308	0.2	1.0	-5.3	0.5	3.9	0.0	2.9	0.1	-7.1	10.0
M	18663 - 18063	0.1	0.0	-3.8	0.2	2.1	0.0	0.9	0.0	-4.7	5.6
N	19877 - 19277	0.1	1.1	-4.0	0.0	7.5	0.0	6.5	0.1	-9.4	15.9
O	18647 - 18047	0.0	-0.1	-4.1	0.0	3.3	0.0	1.8	0.0	-5.9	7.7
P	19840 - 19240	0.0	0.6	-2.2	0.5	9.1	-0.1	8.4	0.0	-10.1	18.5
Q	18628 - 18028	0.0	0.6	-3.6	0.1	4.2	0.0	3.1	0.0	-6.2	9.3
R	19816 - 19216	0.4	4.6	-2.2	1.3	7.7	1.8	10.0	0.0	-7.3	17.4
S	18616 - 18016	-3.8	2.4	-3.0	-1.8	4.8	-0.6	5.6	-4.1	-5.9	11.5
T	18811 - 18011	1.5	2.9	-1.5	2.3	5.8	0.4	7.7	0.9	-5.7	13.4
U	45758 - 45751	-0.5	-1.6	-5.8	-0.7	0.5	1.1	0.0	-1.7	-6.1	6.0
V	50924 - 50921	-0.9	-2.5	0.5	-0.6	0.3	-0.7	0.9	-1.1	-2.7	3.5
W	43278 - 43271	2.4	0.5	-1.6	-0.2	-1.5	-1.7	3.1	1.1	-2.9	5.9
X	50084 - 50081	-0.8	-5.7	-0.7	0.0	0.1	-5.2	4.4	-5.7	-6.0	10.4

[1] Refer to Figure 2.10.2-34 for the identification of the representative sections.

Table 2.10.4-149 $P_m + P_b$ Stresses; 30-Foot Top Corner Drop; Drop Orientation = 24 Degrees; 3-D Top Model; 91.7-Degree Circumferential Location; Condition 1

Condition 1: 100°F Ambient with Contents

		Stress Components (ksi)						Principal Stresses (ksi)			
Section[1]	Node - Node	S_x	S_y	S_z	S_{xy}	S_{yz}	S_{xz}	S1	S2	S3	S.I.
A I	1949 - 1951	1.6	2.6	-0.4	0.0	-0.1	0.3	2.6	1.6	-0.5	3.1
B O	1952 - 93	-1.6	-2.5	1.0	-0.1	0.0	0.3	1.0	-1.6	-2.5	3.6
C I	19925 - 19927	-0.6	1.1	-1.6	0.0	-1.0	-0.1	1.5	-0.6	-1.9	3.4
D O	18683 - 18085	0.6	-1.3	-0.5	-0.1	-0.3	-0.1	0.6	-0.4	-1.4	2.0
E I	18682 - 18082	0.6	0.1	-0.3	0.2	-0.5	-0.3	0.9	0.2	-0.7	1.6
F O	19925 - 19325	-0.2	2.3	2.9	0.4	-1.5	-0.3	4.2	1.1	-0.3	4.5
G I	18680 - 18080	-0.6	0.4	-2.8	0.4	0.2	-0.4	0.5	-0.7	-2.9	3.5
H O	19921 - 19321	0.0	-0.7	-2.9	0.1	-2.2	0.1	0.7	0.0	-4.3	5.0
I I	18676 - 18076	0.0	0.6	-1.6	0.0	0.8	0.0	0.9	0.0	-1.9	2.7
J I	19916 - 19316	0.0	1.9	-3.7	0.0	0.3	0.0	2.0	0.0	-3.7	5.7
K I	18671 - 18071	0.0	0.5	-2.6	0.0	1.3	0.0	1.0	0.0	-3.1	4.0
L I	19908 - 19308	0.2	1.7	-5.0	0.1	4.0	0.0	3.6	0.2	-6.8	10.4
M I	18663 - 18063	0.2	0.8	-3.4	0.1	2.2	0.0	1.7	0.2	-4.4	6.1
N O	19877 - 19277	0.1	1.4	-3.9	0.0	7.5	0.0	6.7	0.1	-9.3	16.0
O I	18647 - 18047	0.0	0.5	-3.8	0.1	3.3	0.0	2.2	0.0	-5.6	7.8
P O	19840 - 19240	-0.1	0.5	-3.8	0.7	10.1	-0.2	8.7	-0.1	-12.0	20.7
Q O	18628 - 18028	0.0	0.0	-5.0	0.0	4.6	0.0	2.8	0.0	-7.8	10.5
R I	19816 - 19216	-0.3	2.3	-10.7	-0.3	8.9	0.0	6.8	-0.3	-15.3	22.0
S I	18616 - 18016	-7.4	-0.4	-10.3	-3.8	6.1	-0.3	3.7	-8.2	-13.6	17.3
T I	18811 - 18011	3.7	5.0	3.8	5.7	9.2	1.5	15.9	2.4	-5.8	21.6
U I	45758 - 45751	-4.7	-1.0	-10.0	-4.0	0.2	2.0	1.6	-6.4	-11.0	12.6
V O	50924 - 50921	3.8	-4.0	0.6	3.4	0.3	-0.8	5.1	0.5	-5.4	10.5
W I	43278 - 43271	9.0	5.4	-3.2	-0.6	-1.3	-2.2	9.4	5.6	-3.8	13.2
X O	50084 - 50081	-23.5	-27.3	9.3	0.5	-0.1	-5.2	10.1	-24.2	-27.4	37.5

[1] Refer to Figure 2.10.2-34 for the identification of the representative sections.

Table 2.10.4-150 P_m Stresses; 30-Foot Top Corner Drop; Drop Orientation = 24 Degrees; 3-D Top Model; 180-Degree Circumferential Location; Condition 1

Condition 1: 100°F Ambient with Contents

		Stress Components (ksi)						Principal Stresses (ksi)			
Section[1]	Node - Node	S_x	S_y	S_z	S_{xy}	S_{yz}	S_{xz}	S1	S2	S3	S.I.
A	1949 - 1951	0.6	1.1	0.0	0.0	0.0	0.2	1.1	0.7	-0.1	1.2
B	1952 - 93	-0.8	-1.3	0.2	-0.1	0.0	0.2	0.3	-0.8	-1.3	1.6
C	31925 - 31927	0.1	0.2	-0.6	0.0	0.0	-0.2	0.2	0.2	-0.7	0.9
D	30683 - 30085	0.0	-0.1	-0.8	0.1	0.0	-0.1	0.1	-0.1	-0.8	0.9
E	30682 - 30082	1.1	0.4	-0.9	0.0	0.1	-0.2	1.1	0.4	-0.9	2.0
F	31925 - 31325	-1.0	0.1	-0.9	0.1	0.0	-0.1	0.2	-0.8	-1.0	1.1
G	30680 - 30080	-0.2	-0.1	-2.0	0.0	0.2	0.1	-0.1	-0.2	-2.0	1.9
H	31921 - 31321	-0.1	-1.4	-2.4	-0.2	0.0	0.1	0.0	-1.5	-2.4	2.4
I	30676 - 30076	0.0	-0.3	-2.1	-0.1	0.2	0.0	0.0	-0.3	-2.1	2.1
J	31916 - 31316	-0.1	-1.2	-2.6	-0.2	0.2	0.0	-0.1	-1.2	-2.6	2.5
K	30671 - 30071	0.0	-0.4	-1.8	-0.1	0.2	0.0	0.0	-0.3	-1.9	1.9
L	31908 - 31308	-0.2	-0.8	-1.0	-0.4	0.4	0.0	0.0	-0.6	-1.4	1.4
M	30663 - 30063	0.0	-0.3	-1.2	-0.1	0.3	0.0	0.0	-0.3	-1.2	1.2
N	31877 - 31277	-0.2	-0.9	2.4	-0.1	0.7	0.0	2.6	-0.2	-1.1	3.6
O	30647 - 30047	0.0	-0.3	-0.2	-0.1	0.3	0.0	0.0	0.0	-0.6	0.6
P	31840 - 31240	-1.0	-2.3	5.2	-0.2	0.9	0.0	5.3	-1.0	-2.5	7.7
Q	30628 - 30028	0.0	-0.9	0.4	-0.1	0.4	-0.1	0.6	0.0	-1.0	1.6
R	31816 - 31216	-0.6	6.6	3.7	1.2	0.3	2.3	7.0	4.5	-1.7	8.7
S	30616 - 30016	-1.6	4.7	-0.1	0.8	0.4	-0.5	4.8	0.0	-1.9	6.6
T	30811 - 30011	-0.9	9.0	-0.6	1.6	0.4	0.3	9.3	-0.5	-1.2	10.5
U	47558 - 47551	-3.1	-3.2	-4.3	-0.1	0.1	-0.6	-2.8	-3.2	-4.6	1.7
V	51524 - 51521	-4.2	-3.5	-0.3	-0.1	0.1	-0.2	-0.3	-3.4	-4.3	4.0
W	43278 - 43271	2.4	0.5	-1.6	-0.2	-1.5	-1.7	3.1	1.1	-2.9	5.9
X	50084 - 50081	-0.8	-5.7	-0.7	0.0	0.1	-5.2	4.4	-5.7	-6.0	10.4

[1] Refer to Figure 2.10.2-34 for the identification of the representative sections.

Table 2.10.4-151 $P_m + P_b$ Stresses; 30-Foot Top Corner Drop; Drop Orientation = 24 Degrees; 3-D Top Model; 180-Degree Circumferential Location; Condition 1

Condition 1: 100°F Ambient with Contents

		Stress Components (ksi)						Principal Stresses (ksi)			
Section[1]	Node - Node	S_x	S_y	S_z	S_{xy}	S_{yz}	S_{xz}	S1	S2	S3	S.I.
A I	1949 - 1951	1.6	2.6	-0.4	0.0	-0.1	0.3	2.6	1.6	-0.5	3.1
B O	1952 - 93	-1.6	-2.5	1.0	-0.1	0.0	0.3	1.0	-1.6	-2.5	3.6
C I	31925 - 31927	-0.8	0.1	-1.2	0.1	0.0	-0.2	0.1	-0.7	-1.3	1.5
D O	30683 - 30085	1.3	0.1	-0.9	0.1	0.1	-0.1	1.3	0.1	-0.9	2.2
E O	30682 - 30082	1.1	0.3	-1.3	0.0	0.3	-0.2	1.1	0.4	-1.4	2.5
F I	31925 - 31325	-1.0	-0.1	-1.7	0.1	0.0	-0.2	-0.1	-0.9	-1.8	1.7
G O	30680 - 30080	-0.2	-0.3	-2.8	0.0	0.2	0.0	-0.1	-0.3	-2.8	2.7
H O	31921 - 31321	-0.1	-1.4	-3.0	-0.2	0.0	0.1	-0.1	-1.5	-3.0	3.0
I O	30676 - 30076	0.0	-0.3	-2.2	0.0	0.1	0.0	0.0	-0.3	-2.2	2.2
J I	31916 - 31316	-0.1	-1.5	-2.7	-0.2	0.2	0.0	-0.1	-1.5	-2.7	2.6
K I	30671 - 30071	0.0	-0.5	-1.9	-0.1	0.2	0.0	0.0	-0.5	-2.0	1.9
L O	31908 - 31308	-0.2	-0.4	-0.9	-0.6	0.4	0.0	0.3	-0.6	-1.3	1.6
M I	30663 - 30063	0.0	-0.4	-1.2	-0.1	0.2	0.0	0.0	-0.3	-1.3	1.2
N O	31877 - 31277	-0.2	-1.0	2.4	-0.1	0.7	0.0	2.5	-0.2	-1.2	3.7
O O	30647 - 30047	0.0	-0.5	-0.2	-0.1	0.3	0.0	0.0	0.0	-0.7	0.7
P I	31840 - 31240	0.1	-1.0	8.5	-0.1	0.9	-0.1	8.6	0.1	-1.1	9.6
Q I	30628 - 30028	0.0	-0.4	1.9	-0.1	0.4	-0.1	2.0	0.0	-0.5	2.5
R O	31816 - 31216	-1.3	6.7	5.6	1.4	0.0	3.8	7.6	6.5	-3.2	10.8
S I	30616 - 30016	-3.1	4.9	1.9	1.0	0.6	-1.4	5.1	2.2	-3.6	8.7
T I	30811 - 30011	-1.5	10.3	3.5	2.0	0.4	1.4	10.7	3.8	-2.1	12.9
U O	47558 - 47551	5.6	1.3	0.8	-0.4	0.2	-2.0	6.4	1.3	0.0	6.4
V I	51524 - 51521	-14.6	-6.0	-0.9	0.4	0.1	-0.3	-0.9	-6.0	-14.7	13.7
W I	43278 - 43271	9.0	5.4	-3.2	-0.6	-1.3	-2.2	9.4	5.6	-3.8	13.2
X O	50084 - 50081	-23.5	-27.3	9.3	0.5	-0.1	-5.2	10.1	-24.2	-27.4	37.5

[1] Refer to Figure 2.10.2-34 for the identification of the representative sections.

Table 2.10.4-152 Primary Stresses; 30-Foot Bottom Corner Drop; Drop Orientation = 24 Degrees; 3-D Bottom Model; 0-Degree Circumferential Location; Condition 1

Condition 1: 100°F Ambient with Contents

Stress Points		Stress Components (ksi)						Principal Stresses (ksi)		
Section[1]	Node	S_x	S_y	S_z	S_{xy}	S_{yz}	S_{xz}	S1	S2	S3
A1	1130	17.5	13.4	-6.5	-0.5	2.1	2.1	17.7	13.6	-6.9
A2	1129	2.2	-0.1	-1.2	0.0	1.5	2.1	3.3	0.5	-2.9
A3	1128	-13.0	-13.6	4.1	0.5	2.0	2.1	4.6	-13.2	-13.9
B1	1185	10.1	3.3	-6.5	-0.5	2.5	2.3	10.4	3.9	-7.3
B2	1184	-3.6	-7.8	-1.9	0.0	1.8	2.3	0.0	-4.9	-8.4
B3	1183	-17.5	-18.8	2.7	0.4	1.9	2.3	3.1	-17.8	-19.0
C1	90	-19.6	-5.7	-24.9	-1.2	-0.7	-5.1	-5.6	-16.6	-28.1
C2	80	-8.8	-1.6	-14.4	-1.0	-0.5	-4.2	-1.4	-6.7	-16.7
C3	70	-5.7	-1.1	-9.1	-0.5	-0.4	-3.8	-1.1	-3.3	-11.6
C4	60	-3.0	-1.2	-5.4	-0.1	-0.4	-3.6	-0.3	-1.2	-8.1
C5	50	6.5	-4.1	-3.5	1.0	-0.2	-2.5	7.2	-4.1	-4.2
C6	40	13.7	-5.5	-3.5	1.6	-0.1	-1.5	14.0	-3.7	-5.6
D1	25	-30.3	-22.9	-31.9	-0.4	-0.6	-8.4	-22.6	-23.0	-39.5
D2	15	-6.7	-18.5	-14.8	0.6	-0.3	-3.8	-5.1	-16.3	-18.5
D3	5	0.5	-22.3	-7.5	1.4	-0.1	-1.2	0.7	-7.6	-22.4
E1	35	10.5	-8.3	-21.9	1.3	-0.4	-3.8	11.0	-8.4	-22.4
E2	34	1.8	-8.9	-17.5	0.7	-0.8	-7.4	4.3	-9.0	-20.0
E3	33	-5.2	-9.1	-11.1	0.3	-0.7	-7.8	0.2	-9.1	-16.5
E4	32	-6.7	-8.4	-6.7	0.1	-0.4	-4.8	-1.9	-8.4	-11.5
E5	31	-7.3	-7.6	-2.5	0.0	-0.3	-2.9	-1.1	-7.6	-8.6
F1	100	-0.1	-2.1	-32.9	-0.1	-0.9	-3.2	0.2	-2.1	-33.2
F2	99	-2.8	1.0	-18.9	-0.4	-0.8	-1.6	1.1	-2.7	-19.1
F3	98	-2.8	2.3	-13.4	-0.5	-0.4	1.0	2.4	-2.7	-13.6
F4	97	0.1	4.6	-8.0	-0.4	-0.4	2.0	4.6	0.5	-8.5
G1	94	0.3	-2.6	-24.2	0.1	-0.4	-1.1	0.4	-2.6	-24.3
G2	93	-0.6	-0.3	-14.8	-0.1	-0.4	-0.5	-0.2	-0.6	-14.9
G3	92	-1.1	1.3	-8.4	-0.2	-0.2	0.1	1.3	-1.1	-8.4
G4	91	-0.5	3.5	-0.7	-0.3	-0.1	0.1	3.5	-0.5	-0.8
H1	330	-0.3	4.0	-13.1	-0.3	-1.0	-0.1	4.1	-0.3	-13.2
H2	329	-0.5	3.8	-16.1	-0.3	-0.9	0.0	3.9	-0.5	-16.1

Table 2.10.4-152 Primary Stresses; 30-Foot Bottom Corner Drop; Drop Orientation = 24 Degrees; 3-D Bottom Model; 0-Degree Circumferential Location; Condition 1 (continued)

Stress Points		Stress Components (ksi)						Principal Stresses (ksi)		
Section[1]	Node	S_x	S_y	S_z	S_{xy}	S_{yz}	S_{xz}	S1	S2	S3
H3	328	-0.5	3.7	-18.8	-0.3	-0.8	0.6	3.8	-0.5	-18.9
H4	327	-0.5	2.9	-24.3	-0.2	-0.7	1.3	3.0	-0.4	-24.4
I1	244	0.0	1.8	-10.1	-0.1	-0.4	-0.1	1.8	0.0	-10.1
I2	243	0.0	2.3	-10.1	-0.2	-0.4	-0.1	2.3	0.0	-10.1
I3	242	0.0	2.7	-9.9	-0.2	-0.3	-0.1	2.8	0.0	-9.9
I4	241	0.0	3.2	-9.9	-0.2	-0.2	-0.1	3.2	0.0	-9.9
J1	550	-0.1	2.5	-10.8	-0.2	-0.7	0.0	2.5	-0.2	-10.8
J2	548	-0.1	4.9	-9.9	-0.4	-0.6	0.0	4.9	-0.1	-9.9
J3	547	0.0	7.1	-9.0	-0.5	-0.6	0.0	7.2	-0.1	-9.0
K1	344	-0.1	-0.3	-7.6	0.0	-0.3	0.0	-0.1	-0.3	-7.6
K2	342	0.0	1.2	-7.0	-0.1	-0.3	0.0	1.2	0.0	-7.0
K3	341	0.0	2.5	-6.4	-0.2	-0.2	0.0	2.6	0.0	-6.5
L1	740	0.1	2.4	-2.9	0.4	-0.2	-0.1	2.4	0.0	-2.9
L2	738	-0.3	4.7	-2.0	-0.9	-0.2	0.0	4.8	-0.5	-2.0
L3	737	0.3	7.2	-0.9	-2.1	-0.2	0.0	7.8	-0.3	-0.9
M1	454	-0.1	-0.9	-3.9	-0.6	-0.2	0.0	0.2	-1.2	-3.9
M2	452	0.2	0.9	-3.2	-0.3	-0.2	0.0	1.0	0.1	-3.2
M3	451	-0.2	2.4	-2.7	0.0	-0.2	-0.1	2.4	-0.2	-2.7
N1	810	-0.1	3.5	-1.4	-0.2	0.2	0.0	3.5	-0.1	-1.4
N2	807	-0.1	6.3	-0.1	-0.4	0.1	0.0	6.3	-0.1	-0.1
O1	524	0.0	-0.7	-1.2	0.0	-0.1	0.0	0.0	-0.6	-1.2
O2	521	0.0	2.0	0.1	-0.1	-0.1	0.0	2.0	0.1	0.0
P1	850	0.0	3.5	-4.0	-0.2	0.4	-0.1	3.6	0.0	-4.0
P2	847	-0.1	5.3	-1.3	-0.3	0.3	0.0	5.4	-0.1	-1.3
Q1	564	0.0	-0.2	-0.2	0.0	0.0	0.0	0.0	-0.2	-0.3
Q2	561	0.0	1.5	0.7	-0.1	0.0	0.0	1.5	0.7	0.0
R1	890	-1.0	-0.2	1.5	0.0	0.2	-0.2	1.5	-0.2	-1.0
R2	887	-1.2	-1.7	-5.2	0.1	0.1	-0.5	-1.1	-1.7	-5.2
S1	604	-0.4	0.3	0.4	0.0	0.0	-0.4	0.6	0.3	-0.6
S2	601	0.0	0.7	0.5	-0.1	-0.1	-0.1	0.7	0.5	0.0
T1	897	0.5	-0.3	-1.6	0.0	0.1	-0.2	0.6	-0.3	-1.6

Table 2.10.4-152 Primary Stresses; 30-Foot Bottom Corner Drop; Drop Orientation = 24 Degrees; 3-D Bottom Model; 0-Degree Circumferential Location; Condition 1 (continued)

Stress Points		Stress Components (ksi)						Principal Stresses (ksi)		
Section[1]	Node	S_x	S_y	S_z	S_{xy}	S_{yz}	S_{xz}	S1	S2	S3
T2	614	0.3	0.2	0.0	0.0	0.0	-0.4	0.5	0.3	-0.3
T3	611	-0.1	0.1	0.0	0.0	-0.1	-0.2	0.2	0.1	-0.3
U1	900	0.7	0.1	-0.4	0.0	0.1	0.1	0.7	0.1	-0.5
U2	910	0.5	-0.2	-0.4	0.0	0.0	0.1	0.5	-0.2	-0.4
V1	920	-0.2	-0.4	-0.3	0.1	0.0	0.1	-0.1	-0.4	-0.4
V2	930	-0.5	-1.0	-0.2	0.2	0.0	0.1	-0.1	-0.5	-1.0
W1	1216	1.2	2.3	-1.0	0.0	0.0	-0.2	2.3	1.2	-1.0
W2	1226	-0.3	-0.1	0.5	0.0	-0.1	-0.1	0.5	-0.1	-0.3
X1	1236	0.1	0.0	-0.6	0.0	-0.1	-0.1	0.1	0.0	-0.6
X2	1246	-1.5	-2.4	1.1	-0.1	0.0	-0.2	1.1	-1.5	-2.5

[1] Refer to Figure 2.10.2-34 for the identification of the representative sections.

Table 2.10.4-153 P_m Stresses; 30-Foot Bottom Corner Drop; Drop Orientation = 24 Degrees; 3-D Bottom Model; 0-Degree Circumferential Location; Condition 1

Condition 1: 100°F Ambient with Contents

		Stress Components (ksi)						Principal Stresses (ksi)			
Section[1]	Node - Node	S_x	S_y	S_z	S_{xy}	S_{yz}	S_{xz}	S1	S2	S3	S.I.
A	1130 - 1128	2.2	-0.1	-1.2	0.0	1.8	2.1	3.4	0.6	-3.1	6.4
B	1185 - 1183	-3.7	-7.8	-1.9	0.0	2.0	2.3	0.0	-4.9	-8.5	8.5
C	90 - 40	-0.5	-2.9	-7.6	0.2	-0.4	-3.2	0.8	-2.9	-8.8	9.6
D	25 - 5	-10.8	-20.5	-17.2	0.5	-0.3	-4.3	-8.6	-19.4	-20.6	12.0
E	35 - 31	-1.3	-8.6	-12.6	0.5	-0.6	-5.8	1.2	-8.6	-15.1	16.3
F	100 - 97	-1.9	1.5	-17.6	-0.4	-0.6	-0.4	1.6	-1.9	-17.6	19.2
G	94 - 91	-0.6	0.5	-11.9	-0.1	-0.3	-0.3	0.5	-0.6	-11.9	12.4
H	330 - 327	-0.5	3.7	-17.9	-0.3	-0.9	0.4	3.7	-0.5	-17.9	21.6
I	244 - 241	0.0	2.5	-10.0	-0.2	-0.3	-0.1	2.5	0.0	-10.0	12.5
J	550 - 547	-0.1	4.8	-9.9	-0.4	-0.6	0.0	4.9	-0.1	-9.9	14.8
K	344 - 341	0.0	1.1	-7.0	-0.1	-0.3	0.0	1.2	0.0	-7.0	8.2
L	740 - 737	-0.1	4.7	-1.9	-0.9	-0.2	0.0	4.9	-0.2	-1.9	6.8
M	454 - 451	0.0	0.9	-3.2	-0.3	-0.2	0.0	0.9	-0.1	-3.2	4.2
N	810 - 807	-0.1	4.9	-0.8	-0.3	0.2	0.0	4.9	-0.1	-0.8	5.7
O	524 - 521	0.0	0.7	-0.6	0.0	-0.1	0.0	0.7	0.0	-0.6	1.3
P	850 - 847	0.0	4.4	-2.6	-0.2	0.4	0.0	4.5	-0.1	-2.6	7.1
Q	564 - 561	0.0	0.6	0.2	0.0	0.0	0.0	0.6	0.2	0.0	0.7
R	890 - 887	-1.1	-1.0	-1.8	0.0	0.2	-0.3	-0.9	-1.0	-2.0	1.1
S	604 - 601	-0.2	0.5	0.4	0.0	0.0	-0.2	0.5	0.5	-0.3	0.8
T	614 - 611	0.1	0.2	0.0	0.0	-0.1	-0.3	0.4	0.2	-0.3	0.6
U	900 - 910	0.6	-0.1	-0.4	0.0	0.1	0.1	0.6	-0.1	-0.5	1.1
V	920 - 930	-0.4	-0.7	-0.2	0.1	0.0	0.1	-0.1	-0.4	-0.7	0.6
W	1216 - 1226	0.5	1.1	-0.3	0.0	0.0	-0.2	1.1	0.5	-0.3	1.4
X	1236 - 1246	-0.7	-1.2	0.3	-0.1	0.0	-0.2	0.3	-0.7	-1.2	1.5

[1] Refer to Figure 2.10.2-34 for the identification of the representative sections.

Table 2.10.4-154 $P_m + P_b$ Stresses; 30-Foot Bottom Corner Drop; Drop Orientation = 24 Degrees; 3-D Bottom Model; 0-Degree Circumferential Location; Condition 1

Condition 1: 100°F Ambient with Contents

			Stress Components (ksi)						Principal Stresses (ksi)			
Section[1]	Node - Node		S_x	S_y	S_z	S_{xy}	S_{yz}	S_{xz}	S1	S2	S3	S.I.
A	I	1130 - 1128	17.5	13.4	-6.5	-0.5	1.8	2.1	17.7	13.5	-6.8	24.5
B	O	1185 - 1183	-17.5	-18.8	2.7	0.4	1.7	2.3	3.1	-17.7	-19.0	22.1
C	I	90 - 40	-14.1	-1.4	-15.6	-1.3	-0.6	-4.7	-1.3	-10.1	-19.7	18.5
D	O	25 - 5	4.6	-20.3	-5.0	1.4	0.0	-0.7	4.7	-5.1	-20.3	25.1
E	I	35 - 31	8.2	-8.9	-23.1	1.2	-0.7	-6.6	9.6	-9.0	-24.4	34.1
F	I	100 - 97	-2.0	-1.5	-29.1	-0.2	-1.0	-3.3	-1.4	-1.7	-29.5	28.1
G	I	94 - 91	-0.1	-2.4	-23.2	0.0	-0.5	-1.0	-0.1	-2.4	-23.2	23.2
H	O	330 - 327	-0.6	3.2	-23.1	-0.2	-0.7	1.1	3.3	-0.5	-23.2	26.5
I	O	244 - 241	0.0	3.2	-9.8	-0.2	-0.2	-0.1	3.2	0.0	-9.9	13.1
J	O	550 - 547	0.0	7.1	-9.0	-0.5	-0.6	0.0	7.2	-0.1	-9.0	16.2
K	O	344 - 341	0.0	2.6	-6.4	-0.2	-0.2	0.0	2.6	0.0	-6.4	9.0
L	O	740 - 737	0.0	7.1	-0.9	-2.1	-0.2	0.0	7.7	-0.5	-0.9	8.6
M	O	454 - 451	-0.1	2.5	-2.6	0.0	-0.2	0.0	2.5	-0.1	-2.6	5.1
N	O	810 - 807	-0.1	6.3	-0.1	-0.4	0.1	0.0	6.3	-0.1	-0.1	6.4
O	O	524 - 521	0.0	2.0	0.1	-0.1	-0.1	0.0	2.0	0.1	0.0	2.1
P	I	850 - 847	0.0	3.5	-4.0	-0.2	0.4	-0.1	3.6	0.0	-4.0	7.6
Q	O	564 - 561	0.0	1.5	0.7	-0.1	0.0	0.0	1.5	0.7	0.0	1.5
R	O	890 - 887	-1.2	-1.7	-5.2	0.1	0.1	-0.5	-1.1	-1.7	-5.2	4.1
S	I	604 - 601	-0.4	0.3	0.4	0.0	0.0	-0.4	0.6	0.3	-0.6	1.1
T	I	614 - 611	0.3	0.2	0.0	0.0	0.0	-0.4	0.5	0.3	-0.3	0.8
U	I	900 - 910	0.7	0.1	-0.4	0.0	0.1	0.1	0.7	0.1	-0.5	1.2
V	O	920 - 930	-0.5	-1.0	-0.2	0.2	0.0	0.1	-0.1	-0.5	-1.0	0.9
W	I	1216 - 1226	1.2	2.3	-1.0	0.0	0.0	-0.2	2.3	1.2	-1.0	3.3
X	O	1236 - 1246	-1.5	-2.4	1.1	-0.1	0.0	-0.2	1.1	-1.5	-2.5	3.6

[1] Refer to Figure 2.10.2-34 for the identification of the representative sections.

Table 2.10.4-155 Critical P_m Stress Summary; 30-Foot Bottom Corner Drop; Drop Orientation = 24 Degrees; 3-D Bottom Model; Condition 1

Condition 1: 100°F Ambient with Contents

Comp. No.[1]	Section Cut Node-Node	P_m Stresses (ksi) S_x	S_y	S_z	S_{xy}	S_{yz}	S_{xz}	Principal Stresses (ksi) S1	S2	S3	S.I.	Allow. Stress	Margin of Safety
1	27- 7	-13.0	-17.0	-3.7	0.1	-0.5	-6.2	-0.6	-16.1	-17.0	16.4	45.6	1.8
2	10140- 10137	0.0	6.4	-12.9	0.0	-6.6	-0.8	8.5	0.0	-14.9	23.4	44.9	0.9
3	10160- 10157	0.0	6.9	-12.5	0.0	-6.6	-0.6	8.9	0.0	-14.6	23.5	66.0	1.8
4	12520- 12517	-0.1	3.0	-9.7	0.0	-7.6	0.0	6.5	-0.1	-13.3	19.8	45.8	1.3
5	12204- 12201	-0.2	2.6	-9.7	0.0	-4.4	-0.2	4.0	-0.2	-11.1	15.1	46.4	2.1
6	14880- 14877	-0.1	1.7	-0.8	-0.1	3.3	0.1	4.0	-0.1	-3.1	7.1	49.3	5.9
7	16900- 16910	-0.2	0.5	-0.8	-0.1	0.6	0.2	0.7	-0.1	-1.1	1.8	48.0	25.2
8	1236- 1246	-0.7	-1.2	0.3	-0.1	0.0	-0.2	0.3	-0.7	-1.2	1.5	94.5	62.0

Locations of the most critical sections for each component are provided in the following:

Comp. No.[1]	Section Location Inside Node x (in)	y (deg)	z (in)	Outside Node x (in)	y (deg)	z (in)
1	37.50	0.0	6.20	37.50	0.0	0.75
2	35.50	45.9	17.40	37.50	45.9	17.40
3	35.50	45.9	18.90	37.50	45.9	18.90
4	35.50	56.5	47.40	37.00	56.5	47.40
5	40.70	56.5	26.40	43.35	56.5	26.40
6	35.50	67.7	172.40	37.50	67.7	172.40
7	35.50	79.4	179.40	35.50	79.4	185.40
8	0.0	0.0	187.40	0.0	0.0	193.71

[1] Refer to Figure 2.10.2-33 for cask component identification.

Table 2.10.4-156 Critical $P_m + P_b$ Stress Summary; 30-Foot Bottom Corner Drop; Drop Orientation = 24 Degrees; 3-D Bottom Model; Condition 1

Condition 1: 100°F Ambient with Contents

Comp. No.[1]	Section Cut Node-Node	$P_m + P_b$ Stresses (ksi) S_x	S_y	S_z	S_{xy}	S_{yz}	S_{xz}	Principal Stresses (ksi) S1	S2	S3	S.I.	Allow. Stress	Margin of Safety
1	1170- 1168	-44.2	-33.1	-4.6	-0.1	-0.1	-0.1	-4.6	-33.1	-44.2	39.6	65.2	0.6
2	14035- 14031	9.1	-3.6	-21.0	5.2	-8.6	-5.2	12.9	-3.6	-24.8	37.7	64.2	0.7
3	10150- 10147	-0.1	4.6	-21.5	0.0	-7.9	-0.7	6.8	-0.1	-23.7	30.5	94.3	2.1
4	12520- 12517	-0.1	5.0	-9.1	0.0	-8.0	0.0	8.6	-0.1	-12.8	21.4	65.5	2.1
5	10204- 10201	-0.3	2.9	-10.6	0.0	-4.3	-0.2	4.2	-0.3	-11.9	16.0	66.4	3.2
6	14880- 14877	-0.1	1.7	-1.8	-0.1	4.0	0.1	4.3	-0.1	-4.4	8.7	70.9	7.1
7	1216- 1226	1.2	2.3	-1.0	0.0	0.0	-0.2	2.3	1.2	-1.0	3.3	69.8	20.2
8	1236- 1246	-1.5	-2.4	1.1	-0.1	0.0	-0.2	1.1	-1.5	-2.5	3.6	135.0	36.5

Locations of the most critical sections for each component are provided in the following:

Comp. No.[1]	Section Location Inside Node x (in)	y (deg)	z (in)	Outside Node x (in)	y (deg)	z (in)
1	14.73	0.0	6.20	14.73	0.0	0.75
2	39.44	67.7	8.20	43.35	67.7	8.20
3	35.50	45.9	18.15	37.50	45.9	18.15
4	35.50	56.5	47.40	37.00	56.5	47.40
5	40.70	45.9	26.40	43.35	45.9	26.40
6	35.50	67.7	172.40	37.50	67.7	172.40
7	0.0	0.0	179.40	0.0	0.0	185.40
8	0.0	0.0	187.40	0.0	0.0	193.71

[1] Refer to Figure 2.10.2-33 for cask component identification.

Table 2.10.4-157 P_m Stresses; 30-Foot Bottom Corner Drop; Drop Orientation = 24 Degrees; 3-D Bottom Model; 45.9-Degree Circumferential Location; Condition 1

Condition 1: 100°F Ambient with Contents

		Stress Components (ksi)						Principal Stresses (ksi)			
Section[1]	Node - Node	S_x	S_y	S_z	S_{xy}	S_{yz}	S_{xz}	S1	S2	S3	S.I.
A	1130 - 1128	2.2	-0.1	-1.2	0.0	1.8	2.1	3.4	0.6	-3.1	6.4
B	1185 - 1183	-3.7	-7.8	-1.9	0.0	2.0	2.3	0.0	-4.9	-8.5	8.5
C	10090 - 10040	0.9	-1.1	-7.2	0.3	-1.8	-2.7	1.9	-0.9	-8.4	10.3
D	10025 - 10005	-7.7	-17.4	-16.8	-0.9	-1.5	-4.0	-6.2	-16.0	-19.6	13.4
E	10035 - 10031	0.4	-5.5	-11.9	1.4	-2.5	-5.4	3.0	-5.7	-14.3	17.3
F	10100 - 10097	-1.4	4.0	-13.5	-0.5	-6.5	-1.0	6.1	-1.3	-15.7	21.8
G	10094 - 10091	-0.8	2.0	-12.1	-0.4	-3.5	-0.7	2.9	-0.8	-13.0	15.9
H	10330 - 10327	-0.4	3.0	-14.0	0.3	-8.0	0.3	6.2	-0.4	-17.2	23.4
I	10244 - 10241	0.0	2.2	-9.9	0.0	-3.5	-0.1	3.2	0.0	-10.9	14.1
J	10550 - 10547	0.0	3.5	-9.5	0.0	-6.1	0.0	5.9	0.0	-11.9	17.8
K	10344 - 10341	0.0	0.9	-7.2	0.0	-2.8	0.0	1.7	0.0	-8.0	9.8
L	10740 - 10737	-0.1	3.5	-4.3	0.1	-2.4	0.0	4.2	-0.1	-5.0	9.2
M	10454 - 10451	0.0	0.7	-4.0	0.0	-1.8	0.0	1.2	0.0	-4.6	5.9
N	10810 - 10807	0.0	3.4	-1.9	0.0	1.2	0.0	3.7	0.0	-2.2	5.9
O	10524 - 10521	0.0	0.4	-1.9	0.0	-0.8	0.0	0.6	0.0	-2.2	2.8
P	10850 - 10847	0.0	3.1	-1.8	0.1	1.2	0.0	4.7	0.0	-3.4	8.1
Q	10564 - 10561	0.0	0.5	-0.9	0.0	-0.4	0.0	0.6	0.0	-1.0	1.6
R	10890 - 10887	-0.5	0.7	-1.2	0.7	1.9	-0.1	2.0	-0.5	-2.5	4.5
S	10604 - 10601	-0.3	1.0	0.0	0.2	-0.3	0.0	1.1	0.0	-0.3	1.5
T	10614 - 10611	0.1	0.5	0.0	0.0	-0.2	-0.1	0.6	0.1	-0.1	0.7
U	10900 - 10910	0.2	0.2	-0.6	-0.3	0.6	0.2	0.6	0.2	-0.9	1.5
V	10920 - 10930	-0.1	-1.0	-0.3	0.1	0.2	0.2	0.0	-0.4	-1.0	1.0
W	1216 - 1226	0.5	1.1	-0.3	0.0	0.0	-0.2	1.1	0.5	-0.3	1.4
X	1236 - 1246	-0.7	-1.2	0.3	-0.1	0.0	-0.2	0.3	-0.7	-1.2	1.5

[1] Refer to Figure 2.10.2-34 for the identification of the representative sections.

Table 2.10.4-158 $P_m + P_b$ Stresses; 30-Foot Bottom Corner Drop; Drop Orientation = 24 Degrees; 3-D Bottom Model; 45.9-Degree Circumferential Location; Condition 1

Condition 1: 100°F Ambient with Contents

		Stress Components (ksi)						Principal Stresses (ksi)			
Section[1]	Node - Node	S_x	S_y	S_z	S_{xy}	S_{yz}	S_{xz}	S1	S2	S3	S.I.
A I	1130 - 1128	17.5	13.4	-6.5	-0.5	1.8	2.1	17.7	13.5	-6.8	24.5
B O	1185 - 1183	-17.5	-18.8	2.7	0.4	1.7	2.3	3.1	-17.7	-19.0	22.1
C I	10090 - 10040	-12.7	0.2	-15.1	-4.7	-4.1	-4.0	2.2	-9.9	-19.9	22.1
D O	10025 - 10005	6.2	-17.7	-4.8	2.0	0.4	-0.8	6.4	-4.9	-17.9	24.3
E I	10035 - 10031	8.5	-6.7	-23.4	3.5	-4.8	-6.2	10.8	-6.9	-25.5	36.3
F I	10100 - 10097	-1.3	-0.5	-30.6	-0.6	-8.8	-3.2	1.9	-1.0	-33.4	35.3
G I	10094 - 10091	-0.4	-1.2	-24.7	-0.6	-5.5	-1.7	0.2	-0.4	-26.0	26.2
H O	10330 - 10327	-0.5	0.8	-19.6	0.5	-7.7	0.9	3.4	-0.4	-22.2	25.6
I I	10244 - 10241	0.0	2.7	-8.9	0.0	-4.1	-0.1	4.0	0.0	-10.2	14.2
J I	10550 - 10547	-0.1	4.8	-9.0	-0.1	-6.5	0.0	7.4	-0.1	-11.6	19.0
K I	10344 - 10341	0.0	1.2	-7.0	-0.1	-3.1	0.0	2.2	0.0	-8.0	10.3
L I	10740 - 10737	0.0	4.5	-4.0	-0.2	-2.4	0.0	5.1	0.0	-4.7	9.8
M I	10454 - 10451	-0.1	1.2	-4.0	0.1	-1.8	0.0	1.7	-0.1	-4.5	6.2
N I	10810 - 10807	0.0	3.8	-2.0	0.0	1.6	0.0	4.2	0.0	-2.4	6.6
O I	10524 - 10521	0.0	1.1	-1.7	-0.1	-0.5	0.0	1.2	0.0	-1.8	3.0
P I	10850 - 10847	0.0	2.9	-2.5	0.1	3.8	-0.1	4.9	0.0	-4.5	9.4
Q O	10564 - 10561	0.0	0.1	-1.3	0.0	-0.8	0.0	0.5	0.0	-1.6	2.1
R I	10890 - 10887	-0.3	0.9	-0.4	0.6	2.4	0.0	2.8	-0.3	-2.3	5.1
S I	10604 - 10601	-0.5	0.7	-1.3	0.3	-0.1	-0.1	0.8	-0.6	-1.4	2.1
T I	10614 - 10611	0.2	0.6	-0.3	-0.1	-0.1	-0.1	0.6	0.2	-0.4	1.0
U I	10900 - 10910	-0.2	0.5	-0.7	-0.6	0.8	0.2	1.1	-0.2	-1.3	2.4
V O	10920 - 10930	0.2	-1.5	-0.2	0.4	0.1	0.1	0.3	-0.3	-1.6	1.9
W I	1216 - 1226	1.2	2.3	-1.0	0.0	0.0	-0.2	2.3	1.2	-1.0	3.3
X O	1236 - 1246	-1.5	-2.4	1.1	-0.1	0.0	-0.2	1.1	-1.5	-2.5	3.6

[1] Refer to Figure 2.10.2-34 for the identification of the representative sections.

Table 2.10.4-159 P_m Stresses; 30-Foot Bottom Corner Drop; Drop Orientation = 24 Degrees; 3-D Bottom Model; 91.7-Degree Circumferential Location; Condition 1

Condition 1: 100°F Ambient with Contents

		Stress Components (ksi)						Principal Stresses (ksi)			
Section[1]	Node - Node	S_x	S_y	S_z	S_{xy}	S_{yz}	S_{xz}	S1	S2	S3	S.I.
A	1130 - 1128	2.2	-0.1	-1.2	0.0	1.8	2.1	3.4	0.6	-3.1	6.4
B	1185 - 1183	-3.7	-7.8	-1.9	0.0	2.0	2.3	0.0	-4.9	-8.5	8.5
C	18090 - 18040	2.6	1.5	-1.6	-0.1	-2.4	-0.3	2.8	2.6	-2.9	5.7
D	18025 - 18005	-2.0	-4.2	-5.2	-3.0	-3.4	-0.6	0.6	-3.0	-9.0	9.6
E	18035 - 18031	3.9	0.8	-2.0	1.7	-5.9	-3.3	8.2	1.4	-6.9	15.1
F	18100 - 18097	-0.1	3.2	-0.5	-0.6	-8.8	-0.7	10.3	0.0	-7.8	18.1
G	18094 - 18091	-0.4	1.8	-2.3	-0.7	-6.0	-0.5	6.2	-0.3	-6.7	12.9
H	18330 - 18327	0.0	0.7	-2.3	0.5	-8.9	0.1	8.2	0.0	-9.8	18.1
I	18244 - 18241	0.0	0.4	-3.4	0.1	-4.7	0.0	3.5	0.0	-6.5	10.1
J	18550 - 18547	0.1	1.1	-4.3	0.0	-6.9	0.0	5.8	0.1	-9.0	14.8
K	18344 - 18341	0.0	0.0	-4.2	0.0	-3.6	0.0	2.1	0.0	-6.3	8.4
L	18740 - 18737	0.1	1.1	-5.4	-0.1	-3.3	0.0	2.5	0.0	-6.8	9.2
M	18454 - 18451	0.0	0.0	-3.9	0.0	-2.4	0.0	1.2	0.0	-5.0	6.2
N	18810 - 18807	0.0	0.8	-4.1	0.1	0.4	0.0	0.8	0.0	-4.1	5.0
O	18524 - 18521	0.0	0.0	-3.0	0.0	-1.4	0.0	0.5	0.0	-3.6	4.1
P	18850 - 18847	0.0	0.3	-2.1	0.1	2.4	-0.1	1.7	0.0	-3.5	5.3
Q	18564 - 18561	0.0	0.2	-2.4	0.0	-1.0	0.0	0.5	0.0	-2.7	3.3
R	18890 - 18887	0.7	2.1	-0.9	0.8	1.7	0.3	3.2	0.4	-1.7	4.8
S	18604 - 18601	-0.1	1.1	-1.3	0.3	-0.2	0.3	1.2	-0.1	-1.4	2.6
T	18614 - 18611	-0.1	0.5	-0.7	0.1	0.2	0.2	0.6	-0.1	-0.8	1.4
U	18900 - 18910	-0.2	0.5	-0.8	0.0	0.6	0.2	0.7	-0.1	-1.0	1.7
V	18920 - 18930	-0.1	-0.9	-0.4	-0.2	0.3	0.2	0.0	-0.3	-1.1	1.1
W	1216 - 1226	0.5	1.1	-0.3	0.0	0.0	-0.2	1.1	0.5	-0.3	1.4
X	1236 - 1246	-0.7	-1.2	0.3	-0.1	0.0	-0.2	0.3	-0.7	-1.2	1.5

[1] Refer to Figure 2.10.2-34 for the identification of the representative sections.

Table 2.10.4-160 $P_m + P_b$ Stresses; 30-Foot Bottom Corner Drop; Drop Orientation = 24 Degrees; 3-D Bottom Model; 91.7-Degree Circumferential Location; Condition 1

Condition 1: 100°F Ambient with Contents

		Stress Components (ksi)						Principal Stresses (ksi)			
Section[1]	Node - Node	S_x	S_y	S_z	S_{xy}	S_{yz}	S_{xz}	S1	S2	S3	S.I.
A I	1130 - 1128	17.5	13.4	-6.5	-0.5	1.8	2.1	17.7	13.5	-6.8	24.5
B O	1185 - 1183	-17.5	-18.8	2.7	0.4	1.7	2.3	3.1	-17.7	-19.0	22.1
C I	18090 - 18040	-8.7	-0.6	-4.4	-5.9	-5.3	-0.5	4.8	-5.5	-13.1	17.8
D I	18025 - 18005	-12.6	-6.9	-10.2	-8.6	-7.1	-2.5	1.3	-8.7	-22.2	23.4
E I	18035 - 18031	9.7	0.9	-6.9	4.8	-8.9	-4.3	14.8	1.7	-12.8	27.5
F I	18100 - 18097	-0.1	0.4	-10.7	-0.8	-10.7	-1.0	6.9	0.0	-17.3	24.1
G I	18094 - 18091	-0.1	0.2	-8.4	-0.9	-7.6	-0.9	4.7	0.0	-12.9	17.6
H O	18330 - 18327	0.0	0.9	-3.4	0.7	-9.8	0.2	8.8	0.0	-11.3	20.1
I O	18244 - 18241	0.0	0.1	-4.2	0.0	-5.0	0.0	3.4	0.0	-7.5	10.9
J O	18550 - 18547	0.1	1.4	-4.3	0.0	-6.9	0.0	6.0	0.1	-8.9	14.9
K I	18344 - 18341	0.0	0.6	-3.9	0.1	-3.7	0.0	2.7	0.0	-5.9	8.6
L I	18740 - 18737	0.2	1.5	-5.1	0.3	-3.5	0.0	3.1	0.1	-6.6	9.6
M I	18454 - 18451	-0.1	0.9	-3.6	-0.1	-2.5	0.0	2.0	-0.1	-4.7	6.8
N I	18810 - 18807	0.0	1.9	-3.7	0.1	0.2	0.0	1.9	0.0	-3.7	5.6
O I	18524 - 18521	0.0	0.5	-2.8	0.0	-1.6	0.0	1.1	0.0	-3.5	4.6
P I	18850 - 18847	0.0	1.3	-1.0	0.1	2.4	0.0	2.8	0.0	-2.5	5.3
Q I	18564 - 18561	0.0	0.6	-1.9	0.0	-1.2	0.0	1.1	0.0	-2.4	3.5
R I	18890 - 18887	0.6	1.5	-3.6	0.7	1.8	0.2	2.4	0.3	-4.2	6.6
S I	18604 - 18601	0.0	0.9	-2.6	0.5	-0.3	0.4	1.1	-0.2	-2.7	3.8
T I	18614 - 18611	-0.2	0.7	-0.9	0.1	0.2	0.3	0.7	-0.1	-1.0	1.7
U I	18900 - 18910	-1.2	0.7	-1.1	-0.2	0.7	0.1	1.0	-1.1	-1.5	2.4
V O	18920 - 18930	0.7	-1.3	-0.3	-0.1	0.2	0.1	0.7	-0.3	-1.4	2.0
W I	1216 - 1226	1.2	2.3	-1.0	0.0	0.0	-0.2	2.3	1.2	-1.0	3.3
X O	1236 - 1246	-1.5	-2.4	1.1	-0.1	0.0	-0.2	1.1	-1.5	-2.5	3.6

[1] Refer to Figure 2.10.2-34 for the identification of the representative sections.

Table 2.10.4-161 P_m Stresses; 30-Foot Bottom Corner Drop; Drop Orientation = 24 Degrees; 3-D Bottom Model; 180-Degree Circumferential Location; Condition 1

Condition 1: 100°F Ambient with Contents

		Stress Components (ksi)						Principal Stresses (ksi)			
Section[1]	Node - Node	S_x	S_y	S_z	S_{xy}	S_{yz}	S_{xz}	S1	S2	S3	S.I.
A	1130 - 1128	2.2	-0.1	-1.2	0.0	1.8	2.1	3.4	0.6	-3.1	6.4
B	1185 - 1183	-3.7	-7.8	-1.9	0.0	2.0	2.3	0.0	-4.9	-8.5	8.5
C	30090 - 30040	1.2	2.5	0.6	0.1	-0.3	1.0	2.6	1.9	-0.2	2.8
D	30025 - 30005	-1.7	2.9	-1.9	0.3	-0.3	0.3	3.0	-1.5	-2.1	5.1
E	30035 - 30031	2.4	3.1	-0.1	0.3	-0.2	-1.7	3.5	2.8	-1.0	4.4
F	30100 - 30097	0.4	2.3	4.8	0.2	-0.7	-0.6	5.1	2.1	0.3	4.8
G	30094 - 30091	0.2	0.8	1.9	0.0	-0.4	0.0	2.1	0.7	0.2	1.9
H	30330 - 30327	-1.1	-2.2	4.3	-0.2	-0.9	0.0	4.4	-1.1	-2.4	6.8
I	30244 - 30241	0.0	-0.5	1.2	-0.1	-0.4	0.0	1.3	0.0	-0.6	1.9
J	30550 - 30547	-0.2	-1.0	1.1	-0.1	-0.7	0.0	1.3	-0.2	-1.2	2.5
K	30344 - 30341	0.0	-0.3	0.3	-0.1	-0.3	0.0	0.5	0.0	-0.4	0.9
L	30740 - 30737	-0.1	-0.9	-1.9	0.0	-0.4	0.0	-0.1	-0.8	-2.0	1.9
M	30454 - 30451	0.0	-0.3	-0.8	0.0	-0.3	0.0	0.0	-0.2	-1.0	0.9
N	30810 - 30807	-0.1	-1.2	-2.9	-0.2	-0.1	0.0	-0.1	-1.2	-2.9	2.8
O	30524 - 30521	0.0	-0.4	-1.7	0.0	-0.2	0.0	0.0	-0.3	-1.7	1.7
P	30850 - 30847	-0.1	-1.5	-2.4	-0.2	0.0	-0.1	0.0	-1.5	-2.4	2.4
Q	30564 - 30561	0.0	-0.4	-2.0	-0.1	-0.2	0.0	0.0	-0.4	-2.0	2.0
R	30890 - 30887	0.4	0.1	-1.3	0.0	0.1	0.1	0.4	0.1	-1.3	1.7
S	30604 - 30601	0.0	0.0	-1.5	0.0	0.0	0.1	0.0	0.0	-1.5	1.6
T	30614 - 30611	-0.1	0.1	-1.0	0.1	0.0	0.2	0.1	-0.1	-1.1	1.2
U	30900 - 30910	0.3	0.2	-0.5	0.0	0.0	0.3	0.4	0.2	-0.6	1.0
V	30920 - 30930	-0.3	0.0	-0.4	0.1	0.0	0.4	0.1	0.0	-0.8	0.9
W	1216 - 1226	0.5	1.1	-0.3	0.0	0.0	-0.2	1.1	0.5	-0.3	1.4
X	1236 - 1246	-0.7	-1.2	0.3	-0.1	0.0	-0.2	0.3	-0.7	-1.2	1.5

[1] Refer to Figure 2.10.2-34 for the identification of the representative sections.

Table 2.10.4-162 $P_m + P_b$ Stresses; 30-Foot Bottom Corner Drop; Drop Orientation = 24 Degrees; 3-D Bottom Model; 180-Degree Circumferential Location; Condition 1

Condition 1: 100°F Ambient with Contents

		Stress Components (ksi)						Principal Stresses (ksi)			
Section[1]	Node - Node	S_x	S_y	S_z	S_{xy}	S_{yz}	S_{zx}	S1	S2	S3	S.I.
A I	1130 - 1128	17.5	13.4	-6.5	-0.5	1.8	2.1	17.7	13.5	-6.8	24.5
B O	1185 - 1183	-17.5	-18.8	2.7	0.4	1.7	2.3	3.1	-17.7	-19.0	22.1
C O	30090 - 30040	8.9	5.5	-0.1	0.0	-0.1	0.8	9.0	5.5	-0.1	9.1
D I	30025 - 30005	-8.4	0.1	-3.5	0.6	-0.4	-0.9	0.2	-3.4	-8.6	8.8
E I	30035 - 30031	5.7	3.9	-1.2	0.1	-0.3	-2.2	6.4	3.9	-1.8	8.2
F O	30100 - 30097	0.5	3.1	8.4	0.4	-0.4	-1.0	8.6	3.1	0.3	8.3
G I	30094 - 30091	0.4	1.6	4.1	0.1	-0.6	0.3	4.3	1.4	0.4	3.9
H I	30330 - 30327	0.1	-0.9	7.2	-0.1	-0.9	0.0	7.3	0.1	-1.0	8.3
I I	30244 - 30241	0.0	-0.2	1.6	0.0	-0.4	0.0	1.7	0.0	-0.3	2.0
J O	30550 - 30547	-0.3	-1.1	1.1	-0.1	-0.7	0.0	1.3	-0.2	-1.3	2.6
K O	30344 - 30341	0.0	-0.6	0.3	-0.1	-0.3	0.0	0.4	0.0	-0.7	1.1
L I	30740 - 30737	-0.2	-1.2	-2.1	-0.3	-0.3	0.0	-0.1	-1.1	-2.2	2.1
M I	30454 - 30451	0.0	-0.3	-0.9	-0.1	-0.3	0.0	0.0	-0.2	-1.0	1.0
N I	30810 - 30807	-0.1	-1.5	-3.0	-0.2	-0.1	0.0	-0.1	-1.6	-3.1	3.0
O I	30524 - 30521	0.0	-0.6	-1.8	-0.1	-0.2	0.0	0.0	-0.6	-1.9	1.8
P O	30850 - 30847	-0.1	-1.4	-2.9	-0.2	0.0	-0.1	0.0	-1.4	-2.9	2.8
Q O	30564 - 30561	0.0	-0.2	-2.0	0.0	-0.1	0.0	0.0	-0.2	-2.0	2.0
R I	30890 - 30887	0.4	-0.2	-2.3	0.0	0.1	0.0	0.4	-0.2	-2.3	2.7
S O	30604 - 30601	-0.1	-0.1	-1.7	0.0	0.0	0.1	-0.1	-0.1	-1.7	1.7
T O	30614 - 30611	0.0	0.1	-1.2	0.0	0.1	0.2	0.1	0.0	-1.2	1.3
U O	30900 - 30910	1.3	0.5	-0.2	0.0	0.0	0.5	1.5	0.5	-0.3	1.8
V I	30920 - 30930	-1.5	-0.3	-0.5	0.1	0.0	0.5	-0.2	-0.3	-1.7	1.5
W I	1216 - 1226	1.2	2.3	-1.0	0.0	0.0	-0.2	2.3	1.2	-1.0	3.3
X O	1236 - 1246	-1.5	-2.4	1.1	-0.1	0.0	-0.2	1.1	-1.5	-2.5	3.6

[1] Refer to Figure 2.10.2-34 for the identification of the representative sections.

Table 2.10.4-163 Primary Stresses; 30-Foot Bottom Oblique Drop; Drop Orientation = 15 Degrees; 3-D Bottom Model; 0-Degree Circumferential Location; Condition 1

Condition 1: 100°F Ambient with Contents

Stress Points		Stress Components (ksi)						Principal Stresses (ksi)		
Section[1]	Node	S_x	S_y	S_z	S_{xy}	S_{yz}	S_{xz}	S1	S2	S3
A1	1130	18.7	15.1	-6.8	-0.5	2.2	2.2	18.9	15.3	-7.2
A2	1129	2.6	1.1	-1.3	0.0	1.6	2.2	3.7	1.5	-2.8
A3	1128	-13.6	-12.9	4.3	0.5	2.1	2.2	4.8	-13.1	-13.9
B1	1185	10.9	4.9	-6.8	-0.6	2.6	2.4	11.3	5.4	-7.7
B2	1184	-3.6	-6.6	-2.0	-0.1	1.9	2.4	0.1	-4.8	-7.6
B3	1183	-18.4	-18.1	2.8	0.4	2.1	2.4	3.3	-18.3	-18.7
C1	90	-21.3	-4.9	-30.1	-1.3	-0.7	-5.7	-4.7	-18.6	-33.0
C2	80	-8.0	0.6	-16.9	-1.0	-0.5	-4.5	0.7	-6.2	-18.8
C3	70	-4.5	1.3	-10.2	-0.6	-0.4	-4.0	1.3	-2.5	-12.3
C4	60	-1.5	1.3	-5.9	-0.1	-0.4	-3.9	1.4	0.7	-8.2
C5	50	9.3	-1.7	-4.1	1.0	-0.2	-2.7	9.9	-1.7	-4.6
C6	40	17.1	-3.2	-4.3	1.7	-0.1	-1.6	17.3	-3.3	-4.4
D1	25	-28.1	-20.8	-33.8	-0.3	-0.7	-8.3	-20.8	-22.1	-39.8
D2	15	-3.9	-16.5	-15.5	0.7	-0.3	-3.8	-2.7	-16.5	-16.7
D3	5	2.9	-21.0	-7.8	1.6	-0.1	-1.2	3.1	-8.0	-21.1
E1	35	13.3	-6.0	-24.0	1.4	-0.4	-4.0	13.8	-6.1	-24.4
E2	34	3.7	-6.4	-18.5	0.7	-0.8	-7.6	6.1	-6.4	-20.9
E3	33	-3.0	-6.2	-11.3	0.2	-0.8	-8.0	1.9	-6.3	-16.2
E4	32	-4.2	-5.2	-6.1	0.1	-0.4	-4.9	-0.1	-5.2	-10.2
E5	31	-4.7	-4.1	-1.0	0.0	-0.3	-3.0	0.7	-4.1	-6.3
F1	100	0.2	-1.4	-40.6	-0.1	-0.8	-3.9	0.5	-1.3	-41.0
F2	99	-2.6	3.4	-20.5	-0.6	-0.7	-2.2	3.5	-2.4	-20.8
F3	98	-2.7	5.7	-11.4	-0.7	-0.4	0.2	5.8	-2.8	-11.4
F4	97	0.0	9.7	1.0	-0.8	-0.3	1.1	9.8	1.6	-0.7
G1	94	0.1	-1.9	-30.9	0.0	-0.4	-2.1	0.2	-1.9	-31.0
G2	93	-1.1	1.6	-17.0	-0.3	-0.4	-1.2	1.6	-1.0	-17.1
G3	92	-1.5	3.6	-9.0	-0.4	-0.2	-0.2	3.6	-1.5	-9.0
G4	91	-0.7	6.3	0.6	-0.5	-0.1	0.0	6.3	0.6	-0.8
H1	330	-0.3	3.3	-12.5	-0.2	-0.7	-0.1	3.4	-0.3	-12.5
H2	329	-0.5	2.7	-16.4	-0.2	-0.7	0.0	2.8	-0.5	-16.4

Table 2.10.4-163 Primary Stresses; 30-Foot Bottom Oblique Drop; Drop Orientation = 15 Degrees; 3-D Bottom Model; 0-Degree Circumferential Location; Condition 1 (continued)

Stress Points		Stress Components (ksi)						Principal Stresses (ksi)		
Section[1]	Node	S_x	S_y	S_z	S_{xy}	S_{yz}	S_{xz}	S1	S2	S3
H3	328	-0.6	2.2	-20.0	-0.2	-0.6	0.6	2.3	-0.6	-20.0
H4	327	-0.6	1.0	-26.6	-0.1	-0.5	1.4	1.0	-0.5	-26.7
I1	244	0.0	2.0	-11.2	-0.1	-0.3	-0.1	2.0	0.0	-11.3
I2	243	0.0	2.3	-11.8	-0.2	-0.3	-0.1	2.3	0.0	-11.8
I3	242	0.0	2.5	-12.3	-0.2	-0.2	-0.1	2.5	0.0	-12.3
I4	241	0.0	2.7	-12.8	-0.2	-0.2	-0.1	2.7	0.0	-12.8
J1	550	-0.1	1.9	-13.2	-0.2	-0.5	0.0	1.9	-0.1	-13.2
J2	548	-0.1	3.5	-12.7	-0.3	-0.5	0.0	3.6	-0.1	-12.7
J3	547	0.0	5.1	-12.2	-0.4	-0.5	0.0	5.1	-0.1	-12.2
K1	344	0.0	-0.4	-9.9	0.0	-0.2	0.0	0.0	-0.4	-9.9
K2	342	0.0	0.7	-9.5	-0.1	-0.2	0.0	0.7	0.0	-9.5
K3	341	0.0	1.8	-9.2	-0.1	-0.2	0.0	1.8	0.0	-9.2
L1	740	0.0	2.1	-6.2	0.2	-0.2	0.0	2.1	0.0	-6.2
L2	738	-0.2	3.4	-5.8	-0.6	-0.2	0.0	3.5	-0.3	-5.8
L3	737	0.2	4.9	-5.2	-1.3	-0.2	0.0	5.2	-0.1	-5.2
M1	454	-0.1	-0.8	-6.3	-0.4	-0.2	0.0	0.1	-1.0	-6.3
M2	452	0.1	0.5	-5.9	-0.2	-0.2	0.0	0.6	0.0	-5.9
M3	451	-0.2	1.5	-5.7	0.0	-0.2	0.0	1.5	-0.2	-5.7
N1	810	-0.1	2.9	-3.4	-0.2	0.0	0.0	2.9	-0.1	-3.4
N2	807	-0.1	4.2	-2.7	-0.3	0.0	0.0	4.2	-0.1	-2.7
O1	524	0.0	-0.7	-3.4	0.0	-0.1	0.0	0.0	-0.7	-3.4
O2	521	0.0	1.2	-2.6	-0.1	-0.1	0.0	1.3	0.0	-2.6
P1	850	0.0	2.7	-3.7	-0.2	0.2	-0.1	2.7	0.0	-3.7
P2	847	0.0	3.5	-2.4	-0.2	0.1	0.0	3.5	0.0	-2.4
Q1	564	0.0	0.1	-1.5	0.0	-0.1	0.0	0.1	0.0	-1.5
Q2	561	0.0	0.7	-1.9	0.0	-0.1	0.0	0.7	0.0	-1.9
R1	890	-0.4	0.6	-0.3	-0.1	0.1	-0.1	0.6	-0.3	-0.5
R2	887	-0.7	-0.1	-3.2	0.0	0.0	-0.2	-0.1	-0.6	-3.2
S1	604	-0.5	0.6	-1.4	0.0	-0.1	-0.1	0.6	-0.5	-1.4
S2	601	-0.1	1.3	0.4	-0.1	-0.1	0.0	1.3	0.4	-0.1
T1	897	0.0	0.4	-1.2	0.0	0.0	0.0	0.4	0.0	-1.2
T2	614	0.1	0.7	-0.6	0.0	-0.1	-0.1	0.7	0.1	-0.6

Table 2.10.4-163 Primary Stresses; 30-Foot Bottom Oblique Drop; Drop Orientation = 15 Degrees; 3-D Bottom Model; 0-Degree Circumferential Location; Condition 1 (continued)

Stress Points		Stress Components (ksi)						Principal Stresses (ksi)		
Section[1]	Node	S_x	S_y	S_z	S_{xy}	S_{yz}	S_{zx}	S1	S2	S3
T3	611	0.0	0.6	-0.3	0.0	-0.1	-0.1	0.6	0.0	-0.3
U1	900	-0.2	0.5	-0.8	0.0	0.0	0.2	0.5	-0.1	-0.8
U2	910	0.9	0.3	-0.5	0.0	0.0	0.3	1.0	0.3	-0.5
V1	920	-0.8	-0.2	-0.5	0.0	0.0	0.3	-0.2	-0.3	-1.0
V2	930	0.3	-0.4	-0.3	0.1	0.0	0.2	0.3	-0.3	-0.4
W1	1216	1.6	2.2	-1.1	0.0	0.1	-0.3	2.2	1.6	-1.1
W2	1226	-0.2	-0.1	0.5	0.0	0.0	-0.1	0.5	-0.1	-0.3
X1	1236	0.1	0.1	-0.6	0.0	0.0	-0.1	0.2	0.1	-0.6
X2	1246	-1.8	-2.1	1.2	0.0	0.1	-0.3	1.2	-1.8	-2.1

[1] Refer to Figure 2.10.2-34 for the identification of the representative sections.

Table 2.10.4-164 P_m Stresses; 30-Foot Bottom Oblique Drop; Drop Orientation = 15 Degrees; 3-D Bottom Model; 0-Degree Circumferential Location; Condition 1

Condition 1: 100°F Ambient with Contents

Section[1]	Node - Node	Stress Components (ksi)						Principal Stresses (ksi)			
		S_x	S_y	S_z	S_{xy}	S_{yz}	S_{xz}	S1	S2	S3	S.I.
A	1130 - 1128	2.5	1.1	-1.2	0.0	1.9	2.2	3.8	1.5	-3.0	6.8
B	1185 - 1183	-3.7	-6.6	-2.0	-0.1	2.1	2.4	0.2	-4.7	-7.7	7.9
C	90 - 40	1.2	-0.6	-8.7	0.2	-0.3	-3.5	2.4	-0.6	-9.8	12.2
D	25 - 5	-8.3	-18.7	-18.2	0.7	-0.3	-4.3	-6.6	-18.7	-19.8	13.1
E	35 - 31	1.0	-5.8	-13.0	0.5	-0.6	-6.0	3.3	-5.8	-15.2	18.5
F	100 - 97	-1.7	4.4	-17.2	-0.6	-0.5	-1.1	4.5	-1.7	-17.3	21.8
G	94 - 91	-1.0	2.4	-13.7	-0.3	-0.3	-0.8	2.5	-1.0	-13.8	16.2
H	330 - 327	-0.5	2.4	-18.6	-0.2	-0.6	0.4	2.4	-0.5	-18.7	21.1
I	244 - 241	0.0	2.4	-12.0	-0.2	-0.3	-0.1	2.4	0.0	-12.0	14.4
J	550 - 547	-0.1	3.5	-12.7	-0.3	-0.5	0.0	3.5	-0.1	-12.7	16.2
K	344 - 341	0.0	0.7	-9.5	-0.1	-0.2	0.0	0.7	0.0	-9.5	10.2
L	740 - 737	0.0	3.4	-5.8	-0.6	-0.2	0.0	3.5	-0.1	-5.8	9.3
M	454 - 451	0.0	0.5	-5.9	-0.2	-0.2	0.0	0.5	-0.1	-5.9	6.5
N	810 - 807	-0.1	3.5	-3.1	-0.2	0.0	0.0	3.6	-0.1	-3.1	6.6
O	524 - 521	0.0	0.3	-3.0	0.0	-0.1	0.0	0.3	0.0	-3.0	3.3
P	850 - 847	0.0	3.1	-3.1	-0.2	0.1	0.0	3.1	0.0	-3.1	6.2
Q	564 - 561	0.0	0.4	-1.7	0.0	-0.1	0.0	0.4	0.0	-1.7	2.1
R	890 - 887	-0.5	0.2	-1.8	0.0	0.1	-0.1	0.2	-0.5	-1.8	2.0
S	604 - 601	-0.3	1.0	-0.5	-0.1	-0.1	0.0	1.0	-0.3	-0.5	1.5
T	614 - 611	0.0	0.7	-0.4	0.0	-0.1	-0.1	0.7	0.1	-0.5	1.1
U	900 - 910	0.4	0.4	-0.6	0.0	0.0	0.2	0.4	0.4	-0.7	1.1
V	920 - 930	-0.3	-0.3	-0.4	0.0	0.0	0.2	-0.1	-0.3	-0.6	0.5
W	1216 - 1226	0.7	1.0	-0.3	0.0	0.0	-0.2	1.0	0.7	-0.3	1.4
X	1236 - 1246	-0.8	-1.0	0.3	0.0	0.0	-0.2	0.3	-0.9	-1.0	1.3

[1] Refer to Figure 2.10.2-34 for the identification of the representative sections.

Table 2.10.4-165 $P_m + P_b$ Stresses; 30-Foot Bottom Oblique Drop; Drop Orientation = 15 Degrees; 3-D Bottom Model; 0-Degree Circumferential Location; Condition 1

Condition 1: 100°F Ambient with Contents

		Stress Components (ksi)						Principal Stresses (ksi)			
Section[1]	Node - Node	S_x	S_y	S_z	S_{xy}	S_{yz}	S_{xz}	S1	S2	S3	S.I.
A I	1130 - 1128	18.7	15.1	-6.8	-0.5	1.9	2.2	18.9	15.2	-7.2	26.1
B O	1185 - 1183	-18.3	-18.1	2.8	0.4	1.8	2.4	3.3	-18.2	-18.7	21.9
C I	90 - 40	-14.2	0.6	-18.2	-1.4	-0.6	-5.1	0.7	-10.8	-21.8	22.5
D O	25 - 5	7.2	-18.8	-5.2	1.6	0.0	-0.7	7.4	-5.2	-18.9	26.2
E I	35 - 31	10.4	-6.7	-25.1	1.2	-0.8	-6.9	11.8	-6.8	-26.5	38.3
F I	100 - 97	-1.6	-0.6	-36.4	-0.3	-0.9	-3.9	-0.5	-1.3	-36.9	36.3
G I	94 - 91	-0.5	-1.4	-28.6	-0.1	-0.5	-2.0	-0.4	-1.4	-28.8	28.4
H O	330 - 327	-0.6	1.3	-25.3	-0.1	-0.5	1.2	1.3	-0.6	-25.4	26.7
I O	244 - 241	0.0	2.7	-12.8	-0.2	-0.2	-0.1	2.7	0.0	-12.8	15.5
J O	550 - 547	0.0	5.1	-12.2	-0.4	-0.5	0.0	5.1	-0.1	-12.2	17.3
K O	344 - 341	0.0	1.8	-9.2	-0.1	-0.2	0.0	1.8	0.0	-9.2	11.0
L O	740 - 737	0.0	4.8	-5.2	-1.3	-0.2	0.0	5.2	-0.3	-5.2	10.4
M O	454 - 451	-0.1	1.6	-5.6	0.0	-0.2	0.0	1.6	-0.1	-5.6	7.2
N O	810 - 807	-0.1	4.2	-2.7	-0.3	0.0	0.0	4.2	-0.1	-2.7	7.0
O O	524 - 521	0.0	1.2	-2.6	-0.1	-0.1	0.0	1.3	0.0	-2.6	3.8
P I	850 - 847	0.0	2.7	-3.7	-0.2	0.2	-0.1	2.7	0.0	-3.7	6.4
Q O	564 - 561	0.0	0.7	-1.9	0.0	-0.1	0.0	0.7	0.0	-1.9	2.6
R O	890 - 887	-0.7	-0.1	-3.2	0.0	0.0	-0.2	-0.1	-0.6	-3.2	3.1
S I	604 - 601	-0.5	0.6	-1.4	0.0	-0.1	-0.1	0.6	-0.5	-1.4	2.1
T I	614 - 611	0.1	0.7	-0.6	0.0	-0.1	-0.1	0.7	0.1	-0.6	1.3
U O	900 - 910	0.9	0.3	-0.5	0.0	0.0	0.3	1.0	0.3	-0.5	1.5
V I	920 - 930	-0.8	-0.2	-0.5	0.0	0.0	0.3	-0.2	-0.3	-1.0	0.8
W I	1216 - 1226	1.6	2.2	-1.1	0.0	0.1	-0.3	2.2	1.6	-1.1	3.3
X O	1236 - 1246	-1.8	-2.1	1.2	0.0	0.1	-0.3	1.2	-1.8	-2.1	3.3

[1] Refer to Figure 2.10.2-34 for the identification of the representative sections.

Table 2.10.4-166 Critical P_m Stress Summary; 30-Foot Bottom Oblique Drop; Drop Orientation = 15 Degrees; 3-D Bottom Model; Condition 1

Condition 1: 100°F Ambient with Contents

Comp. No.[1]	Section Cut Node-Node	P_m Stresses (ksi)						Principal Stresses (ksi)			S.I.	Allow. Stress	Margin of Safety
		S_x	S_y	S_z	S_{xy}	S_{yz}	S_{xz}	S1	S2	S3			
1	14025-14005	-3.9	-11.9	-16.3	-2.3	-3.3	-3.5	-2.8	-10.2	-19.1	16.4	45.6	1.8
2	140-137	0.0	7.3	-16.7	-0.5	-0.5	-0.9	7.4	0.0	-16.8	24.1	44.9	0.9
3	160-157	0.0	7.9	-16.4	-0.6	-0.5	-0.7	7.9	-0.1	-16.4	24.3	66.0	1.7
4	8520-8517	0.0	3.0	-13.3	0.0	-4.3	0.0	4.1	0.0	-14.3	18.5	45.8	1.5
5	8204-8201	-0.1	3.1	-12.1	0.0	-2.3	-0.2	3.4	-0.1	-12.5	15.9	46.4	1.9
6	12880-12877	-0.1	1.3	-1.6	0.0	1.4	0.0	1.9	-0.1	-2.1	4.0	49.3	11.3
7	1216-1226	0.7	1.0	-0.3	0.0	0.0	-0.2	1.0	0.7	-0.3	1.4	48.0	34.3
8	1236-1246	-0.8	-1.0	0.3	0.0	0.0	-0.2	0.3	-0.9	-1.0	1.3	94.5	71.7

Locations of the most critical sections for each component are provided in the following:

Comp. No.[1]	Section Location					
	Inside Node			Outside Node		
	x (in)	y (deg)	z (in)	x (in)	y (deg)	z (in)
1	39.44	67.7	6.20	39.44	67.7	0.75
2	35.50	0.0	17.40	37.50	0.0	17.40
3	35.50	0.0	18.90	37.50	0.0	18.90
4	35.50	35.8	47.40	37.00	35.8	47.40
5	40.70	35.8	26.40	43.35	35.8	26.40
6	35.50	56.5	172.40	37.50	56.5	172.40
7	0.00	0.0	179.40	0.00	0.0	185.40
8	0.00	0.0	187.40	0.00	0.0	193.71

[1] Refer to Figure 2.10.2-33 for cask component identification.

Table 2.10.4-167 Critical $P_m + P_b$ Stress Summary; 30-Foot Bottom Oblique Drop; Drop Orientation = 15 Degrees; 3-D Bottom Model; Condition 1

Condition 1: 100°F Ambient with Contents

Comp. No.[1]	Section Cut Node-Node	$P_m + P_b$ Stresses (ksi) S_x	S_y	S_z	S_{xy}	S_{yz}	S_{xz}	Principal Stresses (ksi) S1	S2	S3	S.I.	Allow. Stress	Margin of Safety
1	1170- 1168	-43.5	-34.0	-4.8	0.0	-0.1	-0.1	-4.8	-34.0	-43.5	38.7	65.2	0.7
2	12035-12031	10.1	-4.2	-24.7	4.5	-6.8	-6.1	13.0	-4.5	-27.3	40.3	64.2	0.6
3	6150- 6147	-0.1	5.2	-25.6	0.0	-3.9	-0.9	5.7	-0.1	-26.1	31.8	94.3	2.0
4	10520-10517	-0.1	3.7	-12.0	0.0	-5.6	0.0	5.5	-0.1	-13.8	19.3	65.5	2.4
5	8204- 8201	-0.3	3.0	-12.1	0.0	-2.7	-0.2	3.5	-0.3	-12.6	16.1	66.4	3.1
6	880- 877	0.1	0.0	-5.0	0.0	0.1	-0.3	0.1	0.0	-5.0	5.1	70.9	12.9
7	1216- 1226	1.6	2.2	-1.1	0.0	0.1	-0.3	2.2	1.6	-1.1	3.3	69.8	20.2
8	1236- 1246	-1.8	-2.1	1.2	0.0	0.1	-0.3	1.2	-1.8	-2.1	3.3	135.0	39.9

Locations of the most critical sections for each component are provided in the following:

Comp. No.[1]	Section Location Inside Node x (in)	y (deg)	z (in)	Outside Node x (in)	y (deg)	z (in)
1	14.73	0.0	6.20	14.73	0.0	0.75
2	39.44	56.5	8.20	43.35	56.5	8.20
3	35.50	26.2	18.15	37.50	26.2	18.15
4	35.50	45.9	47.40	37.00	45.9	47.40
5	40.70	35.8	26.40	43.35	35.8	26.40
6	35.50	0.0	172.40	37.50	0.0	172.40
7	0.00	0.0	179.40	0.00	0.0	185.40
8	0.00	0.0	187.40	0.00	0.0	193.71

[1] Refer to Figure 2.10.2-33 for cask component identification.

Table 2.10.4-168 Primary Stresses; 30-Foot Top Oblique Drop; Drop Orientation = 75 Degrees; 3-D Top Model; 0-Degree Circumferential Location; Condition 1

Condition 1: 100°F Ambient with Contents

Stress Points		Stress Components (ksi)						Principal Stresses (ksi)		
Section[1]	Node	S_x	S_y	S_z	S_{xy}	S_{yz}	S_{xz}	S1	S2	S3
A1	1949	-1.0	1.8	-0.1	-0.2	0.0	-0.2	1.8	-0.1	-1.0
A2	1950	-0.9	1.3	-0.1	-0.2	0.2	-0.2	1.3	-0.1	-0.9
A3	1951	-0.2	-0.1	0.1	-0.1	0.5	-0.1	0.5	-0.2	-0.5
B1	1952	0.0	-0.8	-0.1	-0.2	0.5	-0.1	0.3	-0.1	-1.0
B2	93	0.6	-3.0	0.3	-0.4	0.3	-0.2	0.7	0.2	-3.1
C1	1925	2.5	-2.3	7.5	0.1	-0.5	0.4	7.6	2.5	-2.3
C2	1926	2.4	-3.5	1.5	0.2	-0.2	-0.1	2.4	1.5	-3.6
C3	1927	-1.3	-2.2	0.2	0.1	-0.1	0.2	0.3	-1.3	-2.3
D1	683	2.4	-1.9	0.3	0.5	-0.1	0.8	2.8	0.1	-2.0
D2	85	-3.3	-4.0	0.9	0.8	-0.1	0.2	0.9	-2.8	-4.5
E1	682	-2.0	-3.2	0.1	0.2	-0.1	1.1	0.6	-2.4	-3.3
E2	82	-1.7	-3.6	2.6	0.3	0.2	1.4	3.0	-2.0	-3.6
F1	1925	2.5	-2.3	7.5	0.1	-0.5	0.4	7.6	2.5	-2.3
F2	1325	0.7	-8.4	-13.8	0.6	-0.4	1.1	0.8	-8.4	-13.9
G1	680	2.3	-1.3	10.1	0.2	-0.1	2.0	10.6	1.8	-1.3
G2	80	2.1	-4.5	-2.4	0.4	-0.3	-0.2	2.2	-2.4	-4.5
H1	1921	-0.1	7.3	-2.8	-0.4	-1.3	0.1	7.4	-0.2	-3.0
H2	1321	-0.2	12.0	6.6	-0.7	-1.1	-0.3	12.2	6.5	-0.3
I1	676	-0.1	-0.3	5.4	0.1	-0.6	0.0	5.5	-0.1	-0.4
I2	76	-0.1	3.8	11.1	-0.2	-0.4	0.0	11.1	3.8	-0.1
J1	1916	-0.2	7.6	9.6	-0.6	-0.6	0.0	9.8	7.5	-0.3
J2	1316	-0.2	12.5	13.4	-0.9	-0.6	0.0	13.7	12.3	-0.3
K1	671	-0.1	-1.2	9.9	0.1	-0.4	0.0	9.9	-0.1	-1.3
K2	71	-0.1	5.9	13.3	-0.4	-0.2	0.0	13.3	6.0	-0.1
L1	1908	-0.9	4.5	12.9	-0.4	0.2	0.0	12.9	4.6	-0.9
L2	1308	0.0	11.5	15.9	1.7	0.2	0.0	15.9	11.7	-0.3
M1	663	-1.2	-2.2	10.8	0.1	0.1	0.0	10.8	-1.2	-2.2
M2	63	0.4	8.9	15.8	2.0	0.1	0.0	15.8	9.3	0.0
N1	1877	-0.3	7.4	4.5	-0.6	1.0	0.0	7.8	4.2	-0.4
N2	1477	-0.2	10.0	6.2	-0.8	1.0	0.0	10.3	6.0	-0.2

Table 2.10.4-168 Primary Stresses; 30-Foot Top Oblique Drop; Drop Orientation = 75 Degrees; 3-D Top Model; 0-Degree Circumferential Location; Condition 1 (continued)

Stress Points		Stress Components (ksi)						Principal Stresses (ksi)		
Section[1]	Node	S_x	S_y	S_z	S_{xy}	S_{yz}	S_{xz}	S1	S2	S3
N3	1277	-0.1	12.6	7.9	-0.9	0.9	0.0	12.8	7.7	-0.1
O1	647	-0.1	-1.1	8.3	0.0	0.5	0.0	8.3	-0.1	-1.2
O2	247	-0.1	2.4	9.9	-0.2	0.4	0.0	9.9	2.4	-0.1
O3	47	0.0	5.8	11.5	-0.4	0.3	0.0	11.5	5.8	-0.1
P1	1840	-0.3	7.2	-9.1	-0.5	1.7	0.0	7.4	-0.3	-9.3
P2	1640	-0.2	8.9	-6.3	-0.6	1.6	0.0	9.2	-0.3	-6.4
P3	1440	-0.1	10.6	-3.4	-0.7	1.5	0.0	10.9	-0.1	-3.6
P4	1240	0.1	12.3	-0.6	-0.8	1.5	0.1	12.5	0.1	-0.8
Q1	628	-0.4	0.3	2.2	-0.1	0.7	0.1	2.4	0.0	-0.4
Q2	428	-0.3	2.1	5.0	-0.2	0.6	0.1	5.1	2.0	-0.3
Q3	228	-0.1	3.8	7.7	-0.3	0.5	0.1	7.8	3.8	-0.1
Q4	28	0.0	5.5	10.5	-0.4	0.4	0.0	10.5	5.5	-0.1
R1	1816	-1.0	-9.7	4.1	0.7	1.1	0.2	4.2	-0.9	-9.8
R2	1616	-1.8	-11.9	-4.1	0.9	1.0	-0.1	-1.7	-4.0	-12.1
R3	1416	-4.4	-14.3	-11.7	1.0	0.7	-2.1	-3.8	-11.9	-14.7
R4	1216	-5.1	-16.5	-20.7	1.2	0.3	-5.0	-3.5	-16.5	-22.3
S1	616	5.0	-7.2	-1.8	0.6	0.6	-0.8	5.1	-1.8	-7.3
S2	416	0.3	-7.6	1.3	0.5	0.4	-1.0	1.9	-0.2	-7.7
S3	216	0.5	-6.6	4.3	0.5	0.3	-0.2	4.3	0.5	-6.6
S4	16	0.3	-5.7	7.2	0.4	0.2	0.0	7.2	0.3	-5.8
T1	811	-20.6	-25.0	-17.0	1.0	0.3	-6.4	-12.2	-24.2	-26.3
T2	611	-10.6	-18.8	-5.6	0.9	0.1	-6.4	-1.2	-14.8	-19.0
T3	411	-5.0	-16.3	-2.7	0.9	0.1	-5.5	1.8	-9.4	-16.4
T4	211	-0.6	-14.3	-0.4	1.0	0.1	-3.2	2.7	-3.6	-14.4
T5	11	1.0	-11.8	6.5	0.9	0.1	-1.6	7.0	0.6	-11.8
U1	43058	7.9	2.2	-0.3	0.2	0.1	-0.2	7.9	2.2	-0.3
U2	43057	3.1	-0.1	-0.6	0.1	-0.1	0.0	3.1	0.0	-0.6
U3	43056	0.1	-1.9	-1.3	0.1	0.0	0.1	0.1	-1.3	-1.9
U4	43055	-2.1	-3.6	-2.2	0.1	0.0	-0.2	-2.0	-2.3	-3.6
U5	43054	-4.4	-5.2	-3.0	0.1	-0.1	-1.0	-2.4	-4.9	-5.2
U6	43053	-6.7	-6.8	-3.4	0.1	-0.2	-2.5	-2.0	-6.8	-8.0
U7	43052	-9.6	-8.2	-2.5	0.0	-0.3	-2.9	-1.4	-8.2	-10.7

Table 2.10.4-168 Primary Stresses; 30-Foot Top Oblique Drop; Drop Orientation = 75 Degrees; 3-D Top Model; 0-Degree Circumferential Location; Condition 1 (continued)

Stress Points		Stress Components (ksi)						Principal Stresses (ksi)		
Section[1]	Node	S_x	S_y	S_z	S_{xy}	S_{yz}	S_{zx}	S1	S2	S3
U8	43051	-16.4	-10.9	-0.2	-0.1	0.1	1.5	0.0	-10.9	-16.6
V1	50024	-18.4	-12.7	0.0	-1.1	0.0	0.6	0.0	-12.5	-18.6
V2	50023	-19.7	-15.5	-1.2	-0.8	0.1	1.5	-1.1	-15.4	-20.0
V3	50022	-13.3	-15.8	-1.5	-0.3	0.1	2.0	-1.2	-13.6	-15.8
V4	50021	-17.4	-18.9	-0.4	-0.2	0.1	1.6	-0.3	-17.5	-18.9
W1	43278	-1.6	-5.3	0.1	-0.2	-0.4	0.3	0.1	-1.6	-5.4
W2	43274	-0.6	-5.2	-0.1	-0.1	-0.4	0.3	0.0	-0.7	-5.2
W3	43271	0.2	-2.6	-0.2	0.0	-0.5	0.1	0.2	-0.1	-2.7
X1	50084	9.4	-0.3	-2.6	-0.2	0.2	-2.3	9.8	-0.3	-3.1
X2	50083	2.4	-7.5	-1.7	0.0	0.1	-2.3	3.5	-2.7	-7.5
X3	50081	-10.1	-20.2	5.1	0.4	-0.4	-2.3	5.5	-10.4	-20.2

[1] Refer to Figure 2.10.2-34 for the identification of the representative sections.

Table 2.10.4-169 P_m Stresses; 30-Foot Top Oblique Drop; Drop Orientation = 75 Degrees; 3-D Top Model; 0-Degree Circumferential Location; Condition 1

Condition 1: 100°F Ambient with Contents

		Stress Components (ksi)						Principal Stresses (ksi)			
Section[1]	Node - Node	S_x	S_y	S_z	S_{xy}	S_{yz}	S_{zx}	S1	S2	S3	S.I.
A	1949 - 1951	-0.6	0.9	-0.1	-0.1	0.3	-0.1	1.0	-0.1	-0.7	1.6
B	1952 - 93	0.3	-1.9	0.1	-0.3	0.4	-0.1	0.4	0.0	-2.0	2.4
C	1925 - 1927	1.0	-2.9	1.8	0.2	-0.2	0.1	1.9	1.0	-2.9	4.8
D	683 - 85	-0.4	-2.9	0.6	0.6	-0.1	0.5	0.8	-0.5	-3.1	3.9
E	682 - 82	-1.8	-3.4	1.3	0.2	0.0	1.3	1.8	-2.2	-3.5	5.2
F	1925 - 1325	1.6	-5.3	-3.2	0.4	-0.5	0.7	1.7	-3.2	-5.5	7.2
G	680 - 80	2.2	-2.9	3.8	0.3	-0.2	0.9	4.2	1.8	-2.9	7.1
H	1921 - 1321	-0.2	9.6	1.9	-0.6	-1.2	-0.1	9.8	1.7	-0.2	10.1
I	676 - 76	-0.1	1.8	8.3	-0.1	-0.5	0.0	8.3	1.7	-0.1	8.4
J	1916 - 1316	-0.2	10.1	11.5	-0.7	-0.6	0.0	11.7	9.9	-0.3	12.0
K	671 - 71	-0.1	2.3	11.6	-0.2	-0.3	0.0	11.6	2.3	-0.1	11.7
L	1908 - 1308	-0.5	8.0	14.4	0.6	0.2	0.0	14.4	8.1	-0.5	14.9
M	663 - 63	-0.4	3.3	13.3	1.0	0.1	0.0	13.3	3.6	-0.6	14.0
N	1877 - 1277	-0.2	10.0	6.2	-0.7	1.0	0.0	10.3	6.0	-0.2	10.5
O	647 - 47	-0.1	2.4	9.9	-0.2	0.4	0.0	9.9	2.4	-0.1	10.0
P	1840 - 1240	-0.1	9.8	-4.8	-0.7	1.6	0.0	10.0	-0.2	-5.0	15.0
Q	628 - 28	-0.2	2.9	6.3	-0.2	0.6	0.1	6.4	2.9	-0.2	6.7
R	1816 - 1216	-3.1	-13.1	-8.0	1.0	0.8	-1.5	-2.6	-8.2	-13.4	10.8
S	616 - 16	1.2	-6.9	2.8	0.5	0.4	-0.5	2.9	1.0	-7.0	9.9
T	811 - 11	-6.5	-17.0	-3.5	0.9	0.1	-4.8	0.0	-9.9	-17.1	17.1
U	43058 - 43051	-4.6	-5.0	-1.8	0.0	-0.1	-0.8	-1.6	-4.8	-5.0	3.4
V	50024 - 50021	-17.0	-15.7	-1.0	-0.6	0.1	1.5	-0.8	-15.5	-17.3	16.5
W	43278 - 43271	-0.6	-4.6	-0.1	-0.1	-0.4	0.3	0.1	-0.7	-4.6	4.7
X	50084 - 50081	-0.7	-10.6	0.5	0.1	0.0	-2.3	2.3	-2.5	-10.6	12.9

[1] Refer to Figure 2.10.2-34 for the identification of the representative sections.

Table 2.10.4-170 $P_m + P_b$ Stresses; 30-Foot Top Oblique Drop; Drop Orientation = 75 Degrees; 3-D Top Model; 0-Degree Circumferential Location; Condition 1

Condition 1: 100°F Ambient with Contents

			Stress Components (ksi)						Principal Stresses (ksi)			
Section[1]	Node -	Node	S_x	S_y	S_z	S_{xy}	S_{yz}	S_{xz}	S1	S2	S3	S.I.
A I	1949 -	1951	-1.0	1.8	-0.1	-0.2	0.0	-0.2	1.8	-0.1	-1.1	2.9
B O	1952 -	93	0.6	-3.0	0.3	-0.4	0.3	-0.2	0.7	0.2	-3.1	3.8
C I	1925 -	1927	3.1	-3.2	4.5	0.2	-0.4	0.0	4.5	3.1	-3.2	7.8
D O	683 -	85	-3.3	-4.0	0.9	0.8	-0.1	0.2	0.9	-2.8	-4.5	5.3
E O	682 -	82	-1.7	-3.6	2.6	0.3	0.2	1.4	3.0	-2.0	-3.6	6.6
F O	1925 -	1325	0.7	-8.4	-13.8	0.6	-0.4	1.1	0.8	-8.4	-13.9	14.8
G I	680 -	80	2.3	-1.3	10.1	0.2	-0.1	2.0	10.6	1.8	-1.3	11.8
H O	1921 -	1321	-0.2	12.0	6.6	-0.7	-1.1	-0.3	12.2	6.5	-0.3	12.5
I O	676 -	76	-0.1	3.8	11.1	-0.2	-0.4	0.0	11.1	3.8	-0.1	11.2
J O	1916 -	1316	-0.2	12.5	13.4	-0.9	-0.6	0.0	13.7	12.2	-0.3	13.9
K O	671 -	71	-0.1	5.9	13.3	-0.4	-0.2	0.0	13.3	6.0	-0.1	13.4
L O	1908 -	1308	0.0	11.5	15.9	1.7	0.2	0.0	15.9	11.7	-0.3	16.2
M O	663 -	63	0.4	8.9	15.8	2.0	0.1	0.0	15.8	9.3	0.0	15.8
N O	1877 -	1277	-0.1	12.6	7.9	-0.9	0.9	0.0	12.8	7.7	-0.1	13.0
O O	647 -	47	0.0	5.8	11.5	-0.4	0.3	0.0	11.5	5.8	-0.1	11.6
P I	1840 -	1240	-0.3	7.2	-9.1	-0.5	1.7	0.0	7.5	-0.4	-9.3	16.7
Q O	628 -	28	0.0	5.5	10.5	-0.4	0.4	0.0	10.5	5.5	0.0	10.6
R O	1816 -	1216	-5.6	-16.6	-20.2	1.2	0.4	-4.3	-4.3	-16.5	-21.4	17.1
S O	616 -	16	-0.6	-6.0	7.2	0.4	0.2	0.1	7.2	-0.6	-6.0	13.2
T O	811 -	11	4.0	-11.1	5.8	1.0	0.0	-2.1	7.2	2.7	-11.2	18.4
U O	43058 -	43051	-15.6	-11.3	-2.3	0.0	-0.2	-1.5	-2.2	-11.3	-15.7	13.6
V I	50024 -	50021	-19.5	-13.2	-0.7	-1.0	0.0	1.0	-0.7	-13.0	-19.7	19.0
W I	43278 -	43271	-1.5	-5.9	0.0	-0.2	-0.3	0.3	0.1	-1.6	-6.0	6.1
X O	50084 -	50081	-10.3	-20.4	4.6	0.4	-0.3	-2.3	5.0	-10.6	-20.5	25.5

[1] Refer to Figure 2.10.2-34 for the identification of the representative sections.

Table 2.10.4-171 Critical P_m Stress Summary; 30-Foot Top Oblique Drop; Drop Orientation = 75 Degrees; 3-D Top Model; Condition 1

Condition 1: 100°F Ambient with Contents

Comp. No.[1]	Section Cut Node-Node	P_m Stresses (ksi) S_x	S_y	S_z	S_{xy}	S_{yz}	S_{zx}	Principal Stresses (ksi) S1	S2	S3	S.I.	Allow. Stress	Margin of Safety
1	30683-30085	0.1	3.7	-1.0	0.6	-0.2	-0.6	3.8	0.2	-1.2	5.1	45.6	7.9
2	17924-17324	0.0	2.5	1.0	0.2	-10.7	-0.3	12.5	0.0	-9.0	21.5	44.9	1.1
3	15841-15241	-0.2	3.9	-2.1	0.2	15.9	0.0	17.1	-0.2	-15.3	32.4	66.0	1.0
4	15874-15274	-0.2	3.7	-1.7	0.0	11.6	0.0	12.9	-0.2	-10.9	23.9	45.8	0.9
5	662-62	0.2	2.9	13.3	-2.4	0.1	0.0	13.3	4.3	-1.3	14.5	46.4	2.2
6	403-3	-21.4	-35.5	-1.2	0.6	0.3	3.1	-0.7	-21.9	-35.5	34.8	49.3	0.4
7	43071-43031	-14.7	-10.2	-0.6	-0.1	-0.1	-1.1	-0.5	-10.2	-14.8	14.3	48.0	2.4
8	50101-50104	-19.8	-19.2	-0.5	0.0	-0.1	0.0	-0.5	-19.2	-19.8	19.3	94.5	3.9

Locations of the most critical sections for each component are provided in the following:

Comp. No.[1]	Section Location Inside Node x (in)	y (deg)	z (in)	Outside Node x (in)	y (deg)	z (in)
1	39.44	180.0	6.20	39.44	180.0	0.75
2	35.50	79.4	17.40	37.50	79.4	17.40
3	35.50	67.7	159.90	37.00	67.7	159.90
4	35.50	67.7	142.40	37.00	67.7	142.40
5	40.70	0.0	99.50	43.35	0.0	99.50
6	40.88	0.0	190.15	43.35	0.0	190.15
7	33.71	0.0	185.40	36.46	0.0	185.40
8	40.88	8.3	193.71	40.88	8.3	188.40

[1] Refer to Figure 2.10.2-33 for cask component identification.

Table 2.10.4-172 Critical $P_m + P_b$ Stress Summary; 30-Foot Top Oblique Drop; Drop Orientation = 75 Degrees; 3-D Top Model; Condition 1

Condition 1: 100°F Ambient with Contents

Comp. No.[1]	Section Cut Node-Node	$P_m + P_b$ Stresses (ksi) S_x	S_y	S_z	S_{xy}	S_{yz}	S_{xz}	Principal Stresses (ksi) S1	S2	S3	S.I.	Allow. Stress	Margin of Safety
1	30683-30085	3.0	5.9	-1.2	0.7	-0.2	-0.3	6.1	2.8	-1.2	7.3	65.2	7.9
2	15924-15324	-0.2	1.6	-0.6	0.3	-12.3	0.0	12.9	-0.2	-11.8	24.8	64.2	1.6
3	13842-13242	-0.1	6.6	-3.0	0.0	16.4	0.0	18.9	-0.1	-15.3	34.2	94.3	1.8
4	15874-15274	-0.2	7.1	-0.5	0.0	12.3	0.0	16.2	-0.2	-9.6	25.8	65.5	1.5
5	664-64	-0.1	8.5	16.3	-0.7	0.0	0.0	16.3	8.5	-0.1	16.5	66.4	3.0
6	404-4	-2.0	-26.0	13.2	1.1	0.6	10.4	18.5	-7.3	-26.1	44.5	70.9	0.6
7	43001-43008	-26.3	-14.6	-0.9	-0.6	0.3	1.2	-0.9	-14.6	-26.4	25.5	69.8	1.7
8	50001-50004	-32.0	-20.4	1.2	-0.8	-0.2	-0.2	1.2	-20.3	-32.1	33.2	135.0	3.1

Locations of the most critical sections for each component are provided in the following:

Comp. No.[1]	Section Location Inside Node x (in)	y (deg)	z (in)	Outside Node x (in)	y (deg)	z (in)
1	39.44	180.0	6.20	39.44	180.0	0.75
2	35.50	67.7	17.40	37.50	67.7	17.40
3	35.50	56.5	159.40	37.00	56.5	159.40
4	35.50	67.7	142.40	37.00	67.7	142.40
5	40.70	0.0	93.60	43.35	0.0	93.60
6	40.88	0.0	188.40	43.35	0.0	188.40
7	39.53	0.0	185.40	39.53	0.0	179.40
8	40.88	0.0	193.71	40.88	0.0	188.40

[1] Refer to Figure 2.10.2-33 for cask component identification.

Table 2.10.4-173 Primary Stresses; 30-Foot Bottom Oblique Drop; Drop Orientation = 75 Degrees; 3-D Bottom Model; 0-Degree Circumferential Location; Condition 1

Condition 1: 100°F Ambient with Contents

Stress Points		Stress Components (ksi)						Principal Stresses (ksi)		
Section[1]	Node	S_x	S_y	S_z	S_{xy}	S_{yz}	S_{xz}	S1	S2	S3
A1	1130	3.7	-1.4	-2.0	-0.3	0.6	0.5	3.8	-1.0	-2.4
A2	1129	-0.4	-5.8	-0.4	-0.1	0.4	0.5	0.1	-0.9	-5.9
A3	1128	-4.4	-10.3	1.1	0.0	0.6	0.5	1.2	-4.5	-10.4
B1	1185	1.7	-5.9	-2.1	0.2	0.7	0.6	1.8	-2.1	-6.0
B2	1184	-2.0	-10.2	-0.5	0.3	0.5	0.6	-0.3	-2.2	-10.2
B3	1183	-5.7	-13.8	0.7	0.4	0.5	0.6	0.8	-5.7	-13.8
C1	90	-0.6	-6.6	12.2	-0.1	-0.8	0.5	12.3	-0.6	-6.6
C2	80	-7.6	-10.8	4.6	-0.2	-0.5	-0.5	4.6	-7.6	-10.8
C3	70	-8.1	-12.2	0.9	0.0	-0.3	-0.9	1.0	-8.2	-12.3
C4	60	-8.5	-13.1	-0.4	0.2	-0.2	-0.6	-0.3	-8.6	-13.1
C5	50	-11.2	-15.1	-0.3	0.3	-0.1	-0.2	-0.3	-11.2	-15.2
C6	40	-11.7	-16.0	-0.2	0.4	0.0	-0.1	-0.2	-11.6	-16.1
D1	25	-29.0	-23.5	-8.2	-0.6	-0.2	-4.9	-7.2	-23.5	-30.1
D2	15	-17.6	-20.3	-4.8	-0.3	0.0	-2.2	-4.5	-18.0	-20.4
D3	5	-11.0	-19.5	-2.4	-0.1	0.0	-0.7	-2.3	-11.1	-19.5
E1	35	-8.0	-16.5	-1.5	0.5	-0.1	-1.4	-1.2	-8.3	-16.6
E2	34	-8.6	-17.6	-4.9	0.5	-0.2	-3.2	-3.1	-10.4	-17.7
E3	33	-14.1	-19.4	-5.4	0.3	-0.3	-3.6	-4.1	-15.4	-19.5
E4	32	-16.2	-20.6	-6.9	0.3	-0.2	-2.4	-6.4	-16.8	-20.7
E5	31	-17.0	-21.6	-8.9	0.3	-0.2	-1.4	-8.6	-17.2	-21.6
F1	100	-1.2	-4.7	19.8	0.1	-1.1	1.8	20.0	-1.4	-4.7
F2	99	-2.4	-10.8	-1.2	0.5	-0.9	2.4	0.6	-4.1	-10.9
F3	98	-1.3	-14.3	-15.1	0.9	-0.6	4.0	-0.2	-14.0	-16.5
F4	97	0.7	-21.2	-43.4	1.5	-0.6	5.0	1.3	-21.2	-44.0
G1	94	1.3	-5.2	18.4	0.4	-0.4	4.2	19.4	0.4	-5.2
G2	93	1.8	-9.7	1.4	0.8	-0.3	3.2	4.9	-1.5	-9.8
G3	92	1.6	-10.9	-3.1	0.9	-0.2	1.5	2.1	-3.5	-11.0
G4	91	0.7	-12.4	-8.1	1.0	-0.2	0.6	0.8	-8.2	-12.5
H1	330	-0.3	6.9	-9.1	-0.5	-1.7	0.0	7.1	-0.3	-9.3
H2	329	-0.2	8.6	-5.8	-0.6	-1.6	0.0	8.8	-0.2	-6.0

Table 2.10.4-173 Primary Stresses; 30-Foot Bottom Oblique Drop; Drop Orientation = 75 Degrees; 3-D Bottom Model; 0-Degree Circumferential Location; Condition 1 (continued)

Stress Points		Stress Components (ksi)						Principal Stresses (ksi)		
Section[1]	Node	S_x	S_y	S_z	S_{xy}	S_{yz}	S_{xz}	S1	S2	S3
H3	328	0.0	10.2	-2.6	-0.7	-1.5	0.0	10.4	-0.1	-2.8
H4	327	0.1	11.9	0.7	-0.8	-1.4	-0.2	12.1	0.7	-0.1
I1	244	-0.2	-0.8	-0.9	0.1	-0.8	0.0	0.0	-0.2	-1.7
I2	243	-0.1	0.9	2.2	-0.1	-0.7	-0.1	2.6	0.6	-0.1
I3	242	-0.1	2.6	5.4	-0.2	-0.5	-0.1	5.5	2.5	-0.1
I4	241	0.0	4.1	8.5	-0.3	-0.4	-0.1	8.5	4.1	0.0
J1	550	-0.3	7.6	6.3	-0.6	-0.9	0.0	8.1	5.8	-0.4
J2	548	-0.2	10.1	8.1	-0.8	-0.8	0.0	10.4	7.8	-0.2
J3	547	-0.1	12.4	9.8	-0.9	-0.8	0.0	12.7	9.6	-0.1
K1	344	-0.1	-1.0	7.0	0.0	-0.6	0.0	7.1	-0.1	-1.0
K2	42	-0.1	2.6	8.6	-0.2	-0.4	0.0	8.6	2.5	-0.1
K3	341	0.0	5.9	10.1	-0.5	-0.3	0.0	10.1	5.9	-0.1
L1	740	-0.1	4.9	13.6	0.2	-0.1	-0.1	13.6	4.9	-0.1
L2	738	-0.5	7.6	15.1	-1.2	-0.1	0.0	15.1	7.8	-0.7
L3	737	0.2	10.5	16.7	-2.5	-0.1	0.0	16.7	11.0	-0.4
M1	454	-0.3	-2.0	9.8	-1.9	-0.1	0.0	9.8	0.9	-3.2
M2	452	0.4	3.5	12.5	-0.9	-0.1	0.2	12.5	3.8	0.2
M3	451	-0.7	8.1	14.9	0.0	-0.1	-0.3	14.9	8.1	-0.7
N1	810	-0.3	7.8	9.4	-0.6	0.7	-0.1	9.7	7.6	-0.3
N2	807	-0.2	12.4	12.8	-0.9	0.6	0.0	13.3	11.9	-0.3
O1	524	-0.1	-0.9	9.7	0.1	0.4	0.0	9.7	-0.1	-0.9
O2	521	-0.1	5.7	13.0	-0.4	0.2	0.0	13.0	5.8	-0.1
P1	850	-0.2	7.5	-1.8	-0.4	1.2	-0.1	7.6	-0.2	-1.9
P2	847	-0.2	12.2	7.1	-0.8	1.1	0.3	12.4	6.9	-0.3
Q1	564	-0.1	-0.1	6.3	0.0	0.5	0.0	6.4	-0.1	-0.2
Q2	561	-0.1	4.0	11.1	-0.3	0.3	0.0	11.1	4.0	-0.1
R1	890	-3.2	-3.1	10.2	0.1	0.8	-0.7	10.3	-3.1	-3.3
R2	887	-3.1	-7.7	-10.3	0.4	0.5	-1.6	-2.7	-7.7	-10.7
S1	604	-0.2	-1.3	8.1	0.0	0.2	-1.5	8.4	-0.5	-1.3
S2	601	0.7	-2.7	0.6	0.2	0.1	-0.6	1.2	0.0	-2.7
T1	897	3.2	-3.3	-2.2	0.3	0.3	-1.0	3.4	-2.3	-3.4
T2	614	0.9	-2.1	2.5	0.1	0.0	-1.3	3.2	0.2	-2.2

Table 2.10.4-173 Primary Stresses; 30-Foot Bottom Oblique Drop; Drop Orientation = 75 Degrees; 3-D Bottom Model; 0-Degree Circumferential Location; Condition 1 (continued)

Stress Points		Stress Components (ksi)						Principal Stresses (ksi)		
Section[1]	Node	S_x	S_y	S_z	S_{xy}	S_{yz}	S_{xz}	S1	S2	S3
T3	611	-0.2	-2.5	1.2	0.1	-0.1	-0.7	1.5	-0.5	-2.5
U1	900	5.1	-1.5	2.3	0.2	0.4	-0.1	5.1	2.3	-1.6
U2	910	-2.2	-2.8	0.2	0.1	0.2	-1.0	0.5	-2.5	-2.9
V1	920	2.8	-1.0	0.9	0.4	0.1	-0.8	3.1	0.6	-1.1
V2	930	-4.1	-3.8	0.6	0.6	0.1	-0.2	0.7	-3.3	-4.6
W1	1216	-1.1	1.9	-0.3	-0.1	-0.3	0.1	1.9	-0.3	-1.1
W2	1226	-0.3	0.2	0.1	-0.1	-0.5	0.1	0.6	-0.3	-0.4
X1	1236	0.0	-0.7	-0.1	-0.2	-0.5	0.1	0.3	-0.1	-1.0
X2	1246	0.5	-2.9	0.3	-0.4	-0.3	0.1	0.6	0.3	-3.0

[1] Refer to Figure 2.10.2-34 for the identification of the representative sections.

Table 2.10.4-174 P_m Stresses; 30-Foot Bottom Oblique Drop; Drop Orientation = 75 Degrees; 3-D Bottom Model; 0-Degree Circumferential Location; Condition 1

Condition 1: 100°F Ambient with Contents

		Stress Components (ksi)						Principal Stresses (ksi)			
Section[1]	Node - Node	S_x	S_y	S_z	S_{xy}	S_{yz}	S_{zx}	S1	S2	S3	S.I.
A	1130 - 1128	-0.4	-5.9	-0.4	-0.1	0.5	0.5	0.1	-0.9	-5.9	6.0
B	1185 - 1183	-2.0	-10.0	-0.6	0.3	0.5	0.6	-0.4	-2.2	-10.0	9.6
C	90 - 40	-9.0	-13.2	1.3	0.2	-0.2	-0.4	1.3	-9.0	-13.2	14.5
D	25 - 5	-18.8	-20.9	-5.1	-0.3	-0.1	-2.5	-4.6	-19.2	-21.0	16.3
E	35 - 31	-12.4	-19.0	-5.4	0.4	-0.2	-2.6	-4.5	-13.3	-19.0	14.5
F	100 - 97	-1.3	-12.7	-9.4	0.7	-0.8	3.3	-0.2	-10.2	-13.1	12.9
G	94 - 91	1.5	-9.8	1.1	0.8	-0.3	2.4	3.7	-1.0	-9.9	13.6
H	330 - 327	-0.1	9.4	-4.2	-0.6	-1.5	0.0	9.6	-0.2	-4.4	14.0
I	244 - 241	-0.1	1.7	3.8	-0.1	-0.6	-0.1	4.0	1.5	-0.1	4.1
J	550 - 547	-0.2	10.0	8.0	-0.7	-0.8	0.0	10.4	7.7	-0.2	10.6
K	344 - 341	-0.1	2.5	8.6	-0.2	-0.4	0.0	8.6	2.5	-0.1	8.7
L	740 - 737	-0.3	7.6	15.1	-1.1	-0.1	0.0	15.1	7.8	-0.4	15.6
M	454 - 451	0.0	3.3	12.4	-0.9	-0.1	0.0	12.4	3.5	-0.3	12.7
N	810 - 807	-0.2	10.1	11.1	-0.7	0.7	0.0	11.5	9.8	-0.3	11.8
O	524 - 521	-0.1	2.4	11.3	-0.2	0.3	0.0	11.3	2.4	-0.1	11.4
P	850 - 847	-0.2	9.8	2.7	-0.6	1.2	0.1	10.0	2.5	-0.2	10.3
Q	564 - 561	-0.1	2.0	8.7	-0.1	0.4	0.0	8.8	1.9	-0.1	8.9
R	890 - 887	-3.2	-5.4	0.0	0.2	0.6	-1.1	0.4	-3.5	-5.6	5.9
S	604 - 601	0.2	-2.0	4.4	0.1	0.1	-1.0	4.6	0.0	-2.0	6.6
T	614 - 611	0.3	-2.3	1.9	0.1	0.0	-1.0	2.3	-0.1	-2.3	4.7
U	900 - 910	1.4	-2.2	1.2	0.2	0.3	-0.5	1.9	0.8	-2.2	4.1
V	920 - 930	-0.7	-2.4	0.8	0.5	0.1	-0.5	0.9	-0.7	-2.6	3.5
W	1216 - 1226	-0.7	1.0	-0.1	-0.1	-0.4	0.1	1.1	-0.2	-0.7	1.8
X	1236 - 1246	0.2	-1.8	0.1	-0.3	-0.4	0.1	0.4	0.1	-1.9	2.3

[1] Refer to Figure 2.10.2-34 for the identification of the representative sections.

Table 2.10.4-175 $P_m + P_b$ Stresses; 30-Foot Bottom Oblique Drop; Drop Orientation = 75 Degrees; 3-D Bottom Model; 0-Degree Circumferential Location; Condition 1

Condition 1: 100°F Ambient with Contents

Section[1]	Node - Node	Stress Components (ksi)						Principal Stresses (ksi)			
		S_x	S_y	S_z	S_{xy}	S_{yz}	S_{zx}	S1	S2	S3	S.I.
A O	1130 - 1128	-4.4	-10.3	1.1	0.0	0.5	0.5	1.2	-4.5	-10.4	11.6
B O	1185 - 183	-5.7	-13.9	0.8	0.4	0.4	0.6	0.9	-5.7	-14.0	14.9
C I	90 - 40	-5.3	-9.6	5.1	-0.2	-0.5	-0.5	5.2	-5.3	-9.6	14.8
D I	25 - 5	-27.8	-22.9	-8.0	-0.5	-0.2	-4.6	-7.0	-22.9	-28.9	21.9
E I	35 - 31	-6.6	-16.2	-2.2	0.5	-0.2	-2.7	-0.8	-7.9	-16.2	15.4
F O	100 - 97	-0.3	-20.2	-38.6	1.4	-0.4	5.1	0.5	-20.3	-39.3	39.8
G I	94 - 91	1.8	-6.6	13.0	0.6	-0.4	4.3	14.5	0.4	-6.7	21.1
H I	330 - 327	-0.3	6.9	-9.1	-0.5	-1.7	0.0	7.1	-0.4	-9.3	16.4
I O	244 - 241	0.0	4.2	8.5	-0.3	-0.4	-0.1	8.6	4.2	0.0	8.6
J O	550 - 547	-0.1	12.4	9.8	-0.9	-0.8	0.0	12.7	9.6	-0.1	12.9
K O	344 - 341	0.0	5.9	10.1	-0.5	-0.3	0.0	10.2	5.9	-0.1	10.2
L O	740 - 737	-0.1	10.4	16.7	-2.5	-0.1	0.0	16.7	11.0	-0.7	17.3
M O	454 - 451	-0.3	8.3	14.9	0.0	-0.1	-0.2	15.0	8.3	-0.3	15.2
N O	810 - 807	-0.2	12.4	12.8	-0.9	0.6	0.0	13.3	11.9	-0.3	13.6
O O	524 - 521	-0.1	5.7	13.0	-0.4	0.2	0.0	13.0	5.8	-0.1	13.1
P O	850 - 847	-0.2	12.2	7.1	-0.8	1.1	0.3	12.4	6.9	-0.3	12.8
Q O	564 - 561	-0.1	4.0	11.1	-0.3	0.3	0.0	11.1	4.0	-0.1	11.3
R I	890 - 887	-3.2	-3.1	10.2	0.1	0.8	-0.7	10.3	-3.1	-3.3	13.6
S I	604 - 601	-0.2	-1.3	8.1	0.0	0.2	-1.5	8.4	-0.5	-1.3	9.7
T I	614 - 611	0.9	-2.1	2.5	0.1	0.0	-1.3	3.2	0.2	-2.2	5.4
U I	900 - 910	5.1	-1.5	2.3	0.2	0.4	-0.1	5.1	2.3	-1.6	6.6
V O	920 - 930	-4.1	-3.8	0.6	0.6	0.1	-0.2	0.7	-3.3	-4.6	5.2
W I	1216 - 1226	-1.1	1.9	-0.3	-0.1	-0.3	0.1	1.9	-0.3	-1.1	3.0
X O	1236 - 1246	0.5	-2.9	0.3	-0.4	-0.3	0.1	0.6	0.3	-3.0	3.6

[1] Refer to Figure 2.10.2-34 for the identification of the representative sections.

Table 2.10.4-176 Critical P_m Stress Summary; 30-Foot Bottom Oblique Drop; Drop Orientation = 75 Degrees; 3-D Bottom Model; Condition 1

Condition 1: 100°F Ambient with Contents

Comp. No.[1]	Section Cut Node-Node	P_m Stresses (ksi) S_x	S_y	S_z	S_{xy}	S_{yz}	S_{zx}	Principal Stresses (ksi) S1	S2	S3	S.I.	Allow. Stress	Margin of Safety
1	28- 8	-20.6	-19.0	-1.1	-0.5	-0.1	-2.9	-0.7	-18.9	-21.1	20.5	45.6	1.2
2	16140- 16137	0.0	1.0	0.1	0.0	-12.6	-0.1	13.2	0.0	-12.0	25.2	44.9	0.8
3	14340- 14337	-0.2	3.8	-1.7	0.2	-15.9	0.0	17.2	-0.2	-15.1	32.3	66.0	1.0
4	14520- 14517	-0.2	3.7	-1.3	0.0	-11.5	0.0	13.0	-0.2	-10.6	23.5	45.8	0.9
5	14204- 14201	0.0	1.1	-1.3	0.0	-6.5	-0.1	6.5	0.0	-6.8	13.3	46.4	2.5
6	16880- 16877	-0.1	2.9	1.0	-0.3	10.8	0.3	12.8	-0.1	-8.9	21.6	49.3	1.3
7	14900- 14910	-0.4	-0.1	-0.5	-1.2	3.3	-0.1	3.3	-0.5	-3.8	7.0	48.0	5.9
8	30907- 30927	-0.4	3.6	0.0	0.6	0.2	0.9	3.8	0.7	-1.2	4.9	94.5	18.3

Locations of the most critical sections for each component are provided in the following:

Comp. No.[1]	Section Location Inside Node x (in)	y (deg)	z (in)	Outside Node x (in)	y (deg)	z (in)
1	36.83	0.0	6.20	36.83	0.0	0.75
2	35.50	79.4	17.40	37.50	79.4	17.40
3	35.50	67.7	29.90	37.00	67.7	29.90
4	35.50	67.7	47.40	37.00	67.7	47.40
5	40.70	67.7	26.40	43.35	67.7	26.40
6	35.50	79.4	172.40	37.50	79.4	172.40
7	35.50	67.7	179.40	35.50	67.7	185.40
8	37.00	180.0	185.40	37.00	180.0	193.71

[1] Refer to Figure 2.10.2-33 for cask component identification.

Table 2.10.4-177 Critical $P_m + P_b$ Stress Summary; 30-Foot Bottom Oblique Drop; Drop Orientation = 75 Degrees; 3-D Bottom Model; Condition 1

Condition 1: 100°F Ambient with Contents

Comp. No.[1]	Section Cut Node-Node	$P_m + P_b$ Stresses (ksi) S_x	S_y	S_z	S_{xy}	S_{yz}	S_{xz}	Principal Stresses (ksi) S1	S2	S3	S.I.	Allow. Stress	Margin of Safety
1	27- 7	-33.5	-20.5	0.2	-1.2	-0.3	-3.8	0.6	-20.4	-34.1	34.7	65.2	0.9
2	100- 97	-0.3	-20.2	-38.6	1.4	-0.4	5.1	0.5	-20.3	-39.3	39.8	64.2	0.6
3	12350-12347	-0.1	6.2	-3.2	0.0	-16.4	0.0	18.6	-0.1	-15.6	34.2	94.3	1.8
4	14520-14517	-0.2	6.8	-0.2	0.0	-12.2	0.0	16.0	-0.2	-9.4	25.4	65.5	1.6
5	12204-12201	0.1	1.5	-1.6	-0.2	-8.3	-0.1	8.3	0.1	-8.5	16.8	66.4	3.0
6	14880-14877	-0.2	2.5	-0.2	-0.2	11.8	0.0	13.1	-0.2	-10.7	23.8	70.7	2.0
7	14900-14910	-0.3	0.7	-0.5	-3.0	4.0	0.1	5.1	-0.3	-5.0	10.1	69.8	5.9
8	30920-30930	2.1	5.6	-0.5	0.6	0.2	0.4	5.7	2.0	-0.6	6.3	135.0	20.4

Locations of the most critical sections for each component are provided in the following:

Comp. No.[1]	Section Location Inside Node x (in)	y (deg)	z (in)	Outside Node x (in)	y (deg)	z (in)
1	37.50	0.0	6.20	37.50	0.0	0.75
2	35.50	0.0	15.00	37.50	0.0	15.00
3	35.50	56.5	30.40	37.00	56.5	30.40
4	35.50	67.7	47.40	37.00	67.7	47.40
5	40.70	56.5	26.40	43.35	56.5	26.40
6	35.50	67.7	172.40	37.50	67.7	172.40
7	35.50	67.7	179.40	35.50	67.7	185.40
8	35.50	180.0	187.40	35.50	180.0	193.71

[1] Refer to Figure 2.10.2-33 for cask component identification.

Table 2.10.4-178 Primary + Secondary Stresses; Thermal (Fire) Transient; Time = 30 Minutes; With Contents; 2-D Model

Stress Points		Stress Components (ksi)						Principal Stresses (ksi)		
Section[1]	Node	S_x	S_y	S_z	S_{xy}	S_{yz}	S_{xz}	S1	S2	S3
A1	1	7.8	-0.1	7.8	0.0	0.0	0.0	7.8	7.8	-0.1
A2	2	6.8	-0.1	6.8	0.0	0.0	0.0	6.8	6.8	-0.1
A3	3	5.7	-0.1	5.7	0.0	0.0	0.0	5.7	5.7	-0.1
A4	4	4.5	0.0	4.5	0.0	0.0	0.0	4.5	4.5	0.0
A5	5	3.3	0.0	3.3	0.0	0.0	0.0	3.3	3.3	0.0
B1	6	-0.3	0.0	-0.3	0.0	0.0	0.0	0.0	-0.3	-0.3
B2	7	-0.3	0.0	-0.3	0.0	0.0	0.0	0.0	-0.3	-0.3
B3	8	-0.3	0.0	-0.3	0.0	0.0	0.0	0.0	-0.3	-0.3
B4	9	-0.2	0.0	-0.2	0.0	0.0	0.0	0.0	-0.2	-0.2
B5	10	-0.2	0.0	-0.2	0.0	0.0	0.0	0.0	-0.2	-0.2
C1	251	7.4	0.4	6.6	0.2	0.0	0.0	7.4	6.6	0.4
C2	252	9.1	0.9	6.4	-0.3	0.0	0.0	9.1	6.4	0.8
C3	253	6.8	0.5	4.7	-0.5	0.0	0.0	6.9	4.7	0.5
C4	254	3.1	-0.6	2.1	-0.1	0.0	0.0	3.1	2.1	-0.6
C5	255	-3.8	-1.2	-1.3	0.1	0.0	0.0	-1.2	-1.3	-3.8
D1	306	5.7	19.9	6.3	1.4	0.0	0.0	20.0	6.3	5.6
D2	307	-1.2	8.5	1.5	1.6	0.0	0.0	8.8	1.5	-1.5
D3	308	-1.4	3.2	0.2	0.0	0.0	0.0	3.2	0.2	-1.4
D4	309	-2.3	1.2	-0.6	-0.3	0.0	0.0	1.2	-0.6	-2.3
D5	310	-3.9	0.5	-1.4	-0.2	0.0	0.0	0.5	-1.4	-4.0
E1	305	7.0	22.0	5.5	-3.8	0.0	0.0	23.0	6.1	5.5
E2	315	4.3	7.5	0.4	-1.0	0.0	0.0	7.8	4.0	0.4
E3	325	3.8	1.4	-1.1	-0.3	0.0	0.0	3.9	1.3	-1.1
E4	335	3.3	-4.2	-2.5	-0.1	0.0	0.0	3.3	-2.5	-4.2
E5	345	1.4	-11.6	-5.9	0.2	0.0	0.0	1.4	-5.9	-11.6
E6	355	-0.2	-20.0	-9.5	0.2	0.0	0.0	-0.2	-9.5	-20.0
F1	251	7.4	0.4	6.6	0.2	0.0	0.0	7.4	6.6	0.4
F2	261	6.3	3.7	6.1	-0.3	0.0	0.0	6.3	6.1	3.6
F3	271	7.3	6.6	6.0	-1.7	0.0	0.0	8.7	6.0	5.2
F4	281	9.9	10.0	5.5	-3.0	0.0	0.0	12.9	7.0	5.5
G1	311	5.6	10.5	-19.6	5.0	0.0	0.0	13.6	2.4	-19.6
G2	321	1.1	4.3	-32.0	4.1	0.0	0.0	7.1	-1.7	-32.0

Table 2.10.4-178 Primary + Secondary Stresses; Thermal (Fire) Transient; Time = 30 Minutes; With Contents; 2-D Model (continued)

Stress Points		Stress Components (ksi)						Principal Stresses (ksi)		
Section[1]	Node	S_x	S_y	S_z	S_{xy}	S_{yz}	S_{xz}	S1	S2	S3
G3	331	2.6	5.0	-40.7	2.3	0.0	0.0	6.4	1.2	-40.7
G4	341	-0.4	-8.9	-69.9	1.0	0.0	0.0	-0.2	-9.0	-69.9
G5	351	-7.9	-15.1	-97.3	0.3	0.0	0.0	-7.8	-15.1	-97.3
H1	581	0.0	8.3	2.8	0.1	0.0	0.0	8.3	2.8	0.0
H2	582	0.0	8.7	3.1	0.1	0.0	0.0	8.7	3.1	0.0
H3	583	0.1	9.0	3.3	-0.1	0.0	0.0	9.0	3.3	0.1
H4	584	0.0	10.0	3.8	-0.4	0.0	0.0	10.0	3.8	0.0
I1	589	-0.4	4.4	6.2	0.0	0.0	0.0	6.2	4.4	-0.4
I2	590	-0.2	3.8	5.7	0.0	0.0	0.0	5.7	3.8	-0.2
I3	591	-0.1	3.1	5.2	0.0	0.0	0.0	5.2	3.1	-0.1
I4	592	0.0	0.9	3.3	0.0	0.0	0.0	3.3	0.9	0.0
I5	593	0.0	-1.2	1.4	0.0	0.0	0.0	1.4	0.0	-1.2
J1	971	-0.1	7.5	1.9	0.0	0.0	0.0	7.5	1.9	-0.1
J2	972	-0.1	8.6	2.5	0.0	0.0	0.0	8.6	2.5	-0.1
J3	973	-0.1	9.7	3.2	0.0	0.0	0.0	9.7	3.2	-0.1
J4	974	0.0	10.9	3.9	0.0	0.0	0.0	10.9	3.9	0.0
K1	979	-0.4	3.0	6.8	0.0	0.0	0.0	6.8	3.0	-0.4
K2	980	-0.3	3.0	6.4	0.0	0.0	0.0	6.4	3.0	-0.3
K3	981	-0.1	3.0	6.0	0.0	0.0	0.0	6.0	3.0	-0.1
K4	982	-0.1	1.6	4.3	0.0	0.0	0.0	4.3	1.6	-0.1
K5	983	0.0	0.3	2.7	0.0	0.0	0.0	2.7	0.3	0.0
L1	1601	-0.1	8.1	2.2	0.0	0.0	0.0	8.1	2.2	-0.1
L2	1602	-0.1	8.8	2.7	0.0	0.0	0.0	8.8	2.7	-0.1
L3	1603	0.0	9.5	3.3	0.0	0.0	0.0	9.5	3.3	0.0
L4	1604	0.0	10.2	3.8	0.0	0.0	0.0	10.2	3.8	0.0
M1	1609	-0.4	3.2	7.1	0.0	0.0	0.0	7.1	3.2	-0.4
M2	1610	-0.2	3.1	6.7	0.0	0.0	0.0	6.7	3.1	-0.2
M3	1611	-0.1	3.0	6.2	0.0	0.0	0.0	6.2	3.0	-0.1
M4	1612	-0.1	1.5	4.5	0.0	0.0	0.0	4.5	1.5	-0.1
M5	1613	0.0	0.1	2.9	0.0	0.0	0.0	2.9	0.1	0.0
N1	2216	-0.1	7.6	2.0	0.0	0.0	0.0	7.6	2.0	-0.1
N2	2217	-0.1	8.6	2.5	0.0	0.0	0.0	8.6	2.5	-0.1

Table 2.10.4-178 Primary + Secondary Stresses; Thermal (Fire) Transient; Time = 30 Minutes; With Contents; 2-D Model (continued)

Stress Points		Stress Components (ksi)						Principal Stresses (ksi)		
Section[1]	Node	S_x	S_y	S_z	S_{xy}	S_{yz}	S_{xz}	S1	S2	S3
N3	2218	0.0	9.7	3.0	0.0	0.0	0.0	9.7	3.0	0.0
N4	2219	0.0	10.7	3.5	0.0	0.0	0.0	10.7	3.5	0.0
O1	2224	-0.3	4.0	4.5	-0.1	0.0	0.0	4.5	4.0	-0.3
O2	2225	-0.2	3.6	3.9	-0.2	0.0	0.0	3.9	3.6	-0.2
O3	2226	-0.1	3.0	3.3	-0.3	0.0	0.0	3.3	3.0	-0.1
O4	2227	0.0	1.1	1.3	-0.2	0.0	0.0	1.3	1.2	-0.1
O5	2228	0.0	-0.7	-0.6	-0.1	0.0	0.0	0.0	-0.6	-0.7
P1	2546	-0.4	27.1	7.7	-0.2	0.0	0.0	27.1	7.7	-0.4
P2	2547	-0.3	15.3	4.0	-0.5	0.0	0.0	15.4	4.0	-0.4
P3	2548	-1.1	3.0	0.1	-0.9	0.0	0.0	3.2	0.1	-1.3
P4	2549	0.9	-9.5	-3.1	-1.8	0.0	0.0	1.2	-3.1	-9.8
Q1	2554	-0.4	25.0	24.9	0.2	0.0	0.0	25.0	24.9	-0.4
Q2	2555	-0.2	14.3	20.9	0.4	0.0	0.0	20.9	14.3	-0.2
Q3	2556	-0.2	3.6	16.8	0.9	0.0	0.0	16.8	3.8	-0.4
Q4	2557	-0.1	-9.0	11.4	0.9	0.0	0.0	11.4	0.0	-9.1
Q5	2558	0.0	-22.3	5.8	0.7	0.0	0.0	5.8	0.0	-22.4
R1	2771	3.7	-51.1	42.6	-1.2	0.0	0.0	42.6	3.7	-51.2
R2	2772	9.0	-14.2	51.2	-0.9	0.0	0.0	51.2	9.0	-14.2
R3	2773	20.0	15.2	59.2	2.9	0.0	0.0	59.2	21.3	13.9
R4	2774	34.6	49.1	64.9	7.7	0.0	0.0	64.9	52.4	31.3
S1	2779	21.4	12.6	-16.9	-6.6	0.0	0.0	25.0	9.1	-16.9
S2	2780	16.5	5.9	-34.7	-6.1	0.0	0.0	19.3	3.1	-34.7
S3	2781	8.7	0.7	-52.4	-4.2	0.0	0.0	10.5	-1.1	-52.4
S4	2782	3.9	-8.5	-72.3	-2.3	0.0	0.0	4.3	-8.9	-72.3
S5	2783	0.8	-19.2	-91.3	-1.2	0.0	0.0	0.9	-19.3	-91.3
T1	7066	-21.0	-6.2	10.3	-0.6	0.0	0.0	10.3	-6.1	-21.1
T2	7067	-11.1	1.4	5.4	0.2	0.0	0.0	5.4	1.4	-11.1
T3	7068	-6.4	5.3	-4.0	1.5	0.0	0.0	5.5	-4.0	-6.6
T4	7069	-3.5	3.4	-17.6	2.1	0.0	0.0	3.9	-4.1	-17.6
T5	7070	-0.8	1.9	-32.1	2.0	0.0	0.0	3.0	-1.8	-32.1
T6	7071	-0.9	-6.6	-56.3	1.3	0.0	0.0	-0.6	-6.9	-56.3
T7	7072	-4.4	-10.3	-79.1	0.7	0.0	0.0	-4.3	-10.4	-79.1

Table 2.10.4-178 Primary + Secondary Stresses; Thermal (Fire) Transient; Time = 30 Minutes; With Contents; 2-D Model (continued)

Stress Points		Stress Components (ksi)						Principal Stresses (ksi)		
Section[1]	Node	S_x	S_y	S_z	S_{xy}	S_{yz}	S_{xz}	S1	S2	S3
U1	3051	-0.8	-1.1	-7.5	-0.2	0.0	0.0	-0.7	-1.2	-7.5
U2	3052	2.0	0.1	-4.4	-0.4	0.0	0.0	2.1	0.0	-4.4
U3	3053	2.4	0.0	-2.5	-0.7	0.0	0.0	2.6	-0.2	-2.5
U4	3054	1.8	0.6	-1.2	-1.1	0.0	0.0	2.5	-0.1	-1.2
U5	3055	-0.4	1.7	-0.8	-1.2	0.0	0.0	2.2	-0.8	-0.9
U6	3056	-0.3	2.2	0.1	-0.5	0.0	0.0	2.3	0.1	-0.4
V1	3611	5.0	-0.1	2.0	0.1	0.0	0.0	5.0	2.0	-0.1
V2	3612	3.1	-0.3	1.3	0.2	0.0	0.0	3.1	1.3	-0.3
V3	3613	1.6	-0.8	0.5	0.3	0.0	0.0	1.6	0.5	-0.8
V4	3614	0.2	-1.7	-0.4	0.3	0.0	0.0	0.3	-0.4	-1.8
V5	3615	-1.1	-3.4	-1.5	0.3	0.0	0.0	-1.1	-1.5	-3.4
V6	3616	-2.7	-1.5	-1.7	0.2	0.0	0.0	-1.4	-1.7	-2.8
V7	3617	-5.9	1.5	-2.1	0.1	0.0	0.0	1.5	-2.1	-5.9
W1	3241	0.1	-0.1	0.1	0.0	0.0	0.0	0.1	0.1	-0.1
W2	3242	0.7	-0.1	0.7	0.0	0.0	0.0	0.7	0.7	-0.1
W3	3243	1.4	-0.1	1.4	0.0	0.0	0.0	1.4	1.4	-0.1
W4	3244	2.0	-0.1	2.0	0.0	0.0	0.0	2.0	2.0	-0.1
W5	3245	2.7	0.0	2.7	0.0	0.0	0.0	2.7	2.7	0.0
W6	3246	3.3	0.0	3.3	0.0	0.0	0.0	3.3	3.3	0.0
X1	3801	0.3	0.0	0.3	0.0	0.0	0.0	0.3	0.3	0.0
X2	3802	0.3	0.0	0.3	0.0	0.0	0.0	0.3	0.3	0.0
X3	3803	0.2	0.0	0.2	0.0	0.0	0.0	0.2	0.2	0.0
X4	3804	0.1	0.0	0.1	0.0	0.0	0.0	0.1	0.1	0.0
X5	3805	0.0	0.0	0.0	0.0	0.0	0.0	0.0	0.0	0.0
X6	3806	-0.1	0.0	-0.1	0.0	0.0	0.0	0.0	-0.1	-0.1
X7	3807	-0.2	0.0	-0.2	0.0	0.0	0.0	0.0	-0.2	-0.2

[1] Refer to Figure 2.10.2-34 for the identification of the representative sections.

Table 2.10.4-179 S_n Stresses; Thermal (Fire) Transient; Time = 30 Minutes; With Contents; 2-D Model

		Stress Components (ksi)						Principal Stresses (ksi)			
Section[1]	Node - Node	S_x	S_y	S_z	S_{xy}	S_{yz}	S_{zx}	S1	S2	S3	S.I.
A I	1 - 5	7.9	-0.1	7.9	0.0	0.0	0.0	7.9	7.9	-0.1	8.0
B I	6 - 10	-0.3	0.0	-0.3	0.0	0.0	0.0	0.0	-0.3	-0.3	0.3
C I	251 - 255	10.9	0.4	8.0	-0.2	0.0	0.0	10.9	8.0	0.4	10.6
D I	306 - 310	2.4	19.9	4.1	0.5	0.0	0.0	19.9	4.1	2.4	17.5
E O	305 - 355	-0.2	-18.8	-8.2	-0.8	0.0	0.0	-0.2	-8.2	-18.8	18.6
F I	251 - 281	7.4	0.4	6.5	-1.1	0.0	0.0	7.5	6.5	0.2	7.3
G O	311 - 351	-7.9	-13.4	-88.7	2.5	0.0	0.0	-6.9	-14.4	-88.7	81.8
H O	581 - 584	0.0	9.7	3.7	-0.1	0.0	0.0	9.7	3.7	0.0	9.7
I I	589 - 593	-0.4	5.2	6.9	0.0	0.0	0.0	6.9	5.2	-0.4	7.3
J O	971 - 974	0.0	10.9	3.9	0.0	0.0	0.0	10.9	3.9	0.0	10.9
K I	979 - 983	-0.4	3.7	7.4	0.0	0.0	0.0	7.4	3.7	-0.4	7.8
L O	1601 - 1604	0.0	10.2	3.8	0.0	0.0	0.0	10.2	3.8	0.0	10.2
M I	1609 - 1613	-0.4	3.9	7.7	0.0	0.0	0.0	7.7	3.9	-0.4	8.1
N O	2216 - 2219	0.0	10.7	3.5	0.0	0.0	0.0	10.7	3.5	0.0	10.7
O I	2224 - 2228	-0.3	4.7	5.2	-0.2	0.0	0.0	5.2	4.7	-0.3	5.4
P I	2546 - 2549	-0.4	27.4	7.6	-0.8	0.0	0.0	27.4	7.6	-0.4	27.8
Q O	2554 - 2558	0.0	-21.0	6.6	0.7	0.0	0.0	6.6	0.0	-21.0	27.6
R I	2771 - 2774	3.7	-48.8	43.3	1.8	0.0	0.0	43.3	3.8	-48.8	92.2
S O	2779 - 2783	0.8	-16.7	-90.7	-4.1	0.0	0.0	1.7	-17.6	-90.7	92.4
T O	7066 - 7072	-4.4	-4.5	-67.5	1.2	0.0	0.0	-3.3	-5.6	-67.5	64.2
U I	3051 - 3056	1.8	-3.6	-3.4	-0.8	0.0	0.0	1.9	-3.4	-3.7	5.6
V O	3611 - 3617	-4.7	1.5	-2.6	0.2	0.0	0.0	1.5	-2.6	-4.7	6.2
W O	3241 - 3246	3.3	0.0	3.3	0.0	0.0	0.0	3.3	3.3	0.0	3.3
X I	3801 - 3807	0.3	0.0	0.3	0.0	0.0	0.0	0.3	0.3	0.0	0.4

[1] Refer to Figure 2.10.2-34 for the identification of the representative sections.

Table 2.10.4-180 Critical S_n Stress Summary; Thermal (Fire) Transient; Time = 30 Minutes; With Contents; 2-D Model

Comp. No.[1]	Section Cut Node-Node		P_m Stresses (ksi) S_x	S_y	S_z	S_{xy}	S_{yz}	S_{xz}	Principal Stresses (ksi) S1	S2	S3	S.I.	Allow. Stress	Margin of Safety
1	306-	310	2.4	19.9	4.1	0.5	0.0	0.0	19.9	4.1	2.4	17.5	730.0	40.7
2	311-	351	-7.9	-13.4	-88.7	2.5	0.0	0.0	-6.9	-14.4	-88.7	81.8	730.0	7.9
3	2711-	2714	-0.6	2.3	46.2	3.8	0.0	0.0	46.2	4.9	-3.3	49.5	730.0	13.7
4	926-	929	0.0	11.0	3.7	0.0	0.0	0.0	11.0	3.7	0.0	11.0	730.0	65.1
5	2539-	2543	-22.0	0.4	8.7	-0.3	0.0	0.0	8.7	0.4	-22.0	30.7	730.0	22.8
6	2719-	2723	17.1	-0.2	-77.7	1.5	0.0	0.0	17.3	-0.3	-77.7	95.0	730.0	6.7
7	3021-	3026	1.8	21.6	-13.5	0.6	0.0	0.0	21.6	1.8	-13.5	35.1	730.0	19.8
8	3601-	3607	4.1	-2.7	1.8	0.9	0.0	0.0	4.2	1.8	-2.8	7.1	730.0	102.2

Locations of the most critical sections for each component are provided in the following:

Comp. No.[1]	Section Location Inside Node x (in)	y (in)	Outside Node z (in)	x (in)
1	39.44	6.20	39.44	0.75
2	40.70	14.40	43.35	14.40
3	35.50	171.40	37.50	171.40
4	35.50	52.40	37.00	52.40
5	40.70	159.40	43.35	159.40
6	40.70	171.40	43.35	171.40
7	37.66	179.40	37.66	185.40
8	36.46	188.40	36.46	193.71

[1] **Refer to Figure 2.10.2-33 for cask component identification.**

2.10.5 Inner Shell Buckling Analysis

Code Case N-284 (Metal Containment Shell Buckling Design Methods) of the "ASME Boiler and Pressure Vessel Code" is used to analyze the NAC-STC inner shell and transition sections for structural stability. Structural stability ensures that the inner shell and transition sections do not buckle during cask fabrication, normal conditions of transport, or hypothetical accident conditions. The buckling evaluation requirements of Regulatory Guide 7.6, Paragraph C.5, are shown to be satisfied by the results of the interaction equation calculations of Code Case N-284.

The inner shell buckling design criteria, specifically the criteria of Code Case N-284, are described in detail in Section 2.1.3.4.

2.10.5.1 Buckling Analysis

The structural stability analysis of the NAC-STC inner shell and transition sections is performed by an NAC proprietary computer program in accordance with the ASME Code Case N-284. The data considered for an ASME Code Case N-284 buckling evaluation includes shell geometry parameters, shell fabrication tolerances, shell material properties, theoretical elastic buckling stress values for the shell, and primary plus secondary (P + Q) stresses at the sections of the shell to be evaluated. The axial, hoop, and in-plane shear components of the P + Q stresses in the inner shell and in the transition sections are obtained from the ANSYS finite element analyses for each of the normal conditions of transport and hypothetical accident conditions. Since the inner shell and the transition sections of the primary containment vessel are different materials and have different operating temperatures, a separate buckling evaluation is performed for the inner shell and for the transition sections. The fixity provided by the thick end forgings precludes buckling in the regions of the inner shell immediately adjacent to the forgings.

Nodal P + Q stress components are conservatively used for the buckling evaluation of the inner shell and the transition sections of the directly loaded fuel configuration of the NAC-STC for the heat condition, the cold condition, all of the 1-foot drop conditions, the 30-foot top and bottom end drops, the 30-foot side drop, and the 30-foot top and bottom corner drops (nodal stresses include any peaking effects that are present at the node location). Sectional P + Q stress components, as required by ASME Code Case N-284, are used for the buckling evaluation of the inner shell and the transition sections of the directly loaded fuel configuration of the NAC-STC for the 30-foot top and bottom 75-degree oblique drops and for the 30-foot bottom 15-degree oblique drop. Buckling is evaluated for the canistered fuel configuration of the NAC-STC only

for the 30-foot side drop condition. The 1-foot side drop condition is less critical than the 30-foot side drop condition (refer to Table 2.10.5-1). For the other drop orientations, the directly loaded fuel configuration has been shown to bound the canistered fuel configuration (Sections 2.7.1.1 - 2.7.1.4). For each load condition evaluated, the maximum compressive axial stress component calculated anywhere in the inner shell is combined with the maximum compressive hoop stress component calculated anywhere in the inner shell and the maximum in-plane shear stress component calculated anywhere in the inner shell; this produces a grossly conservative, bounding case buckling evaluation of the inner shell. The same analysis is used in the buckling evaluation of the transition sections. The stress component values used in the buckling evaluations are documented in Table 2.10.5-1.

The maximum temperatures for normal conditions of transport in the inner shell and the transition section are 331°F and 300°F, respectively, for the directly loaded fuel configuration; 311°F and 300°F, respectively, for the Yankee-MPC canistered fuel configuration; and 331°F and 331°F, respectively, for the CY-MPC canistered fuel configuration (Table 3.4-5). Therefore, previously analyzed and conservative higher temperatures are not revised throughout these analyses and a temperature of 353°F is used to determine the values of the modulus of elasticity and yield stress to be used in the buckling evaluation of the Type 304 stainless steel inner shell. Similarly, a temperature of 338°F is used for the transition sections.

2.10.5.2 Analysis Results

The results of the buckling evaluation of the NAC-STC inner shell and transition sections are summarized in Table 2.10.5-1 for the directly loaded fuel configuration and in Sections 2.10.5.4 and 2.10.5.5 for the canistered fuel configurations. All interaction equations yield values less than 1.0. Also, there are no concentrated loads on the inner shell or transition sections that would lead to localized buckling. Therefore, the buckling criteria of Code Case N-284 are satisfied and it is concluded that buckling of the NAC-STC inner shell and transition sections will not occur.

2.10.5.3 Verification of the Code Case N-284 Buckling Evaluation of the NAC-STC Inner Shell and Transition Sections

The results of the proprietary NAC computer program that performs the Code Case N-284 buckling evaluation are verified by a hand calculation of load case "J_T" (Table2.10.5-1). This step-by-step analysis procedure reflects the procedure diagrammed in paragraph-1800 of Code Case N-284. The geometry parameters for the NAC-STC inner shell and transition sections are defined in Table 2.10.5-2.

Step 1

For load case "J_T", the compressive stresses from Table 2.10.5-1 are:

S_f = 16,445 psi

S_q = 10,356 psi

S_{fq} = 14,515 psi

Step 2

For accident conditions, the factor of safety (FS) is 1.34. Multiplying the stress components by this factor of safety yields:

$FS(S_f)$ = 22,036 psi

$FS(S_q)$ = 13,877 psi

$FS(S_{fq})$ = 19,450 psi

Step 3

Capacity reduction factors, calculated per Section 2.1.3.4.3, are as follows for the load case "J_T" transition section temperature of 338°F:

$\alpha_{\phi L}$ = 0.393

$\alpha_{\theta L}$ = 0.8

$\alpha_{\theta\phi L}$ = 0.8

In order to directly use the capacity reduction factors from Table 2.10.5-3, the tolerance requirements of Article NE-4220 of the "ASME Boiler and Pressure Vessel Code," Subsection NE must be satisfied. Article NE-4221.1 and Article NE-4221.2 set forth the "maximum difference in cross-sectional diameters" and "maximum deviation from true theoretical form for external pressure". Table 2.10.5-4 shows that the requirements of Articles NE-4221.1 and NE-4221.2 are satisfied, as long as the maximum tolerances and configuration constraints are met during manufacturing.

Step 4

Plasticity reduction factors are determined using the equations presented in Section 2.1.3.4.4 as follows (S_y available from Table 2.10.5-5):

1. Axial Compression

   S_ϕ (FS)/S_y= (22,036)/(42,600) = 0.5173

   η_ϕ = 1.0

2. Hoop Compression

   S_θ (FS)/S_y= (13,877)/(42,600) = 0.3258

   η_θ = 1.0

3. Shear

$S_{\phi\theta}$ (FS)/S_y = (19,450)/(42,600) = 0.4566

$\eta_{\phi\theta}$ = 1.0

From Section-1600 of Code Case N-284, as an upper limit, the compressive stresses, S_i (ϕ = f or θ), must be less than the yield strength, S_y, divided by the appropriate factor of safety ($S_i < S_y$/FS). Similarly, for shear, $S_{\phi\theta}$ must be less than or equal to 0.6 S_y divided by the appropriate factor of safety ($S_{\phi\theta} < 0.6\ S_y$/FS). As stated in Section 2.1.3.4.1, there is a factor of safety of 2.0 for normal transport conditions and a factor of safety of 1.34 for hypothetical accident conditions. Table 2.10.5-6 presents the elastic upper bound compressive and shear stresses, evaluated using normal and accident condition factors of safety. Under no circumstances can the elastic values presented in the table be exceeded. However, satisfying these limits alone is not sufficient to demonstrate that buckling will not occur. As stated in Section 2.1.3.4.1, the interaction equations must also be satisfied.

Step 5

Compute elastic stress components per the following equation:

$S_{is} = S_i(FS)/\alpha_{iL}$

$S_{\phi s} = S_\phi$ (FS)/$\alpha_{\phi L}$ = (22,036)/(0.393) = 56,071 psi

$S_{\theta s} = S_\theta$ (FS)/$\alpha_{\theta L}$ = (13,877)/(0.8) = 17,346 psi

$S_{\phi\theta s} = S_{\phi\theta}$ (FS)/$\alpha_{\phi\theta L}$ = (19,450)/(0.8) = 24,313 psi

Step 6

Compute inelastic stress components per the following equation:

$S_{ip} = S_{is}/\eta_i$

$S_{\phi p} = S_{\phi s}/\eta_\phi = (56,071)/(1.0) = 56,071$ psi

$S_{\theta p} = S_\theta/\eta_\theta = (17,346)/(1.0) = 17,346$ psi

$S_{\phi\theta p} = S_{\phi\theta s}/\eta_{\phi\theta} = (24,313)/(1.0) = 24,313$ psi

Step 7

For the NAC-STC, the buckling evaluation approach, consistent with the vessel design and method of analysis, is that of paragraph-1710 of Code Case N-284.

Step 8

Theoretical uniaxial buckling values are available from Section 2.1.3.4.2. For the transition section at 338°F, these theoretical values are as follows (Table 2.10.5-7 and Table 2.10.5-8):

$S_{\phi eL} = 668,435$ psi

$S_{\theta eL} = S_{reL} = 49,155$ psi

$S_{\eta eL} = 47,927$ psi

$S_{\phi\theta eL} = 176,487$ psi

Applicable elastic and inelastic interaction equations in paragraph-1713.1.1 and paragraph-1713.2.1 of Code Case N-284 are checked as follows:

1. Elastic Buckling (Paragraph-1713.1.1, Code Case N-284)

a. Axial Compression Plus Hoop Compression

$(S_{\phi s} < 0.5\ S_{\theta s})$

$56,071 > (0.5)(17,346)$; therefore, not applicable.

b. Axial Compression Plus Hoop Compression

$(S_{\phi s} \geq 0.5\ S_{\theta s})$

$$[(S_{\phi s} - 0.5\ S_{heL})/(S_{\phi eL} - 0.5\ S_{heL})] + (S_{\theta s}/S_{heL})^2 \leq 1.0$$

$$\frac{56,071 - (0.5)(47,927)}{668,435 - (0.5)(47,927)} + (17,346/47,927)^2 \leq 1.0$$

$$0.1779 \leq 1.0$$

therefore,

$Q1 = 0.1779 < 1.0$

c. Axial Compression Plus Shear

$$(S_{\phi s}/S_{\phi eL}) + (S_{\phi\theta s}/S_{\phi\theta eL})^2 \leq 1.0$$

$$(56,071/668,435) + (24,313/176,487)^2 \leq 1.0$$

$$0.1029 \leq 1.0$$

therefore,

$Q2 = 0.1029 < 1.0$

d. Hoop Compression Plus Shear

$$(S_{\theta s}/S_{reL}) + (S_{\phi\theta s}/S_{\phi\theta eL})^2 \leq 1.0$$

$$(17,346/49,165) + (24,313/176,487)^2 \leq 1.0$$

$$0.372 \leq 1.0$$

therefore,

$$Q3 = 0.372 < 1.0$$

e. Axial Compression Plus Hoop Compression Plus Shear

$$K = 1 - (S_{\phi\theta s}/S_{\phi\theta eL})^2 = 1 - (24,313/176,487)^2 = 0.981$$

and, therefore, Equation B (above) becomes:

$$+ [(17,346/(0.981)(48,465)]^2 = 0.1832$$

therefore,

$$Q4 = 0.1846 < 1.0$$

2. Inelastic Buckling (Paragraph-1713.2.1, Code Case N-284)

a. Axial Compression Plus Shear

$$(S_{\phi p}/S_{\phi eL})^2 + (S_{\phi\theta p}/S_{\phi\theta eL})^2 \leq 1.0$$

$$(56,071/668,435)^2 + (24,313/176,487)^2 \leq 1.0$$

$$0.026 \leq 1.0$$

therefore,

$Q5 = 0.026 < 1.0$

b. Hoop Compression Plus Shear

$$(S_{\theta p}/S_{reL})^2 + (S_{\phi\theta p}/S_{\phi\theta eL})^2 \leq 1.0$$

$$(17{,}346/49{,}155)^2 + (24{,}313/176{,}487)^2 \leq 1.0$$

$$0.144 \leq 1.0$$

therefore,

$Q6 = 0.144 < 1.0$

The results of the hand calculation of load case "J_T" are identical to the results in Table 2.10.5-1 that were calculated by the NAC proprietary computer program, which performs the Code Case N-284 buckling evaluation. Thus, the computer program results in Table 2.10.5-1 and the buckling stability of the NAC-STC inner shell are verified.

2.10.5.4 Buckling Evaluation of the Inner Shell for the Yankee-MPC Fuel Configuration

In the Yankee-MPC canistered fuel configuration for a side drop load condition, the fuel load is applied to the support disks which transmit the load to the canister and then to the inner shell of the NAC-STC. Thus, the loading on the cask inner shell for a side drop load condition is different than that for the directly loaded fuel configuration where the support disks directly load the cask inner shell. To demonstrate that the NAC-STC will resist buckling of the inner shell in the side drop, the methodology described in 2.10.5.3 will be applied with stresses determined for the side drop using the canistered fuel configuration. The canistered fuel configuration loading on the cask cavity for an end drop condition is essentially the same as for the directly loaded fuel configuration, so no additional evaluation is required.

The section with the maximum compressive stress (hoop and axial) for the inner shell and transition shell occurs at the weld connecting the inner shell to the bottom forging). As a result of computing the linearized stress at this section, the maximum axial stress is -12,800 psi and the maximum hoop stress is -16,200 psi. The corresponding shear stress is 1,100 psi. These values are obtained from Table 2.7.1.2-1. These stresses are for the 30-ft side drop condition and they envelop the 1-ft side drop condition. Thermal compressive forces are included by using the largest thermal membrane stresses from Tables 2.10.4-5, 2.10.4-6, and 2.10.4-7.

Step 1

S_ϕ = -12,800 + (-2,700) = -15,500 psi

S_θ = -16,200 + (-1,800) = -16,700 psi

$S_{\phi\theta}$ = 1,100 + 1,200 = 2, 300 psi

Step 2

$FS(S_\phi)$ = 20,770 psi

$FS(S_\theta)$ = 22,378 psi

$FS(S_{\phi\theta})$ = 3,082 psi

Step 3

$\alpha_{\phi L}$ = 0.393

$\alpha_{\theta L}$ = 0.800

$\alpha_{\phi\theta L}$ = 0.800

Step 4

1. Axial Compression

$S_\phi(FS)/S_y = (20,700)/(42,600) = 0.486$

$\eta_\phi = 1.0$

2. Hoop Compression

$S_\theta(FS)/S_y = (22,378)/(42,600) = 0.525$

$\eta_\theta = 1.0$

3. Shear

$S_{\phi\theta}(FS)/S_y = (3,082)/(42,600) = 0.072$

$\eta_{\phi\theta} = 1.0$

Step 5

$S_{is} = S_i(FS)/\alpha_{iL}$

$S_{\phi s} = S_\phi(FS)/\alpha_{\phi L} = (20,770)/(0.393) = 52,850$ psi

$S_{\theta s} = S_\theta(FS)/\alpha_{\theta L} = (22,378)/(0.800) = 27,973$ psi

$S_{\phi\theta s} = S_{\phi\theta}(FS)/\alpha_{\phi\theta L} = (3,082)/(0.800) = 3,853$ psi

Step 6

$S_{ip} = S_{ip}/\eta_i$

$S_{\phi p} = S_{\phi p}/\eta_{\phi} = (52,850)/(1.0) = 52,850$ psi

$S_{\theta p} = S_{\theta p}/\eta_{\theta} = (27,973)/(1.0) = 27,973$ psi

$S_{\phi\theta p} = S_{\phi\theta p}/\eta_{\phi\theta} = (3,853)/(1.0) = 3,853$ psi

Step 7

For the NAC-STC, the buckling evaluation approach, consistent with the vessel design and method of analysis, is that of Paragraph-1710 of Code Case N-284.

Step 8

From Table 2.10.5-8 the theoretical elastic buckling stresses at 353 °F are:

$S_{\phi eL} = 668,435$ psi

$S_{\theta eL} = S_{rel} = 49,115$ psi

$S_{heL} = 47,927$ psi

$S_{\phi\theta eL} = 176,487$ psi

1. Elastic Buckling (Paragraph-1713.1.1, Code Case N-284)

   a. $52,850 > (0.5)(27,973)$; therefore, not applicable.

   b. $0.381 < 1.0$

   therefore,

   $Q1 = 0.381 < 1.0$

   c. $0.0795 \leq 1.0$

therefore,

Q2 = 0.0795 < 1.0

d. 0.584 ≤ 1.0

therefore,

Q3 = 0.584 < 1.0

e. K = 0.9995

therefore,

Q4 = 0.381 < 1.0

2. Inelastic Buckling (Paragraph-1713.2.1, Code Case N-284)

a. 0.0067 ≤ 1.0

therefore,

Q5 = 0.0067 < 1.0

b. 0.3368 ≤ 1.0

therefore,

Q6 = 0.3368 < 1.0

Using the methodology presented in Section 2.10.5.3, the buckling stability of the inner shell and the transition shell of the NAC-STC for the canistered fuel configuration is verified.

2.10.5.5 Buckling Evaluation of the Inner Shell for the CY-MPC Fuel Configuration

The section with the maximum compressive stress (hoop and axial) for the inner shell and transition shell occurs in the transition shell where the thickness is 2.0 inches. This evaluation conservatively uses a thickness of 1.5 inches for all sections on the inner shell. As a result of computing the linearized stress at this section, the maximum axial stress is –8,490 psi and the maximum hoop stress is –14,740 psi. The corresponding shear stress is 965 psi. These values are obtained from Table 2.7.1.1-2. These stresses are for the 30-foot side drop condition and they envelop the 1-foot side drop event. Thermal compressive forces are included by using the largest thermal membrane stresses from Tables 2.10.4-5, 2.10.4-6 and 2.10.4-7. Use of these thermal stresses is conservative because the heat load in the CY-MPC is less than the heat load in the NAC-STC directly loaded fuel configuration.

Maximum axial stress, S_ϕ = -8,490 + (-2,700) = - 11,190 psi
Maximum hoop stress, S_θ = -14,740 + (-1,800) = - 16,540 psi
Maximum shear stress, $S_{\phi\theta}$ = 965 + 1,200 = + 2,165 psi

Because the stress values for the CY-MPC are less than the corresponding stress values calculated for the Yankee-MPC canistered fuel configuration determined in Section 2.10.5.4.1, the Yankee-MPC configuration evaluated in Section 2.10.5.4 is bounding for the CY-MPC configuration.

Table 2.10.5-1 Buckling Evaluation Results NAC-STC Inner Shell

Load Case	Load Condition	Analysis Section Location	Axial Stress (psi)	Hoop Stress (psi)	Inplane Shear Stress (psi)	Elastic Buckling Interaction Equations Q1	Q2	Q3	Q4	Plastic Buckling Interaction Equations Q5	Q6
A_{IS}	Heat	Inner Shell	-1634	-830	322	.00	.02	.04	.00	.00	.00
B_{IS}	Cold	Inner Shell	-321	-3838	315	.00	.00	.19	.00	.00	.04
C_{IS}	1-Ft Top End	Inner Shell	-5755	-2867	0	.09	.04	.29	.09	.00	.08
D_{IS}	1-Ft Bottom End	Inner Shell	-5988	-2864	0	.10	.04	.30	.10	.00	.09
E_{IS}	1-Ft Side	Inner Shell	-4911	-1829	4338	.04	.07	.10	.04	.01	.01
F_{IS}	1-Ft Top Corner	Inner Shell	-6729	-937	3029	.06	.10	.05	.07	.02	.00
G_{IS}	1-Ft Bottom Corner	Inner Shell	-6819	-847	-2945	.07	.10	.04	.07	.02	.00
H_{IS}	30-Ft Top End	Inner Shell	-10409	-2705	0	.07	.10	.09	.07	.03	.01
I_{IS}	30-Ft Bottom End	Inner Shell	-10649	-2679	0	.08	.10	.09	.08	.03	.01
J_{IS}	30-Ft Side	Inner Shell	-9836	-7346	9724	.12	.10	.26	.13	.08	.13
K_{IS}	30-Ft Top Corner	Inner Shell	-16021	-2484	8083	.13	.16	.09	.13	.72	.02
L_{IS}	30-Ft Bottom Corner	Inner Shell	-15916	-2154	-7853	.13	.16	.08	.13	.65	.01
M_{IS}	30-Ft Top Obliq. (75°)	Inner Shell	-9659	-6848	9460	.11	.10	.24	.12	.07	.11
N_{IS}	30-Ft Bott. Obliq. (15°)	Inner Shell	-16170	-1595	-6427	.13	.16	.06	.13	.81	.01
O_{IS}	30-Ft Bott. Obliq. (75°)	Inner Shell	-10161	-5650	-9286	.10	.10	.20	.10	.07	.08

Table 2.10.5-1 Buckling Evaluation Results NAC-STC Inner Shell (continued)

Load Case	Load Condition	Analysis Section Location	Axial Stress (psi)	Hoop Stress (psi)	Inplane Shear Stress (psi)	Elastic Buckling Interaction Equations				Plastic Buckling Interaction Equations	
						Q1	Q2	Q3	Q4	Q5	Q6
A_T	Heat	Transition	-2956	-5218	-694	.00	.02	.26	.00	.00	.07
B_T	Cold	Transition	-2988	-4135	503	.00	.02	.21	.00	.00	.04
C_T	1-Ft Top End	Transition	-2960	-5727	0	.00	.02	.29	.00	.00	.08
D_T	1-Ft Bottom End	Transition	-2955	-6581	0	.00	.02	.33	.00	.00	.11
E_T	1-Ft Side	Transition	-7482	-3994	6037	.06	.06	.21	.06	.01	.05
F_T	1-Ft Top Corner	Transition	-9626	-1473	3679	.04	.08	.07	.04	.01	.01
G_T	1-Ft Bottom Corner	Transition	-10422	-1704	-3467	.05	.08	.09	.05	.01	.01
H_T	30-Ft Top End	Transition	-2984	-14144	0	.00	.01	.48	.00	.00	.23
I_T	30-Ft Bottom End	Transition	-2973	-14362	0	.00	.01	.48	.00	.00	.23
J_T	30-Ft Side	Transition	-16445	-10356	14515	.17	.10	.37	.18	.03	.14
K_T	30-Ft Top Corner	Transition	-26632	-898	9400	.10	.14	.04	.10	.13	.01
L_T	30-Ft Bottom Corner	Transition	-27565	-2122	-9183	.11	.14	.08	.11	.17	.01
M_T	30-Ft Top Obliq. (75°)	Transition	-13488	-9023	15240	.13	.09	.32	.13	.02	.11
N_T	30-Ft Bott. Obliq. (15°)	Transition	-30799	-1935	-7402	.12	.16	.07	.13	.47	.01
O_T	30-Ft Bott. Obliq. (75°)	Transition	-17164	-10107	-15101	.17	.10	.36	.18	.03	.14

Table 2.10.5-2 Geometry Parameters for the NAC-STC Inner Shell and Transition Sections

Parameter	**Inner Shell**	**Transition Section[1]**
R = radius (in) [to centerline of shell]	36.25	36.25
t = thickness (in)	1.5	1.5
$(Rt)^{0.5}$	7.37	7.37
L_ϕ = length (in)	161.00	161.00
L_θ = 2pR = circumference (in)	227.8	227.8
$M_\phi = L_\phi/(Rt)^{0.5}$	21.83	21.83
$M_\theta = L_\theta/(Rt)^{0.5}$	30.89	30.89
M = lesser of M_ϕ or M_θ	21.83	21.83
ν = Poisson's Ratio	0.275	0.275

1 Conservatively consider the thinner portion of the Transition Section.

Table 2.10.5-3 Capacity Reduction Factors for the NAC-STC Inner Shell and Transition Sections

Capacity Reduction Factor	Temperature (°F)		
	70	**338**	**353**
SA-240, Type 304 Stainless Steel			
$a_{\phi L}$ (axial)	0.67	0.207	0.207
$a_{\theta L}$ (hoop)	0.8	0.8	0.8
$a_{\phi\theta L}$ (shear)	0.8	0.8	0.8
SA-240, Type XM-19 Stainless Steel			
$a_{\phi L}$ (axial)	0.517	0.393	0.389
$a_{\theta L}$ (hoop)	0.8	0.8	0.8
$a_{\phi\theta L}$ (shear)	0.8	0.8	0.8

Table 2.10.5-4 Fabrication Tolerances for the NAC-STC Inner Shell

Requirement	Parameter	Inner Shell Data (inch)
	Maximum Inside Diameter (I.D.)	71.06
	Minimum I.D.	70.96
	Nominal I.D.	71.00
NE-4221.1	a) (Max I.D. - Min I.D.)	0.10
	b) (0.01) x (Nominal I.D.)	0.710
	Tolerance Check	Yes
	(a < b)	(0.10 in < 0.710 in)
	Nominal Shell Thickness	1.50
	Minimum Shell Thickness	1.48
	Shell Length	161.00
	Nominal Shell Outside Diameter (O.D.)	74.00
	Minimum Shell O.D.	73.92
NE-4221.2	c) Permissible Deviation, e	0.54
	(Figure -4221.2-1)	
	d) Actual Deviation[1]	0.04
	Tolerance Check	Yes
	(d < c)	(0.04 in < 0.54 in)

1 (Nominal O.D. - Minimum O.D.)/2 = (74.00 - 73.92)/2 = 0.04.

Table 2.10.5-5 Material Properties for Buckling Analysis Input

Parameter[1]	Temperature (°F)		
	70	**338**	**353**
SA-240, Type 304 Stainless Steel			
E (psi)	28.3×10^6	26.7×10^6	26.7×10^6
S_y (psi)	30.0×10^3	22.0×10^3	21.7×10^3
SA-240, Type XM-19 Stainless Steel			
E (psi)	28.3×10^6	26.7×10^6	26.7×10^6
S_y (psi)	55.0×10^3	42.6×10^3	42.2×10^3

1 Section 2.3.2.

Table 2.10.5-6 Upper Bound Buckling Stresses

Load Condition		Temperature (°F)		
		70	**338**	**353**
SA-240, Type 304 Stainless Steel				
Elastic, Upper Bound Compressive Stress	Normal	15,000	11,320	10,960
S_θ or S_ϕ (psi)	Accident	22,390	16,900	16,343
Elastic, Upper Bound In-Plane Shear Stress	Normal	9,000	6,795	6,580
$S_{\phi\theta}$ (psi)	Accident	13,434	10,140	9,806
(SA-240, Type XM-19 Stainless Steel)				
Elastic, Upper Bound Compressive Stress	Normal	27,500	21,800	21,300
S_θ or S_ϕ (psi)	Accident	41,040	32,550	31,790
Elastic, Upper Bound In-Plane Shear Stress	Normal	16,500	13,080	12,780
$S_{\phi\theta}$ (psi)	Accident	24,620	19,530	19,070

Table 2.10.5-7 Theoretical Elastic Buckling Stress Values (Temperature Independent Form)

Elastic Buckling Stress	Inner Shell	Load Description
$S_{\phi eL}$	0.025035E	axial
$S_{\theta eL} = S_{reL}$	0.001841E	hoop, without end pressure
S_{heL}	0.001795E	hoop, with end pressure
$S_{\theta\phi eL}$	0.00661E	shear

Table 2.10.5-8 Theoretical Elastic Buckling Stresses for Selected Temperatures (SA-240, Type 304 and SA-240, Type XM-19 Stainless Steel)

Parameter	Theoretical Elastic Buckling Stress (psi)		
		Transition Section	Inner Shell
Modulus of Elasticity (E) at Temperature (T)	$E = 28.3 \times 10^6$ T = 70°F	$E = 26.7 \times 10^6$ T = 338°F	$E = 26.7 \times 10^6$ T = 353°F
$S_{\phi eL}$	708,490	669,186	668,435
$S_{\theta eL} = S_{reL}$	52,100	49,213	49,155
S_{heL}	50,800	47,980	47,927
$S_{\phi\theta eL}$	187,060	176,685	176,487

2.10.6 Scale Model Test Program for the NAC-STC

2.10.6.1 Introduction

This section provides a detailed description of the Scale Model Test Program, which was carried out as confirmatory support of the analysis and licensing effort for the design qualification of the directly loaded fuel configuration of the NAC-STC cask. The analyses presented elsewhere in this report demonstrate that the directly loaded fuel configuration of the NAC-STC cask design meets all of the requirements for use in the packaging and transportation of radioactive material (10 CFR 71), PWR spent fuel. The test results presented in this appendix confirm those analyses and provide additional confidence that the cask design provides for the safe transport of spent nuclear fuel. The scale model test program for the directly loaded fuel configuration of the NAC-STC included: (1) quarter-scale model drop tests and (2) eighth-scale model impact limiter quasi-static compression tests. These tests were performed using the redwood and balsa wood impact limiters (redwood impact limiter[s]) described in Licensing Drawings 423-209 and 423-210 and scale model impact limiter Drawings 423-248 and 423-249.

This report revision incorporates the drawings and analyses that demonstrate the design qualification of the canistered configuration of the NAC-STC for Yankee Class fuel or GTCC waste. The cask body is unchanged. The directly loaded fuel basket is replaced by a similar tube and disk design basket structure enclosed in a welded canister. The Yankee-MPC canistered configuration of the NAC-STC includes spacers in the cask cavity that are designed to position the loaded canister such that the package center-of-gravity location is identical to that of the package containing directly loaded fuel. The total weight of the cavity contents for the Yankee-MPC fuel or GTCC waste configuration is just slightly less than that for the directly loaded fuel configuration, 55,590 or 54,271 pounds versus 56,000 pounds. Based on the location of the packaging center-of-gravity and on the cavity contents weight considerations, it is concluded that the confirmatory scale model drop tests and the resulting impact limiter qualification are valid for the Yankee-MPC canistered configuration and for the directly loaded fuel configuration. The scale model tests are not applicable to the Connecticut Yankee MPC (CY-MPC) canistered fuel or GTCC waste configurations since these configurations have a higher contents weight (67,195 pounds) than the scale model test weight (56,000 pounds). The CY-MPC configurations must be transported using the balsa wood impact limiter design (balsa wood impact limiter[s]) shown in Drawings 423-257 and 423-258.

2.10.6.2 Purpose

The purpose of the Scale Model Test Program was to provide confirmatory support for the structural design analyses for the NAC-STC. The test program verified the structural adequacy of the NAC-STC cask packaging in: (1) the performance of its containment function, (2) the performance of the impact limiters, (3) reacting dynamic impact loadings, and (4) resisting puncture by a pin.

2.10.6.3 Discussion

Scale model testing is an accurate means of confirming a proposed packaging design. The packaging comprises the fuel basket, cask body, closure lids, and the redwood impact limiters. The method of performing scale model testing for nonlinear behavior is well accepted. For this application quarter-scale and eighth-scale models were employed. In either case, when the dimensions are scaled, the weight will be adjusted by the $(\text{scale})^3$ and the material properties and drop heights will remain the same as for the full-scale cask. This permits the material employed in the licensed full-scale cask to be used in the scale model testing.

Two types of tests are used in this program, static and dynamic. The tests to confirm the impact limiter design were a combination of eighth-scale model quasi-static compression tests and a quarter-scale model 30-foot drop tests. The packaging design was confirmed by performing 30-foot drop tests and one-meter pin puncture tests using a quarter-scale model that included the fuel basket, fuel assemblies, cask body, lids and impact limiters.

In the overall testing program, the testing of the impact limiter design precedes the quarter-scale testing of the entire package. The impact limiters are the critical component in limiting the impact loads imposed on the cask. Scale model impact limiters were tested as separate components before testing the scale model package assembly. Therefore, the description of the eighth-scale model impact limiter compression tests is presented first, followed by the description of the quarter-scale model drop tests, along with the development of the design changes brought about by the drop tests.

2.10.6.3.1 Scale Model Redwood Impact Limiter Compression Tests

The function of the impact limiter is to limit the maximum acceleration experienced by the cask, regardless of the orientation of the cask. This is accomplished by using an energy absorbing

crushable material which exhibits a minimum degree of rebound once the cask has come to rest. In the NAC-STC redwood impact limiter design, redwood and balsa wood are used as the energy absorbing materials. Measurement of the acceleration resulting from the crushing of the redwood/balsa wood can be accomplished by two means:

1) use of accelerometers to record the accelerations in a dynamic drop test, or
2) measuring the force to crush the impact limiter in the same orientation as the cask would impact the unyielding surface.

In evaluating the impact limiter to determine the deceleration to be experienced by the cask, the latter method is preferred because although the acceleration time histories record the maximum acceleration experienced by the cask as a result of the impact limiter crushing, significant uncertainties may be introduced. The acceleration records may contain high frequency signals which can come from a number of sources: the cable transmitting the accelerometer output to storage, rattling of the model fuel assemblies, or high frequency shell modes. None of these relate to the performance of the impact limiter itself. The static test, in principle, is easier to reproduce and the data acquisition is simpler and is not affected by other transient events during the test. Static testing produces a number of useful results: the acceleration, which is the ratio of the crush force to the model mass; the absorbed energy, which is the area under the force-deformation curve; the crush strain; and the behavior of the impact limiter during crushing.

Static compression tests were performed to simulate an end impact, a corner impact, and a side impact using eighth-scale models impact limiters. The eighth-scale models used redwood/balsa wood as the energy absorbing materials, just as in the full-scale design. The impact limiter shells used in the eighth-scale model tests consisted of 0.031-inch thick stainless steel. The full-scale impact limiter design uses 0.25-inch thick stainless steel shells. Drawings of the eighth-scale model impact limiter are presented in Section 2.10.6.7.

The design of the NAC-STC redwood impact limiter was revised during the quarter-scale drop tests program. The final impact limiter design constrains the redwood during the side and shallow angle oblique drop tests. The eighth-scale model impact limiters represented the redesigned configuration.

The eighth-scale model redwood impact limiter compression tests demonstrated that:

1) The NAC-STC redwood impact limiter, as designed, does not generate deceleration loads larger than those used in the design analyses, and
2) The crush stroke does not exceed the acceptance criteria (the cask body does not come into contact with the impact plane).

2.10.6.3.2 Quarter-Scale Model Drop Tests

The objective of the quarter-scale model drop tests was to confirm the design of the NAC-STC packaging. An important feature of the quarter-scale model is its accuracy in reflecting containment and structural features of the full-scale design. The quarter-scale model packaging was an exact replica of the full-scale design with two exceptions: (1) o-rings in the inner and outer lids were not scaled; and (2) the neutron shield was not modeled, but the weight of the neutron shield was modeled by steel blocks welded to the outer shell. All aspects of the model can be used to reflect the strains, accelerations, and impact limiter crush strokes of the full-scale design. With respect to containment, the model represents the geometrical arrangement and materials used in the full scale design. However, the o-ring dimensions and the leak rate cannot be scaled, which means that the pressure measurements can only be used to indicate the condition of the seals and the adjacent seating surfaces.

The drawings of the detailed quarter-scale model components of the body of the NAC-STC, which were fabricated for use in this test program, are presented in Section 2.10.6.6. The details of the quarter-scale model are described in Section 2.10.6.5.1 (see Figures 2.10.6-1 thru 2.10.6-3).

The test plan called for a series of tests to be conducted at the Winfrith Technology Centre drop test facility, which is located in the United Kingdom. These tests would confirm the NAC-STC design for the nine-meter (30-foot) drop condition and the one-meter (40-inch) drop pin puncture condition. The tests included:

1) Nine-meter (30-foot) top end drop

2) Nine-meter (30-foot) top corner drop (24 degrees from the vertical)

3) Nine-meter (30-foot) side drop

4) Nine-meter (30-foot) bottom end oblique drop (75 degrees from the vertical) to maximize the slapdown effect on the top end)

5) One-meter (40-inch) pin puncture drop at the cask axial mid-point

6) One-meter (40-inch) pin puncture at the center of the outer lid

The test plan included performing a pretest metrology inspection and a post-test metrology inspection to confirm the adequacy of the design. The initial scale-model design used impact limiters with aluminum shells.

For test number 1, the nine-meter (30-foot) top end drop, the aluminum impact limiter shells posed no problems and the cask was shown to meet the acceptance criteria described in Section 2.10.6.5.2 (see Figure 2.10.6-4). The end drop test is not reperformed using scale-model impact limiters with stainless steel shells because the model cask body penetrates into the model impact limiter for the end drop orientation and the effect of the impact limiter shell on this event is negligible. The cask remained upright and no damage was indicated to have occurred to the cask or its components.

For test number 2, the nine-meter (30-foot) top corner drop, it was observed that the accelerations were appropriate, but the limiters did not remain attached to the cask. Testing proceeded to test number 3, which was the nine-meter (30-foot) side drop. The results of test number 3 clearly indicated the inadequacy of the aluminum shell welds to maintain the integrity of the impact limiter shell. It was observed in the high speed films that the redwood was ejected from the limiter at a rate commensurate with the impact speed. As the side drop progressed, the steel blocks representing the neutron shield weight impacted the surface and were displaced into the outer shell of the cask body (see Figure 2.10.6-5). As a result, the inner shell was compressed against the fuel basket. Additionally, the top forging was slightly distorted and the internal pressure was released, even though the lids remained firmly attached to the cask body.

The cask body and basket were submitted to the metrology laboratory for inspection and repair. Hydraulic rams were employed to remove the indentations in the inner shell in conjunction with a machining operation to bring the model back to specifications (see Figures 2.10.6-6 and 2.10.6-7). The first three tests are identified as Test numbers 1, 2 and 3 of Phase 1. While the

indentations due to the steel blocks were on the order of 0.06 to 0.13 inch deep, the maximum strain obtained from the gauges was 0.0018 inch/inch, which would not significantly strain-harden the stainless steel.

The nine-meter (30-foot) side drop (Test No. 3 of Phase 1) demonstrated the integrity of the basket design. Decelerations of about 1200 g were imposed on the basket disks. Outside of the local deformation due to the steel blocks, the basket support disk number 6, which was located opposite the impacted block, was not deformed (see Figure 2.10.6-8). The center basket disk showed no damage. This represents a load factor of 5 over the basket design. Moreover, no out-of-plane or in-plane buckling was observed.

Once the metrology inspection had been completed, and the repairs were made to the model cask body, pin puncture tests were conducted. Since the pin puncture tests were bracketed by before and after metrology inspections, it was determined that the pin puncture tests would be identified as Phase 2 tests. During the performance of these tests, however, the 24-inch long pin deformed excessively, to the extent that maximum damage was not inflicted on the cask body or the outer lid. Therefore, it was determined that the pin puncture tests would be reperformed using an 8-inch tall pin, as specified by regulatory requirements.

Prior to resuming testing, the impact limiter aluminum shell design was replaced with a stainless steel design. This initiated Phase 3 tests, which were planned to include a side drop, an oblique end drop, a top corner drop and two pin puncture tests. Thus, the Phase 3 tests are identified as:

1) Test No. 1 of Phase 3: nine-meter (30-foot) side drop

2) Test No. 2 of Phase 3: nine-meter (30-foot) 75° oblique bottom end drop

3) Test No. 3 of Phase 3: nine-meter (30-foot) top corner drop (24°)

4) Test No. 4 of Phase 3: nine-meter (30-foot) 75° oblique top end drop (added during the test sequence)

5) Test No. 5 of Phase 3 : one-meter (40-inch) drop cask mid-point pin puncture

6) Test No. 6 of Phase 3 : one-meter (40-inch) drop outer lid center pin puncture

The results of the nine-meter (30-foot) top corner drop indicated that the NAC-STC cask model did maintain pressure, and no damage occurred to the fuel basket or the cask body.

For the nine-meter (30-foot) side and oblique drops, the tests indicated a weakness in the impact limiter design. Even with the improved stainless steel shell to contain the redwood, it was observed that the redwood in the side impact region that overlaps the side of the cask was reorienting itself during the crushing action for the side drop impact and the oblique drop slapdown impact. The “overlap” region is that segment of redwood which brings the cask to rest for a side drop impact or an oblique drop slapdown impact. As a result, the redwood effective crush strength was lower than the design values, and the crush stroke was greater than calculated. One of the elements of the acceptance criteria is to ensure that the neutron shield does not come into contact with the impact surface. The full-scale stroke extrapolated from these tests would permit the neutron shield to come into contact with the impact plane. The design analyses do not take into account any impact loading on the neutron shield, so contact with the impact surface is not acceptable. However, neither the top corner drop test, nor the pin puncture drop tests, are affected by the redwood in the overlap region, so those tests are valid. The pin puncture tests at the cask mid-point and at the center of the outer lid were performed with an 8-inch tall puncture pin per regulatory requirements, but without impact limiters on the package model. Additional weight was added in the model cask cavity to obtain the correct scaled mass of the package model. Inspection of the model and the puncture pin after each test revealed: slight deformation of the puncture pin; the outer shell incurred significant local deformation, but was not punctured; essentially no damage occurred to the outer lid; and only a very slight indentation occurred on the inside diameter of the inner shell at its axial midpoint.

After reviewing the unsatisfactory performance of the upper impact limiter in Test Nos. 1 and 2 of Phase 3, Test No. 4, a nine-meter (30-foot), 75° top oblique drop, was added to the test plan to assess the performance of the lower impact limiter (without trunnion cutouts) for a slapdown impact. No significant difference in behavior or crush characteristics was noted, so the trunnion cutouts are negligible.

At the conclusion of the Phase 3 tests, the satisfactory testing results were summarized as follows:

1) Test No. 1 of Phase 1 satisfactorily verified the packaging design for the nine-meter (30-foot) end drop, since the impact limiter shell material has no significant effect on the end drop decelerations.

2) Test No. 3 of Phase 3 satisfactorily verified the packaging design for the nine-meter (30-foot) top corner drop (see Figure2.10.6-9).

3) Test No. 5 and Test No. 6 of Phase 3 satisfactorily verified the packaging design for the pin puncture events. The scaled eight-inch long puncture pin deformed slightly for both orientations of the cask. The degree of deformation was not significant (see Figures 2.10.6-10 and 2.10.6-11) and the pin length satisfied regulatory requirements, so these tests are valid.

A design revision of the NAC-STC impact limiters was developed to better constrain the redwood. Quarter-scale sections of the impact limiter, both with and without the modifications, were tested by quasi-static compression. It was observed that the modification was sufficient to correct previous deficiencies, and that the modification did not significantly affect the crushing of the impact limiter for an end impact or a corner impact.

Prior to initiating the next phase of testing, the inner shell of the model cask body was repaired to remove the pin puncture indentation. This would ensure that the cask model was representative of the full-scale cask body.

Phase 4 required that only the nine-meter (30-foot) bottom oblique and side drop tests be conducted. The nine-meter (30-foot) bottom oblique (top slapdown) drop test was conducted first, since it was expected that the slapdown effect would be maximum for the top impact limiter due to the cutout regions for the trunnions. The cutouts for the trunnions actually reduced, only slightly, the amount of redwood available for crushing.

Test Nos. 1 and 2 of Phase 4 demonstrated that the modified impact limiter design prevents the neutron shield from coming into contact with the impact surface. By defining the margin of safety to be based on the crush stroke and the distance of the crush plane to the edge of the neutron shield, the modified design of the NAC-STC impact limiter allowed a margin of safety of +0.33 for the most severe conditions. Additionally, the measured decelerations indicate that the maximum values are less than those employed for the design analyses of the NAC-STC.

For each of the tests, the pressure and temperature were measured and recorded before and after the test. In all valid tests, closure lid seal integrity was maintained. For the outer lid pin puncture (Test No. 6 of Phase 3), the cavity pressure valve was cracked, but after replacement of the valve, and prior to lid removal, the cask satisfactorily maintained pressure.

In Test Nos. 1 and 2 of Phase 4, diametral measurements indicated that no permanent deformation had been imposed on the cask body. While some of the strain gauges indicated some type of permanent deformation, the level was negligible, when it was compared to the industry accepted value of 0.2 percent strain for material yielding.

It is concluded that the adequacy of the full-scale NAC-STC packaging design is confirmed by the quarter-scale model drop tests.

2.10.6.4 Eighth-Scale Redwood Impact Limiter Compression Tests

A series of quasi-static compression tests were performed with scale model redwood/balsa wood impact limiters to demonstrate that:

1. Force-Deformation curves are as predicted by the RBCUBED computer program.

2. Energy storage (rebound) in the crushed redwood/balsa wood impact limiters is negligible.

3. The impact limiter and cask body geometry effectively causes the impact limiter to stay in position on the cask.

2.10.6.4.1 Force-Deformation Curves for the End, Corner, and Side Impact Orientations

Eighth-scale model impact limiter compression tests were conducted for the end, corner, and side orientations of the cask. These tests were performed using the modified NAC-STC impact limiter design. As indicated previously, the modification has a negligible effect on the crushing of the impact limiter in the end impact and corner impact orientations.

Eighth-scale tests were performed with both aluminum alloy and stainless steel impact limiter shells. The aluminum alloy shells split along the weld seams and came apart as compressive load was applied. The Type 304 stainless steel shells remained ductile and did not split along the weld seams. A full penetration weld was necessary to insure adequate joining of the pieces of the stainless steel shells. The stainless steel shells have a higher weight than the aluminum shells, so initial testing of the quarter-scale model in the nine-meter (30-foot) drops was performed with aluminum alloy impact limiter shells in an effort to reduce the overall cask weight. The weld failures experienced with the aluminum alloy impact limiter shells in the drop tests showed that stainless steel impact limiter shells were, in fact, required. The stainless steel impact limiter shells tested in the eighth-scale quasi-static testing were adopted for the final impact limiter shell design.

Eighth-scale model lower impact limiters were used in the force-deformation compression tests for the NAC-STC impact limiter design. This is primarily because the trunnion cutouts in an eighth-scale model upper impact limiter are extremely difficult to fabricate using the scaled shell thickness. Also, previous analyses, scale model compression tests, and scale model drop tests have all demonstrated that the trunnion cutout regions of the upper impact limiter do not significantly affect the energy absorption capability of the impact limiter.

The eighth-scale model impact limiters were crushed quasi-statically in a tensile test machine which can also apply compressive loads. The tensile test machine capacity limited the maximum size of the test impact limiter to one-eighth scale.

The eighth-scale model impact limiters were not attached mechanically to the cask-shaped test fixtures. Duct tape was used to hold the model impact limiter in place while the compressive test load was applied. The tape relaxed as successively higher loads were applied, demonstrating that the impact limiter geometry produces net crush forces which press the impact limiter against the cask body, regardless of the impact angle.

The force-deformation curve is measured by compressing the model impact limiter and recording the deflections and loads applied to the limiter. The energy storage, or rebound, of the model impact limiter is shown by the load-deformation curve as the test machine is unloaded slowly. The model impact limiter presses against the test machine heads and applies a load proportional to the elastically stored energy. This extra energy component can be restored to a cask in a multiple-impact, oblique drop "slapdown" scenario. The eighth-scale model impact limiter compression tests showed that a maximum of 8.2 percent of the absorbed energy may be stored during crushing and later released.

While each model impact limiter tested was being compressed, two calibrated linear variable differential transformers (LVDT) mechanically attached to test fixtures provided data to an X - Y recorder, which plotted crush force versus deformation. Deformation of the model impact limiter proceeded well into the compression lock-up range of the redwood. As the compression load on the model impact limiter was decreased after the test was stopped, force and deflection continued to be monitored, revealing the amount of elastically stored energy. Based on the results of the quasi-static tests, the force-deformation curve and the energy absorption capacity (area under the curve) of each model impact limiter is presented in Figures 2.10.6-12, 2.10.6-13, and 2.10.6-14. The static force for each data point is multiplied by 1.06, a static to dynamic scaling factor, enabling a direct comparison with the RBCUBED computed values. The dynamic scaling factor is determined from Figure 9 of NUREG/CR-0322, which is based on Sandia National Laboratory

tests. Figures 2.10.6-12, 2.10.6-13 and 2.10.6-14 show for comparison the dynamically scaled forces and the RBCUBED computed values. These figures also show the maximum compression forces that occur for each of the impact orientations.

For the end impact case, the impact limiter compression forces from the quasi-static test are higher than those calculated by the RBCUBED analyses using the maximum tolerance cold temperature crush strength and the minimum tolerance hot temperature crush strength properties of redwood. This difference in compression forces can be attributed to the additional forces on the cask due to the redwood material's resistance to shearing along the periphery of the "backed" area of the cask. The calculated equivalent deceleration force of the full-scale cask, based on the quasi-static eighth-scale model impact limiter test is 54.8 g for the end impact case. This force is greater than the 44.6 g end drop deceleration force obtained from the RBCUBED analysis using the maximum tolerance cold temperature crush strength of redwood, but less than the 56.1 g deceleration force obtained from the RBCUBED analysis using the minimum tolerance hot temperature crush strength of redwood. The higher deceleration force obtained using the minimum tolerance hot temperature crush strength of redwood is a result of the larger deformation and the partial lock-up of the redwood that occurs before the cask is stopped. Based on the area under the dynamically scaled force-deformation curve presented in Figure 2.10.6-12 for the end impact case, all of the energy of a one-eighth scale model of the NAC-STC for a 30-foot drop is absorbed when the impact limiter deformation reaches 1.58 inches (1.63 inches from the static force-deformation curve), which extrapolates to a 12.6-inch deformation for the full-scale NAC-STC impact limiter, or 42 percent of the depth of the impact limiter. The dynamic force-deformation curve for the eighth-scale model impact limiter for the end impact case is extrapolated to full-scale and presented in Figures 2.10.7-5 and 2.10.7-8 for comparison with the RBCUBED calculated force-deformation curves for the NAC-STC impact limiters.

For the corner impact case, the calculated equivalent deceleration force of the full-scale cask, based on the quasi-static eighth-scale model impact limiter test, is 32.6 g. This compares with the 44.0 g deceleration force calculated by the RBCUBED analysis using the maximum tolerance cold temperature crush strength of redwood, and with the 49.3 g deceleration force calculated using the minimum tolerance hot temperature crush strength of redwood. Based on the area under the dynamically-scaled force-deformation curve presented in Figure 2.10.6-13 for the corner impact case, all of the energy of a one-eighth scale model of the NAC-STC for a 30-foot drop is absorbed when the impact limiter deformation reaches 3.22 inches (3.30 inches for the static force-deformation curve), which extrapolates to a 25.76-inch deformation for the full-scale NAC-STC impact limiter, or 70 percent of the depth of the impact limiter. The dynamic force-deformation curve for the eighth-scale model impact limiter for the corner impact case is extrapolated to full-scale and presented in Figures 2.10.7-6 and 2.10.7-9 for comparison with the RBCUBED calculated force-deformation curves for the NAC-STC impact limiters.

For the side impact case, the calculated equivalent deceleration force for the full-scale cask, based on the quasi-static eighth-scale model impact limiter test, is 45.6 g. This force compares with the 51.7 g deceleration force from the RBCUBED analysis using the maximum tolerance cold temperature crush strength of redwood and with the 51.3 g deceleration force using the minimum tolerance hot temperature crush strength of redwood.

Based on the area under the dynamically-scaled force-deformation curve presented in Figure 2.10.6-14 for the side impact case, all of the energy of a one-eighth scale model of the NAC-STC for a 30-foot drop is absorbed when the impact limiter deformation reaches 1.64 inches (1.70 inches for the static force-deformation curve), which extrapolates to a 13.12-inch deformation for the full-scale NAC-STC impact limiter, or 71 percent of the depth of the impact limiter. The dynamic force-deformation curve for the eighth-scale model impact limiter for the side impact case is extrapolated to full-scale and presented in Figures 2.10.7-8 and 2.10.7-11 for comparison with the RBCUBED calculated force-deformation curves for the NAC-STC impact limiters.

Since the force-deformation curves obtained from the quasi-static compression tests are enveloped and reasonably approximated by those force-deformation curves calculated by the RBCUBED program, the NAC-STC transport impact limiters are designed based on RBCUBED analysis runs.

2.10.6.4.2 Conclusion

The results of the eighth-scale model NAC-STC impact limiter quasi-static compression tests clearly demonstrate that the NAC-STC impact limiter design provides the energy absorption capacity to decelerate the cask to a stop for a 30-foot drop accident for the various impact orientations, while maintaining maximum compression forces that are less than the cask design values.

Table 2.10.6-1 shows: (1) the maximum side impact deceleration values determined by RBCUBED using the redwood cold crush strength plus 10 percent, and the hot crush strength minus 10 percent; (2) the deceleration value extrapolated from the eighth-scale quasi-static compression test results as documented above; (3) the actual deceleration value measured during the final quarter-scale model side drop test; and (4) the value used for design calculations. The maximum calculated side impact deceleration determined for the modified impact limiter is within 12 percent of the average value predicted by RBCUBED, and is within 11 percent of the deceleration value measured in the quarter-scale drop test. Therefore, it is concluded that the methodology used above adequately characterizes the structural behavior of the final design of the impact limiter for side impacts, and that the value of maximum side impact deceleration used in the design calculations (55g) is conservative.

2.10.6.5 Quarter-Scale Model Drop Tests

2.10.6.5.1 Model Description

The model of the body of the NAC-STC cask, which was used in the Drop Test Program, was a quarter-scale duplication of the full-scale cask in all aspects, except as described in subsequent paragraphs of this section. The model was fabricated of Type 304 stainless steel inner and outer shells, top and bottom forgings, and inner closure lid; the port covers and the outer closure lid

were Type 17-4PH stainless steel; the gamma shield was Chemical Lead per ASTM B29. The impact limiters were fabricated of redwood and balsa wood. Initially they were enclosed in 6061-T6 aluminum alloy shells, which have subsequently been changed to Type 304 stainless steel. Additionally, the attachment design was changed to include sixteen retaining rods and to allow more flexibility of these retaining rods during an impact loading, which eliminated direct shear failure.

The NAC-STC quarter-scale model lead gamma shield forms an annulus 0.925 inch thick and 40.25 inches long. The lead was enclosed between the 0.375-inch thick, 17.75-inch inside diameter inner shell, and the 0.665-inch thick, 21.68-inch outside diameter outer shell. The ends of the inner shell include 3.00-inch long by 0.505-inch thick transition regions. The bottom forging of the quarter-scale model cask is 1.55 inches thick. The bottom also includes a 0.50-inch thick, 19.77-inch diameter NS-4-FR neutron shielding disk enclosed by a 1.36-inch thick bottom plate. The upper end forging is 4.59 inches thick with an interior that is machined to accept the two closure lids. The main body of the inner closure lid is 2.25 inches thick and 19.750 inches in diameter. A 0.75-inch thick, 1.385-inch wide integral outer rim on the top of the inner lid encloses a 0.50-inch thick layer of NS-4-FR neutron shielding material and a 0.25-inch thick, Type 304 stainless steel coverplate. A bypass port was included in the model inner lid to ensure that the cavity pressure reached the outer lid o-rings for all of the quarter-scale model tests. This bypass port does not exist in the full-scale inner lid design. The model outer lid is 1.313 inches thick and 20.380 inches in diameter. There was a 12.50-inch diameter, 0.015-inch deep recess in the bottom surface of the outer lid to reduce the area that must be polished as a sealing surface. The 42 bolts for the model inner lid are 3/8-24 UNF x 2-1/2 inches long socket head cap screws; the 36 bolts for the model outer lid are 1/4-28 UNF x 1-5/8 inches long socket head cap screws. These bolts were selected to provide a tensile stress area equal to $(1/(4)^2)$ times that of the full-scale closure bolts. Since the impact load factor on the model is four times that applied to the full-scale cask, the proper scaled bolt stress results. The port cover is a 0.72-inch diameter piston-type cylinder with an integral 0.25-inch thick, 1.130-inch diameter coverplate. The model impact limiters are quarter-scale replicas of the full-scale impact limiters with 22.3 pound-per-cubic-foot (average) redwood and 7 to 10 pound-per-cubic-foot (average) balsa wood energy-absorption materials. These model impact limiters produce the properly scaled (4 x full-scale) impact loads on the model cask. The wood material section pie-shapes, joints, and bonds of the scale model impact limiters duplicate those of the full-scale impact limiters. The redwood and balsa wood

materials of the model impact limiters used in the Phase 1 testing were enclosed in 0.12-inch thick, 6061-T6 aluminum alloy shells. For the Phase 3 and Phase 4 testing, the impact limiter shells were changed to 0.062-inch thick Type 304 stainless steel. For the Phase 4 tests, the model impact limiters included modifications to correct deficiencies identified earlier in the test program. Impact limiters were not used for the Phase 2 puncture tests.

The model impact limiters had an outside diameter of 31.0 inches and an overall length of 11.2 inches. The inner cup has an inside diameter of 21.9 inches and a depth of 3.0 inches. The model upper impact limiter has four 2.9-inches wide, 1.6-inch long, 0.9-inch deep cutouts for the lifting trunnions. The model impact limiters are attached to the end surfaces of the cask model with threaded retaining rods and nuts through the ends of the limiters. The model fuel load consisted of 26 steel bars simulating the scaled size and weight of the tubes and fuel assemblies. These "dummy" fuel assemblies fit within an exact quarter-scale model of the fuel basket.

The inner shell, end forging, and the inner lid establish a model cask cavity that is 41.25 inches in length and 17.75 inches in diameter. The weight of the quarter-scale model cask with impact limiters and cavity load is 3884 pounds (approximately 0.5 percent lighter than the scaled design weight).

Three differences do exist between the quarter-scale model cask body and the full-scale cask body: (1) the model does not include the neutron shield; the weight of the neutron shield is simulated on the model by segmented steel bars welded on the exterior surface of the outer shell; the use of segmented weights to simulate the neutron shield prevents the weights from contributing to the strength of the cask, and neglects the stiffening/strengthening effect of the neutron shield shell on the cask body; (2) the inner and outer shells of the model are entirely Type 304 stainless steel, with a yield strength of S_y = 30 ksi and an ultimate strength of S_u = 75 ksi, while the full-scale cask contains Type XM-19 stainless steel inner shell rings at each end of the Type 304 stainless steel inner shell; for Type XM-19 stainless steel, S_y = 55 ksi and S_u = 100 ksi; and (3) the model includes a recessed outer lid that is bolted to the inner lid with the upper impact limiter bolted to the outer lid. The final design of the NAC-STC includes separate inner and outer lids that each bolt directly to the top forging of the cask body. The inner lid and its outer o-ring are defined to be the primary containment boundary. The upper impact limiter attachment to the outer lid remains unchanged.

In the redesigned closure system: (1) inner lid - remains essentially identical to the quarter-scale model, except that it no longer has bolt holes for the outer lid bolts; (2) inner lid bolts - the size and number are unchanged, but the material, SB-637 N07718 (S_u = 185 ksi and S_y = 150 ksi), is considerably stronger than that in the quarter-scale model (S_u = 130 ksi and S_y = 85 ksi); (3) outer lid - material and effective thickness are unchanged, while the diameter is increased and includes a flange with bolt holes; (4) outer lid bolts - the material, size, and number remain unchanged, but the diameter of the bolt circle is increased to accommodate bolting through the flange directly to the top forging; (5) top forging - 2.56 inches shorter, but the thickness has increased from 2.47 inches to 3.79 inches; and (6) inner and outer lid bolt torques - remain unchanged, so the bolt torques specified for the quarter-scale model inner and outer lid bolts are appropriate. Since the redesigned outer lid protects the inner lid (primary containment boundary) and the ring stiffness of the top forging is significantly increased, while the basic configuration of the closure system is unchanged, the quarter-scale model conservatively represents the structural characteristics of the closure region of the full-scale cask.

Based on the foregoing discussion of the significant differences between the quarter-scale model cask body and the full-scale cask body, it is concluded that the NAC-STC quarter-scale model is a conservative, representative replica of the full-scale model.

2.10.6.5.2 Acceptance Criteria for Model Performance

The acceptance criteria for the packaging components is established for the cask body and the impact limiters.

The acceptance criteria for the cask body performance is that cavity pressure be maintained and that the fuel remain in a subcritical configuration. For the cask body this requires that:

1) Permanent deformation must not be observed in the metrology results for the lids and their mating sealing surfaces.

2) Strains in the cask body must not exceed the 0.2 percent offset for determining material yield strength.

3) The pressure test must indicate that there was no loss of pressure during the test.

4) The fuel basket must not exhibit permanent deformation after the tests.

5) The inner and outer lid bolts must not exhibit permanent deformation after the tests.

The function of the impact limiter is to limit the deceleration of the cask body and components during a cask drop event. Then, the impact limiter acceptance criteria requires that:

1) The crush stroke be limited to prevent an impact of the cask body on the impact surface.

2) The accelerations be limited to those used in the design analyses (also verified by the static compression tests).

3) The impact limiters remain attached to the cask body and in position after the impact event.

2.10.6.5.3 Equipment and Instrumentation for the Drop Tests

All drop tests were performed at the Winfrith Technology Centre located in the United Kingdom. The facility, which is an IAEA approved drop test facility, had the capacity to lift the model package to a drop height of 9 meters and had an appropriate unyielding impact surface. The target consisted of a 70 metric ton concrete mass and a 10 foot by 12.5 foot rectangular, 75 mm thick steel plate at the impact surface. Lifting and dropping the model was achieved through a single point suspension system (attaching the cask to the crane hook at a single point) in conjunction with an electromagnetic release. This release mechanism allowed the free fall of the package to be initiated in an unimpeded fashion with minimum perturbation to the angular position of the model.

To assess the model performance against the acceptance criteria, a set of basic data was required to be collected throughout each test. This consisted of:

1) Metrology data - to assess the permanent deformation of the cask body, including the closure lids and the seating area for them. Also included is fuel basket deformation data to determine the response of the basket during the drop.

2) Pressure and temperature data - to assess the retention of pressure by the cask primary containment boundary. The temperature data is needed to correlate pressure changes with an increase or decrease in the temperature while the test is conducted.

3) Strain data - to determine the maximum amount of strain that occurs in the cask body.

4) Acceleration data - to determine the maximum accelerations to which the cask was subjected.

5) Impact limiter deformation data - to evaluate the behavior of the impact limiters, the crush stroke for each orientation, and the condition of the limiter attachment to the cask body after each test.

6) High speed photography - to review and assess the actual angle of impact and the behavior of the cask body and impact limiters during the impact.

A wide range of additional equipment and instrumentation was employed to determine the measurements or capture the test data during the impact event.

1) Cask Body and Fuel Basket Metrology Data

Measurements before the tests and after the test series were performed in a metrology lab, which could determine the measurements within a tolerance of +/- 0.001 inch for all dimensions except the inner diameters in the lower portion of the model cask cavity. Comparison of these sets of measurements permits determination of the presence of any permanent deformation of the diameter of the cask, seating area for the lids, or in the lids themselves.

Certain key dimensions for the fuel basket center support disk (Disk No. 12) were also measured using a metrology bench which was capable of determining the position of a point on a support disk to within 0.001 inch and the out-of-plane position of the disk to within 0.001 inch. After each test, the basket was field inspected to assess any change in the surfaces of the basket support disks.

Definitions of the measurement locations for the cask body and the support disk measurements made by the metrology laboratory are shown in Figures 2.10.6-15 and 2.10.6-16.

2) Pressure and Temperature Data

Through a pressure port located near the cask midpoint (for model only; not in full-scale design), the cask cavity was pressurized to 30 (+2/-0) psi. The pressure in the cask cavity was measured before and after each test. To assist in correlating the pressure change with a change in the cask temperature, the temperature of the cask body was also obtained by Chromel/Constantan thermocouples attached to the cask exterior near the pressure port used to pressurize the cavity.

3) Strain Data

Strain time-histories were recorded for each of the 30-foot drops for the locations shown in Figure 2.10.6-17. Ninety-degree tee-rosettes were mounted on the cask body for all of the drop tests. One gauge of each tee-rosette was positioned in the axial direction and another in the circumferential direction. This allowed the axial and the hoop stresses to be monitored. Later in the testing program, the 90-degree tee-rosettes were exchanged at two of the locations for rosettes with three gauges at 45-degree orientations, which allowed the shear stresses to be determined at the surface. All gauges had at least a 50 kHz response time to ensure that the transient strains could be accurately recorded.

Real time recording was accomplished by a system of strain amplifiers, signal conditioners and a magnetic recording unit to store the data. Strain gauge data was only taken for the 30-foot drop tests. It was concluded that the strain gauge data was not needed for the pin puncture drops.

The strains are converted to axial and hoop stresses by the following expressions:

$$\sigma_a = \frac{E}{1-\nu^2}\left(\varepsilon_a + \nu\varepsilon_h\right) \text{ (axial stress, psi)}$$

$$\sigma_h = \frac{E}{1-\nu^2}\left(\varepsilon_h + \nu\varepsilon_a\right) \text{ (hoop stress, psi)}$$

where

E = Modulus of elasticity = 28.3E+6 psi
ν = 0.3
ε_a = Axial strain
ε_h = Hoop strain

The maximum stress is computed by taking the strain components at the same time point from the strain gauge traces. The time points from each trace (one for the hoop strain gauge and one for the axial strain gauge) are selected to determine a conservative value for the stress.

4) Acceleration Data

Two single-axis accelerometers were mounted on the cask body for each of the 30-foot drop tests. The location and orientation for each test is shown in Figure 2.10.6-18. The directions were altered for each individual test to ensure that the vertical deceleration was measured.

Each accelerometer could measure accelerations up to 20,000 g with an accuracy of 1 percent per 2,000 g. For this application, in which an acceleration level of 300 g was expected, the accuracy was +/- 0.5 g. The frequency response of the accelerometer was from 2 Hz to 15,000 Hz, which would envelope the frequency of the system.

All accelerometer data was conditioned and stored on magnetic media for later processing, which included filtering and integrating to obtain the impact velocities. Acceleration data was only taken for the 30-foot drop tests. It was concluded that the accelerometer data was not needed for the pin puncture drop tests.

5) Limiter Deformation Data

After each test, the limiters were inspected to determine the amount of deformation that had occurred and to determine the condition of the attachment rods and nuts. Photographs of the deformed limiters were taken to record the post-test condition of the limiters.

6) High Speed Photography

Two high speed cameras were used to record the behavior of the quarter-scale model as it impacted the target surface. For the top end drop, both cameras

were operated at 500frames/sec and the cameras were positioned at 90 degrees apart (side and end views). For the final top corner drop, side drop, and oblique slapdown drop, one camera was positioned to capture the overall motion of the cask at 500 frames/sec and the other camera was set to obtain a close up view of the crushing of the impact limiter at 1000 frames/sec.

2.10.6.5.4 Drop Test Sequence

This section describes the test procedures that were used each time the scale model cask was tested. Winfrith personnel were responsible for the model cask preparation; they performed all tasks related to instrumentation and the actual sequence leading up to the drop.

1. Cask Preparation (Winfrith Personnel)

   A. Install the model fuel basket assembly and model fuel assemblies.

   B. Install the model cask inner lid using a new metallic o-ring. The by-pass port plug in the model inner lid has been removed to ensure that the outer lid o-rings will be subjected to the cask cavity pressure.

   C. Torque the 42 model inner lid bolts to 400 (±10) inch-pounds.

   D. Install the model outer lid using new TFE o-rings. The TFE o-rings are inspected for defects prior to installation.

   E. Torque the 36 model outer lid bolts to 80 (±5) inch-pounds.

   F. Verify the model outer lid seals by pressurizing the model cask cavity to 30 (+2/-0) psig. Observe the cavity pressure over a 10 minute period to ensure leak tightness.

G. Attach the model upper and lower impact limiters to the model cask.

Note: For pin puncture drop tests, the basket and fuel assemblies were replaced with equal weight material. Impact limiters were not installed for the pin puncture tests.

2. Performing the Drop Test (Winfrith Personnel)

A. Check umbilical cord connection to data recorders.

B. Ensure the safety of cask release assembly prior to lift and the correct angle of orientation of the cask.

C. Final check to ascertain if all systems are ready for the drop.

D. Turn on the recorders for the strain gauges and accelerometers.

E. Initiate the countdown in preparation for the drop.

F. Start high speed (500 or 1000 frames/second) photography and normal speed photography.

G. When the countdown reaches zero, energize the cask release mechanism. When the cask release mechanism is energized, the assembly restraining the cask allows the cask to initiate its fall unimpeded.

H. Record post-test condition of the model cask body and impact limiters and perform leak test.

I. Continue test sequence as described in this Section.

2.10.6.5.5 Detailed Test Results

Data obtained from the tests consists of both qualitative information with respect to observations about the cask body and the impact limiters, as well as quantitative data obtained by measurements.

For each of the 30-foot drop tests, the data to be presented for each test consists of:

1) Maximum calculated stress for the locations monitored (based on strain measurements), and its location

2) Maximum permanent strain for the locations monitored, and its location (and the strain time-histories for this location)

3) Maximum filtered accelerations (and the acceleration time-histories)

4) Impact limiter deformation and attachment hardware condition (and sketches showing the deformation)

5) Pressure in the cask cavity, measured before and after the test

6) Observations of the impact limiter and cask body behavior

For the pin puncture tests, the data to be presented for each test consists of the pressure measurements and the measurement of the localized deformation due to the pin impact.

Since the model was repaired after the side drop (Test No. 3 of Phase 1), there are four sets of metrology data.

1) Pretest measurements of the cask body and basket.

2) Post-test measurements after the side drop test using the redwood limiter with the aluminum shell (Test No. 3 of Phase 1) and prior to the repair of the cask body.

3) Pretest measurements prior to resuming the tests.

4) Post-test measurements after the completion of the Phase 4 drop tests.

Conclusions about the cask body for the top corner drop, side drop and the oblique drop slapdown tests can only be drawn from metrology data sets (3) and (4).

Metrology data sets (1) and (2) can only be used to evaluate the nature of the damage incurred because of the malfunction of the impact limiters. Conclusions about the top end drop can be drawn by considering the strain data and the observations of the basket obtained in the top end drop.

2.10.6.5.6 Thirty-Foot Top End Drop Using Impact Limiters with Aluminum Shells - Test No. 1 of Phase 1

This was the first drop test to be performed of the four phases of tests using the quarter-scale cask model. The impact limiters used the aluminum shell design, which weighs less than the stainless steel shell design that was used in later tests. The cask model at the time of the top end drop was within 0.5 percent of the design weight of 3906 pounds ($250{,}000/4^3$).

2.10.6.5.6.1 Impact Limiter Deformation and Attachment Data

The impact limiters used in the top end drop had aluminum shells. Essentially all of the crushing occurred within the backed region of the impact limiter. A sketch of the final shape of the impact limiter is shown in Figure 2.10.6-19. Based on viewing the high speed film and the final position of the cask body, the deviation of the cask centerline from the vertical was minimal. The maximum crush for the end drop is summarized in Table 2.10.6-2. The crush deformation was 2.11 inches, corresponding to a crush strain of 23 percent.

2.10.6.5.6.2 Strain Gauge Data

Strain gauge time-histories were obtained for each data channel. The traces shown in Figures 2.10.6-20 and 2.10.6-21 are the axial and hoop direction strains at Location 9. Location 9 corresponds to the instrumented location at which the maximum stress of 8.6 ksi occurs. The hoop strain component was found to be extremely small. All three gauge locations near the top showed similar behavior in the axial and the hoop direction. Some of the strain gauges showed a permanent set of 10 to 15 microstrains, which corresponds to a maximum permanent strain of 0.0015 percent. Since the normal stresses are so low, this offset is not attributed to any yielding of the material. Additionally, only one out of three axial gauges near the top end exhibited this result.

2.10.6.5.6.3 Accelerometer Data

Two accelerometers were mounted 180 degrees apart at the top end of the cask model. The maximum acceleration obtained from a 1000 Hz filtering of the accelerometer trace was 247 g, which corresponds to a full-scale acceleration of 62 g. The accelerometer trace for the top end drop is shown in Figure 2.10.6-22. The cyclic peaks in the accelerometer trace are the first longitudinal vibrational mode of the cask shell.

The filter frequency was computed by considering the first longitudinal vibrational mode, f_1, of the model. This was determined by using the expression from Blevins for a lump mass attached to a cantilevered beam,

$$f_1 = \frac{\lambda}{(2)(n)(L)}\left(\frac{E}{\mu}\right)^{0.5}$$

$$B = \frac{(\mu)(A)(L)}{M}$$

where:

L = Effective length of shell = 161/4 = 40.25 inches
E = Modulus of elasticity = 28.3 x 10^6 psi
μ = Mass density = 0.288/386.4 = .0007453 lb/in^3
M = Total mass = 250,000/[(64)(386.4)] = 1.118 lb/in^3
A = Cross sectional area of shells = 210.5 in^2

Substituting,

B = 5.648

and l must satisfy Bcot(λ) = (λ)

λ = 1.35 satisfies this expression

Substituting for f_1 leads to f_1 = 868 Hz.

Using 1000 Hz for the cut off frequency for the filter is acceptable and is conservative.

2.10.6.5.6.4 Pressure Measurements

The pressure measured after the test showed a slight increase, which would correspond to the small increase in the cask body temperature. Since the temperature data cannot be expanded to determine the temperature of the cavity gas, an accurate calculation of the corresponding increase in the pressure cannot be made. The pressure measurements indicate that there was no loss of pressure.

2.10.6.5.6.5 Test Observations

After the top end drop test, the basket was removed from the cask body to inspect for deformations. In removing the fuel basket, it was observed that the basket was removed without any interference and that no deformation had occurred in the fuel basket or in the dummy fuel assemblies. This indicates the following:

1) Out of plane buckling due to the vertical deceleration loads did not occur.

2) Buckling of the inner shell due to lead slump did not occur.

As evidenced by the nearly uniform crush of the impact limiter and the data from the two axial accelerometers, the load on the lead was essentially uniform around the model circumference. Thus, yielding of the inner shell at one location on the circumference would have precipitated yielding of the larger shell around the entire circumference. There was no evidence of yielding of any model component: lead, basket, lids, or bolts.

2.10.6.5.7 Thirty-Foot Side Drop Using Impact Limiters with Aluminum Shells - Test 3 of Phase 1

The third test in the first phase of testing was the 30-foot side drop test, which used impact limiters with aluminum shells. In this test, it was demonstrated that aluminum welds are inadequate to maintain the integrity of the impact limiter. The impact limiter shells split open and did not constrain the redwood. Thus, neither the model's deceleration, nor the impact limiter's crush stroke, remained within acceptable limits. Consequently, the model cask body struck the impact surface, producing a large impact force.

The most significant benefit from this test was the clear demonstration of the strength of the fuel basket design.

2.10.6.5.7.1 Impact Limiter Deformation and Attachment Data

The high speed film showed that the welds along the edges of the limiters failed immediately upon impact, which allowed the four steel blocks (180 degree location in Figure 2.10.6-17) at the lower edge of the cask to strike the impact surface. The force to decelerate the cask model was concentrated at the four steel blocks. The energy was absorbed by the local deformation of the model cask body shells and the model fuel basket. Based on the high-speed film, the rebound of the cask body was small, indicating that essentially all of the energy was absorbed in the

initial impact. As a result of the localized loading on the cask body shells, the top forging, which serves as the seat for the lids, was deformed and the internal cavity pressure was not maintained. However, the lids remained firmly attached to the cask body during and after the impact. This test served to describe the behavior of the cask body in a guillotine-type impact without a neutron shield.

2.10.6.5.7.2 Strain Gauge Data

Strain gauge data was recorded at nine locations. The permanent strains are listed in Table 2.10.6-3. Since both the hoop and axial directions indicate a permanent strain, an equivalent plastic strain (e_{eq}) is computed for the directions recorded. The e_{eq} is based on the Von Mises and Prandtl-Ruess Flow Rule material representation for material yielding. The e_{eq} is used to assess the amount of work-hardening to which the material was subjected. The maximum value found was 1811 microstrains, or 0.18 percent, at the midpoint of the cask at the point nearest the impact plane. The strain gauges at locations 3 and 9 were approximately 0.25 inches from the edge of the blocks which were displaced into the outer shell. This implies that the strain gauges were able to reflect the maximum strains generated by the impact.

2.10.6.5.7.3 Accelerometer Data

The maximum accelerations recorded were 996 g and 1190 g for accelerometers Nos. 1 and 2, respectively. The trace corresponding to the top end location is shown in Figure 2.10.6-23. The first six or seven milliseconds correspond to the crushing of the redwood, after which the large increase in the deceleration is due to the steel blocks striking the impact surface.

2.10.6.5.7.4 Metrology Data

After this side drop test, the cask was inspected by the metrology laboratory to obtain measurements for the locations shown in Figure 2.10.6-15. The pretest data (prior to Test 1 of Phase 1) and the post test data (after Test 3 of Phase 1) are shown for selected diametral dimensions in Table 2.10.6-4 for the cask body. The

radial deflection was greatest at the lid end of the cask. The inner radius was decreased by 0.126 inches at the 0-180 diameter, which corresponds to the point of impact.

The impact also caused out-of-round deformation of the cask at the other measured locations by approximately 0.06 inch to 0.09 inch on a radius.

The inner and outer lids were inspected for out-of-plane deformation, and the measurement of the out-of-plane dimensions showed that no deformation had occurred during the Phase 1 tests.

The deformation of the model cask body required that the fuel basket be partially disassembled in the cask cavity in order to remove the basket after the side drop test. Support disks Nos. 6 and 12 were submitted to the metrology laboratory for measurements. Support disk No. 6 was the disk loaded by the steel blocks, and support disk No. 12 was the disk at the axial center of the basket. For support disk No. 12, the out-of-plane measurement was 0.001 inch, which is the sensitivity limit of the equipment. For support disk No. 6, a pretest metrology inspection had not been performed. However, the maximum variation in the Z direction (i.e., in the direction perpendicular to the plane of the disk) was 0.004 inch. Figure 2.10.6-8 shows the final shape of support disk No. 6. The impact of the steel blocks into the cask body and basket resulted in the lateral movement of the lower four fuel assembly positions by 0.19 inch. The impact also caused the bottom of support disk No. 6 to be deformed as seen in Figure 2.10.6-24. The pretest metrology data for support disk No. 12 and the post-test metrology data for support disk Nos 6 and 12 are presented in Tables 2.10.6-5 through 2.10.6-7.

The greatest significance of the metrology data is that the center support disk did not experience plastic deformation and that none of the support disks exhibited any out-of-plane buckling. The deformation of the fuel basket near the steel block is not classified as buckling deformation, but rather deformation imposed by the impact of the steel blocks.

2.10.6.5.7.5 Cask Body Repairs

Before proceeding with further testing, the following repairs were performed:

1) The inner radius of the cask inner shell was returned to drawing specification by using a hydraulic jack with a cylindrical seating surface to push the inner shell radially outward (see Figure 2.10.6-6).

2) The damaged basket was replaced with a new basket.

3) The seating surfaces for the lids were machined to return them to drawing specifications.

Since the inner shell was subjected to some small degree of work-hardening, the yield strength was changed slightly. The change in the yield strength is estimated by the product of the tangent modulus (E_t) and the ε_{eq} strain. From NUREG/CR-0481, for Type 304 stainless steel, E_t is 370,000 psi. Using 0.18 percent from Section 2.10.6.5.7.2, the yield strength is increased by 700 psi. The 700 psi change corresponds to a change of about 2 percent for Type 304 stainless steel at 70°F. This change is considered to be insignificant.

2.10.6.5.8 Thirty-Foot Top Corner Drop Using Impact Limiter with Stainless Steel Shells - Test 3 of Phase 3

As a result of the first phase of testing, it was determined that obtaining the designed impact limiter performance required the use of a stainless steel impact limiter shell to enclose the redwood. A top corner drop (Test No. 2 of Phase 1) was initially performed with an aluminum impact limiter shell. The test was reperformed with impact limiters with stainless steel shells. Note, the impact limiters used for this top corner drop had been previously used in a side drop test (Test No. 1 of Phase 2), so they were oriented on the model such that the impact energy was absorbed by the undamaged portion of the model impact limiters. This impact limiter did include the later modification to constrain the redwood. Since the redwood in the overlap region did not get crushed in the corner drop, design

modifications located in that region would not have had any significant effect on the performance of the impact limiter in the corner drop. The top corner drop test was satisfactory.

For the top corner drop test, the cask axial centerline was oriented 24 degrees from the vertical. This corresponded to the center of gravity of the cask being over the edge of the impact limiter.

2.10.6.5.8.1 Impact Limiter Deformation and Attachment Data

The high speed film and the shape of the crushed impact limiter indicated that a small amount of impact limiter rotation occurred during the top corner drop. As the crushing was initiated, a force couple was applied to the impact limiter by the crushing force at the edge of the impact limiter and by a force due to the edge of the cask bottom moving into the impact limiter. This force couple resulted in rotation of the impact limiter away from the cask bottom, which produced the appearance of two crush faces on the bottom of the impact limiter. Initially, the crushed surface of the bottom of the impact limiter was at a 24 degree angle with respect to the uncrushed portion of the limiter (corresponding to the corner drop angle). During the impact, the impact limiter shifted slightly and the angle became smaller.

The maximum permissible deformation was assumed to be the distance from the edge of the redwood at the corner of the limiter to the edge of the limiter nearest the edge of the cask bottom. This was to ensure that the cask corner did not impact the unyielding surface.

The crush stroke for the corner drop was significantly larger than that for the end drop, since the crush area for the corner drop initially started out as a point and increased to the maximum area of 350 square inches (see Figure 2.10.6-25). For the end drop, the crush area remained a constant value of 477 square inches. The decreased crush area and crush force in the corner drop resulted in a much larger crush stroke.

2.10.6.5.8.2 Strain Gauge Data

Strain data was recorded for all locations, but during the post processing, the data for location Nos. 5 thru 9 was inadvertently destroyed. Listed below are the maximum axial strains for location Nos. 1 thru 4 for the top end drop and the top corner drop.

Strain Gauge	Maximum Axial Strain Magnitude (microstrains)	
Location	Top End Drop	Top Corner Drop
1	85	56
2	53	63
3	61	57
4	90	50

The data confirms that the top end drop axial load envelopes that of the top corner drop, except for a spurious reading at location No. 2, which is near the bottom of the model cask and away from the point of impact. The maximum stress computed for the data obtained in the top end drop, 8.6 ksi, thus, envelopes the maximum stress which occurs in the top corner drop.

2.10.6.5.8.3 Accelerometer Data

The accelerometer trace for the vertical acceleration of the top corner drop is shown in Figure 2.10.6-26. The maximum acceleration is listed in Table 2.10.6-8 as 127 g. The trace reflects the gradual increase of the impact limiter crushing area. As the impact limiter crush area increases, the deceleration force also increases. Since the dynamic modes of deformation are similar to those for the end drop, the cut off frequency used for the top end drop is applicable for the top corner drop.

For information purposes, the data for this test was also filtered at 4000 Hz to demonstrate the effects of using higher filter frequencies. The result is that spurious peaks are introduced into the signal.

In comparing the top corner drop to the top end drop, the top corner drop produces significantly lower accelerations. There are two reasons for this. The total crush area for the top end drop was 477 square inches, while the top corner drop utilized 27 percent less area (350 square inches). Additionally, the top corner drop does not subject the redwood to a uniform strain, but rather the crush strain varies from a maximum value to zero.

The top end drop impact force clearly envelopes that of the top corner drop.

2.10.6.5.8.4 Pressure Measurements

The cavity pressure measured after the top corner drop test showed a decrease of 0.2 percent, which results from the 1.5°F decrease measured for the cask body temperature. The pressure measurements indicate that the cavity pressure was maintained during the test.

2.10.6.5.8.5 Test Observations

The lids, lid bolts, basket and fuel assemblies were removed and no damage to any component was observed.

2.10.6.5.9 One-Meter Pin Puncture Drops - Tests 5 and 6 of Phase 3

The purpose of the pin puncture drops is to confirm the ability of the cask design to withstand a pin puncture load in the potentially most damaging orientation. The fuel basket was removed to ensure that the cask shells would not receive any support from the fuel basket during the pin puncture tests. Bags of lead weights were placed in the model cask cavity to replace the weight of the components that were removed.

Two pin puncture tests are performed:

1) Pin puncture at the axial midpoint of the cask

2) Pin puncture at the center of the outer lid

The data of interest to confirm the design are the pressure measurements and any changes in the dimensions of the containment boundary components.

2.10.6.5.8.4 Pressure Measurements

The pressure measurements are summarized in Table 2.10.6-9 for each of the pin puncture drops. The pressure drop observed for the cask mid-point pin puncture event corresponds to the observed temperature drop. In the cask outer lid pin puncture event, the cavity pressure valve cracked, which allowed the cavity pressure to decrease. The cask was refitted with another valve and the cask was repressurized to 3.1997 bar.

At the end of 10 minutes the pressure was still at 3.1995 bar, indicating that the closure lid system had performed satisfactorily. The cavity pressure valve in the model is not a part of the full-scale NAC-STC design, and serves only as a convenient fixture to pressurize the model cavity.

2.10.6.5.9.2 Metrology Data

After the two pin puncture tests, the cask body was submitted to metrology for inspection. The results are summarized in Table 2.10.6-9. The cask mid-point pin puncture resulted in an indentation of 0.33 inch in the outer shell. This did not result in penetration of the outer shell (see Figure 2.10.6-10). The test, however, did result in deformation of the pin itself, but the effect of the deformation of the 8-inch long pin is considered to be negligible.

For the outer lid pin puncture test, the pin was found to have impacted at a location 2.53 inches away from the true center. This corresponds to approximately 10 percent of the diameter, and would produce essentially the same result as if it were at the exact center. The metrology data indicates no permanent deformation of the outer lid for the pin puncture condition at the off-center location. A pin puncture at the center would not be expected to result in permanent deformation of the closure lids, either. Some minor scraping of the outer surface of the outer lid was noted.

2.10.6.5.10 Thirty-Foot Bottom Oblique Drop (Top End Slapdown) using Modified Impact Limiters with Stainless Steel Shells - Test No. 1 of Phase 4

As a result of the side and oblique drop tests performed in Phase 3, it was determined that the redwood in the overlap region of the impact limiter was not maintaining its original position and orientation. A design modification was added to the overlap region of the impact limiter to prevent the redwood in that region from changing its orientation during the side impact. The first test to be conducted in Phase 4 was the bottom oblique drop, since it was observed that the slapdown effect on the upper impact limiter would produce the most critical crush stroke. In this test, the bottom of the cask impacts first causing the top end of the cask to rotate (and slapdown). For a shallow angle oblique impact (near side impact), the slapdown impact usually will result in a higher acceleration than for a side drop due to the angular momentum of the rotating cask.

2.10.6.5.10.1 Impact Limiter Deformation Data

The impact limiter shells were Type 304 stainless steel. The high speed film verified that the model orientation angle was 75 degrees from the vertical. The maximum crush occurred in the top limiter, which was subjected to the slapdown effect. It is required that the maximum crush stroke be limited so as to prevent the neutron shield from coming into contact with the impact surface. For the quarter-scale model this maximum crush stroke distance is 3.22 inches. In the top end slapdown, the maximum crush stroke was 2.41 inches (see Table 2.10.6-10). The deformed upper impact limiter is shown in Figure 2.10.6-27 and the measured impact limiter deformations are shown in Figure 2.10.6-28. The impact limiters remained attached to the cask body (see Figure 2.10.6-29).

2.10.6.5.10.2 Strain Gauge Data

The maximum stress occurred at the top end at the 180 degree location which is location No. 9. The strain gauge time histories are shown in Figure 2.10.6.30 and Figure 2.10.6-31 for the axial and hoop strains at location No. 9. While some permanent strain was recorded, the level was significantly less than 0.2 percent.

2.10.6.5.10.3 Accelerometer Data

The maximum acceleration occurred at the top end of the cask (approximately a 10 percent increase over that at the lower end). The peak acceleration value was 225 g, using a filter frequency of 750 Hz. The acceleration time histories are shown in Figures 2.10.6-32 and 2.10.6-33. The top end accelerometer trace shows a delay of the impact, since the cask was rotating after the impact of the lower limiter. The filter frequency was computed by treating the cask body as a beam, but including a factor to reflect the presence of shear in the beam. The filter frequency was used to reduce the effect of higher frequency signals, which inflate the acceleration levels recorded by instrumentation. Using Blevins, Table 8-15, case # 1, the frequency is given by:

Bending Mode/Shear Beam

$$f_s = \frac{\lambda_1}{2\pi\ell}\left(\frac{kG}{\mu}\right)^{0.5} \text{ (Blevins, Table 8-15, Case \#1)}$$

$$\lambda_1 = \pi$$

$$k = \frac{6\,(1+\nu)\left[1+\left(\frac{20.35}{21.68}\right)^2\right]^2}{(7+6\nu)\left[1+\left(\frac{20.35}{21.68}\right)^2\right]^2 + (20+12\nu)\left(\frac{20.35}{21.68}\right)^2} = 0.5293$$

$$\ell = 48.24 \text{ in}$$

$$\mu = \frac{0.288}{386.4} = 0.000745$$

$$G = 11.1 \times 10^6 \text{ psi}$$

$$f_s = 920 \text{ Hz}$$

Bending Mode/Beam Curvature

$$f_b = \frac{\lambda_1^2}{2\pi\ell^2}\left(\frac{EI}{m}\right)^{0.5} \text{ (Blevins, Table 8-1, Case \#1)}$$

λ_1 = 4.73
ℓ = = 48.24 in
m = 0.21
E = 28.3 x 10^6 psi
I = 38,817 in^4

f_b = 3500 Hz

Combined Mode Frequency

$$\frac{1}{f_c} = \frac{1}{f_s} + \frac{1}{f_b} = \frac{1}{920} + \frac{1}{3500} \text{ (Blevins, page 175)}$$

f_c = 729 Hz

2.10.6.5.10.4 Pressure Measurements

The pressure measured before and after the test remained constant to within the accuracy of the instrumentation. The pressure measurements indicated that no loss of pressure occurred during the test.

2.10.6.5.10.5 Test Observations

The metrology data summarized in Table 2.10.6-11 indicates that for a measurement tolerance of 0.01 inch, none of the diametral dimensions changed. In the process of removing the basket it was observed that the basket was removed without resistance.

2.10.6.5.11 Thirty-Foot Side Drop - Test No. 2 of Phase 4

Upon completing the oblique drop, the side drop was performed for Phase 4. It should be noted that the limiter from the oblique drop test was reused by rotating the limiter 180 degrees. In the slapdown test, the loading was not uniform, as it was in the case of the side drop. In the oblique drop, the loading tends to be concentrated towards the slapdown end. In the side drop the loading tended to be uniformly distributed over the length of the cask and, thus, equally to each impact limiter.

2.10.6.5.11.1 Impact Limiter Deformation Data

The high speed film verified that the cask was horizontal as it approached the impact surface. The maximum crush is summarized in Table 2.10.6-12. The condition of the cask model and limiters following the side drop is shown in Figures 2.10.6-34 and 2.10.6-35. The measured impact limiter deformations are shown in Figure 2.10.6-36. In this test, the amount of stroke was nearly the same for both the top and bottom impact limiters. The criteria for the impact limiter performance during the side drop is the same as that for the oblique drop: a clearance must remain between the neutron shield and the impact surface. The crush data does reflect that a clearance will exist between the neutron shield and the impact plane after the side drop condition.

2.10.6.5.11.2 Strain Gauge Data

The maximum strains and stresses occurred at the 180 degree location of the cask midpoint for the side drop. In fact, the stresses were larger for the side drop than those for the oblique drop, even though the oblique drop deceleration was 10 percent larger. The strain gauge time-histories are shown in Figures 2.10.6-37 and 2.10.6-38.

2.10.6.5.11.3 Accelerometer Data

The accelerometers indicated that the magnitude of the measured accelerations on each end of the cask were nearly the same. This concurs with the crush stroke data. The accelerometer traces are shown in Figures 2.10.6-39 and 2.10.6-40.

2.10.6.5.11.4 Pressure Measurements

The pressure, as measured before and after the test, remained constant to within the accuracy of the instrumentation. The pressure measurements indicated that no loss of pressure occurred during the test.

2.10.6.5.11.5 Test Observations

The metrology data, summarized in Table 2.10.6-11, indicates that for a measurement tolerance of 0.01 inch, none of the diametral dimensions changed. In the process of removing the basket, it was observed that the basket was removed without resistance and no deformations had occurred.

2.10.6.6 NAC-STC Quarter-Scale Model Drawings

423-019, Sheets 1 thru 4	Cask Body-Scale Model, NAC-STC Cask, SAR
423-020	Inner Lid-Scale Model, NAC-STC Cask, SAR
423-023	Model Fuel Assembly, NAC-STC Cask, SAR
423-025	Basket Spacer-Scale Model, NAC-STC Cask, SAR
423-026	Outer Lid-Scale Model, NAC-STC Cask, SAR
423-027	Port Cover-Scale Model, NAC-STC Cask, SAR

423-028	Cask Body Assembly-Scale Model, NAC-STC Cask, SAR
423-029	Instrument Fixture-Scale Model, NAC-STC Cask, SAR
423-248	Upper Limiter-Scale Model, NAC-STC Cask, SAR
423-249	Lower Limiter-Scale Model, NAC-STC Cask, SAR
423-050	26 Element Basket-Scale Model, NAC-STC Cask, SAR
423-098	Model Assembly-Scale Model, NAC-STC Cask, SAR

2.10.6.7 NAC-STC Eighth-Scale Model Drawings

423-236	Impact Limiter, Assy-1/8 Scale Model, Lower, NAC-STC Cask

FIGURE WITHHELD UNDER 10 CFR 2.390

FIGURE WITHHELD UNDER 10 CFR 2.390

FIGURE WITHHELD UNDER 10 CFR 2.390

FIGURE WITHHELD UNDER 10 CFR 2.390

FIGURE WITHHELD UNDER 10 CFR 2.390

FIGURE WITHHELD UNDER 10 CFR 2.390

FIGURE WITHHELD UNDER 10 CFR 2.390

FIGURE WITHHELD UNDER 10 CFR 2.390

FIGURE WITHHELD UNDER 10 CFR 2.390

FIGURE WITHHELD UNDER 10 CFR 2.390

FIGURE WITHHELD UNDER 10 CFR 2.390

FIGURE WITHHELD UNDER 10 CFR 2.390

FIGURE WITHHELD UNDER 10 CFR 2.390

FIGURE WITHHELD UNDER 10 CFR 2.390

FIGURE WITHHELD UNDER 10 CFR 2.390

FIGURE WITHHELD UNDER 10 CFR 2.390

Figure 2.10.6-1 Quarter-Scale Model Package Assembly - Ready for Cavity Pressure Test

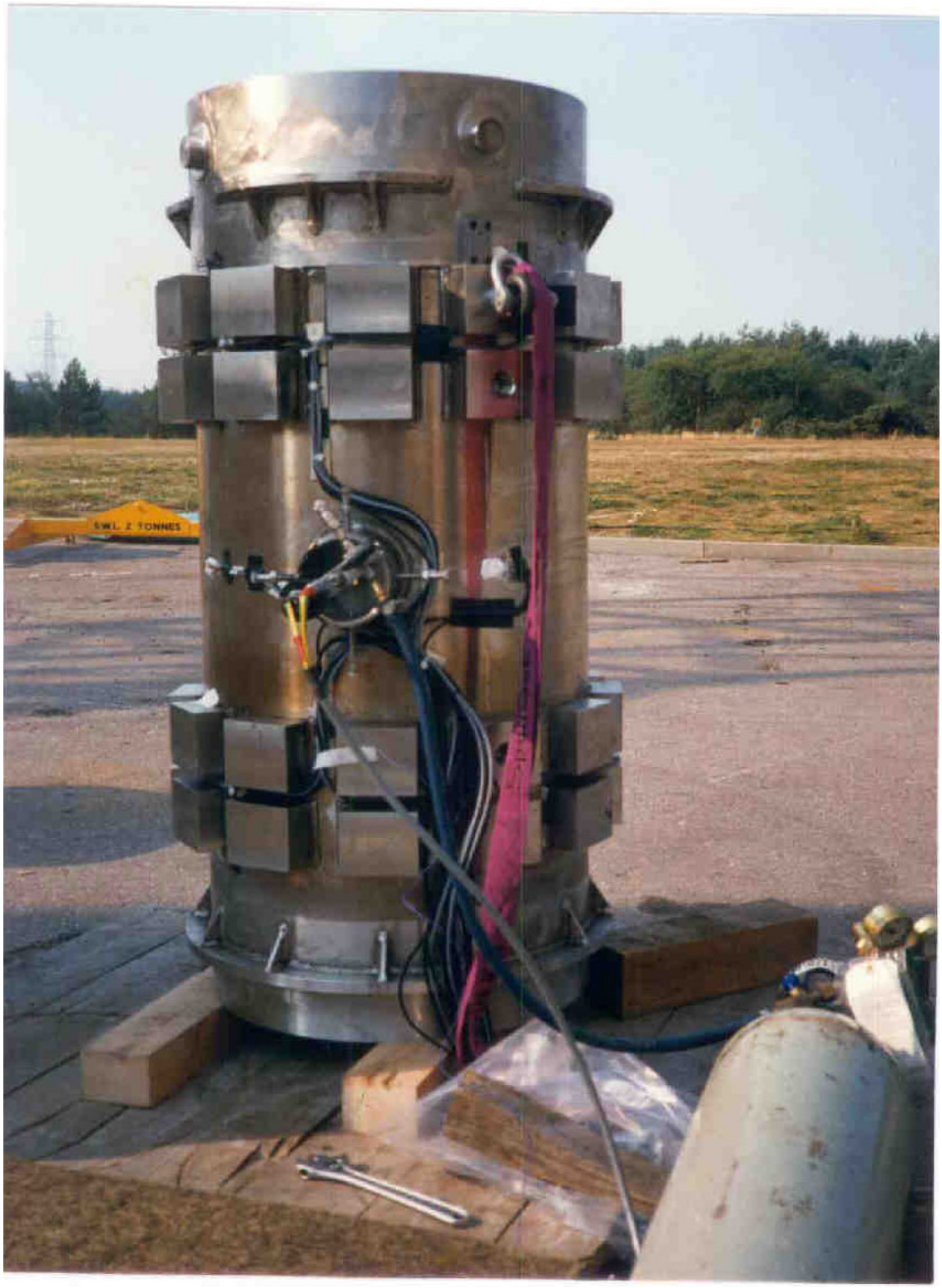

Figure 2.10.6-2 Assembly of Cask - Inner Lid Fitted

Figure 2.10.6-3 Assembly of Cask - Fuel Pin Assemblies Located in Basket

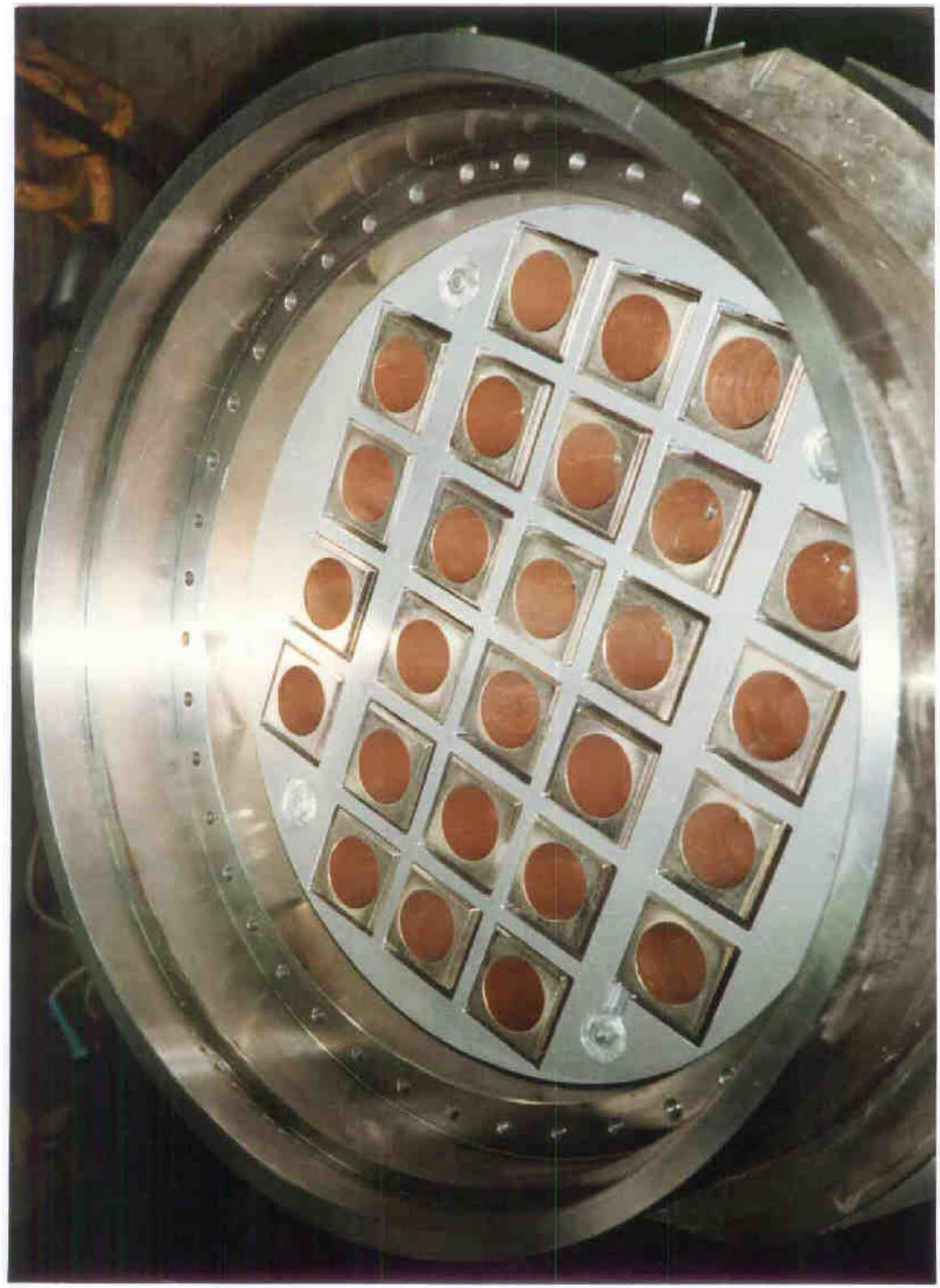

Figure 2.10.6-4 Top End Drop - Cask Penetration into Impact Limiter

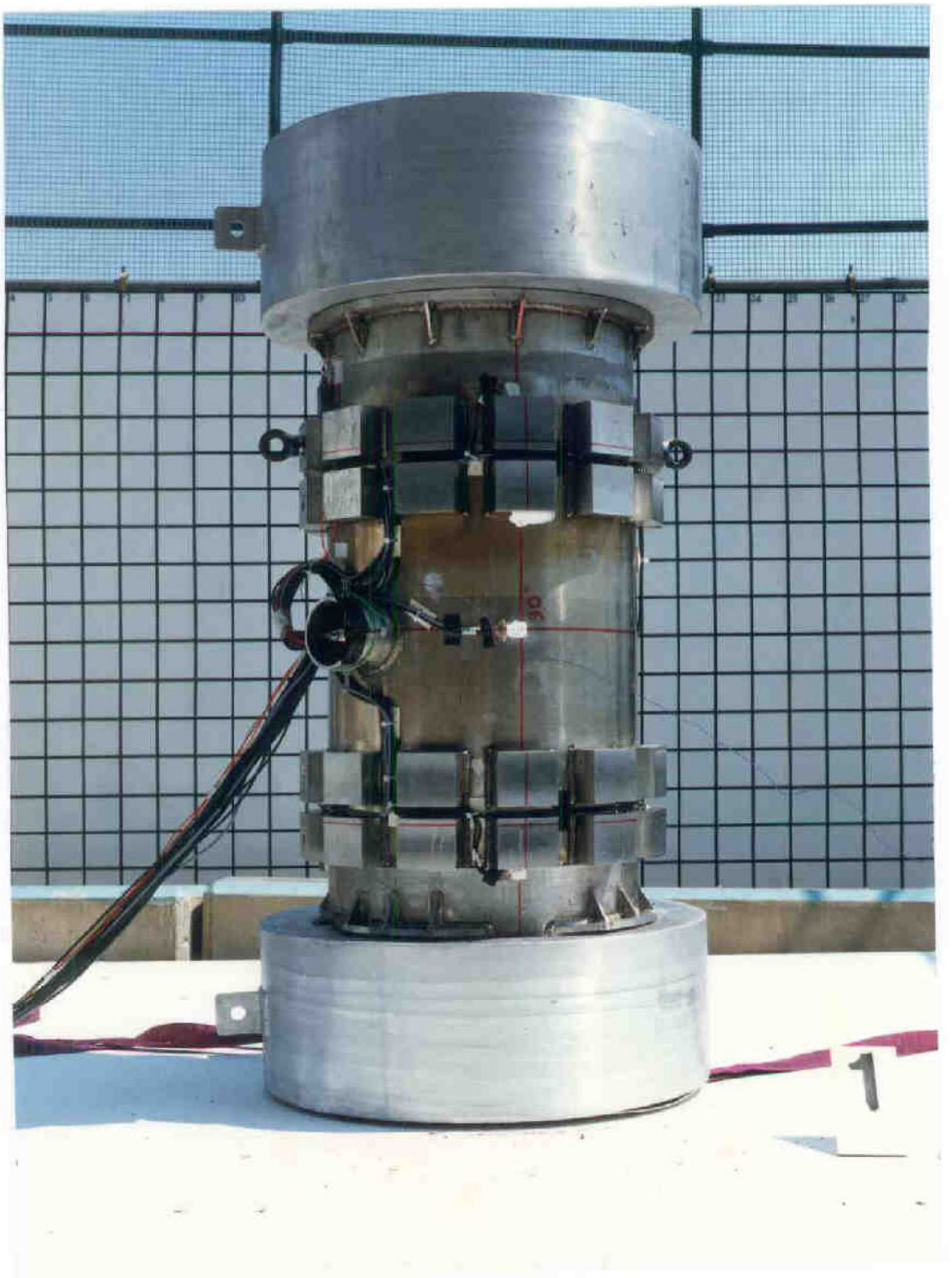

Figure 2.10.6-5 Side Drop - Detail of Shield Block Impact Near Bottom End

Figure 2.10.6-6 Repairs to Cask - 50 Metric Ton Hydraulic Press

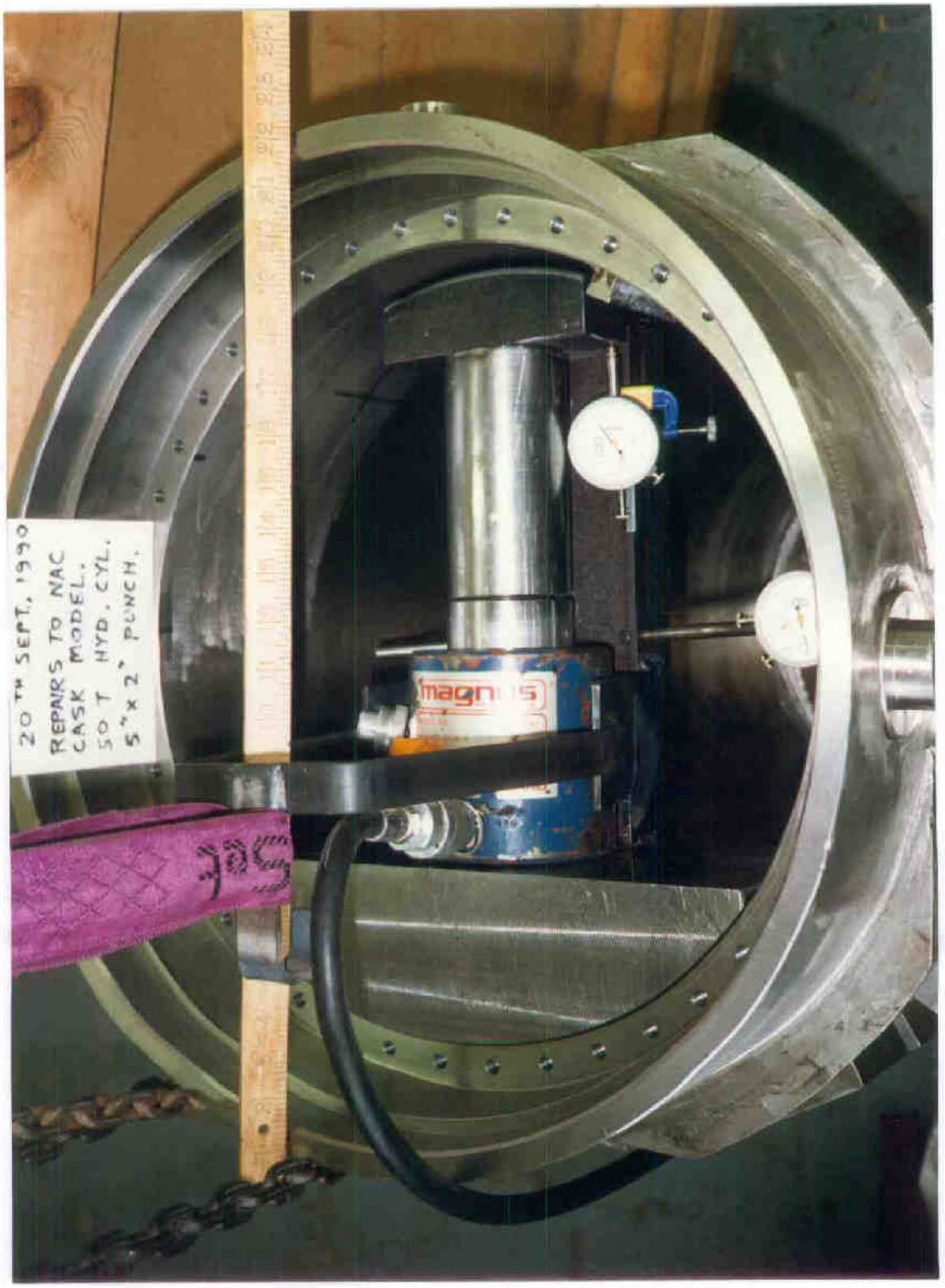

Figure 2.10.6-7 Repairs to Cask - Local Over Pressing

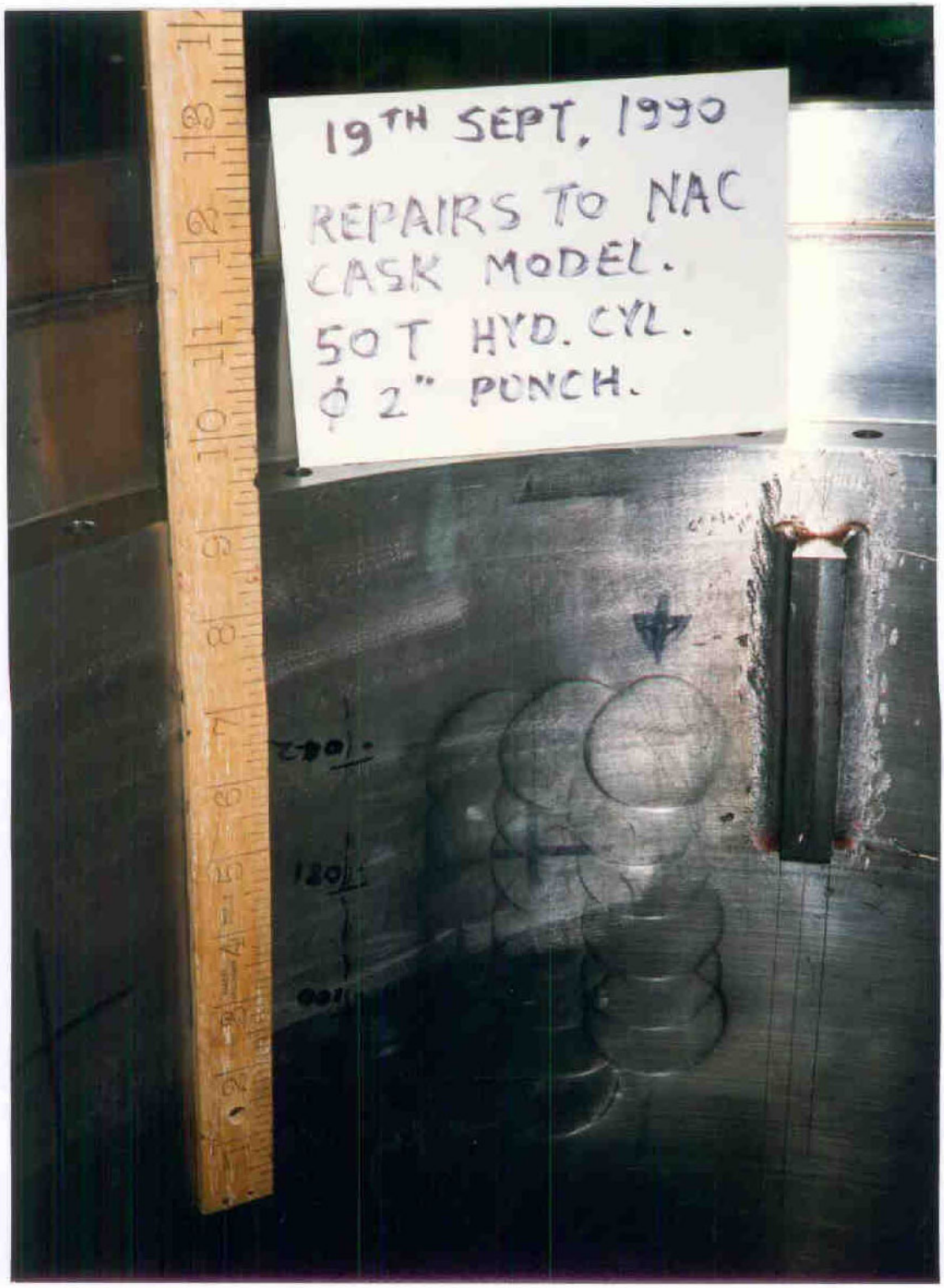

Figure 2.10.6-8 Detail of Distortion to Basket Disk No. 6 - Side Drop

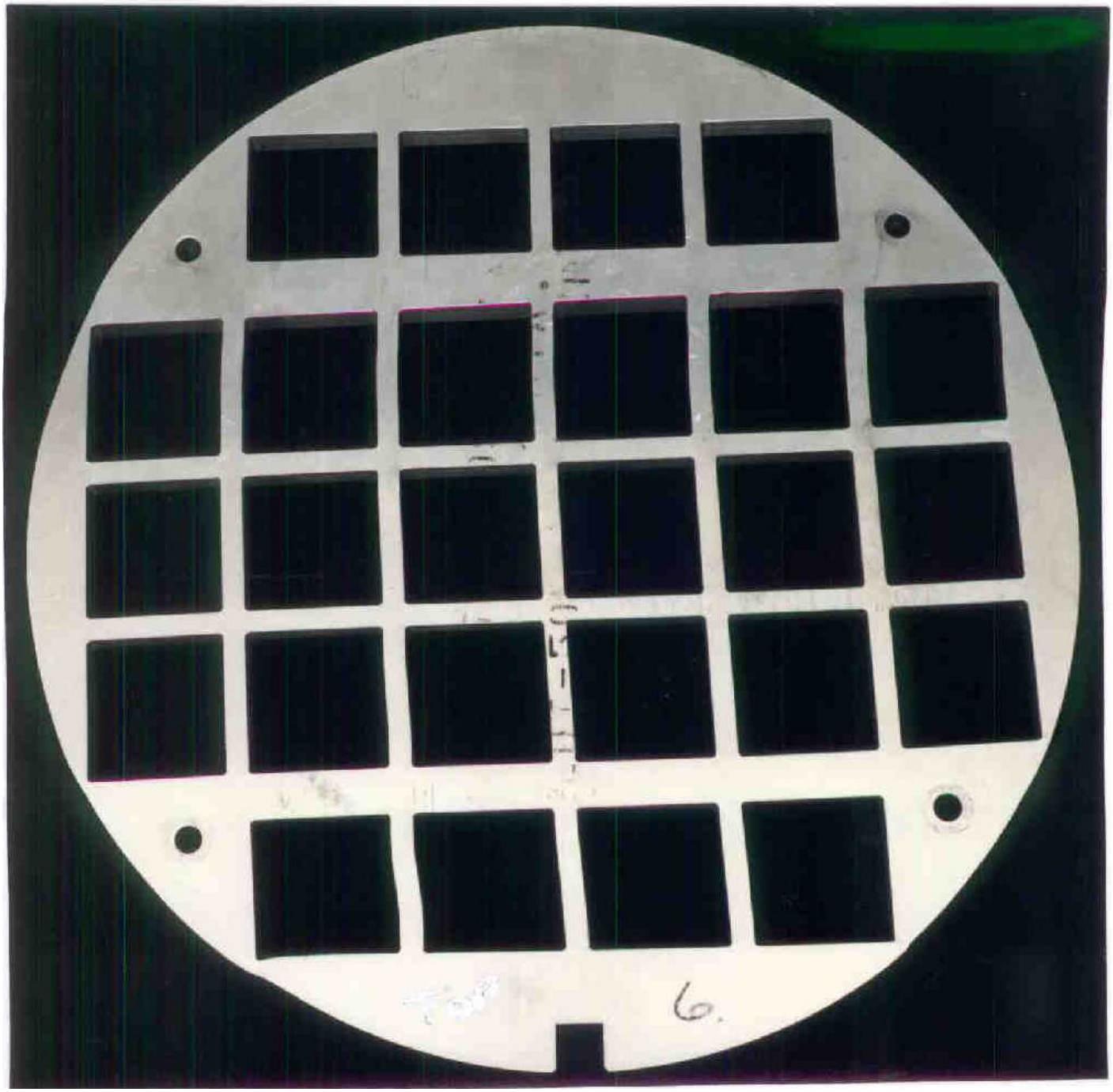

Figure 2.10.6-9 Deformation of Upper Impact Limiter - Top Corner Drop

Figure 2.10.6-10 Cask Midpoint Pin Puncture - Outer Shell Deformation

Figure 2.10.6-11 Center of Outer Lid Pin Puncture - Distortion of Punch

Figure 2.10.6-12 Quasi-Static Force-Deflection Curve, Eighth-Scale Model Impact Limiter - End (0-Degree) Impact

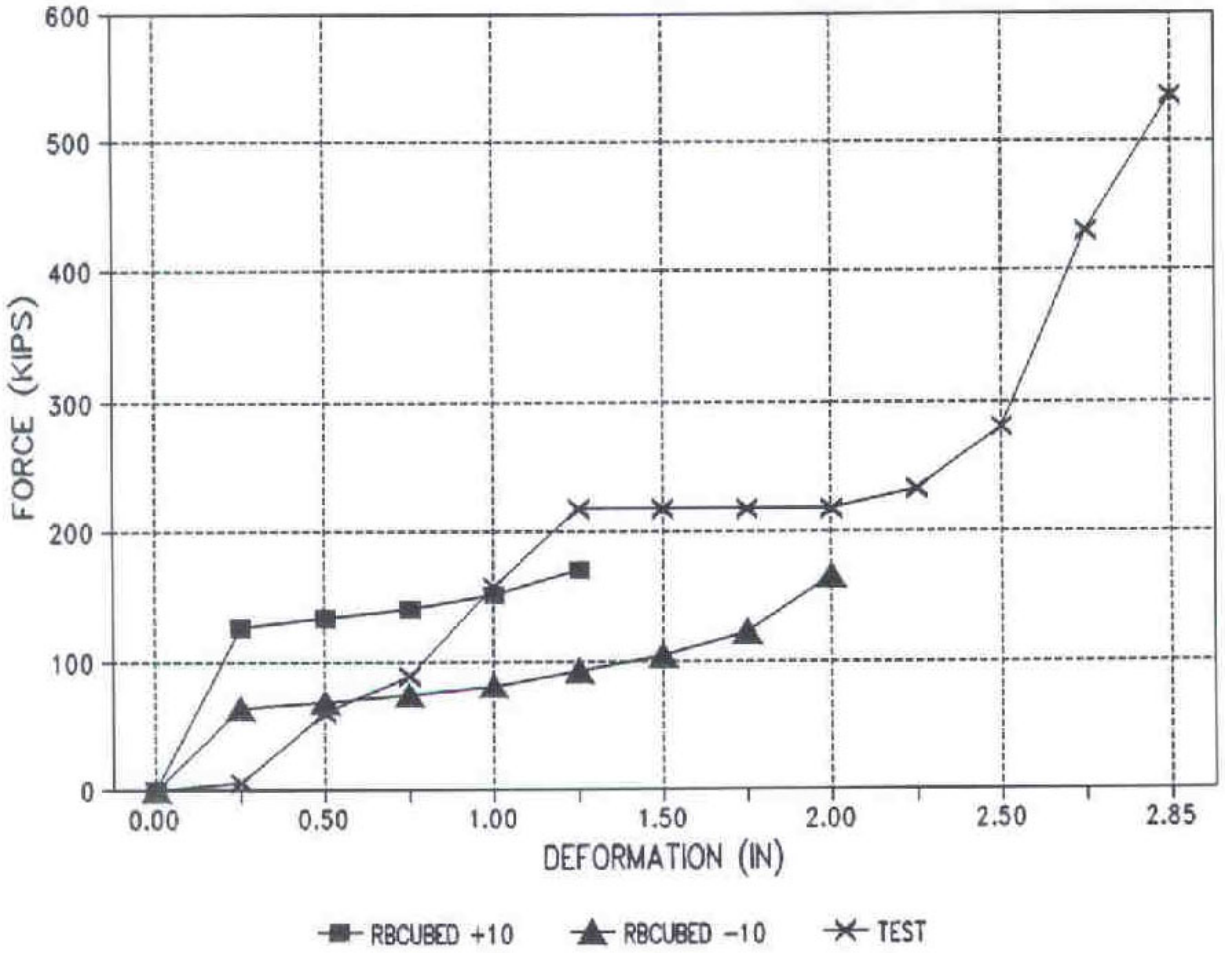

Figure 2.10.6-13 Quasi-Static Force-Deflection Curve, Eighth-Scale Model Impact Limiter - Corner (24-Degree) Impact

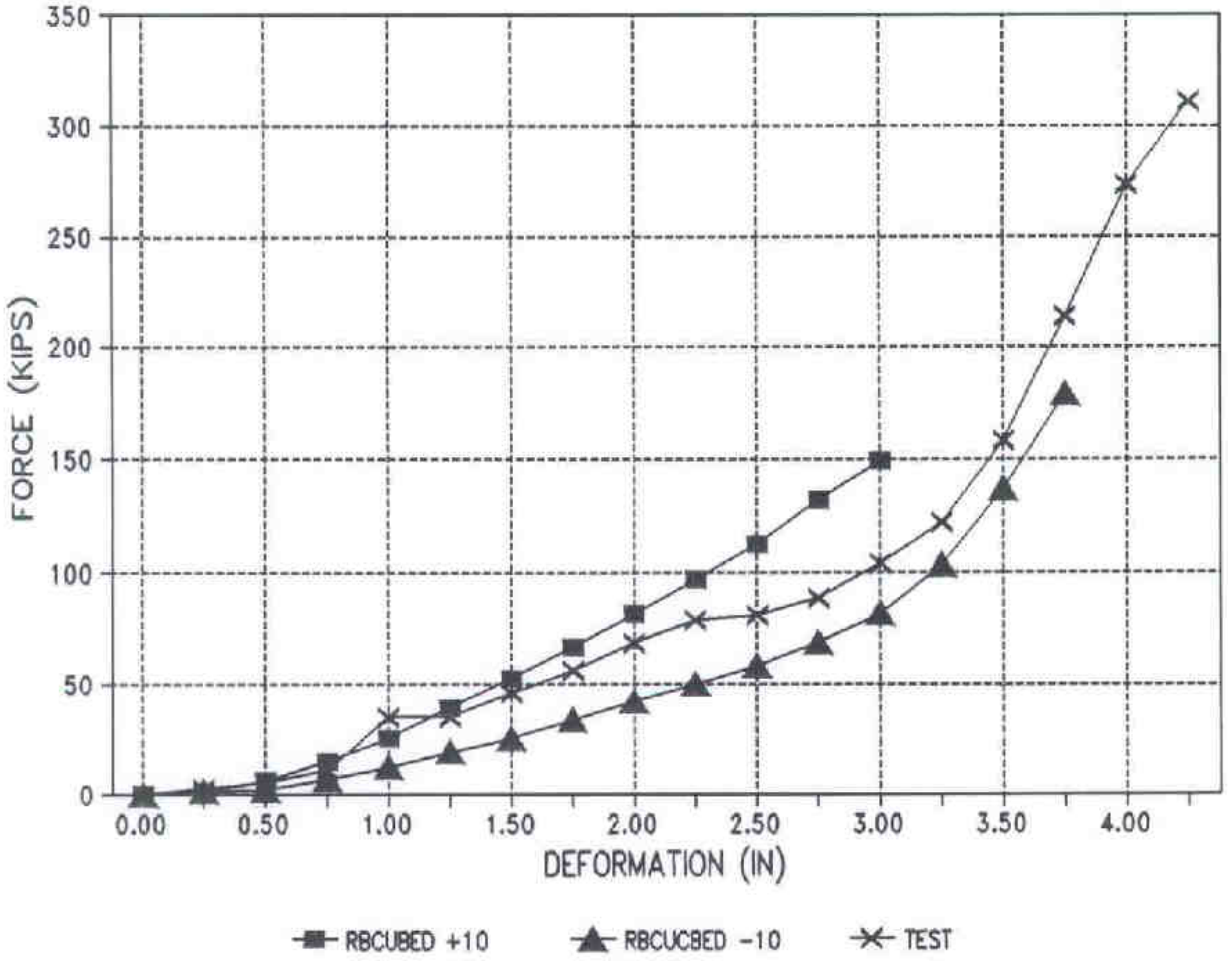

Figure 2.10.6-14 Force-Deformation Curve, Eighth-Scale Model Impact Limiter - Side (90-Degree) Impact

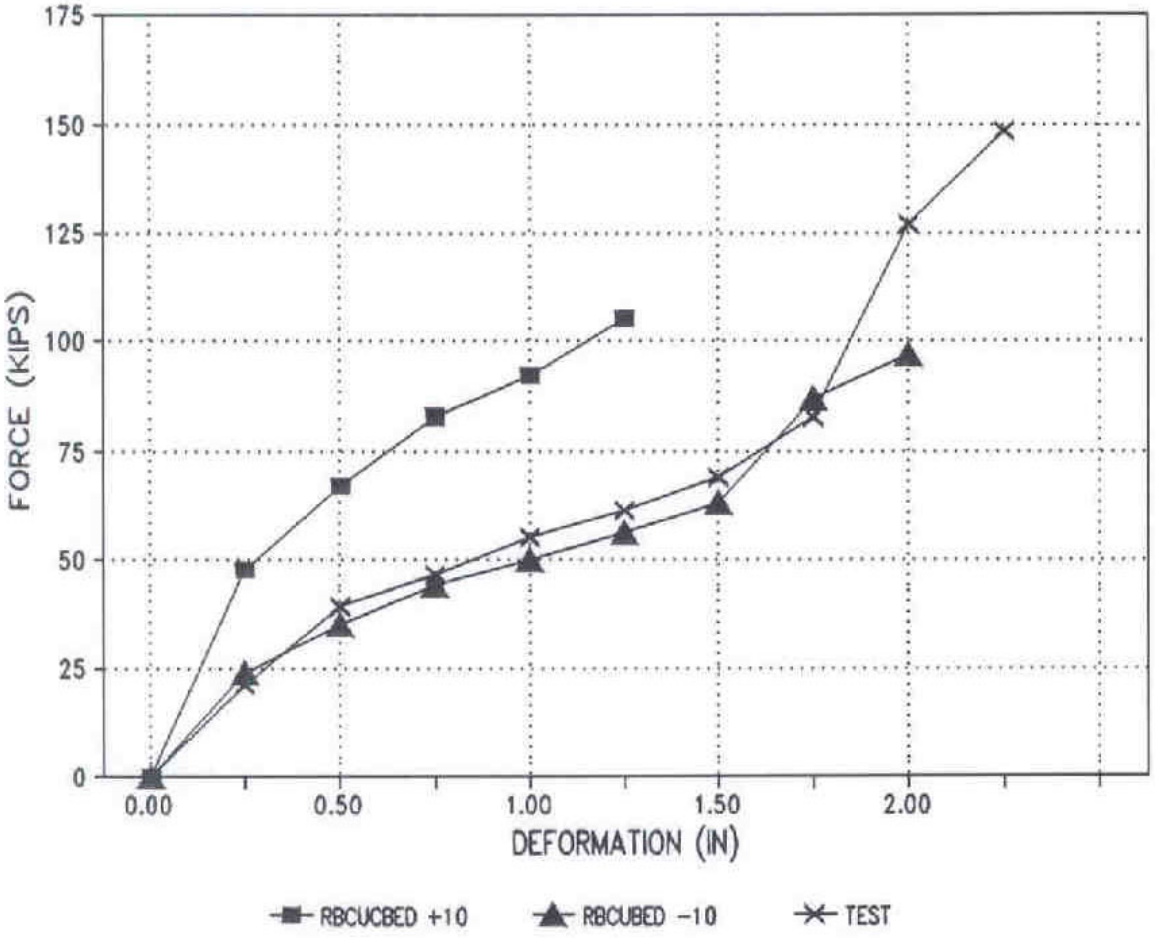

Figure 2.10.6-15 Location of Cask Body Metrology Measurements - Quarter-Scale Model

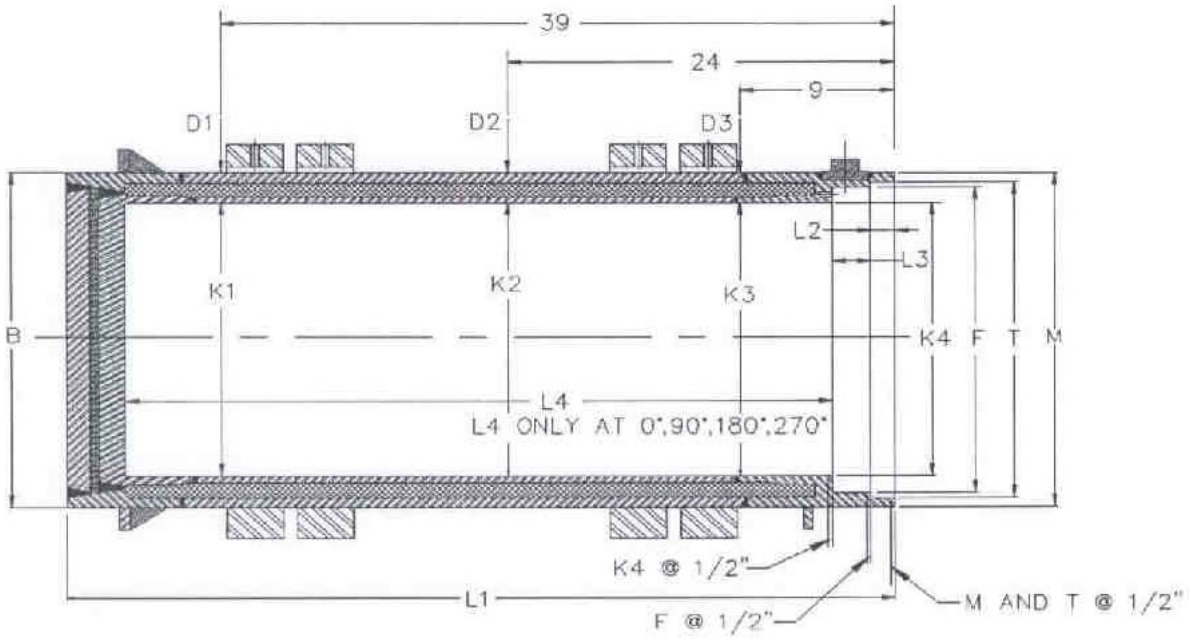

Figure 2.10.6-16 Location of Basket Support Disk Metrology Measurements - Quarter-Scale Model

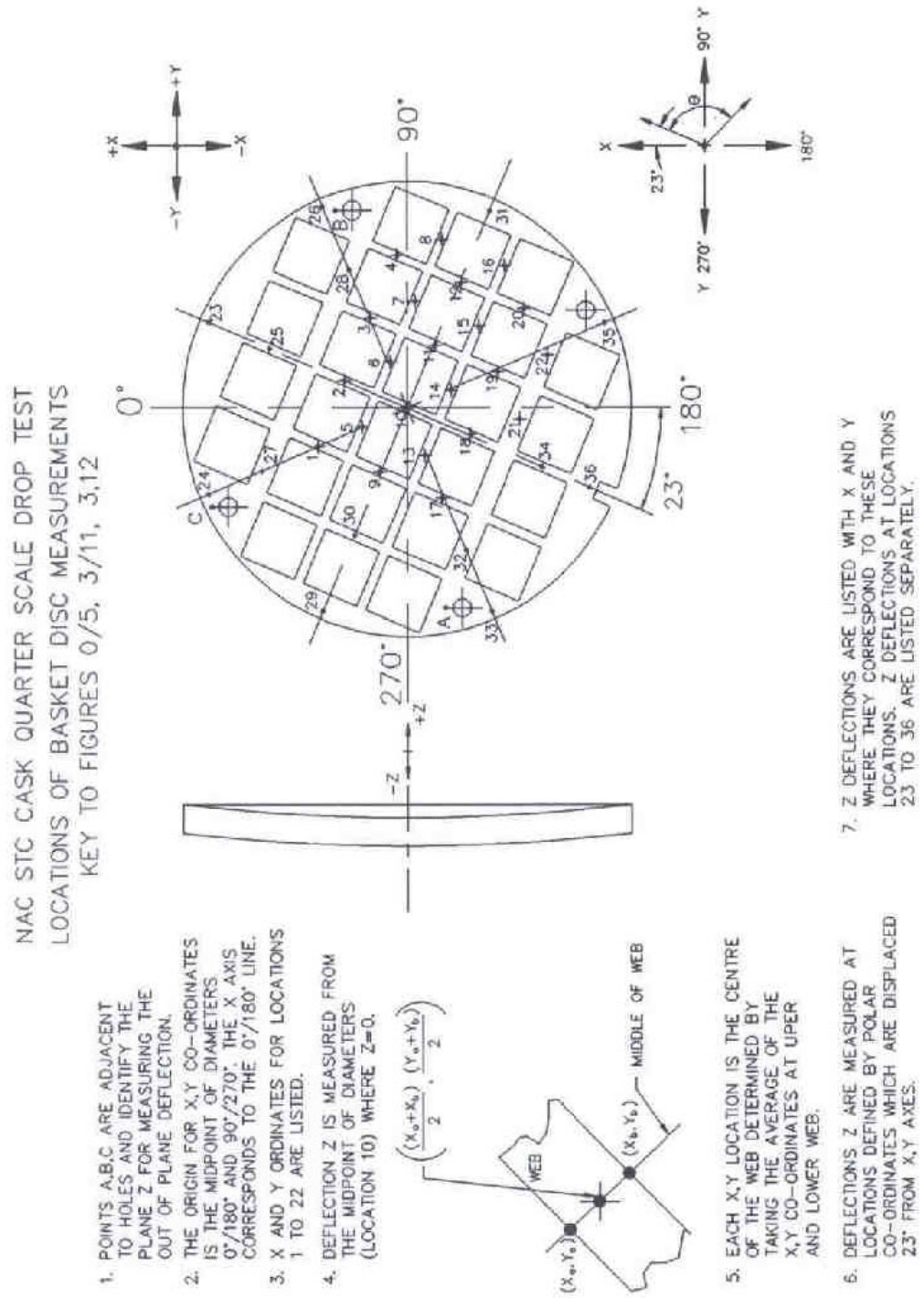

Figure2.10.6-17 Strain Gauge Locations - Quarter-Scale Model

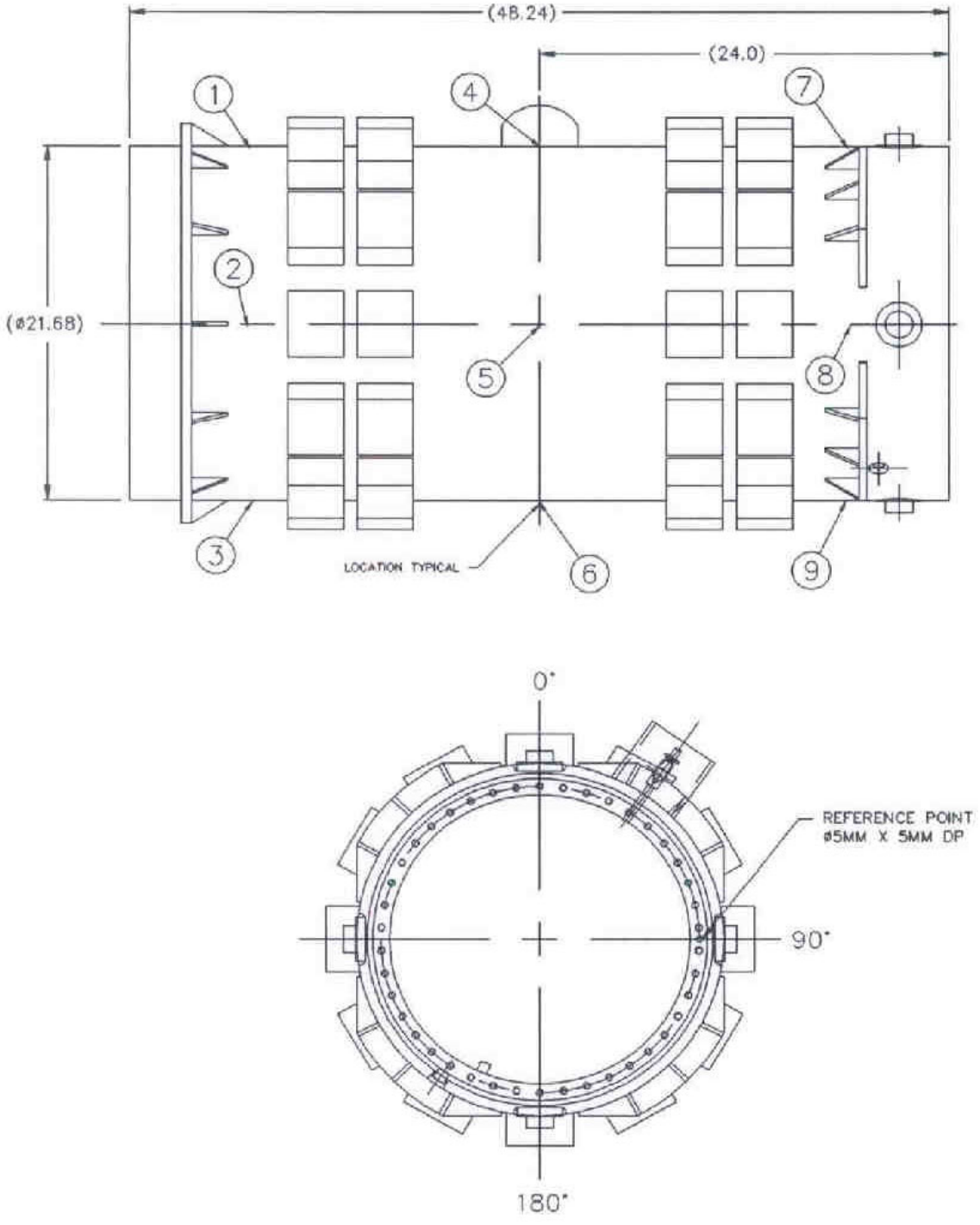

Figure 2.10.6-18 Accelerometer Locations - Quarter-Scale Model

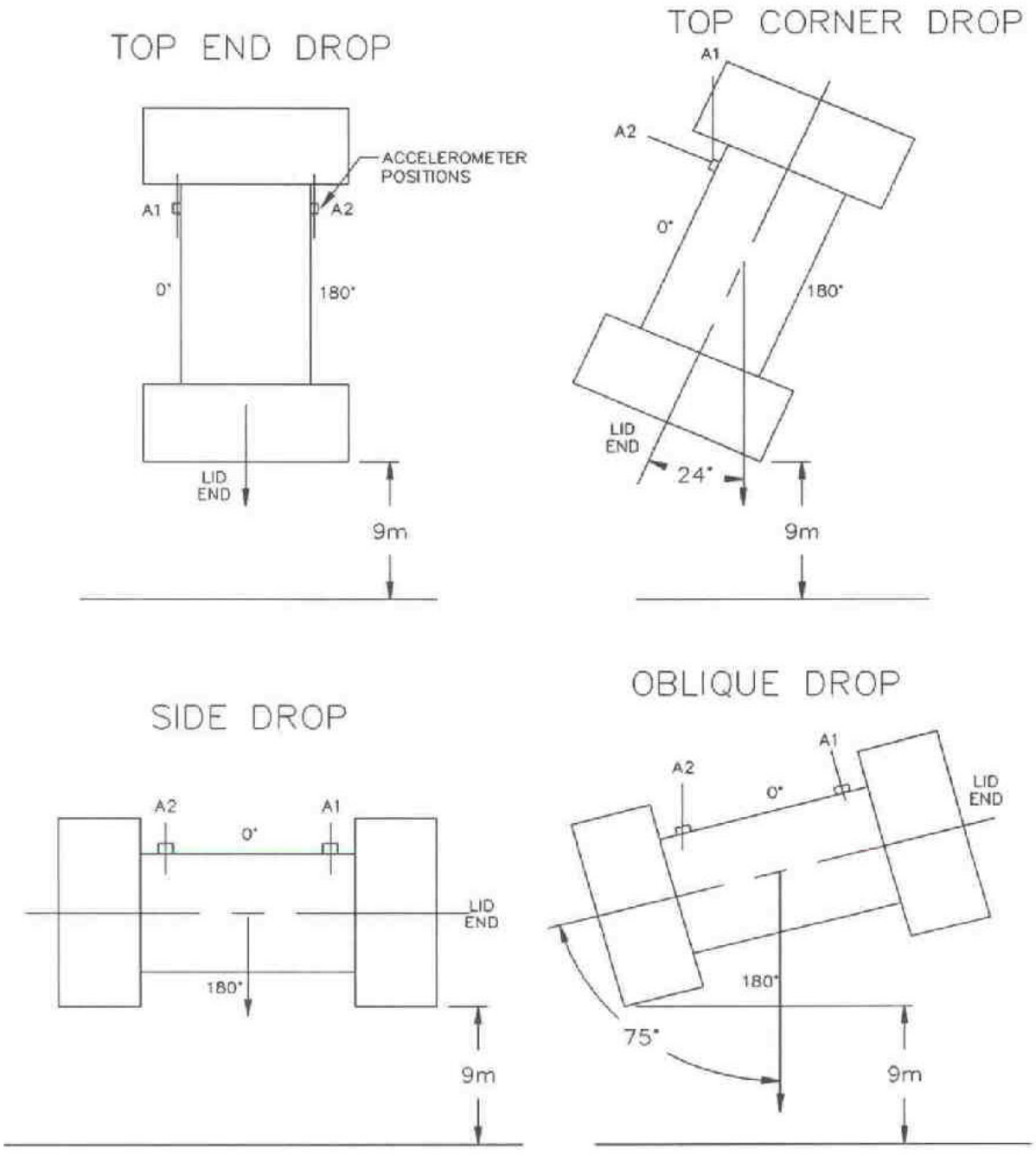

Figure 2.10.6-19 Top End Drop (Test No. 1 of Phase 1) - Upper Impact Limiter Deformation (Using Impact Limiters With Aluminum Shells)

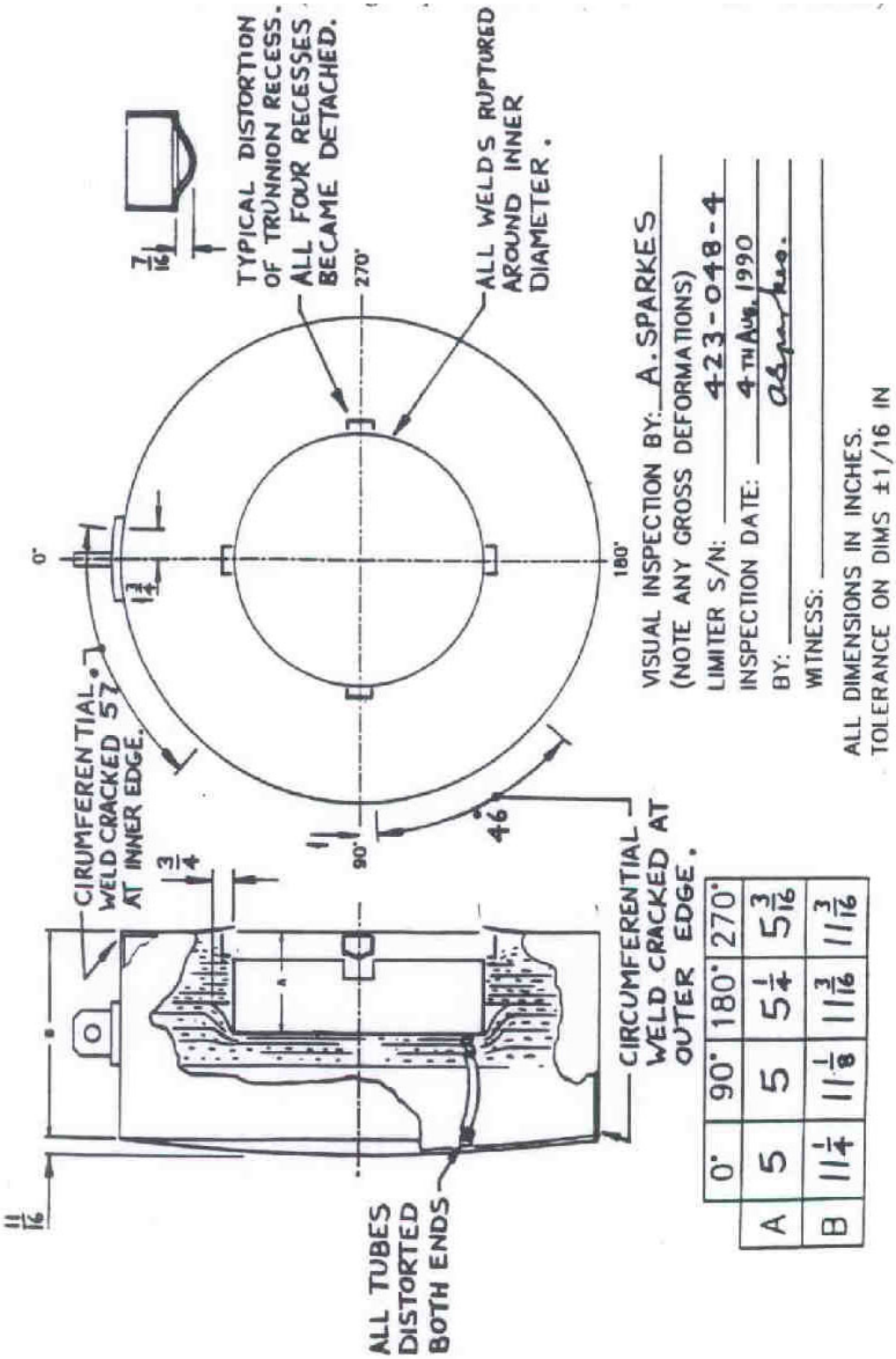

Figure 2.10.6-20 Top End Drop (Test No. 1 of Phase 1) Strain Data - Gauge S9.1 (Axial) (Using Impact Limiters With Aluminum Shells)

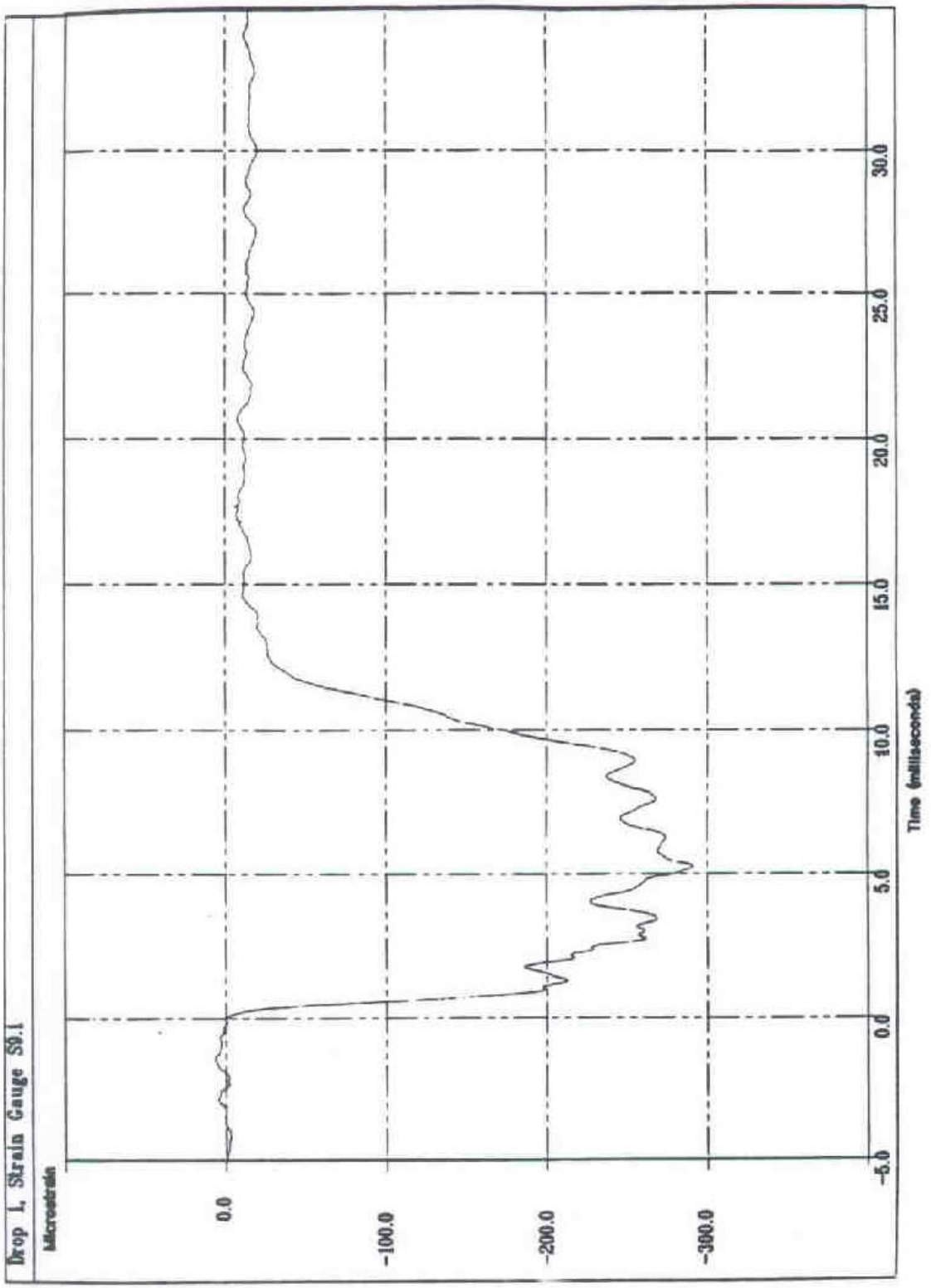

Figure 2.10.6-21 Top End Drop (Test No. 1 of Phase 1) Strain Data - Gauge S9.2 (Hoop) (Using Impact Limiters With Aluminum Shells)

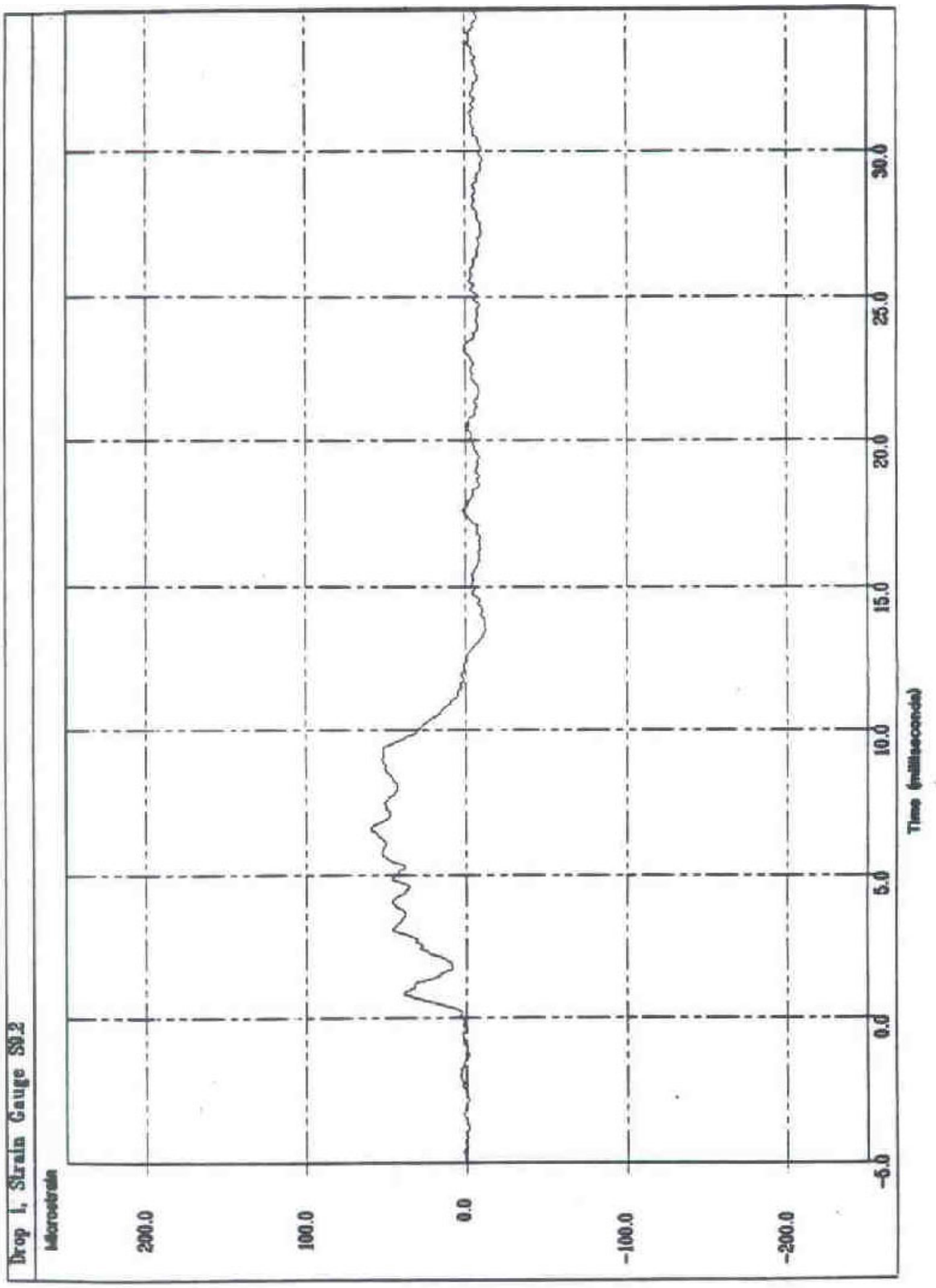

Figure 2.10.6-22 Top End Drop (Test No. 1 of Phase 1) Accelerometer Data - A2 (1 kHz Filter) (Using Impact Limiters With Aluminum Shells)

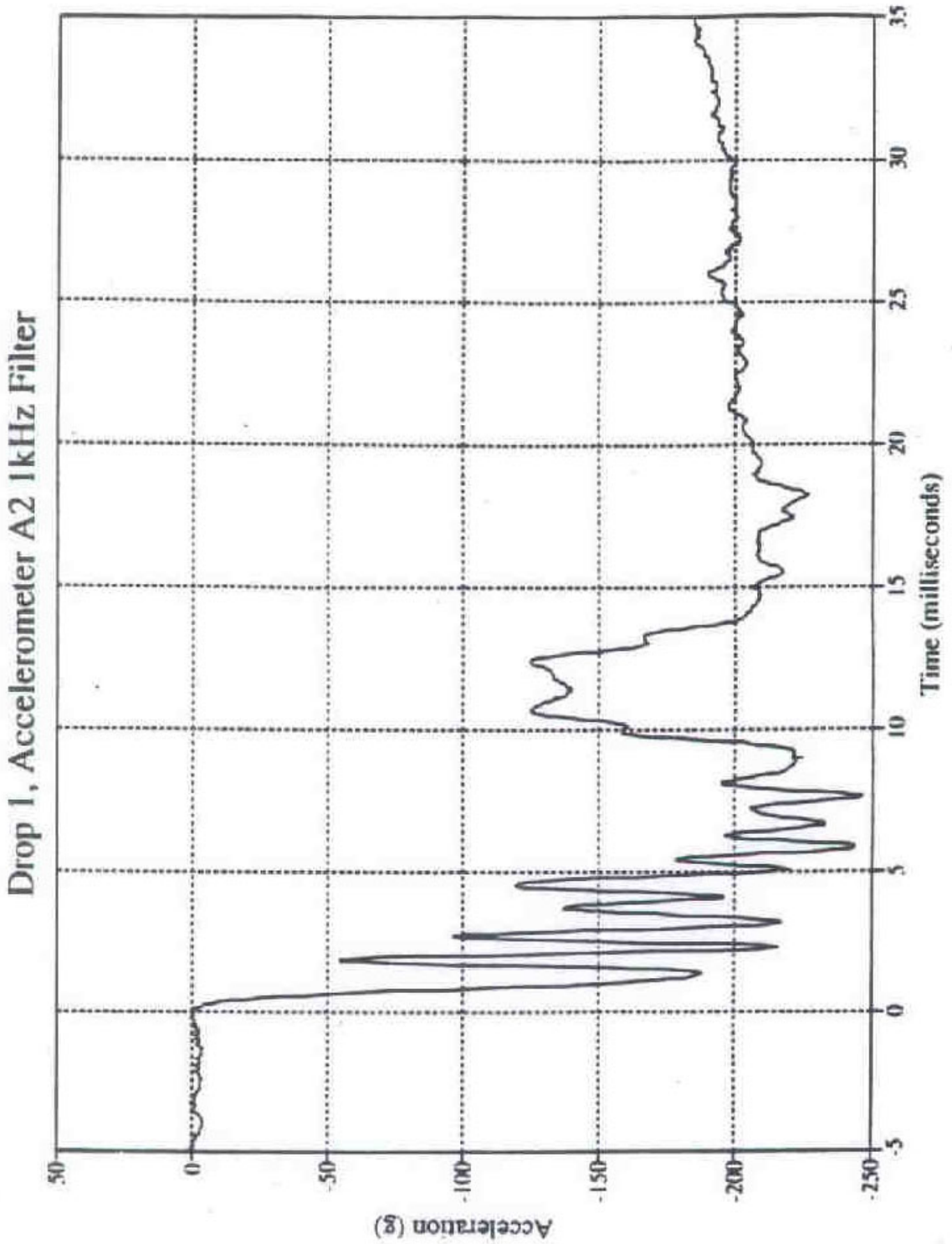

Figure 2.10.6-23 Side Drop Test (Test No. 3 of Phase 1) Accelerometer Data - A2 (Using Impact Limiters With Aluminum Shells)

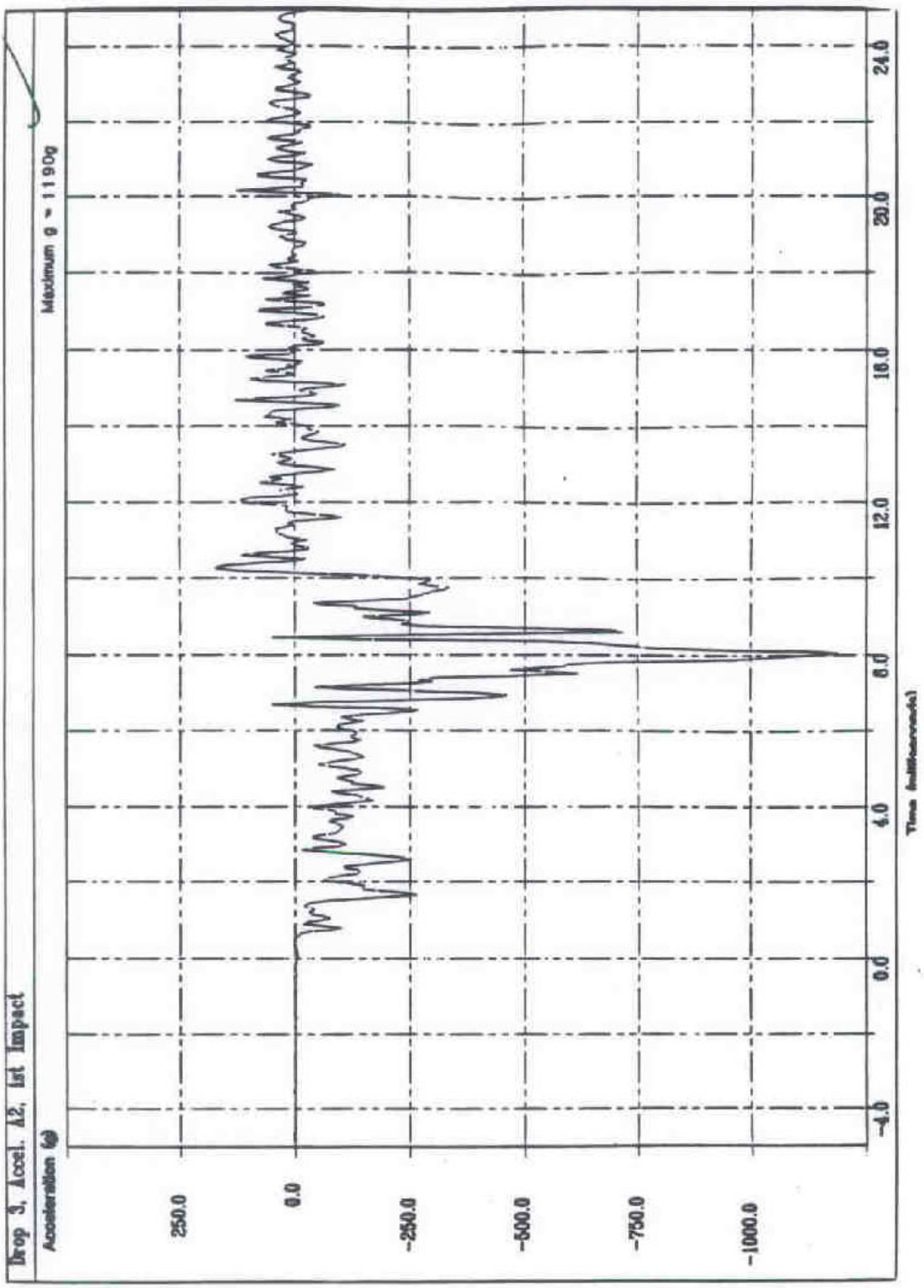

Figure 2.10.6-24 Side Drop Test (Test No. 3 of Phase 1) - Deformation of Support Disk No. 6 (Using Impact Limiters With Aluminum Shells)

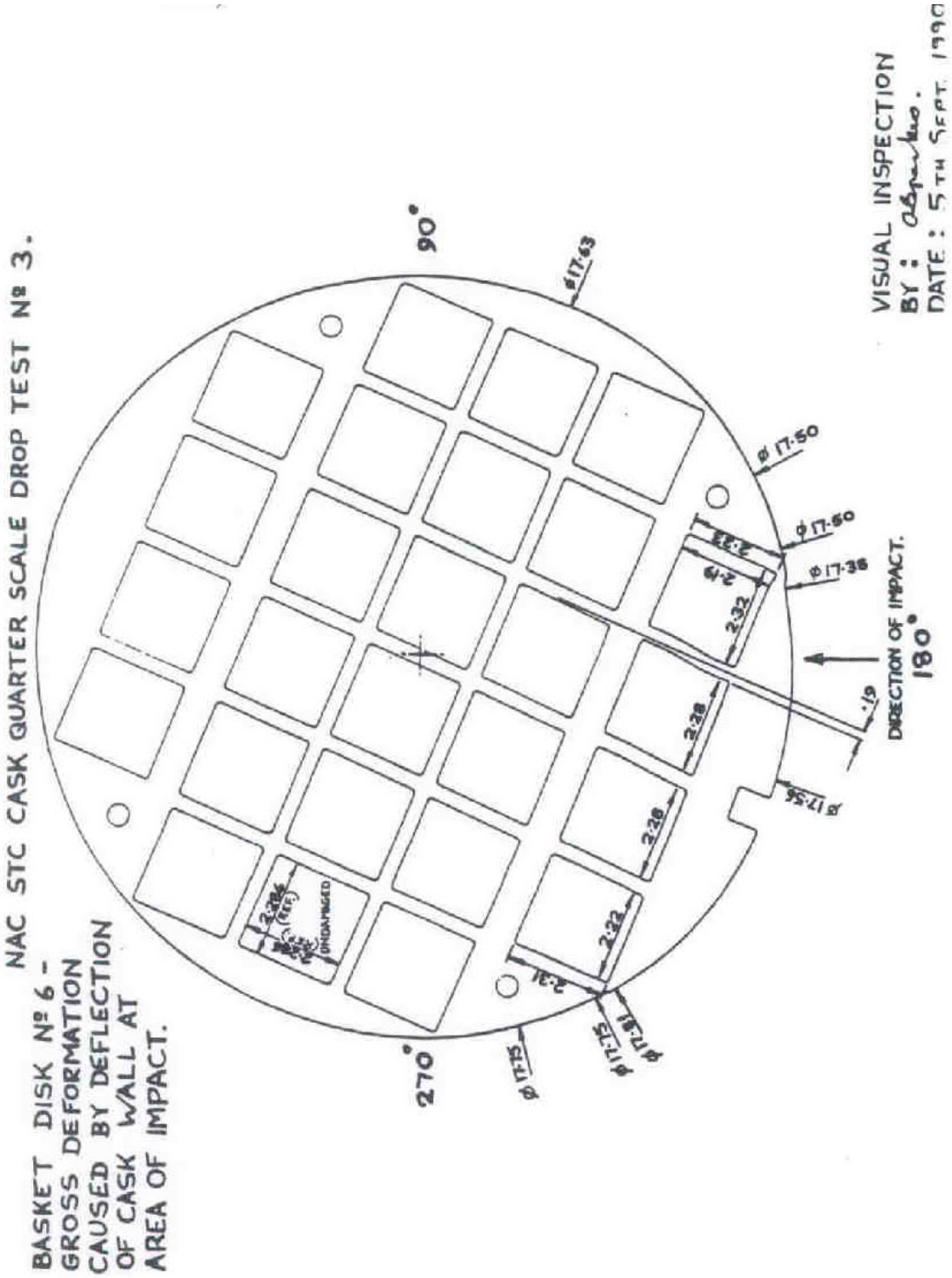

Figure 2.10.6-25 Top Corner Drop Test (Test No. 3 of Phase 3) - Impact Limiter Deformations

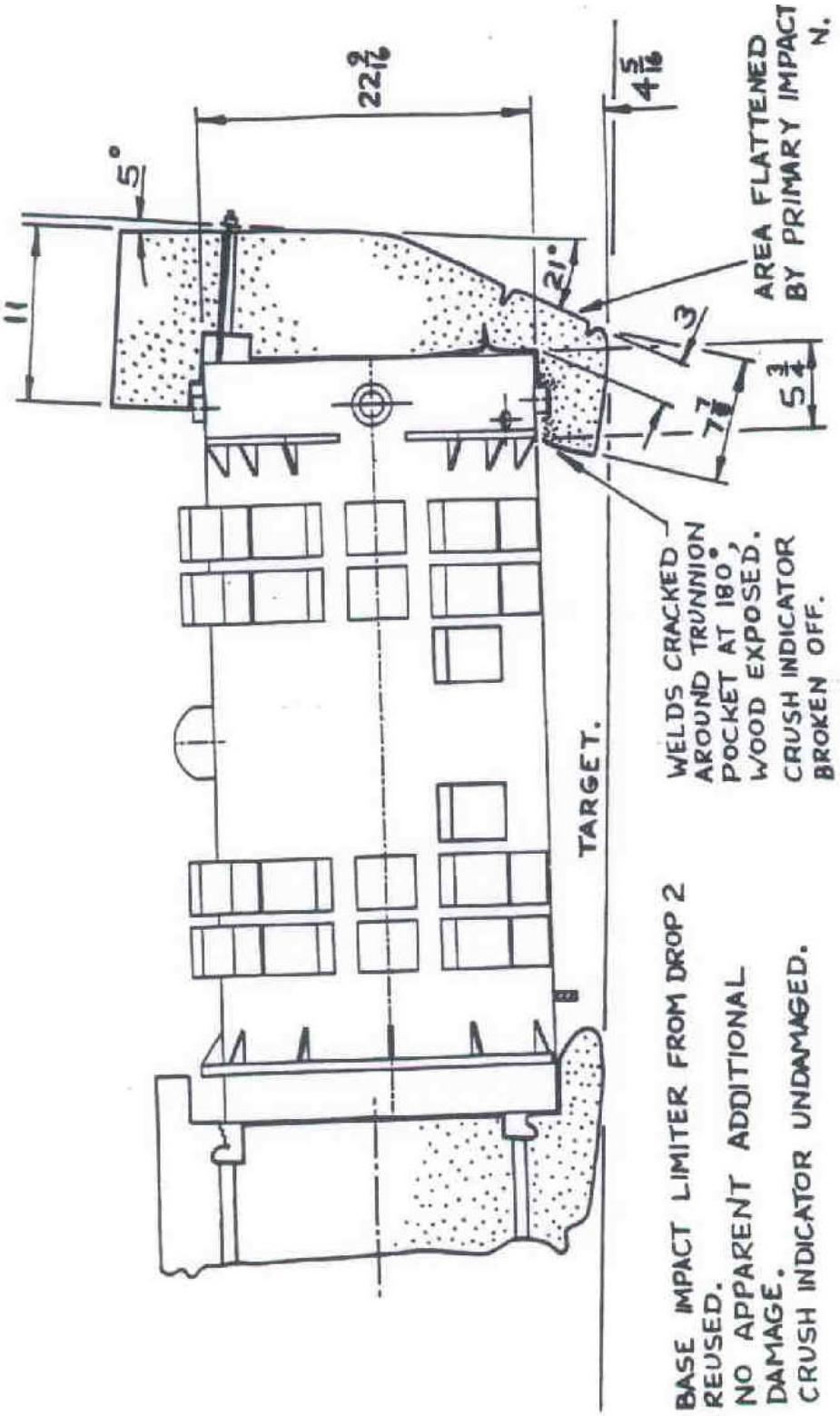

Figure 2.10.6-26 Top Corner Drop Test (Test No. 3 of Phase 3) Accelerometer Data - A1

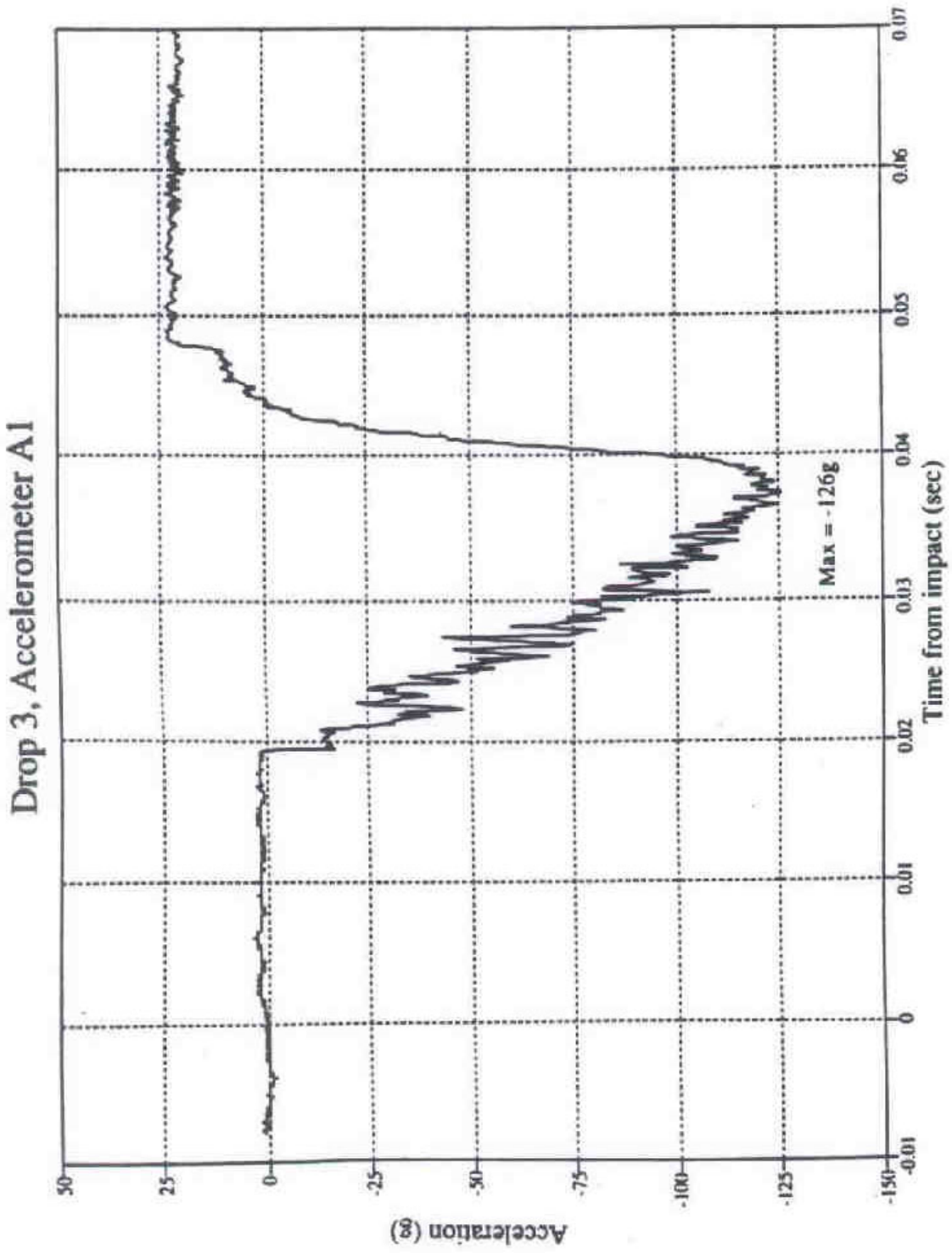

Figure 2.10.6-27 Bottom Oblique Drop Test (Test No. 1 of Phase 4) - Distorted Area of Upper Impact Limiter

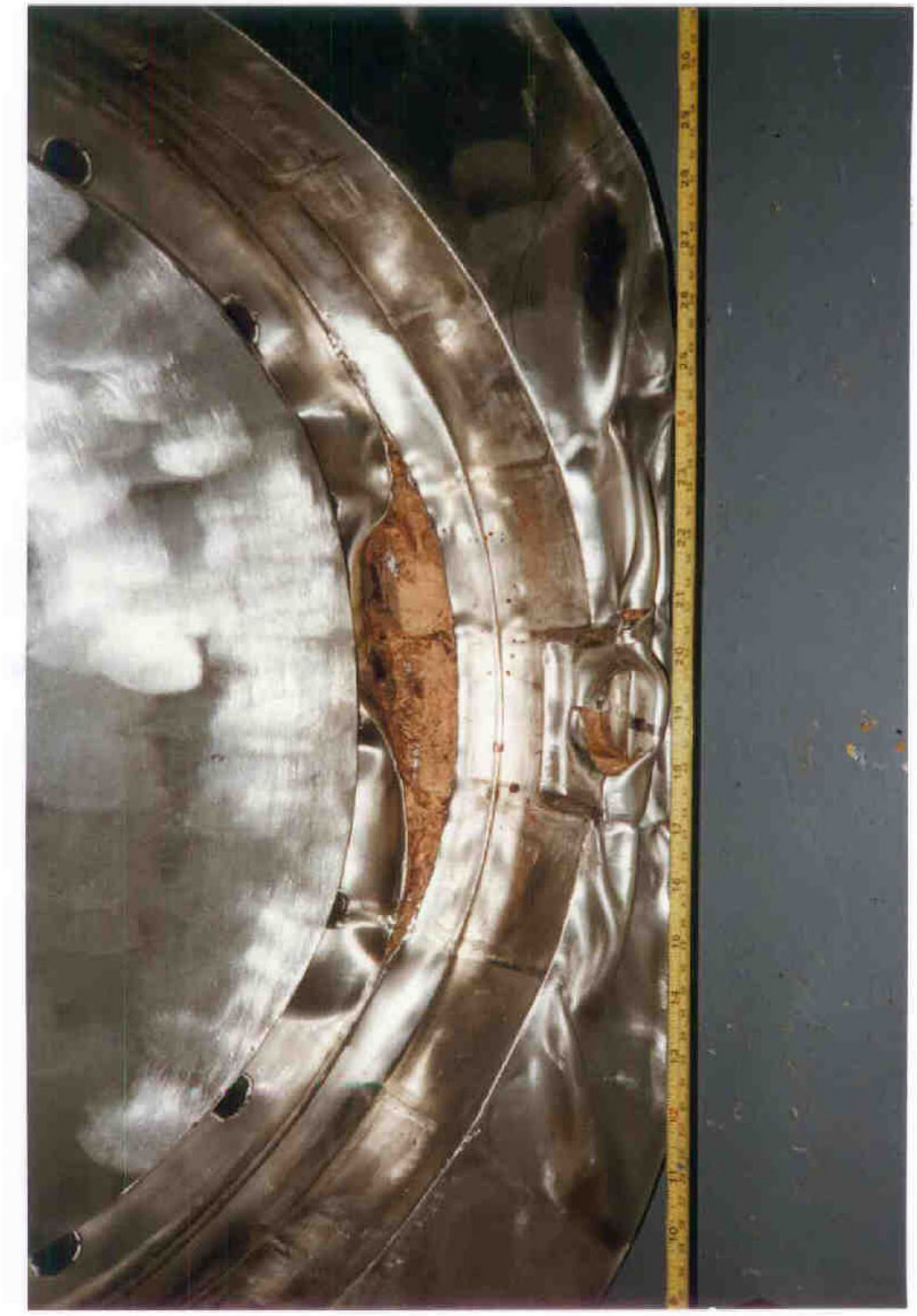

Figure 2.10.6-28 Bottom Oblique Drop Test (Test No. 1 of Phase 4) - Impact Limiter Deformations

FIGURE WITHHELD UNDER 10 CFR 2.390

Figure 2.10.6-29 Bottom Oblique Drop Test (Test No. 1 of Phase 4) - Impact Limiter Attachment Rods Post-Test Condition

Figure 2.10.6-30 Bottom Oblique Drop Test (Test No. 1 of Phase 4) Strain Data - Gauge S9.1 (Axial)

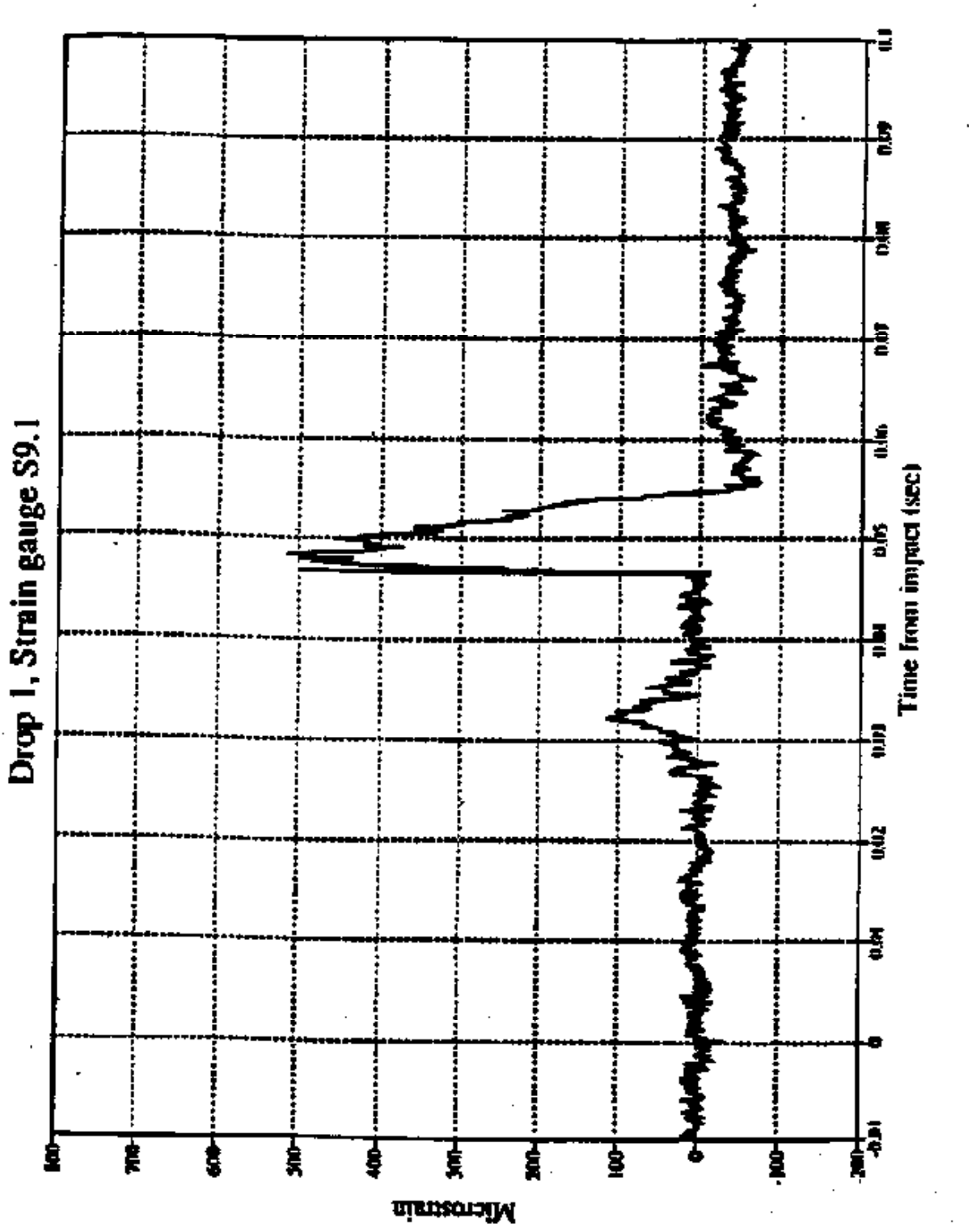

Figure 2.10.6-31 Bottom Oblique Drop Test (Test No. 1 of Phase 4) Strain Data - Gauge S9.2 (Hoop)

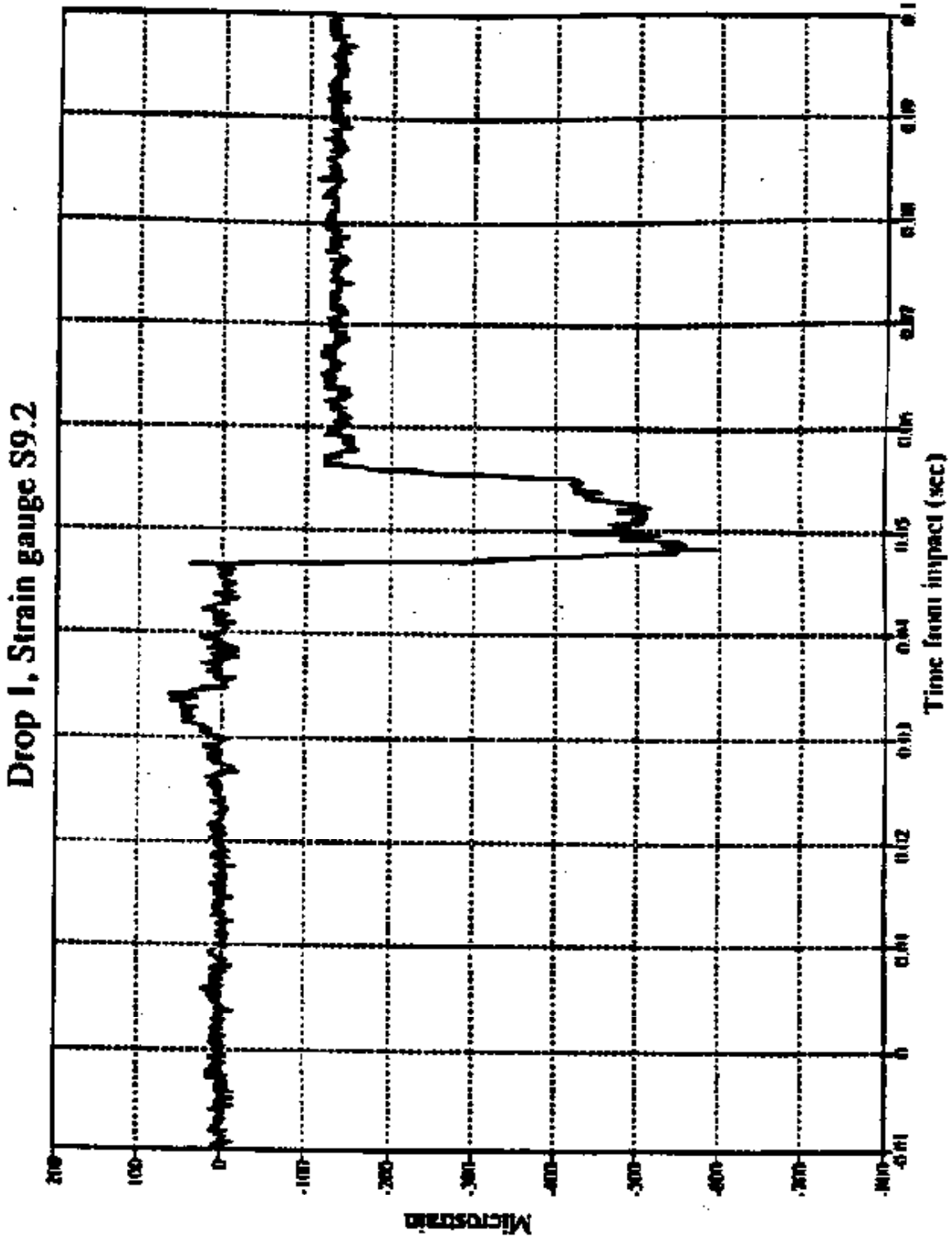

Figure 2.10.6-32 Bottom Oblique Drop Test (Test No. 1 of Phase 4) Accelerometer Data - A1 (750 Hz Filter)

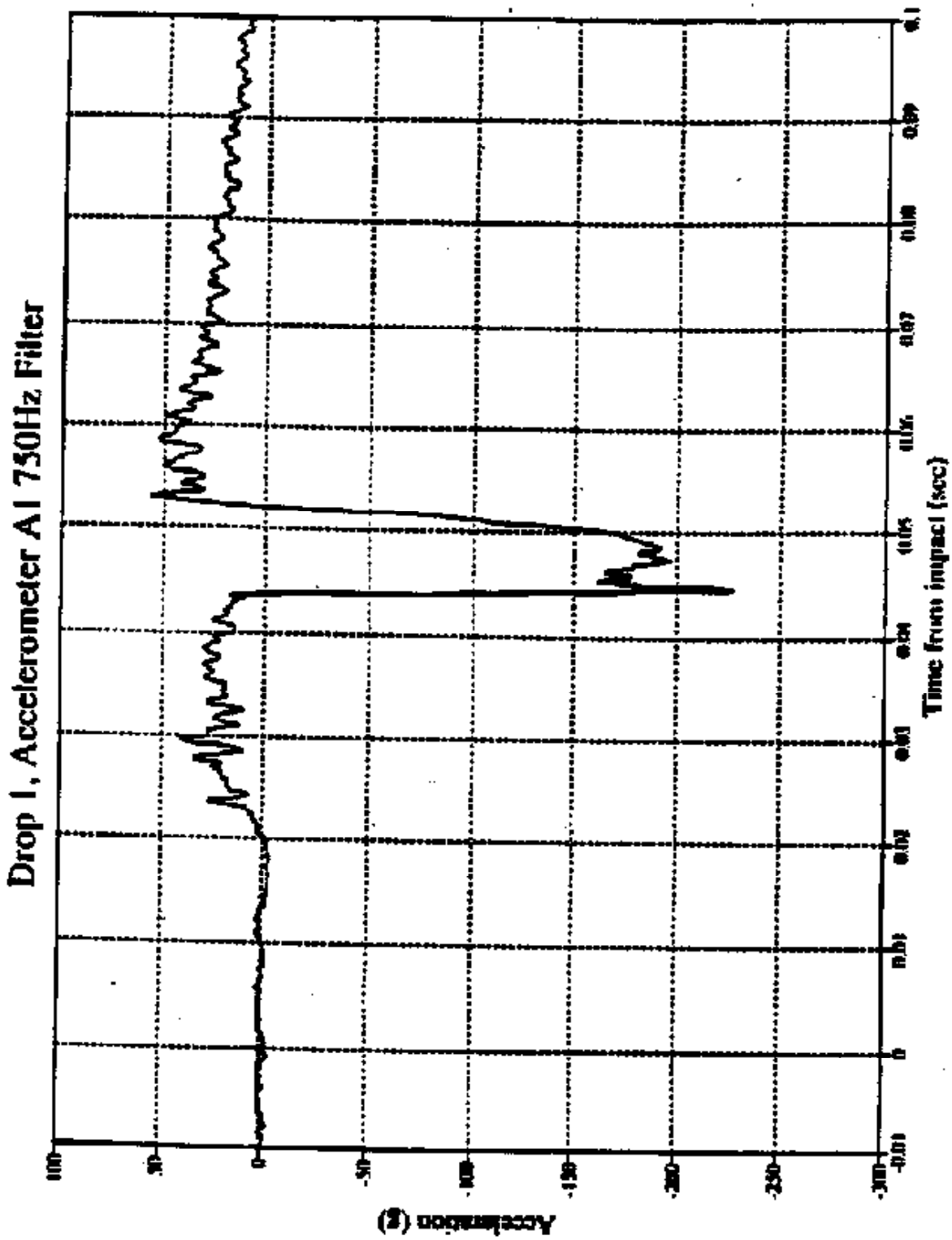

Figure 2.10.6-33 Bottom Oblique Drop Test (Test No. 1 of Phase 4) Accelerometer Data - A2 (750 Hz Filter)

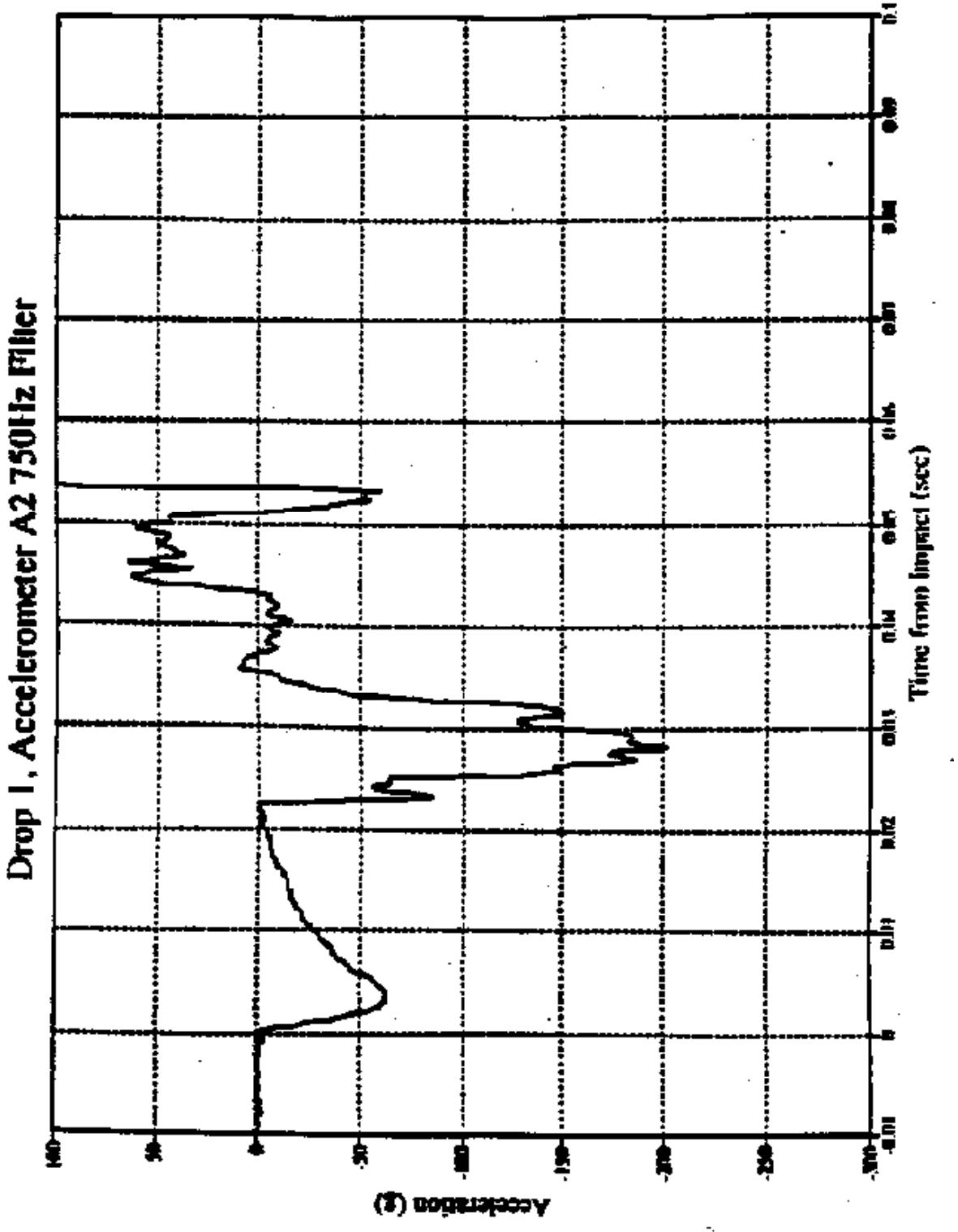

Figure 2.10.6-34 Side Drop Test (Test No. 2 of Phase 4) - Package Immediately After the Drop Test

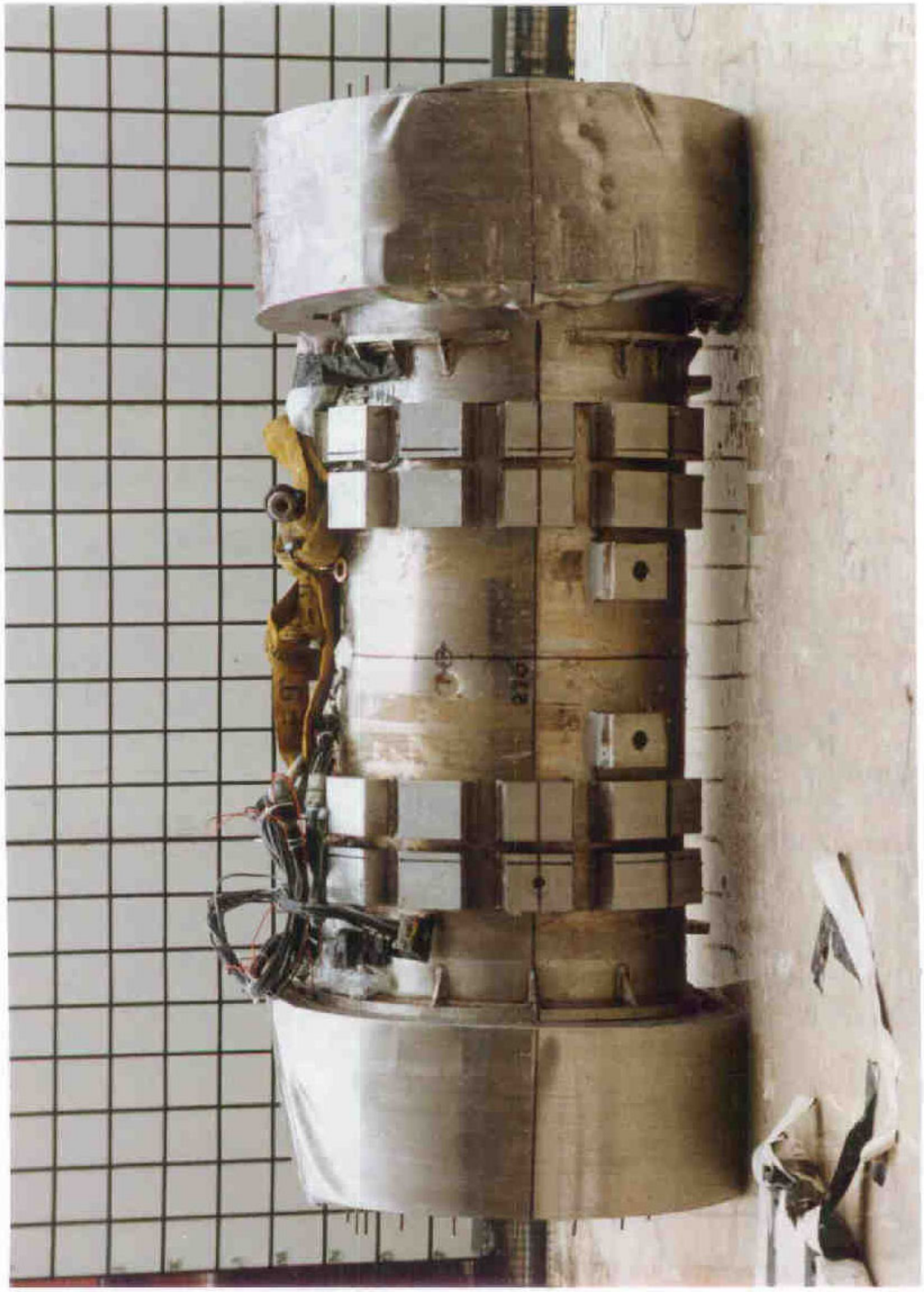

Figure 2.10.6-35 Side Drop Test (Test No. 2 of Phase 4) - Deformed Base Impact Limiter After Removal

Figure 2.10.6-36 Side Drop Test (Test No. 2 of Phase 4) - Impact Limiter Deformations

FIGURE WITHHELD UNDER 10 CFR 2.390

Figure 2.10.6-37 Side Drop Test (Test No. 2 of Phase 4) Strain Data - Gauge S9.1 (Axial)

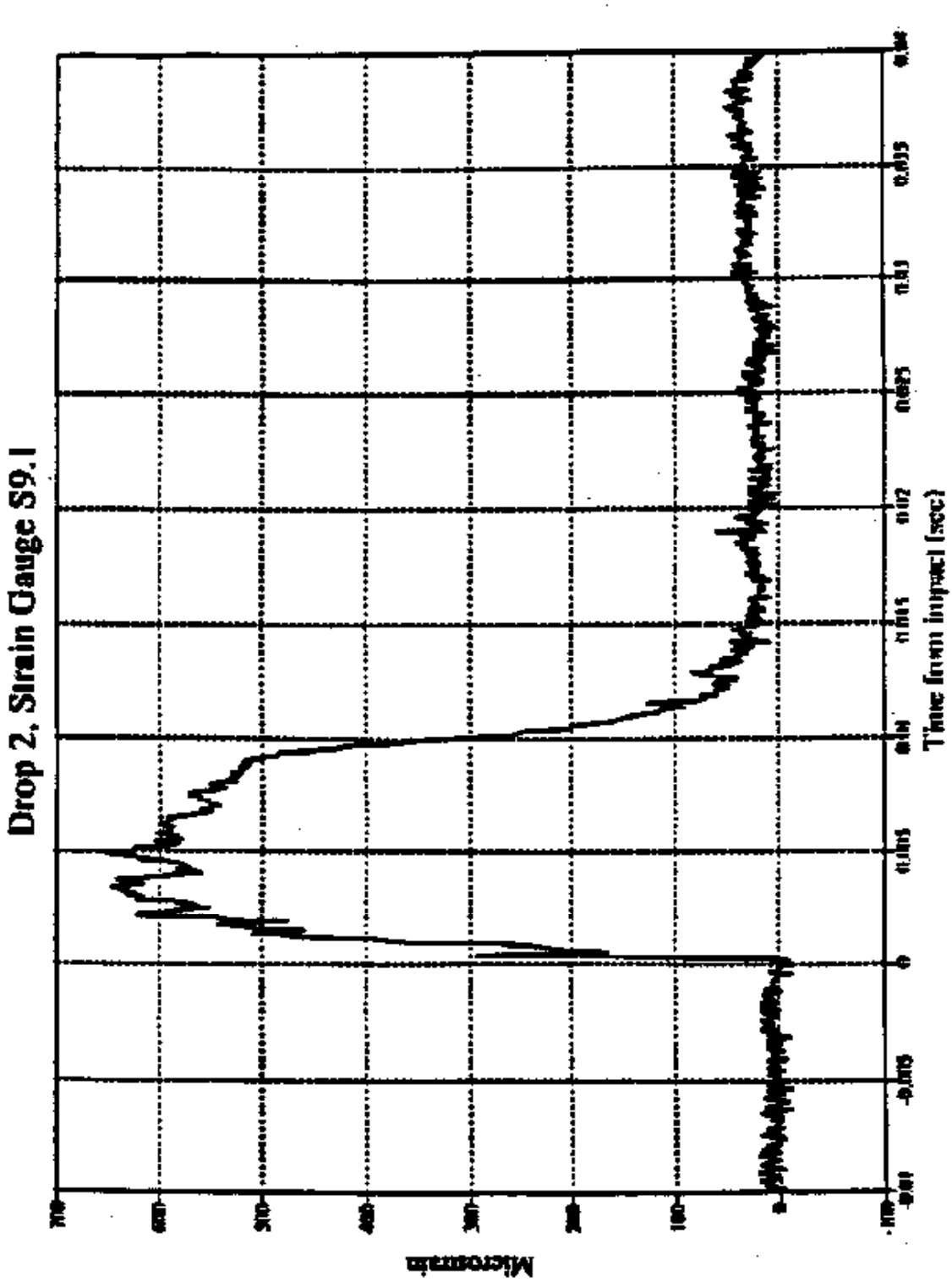

Figure 2.10.6-38 Side Drop Test (Test No. 2 of Phase 4) Strain Data - Gauge S9.2 (Hoop)

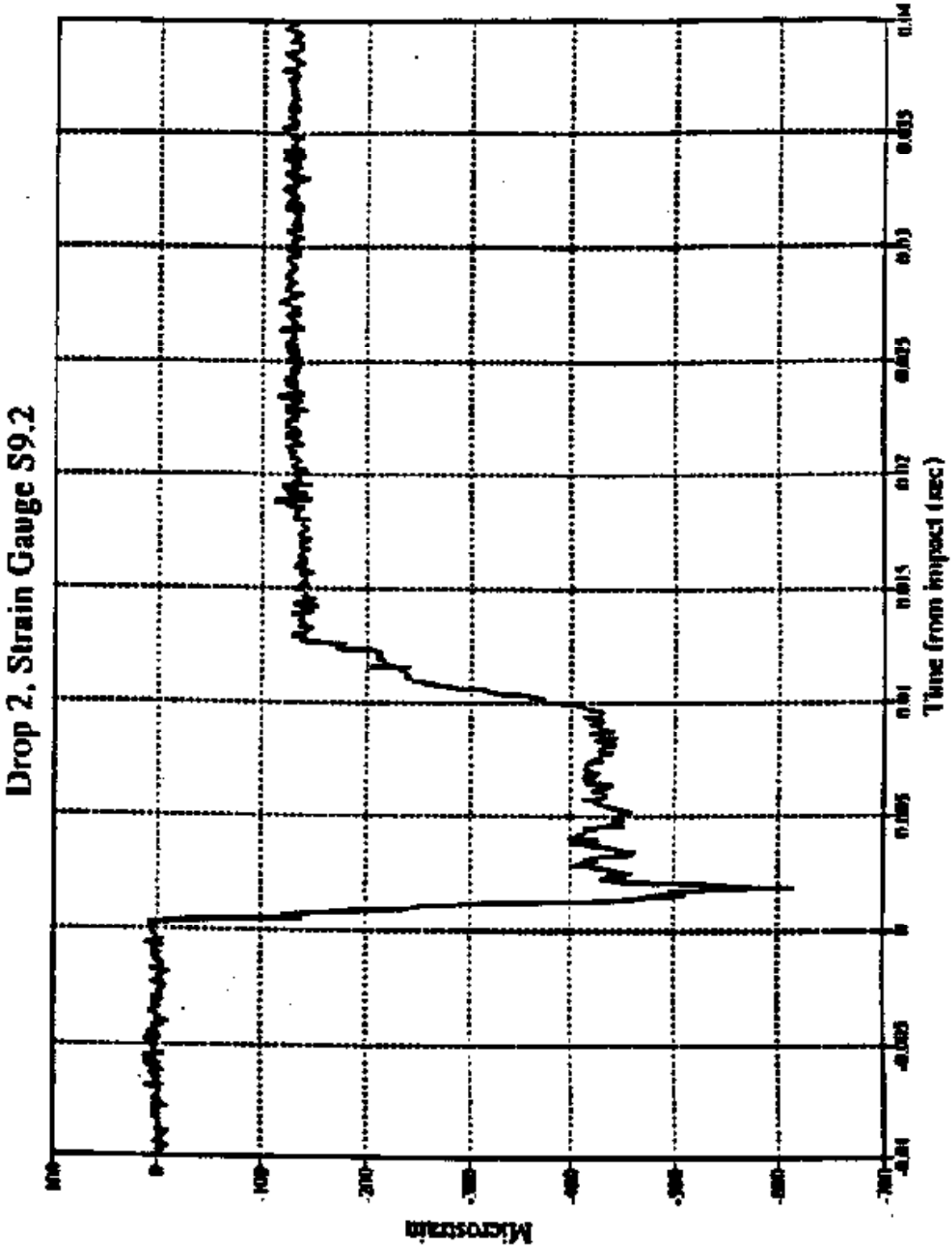

Figure 2.10.6-39 Side Drop Test (Test No. 2 of Phase 4) Accelerometer Data - A1 (1 kHz Filter)

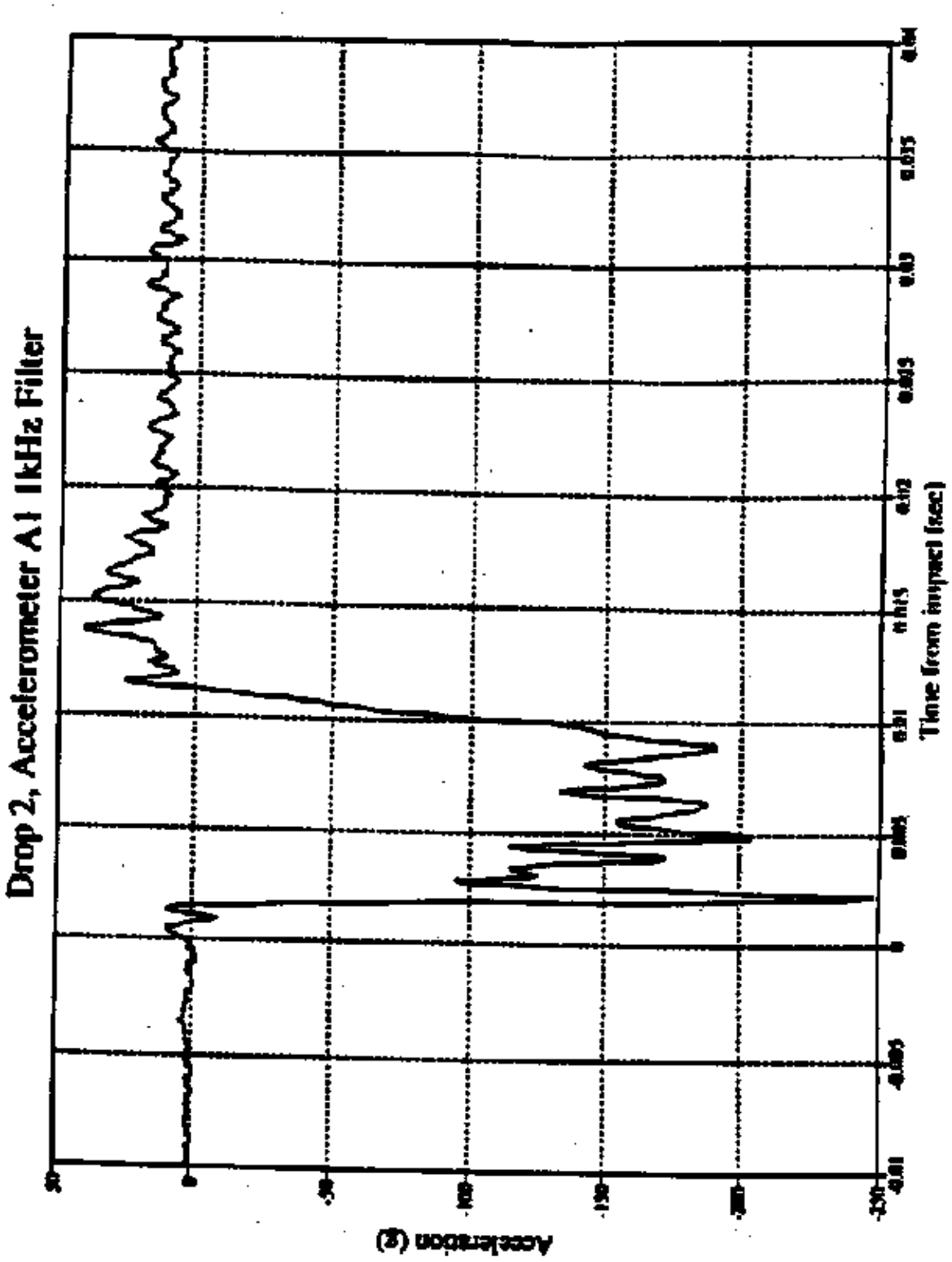

Figure 2.10.6-40 Side Drop Test (Test No. 2 of Phase 4) Accelerometer Data - A2 (750 Hz Filter)

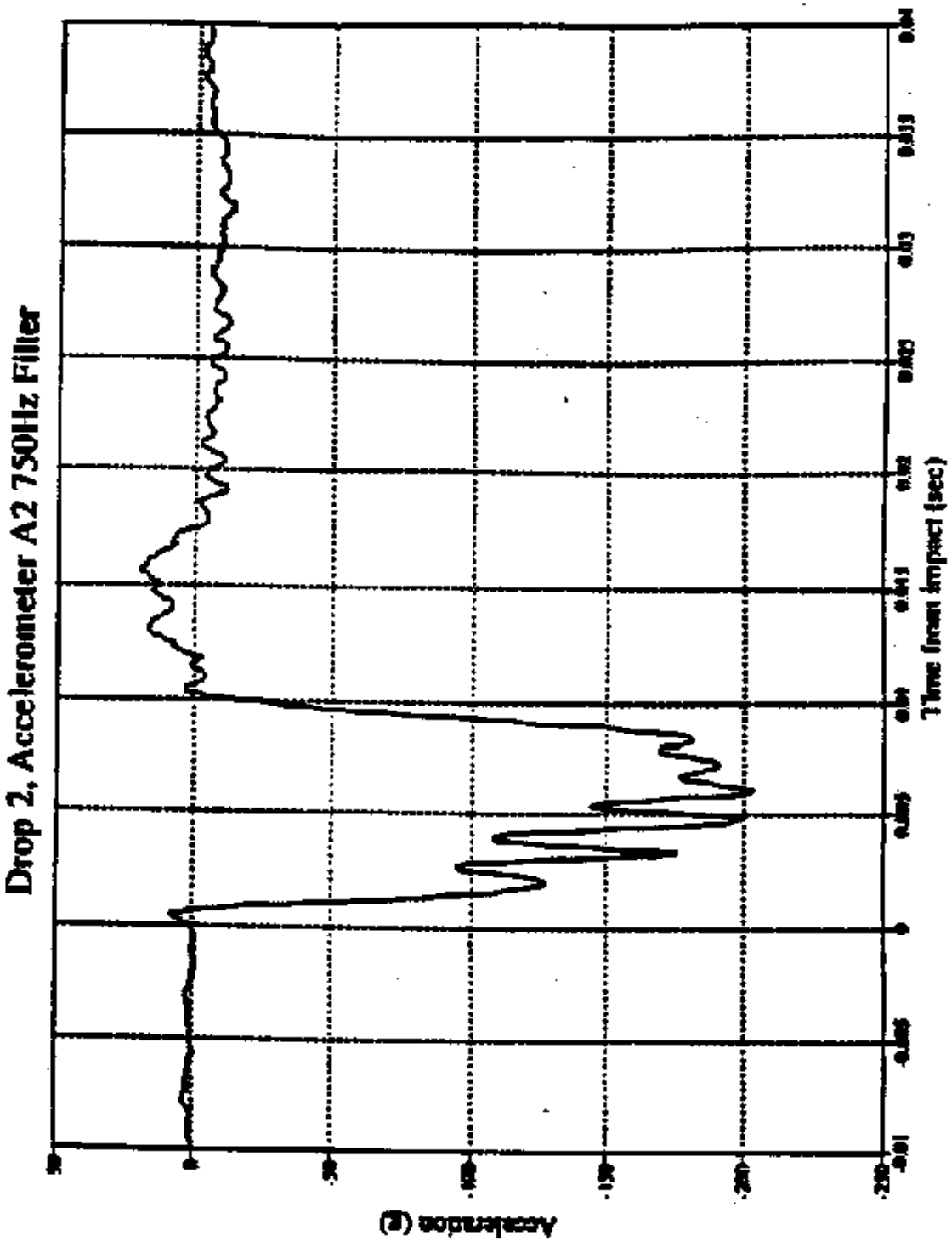

Table 2.10.6-1 Comparison of Full-Scale Deceleration Values for 30-Foot Drop Impacts

	30-Foot Drop Deceleration (g)				
Drop Orientation	RBCUBED[1] (Cold)	RBCUBED[1] (Hot)	Quasi-Static[2] Test	Drop[3] Test	Design[4]
End (0°)	44.6	56.1	54.8	55.6	56.1
Corner (24°)	44.0	49.3	32.6	29.2	55.0
Oblique (75°)	29.9	24.0	-	53.8	55.0
Side (90°)	51.7	51.3	45.6	51.3	55.0

1 Impact g-loads calculated by RBCUBED (NAC's proprietary Impact Limiter Analysis Program).

2 Extrapolated from eighth-scale model impact limiter quasi-static compression tests. Details are provided in Section 2.10.6.4.

3 Extrapolated from quarter-scale model 30-foot drop test results. Details are provided in Section 2.10.6.5.

4 Design g-load values used in the cask and fuel basket analyses.

Table 2.10.6-2 Top End Drop - Test Data (Test No. 1 of Phase 1)

CASK BODY DATA

Maximum Stress (ksi) and Location	8.6	@ Location 9
Maximum Hoop strain (microstrain) and Location	80	@ Location 9
Maximum Acceleration (g) at Location 1 1,000 Hz filter	217	
Maximum Acceleration (g) at Location 2 1,000 Hz filter	247	

Pretest Cavity Conditions

Pressure (bar)	3.276
Temperature (C)	93.6

Post-Test Cavity Pressure (bar)

Pressure (bar)	3.283
Temperature (C)	94.6

IMPACT LIMITER DATA

Maximum Crush Stroke (inches)

Top limiter	2.11
Bottom Limiter	-
Crush strain	23%

Table 2.10.6-3 Permanent Strains Side Drop Test Using Impact Limiters With Aluminum Shells (Test No. 3 of Phase 1)

Location	Axial Plastic Strain (microstrain)	Hoop Plastic Strain (microstrain)	Equivalent Plastic Strain (microstrain)
1	-113	16	122
2	-48	-170	152
3	387	-1279	1510
4	-216	162	328
5	1121	-431	1388
6	601	-1434	1811
7	-145	-83	126
8	-78	-295	265
	-284	338	381
9	500	-963	1288

Table 2.10.6-4 Cask Body and Outer Lid Pretest/Post-Test Metrology Data for Phase 1 Testing

Note: The Points of measurements are identified in Figure2.10.6-15.

PRETEST METROLOGY MEASUREMENTS FOR THE CASK BODY

Angle	K1	K2	K3	K4	D1	D2	D3
0°/180°	17.746	17.752	17.746	17.680	21.657	21.686	21.671
45°/225°	17.739	17.745	17.742	17.716	21.680	Not Made	21.669
90°/270°	17.731	17.730	17.729	17.673	21.691	21.700	21.663
135°/315°	17.752	17.764	17.746	17.717	21.691	21.700	21.655

POST-TEST METROLOGY MEASUREMENTS FOR THE CASK BODY

Angle	K1	K2	K3	K4	D1	D2	D3
0°/180°	17.601	17.605	17.494	17.664	21.585	21.541	21.398
45°/225°	17.814	17.823	17.869	17.751	21.763	Not Made	21.805
90°/270°	17.759	17.827	17.779	17.705	21.720	21.796	21.712
135°/315°	17.780	17.731	17.765	17.698	21.727	21.660	21.689

Table 2.10.6-5 Fuel Basket Support Disk No. 12 Pretest Metrology Data for Phase 1 Testing

Note: The points of measurement are identified in Figure 2.10.6-16.

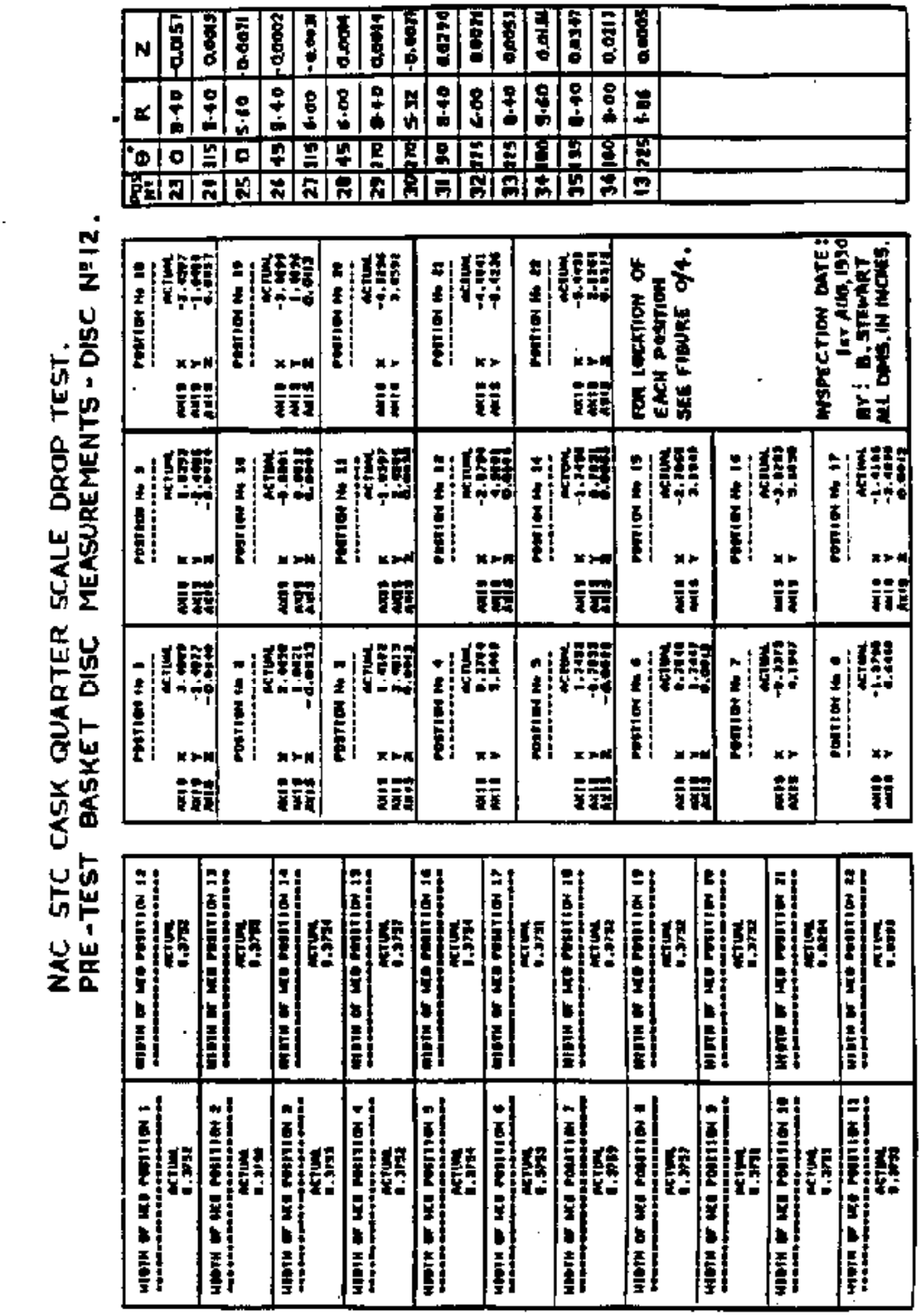

PNT Nº	θ°	R	Z
23	0	8-40	-0.057
24	315	8-40	0.0615
25	0	5-40	-0.0631
26	45	8-40	-0.0002
27	315	6-00	-0.0038
28	45	6-00	0.0004
29	270	8-40	0.0614
30	270	5-32	-0.0078
31	90	8-40	0.0270
32	225	6-00	0.0078
33	225	8-40	0.0053
34	180	5-60	0.0188
35	135	8-40	0.0347
36	180	8-00	0.0211
13	225	1-86	0.0005

Table 2.10.6-6 Fuel Basket Support Disk No. 6 Post-Test Metrology Data for Phase 1 Test 3

Note: The points of measurement are identified in Figure 2.10.6-16.

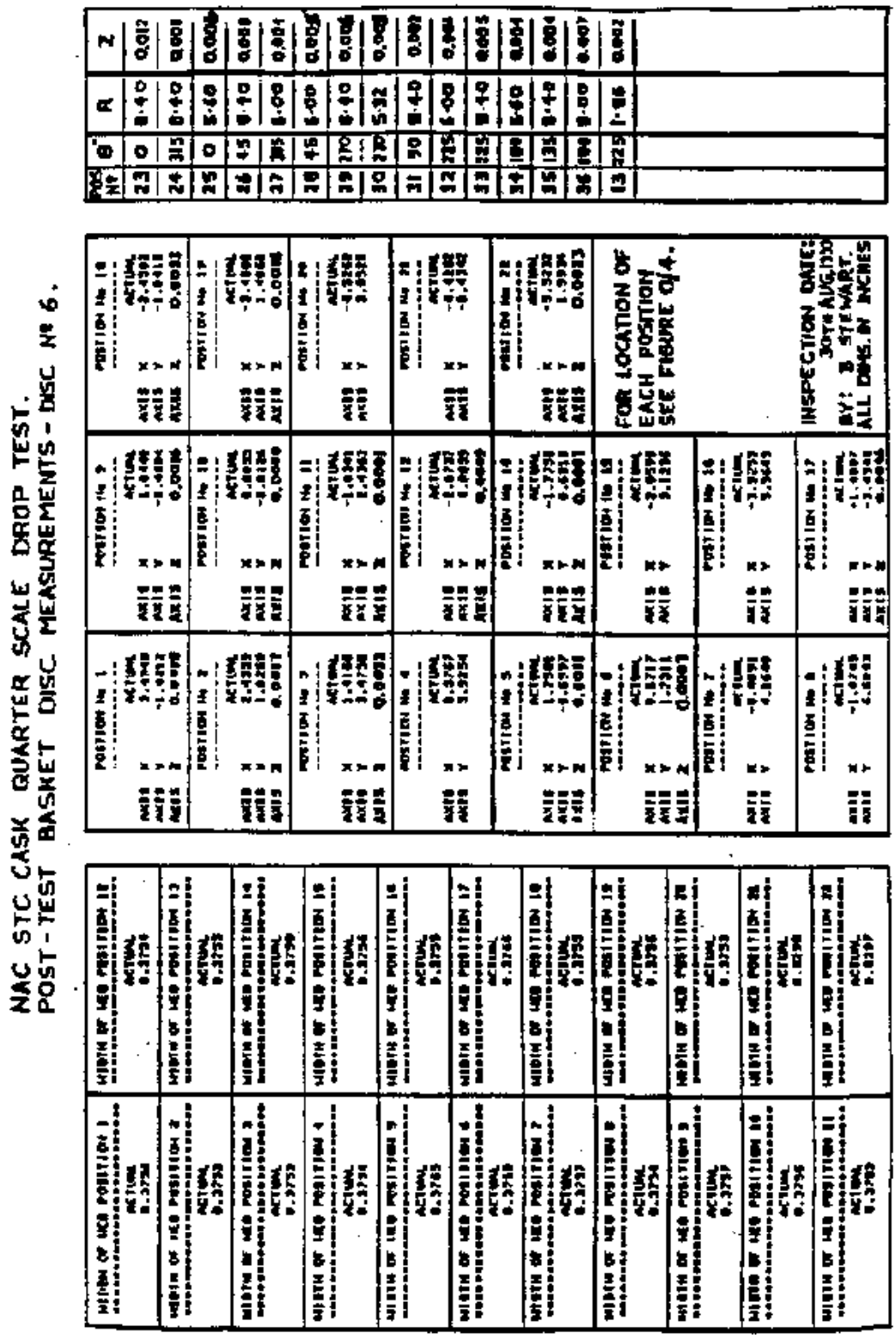

Table 2.10.6-7 Fuel Basket Support Disk No. 12 Post-Test Metrology Data for Phase 1 Test 3

Note: The points of measurement are identified in Figure 2.10.6-16.

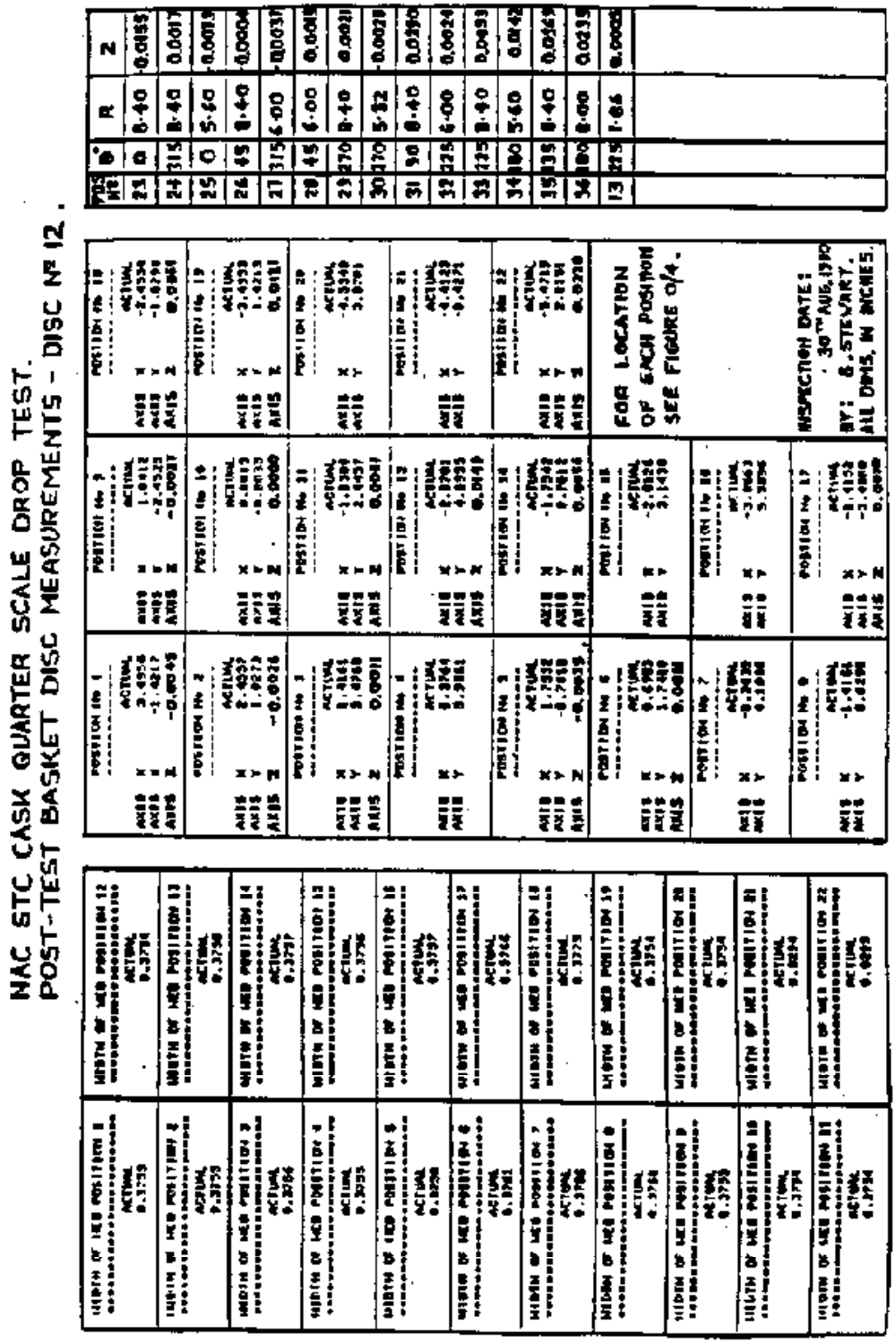

POS Nº	θ°	R	Z
23	0	0-40	-0.0155
24	315	8-40	0.0017
25	0	5-60	-0.0019
26	45	8-40	-0.0004
27	315	6-00	-0.0031
28	45	6-00	0.0018
29	270	8-40	0.0021
30	90	5-52	-0.0029
31	90	8-40	0.0350
32	225	6-00	0.0024
33	225	8-40	0.0453
34	180	5-60	0.0142
35	135	8-40	0.0565
36	180	8-00	0.0215
13	225	1-66	0.0000

Table 2.10.6-8 Top Corner Drop - Test Data (Test No. 3 of Phase 3)

CASK BODY DATA

Maximum Stress (ksi) and Location	3.8	@ Location 9
Maximum Hoop strain (microstrain) and Location	-	
Maximum Vertical Acceleration (g) 4,000 Hz filter	127	
Maximum Cask lateral Acceleration (g) 4,000 Hz filter	107	

Pretest Cavity Conditions

Pressure (bar)	3.2114
Temperature (C)	46.8

Post-Test Cavity Pressure (bar)

Pressure (bar)	3.2045
Temperature (C)	45.3

IMPACT LIMITER DATA

Maximum Crush Stroke

Top limiter	6.4
Bottom Limiter	-

Maximum design stroke (inches)	9.07

Table 2.10.6-9 Pin Puncture Drop Tests (Test Nos. 5 and 6 of Phase 3)

Pressure/Temperature Measurements

	Cask Body Midpoint	Location of Pin Impact	Outer Lid Center
Pretest			
pressure (bar)	3.0070		3.1397
temperature (F)	53.1		45.0
Post-test			
pressure	3.0020		[1]
temperature	45.9		

Metrology Data

Cask Midpoint Pin Puncture

Outer Diameter of Outer shell at pin puncture (inches)	21.30
Outer Diameter of Outer Shell at 5.62 inches from pin (inches)[2]	21.63
Inner Diameter of Inner Shell at pin puncture (inches)	17.509
Inner Diameter of Inner Shell at 5.62 inches from pin (inches)[2]	17.701

Cask Outer Lid Pin Puncture

Maximum out of plane measurement (inches)	
pretest	0.005
post-test	0.007

[1] The cavity valve was broken during the test.

[2] The 5.62 inches is measured in an axial direction parallel to the centerline of the cask body.

Table 2.10.6-10 Bottom Oblique Drop - Test Data (Test No. 1 of Phase 4)

CASK BODY DATA

Maximum Axial Stress (ksi) and Location	+10.41 @ Location 9
Maximum Hoop Stress (ksi) and Location	-12.49 @ Location 9
Maximum Permanent strain (microstrain) and Location	135 @ Location 9
Maximum Top End Acceleration (g)	225
Maximum Bottom End Acceleration (g)	205
Pretest Cavity Conditions	
Pressure (bar)	3.1903
Temperature (F)	47.8
Post-Test Cavity Pressure (bar)	
Pressure (bar)	3.1905
Temperature (F)	47.7

IMPACT LIMITER DATA

Maximum Crush Stroke (inches)	
Top limiter	2.41
Bottom Limiter	1.22
Maximum Permissible stroke (inches)	
Top limiter	3.22
Bottom limiter	3.22

Table 2.10.6-11 Cask Body and Outer Lid Pretest/Post-test Metrology Data for Phase 4 Testing

Pretest Metrology Data[1]

Angle	K1	K2	K3	K4	M	Ka
0°/180°	17.696	17.692	17.856	17.712	21.638	
30°/210°		17.730	17.720	17.716		17.732
90°/270°	17.742	17.778	17.732	17.666	21.619	
120°/300°		17.708	17.721	17.687		17.705

Post-test Metrology Data for the Oblique Drop (Test No. 1 of Phase 4)

Angle	K1	K2	K3	K4	M
0°/180°	17.694	17.692	17.857	17.705	21.618
90°/270°	17.743	17.787	17.741	17.675	21.614

Post-test Metrology Data for the Side Drop (Test No. 2 of Phase 4)

Angle	K1	K2	K3	K4	M
0°/180°	17.702	17.693	17.851	17.704	21.626
90°/270°	17.743	17.779	17.742	17.675	21.614

[1] Definition of dimensions and locations are shown in Figure 2.10.6-15.

Table 2.10.6-12 Side Drop - Test Data (Test No. 2 of Phase 4)

CASK BODY DATA

Maximum Axial Stress (ksi) and Location	+29.5 @ Location 6
Maximum Hoop Stress (ksi) and Location	+17.5 @ Location 6
Maximum Permanent strain (microstrain) and Location	135 @ Location 9
Maximum Top End Acceleration (g)	204
Maximum Bottom End Acceleration (g)	208
Pretest Cavity Conditions	
Pressure (bar)	3.1540
Temperature (F)	49.1
Post-Test Cavity Pressure (bar)	
Pressure (bar)	3.1526
Temperature (F)	49.1

IMPACT LIMITER DATA

Maximum Crush Stroke (inches)	
Top limiter	2.04
Bottom Limiter	2.16
Maximum Permissible stroke (inches)	
Top limiter	3.22
Bottom limiter	3.22

2.10.7 Redwood Impact Limiter Force-Deflection Curves and Data - Directly Loaded Fuel Configuration

As discussed in Section 2.10.6.1 and throughout this report, the center-of-gravity location and the cavity contents weight for the Yankee-MPC configuration of the NAC-STC are essentially identical to those of the directly loaded fuel configuration. Therefore, this evaluation is applicable to both contents configurations of the NAC-STC with the redwood and balsa wood impact limiters (referred to as the redwood impact limiter[s]) described in License Drawings 423-209 and 423-210 and in Section 2.6.7.4.1. The evaluation is not applicable to the balsa wood impact limiter described in License Drawings 423-257 and 423-258 and Section 2.6.7.4.2, used with the CY-MPC configuration. The two impact limiter configurations are described in Section 1.2.1.2.6.

2.10.7.1 Potential Energy and Cask Drop Impact Motion

It is stated in 10 CFR 71 that analyses must show that a spent-fuel shipping cask is capable of sustaining a normal condition test (a 1-foot free drop) followed by a hypothetical accident test (a 30-foot free drop). This has been interpreted to mean that impact limiters must be designed to absorb, or dissipate, the potential energy of the cask, if dropped in any orientation from 30 feet onto an unyielding surface. The cask would not be operated after the occurrence of a 1-foot drop until the impact limiter(s) had been replaced/repaired.

The distance through which the cask free falls is measured from the nearest point on the cask (either impact limiter) to the unyielding surface. This ensures that the center of gravity will translate a minimum of 30 feet before an impact limiter contacts the unyielding surface. Additionally, it is assumed that the cask will always seek a stable orientation on both impact limiters after contacting the unyielding surface. After an end drop, for example, it is assumed that the cask tips over and reaches a stable horizontal orientation. When at rest horizontally on the unyielding surface (a datum surface), the cask is considered to have zero potential energy.

Potential energy is calculated by multiplying the weight of the cask by the height of the center of gravity of the cask above the datum surface. The design weight of the cask, contents and impact limiters is 250,000 pounds. For these analyses, the NAC-STC is considered to be symmetric about the three major axes; therefore, the center of gravity is at the midpoint of the longitudinal centerline of the cask. The center of gravity is a datum point at which all of the mass (weight) of the cask is considered to be located.

2.10.7.1.1 Translational Motion - Side Drop

Figure 2.10.7-1 shows the cask in the horizontal or side drop position. When released in this orientation from 30 feet (360 in), the cask has 9.00×10^7 inch-pounds of potential energy. As shown by the heavy dashed lines in Figure 2.10.7-1, the cask translates in the vertical direction and impacts on an unyielding surface. The deceleration forces that are created by crushing the impact limiters oppose the translational motion of the cask. Impact limiter crushing continues until all of the potential energy of the cask is absorbed, thereby decelerating the cask to rest. Both impact limiters crush simultaneously in a side drop; therefore, the cask is in a stable orientation following a side drop event.

In a side drop, the cask experiences only translational motion in the vertical direction. Ignoring the energy stored elastically in the impact limiter during deceleration, the dissipated energy equals the initial potential energy of the cask. During the side drop, both impact limiters are simultaneously engaged in decelerating the cask; therefore, each impact limiter absorbs the amount of energy shown in Table 2.10.7-1 and labeled E1--"Energy absorbed by the first limiter."

2.10.7.1.2 Translational and End-Rotational Motion - End Drop

Figure 2.10.7-2 shows the cask in the end drop position. End drops are drop angles that range between 0 degree (end drop) and 24 degree (corner drop) and characteristically show translational and end-rotational motion. As in a side drop, a cask in the end drop position translates through a vertical distance of 30 feet and decelerates as a result of an impact on the unyielding surface. Deceleration forces acting on the end of the cask are symmetric and uniform for a flat end drop; therefore, the cask remains vertical during deceleration and after the cask has come to rest. The energy absorbed by one impact limiter, while decelerating the cask during an end impact, equals the initial potential energy of the cask. Considering the package center of gravity to be at the longitudinal midpoint and ignoring deformation, the center of gravity is 128.48 inches above the datum surface for an end impact. The cask comes to rest in the vertical position on the crushed impact limiter.

2.10.7.1.3 Translational, End-Rotational, Mid-Point Rotational Motion - Oblique Drops

Figure 2.10.7-3 shows the cask in an oblique drop orientation. Oblique drops are drop angles that range between the corner drop and the side drop. After its fall is initiated, the cask translates through a vertical distance of 30 feet and impacts on the unyielding surface. The impact limiter, which contacts the unyielding surface first, crushes as it decelerates the leading end of the cask, bringing its velocity to zero. Energy absorbed by the leading impact limiter (E1) decelerates the leading end of the cask to rest. The cask now rotates or pivots on the stopped leading end. However, the energy absorbed by the first impact limiter is less than the initial energy of the cask, leaving the energy remaining (ER) to be absorbed by the second impact limiter.

Simultaneously during deceleration of the leading end of the cask, two other actions are taking place. First, the trailing, or free, end of the cask rotates around the stopped end of the cask and continues to accelerate due to gravity. Second, a component of the deceleration force causes a torque perpendicular to the longitudinal axis of the cask, resulting in the cask beginning to rotate around the center of gravity. Both “actions” contribute to the total amount of energy that must be absorbed by the second impact limiter.

During deceleration of the leading end of the cask, the trailing end continues to accelerate while translating vertically because no deceleration force is applied to it. Newton’s first law, “Every body persists in its state of rest or of uniform motion in a straight line unless it is compelled to change that state by forces impressed on it...” (Resnick, page 75), requires the cask’s trailing end to continue to translate vertically and to be accelerated by gravity until the second impact limiter contacts the unyielding surface. However, because the cask body is rigid, when the leading end of the cask stops, the trailing end of the cask continues translating and the cask begins to pivot on the crushed leading impact limiter. This continues until the second impact limiter contacts the unyielding surface and generates significant deceleration forces as it is crushed.

The second action, occurring while the leading end of the cask is decelerating, is a vector component of the deceleration force at the leading end of the cask, which causes the cask to rotate around its center of gravity. The deceleration force is always perpendicular to the unyielding surface. Depending on the cask angle, the deceleration force can be vectorially broken down into a force component parallel to, and a force component perpendicular to, the cask longitudinal axis. The perpendicular force component acts at a distance of approximately half of the cask length from the cask center of gravity. A torque, equivalent to the perpendicular force

component multiplied by half of the cask length attempts to "spin" the cask around the center of gravity. The spin or rotational velocity can also be thought of as rotational kinetic energy that must be absorbed by the second impact limiter. A detailed explanation of the torque and rotational kinetic energy is presented in the following paragraphs.

Finally, the third component of energy that must be absorbed by the second impact limiter is the energy stored elastically in the first impact limiter. The elastically stored energy produces a force perpendicular to the unyielding surface that augments the rotational velocity of the cask and tends to "lift" the lower end of the cask, which is at rest.

Oblique drops have four distinct quantities of energy that need to be absorbed to bring the cask to rest in a stable, horizontal orientation. These quantities are:

1. Potential energy (E1) absorbed by the impact limiter, which impacts on the unyielding surface first and brings the translational velocity of the leading end of the cask to zero.

2. Potential energy remaining (ER) after the first impact.

3. Potential energy (EP) of the cask by virtue of the height of its center of gravity above the unyielding surface after the first impact.

4. Rotational kinetic energy of the cask produced by the deceleration force and the elastically stored energy (ES), which results from the initial impact of the leading end of the cask.

The total amount of energy (ET) to be dissipated after a cask drop is calculated as:

$$ET = E1 + ER + EP + ES$$

where:

E1 = energy absorbed during the first impact
ER = remaining energy after the first impact
EP = rotational potential energy
ES = elastically stored energy

The sum of the last three terms equals the energy absorbed by the second impact limiter (secondary impact). Terms E1, ER and EP can be calculated; however, testing the redwood and balsa wood in an impact limiter configuration was necessary to determine ES.

The impact limiter evaluation in Section 2.6.7.4 outlines an analysis of the NAC STC impact forces developed during the 30-foot hypothetical accident free drop. That analysis addresses the maximum force imparted to the cask through one impact limiter, resulting from the initial impact with the unyielding surface for various cask orientation angles. The following discussion addresses the primary impact loads (first impact limiter) on the cask structure. It also addresses the adequacy of the second impact limiter to absorb, for an oblique cask orientation, the remaining energy during the secondary impact on the unyielding surface. The geometry of the NAC-STC package is shown in Figure 2.10.7-4.

Based on 30-foot drop testing of a quarter-scale model of the NAC-STC, the secondary impact phenomenon has been reviewed. It has been concluded that elastically stored "rebound" energy (5 to 10 percent of the primary impact energy) may be restored to the cask in such a manner as to cause the leading end of the cask to lift from the ground several inches during the secondary impact (slapdown). Thus, the rebound energy must be dissipated by the second impact limiter.

Table 2.10.7-1 shows that at impact angles of 60 degrees and 75 degrees, the energy dissipated in the impact limiter during the secondary impact (E2) is greater than the energy dissipated in one impact limiter in a side impact, so that the cask "slaps down". This is because the residual drop energy not absorbed in the first impact (energy transformed to rotational energy), impact limiter rebound energy (elastic rebound), and potential energy converted to kinetic energy as the cask rotates to the second impact, all combine to exceed the energy absorbed by one limiter in a pure side drop orientation. Results of the model impact limiter tests show that the impact limiters do have sufficient energy absorption capacity to absorb the energy of the 60-degree and 75-degree oblique secondary impacts.

The calculation of E1 in the proprietary NAC impact limiter analysis program, RBCUBED (Section 2.10.1.2), is performed by solving the equations of motion for the cask. These equations are based on the force developed by the impact limiter as it crushes. The impact limiter force is equal to the crush strength of the redwood and balsa wood multiplied by the "backed" crush area. The RBCUBED program calculates this area as a function of the impact angle and crush depth, using a system of solid geometry subroutines developed by Oak Ridge National Laboratories as

part of the MORSE shielding code. These crush area calculations have been verified by manual calculation of crush area using graphical drafting techniques for several impact angles and crush depths. The accuracy of the area calculation may be shown by inspection of the model impact limiter results presented in Figures 2.10.6-12 through 2.10.6-14, which show that the RBCUBED force (the crush area times the crush strength) accurately tracks the measured force.

The impact limiter force is normal to the unyielding surface and is applied to the cask body, as shown in Figure 2.10.7-3. The cask's weight continues to accelerate the cask downward as the impact limiter decelerates, producing a crush force (FD), which decelerates the cask. During the initial contact of an impact limiter with the unyielding surface, the cask weight causes the net force to accelerate the cask downward until the crush area (footprint) becomes large enough to overcome the cask weight and produce a net deceleration.

The net force applied to the cask produces a force and deceleration parallel to the cask's longitudinal axis as well as a force and angular acceleration perpendicular to the longitudinal axis, as shown in Figure 2.10.7-3. The parallel force component acts on the cask center of mass to slow the cask down, but the perpendicular component transforms translational kinetic energy from the drop into rotational energy that must be absorbed in the secondary impact.

The calculations to determine the energy to be dissipated for each drop angle shown in Table 2.10.7-1 include the potential energy resulting from the cask tipping over to a horizontal position and elastically stored rebound energy from the first impact.

The cask and impact limiters are considered to be a mass (m). When the mass drops from rest, a distance (h), it is accelerated uniformly by gravity (g). Because the mass is not acted upon by any forces while free falling, it will remain in the same orientation that it had when it was released. The change in potential energy equals the change in kinetic energy. The vertical velocity of the mass at the time of contact with the unyielding surface is calculated as:

$$V_i = (2gh)^{0.5}$$

where:

V_i = vertical velocity of cask (ft/sec) at time of impact (t = 0 sec)
g = the gravitational constant (ft/sec^2)
h = the drop height (ft)

The cask may impact at any angle (0° to 90°). In the case of impact orientations from an end drop through a corner drop, the cask could be expected to remain upright after the total energy of the first impact is absorbed; as a result, the center of gravity does not have a moment arm, which would provide a rotational moment about the cask base, causing the cask to tip over. However, the calculated energy shown in Table 2.10.7-1 does include the energy of the tipover for conservatism for the corner drop impact. Ignoring elastically stored energy, the total energy that must be absorbed to bring the cask to rest for a corner impact is:

$$E_T = mg(h + H)$$

where:

E_T = total energy to be absorbed (in-lbf)
m = mass of the cask and limiters (lbm)
g = acceleration due to gravity (ft/sec^2)
h = height of drop (ft)

$$H = \frac{(L/2)}{\cos\left[\mathrm{Tan}^{-1}\left(\frac{D/2}{L/2}\right)\right]}\left[\cos\left|q - \mathrm{Tan}^{-1}\left(\frac{D/2}{L/2}\right)\right|\right] - (D/2)$$

For oblique drops within the range from corner drop to side drop, the total energy absorbed is greater than that for the end to corner range, if one ignores cask tipover and elastically stored energy. Cask impact angles greater than 75 degrees are considered to be side drops because the leading impact limiter stops the cask as the trailing impact limiter begins to absorb energy.

In oblique drops, the center of gravity will fall a distance greater than the drop height, h. The additional distance the center of gravity must fall is L/2 (cosq) (Figure 2.10.7-3), where L is the length of the cask body. Therefore, the total energy that must be absorbed to bring the cask to rest for impact orientations in the range from a corner drop to a side drop is again:

$$E_T = mg(h + H)$$

The total energy to be absorbed is greatest for the corner impact because the cask center of gravity must travel through the greatest distance from the initial impact position to the horizontal position. The total energy absorption capacity required is determined by summing E1 and E2 for each drop angle.

For cask impact orientations beyond a corner drop, the center of gravity of the cask is unsupported. The net crush force is applied at one end of the cask, resulting in a torque (T), possibly causing rotation of the cask about its center of gravity. As the cask is translating vertically while decelerating, it is also rotating around the end that is crushing. The cask is also attempting to rotate around the center of gravity due to the torque applied to the decelerating end of the cask by the perpendicular component ($F_{d^\wedge}$) of the crush force. The applied torque is:

$$T = F_{d\perp}\frac{L}{2}$$

$$= F_d \sin\theta \frac{L}{2}$$

where:

T = torque (in-lb)
L = cask length (in)
F_d = deceleration force (lb)

The impulse equation for an applied torque is:

$$T\Delta t = I\Delta w$$

where:

Δt = increment of time (sec)

I = moment of inertia of a cylinder (cask) about its center of gravity

$$= \frac{mL^2}{12}$$

$\Delta\omega$ = change in angular velocity (rad/sec)

The angular velocity is equal to the rotational velocity change (ΔV_t) divided by the radius:

$$\Delta\omega = \frac{\Delta V_t}{L/2}$$

Substituting for Dw in the impulse equation:

$$T\Delta t = \frac{I\Delta V_t}{L/2}$$

Substituting and solving for ΔV_t:

$$\Delta V_t = \frac{F_d \sin\theta \, \Delta t \, L^2}{4I}$$

Substituting the formula for I for a cylinder yields:

$$\Delta V_t = \frac{F_d \sin\theta \, \Delta t \, 3g}{W_T}$$

Note that the same result for ΔV_t is obtained by regarding the cask as rotating about one end.

This change in transverse velocity is subtracted from the transverse component of the initial velocity to determine the transverse velocity of the cask at the beginning of the next deformation step (δ'). When the sum of the transverse velocity changes equals the initial velocity, the leading end of the cask has been stopped along an axis normal to the longitudinal axis of the cask.

2.10.7.2 Conversion of Potential Energy to Kinetic Energy

Just prior to a drop, the cask is at rest in a given orientation. The uniform gravitational force constantly acts on the cask and accelerates the cask at a constant rate. Gravitational acceleration (g) equals 32.2 feet/second/second. No other forces act on the cask during a drop; therefore, the cask acquires no additional energy during a drop. Uniform forces acting on the cask will not change the orientation of the cask while it is falling. Since energy can't be created or destroyed, the initial potential energy of the cask is converted to kinetic energy. To calculate the velocity at the time the impact limiter contacts the unyielding surface, conservation of energy is used as follows:

$$PE = KE$$

or

$$mgh = \frac{1}{2} mv^2$$

Solving for v:

$$v = (2gh)^{0.5}$$

The initial velocity (at the time crushing begins) is only a function of drop height. For a drop height of 30 feet, the velocity of the cask at the time that the leading impact limiter contacts the unyielding surface is 44.0 feet/second.

The correlation between potential energy and kinetic energy is the foundation on which the computer program RBCUBED is based. Translational velocity (translational kinetic energy), which the cask attains while free falling or while pivoting on end (oblique drop), is a direct function of the initial potential energy of the cask. Rotational velocity (rotational kinetic energy) results during an oblique drop while the leading end of the cask is decelerated; elastically stored energy is a small, calculable quantity of energy. When the total energy absorbed is equal to the sum of the potential energy dissipated during the initial impact, the rotational kinetic energy, and the elastically stored energy of the cask, then the cask is at rest.

2.10.7.3 Deceleration Forces and Energy Absorption Calculation

The following quotation describes how an impact limiter works: "...the kinetic energy of a body in motion is equal to the work it can do in being brought to rest..." (Resnick, page 75). The source of kinetic energy in a cask was established in Section 2.10.7.2. The work done by the force crushing the impact limiter is the magnitude of that force multiplied by the distance (deformation) through which the crush occurs. The units of work are inch-pounds.

The NAC-STC cask redwood impact limiters are right cylindrical stainless steel shells filled with redwood and balsa wood. The wood is used to dissipate the kinetic energy of the cask, and is crushed when a nominal force per unit area is applied to the impact limiter. The redwood and balsa wood show nominal crush strength in the plane that is parallel to the grain direction. The redwood and balsa wood are specified and tested to ensure that the crush strength is within design criteria tolerances. Wedges of wood are bonded together to form a solid cupped cylinder with uniform properties around its circumference. A thin stainless steel shell is welded around each impact limiter to prevent cosmetic, contamination, or decomposition damage.

The wood impact limiter crushes because it is trapped between the cask and the unyielding surface. The initial energy (PE) of the cask will have an equivalent amount of kinetic energy (KE) just before the impact limiter contacts the unyielding surface. When the impact limiter contacts the unyielding surface, it immediately comes to rest; however, the cask continues to move into the impact limiter until it is opposed by a force vector. To explain the work done in stopping the cask, an illustrative example of an end drop is presented:

> The cask weighing 250,000 pounds, is assumed to have been dropped 8.8 inches; PE = KE = 2.2×10^6 inch-pounds. The velocity of the cask when the impact limiter contacts the unyielding surface is 6.87 feet/second (82.5 in/sec).

The cask is a rigid structure and each end has an area of approximately 5,904 square inches. Nominal crush strength of the redwood is 6,240 psi. The cask is rigid and isolates, or "backs", the wood; the backed wood effectively stops the cask. The force required to crush the backed wood is 36.84×10^6 pounds. When the backed wood crushes 0.05 inch, 1.84×10^6 inch-pounds of work is performed:

$$W = (F)(d)$$
$$= 1.84 \times 10^6 \text{ in-lb}$$

where:

$F = 36.84 \times 10^6$ lb
$d = 0.05$ in

Using the definition of work and Newton's second law, F = ma, yields the following derivation:

$$W = \frac{1}{2} mv^2 - \frac{1}{2} mv_o^2$$

where:

W = work performed on a particle, in-lb (work performed on the cask by the wood is negative)
m = mass of the cask (weight of the cask divided by the gravitational constant 32.2 ft/sec^2), lbf-sec^2/ft
v = velocity of the cask after the work is performed, ft/sec
v_o = initial velocity of the cask, ft/sec

Solving for the velocity after an incremental amount of work has been performed:

$$v = \sqrt{\frac{2W}{m} + v_o^2}$$

Substituting for W, m, v_o and adjusting for correct units, the cask velocity after the first crush increment is 2.77 feet/second. Repeating this analysis for another 0.05-inch increment shows that after another fraction of a crush increment, the cask is stopped.

In summary, the force (a vector quantity) that is created by crushing the wood opposes the cask's velocity, which is also a vector quantity. Crushing an incremental amount of wood is a finite quantity of work performed on the cask, decreasing the cask's velocity and kinetic energy. Once the kinetic energy is completely dissipated, the cask velocity equals zero.

RBCUBED, the impact limiter computer program used to design the redwood impact limiters, functions in exactly the same way as the illustrative example. Cask geometry and weight, drop angle, crush increment, wood crush strengths, wood lock-up stroke and wood geometry are entered into the program. RBCUBED calculates an initial velocity (as the limiter touches the unyielding surface), a backed area engaged in crushing, a crush force, the energy absorbed for a crush increment, the elapsed crush time and the cask velocity at the end of the crush increment. The computation cycle is repeated until all the kinetic energy is absorbed and the end of the cask is stopped.

RBCUBED calculates the energy dissipation necessary to stop the translational motion of the end of the cask that first contacts the unyielding surface (both limiters in the side drop). In Table 2.10.7-1, the energy dissipated while reducing the translational velocity of the first end to contact the unyielding surface is the energy absorbed by the first limiter (E1). If E1 is less than the initial kinetic energy of the cask, the difference is reported by RBCUBED as "remaining energy," and shown in Table 2.10.7-1 as energy remaining after first impact (ER).

In oblique drops, at the instant the translational velocity of the first end to contact the unyielding surface is zero, the cask is in position 2 in Figure 2.10.7-3. (Rotation of the cask around its mid-point is addressed in Section 2.10.7.2.) The center of gravity of the cask has a calculable potential energy, which is the energy that increases the velocity of the cask as it pivots on the crushed

("first") impact limiter. In Table 2.10.7-1, the potential energy, which equals the velocity gain as the cask pivots on end, is the potential energy of the cask after the first impact (EP).

The redwood and balsa wood dissipate energy while crushing, but elastically store a small amount of the total energy dissipated. The quantity of elastically stored energy was determined by quasi-static testing of scale model impact limiters (Section 2.10.7.5). The quantity of stored energy ranged between 8.2 percent (side drop) to 7.2 percent (end drop) of the total energy dissipated by the impact limiters tested. As stated above, once the first end of the cask is stopped, the stored energy is released. The force, which the stored energy creates, tends to augment the torque attempting to cause the cask to spin around the center of gravity. This analysis has conservatively ignored the cask spinning and assumes that the energy is absorbed by the second impact limiter. In Table 2.10.7-1, the elastically stored energy (conservatively considered to be 8.2 percent of the total energy dissipated by the leading impact limiter) is the energy stored in the leading impact limiter and absorbed in the second impact limiter while in the side drop orientation (ES).

In summary, the translational velocity of the leading end of the package is reduced to zero by absorbing an amount of energy (E1). The cask will pivot over and absorb--the remaining potential energy (ER), the potential energy resulting from the rotation to a horizontal orientation (EP), and the elastically stored energy (ES)--all in the second impact limiter in the side drop orientation. Table 2.10.7-1 shows that the four components of energy are absorbed by both impact limiters for impact angles from 0 to 90 degrees.

2.10.7.4 RBCUBED Calculated Force-Deflection Graphs

Figures 2.10.7-5 through 2.10.7-11 show the deceleration force as a function of crush depth, calculated using RBCUBED for the full-scale cask impact limiters. Each curve is for either the upper or lower impact limiter, showing the plus and minus tolerance energy absorption profile. Quasi-static tests of eighth-scale model impact limiters further substantiate the RBCUBED calculated values, as described in Section 2.10.6.4. Table 2.10.7-2 provides a comparison of the maximum deceleration values obtained from: (1) the eighth-scale model impact limiter compression tests; (2) RBCUBED impact limiter analysis program; (3) the quarter-scale model drop tests; and (4) the NAC-STC design criteria.

Figure 2.10.7-1 Side Drop

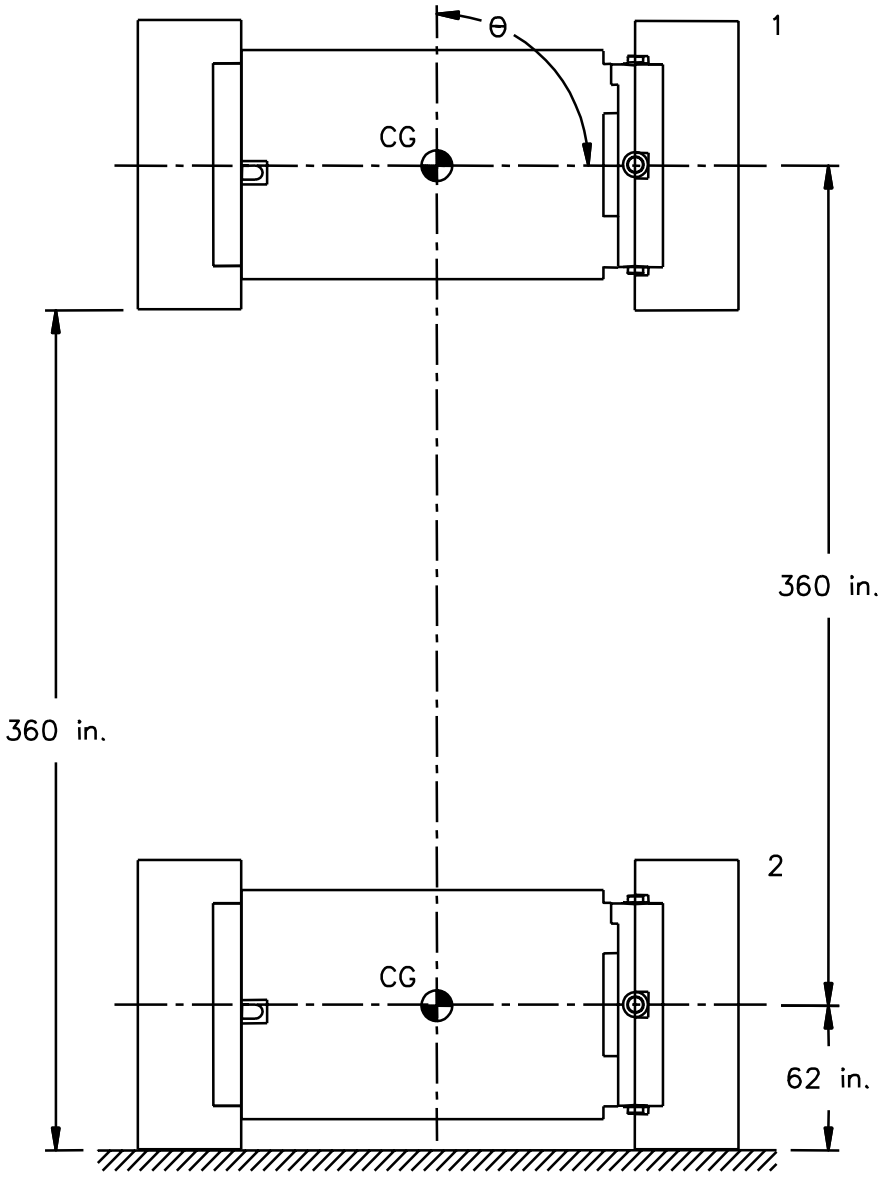

Figure 2.10.7-2 End Drop

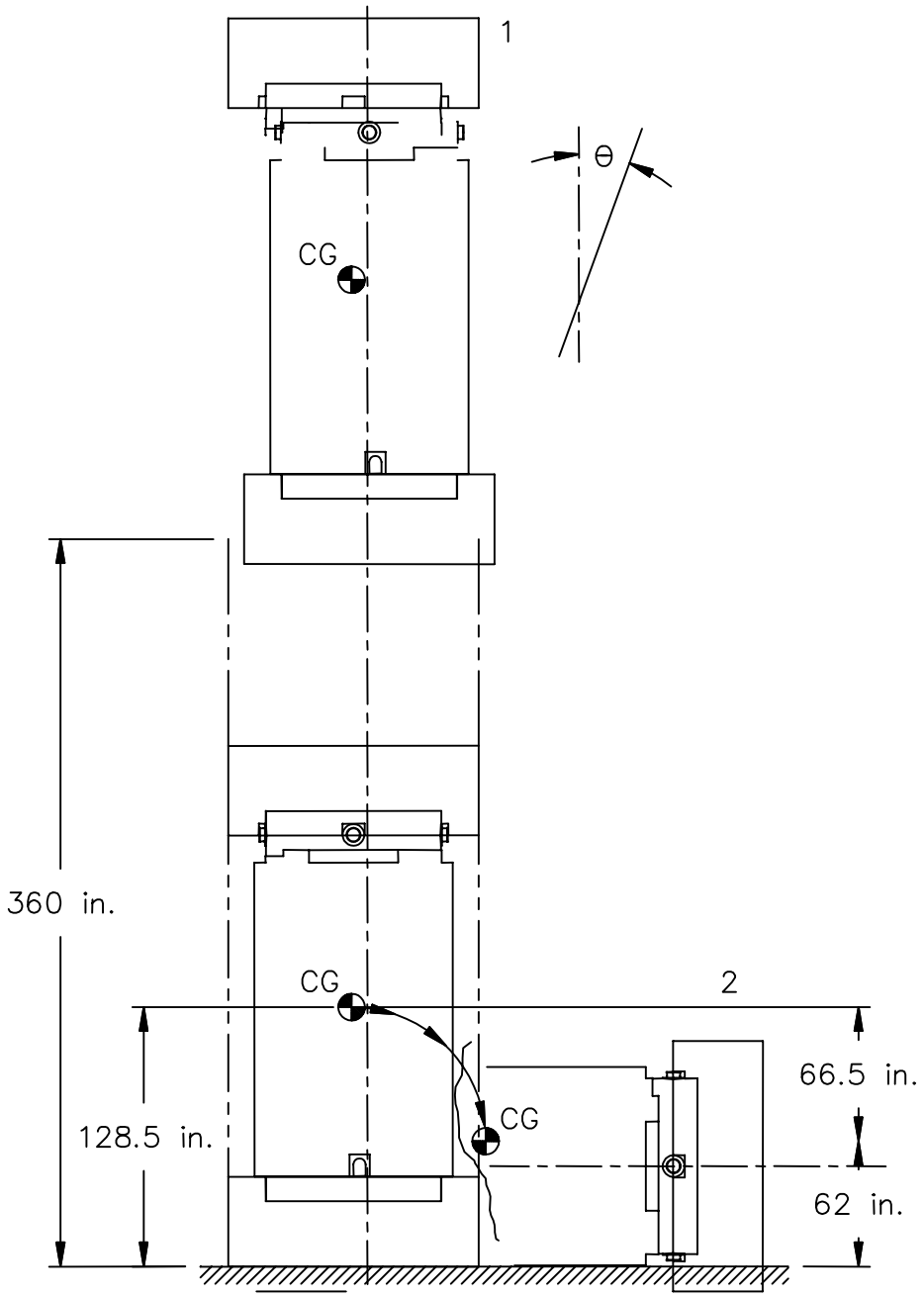

Figure 2.10.7-3 Oblique Drop

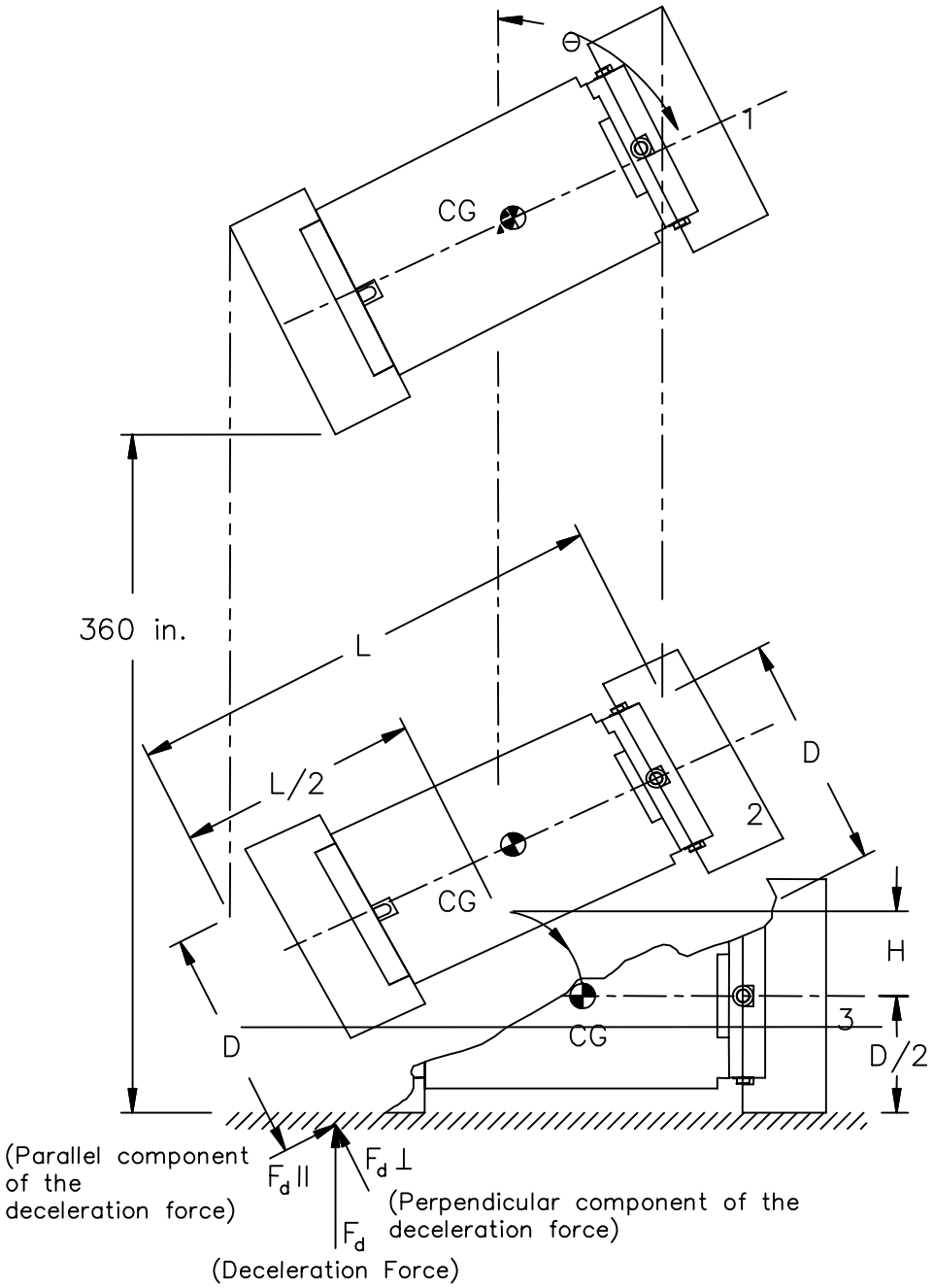

Figure 2.10.7-4 Cask Slapdown Geometry

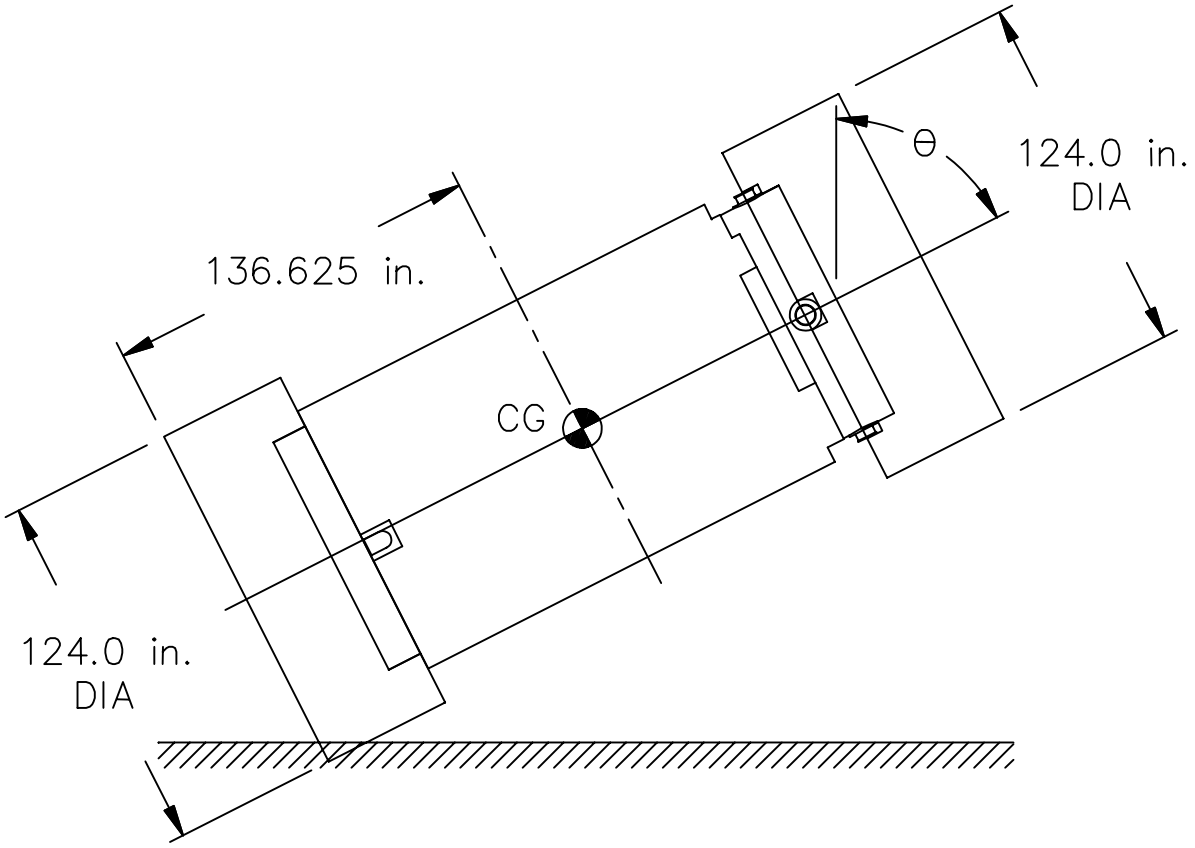

Figure 2.10.7-5 Force-Deformation Curve - Lower Redwood Impact Limiter (Bottom End Impact, 0 Degrees)

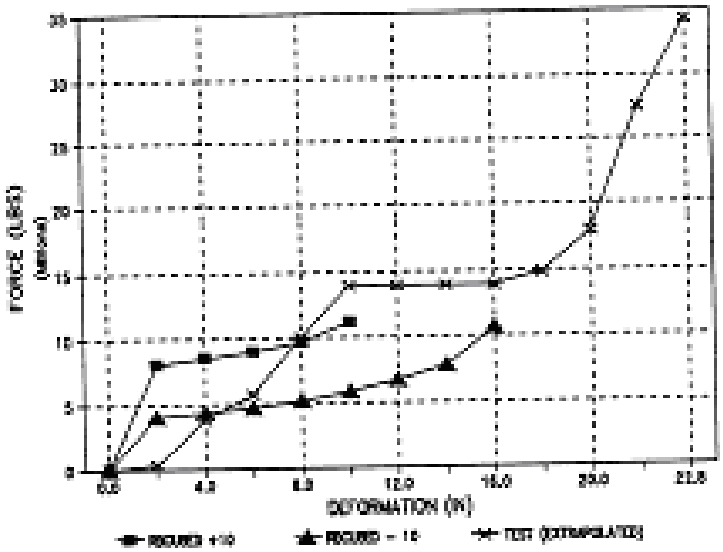

Figure 2.10.7-6 Force-Deformation Curve - Lower Redwood Impact Limiter (Bottom Corner Impact, 24 Degrees)

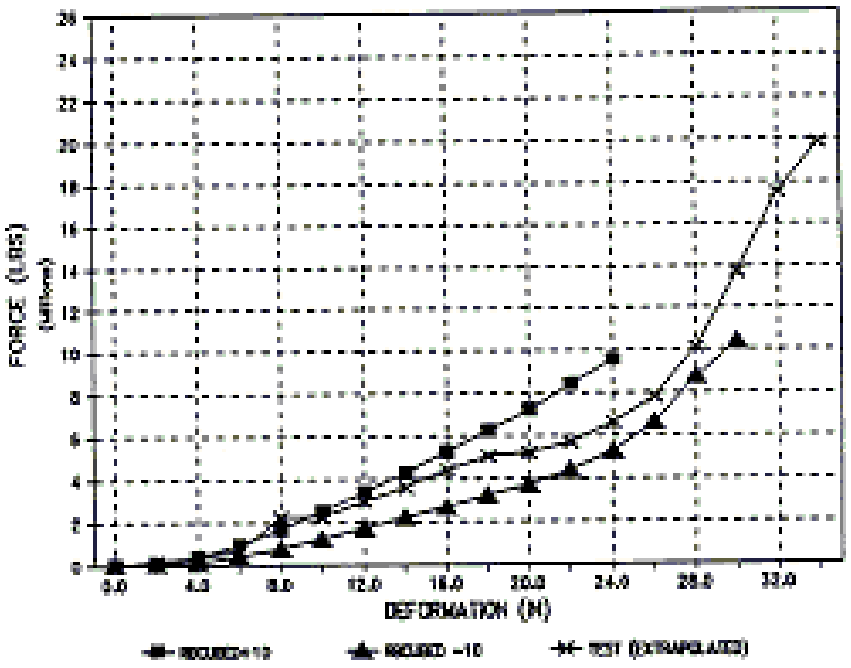

Figure 2.10.7-7 Force-Deformation Curve - Lower Redwood Impact Limiter (Bottom Oblique Impact, 75 Degrees)

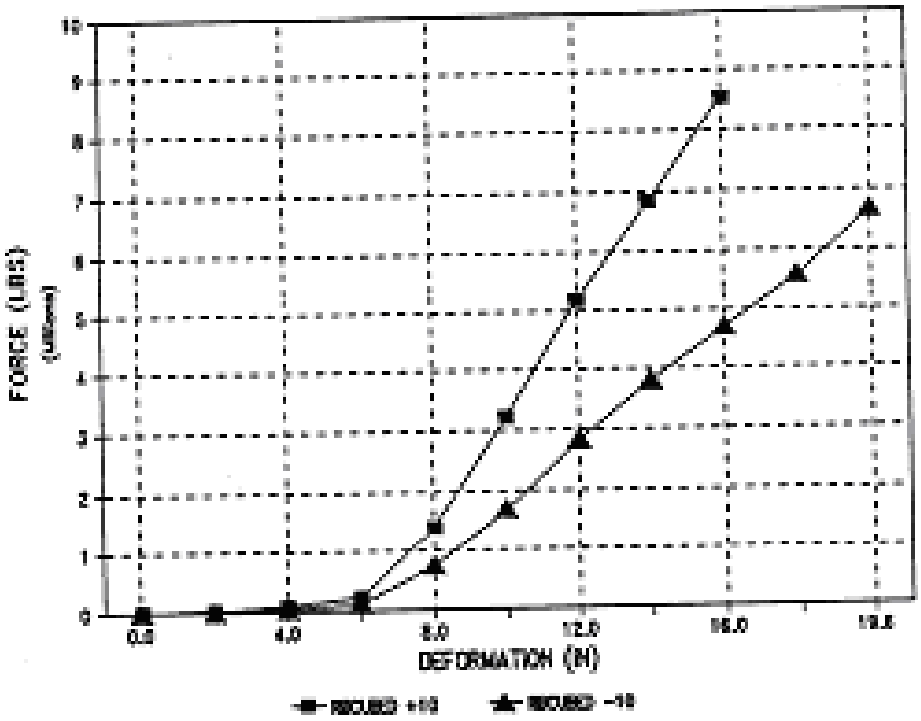

Figure 2.10.7-8 Force-Deformation Curve - Upper Redwood Impact Limiter (Top End Impact, 0 Degrees)

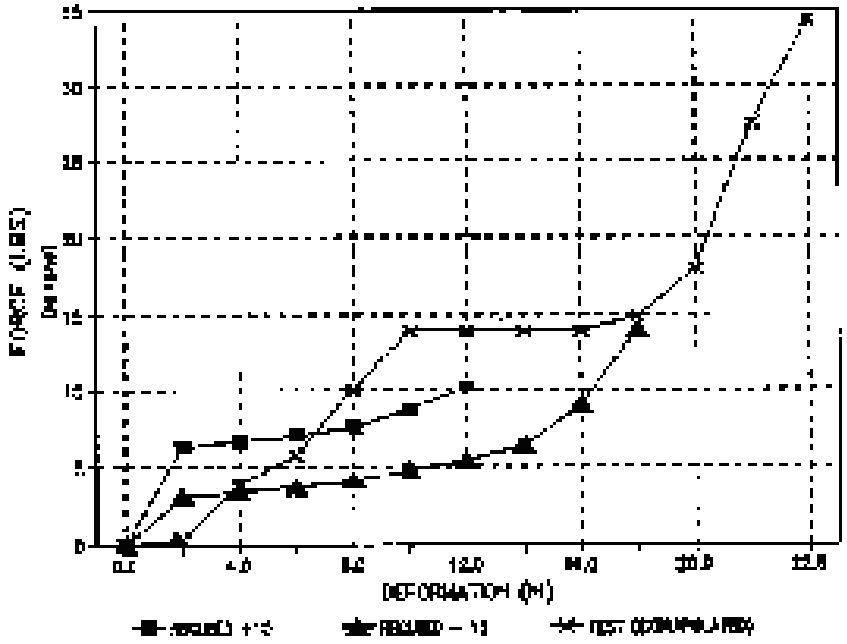

Figure 2.10.7-9 Force-Deformation Curve - Upper Redwood Impact Limiter (Top Corner Impact, 24 Degrees)

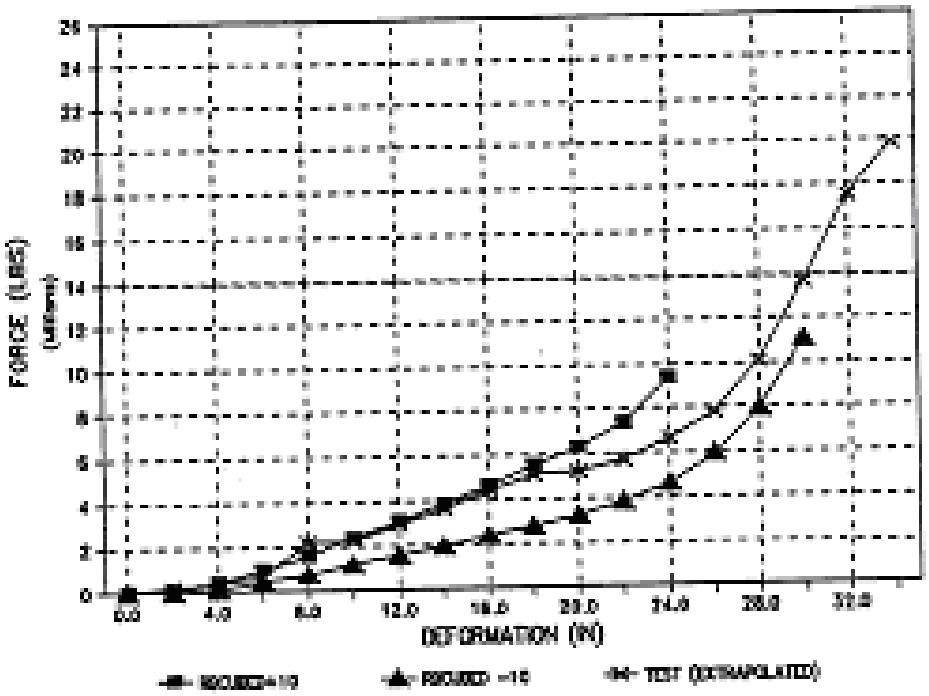

Figure 2.10.7-10 Force-Deformation Curve - Upper Redwood Impact Limiter (Top Oblique Impact, 75 Degrees)

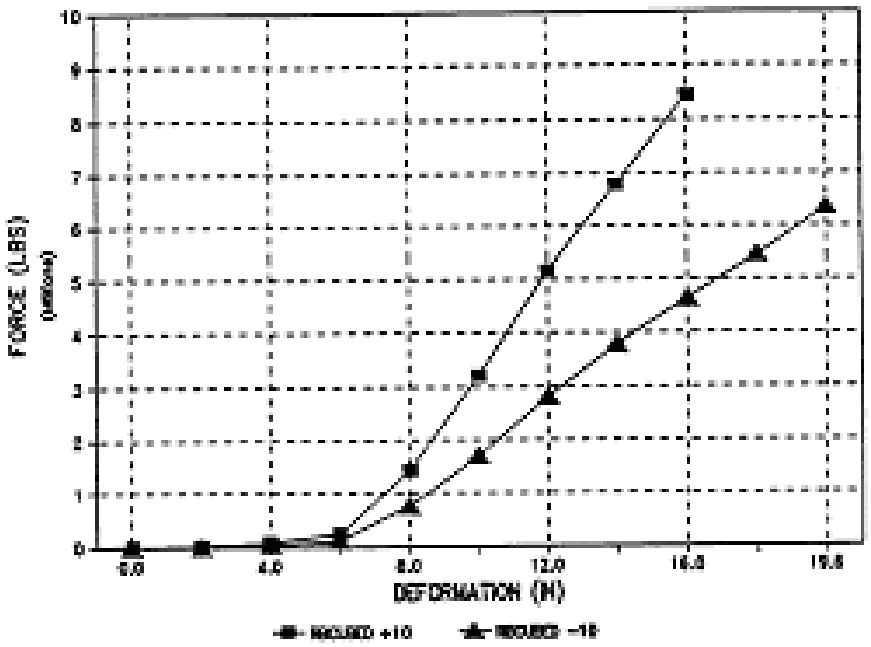

Figure 2.10.7-11 Redwood Impact Limiter Force-Deformation Curve - Side Impact (90 Degrees)

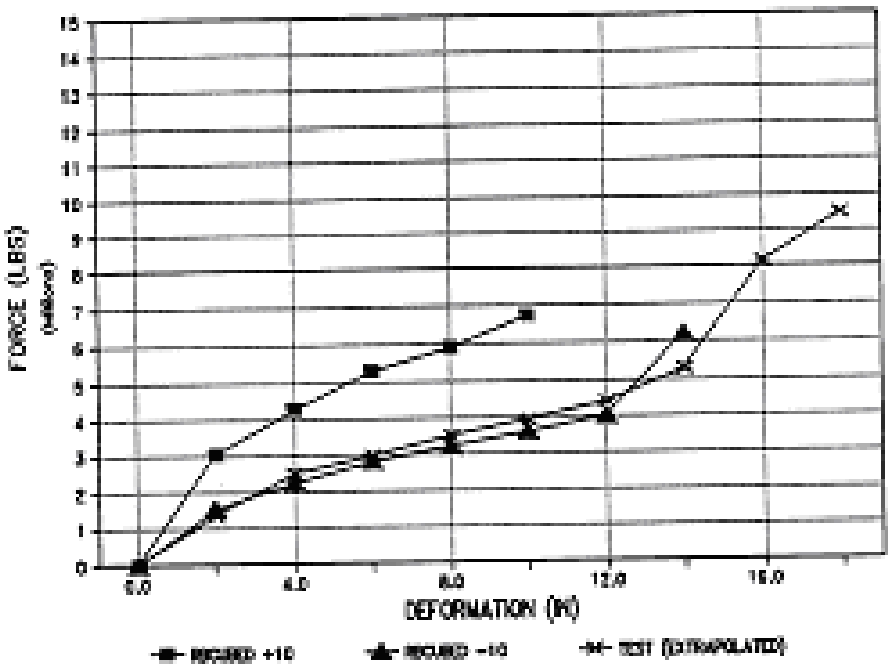

Table 2.10.7-1 Determination of Maximum Energy Remaining for Secondary Impact – Full-Scale Redwood Impact Limiter

DROP ANGLE	**24°**	**30°**	**45°**	**60°**	**75°**
[1]E1 Energy absorbed by first limiter (in-lb)	9.15×10^7	8.66×10^7	7.49×10^7	5.94×10^7	4.38×10^7
[1]ER Energy remaining after first impact (in-lb)	3.99×10^6	8.02×10^6	1.93×10^7	3.21×10^7	4.66×10^7
[2]EP Potential energy of cask after first impact (in-lb)	2.02×10^7	2.01×10^7	1.82×10^7	1.40×10^7	0.78×10^7
[3]ES Energy stored in first limiter; absorbed in second limiter in side drop orientation (in-lb)	7.51×10^6 (8.2%)	7.10×10^6 (8.2%)	6.14×10^6 (8.2%)	4.87×10^6 (8.2%)	3.59×10^6 (8.2%)
E2 Secondary impact total of ER + EP+ ES (in-lb)	3.17×10^7	3.52×10^7	4.36×10^7	5.10×10^7	5.80×10^7
[4]Emax - Side Drop Maximum energy absorption capability of impact limiter in side drop orientation(in-lb)	6.35×10^7	6.35×10^7	6.35×10^7	6.35×10^7	6.35×10^7
Energy Absorption Margin of Safety	+1.01	+0.80	+0.45	+0.24	+0.09

[1] From RBCUBED impact limiter analysis.

[2] Calculated based on Figure 2.10.7-2.

[3] Estimated springback based on quasi-static compression tests.

[4] Extrapolated from quasi-static compression tests.

Table 2.10.7-2 Comparison of Full-Scale Deceleration Values for 30-Foot Drop Impacts

Drop Orientation	30-Foot Drop Deceleration (g)				
	RBCUBED[1] (Cold)	RBCUBED[1] (Hot)	Quasi-Static[2] Test	Drop Test[3]	Design[4]
End (0°)	44.6	56.1	54.8	55.6	56.1
Corner (24°)	44.0	49.3	32.6	29.2	55.0
Oblique (75°)	29.9	24.0	-	53.8	55.0
Side (90°)	51.7	51.3	45.6	51.3	55.0

1. Impact g-loads calculated by RBCUBED (NAC's proprietary Impact Limiter Analysis Program).
2. Extrapolated from eighth-scale model impact limiter quasi-static compression tests. Details are provided in Section 2.10.6.4.
3. Extrapolated from quarter-scale model 30-foot drop test results. Details are provided in Section 2.10.6.5.
4. Design g-load values used in the cask and fuel basket analyses.

2.10.8 Bolts - Closure Lids (Stress Evaluations)

This section presents the analytical methods, assumptions, and detailed example calculations for the evaluation of the stresses in the inner and the outer lid bolts for selected impact orientations. This evaluation is applicable for both the directly loaded fuel and the canistered fuel configurations of the NAC-STC. The bounding load condition for the NAC-STC inner lid bolt evaluation is the combined weight of the loaded CY-MPC, canister spacers and inner lid multiplied by an appropriate acceleration factor. The bounding weight for the outer lid bolts evaluation is the combined weight of the redwood impact limiter and the outer lid.

The detailed analyses of the inner and outer lid bolts consider impact orientations at 5-degree intervals from 0-degrees to 90-degrees. The structural analyses of the inner lid bolts and the outer lid bolts for the normal conditions of transport and the hypothetical accident conditions are presented in Sections 2.6.7.5 and 2.7.1.6, respectively. Tables 2.6.7.5-1 and 2.6.7.5-2 summarize the inner lid bolt stresses for the normal conditions of transport "hot" 1-foot drop and the "cold" 1-foot drop, respectively. Tables 2.6.7.5-3 and 2.6.7.5-4 summarize the outer lid bolt stresses for the normal conditions of transport "hot" 1-foot drop and the "cold" 1-foot drop, respectively. Tables 2.7.1.6-2 through 2.7.1.6-5 summarize the corresponding "hot" and "cold" 30-foot drop accident condition stresses for the inner lid bolts and outer lid bolts. The inner lid bolts and the outer lid bolts are evaluated for the Thermal (fire) accident condition in Section 2.7.3.4.

2.10.8.1 Analysis Approach

The inner and outer lid bolt stress analyses for normal transport and hypothetical accident conditions consider the impact loads, pressure loads, thermal loads and bolt preloads. Each summary table of bolt stresses is preceded with an explicit listing of relevant geometry, mechanical properties and constant loading data (bolt torque, pressure, etc.) taken directly from Sections 2.1, 2.2, 2.3 and the license drawings in Section 1.3.2.

The NAC-STC inner and outer lid bolts are evaluated for the hypothetical accident free drop condition in the following example calculations. Impact loads are expressed in design g acceleration loads as summarized in Tables 2.6.7.4.2-1 and 2.6.7.4.2-2 for the balsa impact limiters and in Tables 2.6.7.4.1-3 and 2.6.7.4.1-4 for the redwood impact limiters.

The "hot" condition temperature of the lid bolts used for the impact evaluations is conservatively defined as 270°F for this example calculation. The "cold" condition temperature of the inner lid bolts is -20°F, per regulatory requirements. Allowable stress limits and material properties for the lid bolts are taken at 270°F and at room temperature (70°F) for the "hot" and the "cold" conditions, respectively. The allowable bolt tensile stress is taken as the material yield strength, S_y, at operating temperature as defined in Tables 2.1.2-1 and 2.1.2-2. For conservatism, external energy absorber reaction forces, which resist separation of the cask lid and body, are completely neglected in all calculations.

An explanatory discussion of bolt stress analysis is found in Section 2.10.8.2. Table 2.7.1.6-2 contains the results of the bolt stress analysis. An example calculation is included with each note to verify the accuracy of the tabular calculation.

The analysis methodology, allowable stress values, and basic assumptions used are consistent with conventional design/analysis codes, such as "AISC Manual of Steel Construction," 8th Edition, and "ASME Boiler and Pressure Vessel Code," Section III, Appendix F, Paragraph F-1335, but this analysis is more conservative. Specifically, this analysis includes stresses associated with the bolt preloads. Conventional design/analysis codes consider only externally applied loads and ignore preloads.

Like the methodology given in the "ASME Boiler and Pressure Vessel Code," Appendix F, Paragraph F-1335, this analysis uses nominal tensile and shear stresses based on the tabulated stress area of the bolts. It should be noted that the elliptic interaction equations of Paragraph F-1335.2 of the "ASME Boiler and Pressure Vessel Code" and the approach used here give nearly identical results when adjustments in loadings are made to account for the differing treatment of preload tension (This approach conservatively includes preloads, whereas the code approach ignores preloads).

2.10.8.2 Inner Lid Closure Bolt Analyses

All numerical examples pertain to the evaluation of the inner lid bolts of the NAC-STC with the CY-MPC canistered fuel under hypothetical accident conditions (Table 2.7.1.6-2). Note that the required minimum preload is evaluated on the basis of the Yankee-MPC end impact condition, which produces the bounding weight × g-load factor result. The Yankee-MPC end impact condition is also used to determine the maximum lid bolt stresses for the end drop. All other drop orientations are bounded by the CY-MPC content weight and g-load factors.

2.10.8.2.1 Bolt Force – Preload

Preload evaluation considers the following factors: (1) an internal pressure force on the closure lid; (2) the o-ring compression force; and (3) the weight of the inner cask lid, canister, and canister contents multiplied by the g-load associated with a 30-foot end drop accident event, which bounds the g-load corresponding to the other drop orientations of the cask.

The required bolt preload to offset the combined static and dynamic loads is determined by:

$$F_b = F_s + F_a$$

where:

F_b = calculated required bolt preload
F_s = total static load
F_a = total dynamic (impact) load

The cask lid closure bolt preload necessary to offset static loads is:

$$\begin{aligned} F_s &= F_{press} + F_{or1} + F_{or2} \\ &= 4{,}578 \text{ lb} + 2{,}208 \text{ lb} + 2{,}250 \text{ lb} \\ &= 9{,}036 \text{ lb} \end{aligned}$$

where:

F_s = total static load per bolt (lb)
F_{press} = internal pressure force per bolt (lb)

$$\left(\frac{PA}{N_b}\right) = \left(45.3 \text{ psig} \times \frac{(73.51 \text{in.})^2 \pi}{4}\right) \div 42 \text{ bolts} = 4{,}578 \text{ lb}$$

where:

P = internal cask lid pressure = 45.3 psi
A = area (in.²) of the cask lid at the o-rings, based on 73.51 in. diameter
N_b = number of cask lid closure bolts
F_{or1} = inner o-ring compression force per bolt (lb)

The higher internal pressure (P) of the Yankee-MPC configuration is conservatively used to determine bolt preload.

$$F_{or1} = \frac{\pi(D_f)(D_{imor})(P_c)}{N_b} = \frac{\pi(1.0)(72.00)(410)}{42} = 2{,}208 \text{ lb}$$

where:

D_{imor} = diameter of inner (metal) o-ring = 72.00 in (71.89 in. actual)
D_f = design factor of Type 321 material = 1.0
P_c = inner o-ring compression force = 410 lb/in
N_b = number of bolts = 42
F_{or2} = outer o-ring compression force per bolt (lb)

$$F_{or2} = \frac{\pi(D_f)(D_{omor})(P_c)}{N_b} = \frac{\pi(1.0)(73.36)(410)}{42} = 2{,}250 \text{ lb}$$

where:

D_{omor} = diameter of outer (metal) o-ring = 73.36 in
P_c = outer o-ring compression force = 410 lb/in
N_b = number of bolts = 42

The axial component of the maximum 30-foot drop acceleration is 56.1g is used to determine the required bolt preload.

The end impact component of the load (F_a) on the cask inner lid is calculated as:

$$F_a = \frac{P_a}{N_b} = \frac{3{,}741{,}309}{42} = 89{,}079 \qquad \text{[Equation 1]}$$

$$P_a = (W_a \times g) = (66{,}690 \text{ lb} \times 56.1g) = 3{,}741{,}309 \text{ lb}$$

where:

W_a = weight of the loaded canister + canister spacer + inner lid = 66,690 lb
g = conservative drop g-load = 56.1g
N_b = number of bolts = 42

Therefore, the calculated required preload per bolt, F_b, is:

$$F_b = F_s + F_a = 9{,}036 \text{ lb} + 89{,}079 \text{ lb} = 98{,}115 \text{ lb}$$

The total torque (T) to develop the required axial bolt preload (F_b) is:

$$T = \left[\left(\frac{d_m}{2d}\right)\left(\frac{\tan\lambda + \mu\sec\alpha}{1 - \mu\tan\lambda\sec\alpha}\right) + 0.625\mu\right](F_b)(d)$$

$$= \left[\left(\frac{1.4375}{3.0}\right)\left(\frac{\tan\lambda + 0.15\sec 30}{1 - (0.15)(\tan\lambda)\sec 30}\right) + 0.625(0.15)\right](98{,}115)(1.5)$$

= 28,036 in.-lb, or 28,036/12 = 2,336 ft-lb

where:

T	=	applied torque in inch-pounds
F	=	preload force in pounds
d	=	bolt diameter = 1.50 in
d_m	=	mean diameter of threads = d-p/2 = 1.4375 in
α	=	one-half the thread angle = 30°
μ	=	coefficient of friction = 0.15
n	=	threads/inch
tan λ	=	1 / (π d_m n)

The design minimum torque is 2,540-200 ft-lb = 2,340 ft-lb

$T_{design} > T_{required}$ = 2,340 ft-lb > 2,336 ft-lb.

Therefore, the design torque is adequate.

The following calculations of bolt stresses are presented in order to verify the values in Table 2.7.1.6-2. The inner lid bolts will be evaluated for the end drop (0°), oblique drop (5°), corner drop (25°), and side drop (90°). The calculation summarized in this section is for the hypothetical accident condition (30-ft drop).

Bolt stress is evaluated by combining the stress from the maximum design installation torque (nominal torque + tolerance) with the maximum static and inertial loads generated by the highest hypothetical accident condition acceleration. The calculated stress is compared to the allowable criteria specified in Table 2.1.2-1.

Derivation of Bolt Stresses - Pivoting Lid Assumed

The derivation of this relationship for tensile bolt stresses assumes the lid pivots about the outer edge of the lid, point "O". The bolts are approximated as a thin, circular ring with a thickness equivalent to (total bolt area) = (ring area).

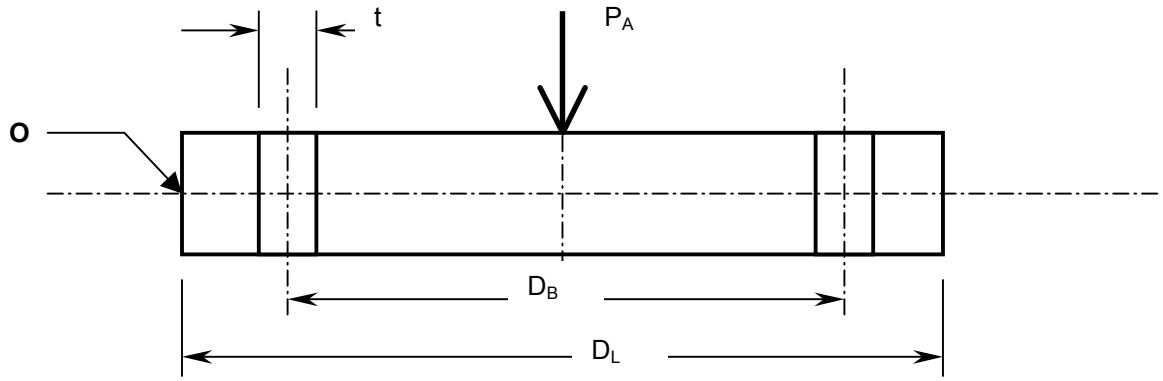

Inner Lid Section

R_B = bolt circle radius = $D_B/2$ = 37.655 in
R_L = lid radius = $D_L/2$ = 39.5 in

Equivalent ring thickness is found as:

$t = A/(\pi D_B) = 0.2649$ in

where:

$A = (42 \text{ bolts})(1.492 \text{ in}^2/\text{bolt}) = 62.66 \text{ in}^2$

The moment of inertia of the bolt ring about point "O" is:

$$I_o = \pi R_B^3 t + A R_L^2 = 142{,}204 \text{ in}^4$$

The applied bending moment about point "O" resulting from the impact force, P_A, is:

$Mc = P_A R_L$

Thus, the bolt stress is found as:

$$f_a = Mc/I = \frac{\left[\left(P_A R_L\right)\left(R_L + R_B\right)\right]}{\pi R_B^3 t + A R_L^2}$$

or

$$F_A = f_a A_b = P_A[R_L(R_L + R_B)/I_o]A_b \qquad \text{[Equation 2]}$$

In this analysis, considering impacts from vertical (end) impacts through side impacts, the two bolt tension relations, equations [1] and [2], must transition from one to the other at some

orientation angle. Both conservatively neglect reaction forces from external energy absorbers. This neglect is extraordinarily conservative for near vertical impacts, but becomes more realistic as the package approaches side impact orientations. Specifically, the center of pressure of the external energy absorber reaction force on the lid moves from the center of the lid towards the impacting corner of the package as the impact orientation moves from near vertical to near horizontal.

For conservatism, this transition from an end relation, [Equation 1], for bolt force to an oblique relation, [Equation 2], is assumed to occur reasonably close to vertical; hence, only the 0-degree case uses the uniform force assumption.

2.10.8.2.2 Top End Drop (0°)

The installation preload bolt force (F_i) is determined by setting torque (T) to the maximum preload torque, 2,540 + 200 = 2,740 ft-lb and solving for (F_i).

$$F_i = \frac{T}{\left[\left(\frac{d_m}{2d}\right)\left(\frac{\tan\lambda + \mu\sec\alpha}{1-\mu\tan\lambda\sec\alpha}\right) + 0.625\mu\right](d)} = 115{,}066 \text{ lb}$$

The total applied external load is:

$$\begin{aligned} P &= F_s\,(\text{static}) + F_a\,(\text{impact}) \\ &= 9{,}306 + 89{,}079 \\ &= 98{,}115 \text{ lb} \end{aligned}$$

where the total static load, F_s, is:

$$\begin{aligned} F_s &= F_{press} + F_{or1} + F_{or2} \\ &= 4{,}578 \text{ lb} + 2{,}208 \text{ lb} + 2{,}250 \text{ lb} \\ &= 9{,}036 \text{ lb} \end{aligned}$$

where:

F_{press} = internal pressure force per bolt (lb)

$$F_{press} = \left(\frac{PA}{N_b}\right) = \left(45.3 \text{ psig} \times \frac{(73.51\text{in.})^2\pi}{4}\right) \div 42 \text{ bolts} = 4{,}578 \text{ lb}$$

and

P = internal cask lid pressure = 45.3 psi
A = area (in.²) of the cask lid at the o-rings, based on 73.51 in. diameter
N_b = number of cask lid closure bolts
F_{or1} = inner o-ring compression force per bolt (lb)

$$F_{or1} = \frac{\pi(D_f)(D_{imor})(P_c)}{N_b} = \frac{\pi(1.0)(72.00)(410)}{42} = 2{,}208 \text{ lb}$$

where:

D_{imor} = diameter of inner (metal) o-ring = 72.00 in (71.89 in. actual)
D_f = design factor of Type 321 material = 1.0
P_c = inner o-ring compression force = 410 lb/in
N_b = number of bolts = 42
F_{or2} = outer o-ring compression force per bolt (lb)

$$F_{or2} = \frac{\pi(D_f)(D_{omor})(P_c)}{N_b} = \frac{\pi(1.0)(73.36)(410)}{42} = 2{,}250 \text{ lb}$$

where:

D_{omor} = diameter of outer (metal) o-ring = 73.36 in
P_c = outer o-ring compression force = 410 lb/in
N_b = number of bolts = 42
F_a= total dynamic load resulting from impact

$$= \frac{P_a}{N_b} = \frac{3{,}741{,}309}{42} = 89{,}079 \text{ lb}$$

where

$$P_a = W_a \times g(\cos\theta) = 66{,}690 \times 56.1(\cos 0) = 3{,}741{,}309 \text{ lb}$$

The net bolt load is:

$F_b = K_b P/(K_b + K_m) + F_i$ (preload) $+F_t$ (thermal)
$= 7{,}656 + 115{,}066 + 13{,}703 = 136{,}425$ lb

where:

K_b = bolt stiffness
$= A_b E_b / L$
$= 4.57 \times 10^6$ lb/in

where:

A_b = 1.492 in^2
E_b = 28.0×10^6
L = total bolt length - ½ bolt head thickness - ½ engagement length
= 9.14 in
K_m = lid stiffness
= $A_L E_{lid} / L_g$
= 5.40×10^7 lb/in

where:

A_L = an assumed cross-sectional area equal to a thick-walled cylinder with an inner diameter equal to the nominal bolt diameter and an outer diameter equal to three times the nominal bolt diameter (Shigley).
= $\pi/4(9d^2 - d^2) = 2\pi d^2$
= 14.14 in^2

and:

E_{lid} = 27.2×10^6 psi
L_g = grip length = 7.12 in
$F_{thermal}$ = bolt differential thermal expansion load
= $A_b\Delta T[\alpha_l - \alpha_b] E_b$ (conservatively assume $E_1 = E_2$)
= 13,703 lb

where:

ΔT = $270^oF - 70^oF = 200^oF$
α_l = 8.94×10^{-6} in/in/^oF
α_b = 7.30×10^{-6} in/in/^oF
E_b = 28.0×10^6 psi

The shear stress in the bolt = 0 because the impact is at 0° with respect to the bolt axis.

The direct tensile stress in the bolt is:

$f_b = F_b/A_b$= 136,425 lb/1.492 in^2 = 91,438 psi

where:

A_b = 1.492 in.^{2}, the bolt tensile area

The margin of safety (M.S.) is:

$$M.S. = \frac{S_y}{f_b} - 1 = \frac{141,700}{91,438} - 1 = +0.55$$

2.10.8.2.3 Oblique Drop (5°)

The impact force (tension) on the bolts is:

$F_A = P_A[R_L(R_L + R_B)/I_o] A_B$
$= 119,085$ lb

where:

$P_A = (n_g)(W_A)(\cos 5^o)$
$= (48)(77,885)(\cos 5^o)$
$= 3,724,254$ lb

R_L = lid radius,
= 39.5 in

R_B = bolt circle radius,
= 37.655 in

I_o = bolt circle moment of inertia = $\pi R^3_B t + A_b N_b R^2_{L,}$
= $\pi (37.655^3)(0.2649) + (1.492)(42)(39.5^2)$
= 142,204 in.^{4}

t = equivalent ring thickness,
= $A_b N_b / (2\pi R_B) = (1.492)(42)/ [(2\pi)(37.655)]$
= 0.2649 in

A_B = bolt stress area
= 1.492 in^2

The total applied external load is:

$P = f_s(\text{static}) + F_A(\text{impact})$
$= 8,308 + 119,085$

= 127,393 lb

where:

f_s = total static load
F_A = total dynamic load resulting from impact

The net bolt tensile load is:

$F_b = K_b P/(K_b + K_m) + F_i$ (preload) $+F_t$ (thermal)
$= 9,940 + 115,066 + 13,703 = 138,709$ lb

The shear force in each bolt is:

$F_L = n_g W_L \sin\theta / N_b$
$= (48)(10,690)(\sin 5^o)/42$
$= 1,065$ lb

where:

n_g = impact acceleration based on impact force
W_L = weight acting in lateral direction = 10,690 lb
N_b = 42, number of bolts

The direct tension stress (f_b) in the bolt is:

$f_b = F_b/A_b$
$= 138,709/1.492$
$= 92,968$ psi

The shear stress (f_v) in the bolt is:

$f_v = F_L/A_b$
$= 1,065/1.492$
$= 714$ psi

The principal stresses are calculated as:

$$\sigma_1, \sigma_2 = \frac{f_b}{2} \pm \sqrt{\left(\frac{f_b}{2}\right)^2 + f_v^2}$$

$$\sigma_1, \sigma_2 = \frac{92{,}968}{2} \pm \sqrt{\left(\frac{92{,}968}{2}\right)^2 + 714^2}$$

$$= 92{,}973 \text{ psi}; - 5 \text{ psi}$$

The stress intensity (SI) is:

$$SI = |\sigma_1 - \sigma_2| = 92{,}978 \text{ psi}$$

The margin of safety (M.S.) is:

$$\text{M.S.} = \frac{S_y}{SI} - 1 = \frac{141{,}700}{92{,}978} - 1 = +0.52$$

2.10.8.2.4 Corner Drop (24°)

The impact force (tension) on the bolts is:

$$F_A = P_A[R_L(R_L + R_B)/I_o]\, A_B$$
$$= 108{,}340 \text{ lb}$$

where:

$$P_A = (n_g)(W_A)(\cos 25^o)$$
$$= (48)(77{,}885)(\cos 25^o)$$
$$= 3{,}388{,}214 \text{ lb}$$

The total applied external load is:

$$P = F_s \text{ (static)} + F_A \text{ (impact)}$$
$$= 8{,}308 + 108{,}340$$
$$= 116{,}648 \text{ lb}$$

where:

F_s = total static load
F_A = total dynamic load resulting from impact

The net bolt load is:

$F_b = K_bP/(K_b + K_m) + F_i$ (preload) $+F_t$ (thermal)
$= 9,102 + 115,066 + 13,703 = 137,871$ lb

The shear force in each bolt is:

$F_L = n_g W_L \sin\theta / N_b$
$= (48)(10,690)(\sin 25^o)/42$
$= 5,163$ lb

where:

n_g = impact acceleration based on impact force
W_L = 10,690, weight acting in lateral direction
N_b = 42

The direct tension stress in the bolt is:

$f_b = F_b/A_b$
$= 137,871/1.492$
$= 92,407$ psi

The shear stress in the bolt is:

$f_v = F_L/A_b$
$= 5,163/1.492$
$= 3,460$ psi

The principal stresses are calculated as:

$$\sigma_1, \sigma_2 = \frac{f_b}{2} \pm \sqrt{\left(\frac{f_b}{2}\right)^2 + f_v^2}$$

$$\sigma_1, \sigma_2 = \frac{92{,}407}{2} \pm \sqrt{\left(\frac{921{,}407}{2}\right)^2 + 3{,}460^2}$$

$$= 92{,}536 \text{ psi}; \; -129 \text{ psi}$$

The stress intensity (SI) is:

$$SI = |\sigma_1 - \sigma_2| = 92{,}665 \text{ psi}$$

The margin of safety (M.S.) is:

$$\text{M.S.} = \frac{S_y}{SI} - 1 = \frac{141{,}700}{92{,}665} - 1 = +0.53$$

2.10.8.2.5 Side Drop (90°)

$F_b = K_b f_s/(K_b + K_m) + F_i$ (preload) $+F_t$ (thermal)
$= 648 + 115{,}066 + 13{,}703 = 129{,}417$ lb

The direct tension stress in the bolt is:

$f_b = F_b/A_b$
$= 129{,}417/1.492$
$= 86{,}741$ psi

The shear force (F_L) in each bolt is:

$F_L = (10{,}690)(55)/42 = 13{,}999$ lb
$f_v = 9{,}383$ psi

The principal stresses are calculated as:

$$\sigma_1, \sigma_2 = \frac{f_b}{2} \pm \sqrt{\left(\frac{f_b}{2}\right)^2 + f_v^2}$$

$$\sigma_1, \sigma_2 = \frac{86{,}741}{2} \pm \sqrt{\left(\frac{86{,}741}{2}\right)^2 + 9{,}383^2}$$

$$= 87{,}744 \text{ psi}; \; -1{,}003 \text{ psi}$$

The stress intensity (SI) is:

$$SI = |\sigma_1 - \sigma_2| = 88{,}747 \text{ psi}$$

The margin of safety (M.S.) is:

$$\text{M.S.} = \frac{S_y}{SI} - 1 = \frac{141{,}700}{88{,}747} - 1 = +0.60$$

2.10.8.3 Outer Lid Closure Bolt Analyses

All numerical examples pertain to the evaluation of the NAC-STC outer lid bolts under hypothetical accident conditions (Table 2.7.1.6-4).

2.10.8.3.1 Outer Lid Bolt Preload

In selecting a preload for the outer lid cask closure bolts, the following loading factors are considered: (1) an internal pressure force on the closure lid of 7.35 psig; (2) the O-ring compression force; and (3) the inertial weight of the outer cask lid and impact limiter due to the 30-foot accident drop condition; and (4) the differential thermal expansion between the outer lid material and the bolt. Based on these loading conditions, an installation torque was selected to be 550 ± 50 foot-pounds.

The required bolt preload to offset the combined static and dynamic loads is determined by:

$$F_b = F_s + F_A$$

where:

F_b = calculated required bolt preload
F_s = total static load
F_A = total dynamic (impact) load

The cask lid closure bolt preload necessary to offset static loads is:

$F_s = F_{pressure} + F_{O\text{-}ring}$
$= 38,635 \text{ lb} + 105,221 \text{ lb}$
$= 143,856/36 = 3,996 \text{ lb/bolt}$; conservatively, use 4,000 lb/bolt

where:

F_s = total static load (lb)
F_{press} = internal pressure force (lb)

$$= (P)(\pi / 4)(D_{or})^2 = \left[(7.35\,\text{psig}) \times \frac{\pi (81.69 \text{ in.})^2}{4} \right] = 38,635 \text{ lb}$$

P = internal cask lid pressure = 7.35 psig
D_{or} = cask outer lid o-ring diameter of 81.69 in.
$F_{o\text{-}ring}$ = o-ring compression force per bolt (lb),

$$= \pi (D_{or})(P)_c = \pi (81.69 \text{in.})(410 \text{lb/in}) = 105,221 \text{ lb}$$

where:

D_{or} = diameter of (metal) o-ring = 81.69 in.
P_c = o-ring compression force = 410 lb/in

The 30-foot drop axial (end drop) acceleration factor, 56.1g, is used for determining the required bolt preload.

F_a = end impact bolt force

$$= \frac{P_a}{N_b} = \frac{952,859}{36} = 26,468 \text{ lb/bolt}$$

where:

$P_a = (W_a \times g)\cos\theta = (16{,}985 \times 56.1)\cos 0^\circ = 952{,}859$ lb

W_a = outer lid (8,120) + impact limiter (8,865) weight = 16,985 lb

g = end drop g-load = 56.1 g

θ = drop angle (from cask axis) = 0°

The impact limiter weight used, 8,865 lbs, is conservative because it considers the weight of the redwood impact limiter, which is heavier than the balsa wood impact limiter specified for the CY-MPC configuration.

Therefore, the calculated required tensile preload per bolt, F_b, is:

$F_b = F_s + F_a$
$= 4{,}000$ lb + 26,468 lb = 30,468 lb

The total torque (T) to develop the required tensile bolt preload (F_b) is:

$$T = \left[\left(\frac{d_m}{2d}\right)\left(\frac{\tan\lambda + \mu\sec\alpha}{1 - \mu\tan\lambda\sec\alpha}\right) + 0.625\mu\right](F)(d) = 5{,}960 \text{ in. lb, or } 5{,}960/12 = 497 \text{ ft-lb.}$$

The minimum design torque is 550 - 50 ft-lb = 500 ft-lb > 497 ft-lb. Therefore, the design installation torque is adequate.

2.10.8.3.2 Top End Drop (0°)

The total applied external load is:

$P = F_s$ (static) + F_A (impact)
$= 4{,}000 + 26{,}468$
= 30,468 lb

where:

F_s = total static load = 4,000 lb

F_A = total dynamic load resulting from impact = 26,468 lb

The net bolt load is:

$$F_b = K_b P/(K_b + K_m) + F_i \text{ (preload)} + F_t \text{ (thermal)}$$
$$= 2{,}267 + 36{,}810 + 0 = 39{,}077 \text{ lb}$$

where:

K_b = bolt stiffness
$= A_b E_b / L$
$= 5.49 \times 10^6$ lb/in

where:

$A_b = 0.606$ in^2
$E_b = 27.2 \times 10^6$
L = total bolt length - ½bolt head thickness - 1/2 engagement length
$= 3.0$ in
K_m = lid stiffness
$= A_L E_l / L_g$
$= 6.83 \times 10^7$ lb/in

where:

A_L = an assumed cross-sectional area equal to a thick-walled cylinder with an inner diameter equal to the nominal bolt diameter and an outer diameter equal to three times the nominal bolt diameter (Shigley).
= $\pi/4(9d^2 - d^2) = 2\pi d^2$
= 6.28 in^2

and,

E_l = 27.2×10^6 psi
L_g = grip length = 2.5 in
$F_{thermal}$ = bolt differential thermal expansion load = 0 because the bolt and the lid are made of the same material.

The shear stress in the bolt = 0 because the impact is at 0° with respect to the bolt axis.

The direct tensile stress in the bolt is:

$$f_b = F_b/A_b = 39{,}077 \text{ lb}/0.606 \text{ in.}^2 = 64{,}483 \text{ psi}$$

where:

A_b = 0.606 in.^{2}, the bolt tensile area

The margin of safety (M.S.) is:

$$M.S. = \frac{S_y}{f_b} - 1 = \frac{94{,}200}{64{,}483} - 1 = +0.46$$

2.10.8.3.3 Oblique Drop (5°)

The impact force (tension) on the bolts is:

$F_A = P_A[R_L(R_L + R_B)/I_o]\ A_B$
$= 34{,}652$ lb

where:

$P_A = (n_g)(W_a)(\cos 5^o)$
$= (55)(16{,}985)(\cos 5^o)$
$= 930{,}620$ lb

R_L = lid radius,
= 43.35 in

R_B = bolt circle radius,
= 41.85 in

I_o = bolt circle moment of inertia = $\pi R^3_B t + A_b N_b R^2_L$,
= $\pi (41.85^3)(0.083) + (0.606)(36)(43.35^2)$
= 60,109 in^4

t = equivalent ring thickness,
= $A_b N_b / (2\pi R_B) = (0.606)(36)/ [(2\pi)(41.85)]$
= 0.083 in

A_B = bolt stress area
= 0.606 in^2

The total applied external load is:

$P = f_s$ (static) + F_A (impact)
= 4,000 + 34,652
= 38,652 lb

where:

f_s = total static load
F_A = total dynamic load resulting from impact

The net bolt tensile load is:

$F_b = K_b P/(K_b + K_m) + F_i$ (preload) $+F_t$ (thermal)
= 2,876 + 36,810 + 0 = 39,686 lb

The shear force in each bolt is:

$F_L = n_g W_L \sin\theta / N_b$
$= (55)(8,120)(\sin 5^o)/36$
= 1,081 lb

where:

n_g = impact acceleration based on impact force
W_L = weight acting in lateral direction = 8,120 lb
N_b = 36

The direct tension stress in the bolt is:

$f_b = F_b/A_b$
$= 39,686/0.606$
= 65,488 psi

The shear stress in the bolt is:

$f_v = F_L/A_b$
= 1,081/0.606
= 1,784 psi

The principal stresses are calculated as:

$$\sigma_1, \sigma_2 = f_b/2 \pm \sqrt{\left[(f_b/2)^2 + f_v^{\,2}\right]}$$
$$= 65{,}488/2 \pm \sqrt{[(65{,}488/2)^2 + (1{,}784)^2]}$$
$$= 65{,}537 \text{ psi}; \; -49 \text{ psi}$$

The stress intensity (SI) is:

$$SI = |\sigma_1 - \sigma_2| = 65{,}586 \text{ psi}$$

The margin of safety (M.S.) is:

$$M.S. = (S_y / SI) - 1$$
$$= (94{,}200/65{,}586) - 1 = +0.44$$

2.10.8.3.4 Corner Drop (24°)

The impact force (tension) on the bolts is:

$$F_A = P_A[R_L(R_L + R_B)/I_o] \, A_B$$
$$= 31{,}526 \text{ lb}$$

where:

$$P_A = (n_g)(W_A)(\cos 25^o)$$
$$= (55)(16{,}985)(\cos 25^o)$$
$$= 846{,}650 \text{ lb}$$

The total applied external load is:

$$P = F_s \text{ (static)} + F_A \text{ (impact)}$$
$$= 4{,}000 + 31{,}526$$
$$= 35{,}526 \text{ lb}$$

where:

F_s = total static load

F_A = total dynamic load resulting from impact

The net bolt load is:

$$F_b = K_bP/(K_b + K_m) + F_i \text{ (preload)} + F_t \text{ (thermal)}$$
$$= 2,643 + 36,810 + 0 = 39,453 \text{ lb}$$

The shear force in each bolt is:

$$F_L = n_g W_L \sin\theta / N_b$$
$$= (55)(8,120)(\sin 24^o)/36$$
$$= 5,243 \text{ lb}$$

where:

n_g = impact acceleration based on impact force
W_L = 8,120 lb, weight acting in lateral direction
N_b = 36

The direct tension stress in the bolt is:

$$f_b = F_b/A_b$$
$$= 39,453/0.606$$
$$= 65,104 \text{ psi}$$

The shear stress in the bolt is:

$$f_v = F_L/A_b$$
$$= 5,243/0.606$$
$$= 8,652 \text{ psi}$$

The principal stresses are calculated as:

$$\sigma_1, \sigma_2 = f_b/2 \pm \sqrt{\left[(f_b/2)^2 + f_v^{\,2}\right]}$$
$$= 65,104/2 \pm \sqrt{[(65,104/2)^2 + (8,652)^2]}$$
$$= 66,234 \text{ psi}; \; -1,130 \text{ psi}$$

The stress intensity (SI) is:

$SI = |\sigma_1 - \sigma_2|$
$= 67,364$ psi

The margin of safety (M.S.) is:

$M.S. = (S_y / SI) - 1$
$= (94,200/67,364) - 1 = +0.40$

2.10.8.3.5 Side Drop (90°)

$F_b = K_b f_s/(K_b + K_m) + F_i$ (preload) $+F_t$ (thermal)
$=298 + 36,810 +0 =37,108$ lb

The shear force in each bolt is:

$F_L = (8,120)(55)/36 = 12,406$ lb
$f_s = 4,000$
$f_b = 37,108/0.606 = 61,234$ psi
$f_v = 12,406/0.606 = 20,472$ psi

The principal stresses are calculated as:

$$\sigma_1, \sigma_2 = f_b/2 \pm \sqrt{\left[(f_b/2)^2 + f_v^2\right]}$$
$$= 61,234/2 \pm \sqrt{[(61,234/2)^2 + (20,472)^2]}$$
$= 67,448;\ -6,214$ psi

The stress intensity (SI) is:

$SI = |\sigma_1 - \sigma_2|$
$= 73,662$ psi

The margin of safety (M.S.) is:

$M.S. = (S_y / SI) - 1$
$= (94,200/73,662) - 1 = +0.28$

THIS PAGE INTENTIONALLY LEFT BLANK

2.10.9 Lead Slump Evaluation

The objective of this lead slump evaluation is to determine the effect of varying the value of the modulus of elasticity of lead used in the 30-foot end drop impact analysis of the NAC-STC at normal operating temperature on: (1) the calculated lead slump distance; and (2) the magnitude of the calculated stresses in the inner and outer shells. A secondary objective of this lead slump evaluation is to verify that the inner and outer shell stresses presented in Section 2.7.1 for the 30-foot drop analyses are conservative (Note: Section 2.7.1 analyses used the modulus of elasticity of lead that reflected a perfectly elastic material throughout the loading event. The lead slump evaluation presented in this section uses the secant modulus, a minimum value of the modulus of elasticity of lead.).

The NAC-STC cask shell is a composite of a 3.70-inch thick lead sandwiched between a 1.50-inch thick stainless steel inner shell and a 2.65-inch thick stainless steel outer shell.

The detailed analysis that follows considers the secant modulus of elasticity of lead to be 27.75 ksi. This value represents a conservative estimate of the strain rate dependent dynamic modulus of elasticity (Evans).

A coefficient of friction of 0.5 is used at the contact surfaces between the stainless steel shells and the lead shielding. According to the Standard Handbook For Mechanical Engineers (Baumeister), the static friction coefficient between lead and steel is 0.95 for dry surface contact and 0.5 for greasy surface contact. Therefore, the 0.5 friction coefficient value adopted for the lead slump evaluation is very conservative.

A uniform temperature of 300°F is conservatively applied to the model. Under normal operating conditions, the temperature spectrum with respect to the longitudinal axis of the composite shell varies from a maximum of 331°F to a minimum of 200°F. The thermal analysis results presented in Section 3.4 define the location of the maximum temperature of the composite shell at the mid-section of the longitudinal axis, with the temperature decreasing at locations away from the mid-section.

This lead slump analysis of the 30-foot end drop impact considers a cask total weight of 250 kips with the maximum deceleration of 56.1 g. Total force at impact is 14.025×10^6 pounds.

2.10.9.1 Methodology/Finite Element Analysis

An ANSYS two-dimensional axisymmetric finite element model was constructed using 2-D isoparametric elements (STIF42), 2-D gap elements (STIF12), and general mass elements (STIF21). The model geometry includes the inner and outer stainless steel shells, neutron shield, lead shielding and the inner and outer lids. The impact limiters were not explicitly modeled. Impact limiter weight was accounted for in the model by discrete lump masses using ANSYS general lump mass elements (STIF21). See Figures 2.10.9-1 and 2.10.9-2 for the finite element model plots.

The weight of the internal contents of the cask, i.e the fuel basket, fuel, and basket spacer, is applied as a pressure load amplified by 56.1 g on the cask model. The total weight of the cask is applied as a 56.1-g impact load to simulate the 30-foot end drop accident. Component stresses--longitudinal, S_y, and circumferential, S_z--are calculated and tabulated for representative locations on the cask body.

Gap elements were introduced at the contact surfaces between the lead shielding and the inner and outer shells. The initial boundary conditions for this evaluation assume that the lead is in contact with both the inner and the outer shells. Gap element stiffness was set to 5.0×10^6 based on elementary classical evaluation of stiffness between the composite shells as detailed in Section 2.6.12.2. As mentioned earlier, a conservative value of 0.5 was used as the coefficient of static friction between the lead and the stainless steel shells. Introduction of a coefficient of friction into the gap elements creates a highly nonlinear problem. To facilitate solution convergence of the ANSYS impact analyses, radial displacement boundary conditions were defined between the contacting surfaces. The nonlinear gap elements were modeled with a contact interference value of 0.001 inch at both the inner and the outer lead/stainless steel contact surfaces.

As previously stated, the analysis approach presented in this section considers a 0.001-inch contact interference at both the inner and the outer lead/stainless steel interface surfaces so that the analytical program, ANSYS, can obtain a converged solution. Thus, there is considered to be no gap present at either interface surface for the normal operating temperature condition at the time the 30-foot end drop accident occurs. There are 121 gap elements spaced at 1.3417-inch intervals modeled on each side of the lead annulus. The normal force at each gap element is approximately 3727 pounds/inch/radian due to the 0.001-inch contact interference modeled at the interface surfaces. (The friction force is 0.5 x the normal force). Then, considering both interface surfaces, the total normal force applied in the finite element model is 7454 pounds/inch/radian. An axisymmetric finite element model evaluation of the differential thermal expansion of the lead and stainless steel shells calculated a gap of 0.0271 inch at the lead/outer shell interface at normal operating temperature and a contact interference at the lead/inner shell interface, which produces a normal force of 14,296 pounds/inch/radian. Therefore, the total interface force modeled in this analysis is conservatively low by a factor of 14,296/7454 = 1.9. Then, the impact lead pressures and resulting inner and outer shell stresses that are calculated by ANSYS in this evaluation are conservative.

2.10.9.2 Analysis Result

2.10.9.2.1 Lead Slump

Figure 2.10.9-3 shows the longitudinal displaced shape due to the 30-foot end drop hypothetical accident condition, corresponding to a deceleration value of 56.1 g, with respect to the full cask weight of 250 kips. The displacement plots show the maximum lead shielding longitudinal settlement is 0.15037 inch at the top. The lead settlement decreases downwards to a value of 0.008354 inch near the bottom of the cask. The deformed shape of the lead shielding after impact clearly concludes that there is no appreciable slump other than a localized maximum compression of 0.15037 inch after the 30-foot end drop hypothetical accident condition.

2.10.9.2.2 Stress Evaluation

Drop tests were carried out on a quarter-scale model of the NAC-STC. The quarter-scale model outer shell was instrumented with three groups of strain gauges, each group consisting of three 90-degree, two-element, rosette type gauges. The strain gauge groups were located longitudinally on the model at 9 inches, 24 inches, and 39 inches from the bottom outer surface of the cask body model. In each group of strain gauges, a 90-degree, two-element, rosette type gauge was located circumferentially at 0°, 90°, and 180° with one element oriented in the cask body axial direction and one element oriented in the circumferential direction. These strain gauges were used to measure strains at each of the above locations on the cask outer shell during impact. Corresponding longitudinal and circumferential component stresses at each location were then calculated based on the generalized Hook's law as follows:

$$Ee_{ij} = [(1+n)s_{ij} - nd_{ij}s_{kk}]$$

where:

n = Poisson's ratio
e = Strain (in)
s = Stress (psi)
E = Elastic Modulus
d = Kronecker Delta ; 1 when $i \neq j$; 0 otherwise

Finite element component stresses and von Mises stresses at similar location to the test strain gauge locations are listed in Tables 2.10.9-1 and 2.10.9-2 for the outer and inner shells, respectively. Figure 2.10.9-4 shows the node locations used in this stress summary. Table 2.10.9-3 provides a comparison of the stresses at selected locations on the outer shell, corresponding to the locations where strain gauges were positioned for the drop tests. The stresses are determined by four different methods, including: (1) SCANS dynamic analysis, using a lead modulus of 2280 ksi, (2) 30-foot end drop test using a quarter-scale cask model, (3) ANSYS analysis using a lead modulus value of 27.0 ksi with the consideration of friction between

the lead and surrounding steel shells, and (4) ANSYS analysis using a lead modulus value of 2280 ksi without the consideration of friction between the lead and the steel shells.

The comparison provided by Table 2.10.9-3 illustrates that the stress evaluations performed using the two different lead modulus values, together with the different considerations of friction, result in similar stress results. The stress results from the ANSYS analysis which uses a lead modulus of 2280 ksi, without friction, are more consistent with the drop test results than the results obtained from the ANSYS analysis using the lead modulus of 27.0 ksi. Therefore, the analysis results documented in Section 2.7, which were performed using a lead modulus of 2280 ksi, are accurate, and adequately represent the behavior of the NAC-STC.

2.10.9.3 Conclusion

A structural analysis using the strain dependent secant modulus of elasticity for lead shows that there is negligible lead slump after the 30-foot end drop hypothetical accident condition. These analytical results closely agree with test results from the quarter-scale model drop test and the elastic analysis results based on Young's modulus for lead used in the analyses of Section 2.7. The NAC-STC cask is, therefore, adequately designed.

Figure 2.10.9-1 Lead Slump - Cask 2D Model Element Plot

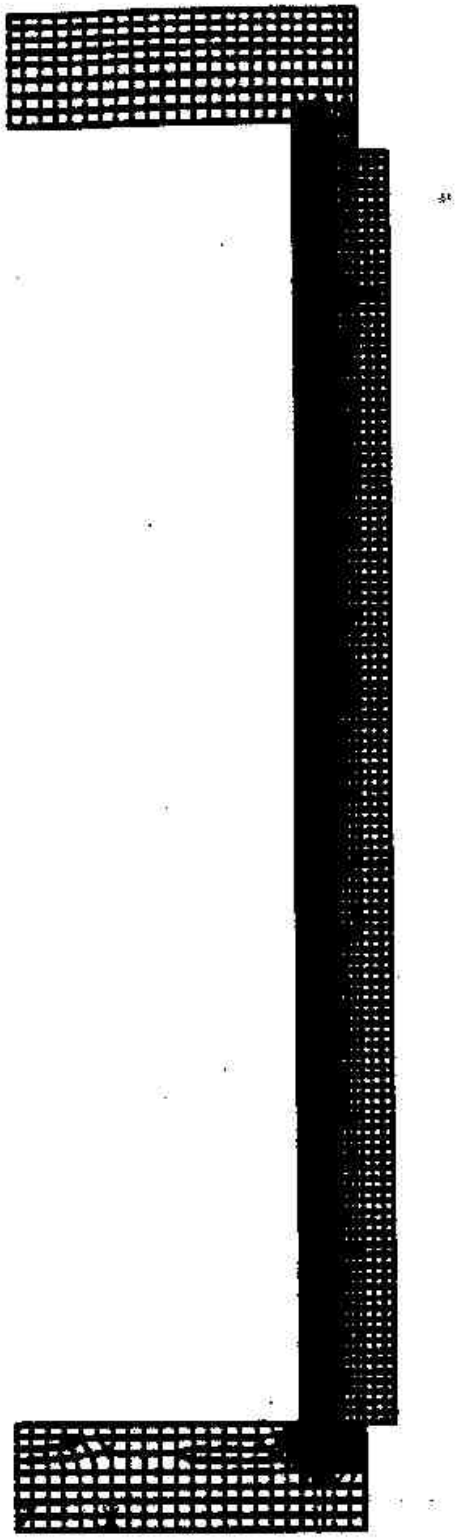

Figure 2.10.9-2 Lead Slump - Gap Element Plot

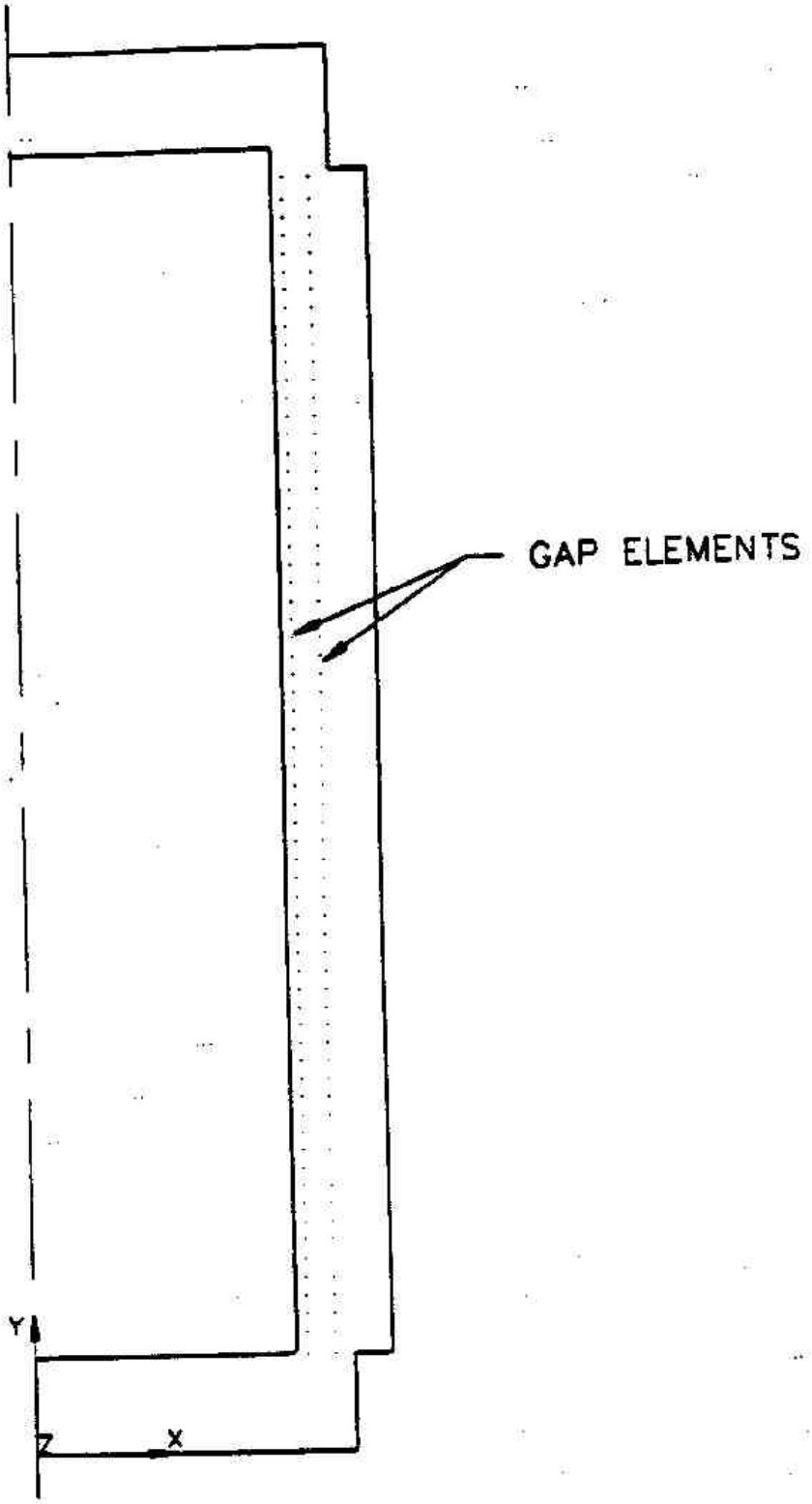

Figure 2.10.9-3 Lead Slump Displacement

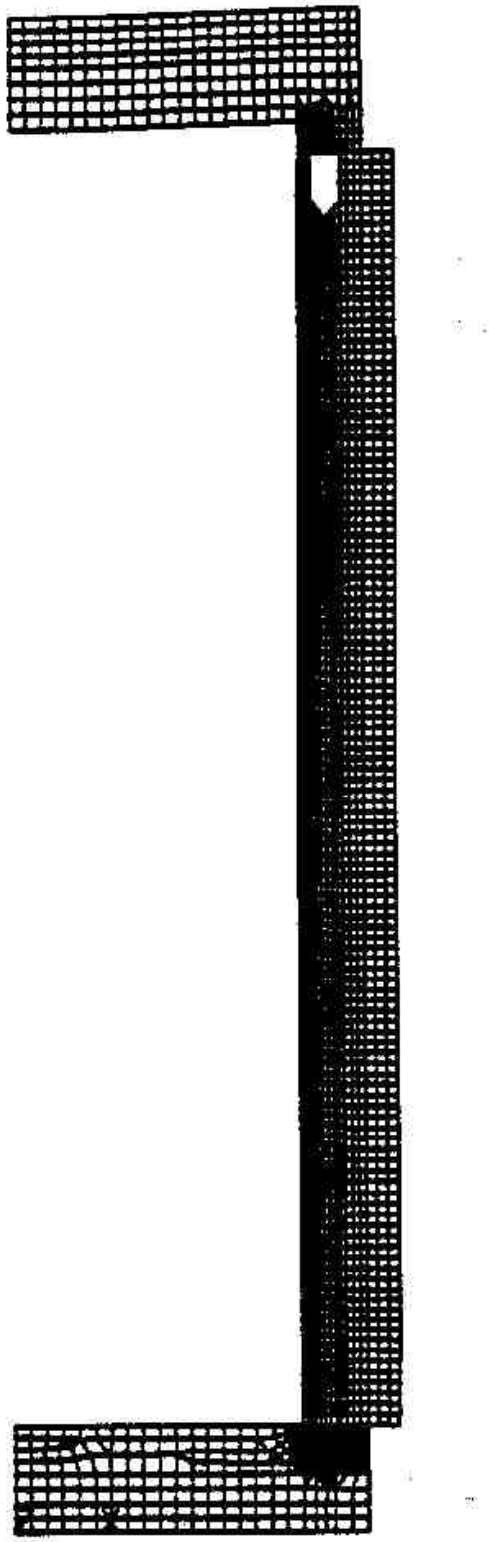

Figure 2.10.9-4 Location of Node Points Used in Stress Summary

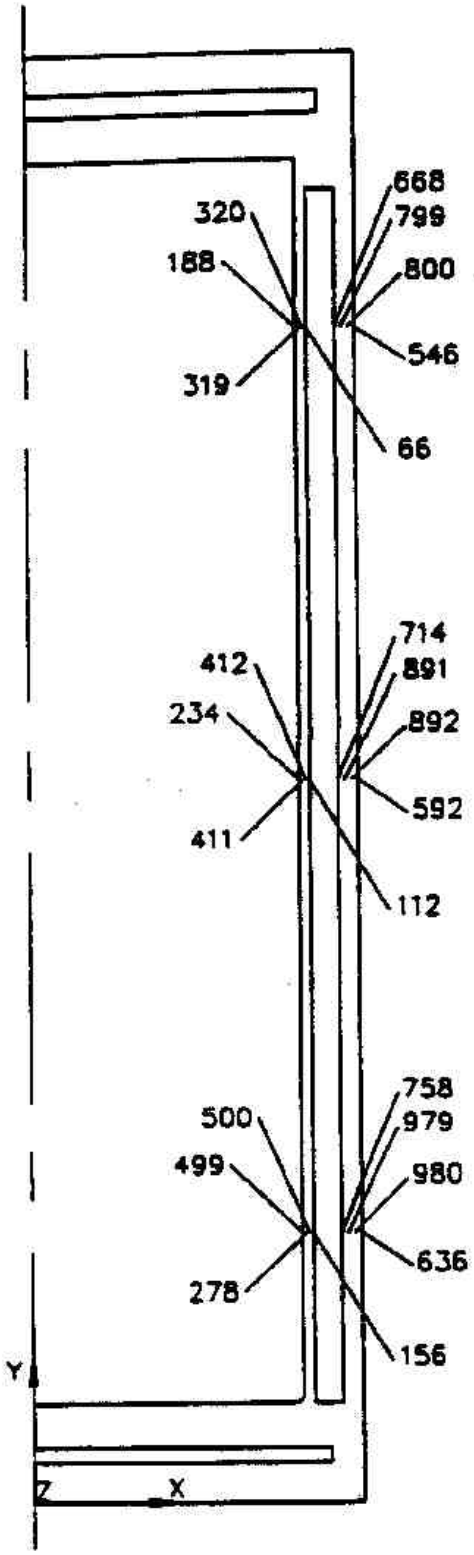

Table 2.10.9-1 Summary of 30-Foot End Drop Stress Results on the Outer Shell of the NAC-STC (ANSYS)

Longitudinal Location (in)	Node #	S_x	S_y	S_z (psi)	S_{xy}	SIGE
156.96	758	1.65	-5510.60	106.49	-22.20	5565.54
	979	0.00	-5668.74	67.06	-18.06	5702.62
	980	0.32	-5588.86	87.10	-23.41	5633.22
	636	1.65	-5510.60	106.49	-22.20	5565.54
96	714	0.0	-4100.67	3.39	-2.04	4102.37
	891	0.0	-4100.68	3.32	-4.02	4102.39
	892	0.13	-4100.69	3.25	-7.93	4102.41
	592	0.19	-4100.70	3.19	-9.74	4102.42
36	668	-0.93	-2338.39	177.04	-2.40	2431.34
	799	1.64	-2452.86	141.99	-4.20	2527.61
	800	2.46	-2564.15	108.36	-7.36	2621.20
	546	3.38	-2676.15	75.50	-8.63	2716.35

Note: See Figure 2.10.9-4 for locations of node numbers listed above S_x, S_y, S_z, S_{xy} and SIGE are the radial, longitudinal, circumferential, shear and von Mises stresses, respectively.

Table 2.10.9-2 Summary of 30-Foot End Drop Stress Results on the Inner Shell of the NAC-STC (ANSYS)

Longitudinal Location (in)	Node #	S_x	S_y	S_z (psi)	S_{xy}	SIGE
156.96	278	-0.2	-7146.9	-2176.69	-7.52	345.33
	499	-30.20	-7145.84	-2146.40	-14.70	6329.15
	500	-59.05	-7144.69	-2117.33	-28.83	6313.94
	156	-86.71	-7143.51	-2089.40	-35.48	6299.59
96	234	00.00	-4422.21	-1571.61	-5.43	3883.04
	411	-21.79	-4422.31	-1549.98	-10.67	3870.15
	412	-42.63	-4422.34	-1529.22	-21.10	3858.09
	112	-62.61	-4422.30	-1509.27	-26.07	3846.70
36	188	1.02	-2091.81	-1073.98	-4.24	1812.99
	319	-13.52	-2055.79	-1049.27	-7.91	1769.07
	320	-27.17	-2021.25	-1025.65	-14.42	1727.38
	66	-40.38	-1985.03	-1002.32	-17.12	1684.70

Note: See Figure2.10.9-4 for location of node numbers listed above. S_x, S_y, S_z, S_{xy} and SIGE are the radial, longitudinal, circumferential, shear and von Mises stresses, respectively.

Table 2.10.9-3 Comparison of Outer Shell Stresses for 30-Foot End Drop

Location[1]			Stress (ksi)			
Longitudinal (inch)	**Circumferential (degree)**		**SCANS[3] (51.4g)**	**Drop Test (55.6g)**	**ANSYS[4] (56.1g)**	**ANSYS[5] (56.1g)**
156.96	0	S_z	-7.17	-8.27	-5.67	-6.0
		S_t	1.88	1.68	0.10	1.1
	90	S_z	-7.17	-5.66	-5.67	-6.0
		S_t	1.88	1.04	0.10	1.1
	180	S_z	-7.17	-5.88	-5.67	-6.0
		S_t	1.88	2.01	0.10	1.1
96.0	0	S_z	-5.0	-4.74	-4.10	-3.2
		S_t	1.28	1.76	0.0	0.0
	90	S_z	-5.0	-4.54	-4.10	-3.2
		S_t	1.28	1.42	0.0	0.0
	180	S_z	-5.0	-3.95	-4.10	-3.2
		S_t	1.28	1.71	0.0	0.0
36.0	0	S_z	-2.7	-1.86	-2.68	-1.9
		S_t	0.35	1.42	0.20	0.3
	90	S_z	-2.7	-1.79	-2.68	-1.9
		S_t	0.35	1.49	0.20	0.3
	180	S_z	-2.7	-1.67	-2.68	-1.9
		S_t	0.35	1.56	0.20	0.3

1 Locations where the strain gauges were positioned for the NAC-STC drop tests. Longitudinal location is measured from the cask bottom; circumferential location is the angular position on the cask circumference. (Note that the 0-degree circumferential location for the analyses is the 180 degrees circumferential location for the specification of gauge location.

2 S_z (longitudinal) and S_t (circumferential) are normal stresses.

3 Lead modulus 2280 ksi was used in the SCANS dynamic evaluation.

4 Lead modulus 27.75 ksi with friction was used in the ANSYS non-linear evaluation.

5 Lead modulus 2280 ksi was used in the ANSYS impact evaluation in Section 2.10.4, Table 2.10.4-14.

2.10.10 Assessment of the Effect of the Revised Temperature Distribution on Structural Qualification

Finite element structural analysis of the directly loaded fuel configuration of the cask for normal and accident condition loads had been completed based on temperature distributions obtained using analytical thermal boundaries different than those currently documented in the heat transfer analyses in Chapter 3. Therefore, an evaluation of the effect of the revised temperature distribution on the cask structural qualification is performed to evaluate the adequacy of the previously completed structural analyses. The following discussion presents the methodology, and data evaluation used to investigate the dependence of the structural analyses on the temperature distribution in the cask. From this evaluation it is concluded that the structural analyses are conservative and that the calculated stress intensity values are higher than those that would be obtained using the revised thermal distribution. Therefore, revision of the structural analyses of the cask to reflect the revised temperature distributions is not required. Note: Separate thermal analyses have been performed for the canistered fuel configuration of the NAC-STC (refer to Chapter 3).

2.10.10.1 Evaluation Methodology

The cask temperature distribution influences the structural analyses through temperature dependent material properties and through induced secondary stress resulting from temperature gradients. These parameters are expressed as a function of temperature in the following generalized relationship for calculating temperature induced stress in structural members:

$$S = C\, E_{(T)}\, \alpha_{(T)}\, \Delta T$$

where

S = thermal induced stress
C = problem configuration constant

$E_{(T)}$= temperature dependent modulus of elasticity

$\alpha_{(T)}$ = temperature dependent coefficient of thermal expansion
ΔT = temperature difference between two points in the structure (through the thickness of the component or between adjacent components).

The problem configuration constant is not dependent on the temperature distribution in a structure and will not have an effect on the stress results obtained for a constant cask geometry subjected to different heat transfer results. Therefore, C, the problem configuration constant does not enter into the following evaluation.

The modulus of elasticity, $E_{(T)}$, is a temperature dependent material property which produces a direct proportional response in the resultant stress. However, it is important to note that this material property is temperature dependent and that its value has an inverse relationship with temperature for all cask component materials presented in Section 2.3. As the temperature increases the modulus of elasticity becomes smaller. Therefore, as the average temperature of the cask components change, the component stress will change as an inverse relationship. It is also important to note that the modulus of elasticity is the only temperature dependent material property that effects primary stress results.

The coefficient of thermal expansion, $\%_{(T)}$, is also a temperature dependent material property that, unlike the modulus of elasticity, increases with temperature. Influence of the coefficient of thermal expansion on the resultant stress components is only included as a stress component in combination with the temperature difference between adjacent points in the structure, ΔT. Therefore, to obtain an assessment of the influence of the coefficient of thermal expansion on the resultant stress values it must be evaluated in combination with the respective temperature difference between two adjacent points. Thus, the combined function ($\%_{(T)}\ \Delta T$) is a temperature dependent set influencing this evaluation.

From the above general equation, secondary temperature dependent stress is directly dependent on the difference in temperature, ΔT, between adjacent points in the cask. Boundary conditions used in the heat transfer analysis have a significant influence on the actual temperatures

throughout the cask. Therefore, to perform an assessment of the influence of these different parameters on the completed structural analyses, the cask component average temperatures and temperature gradients resulting from the original and revised heat transfer analyses are summarized for the different cask components.

In addition to the temperature effects on the stress results, as discussed above, allowable stress limits are based on temperature dependent yield and ultimate material strengths. Material strength for each structural component in the cask has an inverse relationship with temperature as shown in the material property tables presented in Section 2.3. Therefore, in addition to evaluating the effect of the change in temperature on the resultant stress intensity for both the normal and accident condition loadings, the influence of temperature on the allowable stress values is performed for comprehensive assessment of the revised heat transfer analysis on the structural qualification of the NAC-STC.

2.10.10.2 Temperature Dependent Stress Results

Tables 2.10.10-1 and 2.10.10-2 present the comparison of the temperature results between the original heat transfer analysis that was used in the structural qualification to the revised heat transfer analysis that is documented in Chapter 3. The original heat transfer analysis represented boundary conditions: (1) without the gap between the basket and inner shell wall; (2) without the influence of the attached impact limiters; and (3) with surface convection based on a vertical circular cylinder. The original heat transfer analysis results were obtained from a two-dimensional finite difference model analyzed using HEATING5 (Turner). The revised heat transfer analysis represents boundary conditions: (1) with the gap between the basket and inner shell wall; (2) with the influence of both installed impact limiters; (3) with convection based on a horizontal circular cylinder; (4) with air as the cavity gas; and (5) with the revised fuel tube design. The revised heat transfer analysis results have been obtained from a three-dimensional finite element model analyzed using ANSYS.

The following observations and conclusions are made from a review of the data presented in Tables 2.10.10-1 and 2.10.10-2.

1. The average temperature of the cask components enclosed by the impact limiters increased significantly. The average temperature for the inner lid increased approximately 50EF, and the bottom plate and forging increased approximately 210EF and 250EF, respectively.

2. As noted in Section 2.10.10.1, the modulus of elasticity is a temperature dependent material property that reduces in value as the temperature increases. The evaluation of the change in stress resulting from the effect of modulus of elasticity is performed by calculating the ratio of the material property values for the component having the greatest change in average temperature. Therefore, for the bottom forging this calculation is:

$$\frac{E_{(T\text{-Revised})}}{E_{(T\text{-Original})}} = \frac{E_{(425)}}{E_{(150)}} = \frac{26.33 \times 10^6 \text{ psi}}{27.9 \times 10^6 \text{ psi}} = 0.94$$

   Based on this calculation for the cask component having the greatest increase in temperature, it is concluded that the change in the modulus of elasticity resulting from the revised heat transfer analysis will lower the stress results to as much as 94 percent of the stress calculated using the temperature from the original heat transfer analysis. Therefore, the current structural qualification as influenced by the modulus of elasticity is conservative.

3. Temperature gradients are small through the thickness of the individual components. Therefore, evaluating the influence of the change in temperature on stress results produced from the combined coefficient of thermal expansion and temperature gradient is performed for both the top and bottom of the cask relative to the shell. The temperature gradients are defined in Table 2.10.10-2.

   To compare the structural influence of the differential thermal expansion of the inner shell and forging ends using previous thermal analysis with the differential expansion using the revised thermal analysis, the general expression is:

$$\frac{(\alpha_{(T)}\,\Delta T)_{Revised}}{(\alpha_{(T)}\,\Delta T)_{Original}}$$

where)T = (average temperature of forging) - (average temperature of inner shell)

For the bottom of the cask, this expression becomes:

$$\frac{(\alpha_{(425)}\,\Delta T)}{(\alpha_{(150)}\,\Delta T)} = \frac{(9.24 \times 10^{-6} \times 53)}{(8.67 \times 10^{-6} \times 153)} = 0.37$$

For the top of the cask, this expression becomes:

$$\frac{(\alpha_{(225)}\,\Delta T)}{(\alpha_{(200)}\,\Delta T)} = \frac{(8.85 \times 10^{-6} \times 88)}{(8.79 \times 10^{-6} \times 113)} = 0.78$$

This calculation shows that the effect of the revised heat transfer analysis on stress resulting from the difference in average temperature between adjacent cask components will be less than that produced from the original heat transfer analysis. Therefore, that portion of the secondary stress results, which are produced from the coefficient of thermal expansion and temperature gradients in the cask structural qualification are conservative.

4. In addition to the above direct stress component effects, the allowable stress limits are influenced by the maximum component temperature. The following is a comparison of the revised and original temperature dependent material yield strength for the cask component experiencing the greatest change in temperature (the bottom plate of the cask). This comparison is representative of the revised temperature influence on the allowable stress values (independent of the specific evaluation), which are a function of S_m, S_y, or S_u.

$$\frac{S_{y(350)}}{S_{y(150)}} = \frac{21.6}{26.2} = 0.83$$

Based on this evaluation it is concluded that the allowable stress limits for both normal and accident condition structural evaluations for the revised heat transfer results may be as much as 20 percent less than stress allowable based on the original heat transfer analysis. Therefore, allowable stress and margins of safety are revised throughout the structural qualification based on the temperature results from the revised heat transfer analysis.

5. Further evaluation of the effect of the temperature increase throughout the cask considers the enclosed non-structural members of the cask, i.e., the chemical lead gamma shield and the BISCO NS4FR neutron shield.

The average temperature of the lead gamma shield has effectively not changed over the average temperature of the lead defined from the original heat transfer analysis and used in the finite element structural analyses of the cask. This result represents the combined influence of including gaps and reducing the heat load. These changes tend to cancel each other. Therefore, it is concluded that the influence of the revised temperature in the cask shell wall has no impact on the structural qualification of the NAC-STC cask.

The most significant increase in a cask component temperature is in the bottom where heat loss has been significantly reduced by the modeling of the bottom impact limiter. Although this has reduced temperature gradients in this region, the temperature of the bottom neutron shield has increased to 403EF. The neutron shield will be sized such that no stress will be induced into the cask structure from thermal expansion of the neutron shield. Additionally, off-gas from the neutron shield material between the inner lid top plate and the inner lid, and between the bottom plate and bottom forging will not be released. Considering the neutron shield cavity in both cask ends to be completely filled with off-gas experiencing temperature increases from 70EF to their respective steady state temperatures will result in an induced stress of 3200 psi in the inner lid top plate and 240 psi in the bottom. These stress levels are insignificant with respect to the structural qualification of the cask and have been neglected.

2.10.10.3 Conclusions - Revised Temperature Distribution Evaluation

From the above evaluation it is seen that each of the different temperature parameters will have a positive margin of safety impact on the current structural analyses. The evaluation of the influence of the modulus of elasticity effect shows that the current set of stress results are conservative. The evaluation of the influence of the coefficient of thermal expansion in combination with the thermal gradients between the cask components shows a 20 to 80 percent conservatism for the interaction between the cask shell and the cask ends. In addition to the conservative changes in stresses, adjusting the allowable stress values to those representative of the maximum component temperature based on the revised thermal conditions provides qualification of conservative structural analyses. Therefore, it is concluded from this evaluation that the detailed finite element analyses performed for normal and accident condition loads using the original temperature distributions are conservative. Revisions to the structural qualification of the cask resulting from the revised heat transfer analyses are limited to changes in the allowable stress and the margins of safety in the stress summary tables in Section 2.10.4.

Figure 2.10.10-1 Identification Applicable to Temperature Summary

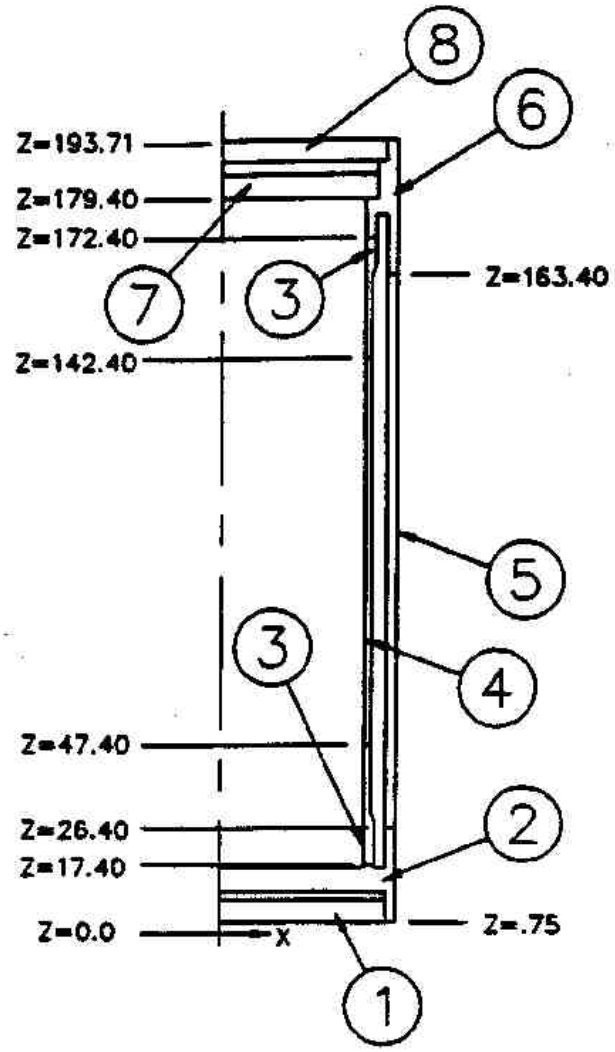

1 - Bottom Plate
2 - Bottom Forging and Bottom Ring Forging
3 - Transition Shell
4 - Inner Shell
5 - Outer Shell
6 - Top Forging
7 - Inner Lid
8 - Outer Lid

Figure 2.10.10-2 Component Wall Gradient Locations

FIGURE WITHHELD UNDER 10 CFR 2.390

Table 2.10.10-1 Comparison of Cask Component Temperatures (Directly Loaded Fuel Configuration)

			Original 2D Head Transfer Analysis			Revised 3D Heat Transfer Analysis[3]		
Component[1] I.D.	Description	Wall[2] Gradient Location	Maximum Temp. (°F)	Average Temp. (°F)	Wall Grad. °F/in	Maximum Temp. (°F)	Average Temp. (°F)	Wall Grad. °F/in
1	Bottom Plate	B	140	124	2.57	350	319	0.48
2	Bottom forging	A	165	158	2.65	418	329	2.57
3	Upper Transition Shell	P	247	225	1.3	255	224	1.06
3	Lower Transition Shell	H	222	171	1.3	300	282	1.0
4	Inner Shell	L	351	311	2.11	311	276	3.73
5	Outer Shell	M	324	250	2.83	286	254	2.90
6	Top Forging	T	217	198	0.82	211	188	0.62
7	Inner Lid	W	181	180	0.66	223	175	0.18
8	Outer Lid	X	180	174	1.33	178	159	0.43

[1] Refer to Figure 2.10.10-1 for component definitions.

[2] Refer to Figure 2.10.10-2 for wall gradient locations.

[3] The temperature reported below corresponds to the condition of a heat load of 22.1 kW, solar insolation, 100°F ambient condition with air in the cask cavity.

Table 2.10.10-2 Comparison of Cask Component Average Temperature Difference (Directly Loaded Fuel Configuration)

Component I.D.	Description	Original 2D Heat Transfer Analysis Average Temp. °F	Original 2D Heat Transfer Analysis Temperature Difference (4-2 or 4-6)	Revised 3D Heat Transfer Analysis Average Temp. °F	Revised 3D Heat Transfer Analysis Temperature Difference (4-2 or 4-6)
2	Bottom Forging	158		329	
4-2			153		53
4	Inner Shell	311		276	
4-6			113		88
6	Top Forging	198		188	

THIS PAGE INTENTIONALLY LEFT BLANK

2.10.11 Sensitivity Studies of the Yankee-MPC Canistered Fuel Basket Analysis

This section presents the results of various sensitivity studies and provides supplemental data for the Yankee-MPC canistered fuel basket support disk evaluation. Section 2.10.11.1 presents the justification of considering the 0° and 45° basket drop orientations as bounding cases for the support disk side drop evaluations. Section 2.10.11.2 shows that the stress results of the support disk evaluation are not sensitive to the value of the gap stiffness used in the support disk side drop models. Section 2.10.11.3 demonstrates that the finite element mesh used for the disk ligaments is adequate to determine maximum stress of the ligaments. The CY-MPC fuel baskets are very similar in design to the Yankee-MPC fuel basket, differing primarily in the overall length dimension.

2.10.11.1 Yankee-MPC Fuel Basket Drop Orientation

As described in Section 2.6.14.1, three basket drop angles, 0°, 22.9° and 45° (shown in Figure 2.10.11-1) are considered in the support disk evaluation for the side drop condition. The angles 22.9° and 45° are selected because a minimal ligament between the corner of the fuel assembly slot and the disk outer radius occurs at these orientations. This section shows that the worst case stress occurs in the 45° drop orientation, and that the 0° and 45° drop orientations are the bounding cases for the support disk evaluation.

As shown in Figure 2.10.11-2, a finite element model for the support disk is generated using the ANSYS program to perform analyses for six-side impact cases:

Case No.	Side Impact Acceleration (g)	Basket Drop Orientation (Degree)
1	20	0
2	20	22.9
3	20	45
4	55	0
5	55	22.9
6	55	45

The model consists of a support disk and a section of the canister shell, as shown in Figure 2.10.11-2. ANSYS SHELL63 elements are used to model the disk and canister. The disk ligaments are modeled using the same number of elements and mesh ratio as those in the three dimensional support disk side drop models described in Section 2.6.14.2. As shown in Figure

2.10.11-3, CONTAC52 elements are used between the disk and canister to simulate the interface between the support disk and the canister shell. A value of 1.0 x 10^6 lb./inch is used for the stiffness of CONTAC52 elements. BEAM3 elements with very small properties (Area = 5 x 10^{-4} $inch^2$, Izz = 5 x 10^{-2} $inch^4$, Modulus of Elasticity = 1 psi) are applied, at the same locations as the CONTAC52 elements, to prevent rigid body motion of the model. The canister shell outer diameter is constrained to prevent translation of the canister. The fuel assembly and tube weight is simulated by applying a concentrated load (with the acceleration factor) at the mid-span of each ligament. The value of the force varies according to the drop orientation. There is no fuel assembly in the center slot of the basket, therefore, no forces are applied at the ligaments of the center slot.

The maximum nodal stress intensity for each basket drop angle (0°, 22.9° and 45° (20 g and 55 g)) is summarized in the table below. The worst case stress intensity occurs in the 45° drop orientation cases. The stresses in the 22.9° drop cases are bounded by those of the 45° drop cases. Therefore, it is concluded that the 0° and 45° drop orientation are the bounding cases for the support disk evaluations for side drop conditions.

Basket Side Drop Orientation	Maximum Stress Intensity (ksi)	
	20 g	55 g
0°	33.3	84.1
22.9°	48.1	81.8
45°	48.9	85.3

2.10.11.2 Gap Stiffness

CONTAC49 and CONTAC52 gap elements are used in the support disk side drop models described in Section 2.6.14.2. A value of 1.0 x 10^6 pound/inch is used as the gap stiffness in the models. This section shows that there is insignificant change in the stress results if the gap stiffness is reduced by 50 percent (0.5 x 10^6 pound/inch). The stress results are not sensitive to the value of the gap stiffness.

The analysis results of the cases for the normal condition, 45° basket drop orientation, thermal condition 3 presented in Section 2.6.14.2, are used as the basis for comparison. A new analysis is performed using the same ANSYS input files as is used in Section 2.6.14.2, except using a gap stiffness of 0.5 x 10^6 pound/inch.

The comparison of the maximum nodal stress intensity for the support disks for the two analyses using different gap stiffness is:

Gap Stiffness (pound/inch)	Maximum Nodal Stress Intensity (ksi)	Location (Node No.)
1.0×10^6	62.1	19643
0.5×10^6	62.7	19643

As shown, the maximum nodal stress intensity increases by less than 1 percent (62.7/62.1=1.0097) when the gap stiffness decreases by 50 percent. The maximum stress intensity occurred at the same nodal location. Therefore, it is concluded that the stress results of the support disks for the side drop evaluation are not sensitive to the value of the gap stiffness used in the model.

2.10.11.3 Finite Element Mesh for the Support Disk Ligaments

As described in Section 2.6.14.2, the support disks are modeled using ANSYS SHELL63 elements. Each ligament of the disk is modeled with 20 elements, ten along the length and two through the width. Since the majority of the stresses are due to the displacement of the disk, the maximum stress in the ligament always occurs at one end of the ligament. Therefore, in the model a higher mesh density is used at the ends of the ligaments. To demonstrate that this finite element mesh is sufficient to accurately determine the stresses, stress analyses are performed for a single disk ligament using two different models: a shell model with SHELL63 elements and a beam model with BEAM4 elements. Linearized sectional stresses from the shell element model are then compared with the solutions from the beam element model.

There are three different widths for the ligaments in a support disk (thickness and length are the same for all ligaments). Therefore, three cases are considered.

Case Number	Ligament Width (inch)	Ligament Thickness (inch)	Ligament Length (inch)
1	0.875	0.5	8.254
2	0.81	0.5	8.254
3	0.75	0.5	8.254

As described above and as shown in Figure 2.10.11-4, two ANSYS models are used to perform the analysis for each case. The first model is generated using SHELL63 elements and the second model using BEAM4 elements. Each model represents a single ligament. The shell model uses the same mesh density as that for the ligaments in the model described in Section 2.6.14.2. Both ends of the ligament are considered to be restrained to preclude rotation and translation. Two boundary conditions (force and displacement) are applied to each model: (1) a concentrated force of 630 lb. (-Y direction) at the mid-span of the ligament; and, (2) a displacement of 0.057 inches (-Y direction) at one end of the ligament. These boundary conditions are based on the support disk side drop evaluation worst case as presented in Section 2.6.14.7. As shown in Tables 2.6.14.7-1 and 2.6.14.7-7, the worst case stress occurs at Section 19 (minimum margin of safety = 0.09) for 1-foot side drop, thermal condition 2, and basket drop orientation of 45 degrees. The applied force and calculated displacements (from the analysis results) of the corresponding ligament containing Section 19 are used. The force at the ligament representing the weight of the fuel assembly and fuel tube (for the 45° drop orientation), with 20 g acceleration, is 629.96 pounds (≈ 630 pounds). Based on the analysis results, the displacements at both ends of the ligament containing Section 19 (perpendicular to the ligament, downward) are 0.314-inch and 0.371-inch, respectively. The relative displacement, 0.057 inch, is applied to the models at the right end of the ligament. For both models, 29 x 10^6 psi is used for the Modulus of Elasticity. A shear factor of 1.2 is used for the beam element.

Maximum stress occurs at the left end of the ligament. Maximum section stresses from the shell model, compared to the beam model results, are:

Case	Beam Model Max. Stress, S_b, (ksi)	Shell Model Max. Section Stress[1], S_s, (ksi)	Percentage Difference (S_b vs S_s)
1	71.7	71.6	0.1%
2	69.1	68.8	0.4%
3	67.1	66.6	0.7%

[1] Section is defined at Nodes 17 and 4 (see Figure 2.10.11-4).

As shown, the difference in maximum stresses between the results from the shell model and those of the beam model is less than 1 percent. Therefore, the mesh for the ligaments of the support disk in the models presented in Section 2.6.14.2 is sufficient to accurately determine the maximum stresses of the support disk ligaments.

Figure 2.10.11-1 Yankee-MPC Fuel Basket Drop Orientation

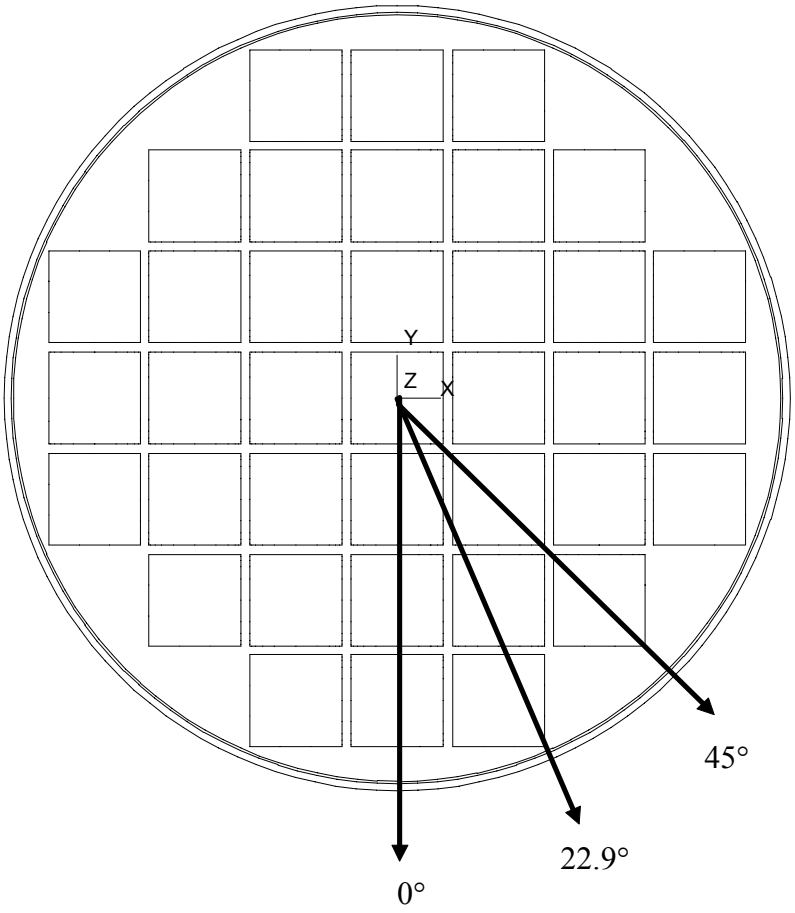

Figure 2.10.11-2 ANSYS Model for the Yankee-MPC Fuel Basket Support Disk

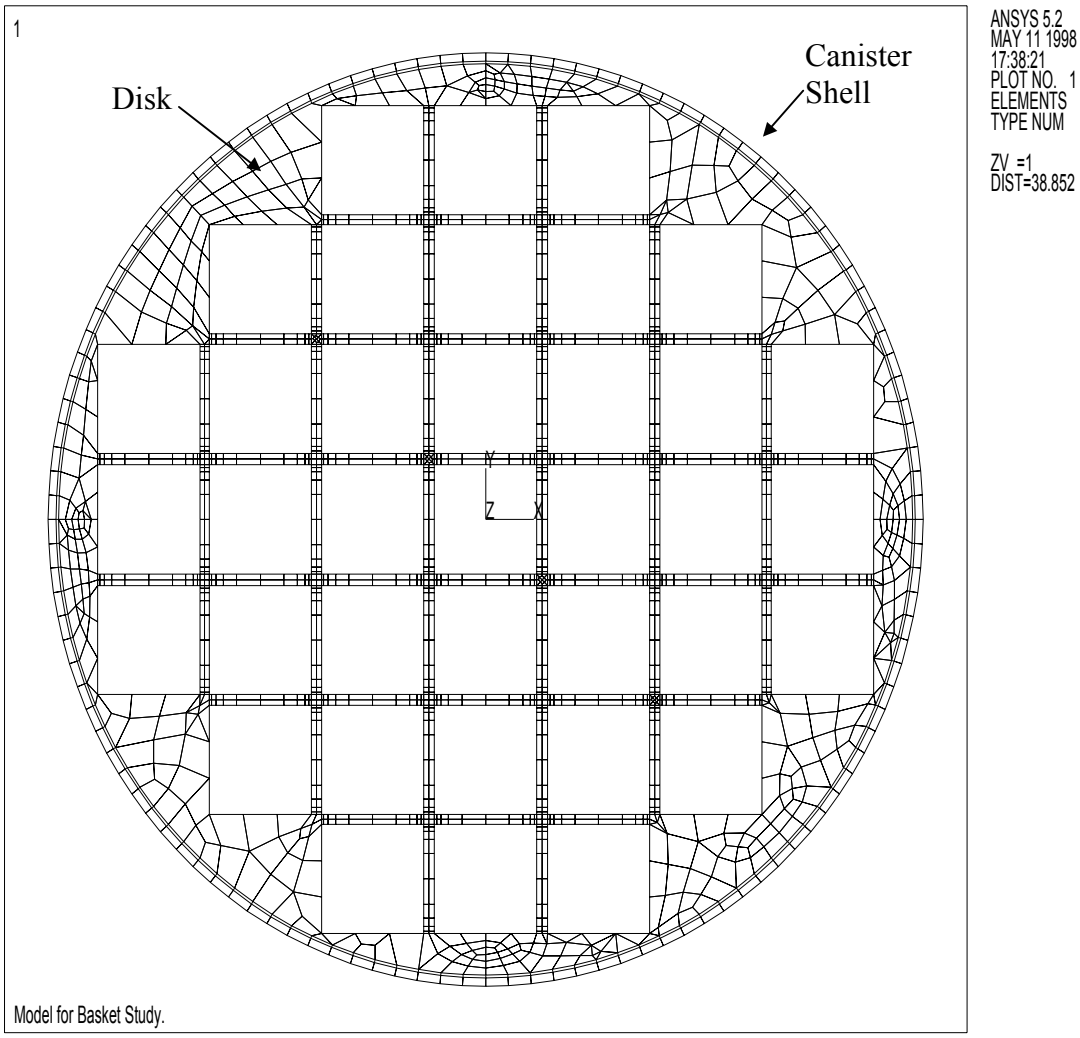

Figure 2.10.11-3 ANSYS Model for the Yankee-MPC Fuel Basket Support Disk (Detail)

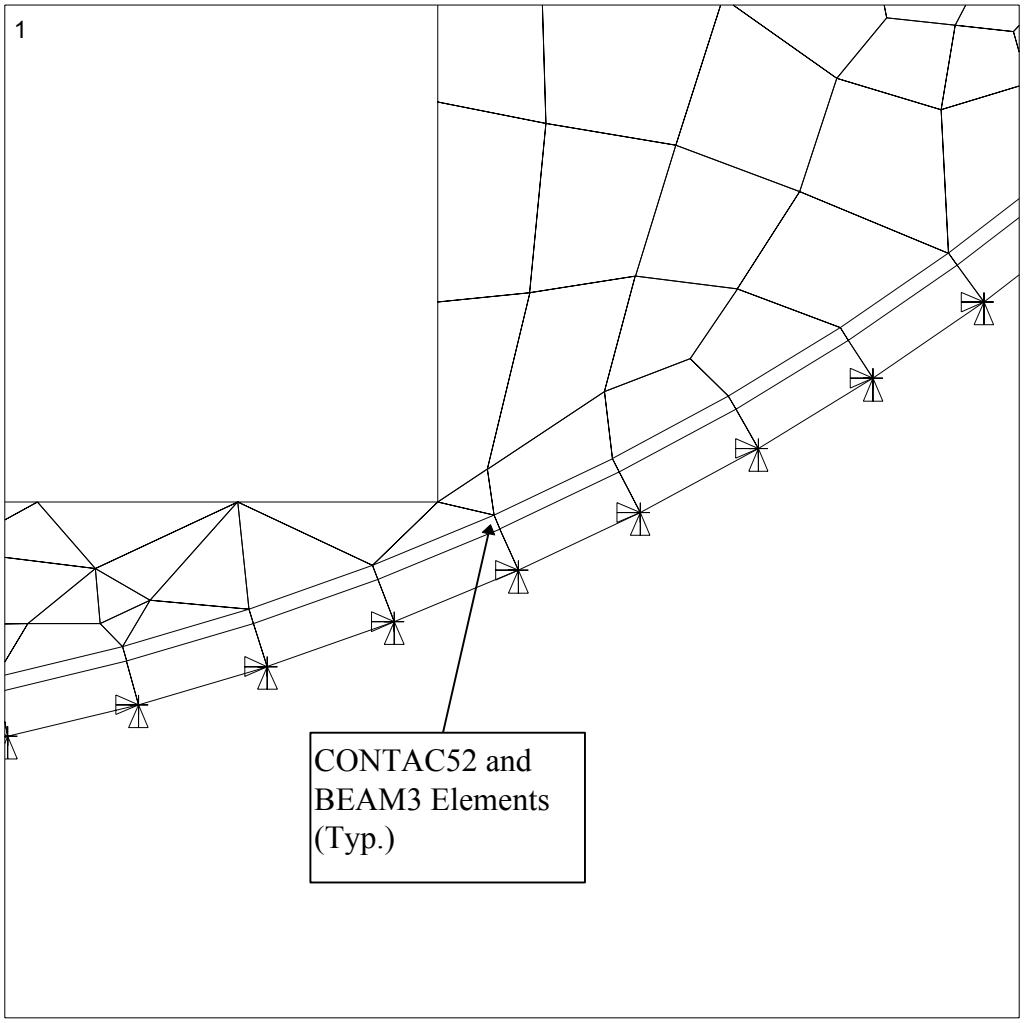

Figure 2.10.11-4 ANSYS Models for Yankee-MPC Support Disk Ligament Mesh

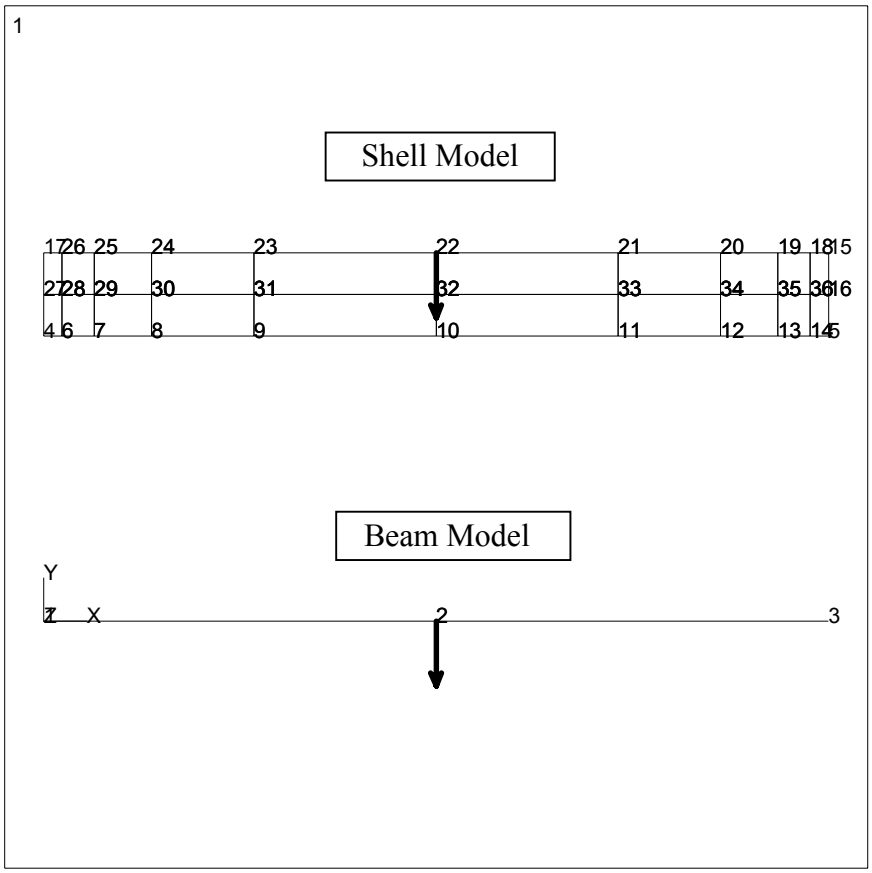

2.10.12 Confirmatory Testing Program – Balsa Impact Limiters and Attachments

This section provides a description of the scale model test program, which was carried out as confirmatory support of the analysis and licensing effort for the design qualification of the balsa impact limiters and attachments. More specifically, the purpose of the balsa impact limiter scale model test program was to confirm the capability of the impact limiters to restrict the deceleration of the cask to the design limits used in the structural evaluation, show that the impact limiters remain attached to the cask body and show that the crush depth is limited to prevent an impact of the cask body on the impact surface.

The test results confirm the impact limiter analysis and provide physical evidence that the balsa impact limiters will function as designed to limit the deceleration applied to the cask and its contents and to remain attached to the transport cask during an accident condition impact.

The scale model test program included 30-foot drops of a quarter-scale model of the NAC-STC cask in the top end, side, and top corner impact orientations. The total weight of the quarter-scale model and impact limiters (4,140 pounds) corresponded to that of the full-scale cask and impact limiters of 265,000 pounds, which bounded the design limit of 260,000 pounds for all transport configurations.

This section presents the scale model impact limiter and attachment drawings, the test descriptions, test results, and conclusions that demonstrate the design qualification of the impact limiters and their attachments.

2.10.12.1 Confirmatory Testing Program Results Summary

Three 30-foot drop tests were performed for the NAC-STC transport cask scale model test program. The top end drop, top corner drop and side drop tests were performed at the drop test facility at the Sandia National Laboratory (SNL) in October 2001.

Since the purpose of the test program was to confirm the design of the balsa impact limiters and attachments, the design of the scale model package focused on the limiters and their attachments to the cask body. The scale model body was designed to accurately represent the interface between the cask body and the impact limiters, as well as the weight and CG of the cask body and the maximum contents weight. The use of a scale model is appropriate to perform these tests and the scale selected for the tests was a quarter-scale model. Using a smaller scale model

presents fabrication difficulties, while use of a larger scale model would increase the drop pad requirement (mass and geometric size). The drop pad at SNL meets the requirements of the IAEA for simulating an essentially unyielding surface.

The test data consisted of measurements of the deformations of the impact limiters, recordings of the package accelerations, and inspections of the retaining rods. Impact limiter measurements were performed before and after each test to determine the crush depth of the impact limiters. The measured crush depths are used to demonstrate that the impact limiter design calculations are bounding. The accelerations are recorded by accelerometers attached to the model body. The accelerometers are positioned and oriented so that the acceleration in each direction is recorded. The acceleration data obtained from the accelerometers contained some contributions to the acceleration signal that were extraneous, based on the frequencies of the contributions. For this reason, the acceleration data was filtered to extract appropriate accelerations, which were compared to the accelerations calculated by the LS-DYNA finite element analysis program. The LS-DYNA analyses for the quarter-scale model are presented in Section 2.10.12.7. Additional test documentation included high-speed photography that confirmed the orientation of the cask at impact and still photographs of the scale model, impact limiters, and the impact limiter retaining rods. Post-test inspection of the retaining rods and the impact limiters confirmed that the impact limiters have a significant margin of safety for remaining attached to the cask body during and after a 30-foot drop test impact.

The quarter-scale model 30-foot drop test acceleration values and the LS-DYNA predicted (calculated) values are summarized in the following table:

Cask model Drop Orientation	Quarter-Scale Drop Test Results (g)		LS-DYNA Prediction (g)		Design Basis Acceleration (g)
	Top Accelerometer	Bottom Accelerometer	Top Accelerometer	Bottom Accelerometer	
Top Corner	126	N/A	137	N/A	192
Top End	122	N/A	128	N/A	192
Side	150	164	184	179	220

The drop test measured crush depths and the LS-DYNA predicted (calculated) values are summarized in the following table:

Cask Model Drop Orientation	Quarter-Scale Drop Test Results (inch)			LS-DYNA Prediction (inch)		
	Original Thickness	Final Thickness	Measured Crush Depth	Original Thickness	Final Thickness	Total Crush Depth
Top End Drop	—	—	5.50	—	—	5.68
Top Corner Drop	—	—	4.40	—	—	4.62
Side Drop–Under The trunnion	4.25	1.12	3.13	4.25	0.92	3.33
Side Drop–Bottom Impact limiter	5.00	2.00	3.00	5.00	1.66	3.34

These results of the balsa impact limiter drop test program confirm that the design-basis accelerations and crush depths used for the evaluation of the transport cask are bounding. The table also shows that LS-DYNA accurately predicts the amount of crush experienced during the drop tests except in regions where extreme irregular deformations occur (i.e., directly below the trunnions and corner.

2.10.12.2 Acceptance Criteria for Model Performance

Acceptance criteria were established only for the scale model impact limiters and their attachment components, since the purpose of the scale model test program was to confirm their performance capabilities. The function of the scale model impact limiters is to limit the deceleration of the scale model package during the 30-foot drop event, while remaining firmly attached to the cask body. The impact limiter acceptance criteria require that:

1. The crush depth be limited to prevent an impact of the cask body on the impact surface.
2. The accelerations be limited to be less than or equal to those used in the design analysis.
3. The impact limiters remain attached to the cask body and in position after the impact event.

The results of the balsa impact limiter drop test program confirm:

1. The scale model body did not impact the pad surface confirming that the impact limiters possess a sufficient depth of wood to absorb all of the energy of a 30-foot drop in any orientation.

2. The maximum accelerations determined from the scale model tests are less than the design-basis values used to evaluate the NAC-STC transport cask components for a 30-foot drop accident.

3. The impact limiters remain attached to the transport cask body.

2.10.12.3 Description of 30-Foot Drop Tests Performed at SNL

A quarter-scale model was used for the confirmatory testing of the balsa impact limiters and attachments for the top end drop, top corner drop and side drop. These drop tests were performed at the Sandia National Laboratory (SNL) in October 2001. The acceptance criteria for the testing were primarily concerned with the impact limiters. Therefore, the quarter-scale model was only required to represent the appropriate cask body weight, center of gravity, and attachment interface to the impact limiters.

The cask body used for the balsa impact limiter quarter scale model testing was the quarter scale model body described in Section 2.10.6.5 except with modifications for the cask ends and the additional weight for the contents. The actual cask body used in the quarter scale model testing for the directly loaded fuel was used in the quarter scale model testing for the balsa impact limiters. The revised quarter scale model is shown in the model drawings 423-355, Sheets 1 through 4. The closure end of the cask quarter scale model used a 4.49 inch thick plate welded to the cask body. To represent the contents weight, a 10-inch, schedule 120 pipe was filled with poured lead. This pipe was extended from the bottom plate to the inner surface of the closure end plate and was attached to the end plates by welds. The thickness of the two end plates was adjusted to allow the CG of the quarter scale model to match the location of the CG in the full-scale design.

The total weight of the quarter-scale model including the impact limiters was 4,140 pounds. This closely approximates $(1/4)^3 = 1/64$ of the full-scale transport cask weight of 265,000 pounds which bounds the maximum design weight of the transport configurations of 260,000 pounds.

Since the top end drop and top corner drop tests involve only the top end of the model, there was no need to include a bottom impact limiter on the model for these tests. To ensure that the total scale model package weight and CG were properly represented for the top end and top corner drop tests, a steel plate corresponding to the weight of the bottom impact limiter was designed, fabricated, and bolted to the bottom end of the model.

The model impact limiters were quarter-scale representations of the full-scale impact limiters. The redwood and balsa wood used in the model limiters met the same specifications that are defined for the full-scale limiters. The wood section shapes, joints, and bonds of the scale model impact limiters duplicate those of the full-scale impact limiters. The grain orientation of the redwood and balsa wood in the scale model impact limiters is identical to that as designed in the full-scale impact limiters. The scale model impact limiter shells and gussets were fabricated from 16 gauge (0.0625-inch thick) Type 304 stainless steel sheets and the screw tubes, which serve as the penetrations for the impact limiter retaining rods, were fabricated from 0.035-inch thick, 0.75-inch diameter tubes. Each model impact limiter is attached to the cask by sixteen quarter-scale retaining rods fabricated from ASME SA-193 Grade B8S stainless steel.

The model impact limiter shells - i.e., material thickness, geometry, and welds - are appropriately quarter-scale. The diameter of the screw tubes is quarter-scale, but the tube wall thickness is full-scale due to fabricability and material availability limitations. The use of the thicker tube is considered to have an insignificant effect, since the tubes are not located in the primary crush regions of the impact limiter for any of the drop orientations.

2.10.12.3.1 Equipment and Instrumentation for the Tests Conducted at SNL

The drop pad at the SNL functions as an essentially unyielding impact surface. The surface of the drop pad consists of armor plate measuring 34 feet by 16 feet and has a varying thickness from 8 inches to 4 inches. The plate is attached to reinforced concrete that allows the total mass of the system to be 1,000 tons. The total mass of the target is approximately 500 times that of the quarter-scale test model, which is large compared to the ratio of 30 recommended by IAEA. The pad at SNL is considered to meet the IAEA requirements for a drop test pad.

Lifting and dropping the model was performed with a system of cables to provide sufficient restraint from lateral motion of the cask, as well as to limit the motion of the cables upon release of the cask model. The cask model was attached to the cable system via a single point, and an explosive bolt mechanism was used to release the cask from the cables. This mechanism allowed the free fall of the package to be initiated in an unimpeded fashion with minimum perturbation to the position of the cask model.

To assess the model performance with respect to the acceptance criteria, a set of basic data was required to be collected throughout each test. This data included:

1. Acceleration data – to determine the maximum impact acceleration of the cask. All of the accelerometers used in the drop tests were the same model and they were calibrated to NIST traceable standards corresponding to frequencies ranging from 30 Hz to 350 kHz. Accelerometers were mounted on steel blocks bolted to the cask model at three locations 90° apart at the end of the test model, as shown below. Locations 1, 2 and 3 were 7.5 inches from the top end of the model, and accelerometers 4, 5 and 6 were 7.5 inches from the bottom end of the model. At each of the six locations, two accelerometers were mounted to record a lateral acceleration and an axial acceleration. The X and Y directions of the accelerations remained the same for all the drop tests. The locations of the accelerometers and the directions are shown in the following.

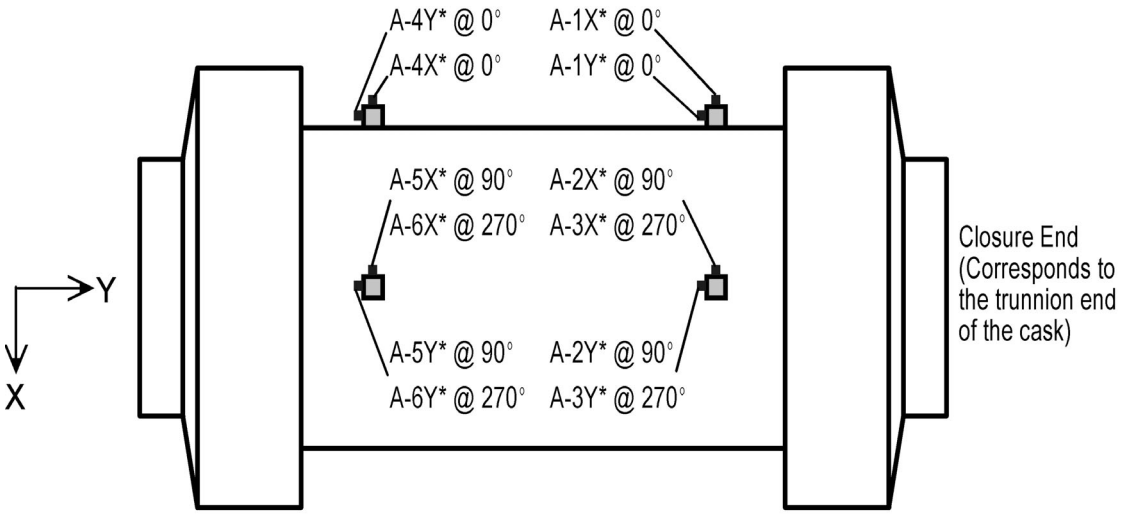

*Indicates label for accelerometer channels to identify plot

The acceleration time histories were stored electronically, which permitted them to be filtered after the tests were completed. The unfiltered data consisted of acceleration (in units of gravity "g") points corresponding to time increments of 2 microseconds.

2. Impact limiter deformation data – to evaluate the behavior of the impact limiters, the crush depth for each orientation and the condition of the limiter attachment to the model body after each test. After each test, the impact limiters were inspected to determine the amount of deformation that had occurred (the crush depth) and to determine the condition of the retaining rods. Photographs were taken to record the post-test condition of the impact limiters and retaining rods.

3. High speed photography – to review and assess the actual angle of impact and the behavior of the cask body and impact limiters during the impact.

Several high-speed cameras were used to record the behavior of the quarter-scale model as it impacted the target surface. Film speeds were 500 frames/second or greater. One camera was positioned and focused to obtain a close up view of the impact deformation. The other camera was focused to record an overall view of the impact and to verify the orientation of the cask as the impact was initiated.

2.10.12.3.2 Filter Frequency Identification for Accelerometer Data

Accelerometers can be sensitive to high frequency vibrations in parts of the structure that could be considered to be remote from the actual location of the accelerometer. The purpose of the accelerometer is to determine the rigid body deceleration of the model body during the impact, not the high frequency vibration dynamic response of other components of the model body. High frequency vibrations typically correspond to mode shapes, which are excited by the impact. Since these high frequency vibration dynamic responses are a function of the loadings on the model body, separate filter frequencies are determined and applied for each of the different drop orientations. The corner drop impact orientation produces an axial loading on the cask components in a manner similar to the end drop. The filter frequencies are determined at the test site using Fast Fourier Transforms (FFT) that is embedded in the software used to record the acceleration data during the drop test. The FFT identifies the frequency content of the unfiltered data as a function of the frequency.

2.10.12.3.3 Scale Model Drawings

The drawings for the SNL quarter-scale models are included in this section for reference. The detailed dimensions, welding and materials are shown on the drawings of the model body and impact limiters used in the SNL drop test.

Drawing Number	Number of Sheets	Revision	Title
423-354	2	2	Drop Test Assembly, ¼ Scale Model, NAC-STC Cask
423-355	4	2	Cask Body-Scale Model, 2nd Generation, NAC-STC Cask
423-357	1	0	Balsa Impact Limiter, Upper, ¼ Scale, NAC-STC Cask
423-358	1	0	Balsa Impact Limiter, Lower, ¼ Scale, NAC-STC Cask

2.10.12.4 Results/Evaluation for the 30-Foot Side Drop Test

Prior to lifting the scale model package to the 30-foot drop height, the torque for the retaining rods and nuts was verified to ensure that the torque specifications were met.

Several high-speed cameras were used to record the side drop impact. The high speed camera used to record an overall view of the drop test showed that the scale model's longitudinal axis was essentially horizontal and that the model impacted the drop test facility pad as targeted. The high-speed camera also showed that the model rebounded an estimated 4 to 6 inches into the air after the initial 30-foot drop impact.

2.10.12.4.1 Impact Limiter Deformation and Attachment Data

After the side drop test the scale model package was lifted off the ground to remove the impact limiters. During the impact limiter removal, it was observed that none of the retaining rods were broken. This confirms that the impact limiters remained attached to the cask body during and after the 30-foot side drop.

Measurements of the deformed model impact limiter dimensions were obtained after the side drop test to determine the crush depth that occurred. These dimensions are tabulated in Section 2.10.12.1, but for convenience are presented below, along with the crush depth calculated by LS-DYNA for the quarter-scale model (The description of the LS-DYNA analyses supporting these values is presented in Section 2.10.12.7).

Location	Model Drop Test Crush Depth (in.)			LS-DYNA Crush Depth Prediction (in.)		
	Original Thickness	Final Thickness	Measured Crush	Original Thickness	Final Thickness	Total Crush
Side Drop–Under The Trunnion	4.25	1.12	3.13	4.25	0.92	3.33
Side Drop–Bottom Impact Limiter	5.00	2.00	3.00	5.00	1.66	3.34

2.10.12.4.2 Accelerometer Data

The unfiltered accelerometer traces were electronically stored to permit filtering after the tests. Three acceleration traces were obtained near the bottom of the model and three acceleration traces were obtained near the top of the model. The acceleration time histories, both the filtered and the unfiltered data with maximum accelerations, are shown in Figure 2.10.12-1 for the top

end. The unfiltered acceleration data was filtered at 450 Hz. The FFT for the unfiltered data is shown in Figure 2.10.12-2, which shows there is insignificant frequency content after 300 Hz. Therefore the use of 450 Hz as the filter frequency is acceptable. Figure 2.10.12-3 shows the acceleration trace containing the maximum acceleration for the top end along with the acceleration time history computed by LS-DYNA (as described in Section 2.10.12.7). A similar set of curves is shown in Figure 2.10.12-4 for the bottom end of the cask that compares the maximum acceleration obtained from testing to the acceleration time history obtained from the LS-DYNA analysis in Section 2.10.12.7. The peak accelerations for the quarter-scale model are shown below.

Cask Model Drop Orientation	Model Acceleration Results (g)		LS-DYNA Acceleration Prediction (g)		Design Basis Acceleration (g)
	Top Accelerometer	Bottom Accelerometer	Top Accelerometer	Bottom Accelerometer	
Side	150	164	184	179	220

2.10.12.4.3 Energy Absorption Capacity of the Impact Limiter in the 30-Foot Side Drop

The capacity to absorb energy is the function of the impact limiter. For a side impact, the energy absorption of the impact limiter can be obtained from the 30-foot side drop test results. Similarly, the results of the static test for the end drop orientation can be used to determine the energy absorption for the end orientation. The side drop acceleration time history can be integrated twice to obtain the displacement, which can be plotted versus the force (the product of the acceleration time history and the model weight, i.e., the acceleration time history in units of g). This force versus displacement time history is shown in Figure 2.10.12-5. The area under this curve corresponds to 1.50E6 inch-pounds, which is within 2% of the total energy (TE) of the side drop test (1.47E6 inch-pounds). The total energy is obtained by multiplying the model weight of 4,140 pounds times the total distance traversed.

2.10.12.4.4 Summary of the Side Drop Test

The comparison of the maximum test accelerations to those computed by LS-DYNA is considered to be acceptable. The LS-DYNA results show that the predicted accelerations are conservative over the test values by approximately 20%. Additionally, the design acceleration corresponding to the quarter-scale model is 220g. This indicates that, not only is there a margin between LS-DYNA and the design basis acceleration, but there is considered to be additional 20% margin between the predicted values and the test data. With respect to maximum crush depth, LS-DYNA was shown to provide a conservative prediction. Using the dynamic force-

deflection curve, the balsa impact limiter design is shown to have an additional 25% energy absorption capacity required to decelerate the transport cask. The side drop test performed at Sandia National Laboratory confirms that the balsa impact limiters are adequate to limit the cask component accelerations well within the design basis accelerations.

2.10.12.5 Results/Evaluation for the 30-Foot Top Corner Drop Test

The 30-foot top corner drop test was performed using the NAC-STC quarter-scale model. Prior to lifting the scale model package to the 30-foot drop height, the torque for the retaining rods and nuts were confirmed to ensure that the torque specifications were met.

Only the upper impact limiter was attached to the cask model. The bottom end of the scale model used the same test weight that was to be used for the top end drop. This test weight was a substitute for a bottom impact limiter and ensures that the tested package has the proper weight and CG location to bound all transport configurations.

Several high-speed cameras were used to record the top corner drop impact. One of the high-speed cameras recorded a close-up view of the impact limiter crush in the region of the impact plane. The other camera recorded an overall view of the drop test and showed that the cask orientation was very close to the target angle of 15° from vertical.

2.10.12.5.1 Impact Limiter Deformation and Attachment Data

After the top corner drop test the scale model package was lifted off the ground to remove the impact limiters. During the impact limiter removal, it was observed that none of the retaining rods were broken. This confirms that the impact limiters remained attached to the cask body during and after the 30-foot top corner drop.

Measurements of the deformed model impact limiter dimensions were obtained after the top corner drop test to determine the crush depth that occurred. These dimensions are tabulated below, along with the crush depth calculated by LS-DYNA for the quarter-scale model (The description of the LS-DYNA analyses supporting these values is presented in Section 2.10.12.7).

Location	Model Drop Test Crush Depth (in.)			LS-DYNA Crush Depth Prediction (in.)		
	Original Thickness	Final Thickness	Measured Crush	Original Thickness	Final Thickness	Total Crush
Top Corner Drop	9.75	4.25	5.5	9.75	4.07	5.68

2.10.12.5.2 Accelerometer Data

An initial observation is that significant "noise" vibrations associated with the accelerations do exist and that filtering of the accelerometer data is appropriate. The typical unfiltered result is shown in Figure 2.10.12-6 while the filtered data is shown in Figure 2.10.12-7. The filter frequency was selected to be 450 Hz. The comparison of the accelerometer data test results and the LS-DYNA results is shown in Figure 2.10.12-8. The results from the LS-DYNA finite element analysis program, and the maximum acceleration determined from the three accelerometer traces are:

Location	Quarter-Scale Model Acceleration (g)	LS-DYNA Calculated Acceleration (g)
Top Impact Limiter	126	137

The acceleration determined from the quarter-scale model top corner drop test is enveloped by the LS-DYNA calculated design basis accelerations.

2.10.12.5.3 Energy Absorption Capacity of the Impact Limiter in the 30-Foot Top Corner Drop

The capacity to absorb energy is the function of the impact limiter. For a top corner impact, the energy absorption of the impact limiter can be obtained from the 30-foot top corner drop test results. Similarly, the results of the static test for the end drop orientation can be used to determine the energy absorption for the end orientation. The corner drop acceleration time history can be integrated twice to obtain the displacement, which can be plotted versus the force (the product of the acceleration time history and the model weight, i.e., the acceleration time history in units of g). This force versus displacement time history is shown in Figure 2.10.12-9. The area under this curve corresponds to 1.49E6 inch-pounds, which is within 1% of the total energy (TE) of the side drop test (1.47E6 inch-pounds). The total energy is obtained by multiplying the model weight of 4,140 pounds times the total distance traversed.

2.12.3.5.4 Summary of the Top Corner Drop Test Results

The crush depth and impact accelerations determined from the 30-foot top corner drop test of the NAC-STC quarter-scale model are enveloped by the LS-DYNA calculated design-basis analysis data used in the SAR. The NAC-STC impact limiters are confirmed to provide adequate design margin to limit the acceleration and the crush depth of the transport cask for the 30-foot top

corner drop. Thus, the NAC-STC cask body will not contact the impact plane during the 30-foot top corner drop.

2.10.12.6 Results/Evaluation for the 30-Foot Top End Drop Test

Two 30-foot top end drop tests were performed using the NAC-STC quarter-scale model. In the first test of the top end drop, the accelerometer traces demonstrated that the accelerometers attached to the cask body had experienced a resonance condition. This resulted in large spurious signals in the traces, which were on the order of several thousand g's even though the limiter performed as intended. To correct this accelerometer performance the accelerometers in the first end drop test which had a resonance frequency of 160 kHz were replaced with accelerometers with a resonance frequency of 350 kHz. The new accelerometers were subjected to the same calibration and traceability criteria as the initial accelerometers. The use of the new accelerometers resolved the resonance problem. The results presented in this section correspond to the second top end drop. The first end drop employed an unused impact limiter. The second end drop was done using the top end impact limiter from the side drop. In the side drop test, the balsa portion of the impact limiter, which protects in the end drop, was not deformed. This impact limiter was inspected to verify that the dimensions for the balsa section corresponded to those for an unused impact limiter intended for an end drop orientation. Therefore, the second end drop test is considered to be acceptable for confirming the design of the balsa impact limiter for the end drop.

In each test, prior to lifting the scale model package to the 30-foot drop height, the torque for the retaining rods and nuts were confirmed to ensure that the torque specifications were met.

Only the upper impact limiter was attached to the cask model. The bottom end of the scale model used the same test weight that was used for the top end drop. This test weight is an inexpensive substitute for a bottom impact limiter and ensures that the tested package has the proper weight and CG location to bound all transport configurations.

Several high-speed cameras were used to record the top corner drop impact. One of the high-speed cameras recorded a close-up view of the impact limiter crush in the region of the impact plane. The other camera recorded an overall view of the drop test and showed that the cask orientation was very close to being perpendicular with the target.

2.10.12.6.1 Impact Limiter Deformation and Attachment Data

After the top end drop test, the scale model package was lifted off the ground to remove the impact limiter.

Measurements of the model impact limiter dimensions after the top end drop test were obtained to determine the crush depth. The measured crush depth is tabulated as follows, along with the LS-DYNA calculated crush depth.

Location	Quarter-Scale Model Impact Limiter Crush Depth (inch)	LS-DYNA Calculated Crush Depth (inch)
Top Impact Limiter	4.4	4.6

The resulting crush depth determined from the quarter-scale model top end drop test is enveloped by the LS-DYNA calculated design-basis crush depths for the full-scale NAC-STC transport cask for a 30-foot top corner drop with impact limiters.

2.10.12.6.2 Accelerometer Data

An initial observation is that significant "noise" vibrations associated with the accelerations do exist and that filtering of the accelerometer data is appropriate. The typical unfiltered trace is shown in Figure 2.10.12-10, while the filtered result is shown in Figure 2.10.3-12. The filter frequency was selected to be 450 Hz. The FFT of the end drop time history is shown in Figure 2.10.12-11 and it confirms that the use of 450 Hz as the filter frequency is acceptable. The comparison of the LS-DYNA results and the test results are shown in Figure 2.10.12-13. The results from the LS-DYNA finite element analysis program, and the maximum acceleration determined from the three accelerometer traces are:

Location	Quarter-Scale Model Acceleration (g)	LS-DYNA Calculated Acceleration (g)
Top Impact Limiter	122	128

The acceleration determined from the quarter-scale model top corner drop test is enveloped by the LS-DYNA calculated design basis accelerations.

2.10.12.6.3 Energy Absorption Capacity of the Impact Limiter in the 30-Foot Top End Drop

The capacity to absorb energy is the function of the impact limiter. For a top end impact, the energy absorption of the impact limiter can be obtained from the 30-foot top end drop test results. Similarly, the results of the static test for the end drop orientation can be used to determine the energy absorption for the end orientation. The end drop acceleration time history can be integrated twice to obtain the displacement, which can be plotted versus the force (the product of the acceleration time history and the model weight, i.e., the acceleration time history in units of g). This force versus displacement time history is shown in Figure 2.10.12-14. The area under this curve corresponds to 1.49E6 inch-pounds, which is within 1% of the total energy (TE) of the side drop test (1.47E6 inch-pounds). The total energy is obtained by multiplying the model weight of 4,140 pounds times the total distance traversed.

2.10.12.6.4 Summary of the Top End Drop Test Results

The crush depth and impact accelerations determined from the 30-foot top end drop test of the NAC-STC quarter-scale model are enveloped by the LS-DYNA calculated design-basis analysis data used in the SAR. The NAC-STC impact limiters are confirmed to provide adequate design margin to limit the acceleration and the crush depth of the transport cask for the 30-foot top end drop. Thus, the NAC-STC cask body will not contact the impact plane during the 30-foot top end drop.

2.10.12.7 LS-DYNA Analyses of the NAC-STC Quarter-Scale Model

The finite element model of the quarter-scale NAC-STC cask equipped with balsa impact limiters was built using LS-DYNA's Finite Element Model Builder. The top end, top corner, and side impact analyses were performed using the LS-DYNA program. The model is constructed of 8-node brick and 4-node shell elements. Using the symmetry planes that exist for the various drop orientations, the model was simplified so that only a half-model was necessary for the analyses. The finite element model used in the analyses corresponds to the quarter-scale cask body and impact limiters. The complete finite element model is shown in Figure 2.10.12-15.

The cask body section of the model consists of a single shell using an elastic material. The elastic modulus of the cask body was adjusted to allow the cross sectional modulus of the finite element model to be equal to that of the quarter-scale model. As shown in Figure 2.10.12-15, the model contains a detailed representation of the trunnion and the cut out (trunnion pocket) in the

top impact limiter. The impact limiters are attached to the cask ends by beam elements corresponding to the attachment bolts for the impact limiter. The redwood and the balsa wood were modeled as an isotropic foam material. The room temperature stress-strain curves used as input into the LS-DYNA model were obtained by dynamic crush testing of redwood and balsa wood specimens as described in section 2.6.7.4.2.4.

To account for the deformation of the Type 304 stainless steel shells and gussets, these components were modeled with an elasto-plastic material. The LS-DYNA material Type 24 was used ("Piecewise_Linear_Plasticity"). The required input data for the stainless steel consists of the stress-strain data contained in Section 2.6.7.4.2.5.

2.10.12.7.1 Boundary Conditions and Initial Conditions

LS-DYNA "Surface_to_Surface" contact interfaces are employed between the cask body and the impact limiter shells. The unyielding surface is modeled as being flat using the Rigidwall_Geometric_Flat" option in LS-DYNA. Symmetry boundary conditions are imposed on the nodes in the X-Z plane for all drops. An initial velocity of 527.4 in/sec is applied to the entire model to represent the 30-foot drops. A uniform gravitational field corresponding to 386.4 in/sec^2 is also applied in the direction of the drop.

Three drop orientations are considered in this evaluation: top end, CG over top corner, and side drop. The end drop provides the maximum axial accelerations. The corner drop results in the largest crush depth of the limiter. The side drop provides the maximum acceleration in the lateral direction of the cask.

2.10.12.7.2 Results

To obtain results from LS-DYNA, nodes of interest are used to record output data. The nodes are located on the cask body at the plane of symmetry approximately 10 inches from the impact limiters. These data nodes correspond to the location of the accelerometers mounted on the quarter-scale model. For the side drop, the nodes record the lateral acceleration, and for the end drop they record the axial acceleration. For the CG over corner orientation, the output acceleration corresponds to the direction of the drop.

The LS-DYNA output is in the form of displacement and acceleration time histories. However, the acceleration time histories contain high frequency components that do not represent the

response of the cask to the external impact. Therefore, the acceleration time histories are filtered to obtain true accelerations corresponding to the impact. For this evaluation, the Butterworth low-pass filter in LS-DYNA's post-processor is used with a filter frequency of 450 Hz for the lateral direction axial directions. The Butterworth filter is used in NUREG/CR-6608 to filter the acceleration of the impact tests for a steel billet in the side drop and end drop orientation.

The following table shows the maximum accelerations for the three 30-foot drop cases.

Cask model Drop Orientation	Quarter-Scale Drop Test Results (g)		LS-DYNA Prediction (g)	
	Top Accelerometer	Bottom Accelerometer	Top Accelerometer	Bottom Accelerometer
Top Corner	126	N/A	137	N/A
Top End	122	N/A	128	N/A
Side	150	164	184	179

As the table shows, the maximum predicted acceleration of 184g occurs during the side drop. Acceleration time-history plots are provided in Figures 2.10.12-3 and 2.10.12-4 for the side drop and Figures 2.10.12-8 and 2.10.12-13 for the top corner and top end drops, respectively. In all cases, the LS-DYNA prediction is greater than the quarter-scale drop test results.

A comparison of the predicted crush depth to the actual crush depth is provided in Section 2.10.12.1 and shows that LS-DYNA accurately predicts the amount of crush experienced during the drop tests except in regions where extreme irregular deformations occur (i.e. directly below the trunnion and corner).

Figure 2.10.12-1 Typical Filtered Acceleration Time History for the Quarter-Scale Model Side Drop, Overlayed with the Unfiltered Data for the Top End of the Model

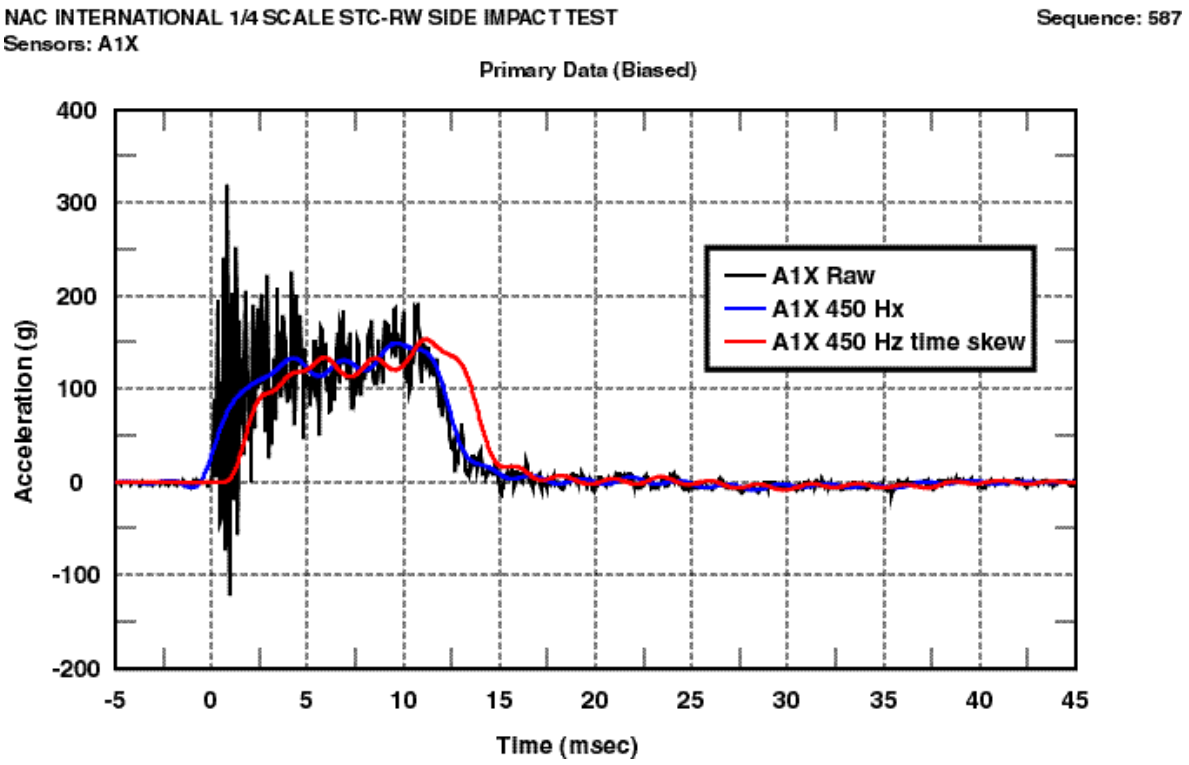

Figure 2.10.12-2 The FFT for the Unfiltered Accelerometer Time History in Figure 2.10.12-1

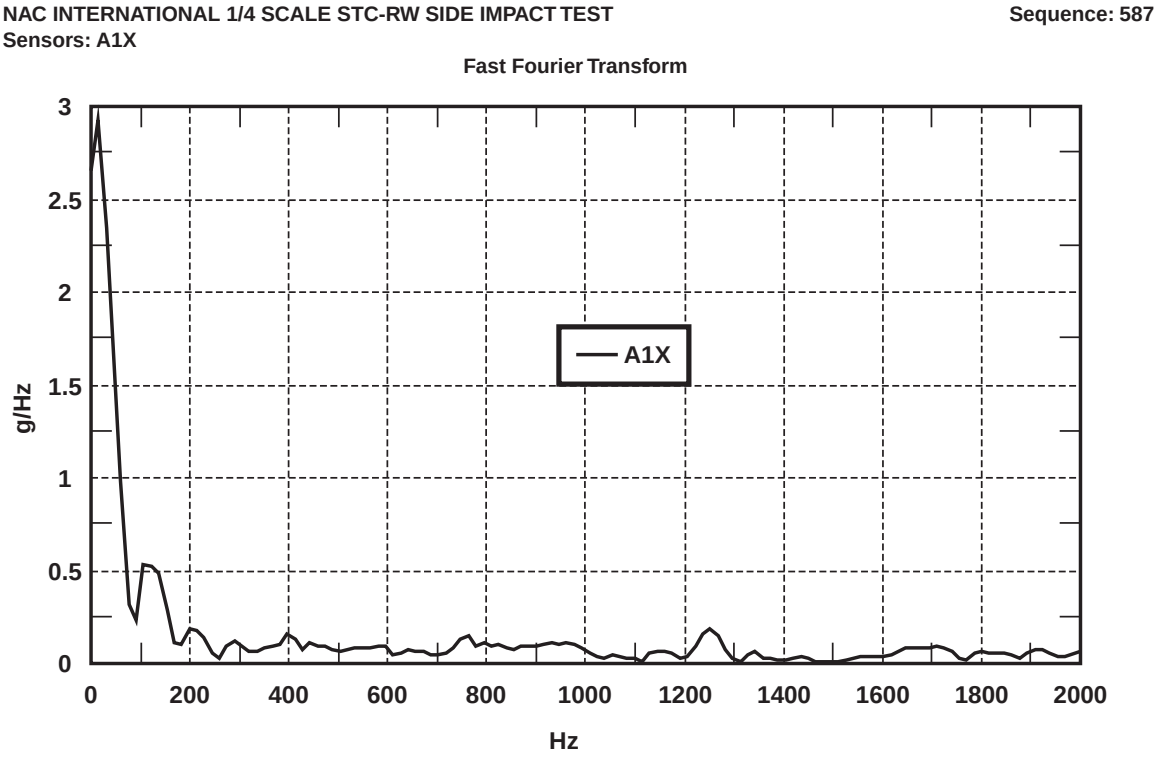

Figure 2.10.12-3 Typical Filtered Acceleration Time History for the Quarter-Scale Model Side Drop, Overlaid with the LS-DYNA Filtered Time History for the Top End of the Model

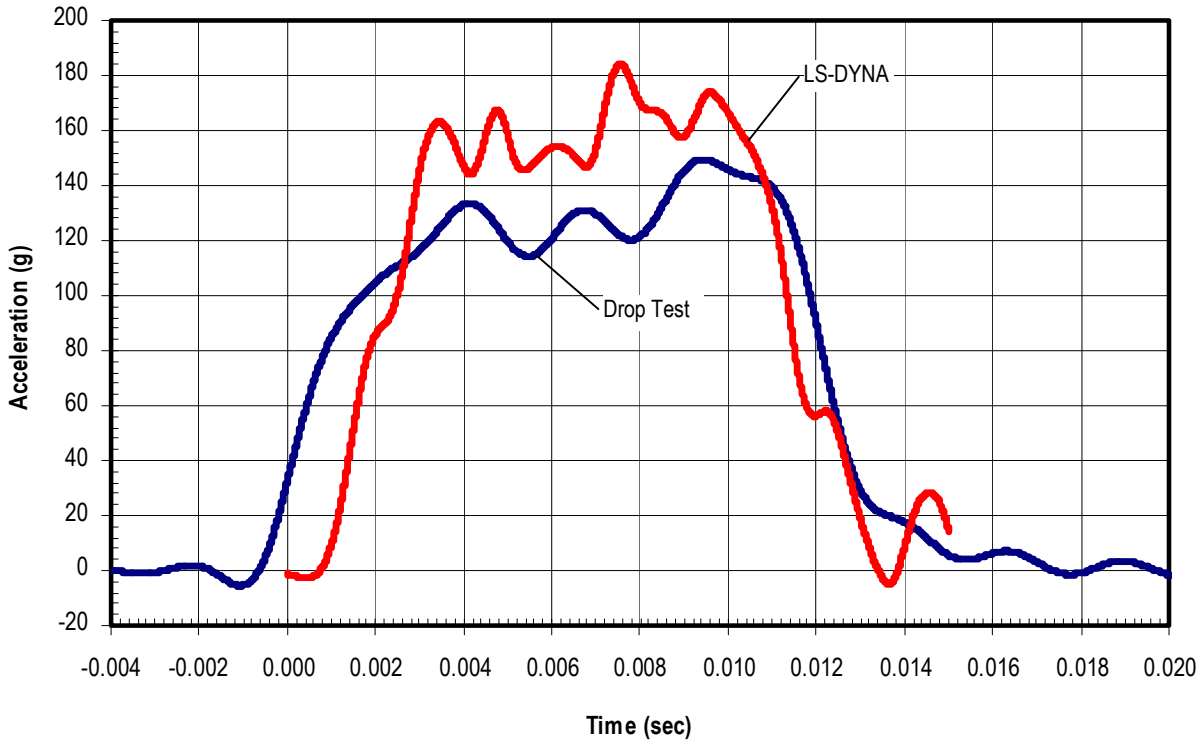

Figure 2.10.12-4 Typical Filtered Acceleration Time History for the Quarter-Scale Model Side Drop, Overlaid with the LS-DYNA Filtered Time History for the Bottom End of the Model

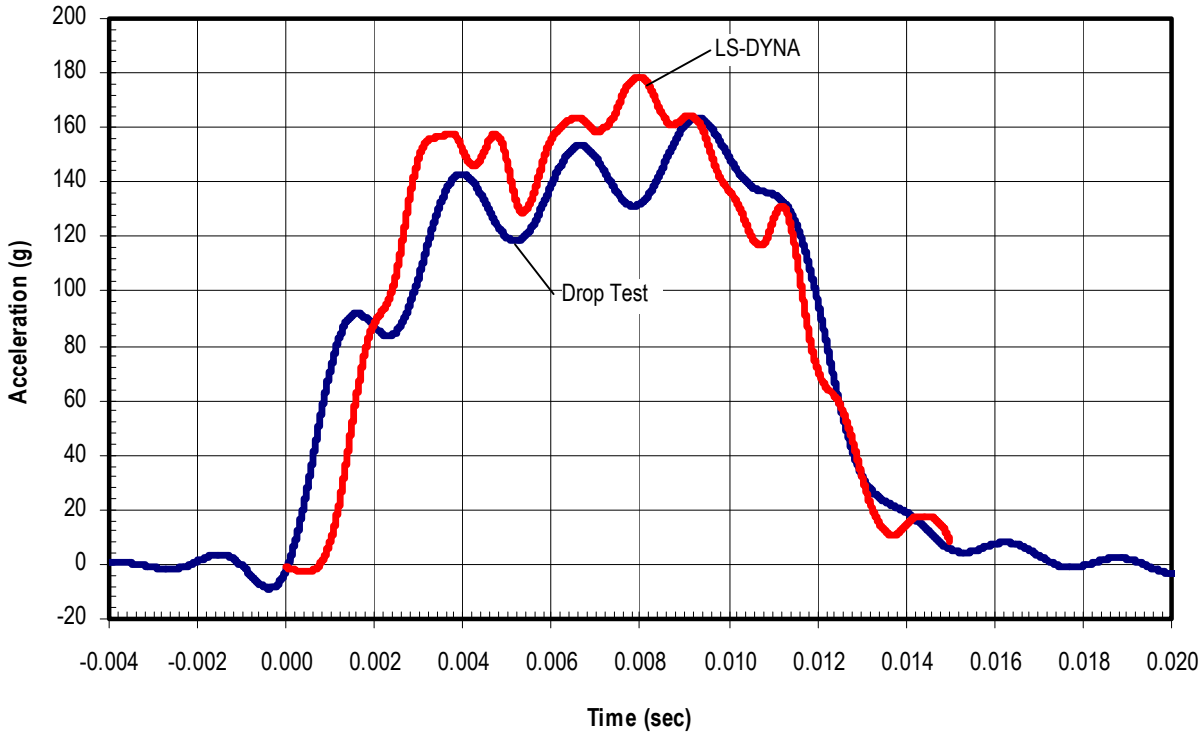

Figure 2.10.12-5 Force Deflection Curve for the 30-Foot Side Drop Test

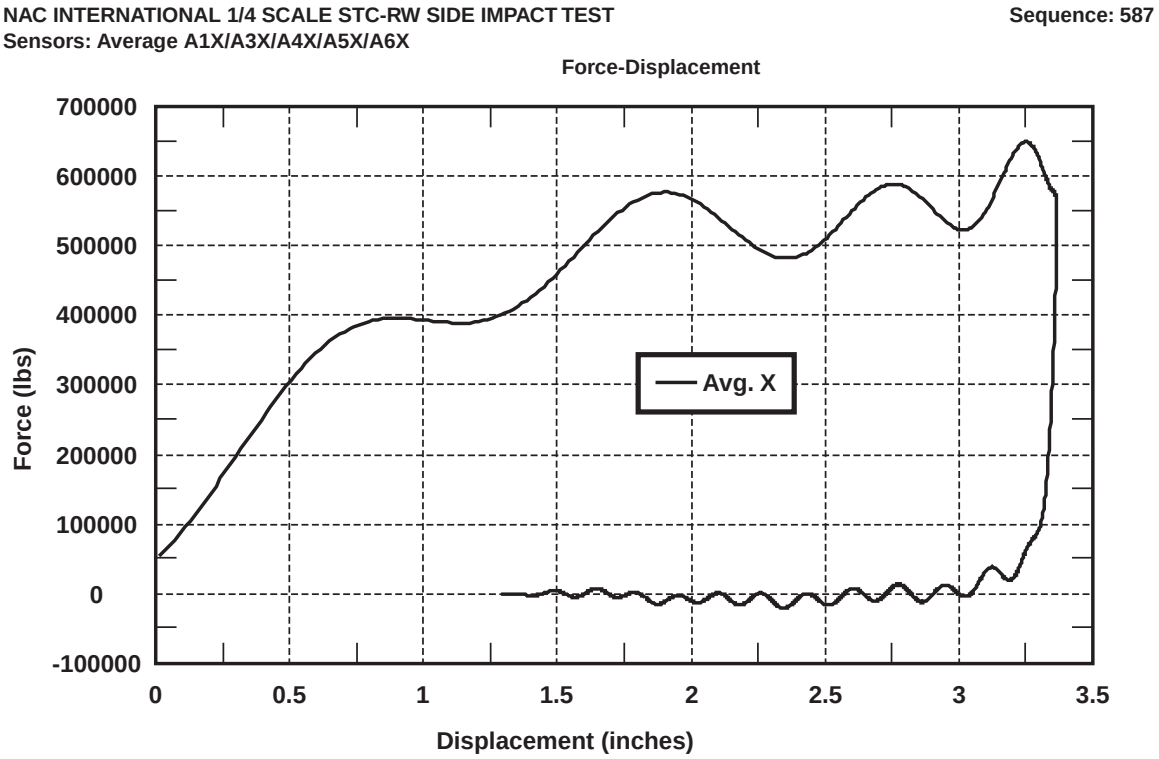

Figure 2.10.12-6 Typical Unfiltered Acceleration (Top Accelerometer) Time History for the Quarter-Scale Model Top Corner Drop

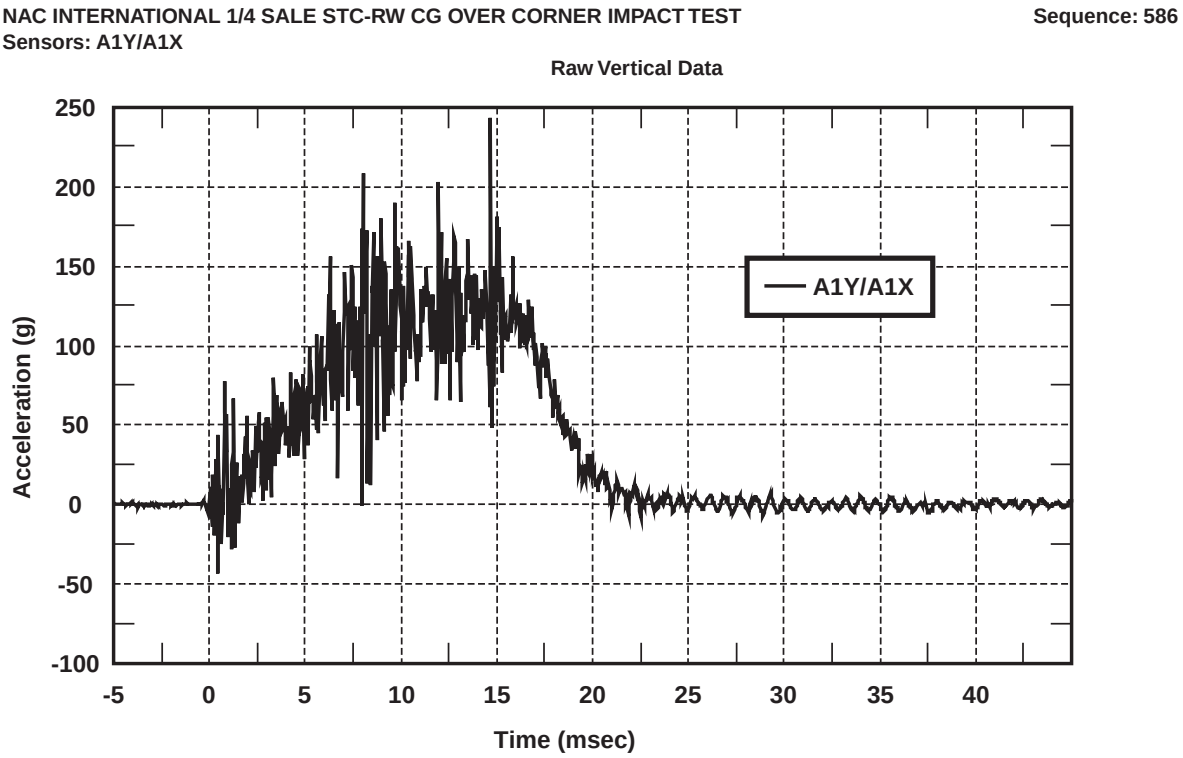

Figure 2.10.12-7 Typical Filtered Acceleration (Top Accelerometer) Time History for the Quarter-Scale Model Top Corner Side Drop

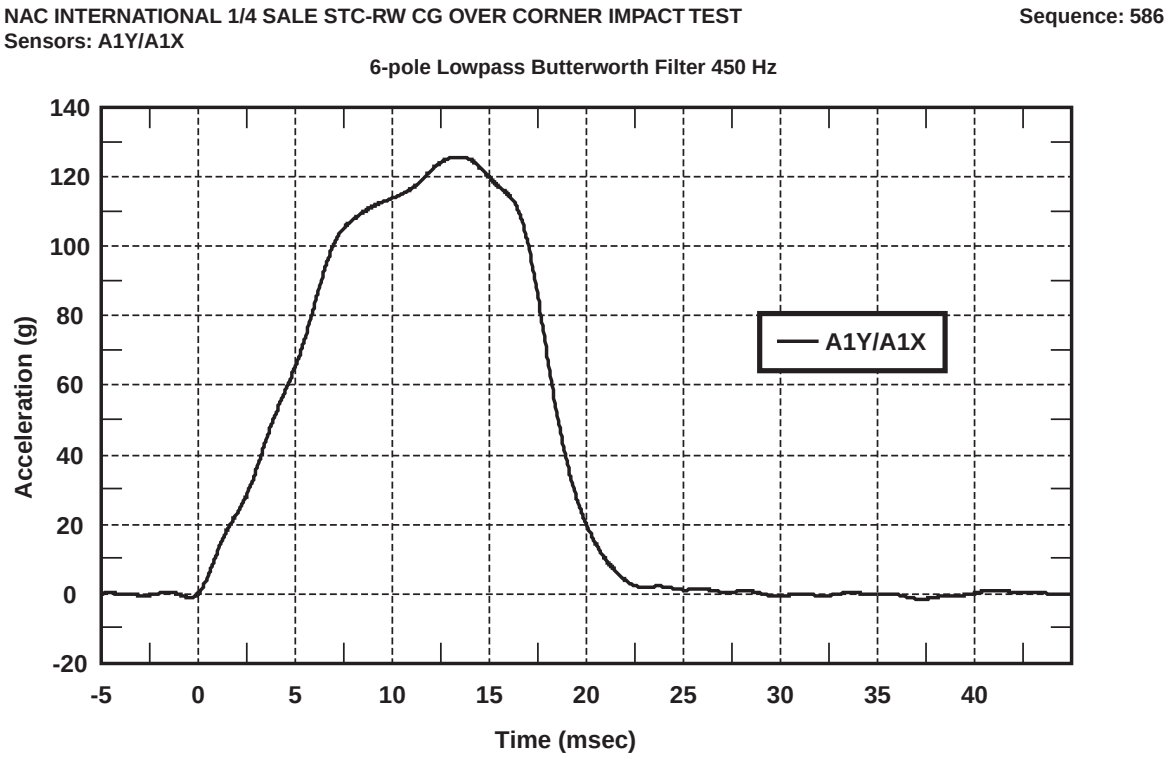

Figure 2.10.12-8 Comparison of Quarter-Scale Top Corner Drop (LS-DYNA and Drop Test) Results (Upper Accelerometer)

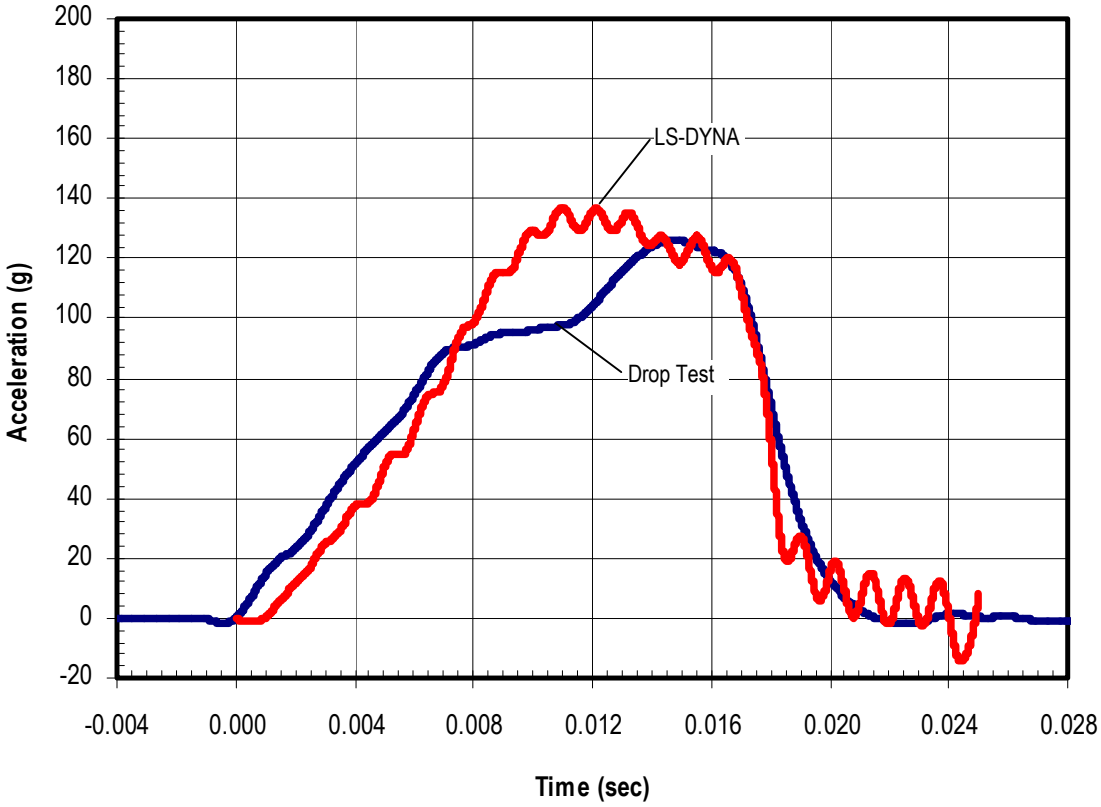

Figure 2.10.12-9 Force Deflection Curve for the Top Corner Drop

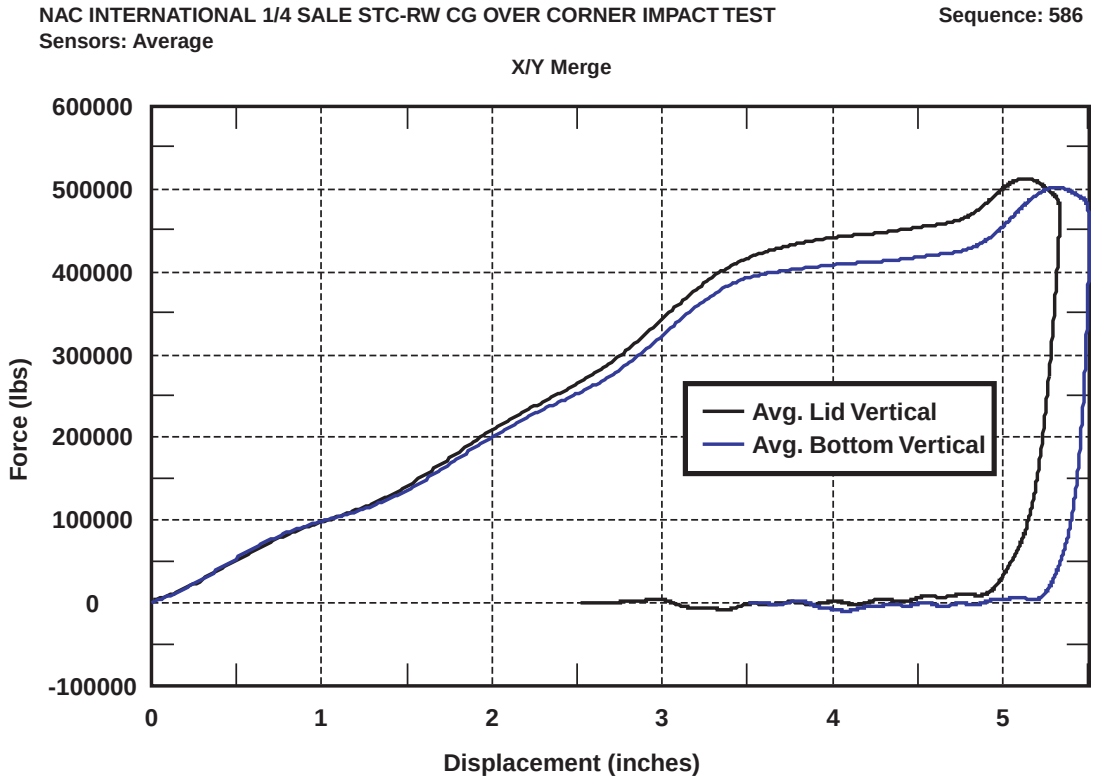

Figure 2.10.12-10 Typical Unfiltered Acceleration (Top Accelerometer) Time History for the Quarter-Scale Model Top End Drop

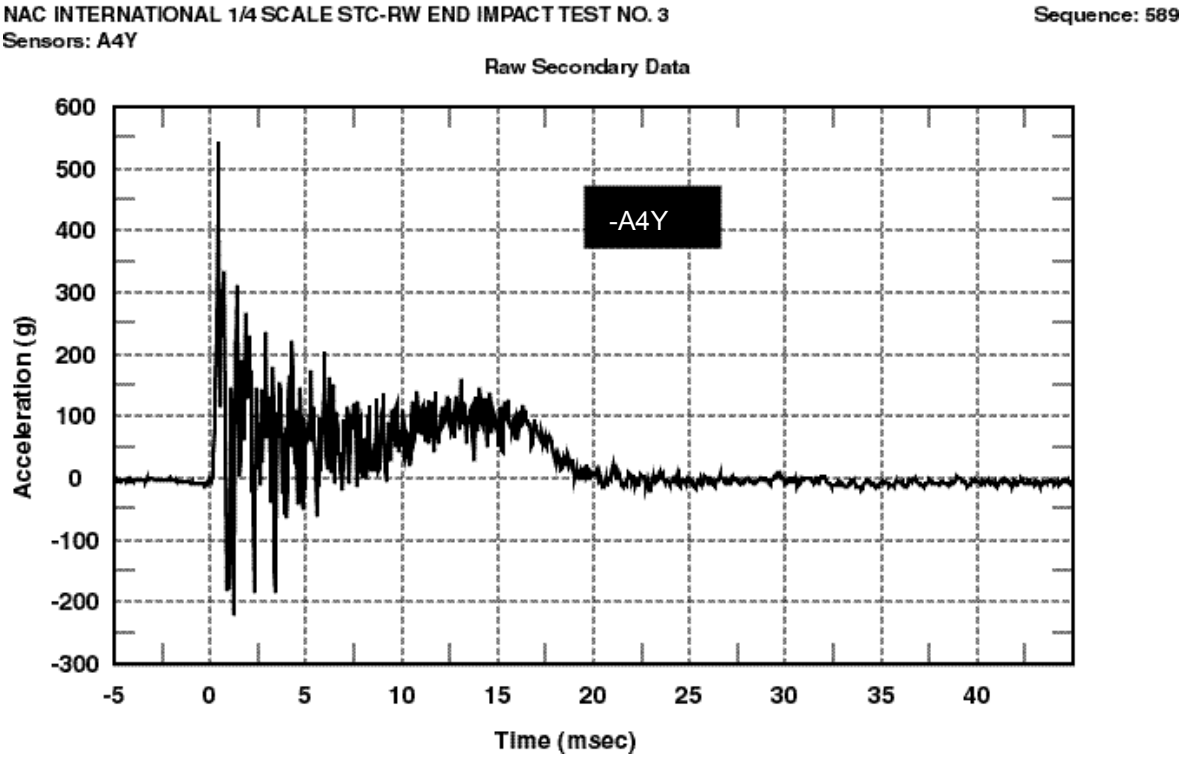

Figure 2.10.12-11 The FFT for the Unfiltered Accelerometer Time History in Figure 2.10.12-10

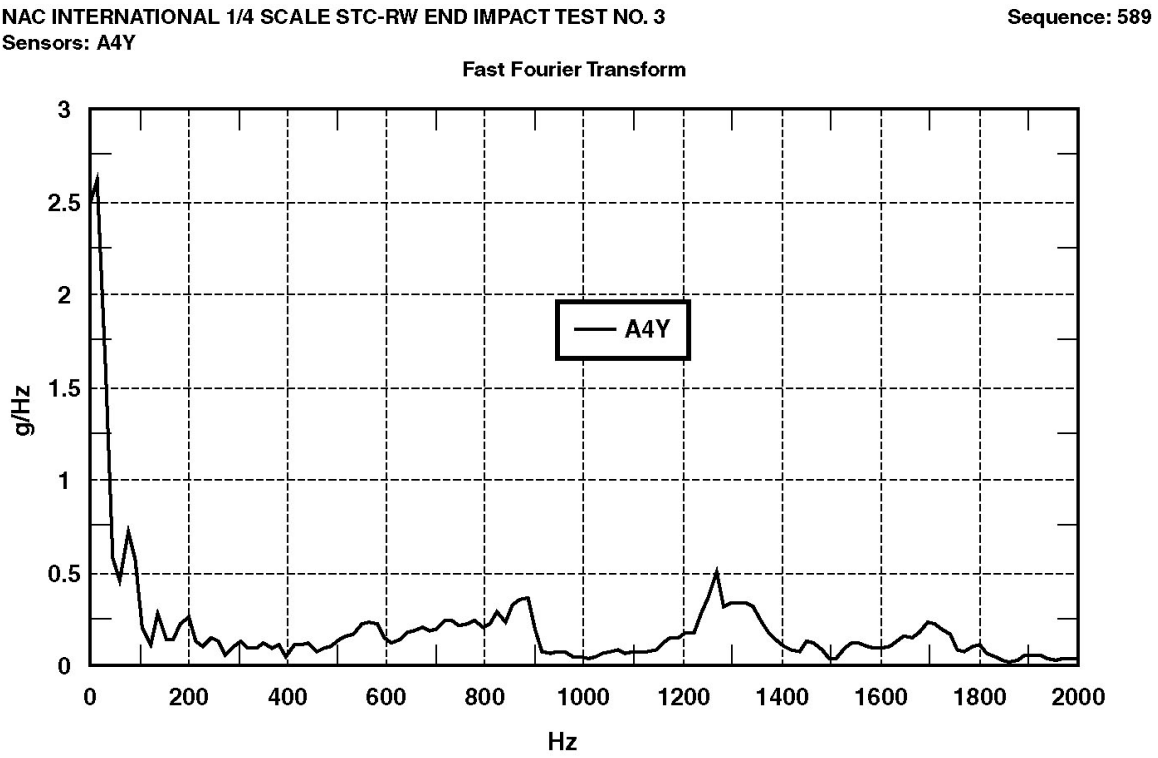

Figure 2.10.12-12 Typical Filtered Acceleration (Top Accelerometer) Time History for the Quarter-Scale Model Top End Drop

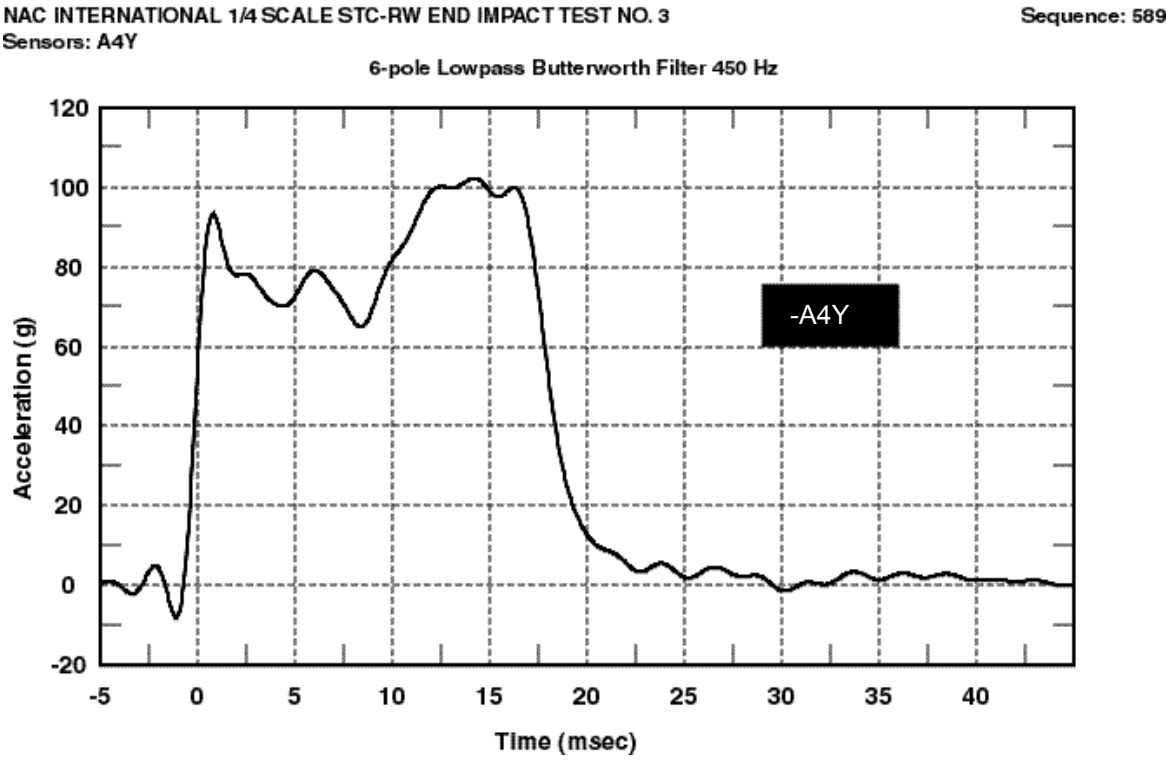

Figure 2.10.12-13 Comparison of Quarter-Scale Top End Drop (LS-DYNA and Drop Test) Results (Upper Accelerometer)

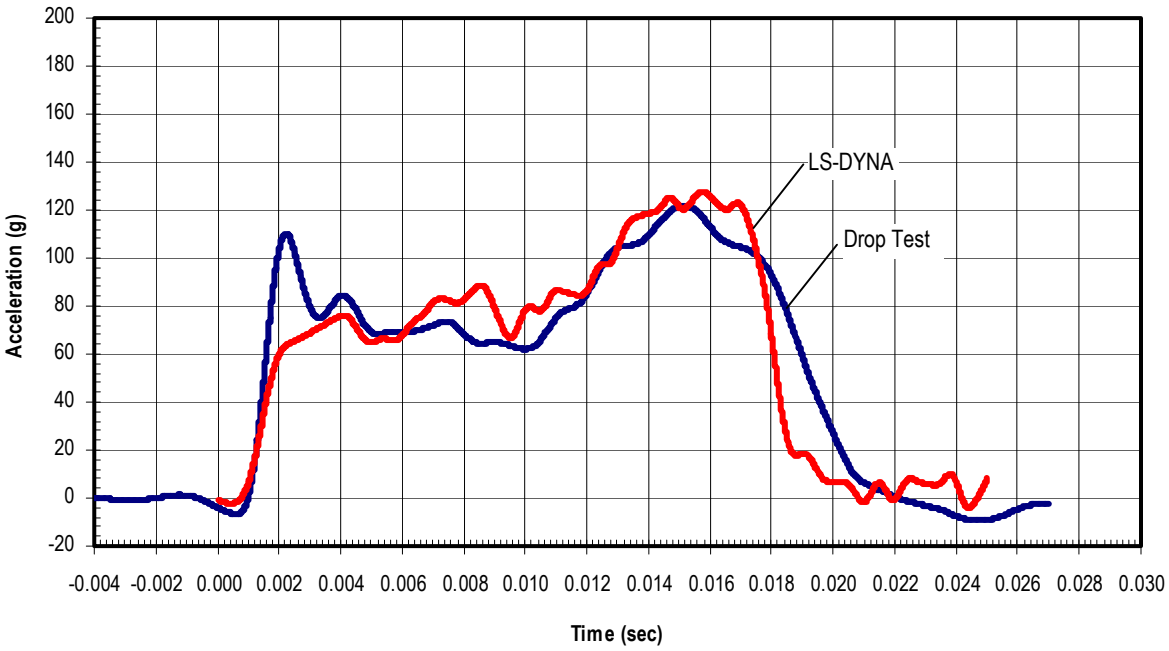

Figure 2.10.12-14 Force Deflection Curve for the Top End Drop

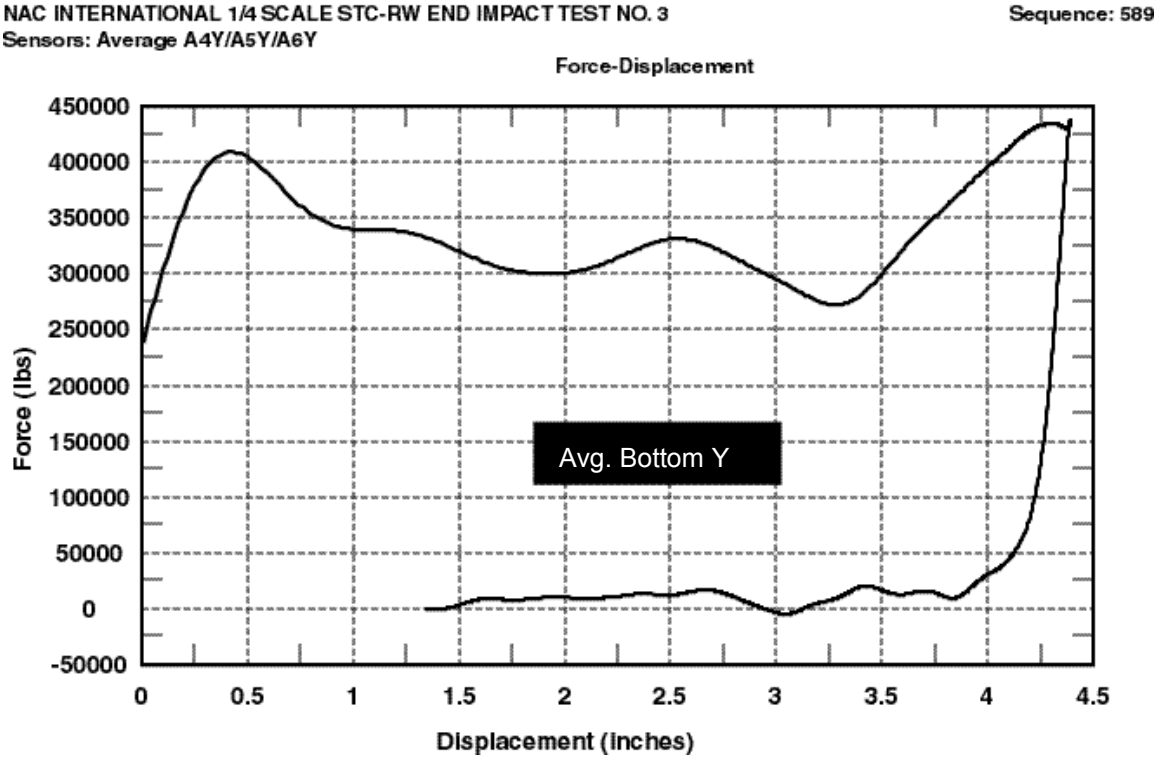

Figure 2.10.12-15 LS-DYNA Quarter-Scale Model

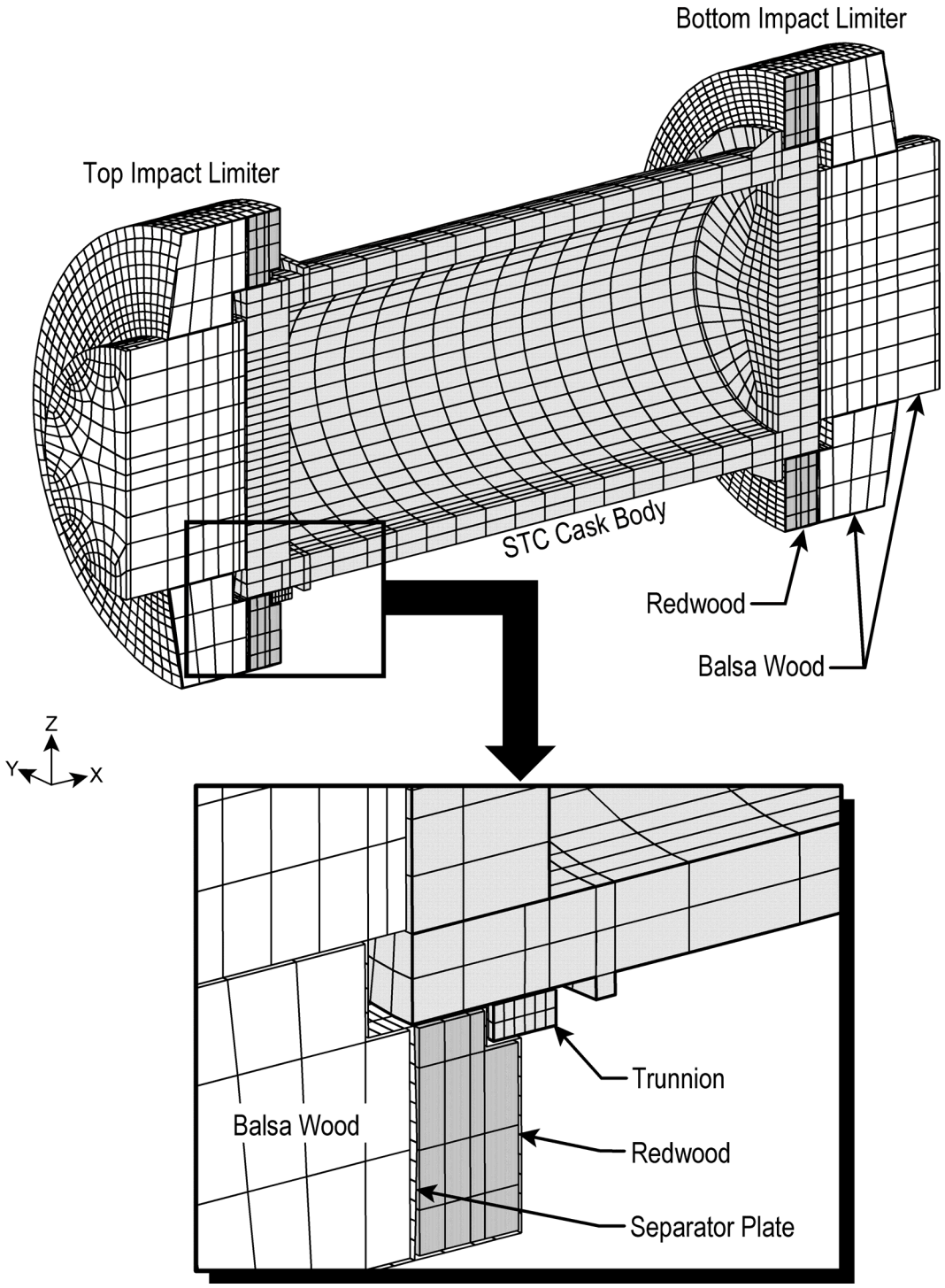

THIS PAGE INTENTIONALLY LEFT BLANK

FIGURE WITHHELD UNDER 10 CFR 2.390

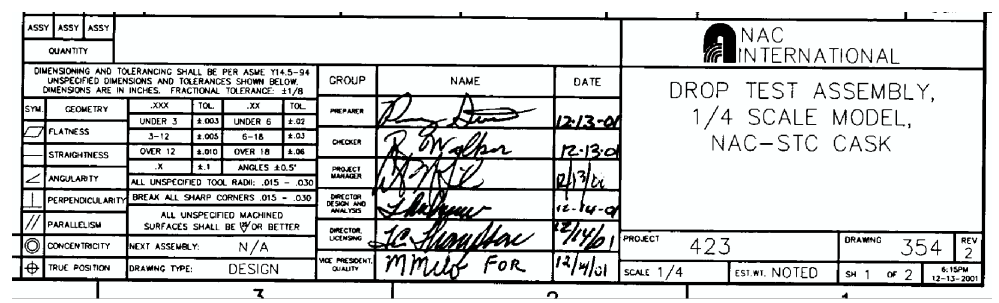

FIGURE WITHHELD UNDER 10 CFR 2.390

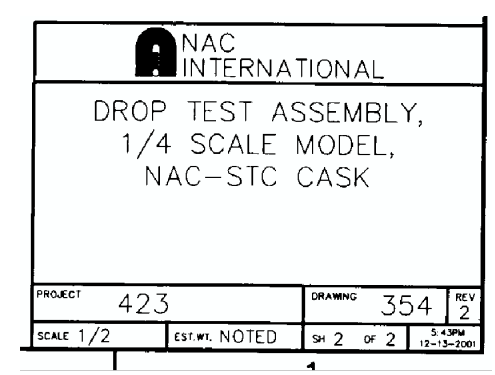

FIGURE WITHHELD UNDER 10 CFR 2.390

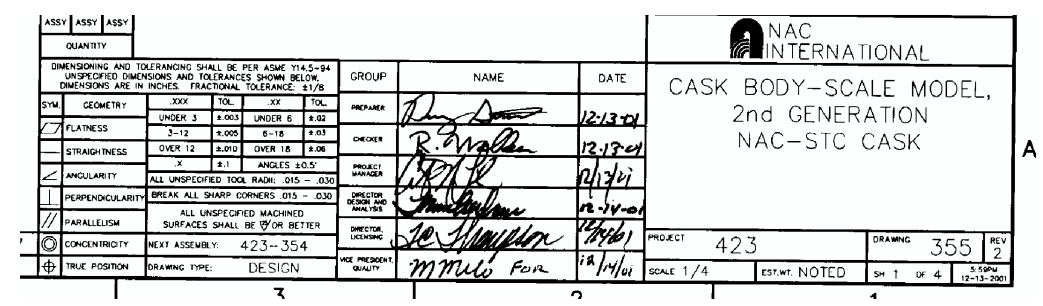

FIGURE WITHHELD UNDER 10 CFR 2.390

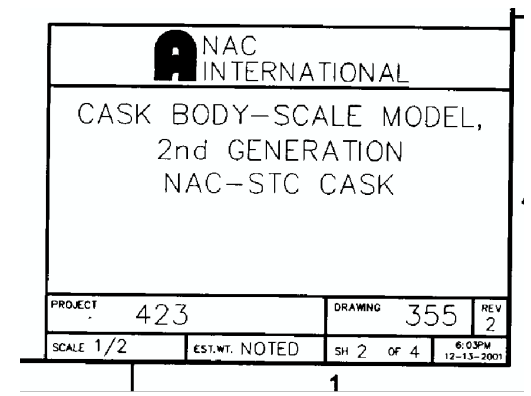

FIGURE WITHHELD UNDER 10 CFR 2.390

NAC INTERNATIONAL

CASK BODY–SCALE MODEL
2nd GENERATION
NAC–STC CASK

PROJECT 423		DRAWING 355	REV 2
SCALE 1/2	EST.WT. NOTED	SH 3 OF 4	6:04PM 12-13-2001

1

FIGURE WITHHELD UNDER 10 CFR 2.390

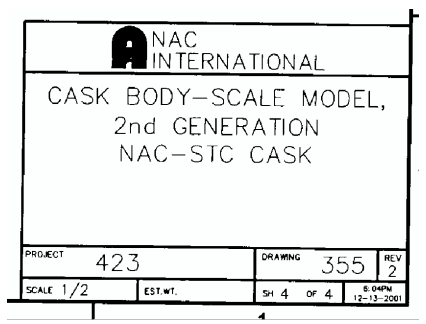

FIGURE WITHHELD UNDER 10 CFR 2.390

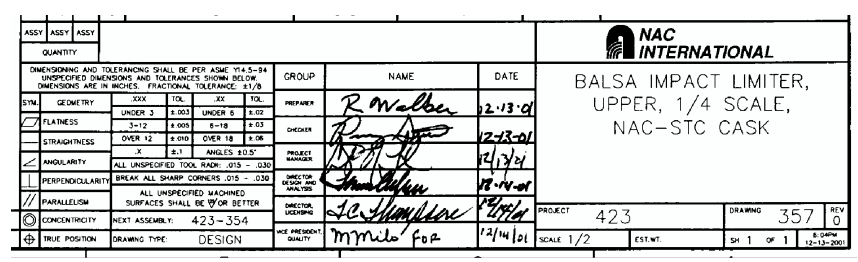

FIGURE WITHHELD UNDER 10 CFR 2.390

ASSY	ASSY	ASSY
QUANTITY		

DIMENSIONING AND TOLERANCING SHALL BE PER ASME Y14.5-94
UNSPECIFIED DIMENSIONS AND TOLERANCES SHOWN BELOW.
DIMENSIONS ARE IN INCHES. FRACTIONAL TOLERANCE: ±1/8

SYM	GEOMETRY	.XXX	TOL.	.XX	TOL.
⏥	FLATNESS	UNDER 3	±.003	UNDER 6	±.02
—	STRAIGHTNESS	3-12	±.005	6-18	±.03
∠	ANGULARITY	OVER 12	±.010	OVER 18	±.06
⊥	PERPENDICULARITY	.X	±.1	ANGLES ±0.5°	
//	PARALLELISM	ALL UNSPECIFIED TOOL RADII: .015 - .030			
◎	CONCENTRICITY	BREAK ALL SHARP CORNERS .015 - .030			
⊕	TRUE POSITION	ALL UNSPECIFIED MACHINED SURFACES SHALL BE ▽ OR BETTER			

NEXT ASSEMBLY: 423-354
DRAWING TYPE: DESIGN

GROUP	NAME	DATE
PREPARER	[signature]	12/13/01
CHECKER	R. Walker	12-13-01
PROJECT MANAGER	[signature]	12/13/01
DIRECTOR DESIGN AND ANALYSIS	[signature]	12-14-01
DIRECTOR LICENSING	J.C. Thompson	12/14/01
VICE PRESIDENT, QUALITY	M Mills FOR	12/14/01

NAC INTERNATIONAL

BALSA IMPACT LIMITER, LOWER, 1/4 SCALE, NAC-STC CASK

PROJECT 423 | DRAWING 358 | REV 0
SCALE 1/2 | EST.WT. NOTED | SH 1 OF 1 | 6:36PM 12-13-2001